Experimental Investigations of Piping Erosion and Suffusion of Soils in Embankment Dams and their Foundations

by

Chi Fai Wan

A thesis submitted in partial fulfilment
of the requirements for the degree of
Doctor of Philosophy

Volume 1

School of Civil and Environmental Engineering

The University of New South Wales

June 2006

ABSTRACT

This thesis presents the findings of an investigation on internal erosion in embankment dams and their foundations by piping and suffusion. The development of internal erosion in a dam can be divided into the Initiation Phase, the Continuation Phase, the Progression Phase, and the Failure Phase. The current study focuses on the Initiation Phase, and involves laboratory investigations of erosion in a concentrated leak, and suffusion processes, which are two main initiation mechanisms of internal erosion.

The slot erosion test and the hole erosion test have been developed for studying piping erosion in cracks in embankment dams. The two laboratory tests characterise the erosion properties of a soil by the erosion rate index, which measures the rate of erosion, and the critical shear stress, which represents the minimum shear stress when erosion starts. Values of the erosion rate index span from 0 to 6, indicating that soils can differ in their rates of erosion by up to 10^6 times. The erosion rate index is dependent on the soil fines and clay sized content, plasticity, and dispersivity; compaction water content, density and degree of saturation; clay mineralogy, and cementing materials. Coarse-grained, non-cohesive soils, in general, erode more rapidly and have lower critical shear stresses than fine-grained cohesive soils.

Suffusion is defined as an internal erosion process by which finer soil particles are moved through constrictions between larger soil particles by seepage forces. There is no general consensus on the use of the word "suffusion". German and Canadian literature uses the word "suffosion" or "suffossion". Suffusion leads to a coarser soil structure, increased seepage, progressive deterioration of a dam or its foundation, and potential instability of the downstream slope of the dam. Laboratory investigation of the suffusion process involved conducting two tests, namely the downward flow (DF) seepage test and the upward flow (UF) seepage test. The DF test identifies soils that are susceptible to suffusion, whereas the UF test identifies the hydraulic gradient at which suffusion is initiated. Based on the analysis of the results of the two series of seepage tests, and similar seepage tests conducted by previous investigators, new procedures are developed for assessing the suffusion characteristics of clay-silt-sand-gravel and silt-sand-gravel soils.

ACKNOWLEDGEMENTS

This thesis marks the completion of my research at the School of Civil and Environmental Engineering, the University of New South Wales. The research was part of a project on the investigation of the likelihood on internal erosion and piping in embankment dams and their foundations initiated by Professor Robin Fell. I have developed an interest in internal erosion problems in embankment dams ever since I started my career in dams engineering. Thanks to Professor Fell for offering me the opportunity to carry out an in-depth study on internal erosion in dams. Without his vision and enthusiasm, the research project would not have been possible.

I would like to express my most heartily thanks to Professor Fell, who patiently supervised my research and the preparation of this thesis in the past few years. He has made himself available at all time for giving me valuable advice and direction. Working under his supervision has greatly broadened my knowledge in geotechnical engineering and dams, and has given me much pleasure and satisfaction. I would also like to express my appreciation to my co-supervisor, Dr. Nasser Khalili-Naghadeh, who introduced me to the research project, and provided continuous encouragement and support throughout the course of my study. Special thanks are further due to Dr. Mark Foster for his thoughtful discussion in the development of the laboratory tests, and his valuable comments on my work.

I am grateful to the Australian Research Council and the eighteen industry sponsors for providing financial support to the research. The industry sponsors are:

- ACTEW Corporation
- BC Hydro and Power Authority, Canada
- Damwatch Services Ltd, New Zealand

- Dams Safety Committee of NSW
- Department of Land and Water Conservation
- Department of Sustainability and Environment
- GHD Services Pty Ltd
- Goulburn Murray Water
- Hydro Tasmania
- Melbourne Water Corporation
- NSW Department of Commerce (formerly NSW Department of Public Works and Services)
- Pacific Power
- Snowy Hydro Ltd
- Snowy Mountains Engineering Corporation
- South Australia Water Corporation
- US Department of the Interior, Bureau of Reclamation, USA
- Vattenfall Vattenkraft AB, Sweden
- Water Corporation

I especially want to thank the personnel within the above sponsoring organisations for their time and efforts in providing valuable case study information, supplying soil samples for laboratory testing, and feedback and discussion on various aspects of the research work.

Thanks are extended to the staff of the School of Civil and Environmental Engineering of the University of New South Wales for their efficient services throughout the course of my study. In particular, I acknowledge with pleasure the assistance of the laboratory staff, Messrs. Lindsay O'Keeffe, Paul Gwynne, Tony Macken, Richard Berndt and Sajid Rehman in setting up the test apparatus and carrying out the experimental work.

The friendship and support of my colleagues within the School of Civil and Environmental Engineering is acknowledged. Their keen interest and enthusiasm in my research project have been one of the key driving forces for the completion of this thesis. In particular, I appreciate very much the friendship of Mr. Seok San Lim. Lim and I both investigated the erosion characteristics of soils. Lim has provided valuable

comments on my work, and shared with me the findings of his own testing and investigations.

Last, but not least, I recognise a great personal debt to my wife, Annie and my son, Samuel. The time I spent on the study was at the expense of time spent with them. Unbounded thanks are due to Annie, for her patience and understanding during the countless days when I indulged myself in the research project.

TABLE OF CONTENTS

VOLUME 1

ABSTRACT ..... **i**

ACKNOWLEDGEMENT ..... **ii**

TABLE OF CONTENTS ..... **v**

CHAPTER 1 ..... **1**

INTRODUCTION **1**

1.1 INTRODUCTION 1
1.2 BACKGROUND 1
1.3 TERMINOLOGY 2
1.3.1 Internal erosion 2
1.3.2 Piping 2
1.3.3 Backward erosion 4
1.3.4 Suffusion and internal instability 5
1.3.5 Heave, sand boils and blowout 5
1.4 ANALYSIS OF INTERNAL EROSION AND PIPING USING EVENT TREE METHODS 6
1.5 INFLUENCE OF SOIL ERODIBILITY ON INTERNAL EROSION AND PIPING 8
1.6 OBJECTIVE OF THIS THESIS 12
1.7 STRUCTURE OF THIS THESIS 12

CHAPTER 2 14

LABORATORY TESTS ON PIPING EROSION 14

2.1 INTRODUCTION 14
2.1.1 Overview 14
2.1.2 Needs for research on erodibility of soils 14
2.1.3 Definition of the erodibility of a soil 15
2.1.4 Layout of Chapter 2 17
2.2 RESEARCH ON SOIL EROSION BY OTHERS 18
2.2.1 Overview 18
2.2.2 Type of erosion tests 18
2.2.3 Flume tests 18
2.2.4 Rotating cylinder tests 37
2.2.5 Jet erosion tests 50
2.2.6 Tests measuring the dispersivity of a soil 57
2.2.7 Other types of erosion tests 64
2.2.8 Summary 77
2.3 EXPERIMENTAL INVESTIGATION OF PIPING EROSION OF SOILS AT THE UIVERSITY OF NEW SOUTH WALES 81
2.3.1 Objectives of experimental investigation 81
2.3.2 Slot Erosion Test 81
2.3.3 Measurement and control of test variables in a SET 91
2.3.4 Hole Erosion Test 93
2.3.5 Measurement and control of test variables in a HET 101
2.3.6 Special Slot Erosion Test and Hole Erosion Test 102
2.4 PROPERTIES OF SOIL SAMPLES USED IN SLOT EROSION TESTS AND HOLE EROSION TESTS 104
2.4.1 Origins of soil samples 104
2.4.2 Basic information on engineering classification of soil samples 106
2.4.3 Soil dispersivity 108
2.4.4 Mineralogy 108
2.5 ANALYSIS OF TEST RESULTS 112

2.5.1 Summary of interpreted test data 112
2.5.2 Graphical presentation of test results 112
2.5.3 Statistical correlation between test results and soil properties 146
2.5.4 Effects of soil mineralogy on the Erosion Rate Index 171
2.5.5 Effects of cementing materials on erosion rate 177
2.5.6 Special tests 178
2.6 COMMENTS AND DISCUSSIONS 187
2.6.1 General comparison between the SET and the HET 187
2.6.2 Estimating erosion characteristics using SET and HET 188
2.6.3 Estimating resistance against initiation of erosion using the HET ... 189
2.6.4 Accuracy of the SET and the HET 190
2.7 SUMMARY OF FINDINGS AND CONCLUSIONS 191
2.7.1 General 191
2.7.2 Apparent relationship between Erosion Rate Index, soil dry density and water content 191
2.7.3 Correlation between Erosion Rate Index and other soil properties 192
2.7.4 Multiple linear regression analysis on test data 193
2.7.5 Effects of soil mineralogy on the erosion rate index 193
2.7.6 Estimation of Critical Shear Stress from the Slot Erosion Test and the Hole Erosion Test 193
2.7.7 Comparison between the Representative Erosion Rate Indices of the Slot Erosion Test and the Hole Erosion Test 194
2.7.8 Special tests 194
2.8 RECOMMENDATIONS 196
2.8.1 Use of the Hole Erosion Test 196
2.8.2 Use of the Slot Erosion Test 198
2.8.3 Prediction of the Erosion Rate Index 198

CHAPTER 3 202

INTERNAL INSTABILITY OF SOILS 202

3.1 INTRODUCTION 202
3.1.1 Objectives 202
3.1.2 Definitions 202
3.1.3 Problems associated with Suffusion in Embankment Dams and Their Foundations 204
3.1.4 Layout of this Chapter 205
3.2 LITERATURE REVIEW 206
3.2.1 Overview 206
3.2.2 Frequently used symbols 206
3.2.3 Investigations on internal instability of cohesionless soils by others 207
3.2.4 Investigations on internal instability of cohesive soils by others 228
3.2.5 Investigations of soils which do not self filter 231
3.2.6 Summary 233
3.3 EXPERIMENTAL INVESTIGATION OF INTERNAL INSTABILITY OF SOILS AT UNSW 237
3.3.1 Objective of experimental investigation 237
3.3.2 Downward flow (DF) seepage test 237
3.3.3 Upward flow (UF) seepage test 243
3.3.4 Properties of soil samples 245
3.3.5 Interpretation of test data 252
3.4 ANALYSIS OF THE RESULTS OF DOWNWARD FLOW TESTS 257
3.4.1 Interpretation of test data 257
3.4.2 Identification of the factors influencing internal instability 257
3.4.3 Prediction of the internal instability of the UNSW test samples using currently available methods 262
3.4.4 Prediction of the fraction of materials loss by suffusion and the size of the largest particles eroded 276
3.4.5 Summary 278
3.5 ANALYSIS OF THE RESULTS OF UPWARD FLOW TESTS 281
3.5.1 Overview 281
3.5.2 Definitions 282

3.5.3 Relationship between the hydraulic gradient causing erosion and the coefficient of uniformity of the soil 284
3.5.4 Relationship between the hydraulic gradient causing erosion and the minimum stability number H/F of the soil 285
3.5.5 Relationship between the hydraulic gradient causing erosion and the fines content of the soil 286
3.5.6 Relationship between the hydraulic gradient causing erosion and the porosity of the soil 287
3.5.7 Effects of plastic fines on the hydraulic gradient causing erosion 288
3.5.8 Effects of dry density on the hydraulic gradient causing erosion 290
3.5.9 Effects of gap-grading on the hydraulic gradient causing erosion 291
3.5.10 Summary 291
3.6 PROPOSED METHODS FOR PREDICTION OF INTERNAL INSTABILITY 293
3.6.1 Fine particles and the primary soil fabric in an internally unstable soil 293
3.6.2 Proposed methods for predicting internal instability 297
3.6.3 Proposed methods for estimating the maximum fraction of erodible particles and the size of the largest erodible soil particles 302
3.6.4 Estimating the actual fraction of materials eroded by suffusion 305
3.7 CONCLUSIONS 306
3.7.1 Factors influencing whether a soil is internally unstable 306
3.7.2 Currently available methods for assessing internal instability 307
3.7.3 Proposed methods for assessing internal instability 308
3.7.4 Currently available method for predicting the fraction of fine materials and the size of the largest particles eroded by the suffusion process 309
3.7.5 Proposed method for predicting the fraction of fine materials and the size of the largest particles eroded by the suffusion process 309
3.7.6 Hydraulic gradients causing internal instability in silt-sand-gravel and clay-silt-sand-gravel mixtures 310

CHAPTER 4 312

APPLICATIONS 312

4.1 OVERVIEW 312

4.2 PREDICTION OF INITIATION OF EROSION ALONG A CRACK OR CONCENTRATED LEAK 312

4.2.1 Background 312

4.2.2 Hydraulic Shear Stress along the Walls of a Crack 313

4.2.3 Hole Erosion Test and Initial Shear Stress 317

4.3 PREDICTION OF THE RATE OF EROSION ALONG A CONCENTRATED LEAK 320

4.3.1 Background 320

4.3.2 Details of a hypothetical dam suffering from piping 320

4.3.3 Numerical modeling of piping erosion 321

4.3.4 Results of Numerical Analysis 324

4.4 PREDICTION OF INTERNAL INSTABILITY AND EROSION OF FINE MATERIALS BY SUFFUSION 328

4.4.1 Background 328

4.4.2 Assessing the Probability of Internally Instability 329

4.4.3 Assessment of the Fraction of Materials Eroded 331

CHAPTER 5 333

CONCLUSIONS AND RECOMMENDATIONS 333

5.1 LABORATORY INVESTIGATION OF PIPING EROSION 333

5.1.1 Relationship between erosion rate and hydraulic shear stress 333

5.1.2 Effects of dry density and water content on Erosion Rate Index 333

5.1.3 Correlation between Erosion Rate Index and other soil properties 334

5.1.4 Multiple linear regression analysis on test data 335

5.1.5 Effects of soil mineralogy on erosion properties 335

5.1.6 Estimation of Critical Shear Stress from the SET and the HET 335
5.1.7 Comparison between the Representative Erosion Rate Indices of the Slot Erosion Test and the Hole Erosion Test 336
5.1.8 Special tests 336
5.2 INVESTIGATION OF INTERNAL INSTABILITY OF SOILS 338
5.2.1 Factors influencing whether a soil is internally unstable 338
5.2.2 Methods for assessing internal instability 339
5.2.3 Fraction of fine particles eroded by the suffusion process 340
5.2.4 Hydraulic gradients causing internal instability in silt-sand-gravel and clay-silt-sand-gravel mixtures 341
5.3 RECOMMENDATIONS 343
5.3.1 Applications of the Hole Erosion Test and the Slot Erosion Test 343
5.3.2 Recommended method for predicting internal instability 345
5.3.3 Proposed further research 346

CHAPTER 6 349

REFERENCES 349

TABLE OF CONTENTS

VOLUME 2

LIST OF APPENDICES

APPENDIX A: SUMMARY OF INTERPRETED RESULTS OF ALL SLOT EROSION TESTS

APPENDIX B: SUMMARY OF INTERPRETED RESULTS OF ALL HOLE EROSION TESTS

APPENDIX C: NON-LINEAR REGRESSION MODELS FOR PREDICTING I_{SET} AND I_{HET} FOR SPECIMEN COMPACTED TO 95% COMPACTION AT OPTIMUM WATER CONTENT

APPENDIX D: CONTOUR PLOTS OF I_{SET} AND I_{HET}

APPENDIX E: PLOTS OF EROSION RATE INDEX AGAINST DRY DENSITY, WATER CONTENT, PERCENTAGE COMPACTION, RATIO OF WATER CONTENT TO OWC, AND DEGREE OF SATURATION

APPENDIX F: PLOTS OF EROSION RATE INDEX AGAINST SAND CONTENT, FINES CONTENT, AND CLAY CONTENT

APPENDIX G: PLOTS OF EROSION RATE INDEX AGAINST LIQUID LIMIT, PLASTICITY INDEX, AND ACTIVITY

APPENDIX H: PLOTS OF EROSION RATE INDEX AGAINST PINHOLE TEST CLASSIFICATION, EMERSON CLASS TEST CLASSIFICATION, PERCENTAGE DISPERSION, *SAR*, AND MAJOR CATION CONTENT

APPENDIX I: SLOT EROSION TEST PROCEDURE

APPENDIX J: HOLE EROSION TEST PROCEDURE

APPENDIX K: X-RAY POWDER DIFFRACTION ANALYSIS OF SOIL SAMPLES

APPENDIX L: REPORT ON THE IDENTIFICATION OF COMPONENTS WITHIN TWO CLAYS FROM THE BUFFALO DAM, VICTORIA BY HENSEL, H.D.

APPENDIX M: SUMMARY OF GRADING INFORMATION OF SOIL SAMPLES TESTED FOR INTERNAL STABILITY BY OTHERS

APPENDIX N: RECORD OF DOWNWARD FLOW SEEPAGE TESTS

APPENDIX O: DOWNWARD FLOW SEEPAGE TESTS – ESTIMATING THE FRACTION OF MATERIALS LOSS BY SUFFUSION USING CURVE MATCHING TECHNIQUE

APPENDIX P: RECORDS OF UPWARD FLOW SEEPAGE TESTS

LIST OF FIGURES

Figure 1.1: Piping through a concentrated leak within the embankment or in the foundation. 3
Figure 1.2: Backward erosion initiated at an open seepage exit or at the interface between the core and the downstream filter 4
Figure 1.3: Internal erosion by the process of suffusion within the embankment. 5
Figure 1.4: Heave (blowout) at the downstream toe of the embankment. 6
Figure 1.5: Models showing the four phases of development of failure by internal erosion and piping (Foster and Fell 1999b). 9
Figure 1.6: Failure path diagram for failure by piping through the embankment (Foster and Fell 1999b). 10
Figure 1.7: Event tree for piping through an embankment dam (Foster and Fell 1999b). 11
Figure 2.1: Graphical illustration of the meaning of Critical Shear Stress and Coefficient of Soil Erosion. 16
Figure 2.2: Relationship between Tractive Force (Critical Shear Stress), Natural Dry Density and Liquid Limit (Gibbs 1962) 20
Figure 2.3: Suggested Trend of Erosion Resistance (as measured by Critical Shear Stress) for Fine-grained Cohesive Soils with respect to Plasticity (Gibbs 1962). 21
Figure 2.4: Soil erodibility, as measured by Critical Shear Stress, versus Plasticity (Arulanandan and Perry 1983). 25
Figure 2.5: Schematic drawing of flume and sample containers 29
Figure 2.6: Scour hole next to a cylindrical pier in clay during a flume test (http://tti.tamu.edu/geotech/scour/). 34
Figure 2.7: EFA Conceptual Diagram (Briaud et al. 2001a). 34
Figure 2.8: Photographs of the Erosion Function Apparatus (Briaud et al. 2003). 35
Figure 2.9: Critical Shear Stress versus Mean Grain Diameter (Briaud et al. 2003). .. 36
Figure 2.10: Cross-sectional View of Rotating Cylinder Test Apparatus. 40

Figure 2.11: Sodium Adsorption Ratio versus Total Cation Concentration - Boundary between flocculated and deflocculated states (Sargunan 1977). 45
Figure 2.12: Improved Rotating Cylinder Test Apparatus 46
Figure 2.13: Erosion rate versus hydraulic shear stress (Chapuis 1986a). 49
Figure 2.14: Schematic of Jet Index Test Apparatus (Hanson 1992). 53
Figure 2.15: Determination of the Emerson Class Number (AS1289.3.8.1 – 1997). 58
Figure 2.16: Pinhole Test – Setup and Evaluation of Results (Sherard, Dunnigan, Decker and Steele 1976). 60
Figure 2.17: Consolidation Cylinder (Atkinson et al. 1990). 63
Figure 2.18: Crack, Leakage and Erosion Apparatus (Hjeldnes and Lavania 1980)..... 67
Figure 2.19: Schematic representation of triaxial erosion test apparatus (Sanchez, Strutynsky, and Silver 1983)..... 69
Figure 2.20: Physical conditions modeled in cracked earth dam core material erosion studies (Sanchez, Strutynsky, and Silver 1983). 69
Figure 2.21: Crack erosion test setup (Maranha das Neves 1989). 71
Figure 2.22: Schematic diagram showing the UNSW Slot Erosion Test Apparatus (Cedeño 1998)..... 74
Figure 2.23: Schematic diagram of the Slot Erosion Test Assembly. 83
Figure 2.24: Slot Erosion Test Apparatus. Water re-circulation system not shown. 84
Figure 2.25: Slot Erosion Test on soil sample taken from Jindabyne Dam. 84
Figure 2.26: Cross-section of a SET test specimen showing enlargement of pre-formed slot due to erosion. 85
Figure 2.27: Width of pre-formed slot versus time in a Slot Erosion Test using Test BDSET4 on soil sample Bradys as an example. 89
Figure 2.28: Average cross-sectional area and average wetted-perimeter of pre-formed slot versus time in Slot Erosion Test BDSET4 on soil sample Bradys. 89
Figure 2.29: Estimated rate of mass removal per unit area and estimated shear stress versus time in Slot Erosion Test BDSET4 on soil sample Bradys. 90
Figure 2.30: Estimated rate of mass removal per unit area versus estimated shear stress in Slot Erosion Test BDSET4 on soil sample Bradys..... 90
Figure 2.31: Schematic diagram of the Hole Erosion Test Assembly..... 94

Figure 2.32: Hole Erosion Test apparatus. 94
Figure 2.33: Hole Erosion Test on soil sample from Jindabyne Dam. Photograph of test specimen after test. 95
Figure 2.34: Cross-section of a HET test specimen showing enlargement of the pre-formed pipe due to erosion. 96
Figure 2.35: Estimation of diameter of pre-formed hole in a Hole Erosion Test using Test HDHET9 on soil sample Hume as an example 100
Figure 2.36: Estimated rate of mass removal per unit area and shear stress versus time in Hole Erosion Test HDHET9 on soil sample Hume 100
Figure 2.37: Estimated rate of mass removal per unit area versus estimated shear stress in Hole Erosion Test HDHET9 on soil sample Hume. 101
Figure 2.38: Plasticity Chart showing plasticity of soil samples. Lyell, Pukaki and Rowallan are non-plastic (NP) and not shown on the chart 107
Figure 2.39: Particle Size Distribution Curves for the 13 Soil Samples. 107
Figure 2.40: Summary of I_{SET} for all successful Slot Erosion Tests. 113
Figure 2.41: Summary of I_{HET} for all successful Hole Erosion Tests 114
Figure 2.42: Erosion Rate Indices, I_{SET} based on SETs on soil sample Fattorini. 117
Figure 2.43: Erosion Rate Indices, I_{HET} based on HETs on soil sample Fattorini. 118
Figure 2.44: Erosion Rate Indices, I_{SET} based on SETs on soil sample Jindabyne. 118
Figure 2.45: Erosion Rate Indices, I_{HET} based on HETs on soil sample Jindabyne 119
Figure 2.46: Erosion Rate Index (I_{SET}) from Slot Erosion Test versus Percentage Compaction ($\rho_d / \rho_{d_{max}}$). (Same as Figure E3a in Appendix E) 121
Figure 2.47: Erosion Rate Index (I_{SET}) from Slot Erosion Test versus Percentage Compaction ($\rho_d / \rho_{d_{max}}$). Soil samples classified into fine-grained soils and coarse-grained soils. (Same as Figure E3b in Appendix E) 122
Figure 2.48: Erosion Rate Index (I_{HET}) from Hole Erosion Test versus Percentage Compaction ($\rho_d / \rho_{d_{max}}$). (Same as Figure E4a in Appendix E) 122
Figure 2.49: Erosion Rate Index (I_{HET}) from Hole Erosion Test versus Percentage Compaction ($\rho_d / \rho_{d_{max}}$). Soil samples classified into fine-grained soils and coarse-grained soils. (Same as Figure E4b in Appendix E) 123
Figure 2.50: Erosion Rate Index (I_{SET}) from Slot Erosion Test versus 124

Figure 2.51: Erosion Rate Index (I_{SET}) from Slot Erosion Test versus Water Content Ratio ($\Delta\omega_r$). Soil samples classified into fine-grained soils and coarse-grained soils. (Same as Figure E7b in Appendix E) 125

Figure 2.52: Erosion Rate Index (I_{HET}) from Hole Erosion Test versus 125

Figure 2.53: Erosion Rate Index (I_{HET}) from Hole Erosion Test versus Water Content Ratio ($\Delta\omega_r$). Soil samples classified into fine-grained soils and coarse-grained soils. (Same as Figure E8b in Appendix E) 126

Figure 2.54: Erosion Rate Index (I_{SET}) from Slot Erosion Test versus Degree of Saturation. (Same as Figure E9a in Appendix E) 126

Figure 2.55: Erosion Rate Index (I_{SET}) from Slot Erosion Test versus Degree of Saturation. Soil samples classified into fine-grained soils and coarse-grained soils. (Same as Figure E9b in Appendix E) 127

Figure 2.56: Erosion Rate Index (I_{HET}) from Hole Erosion Test versus Degree of Saturation. (Same as Figure E10a in Appendix E) 127

Figure 2.57: Erosion Rate Index (I_{HET}) from Hole Erosion Test versus Degree of Saturation. Soil samples classified into fine-grained soils and coarse-grained soils. (Same as Figure E10b in Appendix E) 128

Figure 2.58: Predicted Erosion Rate Index ($\tilde{I}_{SET}$) from Slot Erosion Test versus Degree of Saturation. (Same as Figure E9c in Appendix E) 128

Figure 2.59: Predicted Erosion Rate Index ($\tilde{I}_{HET}$) from Hole Erosion Test versus Degree of Saturation. (Same as Figure E10c in Appendix E) 129

Figure 2.60: Representative Erosion Rate Index ($\tilde{I}_{SET}$) from Slot Erosion Test versus Standard Maximum Dry Density ($\rho_{d_{max}}$) and Optimum Water Content (*OWC*). (Same as Figure E11a in Appendix E) 129

Figure 2.61: Representative Erosion Rate Index ($\tilde{I}_{HET}$) from Hole Erosion Test versus Standard Maximum Dry Density ($\rho_{d_{max}}$) and Optimum Water Content (*OWC*). (Same as Figure E11b in Appendix E) 130

Figure 2.62: Erosion Rate Index (I_{SET}) from Slot Erosion Test versus Fines Content. (Same as Figure F3a in Appendix F) 132

Figure 2.63: Erosion Rate Index (I_{SET}) from Slot Erosion Test versus Fines Content. Soil samples classified into fine-grained soils and coarse-grained soils. (Same as Figure F3b in Appendix F) 133

Figure 2.64: Erosion Rate Index (I_{HET}) from Hole Erosion Test versus Fines Content. (Same as Figure F4a in Appendix F) 133

Figure 2.65: Erosion Rate Index (I_{HET}) from Hole Erosion Test versus Fines Content. Soil samples classified into fine-grained soils and coarse-grained soils. (Same as Figure F4b in Appendix F) 134

Figure 2.66: Predicted Representative Erosion Rate Index ($\tilde{I}_{SET}$) from Slot Erosion Test versus Fines Content. (Same as Figure F3c in Appendix F) 134

Figure 2.67: Predicted Representative Erosion Rate Index ($\tilde{I}_{HET}$) from Hole Erosion Test versus Fines Content. (Same as Figure F4c in Appendix F) 135

Figure 2.68: Predicted Erosion Rate Index ($\tilde{I}_{SET}$) from Slot Erosion Test versus Pinhole Test Classification. (Same as Figure H1c in Appendix H) 138

Figure 2.69: Predicted Erosion Rate Index ($\tilde{I}_{HET}$) from Hole Erosion Test versus Pinhole Test Classification. (Same as Figure H2c in Appendix H) 139

Figure 2.70: Predicted Erosion Rate Index ($\tilde{I}_{SET}$) from Slot Erosion Test versus Emerson Class. (Same as Figure H3c in Appendix H) 139

Figure 2.71: Predicted Erosion Rate Index ($\tilde{I}_{HET}$) from Hole Erosion Test versus Emerson Class. (Same as Figure H4c in Appendix H) 140

Figure 2.72: Predicted Erosion Rate Index ($\tilde{I}_{SET}$) from Slot Erosion Test versus Percentage Dispersion. (Same as Figure H5c in Appendix H) 140

Figure 2.73: Predicted Erosion Rate Index ($\tilde{I}_{HET}$) from Hole Erosion Test versus Percentage Dispersion. (Same as Figure H6c in Appendix H) 141

Figure 2.74: Summary of Critical Shear Stresses obtained from Slot Erosion Tests on all soil samples 142

Figure 2.75: Summary of Critical Shear Stresses obtained from Hole Erosion Tests on all soil samples 143

Figure 2.76: Erosion Rate Index (I_{SET}) versus Critical Shear Stress (τ_{cSET}) based on Slot Erosion Test data. Samples classified into fine and coarse-grained soils. 143

Figure 2.77: Erosion Rate Index (I_{HET}) versus Critical Shear Stress (τ_{cHET}) based on Hole Erosion Test data. Soil samples classified into fine-grained and coarse-grained soils. 144

Figure 2.78: Minimum Test Heads and the corresponding Initial Shear Stresses in Hole Erosion Tests 144

Figure 2.79: Initial Shear Stresses (τ_o) versus Representative Erosion Rate Index ($\tilde{I}_{HET}$) from Hole Erosion Tests. 146

Figure 2.80: Erosion Rate Indices ($\hat{I}_{SET}$) predicted by Multiple Linear Regression Model versus Erosion Rate Indices (I_{SET}) from Slot Erosion Tests on Coarse-grained Soil Samples. 160

Figure 2.81: Erosion Rate Indices ($\hat{I}_{HET}$) predicted by Multiple Linear Regression Model versus Erosion Rate Indices (I_{HET}) from Hole Erosion Tests on Coarse-grained Soil Samples. 161

Figure 2.82: Erosion Rate Indices ($\hat{I}_{SET}$) predicted by Multiple Linear Regression Model versus Representative Erosion Rate Indices ($\tilde{I}_{SET}$) predicted by Non-linear Regression Models for each Coarse-grained Soil Samples. .. 162

Figure 2.83: Erosion Rate Indices ($\hat{I}_{HET}$) predicted by Multiple Linear Regression Model versus Representative Erosion Rate Indices ($\tilde{I}_{HET}$) predicted by Non-linear Regression Models for each Coarse-grained Soil Samples. .. 163

Figure 2.84: Erosion Rate Indices ($\hat{I}_{SET}$) predicted by Multiple Linear Regression Model versus Erosion Rate Indices (I_{SET}) from Slot Erosion Tests on Fine-grained Soil Samples. 165

Figure 2.85: Erosion Rate Indices ($\hat{I}_{HET}$) predicted by Multiple Linear Regression Model versus Erosion Rate Indices (I_{HET}) from Hole Erosion Tests on Fine-grained Soil Samples. 166

Figure 2.86: Erosion Rate Indices ($\hat{I}_{SET}$) predicted by Multiple Linear Regression Model versus Representative Erosion Rate Indices ($\tilde{I}_{SET}$) predicted by Non-linear Regression Models for each Fine -grained Soil Samples. 167

Figure 2.87: Erosion Rate Indices ($\hat{I}_{HET}$) predicted by Multiple Linear Regression Model versus Representative Erosion Rate Indices ($\tilde{I}_{HET}$) predicted by Non-linear Regression Models for each Fine-grained Soil Samples. 168

Figure 2.88: Critical Shear Stresses ($\hat{\tau}_{c\ HET}$) predicted by Multiple Linear Regression Model versus Critical Shear Stresses (τ_{cHET}) from Hole Erosion Tests on Coarse-Grained Soil Samples. 169

Figure 2.89: Representative Erosion Rate Index based on Hole Erosion Tests versus Representative Erosion Rate Index based on Slot Erosion Tests. 170

Figure 2.90: (a) Single silica tetrahedron; (b) Sheet structure of silica tetrahedrons arranged in a hexagonal network. (Grim 1953). 172

Figure 2.91: (a) Single octahedral unit; (b) Sheet structure of the octahedral units. (Grim 1953). 173

Figure 2.92: (a) Structure of kaolinite layer (Grim 1953); (b) Schematic diagram of the structure of kaolinite (Mitchell 1976). 174

Figure 2.93: (a) Structure of smectite (Grim 1953); (b) Schematic diagram of the structure of smectite (Mitchell 1976) 174

Figure 2.94: (a) Structure of muscovite/illite (Grim 1953); (b) Schematic diagram of the structure of illite (Mitchell 1976) 175

Figure 2.95: Schematic diagram of the structure of vermiculite (Mitchell 1976) 176

Figure 2.96: Schematic diagram of the structure of chlorite (Mitchell 1976). 177

Figure 3.1: Soil gradation types which are internally unstable and are susceptible to suffusion (Foster and Fell 1999). 203

Figure 3.2: Soil types which have experienced a lack of self filtering (based on Sherard 1979) 204

Figure 3.3: Some failure modes due to suffusion (adapted from CFGB 1997) 204

Figure 3.4: Examples of grain-size distribution curves according to Fuller & Thompson (1907) criterion for maximum density. 208

Figure 3.5: Grain-size distribution curve normalised against maximum particle size based on Fuller & Thompson (1907) criterion of maximum density. 209
Figure 3.6: Lubochkov (1965) analytical method for determining the range of grains susceptible to suffusion. 211
Figure 3.7: Linearly-graded soil samples tested to be internally stable 214
Figure 3.8: Non-linearly graded soil samples tested to be internally stable 214
Figure 3.9: Soil sample, having irregular grain-size distribution curve, tested to be internally unstable by Kenney et al. (1983). 215
Figure 3.10: Gap-graded gravel-sand mixtures tested by Kenney et al. (1984). 216
Figure 3.11: Soil samples tested by Kenney and Lau (1985). 217
Figure 3.12: Shape curves of (a) unstable and (b) stable gradings of soil samples tested by Kenney and Lau (1985). 218
Figure 3.13: Alternative method to evaluate the potential for grading instability (Kenney & Lau 1985). 219
Figure 3.14: Shape curves of selected unstable and stable gradings and the revised boundary between stable and unstable gradings (Kenney and Lau 1986).220
Figure 3.15: Grain-size distribution curves of materials tested for internal instability by Lafleur et al. (1989) 221
Figure 3.16: Classification of Gradation Curves of Broadly Graded Soils 222
Figure 3.17: Classification of suffusive and non-suffusive soil compositions (Burenkova 1993). 223
Figure 3.18: Eight soil samples tested by seepage tests (Burenkova 1993). 224
Figure 3.19: Upward flow seepage cell (Skempton and Brogan 1994) 225
Figure 3.20: Soil samples tested by Skempton and Brogan (1994) 225
Figure 3.21: Samples selected for seepage tests (Chapuis et al. 1996). 228
Figure 3.22: Soil samples tested to be internally stable by Sun (1989) 229
Figure 3.23: Soil samples tested to be internally unstable by Sun (1989) 230
Figure 3.24: Schematic drawing showing setup of test equipment (Sun 1989). 230
Figure 3.25: Assessment of internal stability (Sun 1989). 231
Figure 3.26: Simple test on grain size curve to check unacceptable skip-grading with respect to internal erosion (de Mello 1975). 232
Figure 3.27: Schematic diagram of the downward flow seepage test assembly 240
Figure 3.28: Downward flow seepage test apparatus. 241

Figure 3.29: Schematic diagram of the upward flow seepage test assembly. 244
Figure 3.30: Upward flow seepage test apparatus. 245
Figure 3.31: Grain-size distribution curves of the materials used for blending for the test samples. 247
Figure 3.32: Grain-size distribution curves of sample "RD" and well-graded samples of silt-sand-fine gravel mixtures or clay-silt-sand-fine gravel mixtures.. 250
Figure 3.33: Grain-size distribution curves of gap-graded test samples made of silt-sand-fine gravel or clay-silt-sand-fine gravel mixtures. 250
Figure 3.34: Grain-size distribution curves of test samples made of silt-sand-coarse gravel mixtures. 251
Figure 3.35: DF test No. 8 on Sample 10 - Post-test grain-size distribution analysis on sub-samples taken from various depths of the test sample. 254
Figure 3.36: DF test No. 8 on Sample 10 – Curve matching for finding the fraction of materials loss by suffusion and the size of the largest erodible particles. 255
Figure 3.37: UF test No. 8 on Sample No. 10 – Temporal variation of hydraulic gradient and flow rate. 256
Figure 3.38: UF test No. 8 on Sample No. 10 – Average flow velocity versus hydraulic gradient. 256
Figure 3.39: Actual fraction of materials loss by suffusion is plotted against the fraction finer than the largest eroded particles. 259
Figure 3.40: Plot of gravel content versus fines content for all test samples. 260
Figure 3.41: Coefficient of curvature versus coefficient of uniformity for 20 UNSW soil samples. 264
Figure 3.42: Coefficient of curvature versus coefficient of uniformity for all available internal instability test data. 265
Figure 3.43: d_{C15}/d_{f95} versus dividing point, d for all internally unstable samples tested by UNSW. 267
Figure 3.44: d_{C15}/d_{f95} versus dividing point, d for all internally stable samples tested by UNSW. 267
Figure 3.45: d_{C15}/d_{f95} versus dividing point, d for soil samples tested by Kenney & Lau (1984). 268

Figure 3.46: *H-F* plots for unstable samples tested by UNSW. 269
Figure 3.47: *H-F* plots for stable samples tested by UNSW. 270
Figure 3.48: Plot of minimum *H/F* ratios (UNSW test data). 270
Figure 3.49: Plot of minimum *H/F* ratios for all available test data on silt-sand-gravel and clay-silt-sand-gravel soils. 271
Figure 3.50: Classification of suffusion characteristics based on Burenkova (1993) method (UNSW test data). 272
Figure 3.51: Classification of suffusion characteristics for all available test data on silt-sand-gravel and clay-silt-sand-gravel using Burenkova (1993) method. 273
Figure 3.52: F_C^* versus D_C^*/d_{F50} based on Sun (1989) method for all UNSW internal instability test samples. 274
Figure 3.53: F_C^* versus D_C^*/d_{F50} based on Sun (1989) method for all available internally instability test data. 275
Figure 3.54: Actual fraction of materials loss by suffusion versus maximum fraction of erodible materials (all unstable soil samples in data set) 276
Figure 3.55: Sizes of largest particles eroded predicted by Lubochkov (1965) method versus sizes of largest particles eroded estimated by the curve-matching technique for all samples tested to be internally unstable. 277
Figure 3.56: d_{dv} estimated by Burenkova (1993) method versus size of largest erodible particles estimated by curve matching technique (all unstable soil samples in data set). 279
Figure 3.57: Average hydraulic gradient across the test sample at which erosion of fine particles started against coefficient of uniformity. 284
Figure 3.58: Average hydraulic gradient across the test sample at which "boiling" started against coefficient of uniformity. 285
Figure 3.59: Average hydraulic gradient across the test sample at which erosion of fine particles started against Minimum *H/F* ratio. 286
Figure 3.60: Average hydraulic gradient across the test sample at which erosion of fine particles started against fines content (% finer than 0.075mm). 287
Figure 3.61: Average hydraulic gradient across the test sample at which erosion of fine particles started against porosity. 288

Figure 3.62: Effects of fines content and plasticity of fines on average hydraulic gradient when erosion of fine particles started in non gap-graded samples 289
Figure 3.63: Effects of fines content and plasticity of fines on average hydraulic gradient when erosion of fine particles started in gap-graded samples. .. 289
Figure 3.64: Effects of compaction density on average hydraulic gradient when erosion of fine particles started. 290
Figure 3.65: Effects of gap-grading on average hydraulic gradient when erosion of fine particles started. 291
Figure 3.66: Phase diagram showing volume and weight relationships between the primary fabric, and the fine erodible particles in an internally unstable soil 293
Figure 3.67: Contours of the probability of internal instability for silt-sand-gravel soils and clay-silt-sand-gravel soils of limited clay content and plasticity. 300
Figure 3.68: Contours of the probability of internal instability for sand-gravel soils with less than 10% non-plastic fines passing 0.075 mm. 301
Figure 3.69: Predicted maximum fraction of erodible particles based on $H/F < 1.3$ versus maximum fraction of erodible particles assessed from test data. . 303
Figure 3.70: Predicted size of largest erodible particles based on $H/F < 1.3$ versus size of largest erodible particles assessed from test data. 304
Figure 4.1: Diagram showing the forces acting on a segment of eroding fluid within a cylindrical leak. 314
Figure 4.2: Diagram showing the forces acting on a segment of eroding fluid within an open crack or gap. 315
Figure 4.3: Initial Shear Stresses, τ_o versus Representative Erosion Rate Index, $\tilde{I}_{HET}$ (Reproduced from Figure 2.79. of Chapter 2) 318
Figure 4.4: Details of a hypothetical embankment dam suffering from piping 321
Figure 4.5: Storage level and diameter of concentrated leak versus time for Scenario 1 - $I_{HET} = 4$, and diameter of emergency discharge pipe = 1.2 m 325

Figure 4.6: Storage level and diameter of concentrated leak versus time for Scenario 2 - I_{HET} = 4, and diameter of emergency discharge pipe = 0.6 m. 326

Figure 4.7: Storage level and diameter of concentrated leak versus time for Scenario 3 - I_{HET} = 5, and diameter of emergency discharge pipe = 1.2 m. 327

Figure 4.8: Storage level and diameter of concentrated leak versus time for Scenario 4 - I_{HET} = 5, and diameter of emergency discharge pipe = 0.6 m. 328

Figure 4.9: Particle size distribution curves of proposed filter materials..... 329

Figure 4.10: Assessment of the internal instability of the proposed filter materials using Kenney and Lau (1985, 1986) method. 330

Figure 4.11: Assessment of the internal instability of the proposed filter materials using Burenkova (1993) method..... 330

Figure 4.12: Assessment of the probability of internal instability of the proposed filter materials using the method proposed by the Author..... 331

LIST OF TABLES

Table 2.1: Physical properties of soils tested (Lyle and Smerdon (1965)). 21
Table 2.2: Correlation between critical shear stress, rate of erosion with soil and water properties (based on Briaud et al. 2001a)..... 37
Table 2.3: Properties of tested natural samples : mean values (m) and standard deviations (σ) (Chapuis 1986b)..... 48
Table 2.4: Summary of physical properties of soil samples (Hanson 1991)..... 54
Table 2.5: Description of soils tested (Christensen and Das 1973). 64
Table 2.6: Properties of soil samples tested by Maranha das Neves (1989). 72
Table 2.7: Source and origin of soil samples used in Slot Erosion Tests 104
Table 2.8: Engineering classification of soil samples. 109
Table 2.9: Dispersivity and physiochemical properties of saturation extracts of the soil samples. 110
Table 2.10: Summary of soil sample mineralogy..... 111
Table 2.11: Regression Models for predicting I_{SET} and I_{HET} from percentage compaction and water content. 116
Table 2.12: Correlations between Erosion Rate Indices from Slot Erosion Tests and Individual Soil Parameters. 147
Table 2.13: Correlations between Erosion Rate Indices from Hole Erosion Tests and Individual Soil Parameters. 148
Table 2.14: Correlations between Critical Shear Stresses from Hole Erosion Tests and Individual Soil Parameters. 149
Table 2.15: Critical values of the Pearson's Correlation Coefficient at a Level of Significance of 5% and 1%. 150
Table 2.16: Summary of Linear Regression Models for prediction of Erosion Rate Indices and Critical Shear Stresses for coarse-grained soils. 156
Table 2.17: Summary of Linear Regression Models for prediction of Erosion Rate Indices and Critical Shear Stresses for fine-grained soils. 158
Table 2.18: Effects on Erosion Rate Index (I_{SET}) of prior soaking of test specimens in Slot Erosion Tests. 181

Table 2.19: Effects on Erosion Rate Index (I_{HET}) of prior soaking of test specimens in Hole Erosion Tests..... 182
Table 2.20: Effects on Erosion Rate Index (I_{SET}) due to the use of 0.02M Sodium Chloride Solution as the Eroding Fluid in Slot Erosion Tests..... 183
Table 2.21: Effects on Erosion Rate Index (I_{HET}) of the use of 0.02M Sodium Chloride Solution as the Eroding Fluid in Hole Erosion Tests..... 184
Table 2.22: Effects on Erosion Rate Index (I_{HET}) of to the use of 0.005M Sodium Chloride Solution as the Eroding Fluid in Hole Erosion Tests..... 185
Table 2.23: Effects on Erosion Rate Index (I_{SET}) of Pausing Flow during a Slot Erosion Test..... 186
Table 2.24: Summary of Predicted Representative Erosion Rate Indices at 95% Compaction and Optimum Water Content based on Results of Slot Erosion Tests and Hole Erosion Tests, and Soil Properties..... 197
Table 2.25: Proposed Rules for Preliminary Estimation of the Representative Erosion Rate Index of a Soil..... 201
Table 3.1: Meaning of mathematical symbols..... 206
Table 3.2: Results of seepage tests (from Skempton and Brogan 1994)..... 227
Table 3.3: Summary of investigations on internal instability of soils by others..... 235
Table 3.4: Schedule of DF tests and UF tests..... 246
Table 3.5: Mix proportions for test samples in downward flow tests and upward flow tests..... 248
Table 3.6: Grading characteristics of the test samples..... 249
Table 3.7: Summary of soil particle densities..... 251
Table 3.8: Results of standard compaction tests..... 253
Table 3.9: Summary of the results of downward flow tests..... 258
Table 3.10: Fraction of material loss by suffusion and size of largest erodible particles assessed by grain-size distribution curve matching technique..259
Table 3.11: Assessment of internal stability of the 20 soil samples using currently available methods..... 263
Table 3.12: Accuracy of various methods used for the prediction of the internal stability of a soil..... 280
Table 3.13: Summary of the results of the 18 UF tests on 14 test samples..... 283

Table 3.14: Maximum and minimum densities for granular soils (from Lambe & Whitman 1979). 297

Table 3.15: Classification of all test samples using Kenney & Lau (1985, 1986) method and Burenkova (1993) method 298

Table 3.16: Method for assessing the likelihood of internal instability of silt-sand-gravel and clay-silt-sand-gravel mixtures using Burenkova (1993) and Kenney and Lau (1985, 1986) methods. 299

Table 4.1: Estimated hydraulic shear stress (N/m^2) from water flowing in an open crack, versus crack width and flow gradient. 317

Table 4.2: Proposed Guidelines for Preliminary Estimation of the Representative Erosion Rate Index of a Soil (Reproduced from Table 2.25 of Chapter 2). 319

Table 4.3: Results of numerical modeling of the rate of piping erosion. 325

LIST OF SYMBOLS

Upper case

A	Cross-section area of flow.
C_C	Coefficient of curvature of a soil defined as $D_{30}{}^2/(D_{60} \times D_{10})$
C_e	Coefficient of soil erosion. A parameter defined by the Author.
C_U	Coefficient of uniformity of a soil defined as D_{60}/D_{10} .
D	Diameter, or size of a soil particle, in [mm]. Also used to denote depth of the artificial slot in a test sample of the Slot Erosion Test.
D_C	Constriction size approximately equal to 0.25 of the particle size, D.
$D_C{}^*$	Controlling constriction defined by Sun (1989) as the constriction size D_C when the ratio D_C/d_{F50} is maximised.
D_x	Particle size for which X% by weight is finer, in [mm].
F	The fraction by weight of a soil finer than a specified particle size D, usually shown as a percentage. Also denotes a random variable which follows the F distribution in statistics.
$F_{d\,max\_erod}$	Fraction by weight of a soil with particle sizes finer than the maximum size of the particles eroded in the process of suffusion.
$F_C{}^*$	The fraction by weight of soil particles finer than size $D_C{}^*$.
F_L	Fraction by weight of a soil lost by the process of suffusion.
$\hat{F}_{max}$	The predicted maximum fraction of materials eroded in the process of suffusion.
G_s	Soil grain density.
G_{s_avg}	Average soil grain density of a mixture of more than one type of soils.
H	Total head in hydraulics analysis.

	Also used to denote the fraction by weight of a soil with particle sizes between D and $4D$ in the analysis of the internal instability of a soil using Kenney and Lau (1985, 1986) method..
H_f	Head loss in pipe flow.
I_{HET}	Erosion rate index obtained by the Hole Erosion Test (HET)
I_P	Plasticity index of a soil, in [%].
I_{SET}	Erosion rate index obtained by the Slot Erosion Test (SET).
$\tilde{I}_{HET}$	Representative erosion rate index for a soil sample at 95% compaction and at *OWC*, estimated from non-linear regression using test data obtained from Hole Erosion Tests.
$\tilde{I}_{SET}$	Representative erosion rate index for a soil sample at 95% compaction and at *OWC*, estimated from non-linear regression using test data obtained from Slot Erosion Tests.
$\hat{I}_{HET}$	Representative erosion rate index for a soil sample at 95% compaction and at *OWC*, predicted from multiple linear regression formula using the soil classification parameters as the independent variables, and using multiple linear regression formula based on test data obtained from Hole Erosion Tests.
$\hat{I}_{SET}$	Representative erosion rate index for a soil sample at 95% compaction and at *OWC*, predicted from multiple linear regression formula using the soil classification parameters as the independent variables, and using multiple linear regression formula based on test data obtained from Slot Erosion Tests.
K	Coefficient of permeability in [m/s].
L	Length of flow path. In many case is the length of the soil sample being tested.
LL	Liquid limit of a soil, in [%].
M	Mass of a soil.
N	Sample size.
P_f	The estimated probability that a soil is internally unstable.

Pinhole	The Pinhole Dispersion Test classification index expressed as an ordinal number, i.e. '1' for Class D1, '2' for Class D2, '3' for Class PD1, '4' for Class PD2, '5' for Class ND2, and '6' for Class ND1.
Q	Flow rate, in [m^3/s]
R	Coefficient of correlation in a multiple linear regression.
R^2	Coefficient of determination in a multiple linear regression.
R_e	Reynold's number.
S	Degree of saturation.
SAR	Sodium Adsorption Ratio.
$\overline{V}$	Average flow velocity.
V_l	Volume of the loose fine particles of a soil mass that are washed out of the soil in the suffusion process.
V_p	Volume of the primary fabric of a soil mass.
W	Width of the artificial slot in a test sample of the Slot Erosion Test.
W_l	Weight of the loose fine particles of a soil mass that are washed out of the soil in the suffusion process.
W_p	Weight of the primary fabric of a soil mass.
X_i	Independent variable, also called predictor variable, in a multiple linear regression.
Y	Dependent variable in a multiple linear regression.
Z	The dependent variable in a logistic regression equation.

Lower case

c_i	Coefficients for independent variable X_i in linear multiple regression.
d_{cx}	Particle size for which X% by weight is finer, when only the coarse (c) fraction of a soil is considered. The soil is divided into a coarse fraction and a fine fraction at a point represented by size d_{dv}, and that part of the grain-size distribution curve for the coarse fraction is adjusted to give a minimum size equal to d_{dv}.

d_{dv} The size of the largest particles representing the limit between the fraction building the soil skeleton and the loose soil grains in an internally unstable soil.

d_{fx} Particle size for which X% by weight is finer, when only the fine (f) fraction of a soil is considered. The soil is divided into a coarse fraction and a fine fraction at a point represented by size d_{dv}, and that part of the grain-size distribution curve for the fine fraction is adjusted to give a maximum size equal to d_{dv}.

d_{F50} The size at which 50% by weight of the fine fraction of a soil is finer. The soil is divided into a coarse fraction and a fine fraction for assessing internal instability of a soil using Sun (1989) method.

d_{max_erod} The maximum size of the soil particles eroded in a suffusion process.

$\hat{d}_{max\_erod}$ The predicted maximum size of the soil particles eroded in a suffusion process.

d_x Particle size for which X% by weight is finer, in [mm]. Same meaning as D_x.

e Void ratio of a soil.

f The friction loss factor in pipe flow.

f_i Fraction by weight of the i^{th} soil type used in a mixture formed by blending two or more types of soils together.

f_L The proportional constant between the hydraulic shear stress and the mean flow velocity during laminar flow condition.

f_T The proportional constant between the hydraulic shear stress and the square of the mean flow velocity during turbulent flow condition.

g Acceleration due to gravity, equal to 9.81 m/s^2.

h' Equal to d_{90}/d_{60} in the classification of internally unstable and stable soils using the method by Burenkova (1993).

h'' Equal to d_{90}/d_{15} in the classification of internally unstable and stable soils using the method by Burenkova (1993).

i_c The critical hydraulic gradient causeing a zero effective stress condition within a granular cohesionless material.

i_{start} The minimum hydraulic gradient at which erosion of fine soil particles is first observed in an upward flow seepage test.

i_{boil} The minimum hydraulic gradient at which "boiling" at the surface of a test specimen is observed in an upward flow seepage test.

p Hydraulic pressure.

r Coefficient of correlation between two variables in a linear regression.

r^2 Coefficient of determination in a linear regression.

s Hydraulic gradient.

t Time, in [s].

Creek Letter

$\dot{\varepsilon}$ Rate of piping erosion in a soil, in [kg/s].

ϕ The diameter of the pre-formed hole through the test sample in a Hole Erosion Test.

η Porosity of a soil.

μ Coefficient of dynamic viscosity. For water, μ is equal to 10^{-3} kg/ms at 20 °C.

ρ_d The dry density of a soil, in [Mg/m^3].

$\rho_{d\,max}$ The maximum dry density of a soil obtained from the standard compaction test, in [Mg/m^3].

ρ_w Density of water, equal to 1,000 kg/m^3 at 4 °C.

τ Hydraulic shear stress, in [kN/m^2].

τ_c Critical hydraulic shear stress, defined as the shear for initiation of erosion in a soil.

τ_{cHET} The critical shear stress of a soil obtained from the Hole Erosion Test.

τ_{cSET} The critical shear stress of a soil obtained from the Slot Erosion Test.

$\hat{\tau}_{cHET}$ Representative critical shear stress for a soil sample at 95% compaction and at *OWC*, predicted from multiple linear regression formula using the

soil classification parameters as the independent variables, and using multiple linear regression formula based on test data obtained from Hole Erosion Tests.

$\hat{\tau}_{cSET}$ Representative critical shear stress for a soil sample at 95% compaction and at *OWC*, predicted from multiple linear regression formula using the soil classification parameters as the independent variables, and using multiple linear regression formula based on test data obtained from Hole Erosion Tests.

τ_o The initial shear stress along the pre-formed hole at the start of a Hole Erosion Test.

ω The water content of a soil.

ω_o The optimum water content of soil, also denoted as *OWC*, obtained from the standard compaction test.

Ψ The wetted area, equal to the wetted perimeter × the length of the sample, i.e. $\Psi = \wp \times L$, in [m^2].

Other symbols

$\wp$ The wetted perimeter, in [m].

Δh Difference in head across a flow path, in [m].

ΔP Difference in pressure across a given length of flow path, in [kN/m^2].

$\Delta\omega_r$ Water content ratio defined as $(\omega - OWC)/OWC \times 100\%$.

$\left[N_a^+\right]$ Concentration of ion, e.g. N_a^+ , in a solution, in [meq/l].

%Clay The clay content of a soil, defined as the fraction by weight of the clay-sized particles of the soil.

%Clay(UK) The clay content of a soil, as defined by UK engineers as the fraction by weight of the particles finer than 0.002 mm.

%Clay(US) The clay content of a soil, as defined by US engineers as the fraction by weight of the particles finer than 0.005 mm.

%Fines Fines content of a soil, also denoted as *Fines*, is defined as the fraction by weight of the soil finer than 0.075 mm.

%Gravel	The gravel content of a soil, defined as the fraction by weight of the soil particles of sizes between 4.75 mm and 75 mm.
%Sand	The sand content of a soil, defined as the fraction by weight of the soil particles of sizes between 0.075 mm and 4.75 mm.

CHAPTER 1

INTRODUCTION

1.1 INTRODUCTION

This thesis presents the findings of an investigation on piping erosion and internal instability of soils in embankment dams and their foundation. The investigation formed part of the research project "Estimation of the Probability of Failure of Embankment Dams by Piping and Internal Erosion" funded by the Australian Research Council and eighteen industry sponsors. The investigation is an extension of the research carried out by Dr. Mark Foster in the earlier stage of the project, and is focused on the study of the factors that influence the initiation of internal erosion and the rate of piping erosion through extensive laboratory testing.

1.2 BACKGROUND

There is a growing trend in Australia and some overseas countries in the use of quantitative risk assessment (QRA) techniques in the management of dam safety. The process of a QRA for a dam involves the estimation of the probability of failure, and the consequences due to the failure of the dam, such as loss of lives and properties. One of the main causes of failures in embankment dams is internal erosion and piping. According to Fell et al. (2001, 2003), about 0.5% (1 in 200) of embankment dams failed by internal erosion and piping, and about 1.5% (1 in 60) experienced an internal erosion incident. Von Thun (1996) studied the relative risk of failure of dams in USA, and revealed that 60% of the failures among embankment dams higher than 15.2 m in western USA were due to piping. The research project sets out to improve the state of the art of the methods for estimating the probability of failure of embankment dams by internal erosion and piping for application in the QRA process. It does this by investigating the physical processes of erosion in cracks in dams, and suffusion of soils in dams and their foundations.

1.3 TERMINOLOGY

A number of terms such as piping, suffusion, internal instability, sand boils, heave, etc. have been used by dam engineers to describe different internal erosion phenomena. There have been no universally accepted definitions for these terms. Many internal erosion incidents were too generally described as piping. Some of these commonly used terms are defined in this section to avoid misunderstanding of their meaning in this thesis.

1.3.1 Internal erosion

In the present study, internal erosion is defined as the situation when soil particles within the body of an embankment dam or its foundation are carried downstream by flow from the reservoir or groundwater. There are two fundamental types of internal erosion, viz. *piping* and *suffusion*, which differ in the ways that eroded particles are transported out of an embankment or its foundation.

1.3.2 Piping

Piping describes those incidents involving the formation and the sustenance of a continuous tunnel, usually called a "pipe", between the upstream and the downstream side of an embankment dam. Figure 1.1 shows a schematic diagram on piping through a dam and its foundation. Piping erosion describes the process in which erosion of soils takes place along the walls of a "pipe".

Piping may be initiated by backward erosion at locations where the exit gradient is high enough to cause detachment of soil particles. Such locations may be found at the downstream side of a homogeneous embankment, at the interface between the dam core and a coarser downstream zone in central core earth and rockfill dams, at the interface between an upstream zone of finer materials and a downstream zone of coarser materials

in the foundation, or at the interface between the embankment and the foundation. Erosion gradually works its way towards the upstream side of the dam until a continuous pipe is formed.

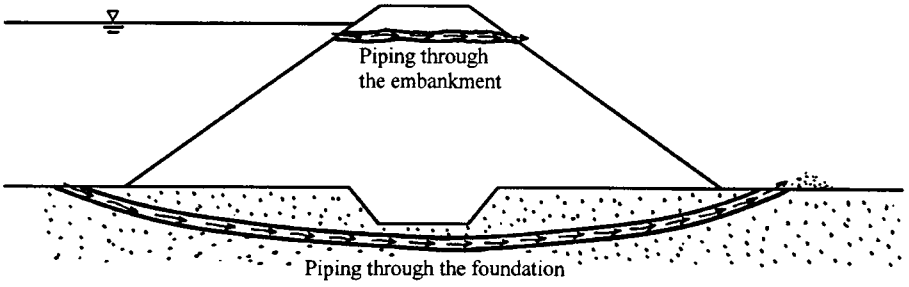

(a) Piping through the foundation of an embankment dam

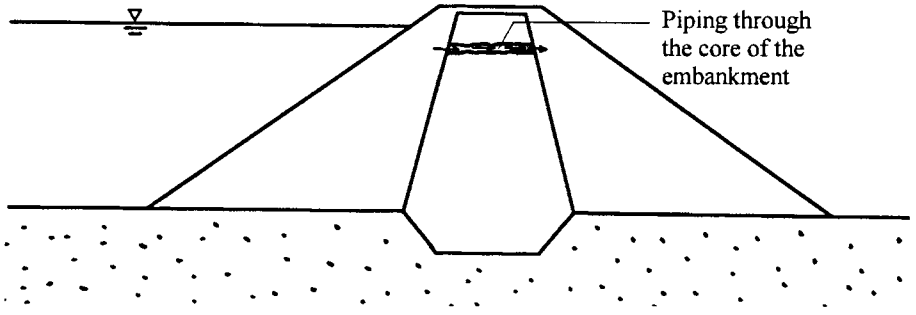

(b) Piping through the core of an embankment dam

Figure 1.1: Piping through a concentrated leak within the embankment or in the foundation.

Piping may also form along a concentrated leak through the embankment. The concentrated leak may be a crack through the dam core caused probably by differential settlement and/or hydraulic fracturing (Kjaernsli and Torblaa (1968), Sherard (1973 and 1985)), or may be a continuous permeable zone containing coarse and/or poorly compacted materials. Many concentrated leaks initiate along poorly compacted zones or cracks or voids around a conduit through an embankment dam.

A study of dam incidents revealed that piping could develop within the embankment, within the dam foundation, or from the embankment into the foundation.

1.3.3 Backward erosion

This involves the erosion of soils particles at the exit end of a seepage path due to a high exit velocity. The exit of the seepage path may situate at a free surface, such as the ground surface downstream of a soil foundation or the downstream face of a homogeneous embankment, or at the interface between the clay core and the downstream filter of a central core earthfill or rockfill embankment dam. A schematic diagram of piping initiated by backward erosion is shown in Figure 1.2. The detached particles are transported away by the seepage flow. The process gradually works its way towards the upstream side of the embankment or its foundation until a continuous pipe is formed.

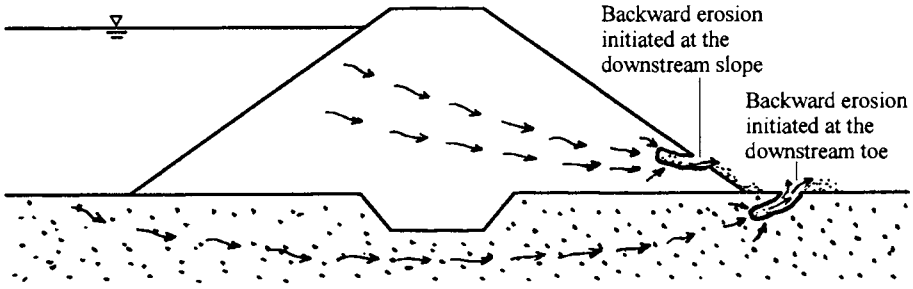

(a) Backward erosion initiated at the downstream side of the embankment

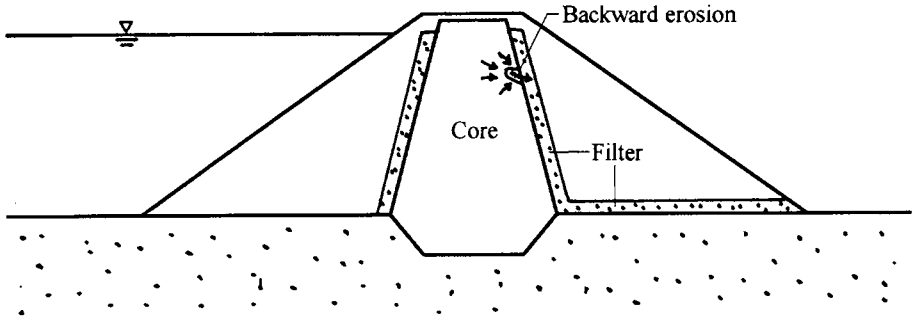

(b) Backward erosion initiated at the interface between the core and the downstream filter

Figure 1.2: Backward erosion initiated at an open seepage exit or at the interface between the core and the downstream filter.

1.3.4 Suffusion and internal instability

Suffusion is an internal erosion process involving the selective erosion of fine particles from a soil whose particle size distribution does not satisfy self-filtering conditions. The finer soil particles are fine enough to be removed through the constrictions between the larger particles by flow leaving behind an intact soil skeleton formed by the coarser soil particles. A schematic diagram showing the suffusion process in a dam is presented in Figure 1.3. Coarse widely graded or gap-graded soils (e.g. some sandy gravels, glacial tills) are more prone to internal erosion by suffusion. Soils that are susceptible to suffusion are often described as internally unstable.

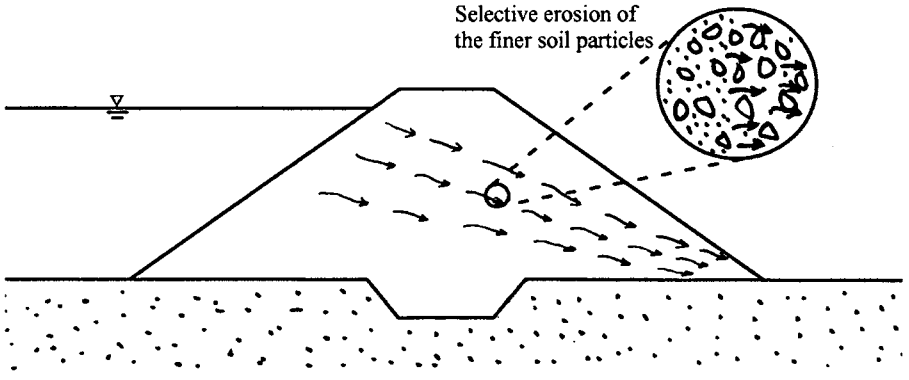

Figure 1.3: Internal erosion by the process of suffusion within the embankment.

It should be noted that there is no consensus on the use of the word "suffusion". German and Canadian literature for example, uses the word "suffosion" or "suffossion".

1.3.5 Heave, sand boils and blowout

Heave and sand boils are often considered as a special type of piping. Terzaghi and Peck (1948, 1967) classified piping failures into two types, namely failure by subsurface erosion and failure by heave.

Failure by heave usually occurs in a foundation of relatively permeable cohesionless soils. It refers to the situation when an excessive seepage gradient reduces the effective stress of the soils at the downstream toe of a dam to zero, hence causing instability. It is

often characterised by the presence of "boils" of sand at the toe of a dam because the same condition initiates backward erosion. Heave is called blow-out by Cedergren (1973) and Von Thun (1996). Figure 1.4 shows an example of heave occurring at the downstream toe of an embankment dam, leading to the initiation of backward erosion.

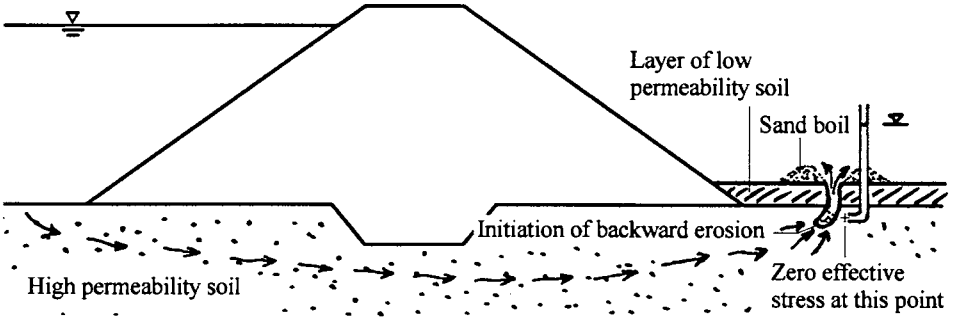

Figure 1.4: Heave (blowout) at the downstream toe of the embankment.

Heave may however also initiate suffusion as well as backward erosion. In some cases, however, instability and backward erosion or suffusion does not occur because the formation of some localised sand boils partially relieves the excessive uplift pressure and the exit gradients reduce.

Failure by "subsurface erosion", according to Terzaghi and Peck (1948, 1967), is similar in meaning to piping in the foundation initiated by backward erosion as described in the previous section.

1.4 ANALYSIS OF INTERNAL EROSION AND PIPING USING EVENT TREE METHODS

For internal erosion by heave and sand boils, a factor of safety against instability by heave can be estimated using some basic theories on seepage and effective stress. The method of finding the factor of safety can be found in books on classical soil mechanics. Rigorous theoretical approaches, however, are not available for the analysis of the majority of internal erosion problems. This is because most internal erosion incidents involve complex initiation and development processes which are not amenable to

theoretical analysis. Each of these processes is influenced by a number of internal and external factors, whose effects are often difficult to quantify. Some of the more important factors are:

- the potential of cracking through the dam;
- the possibility of poor construction that may result in erosion susceptible zones in the embankment;
- the ability of the embankment soils to heal a crack, for example by swelling as the soil wets up;
- the resistance of the soils against erosion;
- the reservoir storage and the variability of the permeability of the embankment soils that influence the distribution of the hydraulic gradient across the dam and the exit gradient;
- the speed of filling up the reservoir (rapid filling will cause the formation of very high local hydraulic gradient which may cause hydraulic fracturing of the core of the dam);
- the presence or absence of a filter, and the effectiveness of the filter for protecting the embankment materials against erosion;
- the ability of the core soils to sustain the roof of an open pipe;
- the possibility of crack filling action due to upstream materials being washed into a crack, hence slowing down the speed of piping erosion;
- the ability of the embankment to discharge safely the flow through the pipe;
- the possibility of human intervention; etc.

The State of the Art approach for analysing internal erosion uses event tree techniques to represent the series of processes involved in internal erosion, such as those listed above. The various sub-branches of an event tree represent all possible pathways that internal erosion might lead to failure or not failure. The use of the event tree method in the analysis of the likelihood of internal erosion and piping has been investigated in the earlier stage of the research project and findings are presented in Foster (1999), Foster and Fell (1999b, 2000), and Foster et al. (2001). In their proposed event tree methods, Foster and Fell (1999b), developed further the idea initially proposed by Von Thun

(1996), of sub-dividing the internal erosion process into four phases of development. The four phases are:

Initiation: Internal erosion may initiate in a concentrated leak, or by backward erosion or suffusion.

Continuation: Internal erosion may or may not continue depending on whether or not there are filters capable of stopping the erosion process.

Progression: The progress of internal erosion into a pipe.

Breach: Further internal erosion leading to dam breach and uncontrolled release of the storage.

Diagrammatic models are shown in Figure 1.5 to illustrate the four phases of development of internal erosion in the cases of piping initiated along a concentrated leak and piping initiated by backward erosion. Foster and Fell (1999b) identified the various factors that would affect the process mechanisms of each of the four phases of development, and set up a framework, based on event tree and fault tree techniques, for estimating the likelihood of internal erosion and piping in an embankment dam. Figure 1.6 presents an example of a failure path diagram which shows the processes involved in the four phases of development of internal erosion in an embankment dam. An example of an event tree for piping through an embankment dam is shown in Figure 1.7.

1.5 INFLUENCE OF SOIL ERODIBILITY ON INTERNAL EROSION AND PIPING

According to the framework of Foster and Fell (1999), the erodibility of the soil in the core of an embankment dam and its foundation has a significant influence on the Initiation Phase and the Progression Phase of internal erosion. The significant influence is in the following aspects:

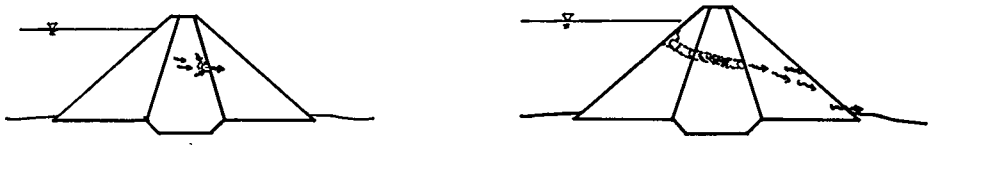

INITIATION →	CONTINUATION →	PROGRESSION →	BREACH/FAILURE
Leakage exits on d/s side of core and backward erosion initiates	Continuation of erosion	Backward erosion progresses back to the reservoir	Breach mechanism forms

(a) Piping in the Embankment Initiated by Backward Erosion

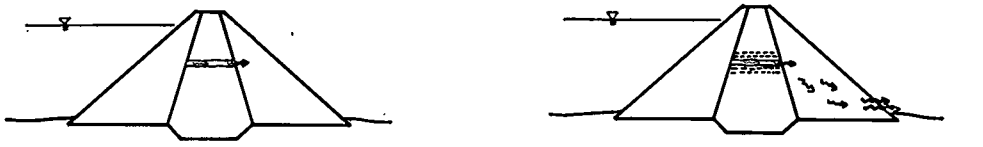

INITIATION →	CONTINUATION →	PROGRESSION →	BREACH/FAILURE
Concentrated leak forms and erosion initiates along walls of crack	Continuation of erosion	Enlargement of concentrated leak	Breach mechanism forms

(b) Piping in the Embankment Initiated by Erosion in a Concentrated Leak

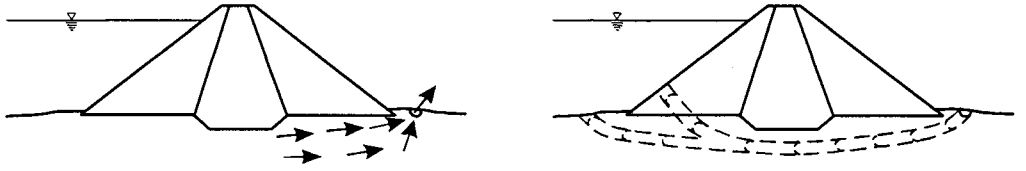

INITIATION →	CONTINUATION →	PROGRESSION →	BREACH/FAILURE
Leakage exits from the foundation and backward erosion initiations	Continuation of erosion	Backward erosion in progresses to form a pipe	Breach mechanism forms

(c) Piping in the Foundation initiated by Backward Erosion

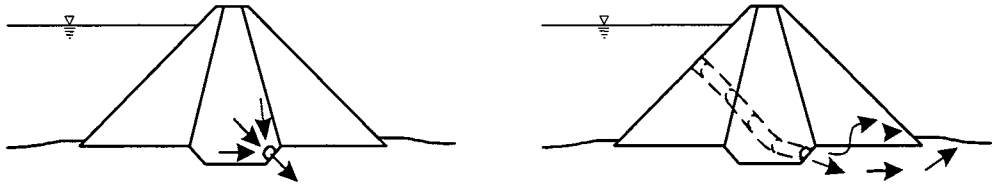

INITIATION →	CONTINUATION →	PROGRESSION →	BREACH/FAILURE
Leakage exits the core into the foundation and backward erosion initiates as core erodes into the foundation	Continuation of erosion	Backward erosion progresses to form a pipe. Eroded soil is transported in the foundation	Breach mechanism forms

(d) Piping from the Embankment to Foundation Initiated by Backward Erosion

Figure 1.5: Models showing the four phases of development of failure by internal erosion and piping (Foster and Fell 1999b).

Initiation phase

The erodibility of the soil in the core of an embankment dam or its foundation will decide whether or not internal erosion will initiate in a crack developed through the core or the foundation of an embankment dam under the imposed hydraulic conditions and physiochemical environment. For erosion in a crack, the erodibility is measured as the critical hydraulic shear stress at which erosion initiates. In internally unstable soils, it is measured by the seepage gradient at which the suffusion process begins.

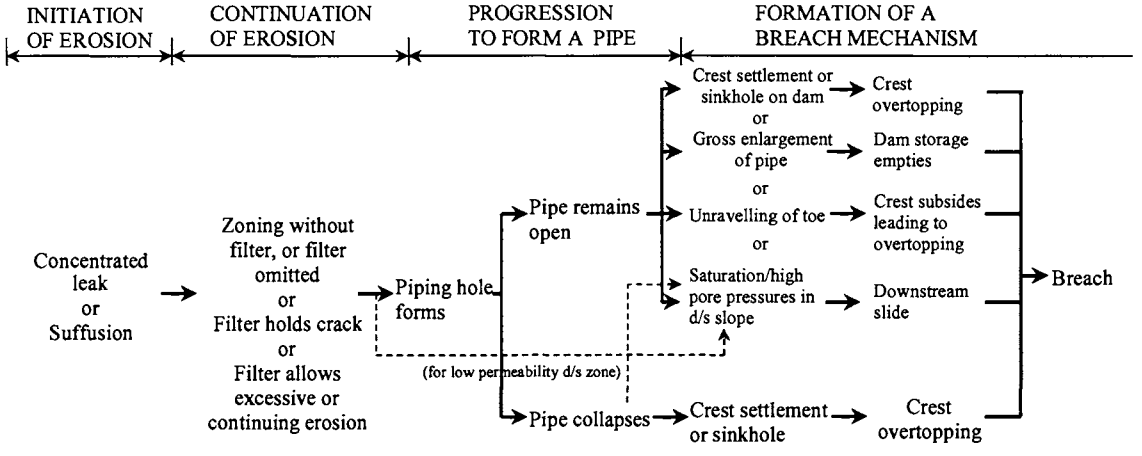

Figure 1.6: Failure path diagram for failure by piping through the embankment (Foster and Fell 1999b).

Progression Phase

Knowledge of the rate of erosion of the soil under the hydraulic gradient presents in a crack or pipe in the core of an embankment dam or its foundation will help assessing the rate of progression of internal erosion given internal erosion has already initiated. If the erosion rate of the soil is so slow that cracks might be sealed due to swelling of the soil around cracks or permeable zones, or filling of the cracks by upstream materials, progression of internal erosion might be less likely.

A slow rate of erosion might also increase the chance of a successful intervention or repair. Furthermore, a slow rate of erosion might increase the chance of lowering the reservoir to a safe level before a breach mechanism develops.

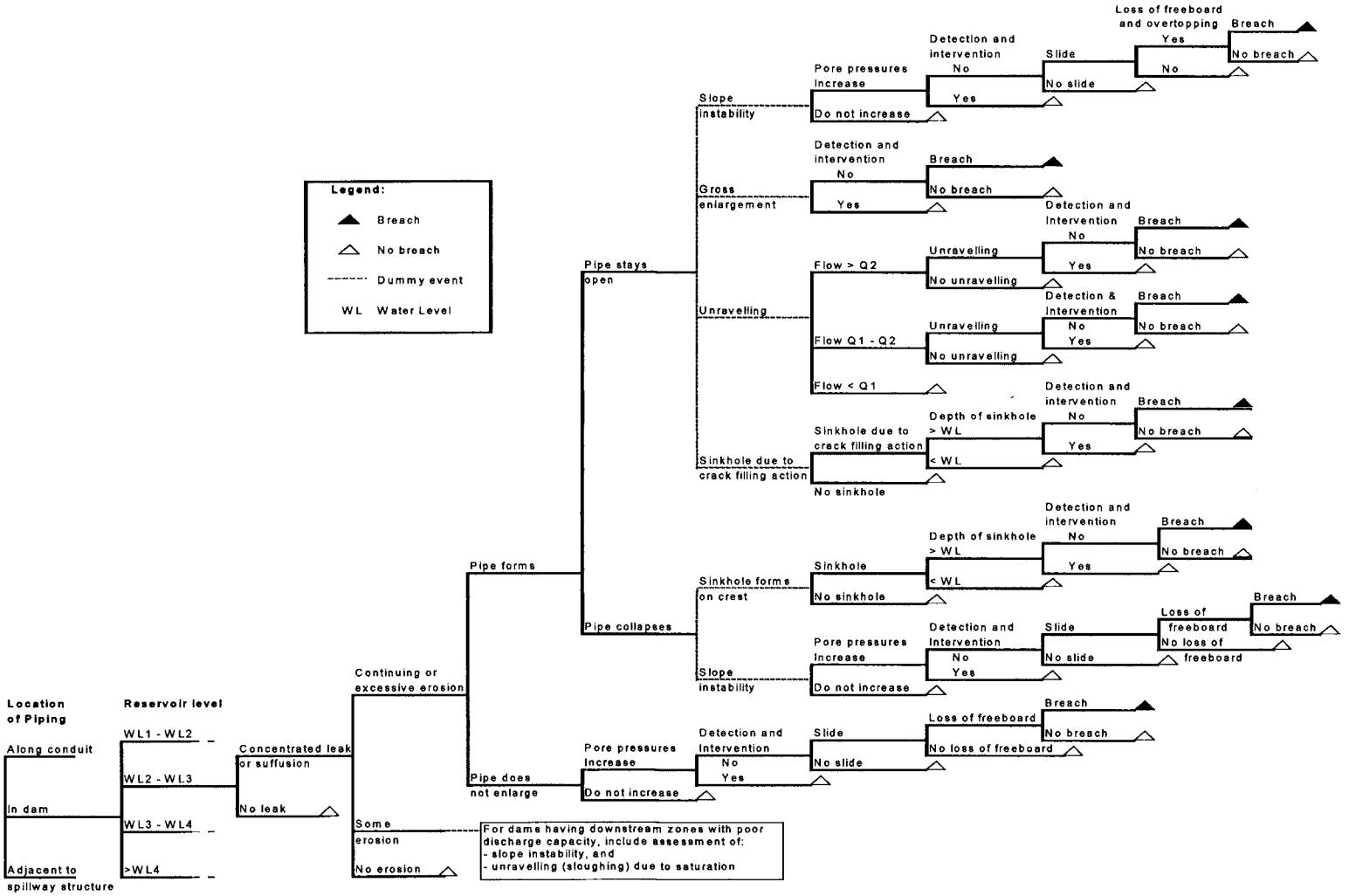

Figure 1.7: Event tree for piping through an embankment dam (Foster and Fell 1999b).

Warning Time for a Dam Breach

According to Fell et al. (2001), the rate of erosion also has a significant influence on the time for progression of piping and development of a breach. This affects the amount of warning time available to evacuate the population at risk downstream of the dam, and hence has important implications for the management of dam safety.

1.6 OBJECTIVE OF THIS THESIS

The objective of this thesis is to present the findings of the investigations on piping erosion, and the internally instability of soils in embankment dams and their foundations. The investigations included development of the slot erosion tests and the hole erosion tests to investigate the factors which affect the critical shear stress and the rate of erosion of cohesive soils. They also used downflow and upflow seepage tests on cohesionless soils to investigate the particle size distribution of soils which are internally unstable, and the hydraulic gradients at which suffusion begins. These results were combined with published data to provide aids to judgment in the assessment of the probabilities of initiation and progression of internal erosion and piping in an embankment dam and its foundation in the QRA process.

1.7 STRUCTURE OF THIS THESIS

This thesis comprises two volumes. Volume 1 of the thesis presents the main findings of the investigation, and comprises of six chapters:

Chapter 1 is the current chapter which states the objectives of the thesis, and introduces the background of the research project.

Chapter 2 describes the investigation of piping erosion. It describes the Slot Erosion Test and the Hole Erosion Test, developed at the University of New South Wales for studying the erosion characteristics of a soil. It presents the findings of the two tests, and discussed the factors which are likely to affect the erosion characteristics of a soil.

Methods are proposed for approximately estimating the erosion characteristics based on known parameters of the soil.

Chapter 3 describes the investigation of internal instability of soils. The investigation involved conducting two series of laboratory suffusion tests, namely the downward flow seepage test and the upward flow seepage test, for identifying the properties of those soils that are susceptible to suffusion, and the hydraulic gradient at which suffusion is initiated. The chapter presents the analysis of the results of the two series of tests, and the review of the results of similar seepage tests conducted by previous investigators. The chapter also presents new procedures for assessing the likelihood of internal instability of clay-silt-sand-gravel or silt-sand-gravel mixtures.

Chapter 4 describes, using examples, on how the findings presented in Chapter 2 and Chapter 3 can be applied in the assessment of the likelihood of internal erosion and piping in a QRA process.

Chapter 5 presents the main conclusions of the thesis, and recommends areas where further research related to internal erosion in embankment dams and their foundations should be carried out.

Chapter 6 presents a list of references.

Volume 2 of the thesis consists of Appendices where test records, graphical presentation of test results, detailed test procedures, and drawings of test apparatus are presented.

An electronic version of this thesis in portable file format (PDF) can be found in the compact disc at the back cover of the thesis.

CHAPTER 2

LABORATORY TESTS ON PIPING EROSION

2.1 INTRODUCTION

2.1.1 Overview

This Chapter presents the findings of the experimental investigation on the erosion resistance of soils in the core or the foundations of embankment dams. The main objectives of the investigation were to experiment the use of two laboratory tests, namely the Slot Erosion Test (SET) and the Hole Erosion Test (HET) to find out the erosion characteristics of a soil, and to study the influence of the various basic engineering properties of a soil on its erosion characteristics.

This Chapter provides an overview of the research on soil erosion by others, explains the needs of further research, introduces the theoretical basis of the SET and the HET, and presents the results of analysis and the findings of the laboratory testing.

2.1.2 Needs for research on erodibility of soils

Over the years, a lot of research on the erodibility of soils has been carried out by engineers, geomorphologists and hydrologists. Nevertheless, there has been no unified method for predicting the erodibility of soils. This may reflect the fact that no one test simulates all erosion conditions, but is also because most research was confined to investigate only a few aspects of the erosion problem. For instances, some focused on the influence of pore fluid chemistry on the erodibility of saturated remoulded clay, while others aimed at studying the influence of the soil's mechanical properties. Some research involved testing blended artificial soils, while others studied natural soils in particular size ranges. Some carried out external erosion tests such as the Jet Erosion Index Test, the Rotating Cylinder Test and the Flume Test, whereas some carried out

internal erosion tests to investigate erosion within a soil mass with or without the formation of a pipe. As different test methods were used involving different erosion and particle transport mechanisms, and applied to different types of soils, their results are difficult to compare or combine. An overview of the research work on erodibility of soils by others is presented in Section 2.2 of this report.

In order to be able to quantify the relative erodibility of various types of soils commonly found in embankment dams, a sufficiently wide range of soils should be investigated by the same erosion test. The chosen test should be able to provide adequate control over the various physiochemical and mechanical properties believed to influence erodibility. External and internal erosion processes are different as they involve different particle transport mechanisms although they may both be influenced by the same properties of the soil. Therefore, for investigating erosion in cracks or pipes in dams, the chosen test should preferably be an internal erosion test that can simulate erosion along a crack or pipe within a dam core. In the present study, two tests, namely the Slot Erosion Test and the Hole Erosion Test have been specially designed based on the above considerations.

2.1.3 Definition of the erodibility of a soil

The erodibility of a soil can be described in terms of the soil's behaviour in two aspects, namely

- the rate of erosion when a given hydraulic shear stress is applied to the soil;
- the ease of initiating erosion in the soil;

Rate of Erosion – the Slope of the graph of Erosion Rate versus Hydraulic Shear Stress

There are a number of different methods for quantifying the rate of erosion in a soil. For instance the rate can be expressed as the eroded depth in a soil sample in a specified period of time under a specified hydraulic shear stress; the volume of soil eroded per unit time and area under a given shear stress; the mass of soil eroded per unit time and area under a given shear stress, etc. The rate of mass removal per unit area is considered

a better representation of the erosion rate as it takes into account the density and the porosity of the soil mass. Since the rate of erosion depends on the level of the hydraulic shear stress due to the traction of the eroding fluid, the rate of erosion is usually normalised against the hydraulic shear stress. Research by others shows that, for some soils, the rate of erosion per unit area is approximately linearly proportional to the level of shear stress. The slope of the best-fit straight line that approximates the linear relationship between the mass rate of erosion per unit area and the hydraulic shear stress, therefore, represents the normalised rate of erosion per unit area. For simplicity, the slope of the best-fit straight line is called the *Coefficient of Soil Erosion* (C_e) in this report. The meaning of C_e is illustrated graphically in Figure 2.1.

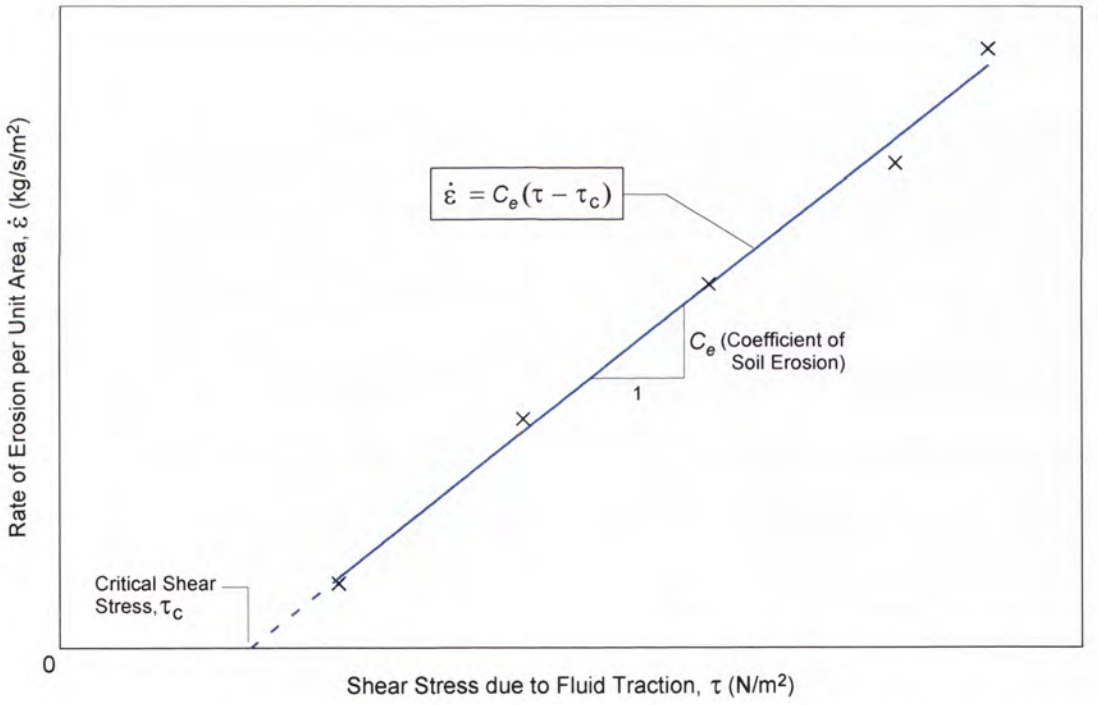

Figure 2.1: Graphical illustration of the meaning of Critical Shear Stress and Coefficient of Soil Erosion.

Ease of Initiating Erosion – the Critical Shear Stress

The ease of initiating erosion in a soil can be quantified by the Critical Hydraulic Shear Stress, τ_c, or simply called the Critical Shear Stress, which has the physical meaning of

the value of the hydraulic shear stress for which erosion initiates. τ_c is often obtained by extrapolating a graph of observed erosion rate, $\dot{\varepsilon}$, versus hydraulic shear stress, τ, as illustrated by Figure 2.1. This assumes a constant value C_e which, as discussed later, may not apply to all soils.

Section 2.2 of this Chapter describes some other methods of quantifying the ease of initiating erosion in a soil. Among the various methods, the Critical Shear Stress is, by far, the most commonly used parameter.

2.1.4 Layout of Chapter 2

After this introduction, Section 2.2 is a literature review providing a brief account of the research work by others on soil erosion. Section 2.3 explains the theories behind the SET and the HET, and the procedures for analysing the raw data obtained from the tests. The origins of the soil samples used in the laboratory erosion tests, their mineralogy compositions, and their basic engineering properties are summarised in Section 2.4. Section 2.5 presents the results of correlation and regression analysis for the purpose of finding relationships between the erosion parameters and the basic engineering properties of the soil samples. Section 2.6 comments on and discusses the results of the analysis. The findings of the experimental investigation on piping erosion are summarised and concluded in Section 2.7. Some recommendations are made in Section 2.8 on the applications of the erosion tests and the use of the findings of the experimental investigation.

2.2 RESEARCH ON SOIL EROSION BY OTHERS

2.2.1 Overview

This Section presents a detailed literature review on studies of the factors that affect the erodibility of soils in embankment dams and their foundations, and the tests which are available to measure erodibility. A summary of the literature review is presented in Section 2.2.8.

2.2.2 Type of erosion tests

Field or laboratory tests commonly used by researchers for studying the erosion resistance of soils are:

- laboratory hydraulic flume test, or large scale channel erosion test,
- rotating cylinder test,
- field or laboratory submerged jet erosion test, and
- tests for measuring the dispersivity of a soil.

These four types of tests are described in Sections 2.2.3, 2.2.4, 2.2.5 and 2.2.6 respectively. Other types of erosion tests are described in Section 2.2.7.

2.2.3 Flume tests

Use of the flume test has been described in the following literature:

- Gibbs (1962)
- Lyle and Smerdon (1965)
- Kandiah and Arulanandan (1974)
- Arulanandan and Perry (1983)
- Shaikh, Ruff, and Abt (1988)

- Shaikh, Ruff, Charlie, and Abt (1988)
- Ghebreiyessus, Gantzer, Alberts and Lentz (1994)
- Briaud, Ting, Chen, Gudavalli, Perugu and Wei (1999), Briaud, Ting, Chen, Cao, Han and Kwak (2001a), Briaud, Chen, Kwak, Han and Ting (2001b) and Briaud, Chen, Li, Nurtjahyo and Wang (2003)

Gibbs (1962)

Gibbs reviewed past studies in erosion and tractive forces on fine-grained cohesive soils, and attempted to generalise the soil mechanics properties with respect to the erosion test findings.

Gibbs acquired information on 45 case studies on canal banks. He collected undisturbed samples from canal banks for evaluation of in-place density and carried out hydraulic flume tests in the laboratory. The soil samples were mostly low plasticity silts (ML) or clays (CL). Results of his hydraulic flume tests were correlated with plasticity, density and gradation of tested soil samples.

Gibbs main findings were:

- erosion resistance as measured by the critical shear stress for the samples tested were in the range of 0.015 – 0.060 lb/ft^2 (0.72 – 2.87 Pa). Gibbs called this the "Tractive Force";
- clayey soils were more erosion-resistant than silty and clayey sands;
- plasticity of a soil was the principal characteristic that influenced erosion resistance;
- gradation had great influence on erosion resistance among sand and coarse-grained soils, whereas plasticity data have larger effects on the erosion resistance among fine-grained soils;
- the Liquid Limit had a greater influence than the density on the tractive force resistance. Soils with higher liquid limits had higher critical shear stress than soils with lower liquid limits as shown in Figure 2.2.

Gibbs grouped his canal bank cases into zones according to their critical shear stresses on the A-line plasticity chart as shown in Figure 2.3. Criteria were given for evaluating the erosion potential of fine-grained soils on the basis of plasticity characteristics.

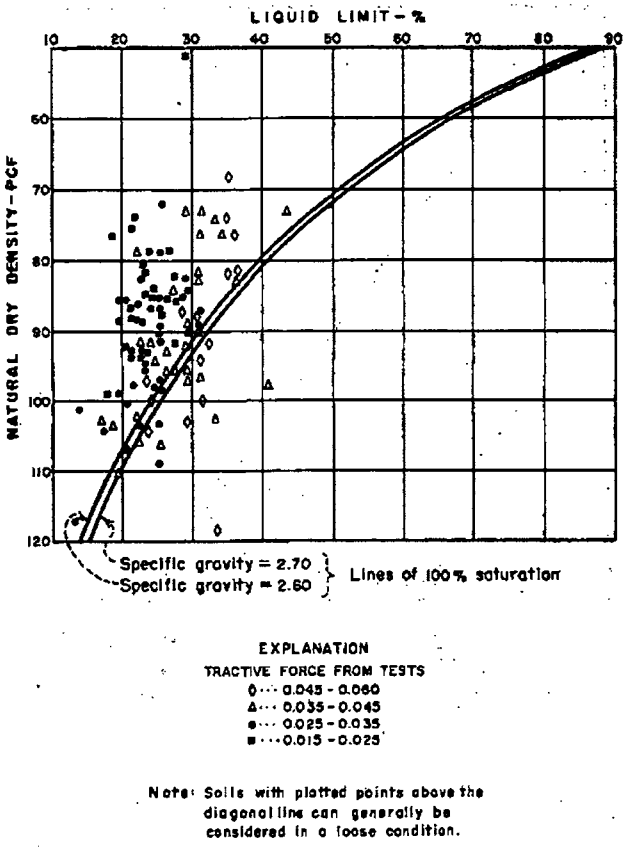

Figure 2.2: Relationship between Tractive Force (Critical Shear Stress), Natural Dry Density and Liquid Limit (Gibbs 1962).

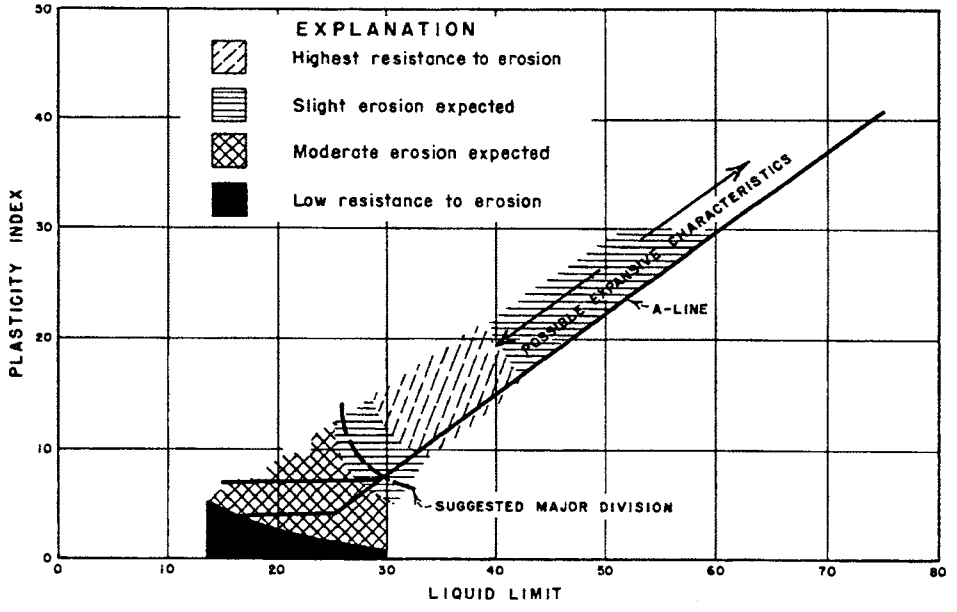

Figure 2.3: Suggested Trend of Erosion Resistance (as measured by Critical Shear Stress) for Fine-grained Cohesive Soils with respect to Plasticity (Gibbs 1962).

Lyle and Smerdon (1965)

Lyle and Smerdon carried out flume tests on seven Texan soils whose properties are summarised in Table 2.1.

Table 2.1: Physical properties of soils tested (Lyle and Smerdon (1965)).

Soil	Amarillo fine sandy loam	Lufkin fine sandy loam	Reagan sandy clay loam	Lufkin clay	Houston clay	Lake Charles clay	San Saba clay
Soil No.	K853	K114	K810	K116	K117	K319	.....
Plasticity index, I_w	Non-plastic	Non-plastic	9.9	23.7	23.2	34.4	25.7
Percent clay, P_c	13.5	11.5	29.8*	44.0	36.0	50.5	50.0
Mean particle size, M	0.096	0.075	0.0071	0.0084	0.0033	0.0019	0.0020
Dispersion ratio, D_r, percent	71	35	72	16	10	15	16
Vane shear strength, S_v†, lb/ft²	43	93	18	162	165	618	470
Percent organic matter, P_{om}	0.8	1.8	1.9	0.9	3.3	3.9	3.3
Cation exchange capacity, CEC me/100 gm	8.7	11.5	18.2	29.0	58.2	41.6	53.6
Calcium-sodium ratio, R_{cn}	9.0	15.0	3.24	7.2	279.5‡	34.2	285.5‡

* Value supplied by Dr. George Kunze, soil and crop sciences department, Texas A&M University.
† Values of shear strength for sandy soils K853 and K114 were taken at a 20 percent moisture content with a void ratio of 0.8. Shear strength for the other soils (clays) was taken at approximately 38 percent moisture and at a void ratio of 1.5.
‡ Estimated values.

Lyle and Smerdon tested each soil samples at three different degrees of compaction in a hydraulic flume. They defined Critical Tractive Force, T_c as the hydraulic shear stress which caused noticeable channel erosion.

Their findings were:

- typical values of T_c were approximately 0.02 lb/ft^2 (0.96 Pa);
- T_c decreased linearly with void ratio (e);
- T_c increased with Plastic Index;
- at a given void ratio (e), T_c was best correlated to the soil properties in the following order:
    i. Plastic Index,
    ii. Dispersion ratio obtained from the SCS Laboratory double-hydrometer test,
    iii. Percentage organic matter,
    iv. Vane shear strength,
    v. Cation exchange capacity,
    vi. Mean particle size,
    vii. Calcium-sodium ratio,
    viii. Clay size percentage.

The Author notes that Lyle and Smerdon have neglected the important influence of the moulding water content and the dry density ratio (i.e. the ratio of the dry density to the standard maximum dry density (SMDD)) of a test sample on its erosion resistance.

Kandiah and Arulanandan (1974)

Kandiah and Arulanandan carried out erosion tests on saturated and unsaturated clay using the flume test and the rotating cylinder test.

They tested Yolo loam clay (11% clay, 49% silt, 40% sand, the clay minerals being montmorillonite, kaolinite, mica and vermiculite). Soil samples tested were mixed with solutions of known Sodium Adsorption Ratio (*SAR*) and salt concentration, and samples were mixed with water to obtain the desired water content. *SAR* is defined as:

$$SAR = \frac{[Na^+]}{\sqrt{\frac{1}{2}([Ca^{2+}]+[Mg^{2+}])}}$$

where $[Na^+]$, $[Ca^{2+}]$, and $[Mg^{2+}]$ represent the concentration in [meq/l] of the cations Na^+, Ca^{2+}, and Mg^{2+}, respectively.

Both saturated and compacted samples were tested in a flume apparatus, but only saturated samples were tested in a rotating cylinder apparatus.

Their aims were to:

- compare critical shear stresses obtained by the rotating cylinder test and the flume test;
- examine the effect of compaction water content on the critical shear stress, τ_c; and
- investigate the influence of structure and water content on the slaking (or flaking) of cohesive soil systems.

Their findings were:

- the rate of erosion, $\dot{\varepsilon}$, defined as the mass of materials eroded per unit surface area per unit time, increased as the shear stress, τ, was increased;
- at different *SAR*s, τ_c obtained by the flume test were the same as those obtained by the rotating cylinder test;
- $\dot{\varepsilon}$ obtained by the flume test were lower than those obtained by the rotating cylinder test;
- at a given salt concentration, τ_c decreased, but $\dot{\varepsilon}$ increased as *SAR* increased;
- in saturated samples prepared at low SAR, the water content had little effect on τ_c. When τ_c was exceeded, $\dot{\varepsilon}$ increased as water content increased;
- in compacted unsaturated soil samples, τ_c was highly dependent on water content. The higher the water content, the lower the swell, and the higher the τ_c;
- slaking (or flaking) was instantaneous for samples compacted drier than optimum. τ_c for these soil samples was zero;

- for compacted samples, the slaking rate decreased as the water content increased, and became negligible when the water content reached 19.3% (about 4.5% above optimum water content);
- soils with more dispersed structure (e.g. montmorillonite) had longer slaking times (due possibly to lower permeability and longer time for water to enter pores);
- soils with higher *SAR* in the saturated state took longer time to slake, as they developed less flocculated structure.

Kandiah and Arulanandan proposed that:

- the mechanism causing erosion was thought to be swelling;
- in saturated samples, swelling was due to differences in concentration between pore fluid and eroding fluid;
- in compacted soils, τ_c was highly dependent on water content. The higher the water content, the lower the swell and hence the higher the τ_c;
- the rate of slaking was controlled by permeability. The lower the permeability, the longer the slaking time.

Arulanandan and Perry (1983)

Arulanandan and Perry reviewed filter design practice of that time and investigated the significance of the erodibility of core material to filter design. They also investigated the use of critical shear stress, τ_c, to quantify the erodibility of core material. They proposed a procedure for evaluating successful performance of filter with respect to erodibility of core material.

Arulanandan and Perry commented that assessing the erosion resistance of a soil using Gibbs (1962) A-line plasticity chart was inadequate as some important factors which affected erodibility, such as the clay mineralogy of the soil and the chemical compositions of pore and eroding fluid, were not considered. Some dams failed by piping but their core materials would be classified as having highest resistance to erosion according to their Atterberg Limits using Gibbs' A-line chart in Figure 2.4.

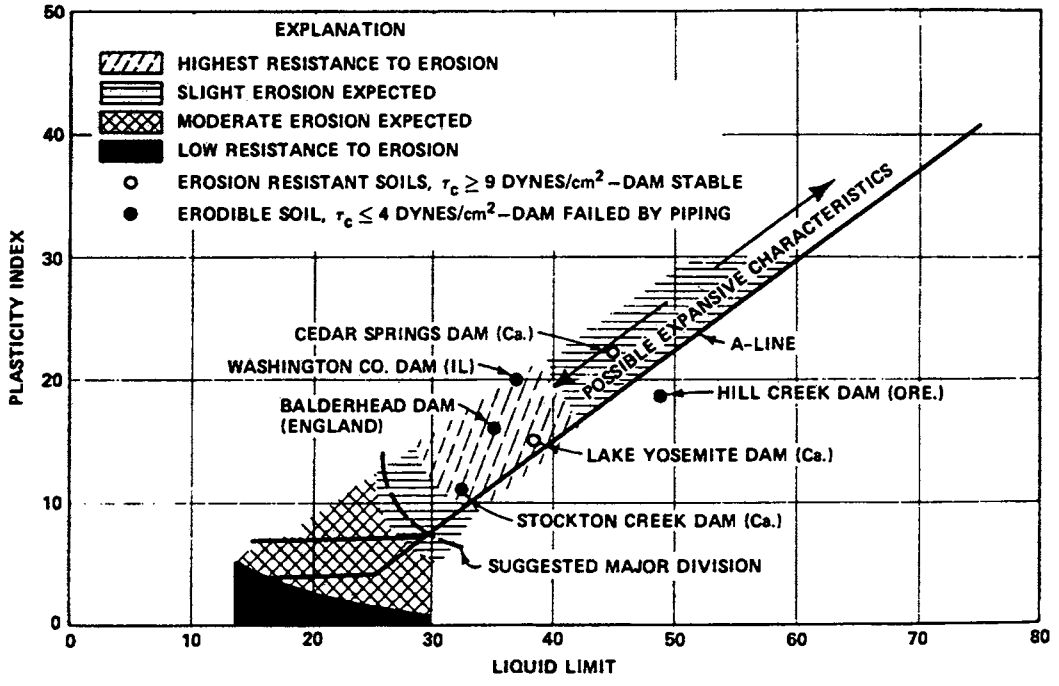

Figure 2.4: Soil erodibility, as measured by Critical Shear Stress, versus Plasticity (Arulanandan and Perry 1983).

Arulanandan and Perry commented that some commonly used tests for finding the dispersivity of a soil, such as the Crumb Test, SCS Dispersion Ratio Test and Pinhole Test did not take into account some soil characteristics which would affect erodibility. Some soils were not classified as dispersive but they were very erodible.

Arulanandan and Perry proposed to quantify erodibility based on the Critical Shear Stress, τ_c, defined as the value of the stress for zero sediment discharge. τ_c would be obtained by extrapolating a graph of observed erosion rate, $\dot{\varepsilon}$, versus shear stress, τ, (Shields, 1936). Arulanandan and Perry measured τ_c of remoulded or undisturbed soil samples using a rotating cylinder apparatus, and a hydraulic flume. They suggested that τ_c could also be estimated indirectly by the composition index called Dielectric Dispersion, $\Delta\varepsilon_0$, in conjunction with pore fluid concentration, and *SAR* (i.e. $\Delta\varepsilon_0$ depends on clay mineralogy and amount). $\Delta\varepsilon_0$ is the difference in dielectric constant measured at say, 10^6 and 10^8 Hz, and is a function of the Cation Exchange Capacity (*CEC*).

Arulanandan and Perry presented graphs for remoulded saturated soils showing τ_c as a function of $\Delta\varepsilon_0$ and *SAR*, given soil pore fluid concentration, and assuming that distilled water was the eroding fluid. They found out that τ_c was influenced by the following factors:

- clay mineralogy and clay fraction percentage;
- chemical compositions of pore and eroding fluid (τ_c would be higher as concentration of the eroding fluid increased);
- pH;
- temperature;
- organic matter;

In addition, Arulanandan and Perry found that, under the same τ, $\dot{\varepsilon}$ would increase as the salt concentration of eroding fluid decreased (i.e. distilled water gives the highest erosion rate).

Arulanandan and Perry studied 29 dams with both dispersive and non-dispersive soils, and found that dams which had experienced piping, in general, had τ_c less than or equal to 4 dynes/cm^2 (0.4 Pa), whereas dams which had not experienced piping had τ_c higher than 4 dynes/cm^2 (0.4 Pa). Their case studies showed that some non-dispersive soils could also show low erosion resistance. The τ_c values were estimated from $\Delta\varepsilon_0$ values which were predicted from CEC values given in the literature on the 29 dams.

Based on the results of the case studies, Arulanandan and Perry proposed a classification of the erosion resistance of soils:

Category 1: Erodible soils $\tau_c \leq 4$ dynes/cm^2 (0.4 Pa). Extensive filter tests would be necessary to ensure that the proposed filter materials could stop the migration of fines out of the base soil.

Category 2: Moderately erodible soils $4 < \tau_c < 9$ dynes/cm^2 ($0.4 < \tau_c < 0.9$ Pa). Filter tests would be required for the proposed filter materials same as for Category 1.

Category 3: Erosion resistant soils $\tau_c \geq 9$ dynes/cm^2 (0.9 Pa). Filter design according to current grading criteria (i.e. Terzaghi's design criteria for filters).

Acciardi (1984), in discussion on the paper, commented that the boundary shear stress in the Pinhole Test significantly exceeded the Critical Shear Stress values for erosion resistant soils reported by Arulanandan and Perry. Therefore, soils classified by them as "erosion-resistant" could classify as "dispersive" in the Pinhole Test. Arulanandan and Perry replied that although a soil sample would be exposed to very high boundary shear stress in the Pinhole Test, the rate of change of erosion and the rate of erosion would be small for erosion-resistant soils. These erosion-resistant soils would not show appreciable erosion in a Pinhole Test. On the other hand, erodible soils would have high rate of change of erosion rate. Arulananandan and Perry also commented that the Pinhole Test was not a reliable test to evaluate the erodibility characteristics of soils in terms of critical shear stress, because the surface of the pinhole was not clearly defined during the test (e.g. hole diameter reduced as the soil sample was wetted and swelled).

Kenney (1984) commented that at the start of erosion, "slaking" was responsible which required zero velocity of flow and only the presence of water. He believed that, in the early stages, the key process affecting dislodgement of particles was slaking rather than dislodgement by flow water. He said that filters should therefore be able to prevent the loss of particles due to slaking at the early stage. Arulanandan and Perry replied that τ_c was zero when slaking occurred, and τ_c would be a better parameter to define particle detachment than flow velocity.

The Author has reservations regarding the way that Arulanandan and Perry related their test results to dam incidents. They drew an equivalence between the erodibility of the soil in a dam and the potential of piping. While their conclusion based on the studies of 29 dams might be correct, they failed to acknowledge that just because a dam had not experienced piping did not mean the soils in the dam were not erodible. The Author is of the view that the occurrence of piping is not just influenced by the erodibility of the soil in the dam, but also by a lot of other factors that influence the various phases of

development of internal erosion, viz. (1) initiation of erosion by concentrated leak, backward erosion, suffusion or blow-out, (2) continuation of erosion, (3) progression to form a pipe, and (4) formation of a breach mechanism. In addition, their estimation of critical shear stresses from $\Delta\varepsilon_0$, which were predicted from CEC values given in the literature on the 29 dams would bring some uncertainty to the estimated values.

Shaikh, Ruff, and Abt (1988)

Shaikh, Ruff and Abt used a hydraulic flume (L 2.5 m x W 15.5 cm x D 11 cm) to study the influence of clay content and compaction water content on erodibility of soil. The eroding fluid was tap water (Total Dissolved Solids (*TDS*) < 2.2 meq/l, pH = 7.7, at $18 \pm 1\,^{\circ}C$). Flow rate was measured by a venturi meter and the flow depth was maintained uniform. Flow velocity profile was measured by a Pitot tube. The set up of the test is shown schematically at Figure 2.5.

They proposed an empirical relationship between erosion rate (mass per unit area per unit time), hydraulic shear stress and percentage clay.

They tested unsaturated compacted samples of Na-montmorillonite clays. Na-montmorillonite clay was mixed with silica to produce samples of varying Na-montmorillonite clay content (100, 70, 40 and 10% by dry weight). Samples of soils were compacted statically under 700 Pa at different degrees of moisture content ($\pm 5\%$ of optimum moisture content). The Liquid Limit, Plastic Index, Optimum Moisture Content and Maximum Dry Density of the soil samples were measured prior to the flume tests. 9 tests were carried out for each soil sample.

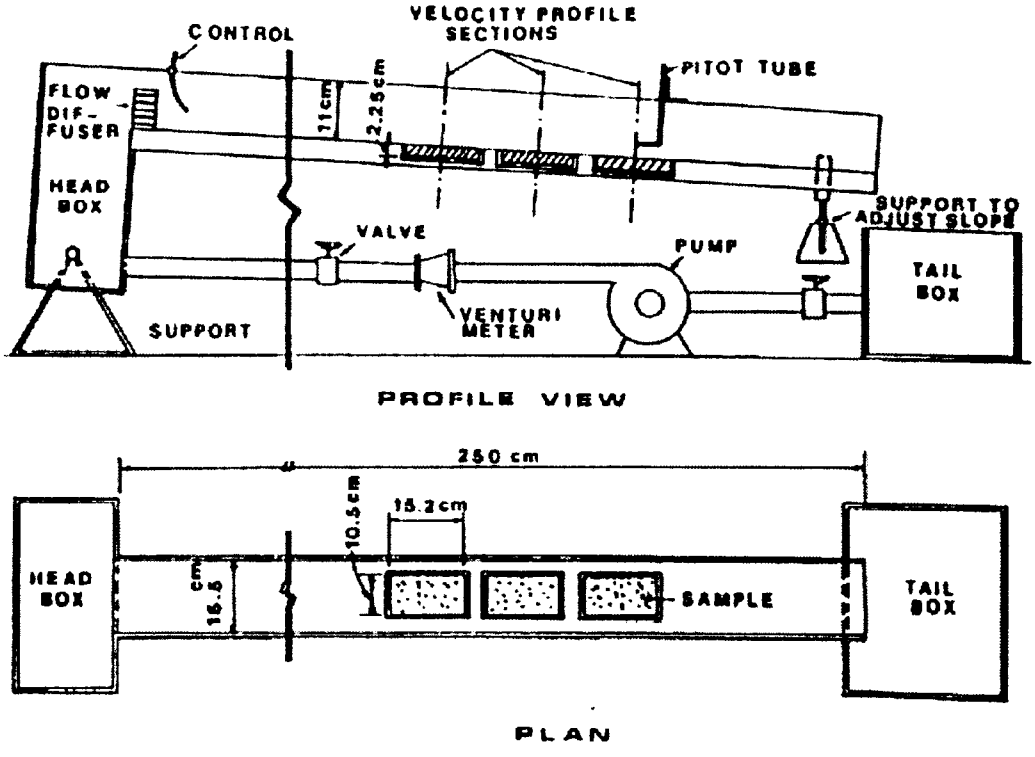

Figure 2.5: Schematic drawing of flume and sample containers (Shaikh, Ruff and Abt 1988).

Their findings were:

- weight loss progressed linearly with time (i.e. erosion rate was constant). Weight loss was defined as difference in dry weights of the samples before and after test;
- the relationship between erosion rate, $\dot{\varepsilon}$, and tractive stress, τ, was approximately linear, and the straight line passed through the origin ($\dot{\varepsilon} = C \cdot \tau$). The critical shear stress was, therefore, zero for unsaturated compacted Na-Montmorillonite soil samples;
- the coefficient of erosion rate (C) decreased as the clay percentage increased, implying that $\dot{\varepsilon}$ increased as clay content of the soil sample decreased;
- the coefficient of erosion rate (C) decreased as Vane Shear Strength increased, but this finding might not be generalised for all type of soils;
- the compaction water content had no obvious effect on $\dot{\varepsilon}$.

The Author notices that the dry density (or the degree of compaction) of the test samples was not considered by Shaikh, Ruff and Abt to be an important factor that would

influence the erosion rate and the critical tractive stress. Although the test samples were all compacted statically at 700 kPa, their dry densities would be different due to their having different water content. The compactness of the test samples was inadequately defined using only the water content.

Shaikh, Ruff, Charlie, and Abt (1988)

Shaikh, Ruff, Charlie, and Abt tested Ca-montmorillonite (non-dispersive) and Na-montmorillonite (dispersive) in a hydraulic flume (same as the one shown in Figure 2.5) to assess rate of surface erosion on unsaturated samples. Their aim was to investigate the relationship between surface erosion rate, $\dot{\varepsilon}$, and dispersibility (dispersivity).

They controlled the *SAR* of the soil samples by mixing the soils with salt solution. Soil samples of varying compaction moisture contents ($\pm 5\%$ of optimum moisture content) were tested. Soil samples were compacted by static pressing at 700 kPa. The eroding fluid was tap water (*TDS* < 2.2 meq/l, pH = 7.7, at $18 \pm 1\,^{\circ}C$). The *SAR* and *TDS* of Ca-Montmorillonite was varied by adding $CaCl_2$ (increase *TDS*) or Na_2CO_3 (increase *SAR*).

Dispersibility (dispersivity) of the test specimens was measured by four tests, namely (1) soluble salts in pore water (dispersivity depends on *TDS* and percentage sodium (i.e. (*Na*/*TDS*)), (2) the SCS Laboratory Dispersion Test (double hydrometer test), (3) the Crumb test (Emerson Class Test), and (4) the Pinhole test. Na-Montmorillonite was classified as dispersive by Tests 1 and 3. Ca-Montmorillonite was classified as non-dispersive by all 4 tests.

Their findings from tests on Na-Montmorillonite were:

- weight loss per unit area increased linearly with time, and the slope of the straight line represented the rate of surface erosion;
- the erosion rate was found to vary linearly with tractive stress, and the straight line passed through the origin. Erosion rate coefficient, *C*, was defined as erosion rate (N/m^2/min.) over tractive stress (N/m^2);
- the rate of surface erosion was independent of compaction water content.

Their findings from tests on Ca-Montmorillonite were:

- the results were similar to those for Na-montmorillonite, but more scattered at high erosion rates;
- The erosion rate coefficient, C, was high (11.8 per min.) for Ca-Montmorillonite (or treated with $CaCl_2$), but low (0.064 per min.) for Na-Montmorillonite. Treatment of Ca-Montmorillonite with $CaCl_2$ had no appreciable influence on erosion rate of Ca-Montmorillonite.

Shaikh et al conclude that:

- pore-water chemistry was the controlling factor of erosion behaviour of montmorillonite clays;
- pore-water chemistry was characterised by *TDS* (meq/l), and *SAR* $(meq/l)^{1/2}$, the proposed relationship between the erosion rate coefficient, C, and sodium adsorption ration (*SAR*) was

$$C = 4.41\,(SAR)^{-1.34}$$

- slaking had greater influence on surface erosion of an unsaturated soil than dispersivity (i.e. colloidal dispersion of saturated samples) did. Ca-Montmorillonite slaked, but Na-Montmorillonite did not slake;
- non-dispersive samples showed a much higher surface erosion rate than samples classified as dispersive. This suggested that dispersive clays were not always highly erodible soils, and non-dispersive clays could be highly erodible.

Gray (1989) commented that the rate of erosion would depend on the type of tests. Flume test would result in higher erosion rate than Pinhole test because in the former test, particles would be discharged into a relatively large volume of water, whereas particles in the Pinhole test would be discharge into a relatively small, constricted volume of fluid. He pointed out that the time allowed to equilibrate in the flume before starting the pump might affect the results. It was because Na-Montmorillonite, initially having much higher negative pore pressure and lower hydraulic conductivity, might take longer equilibration time in water. He also commented that, in general, highly dispersive soils were also highly erodible, but whether or not there was observable

erosion would depend on pore water chemistry and the nature of the flow regime. He suggested to do further erosion test on other soils such as Na-illite.

Shrestha and Arulanandan (1989) commented that the four tests on dispersivity did not take into account some of the factors that influence erodibility. For instance, the soluble salts test did not consider soil structure, cementation and mineralogy. They suggested that the faster erosion rate in Ca-Montomorillonite than in Na- Montomorillonite was because the former, having a *SAR* of 0.4 $(meq/l)^{1/2}$ (c.f. *SAR* = 19.8 $(meq/l)^{1/2}$), was in a relatively flocculated state, and slake faster than the latter.

The Author is of the view that there was inadequate control over the density of the test specimens. Although all the test specimens were compacted statically under the same pressure of 700 kPa, differences in the moulding water content and the ion contents of the moulding water would result in test specimens having different densities.

Ghebreiyessus, Gantzer, Alberts and Lentz (1994)

Ghebreiyessus et al. investigated the differences in erodibility for Mexico silt loam soil (fine, montmorillonite, mesic Udolloc Ochraqualf) packed at 2 different bulk densities. Regression equations were proposed for predicting detachment rate, as mass per unit area per unit time, by hydraulic shear stress, bulk density and Vane Shear Strength.

The Author is of the view that the degree of compactness and the moisture condition of a test sample are not adequately defined by the bulk density alone. In addition, the relationship between detachment rate, shear stress and bulk density obtained by multiple regression might not be generalised to describe the erosion characteristics of other types of soils. The Author also notices that the proposed linear relationship between the amount of soil detachment and the duration of erosion for each test specimen was only based on limited information provided by the results of 3 tests.

Briaud, Ting, Chen, Gudavalli, Perugu and Wei (1999), Briaud, Ting, Chen, Cao, Han and Kwak (2001a), Briaud, Chen, Kwak, Han and Ting (2001b), and Briaud, Chen, Li, Nurtjahyo and Wang (2003)

Briaud and his coworkers developed a method called SRICOS to predict the scour depth in cohesive soils around cylindrical bridge piers in rivers. SRICOS stands for scour rate in cohesive soils. The method uses the Erosion Function Apparatus (EFA) invented by Briaud et al. (1999) to study the relationship between scour rate and the hydraulic shear stress for soil samples taken from around bridge piers.

Application of the SRICOS method consists of the following steps:

- use the EFA to obtain the relationship between scour rate, $\dot{z}$ and shear stress, τ, for a soil sample taken from the bottom of a bridge pier;
- predict the maximum shear stress, τ_{max} at the bottom of the bridge piers;
- based on the laboratory EFA results, predict the initial scour rate, $\dot{z}$, based on the estimated τ_{max};
- estimate the maximum scour, z_{max};
- predict the scour z versus time, t;
- estimate the scour z from the z versus t curve for a flood of a given duration and magnitude.

Figure 2.6 illustrates the problem of scour around bridge pier investigated by Briaud et al. (1999, 2001a, 2001b and 2003), and Figure 2.7 shows a schematic diagram of the Erosion Function Apparatus (EFA) (Briaud et al. 1999).

Figure 2.6: Scour hole next to a cylindrical pier in clay during a flume test (http://tti.tamu.edu/geotech/scour/).

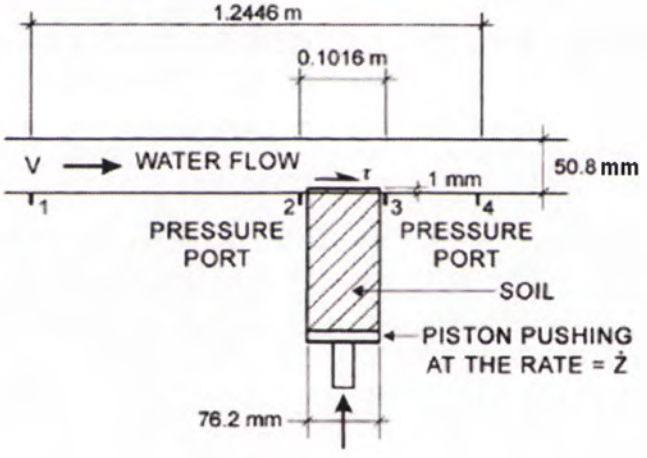

Figure 2.7: EFA Conceptual Diagram (Briaud et al. 2001a).

The EFA is basically a flume test apparatus. A 76 mm-diameter soil sample in a Shelby tube is fitted through a tight opening at the bottom of a flume which has a rectangular cross-section (width 101.6 mm, depth 50.8 mm, and length 1.22 m). Water is pumped through the flume and erodes the soil sample which protrudes 1 mm above the channel flow. Erosion of the soil sample is observed through the observation chamber of the flume. The rate at which the sample erodes is measured as scour depth per unit time (mm/hr.). The velocity of the flow is measured, and the hydraulic shear stress is assessed from the Moody Diagram based on the measured flow velocity. Figure 2.8 shows photographs of the EFA.

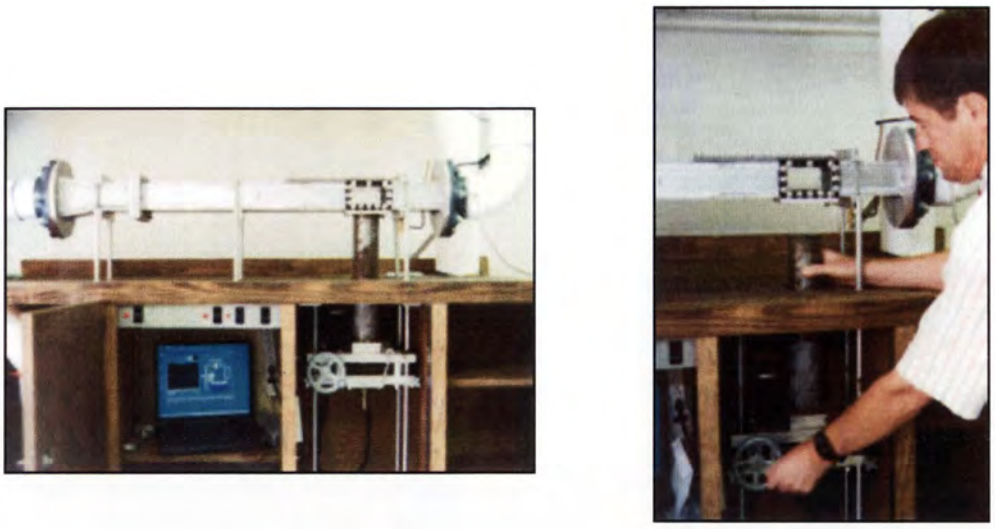

(a) (b)

Figure 2.8: Photographs of the Erosion Function Apparatus (Briaud et al. 2003). (a) General view; (b) Close up of the test section

Plot of erosion rate versus shear stress obtained from the test indicates the critical shear stress at which erosion starts, and the rate of erosion beyond the critical shear stress. Some of the major assumptions made by Briaud et al. (1999) in the tests using the EFA are as follows:

- the shear stress, τ, applied by the water to the soil at the soil/water interface is the major parameter causing erosion in a scour test using the EFA;
- the concept of the critical shear stress which represents the stress below which soil particles are not eroded is theoretically incorrect, but practically useful. The critical shear stress, τ_c, is defined as one corresponding to a standardised small erosion rate of 1mm/hr. in a scour test using the EFA;
- The hydraulic shear stress is estimated from the flow velocity, V, based on the Moody Diagram:

$$\tau = \frac{1}{8} f \rho_w V^2$$

where f is the friction coefficient based on the roughness, ε/D, and the Reynolds No., R_e, and is estimated from the Moody Diagram;

ε is the depth of soil surface asperities, assumed to be 0.5 D_{50} (mm)

D is the equivalent hydraulic diameter of the rectangular flume

ρ_w is the density of water (1000 kg/m^3)

Briaud et al. (2001a, 2003) attempted to correlate the critical shear stress and the rate of scour obtained from the EFA with other soil parameters. They found that, for granular cohesionless soils, the critical shear stress is approximately equal to the mean particle size of the soil:

$$\tau_c \cong D_{50}$$

where τ_c: is the critical shear stress [N/m^2]

D_{50}: is the mean particle size (50% finer) of the soil [mm]

Figure 2.9 presents curves of critical shear stress, τ_c, versus mean soil grain diameter, D_{50} (Briaud et al. 2003). The curves show a good linearly relationship between τ_c and D_{50} for coarse-grained soils, but the test data show considerable scattering for fine-grained soils.

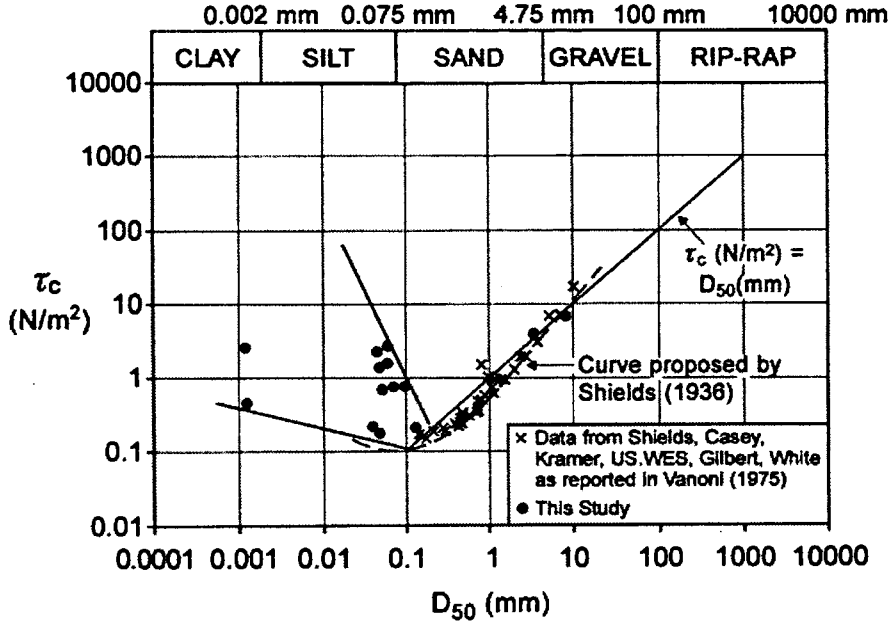

Figure 2.9: Critical Shear Stress versus Mean Grain Diameter (Briaud et al. 2003).

For fine-grained soils, the correlation analysis between τ_c and the rate of erosion, indicated by the initial slope, S_i, of the scour rate, $\dot{z}$ (mm/hr.) versus τ_c plot is

summarised in Table 2.2. Briaud et al. (2001a, 2003) also studied the correlations between τ_c and S_i, and other parameters, such as the mean grain size (D_{50}), the water content of the soil (ω), the Cation Exchange Capacity (*CEC*), the Sodium Adsorption Ratio (*SAR*), the pH value of the water, and the chemical composition of the water. The correlations between τ_c and S_i, and the individual predictor variables were poor, as indicated by the low coefficient of determination, r^2. The best r^2 was only 0.348 (11 data points) obtained between τ_c and the undrained shear strength.

Table 2.2: Correlation between critical shear stress, rate of erosion with soil and water properties (based on Briaud et al. 2001a).

Scour parameters	**Predictor variables (soil, water parameters)**		**Apparent relationship**
	Symbol	**Meaning**	
Critical shear stress, τ_c	γ	Soil unit weight	τ_c increases as the value of the predictor variable increases.
	I_p	Plasticity Index	
	%Fines	Fines content (% finer than 0.075mm)	
	S_u	Undrained strength	
	e	Void ratio	τ_c decreases as the value of the predictor variable increases.
	DR	Dispersion ratio	
	Swell	Soil swell	
	T_s	Temperature of soil	
	T_w	Temperature of water	
Initial slope of scour rate versus shear stress, S_i	τ	Applied hydraulic shear stress	S_i increases as the value of the predictor variable increases.
	T_s	Temperature of soil	
	T_w	Temperature of water	
	%Clay	Clay content (% finer than 0.005mm)	S_i decreases as the value of the predictor variable increases.

2.2.4 Rotating cylinder tests

The use of the Rotating Cylinder Tests has been described in the following literature:

- Moore and Masch (1962)
- Arulanandan, Sargunam, Loganathan and Krone (1973)
- Kandiah and Arulanandan (1974)
- Arulanandan, Loganathan and Krone (1975)
- Sargunan (1977)
- Arulanandan and Perry (1983)
- Chapuis and Gatien (1986)
- Chapuis (1986a)
- Chapuis (1986b)

Moore and Masch (1962), Masch, Espey and Moore (1965)

Moore and Masch explored the use of the rotating cylinder test and the submerged jet test for measuring erosion resistance of cohesive soils. The original rotating cylinder test apparatus was developed by Masch, Espey and Moore (1965). Their work on the submerged jet test will be described in Section 2.2.5.

Moore and Masch tried the rotating cylinder test as they were of the view that other tests, such as the submerged jet test and the flume test, could not allow accurate determination of the shear stress because:

- the variation of the temporal shear stress over the erosion surface of the soil sample would be difficult to determine under turbulent flow conditions. Usually shear stresses would be averaged over time and space, but it was the peak values of the instantaneous shear stresses that were responsible for removal of soil particles from the sample;
- the surface roughness of the sample would change as soon as erosion of the sample began.

The rotating cylinder test, based on the principal of certain type of viscosimeters, was used to measure shear stress induced by an eroding fluid on the surface of a cylindrical soil sample. In a rotating cylinder test, the shear stress would be uniform at all points around the surface of the cylindrical soil sample. The rotating speed of the cylinder was gradually increased until erosion was observed. The torque on the soil sample was

recorded and used to compute the shear stress on the cylindrical surface of the soil sample.

Trial tests were carried out on soil samples with 60% clay (montmorillonite) and 40% sand, compacted in layers in a 3" (76 mm) diameter mould. Typical values of critical shear stress were between 0.2 – 0.3 lb/ft^2 (9.6 – 14.4 Pa).

Moore and Masch proposed future investigations on the use of the rotating cylinder tests for measuring the rate of erosion as well as the critical shear stress, and for investigating the influence of some soil parameters, such as moisture content, density and cohesive properties.

Arulanandan, Sargunam, Loganathan and Krone (1973), and Arulanandan, Loganathan and Krone (1975)

Arulanandan et al. used a modified rotating cylinder test apparatus, as shown in Figure 2.10, to investigate the influence of clay mineralogy and amount, and the composition of pore and eroding fluid on the erodibility of remoulded saturated soils. The original rotating cylinder test apparatus was developed by Masch, Espey and Moore (1965).

Arulanandan et al. summarised laboratory data on the influence of pore and eroding fluid composition on erodibility, and provided new data showing the influence of the type and amount of clay minerals on erodibility.

In their modified rotating cylinder apparatus, the outer cylinder containing the eroding fluid (distilled water) was rotated at constant speed, and the shear stress on the surface of the soil sample was calculated from the torsional displacement (measured torque) of the inner cylinder containing the soil sample. Erosion was determined from the difference in weight in the soil sample before and after the test, for various periods of erosion. Critical shear stress, τ_c, was defined as the shear stress required for zero erosion rate.

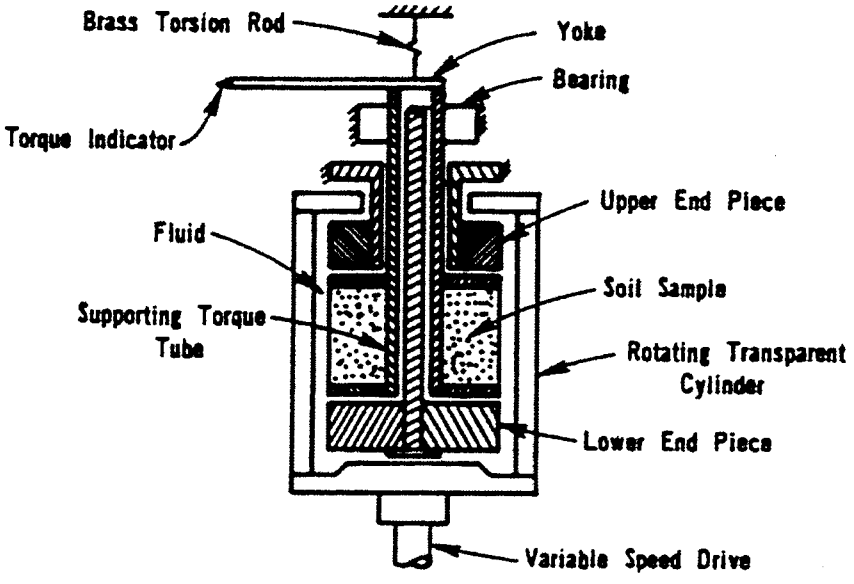

Figure 2.10: Cross-sectional View of Rotating Cylinder Test Apparatus. (Arulanandan, Loganathan and Krone 1975)

They tested Yolo loam which had the following properties:

- cohesive soil composed of 46% sand, 35% silt and 19% clay
- the clay were montmorillonite, kaolinite, mica and vermiculite
- Cation Exchange Capacity, CEC = 19.8 meq/100g
- pH = 8.2
- LL = 46% and PL = 23%.

The controlled parameters in the tests were (1) the type and amount of clay minerals; (2) the pore fluid composition; and (3) the eroding fluid composition. The type and amount of clay minerals were quantified by the parameter called Dielectric Dispersion ($\Delta\varepsilon_o$). According to Arulanandan et al., $\Delta\varepsilon_o$ depended on frequency, soil type and amount, and the moisture content. $\Delta\varepsilon_o$ varied across different clay mineralogy and amount, but did not vary much with moisture content at constant clay composition. $\Delta\varepsilon_o$ was a measure of the average compositional and environmental property of clay-water-electrolyte system. Arulanandan et al. indicated that the Plasticity Index or the Activity or both could not provide similar evaluation of the soil composition as $\Delta\varepsilon_o$. Salt concentration in the fluid composition was measured by electrical conductivity. Types

of ions were indicated by Sodium Adsorption Ratio, *SAR*, based on analysis by an Atomic Absorption Spectrometer. The salt (NaCl) concentration in the eroding fluid was measured by electrical conductivity.

The findings of Arulanandan et al. were:

- erosion increased linearly with time. The slope of the straight-line plot gave the erosion rate, $\dot{\varepsilon}$;
- $\dot{\varepsilon}$ increased linearly with shear stress, τ, and the straight-line plot was defined by $\dot{\varepsilon} = m(\tau - \tau_c)$;
- m, representing slope of the straight line, increased with *SAR* (i.e. $\dot{\varepsilon}$ increased with increase in *SAR*);
- τ_c, the x-intercept called the critical shear stress, decreased non-linearly with increase in *SAR*;
- τ_c decreased as salt concentration (electrical conductivity) of pore fluid increased, at given *SAR*;
- τ_c decreased non-linearly with increase in *SAR* at a given salt concentration. Arulanandan et al. suggested that as *SAR* increased, or salt concentration in pore fluid decreased, degree of flocculation decreased, and the interparticle bonds become weakened, and hence the soil became more erodible;
- τ_c increased, and m decreased as salt concentration in the eroding fluid increased, given that *SAR*, salt concentration in pore fluid and moisture content remained constant. Arulanandan et al. suggested that it was because erosion was dependent on the osmotic pressure gradient between the pore fluid and the eroding fluid;
- τ_c decreased non-linearly as $\Delta\varepsilon_o$ decreased. (i.e. τ_c decreased in the order of montmorillonitic ($\Delta\varepsilon_o = 40$), illitic ($\Delta\varepsilon_o = 32$) and kaolinitic ($\Delta\varepsilon_o = 24$) clays), given that *SAR*, clay content, salt content in pore fluid and moisture content remained constant. Highly swelling montmorillonitic clay had a higher τ_c;
- τ_c decreased non-linearly with increase in *SAR* for the same clay mineralogy.

Arulanandan, Loganathan and Krone (1975) used the same rotating cylinder apparatus to investigate the influence of pore fluid composition and salt concentration of the

eroding fluid on the erodibility of remoulded saturated soils. They altered the degree of flocculation of a clayey soil by the following methods:

- adding salt to increase the electrolyte concentration so as to decrease permeability by causing swelling and dispersion.
- changing cations to one of a higher valence (e.g. replace Na^+ by Ca^{2+}. Na-clay has a large hydrated radius than Ca or Mg-clay, and Na-clay is more dispersive).

Tests were carried out on Yolo loam which was conditioned to have varying pore fluid compositions by mixing with solutions of varying *SAR* and salt concentrations. Effluents collected from the consolidating soil samples were taken for analysis of cation contents (by Perkin-Elmer Atomic Absorption Spectrometer), and salt concentration (by measuring electrical conductivity). Consolidated soil samples were also analysed for moisture content.

The findings by Arulanandan. Loganathan and Krone (1975) were:

- at a given salt concentration and moisture content, the $\dot{\varepsilon}$ increased linearly with τ, and the straight-line plot could be represented by $\dot{\varepsilon} = m(\tau - \tau_c)$. m, the slope of the straight line, increased with *SAR*. τ_c, the x-intercept called the critical shear stress, decreased non-linearly with increase in *SAR*. At low *SAR*, τ_c decreased more rapidly for a small increase in *SAR*;
- at a given *SAR*, τ_c increased with salt concentration (as high salt concentration implied flocculation). Effects of salt concentration were more pronounced at low values of *SAR*. Uptake of water (swell) with time by a soil sample was higher if *SAR* was higher (i.e. higher *SAR* implies higher dispersion, higher swell, and smaller interparticle bonding force). τ_c increased, and m decreased as salt concentration in eroding fluid increased (given same *SAR*, same salt concentration in pore fluid and same moisture content). The explanation by Arulanandan, Loganathan and Krone was that water would move into the surface of clay particles by osmosis causing swelling, and weakening of interparticle bonds if the salt concentration in the eroding fluid was lower than that in the pore fluid.

The Author notices that the rotating cylinder apparatus used by Arulanandan et al. was used to test remoulded saturated soil samples. The dry densities of the various soil samples prepared by the static consolidation procedure might be different. The Author considers that the dry density of a soil might be an important controlling parameter, but Arulanandan et al. did not consider dry density as a controlling parameter.

Kandiah and Arulanandan (1974)

Kandiah and Arulanandan carried out erosion tests on Yolo loam clay (saturated or unsaturated) using both the flume test and the rotating cylinder test. Only saturated samples could be tested by their rotating cylinder apparatus. A brief summary of their works and findings has already been presented in Section 2.2.3 on flume tests.

Sargunan (1977)

Sargunan used the rotating cylinder test to examine the erosion behaviour of consolidated cohesive soils. He attempted to define a boundary between the flocculated and deflocculated states. The controlling parameters in the erosion tests were clay mineralogy, cation ratio, and total salt concentration for the soil samples studied.

Soil samples tested were formed by blending 80% silt (taken from Yolo loam) and 20% clay (kaolinite or illite). The samples were conditioned by solutions of NaCl, $CaCl_2$ and $MgCl_2$ to produce specimens of a range of salt concentrations and *SAR*s. The soil specimens were consolidated from slurries and the saturation extracts were analysed for electrical conductivity and cation ratio.

Sargunan's findings were:

- the erosion rate varied linearly with shear stress;
- τ_c decreased non-linearly with increase in *SAR* (i.e. achieved by replacement of Ca or Mg or both by Na),
- at a given *SAR*, τ_c increased with salt concentration;
- unconfined compression tests on specimens showed that, at low *SAR*, Ca or Mg-saturated specimens showed higher shear strengths at relatively lower shear strains, suggesting an initially flocculated structure, whereas at high *SAR*, Na-

saturated specimens showed lower shear strengths mobilised at relatively higher shear strains, suggesting an initially dispersed structure.

From the test results, Sargunan suggested that the high τ_c, lower erosion rate, lower strain required to develop peak shear strength associated with Ca-saturated specimens indicated stronger particle bonds, and less hydration in these specimens, whereas the low τ_c, higher erosion rate, higher shear strain mobilised to produce peak shear strength shown by Na-saturated specimen indicated a system that was readily or spontaneously dispersible.

Sargunan extrapolated the τ_c versus *SAR* curves to obtain *SAR* values corresponding to $\tau_c = 0$, and called these *SAR* values the *Threshold SAR*s. He suggested that zero τ_c represented a state of soil condition at which the system would be sufficiently deflocculated, or dispersed (i.e. a condition of metastable equilibrium) where failure conditions would be imminent at the surface. He noticed that the *Threshold SAR*s were apparently dependent on total cation concentration (in meg/l). He proposed that, for each type of soil, a curve could be produced by plotting *Threshold SAR* against total cation concentration. Region below the curve represented a zone of flocculated condition, whereas region above the curve represented a zone of complete dispersion. Sargunan's plot of *SAR* against total cation concentration is shown in Figure 2.11.

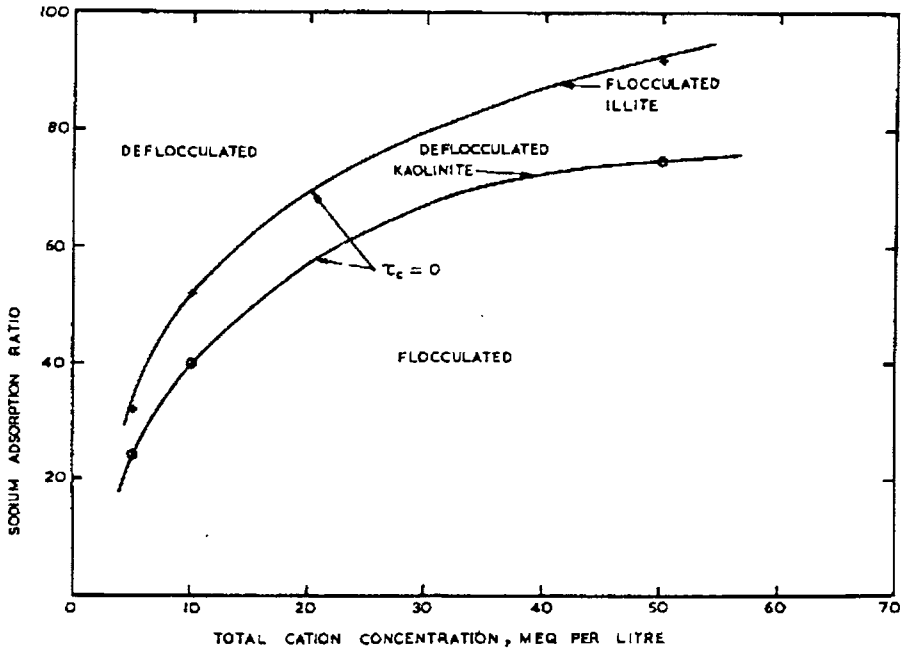

Figure 2.11: Sodium Adsorption Ratio versus Total Cation Concentration - Boundary between flocculated and deflocculated states (Sargunan 1977).

Arulanandan and Perry (1983)

Arulanandan and Perry used the flume test and the rotating cylinder test to find out the critical shear stress, τ_c, and the erosion rate of a soil. Their findings and conclusions have been discussed in Section 2.2.3. They tested both remoulded saturated and unsaturated soil samples by the flume test, but only saturated remoulded samples could be tested by their rotating cylinder apparatus.

Chapuis and Gatien (1986), Chapuis (1986a and 1986b)

Chapuis and Gatien (1986) described the study of the erosion resistance of solid clays using improved rotating cylinder techniques. They tested intact or remoulded samples taken from three Quebec clays. The improved apparatus, unlike old designs, was capable of testing intact soil samples. Chapuis (1986a) described the modified rotating device. Results of their tests were presented by Chapuis (1986b). The improved rotating cylinder test apparatus used by Chapuis and Gatien is shown in Figure 2.12.

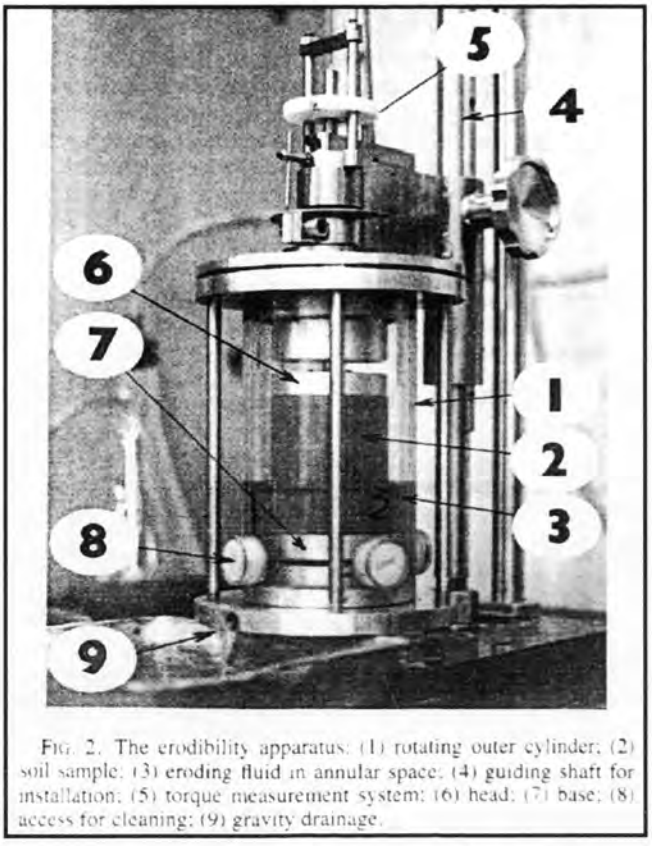

FIG. 2. The erodibility apparatus: (1) rotating outer cylinder; (2) soil sample; (3) eroding fluid in annular space; (4) guiding shaft for installation; (5) torque measurement system; (6) head; (7) base; (8) access for cleaning; (9) gravity drainage.

Figure 2.12: Improved Rotating Cylinder Test Apparatus (Chapuis and Gatien 1986).

According to Chapuis and Gatien (1986), the improved rotating cylinder device could simulate various physical and mechanical environmental conditions, such as:

- both intact or remoulded samples could be tested;
- the water quality of eroding fluid could be controlled;
- the boundary shear stress applied to the clay surface could be directly and accurately measured;
- the dry weight of the eroded soil per unit time and surface could be directly measured;
- the influence of water quality (pH, pollutants, etc.) could be quantitatively determined.

Chapuis (1986a) and Chapuis and Gatien (1986) summarised some of the most popularly used external erosion test methods, and comment on the drawbacks of the

submerged water jets, the open flume tests and the channel tests. They commented that tests carried out by others using older rotating cylinder apparatus were inadequate in the following aspects:

- the old rotating cylinder devices could only test remoulded and reconsolidated samples. Undisturbed natural soils could not been tested;
- previous rotating cylinder tests did not measure shear stress accurately as friction in the device was not accounted for;
- previous rotating cylinder tests did not measure erosion rate accurately, as erosion was determined by measuring the change in weight of the wet soil sample. Measurement was inaccurate and the sample was disturbed after repetitive manipulations. Negative erosion rates were often measured at low shear stress.

According to Chapuis (1986a), his modified rotating cylinder device had the following advantages over rotating devices used by others:

- the device did not have a central shaft through the soil sample. The soil sample was mounted between two metallic short cylinders (base and head plates) so that intact samples could be tested;
- torque was accurately measured directly by a pulley-weight system;
- erosion was measured accurately by draining away the eroding fluid from the outer cylinder, evaporating the fluid inside an oven, and measuring the weight of the oven-dried residue (i.e. the eroded material). The soil sample did not have to be taken out of the device.

Chapuis and Gatien (1986) tested 3 natural clays from northern Quebec on the improved rotating cylinder device. The 3 clays had the following properties:

Table 2.3: Properties of tested natural samples : mean values (m) and standard deviations (σ) (Chapuis 1986b).

Property		Natural clay No. 1	2	3
Water content W (%)	m	25.4	53.0	18.0
	σ	1.0	3.0	1.3
Liquid limit W_L (%)	m	26.6	44.4	28.0
	σ	1.2	0.7	1.7
Plastic limit W_P (%)	m	15.4	22.2	17.6
	σ	0.5	0.7	1.0
Plasticity index I_P (%)	m	11.2	22.2	10.4
	σ	1.4	0.7	1.0
Clay content (2 μm)	m	36.7	65.6	24.3
	s	1.1	1.3	3.7
Silt content (74 μm)	m	48.7	27.6	56.4
	σ	1.5	2.1	4.0
Sand content	m	12.0	6.8	13.6
	σ	0.7	1.2	2.5
Gravel content	m	2.6	0.0	5.7
	σ	0.9	0.0	2.9
Preconsolidation (kPa)		165–210	140	180–195

Chapuis (1986a, b) presented complete curves of τ versus $\dot{\varepsilon}$ including, $\dot{\varepsilon}$ values for shear stresses smaller or greater than the critical shear stress. He compared his results with τ_c and $\dot{\varepsilon}$ obtained by others. He noticed the wide variations in the results by others. He attributed the wide variations to widely varying types of equipment; arbitrary criteria for failure conditions (i.e. τ_c), inadequate control over the geotechnical properties of soil samples, and failure to consider the influence of some important physiochemical parameters.

The findings of Chapuis (1986a, b) were:

- the method of sample preparation influenced the results probably due to surface disturbance. Samples prepared by consolidation in a triaxial cell had a smoother and less erodible surface than samples cut from the same clay. τ_c was higher for the triaxially prepared samples, and $\dot{\varepsilon}$ at given τ (where $\tau < \tau_c$) was higher for cut samples. τ on surface depended on surface roughness which varied throughout the test;

- for remoulded samples, τ_c increased as consolidation pressure increased; and $\dot{\varepsilon}$ at τ lower than τ_c decreased when consolidation pressure increased;
- complete graphs of $\dot{\varepsilon}$ versus τ were obtained for shear stresses smaller or greater than τ_c. The graphs were bi-linear. τ_c for the 3 clays were in the range of 4.2 – 8.0 Pa. In the bilinear graph, τ_c was indicated by the point at which there was a marked increase in the rate of erosion. The bilinear plot is shown in Figure 2.13(b);

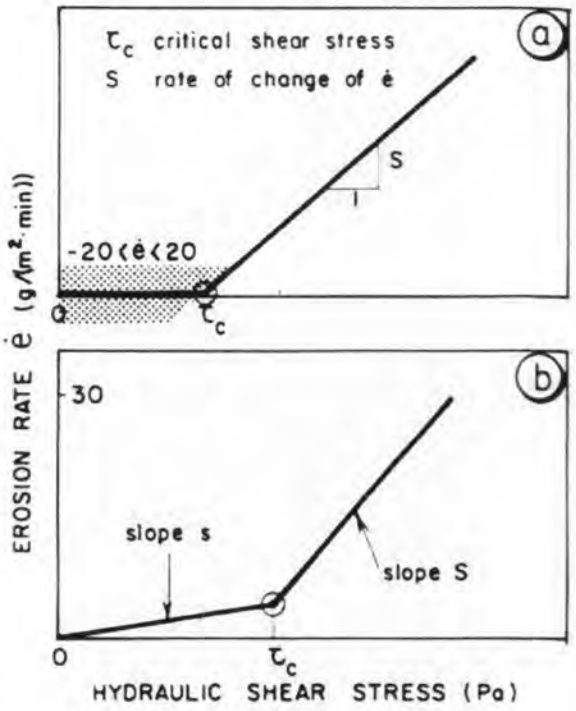

(a) former test apparatus (for testing remoulded sample only)

(b) improved apparatus (for testing intact or remoulded samples).

Figure 2.13: Erosion rate versus hydraulic shear stress (Chapuis 1986a).

- the erosion resistance of cohesive soils was found to be influenced by the electrochemical bonds between the fine particles, and these depended on soil and pore water properties and also strongly influenced by the physiochemical nature of the eroding fluid;

Chapuis (1986b) further commented that previous research works focused mainly on initiation of erosion. Laboratory tests usually lasted less than 30 minutes, but field observations showed that erosion resistance might increase with time. He also noticed

that while laboratory tests prevented secondary flows and blotted out waves, both of them were significant field factors.

The Author notices that the Critical shear stresses obtained by Chapuis' modified rotating cylinder device had a slightly different meaning to the critical shear stresses obtained by the older rotating cylinder device, or other test methods. The former corresponded to the point of a marked increase in erosion rate, whereas the latter corresponded to the intercept on the shear stress axis by extrapolating the straight-line plot of erosion rate versus shear stress.

2.2.5 Jet erosion tests

Use of the Jet Erosion Tests has been described in the following literature:

- Dunn (1959)
- Moore and Masch (1962)
- Hanson (1991)
- Hanson (1992)
- Hanson and Robinson (1993)
- ASTM D5852-95

Dunn (1959)

Dunn (1959) proposed the use of the Jet Erosion Test to measure the "tractive resistance" of cohesive channel beds. Dunn's jet test apparatus directed a submerged vertical jet of water perpendicular at the soil surface. The head of the water jet was gradually raised until continuous erosion was noticed in the soil sample. The maximum shear stress and the beginning point of erosion were found to occur at a small distance from the centre of the soil sample at where the perpendicular jet of water was directed. In addition, the position of the maximum shear stress and the beginning point of erosion were found to remain unchanged when the head or the elevation of the nozzle above the soil was altered. The shear stress was measured by replacing the soil surface with a steel plate which was coated with soil grains and which contained a one inch square shear plate in the position of the maximum shear stress for measuring the shear stress.

Dunn plotted the measured maximum shear stresses at the initiation of erosion against the measured vane shear strengths of the soil samples. His findings were:

- the shear stress at the initiation of erosion was linearly proportional to the vane shear strength (i.e. the undrained strength);
- the slope of straight line plots between the maximum shear stress and the vane shear strength was apparently related to the silt and clay fraction (< 0.06 mm) of the soil;
- the slope of straight line plots between the maximum shear stress and the vane shear strength was apparently also related to the plastic index of the soil, or the Dos Santos' statistics '*t*' which related a soil's Liquid Limit and Plastic Index to its particle size distribution;
- the slope of straight line plots between the maximum shear stress and the vane shear strength was apparently also related to the statistics which described the mean size (M_ϕ), standard deviation (σ_ϕ) and the skew (k_ϕ) of the particle size distribution of the soil.

Moore and Masch (1962)

Moore and Masch explored the use of submerged jet tests and the rotating cylinder tests to measure the erosion resistance of cohesive soils. Their tests using a rotating cylinder device have been described in Section 2.2.4.

The main procedures of the submerged jet test carried out by Moore and Masch at the University of Texas were as follows:

- impinging a submerged vertical jet on the horizontal surface of a sediment sample (5" (127 mm) diameter and 4" (102 mm) deep),
- scour at constant jet velocity for at least 60 minutes,
- measure weight loss every 10 minutes,
- calculate mean depth of scour ($\bar{s}$),
- increase jet velocity and repeat the procedure.

Moore and Masch found that the depth of scour, s was a function of a number of variables, viz.

- elevation of the jet above the sample, h,
- diameter of the jet, d,
- jet velocity, V,
- time, t,
- mass density of the eroding fluid, ρ,
- dynamic viscosity of the eroding fluid, μ,
- scour resistance property of the soil lumped into a single parameter, σ_s (assumed to be constant throughout the test).

Moore and Masch found that:

- $\bar{s}/h$ increased linearly with $(t\mu)/\rho d^2$ for different jet velocities. Slope of the straight-line plot was called the Scour Rate Index, K_s;
- for each sediment, K_s varies approximately linearly with the Reynolds no., N_R, and $N_R = Vd\rho/\mu$. Slope of the straight-line plot was m, and the Reynolds no. at the point of incipient scour was N_{R_o} (x-intercept);
- tests by varying the nozzle height showed that, for any N_R, maximum K_s (i.e. max. amount of scour) occurred at $h/d \approx 8.0$;
- more scour resistant sediments would normally have lower m and higher N_{R_o}, but some samples with high N_{R_o} eroded rapidly once initial scour took place.

Moore and Masch commented that the test was only a scour test to measure relative scour resistance, and was not a test to measure shear stress (tractive stress) at the soil surface.

Martin (1962) commented that the accuracy in the estimation of dynamic viscosity and the Reynolds no. was doubtful as the kinematic viscosity of water would change by an order of magnitude when a small amount of clay was present, or if the pH was slightly altered. He suggested that the nature of the clay and pore fluid would have significant

influence on the critical shear stress. He also proposed to measure scour depth, s directly rather than estimating the mean scour depth, $\bar{s}$, indirectly from volume of soil removed.

Hanson (1991, 1992), ASTM D5852-95

Hanson described the use of the site-specific submerged jet testing device to carry out scour studies of non-cohesive and cohesive soils. His tests resulted in the use of a Jet Index to express erosion resistance. The test apparatus used by Hanson is shown in Figure 2.14.

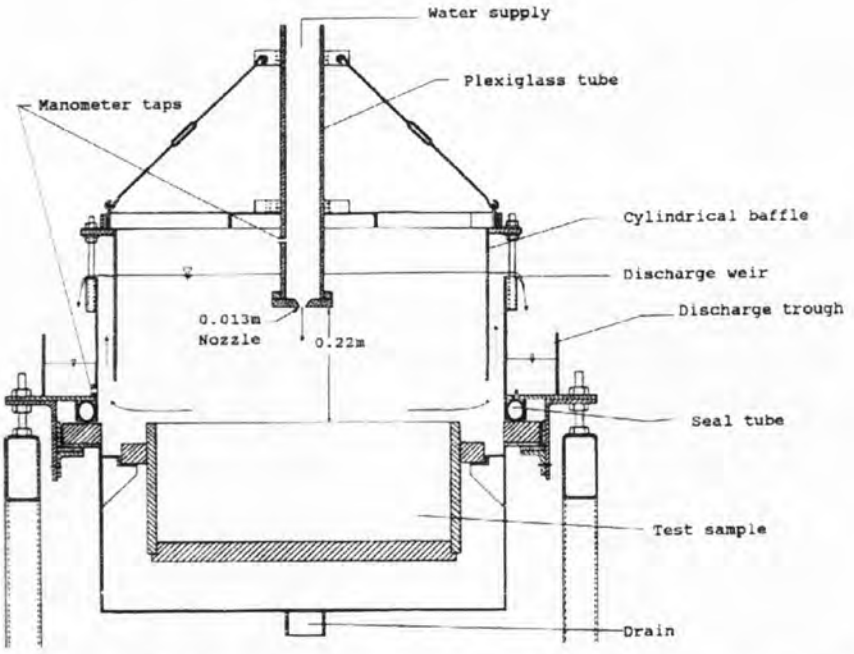

Figure 2.14: Schematic of Jet Index Test Apparatus (Hanson 1992).

In the submerged jet device:

nozzle diameter, d = 13 mm

jet height, h = 0.22 m

jet velocity, U_o = 166 – 731 cm/s

Hanson found that the peak stress, τ_{om} [Pa] along the soil boundary in his submerged jet device was solely a function of the jet velocity U_o [cm/s] at the nozzle:

$$\tau_{om} = 0.0014\, U_o^{1.5}$$

In the jet erosion tests, Hanson measured the maximum depth of scour, D_s at predetermined time intervals during the test duration of 4 hours. The test was repeated for various jet velocities.

Hanson tested four soils whose following properties are shown in Table 2.4.

Table 2.4: Summary of physical properties of soil samples (Hanson 1991).

Physical properties	Soil A	Soil B	Soil C	Soil D
Liquid limit	21	37	26	–
Plastic limit	17	19	20	NP
Plasticity index	4	18	6	0
% Sand > 0.05 mm	57	37	48	67
% Silt > 0.002 mm	27	36	33	26
% Clay < 0.002 mm	16	27	19	7
U.S.C.	CL-ML	CL	CL-ML	SM
A.S.C.	sandy loam	clay loam	loam	sandy loam

The findings of Hanson (1991, 1992) were:

- D_s increased with time, t. At a given time t, higher jet velocity U_o would result in higher D_s;
- log-log plot of D_s/t (average scour over time) against t for a particular soil gave parallel sets of straight lines with negative slopes. Each straight-line plot corresponded to a particular U_o. The higher the U_o, the higher the intercept at the time axis;
- combining the variables D_s, t and U_o into one equation gave:

$$\frac{D_s}{t} = J_i U_o \left(\frac{t}{t_1}\right)^{-0.931}$$

where J_i : a dimensionless coefficient called the *Jet Index*,

t_1 : time equal 1 s.

- plotting D_s/t against $U_o(t/t_1)^{-0.931}$ for all scour durations and jet velocities, and performing linear regression gave a straight line with slope equal to J_i. Data scatter was noticed at low jet velocities. It was speculated that those scattered data points corresponded to regions in which critical stress was significant. J_i were found for each of the 4 soils tested;
- erodibility coefficient, k (cm^3/Ns) had been determined in open channel tests by Hanson for the 4 soils. In open channel erosion tests, rate of erosion was usually related to shear stress by

$$\dot{\varepsilon} = k\left(\tau_e - \tau_c\right)$$

where $\dot{\varepsilon}$: rate of erosion (volume/unit area/unit time)

k : erodibility coefficient

τ_e : effective shear stress

τ_c : critical tractive stress

The plotting of log(k) versus log(J_i) produced a straight line represented by the equation:

$$k = 0.003e^{385J_i}$$

- the above equation implied that a higher J_i means higher k, and less resistant to erosion;
- the *Jet Index* (J_i) might be used for expressing erosion resistance.

Hanson and Robinson (1993)

Hanson and Robinson carried out laboratory submerged jet tests to derive the Jet Index, for comparing changes in the erosion resistance of a soil at different compaction dry densities and compaction moisture contents. Results were compared with large-scale open channel tests on the same soils.

The soil tested had the following properties:

- LL = 23%, PL = 12 – 16%, PI = 7 – 12%
- USCS classification : CL, CL-ML
- 34% sand, 39% silt, 27% clay
- 44% Dispersion (dispersivity confirmed by Pinhole test and Crumb test)
- maximum dry density = 1.92 g/cm^3
- optimum moisture content = 12.5%

Compaction of soil was carried out by either dynamic method (79.4 kg hammer fell over 0.3 m, and controlling number of blows) or static method (by 300 Pa applied pressure). The soil was compacted in 0.44 m diameter by 0.18 m high moulds at various moisture contents and dry density. Samples were wetted for 20 hours prior to jet testing. 29 soil samples were tested. 9 out of the 29 samples were prepared by dynamic compaction method.

Results of the tests by Hanson and Robinson showed that:

- at a given compaction moisture content, an increase of dry density (ρ_d) would result in an increase in erosion resistance (i.e. J_i decreased;.
- at the same dry density, higher compaction moisture content would result in an increase in erosion resistance (i.e. J_i decreased), but for saturated samples, higher compaction moisture content would cause a decrease in erosion resistance (i.e. higher J_i). This was consistent with the phenomenon that there would usually be an optimum moisture content slightly less than saturation;
- soils compacted at similar densities and moisture contents showed little difference in performance whether they were dynamically or statically compacted;
- results of Jet Index tests were consistent with the results of open channel tests carried out on the same soils in 1988 and 1989 (i.e. soils compacted to lower dry densities experienced more severe gully head cut than soils compacted to higher dry densities under the same constant flow rate.

It is important to recognise that this "head cut" mechanism, where after initial surface erosion on an open channel, a vertical face forms, which gradually deepens and

progresses upstream. The flow of water over the vertical cut is what is being simulated in the Jet Erosion Test.

2.2.6 Tests measuring the dispersivity of a soil

The three most popular tests for estimating the dispersivity of a soil are the Emerson Class Test (Emerson 1967, AS1289.3.8.1 1997) which is also known as the Crumb Test, the Pinhole Erosion Test (Sherard et al. 1976, AS1289.3.8.3 1997), and the Soil Conservation Service Laboratory Dispersion Test (Sherard et al. 1972, 1976, Decker and Dunnigan 1977, AS1289.3.8.2 1997). Atkinson, Charles and Mhach (1990) proposed a modified form of Crumb Test called the Cylinder Dispersion Test. Details of these tests are described in the following sections.

Emerson Class Test (Emerson 1967, Sherard, Dunnigan and Decker 1976, AS1289.3.8.1 - 1997)

Emerson classified soil aggregates of soil particles into 8 classes. 7 out of the 8 classes could be distinguished by observing the coherence of the clay fraction after reacting aggregates with water. Three types of reactions were observed, namely

- reaction by immersion of dry aggregates in water;
- reaction by immersion of wet remoulded aggregates in water; and
- suspension of aggregates in water.

The remaining class was used to describe the presence of carbonates or gypsums.

Emerson presented the scheme for determining class numbers in the form of a decision tree as shown in Figure 2.15.

Emerson indicated that the detection of Class 1 aggregates in the field is important in the prevention of the failure of earth dams by piping.

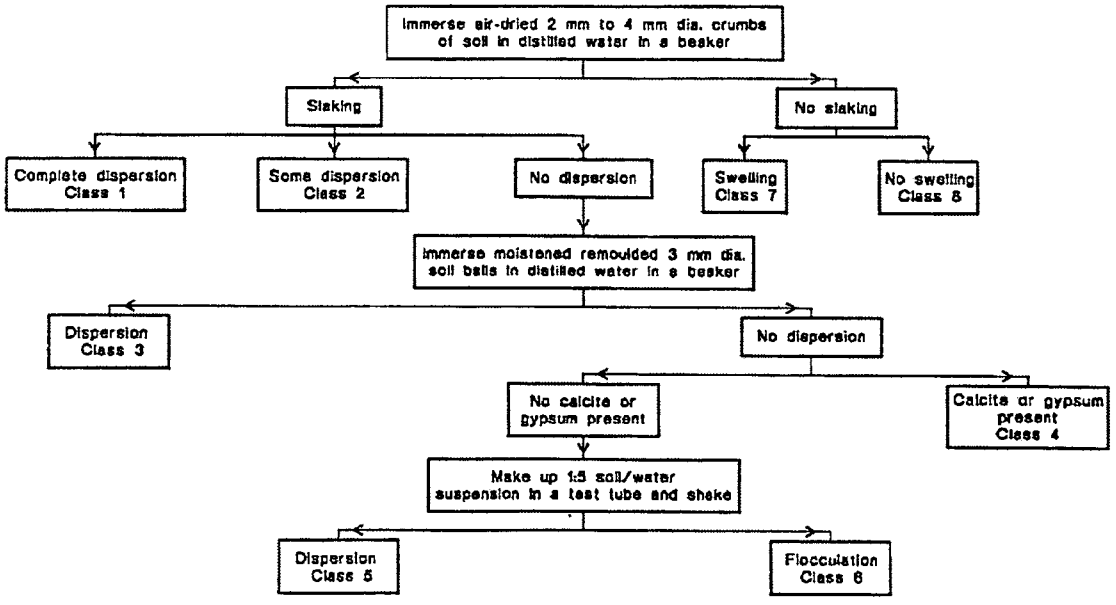

NOTES:

1 *Slaking*—most dry soil crumbs slake (break up and run out along the bottom of the beaker in a flat pile) when immersed in water.

2 *Dispersion*—describes the tendency for the clay fraction of a soil to go into colloidal suspension in water.

3 *Calcite* is chemically calcium carbonate.

4 *Gypsum* is chemically calcium sulfate.

Figure 2.15: Determination of the Emerson Class Number (AS1289.3.8.1 – 1997).

Sherard, Dunnigan and Decker (1976) compared four methods of identification of the dispersivity of a soil, viz. Pinhole Test, soluble salts in pore water, SCS Laboratory Dispersion Test, and the Crumb Test. When correlating the test results to field behaviour, they found that the Crumb Test using distilled water was a very good indicator of dispersivity of a soil. If the Crumb Test indicated dispersion, it would be very probable that the soil would be dispersive in the Pinhole test, but the reverse might not be true. They indicated that 40% of the dispersive soils had non-dispersive reactions in the Crumb Test.

Pinhole Erosion Test (Sherard, Dunnigan, Decker and Steele 1976, Sherard, Dunnigan and Decker 1976, Statton and Mitchell 1977, AS1289.3.8.3 - 1997)

Sherard, Dunnigan, Decker and Steele (1976) introduced a new laboratory test, the Pinhole test, for direct measurement of the dispersivity (colloidal erodibility) of compacted fine-grained soils. The test involved passing distilled water through a small hole punched through a soil sample and observing the erosion of the hole. The purpose

of the test was for identification and improved understanding of dispersive high sodium highly erodible fine-grained soils.

The principal differences between dispersive clays and non-dispersive clays are the clay mineralogy and the nature of the cations in the pore water. Dispersive clays are montmorillonites and illites. Dispersion is more likely if there is a preponderance of sodium ions in the pore water, whereas non-dispersive clays have a preponderance of calcium and magnesium cations in the pore water.

The test was devised in the laboratory simulating the action of a leak in a clay dam. The test was intended to gain experience, without the necessity of having actual records of the behaviour of dams with leaks in them.

The Pinhole test involved the following procedures:

- distilled water was caused to flow through a nominal 1.0 mm diameter hole in a 1" (25 mm) long specimen of clay. The diameter of the hole in the Pinhole test might vary. It might be bigger than 1mm in case there was lateral movement of the pin when the hole was punched. The hole diameter could be smaller than 1 mm because of swelling of the specimen after the hole was formed;
- initially the hydraulic head was 2" (51 mm). For a dispersive clay, the flow emerging from the specimen was visibly coloured with a colloidal cloud, and did not clear with time. For a non-dispersive clay, the flow emerging from the specimen was completely clear or became completely clear in a few seconds;
- the hydraulic head was raised in steps for 5 minutes each to 7" (178 mm), 15" (381 mm) and 40" (1016 mm). At each progressively higher gradient, the rate of flow was measured and the colour of water was observed;
- the test result was evaluated from the appearance of the water, the rate of flow, and final size of the hole in the specimen;
- the test was normally used for recompacted specimens, but could be applied to undisturbed samples.

Figure 2.16 (a) shows the setup of the Pinhole test, and Figure 2.16 (b) shows the criteria for evaluating results.

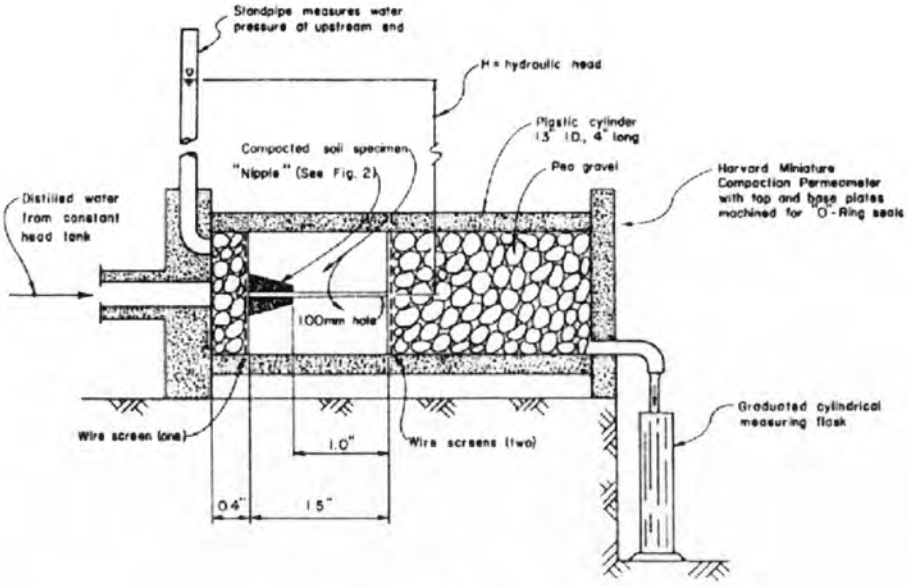

(a) Pinhole Test Apparatus.

Classification (Table 1) (1)	Head, in inches (2)	Test time for given head, in minutes (3)	Visual final flow through specimen, in milliliters per second (4)	Color of flow at end of test (cloudy or color) (5)	Hole size after test (needle diameter) (6)
D1	2	5	>1.5	Very distinct	2x
D2	2	10	>1.0	Distinct to slight	2x
ND4	2	10	<0.8	Slight but easily visible	1.5x
ND3	7–15	5	>2.5	Slight but easily visible	2x
ND2	40	5	>3.5	Clear or barely visible	2x
ND1	40	5	<5.0	Crystal clear	No erosion

Note: 1 in. = 25.4 mm.

(b) Summary of criteria for evaluating results.

Figure 2.16: Pinhole Test – Setup and Evaluation of Results (Sherard, Dunnigan, Decker and Steele 1976).

Sherard et al. (1976) assumed that flow through the hole was laminar. The computed Reynolds numbers exceeded 2000 for the higher heads, but they commented that flow appeared to remain laminar even at Reynolds numbers up to 4000.

Sherard et al. (1976) commented on the effects of compaction water content and density on the results of the Pinhole test as follows:

- most tests were carried out at with compaction moisture content near the plastic limit;
- for highly dispersive clays, erosion would be rapid regardless of water content or density;
- for most erosion-resistant soils (ND1, ND2), Pinhole test results were not changed by moderate differences in the compaction moisture content;
- results of the several hundred tests indicated that most soils belonged to the non-dispersive (ND1, ND2) or dispersive (D1, D2) categories, and only a small group of soils were in the intermediate categories ND3 or ND4. It would be possible that moderate differences in the compaction moisture content would have important influence on the results in this small group of ND3, ND4 soils.

Sherard, Dunnigan and Decker (1976) found a strong correlation between pinhole test results and pore-water sodium content. They advised that for evaluation of a given soil, both pinhole tests and tests of pore water salts should be made.

Statton and Mitchell (1977) used the Pinhole test to determine the boundaries between dispersive and non-dispersive behaviour for a clay shale with respect to acidity and salt concentration in the erosion solution. They found that soils changed from dispersive to non-dispersive when the pH was lowered to below 4 or raised to above 11. They also found that increasing the salt concentration of the erosion solution caused erosion to stop (i.e. change the soil from dispersive to non-dispersive).

The Author considers that the Pinhole test is basically an internal erosion test, but it is often used for identification of dispersive clays in surface erosion problems. The Pinhole test will rate some non-plastic silty soils as highly dispersive (Class D1) reflecting that the soil is very erodible rather than chemically dispersive. Sherard et al. (1976) did not attempt to quantify the dispersivity of a soil based on quantitative measurement of erosion although pressure readings and flow rates were recorded during

a Pinhole test. The pressure and flow measurements were used only to aid judgment. The test can be considered a semi-quantitative test on dispersivity.

Soil Conservation Service Laboratory Dispersion Test (Sherard, Decker and Ryker 1972, Sherard, Dunnigan and Decker 1976, Decker and Dunnigan 1977, AS1289.3.8.2-1997)

Decker and Dunnigan (1977) introduced the Soil Conservation Service (SCS) Dispersion Test which had been extensively used to identify dispersive clay soils since the test was reported in 1937. The test evolved from the correlation of earth-structure failures and physiochemical soil characteristics. The degree of dispersion (Percentage Dispersion) is defined as:

$$Degree\ of\ Dispersion = \frac{\%\ finer\ than\ 0.005\,mm\ without\ chemical\ dispersant}{\%\ finer\ than\ 0.005\,mm\ with\ chemical\ dispersant}$$

where the fractions of the soil finer than 0.005mm were found out from hydrometer tests on the suspensions of the fine fraction of the soil with and without the treatment of a dispersing chemical.

Decker and Dunnigan compared the results of the SCS Dispersion test with field performance, and with the results of the Pinhole test. Their findings were:

- about 85% of the soil which showed 30% or more dispersion were subject to dispersive erosion in the field. 95% of the soils which showed 60% or more dispersion were subject to dispersive erosion in the field;
- the Pinhole test was the best test for identifying soils that were subject to dispersive erosion, but there were some physiographic areas where field performance characteristics correlate very closely with the results of the dispersion test.

Sherard, Dunnigan and Decker (1976) noticed that:

- for soils showing more than 50% dispersion in the SCS dispersion test, the greater majority were also dispersive in the pinhole test;

- the SCS dispersion test apparently failed to identify dispersive clay in a small percentage of cases;
- the SCS dispersion test was generally a reliable test for testing the dispersivity of a soil.

Cylinder Dispersion Test (Atkinson, Charles and Mhach (1990))

Atkinson et al. introduced a qualitative test called the Cylinder Dispersion Test, for the identification of dispersive soils.

The Cylinder Dispersion Test was intended to examine the dispersive behaviour of soils at near zero effective stress. Achievement of zero effective stress was by means of triaxially consolidating the soil sample in a consolidating cylinder with all-round drainage as shown in Figure 2.17. The sample was then saturated and pore pressure was equal to external water pressure before being lowered into a beaker of water with the required chemical composition.

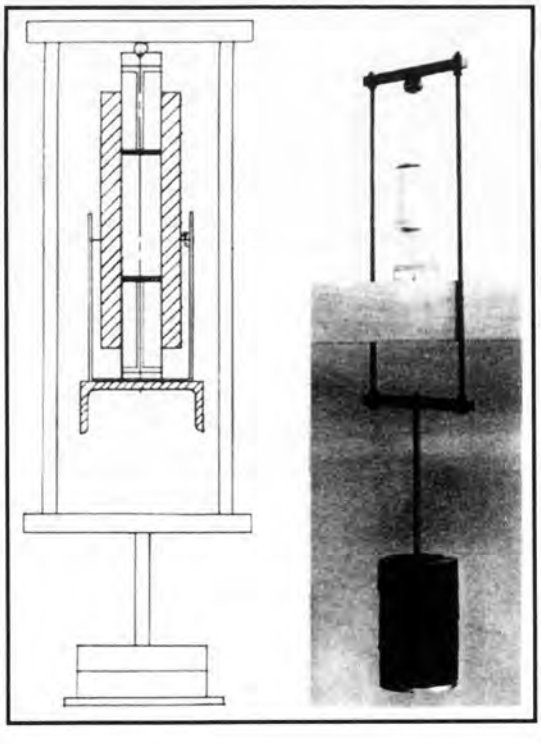

Figure 2.17: Consolidation Cylinder (Atkinson et al. 1990).

According to Atkinson et al., the Cylinder Dispersion Test was able to demonstrate the major influence of the pore water chemistry on the true cohesion and dispersion properties of the soils tested. Tests on puddle clay samples taken from South Wales, West Yorkshire (1) and West Yorkshire (2) indicated that samples classified as dispersive when tested with distilled water were classified as non-dispersive when tested with reservoir water or brine. This behaviour is consistent with what would be shown in Pinhole or Crumb Tests using distilled and salt water.

2.2.7 Other types of erosion tests

Christensen and Das (1973) – Hole erosion test on cohesive clay

Christensen and Das investigated the erosion of cohesive clays formed with a smooth surface as a 1/8 in. (3 mm) thick lining on the inside of an outer brass tube. The tube had an inside diameter of 3/4 in. (19 mm) and a length of 4 in. (102 mm). They attempted to determine the relationship between rate of erosion and critical hydraulic shear stress.

They carried out three series of tests on soils containing kaolinite and grundite with Ottawa sand added to some soil samples. The soil properties were summarised in Table 2.5.

Table 2.5: Description of soils tested (Christensen and Das 1973).

Soil	<No. 40 Sieve (percent)	<No. 200 Sieve (percent)	<2 Microns (percent)	Liquid Limit	Plastic Limit	Plasticity Index
Kaolinite	100	100	53	43	29	14
Grundite	100	96	62	51	30	21
Ottawa sand	2	–	–	–	–	–

The soil lining was moulded inside the brass cylinder by static compression.

According to Christensen and Das, the hydraulic shear stress on the inside surface of the soil lining was given by:

$$\tau = \frac{f\rho}{8}V^2$$

where τ : hydraulic shear stress

ρ : density of eroding fluid (water)

V: velocity of flow

f: friction factor

Friction factor, f, was dependent on Reynolds number, R_e, and relative roughness, ε/D, of the soil lining surface with D being the diameter of the soil lining. It was assumed that the soil lining surface was so smooth that ε would be within the range of values corresponding to wrought iron and drawn tube. R_e was controlled to within 4000 – 8000 by adjusting the rate of flow. Christensen and Das stated that test data were disregarded when erosion became excessive, and surface of soil lining became too rough.

The controlled variables in the tests were:

- hydraulic shear stress, τ
- moulding moisture content, ω
- temperature of flowing water, T

The findings of Christensen and Das were:

- erosion proceeded in 3 stages. The first stage showed decreasing erosion rate with time. The second stage showed steady erosion rate, and the third stage showed rapid increase in erosion rate. Christensen and Das commented that the initial stage of low and decreasing erosion rate was probably due to the removal of loose particles on the surface. The initial stage was followed by a fairly short duration of steady-state condition during which the soil surface was gradually roughened by erosion. During the third stage, after the soil surface had been significantly roughened, the rate of erosion was relatively faster than the first two stages;
- when plotting steady-state erosion rate against hydraulic shear stress, a bi-linear graph was obtained. The steady-state erosion rate increased rapidly beyond a certain hydraulic shear stress level, which was called the critical hydraulic shear stress, τ_c;

- at constant duration, t, temperature, T, and shear stress, τ, increasing the moulding moisture content would reduce erosion;
- at constant duration, t, molding moisture content, ω, and shear stress, τ, increasing the temperature, T, of the eroding fluid would increase the rate of erosion. Christensen and Das varied the temperature of the eroding fluid from 13 °C to 40 °C, and found that the rate of erosion would be increased by 10 times. They, however, stated that there might be errors in the results of the tests as the temperature in the soil lining might not have reached complete equilibrium with the temperature of the eroding water;
- Christensen and Das attempted to treat the erosion process of saturated cohesive soils as a shearing process and explained the phenomena by Rate Process Theory. They found that the values of the rate process parameters were consistent with those obtained for steady-state creep.

Christensen and Das concluded that:

- the erosion rate was dependent on soil composition, and both clay-size percentage and clay mineralogy were important variables;
- other controlling variables were surface roughness, flow rate, hydraulic shear stress and duration of flow;
- in saturated clays, increasing density might not increase resistance to erosion. Surface roughness, which would be related to placement conditions, might overshadow the effects of increased density.

Hjeldnes and Lavania (1980) – Crack, Leakage and Erosion Test

Hjeldnes and Lavania (1980) constructed a test device for observing simultaneously the cracking, leakage and erosion behaviour of a soil. A sketch of the test device is shown in Figure 2.18.

Soil was compacted at a known water content using standard Proctor compaction effort. The test apparatus was then given a pull at a predetermined rate of tensile deformation to develop cracking in a horizontal plane through the soil specimen at the mid-height. The desired hydraulic gradient was applied across the fracture plane. Leak discharge and the eroded soil were collected and measured.

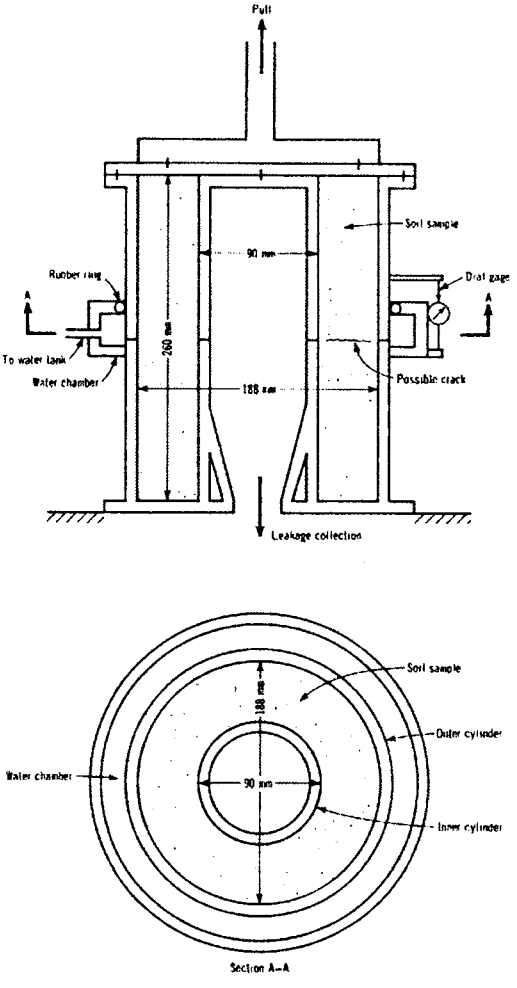

Figure 2.18: Crack, Leakage and Erosion Apparatus (Hjeldnes and Lavania 1980)

Hjeldnes and Lavania (1980) tested two soils, namely a well graded silty-gravelly sand (glacial moraine) and a silty-clayey sand. The test findings were:

- the glacial moraine exhibited a self-healing characteristic. Erosion, measured as the volume of the soil content of the flow discharge (V_s), diminished and eventually stopped. The soil sample compacted 3% dry of optimum water content cracked at a smaller tensile deformation, and showed more leakage and erosion when compared to the sample compacted at optimum water content. The sample compacted at 3% wet of optimum did not cracked at the same rate of tensile deformation;
- the silty-clayey sand did not exhibit self-healing characteristics. Erosion started at certain tensile deformation and increased with time. The sample compacted 3% wetter than optimum showed sudden large increase in erosion (blow off) at smaller tensile deformation when compared to the samples compacted at optimum water content or 3% drier than optimum. The sample compacted 3% dry of

optimum required larger tensile deformation to initiate leakage, and took longer time to reach the final blow off when compared to the sample compacted at optimum water content. The rate of erosion in the sample compacted 3% dry of optimum was about the same as that in the sample compacted at optimum water content.

The Author notes that Hjeldnes and Lavania (1980) did not attempt to assess or monitor the dimension of the crack induced by tensile deformation. The observed self-healing characteristics of the glacial moraine suggested that the actual width of the induced crack might be smaller than the tensile deformation of the mould, and might not be uniform across the thickness of the soil sample. Hjeldnes and Lavania did not assess the hydraulic shear stress along the crack. Assessment of the hydraulic shear stress would be difficult due to uncertainty in the crack width.

Sanchez, Strutynsky, and Silver (1983) – Triaxial Erosion Test

Sanchez et al. tested 5 typical embankment dam core materials ranging from silty to clayey soils using a triaxial erosion test apparatus. The apparatus, modified from an ordinary triaxial test apparatus, was used to reproduce the stress condition in the field. Figure 2.19 shows the set up of the triaxial erosion test, and Figure 2.20 illustrates the field stress condition that the apparatus was used to simulate.

The test specimen was compacted in a cylindrical split compaction mould (diameter 7.1 cm and height 5.5 cm). A thin blade (2.3 cm by 0.2 cm) was used to form a slot along the axis of the test specimen. Forming nozzles were attached at both ends of the test specimen to facilitate the formation of the slot, and for directing eroding fluid through the slot.

Raw data from the erosion tests were analysed to obtain the values of the erosion rate, measured as the weight lost per unit cross-sectional area of the slot per unit time, as a function of the eroding fluid shear stress.

To compute erosion rate and fluid shear stress requires the knowledge of the surface area and the cross-sectional area of the slot. As there was no direct measurement of

these areas during the test, Sanchez et al. assumed that the cross-section of the slot remained rectangular and related the cross-sectional area to the initial dimensions of the slot and the cumulated loss of weight of the test specimen during the course of the test. They, however, noted that the cross-section of the slot at the end of the test was elliptical among most of the soil specimens tested.

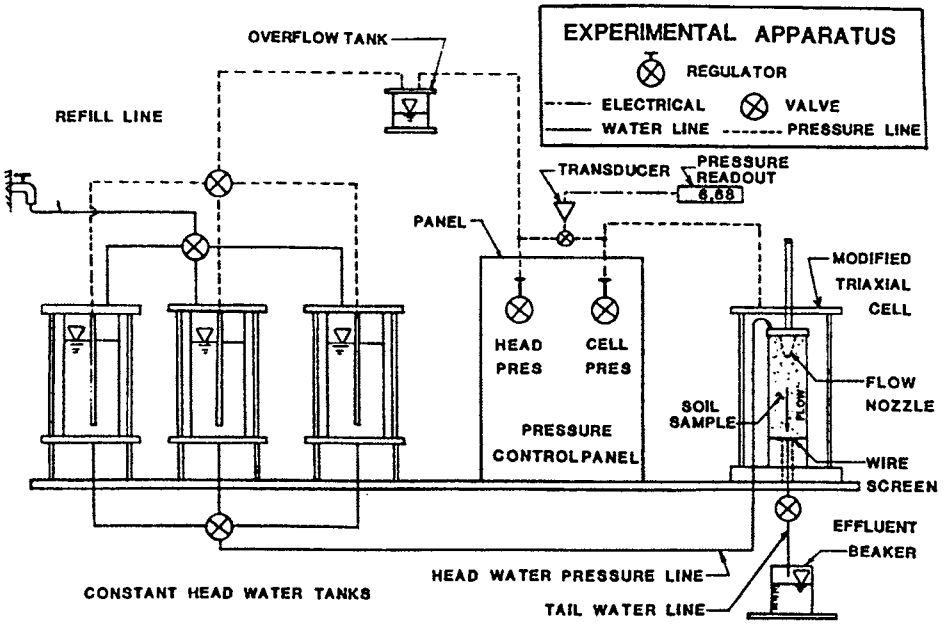

Figure 2.19: Schematic representation of triaxial erosion test apparatus (Sanchez, Strutynsky, and Silver 1983).

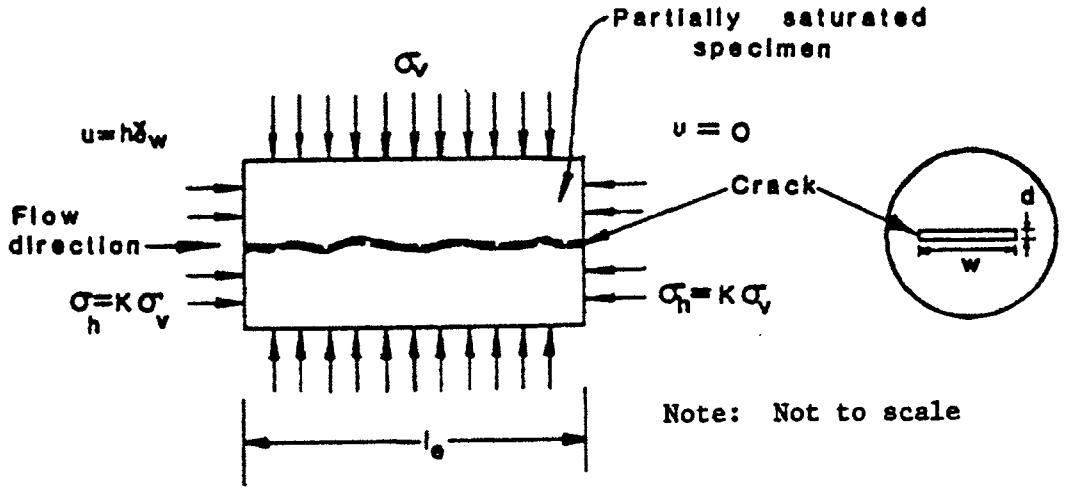

Figure 2.20: Physical conditions modeled in cracked earth dam core material erosion studies (Sanchez, Strutynsky, and Silver 1983).

The findings of Sanchez et al. were:

- varying the compacted density had little effect on erosion for silt materials compacted at the optimum water content. For clay materials, the erosion rate increased as the density decreased from 95% to 90% of standard Proctor maximum dry density;
- varying the moulding water content had a significant effect on the erodibility of silt materials, but this effect was less important for clay materials;
- minimum erosion occurred when the soil was compacted at or slightly above the optimum water content. Erosion was more severe in specimens compacted dry of optimum;
- erosion rate increased slightly with a decrease in eroding fluid ionic concentration. This increase was more significant for silt materials than for clay materials.

The Author notes that the actual initial dimensions of the pre-formed slot in the soil specimen might be different from the assumed initial dimensions because application of vertical and horizontal stresses to the test specimen might have deformed the pre-formed slot before the erosion test started.

Maranha das Neves (1987, 1989) – Crack erosion test

Maranha das Neves described the Crack Erosion Test for demonstrating the mechanism of crack erosion, transportation of eroded materials to the filter face, and filtering action at the filter layer. Figure 2.21 shows the preparation of soil sample, and the setup of the Crack Erosion Test.

The test procedure is as follows:

- soil was compacted in a Proctor mould at optimum moisture content. The compacted sample was taken out of the mould and split along a diameter into half-cylinders;
- one half-cylinder was placed into a half-cylinder Perspex permeameter, leaving a 5 mm (or 2.5 mm) gap between the flat split surface of the half-cylinder soil sample and the flat perspex cover plate of the permeameter;

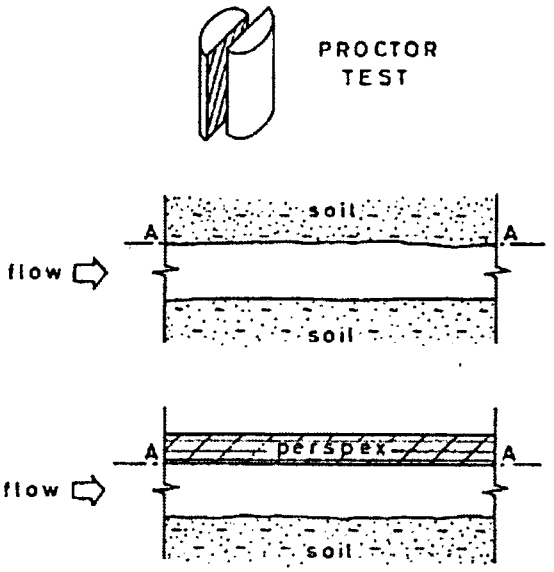

(a) : Sample preparation for the Crack Erosion Test.

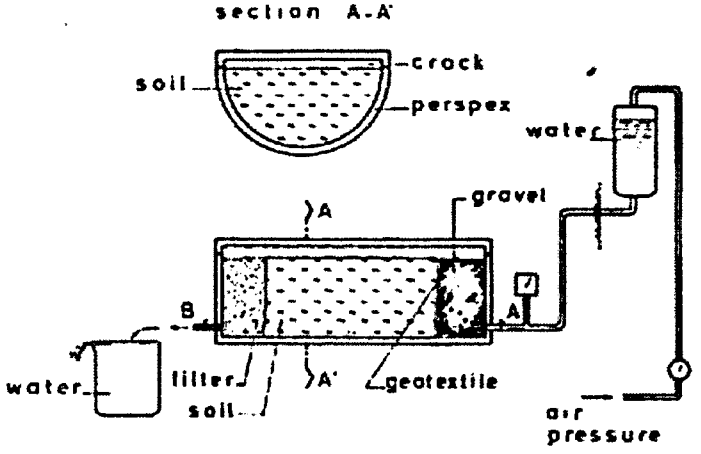

(b) : Setup of the Crack Erosion Test.

Figure 2.21: Crack erosion test setup (Maranha das Neves 1989).

- at the upstream end of the half-cylinder soil sample, gravel enwrapped by a geotextile was used to make the flow more uniform. At the downstream end, filter materials were placed to filter the flow emerging from the gap and the soil sample;

- water was passed through the permeameter. Flow velocity and hydraulic gradient were measured. Observation of the erosion of the half-cylinder soil sample and the filter action of the downstream filter materials were also made;
- the slope of the permeameter (i.e. slope of the aperture) was varied across various tests.

Two soils commonly used as core materials in Portuguese dams were tested. The properties of the two soils are summarised in Table 2.6.

Table 2.6: Properties of soil samples tested by Maranha das Neves (1989).

Soil	Origin	% clay	% silt	% sand	% gravel
A	Residual soils (schist)	10	40	48	2
B	Residual soils (granite)	10	15	50	25

The following quantities were recorded from the test:

- initial flow velocity was calculated from the measured flow rate and the known dimension of the gap/aperture between the half-cylinder soil sample and the cover plate of the perspex permeameter;
- final flow velocity was calculated from the measured flow rate and the measured aperture at the end of the test;
- the velocity of flow during the test was not measured, as the aperture as well as the roughness of sample, both of which would affect the flow, changed. Low flow velocities and low hydraulic gradients were used because the authors claimed that in real cracks, gradient could not be so high as 1000 to 2000 as predicted by Sherard et al. (1984). It was because the flow would become turbulent at high velocity so that flow would be influenced by surface roughness. The resulting hydraulic gradient would be more than 10 times less than predicted by Sherard et al.

The findings of Maranha das Neves' crack erosion tests were:

- at low flow velocity, erosion was influenced by slope of the aperture (i.e. gravity action);
- initiation of the erosion process was decided by the initial flow velocity;
- at the start of the test, even conservative filters would be unable to retain fine particles before self-filtering action had developed;
- in the study, time effect would be important for comparison between test results.

The Author notices that the crack erosion test tried to model erosion and filter actions in one set-up. The test might simulate internal erosion in a dam core with downstream filter, but would not be suitable for investigating the erosion mechanism due to the influence of the filtering materials. An advantage of the test was that it allowed for observation of the erosion process. The arguments that hydraulic gradient along a crack in the core of a dam would not be too high contradicted the predictions by Sherard et al. (1984), and would not be true near the exit of a crack.

Cedeño (1998) – UNSW Slot Erosion Test

Cedeño, under the direction of Professor Robin Fell, set up an apparatus in the laboratory of the School of Civil and Environmental Engineering at the University of New South Wales, Australia, attempting to simulate piping erosion through core materials in embankment dams. The apparatus was used to assess the rate of progression of piping through a pre-formed slot in a compacted unsaturated soil sample. A schematic diagram of the test apparatus is shown at Figure 2.22, and was called the UNSW Slot Erosion Test. It was the prototype of the current Slot Erosion Test used in this research work.

Cedeño investigated the effects of moisture content at compaction, and the degree of compaction on the rate of piping erosion. He carried out 11 tests on a sandy gravel clay of medium plasticity obtained from residual soil and weathered rock overlying shale from Glenmore Park, Sydney. The properties of the sandy gravel clay from Glenmore Park are as follows:

- geological origin : shale residual
- Liquid Limit 42%, Plastic Limit 21%, and Plastic Index : 21%
- Pinhole dispersion : PD1 – PD2,

- Emerson Class : 2,
- optimum moisture content 18%
- maximum dry density 1.802 Mg/m^3

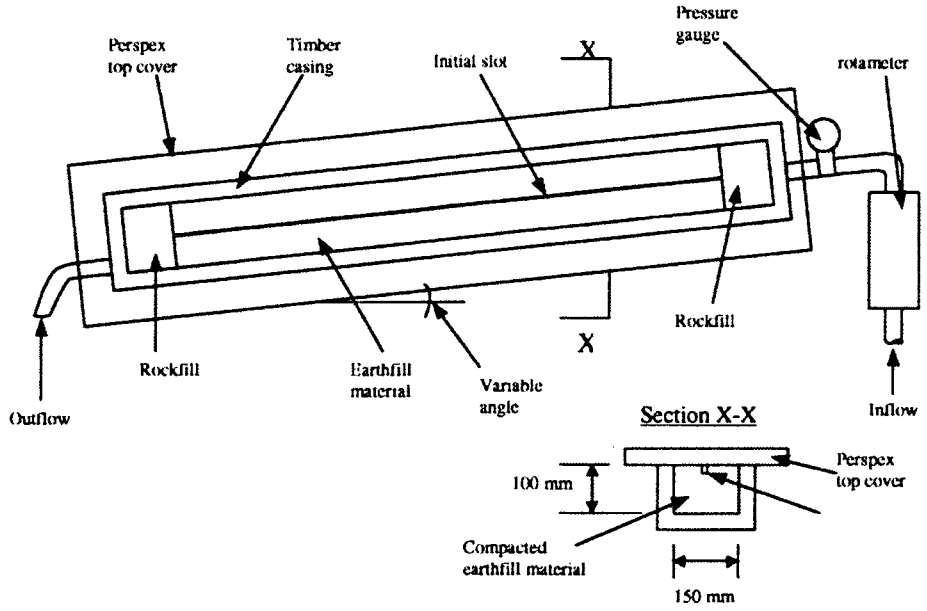

Figure 2.22: Schematic diagram showing the UNSW Slot Erosion Test Apparatus (Cedeño 1998).

Cedeño's major findings were:

- soil samples compacted at a higher moisture content relative to the optimum moisture content, and samples with a relatively higher degree of compaction were more resistant to piping erosion;
- soil samples compacted at a lower moisture content relative to the optimum moisture content, and samples with a relatively lower degree of compaction were less resistant to piping erosion;
- the effect of stopping and then restarting the flow was a sudden increase in the erosion rate;
- testing while placing the soil sample at an angle to the horizontal appeared to influence the rate of erosion.

Reddi, Lee and Bonala (2000) – Internal and surface erosion using flow pump tests

Reddi et al. attempted to assess the difference between surface erosion and internal erosion processes using results from flow pump tests. The main objective was to understand how well the surface erosion parameters (i.e. critical shear stress, τ_c, and rate of erosion) represented the internal erosion process.

Reddi et al. commented that currently available methods for investigating erodibility were either qualitative in nature (e.g. SCS Dispersion Test, Crumb Test and Pinhole Test), or directed towards the study of external erosion (e.g. flume test, flow-through-slot test, rotating cylinder test). Internal erosion, however, would be significantly affected by the processes subsequent to particle detachment in the interior of the soil, viz., re-deposition of the particles on pore walls and clogging of pores.

The flow pump tests were carried out on mixture of 70% Ottawa sand (size 2 mm) and 30% kaolinite (mean particle size 0.77 μm). Moisture content of specimens was 12% (which was wetter than optimum moisture content) and the compacted dry density was 18.9 kN/m^3. The specimens were saturated with the eroding fluid before the flow pump tests.

Details of the flow pump test described by Reddi et al. are as follows:

- the surface erosion test was basically a flow-through-hole test, the eroding fluid was pumped through a cylindrical hole of 7mm diameter;
- in the internal erosion test, the eroding fluid was pumped through intact compacted specimens in compaction permeameters in such a way that the flow rate was increased linearly from 0 to 200 ml/min. in 15 minutes;
- the eroding fluid (permeant) used was distilled water or salt solution having a concentration of 0.01N or 0.001N. The experiments were flow rate-controlled, and a flow rate of 0 – 200 ml/min. was used;
- the effluent from the cells was diverted to a continuous flow turbidimeter. The measured nephelometric turbidity units (NTU) were converted to kaolinite particle concentrations.

For the external erosion test, which was a flow-through-hole test. The initial diameter of the pre-formed hole through the soil sample was chosen to be 7 mm. Flow was described by the Poiseuille's equation for laminar flow, and viscous flow equations. Shear stress, τ would be given by:

$$\tau = \left(\frac{\Delta p}{L}\right)\frac{R}{2}$$

where $\frac{\Delta p}{L}$: pressure gradient (kN/m^2/m)

R : radius of the hole through the specimen (m).

For the internal erosion test, the soil was idealised as an ensemble of pore tubes. The shear stress in a pore tube was estimated by:

$$\tau = 1.414\left(\frac{\Delta p}{L}\right)\left(\frac{k}{n}\right)^{1/2}$$

where n : porosity of the soil specimen

k : intrinsic permeability of the specimen.

$$k = \frac{K\eta}{\rho g}$$

where K : hydraulic conductivity

η : viscosity of the eroding fluid

ρ : mass density of the eroding fluid

g : acceleration due to gravity.

The findings of the flow pump tests were:

- in the surface erosion tests (flow-through-hole tests), the critical shear stresses for the tested samples were in the range of 0.037 – 0.060 Pa for various concentrations of eroding fluid;
- for internal erosion tests (flow through intact sample tests), the critical shear stresses were in the range of 1.23 – 3.35 Pa, which were several orders of magnitude greater than those in the surface erosion experiments.

The Author notes that the critical shear stresses presented by Reddi et al. were derived from the results of the tests. The validity of the results would depend on the validity of the models and theories used for predicting the critical shear stresses. The Author also notices that Reddi et al. used the term internal erosion to describe erosion within an intact soil mass, whereas the normal use of the term is where erosion initiates on cracks or in poorly compacted zones in the earthfill.

2.2.8 Summary

Erosion Tests on Soils

The various site and laboratory tests described in this report can be broadly summarised into three main categories, viz.

Category 1 : Surface erosion tests

- laboratory hydraulic flume tests, or large scale channel erosion tests
  (e.g. Gibbs 1962, Kandiah & Arulanandan 1974, Arulanandan & Perry 1983, Shaikh et al. 1988a, 1988b, Ghebreiyessus et al. 1994, Briaud et al. 1999, 2001a, 2001b and 2003)
- rotating cylinder tests
  (e.g. Moore & Masch 1962, Kandiah & Arulanandan 1974, Arulanandan et al. 1975, Sargunan 1977, Arulanandan & Perry 1983, Chapuis 1986a, 1986b, Chapuis & Gatien 1986.)
- site or laboratory submerged jet erosion tests
  (e.g. Moore & Masch 1962, Hanson 1991, 1992, Hanson & Robinson 1993, ASTM D5852-95 1995.)

Category 2 : Internal erosion tests:

- hole/aperture erosion tests

(e.g. Christensen & Das 1973, Hjeldnes and Lavania 1980, Sanchez, Strutynsky and Silver 1983, Maranha das Neves 1987, 1989, Cedeño 1998, Reddi et al. 2000,)

- flow through intact sample tests
  (e.g. Reddi et al. 2000.)

Category 3 : Dispersivity tests:

- Emerson Class Test (also called Crumb test) (Emerson 1967, AS1289.3.8.1-1997)
- Pinhole test (Sherard et al. 1976, AS1289.3.8.3-1997)
- SCS Laboratory Dispersion test (also called the double-hydrometer test) (Decker & Dunnigan 1976, AS1289.3.8.2-1997)
- Cylinder dispersion test (Atkinson et al. 1990)

Hydraulic flume tests have been widely used for investigating surface erosion in unlined canals and river channels which they physically model. The main disadvantages of the test are: (1) erosion is visually assessed without quantitative measurements, and (2) hydraulic shear (tractive) stresses are not measured but derived indirectly from measured flow velocity. Reproduceability of results is apparently difficult probably because geotechnical properties and surface roughness of samples were not adequately controlled. Briaud et al. (1999, 2001a, 2001b and 2003) carried out extensive flume testing using the Erosion Function Apparatus. Their study, however, was focused on surface scour around bridge piers.

The rotating cylinder test provides a relatively accurate means of measuring the critical shear stress and the coefficient of soil erosion. The equipment is complicated, expensive to construct, and has only been used in a few research laboratories over the world. Considerable skill is required in sample preparation, and in the operation of the test apparatus and the supporting equipment. Chapuis (1986a, 1986b) reported that the test was sensitive to surface roughness of the specimen. The way that the specimen is prepared (i.e. in the form of a cut sample or triaxially consolidated sample) will, therefore, influence the results.

The submerged jet erosion test uses a parameter called the Jet Index to measure the relative erodibility of soils. The test is not popular, despite the fact that it has become an ASTM standard, and has a relatively simple set up. This is probably because the test has not been adequately calibrated with accurate field measurements of shear stress in different types of soils. It is stated in the ASTM D5852-95 that the precision and bias of the test has not yet been determined. It probably best simulates the head-cutting erosion action which occurs in inclined spillway channels in small dams.

Dispersivity tests measure the tendency of dispersion of soil particles in water. They do not provide a measure of erodibility directly, but it is generally agreed that a dispersive soil is more erodible than a non-dispersive soil in terms of the ease that erosion can be initiated in the soil. The Pinhole test is actually a kind of internal erosion test, which was designed to simulate erosion along a crack through an embankment dam core.

It must be recognised that there are several mechanisms of erosion which the various tests are simulating, i.e. Flume Tests for erosion in open channels, and Jet Erosion Tests for erosion in unlined spillway channels subject to headward erosion. Dispersivity tests are not meant to measure erosion (i.e. the critical shear stress, or the coefficient of soil erosion), but are used to identify soils which display dispersion in the field. The Rotating Cylinder Tests, and internal erosion tests do set out to measure critical shear stress and erosion rate for surface erosion, and can be regarded as simulating conditions along a crack, or a erosion pipe in a dam. However, the Authors believe that the Rotating Cylinder Tests are too complex for routine testing, and set out to develop the Slot and Hole Erosion Tests which are relatively simple to do, and simulate erosion in a crack or pipe in a dam.

It is noticeable that most of the more fundamental research has been directed towards the critical shear stress. It is the Author's view that while this is important, it is likely that the critical shear stress will be exceeded in many cracked dams, and hence it is the rate of erosion which is at least equally important for the reason outlined in Section 1.5.

Factors affecting the erodibility of a soil

The important findings of the various tests are:

- a critical shear stress exists for a given soil-eroding water system below which surface erosion was absent or very slow;
- for compacted soils, erosion resistance, represented by critical shear stress, increases with the compaction moisture content and the compaction effort, and rate of erosion decreases with increase in compaction moisture content and compaction effort;
- the critical shear stress decreased with an increase in the *SAR* of the pore fluid;
- the critical shear stress increases as salt concentration in the eroding fluid increased;
- the erosion resistance is affected by the salt concentration gradient between pore fluid and the eroding fluid;
- the rate of erosion increased linearly with applied hydraulic shear (tractive) stress;
- the rate of erosion is influenced by clay mineralogy and clay size percentage;
- erosion resistance is also influenced by other factors, such as test methods, temperature of the eroding fluid, and surface roughness, which would depend on the method of sample preparation.

2.3 EXPERIMENTAL INVESTIGATION OF PIPING EROSION OF SOILS AT THE UIVERSITY OF NEW SOUTH WALES

2.3.1 Objectives of experimental investigation

The objectives of experimental investigation are two-fold, namely

- to investigate the use of relatively simple laboratory tests, namely the Slot Erosion Test (SET) and the Hole Erosion Test (HET) for finding the erosion characteristics of a soil;
- to study the relationships between the basic engineering properties and the erosion characteristics of a soil.

Most of the work is directed towards the assessment of the rate of erosion, as measured by the mass of soil eroded per unit area per unit time, with a lesser emphasis on the critical shear stress.

2.3.2 Slot Erosion Test

Introduction

The Slot Erosion Test (SET) has been designed to simulate piping erosion along a concentrated leak within an earth embankment. In a SET, a 2.2 mm wide x 10 mm deep x 1 m long slot is artificially formed along one surface of an unsaturated soil sample compacted inside a 0.15 m wide x 0.1 m deep by 1 m long rigid sample box made of aluminium. The pre-formed slot is in contact with a transparent perspex cover plate of the sample box through which erosion of the slot can be observed during the test. An eroding fluid is passed through the soil sample to initiate erosion of the soil along the pre-formed slot. The width of the pre-formed slot, as it is widened by erosion, is measured at chosen time intervals.

More than 95% of the SETs were carried out using Sydney tap water as the eroding fluid. The remaining SETs used dilute sodium chloride solutions as the eroding fluid so

as to investigate the effects of water chemistry on the erosion characteristics of a soil. It should however be noted that Sydney tap water contains a small amount of dissolved salts in the order of 35 to 100 mg/l which is high enough to inhibit dispersion.

A schematic diagram of the SET apparatus is shown at Figure 2.23. Figure 2.24 shows the actual test setup, and Figure 2.25 shows an example of an eroded soil sample during the course of a SET. Appendix I presents the detailed geometry and procedure of the SET.

Theory

Some fundamental theories in hydraulics can be used to model the flow of the eroding fluid along the pre-formed slot.

Considering force equilibrium on the body of eroding fluid along the pre-formed slot at a particular time t:

$$\tau_t \cdot \wp_t \cdot L = \Delta P_t \cdot A_t \qquad \text{Eqn 2.1}$$

$$\Delta P_t = \rho_w g \Delta h_t = \rho_w g s_t L \qquad \text{Eqn 2.2}$$

where the meaning of the various symbols are given in Figure 2.26.

- τ_t is the shear stress due to the eroding fluid on the surface of the pre-formed slot at time t,
- ΔP_t is the pressure difference across the 1m long soil sample at time t,
- ρ_w is the density of the eroding fluid,
- g is the acceleration due to gravity (9.806 m/s^2),
- $\wp_t$ is the wetted perimeter of the pre-formed slot at time t,
- Δh_t is the head difference across the soil sample at time t measured by pressure gauges,
- s_t is the hydraulic gradient across the 1m long soil sample at time t.
- A_t is the cross-sectional area of the pre-formed slot at time t.

Combining equations 2.1 and 2.2 gives

$$\tau_t = \rho_w g s_t \frac{A_t}{\wp_t} \qquad \text{Eqn 2.3}$$

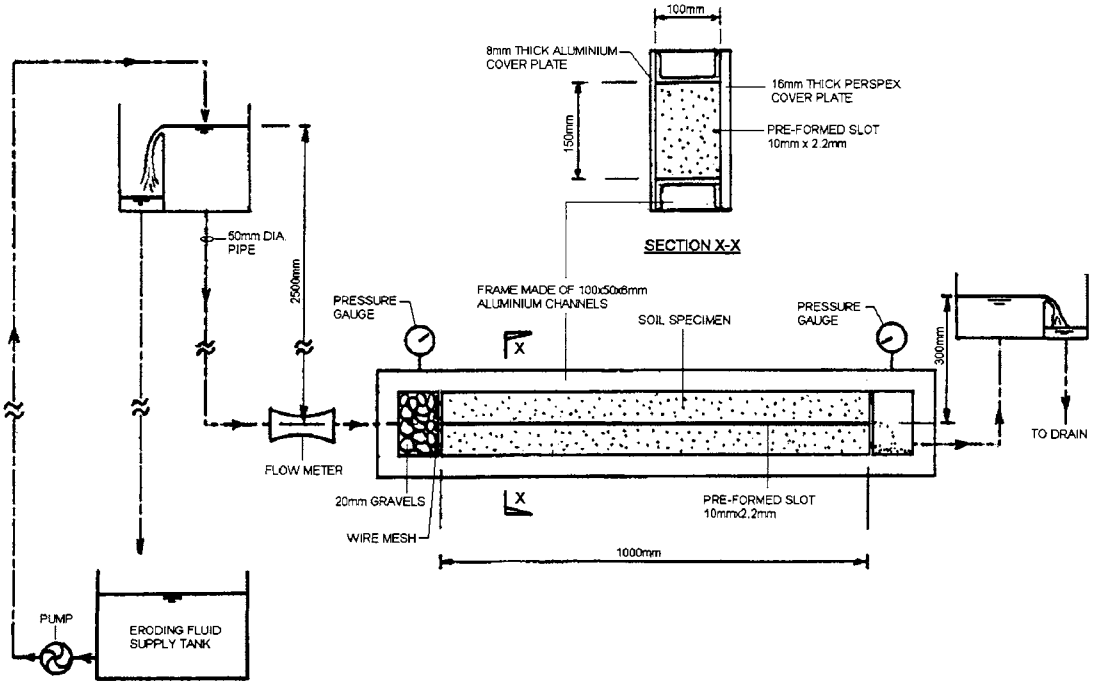

Figure 2.23: Schematic diagram of the Slot Erosion Test Assembly.

The rate of erosion per unit surface area of the slot at time t, denoted by $\dot{\varepsilon}_t$, is given by

$$\dot{\varepsilon}_t = \frac{1}{\Psi_t}\frac{dM_t}{dt} \qquad \text{Eqn 2.4}$$

$$\Psi_t = \wp_t \cdot L \qquad \text{Eqn 2.5}$$

$$dM_t = \rho_d L dA_t \qquad \text{Eqn 2.6}$$

where

Ψ_t is the surface area of the pre-formed slot at time t,

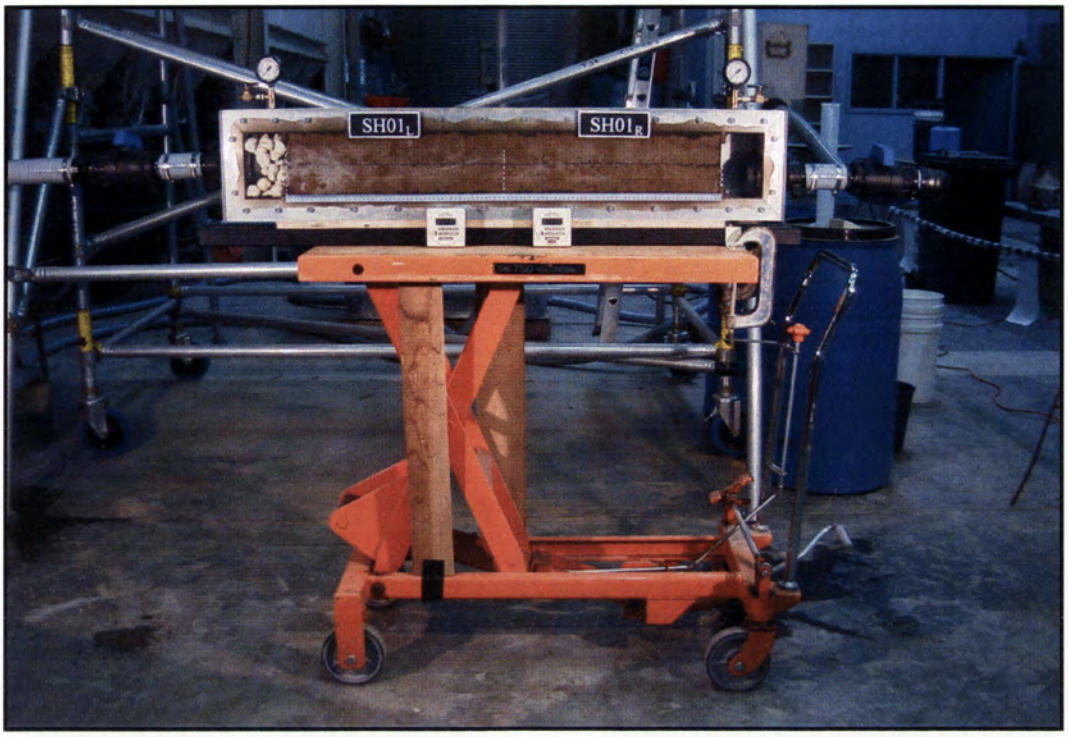

Figure 2.24: Slot Erosion Test Apparatus. Water re-circulation system not shown.

Figure 2.25: Slot Erosion Test on soil sample taken from Jindabyne Dam.

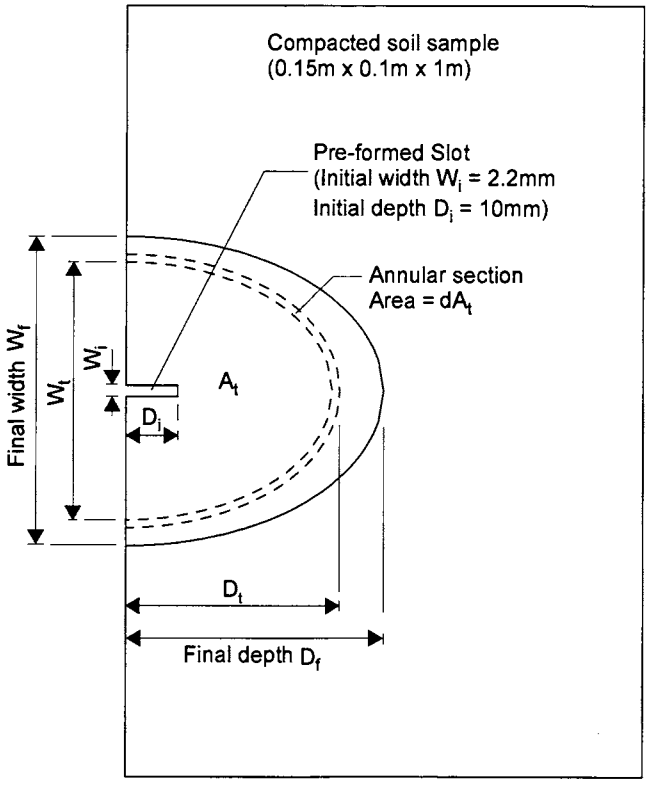

Figure 2.26: Cross-section of a SET test specimen showing enlargement of pre-formed slot due to erosion.

dM_t/dt is the rate of soil mass removal due to erosion at time *t*.

L is the length of the soil sample (1m),

ρ_d is the dry density of the soil.

Combining equations 2.4, 2.5 and 2.6 gives

$$\dot{\varepsilon}_t = \frac{\rho_d}{\wp_t}\frac{dA_t}{dt} \qquad \text{Eqn 2.7}$$

The underlying assumptions behind equations 2.3 and 2.7 are that:

i. the pre-formed slot has a uniform cross-section along the length of the soil sample,

ii. only the soil surface along the pre-formed slot offers shear resistance to flow, the shear resistance due to the perspex cover plate is negligible.

Parameters ρ_w, s_t, ρ_d and L in equations 2.1 and 2.2 are measured during a SET.

There are, however, no simple methods to measure the cross-sectional area A_t, and the wetted perimeter $\wp_t$ of the pre-formed slot. In order to estimate τ_t and $\dot{\varepsilon}_t$, both of which depends on A_t and $\wp_t$, two further assumptions are made regarding the shape of the pre-formed slot, viz:

iii. the pre-formed slot has an elliptical cross-section soon after erosion starts, and the elliptical cross-section is uniform along the length of the soil sample,

iv. the depth D_t of the pre-formed slot at time t is proportional to t^2.

Measurement of the pre-formed slot after each SET indicated that the slot had an approximately semi-elliptical shape, as shown in Figure 2.26. Sanchez et al. (1983), when introducing their triaxial erosion test, also described that the final eroded shape of an initially rectangular slot was approximately elliptical. Based on the fourth assumption, the depth of the pre-formed slot D_t at time t can be interpolated between the initial value D_o = 2.2 mm and the final depth D_f directly measured after the test. Widening of the pre-formed slot can be observed through the transparent perspex cover during the test, and the width of the pre-formed slot W_t can be measured at regular time intervals.

Based on assumptions iii. and iv., the cross-sectional area, A_t, and the wetted perimeter, $\wp_t$, of the pre-formed slot can be estimated using the formulae for a half-ellipse:

$$A_t = \frac{\pi}{4} W_t D_t \qquad \text{Eqn 2.8}$$

$$\wp_t = \sqrt{\frac{\pi^2}{2}\left[\left(\frac{W_t}{2}\right)^2 + D_t^2\right]} \qquad \text{Eqn 2.9}$$

The shear stress, τ_t, and the rate of erosion per unit area, $\dot{\varepsilon}_t$, along the pre-formed slot can then be estimated using equations 2.3, 2.7, 2.8 and 2.9. When $\dot{\varepsilon}_t$ is plotted against τ_t, the rising portion of the plotted curve can be approximated by a straight line which can be represented by the following linear equation:

$$\dot{\varepsilon}_t = C_e(\tau_t - \tau_c) \qquad \text{Eqn 2.10}$$

where C_e is a proportionality constant named by the Author as the *Coefficient of Soil Erosion*,

τ_c is the intercept of the straight line at the horizontal axis representing $\dot{\varepsilon}_t = 0$. In the literature, τ_c is often called the *Critical Shear Stress*.

C_e obtained for the various SETs are small numbers in the order of 10^{-1} to 10^{-6} having the unit [s/m] which is simplified from [kg/s/m^2 per N/m^2]. Since $\log(C_e)$ is more often used in correlation analysis and plotting of results, another parameter named by the Authors the *Erosion Rate Index* (I_{SET}), is used in lieu of C_e. I_{SET} is defined as

$$I_{SET} = -\log(C_e) \qquad \text{Eqn 2.11}$$

I_{SET} has an order of magnitude in the range of 0.1 to 6. A smaller value of I_{SET} implies a more rapidly erodible soil. The following section shows an example on how C_e, τ_c and I_{SET} are estimated from SET test data.

Analysis of raw data obtained from the SET

Analysis of the raw data of test BDSET4 on soil sample Bradys is presented in this section to demonstrate the application of the theory on SET described in preceding Section. The analysis involves the following steps:

- plot width of pre-formed slot measured during the SET against time as shown in Figure 2.27,
- estimate the average cross-sectional area and the wetted-perimeter of the pre-formed slot using equations 2.8 and 2.9 respectively and plot the two parameters against time as shown in Figure 2.28,

- plot the rate of mass removal per unit area, $\dot{\varepsilon}_t$, and the shear stress, τ_t against time as shown in Figure 2.29. τ_t and $\dot{\varepsilon}_t$ are estimated using equations 2.3 and 2.7 respectively. The derivative dA_t/dt in equation 2.7 can be approximated by $\Delta A_t/\Delta t$ using numerical differentiation techniques, where ΔA_t represents the change in A_t over a short time interval Δt,
- plot $\dot{\varepsilon}_t$ against τ_t as shown in Figure 2.30. The *Coefficient of Soil Erosion*, C_e, is the slope of straight line approximating the rising part of the curve. The intercept of the straight line on the horizontal axis represents the *Critical Shear Stress*, τ_c. The initial section of the curve in Figure 2.30 shows a decrease in erosion rate per unit area with an increase in the shear stress. This is due to the removal of the loose, disturbed soils around the pre-formed slot at the early stage of the test. After this early stage, the erosion rate increases steadily with shear stress. The initial section of the curve in Figure 2.30 shows a negative slope. This section of the curve corresponds to the initial section of the curve in Figure 2.29 which shows a decreasing rate of erosion. The slowing down of the rate of erosion after the early stage is due to the disturbed and relatively loose materials around the pre-formed slot being less erosion-resistant than the relatively intact materials further away from the slot. The erosion rate, therefore, reduces as the materials become harder and harder to erode. The erosion rate gradually increases with the shear stress when the loose materials have been removed. Christensen and Das (1973) also recorded a decreasing erosion rate with time in the early stage of their hole erosion test on cohesive clay.
- the *Erosion Rate Index*, I_{SET}, is equal to $-\log(C_e)$.

The above procedure has been followed for analysing test data of the SET. A summary of the interpreted results of all SETs is shown in Appendix A.

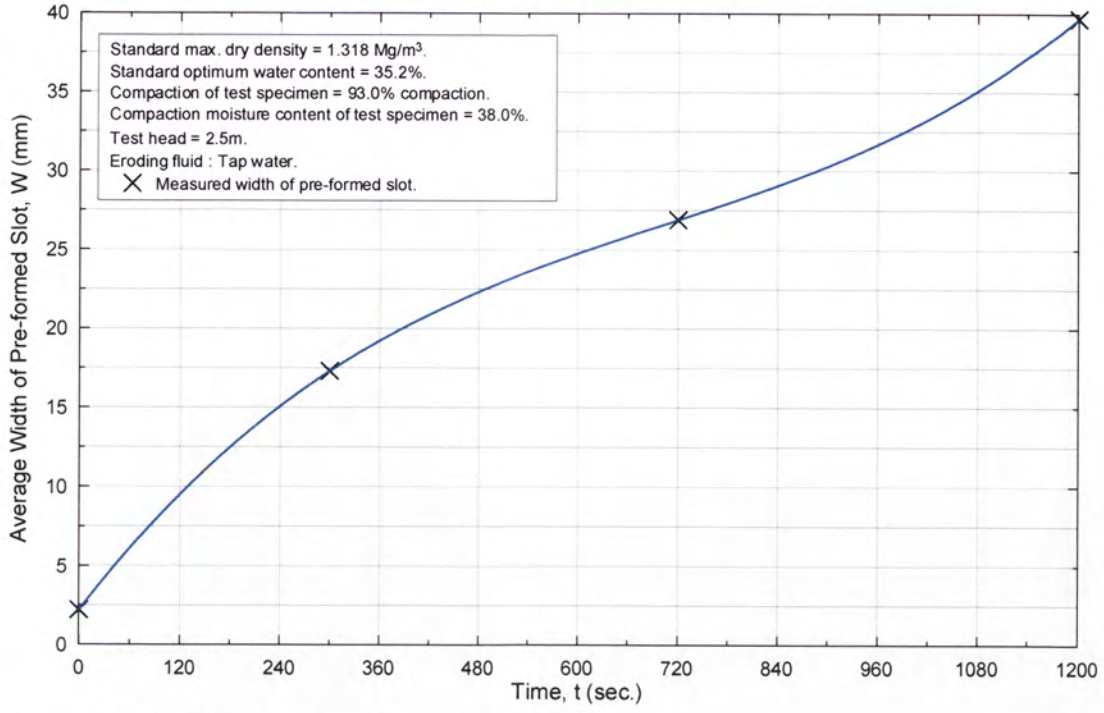

Figure 2.27: Width of pre-formed slot versus time in a Slot Erosion Test using Test BDSET4 on soil sample Bradys as an example.

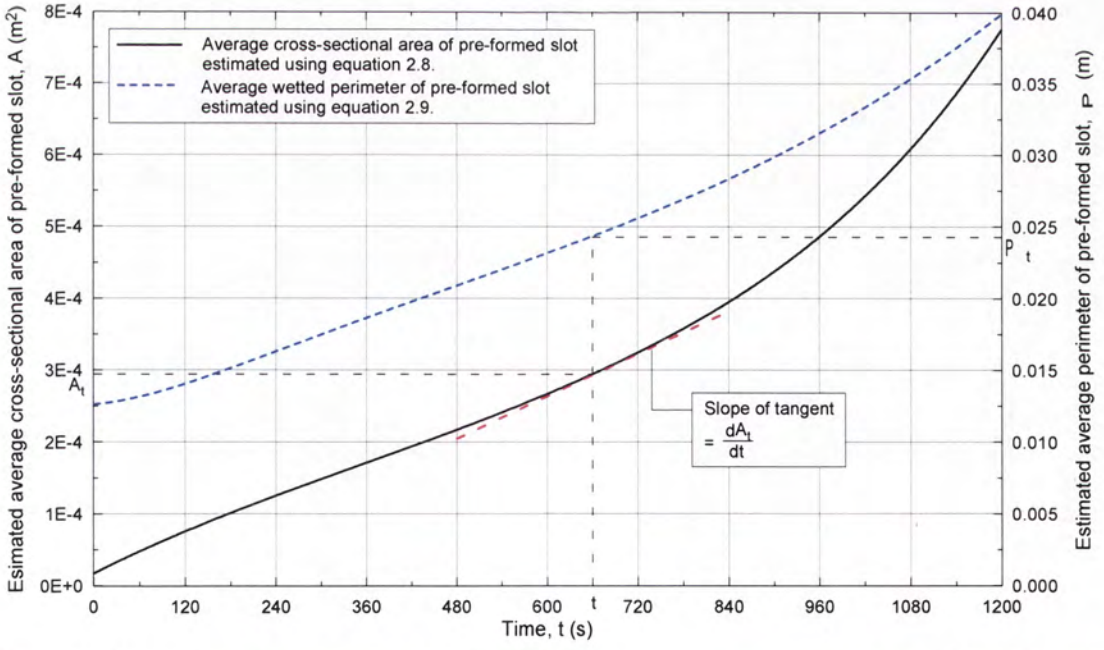

Figure 2.28: Average cross-sectional area and average wetted-perimeter of pre-formed slot versus time in Slot Erosion Test BDSET4 on soil sample Bradys.

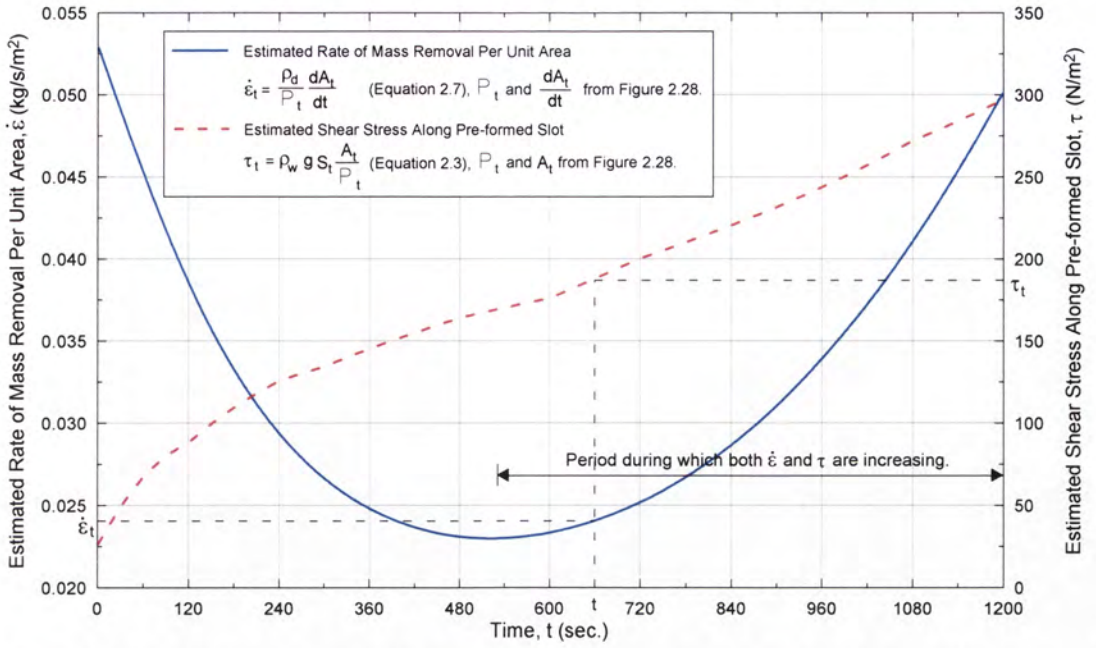

Figure 2.29: Estimated rate of mass removal per unit area and estimated shear stress versus time in Slot Erosion Test BDSET4 on soil sample Bradys.

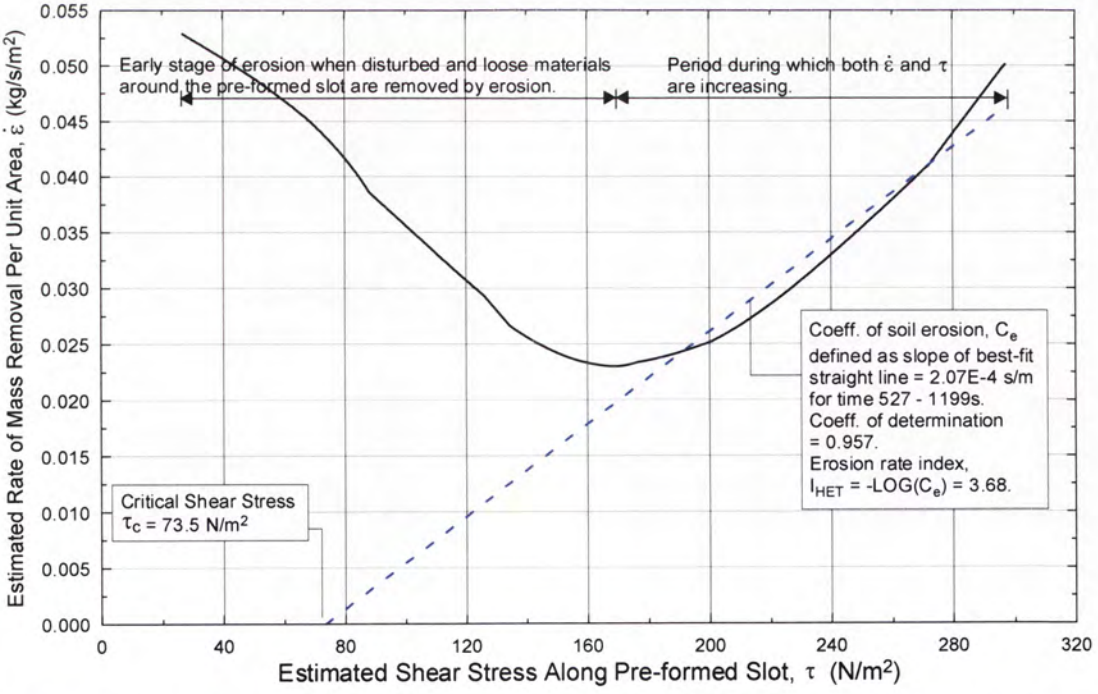

Figure 2.30: Estimated rate of mass removal per unit area versus estimated shear stress in Slot Erosion Test BDSET4 on soil sample Bradys.

2.3.3 Measurement and control of test variables in a SET

The test variables, which were measured or controlled before or during a SET, are as follows:

Basic information of the soil samples

Standard soil classification tests were carried out on the soil samples according to relevant Australian Standards to obtain basic classification information, namely soil particle density, particle size distribution, and Atterberg's limits.

Standard compaction tests were carried out on each of the soil samples to obtain information on standard maximum dry density and optimum water content. This information was essential for controlling the dry density and moulding water content of the test specimens.

Three different tests were used to measure the dispersivity of the soil samples, namely the Pinhole Dispersion Test (Sherard et al. 1976), Emerson Class Test (Emerson 1967), and the US Soil Conservation Services Percentage Dispersion Test.

The electro-chemical properties of the soil samples were also assessed by measuring the cation content, the electrical conductivity, and the pH of the saturation extracts of the soil samples. The saturation extracts were pore fluids extracted from the soil samples wetted up to their liquid limits. Extraction of pore fluid was carried out by means of a vacuum flask and a Buechner funnel (Sherard et al. 1972).

Moulding water content and dry density of test specimens

Test specimens were usually prepared at one of five different levels of moulding water content. The five levels were -2%, -1%, +0%, +1% and +2% of the standard optimum water content (OWC). To achieve the desired moulding water content, the appropriate amount of water was added to the soil sample, which was then cured for at least two days before a test specimen of the soil was prepared. Water content tests were carried out on soils trimmed from the compaction mould so as to find out the actual moulding water content of the test specimen.

Test specimens were usually prepared at one of three different levels of dry density. The three levels were represented by 92%, 95% and 98% of the standard maximum dry density (SMDD) of the soil sample. The dry density of a test specimen was controlled by controlling the total mass of soil of known water content to be used for forming the compacted test specimen. Known amount of soil was compacted to a pre-calculated thickness corresponding to the desired dry density. Finally, the mass of the completed test specimen was measured so as to calculate the actual dry density of the specimen.

Salt content and temperature of the eroding fluid

About 95% of the SETs were carried out using Sydney tap water as the eroding fluid. This contains approximately 35 to 100 mg/l of dissolved solids. This is insufficiently pure to inhibit dispersion some what in Emerson Crumb Tests. The remaining 5% of the tests were carried out using salt water in place of tap water. The salt water was prepared by adding sodium chloride into tap water. Two salt solutions of different concentration were used. One was a 0.005M salt solution (0.292 g of NaCl per litre of distilled water), and the other was a 0.02M salt solution (1.169 g of NaCl per litre of distilled water). Samples of tap water and the salt solutions were taken from the constant head tank for confirmation of the salt concentration of the eroding fluid.

The temperature of the eroding fluid was measured immediately before and after the SET so that the effect of temperature on the viscosity of the eroding fluid could be considered if necessary.

Monitoring of hydraulic gradient and flow rate during a SET

Nearly all the SETs were carried out with an upstream water head of 2.5 m. This head corresponded to a hydraulic gradient of about 2.2 across the 1m long pre-formed slot, taking into account the 0.3 m tailwater at the outlet end of the apparatus. As the pre-formed slot widened, the flow rate increased causing increased head loss across the test specimen. The hydraulic gradient across the slot, therefore, did not remain constant throughout the test. The pressure difference across the pre-formed slot was however, monitored by pressure gauges installed immediately upstream and downstream of the pre-formed slot.

Flow rate was measured as a check against the possibility of undetected alternative erosion path through the test specimen.

2.3.4 Hole Erosion Test

Introduction

The Hole Erosion Test (HET) has been developed to be a faster and more economical alternative to the SET. The setup of the HET is similar to that of the SET except a much smaller soil specimen is tested at a relatively lower water head. In the HET, the soil specimen is compacted inside a standard mould used for the Standard Compaction Test. A 6mm-diameter hole is drilled along the longitudinal axis of the soil sample to simulate a concentrated leak. The HET uses flow rate as an indirect measurement of the diameter of the pre-formed pipe.

A schematic diagram of the HET assembly is shown at
Figure 2.31. Figure 2.32 shows the actual test apparatus, and Figure 2.33 shows an eroded test specimen after a HET. Appendix J presents the detailed geometry and procedure of the HET.

Theory

The diameter of the pre-formed pipe can be indirectly estimated from the measured flow rates based on some fundamental theories in hydraulics.

Similar to flow through a pre-formed slot, the shear stress, τ_t along the surface of a circular pipe at time t can be predicted by equation 2.3.

$$\tau_t = \rho_w g s_t \frac{A_t}{\wp_t} \qquad \text{Eqn 2.3}$$

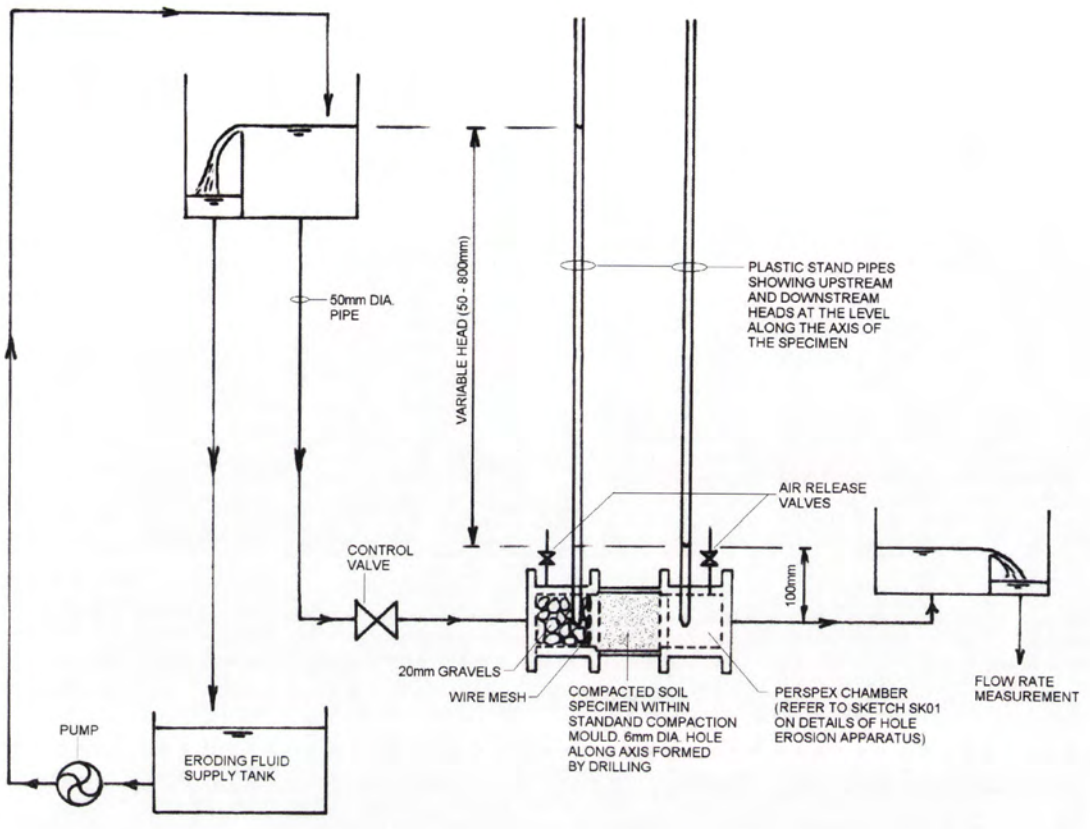

Figure 2.31: Schematic diagram of the Hole Erosion Test Assembly.

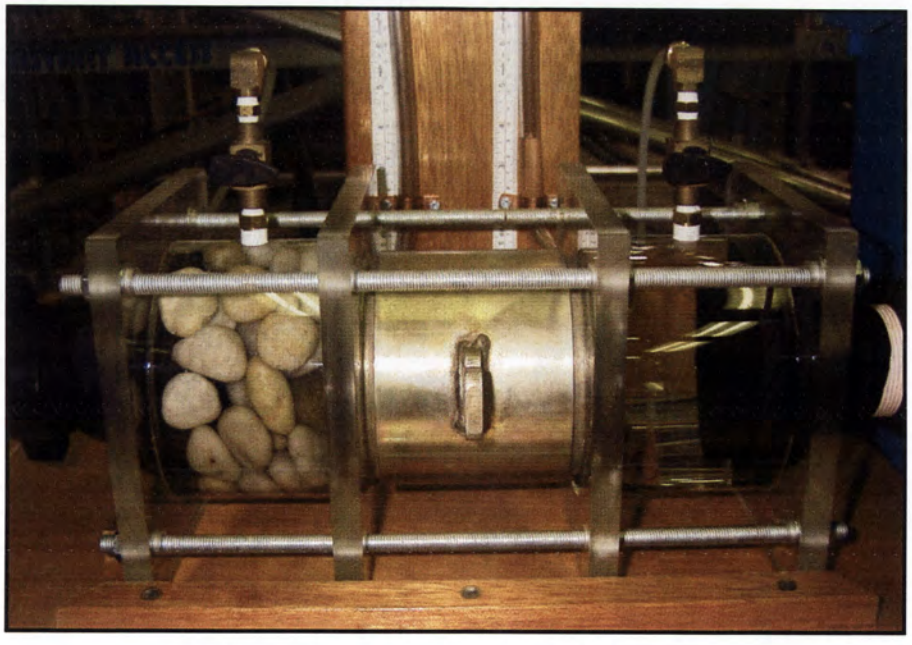

Figure 2.32: Hole Erosion Test apparatus.

Water recirculation system not shown.

For flow through a circular pipe, $A_t / \wp_t$ is simply ϕ_t / L, where ϕ_t is the diameter of the pipe at time t, and L is the length of the circular pipe. Equation 2.3 is, therefore, simplified to

$$\tau_t = \rho_w g s_t \frac{\phi_t}{4} \qquad \text{Eqn 2.12}$$

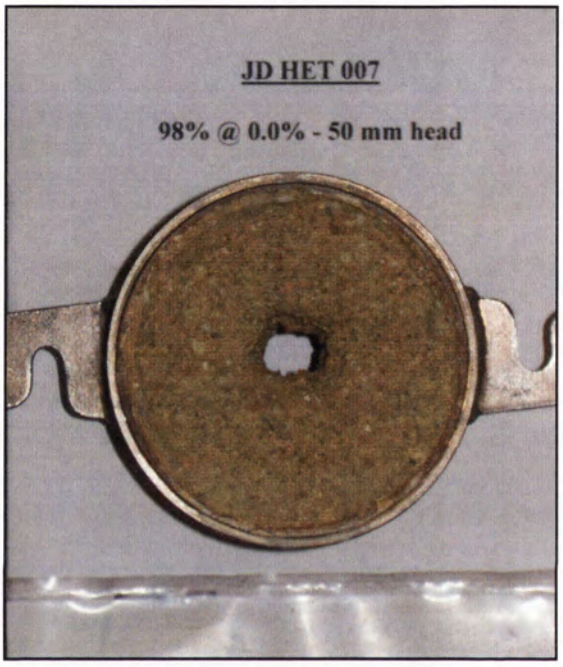

Figure 2.33: Hole Erosion Test on soil sample from Jindabyne Dam. Photograph of test specimen after test.

Similarly, equation 2.7 can also be used to predict the rate of erosion per unit surface area of the pipe at time t.

For a circular pipe, $dA_t = (\pi \phi_t d\phi_t)/2$ is the area of the annular section shown in Figure 2.34, and $\wp_t = \pi \phi_t$. Equation 2.7 is, therefore, simplified to

$$\dot{\varepsilon}_t = \frac{\rho_d}{2} \frac{d\phi_t}{dt} \qquad \text{Eqn 2.13}$$

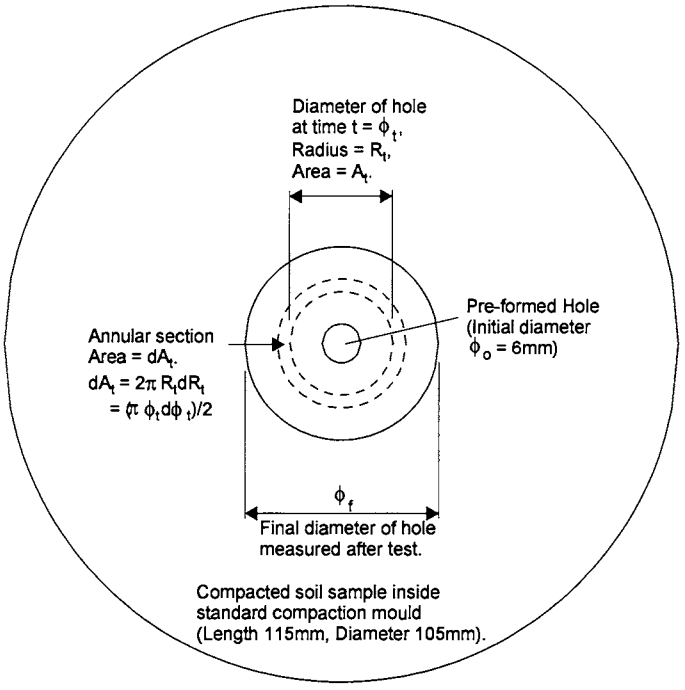

Figure 2.34: Cross-section of a HET test specimen showing enlargement of the pre-formed pipe due to erosion.

Equations 2.12 and 2.13 show that the shear stress along the pre-formed pipe and the rate of erosion per unit area of the hole depend on the diameter of the pipe and the rate of change of the diameter respectively. The diameter of the pipe was not measured directly during the HET, but can be estimated indirectly from the measured flow rate and the hydraulic gradient.

If the flow condition is laminar, shear stress, τ is proportional to the mean velocity of flow, $\overline{V}$, so that

$$\tau = f_L \overline{V} \qquad \text{Eqn 2.14}$$

where f_L : is a friction factor for laminar flow condition.

If the flow condition is turbulent, τ is proportional to the square of $\overline{V}$ so that

$$\tau = f_T \overline{V}^2 \qquad \text{Eqn 2.15}$$

where f_T : is a friction factor for turbulent flow condition.

The mean velocity of flow, $\overline{V}$, can be estimated from the measured flow rate, Q by

$$\overline{V} = \frac{4Q}{\pi\phi^2} \qquad \text{Eqn 2.16}$$

Combining equations 2.13, 2.14, 2.15 and 2.16 gives

$$f_L = \frac{\rho_w g \pi s}{16} \frac{\phi^3}{Q} \qquad \text{Eqn 2.17}$$

and $$f_T = \frac{\rho_w g \pi^2 s}{64} \frac{\phi^5}{Q^2} \qquad \text{Eqn 2.18}$$

At a particularly time t, the diameter ϕ_t of the pipe can therefore be estimated from s_t, Q_t, f_{Lt} and f_{Tt}.

If laminar flow conditions apply, rearranging equation 2.18 gives

$$\phi_t = \left(\frac{16 Q_t f_{Lt}}{\pi \rho_w g s_t} \right)^{1/3} \qquad \text{Eqn 2.19}$$

If turbulent flow conditions apply, rearranging equation 2.19 gives

$$\phi_t = \left(\frac{64 Q_t^2 f_{Tt}}{\pi^2 \rho_w g s_t} \right)^{1/5} \qquad \text{Eqn 2.20}$$

During a HET, s and Q were measured at regular time intervals. The diameter of the pipe ϕ was known to be 6mm at the start of the test ($t = 0$), and was measured directly immediately after the test ($t = t_f$). The friction factors f_L and f_T both at the start and at the end of the test can, therefore, be estimated from equations 2.17 and 2.18.

In order that the diameter of the pipe at any time t during a HET can be estimated, the following three assumptions have been made:

i. the pre-formed pipe has a uniform cross-section along the length of the soil sample,

ii. the friction factor f_L or f_T vary linearly with time between its initial value at time $t = 0$, and its final value at $t = t_f$,

iii. the flow through the soil matrix is so small compared to the flow through the pre-formed hole that the former can be neglected.

The flow condition (i.e. laminar or turbulent) during the HET will determine the use of either equation 2.19 or 2.20 for estimating the pipe diameter. It has been assumed that flow is turbulent if Reynolds number R_e is larger than 5000. In most of the HETs so far carried out at a test head greater than 100mm, the flow condition was turbulent. R_e is defined by

$$R_e = \frac{\rho_w \bar{V} \phi}{\mu} \qquad \text{Eqn 2.21}$$

where μ is the coefficient of dynamic viscosity (10^{-3} kg/ms at 20 °C).

After calculating the diameter of the pre-formed pipe, the shear stress, τ_t, and the rate of erosion per unit area, $\dot{\varepsilon}_t$, along the pipe can then be estimated using equations 2.12 and 2.13. When $\dot{\varepsilon}_t$ is plotted against τ_t, the rising portion of the plotted curve can be approximated by a straight line, whose gradient and horizontal-intercept represent the Coefficient of Soil Erosion, C_e, and the Critical Shear Stress, τ_c, respectively as described by equation 2.10.

For HET, the *Erosion Rate Index* is designated as I_{HET}, and is defined by equation 2.11.

The following Section shows an example on how C_e and τ_c are estimated from HET test data.

Analysis of raw data obtained from a Hole Erosion Test

Analysis of the raw data of test HDHET9 on soil sample Hume is presented in this section to demonstrate the application of the theory on HET described in the preceding Section. The analysis involves the following steps:

- estimate the initial and final friction factors f_L and f_T based on the initial diameter, D_o, of the pre-formed hole (i.e. 6mm) and the measured final diameter of the widened hole, D_f, using equations 2.17 and 2.18,
- estimate the diameter of hole, ϕ_t, at any time, t, based on the measured flow rate, Q_t, the measured hydraulic gradient, s_t, and the estimated friction factor, f_L or f_T, at time t using equations 2.19 or 2.20,
- plot a curve of the estimated diameter of the hole against time, and estimate the slope of the curve at time t as shown in Figure 2.35,
- plot the rate of mass removal per unit area, $\dot{\varepsilon}_t$, and the shear stress, τ_t, against time as shown in Figure 2.36. τ_t and $\dot{\varepsilon}_t$ are estimated using equations 2.12 and 2.13 respectively. The derivative $d\phi_t/dt$ in equation 2.13 can be approximated by $\Delta\phi_t/\Delta t$ using numerical differentiation techniques, where $\Delta\phi_t$ represents the change in ϕ_t over a short time interval Δt,
- plot $\dot{\varepsilon}_t$ against τ_t as shown in Figure 2.37. The *Coefficient of Soil Erosion, C_e,* is the slope of straight line approximating the rising part of the curve. The intercept of the straight line on the horizontal axis represents the *Critical Shear Stress, τ_c*. Similar to the SETs, the initial section of the curve in Figure 2.37 shows a decrease in the erosion rate per unit area with an increase in shear stress. This early section of the curve corresponds to the removal of the loose, disturbed soils along the per-formed hole.
- the *Erosion Rate Index, I_{HET},* is equal to $-\log(C_e)$.

Similar to Figure 2.30 for the Slot Erosion Test, the initial section of the curve in Figure 2.37 shows a negative slope. This section of the curve corresponds to the erosion of the disturbed and relatively loose materials around the pre-formed hole at the early stage of the test.

The above procedure has been followed for analysing test data of the HET. A summary of the interpreted results of all HETs is shown in Appendix B.

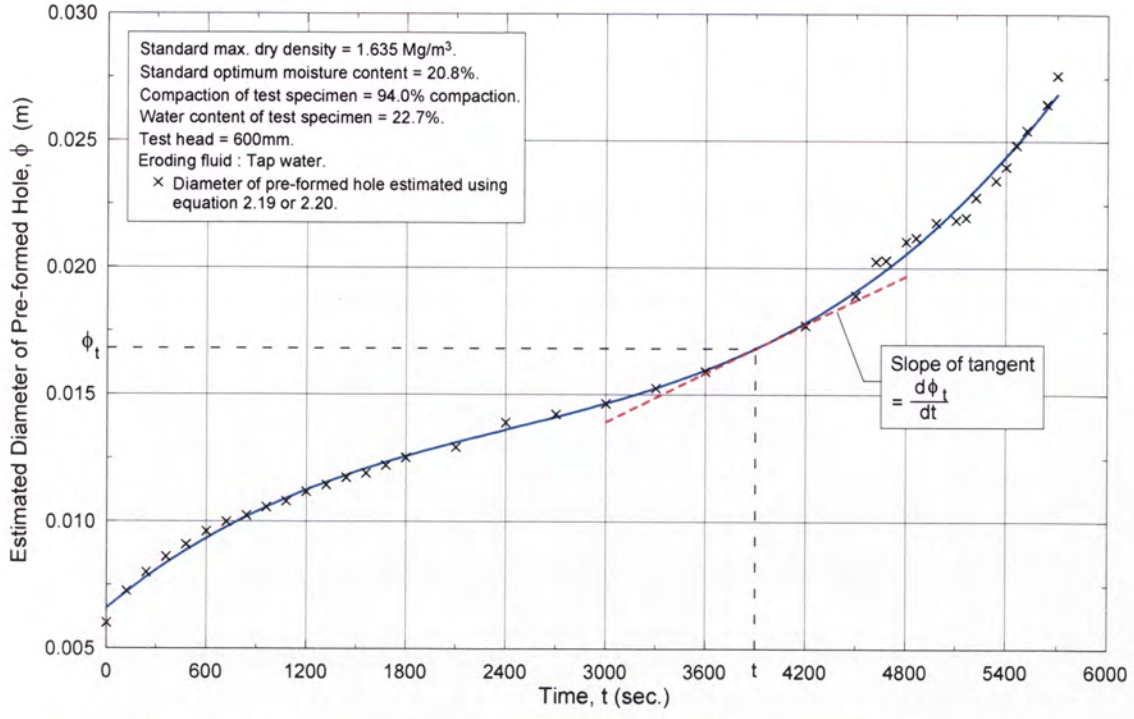

Figure 2.35: Estimation of diameter of pre-formed hole in a Hole Erosion Test using Test HDHET9 on soil sample Hume as an example.

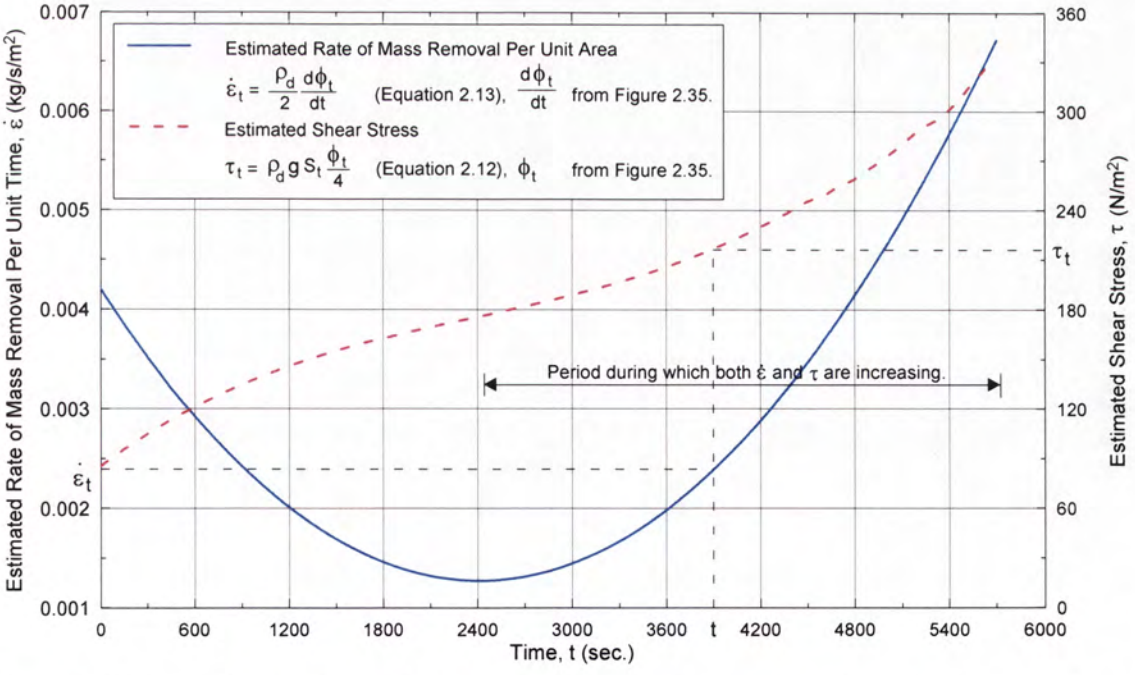

Figure 2.36: Estimated rate of mass removal per unit area and shear stress versus time in Hole Erosion Test HDHET9 on soil sample Hume.

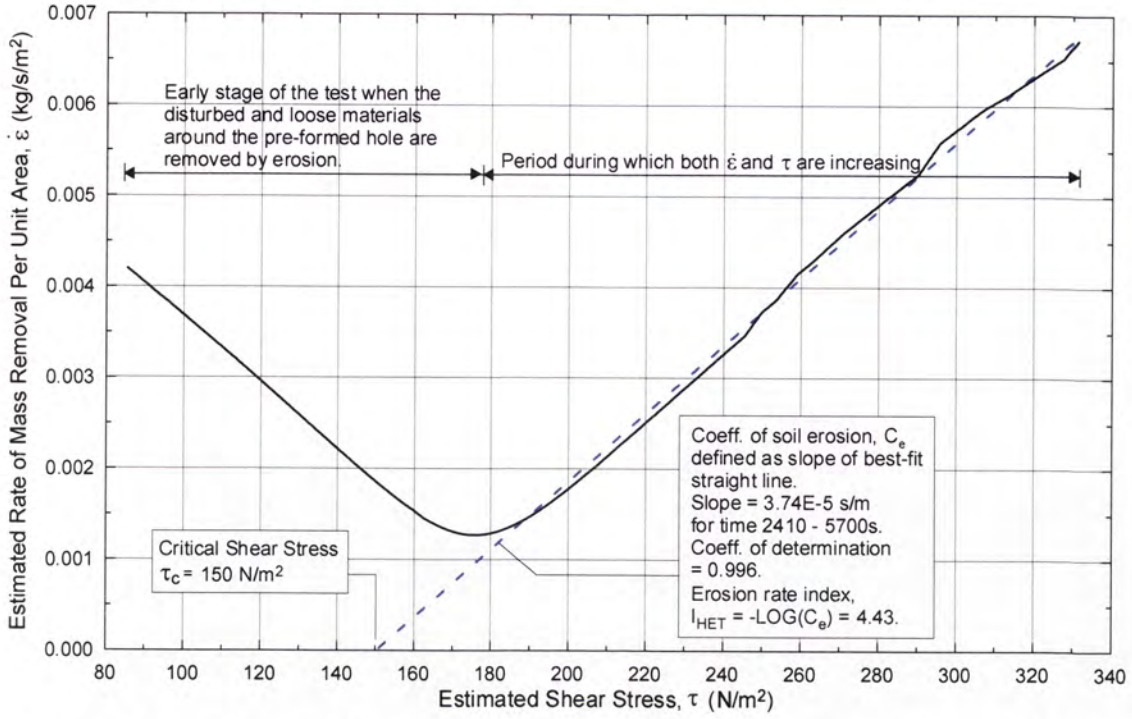

Figure 2.37: Estimated rate of mass removal per unit area versus estimated shear stress in Hole Erosion Test HDHET9 on soil sample Hume.

2.3.5 Measurement and control of test variables in a HET

The test variables controlled and measured in HETs are similar to those in SETs discussed under Section 2.3.3.

In HETs, however, the test head varied between soil samples rather than remained constant at 2.5 m as in SETs. The test head for HETs ranged from 50 mm for very erodible soils to 1200 mm for very erosion resistant soils. The test head can also vary between different specimens of the same soil sample.

Unlike the SET during which the erosion process can be monitored by measuring directly the average width of the pre-formed slot, the enlargement of the pre-formed hole in a HET test specimen cannot be observed during a HET. Therefore, the flow rate in HET is used as an indirect measurement of the erosion rate.

2.3.6 Special Slot Erosion Test and Hole Erosion Test

Apart from the normal SETs and HETs, three types of special tests were carried out, namely soaked tests, salt water tests and paused tests.

Soaked tests

The soaked tests were designed for studying the effects of prior wetting up on the erosion characteristics of a soil.

In a soaked SET, the test specimen with the slot formed was soaked in water for at least 18 hours prior to the erosion test. The erosion test was then carried out in the same manner as in a normal test. In a soaked HET, the test specimen together with the mould were soaked in water under a normal pressure of 6.9 kN/m^2 (1 psi). Any swelling of the specimens in the semi-confined longitudinal direction was measured by a dial-gauge. When the dial-gauge indicated no further swelling, the specimen was taken out of water. A 6mm diameter hole was then drilled along the axis, and the erosion test was then carried out.

Salt water tests

The salt water tests were designed for studying the effects of salt concentration of the eroding fluid on the erosion characteristics of a soil.

Sodium chloride (NaCl) solution was used as the eroding fluid. For SETs, 0.02M (1.169 g of NaCl per litre of water) solution was used. For HETs, both 0.02M and 0.005M (0.292 g/l) solutions were used.

Tap water was used for preparing the NaCl solutions. Tap water in the domestic water supply system contained approximately 60 mg/l of dissolved solids. This quantity does not significantly affect the concentration of the salt solutions. The concentration of the salt solutions were confirmed by testing the Na^+ concentration in solution samples collected from the source tank during the salt tests.

Paused tests

The paused tests were designed to study the effects of intermittent water supply on the erosion characteristics of a soil.

In a paused test, water was supplied intermittently so that there was a 15-minute pause period after each 15-minute period of erosion.

2.4 PROPERTIES OF SOIL SAMPLES USED IN SLOT EROSION TESTS AND HOLE EROSION TESTS

2.4.1 Origins of soil samples

SETs and HETs were carried out on thirteen soil samples. The source and origin of these soil samples are summarised in Table 2.7.

Table 2.7: Source and origin of soil samples used in Slot Erosion Tests and Hole Erosion Tests.

Geological origin	Soil sample		Location	Unified Soil Classification System (USCS)	Supplied by
Alluvial	Hume		Borrow area at Lake Hume, Albury	CL	DPWS, NSW
	Waranga Basin		Waranga Basin dam site near Shepparton, Vic.	CL	Goulburn-Murray Water
Colluvial	Fattorini		Borrow area at Fattorini Dam, Kempsey, NSW	CL	DPWS, NSW
Residual	Bradys	Derived from dolerite and basalt	Near Bradys Dam, Tasmania	CH	Hydro-electric Corporation
	Buffalo	From metamorphosed sediments and granite.	Core of Lake Buffalo Dam, near Myrtleford, Vic.	CL	Goulburn-Murray Water
	Jindabyne	From granite	Jindabyne Dam site on Snowy River near Cooma, NSW	SC	Snowy Mountain Hydro-electric Authority
	Lyell	From granite	Lyell Dam site near Lithgow, NSW	SM	
	Matahina	From greywacke sandstones	Matahina Dam, North Island, NZ	CL-ML	Damwatch Services Ltd.
	Shellharbour	From sandstones of andesitic/basaltic origin	Construction site, Shellharbour, NSW	CH	
	Waroona	From gneiss	Waroona Dam site on Drakes Brook near Waroona, WA	CL	Water Corporation
Glacial	Pukaki		Pukaki Dam site, South Island, NZ	SM	Damwatch Services Ltd.
	Rowallan		Rowallan Dam site, Tasmania	SM	Hydro-electric Corporation
Aeolian	Teton		Borrow area at Teton Dam, Idaho, USA	CL, ML	US Bureau of Reclamation

Soil sample 'Bradys', abbreviated 'BD', is a high plasticity sandy clay (CH). It is a yellow brown residual soil derived from dolerite and basalt, and was taken from a clay pit between Woodwards Marsh and Brady's Marsh north of Brady's Creek, Tasmania.

Soil sample 'Buffalo', abbreviated 'BuD', is a low plasticity clay (CL). It was taken from the upper part of the core of Lake Buffalo Dam located 20km south of Myrtleford, Victoria. It is a red brown residual soil from weathering of fluvial deposits which were breakdown products of metamorphosed sediments and the granites of the catchment.

Soil sample 'Fattorini', abbreviated 'FT', is a medium plasticity sandy clay (CL). It is a grey brown colluvium taken from a borrow area for the construction works at Fattorini Dam, Kempsey, NSW. The sample is also designated as Fattorini (b) in the test records so as to distinguish it from another soil sample taken from the same area a few years ago for doing No Erosion Filter Tests and Continuous Erosion Filter Tests.

Soil sample 'Hume', abbreviated 'HD', is a low plasticity sandy clay (CL). It is a grey brown Tertiary alluvium, and was obtained from a borrow area at Lake Hume, Albury in early 2000. The sample is also designated Lake Hume (b) in the test records so as to distinguish it from another soil sample taken from Lake Hume a few years ago for doing No Erosion Filter Tests and Continuous Erosion Filter Tests.

Soil sample 'Jindabyne', abbreviated 'JD', is a clayey sand (SC). It is a grey yellow residual soil derived from weathering of granite, and was obtained from Jindabyne Dam site located along Snowy River about 50km west of Cooma, NSW.

Soil sample 'Lyell', abbreviated 'LD', is a silty sand (SM). It is a grey residual soil derived from granites. It was taken from the abutment of Lyell Dam located approximately 7km south-west of Lithgow, NSW.

Soil sample 'Matahina', abbreviated 'MD', is a low plasticity clay (CL). It is a brown yellow residual soil derived from deep in-situ weathering of greywacke sandstones. It was taken from the core of Matahina Dam located on the Rangitaiki River in the Bay of Plenty Region in the North Island of New Zealand.

Soil sample 'Pukaki', abbreviated 'PD', is a silty sand (SM). It is a grey glacial till taken from the right abutment of Pukaki Dam located near Twizel in the middle of the South Island of New Zealand.

Soil sample 'Rowallan', abbreviated 'RD', is a silty sand (SM). It is a grey brown fine-grained glacial deposit obtained from a place approximately 100m downstream of Rowallan Dam, Tasmania.

Soil sample 'Shellharbour', abbreviated 'SH', is a high plasticity clay (CH) with some sand. It is a brown residual soil derived from sandstones, and was obtained from Shellharbour near Wollongong. The sandstones are of andesitic and basaltic origin.

Soil sample 'Teton', abbreviated 'TD', is a low plasticity clay (CL). It is a brown grey aeolian deposit taken from a borrow area north of the right abutment of Teton Dam, Idaho, USA.

Soil sample 'Waranga Basin', abbreviated 'WB', is a low plasticity clay (CL). It is a brown red alluvial deposit of the Shepparton Formation. The soil was taken from a test pit at the downstream slope of Waranga Basin Dam located 38km south west of Shepparton, Victoria.

Soil sample 'Waroona', abbreviated 'WD', is a low plasticity clay (CL). It is a yellow brown residual soil derived from gneiss. The soil was taken from test pits immediately downstream of Waroona Dam located on Drakes Brook, some 5.5km east of the town of Waroona, WA.

2.4.2 Basic information on engineering classification of soil samples

Detailed results of classification tests on the 13 soil samples are presented in the Factual Data Report. A summary of the results of engineering classification is shown in Table 2.8. The various soil samples, except Lyell, Pukaki and Rowallan, are plotted on the plasticity chart in Figure 2.38, and their particle size distribution curves are shown in Figure 2.39. Liquid Limit and Plastic Limit tests showed that Lyell, Pukaki and Rowallan are non-plastic soils designated NP.

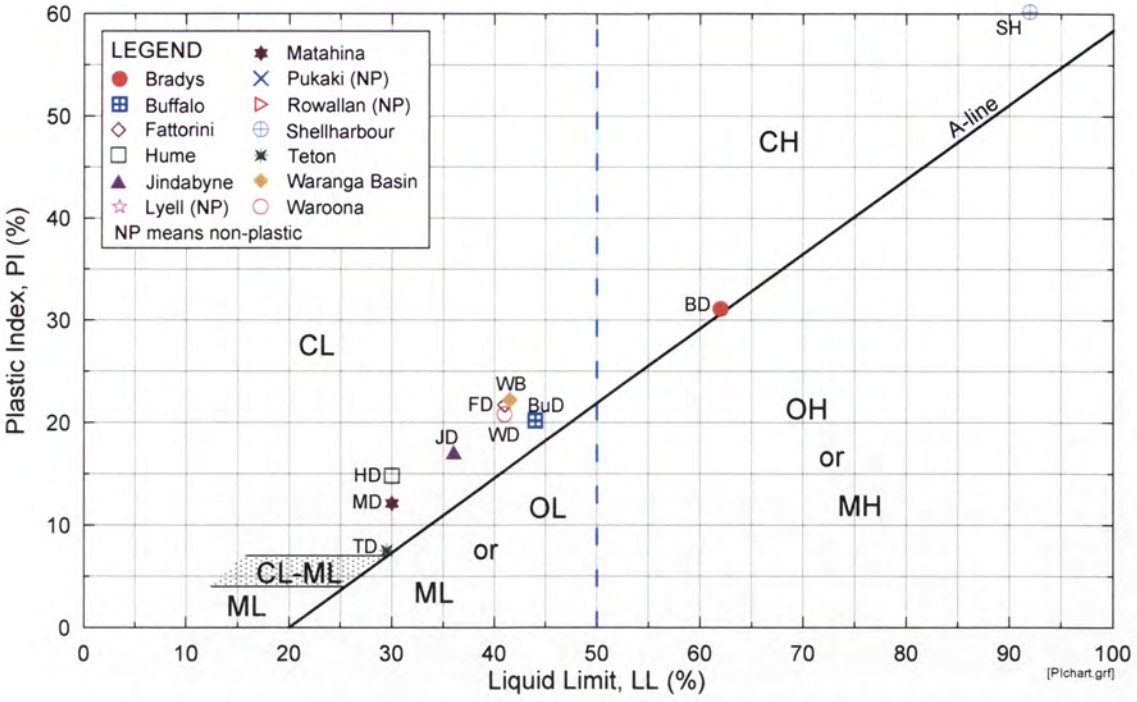

Figure 2.38: Plasticity Chart showing plasticity of soil samples. Lyell, Pukaki and Rowallan are non-plastic (NP) and not shown on the chart.

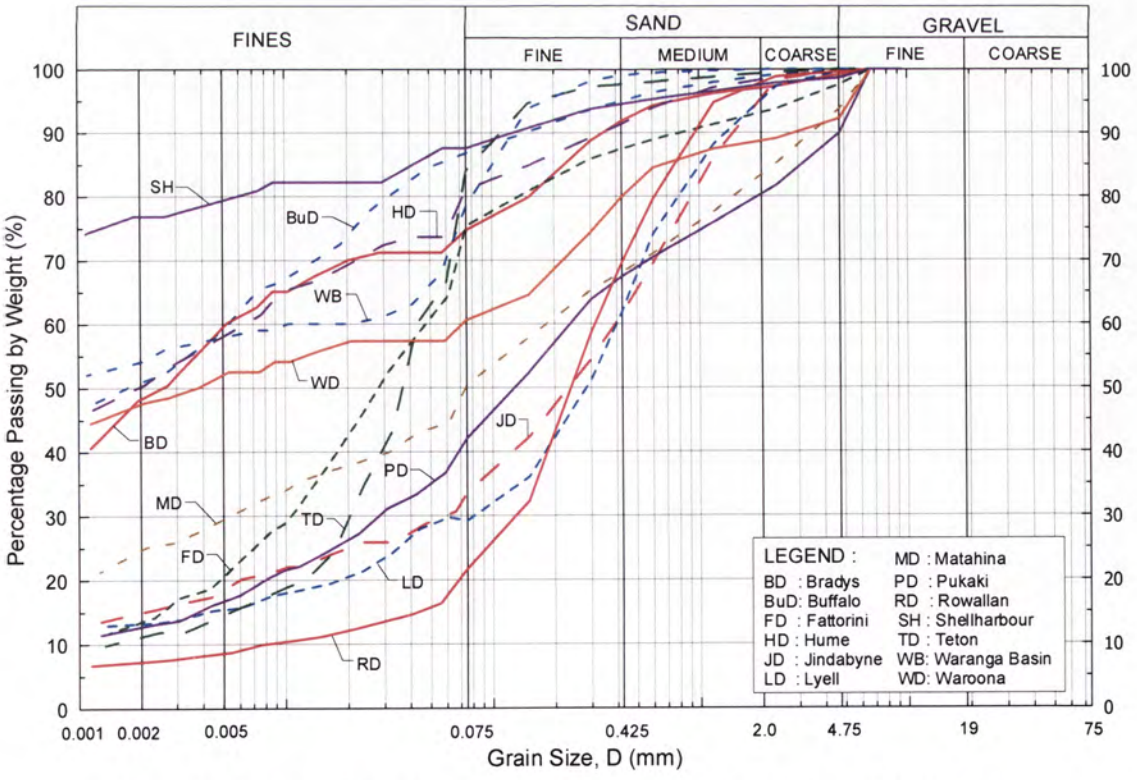

Figure 2.39: Particle Size Distribution Curves for the 13 Soil Samples.

2.4.3 Soil dispersivity

A summary of the results on dispersivity tests is shown in Table 2.9. Also presented in the table are the Sodium Adsorption Ratios, *SAR*s, the major cation contents, pH and electrical conductivity of the saturation extracts of the soil samples. The *SAR*s are calculated from the major cation contents of the saturation extracts of the soil samples.

2.4.4 Mineralogy

X-ray Powder Diffraction Analysis on the 13 soil samples has been carried out by the School of Geology, UNSW. Reports on the analysis are included in Appendix K of this report. Table 2.10 summarises the results of the X-ray Powder Diffraction Analysis. Also shown in the table are the mass fractions of the clay size (i.e. < 0.002 mm) particles in each soil samples obtained from hydrometer analysis.

It should be noted that crystals of clay minerals are not necessarily finer than 0.002 mm, and soils particles finer than 0.002 mm are not necessarily crystals of clay minerals. A detailed study on the clay mineralogy of soil sample "Buffalo" has been undertaken by Hensel, H.D. (2001), and a copy of his report is presented at Appendix L.

Table 2.8: Engineering classification of soil samples.

Soil Sample	Soil Particle density	Particle Size Distribution					Unified Soil Classification System (USCS)	Standard Max. Dry Density	Optimum Water Content	Atterberg's Limit		Activity (Note 2)
		%Gravel	%Sand	%Fines (Silts and Clay)	%Clay_US (Note 1) %<0.005mm	%Clay_UK (Note 1) %<0.002mm				Liquid Limit	Plasticity Index	
	Mg/m^3							Mg/m^3	OWC (%)	%	%	
Bradys	2.74	1%	24%	75%	60%	48%	CH	1.32	35.0%	62%	31%	0.65
Buffalo	2.72	0%	13%	87%	59%	50%	CL	1.72	19.5%	44%	20%	0.40
Fattorini	2.68	2%	22%	75%	20%	14%	CL	1.70	18.5%	41%	22%	1.53
Hume	2.71	0%	19%	81%	59%	51%	CL	1.64	21.0%	30%	15%	0.29
Jindabyne	2.68	0%	66%	34%	18%	15%	SC	1.75	16.0%	36%	17%	1.11
Lyell	2.61	0%	70%	29%	15%	13%	SM	1.96	10.0%	NP	NP	---
Matahina	2.67	6%	43%	50%	29%	25%	CL	1.81	16.5%	30%	12%	0.48
Pukaki	2.70	10%	48%	42%	17%	13%	SM	2.15	8.5%	NP	NP	---
Rowallan	2.82	0%	78%	22%	9%	7%	SM	1.87	13.5%	NP	NP	---
Shellharbour	2.75	1%	11%	88%	80%	77%	CH	1.25	41.0%	92%	60%	0.78
Teton	2.67	0%	16%	84%	14%	12%	CL	1.64	18.5%	30%	8%	0.63
Waranga Basin	2.69	0%	21%	79%	58%	54%	CL	1.67	19.0%	42%	22%	0.41
Waroona	2.61	8%	32%	61%	52%	48%	CL	1.59	23.0%	41%	21%	0.44

Note

1 In US, soil particles finer than 0.005mm are described as clay-size particles. The mass fraction of the soil finer than 0.005mm is designed %Clay_US.
In UK, soil particles finer than 0.002mm are described as clay-size particles. The mass fraction of the soil finer than 0.002mm is designed %Clay_UK.

2 Activity is defined as the ratio between the Plastic Index (%) and the mass fraction (%) finer than 0.002mm.

Table 2.9: Dispersivity and physiochemical properties of saturation extracts of the soil samples.

Soil Sample	Dispersivity			Tests on Saturation Extract		
	Pinhole Test	Emerson Class	SCS Dispersion Test % Dispersion	Sodium Adsorption Ratio (SAR)	pH	Electrical conductivity (mS)
Bradys	PD1/PD2	5	22%	0.83	7.3	109
Buffalo	ND1	6	4%	0.70	6.3	105
Fattorini	ND2	5	58%	4.95	6.7	239
Hume	D1	1	75%	18.32	8.6	1705
Jindabyne	D1	3	46%	1.31	7.1	71
Lyell	D1	5	25%	0.87	6.5	426
Matahina	D1	3	60%	1.72	7.6	246
Pukaki	D1	5	35%	0.49	8.0	968
Rowallan	D1	5	34%	0.39	7.1	206
Shellharbour	ND1	5	8%	6.60	7.6	426
Teton	PD2	5	25%	2.32	9.0	405
Waranga Basin	D1	1	69%	29.58	8.8	13
Waroona	ND1	6	4%	1.90	7.3	127

Table 2.10: Summary of soil sample mineralogy.

Soil Sample	Fraction finer than 0.002mm from hydrometer test	Non-clay minerals		Clay minerals						Other soil minerals						
		Quartz	Feldspars	Kaolinite	Chlorite	Illite/mica	Smectite	Vermiculite or Vermiculite/Chlorite	Mixed layer mica/smectite	Anatase	Calcite	Goethite	Hematite	Gypsum	Jarosite	Siderite
Bradys	48%	A	T	M		T	S			T	T?					
				79%			21%									
Buffalo	50%	D	T-S	S	S	S		T		T-S		T	T	T?	T?	
				25%		52%		23%								
Fattorini	14%	A	S	S		T	S-T		T	S		S				
				23%		57%	20%									
Hume	51%	A-M	S	M-S		M-S	S-T			T		T-S				T
				30%		51%	19%									
Jindabyne	15%	A	M	S		M	T-S			T					T	
				53%		30%	17%									
Lyell	13%	M	A	S-T				T		T					T	
				D				S								
Matahina	25%	A	A-M	S		S	S			T?	T?			T	T?	
				14%		59%	27%									
Pukaki	13%	A	A		S	S	T	T								T?
					14%	50%		36%								
Rowallan	7%	A	M	S	S	S				T?						
				M	A (may contain some expandable layers)		T									
Shellharbour	77%	M	A-M	M		T			T	T	T?	S	S			
				D (mainly Halloysite)					T							
Teton	12%	A	S	S	T	S	S			T?	S	T?	T-S		T?	T-S
				17%		29%	54%									
Waranga Basin	54%	A	T	S		S	T			T?		T	T?			T?
				23%		59%		17%								
Waroona	48%	A	S-T	M		T						T				
				87% (Mainly Gibbsite)		13%										

Notes :

1 D = dominant (>60%)
A = abundant (60 - 40%)
M = moderate (40 - 20%)
S = small (20 - 5%)
T = traces (<5%)

2 The given percentage composition of clay minerals are semi-quantitative estimates based on the method by Griffin (1970).

2.5 ANALYSIS OF TEST RESULTS

2.5.1 Summary of interpreted test data

All raw data from the SETs and HETs have been analysed according to the procedures described in Sections 2.3.2 and 2.3.4. Appendix A summarises the test parameters and the major outcomes of the analysis of the SET data, namely the *Coefficient of Soil Erosion,* C_e, and the *Critical Shear Stress,* τ_c. Appendix B shows a similar summary, but for the HET data. The summaries include interpreted results of both successful and unsuccessful tests, and the normal and special tests. Special tests are soaked tests, salt water tests and paused tests described in Section 2.3.6.

2.5.2 Graphical presentation of test results

Erosion Rate Indices versus soil samples

Figure 2.40 and Figure 2.41 show the Erosion Rate Indices based on the SETs and HETs respectively. In order to allow for observation of trends, results of the special tests are not included in these Figures. Results of the special tests are discussed in later sections.

The 13 soil samples are divided into two groups, namely fine-grained soils and coarse-grained soils. Fine-grained soils have a fines content exceeding 50% by mass. Fines means soil particles finer than 0.075 mm. The nine fine-grained soil samples are Bradys, Buffalo, Fattorini, Hume, Matahina, Shellharbour, Teton, Waranga Basin and Waroona. Coarse-grained soils are soils with a fines content of less than 50% by mass. The five coarse-grained soil samples are Jindabyne, Lyell, Pukaki, Rowallan and Matahina. For the purpose of this experimental investigation, Matahina is considered both a fine-grained soil and a coarse-grained soil, as its fines content (50.5%) is only marginally above 50%.

Figure 2.40 and Figure 2.41 show considerable range of the Erosion Rate Indices for each of the soil samples. The Erosion Rate Indices of two different tests on the same

soil sample can differ in value by 2 to 3, representing a difference of approximately 100 to 1000 times in the *Coefficient of Soil Erosion,* C_e. The range is due mainly to the fact that test specimens were compacted to different degree of compaction at different water contents. Some specimens were compacted to 92% or lower of the standard maximum dry density, and a few percent dry of optimum water content, whereas some were compacted to as high as 99% of standard maximum dry density and wet of optimum.

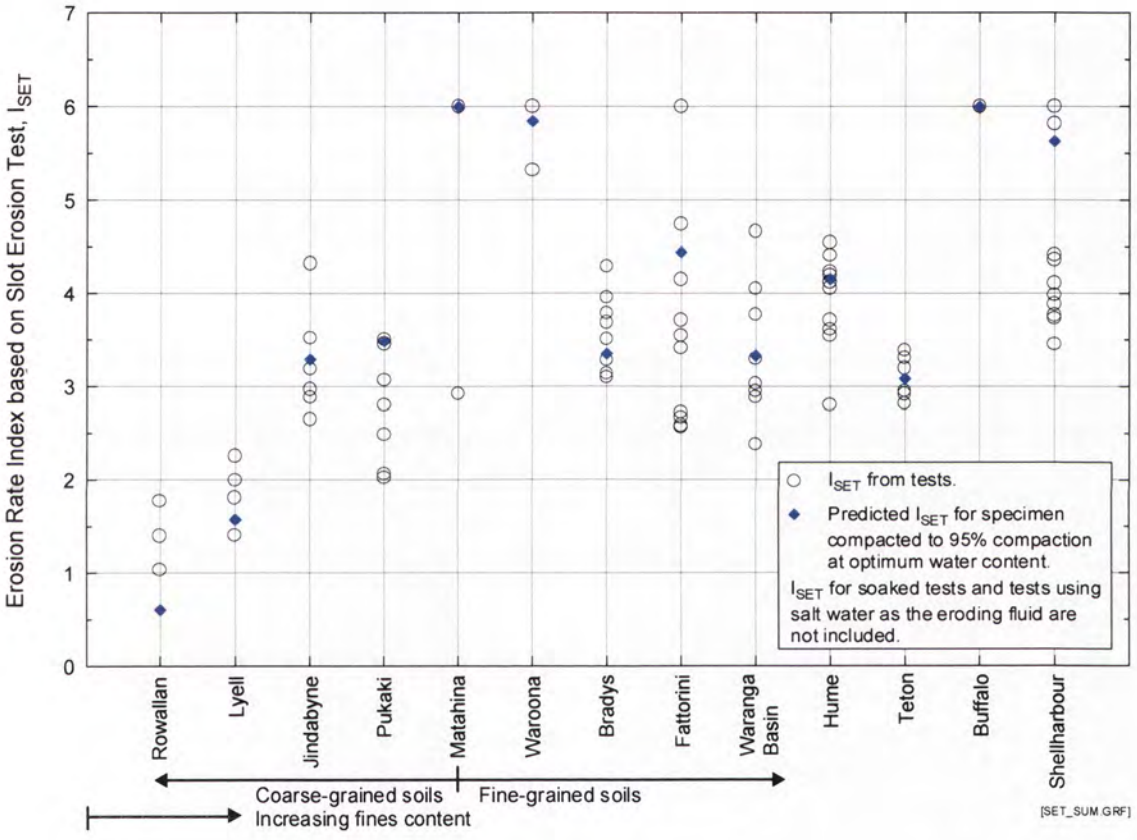

Figure 2.40: Summary of I_{SET} for all successful Slot Erosion Tests.

Figure 2.40 and Figure 2.41 reveal that the coarse-grained soil samples, in general, have lower Erosion Rate Indices than the fine-grained soil samples, that is they erode more rapidly. Most of the tests on coarse-grained soil samples resulted in Erosion Rate Indices less than 4, and most of the tests on fine-grained samples resulted in Erosion Rate Indices higher than 2.

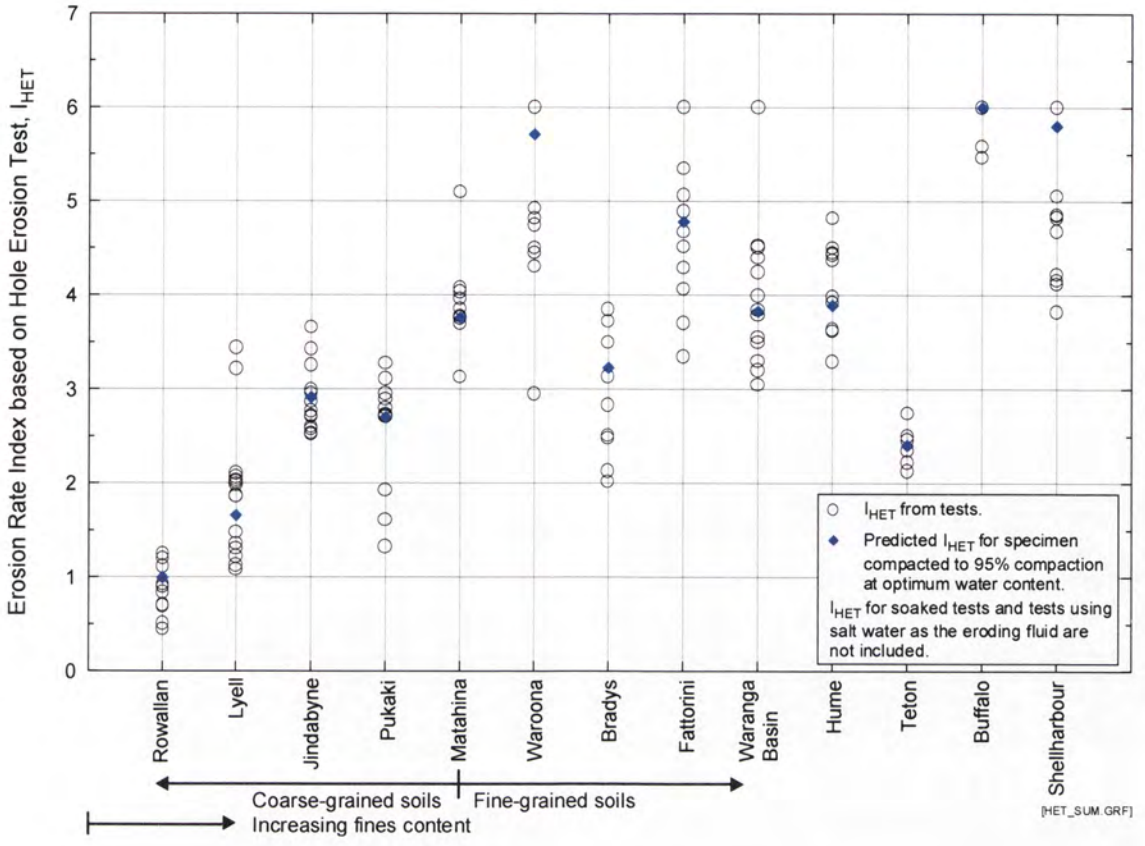

Figure 2.41: Summary of I_{HET} for all successful Hole Erosion Tests.

Figure 2.40 and Figure 2.41 also reveal the trend that the Erosion Rate Indices of the coarse-grained soil samples increase with the fines content. In other words, coarse-grained soils are more erosion-resistant as their fines content increases. The same trend is, however, not observed among the fine-grained soil samples.

Also shown in Figure 2.40 and Figure 2.41 are the predicted Erosion Rate Indices at 95% compaction and optimum water content (OWC) for each soil sample. The predicted indices ($\tilde{I}_{SET}$ for SET and $\tilde{I}_{HET}$ for HET) at 95% compaction and OWC are used to represent the erosion characteristics of a particular soil sample. Detailed discussions on how $\tilde{I}_{SET}$ and $\tilde{I}_{HET}$ are estimated are given in following Section.

Representative Erosion Rate Index

The wide variation in the values of the Erosion Rate Index of a soil makes it difficult to compare the erodibility of various soil samples. Instead of comparing two ranges of Index values, it is more convenient comparing two Erosion Rate Indices which are representative of the soil samples. As earth embankments are generally specified to be compacted to at least 95% of the standard maximum dry density at around OWC, a reasonable choice of the representative Erosion Rate Index is the one corresponding to 95% compaction at OWC. This representative index is designated $\tilde{I}_{SET}$ for SET, and $\tilde{I}_{HET}$ for HET.

Preferably a SET or HET should be carried out at 95% compaction and OWC for finding $\tilde{I}_{SET}$ or $\tilde{I}_{HET}$. It is, however, not uncommon that the density and moisture conditions of the test specimen will deviate slightly from the desired 95% compaction and OWC due to slight errors in compaction and moisture control. Regression models were, therefore, developed to predict $\tilde{I}_{SET}$ or $\tilde{I}_{HET}$ from all available values of I_{SET} or I_{HET} for test specimens at and around 95% compaction and OWC. Even if an index were successfully obtained from a test on a specimen prepared to exactly 95% compaction and OWC, it would still be desirable to estimate the representative index from all available indices by the regression method to avoid the risk of adopting directly the index value from a single test.

Proposed regression models for predicting I_{SET} or I_{HET} from the degree of compaction and water content are presented in Table 2.11.

For each soil sample, the model coefficients of each of the 9 proposed regression models were evaluated by substituting relevant data points (X, Y, I) into the models, and applying the method of least squares to minimise the sum of squared errors in I. Relevant data points include the results of all successful tests on specimens prepared at or around 95% compaction and OWC. This usually covers a dry density range of 92% to 99% of the standard maximum dry density, and a water content range of OWC $\pm$ 3%. A non-linear regression analysis program called NONLIN (Dennis et al 1981) was used to evaluate the model coefficients. Each model was then used to prepare a contour

diagram of predicted I values, with X and Y as the independent variable. The regression model that produced the most reasonable contour pattern and the best correlation coefficient was chosen to represent the soil sample. The chosen model was then used to predict $\tilde{I}_{SET}$ and $\tilde{I}_{HET}$ by putting $X = 95\%$ and $Y = 0$. The chosen regression models and the corresponding model coefficients for the 13 soil samples are summarised in Tables C1 and C2 at Appendix C. Also found in the tables are the predicted $\tilde{I}_{SET}$ and $\tilde{I}_{HET}$ for each soil sample.

Table 2.11: Regression Models for predicting I_{SET} and I_{HET} from percentage compaction and water content.

Regression Model No.	Model coefficients					
	$I = a + b \cdot X + c \cdot Y + d \cdot X \cdot Y + e \cdot X^2 + f \cdot Y^2$ for models 1 - 8					
	a	b	c	d	e	f
1	√	√	√			
2	√	√	√	√		
3	√	√	√	√	√	
4	√	√	√		√	
5	√	√	√			√
6	√	√	√	√		√
7	√	√	√		√	√
8	√	√	√	√	√	√
	$I = a + b \cdot \log(\rho_d) + c \cdot \log(\omega/100)$ for model 9					
9	√	√	√			

Notes :

1. I represents the Erosion Rate Index I_{SET} or I_{HET}, depending on whether the non-linear regression is carried out on Slot Erosion Test data or Hole Erosion Test data.
2. A tick '√' below the model coefficient means that the coefficient is assumed non-zero, and whose value is obtained during the non-linear multivariate regression analysis.
3. For models 1 – 8, $X = (\rho_d / \rho_{d_{max}}) * 100\%$, where ρ_d [Mg/m^3] is the dry density of the test specimen, and $\rho_{d_{max}}$ [Mg/m^3] is the standard maximum dry density. Y represents the deviation of the water content, ω from the optimum water content, ω_o (i.e. $Y = \omega - \omega_o$). Both ω_o and $\rho_{d_{max}}$ are obtained from a standard compaction test. X, Y, ω and ω_o are in %.

Figure 2.42 and Figure 2.43 show the Erosion Rate Indices obtained from SETs and HETs on soil sample "Fattorini" as well as the dry densities and water contents at which the test specimens were prepared. In these figures, contour lines are plotted to show how the Erosion Rate Indices vary with dry density and water content. These contour lines are based on Erosion Rate Indices predicted by regression models described earlier. Figure 2.44 and Figure 2.45 show similar plots, but for soil sample "Jindabyne". Similarly plots for all 13 soil samples are presented in Appendix D.

Figures D1 to D13 in Appendix D reveal in most of the soil samples, the trend that the lower the degree of saturation of a test specimen, the lower will be the Erosion Rate Index, i.e. the rate of erosion is higher. This trend, however, is not observed in the non-plastic coarse-grained soil samples Lyell, Pukaki and Rowallan. For Lyell, Pukaki and Rowallan, it appears that test specimens compacted at low density but high water content will also produce lower Erosion Rate Indices, with the highest index for specimens compacted at optimum water content.

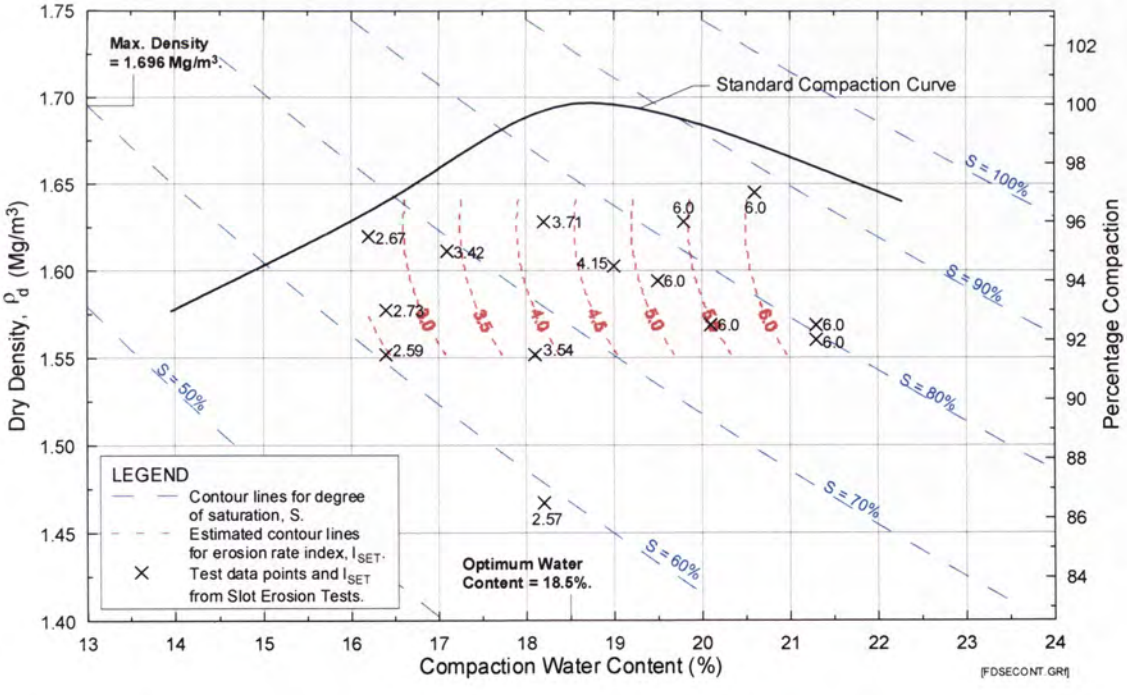

Figure 2.42: Erosion Rate Indices, I_{SET} based on SETs on soil sample Fattorini.

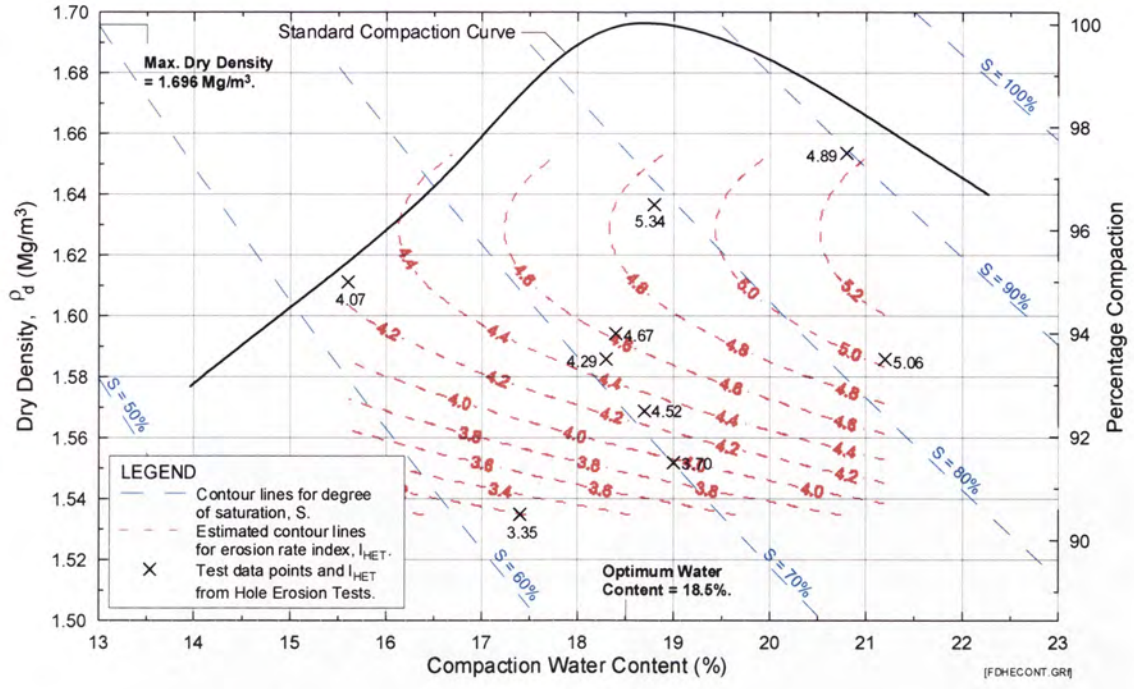

Figure 2.43: Erosion Rate Indices, I_{HET} based on HETs on soil sample Fattorini.

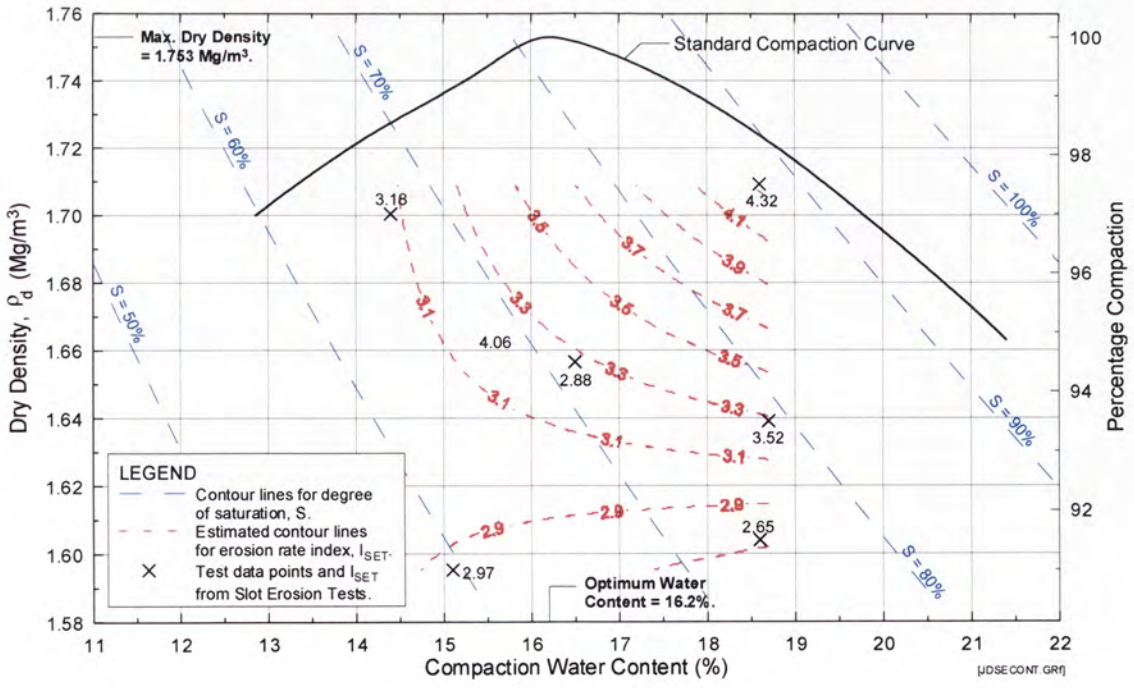

Figure 2.44: Erosion Rate Indices, I_{SET} based on SETs on soil sample Jindabyne.

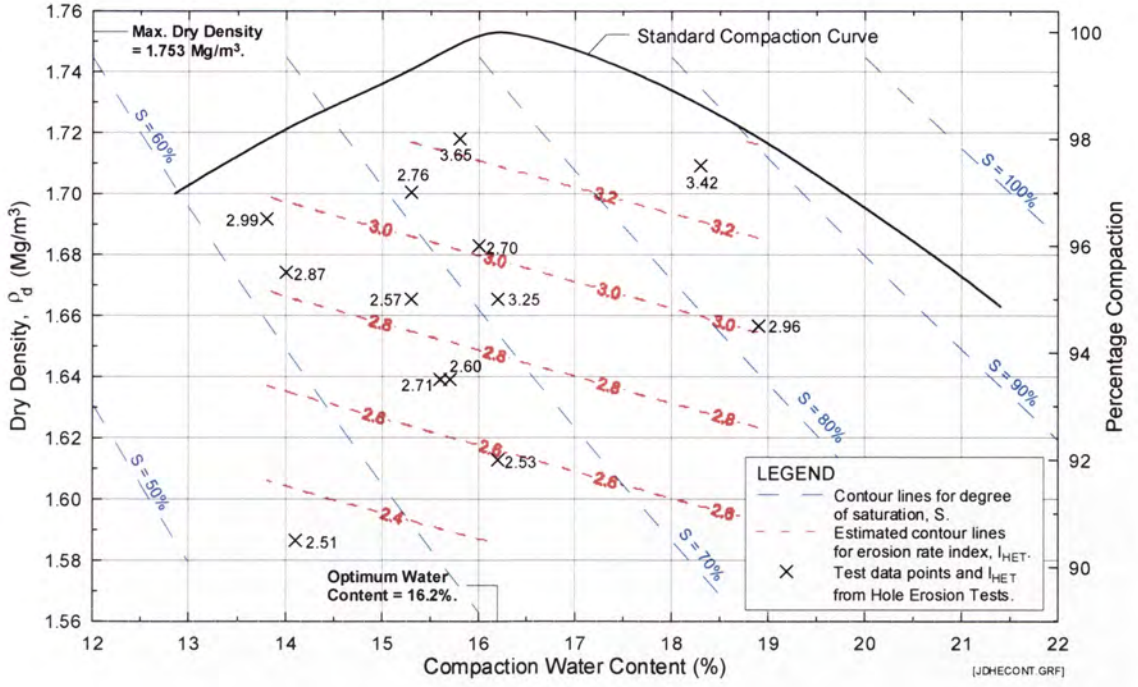

Figure 2.45: Erosion Rate Indices, I_{HET} based on HETs on soil sample Jindabyne.

The accuracy of the non-linear regression models and the contour diagrams for the Erosion Rate Indices depends on the number of available data points used for developing the regression models, and the distribution of the data points throughout the dry density – water content domain. In many cases the contours are based on limited data and are a statistical fit to the data, not necessarily the true picture of the relationship between Erosion Rate Index, Percentage Compaction and Water Content. The more data points available for developing the regression model, and the more uniform these data points are distributed throughout the dry density – water content domain, the more accurate will be the regression model. The regression model should not be used to predict Erosion Rate Indices at regions of very high or very low dry density, or at regions of very high or very low water content, as there are usually insufficient data points at these regions to define accurately the pattern of variations of the Erosion Rate Indices.

It will be noted that the Erosion Rate Index (reflecting the rate of erosion) covers nearly 6 orders of magnitude on the soil samples tested, with some soil samples eroding very

rapidly (e.g. Rowallan, Lyell), and others with very slow rates (virtually non-erodible) (e.g. Buffalo, Shellharbour, and Waroona). Four of the dams represented have experienced internal erosion and piping:

- Rowallan – piping incident soon after first filling;
- Matahina – two piping incidents involving the discovery of large sinkholes;
- Waranga Basin – several piping incidents on first filling;
- Teton – piping failure on first filling.

Erosion Rate Indices versus soil properties

Some basic soil parameters are believed to influence the erosion characteristics of a soil. These parameters are classified into four main groups. The first group, which includes parameters that define the density and moisture conditions of a soil, consists of dry density (ρ_d), compaction water content (ω), ratio of dry density to standard maximum dry density ($\rho_{d_{max}}$) (i.e. $\rho_d / \rho_{d_{max}}$) (or simply called percentage compaction), deviation of ω from optimum water content (*OWC*) expressed as a percentage of the *OWC* (i.e. $(\omega - OWC)/OWC$) (or simply called water content ratio, $\Delta\omega_r$), and the degree of saturation (*S*). The second group consists of parameters that define the particle size distribution of a soil, viz. gravel content, sand content, fines content and clay content. The third group consists of the Atterberg's limits (i.e. Liquid Limit and Plasticity Index) and Activity. Parameters that define the dispersivity of a soil, namely the Pinhole Test Classification, Emerson Class, SCS Percentage Dispersion, Sodium Adsorption Ratio, *SAR* and the Major Cation Content, are included in the fourth group. Those soil parameters in the first group vary between test specimens, whereas those parameters in the other three groups vary only between soil samples.

Group 1 parameters : Density and moisture conditions

The Erosion Rate Indices are plotted against the dry density (ρ_d), the percentage compaction ($\rho_d / \rho_{d_{max}}$), the water content (ω), the water content ratio ($\Delta\omega_r$), and the degree of saturation, *S* in Figures E1 to E10 at Appendix E. In addition, the Representative Erosion Rate Indices of the 13 soil samples are plotted against their respective standard maximum dry density and optimum water content in Figures E11a and E11b in Appendix E.

The plots show considerable scattering of the data points. Observations from the plots are summarised as follows:

- I_{SET}, I_{HET} versus dry density (ρ_d) in Figures E1 and E2 in Appendix E

  No relationship between the Erosion Rate Indices and the dry density is observed. The plots only show that, in general, coarse-grained soil samples usually have higher dry densities than the fine-grained soil samples. There is also no obvious relationship between the Representative Erosion Indices ($\tilde{I}_{SET}$ and $\tilde{I}_{HET}$) and the dry density as shown in Figures E1c and E2c.

- I_{SET}, I_{HET} versus percentage compaction ($\rho_d / \rho_{d_{max}}$) in Figures E3 and E4

  No relationship between the Erosion Rate Indices and the dry density is observed as shown in Figure 2.46, Figure 2.47 and Figure 2.48, and Figure 2.49.

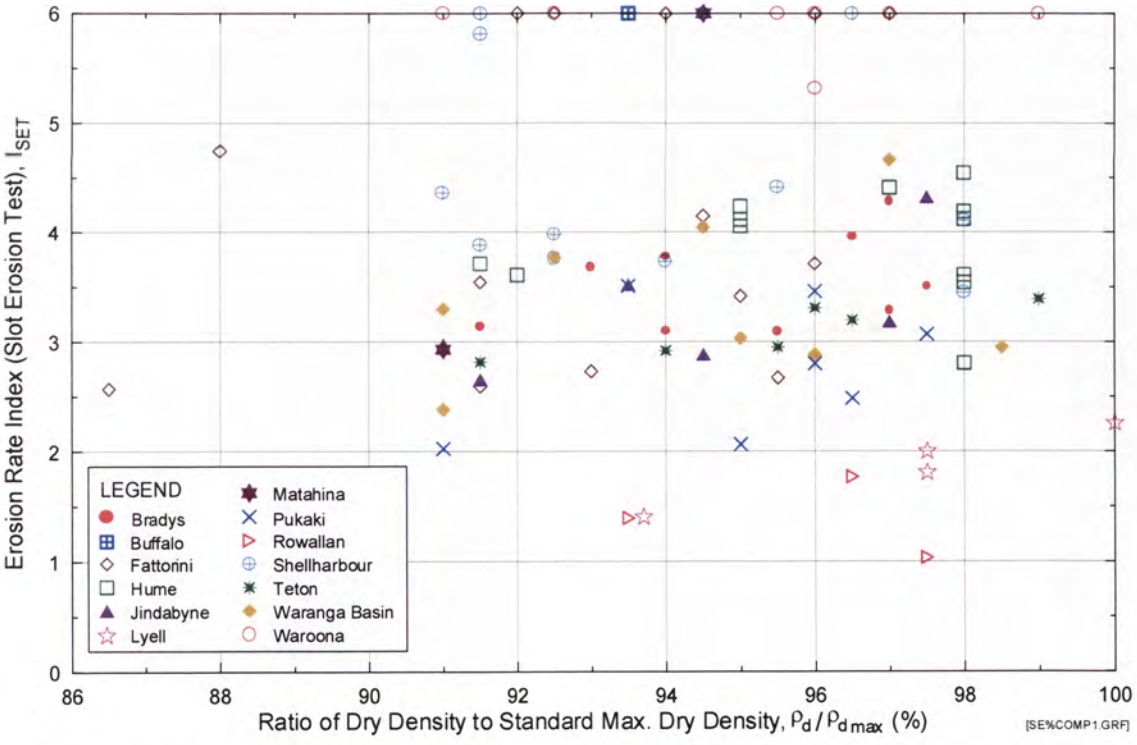

Figure 2.46: Erosion Rate Index (I_{SET}) from Slot Erosion Test versus Percentage Compaction ($\rho_d / \rho_{d_{max}}$). (Same as Figure E3a in Appendix E)

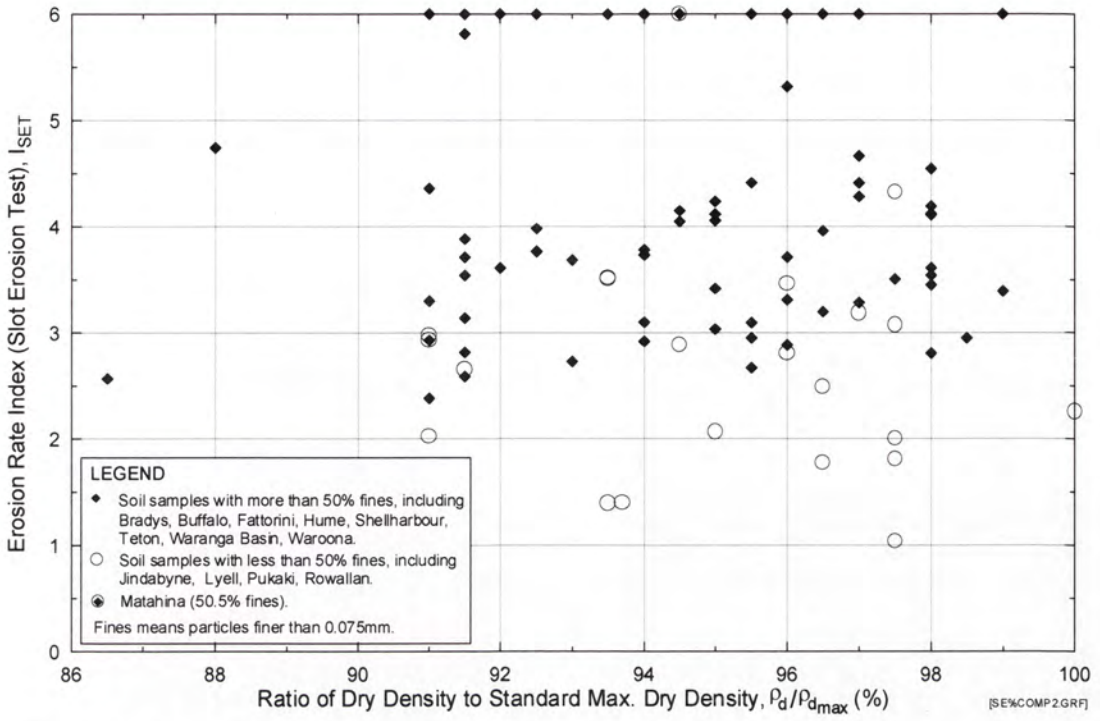

Figure 2.47: Erosion Rate Index (I_{SET}) from Slot Erosion Test versus Percentage Compaction ($\rho_d / \rho_{d_{max}}$). Soil samples classified into fine-grained soils and coarse-grained soils. (Same as Figure E3b in Appendix E)

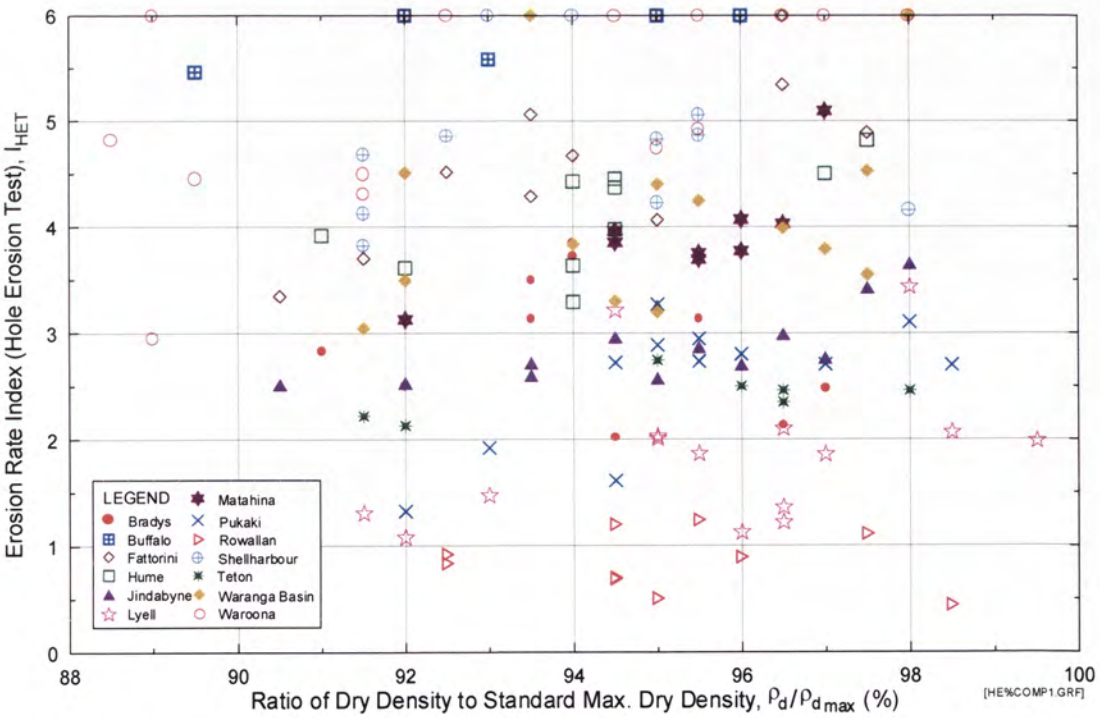

Figure 2.48: Erosion Rate Index (I_{HET}) from Hole Erosion Test versus Percentage Compaction ($\rho_d / \rho_{d_{max}}$). (Same as Figure E4a in Appendix E)

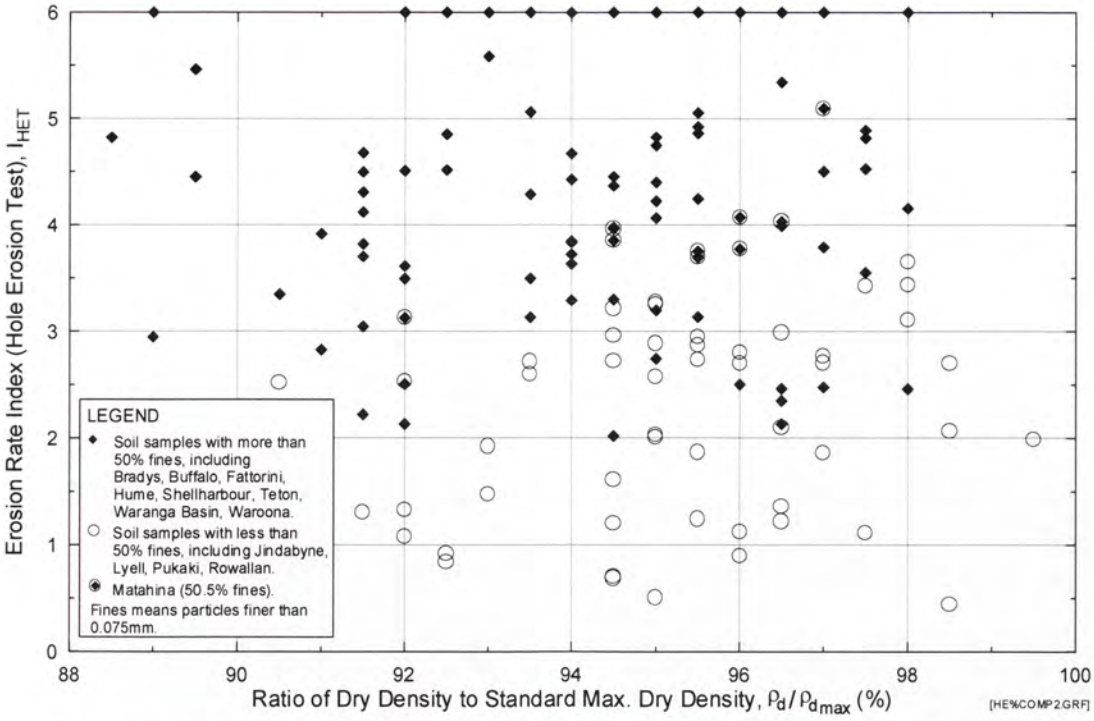

Figure 2.49: Erosion Rate Index (I_{HET}) from Hole Erosion Test versus Percentage Compaction ($\rho_d / \rho_{d_{\max}}$). Soil samples classified into fine-grained soils and coarse-grained soils. (Same as Figure E4b in Appendix E)

- I_{SET} , I_{HET} versus water content (ω) in Figures E5 and E6

  No relationship between the Erosion Rate Indices and the water content is observed. The plots only show that, in general, coarse-grained soil samples usually have lower compaction water content than the fine-grained soil samples. There is also no obvious relationship between the Representative Erosion Indices ($\tilde{I}_{SET}$ and $\tilde{I}_{HET}$) and the compaction water content as shown in Figures E5c and E6c.

- I_{SET} , I_{HET} versus water content ratio ($\Delta\omega_r$) in Figures E7 and E8

  No relationship between the Erosion Rate Indices and the dry density is observed as shown in Figure 2.50, Figure 2.51 and Figure 2.52, Figure 2.53.

- I_{SET} and I_{HET} versus degree of saturation (S) in Figures E9 and E10

  Tests on specimens having a lower degree of saturation apparently gave relatively lower Erosion Rate Indices as shown in Figure 2.54, Figure 2.55 and Figure 2.56, Figure 2.57. The plots of the Representative Erosion Indices versus

the degree of saturation corresponding to the optimum water content in Figure 2.58, Figure 2.59 show that the Erosion Rate Index increases with the degree of saturation (i.e. slower erosion rate at a higher degree of saturation). A good linear relationship between the Representative Erosion Indices and the degree of saturation is observed among the coarse-grained soil samples.

- Representative Erosion Rate Indices ($\tilde{I}_{SET}$ and $\tilde{I}_{HET}$) versus standard maximum dry density ($\rho_{d_{\max}}$) and optimum water content (OWC) in Figures E11a and E11b The predicted Representative Erosion Rate Indices are marked against the OWC and $\rho_{d_{\max}}$ of the respective soil samples in Figure 2.60 and Figure 2.61. No obvious relationship is observed between $\tilde{I}_{SET}$, $\tilde{I}_{HET}$, OWC and $\rho_{d_{\max}}$.

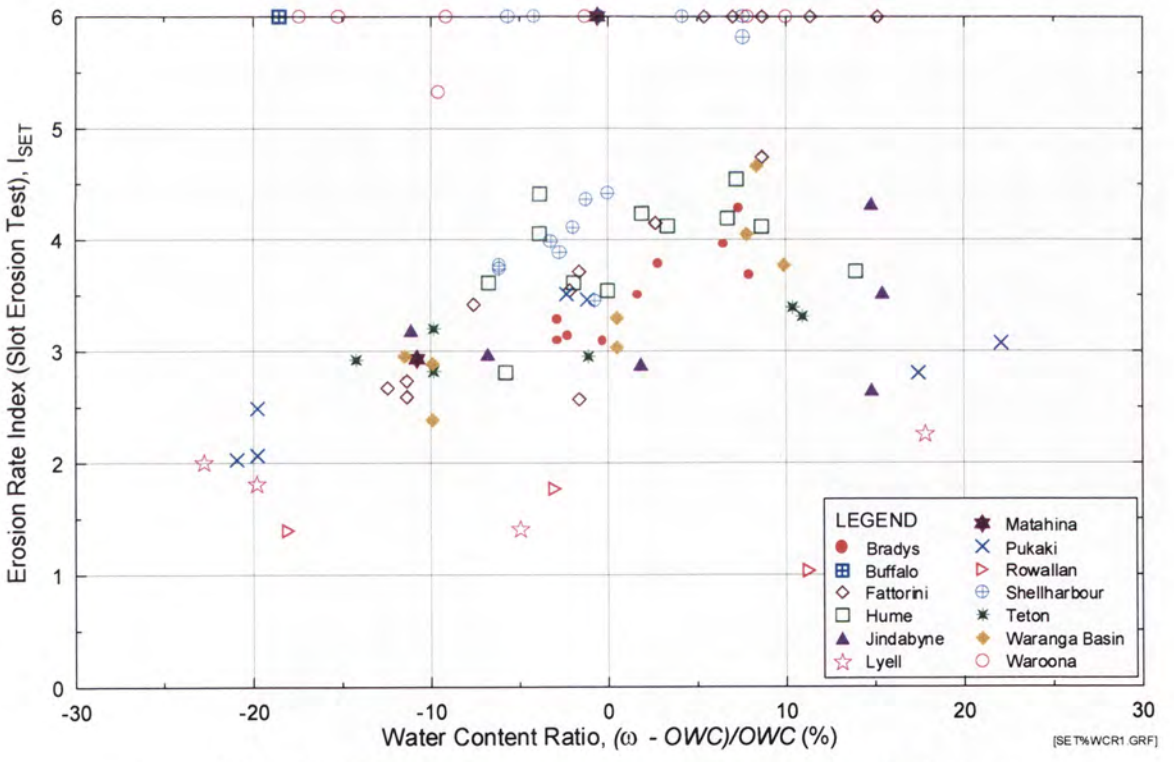

Figure 2.50: Erosion Rate Index (I_{SET}) from Slot Erosion Test versus Water Content Ratio ($\Delta\omega_r$). (Same as Figure E7a in Appendix E)

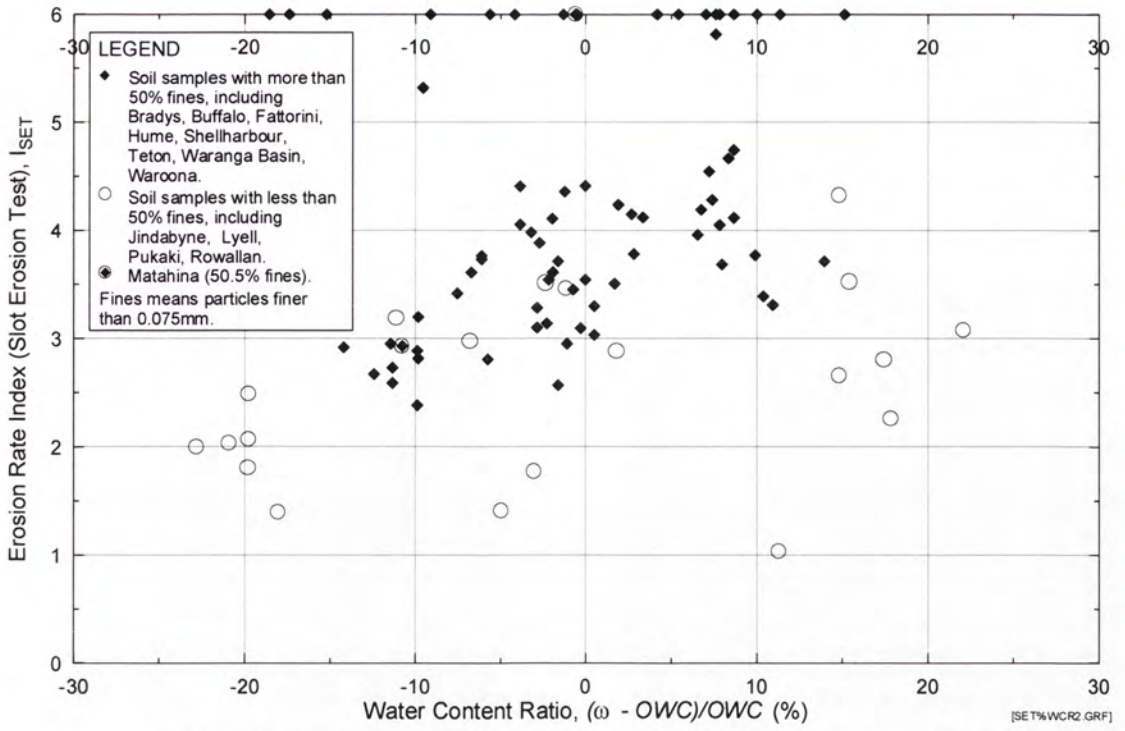

Figure 2.51: Erosion Rate Index (I_{SET}) from Slot Erosion Test versus Water Content Ratio ($\Delta\omega_r$). Soil samples classified into fine-grained soils and coarse-grained soils. (Same as Figure E7b in Appendix E)

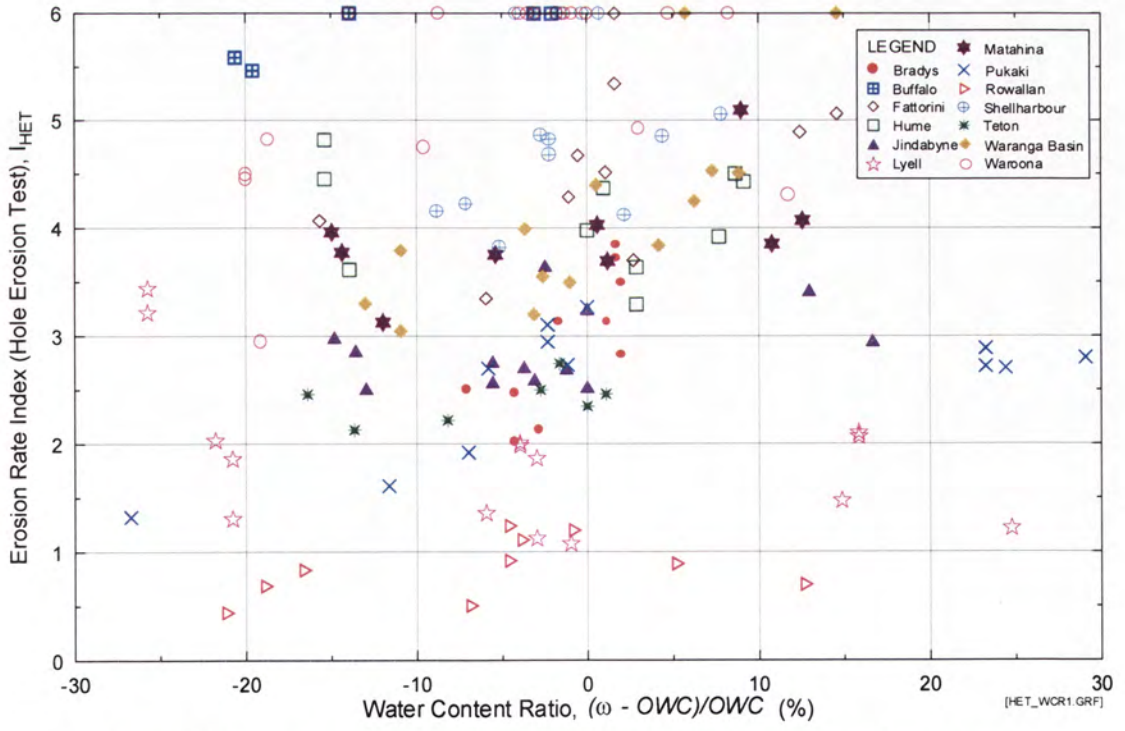

Figure 2.52: Erosion Rate Index (I_{HET}) from Hole Erosion Test versus Water Content Ratio ($\Delta\omega_r$). (Same as Figures E8a in Appendix E)

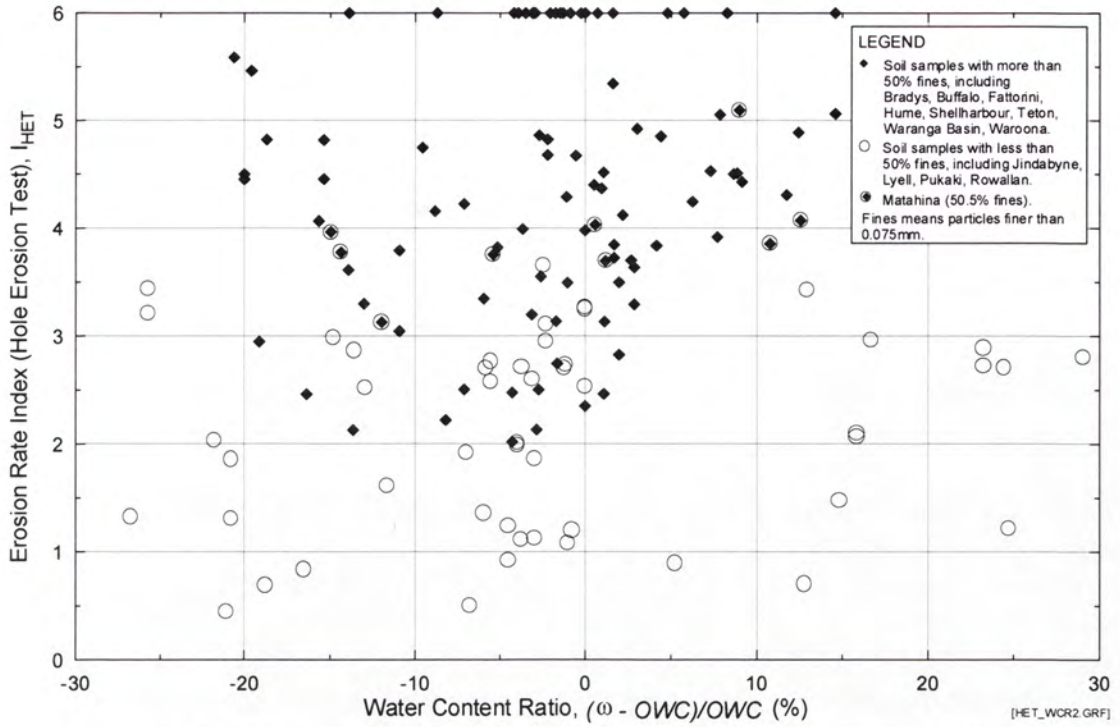

Figure 2.53:Erosion Rate Index (I_{HET}) from Hole Erosion Test versus Water Content Ratio ($\Delta\omega_r$). Soil samples classified into fine-grained soils and coarse-grained soils. (Same as Figure E8b in Appendix E)

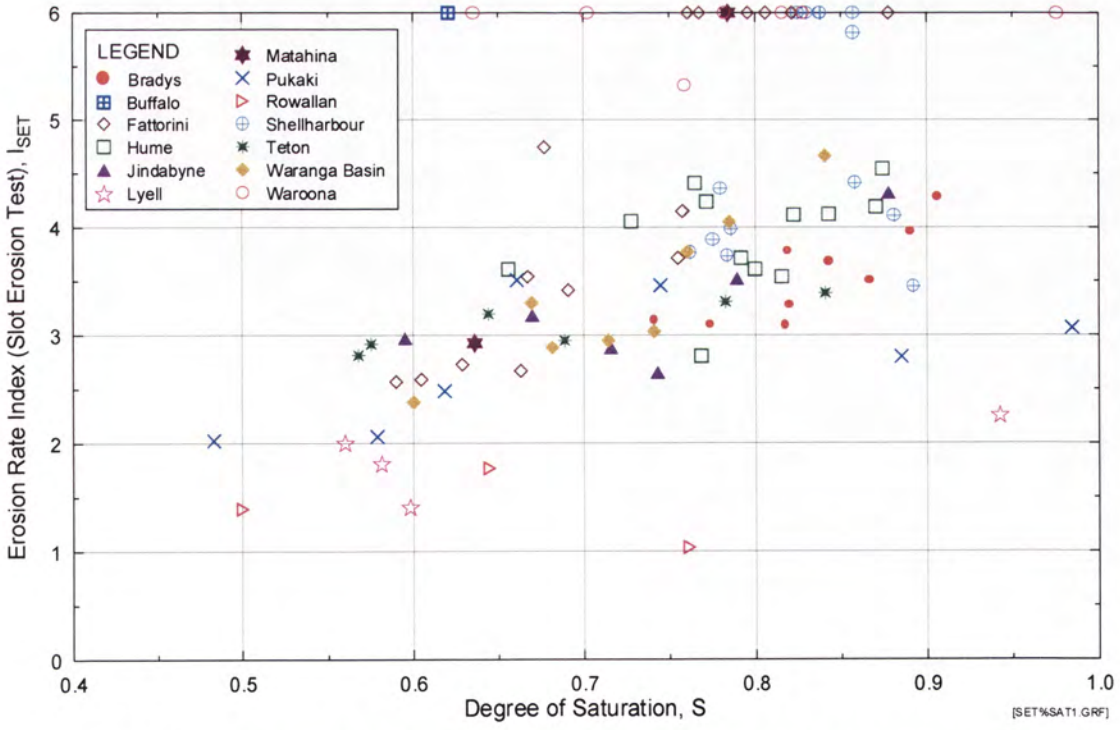

Figure 2.54: Erosion Rate Index (I_{SET}) from Slot Erosion Test versus Degree of Saturation. (Same as Figure E9a in Appendix E)

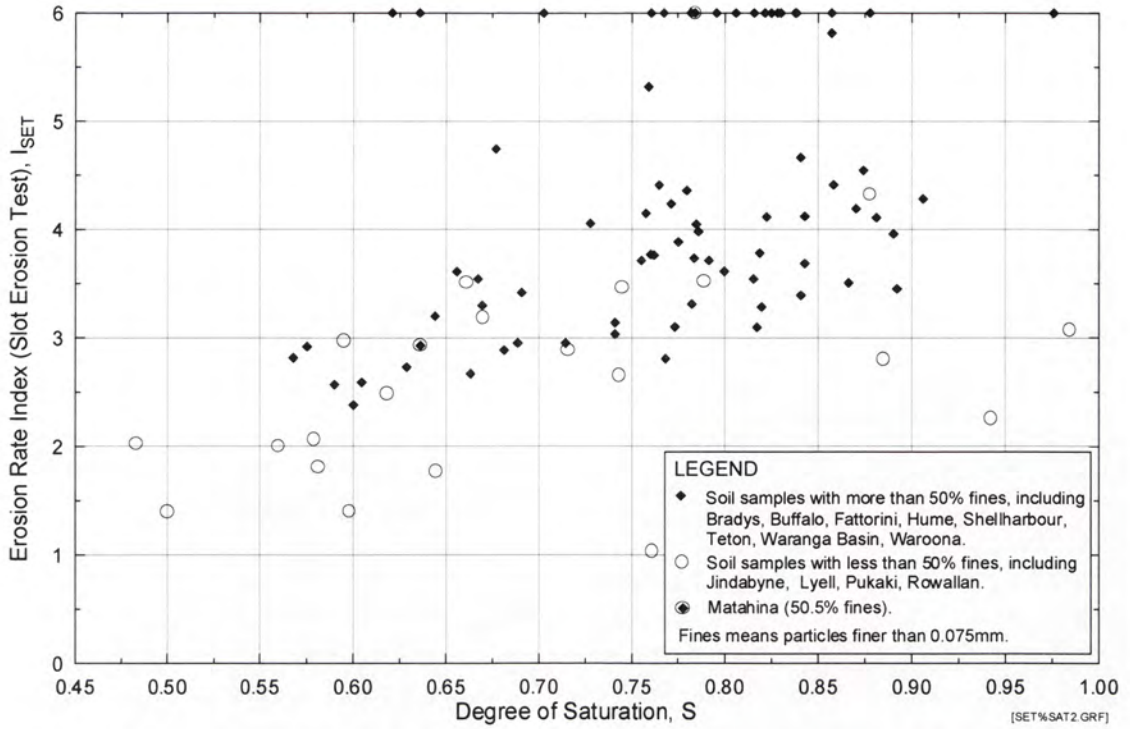

Figure 2.55: Erosion Rate Index (I_{SET}) from Slot Erosion Test versus Degree of Saturation. Soil samples classified into fine-grained soils and coarse-grained soils. (Same as Figure E9b in Appendix E)

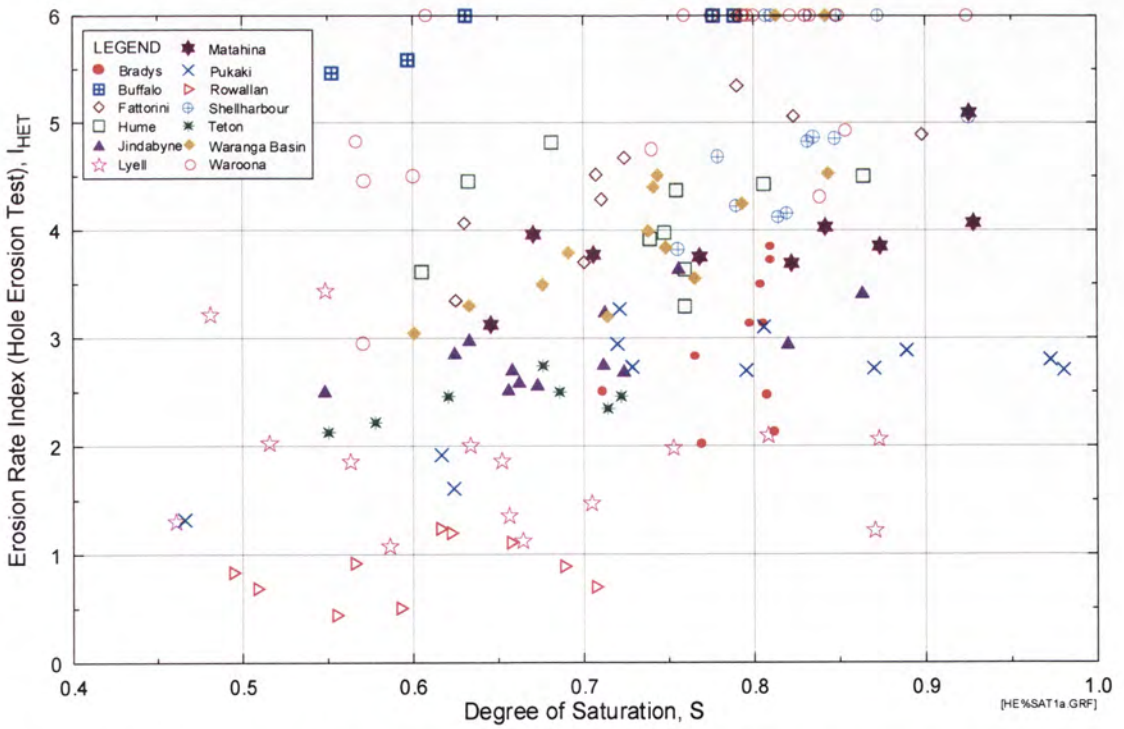

Figure 2.56: Erosion Rate Index (I_{HET}) from Hole Erosion Test versus Degree of Saturation. (Same as Figure E10a in Appendix E)

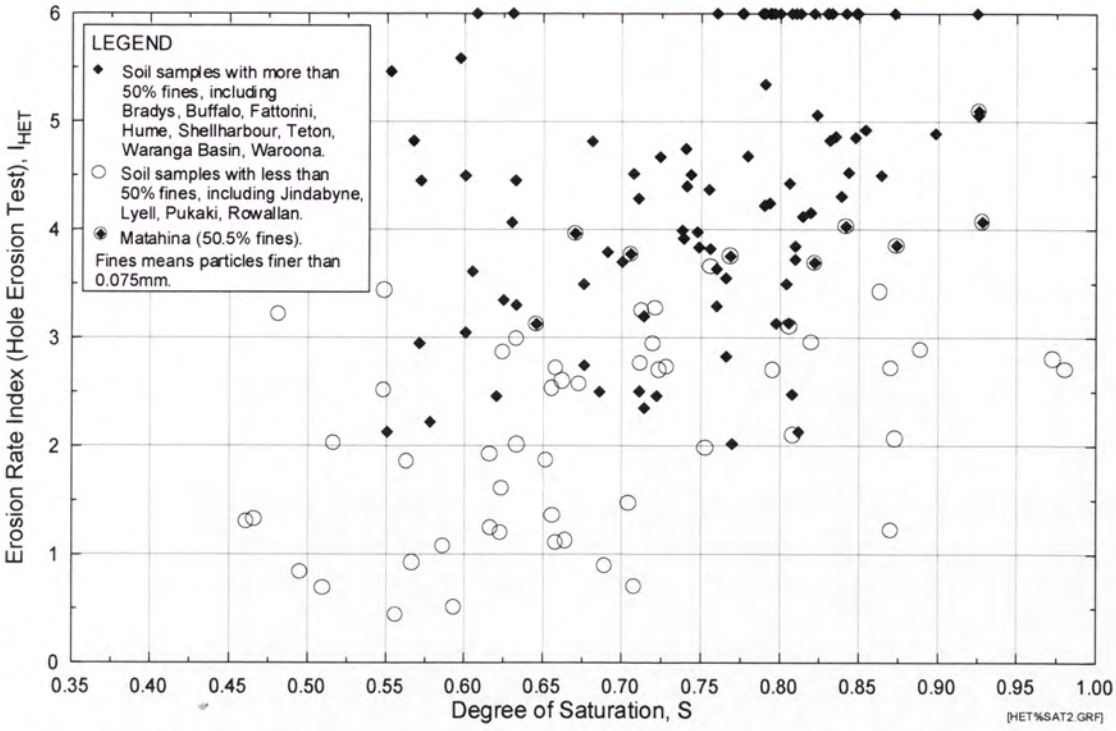

Figure 2.57: Erosion Rate Index (I_{HET}) from Hole Erosion Test versus Degree of Saturation. Soil samples classified into fine-grained soils and coarse-grained soils. (Same as Figure E10b in Appendix E)

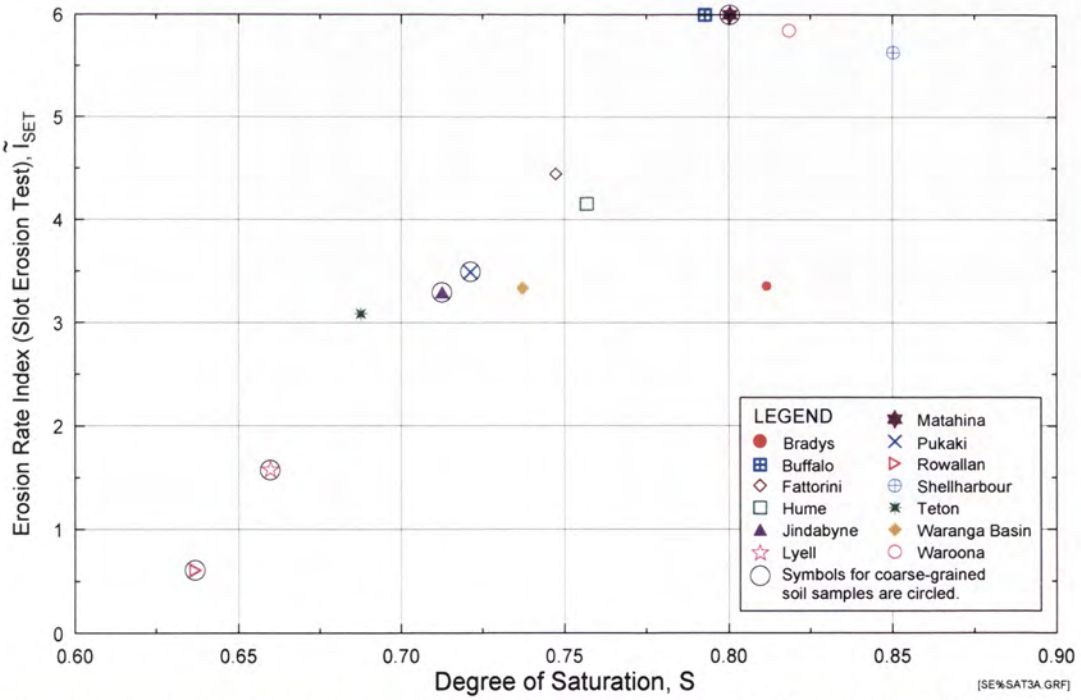

Note : Erosion rate indices presented are predicted indices for specimens at 95% compaction and Optimum Water Content.

Figure 2.58: Predicted Erosion Rate Index ($\tilde{I}_{SET}$) from Slot Erosion Test versus Degree of Saturation. (Same as Figure E9c in Appendix E)

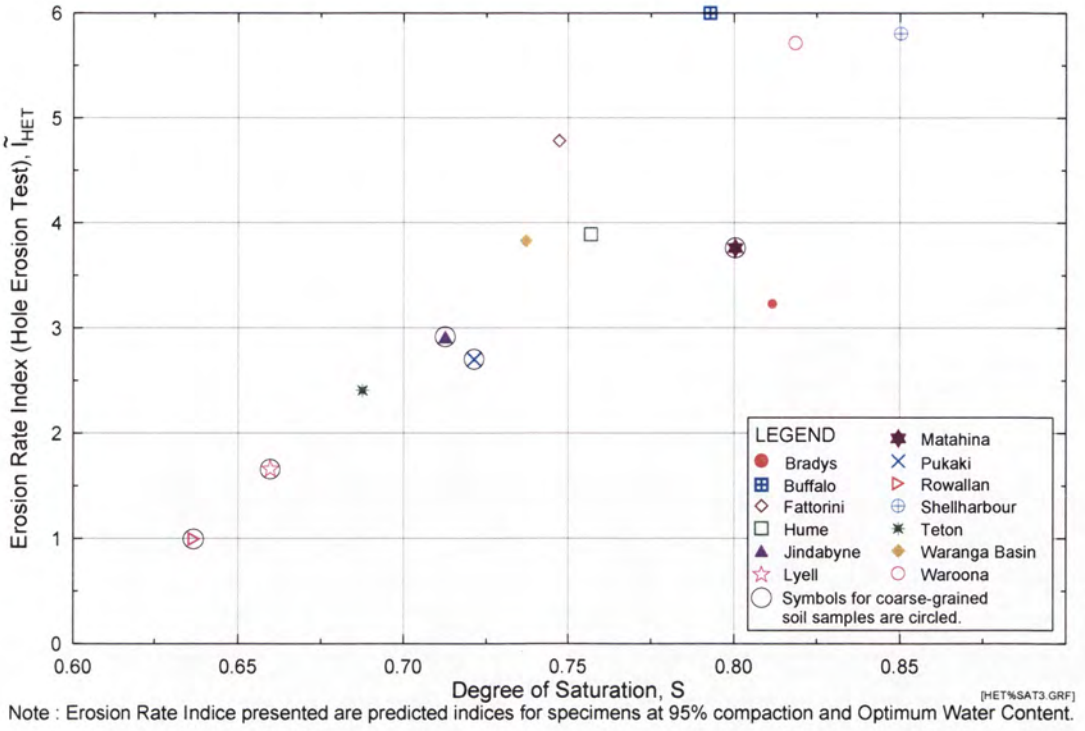

Figure 2.59: Predicted Erosion Rate Index ($\tilde{I}_{HET}$) from Hole Erosion Test versus Degree of Saturation. (Same as Figure E10c in Appendix E)

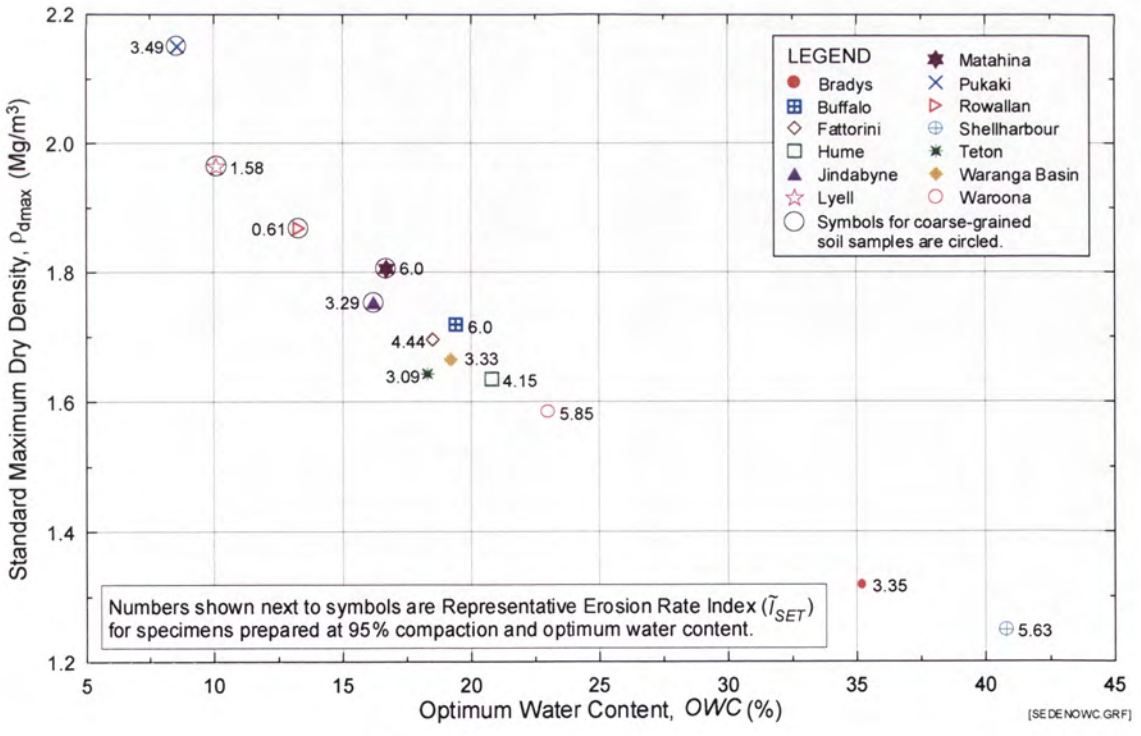

Figure 2.60: Representative Erosion Rate Index ($\tilde{I}_{SET}$) from Slot Erosion Test versus Standard Maximum Dry Density ($\rho_{d_{max}}$) and Optimum Water Content (*OWC*). (Same as Figure E11a in Appendix E)

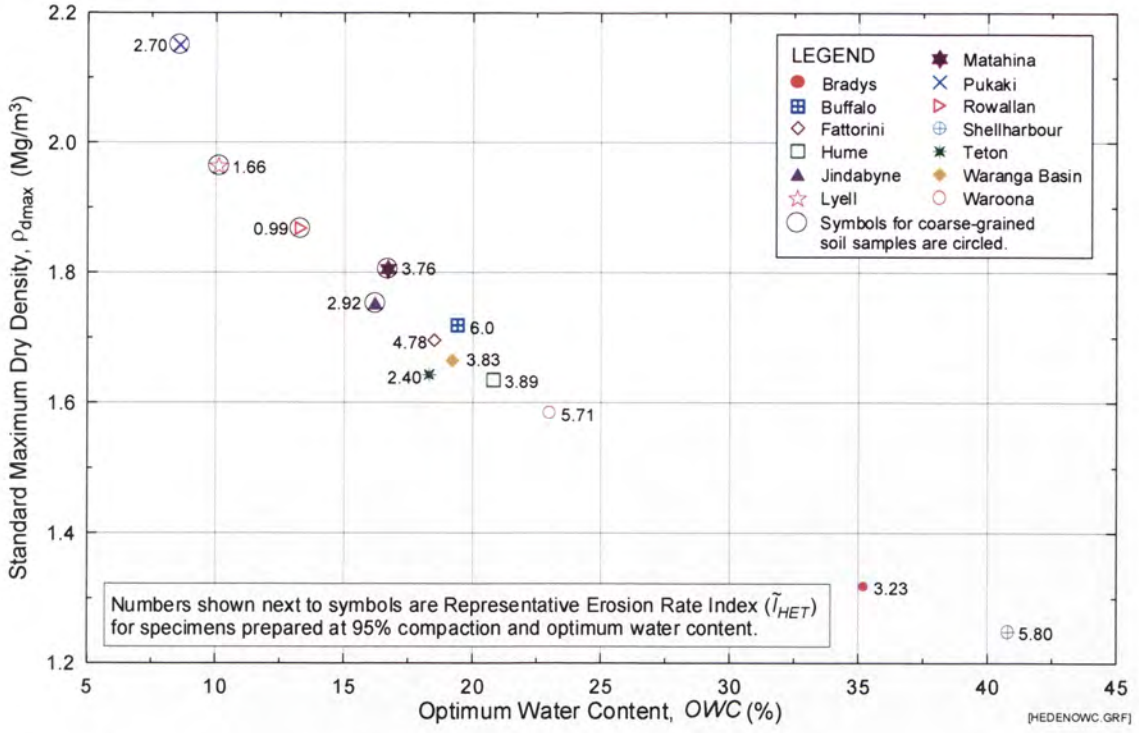

Figure 2.61: Representative Erosion Rate Index ($\tilde{I}_{HET}$) from Hole Erosion Test versus Standard Maximum Dry Density ($\rho_{d_{\max}}$) and Optimum Water Content (*OWC*). (Same as Figure E11b in Appendix E)

Group 2 parameters : Grading properties which vary between soil samples only

The parameters commonly used to represent grading properties are gravel content (%gravel), sand content (%sand) and fines content (%fines). For a given soil, these three quantities add up to 100%. The amount of gravel in the 13 soil samples is insignificant, and plots of Erosion Rate Indices against gravel content reveal no relationship between the two parameters. As the erosion resistance of fine-grained soils is believed to be influenced by electro-chemical forces among clay particles, the relationship between erodibility and the clay content (%clay) of a soil should also be investigated. There are two slightly different definitions of clay-size particles. US engineers define clay-size particles as those finer than 0.005mm, whereas UK engineers define clay-size particles as those finer than 0.002mm. The clay contents based on the two slightly different definitions on clay-size particles are denoted by %clay(US) and %clay(UK). It should, however, be noted that clay-size particles may include non-clay minerals, and crystals of clay minerals are not necessarily finer than the clay-size minerals of 0.002 or 0.005 mm.

Plots of the Erosion Rate Indices against the grading properties are shown in Figures F1 to F8 at Appendix F. Comments on the plots are as follows:

- I_{SET} and I_{HET} versus Sand Content (%sand) in Figures F1 and F2

  Figures F3a, b and F4a, b show considerable scattering of the data points. The plots, however, show an obvious trend that the higher the Sand Content, the lower would be the Erosion Rate Indices (i.e. higher erosion rates). The coarse-grained soil samples have relatively higher Sand Content than the fine-grained soil samples. Figures F3c, and F4c, show an apparent linear relationship between the indices and the Sand Content of the coarse-grained soil samples.

- I_{SET} and I_{HET} versus Fines Content (%fines) in Figures F3 and F4

  Plots of I_{SET}, I_{HET} against Fines Content show considerable scattering of the data points. However the plots, as shown in
  Figure 2.62, Figure 2.63 and Figure 2.64, Figure 2.65, do reveal the trend that the higher the Fines Content, the higher would be the Erosion Rate Indices (i.e. lower erosion rates). The coarse-grained soil samples have relatively lower Fines Content than the fine-grained soil samples. Figure 2.66 and Figure 2.67 also show an apparent linear relationship between the Representative Erosion Indices and the Fines Content of the coarse-grained soil samples, but no correlation for the fine-grained soil samples. As all the soil samples tested have low gravel content, and are mainly composed of sands and fines, the existence of a relationship between the indices and the sand content implies that the indices and the fines content are also related.

- I_{SET} and I_{HET} versus Clay Content (%clay(US)) in Figures F5 and F6

  Figures F7a, b and F8a, b show considerable scattering of the data points. The figures, however, show the trend that the higher the clay content, the higher would be the Erosion Rate Indices. Figures F5c, and F6c also show that the Erosion Rate Indices are approximately linearly related to the Clay Content of the coarse-grained soils.

- I_{SET} and I_{HET} versus Clay Content (%clay(UK)) in Figures F7 and F8

  The plots of Erosion Rate Indices against Clay Content (UK definition) in Figures F7 and F8 are very similar to the plots of the indices against Clay

Content (US definition) in Figures F5 and F6. The Erosion Rate Indices are approximately linearly related to the Clay Content of the coarse-grained soils, but as for fines content, there is no correlation for fine-grained soils.

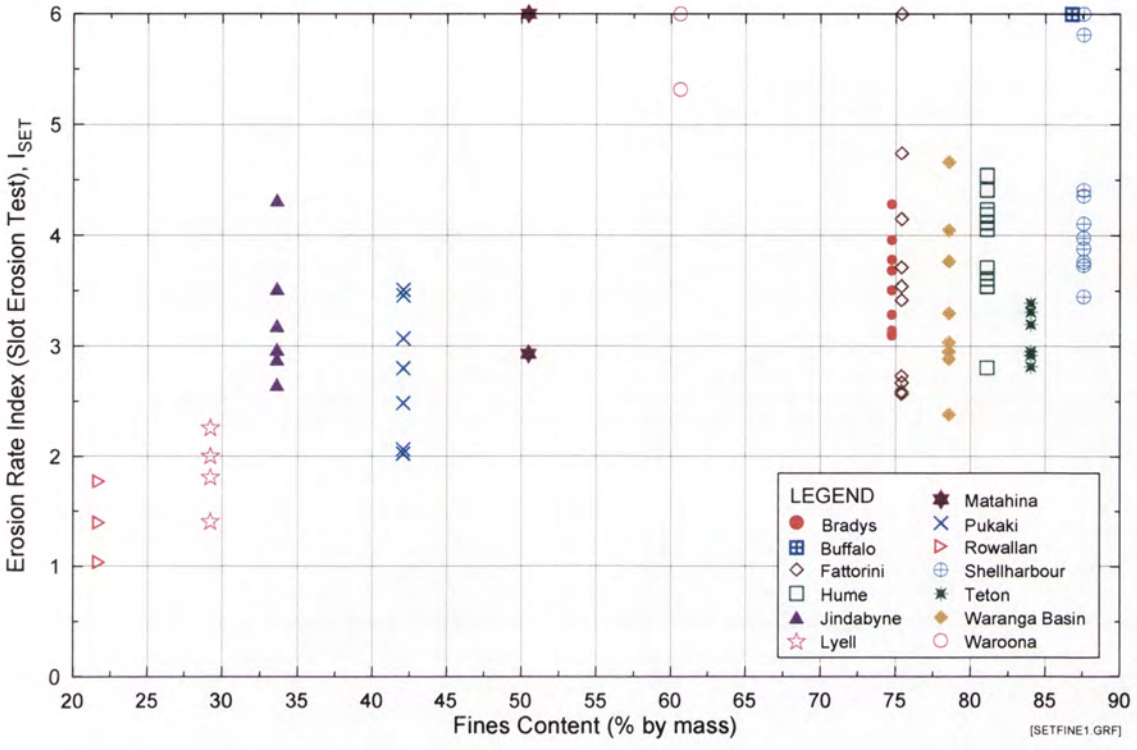

Figure 2.62: Erosion Rate Index (I_{SET}) from Slot Erosion Test versus Fines Content. (Same as Figure F3a in Appendix F)

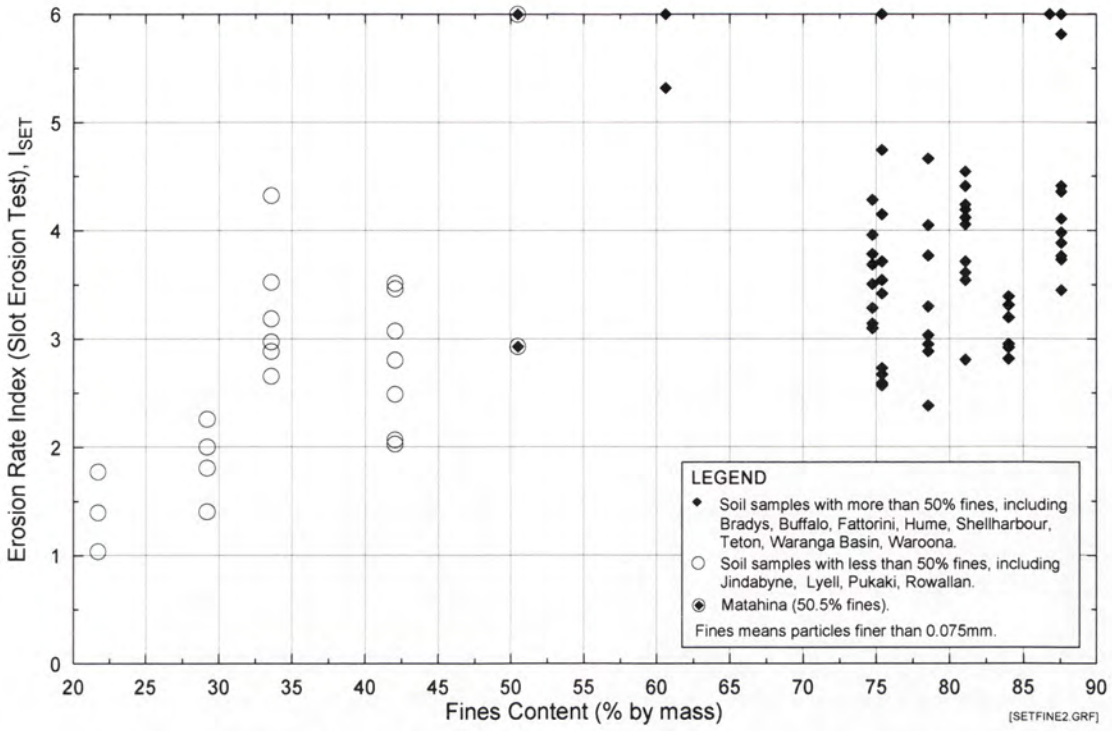

Figure 2.63: Erosion Rate Index (I_{SET}) from Slot Erosion Test versus Fines Content. Soil samples classified into fine-grained soils and coarse-grained soils. (Same as Figure F3b in Appendix F)

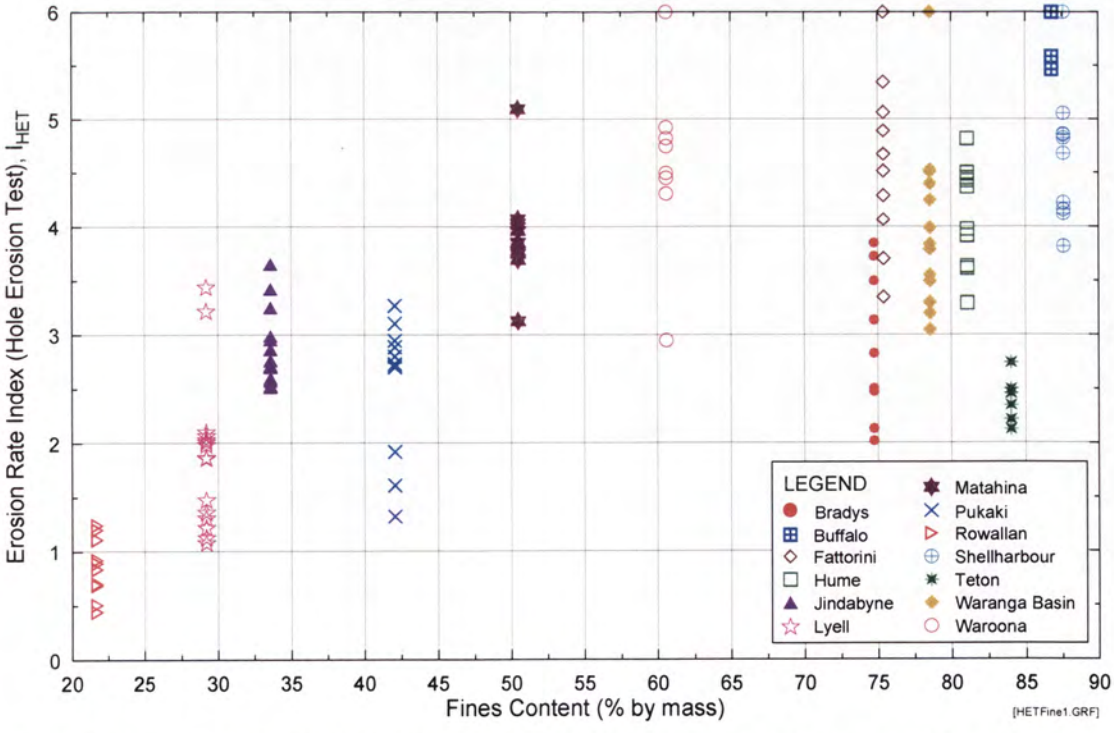

Figure 2.64: Erosion Rate Index (I_{HET}) from Hole Erosion Test versus Fines Content. (Same as Figure F4a in Appendix F)

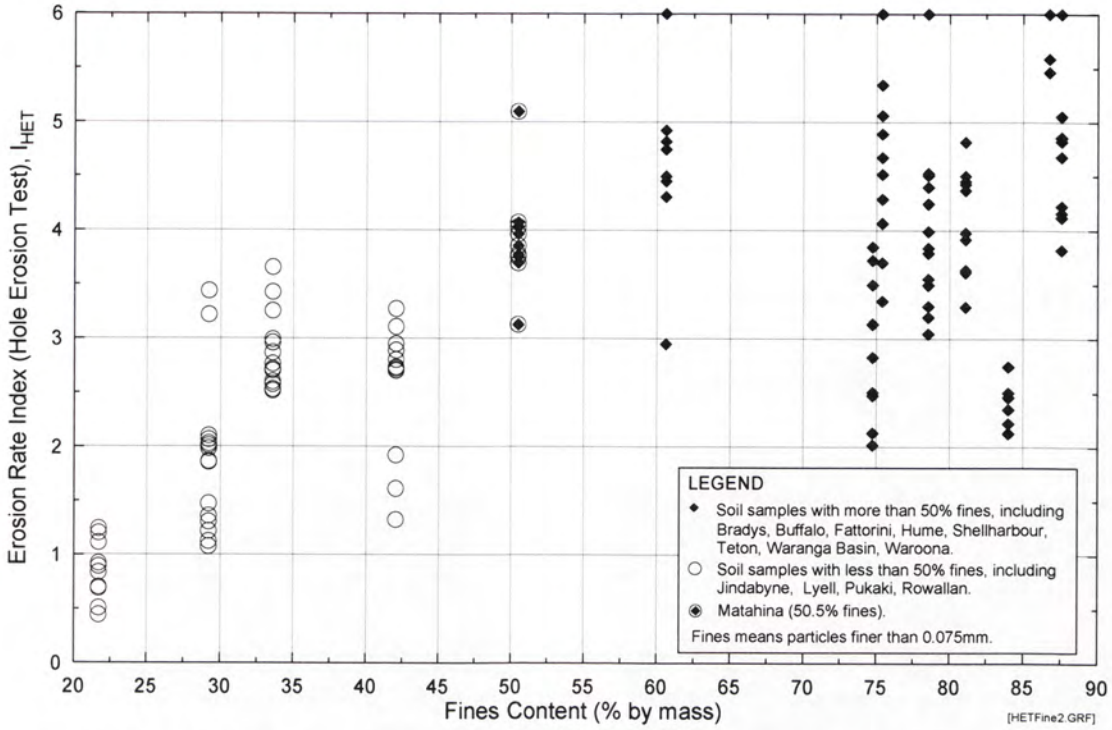

Figure 2.65: Erosion Rate Index (I_{HET}) from Hole Erosion Test versus Fines Content. Soil samples classified into fine-grained soils and coarse-grained soils. (Same as Figure F4b in Appendix F)

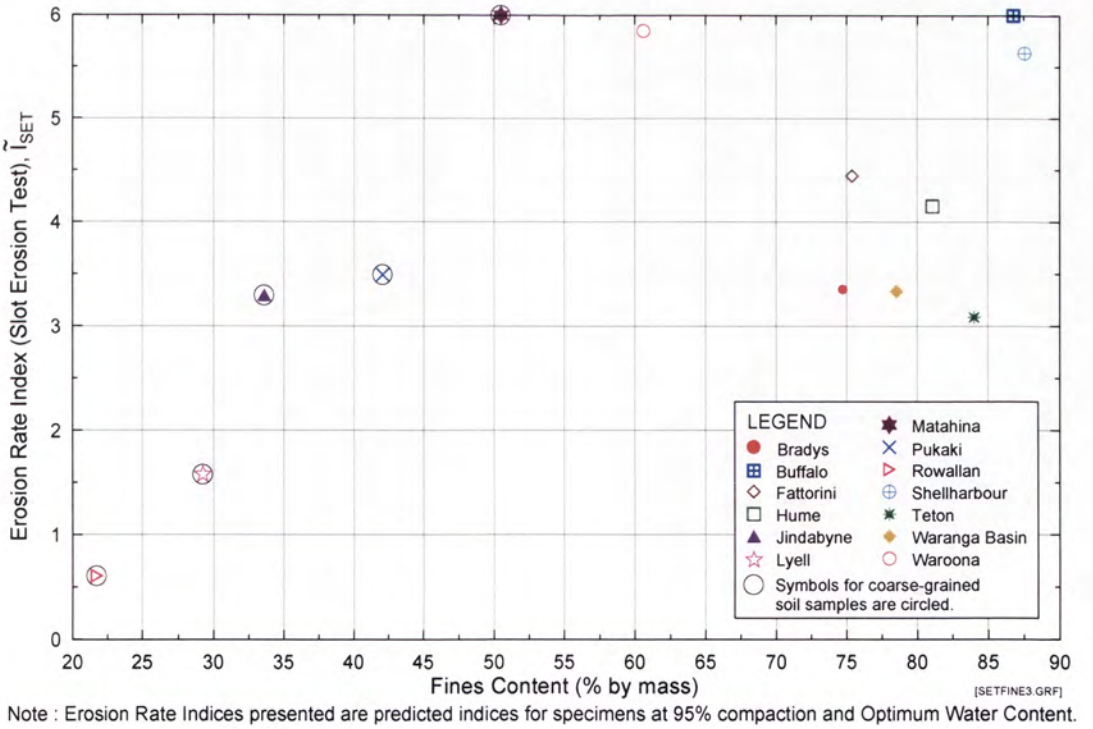

Note : Erosion Rate Indices presented are predicted indices for specimens at 95% compaction and Optimum Water Content.

Figure 2.66: Predicted Representative Erosion Rate Index ($\tilde{I}_{SET}$) from Slot Erosion Test versus Fines Content. (Same as Figure F3c in Appendix F)

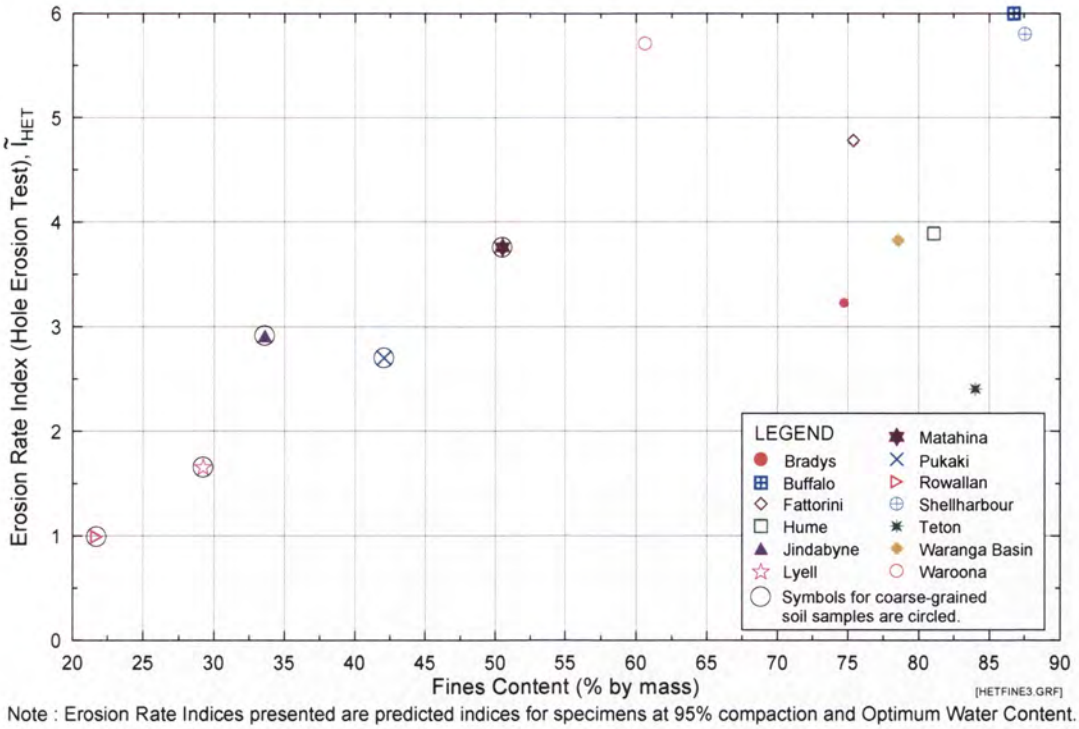

Note : Erosion Rate Indices presented are predicted indices for specimens at 95% compaction and Optimum Water Content.

Figure 2.67: Predicted Representative Erosion Rate Index ($\tilde{I}_{HET}$) from Hole Erosion Test versus Fines Content. (Same as Figure F4c in Appendix F)

Group 3 parameters : Atterberg limits which vary between soil samples only

Plots of the Erosion Rate Indices against Liquid Limits, Plasticity Indices and Activity are shown in Figures G1 to G6 at Appendix G. Activity is defined as the ratio between the Plastic Index and the Clay Content (fraction finer than 0.002 mm) (Skempton 1953).

- I_{SET} and I_{HET} versus Liquid Limit in Figures G1 and G2

  Figures G1 and G2 show that the non-plastic soil samples have relatively lower Erosion Rate Indices. Other soil samples which have Liquid Limits at 30% or higher do not show any obvious relationship between their Erosion Rate Indices and their Liquid Limits.

- I_{SET} and I_{HET} versus Plasticity Index in Figures G3 and G4

  Figures G3 and G4 show that the non-plastic soil samples have relatively lower Erosion Rate Indices. The plastic soil samples do not show any obvious relationship between their Erosion Rate Indices and their Plasticity Indices.

- I_{SET} and I_{HET} versus Activity in Figures G5 and G6

Figures G5 and G6 show that the non-plastic soil samples have relatively lower Erosion Rate Indices. The plastic soil samples do not show any obvious relationship between the Erosion Rate Indices and their Activity.

Group 4 parameters : Dispersivity which varies between soil samples only

The three commonly used laboratory tests for determining the dispersivity of a soil are the Pinhole Erosion Test (AS1289.3.8.3 1997, Sherard et al 1976), Emerson Class Test (AS1289.3.8.1 1997, Emerson 1967), and the SCS Laboratory Dispersion Test (AS1289.3.8.2 1997, Decker and Dunnigan 1977, Sherard et al 1972) which is also known as the Double-hydrometer Test. The Sodium Adsorption Ratio, *SAR* and the major cation content of the saturation extract of a soil are also believed to be good indicators of the degree of dispersivity. *SAR* is defined as

$$SAR = \frac{[Na^+]}{\sqrt{\frac{[Ca^{2+}]+[Mg^{2+}]}{2}}} \qquad \text{Eqn 2.22}$$

and the major cation content is the total amount of metallic ions (Na^+, Ca^{2+}, Mg^{2+} and K^+) in the saturation extract of a soil. The amount of individual cations is expressed in milliequivalents per litre (meq/l). The saturation extract is a small quantity of pore fluid extracted from a saturated soil paste with water content approximately equal to its Liquid Limit. Plots of the Erosion Rate Indices against Pinhole Class, Emerson Class, percentage dispersion, *SAR* and cation contents are shown in Figures H1 to H10 at Appendix H.

- I_{SET} and I_{HET} versus Pinhole Test Classification in Figures H1 and H2

  All coarse-grained soil samples and two fine-grained soil samples (Hume and Waranga Basin) were classified as D1 by the Pinhole Test. The remaining fine-grained soil samples were classified from PD1/PD2 to ND1. The plots do not show any obvious relationship between the Erosion Rate Indices and the Pinhole Test Classifications when considered as a whole, but if the fine-grained soils are considered separately, there is an apparent trend of higher I_{SET} and I_{HET} with decreasing dispersivity, which is what would be expected. The plots of the

predicted Representative Erosion Rate Indices versus Pinhole Test Classifications are shown in Figure 2.68 and Figure 2.69.

- I_{SET} and I_{HET} versus Emerson Class in Figures H3 and H4

  Hume and Waranga Basin, the only two fine-grained soil samples classified as highly dispersive (D1) by the Pinhole Test, were also classified as dispersive (Class 1) by the Emerson Class Test. Nevertheless, unlike the Pinhole Test, the Emerson Class Test did not classify the coarse-grained soil samples as highly dispersive. Some of the coarse-grained soil samples have the same Emerson Class rating as some relatively erosion-resistant fine-grained soil samples. The plots in Figures H3 and H4 do not show any obvious relationship between the Erosion Rate Indices and the Emerson Classes. The plots of the predicted Representative Erosion Rate Indices versus Emerson Classes are shown in Figure 2.70 and Figure 2.71.

- I_{SET} and I_{HET} versus Percentage Dispersion in Figures H5 and H6

  With very high Percentage Dispersion values, Waranga Basin and Hume are also shown by the SCS Laboratory Dispersion Test to be highly dispersive soils. The relatively erodible coarse-grained soil samples have Percentage Dispersion values within the range of 25 – 60%, whereas those relatively non-erodible fine-grained soil samples having high Erosion Rate Indices have relatively lower Percentage Dispersion values. Overall, the plots in Figures H5 and H6 do not show any obvious relationship between the Erosion Rate Indices and the Percentage Dispersion values. The plots of the predicted Representative Erosion Rate Indices versus Pinhole Percentage Dispersion values are shown in Figure 2.72 and Figure 2.73.

- I_{SET} and I_{HET} versus SAR in Figures H7 and H8

  Waranga Basin and Hume, classified as highly dispersive by other tests, have the highest SAR values among other soil samples. The coarse-grained soil samples have relatively low SAR values compared with the fine-grained soil samples. Overall, the plots in Figures H7 and H8 do not show any obvious relationship between the Erosion Rate Indices and the SAR values.

- I_{SET} and I_{HET} versus Major Cation Content in Figures H9 and H10

The Major Cation Contents of Waranga Basin and Hume, being 145 and 28 meq/l respectively, are the highest among all soil samples. Other soil samples have values below 15 meq/l. The plots in Figures H9 and H10 do not show any obvious relationship between the Erosion Rate Indices and the Major Cation Contents.

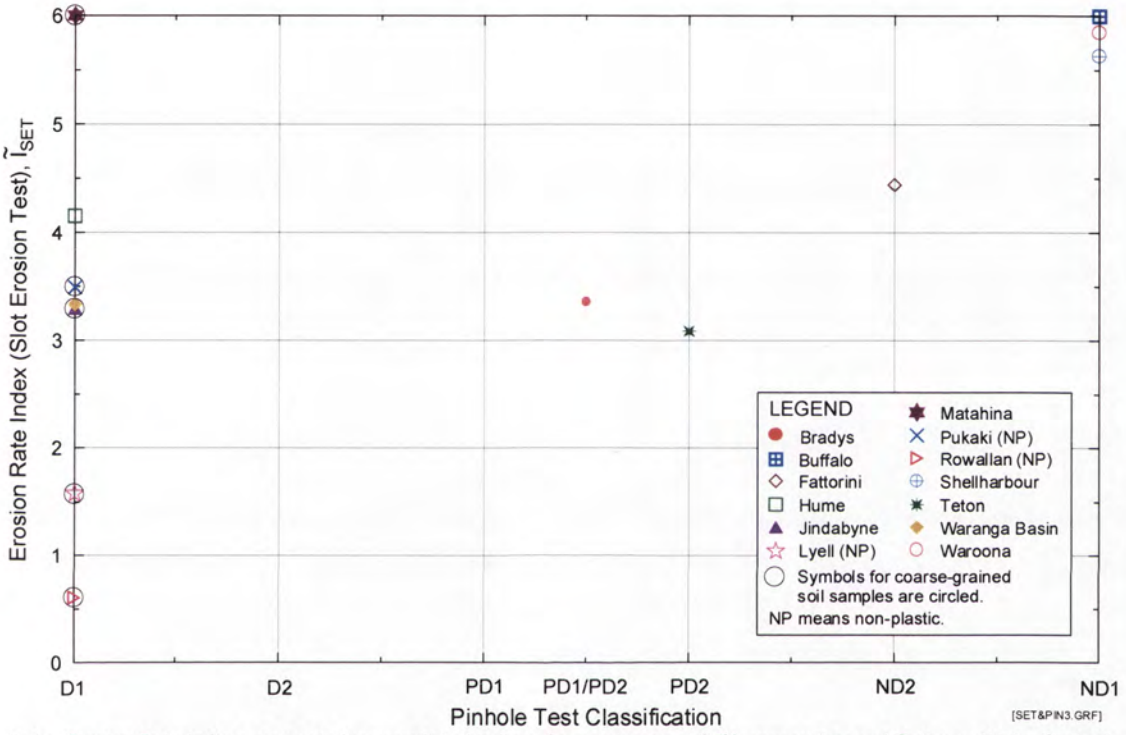

Note : Erosion Rate Indices presented are predicted indices for specimens at 95% compaction and Optimum Water Content.

Figure 2.68: Predicted Erosion Rate Index ($\tilde{I}_{SET}$) from Slot Erosion Test versus Pinhole Test Classification. (Same as Figure H1c in Appendix H)

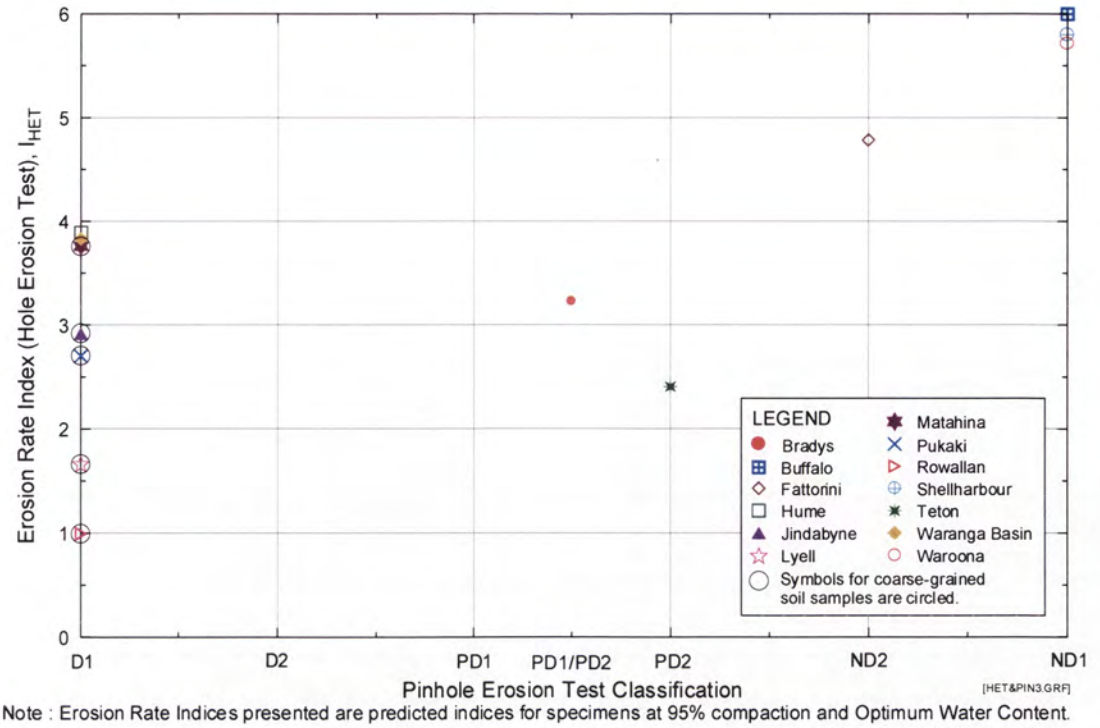

Note : Erosion Rate Indices presented are predicted indices for specimens at 95% compaction and Optimum Water Content.

Figure 2.69: Predicted Erosion Rate Index ($\tilde{I}_{HET}$) from Hole Erosion Test versus Pinhole Test Classification. (Same as Figure H2c in Appendix H)

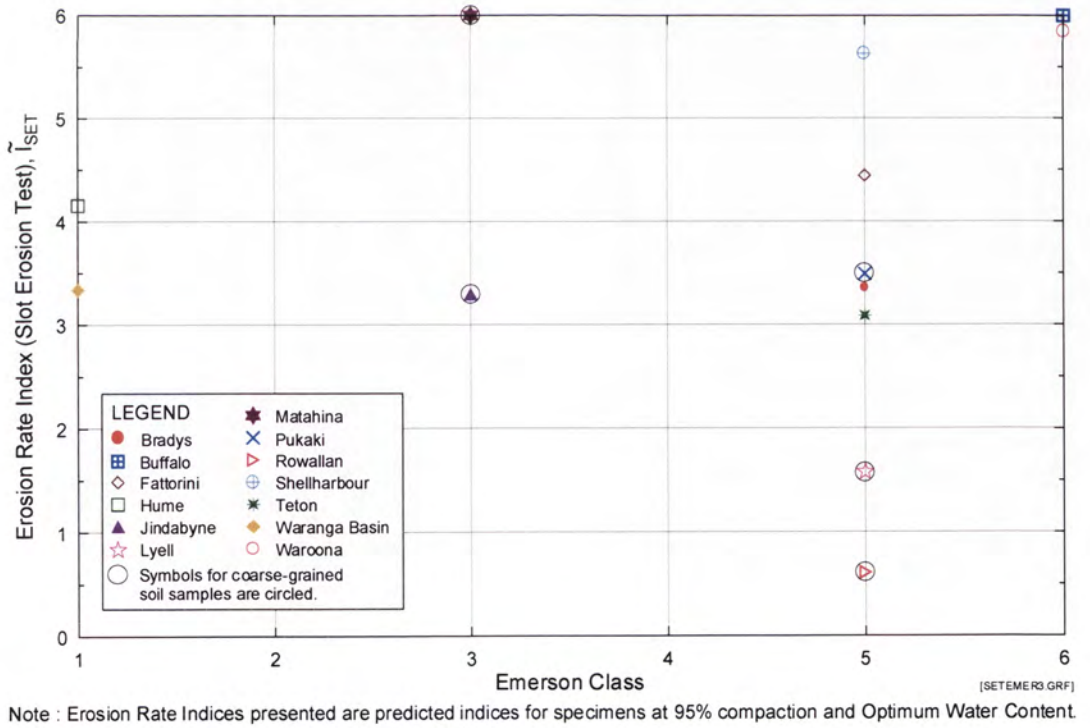

Note : Erosion Rate Indices presented are predicted indices for specimens at 95% compaction and Optimum Water Content.

Figure 2.70: Predicted Erosion Rate Index ($\tilde{I}_{SET}$) from Slot Erosion Test versus Emerson Class. (Same as Figure H3c in Appendix H)

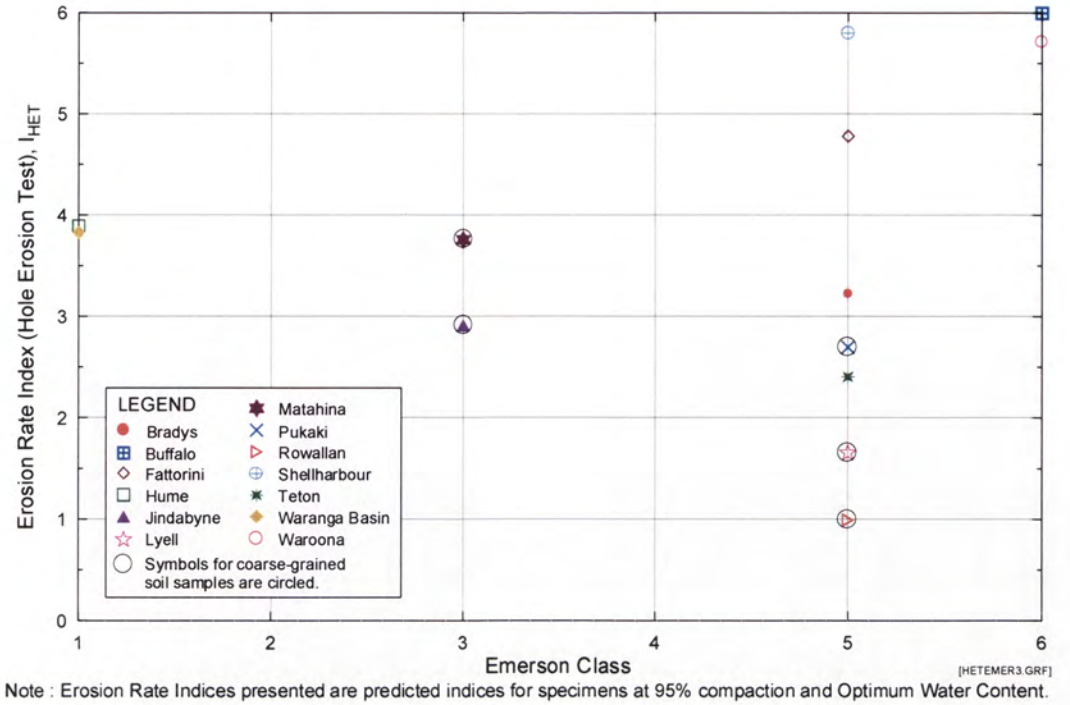

Note : Erosion Rate Indices presented are predicted indices for specimens at 95% compaction and Optimum Water Content.

Figure 2.71: Predicted Erosion Rate Index ($\tilde{I}_{HET}$) from Hole Erosion Test versus Emerson Class. (Same as Figure H4c in Appendix H)

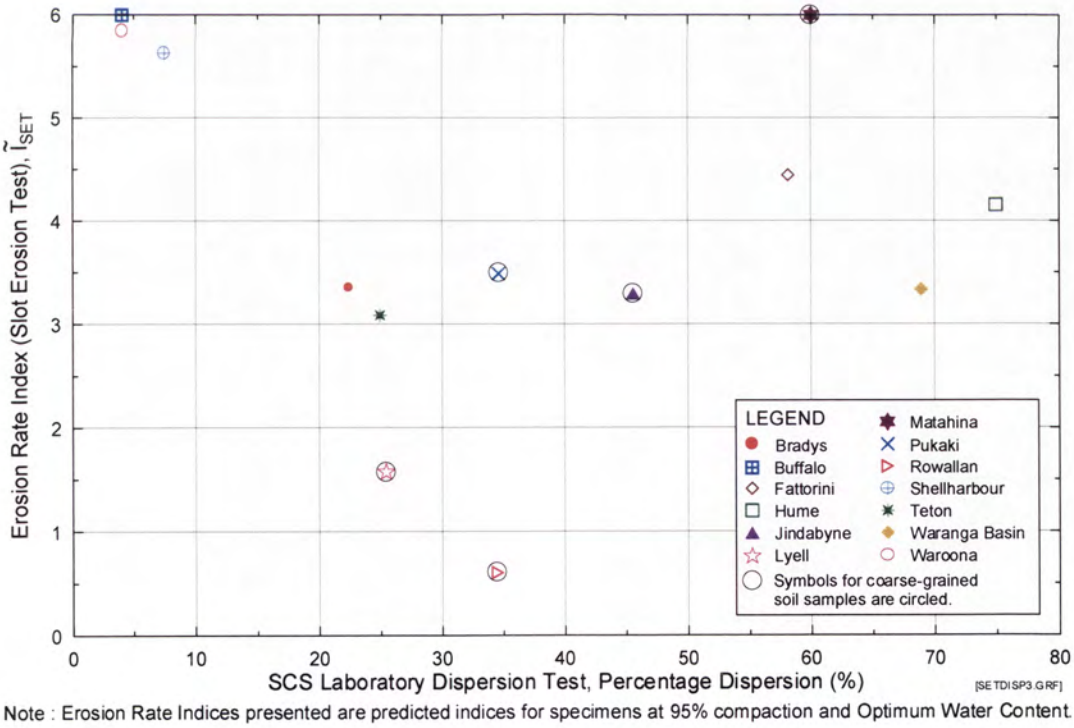

Note : Erosion Rate Indices presented are predicted indices for specimens at 95% compaction and Optimum Water Content.

Figure 2.72: Predicted Erosion Rate Index ($\tilde{I}_{SET}$) from Slot Erosion Test versus Percentage Dispersion. (Same as Figure H5c in Appendix H)

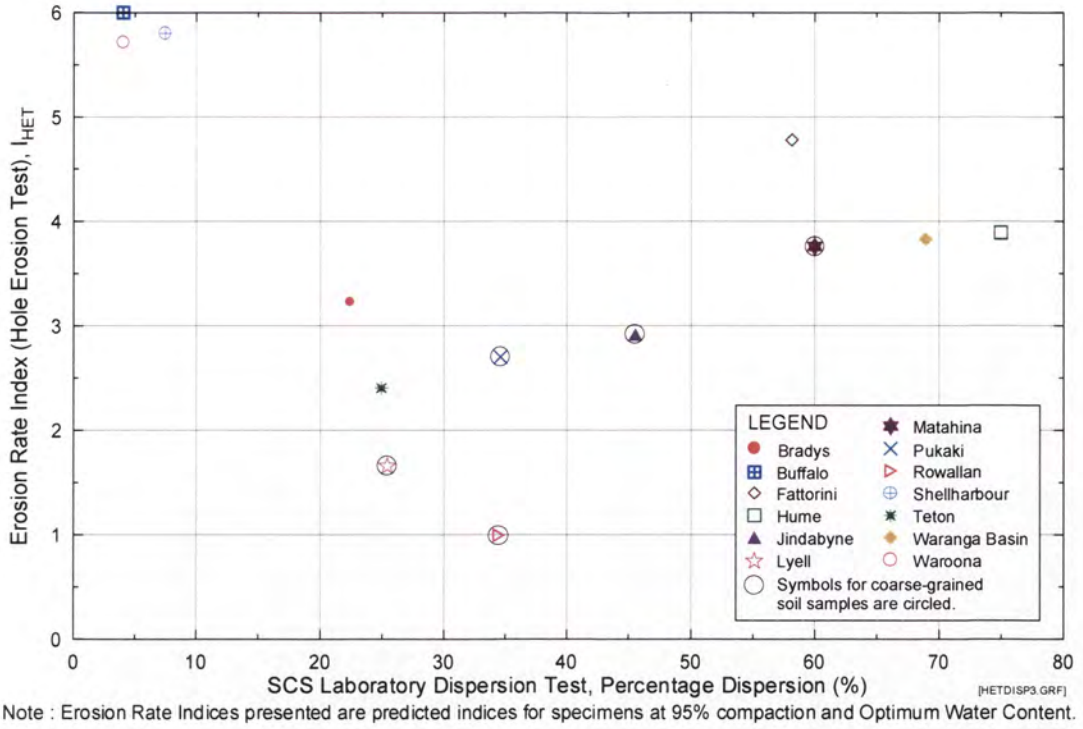

Figure 2.73: Predicted Erosion Rate Index ($\tilde{I}_{HET}$) from Hole Erosion Test versus Percentage Dispersion. (Same as Figure H6c in Appendix H)

Critical shear stresses versus soil properties

The Critical Shear Stress is not directly measured from an erosion test. It is the horizontal-intercept of the best-fit straight line approximating the relationship between the rate of erosion per unit area and the shear stress due to the eroding fluid. This horizontal-intercept is assigned the physical meaning of "the threshold shear stress to cause erosion". Procedures for finding the Critical Shear Stress have been described in Sections 2.3.2 and 2.3.4 of this report.

In Figure 2.74 and Figure 2.75, Critical Shear Stresses are plotted against the soil samples arranged in the order of increasing fines content, whereas in Figure 2.76 and Figure 2.77, they are plotted against the Erosion Rate Indices.

Figure 2.77 shows that the Critical Shear Stresses, τ_{cSET} obtained from Slot Erosion Tests on a soil sample can assume a wide range of values, positive and negative, but spread relatively evenly about zero. Except for Hume and Shellharbour which have

higher Critical Shear Stresses up to 400 N/m^2, other soil samples do not show large differences in their Critical Shear Stresses.

Figure 2.78 shows that the Critical Shear Stresses, τ_{cHET}, based on the HET test data. These are considered to be more reliable than for the Slot Erosion Tests. It shows that τ_{cHET} obtained from different tests on the same soil samples can vary considerably, but some soils clearly have very low (zero) Critical Shear Stresses (Rowallan, Lyell, Jindabyne, Pukaki, Teton, Bradys), while others clearly have high Critical Shear Stresses. One obvious reason for the scatter is that the different test specimens of the same soil samples were having different conditions of compaction and water content, but the measurement of the τ_{cHET} is in itself uncertain. The plot shows that the τ_{cHET} of the coarse-grained soil samples are, in general, lower than the τ_{cHET} of the fine-grained soil samples. τ_{cHET}, however, does not appear to be dependent on fines content.

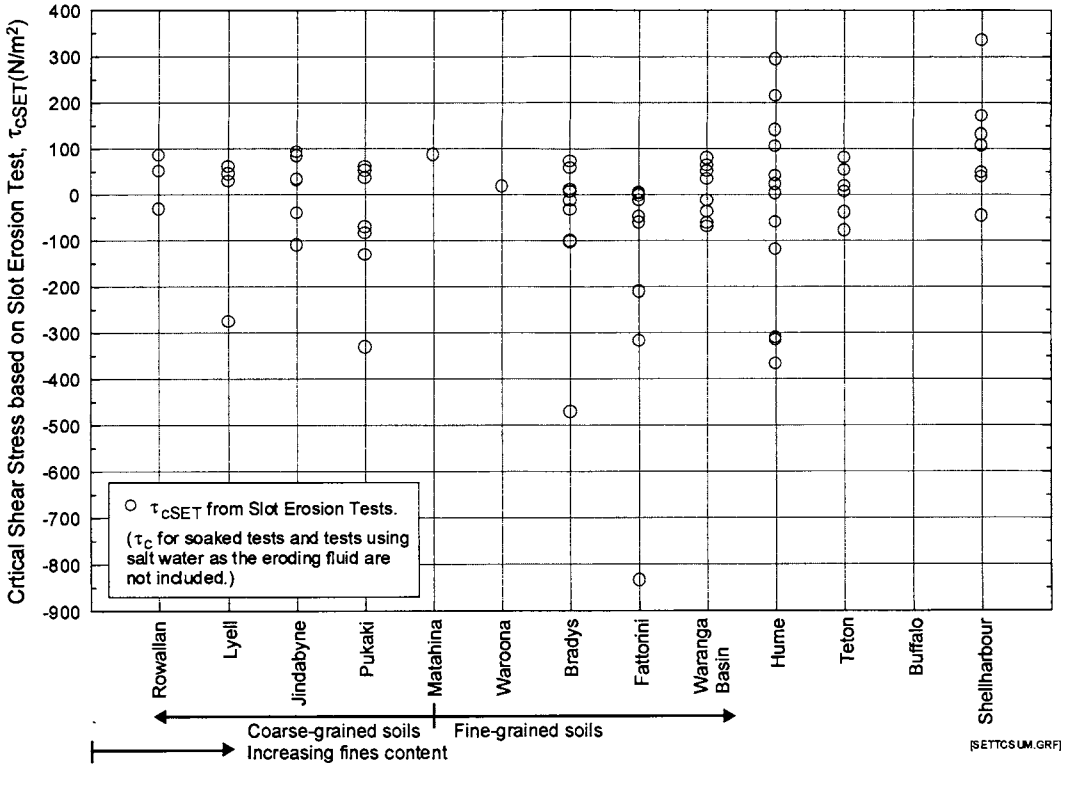

Figure 2.74: Summary of Critical Shear Stresses obtained from Slot Erosion Tests on all soil samples.

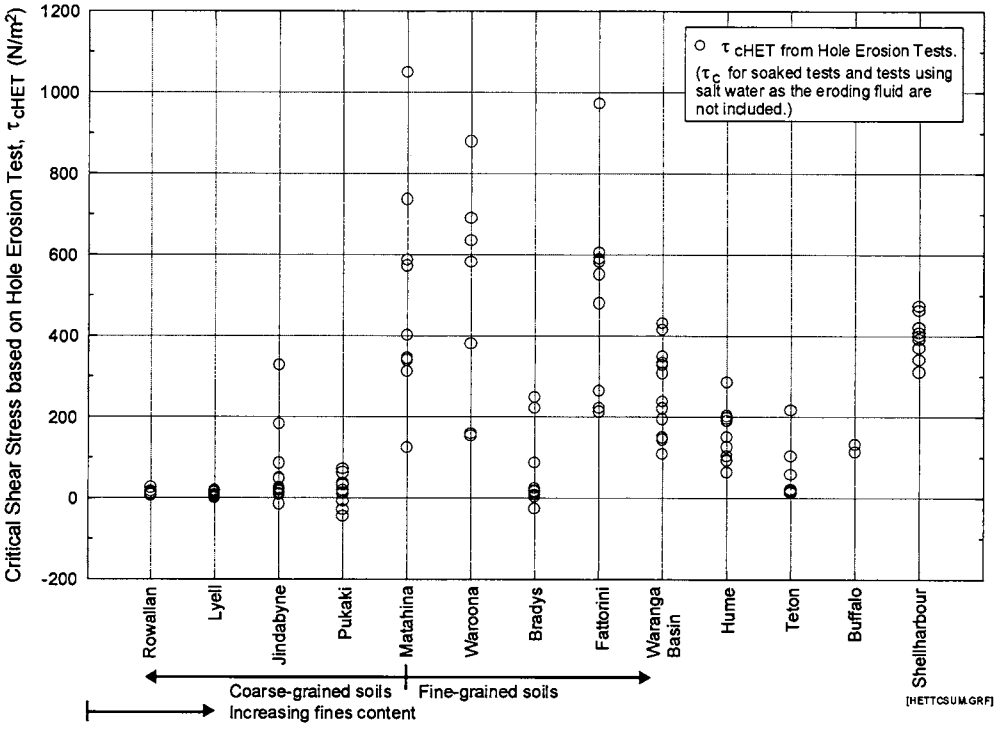

Figure 2.75: Summary of Critical Shear Stresses obtained from Hole Erosion Tests on all soil samples.

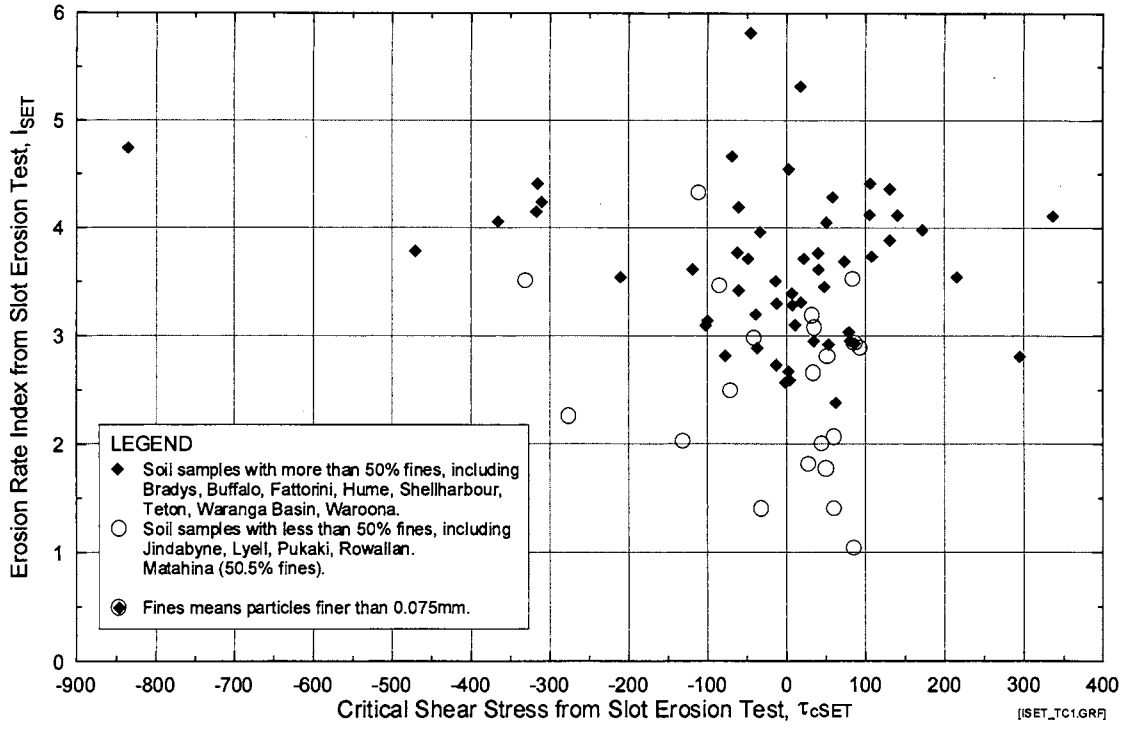

Figure 2.76: Erosion Rate Index (I_{SET}) versus Critical Shear Stress (τ_{cSET}) based on Slot Erosion Test data. Samples classified into fine and coarse-grained soils.

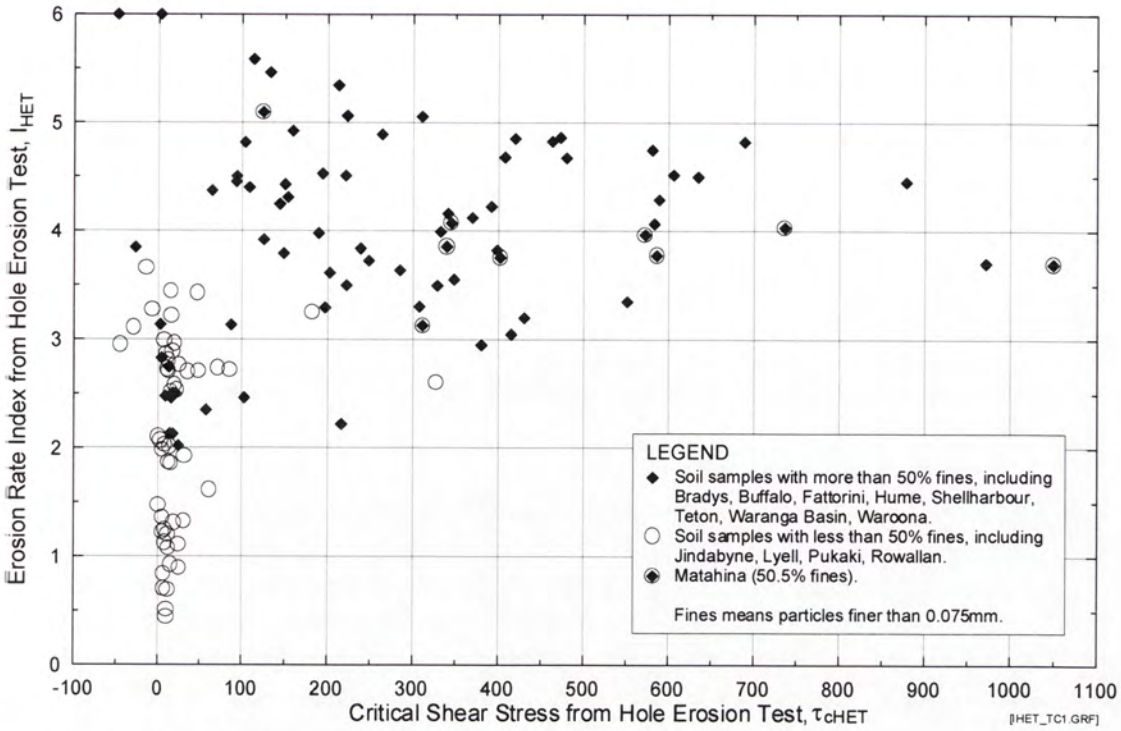

Figure 2.77: Erosion Rate Index (I_{HET}) versus Critical Shear Stress (τ_{cHET}) based on Hole Erosion Test data. Soil samples classified into fine-grained and coarse-grained soils.

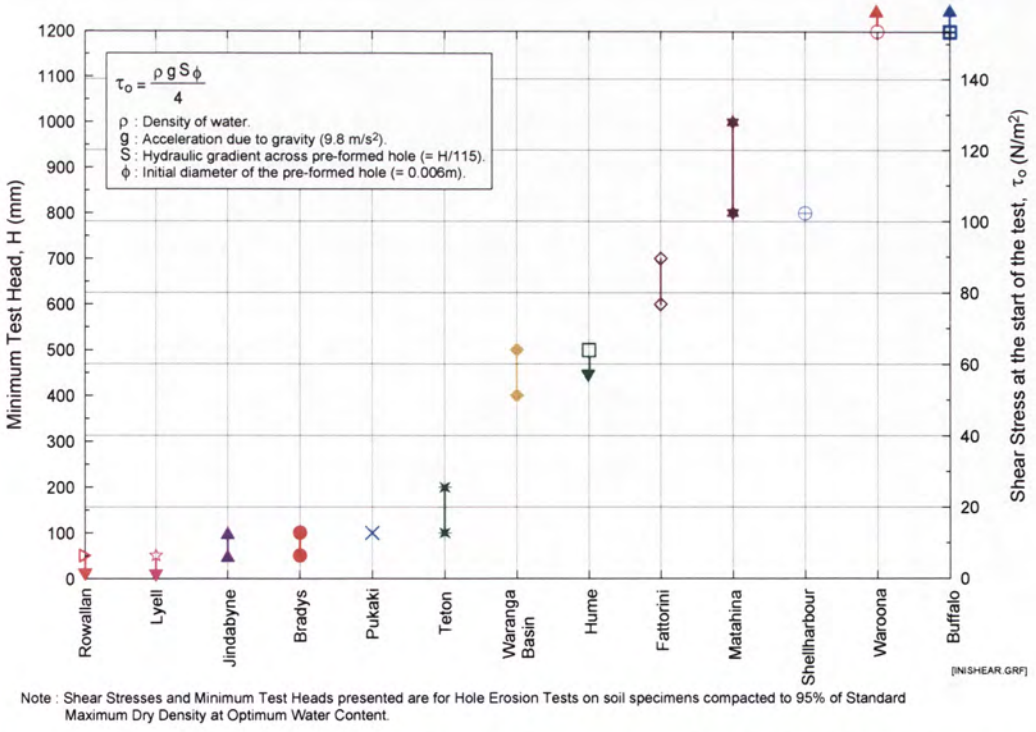

Note : Shear Stresses and Minimum Test Heads presented are for Hole Erosion Tests on soil specimens compacted to 95% of Standard Maximum Dry Density at Optimum Water Content.

Figure 2.78: Minimum Test Heads and the corresponding Initial Shear Stresses in Hole Erosion Tests

Figure 2.76 and Figure 2.77 do not show any obvious relationship between the I_{SET} and the τ_{cSET}, or between I_{HET} and τ_{cHET}. Figure 2.77 does show that coarse-grained soils, in general, have lower τ_{cHET} values than fine-grained soils.

τ_{cSET} and τ_{cHET} have also been plotted against the basic soil parameters as for the Erosion Rate Indices. As none of these plots shows any obvious trend or relationship, they are not presented in this thesis.

In Figure 2.78, the test heads and the corresponding initial shear stresses, τ_o, in Hole Erosion Tests on soil specimens prepared at 95% compaction and optimum water content are presented for the 13 soil samples. The test heads presented were the minimum head under which erosion was detected in the Hole Erosion Tests. τ_o is a simple function of the test head and the initial diameter of the pre-formed hole in the test specimen as described by equation 2.12 in Section 2.3.4. τ_o, therefore, similar to τ_{cHET}, can serve as an indicator of the relative resistance of a soil for against initiation of piping erosion. There is quite good agreement in trend terms between Figure 2.75 and Figure 2.78, but it is considered that this method is a more reliable way to determine the Critical Shear Stress than the extrapolation method used for Figure 2.75.

The initial shear stresses, τ_o, are also plotted against the Representative Erosion Rate Index, $\tilde{I}_{HET}$, in Figure 2.79. The plot shows the broad trend that coarse-grained soils have lower τ_o values than the fine-grained soils, and that τ_o value of a fine-grained soil increases as its Erosion Rate Index increases.

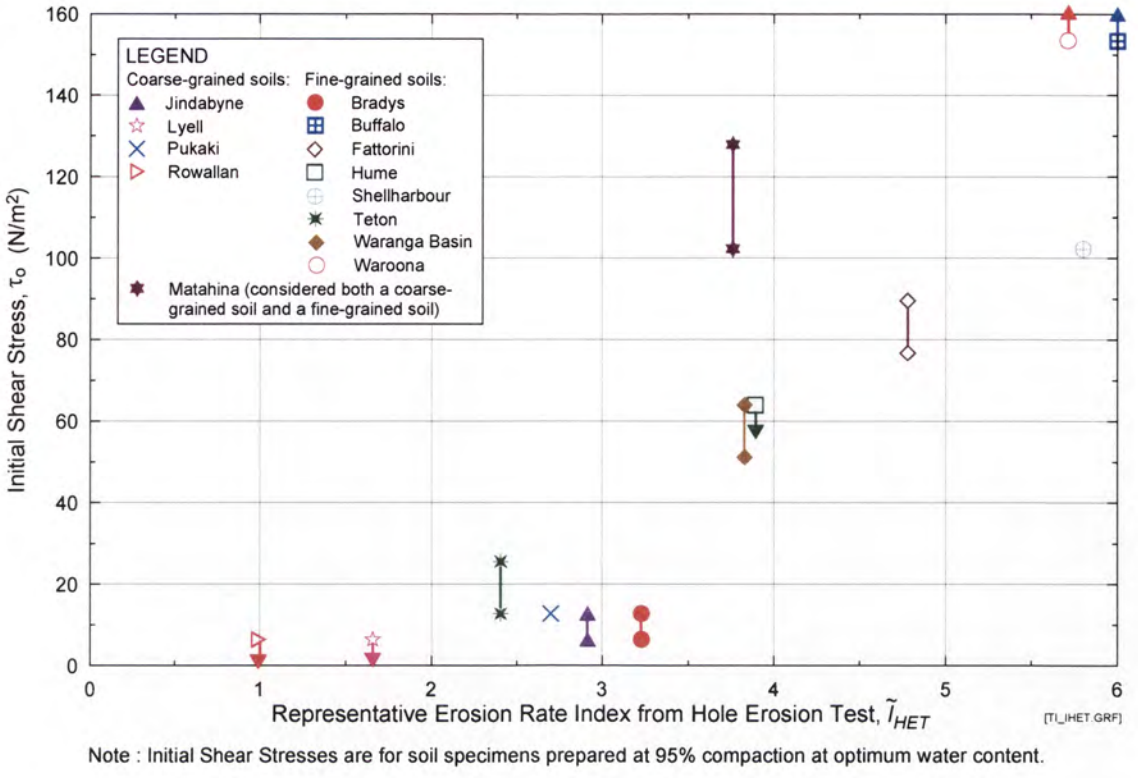

Figure 2.79: Initial Shear Stresses (τ_o) versus Representative Erosion Rate Index ($\tilde{I}_{HET}$) from Hole Erosion Tests.

2.5.3 Statistical correlation between test results and soil properties

Correlation of Erosion Rate Indices and Critical Shear Stresses with individual soil parameters

In order to reveal any possible links between the Erosion Rate Indices, the Critical Shear Stresses and the basic soil parameters, Erosion Rate Indices and Critical Shear Stresses have been correlated with individual soil parameters. The correlation analysis was carried out using the statistics package SPSS Ver.10, and the results are summarised in Table 2.12, Table 2.13 and Table 2.14.

In Table 2.12, Table 2.13 and Table 2.14, the strength of correlation is indicated by the Pearson's Coefficient of Correlation Coefficient (r), the Coefficient of Determination (r^2), and the Level of Significance. r = 0 means that two parameters are totally

unrelated, whereas r = 1 or -1 represents a perfect correlation. The square of the Pearson's Coefficient (r^2), sometimes called the Coefficient of Determination, indicates the percentage of variations in one parameter that can be explained by the other parameter. For example, $r^2 = 0.6$ means that 60% of the variations in one parameter can be explained by the other parameter. The Level of Significance of a correlation indicates the probability that an error is made by assuming that there is a relationship between two parameters while in actual fact they are unrelated. In the language of statistics, the Level of Significance represents the probability that a Type I Error is committed by rejecting a Null Hypothesis which states that two variables are not related.

Table 2.12: Correlations between Erosion Rate Indices from Slot Erosion Tests and Individual Soil Parameters.

Parameters	Unit		Erosion Rate Index from test			Predicted representative index for each soil sample		
			I_{SET} of all soil samples	I_{SET} of all coarse-grained soil samples	I_{SET} of all fine-grained soil samples	$\tilde{I}_{SET}$ of all soil samples	$\tilde{I}_{SET}$ of all coarse-grained soil samples	$\tilde{I}_{SET}$ of all fine-grained soil samples
		Sample size (N)	94	22	74	13	5	9
Dry Density	Mg/m^3	Correlation coefficient, r	-0.42					
		Coeff. of determination, r^2	0.17					
		Level of significance	2.9E-05					
Percentage Compaction	%	Correlation coefficient, r	-0.05	-0.08	0.03	—	—	—
		Coeff. of determination, r^2	0.00	0.01	0.00	(Note 1)	(Note 1)	(Note 1)
		Level of significance	6.4E-01 *	7.1E-01 *	7.9E-01 *			
Water Content	%	Correlation coefficient, r	0.44	0.44				
		Coeff. of determination, r^2	0.19	0.19				
		Level of significance	1.1E-05	4.2E-02				
Water Content Ratio	%	Correlation coefficient, r	0.28	0.30	0.29	—	—	—
		Coeff. of determination, r^2	0.08	0.09	0.08	(Note 2)	(Note 2)	(Note 2)
		Level of significance	7.2E-03	1.7E-01 *	1.2E-02			
Degree of Saturation	%	Correlation coefficient, r	0.49	0.44	0.43	0.88	1.00	0.69
		Coeff. of determination, r^2	0.24	0.19	0.19	0.77	1.00	0.47
		Level of significance	6.4E-07	4.3E-02	1.2E-04	8.7E-05	4.2E-05	4.2E-02
Sand Content	%	Correlation coefficient, r	-0.49	-0.52		-0.66	-0.91	
		Coeff. of determination, r^2	0.24	0.27		0.43	0.82	
		Level of significance	5.9E-07	1.3E-02		1.5E-02	3.3E-02	
Fines Content	%	Correlation coefficient, r	0.44	0.64		0.59	0.97	
		Coeff. of determination, r^2	0.19	0.41		0.34	0.94	
		Level of significance	8.8E-06	1.4E-03		3.5E-02	6.8E-03	
Clay Content (US definition)	%	Correlation coefficient, r	0.42	0.74		0.60	0.96	
		Coeff. of determination, r^2	0.17	0.54		0.35	0.93	
		Level of significance	2.8E-05	9.2E-05		3.2E-02	8.9E-03	
Clay Content (UK definition)	%	Correlation coefficient, r	0.41	0.71		0.59	0.94	
		Coeff. of determination, r^2	0.17	0.51		0.34	0.88	
		Level of significance	3.8E-05	2.0E-04		3.5E-02	1.8E-02	
Liquid Limit	%	Correlation coefficient, r	0.49	0.57		0.61		
		Coeff. of determination, r^2	0.24	0.32		0.37		
		Level of significance	5.9E-07	5.7E-03		2.7E-02		
Plasticity Index	%	Correlation coefficient, r	0.46	0.54	0.24	0.55		
		Coeff. of determination, r^2	0.21	0.29	0.06	0.31		
		Level of significance	2.5E-06	9.3E-03	4.0E-02	5.0E-02		
Activity		Correlation coefficient, r	0.32	0.47				
		Coeff. of determination, r^2	0.10	0.22				
		Level of significance	1.5E-03	2.9E-02				
Pinhole Test Classification	As ordinal no.	Correlation coefficient, r	0.56		0.41	0.60		
		Coeff. of determination, r^2	0.32		0.16	0.36		
		Level of significance	3.8E-09		3.4E-04	3.1E-02		
Emerson Class	As ordinal no.	Correlation coefficient, r			0.34			
		Coeff. of determination, r^2			0.12			
		Level of significance			2.9E-03			
Percentage Dispersion	%	Correlation coefficient, r	-0.21		-0.33			
		Coeff. of determination, r^2	0.04		0.11			
		Level of significance	4.3E-02		3.6E-03			
SAR		Correlation coefficient, r			-0.26			
		Coeff. of determination, r^2			0.07			
		Level of significance			2.4E-02			
Cation Content	meq/L	Correlation coefficient, r			-0.29			
		Coeff. of determination, r^2			0.08			
		Level of significance			1.3E-02			

Notes:

1 When Representative Erosion Indices are being studied, Percentage Compaction becomes a constant = 95%, but not a variable.

2 When Representative Erosion Indices are being studied, Water Content Ratio becomes a constant = 0, but not a variable.

3 Asterisk '*' means that the Level of Significance is greater than 0.05.

Table 2.13: Correlations between Erosion Rate Indices from Hole Erosion Tests and Individual Soil Parameters.

Parameters	Unit		Erosion Rate Index from test			Predicted representative index for each soil sample		
			I_{HET}	I_{HET}	I_{HET}	$\tilde{I}_{HET}$	$\tilde{I}_{HET}$	$\tilde{I}_{HET}$
			of all soil samples	of all coarse-grained soil samples	of all fine-grained soil samples	of all soil samples	of all coarse-grained soil samples	of all fine-grained soil samples
		Sample size (N)	148	59	98	13	5	9
Dry Density	Mg/m^3	Correlation coefficient, r	-0.49					
		Coeff. of determination, r^2	0.24					
		Level of significance	1.7E-10					
Percentage Compaction	%	Correlation coefficient, r	-0.05	0.20	0.11	-----	----	----
		Coeff. of determination, r^2	0.00	0.04	0.01	(Note 1)	(Note 1)	(Note 1)
		Level of significance	5.4E-01 *	1.2E-01 *	3.0E-01 *			
Water Content	%	Correlation coefficient, r	0.50	0.44		0.55		
		Coeff. of determination, r^2	0.25	0.20		0.30		
		Level of significance	1.1E-10	4.3E-04		5.1E-02 *		
Water Content Ratio	%	Correlation coefficient, r	0.09	0.15	0.14	----	----	----
		Coeff. of determination, r^2	0.01	0.02	0.02	(Note 2)	(Note 2)	(Note 2)
		Level of significance	2.9E-01 *	2.4E-01 *	1.8E-01 *			
Degree of Saturation	%	Correlation coefficient, r	0.47	0.53	0.36	0.85	0.97	0.65
		Coeff. of determination, r^2	0.22	0.28	0.13	0.73	0.94	0.42
		Level of significance	1.8E-09	1.9E-05	3.1E-04	2.1E-04	6.1E-03	5.8E-02 *
Sand Content	%	Correlation coefficient, r	-0.68	-0.71		-0.73		
		Coeff. of determination, r^2	0.47	0.51		0.54		
		Level of significance	1.7E-19	6.8E-11		4.5E-03		
Fines Content	%	Correlation coefficient, r	0.64	0.80		0.69	0.93	
		Coeff. of determination, r^2	0.41	0.64		0.48	0.87	
		Level of significance	1.7E-19	1.5E-17		8.9E-03	2.1E-02	
Clay Content (US definition)	%	Correlation coefficient, r	0.67	0.84	0.31	0.74	0.93	
		Coeff. of determination, r^2	0.45	0.71	0.10	0.54	0.87	
		Level of significance	1.7E-19	1.5E-17	1.6E-03	4.0E-03	2.2E-02	
Clay Content (UK definition)	%	Correlation coefficient, r	0.66	0.82	0.34	0.73	0.90	
		Coeff. of determination, r^2	0.44	0.68	0.12	0.53	0.82	
		Level of significance	1.7E-19	1.5E-17	5.2E-04	4.5E-03	3.5E-02	
Liquid Limit	%	Correlation coefficient, r	0.62	0.64		0.72		
		Coeff. of determination, r^2	0.39	0.41		0.53		
		Level of significance	4.2E-18	5.3E-08		5.1E-03		
Plasticity Index	%	Correlation coefficient, r	0.59	0.60	0.25	0.70		
		Coeff. of determination, r^2	0.34	0.36	0.06	0.49		
		Level of significance	1.9E-15	4.8E-07	1.2E-02	7.6E-03		
Activity		Correlation coefficient, r	0.37	0.49				
		Coeff. of determination, r^2	0.14	0.24				
		Level of significance	3.0E-06	7.7E-05				
Pinhole Test Classification	As Ordinal No.	Correlation coefficient, r	0.65		0.45	0.76		0.66
		Coeff. of determination, r^2	0.42		0.20	0.57		0.43
		Level of significance	1.7E-19		3.9E-06	2.7E-03		5.5E-02 *
Emerson Class	As Ordinal No.	Correlation coefficient, r			0.27			
		Coeff. of determination, r^2			0.07			
		Level of significance			8.1E-03			
Percentage Dispersion	%	Correlation coefficient, r	-0.16		-0.32			
		Coeff. of determination, r^2	0.03		0.10			
		Level of significance	4.9E-02		1.5E-03			
SAR		Correlation coefficient, r						
		Coeff. of determination, r^2						
		Level of significance						
Cation Content	meq/L	Correlation coefficient, r						
		Coeff. of determination, r^2						
		Level of significance						

Notes:

1 When Representative Erosion Indices are being studied, Percentage Compaction becomes a constant = 95%, but not a variable.

2 When Representative Erosion Indices are being studied, Water Content Ratio becomes a constant = 0, but not a variable.

3 Asterisk ' * ' means that the Level of Significance is greater than 0.05.

The Level of Significance is usually set at 5% or lower. That means we allow for a 5% probability of making an error by assuming that two parameters are related while in fact they are not. In Table 2.12, Table 2.13 and Table 2.14, only the results of the correlation analysis which resulted in a Level of Significance of 5% or lower are presented.

The Level of Significance depends on the value of the Pearson's Correlation Coefficient (r) and the Sample Size (N). Table 2.15 indicates the critical value of r for satisfying

the requirement of a 5% or 1% Level of Significance. In the table, the Sample Size (*N*) is the number of data points obtained from the erosion tests as shown in Table 2.12, Table 2.13 and Table 2.14.

Table 2.14: Correlations between Critical Shear Stresses from Hole Erosion Tests and Individual Soil Parameters.

Parameters	Unit		Critical Shear Stress from Slot Erosion Tests			Critical Shear Stress from Hole Erosion Tests		
			of all soil samples	of all coarse-grained soil samples	of all fine-grained soil samples	of all soil samples	of all coarse-grained soil samples	of all fine-grained soil samples
		Sample size (N)	75	21	55	125	59	75
Dry Density	Mg/m^3	Correlation coefficient, r				-0.37	-0.33	
		Coeff. of determination, r^2				0.14	0.11	
		Level of significance				2.4E-05	1.2E-02	
Percentage Compaction	%	Correlation coefficient, r	0.22	-0.10	0.28	-0.32	-0.03	-0.25
		Coeff. of determination, r^2	0.05	0.01	0.08	0.10	0.00	0.06
		Level of significance	5.4E-02 *	6.6E-01 *	4.0E-02	2.9E-04	8.3E-01 *	3.2E-02
Water Content	%	Correlation coefficient, r				0.28	0.46	
		Coeff. of determination, r^2				0.08	0.21	
		Level of significance				1.4E-03	2.5E-04	
Water Content Ratio	%	Correlation coefficient, r	-0.09	-0.04	-0.15	-0.11	-0.02	-0.18
		Coeff. of determination, r^2	0.01	0.00	0.02	0.01	0.00	0.03
		Level of significance	4.4E-01 *	8.7E-01 *	2.6E-01 *	2.3E-01 *	8.6E-01 *	1.2E-01 *
Degree of Saturation	%	Correlation coefficient, r						
		Coeff. of determination, r^2						
		Level of significance						
Sand Content	%	Correlation coefficient, r				-0.44	-0.53	0.34
		Coeff. of determination, r^2				0.19	0.28	0.11
		Level of significance				2.8E-07	1.6E-05	3.2E-03
Fines Content	%	Correlation coefficient, r				0.40	0.62	-0.40
		Coeff. of determination, r^2				0.16	0.38	0.16
		Level of significance				3.0E-06	2.1E-07	3.5E-04
Clay Content (US definition)	%	Correlation coefficient, r			0.29	0.35	0.74	
		Coeff. of determination, r^2			0.08	0.12	0.54	
		Level of significance			3.5E-02	7.0E-05	3.9E-12	
Clay Content (UK definition)	%	Correlation coefficient, r	0.24		0.33	0.36	0.75	
		Coeff. of determination, r^2	0.06		0.11	0.13	0.56	
		Level of significance	3.7E-02		1.5E-02	4.2E-05	5.9E-13	
Liquid Limit	%	Correlation coefficient, r				0.45	0.46	
		Coeff. of determination, r^2				0.20	0.22	
		Level of significance				1.9E-07	2.1E-04	
Plasticity Index	%	Correlation coefficient, r				0.44	0.40	
		Coeff. of determination, r^2				0.19	0.16	
		Level of significance				3.9E-07	1.8E-03	
Activity		Correlation coefficient, r				0.40		0.29
		Coeff. of determination, r^2				0.16		0.08
		Level of significance				3.2E-06		1.2E-02
Pinhole Test Classification	As Ordinal No.	Correlation coefficient, r				0.45		
		Coeff. of determination, r^2				0.20		
		Level of significance				1.3E-07		
Emerson Class	As Ordinal No.	Correlation coefficient, r						
		Coeff. of determination, r^2						
		Level of significance						
Percentage Dispersion	%	Correlation coefficient, r						
		Coeff. of determination, r^2						
		Level of significance						
SAR		Correlation coefficient, r						
		Coeff. of determination, r^2						
		Level of significance						
Cation Content	meq/L	Correlation coefficient, r						
		Coeff. of determination, r^2						
		Level of significance						

Note:

1 Asterisk ' * ' means that the Level of Significance is greater than 0.05.

Table 2.15: Critical values of the Pearson's Correlation Coefficient at a Level of Significance of 5% and 1%.

Sample	Sample Size	Degree of freedom	Critical value of Pearson's Correlation Coefficient, r		Critical value of the Coefficient of Determination, r^2	
			Level of Significance		Level of Significance	
	N	N - 2	5%	1%	5%	1%
Successful SETs on all soil samples	94	92	0.20	0.27	0.04	0.07
Successful SETs on coarse-grained soil samples	22	20	0.42	0.54	0.18	0.29
Successful SETs on fine-grained soil samples	74	72	0.23	0.30	0.05	0.09
Successful HETs on all soil samples	148	146	0.20	0.25	0.04	0.06
All successful HETs on coarse-grained soil samples	59	57	0.26	0.33	0.07	0.11
Successful HETs on fine-grained soil samples	98	96	0.20	0.26	0.04	0.07
All soil samples	13	11	0.55	0.68	0.30	0.46
Coarse-grained soil samples	5	3	0.88	0.96	0.77	0.92
Fine-grained soil samples	9	7	0.67	0.80	0.45	0.64

Findings of the correlation analysis are summarised as follows:

- Correlation using data from Slot Erosion Tests

  Table 2.12 shows that many soil parameters are correlated with I_{SET} at the 5% significance level, but none of them shows a particularly strong correlation if all soils are considered together.

  If only the test data on the coarse-grained soils are analysed, Table 2.12 shows that fines content and clay content have moderately good correlations with I_{SET}, with Pearson's correlation coefficients (r) higher than 0.63. The degree of saturation and the Atterberg's limits also show some degree of correlation with I_{SET}. In the correlation analysis, Matahina is considered both a coarse-grained soil and a fine-grained soil.

  If only the test data on the fine-grained soils are analysed, Table 2.12 shows that the degree of saturation, the Pinhole Test classification, the Emerson Class and the Percentage Dispersion exhibit some degree of correlation with I_{SET}, but the correlations are weak.

Correlation of the Erosion Rate Indices with either the Percentage Compaction, or the Water Content Ratio is insignificant.

- Correlation using all data from Hole Erosion Tests

  Table 2.13 shows that many soil parameters are correlated with I_{HET} at the 5% significance level, but none of them shows a particularly strong correlation if all soils are considered together.

  If only the test data on the coarse-grained soils are considered, correlation analysis shows that sand content, fines content and clay content have good correlations with I_{HET} with r values greater than 0.71. The water content, the degree of saturation and the Atterberg's Limits show some, but weak correlation with I_{HET}.

  If only the test data on the fine-grained soils are considered, correlation shows that the degree of saturation, the clay content, the Pinhole Test classification, the Emerson Class, the Percentage Dispersion show some degree of correlation with I_{HET}, but the correlations are not strong.

  Correlation of the Erosion Rate Indices with either the Percentage Compaction, or the Water Content Ratio is insignificant.

- Correlations between soil parameters and representative erosion rate indices ($\tilde{I}_{SET}$ and $\tilde{I}_{HET}$) predicted from non-linear regression models

  Table 2.12 shows that , based on SET data for coarse-grained soils, $\tilde{I}_{SET}$ have a very strong correlation with the degree of saturation, the fines content and the clay content with r values greater than 0.96. Similarly, $\tilde{I}_{HET}$ also shows a very strong correlation with the degree of saturation, the fines content and the clay content with r values greater than 0.93 when the HET data are considered.

For fine-grained soils, $\tilde{I}_{SET}$ shows moderately good correlation with the degree of saturation with r value = 0.69 as shown in the Table 2.12. When the HET data were analysed, $\tilde{I}_{HET}$ shows moderately good correlation with the degree of saturation and the Pinhole Test Classification, with r values at about 0.65 as shown in Table 2.13.

- Correlations between Critical Shear Stresses and soil parameters
  Table 2.14 shows weak correlations between the Critical Shear Stresses, τ_{cSET}, obtained from Slot Erosion Tests on fine-grained soil samples and the clay content, and between τ_{cSET} and the Percentage Compaction. Apart from that, τ_{cSET} do not show any significant correlation with any of the other soil parameters. Table 2.14 also shows that the Critical Shear Stresses, τ_{cHET}, obtained from Hole Erosion Tests on coarse-grained soil samples have moderately good correlation with the fines content and the clay content. τ_{cHET} for fine-grained soils do not show particularly good correlation with any of the soil parameters.

The correlation analysis shows that the Erosion Rate Indices and the Critical Shear Stresses cannot be satisfactorily explained by a single soil parameter in that none of the correlations is particularly strong. This observation is consistent with the plots of Erosion Rate Indices against individual soil properties in Appendices E, F, G and H which show considerable scattering of the data points. Plots of Critical Shear Stresses in Figure 2.74 to Figure 2.77 also show considerable scattering of the data points. A multivariate analysis is required for studying the relationship between the Erosion Rate Indices or the Critical Shear Stresses and a group of soil parameters. The following Section describes the multivariate analysis.

Multiple linear regression analysis between erosion rate indices, critical shear stresses and soil parameters

The main purpose of multiple linear regression analysis is to find out any possible link between the Erosion Rate Indices or the Critical Shear Stresses with one or more of the basic soil parameters. A multiple linear regression equation relates a dependent variable Y with a number of independent variables X and takes the form:

$$Y = c_0 + c_1 X_1 + c_2 X_2 + \cdots + c_i X_i \qquad \text{Eqn 2.23}$$

where Y is the dependent variable, which may be the Erosion Rate Index, or the Critical Shear Stress,

$X_1 \cdots X_i$ are the independent variables (also called the predictor variables) which, for example, may be water content, or dry density, etc.

$c_1 \cdots c_i$ are the model coefficients which are to be found out from the regression analysis.

The independent variables used for defining a regression equation can be selected manually based on their degree of correlation with the dependent variable as revealed by the results of correlation analysis in the preceding Section. In addition, there are three systematic methods for selecting or rejecting independent variables in a regression analysis. The three methods are forward selection, backward elimination and stepwise regression.

In brief, the forward selection procedure starts with no independent variable in the regression equation. The first independent variable considered for insertion into the equation is one which will cause the biggest increase in the coefficient of determination. Independent variables are then added one by one until the addition of a new independent variable has caused no significant improvement in the correlation. The backward elimination is the opposite of the forward selection procedure. All the independent variables start in the equation are eliminated one at a time. At each stage the independent variable least important to the correlation will be removed from the

equation. The stepwise regression procedure is an improved version of forward selection. In this procedure, the variables already in the equation are re-evaluated at each stage. Due to inter-correlation, a variable that is important at an earlier stage may become not important at a later stage. Therefore, before a variable is added in the stepwise regression process, the least important variable identified during the re-evaluation process will be removed.

Using the above methods for selecting independent variables, and with the use of the statistics package SPSS Ver. 10, regression equations were obtained for the Erosion Rate Indices and the Critical Shear Stresses.

As the plots in Appendices E – H and the correlation analysis in the preceding Section show that the Erosion Rate Indices and the Critical Shear Stresses of the coarse-grained soils and the fine-grained soils are influenced by different sets of soil parameters, there is a need to analyse separately the data for the coarse-grained soil samples and the data for the fine-grained soil samples. The various linear models obtained from the multiple regression analysis are summarised in Table 2.16 and Table 2.17.

The strength of the correlations between the dependent and the independent variables in the regression equations in Table 2.16 and Table 2.17 are described by the parameters R, R^2, Adjusted R^2, F and the level of significance. R is the correlation coefficient similar to the Pearson's Correlation Coefficient, r, in a correlation analysis between 2 variables. R^2 is the Coefficient of Determination when the predicted values of the dependent variable are correlated with their actual values. To obtain an unbiased estimate of R^2 for the population, the Adjusted R^2 is used instead of R^2. The Adjusted R^2 takes account of the number of independent variables in the regression equation. The Adjusted R^2 is always less than R^2, and the difference between the Adjusted R^2 and R^2 increases as more independent variables are added to the regression equation. A large value of Adjusted R^2 means a better correlation. The level of significance is the probability that an error is made by assuming that the variables are correlated while in actual fact they are not. The level of significance is dependent upon the F statistics, the sample size and the number of independent variables in the regression equation. Usually a large F

indicates a better correlation between the independent variables and the dependent variable.

The regression equations in Table 2.16 and Table 2.17 have been used to predict values of Erosion Rate Indices and Critical Shear Stresses. In Figure 2.80 and Figure 2.81 the predicted Erosion Rate Indices for the coarse-grained soil samples are plotted against the actual values obtained from tests. The plots show moderately good correlation between the predicted and the actual values. The same regression equations were also used to predicted values of the Representative Erosion Rate Index corresponding to 95% compaction and optimum water content. These predicted values of the Erosion Rate Index ($\hat{I}_{SET}$ and $\hat{I}_{HET}$) are compared with the Representative Erosion Rate Indices ($\tilde{I}_{SET}$ and $\tilde{I}_{HET}$) predicted from non-linear regression models described in Section 2.5.2. The non-linear models were developed for each soil samples using only the dry density and the water content as the independent variables. The plots in Figure 2.82 and Figure 2.83 show very good match between $\hat{I}_{SET}$ and $\tilde{I}_{SET}$, and between $\hat{I}_{HET}$ and $\tilde{I}_{HET}$.

Table 2.16: Summary of Linear Regression Models for prediction of Erosion Rate Indices and Critical Shear Stresses for coarse-grained soils.

Dependent variable	Data set	No. of data points	Correlation statistics						Independent variables	Unit	Model Coefficient
			Correlation Coefficient, R	R^2	Adjusted R^2	Standard error of the estimate	F	Level of significance			
$\hat{I}_{SET}$	All SET data on coarse-grained soil samples	22	0.856	0.732	0.625	0.673	6.831	1.2×10^{-3}	Constant		-8.836
									Percentage Compaction (Note 1)	%	-0.120
									Dry density	Mg/m^3	6.904
									Water Content Ratio (Note 2)	%	-0.0745
									Water content	%	0.386
									Degree of saturation	%	0.0558
									Clay content (US)	%	0.0880
$\hat{I}_{HET}$	All HET data on coarse-grained soil samples	59	0.891	0.793	0.769	0.519	33.253	3.8×10^{-16}	Constant		6.623
									Percentage Compaction (Note 1)	%	-0.104
									Dry density	Mg/m^3	-0.0160
									Water Content Ratio (Note 2)	%	-0.0736
									Water content	%	-0.0443
									Degree of saturation	%	0.113
									Clay content (US)	%	0.0611

Dependent variable	Data set	No. of data points	Correlation statistics						Independent variables	Unit	Model Coefficient
			Correlation Coefficient, R	R^2	Adjusted R^2	Standard error of the estimate	F	Level of significance			
$\hat{\tau}_{c\,SET}$	All SET data on coarse-grained soil samples	21	No regression model found at a level of significance of 5% or better.								
$\hat{\tau}_{c\,HET}$	All HET data on coarse-grained soil samples	59	0.838	0.705	0.683	115.38	32.296	9.0×10^{-14}	Constant		-446.530
									Degree of Saturation	%	-1.024
									Percentage Dispersion	%	12.339
									Activity		-268.609
									SAR	$(meq/l)^{1/2}$	240.563

Notes :

1. Percentage Compaction is the ratio of Dry Density to the Standard Max. Dry Unit Weight (i.e. $\rho_d / \rho_{d_{max}}$).

2. Water Content Ratio is the deviation of Water Content from the Optimum Water Content divided by the Optimum Water Content (i.e. $(\omega - OWC)/OWC$).

Table 2.17: Summary of Linear Regression Models for prediction of Erosion Rate Indices and Critical Shear Stresses for fine-grained soils.

Dependent variable	Data set	No. of data points	Correlation statistics						Independent variables	Unit	Model Coefficient
			Correlation Coefficient, R	R^2	Adjusted R^2	Standard error of the estimate	F	Level of significance			
$\hat{I}_{SET}$	All SET data on fine-grained soil samples	74	0.820	0.672	0.626	0.734	14.573	1.7×10^{-12}	Constant		-9.153
									Percentage Compaction (Note)	%	-0.194
									Dry density	Mg/m^3	16.528
									Water Content Ratio (Note)	%	0.0209
									Water content	%	0.240
									Fines content	%	-0.0293
									Clay content (US)	%	0.0478
									Liquid Limit	%	-0.0107
									Plasticity Index	%	0.00815
									Pinhole Test Classification		0.558
$\hat{I}_{HET}$	All HET data on fine-grained soil samples	98	0.867	0.753	0.727	0.620	29.736	4.5×10^{-23}	Constant		-10.201
									Percentage Compaction (Note)	%	-0.0415
									Dry density	Mg/m^3	9.572
									Water Content Ratio (Note)	%	0.00966
									Water content	%	0.103
									Fines content	%	-0.00564
									Clay content (US)	%	0.0418
									Liquid Limit	%	-0.0904
									Plasticity Index	%	0.111
									Pinhole Test Classification		0.443

Dependent variable	Data set	No. of data points	Correlation statistics						Independent variables	Unit	Model Coefficient
			Correlation Coefficient, R	R^2	Adjusted R^2	Standard error of the estimate	F	Level of significance			
$\hat{\tau}_{c\ SET}$	All SET data on fine-grained soil samples	55	<= 0.588	<= 0.345	<= 0.185	>= 166.9	<= 5.158	>= 8.0×10^{-3}	Models are unsatisfactory as revealed by low values of Adjusted R^2 (all less than 0.6).		
$\hat{\tau}_{c\ HET}$	All HET data on fine-grained soil samples	75	<= 0.801	<= 0.641	<= 0.589	>= 151.8	<= 17.556	>= 3.7×10^{-12}	Models are unsatisfactory as revealed by low values of Adjusted R^2 (all less than 0.6).		

Note : Refer to Notes for Table 2.16 for the meaning of Percentage Compaction and Water Content Ratio.

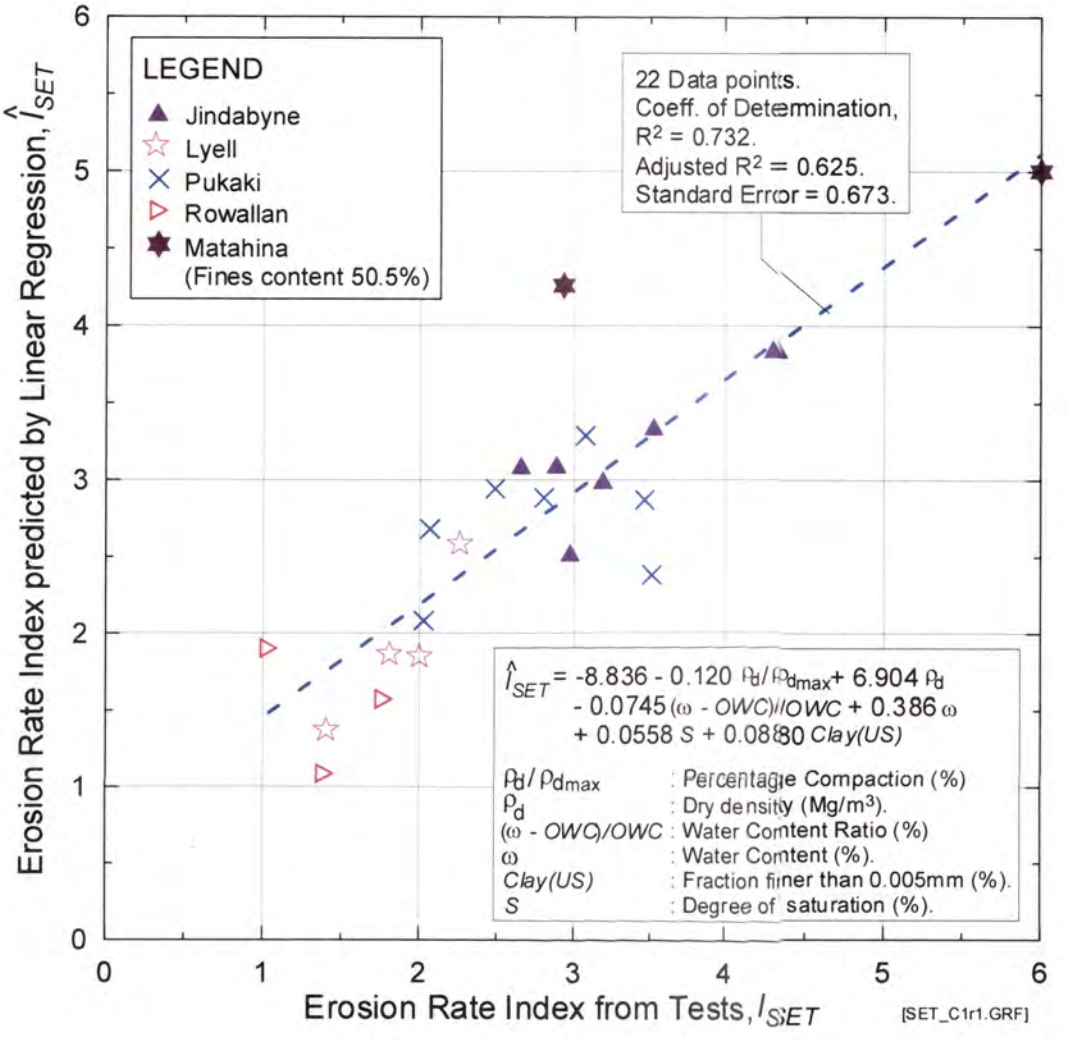

Figure 2.80: Erosion Rate Indices ($\hat{I}_{SET}$) predicted by Multiple Linear Regression Model versus Erosion Rate Indices (I_{SET}) from Slot Erosion Tests on Coarse-grained Soil Samples.

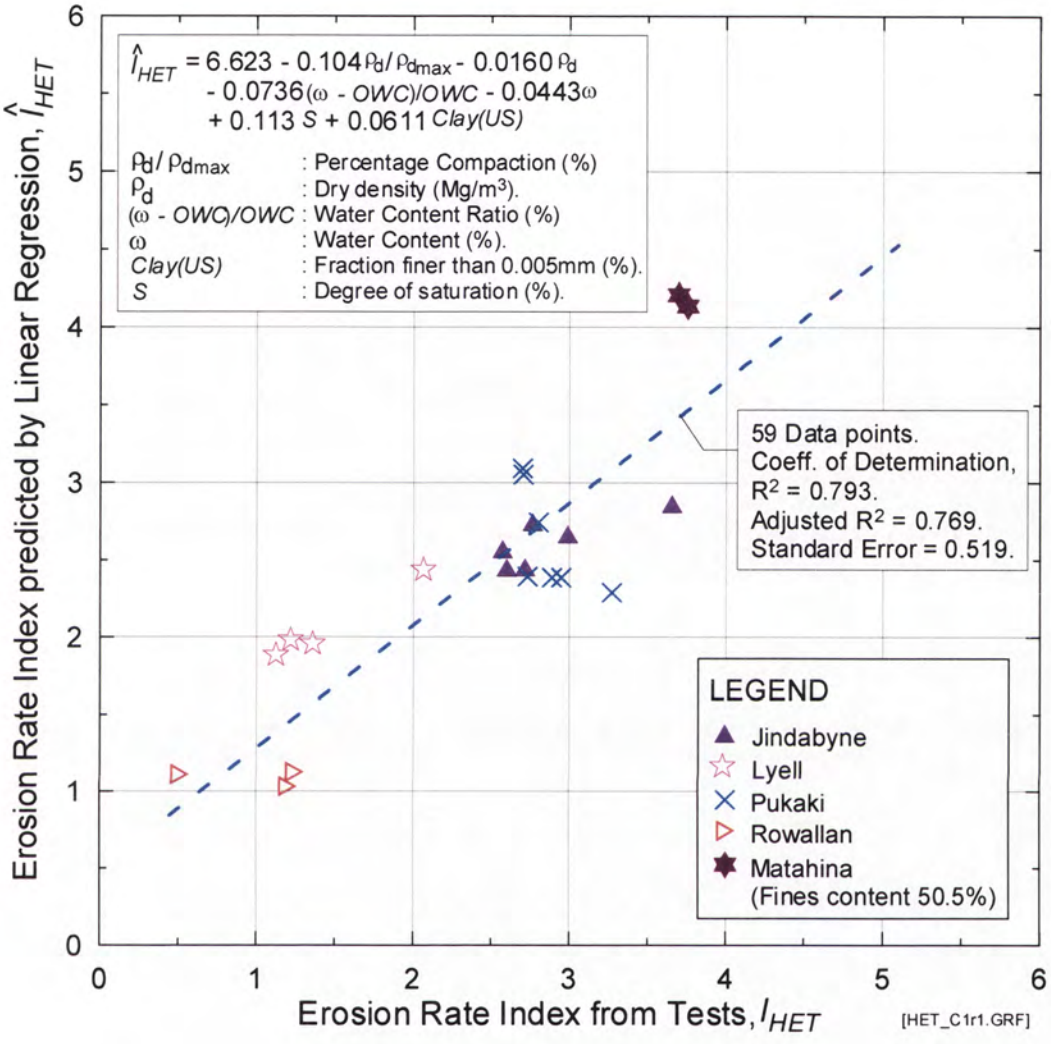

Figure 2.81: Erosion Rate Indices ($\hat{I}_{HET}$) predicted by Multiple Linear Regression Model versus Erosion Rate Indices (I_{HET}) from Hole Erosion Tests on Coarse-grained Soil Samples.

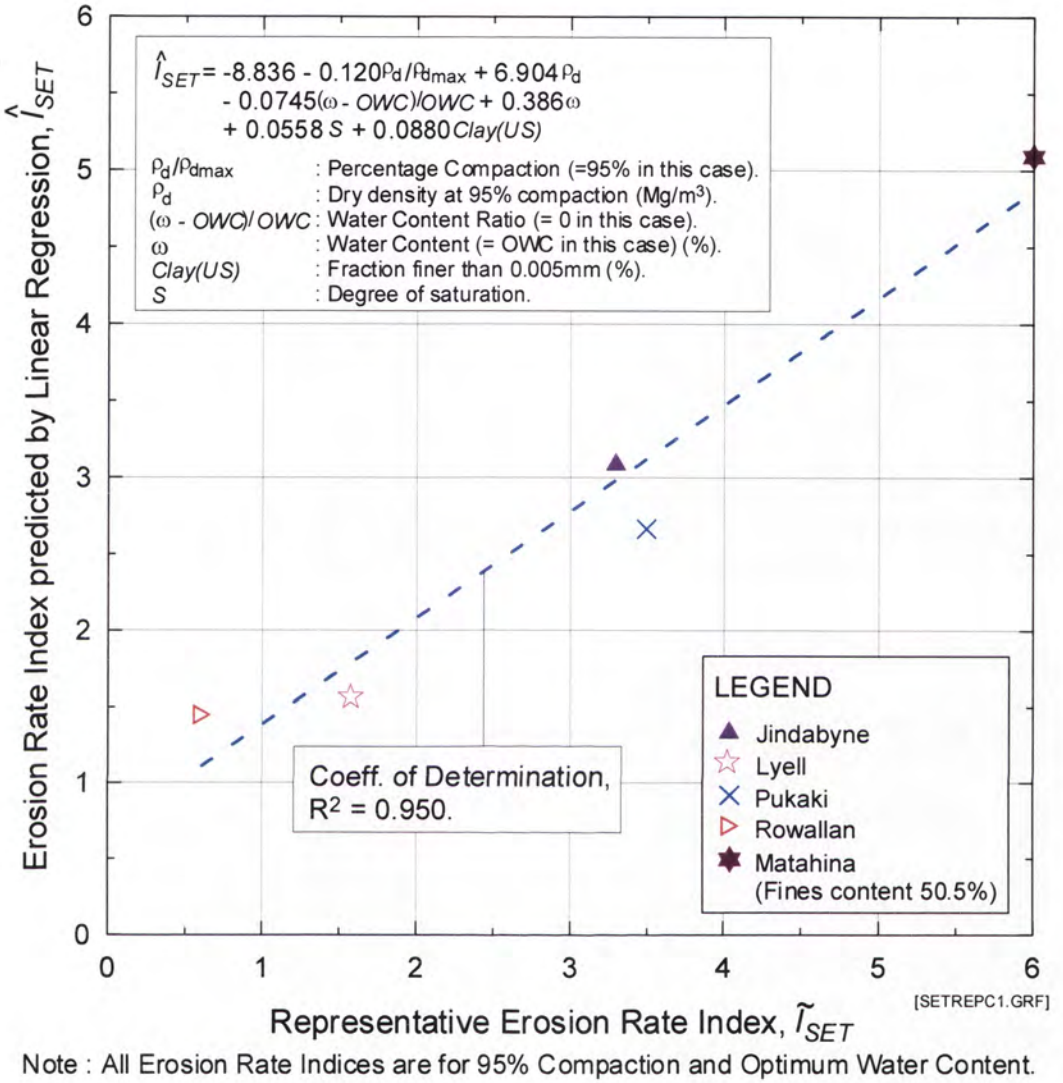

Note : All Erosion Rate Indices are for 95% Compaction and Optimum Water Content.

Figure 2.82: Erosion Rate Indices ($\hat{I}_{SET}$) predicted by Multiple Linear Regression Model versus Representative Erosion Rate Indices ($\tilde{I}_{SET}$) predicted by Non-linear Regression Models for each Coarse-grained Soil Samples.

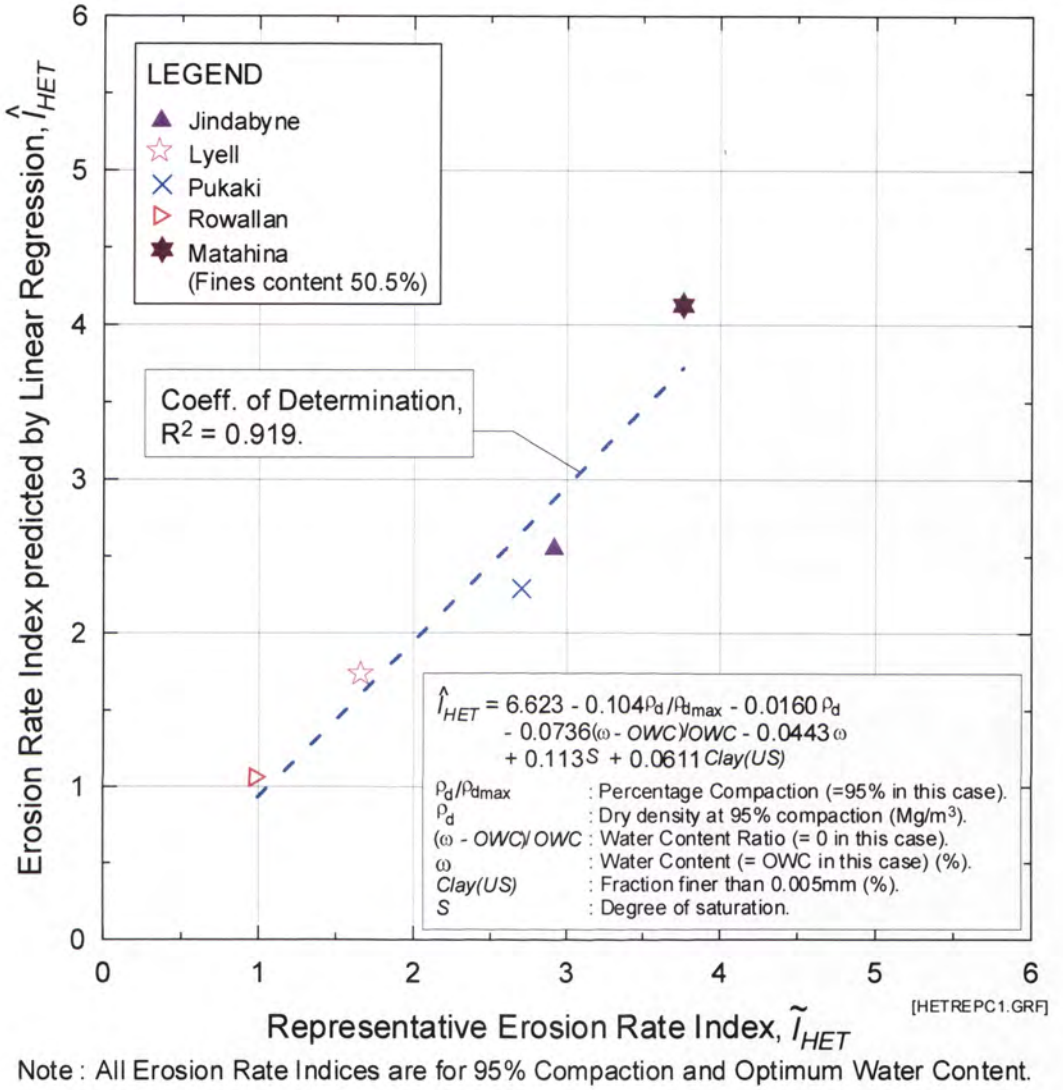

Note : All Erosion Rate Indices are for 95% Compaction and Optimum Water Content.

Figure 2.83: Erosion Rate Indices ($\hat{I}_{HET}$) predicted by Multiple Linear Regression Model versus Representative Erosion Rate Indices ($\tilde{I}_{HET}$) predicted by Non-linear Regression Models for each Coarse-grained Soil Samples.

In Figure 2.84 and Figure 2.85 the predicted Erosion Rate Indices for the fine-grained soil samples are plotted against the actual values obtained from tests. Figure 2.84 reveals that the predicted Erosion Rate Indices do not show a particularly strong correlation with the actual values obtained from Slot Erosion Tests on the fine-grained soil samples. The plot in Figure 2.85 however, shows moderately good correlation between the predicted Indices and the actual values obtained from Hole Erosion Tests on the fine-grained soil samples. The predicted values of Erosion Rate Indices at 95% compaction and optimum water content are plotted against the Representative Erosion Rate Indices for the fine-grained soil samples in Figure 2.86 and. Figure 2.87. Figure 2.86 does not show a particularly good correlation between $\hat{I}_{SET}$ and $\tilde{I}_{SET}$ based on the Slot Erosion Test data. Figure 2.87 on the other hand, shows very good correlation between $\hat{I}_{HET}$ and $\tilde{I}_{HET}$.

Figure 2.88 shows a plot of the predicted Critical Shear Stresses, $\hat{\tau}_{c\,HET}$, against the Critical Shear Stresses, τ_{cHET}, obtained from Hole Erosion Test data on the coarse-grained soil samples using the extrapolation method. The independent variables of the model, namely the Degree of Saturation, Activity, Percentage Dispersion and the Sodium Adsorption Ratio, appear to be reasonable predictors of the Critical Shear Stress. The plot in Figure 2.88 however, does not indicate a good match between the predicted values and the actual values of the Critical Shear Stress. Regression analysis of the Slot Erosion Test data indicated poor correlation between τ_{cSET} and other soil parameters (values of Adjusted R^2 of all tested models are less than 0.6). Regression analysis of the Hole Erosion Test data for the fine-grained soil samples was also unable to produce satisfactory regression model for predicting Critical Shear Stresses.

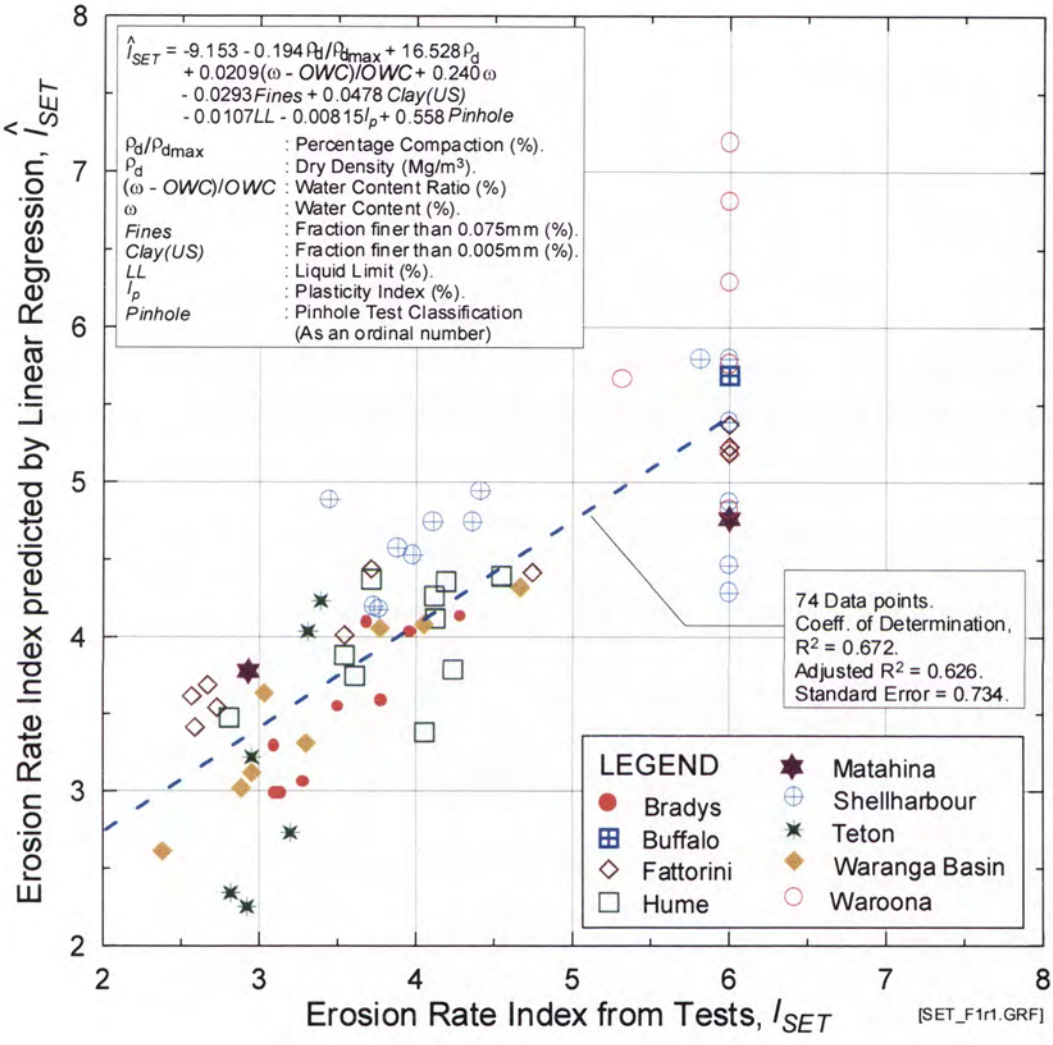

Figure 2.84: Erosion Rate Indices ($\hat{I}_{SET}$) predicted by Multiple Linear Regression Model versus Erosion Rate Indices (I_{SET}) from Slot Erosion Tests on Fine-grained Soil Samples.

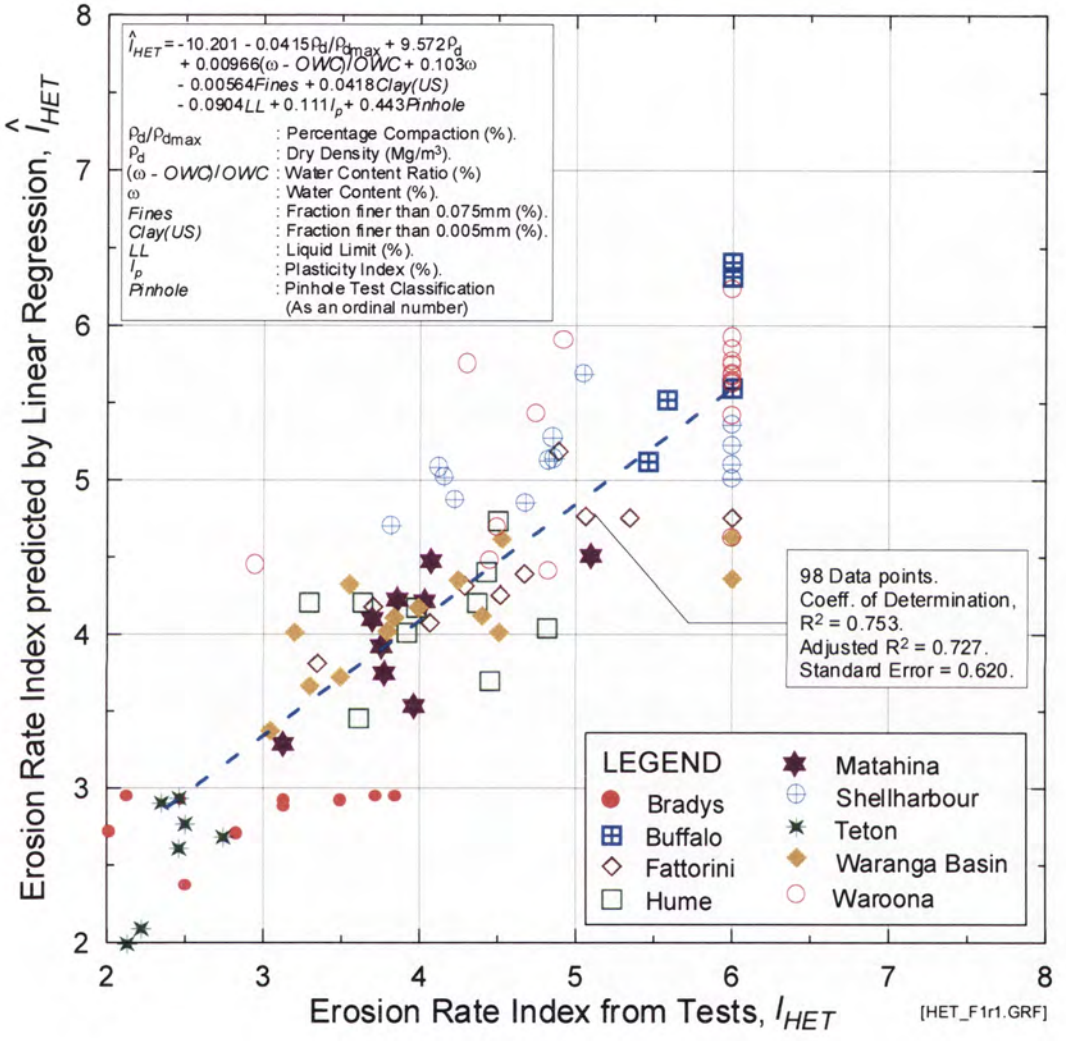

Figure 2.85: Erosion Rate Indices ($\hat{I}_{HET}$) predicted by Multiple Linear Regression Model versus Erosion Rate Indices (I_{HET}) from Hole Erosion Tests on Fine-grained Soil Samples.

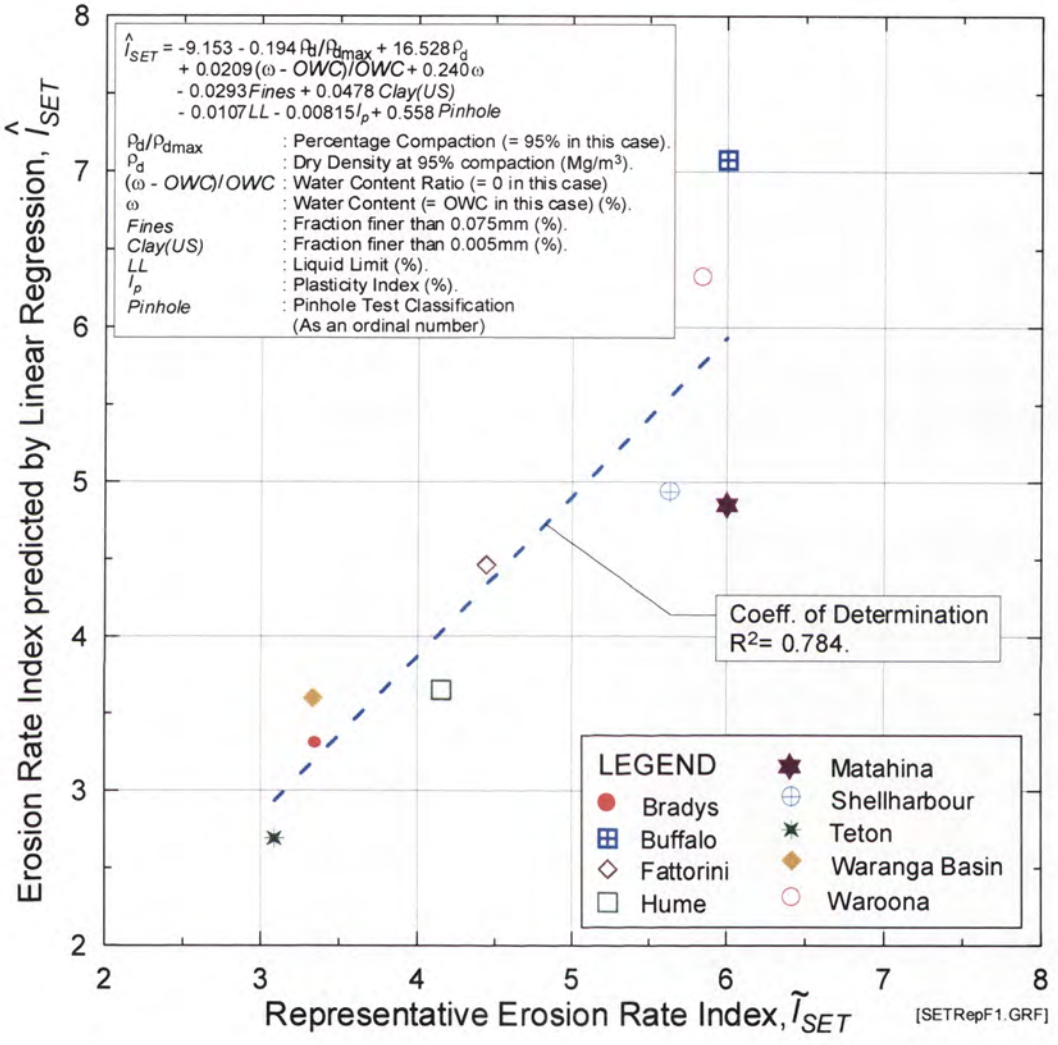

Figure 2.86: Erosion Rate Indices ($\hat{I}_{SET}$) predicted by Multiple Linear Regression Model versus Representative Erosion Rate Indices ($\tilde{I}_{SET}$) predicted by Non-linear Regression Models for each Fine -grained Soil Samples.

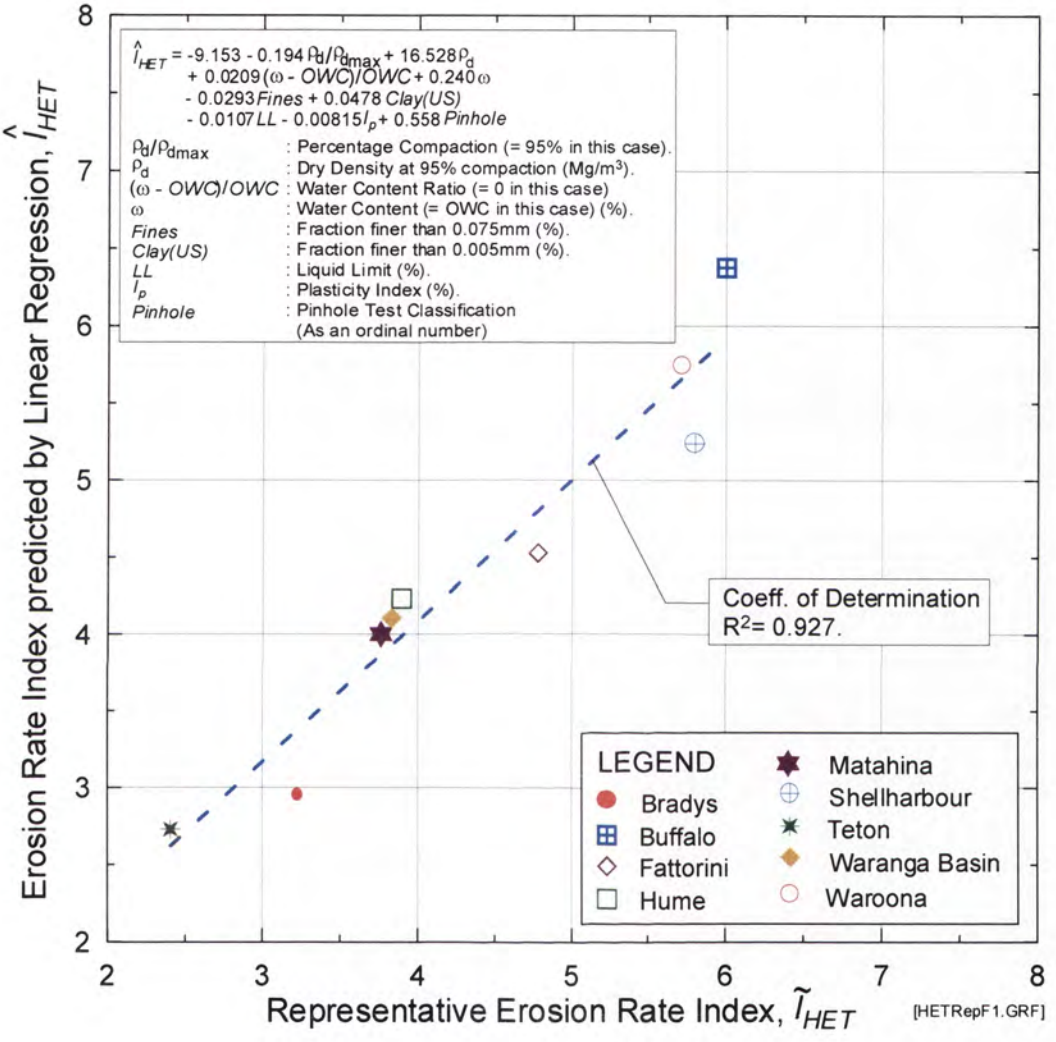

Figure 2.87: Erosion Rate Indices ($\hat{I}_{HET}$) predicted by Multiple Linear Regression Model versus Representative Erosion Rate Indices ($\tilde{I}_{HET}$) predicted by Non-linear Regression Models for each Fine-grained Soil Samples.

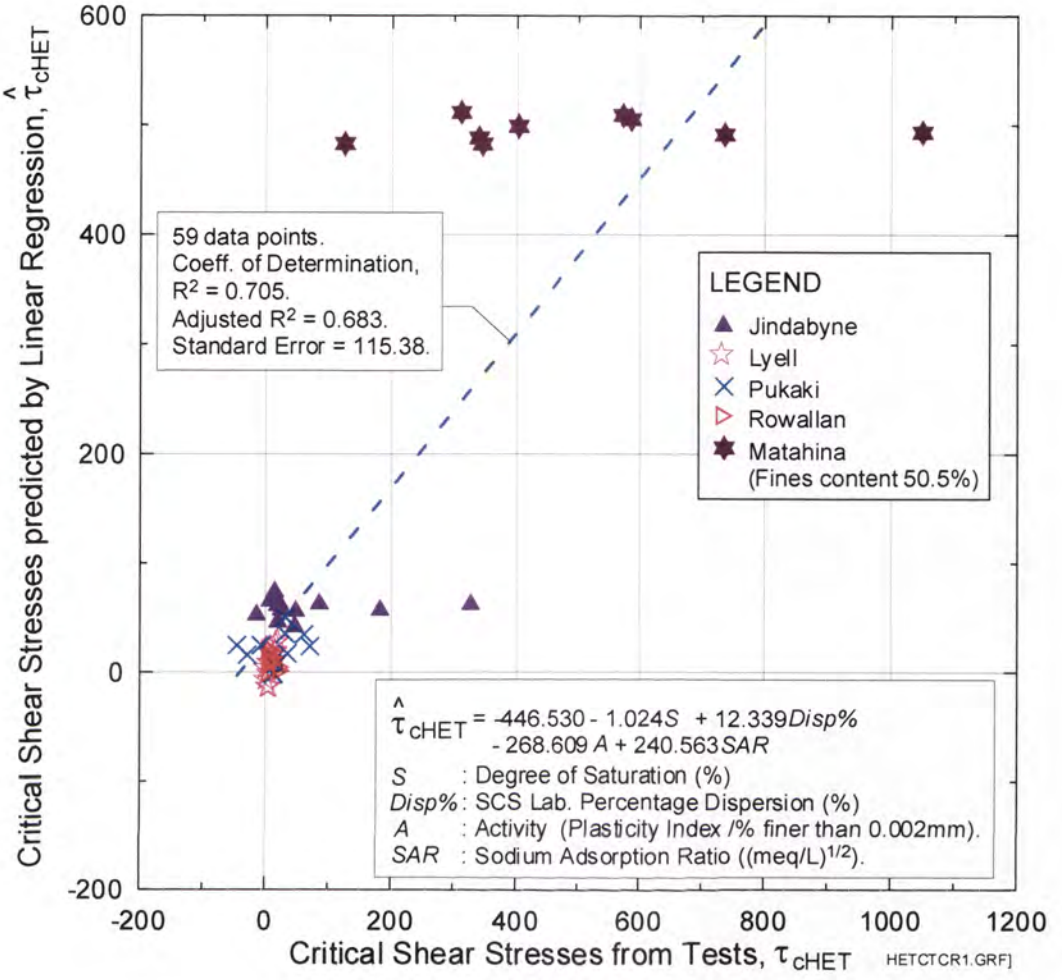

Figure 2.88: Critical Shear Stresses ($\hat{\tau}_{c\,HET}$) predicted by Multiple Linear Regression Model versus Critical Shear Stresses (τ_{cHET}) from Hole Erosion Tests on Coarse-Grained Soil Samples.

Correlation between the SET and the HET

Erosion Rate Indices obtained from Slot Erosion Tests cannot be directly compared with Erosion Rate Indices obtained from Hole Erosion Tests simply because the test parameters, namely the dry density and the water content, vary from test to test. It is, however, quite reasonable to compare the Representative Erosion Indices, $\tilde{I}_{SET}$, based on Slot Erosion Tests with the Representative Erosion Indices, $\tilde{I}_{HET}$, based on Hole Erosion Tests for each soil samples, because both predicted indices correspond to the

standard conditions of 95% compaction and optimum water content. Values of $\tilde{I}_{SET}$ and $\tilde{I}_{HET}$ for the 13 soil samples are shown in Table C1 at in Appendix C.

Figure 2.89 shows a plot of $\tilde{I}_{HET}$ against $\tilde{I}_{SET}$ for the 13 soil samples. The plot shows very good correlation between the two Indices. The correlation, however, does not include the data points for Buffalo and Matahina because regression models for predicting $\tilde{I}_{SET}$ are not available for these two soils due to insufficient Slot Erosion Test data. The $\tilde{I}_{SET}$ representing Buffalo and Matahina in the plots are values estimated from limited test data and may not be representative of the index values at 95% compaction and optimum water content.

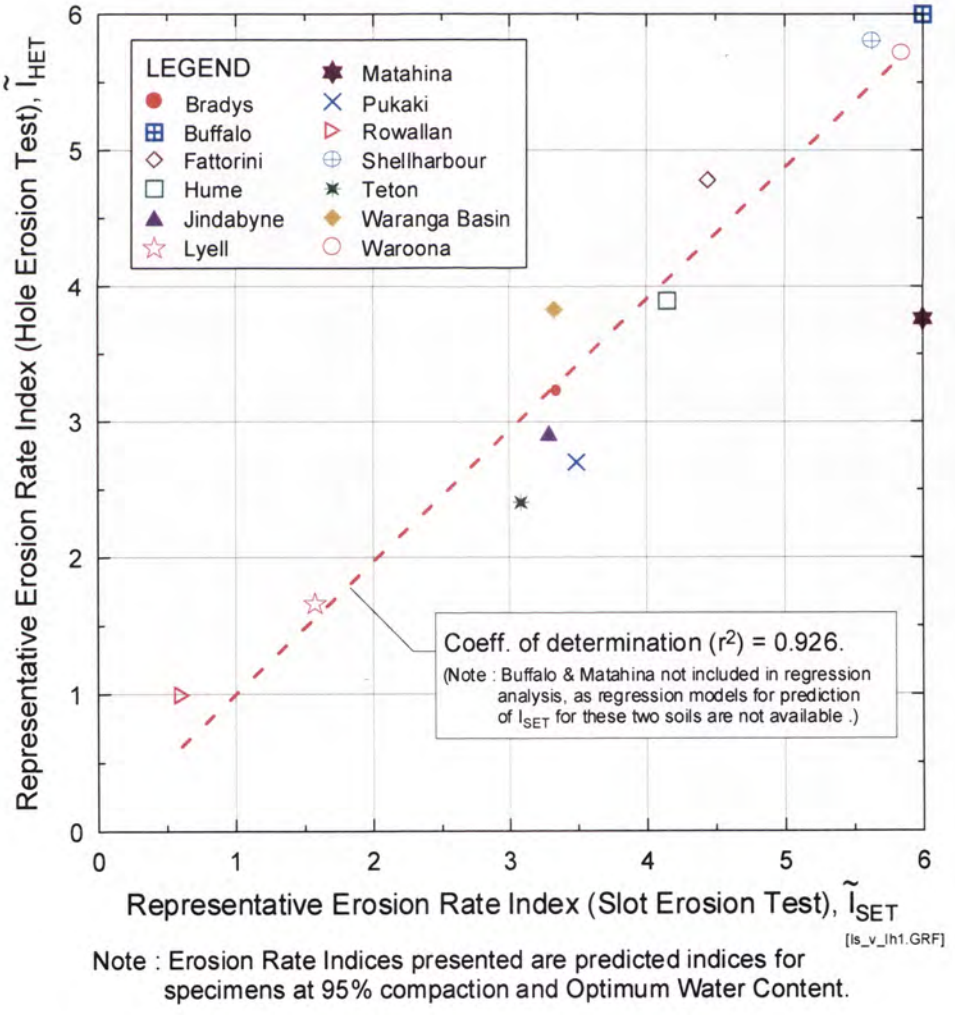

Figure 2.89: Representative Erosion Rate Index based on Hole Erosion Tests versus Representative Erosion Rate Index based on Slot Erosion Tests.

Figure 2.89 also shows that the $\tilde{I}_{SET}$ and $\tilde{I}_{HET}$ of the same soil are in the same order of magnitudes. The maximum differences between the two predicted indices of the same soil are 0.8 for Pukaki and 0.7 for Teton. In other words, the Slot Erosion Test and the Hole Erosion Test will provide a very similar rating on erosion rate when applied to the same soil prepared at the standard conditions of 95% compaction and optimum water content.

2.5.4 Effects of soil mineralogy on the Erosion Rate Index

As shown in earlier analysis, the Erosion Rate Indices of the coarse-grained soil samples are more satisfactorily predicted from the basic soil parameters than the Erosion Rate Indices of the fine-grained soil samples. The Erosion Rate Indices of the fine-grained soil samples do not show any strong relationship with the fines content, nor with any other soil parameters. It is believed that in fine-grained soils, the complex electro-chemical forces acting among clay particles and the cations in water have an important effect on their erosion characteristics. An attempt has been made to account for the differences in erosion rates among the fine-grained soil samples from the point of view of clay mineralogy.

Effects of composition of soil minerals of fine-grained soil samples on the erosion rate index

A comparison of the Erosion Rate Indices of the fine-grained soil samples shows that Waroona, Shellharbour and Buffalo are more erosion-resistant than the other fine-grained soil samples. A close examination of the compositions of soil minerals of the various soil samples in Table 2.10. reveals that soil samples Waroona and Shellharbour have kaolinites as the predominant clay minerals, and do not contain any smectites or vermiculites, whereas Buffalo has no smectites and only a trace of vermiculites. In Shellharbour, the kaolinites are halloysites which explain the high Atterberg's limits of the soil. All of the remaining 7 fine-grained soil samples contain smectites and some

vermiculites too. Hence one possible explanation for the difference in erodibility between the soil samples is that the presence of smectites and possibly vermiculites in a soil makes it more erodible. Following this Section is a discussion of the structure and the bonding of the commonly found clay minerals, namely kaolinites, illites, smectites, vermiculite and chlorite. This shows that kaolinites, illites and chlorite have strong interlayer bonds, and have low tendency to expand in water. Smectites and vermiculites, on the other hand, tend to expand in water leading to weakening of bonding between clay mineral crystals. The proposition that soils containing smectites and possibly vermiculites are more erodible, therefore, sounds reasonable.

Basic structures of clay minerals

Individual clay mineral crystals usually look like tiny plates. These plates consist of many crystal sheets which have a repeated atomic structure. The fundamental building blocks of the repeated atomic structure are the silica (or tetrahedral) sheet and the alumina (or octahedral) sheet. Figure 2.90 and Figure 2.91 show the structure of the silica sheet and the alumina sheet respectively. Different ways of stacking together of these fundamental sheets, different bonding types, and different metallic ions in the crystal lattice result in different types of clay minerals.

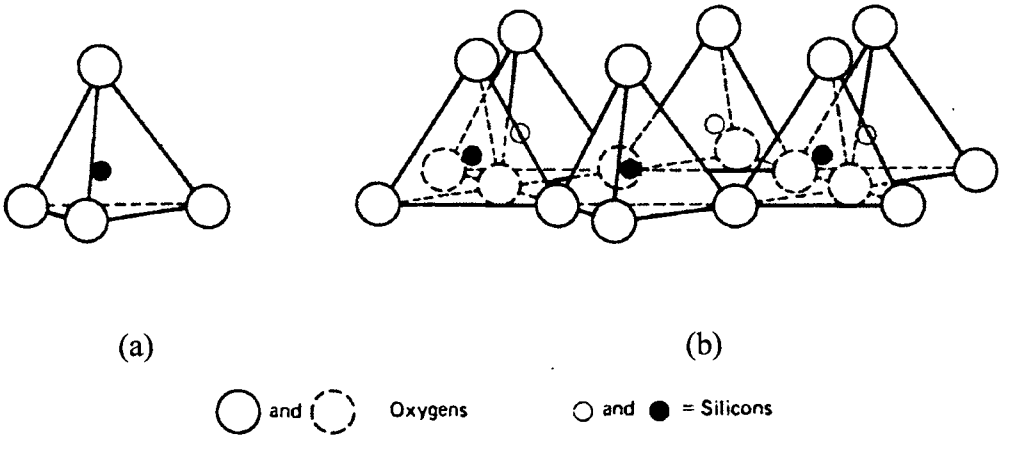

Figure 2.90: (a) Single silica tetrahedron; (b) Sheet structure of silica tetrahedrons arranged in a hexagonal network. (Grim 1953).

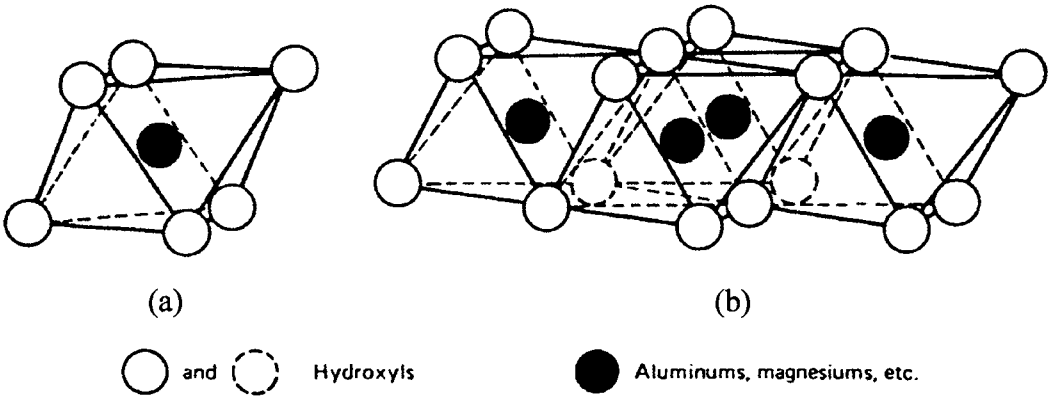

Figure 2.91: (a) Single octahedral unit; (b) Sheet structure of the octahedral units. (Grim 1953).

The five commonly found clay minerals in soils are kaolinite, illite, vermiculite, smectite, and chlorite. Some of the important properties of these minerals are summarised from Mitchell (1976) as follows:

Kaolinite

Kaolinite is composed of alternating silica (tetrahedral) and alumina (octahedral) sheets. A sketch showing the structure of a basic kaolinite layer is shown in Figure 2.92a, and a schematic diagram of the structure of kaolinite is shown in Figure 2.92b. The bonding between successive layers is by both van der Waals forces and hydrogen bonds. The bonding is so strong that there is no interlayer swelling in the presence of water.

Smectite

The basic structural unit for smectite (montmorillonite) is a three-layer sandwich. The middle layer can be either a gibbsite sheet (as in montmorillonites) or a brucite sheet (as in saponites). A sketch of the structure of smectite is shown in Figure 2.93a , and a schematic diagram of the structure is shown in Figure 2.93b. Bonding between successive layers is by van der Waals forces and by readily exchangeable cations which balance charge deficiencies in the structure. The charge deficiencies occur due to isomorphous substitution of the cations within the crystal structure leading to net negative charge on the clay crystal surface. The bonding by van der Waals forces is weak and easily separated by cleavage or adsorption of water. A water molecule has a

dipolar positive and negative charge which allows the molecule to be attracted to the negatively charged clay surface, and with the cations. Montorillonite is the most expansive and potentially dispersive of all clay minerals.

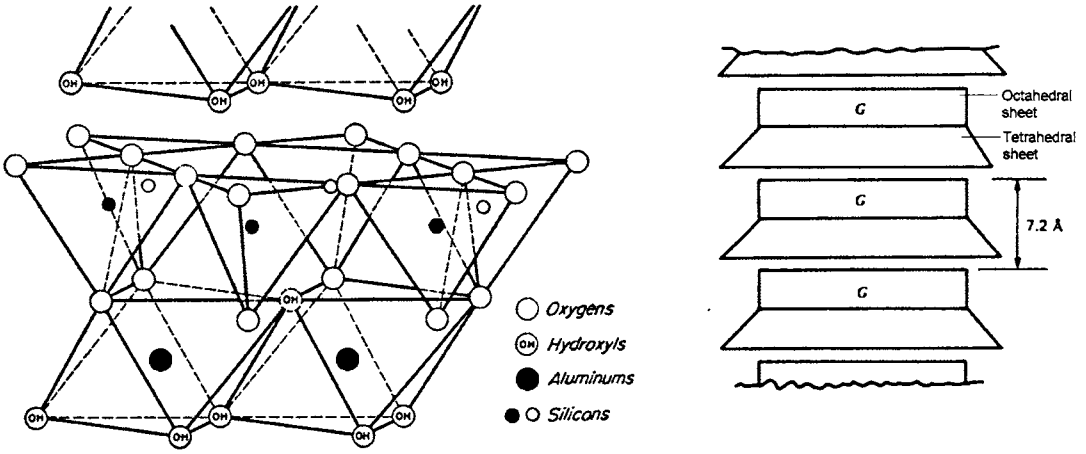

(a) (b)

Figure 2.92: (a) Structure of kaolinite layer (Grim 1953); (b) Schematic diagram of the structure of kaolinite (Mitchell 1976).

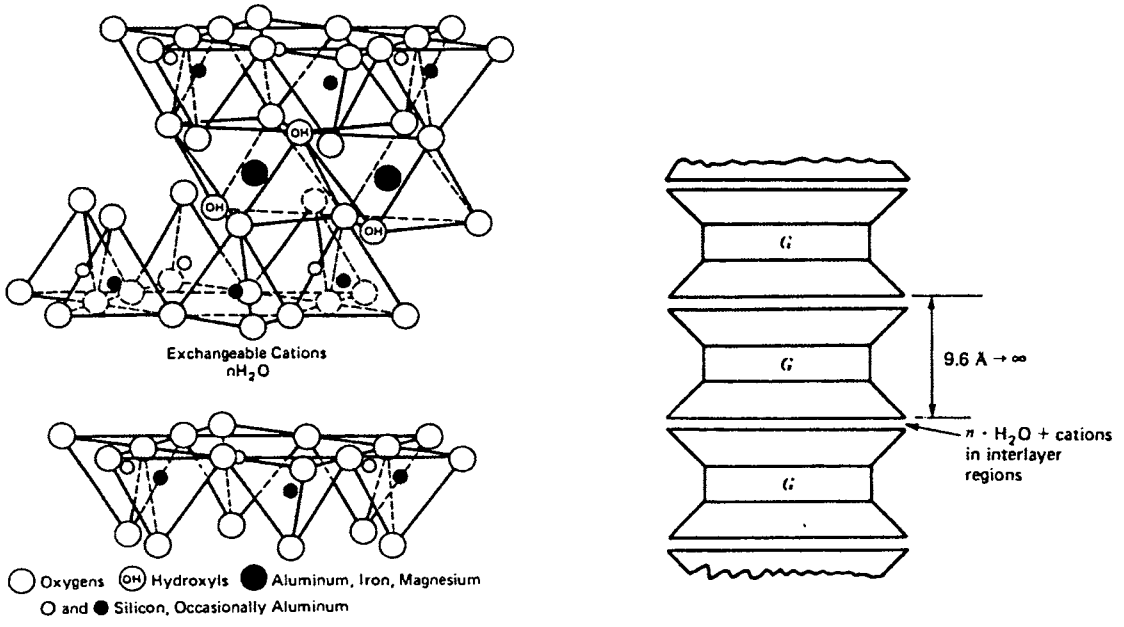

(a) (b)

Figure 2.93: (a) Structure of smectite (Grim 1953); (b) Schematic diagram of the structure of smectite (Mitchell 1976).

Illite

The basic structural unit for illite is the three-layer silica-gibbsite-silica sandwich similar to that of smectite. A gibbsite sheet is an octahedral sheet in which the cations are mainly aluminium. One-quarter of the silicon positions in the silica sheet are filled by aluminium. The resulting charge deficiency is balanced by potassium ions between the layers. The potassium ion fits itself nicely into the hexagonal hole formed by the bases of the silica tetrahedrals. A sketch of the structure of illite is shown in Figure 2.94a, and a schematic diagram of the structure is shown in Figure 2.94b The bonding between successive layers is by both van der Waals forces, and the potassium ion. Some isomorphous substitution may occur (as for montorillonite) giving a negatively charged surface, and a tendency to attract cations and water. The bonding by potassium is, however, sufficiently strong that illite does not swell much in the presence of water.

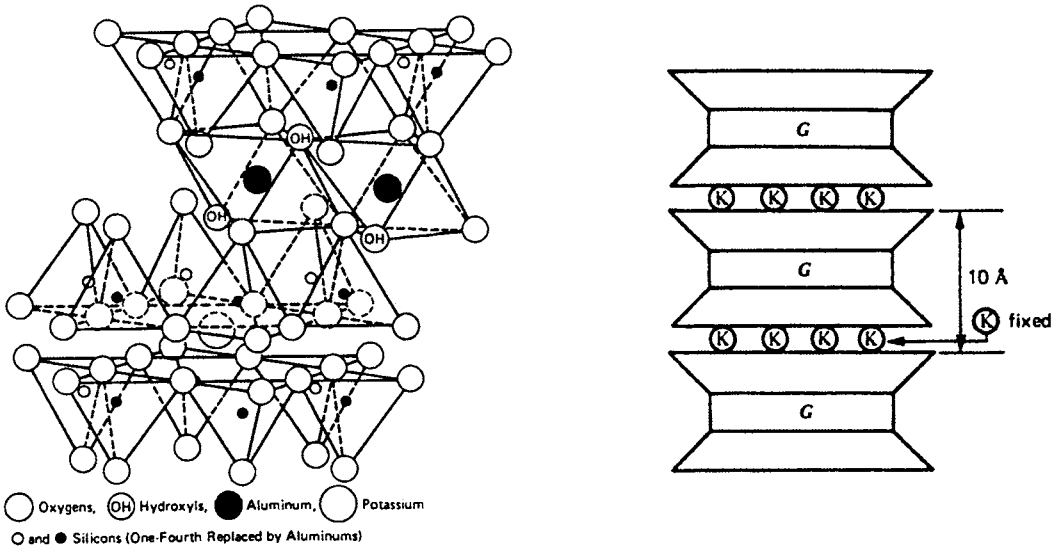

(a) (b)

Figure 2.94: (a) Structure of muscovite/illite (Grim 1953); (b) Schematic diagram of the structure of illite (Mitchell 1976).

Vermiculite

The basic structural unit for vermiculite is the three-layer silica-brucite-silica sandwich. A brucite sheet is an octahedral sheet in which the cations are mainly magnesium. In between the three-layer units, there are double molecular layers of water. The thickness of the water layer depends on the cation presents in this region for balancing charge deficiencies. With magnesium and calcium as the balancing cations, there are two water layers. A schematic diagram of the structure of vermiculite is shown in Figure 2.95 The bonding between successive layers is by both van der Waals forces, and the magnesium and calcium ions. The interlayer cations are exchangeable, and vermiculite can dehydrate or re-hydrate easily. The interlayer bonding is weak and depends on the type of interlayer cations. The minerals can expand easily upon re-hydration when exposed to moist air.

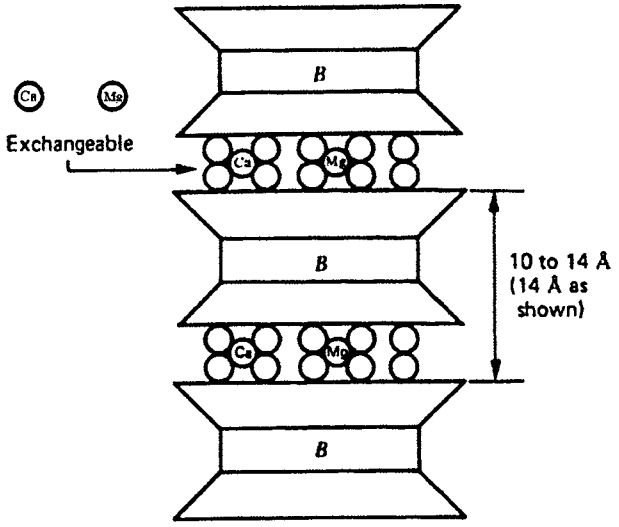

Figure 2.95: Schematic diagram of the structure of vermiculite (Mitchell 1976).

Chlorite

The basic structural unit for chlorite is a three-layer sandwich similar to that of illite, but the middle layer usually has magnesium as the predominant cation. The magnesium ions can be partially substituted by ferrous, ferric or aluminium ions. The three-layer units are connected together by a brucite sheet. A schematic diagram of the structure of chlorite is shown in

Figure 2.96. Bonding between successive layers by van der Waals forces and the brucite sheet is strong so that the structure does not expand significantly when exposed to water.

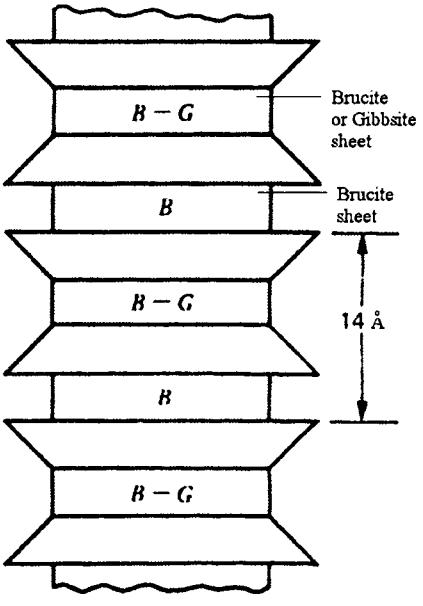

Figure 2.96: Schematic diagram of the structure of chlorite (Mitchell 1976).

2.5.5 Effects of cementing materials on erosion rate

If the presence of smectites and vermiculites makes a soil more erodible, soil sample Buffalo should have a lower Erosion Rate Index than Waroona and Shellharbour, as it contains vermiculites. Results from both SETs and HETs, however, show that Buffalo has the highest Erosion Rate Indices among all the soil samples tested. This finding suggests that either the proposition that the presence of vermiculites makes a soil more erodible is wrong, or there are some other factors that cause the high erosion-resistance of Buffalo.

A detailed report by Hensel (2001) on the soil mineralogy of Buffalo indicated that the soil contained iron oxides as a cementing material. The iron oxides formed a hard crust around the clay minerals, and might have improved the erosion resistance of the soil.

For the same reason, other type of cementing agents which may be found in a soil, such as gypsum, might also improve the erosion resistance of the soil.

A copy of the report on the soil mineralogy of Buffalo by Hensel (2001) can be found in Appendix L of this report.

It is notable that Waroona, Buffalo and Shellharbour, as well as having the above characteristics, are characterised by a red colour from iron oxides. Waroona is a lateritic soil. Buffalo is fluvial soils which are weathered and oxidised and in parts cemented from fluctuating water table.

2.5.6 Special tests

Effects of soil saturation on erosion rate – soaked tests

13 Slot Erosion Tests have been carried out in such a way that the soil specimens were soaked in water for at least 18 hours prior to testing. The aim of these tests is to investigate the effects of soaking/saturating the soil specimen on erosion rate. The tests were carried out on 7 soil samples, and the results are summarised in Table 2.18. Only Five out of the thirteen 13 tests were successful in producing results as the other tests showed no erosion due to blockage of the pre-formed slot before or during the erosion test.

Out of the 5 successful tests, 2 tests, on Fattorini and Waranga Basin, produced a higher Erosion Rate Index, meaning that the soaked specimen eroded at a slower rate than one without soaking. 1 test on Rowallan, however, gave a lower Erosion Index than that from an un-soaked specimen. The remaining 2 successful tests on Fattorini resulted in Erosion Rate Indices which did not differ by more than 0.5 from the index of an un-soaked specimen. As shown in Table 2.18, a "neutral" rating is given for these two tests in that the small difference in the index values might be due to measurement errors or errors in the predicting the index of the un-soaked specimen.

It should be noted that controlled tests on un-soaked specimens prepared at the same conditions of compaction and water content as the soaked specimens have not been carried out due to limited amount of soils available for testing. The Erosion Rate Indices for the un-soaked specimens used for comparing with the Indices obtained from the soaked tests are actually predicted values using the non-linear regression model described in Section 2.5.2.

24 Hole Erosion Tests have been carried out on specimens which had been soaked in water under a surcharge of 6.89 kPa (1 psi) until no further swelling of the specimen was recorded by dial gauges. Moisture content tests on some of these soaked specimens indicated that a degree of saturation close to or above 90% could be achieve by of this method of soaking. The 24 tests were carried out on all the 13 soil samples. Results of the tests are summarised in Table 2.19.

7 out of the 24 tests were unsuccessful as the pre-formed hole of the test specimen was blocked before or during the test. Three tests on Fattorini, Hume and Waranga Basin indicated that the Erosion Rate Index of the soaked specimen was higher than that of the un-soaked specimen, meaning that prior soaking might have reduced the erosion rate. 4 tests on Lyell, Shellharbour, Teton and Waroona respectively, showed a lower Erosion Rate Index than expected from an un-soaked specimen. The remaining ten tests showed no significant difference between the Erosion Rate Index of the soaked specimen and that of the un-soaked specimen.

The number of cases with an increased in the value of the Erosion Rate Index due to prior soaking of the test specimen is almost equal to the number of cases for a decreased value of the Erosion Rate Index. In view of this, a conclusion cannot be drawn at this stage regarding the effects of prior soaking/saturation on the erosion rate of a soil. Testing of soaked specimens of the non-plastic/low plasticity soil samples were difficult in that the pre-formed hole easily collapsed as soon as water was applied to the specimen. Two of the soil samples which experienced a reduction in Erosion Rate Index were non-plastic or of low plasticity, suggesting that prior soaking made specimens of non-plastic coarse-grained soils more erodible.

Effects of salt concentration of eroding fluid on erosion rate – salt tests

Research by others showed that pure water or water with a very low concentration of dissolved solids would cause faster erosion in some soils than water which had a higher concentration of dissolved solids. The effects of salt concentration in the eroding fluid on erosion rate would also depend on the electrochemical properties of the soil being eroded. Some Slot Erosion Tests and Hole Erosion Tests have been carried out using dilute sodium chloride solution as the eroding fluid. The purpose was to investigate the effects of salt concentration on the erosion rate of various soil samples.

6 SETs have been carried out on specimens of 6 soil samples using 0.02M NaCl solution as the eroding fluid. Results of the test are summarised in Table 2.20. 1 out of the 6 tests was unsuccessful in that the slot was blocked during the test. 4 out of the 5 successful tests did not show significance differences between the values of the Erosion Rate Index obtained from the tests and the predicted values of the Erosion Rate Index for normal tests with tap water as the eroding fluid. A test on Rowallan showed a higher Erosion Rate Index than that expected from a normal test.

12 HETs have been carried out on specimens of 12 soil samples using 0.02M NaCl solution as the eroding fluid. The test results are summarised in Table 2.21. 3 out of the 12 tests were unsuccessful in that the pre-formed hole of the test specimen was blocked or collapse during the test. The test on Lyell showed that the Erosion Rate Index was higher than the normal test, meaning that the erosion rate was relatively lower using 0.02M NaCl solution as the eroding fluid. Three tests on specimens of Hume, Pukaki and Shellharbour resulted in Erosion Rate Indices higher than that from normal tests on these specimens. There were 5 tests which produced Erosion Rate Indices not significantly different from normal tests on the same test specimens.

Table 2.18: Effects on Erosion Rate Index (I_{SET}) of prior soaking of test specimens in Slot Erosion Tests.

Soil Sample	Erosion Rate Indices for soil specimens soaked in water for at least 18 hours before testing.				Predicted Erosion Rate Indices for imaginary soil specimens with the same conditions of compaction and water content.		Comparison of I_{SET} for soaked specimen with predicted I_{SET} of imaginary, unsoaked specimen having same conditions of compaction and water content as the soaked specimen.	
	Test No.	Percentage Compaction	Water Content	I_{SET} from Test	Regression Model (Note 1)	Predicted I_{SET} based on regression model	I_{SET} for soaked specimen higher than Predicted I_{SET} for specimen without prior soaking?	Comments
Bradys	9	96.0%	35.6%	Slot blocked	2	3.49	---	Cannot compare.
Fattorini	13	90.5%	16.7%	3.95	4	2.52	Yes	The I_{SET} based on test on a soaked specimen is higher than the predicted I_{SET} for a similar specimen without prior soaking.
Fattorini	14	93.0%	17.5%	3.56	4	3.53	Neutral	The I_{SET} based on test on a soaked specimen is higher than the predicted I_{SET} for a similar specimen without prior soaking. The difference in the I_{SET} values is insignificant.
Fattorini	15	97.5%	16.8%	3.58	4	3.11	Neutral	The I_{SET} based on test on a soaked specimen is higher than the predicted I_{SET} for a similar specimen without prior soaking. The difference in the I_{SET} values is insignificant.
Hume	13	97.0%	22.8%	Slot blocked	3	4.61	---	Cannot compare.
Hume	14	93.0%	19.7%	Slot blocked	3	3.87	---	Cannot compare.
Hume	15	92.5%	17.6%	Slot blocked	3	3.66	---	Cannot compare.
Jindabyne	8	94.0%	16.4%	Slot blocked	2	3.19	---	Cannot compare.
Rowallan	7	96.0%	13.6%	Slot blocked	1	0.99	---	Cannot compare.
Rowallan	8	98.0%	11.1%	1.86	1	3.91	No	The I_{SET} based on test on a soaked specimen is lower than the predicted I_{SET} for a similar specimen without prior soaking.
Shellharbour	14	94.5%	37.4%	Slot blocked before test	4	4.26	---	Cannot compare.
Shellharbour	15	91.0%	38.2%	Slot blocked before test	4	3.21	---	Cannot compare.
Waranga Basin	9	95.5%	19.5%	4.49	4	3.54	Yes	The I_{SET} based on test on a soaked specimen is higher than the predicted I_{SET} for a similar specimen without prior soaking.

Notes :

1 Details of the regression models can be found in Section 2.5.2.

2 A 'neutral' rating is given when the Erosion Rate Index of the soaked test and the predicted Index of an un-soaked specimen do not differ by more than 0.5.

Table 2.19: Effects on Erosion Rate Index (I_{HET}) of prior soaking of test specimens in Hole Erosion Tests.

Soil Sample	Erosion Rate Indices for soil specimens soaked in water until no further swelling before testing.					Predicted Erosion Rate Indices for imaginary soil specimens with the same conditions of compaction and water content.		Comparison of I_{HET} for soaked specimen with predicted IH_{ET} of imaginary, unsoaked specimen having same conditions of compaction and water content as the soaked specimen.	
	Test No.	Percentage Compaction	Water Content	I_{HET} from Test	Sample swell (mm) during soaking	Regression Model (Note 1)	Predicted I_{HET} based on regression model	I_{SET} for soaked specimen higher than Predicted I_{SET} for specimen without prior soaking?	Comments
Bradys	16	94.5%	35.7%	3.55	2.118	6	3.72	Neutral	The two I_{HET} values do not differ significantly.
	20	94.0%	35.6%	3.41	2.972	6	3.43	Neutral	The two I_{HET} values do not differ significantly.
	4	95.0%	18.7%	6.00	0.436	9	6.02	Neutral	The two I_{HET} values do not differ significantly.
	8	89.0%	15.3%	6.00	1.670	9	5.55	Neutral	The two I_{HET} values do not differ significantly.
Fattorini	14	95.5%	17.7%	6.00	1.040	4	4.67	Yes	The I_{HET} based on test on a soaked specimen is higher than the predicted I_{HET} for a similar specimen without prior soaking.
Hume	11	95.5%	20.3%	4.44	3.096	5	3.93	Yes	The I_{HET} based on test on a soaked specimen is higher than the predicted I_{HET} for a similar specimen without prior soaking.
Jindabyne	17	94.5%	15.9%	Hole blocked	1.526	1	2.84	---	Cannot compare.
	20	96.0%	15.9%	Hole blocked	1.332	1	3.01	---	Cannot compare.
	21	94.5%	16.4%	3.03	1.026	1	2.87	Neutral	The two I_{HET} values do not differ significantly.
Lyell	15	95.0%	9.8%	1.71	0.000	9	1.73	Neutral	The two I_{HET} values do not differ significantly.
	18	95.0%	7.5%	1.72	-0.016	9	2.33	No	The I_{HET} based on test on a soaked specimen is lower than the predicted I_{HET} for a similar specimen without prior soaking.
Matahina	12	95.0%	16.2%	4.07	0.568	4	3.73	Neutral	The two I_{HET} values do not differ significantly.
	17	97.5%	17.3%	Hole blocked	0.230	4	4.84	---	Cannot compare.
Pukaki	15	96.0%	8.8%	2.53	-0.020	5	2.85	Neutral	The two I_{HET} values do not differ significantly.
	18	96.5%	8.4%	3.05	0.000	5	2.78	Neutral	The two I_{HET} values do not differ significantly.
Rowallan	16	98.5%	10.0%	Hole blocked	0.000	6	0.21	---	Cannot compare.
Shellharbour	14	95.5%	40.0%	4.34	1.446	5	5.75	No	The I_{HET} based on test on a soaked specimen is lower than the predicted I_{HET} for a similar specimen without prior soaking.
	17	94.5%	40.2%	6.00	1.440	5	5.54	Neutral	The two I_{HET} values do not differ significantly.
Teton	19	96.5%	17.8%	Hole blocked	0.028	5	2.60	---	Cannot compare.
	22	95.0%	18.2%	2.25	0.002	5	2.43	No	The I_{HET} based on test on a soaked specimen is lower than the predicted I_{HET} for a similar specimen without prior soaking.
Waranga Basin	12	92.0%	18.3%	Hole blocked	3.074	5	3.07	---	Cannot compare.
	13	95.0%	18.5%	Hole blocked	1.660	5	3.57	---	Cannot compare.
	19	95.4%	18.6%	5.01	0.734	5	3.66	Yes	The I_{HET} based on test on a soaked specimen is higher than the predicted I_{HET} for a similar specimen without prior soaking.
Waroona	17	94.0%	23.2%	4.69	0.186	9	5.59	No	The I_{HET} based on test on a soaked specimen is lower than the predicted I_{HET} for a similar specimen without prior soaking.

Notes :

1 Details of the regression models can be found in Section2.5.2.

2 A "neutral" rating is given when the Erosion Rate Index of the specimen in the salt test and the predicted index of a normal test do not differ by more than 0.5.

Table 2.20: Effects on Erosion Rate Index (I_{SET}) due to the use of 0.02M Sodium Chloride Solution as the Eroding Fluid in Slot Erosion Tests.

Soil Sample	Erosion Rate Indices for specimens tested with Salt Solution (0.02M NaCl) as the eroding fluid.				Predicted Erosion Rate Indices for imaginary soil specimens with the same conditions of compaction and water content.		Comparison of I_{SET} from salt water test with predicted I_{SET} of imaginary specimen having same conditions of compaction and water content.	
	Test No.	Percentage Compaction	Water Content	I_{SET} from Test	Regression Model (Note 1)	Predicted I_{SET} based on regression model	I_{SET} for salt water test higher than Predicted I_{SET} for tap water test?	Comments
Bradys	11	94.5%	35.2%	3.54	2	3.34	Neutral	The two I_{SET} values do not differ significantly.
Jindabyne	9	93.5%	16.5%	Slot blocked	2	3.13	—	Cannot compare.
Lyell	8	95.5%	9.8%	2.02	1	1.64	Neutral	The two I_{SET} values do not differ significantly.
Rowallan	12	96.0%	13.2%	1.80	1	1.27	Yes	The I_{SET} based on the salt water test is slightly higher than the predicted I_{SET} for a similar specimen.
Shellharbour	17	94.0%	41.4%	6.00	4	5.82	Neutral	The two I_{SET} values do not differ significantly.
Waranga Basin	10	96.0%	18.8%	3.69	4	3.32	Neutral	The two I_{SET} values do not differ significantly.

Notes :

1 Details of the regression models can be found in Section 2.5.2.

2 A "neutral" rating is given when the Erosion Rate Index of the specimen in the salt test and the predicted index of a normal test do not differ by more than 0.5.

6 HETs have been carried out on specimens of 6 soil samples using 0.005M NaCl solution as the eroding fluid. Results of the tests are summarised in Table 2.22. All the 6 tests were successful, but 4 out of which did not show significant differences between the Erosion Rate Indices obtained from the tests and the Indices expected from normal tests on similar specimens. The test on Bradys gave a lower Erosion Rate Index than expected from a normal test, whereas the test on Matahina showed a higher Erosion Rate Index than expected from a normal test.

The SETs and HETs using salt water as the eroding fluid do not provide sufficient evidence to prove the effects of salt concentration of the eroding fluid on the erosion rate. Most of the tests did not show a significant difference in the Erosion Rate Index obtained from the test and the Index expected from a normal test on a similar test specimen. There were a few tests that showed positive results (i.e. salt water caused slower erosion than tap water), but there were also as many tests that showed negative results (i.e. salt water caused faster erosion than tap water). It is notable however that on the available evidence the effect on erosion rate is small. This contrasts to the marked effect saline solution has in suppressing dispersion as measured in Emerson

Crumb and Pinhole Tests. It should however be noted that Sydney tap water has a small concentration of dissolved solids, and this has been noted to be sufficient to some what inhibit dispersion in Emerson Crumb Tests, e.g. an Emerson Class 1 may become Class 2. Hence for a more definitive assessment, tests would be carried out using distilled water. This could not be done as part of this study.

Table 2.21: Effects on Erosion Rate Index (I_{HET}) of the use of 0.02M Sodium Chloride Solution as the Eroding Fluid in Hole Erosion Tests.

Soil Sample	Erosion Rate Indices for specimens tested with Salt Solution (0.02M NaCl) as the eroding fluid.				Predicted Erosion Rate Indices for imaginary soil specimens with the same conditions of compaction and water content.		Comparison of I_{HET} from salt water test with predicted I_{HET} of imaginary specimen having same conditions of compaction and water content.	
	Test No.	Percentage Compaction	Water Content	I_{HET} from Test	Regression Model No. (Note 1)	Predicted I_{HET} based on regression model	I_{HET} for salt water test higher than Predicted I_{HET} for tap water test?	Comments
Bradys	17	95.0%	33.1%	Hole blocked	6	2.14	—	Cannot compare.
Buffalo	5	94.5%	20.0%	6.00	9	>6	Neutral	The two I_{HET} values do not differ significantly.
Hume	12	94.0%	20.3%	2.89	5	3.71	No	The I_{HET} based on the salt water test is lower than the predicted I_{HET} for a similar specimen.
Jindabyne	18	94.0%	16.8%	2.43	1	2.84	Neutral	The two I_{HET} values do not differ significantly.
Lyell	16	97.0%	9.8%	1.76	9	0.77	Yes	The I_{HET} based on the salt water test is higher than the predicted I_{HET} for a similar specimen.
Matahina	13	95.5%	15.6%	Hole blocked and collapsed later	4	3.85	—	Cannot compare.
Pukaki	16	95.0%	8.8%	2.06	5	2.75	No	The I_{HET} based on the salt water test is lower than the predicted I_{HET} for a similar specimen.
Rowallan	14	95.5%	12.1%	1.43	6	0.94	Neutral	The two I_{HET} values do not differ significantly.
Shellharbour	15	95.0%	40.1%	5.07	5	5.65	No	The I_{HET} based on the salt water test is lower than the predicted I_{HET} for a similar specimen.
Teton	20	95.0%	17.3%	Hole blocked	5	2.54	—	Cannot compare.
Waranga Basin	17	96.0%	18.0%	3.82	5	3.61	Neutral	The two I_{HET} values do not differ significantly.
Waroona	18	95.0%	22.5%	5.43	9	5.25	Neutral	The two I_{HET} values do not differ significantly.

Notes :

1 Details of the regression models can be found in Section 5.2.2.

2 A "neutral" rating is given when the Erosion Rate Index of the specimen in the salt test and the predicted index of a normal test do not differ by more than 0.5.

Table 2.22: Effects on Erosion Rate Index (I_{HET}) of to the use of 0.005M Sodium Chloride Solution as the Eroding Fluid in Hole Erosion Tests.

Soil Sample	Erosion Rate Indices for specimens tested with Salt Solution (0.005M NaCl) as the eroding fluid.				Predicted Erosion Rate Indices for imaginary soil specimens with the same conditions of compaction and water content.		Comparison of I_{HET} from salt water test with predicted I_{HET} of imaginary specimen having same conditions of compaction and water content.	
	Test No.	Percentage Compaction	Water Content	I_{HET} from Test	Regression Model No. (Note 1)	Predicted I_{HET} based on regression model	I_{HET} for salt water test higher than Predicted I_{HET} for tap water test?	Comments
Bradys	18	95.5%	34.3%	1.68	6	2.50	No	The I_{HET} based on the salt water test is lower than the predicted I_{HET} for a similar specimen.
Buffalo	6	95.0%	19.7%	6.00	9	>6	Neutral	The two I_{HET} values do not differ significantly.
Matahina	14	94.5%	16.1%	4.18	4	3.59	Yes	The I_{HET} based on the salt water test is slightly higher than the predicted I_{HET} for a similar specimen.
Pukaki	17	95.0%	8.9%	3.03	5	2.78	Neutral	The two I_{HET} values do not differ significantly.
Rowallan	15	94.5%	13.0%	1.14	6	0.98	Neutral	The two I_{HET} values do not differ significantly.
Waranga Basin	18	95.5%	18.7%	4.04	5	3.70	Neutral	The two I_{HET} values do not differ significantly.

Notes :
1 Details of the regression models can be found in Section 5.2.2.
2 A "neutral" rating is given when the Erosion Rate Index of the specimen in the salt test and the predicted index of a normal test do not differ by more than 0.5.

Effects of pausing flow during an erosion test on erosion rate – paused tests

3 Slot Erosion Tests were carried out to investigate the effects of pausing flow on erosion rate. The results are summarised tabulated in Table 2.23. Two out of the three tests indicates that pausing might have reduced the erosion rate of the soil. For these paused tests, the erosion rate was calculated on the basis of effective time of erosion, which means the actual duration of the test minus the time periods during which the test was paused. As only three tests were carried out, a firm conclusion regarding the effects of pausing on erosion rate cannot be drawn.

What is observed in paused tests is that slaking/separation of soil from the surface of the pipe occurs during the pause, resulting in an apparent fluent period of erosion on re-starting the flow.

Table 2.23: Effects on Erosion Rate Index (I_{SET}) of Pausing Flow during a Slot Erosion Test.

Soil Sample	Erosion Rate Indices for specimens tested with 15-minute pauses after each 15-minute period of erosion.				Predicted Erosion Rate Indices for imaginary soil specimens with the same conditions of compaction and water content.		Comparison of I_{SET} for paused test with predicted I_{SET} for normal test on an imaginary specimen having same conditions of compaction and water content.	
	Test No.	Percentage Compaction	Water Content	I_{SET} from Test	Regression Model (Note 1)	Predicted I_{SET} based on regression model	I_{SET} from paused test higher than Predicted I_{SET} for a normal test on a similar specimen?	Comments
Fattorini	16	98.5%	17.5%	6.00	4	3.56	Yes	The I_{SET} based on paused test is higher than the predicted I_{SET} for a similar specimen.
Hume	12	94.0%	21.3%	3.31	3	4.18	No	The I_{SET} based on paused test is lower than the predicted I_{SET} for a similar specimen.
Shellharbour	12	97.0%	39.5%	6.00	4	4.63	Yes	The I_{SET} based on paused test is higher than the predicted I_{SET} for a similar specimen.

Note :

1 Details of the regression models can be found in Section 2.5.2.

2.6 COMMENTS AND DISCUSSIONS

2.6.1 General comparison between the SET and the HET

Both the SET and the HET use simple apparatus which are easy to fabricate, and can be easily set up in a soil laboratory. The results of the two tests are reproducible.

A SET requires two or more persons to operate due to the weight of the soil specimen and the mould. A soil specimen of the SET weighs about 30 kg. Compared to the SET, the HET is a more economical and productive test. The test specimen of a HET weights only about 2 kg and is relatively easy to prepare. The HET requires only one person to operate.

HET is a more economical and feasible test for investigating the effects of salt concentration in the eroding fluid on erosion characteristics as the test consumes a lot less eroding fluid than the SET.

HET is also a better test for investigating the effects of prior soaking/saturation of a specimen on erosion characteristics because the soaking process in the HET is better controlled than in the SET. In addition, the pre-formed hole can be drilled after completion of the soaking process, hence reducing the chance of blocking of the hole during the soaking process. In the case of the SET, the pre-formed slot often closed up due to slaking or soil swell during the soaking process, and the subsequent test failed to show any erosion.

It is viable to perform replicate tests in HET to validate test results. Performing replicate tests in SET is relatively not so viable economically.

The SET, on the other hand, has two advantages over the HET. First, the SET allows witnessing the erosion process, as the widening of the pre-formed slot by erosion can be observed through the transparent perspex cover plate. Second, the SET is less affected

by undesirable end effects due to loss of soil by detachment of soils at the upstream and downstream faces of the test specimen as in the case of the HET.

2.6.2 Estimating erosion characteristics using SET and HET

Both the SET and the HET are reliable tests for assessing the rate of erosion in a soil sample. The rate of erosion is normalised against the level of shear stress, and is defined in terms of an Erosion Rate Index. Correlation analysis shows that, for a given soil, the Erosion Rate Index, I_{SET}, obtained from a SET is in the same order of magnitude as the Erosion Rate Index, I_{HET}, obtained from a HET. There is a strong correlation between the two indices obtained for test specimens at the standard conditions of 95% compaction and optimum water content.

The SET and the HET, however, provide scattered results of the Critical Shear Stress, τ_c, which represents the minimum shear stress to initial erosion. Some possible causes of the scattered results are:

- Extrapolating too far back to the horizontal axis

  τ_c is the horizontal intercept of the best-fit straight line through the data points in a plot of erosion rate per unit area versus shear stress. If the data points are mostly within the high stress – high erosion rate region, finding the horizontal intercept by extrapolating the best-fit straight line from the high stress – high erosion rate region too far back to the horizontal axis will give rise to large error in the estimated horizontal intercept. SET and HET, however, are usually operated at a high stress level in order to achieve the conditions of increasing erosion rate and shear stress.
- Large error bounds in the horizontal intercept due to extrapolating a best-fit straight line with a very flat slope

  For soil samples which show very small change in erosion rate with increase in shear stress, the best-fit straight line has a very flat slope. For these soils, there

are large error bounds in the horizontal intercepts obtained by extrapolating the best-fit straight lines.

- Deviation from linearity

  The definition of the Coefficient of Soil Erosion, C_e, and the Critical Shear Stress, τ_c, in Figure 2.1 has based upon the assumption that the erosion rate per unit area, $\dot{\varepsilon}$, is a linear increasing function of the shear stress, τ. The actual relationship between $\dot{\varepsilon}$ and τ may not be perfectly linear. C_e and τ_c may vary with the shear stress level, and may also depend on some other unknown factor.

- Errors due to simplifying assumptions

  The methods of analysing SET and HET data were based on a number of simplifying assumptions regarding the size and shape of the man-made defect (pre-formed slot or hole) during the erosion process. Large errors may be found in the estimated τ_c if the actual behaviour of the test specimen deviates considerably from the assumptions.

2.6.3 Estimating resistance against initiation of erosion using the HET

As discussed in Section 2.6.2, both the SET and the HET provided scattered results on the Critical Shear Stresses, τ_c. There might also be large inherent errors in the estimated values for τ_c. The HET, however, can be used to measure the relative resistance of a soil against initiation of erosion. By testing different test heads on specimens of a soil, it is possible to find a minimum test head below which there is no measurable erosion of the specimen. The Initial Shear Stress, τ_o, at the start of the HET with the minimum test head is an approximate measure of the resistance against initiation of erosion of the soil. Although the definition of τ_o is different from that of τ_c, the physical meanings of the two parameters are similar. A plot of the minimum test heads and the corresponding Initial Shear Stresses of the 13 soil samples tested by HETs is shown in Figure 2.78. These results are considered a more reliable assessment of the hydraulic shear stress at which measurable erosion will initiate.

2.6.4 Accuracy of the SET and the HET

The accuracy of an erosion test depends on the accuracy in the measurement of the erosion rate and the shear stress during the erosion process. In the case of the SET and the HET, the erosion rate per unit area, $\dot{\varepsilon}$, and the shear stress, τ, are not directly measured, but are estimated indirectly from recorded pressures, flow rates and sizes of the man-made defect (slot or hole). The estimation involves simplifying assumptions which describe the shape of the man-made defect during the erosion process, and approximations in the measurement of the final size and shape of the defect at the end of the test. The simplifying assumptions and the approximate measurements unavoidably incur errors in the Erosion Rate Index and the Critical Shear Stress estimated from the tests. The SET and the HET, therefore, are not intended to provide accurate measurements of Erosion Rate Indices and the Critical Shear Stresses. They are intended to be fast and simple tests for comparing erosion resistance, as measured by the rate of erosion, and the hydraulic shear stress at which erosion will initiate, among different types of soils, and the effects of compaction density and water content.

2.7 SUMMARY OF FINDINGS AND CONCLUSIONS

2.7.1 General

Experimental investigations show that the Slot Erosion Test (SET) and the Hole Erosion Test (HET) can successfully measure the rate of piping erosion of a soil. The tests express erosion rate in the form of an Erosion Rate Index, I defined by:

$$I = -\log(C_e)$$

$$\dot{\varepsilon} = C_e(\tau - \tau_c)$$

where $\dot{\varepsilon}$ is the erosion rate per unit area [kg/s/m^2],
τ is the hydraulic shear stress causing the erosion [N/m^2 or Pa],
C_e is the Coefficient of Soil Erosion [s/m or kg/s/m^2/Pa],
τ_c is the Critical Hydraulic Shear Stress for initiation of erosion.

Tests on 13 soil samples show that C_e is in the order of 10^{-1} to 10^{-6} kg/s/m^2/Pa. The corresponding range of values for the Erosion Rate Index, I, is > 0 to 6. Soils that erode rapidly have lower I values than soils that erode slowly.

2.7.2 Apparent relationship between Erosion Rate Index, soil dry density and water content

The Erosion Rate Index of a soil is influenced strongly by the degree of compaction and the water content of the soil. In most of the soil samples tested, a specimen compacted to a higher dry density, and to the wet side of the optimum water content has a higher Erosion Rate Index (higher erosion resistance) than another specimen of the same soil compacted to a lower dry density, and to the dry side of the optimum water content.

Some coarse-grained, non-plastic soil samples, for examples Rowallan, Lyell and Pukaki, appeared to behave differently. These soils have a highest Erosion Rate Index when compacted to a high dry density and to the dry side of optimum.

The erosion resistance of a soil can conveniently be represented by $\tilde{I}$, the Erosion Rate Index corresponding to 95% compaction and optimum water content. $\tilde{I}$ is called the Representative Erosion Rate Index of the soil. $\tilde{I}$ can be obtained directly from a test on a specimen at 95% compaction and optimum water content, or estimated from results of tests on specimens of different dry densities and water contents using a second order non-linear regression with the dry density and the water content as the independent variables.

2.7.3 Correlation between Erosion Rate Index and other soil properties

For coarse-grained soils, the Erosion Rate Indices show good correlation with water content, the degree of saturation, fines content, and the fraction of the soil finer than 0.005 mm.

For fine-grained soils, the Erosion Rate Indices show moderately good correlations with the degree of saturation, and dispersivity ratings based on the Pinhole Dispersion Test, Emerson Class Test, SCS Laboratory Dispersion Test and the Sodium Adsorption Ratio.

Correlation analysis indicates that the Representative Erosion Rate Indices of the coarse-grained soil samples show very good correlation with the degree of saturation, the fines content, and the fraction of the soil finer than 0.005 mm. For fine-grained soil samples, only a moderately good correlation exists between the Representative Erosion Rate Indices and the degree of saturation.

2.7.4 Multiple linear regression analysis on test data

Multiple linear regression analysis has been carried out to investigate any possible relationship between the Erosion Rate Index and a group of two or more soil parameters. The analysis provided separate linear regression equations for predicting the Erosion Rate Index for coarse-grained soils and for fine-grained soils. Details of these regression equations are shown in Table 2.16 and Table 2.17 in Section 2.5.3.

The erosion tests on fine-grained soils show more scattering results. The regression models for the coarse-grained soils provide more satisfactory predictions than the regression models for the fine-grained soils.

2.7.5 Effects of soil mineralogy on the erosion rate index

Examination of the soil mineral compositions of the soil samples revealed that soils containing smectites and vermiculites appeared to have lower Erosion Rate Indices (lower erosion resistance). This does not explain the behavior of soil sample "Buffalo" which contains vermiculites, but is the most erosion-resistant soil among all soil samples tested. It is possible the high Erosion Rate Index of "Buffalo" is due to the presence of iron oxides, a cementing material, in the soil.

2.7.6 Estimation of Critical Shear Stress from the Slot Erosion Test and the Hole Erosion Test

The Critical Shear Stresses, τ_c, obtained from the SETs and the HETs by extrapolating the graphical plot of erosion rate against shear stress do not show any form of strong relationship with other soil properties. The values of τ_c obtained for different specimens of the same soil also vary considerably. It appears that there is a large degree of inaccuracy in the estimation of τ_c from the SET or the HET data.

The HET, however, can be used to estimate the minimum test head required to initiate erosion in a soil. The initial shear stress, τ_o corresponding to the minimum test head can be used as an indicator of the soil's resistance against initiation of erosion.

Results of HETs on specimens of the 13 soil samples compacted to 95% standard maximum dry density at optimum water content show the broad trend that coarse-grained soils have lower τ_o values than the fine-grained soils, and that τ_o value of a fine-grained soil increases as its Erosion Rate Index increases.

2.7.7 Comparison between the Representative Erosion Rate Indices of the Slot Erosion Test and the Hole Erosion Test

The Representative Erosion Rate Indices, $\tilde{I}_{SET}$, based on the test data of the Slot Erosion Tests show very strong correlation with the Representative Erosion Rate Indices, $\tilde{I}_{HET}$, based on the data of the Hole Erosion Test. In addition, $\tilde{I}_{SET}$ and $\tilde{I}_{HET}$ of the same soil have the same order of magnitude. It implies that the two erosion tests will give a similar rating on the erosion rate to the same soil at the standard condition of 95% compaction and optimum water content. In addition, one test can provide a check on the results of the other test.

2.7.8 Special tests

Special tests have been carried out to investigate the effects of prior soaking/saturation (soaked test), salt concentration in the eroding fluid (salt test), and pausing (paused test) on the erosion rate of a soil.

For the soaked tests, the number of cases showing an increase in the value of the Erosion Rate Index due to prior soaking of the test specimen is almost equal to the number of cases showing a decrease in the value of the Erosion Rate Index.

Similarly, for the salt tests, although there were a few tests that showed positive results (i.e. salt water caused slower erosion than tap water), there were as many tests that showed negative results (i.e. salt water caused faster erosion than tap water).

For the paused tests, two out of a total of three tests gave positive results (i.e. pausing caused slower erosion).

Due to the limited number of successful tests, conclusions regarding the special tests cannot be made at this stage.

2.8 RECOMMENDATIONS

2.8.1 Use of the Hole Erosion Test

The Hole Erosion Test (HET) is recommended as a fast and simple test for assessing the rate of erosion of a soil. The HET assigns an Erosion Rate Index, I_{HET}, to a soil. I_{HET} has values in the range of 0 – 6. The smaller the index, the faster is the rate of erosion for a given shear stress caused by the eroding fluid.

When an Erosion Rate Index, I_{HET}, is quoted for a soil, the percentage compaction and the water content of the test specimen of the soil should also be stated, as I_{HET} is strongly influenced by the degree of compaction and the water content. The Index corresponding to 95% compaction and optimum water content is called the Representative Erosion Rate Index, $\tilde{I}_{HET}$, of the soil.

Soils can be classified into 6 groups according to their Representative Erosion Rate Index, $\tilde{I}_{HET}$. The 6 groups are :

Group No.	Erosion Rate Index	Description
1	< 2	Extremely rapid
2	2 – 3	Very rapid
3	3 – 4	Moderately rapid
4	4 – 5	Moderately slow
5	5 – 6	Very slow
6	> 6	Extremely slow

Table 2.24 shows the above classification scheme using the 13 soil samples tested as examples.

Table 2.24: Summary of Predicted Representative Erosion Rate Indices at 95% Compaction and Optimum Water Content based on Results of Slot Erosion Tests and Hole Erosion Tests, and Soil Properties.

Soil Sample	Representative I_{SET} and I_{HET} at 95% Compaction and Optimum Water Content (Note 2)	Range of Erosion Rate Indices I_{SET} or I_{HET} (Note 1)	Descriptions on Rate of Erosion	USCS Classification	Atterberg's Limits		Fines Content	Geological origin of soil	Dispersivity				Major Cation Content (meq/L)
					Liquid Limit (%)	Plasticity Index (%)	(% < 0.075mm)		Pinhole Erosion	Emerson Class	Percentage dispersion (%)	Sodium Adsorption Ratio (SAR)	
Rowallan	0.6, 1.0	<2	Extremely rapid	SM	NP	NP	22%	Glacial till	D1	5	34	0.4	1.8
Lyell	1.6, 1.7			SM	NP	NP	29%	Residual (granite)	D1	5	25	0.9	3.6
Teton	3.1, 2.4	2 - 4	Very rapid to Moderately rapid	CL	30%	8%	84%	Aeolian	PD2	5	25	2.3	4.7
Pukaki	3.5, 2.7			SM	NP	NP	42%	Glacial till	D1	5	35	0.5	13.8
Jindabyne	3.3, 2.9			SC	36%	17%	34%	Residual (granite)	D1	3	46	1.3	0.9
Bradys	3.4, 3.2	3 - 4	Moderately rapid	CH	62%	31%	75%	Residual (dolerite, basalt)	PD1/PD2	5	22	0.8	1.1
Waranga Basin	3.3, 3.8			CL	42%	22%	79%	Alluvium	D1	1	69	29.6	144.5
Hume	4.2, 3.9	3 - 5	Moderately rapid to Moderately slow	CL	30%	15%	81%	Alluvium	D1	1	75	18.3	28.2
Matahina	6.0, 3.8	3 - 6	Moderately rapid to Very slow	CL	30%	12%	50%	Residual (greywacke sandstone)	D1	3	60	1.7	2.5
Fattorini	4.4, 4.8	4 - 5	Moderately slow	CL	41%	22%	75%	Colluvium	ND2	5	58	4.9	2.3
Waroona	5.9, 5.7	5 - 6	Very slow	CL	41%	21%	61%	Residual (granite)	ND1	6	4	1.9	1.0
Shellharbour	5.6, 5.8			CH	92%	60%	88%	Residual (sandstone of andesitic, basaltic origin)	ND1	5	8	6.6	3.3
Buffalo	>6, >6	>6	Extremely slow	CL	44%	20%	87%	Alluvium (metamorphosed sediments, granite)	ND1	6	4	0.7	0.9

Notes :

1 I_{SET} or I_{HET} is defined as -LOG(C_e), where C_e is the Coefficient of Erosion of the soil obtained from a Slot Erosion Test or a Hole Erosion Test.
C_e is defined as the slope of the rising portion of the curve obtained by plotting the erosion rate per unit surface area, $\dot{\varepsilon}$ [kg/s/m^2] against shear stress, τ [N/m^2].

2 2nd order non-linear regression models based on test data were used to predict the Representative I_{SET} or I_{HET}.

The HET can be used as an approximate test to estimate the erosion resistance of a soil against initiation of erosion. By trying different test heads on different test specimens of a soil, the HET can identify a minimum test head below which the specimen shows no measurable erosion. The Initial Shear Stress, τ_o, can serve as an indicator of the soil's resistance against initiation of erosion. Discussions on the use of τ_o can be found in Section 2.6.3.

2.8.2 Use of the Slot Erosion Test

The Slot Erosion Test (SET) can also be used to assess the rate of erosion of a soil as a check against the results of the HET. The Erosion Rate Index, I_{SET}, obtained from the SET on the same soil at the standard conditions of 95% compaction and optimum water content is expected to be in the same order of magnitude as, I_{HET}, obtained from the HET.

2.8.3 Prediction of the Erosion Rate Index

If erosion tests have not been carried out to assess the erosion resistance of a soil, predictive equations as described in Section 2.5.3 can be used to provide a preliminary estimate of the Erosion Rate Index. The predictive equations are:

For coarse-grained soils:

$$\hat{I}_{HET} = 6.623 - 0.016\rho_d - 0.104\,\rho_d/\rho_{d_{max}} - 0.044\omega - 0.074\Delta\omega_r + 0.113S + 0.061Clay(US) \quad \text{Eqn 2.24}$$

$$\hat{I}_{SET} = -8.836 + 6.904\rho_d - 0.120\,\rho_d/\rho_{d_{max}} + 0.386\omega - 0.075\Delta\omega_r + 0.056S + 0.088Clay(US) \quad \text{Eqn 2.25}$$

where

$\hat{I}_{HET}$ is the predicted Erosion Rate Index for the Hole Erosion Test,

$\hat{I}_{SET}$ is the predicted Erosion Rate Index for the Slot Erosion Test,

ρ_d is the dry density of the soil in Mg/m^3,

$\rho_d / \rho_{d_{max}}$ is the percentage compaction in %,

ω is the water content in %,

$\Delta\omega_r$ is the water content ratio in %, and

$$\Delta\omega_r = \frac{(\omega - OWC)}{OWC} * 100\%$$

S is the degree of saturation in %,

$Clay(US)$ is the mass fraction finer than 0.005mm in %.

For fine-grained soils:

$$\hat{I}_{HET} = -10.201 + 9.572\rho_d - 0.042\,\rho_d / \rho_{d_{max}} + 0.103\omega + 0.0097\Delta\omega_r - 0.0056Fines + 0.042Clay(US) - 0.090LL + 0.111I_P + 0.443Pinhole$$

Eqn 2.26

$$\hat{I}_{SET} = -9.153 + 16.528\rho_d - 0.194\,\rho_d / \rho_{d_{max}} + 0.240\omega + 0.021\Delta\omega_r - 0.0293Fines + 0.048Clay(US) - 0.011LL + 0.0082I_P + 0.558Pinhole$$

Eqn 2.27

where

Fines is the fines content (< 0.075 mm) of the soil in %,

LL is the Liquid Limit in %,

I_P is the Plasticity Index in %,

Pinhole is the Pinhole Test Classification expressed as an ordinal number, i.e. '1' for Class D1; '2' for Class D2, '3' for Class PD1, ..., '6' for Class ND1).

Equations 2.24 to 2.27 represent multiple linear regression models obtained from statistical analysis of the test data of the SET and the HET. They do not necessarily imply any causal link between the predictor variables and the Erosion Rate Indices. The Author strongly recommends carrying out HET rather than using these equations, as the equations are, so far, based on a limited number of soils. The results are sensitive to the input data, and in any case, it will be more economical to do the HET than the other tests to find out the unknown parameters in the equations.

A qualitative approach is also proposed for predicting the Representative Erosion Rate Index of a soil. A number of soil parameters, namely the degree of saturation, the fines content (< 0.075 mm), the clay content (< 0.005 mm) and the Atterberg's limits, which individually show good correlation with the Representative Erosion Rate Index are used as predictor variables. These predictor variables are used independently to estimate the Representative Erosion Rate Index according to the guidelines in Table 2.25. A judgment is made on the final estimated value of the Representative Erosion Rate Index after considering all the values predicted by the individual predictor variables. This table may be used as an aid to judgment in conjunction with the multiple regression equations. The Author considers that this approach is not as good as doing a HET or SET, but is more reliable than using the predictive equations above.

Table 2.25: Proposed Rules for Preliminary Estimation of the Representative Erosion Rate Index of a Soil.

Parameters	Values	Erosion Rate Index (See Note 1)					
		Extremely rapid	Very rapid	Moderately rapid	Moderately slow	Very slow	Extremely slow
		<2	2 - 3	3 - 4	4 - 5	5 - 6	>6
Predictions for coarse-grained soils (See Note 3):							
USCS Classification	SM	Very likely	Likely	Likely - Neutral	Unlikely	Very unlikely	
(See Note 2)	SC	Neutral - Likely	Very likley		Likely - Neutral	Unlikely	Very unlikely
Degree of Saturation	<70%	Very likely	Likely	Neutral - Unlikely	Unlikely	Very unlikely	
	70 - 80%	Likely	Very Likely		Likely	Unlikely	Very unlikely
	>80%	Neutral	Likely	Very likely	Likely - Neutral	Unlikely	Very unlikely
Fines Content (<0.075mm)	<30%	Very likely	Likely - Neutral	Unlikely	Very unlikely		
	30 - 40%	Neutral - Likely	Very Likely		Likely - Neutral	Unlikely	Very unlikely
	40 - 50%	Unlikely - Neutral	Likely	Very likely	Likely	Neutral - Unlikely	Unlikely
Clay Content (<0.002mm)	<10%	Very likely	Likely - Neutral	Unlikely	Very unlikely		
	10 - 20%	Very likely			Likely - Neutral	Unlikely	Very unlikely
	>20%	Unlikely	Likely - Neutral	Very likely	Likely - Neutral	Unlikely	
Predictions for fine-grained soils (See Note 3):							
USCS Classification	CH	Very unlikely	Unlikely - Neutral	Likely		Very likely	
	MH	Unlikely	Likely	Very likely		Likely	
	CL	Unlikely - Neutral	Likely	Very likely	Likely		
	CL - ML	Neutral - Likely	Very likely		Neutral - Likely	Unlikely	
	ML	Likely	Very likely	Likely - Neutral	Unlikely	Very unlikely	
Degree of Saturation	<70%	Likely - Neutral	Very likely		Likely - Neutral	Unlikely	Very unlikely
	70 - 80%	Unlikely	Neutral - Likely	Very likely		Likely	
	>80%	Unlikely	Unlikely - Neutral	Likely		Very likely	
Soil mineralogy	Kaolinites or illites or chlorites only	Unlikely			Neutral - Likely	Very likely	Likely
	Some smectites or vermiculites	Unlikely	Likely	Very likely		Likely	Unlikely
	With cementing materials (e.g. iron oxides, aluminium oxides, gypsum, etc.)	Unlikely			Neutral - Likely	Very likely	

Notes :

1 Erosion Rate Index is taken as the negative LOG of the Coefficient of Soil Erosion, which is defined as the slope of the rising portion of the curve obtained by plotting the rate of mass removal per unit area against shear stress.

2 Soils used for construction of dam cores usually contains a considerable fraction of fines. Coarse-grained soils used for construction of a dam core are usually SC or SM. It is less common to find dam core materials belonging to GW,GP, GM, GC, SW, or SP.

3 Fine-grained soils means soils containing more than 50% by mass of fines (namely silts and clays). Fines means soil particles finer than 0.075mm. Coarse-grained soils means soils containing less than 50% by mass of fines (namely gravels and sands).

CHAPTER 3

INTERNAL INSTABILITY OF SOILS

3.1 INTRODUCTION

3.1.1 Objectives

This Chapter presents the findings of an experimental investigation and analysis of published data on the internal stability of soils in embankment dams and their foundations. The main objectives of the experimental investigation are:

i. to investigate the factors which affect the internal stability of soils;
ii. to investigate the validity of applying currently available methods in assessing the internal stability of silt-sand-gravel or clay-silt-sand-gravel mixtures, and to propose appropriate methods for assessing the internal stability of these soils; and
iii. to study the hydraulic conditions at which erosion of fine particles from within the coarse soil matrix occurs in an internally unstable soil.

The study mainly considers cohesionless soils consisting of mixtures of silt, sand and gravel. There is also a short discussion on the potential for internal instability of low plasticity clay-silt-sand-gravel mixtures.

3.1.2 Definitions

Suffusion and internal instability

Suffusion is defined as an internal erosion process which involves selective erosion of fine particles from the matrix of a soil made up of coarse particles. The fine particles are removed through the voids between the larger particles by seepage flow, leaving

behind an intact soil skeleton formed by the coarser particles. Soils which are susceptible to suffusion are *internally unstable*. Coarse widely graded or gap-graded soils such as those shown schematically in Figure 3.1 are susceptible to suffusion.

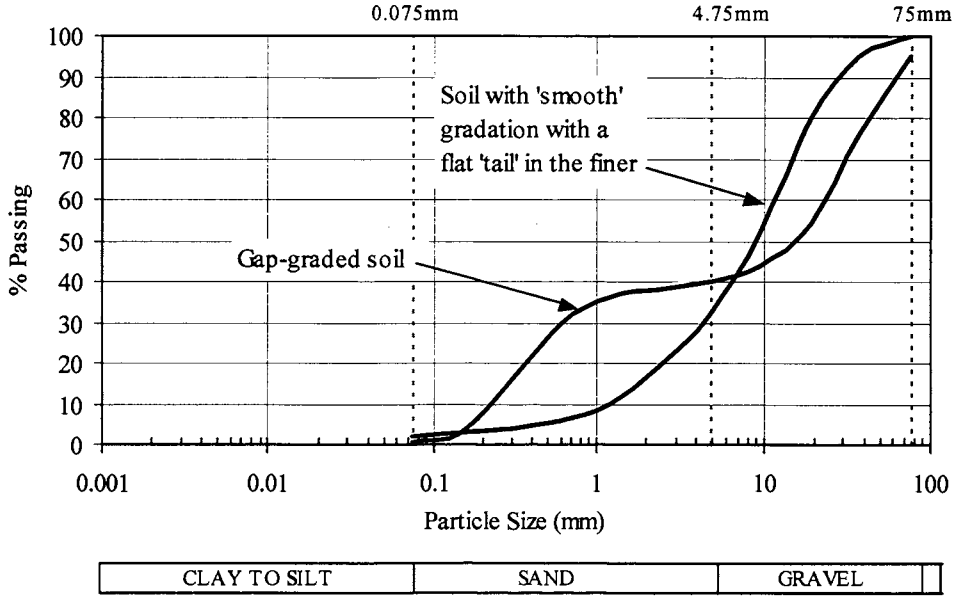

Figure 3.1: Soil gradation types which are internally unstable and are susceptible to suffusion (Foster and Fell 1999).

There is no consensus on the use of the word "suffusion". German and Canadian literature, for example, uses the word "suffosion" or "suffossion" instead of "suffusion". The word "colmatation" is also used in some literature, but "colmatation" is synonymous to clogging which is contradictory to the meaning of suffusion defined in the current study.

Self filtering

In soils which self filter, the coarse particles prevent the internal erosion of the medium particles, which in turn prevent erosion of the fine particles. Soils which potentially will not self filter include those which are susceptible to suffusion/internal instability, and very broadly graded soils such as the glacial tills shown in Figure 3.2.

Sherard (1979) indicated that the soils shown in Figure 3.2 were subject to internal erosion and piping initiated in concentrated leaks. He described the soils as being

subject to a "type of internal instability" in that they did not self filter. These soils that do not self filter are not internally unstable within the definition used in this thesis.

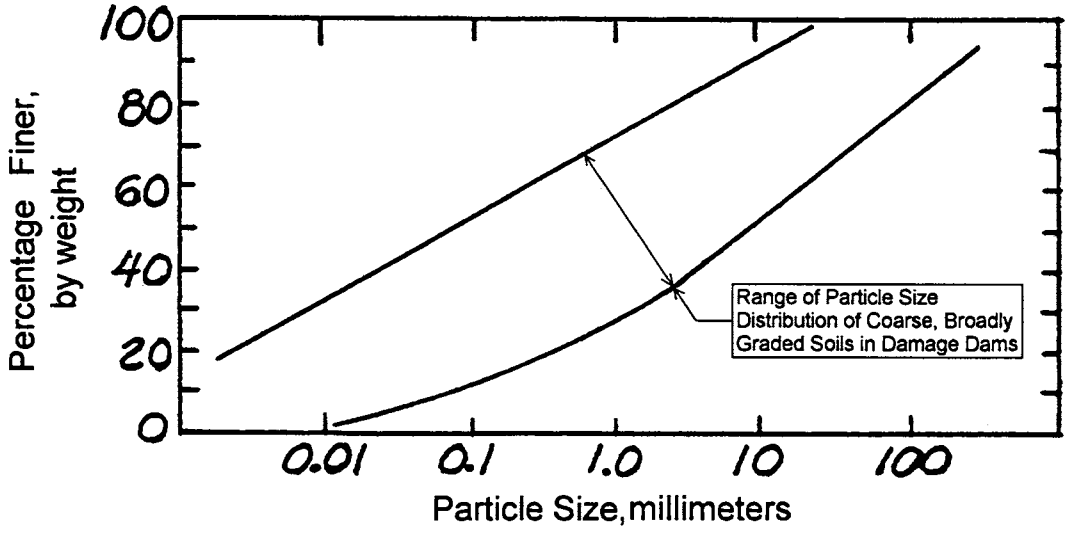

Figure 3.2: Soil types which have experienced a lack of self filtering (based on Sherard 1979).

3.1.3 Problems associated with Suffusion in Embankment Dams and Their Foundations

A number of embankment dams in France were reported to have suffered from internal erosion due to suffusion (CFGB 1997).

Figure 3.3 illustrates some of the likely problems associated with internal erosion by the process of suffusion within an embankment dam or its foundation.

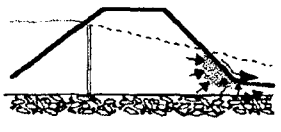

(a) Instability due to increased pore pressure

b) Settlement leading to overtopping

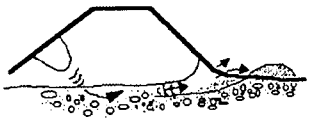

(c) Development of a sinkhole into the embankment

Figure 3.3: Some failure modes due to suffusion (adapted from CFGB 1997).

In the case of suffusion occurring within the foundation of a dam, the selective removal of fine soil particles will result in a coarser soil structure, leading to increased seepage and progressive deterioration of the foundation. The process may result in settlement, or development of pipes or cracks in an embankment dam or its foundation. Increased permeability also implies a higher risk of toe instability.

A filter layer constructed of internally unstable materials may have a tendency for migration of the finer particles, rendering the filter coarser and less effective in protecting the core materials from erosion.

3.1.4 Layout of this Chapter

Following this introduction, Section 3.2 provides a brief account of the research work by others on internal stability of soils. Section 3.3 describes the two types of seepage tests carried out as part of this research project, namely downward flow seepage tests and upward flow seepage tests, designed for studying the internal stability of soils, and the type of materials tested. Section 3.4 presents the test data of the downward flow seepage tests and the results of analysis of the data. Section 3.5 presents the test data and the results of analysis of the upward flow seepage test. It is followed by discussions of the analysis and proposed methods of assessing internal stability in Section 3.6. The findings of the investigation are concluded in Section 3.7.

3.2 LITERATURE REVIEW

3.2.1 Overview

This Section provides a brief review of the findings of previous investigations of internal instability of soils, and of self filtering.

The phenomenon of suffusion of cohesionless sand-gravel soils has been studied by a number of investigators, including the US Army Corps of Engineers (1953), Istomina (1957), Lubochkov (1962, 1965), Kenney and Lau (1985, 86), Lafleur et al. (1989), Burenkova (1993), Skempton and Brogan (1994), Schuler (1995) and Chapuis et al. (1996). Sun (1989) carried out tests on cohesive clay-silt-sand soils.

Kézdi (1969), de Mello (1975), and Sherard (1979) discussed soils which were not self filtering.

3.2.2 Frequently used symbols

Some mathematical symbols which are used in this Chapter are explained in Table 3.1.

Table 3.1: Meaning of mathematical symbols.

Symbol	Meaning
C_C	Coefficient of curvature equal to $D_{30}^{\ 2}/(D_{60} \times D_{10})$.
C_U	Coefficient of uniformity equal to D_{60}/D_{10}.
d_X or D_X	Particle size for which X% by weight is finer (in mm).
d_0 or D_0	Minimum particle size (in mm).
d_{100} or D_{100}	Maximum particle size (in mm).

Symbol	Meaning
d_{BX} or D_{BX}	Particle size for which X% by weight is finer, for a base material (B) which is protected against internal erosion by a filter (in mm).
d_{FX} or D_{FX}	Particle size for which X% by weight is finer, for a filter material (F) which is protecting a base material against internal erosion (in mm).
d_{cX} or D_{cX}	Particle size for which X% by weight is finer, when only the coarse (c) fraction of a soil is considered. The soil is divided into a coarse fraction and a fine fraction at a point represented by size d_{dv}, and that part of the grain-size distribution curve for the coarse fraction is adjusted to give a minimum size of d_{dv} (in mm).
d_{fX} or D_{fX}	Particle size for which X% by weight is finer, when only the fine (f) fraction of a soil is considered. The soil is divided into a coarse fraction and a fine fraction at a point represented by size d_{dv}, and that part of the grain-size distribution curve for the fine fraction is adjusted to give a maximum size of d_{dv} (in mm).
F_d or F_D	The fraction by weight (in %) of a soil which is finer than size d (or D).
%Fines	Fines content of a soil (i.e. percentage by weight finer than 0.075mm).

3.2.3 Investigations on internal instability of cohesionless soils by others

Fuller and Thompson (1907) and Schuler (1995)

Schuler (1995) suggested that soils would be safe from suffusion if their grading resulted in a soil with minimum porosity. The grading of such a soil can be represented by equation 3.1 from Fuller and Thompson (1907) who presented the results of a series of tests on the density of different mixtures of aggregates and cement for the purpose of studying the rules of proportioning for maximum density with different materials. Their test results showed that the densest mixtures of cement and aggregate had a mechanical

analysis curve (i.e. grain-size distribution curve) resembling a parabola. The grain-size distribution curve of the densest mixtures can be represented by:

$$F_d = \left(\frac{d}{d_{100}} \right)^n \times 100\% \qquad \text{Eqn 3.1}$$

with n approximately equal to 0.5.

Figure 3.4 shows theoretically stable grain-size distribution curves for soils having maximum particle sizes of 19 mm and 75 mm, respectively according to equation 3.1. Figure 3.5 presents a theoretically stable grain-size distribution normalised against the maximum particle size.

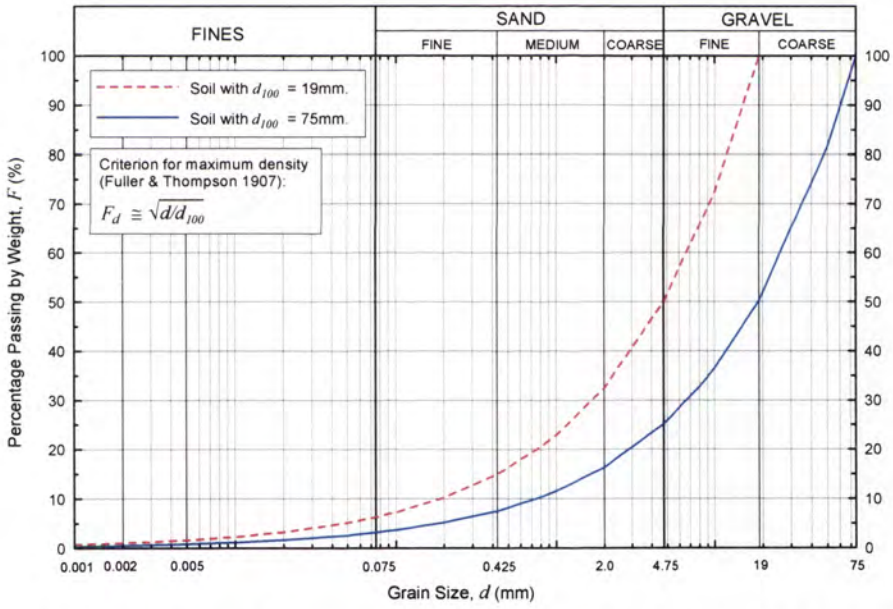

Figure 3.4: Examples of grain-size distribution curves according to Fuller & Thompson (1907) criterion for maximum density.

Kenney and Lau (1986) compared their recommended criterion for internal instability with Fuller & Thompson (1907) ideal curve for maximum density, and remarked that their criterion, represented by $H / F < 1.0$, was similar to Fuller and Thompson's ideal curve for $F < 0.3$. Neither Kenney and Lau (1986) nor Schuler (1995) commented on

the internal stability of those soils which did not satisfy Fuller and Thompson (1907) criterion for maximum density.

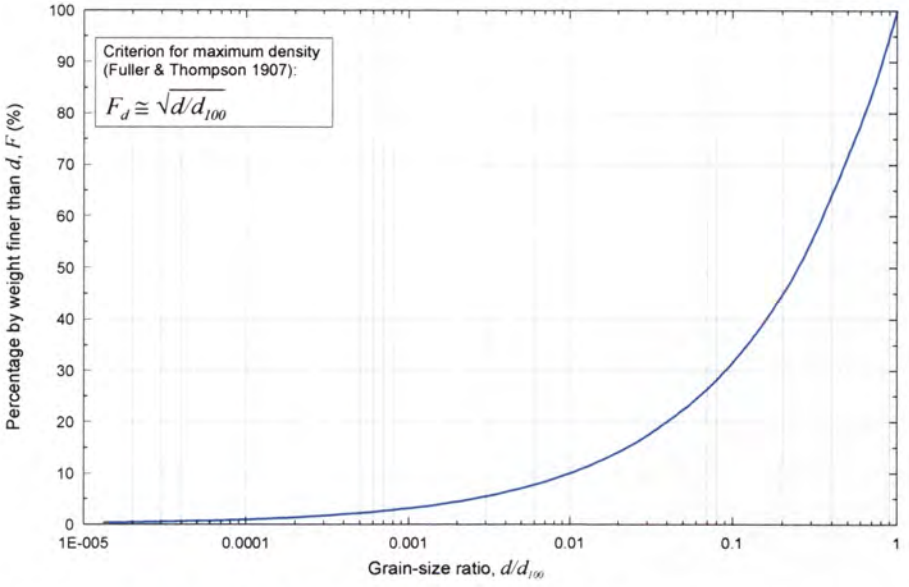

Figure 3.5: Grain-size distribution curve normalised against maximum particle size based on Fuller & Thompson (1907) criterion of maximum density.

U.S. Army Corps of Engineers (1953)

The U.S. Army Corps of Engineers (1953) carried out downward flow seepage tests on granular filter materials, and proposed that suffusion would occur in cohesionless filter materials if (1) the flow condition is turbulent; (2) the hydraulic gradient is higher than 5; and (3) the coefficient of uniformity of the soil, $C_U > 20$. Their experimental data are not available for analysis in the current study.

Istomina (1957)

Istomina (1957) defined the likelihood of suffusion in terms of the uniformity coefficient, C_U of the soil. Istomina classification scheme, according to Kovács (1981), is as follows.

No suffusion if	$C_U \leq 10$;
Transition condition	$10 \leq C_U \leq 20$;

Suffusion is liable if $C_U \geq 20$.

Lubochkov (1962, 1965)

Lubochkov (1962) proposed that not all materials having $C_U \geq 20$ were liable to suffusion, as the possibility of movement of the fine grains depended on the shape of the grain-size distribution curve.

Lubochkov (1965) proposed that a soil would not be susceptible to suffusion when the slope of the grain-size distribution curve was equal to, or smaller than a given limit in each grain-size interval. This condition is presented in mathematical form by Kovács (1981) as:

if $$\frac{D_{n-1}}{D_n} = \frac{D_n}{D_{n+1}} = 10; \quad \frac{\Delta S_1 / \Delta S_2}{4.0} \leq 1$$ Eqn 3.2a

if $$\frac{D_{n-1}}{D_n} = \frac{D_n}{D_{n+1}} = 5; \quad \frac{\Delta S_1 / \Delta S_2}{2.6} \leq 1$$ Eqn 3.2b

if $$\frac{D_{n-1}}{D_n} = \frac{D_n}{D_{n+1}} = 2.5; \quad \frac{\Delta S_1 / \Delta S_2}{1.7} \leq 1$$ Eqn 3.2c

where D_n is an arbitrary grain-size on the distribution curve;

D_{n-1}, D_{n+1} are determined from D_n by multiplying or dividing it by 10, 5 or 2.5;

$\Delta S_1 = S_{n-1} - S_n$ is the difference between the percentage in weight for grain sizes D_{n-1} and D_n;

$\Delta S_2 = S_n - S_{n+1}$ is the difference between the percentage in weight for grain sizes D_n and D_{n+1};

An example on the application of Equations (3.2a, b, c), and the use of the method to estimate the range of grains which would likely be eroded by the process of suffusion is shown in Figure 3.6.

The upper part of Figure 3.6 shows the grain-size distribution curve of a soil which is

deficient in materials between 0.1 and 1 mm. The grain-size distribution curve is divided at an arbitrary point denoted by size D_n. For a chosen grain-size interval represented by $X = 10$, sizes D_{n-1} and D_{n+1}, and the ratio $(\Delta S_1/\Delta S_2)/F$ are calculated according to equation 3.2a. F is equal to 4.0 for $X = 10$. The calculations are repeated for all valid dividing points D_n along the grain-size distribution curve. $(\Delta S_1/\Delta S_2)/F$ is then plotted against D_n as shown in the lower part of Figure 3.6. The lower part of Figure 3.6 shows two other curves for smaller size fraction ratios represented by $X = 5.0$ and $F = 2.6$ (equation 3.2b), and $X = 2.5$ and $F = 1.7$ (equation 3.2c). According to Lubochkov (1965), the soil is internally unstable as all three curves are plotted above the horizontal line represented by $(\Delta S_1/\Delta S_2)/F = 1$. The curves cross the horizontal line at 1.7, 1.9 and 2.1 mm, indicating that grain-sizes finer than 1.7 to 2.1 mm are susceptible to erosion by suffusion.

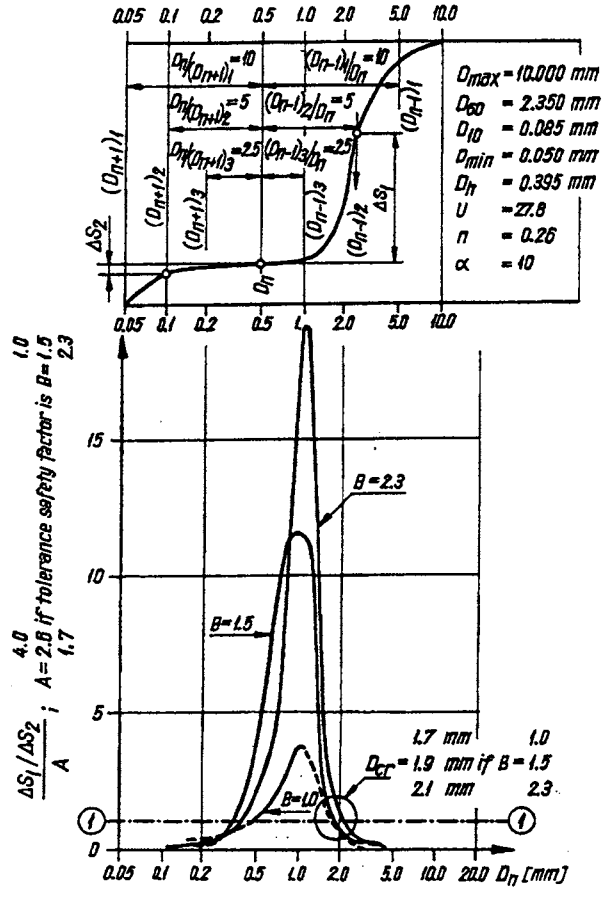

Figure 3.6: Lubochkov (1965) analytical method for determining the range of grains susceptible to suffusion.

Kenney, Lau and Clute (1983), and Kenney, Chahal, Chiu, Ofoegbu, Omange and Ume (1985)

Kenney et al. (1983, 1985) carried out downward flow filter tests on granular materials to investigate the controlling constriction size of different granular cohesionless materials, and the internal stability of granular materials.

Kenney et al. (1983, 1985) defined the constriction size, D_C, as the diameter of the largest spherical particle that could pass through a void between particles in the soil. The controlling constriction size, D_C^*, of a porous material, or soil was defined as the diameter of the largest particle which could be transported through the material. A constriction is different from a pore in that the latter is the volumetric space between four or more soil grains, whereas the former is an opening connecting two pores.

Kenney et al. (1983, 1985) carried out filter tests on linearly-graded materials with coefficients of uniformity, C_U, of 1.2, 3, 6 and 12. They found that, for filter materials with minimum particle size, D_o, > 0.2 mm, the ratio D_C^*/D_o, which limits whether the filter will control erosion, is approximately a constant. For a filter with C_U = 1.2, $D_C^*/D_o \cong 0.18$, and for filters with C_U = 3, 6 and 12, $D_C^*/D_o \cong 0.26$. Their filter tests on 8 non-linearly-graded filter materials having various C_U values showed that D_C^* was best correlated with D_5, and that filters satisfying equations 3.3 and 3.4 would control erosion.

$$\frac{D_C^*}{D_5} \leq 0.25 \qquad \text{Eqn 3.3}$$

$$\frac{D_C^*}{D_{15}} \leq 0.20 \qquad \text{Eqn 3.4}$$

Kenney et al. (1983, 1985) concluded that that D_C^* was strongly dependent on the fine fraction (e.g. D_5) of the filter material, but not on filter thickness or the shape of the grain-size distribution curve.

Filters for soils with a minimum particle size, D_o < 0.2 mm, have smaller ratios of D_C^*/D_5 than those indicated by equations 3.3 and 3.4. Kenney et al. (1983, 85) explained that the hydrodynamic conditions within these filter materials during the tests were not severe enough to mobilise particles as large as size D_C^*. According to Kenney et al. (1983, 85), for particles of sizes up to D_C^* to be mobilised, the hydrodynamic number, R', had to be greater than 10. Hydrodynamic number, R', is defined as:

$$R' = \frac{qD_5}{\eta \nu} \qquad \text{Eqn 3.5}$$

where q: is the discharge rate divided by the total cross-sectional area [mm/s];

D_5: in [mm];

η: is the porosity of the filter material;

ν: is the kinematic viscosity of water (approximately 1 mm^2/s).

Kenney et al. (1983) carried out downward flow seepage tests on the filter materials to find out whether or not fine particles in the filters might be moved by seepage water, rendering the filters coarser and less effective (i.e. whether the filters were internally unstable). The test samples, having a maximum grain size of 25 mm, were compacted to 230 – 270 mm thick inside a seepage cell of 245 mm diameter. The tests were carried out under a hydraulic gradient of less than 5. The filter materials, with grain-size distribution curves shown in Figure 3.7 and Figure 3.8, were found to be internally stable. Kenney et al. (1983) also presented the grain-size distribution curve of a granular material, as in Figure 3.9, which was tested to be internally unstable.

Kenney et al. (1983) proposed that internal instability was associated with the following conditions:

- soil/filter consisted of a primary fabric of particles which carried the effective stresses imposed on the filter;
- loose particles within the void spaces of the primary fabric which were free to move;

- constrictions leading from the void spaces were larger than some of the loose particles.

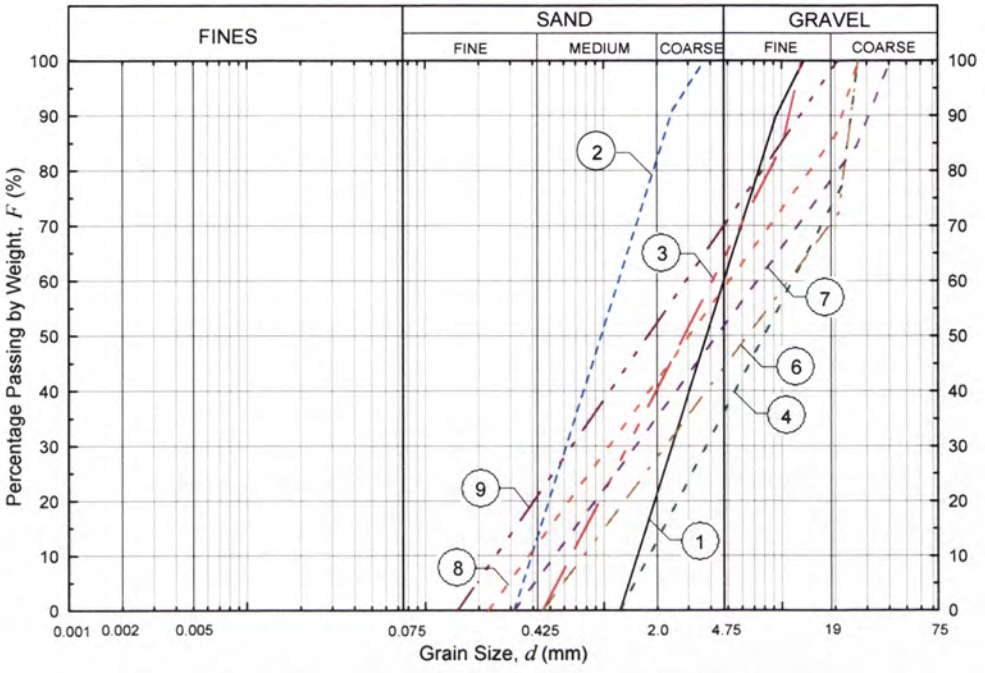

Figure 3.7: Linearly-graded soil samples tested to be internally stable by Kenney et al. (1983).

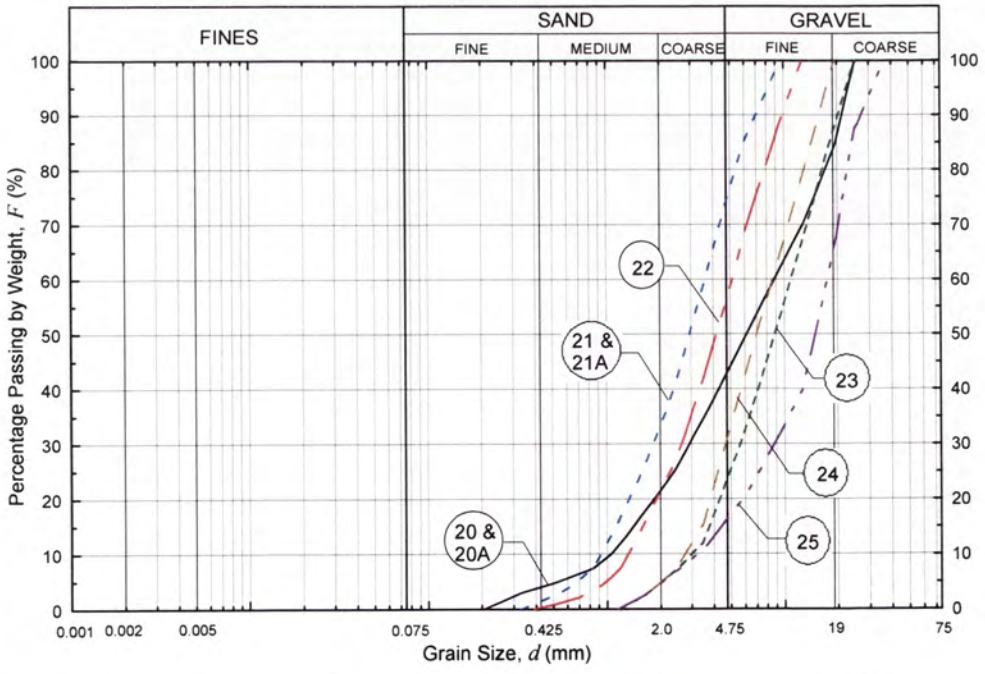

Figure 3.8: Non-linearly graded soil samples tested to be internally stable by Kenney et al. (1983).

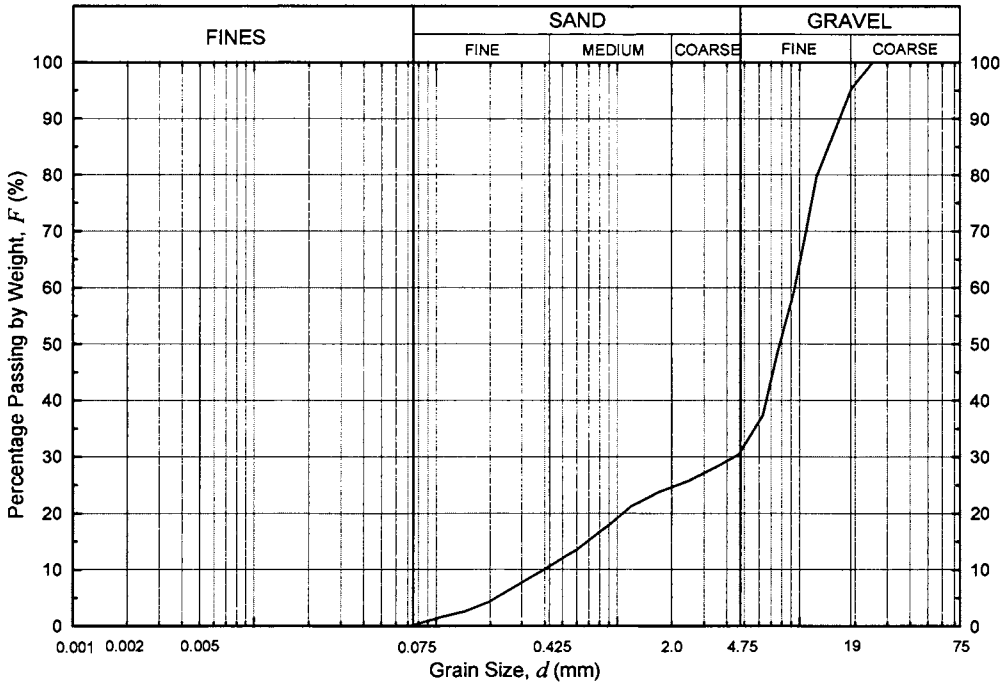

Figure 3.9: Soil sample, having irregular grain-size distribution curve, tested to be internally unstable by Kenney et al. (1983).

Kenney, Lau and Clute (1984)

Kenney et al. (1984) considered the stability of gradings from the point of view of filtration. They treated the primary fabric of a compacted material as made up of the coarser soil particles which act as a filter to the finer loose particles. They hypothesized that a soil would behave as a stable system when the sizes of the loose particles were larger than the controlling constriction size, D_C^*, of the primary fabric. Kenney et al. (1984) verified their hypothesis by applying downward flow seepage tests to gap-graded granular filters made by mixing uniform gravel (material A) and uniform sand (material B, C or D). Material A was the coarse material forming the primary fabric of the blended soil. Materials B, C or D were added to A to form 3 different mixtures. The grain-size distribution curves of the 3 mixtures are shown in Figure 3.10. Most of the particles of material B were larger than D_C^* of the coarse material A. Mixture A-B was predicted to be stable. Most of the particles in material C were smaller than D_C^*, and material D was substantially finer than D_C^*. Mixtures A-C and A-D were predicted to be unstable. Results of the seepage tests showed that their predictions were correct.

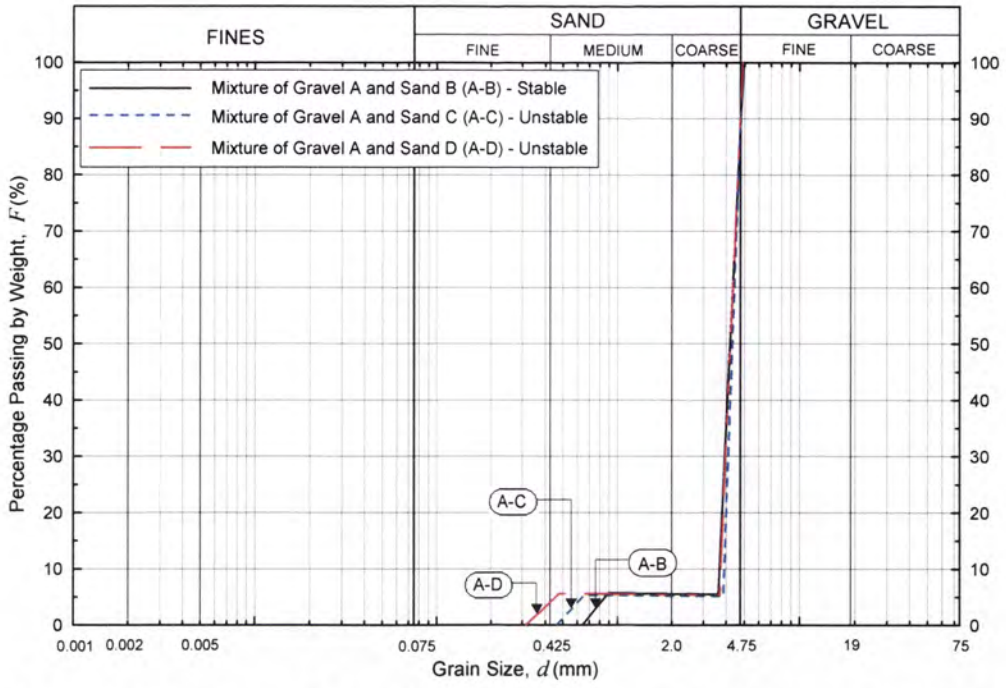

Figure 3.10: Gap-graded gravel-sand mixtures tested by Kenney et al. (1984).

Kenney and Lau (1984, 1985, 1986)

Kenney and Lau (1984, 85) postulated that materials finer than size d (having a weight fraction, F), will likely be washed out from a soil if there was not enough materials in the size range d to $4d$ (having a weight fraction, H). Both F and H can be obtained from the grain-size distribution curve of the material for any given particle size d, with $H = F_{4d} - F_d$.

To verify their theory, Kenney and Lau (1984, 85) carried out downward flow seepage tests on 14 cohesionless sand-gavel soil samples with a maximum particle size of up to 100 mm. The grain-size distribution curves of the test samples are shown in Figure 3.11a and Figure 3.11b. The soil samples were tested in seepage cells of either 245 mm or 580 mm diameters. The compacted thicknesses of the test samples were 580 mm for the smaller seepage cell, and 860 mm for the larger seepage cell. The tests were carried out under flow conditions corresponded to hydrodynamic numbers R' (equation 3.5) of greater than 10. Six out of the 14 test samples showed signs of internal instability. Kenney and Lau (1984, 85) examined the shape curves (H-F plots) of the test samples and proposed that an internally unstable soil will have part or the whole of its shape

curve plotted below the line represented by $H = 1.3F$, within the region $0 < F < X$. For Narrowly-Graded (NG) soils (i.e. soils with $C_U \leq 3$), X is equal to 0.3, whereas for Widely-Graded (WG) soils (i.e. soils with $C_U > 3$), X is equal to 0.2.

Shape curves for the unstable and stable samples tested by Kenney and Lau are shown in Figure 3.12a and Figure 3.12b, respectively.

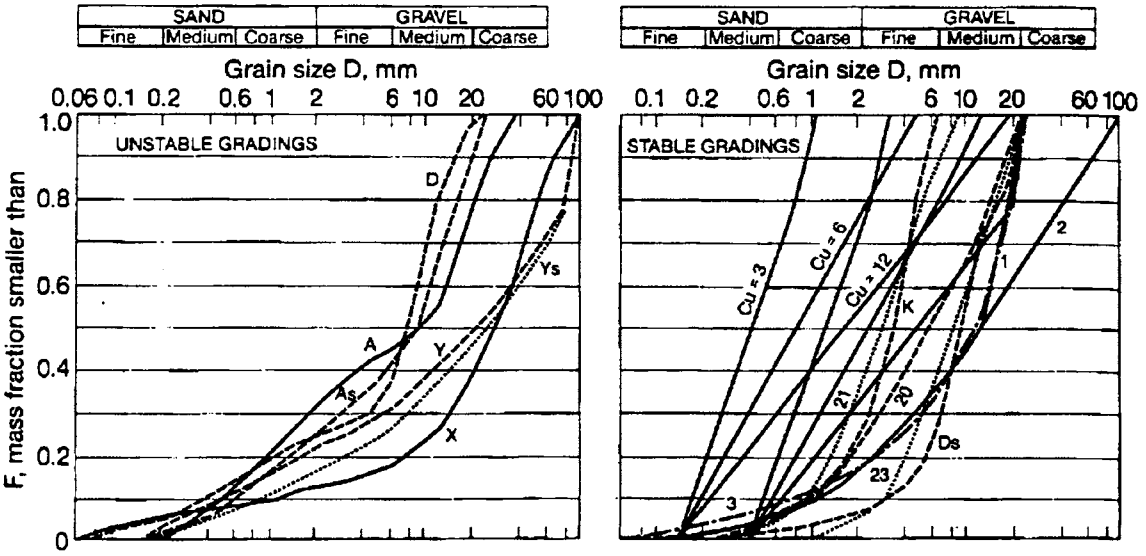

(a) Gradings of unstable materials. (b) Gradings of stable materials.

Figure 3.11: Soil samples tested by Kenney and Lau (1985).

Kenney and Lau (1984, 85) stated that their proposed boundary represented by $H = 1.3F$ coincided with Lubochkov (1965) "lower-limit" condition for stable soils in a medium-dense to dense condition having a porosity value of 0.23. According to Kenney and Lau (1984, 85), Lubochkov (1965) "lower-limit" could be approximated by the equation:

$$F_d = 0.6(d/d_{60})^{0.6} \qquad \text{Eqn 3.6}$$

Since $F_{4d} = 0.6(4d/d_{60})^{0.6} = F_d(4)^{0.6}$ according to equation 2.6, $H = F_{4d} - F_d$ is equal to $F_d(4)^{0.6} - F_d$, which can be simplified to $H = 1.3F$.

Kenney and Lau (1985) suggested an alternative graphical method to assess the potential of instability. As illustrated in Figure 3.13, H values are calculated from F values based on the boundary line $H = 1.3F$ for F between 0 and 0.2. The upper grading curve shown in Figure 3.13 lies below the points marked H_{10}, H_{15}, H_{20}, etc., and the material is assessed as potentially unstable.

Kenney and Lau (1985) also stipulated that as long as the materials were composed of particles coarser than silt size, and the transport conditions within the void network corresponded to a hydrodynamic number $R' \geq 10$ (Kenney et al. 1983, 1985), coupled with light vibration, the absolute sizes of the particles were of little importance in comparison with the shape of the grading curve.

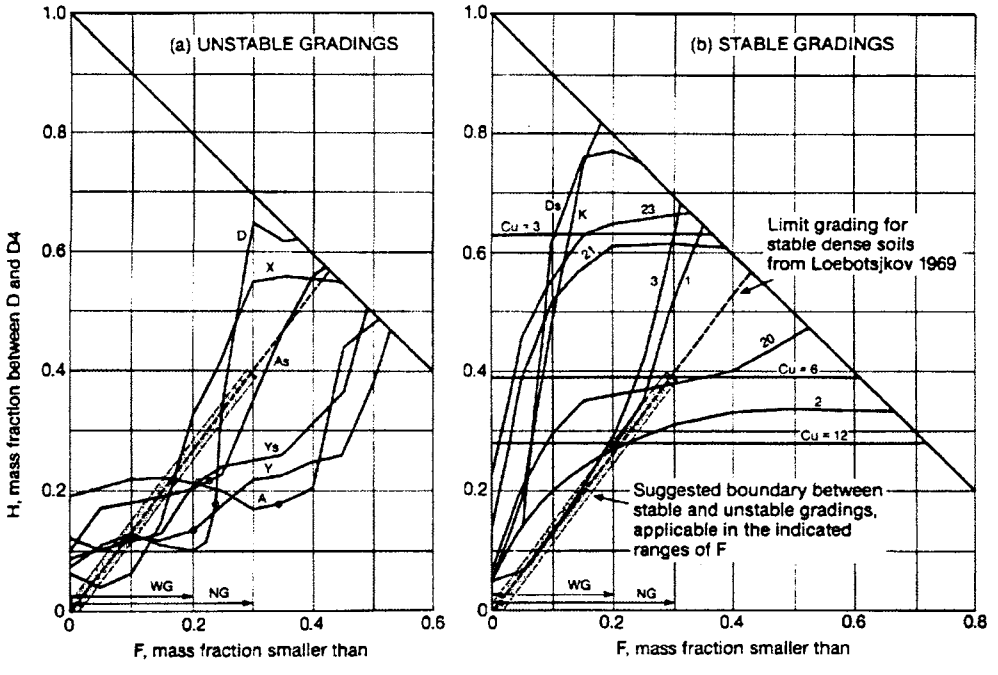

Figure 3.12: Shape curves of (a) unstable and (b) stable gradings of soil samples tested by Kenney and Lau (1985).

Upon considering the comments by others and the results of further laboratory testing, the originally proposed boundary $H = 1.3F$ was revised to $H = 1.0F$ (Kenney and Lau 1986) as shown in Figure 3.14. The revised boundary is slightly less conservative than the original, and is consistent with Fuller and Thompson (1907) grading for minimum

porosity represented by $F_d = \sqrt{d/d_{100}}$ (equation 3.1). Substituting $F_{4d} = \sqrt{4d/d_{100}}$ in $H = F_{4d} - F_d$ gives $H = 1.0F$. The zone between the boundaries represented by $H = 1.3F$ and $H = 1.0F$ is a transition zone between stable and unstable gradings.

The Kenney and Lau (1986) method is widely used for predicting the internal stability of cohesionless sand-gravel soils. In the Author's experience, the method has been applied to silt-sand-gravel soils which are outside the range of soils tested by Kenney and Lau (1984, 85 and 86).

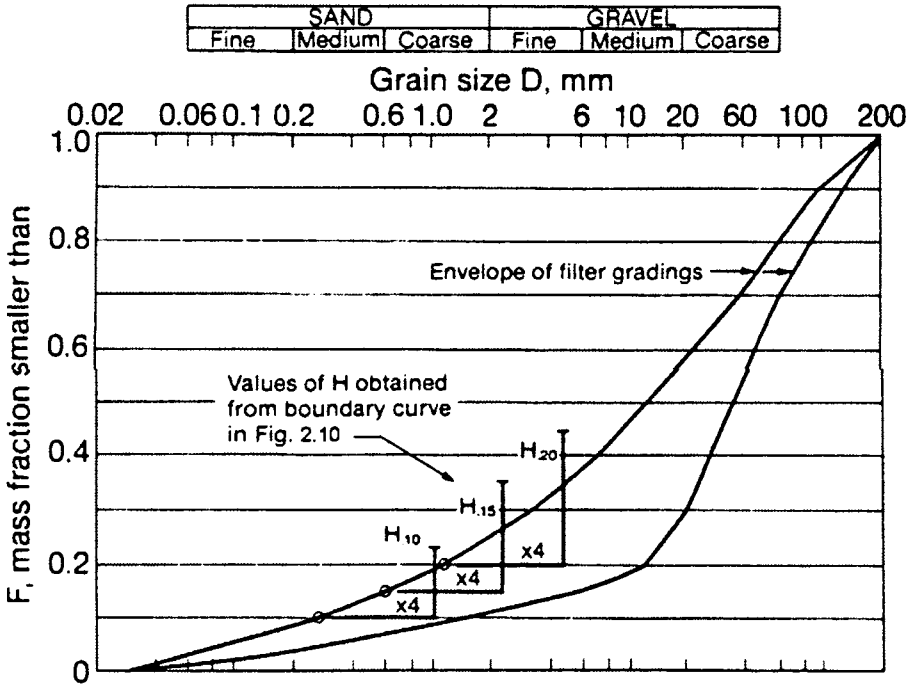

Figure 3.13: Alternative method to evaluate the potential for grading instability (Kenney & Lau 1985).

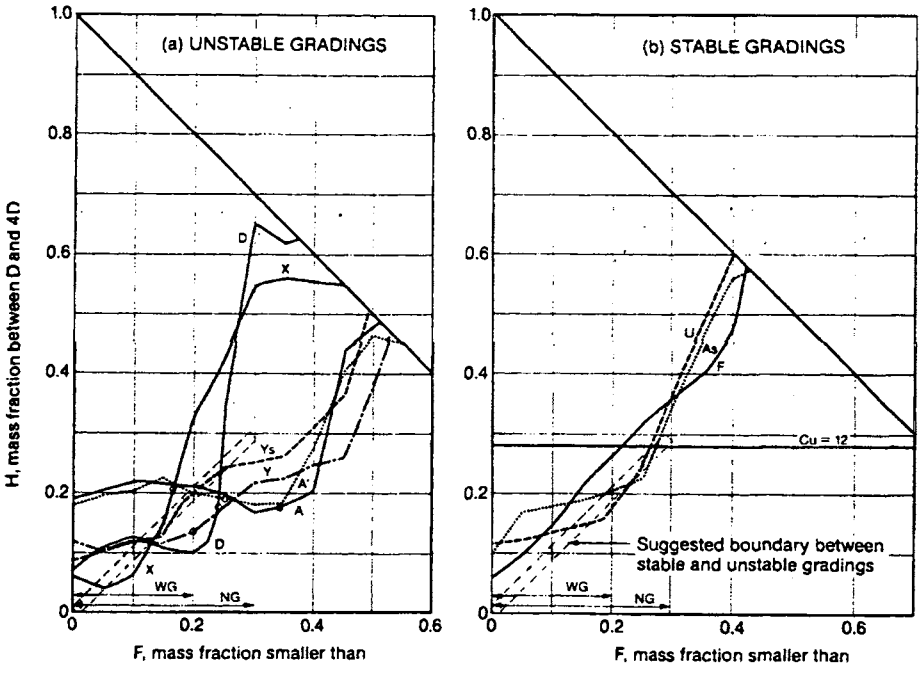

Figure 3.14: Shape curves of selected unstable and stable gradings and the revised boundary between stable and unstable gradings (Kenney and Lau 1986).

Lafleur, Mlynarek and Rollin (1989, 1993)

Lafleur et al. (1989) reviewed the filter design criteria for broadly-graded core materials taking into account suffusion of the finer particles within the core materials. Lafleur et al. (1989) conducted two series of tests. The first series of tests, the screen tests, served to identify those base materials in which migration of particles would occur. Three gradings, as shown in Figure 3.15, of base materials formed by blending artificial glass beads were tested for internal stability by downward flow seepage tests. In these seepage tests, the test samples were compacted to a thickness of approximately 230 mm inside a seepage cell of 197 mm diameter, and then subjected to hydraulic gradients ranging from 2.5 to 6.5. Sample M42 was tested to be internally stable, whereas samples M6 and M8 were tested to be internally unstable. The second series of tests, the compatibility tests, were a series of filter tests for determining the indicative size of the filters which caused insignificant losses of particles in the base materials.

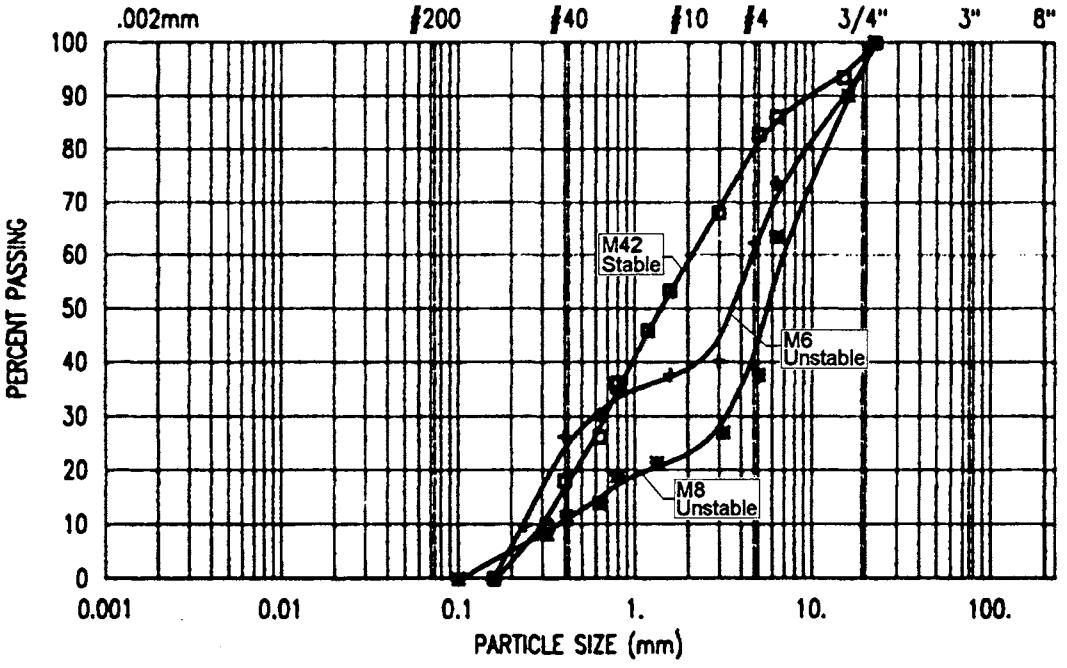

Figure 3.15: Grain-size distribution curves of materials tested for internal instability by Lafleur et al. (1989).

Lafleur et al. (1989) commented on the internal stability of soils that could be represented by 3 general shapes of grading curves as shown in Figure 3.16:

- Linearly graded (curves 1 and 2): Included soils with all the particles uniformly distributed (curve 1), soils with the fine particles uniformly distributed (curve 2), and soils with appreciable amount (< 40%) of coarse particles floating within a finer linearly graded matrix. Soils in this group are internally stable.
- Gap-graded (curve 3): Particles within an intermediate range of size were missing. There is a horizontal or sub-horizontal portion in the 30% or less finer particles. Gap-graded soils can be either internally stable or unstable.
- Concave upward (curve 4): Soils in this group are internally unstable.

The grading curves in Figure 3.16 are conceptual, and do not represent actual boundaries between internally stable and unstable soils.

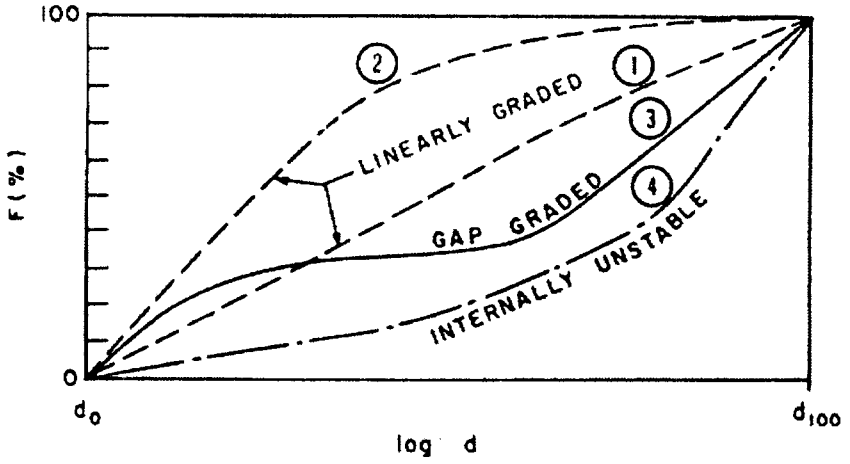

Figure 3.16: Classification of Gradation Curves of Broadly Graded Soils (Lafleur et al. 1989, 1993).

Burenkova (1993)

Burenkova (1993) proposed a predictive method based on the results of laboratory tests on 22 cohesionless sand-gravel soils of maximum particle sizes up to 100 mm, and coefficients of uniformity, C_U, up to 200.

Burenkova's test involves dry mixing various size fractions of a soil. The basic assumption was that a smaller size fraction did not form part of the basic soil skeleton if it did not cause volume increase when mixed with a coarser size fraction. During the test, the coarsest size fraction was put into a container and the volume of the specimen was measured. The next finer size fraction was then added to the container, and the volume of the mixture was measured again. The tests followed this procedure until all prepared fractions were included in the specimen. If the volume of the specimen increased after addition of a finer fraction, this finer fraction was estimated as belonging to the soil skeleton. If the additional fraction did not increase the volume of the specimen, the fraction was considered as belonging to the loose particles which could be subject to suffusion.

According to Burenkova (1993), the internal stability of a soil depends on the conditional factors of uniformity, h' and h'' defined as:

$$h'' = d_{90}/d_{15} \qquad \text{Eqn 3.7a}$$

$$h' = d_{90}/d_{60} \qquad \text{Eqn 3.7b}$$

On a plot of h' against $\log(h'')$ as shown in Figure 3.17, Burenkova (1993) defined boundaries separating "Suffusive Soils" from "Non-suffusive Soils". According to Burenkova (1993), Zones I and III represent zones of suffusive compositions; Zone II represents a zone of non-suffusive compositions; and Zone IV represents a zone of artificial soils. The domain for non-suffusive soils (i.e. Zone II) is approximately described by the following inequality:

$$0.76\log(h'')+1 < h' < 1.86\log(h'')+1 \qquad \text{Eqn 3.8}$$

Burenkova (1993) also proposed a method, as shown in equation (3.9), for predicting the size of the largest particles, d_{dv}, representing the limit between the fraction building the soil skeleton, and the loose grains.

$$0.55(h'')^{-1.5} < \frac{d_{dv}}{d_{100}} < 1.87(h'')^{-1.5} \qquad \text{Eqn 3.9}$$

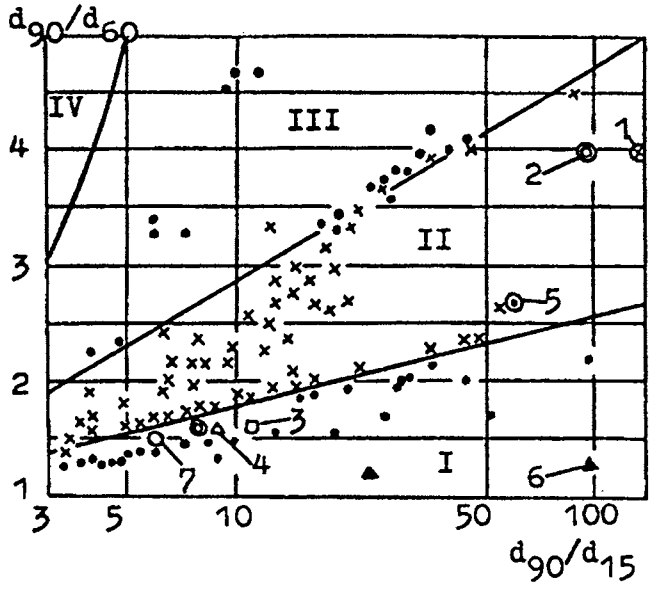

(Zones I and III – Suffusive; Zone II – Non-suffusive; Zone IV – Artificial Soils.)

Figure 3.17: Classification of suffusive and non-suffusive soil compositions (Burenkova 1993).

Burenkova (1993) also carried out a series of seepage tests to study the effects of suffusion. The sizes of the eroded particles in the seepage tests were similar to those predicted by equation 3.9. Among the series of seepage tests carried out by Burenkova (1993), eight tests were clearly documented. The eight tests confirmed 4 suffusive and 4 non-suffusive soil samples whose grain-size distribution curves are shown in Figure 3.18. The seepage tests were carried out at hydraulic gradients up to 2.5.

Skempton and Brogan (1994)

Skempton and Brogan (1994) carried out laboratory seepage tests to study the internal instability in sandy gravels. They attempted to find out the critical hydraulic gradient at which migration of fines would start. They used an upward flow seepage cell of 139 mm diameter to investigate internal instability in sandy gravels. A 155 mm length soil sample in the seepage cell was saturated by a small initial flow before the test began. Each test lasted for about 1.5 hr., during which fines were collected, dried and weighed at the end of the test. The test set up is shown in Figure 3.19. Four samples formed by mixing gravels with uniform sand and in the size range of 0.06 – 10 mm were tested in the seepage cell. The grain-size distribution curves of the 4 samples are shown in Figure 3.20.

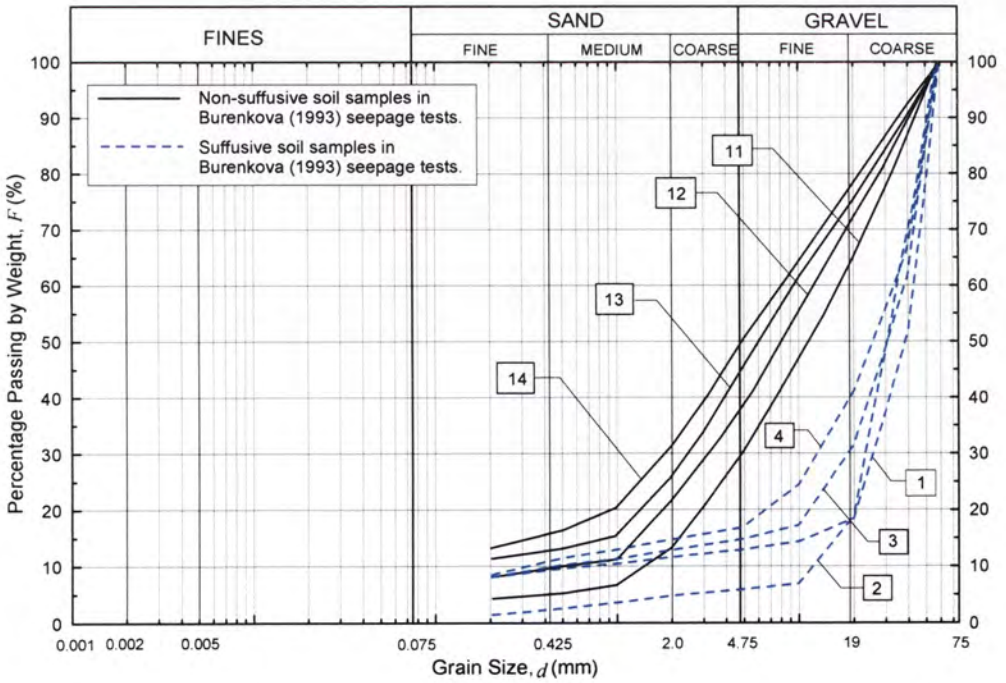

Figure 3.18: Eight soil samples tested by seepage tests (Burenkova 1993).

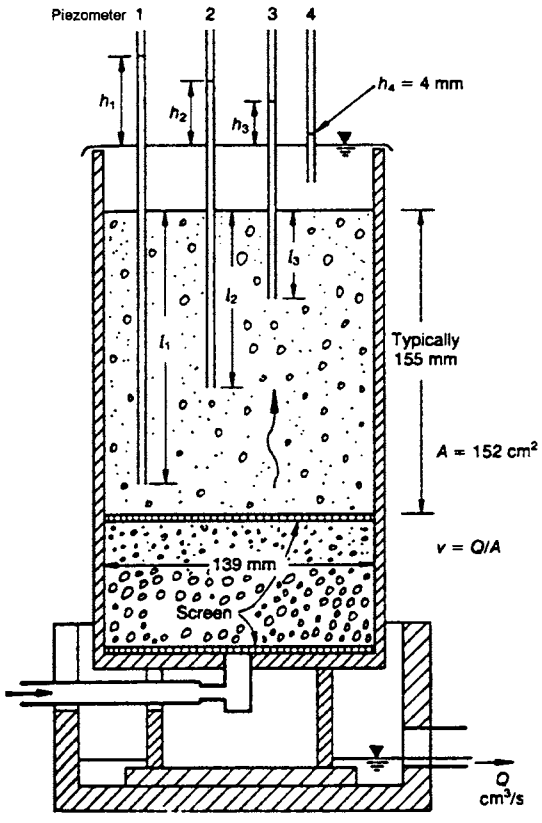

Figure 3.19: Upward flow seepage cell (Skempton and Brogan 1994).

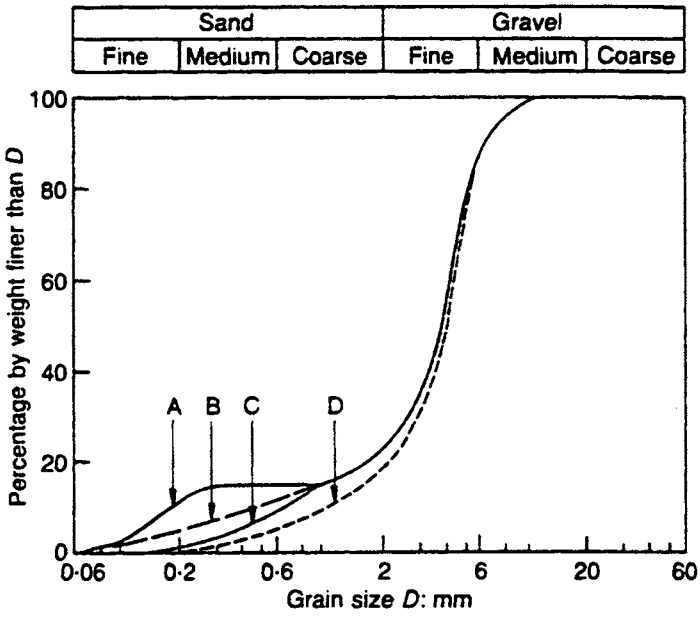

Figure 3.20: Soil samples tested by Skempton and Brogan (1994).

Skempton and Brogan plotted critical hydraulic gradient (i_c) against stability index (*H/F*) (Kenney and Lau 1985, 1986), and noticed that i_c increased rapidly from a low value to a high value across the line represented by $H/F = 1$, which represented the boundary between stable and unstable gradings. They, however, commented that the relationship required further investigations, and the influence of density of packing and proportions of sand to gravels had to be investigated.

They also noticed that, in unstable sandy gravels (samples A and B), erosion of the sand grains could occur at hydraulic gradients 1/3 to 1/5 of the theoretical critical gradient for a homogeneous granular material of the same porosity. The critical hydraulic gradient, corresponding to zero effective stress, is defined as:

$$i_c = (1-\eta)(G_s - 1) = \frac{\gamma'}{\gamma_w} \qquad \text{Eqn 3.10}$$

where i_c : critical hydraulic gradient,

η : porosity of the material,

G_s : specific gravity of the soil grains,

γ' : submerged unit weight of the soil,

γ_w : unit weight of water.

The observed critical hydraulic gradients were far less than the theoretical critical gradient for a sample composed entirely of the sand component. Skempton and Brogan suggested that, in an internally unstable soil, overburden load was probably carried on a primary fabric so that sand was under relatively small pressure. Table 3.2 summarises the properties of the soil samples and the results of the 4 seepage tests carried out by Skempton and Brogan (1994).

Chapuis, Constant and Baass (1996)

Chapuis et al. (1996) investigated the effects of compaction methods on the migration of fines in 0 - 20mm crushed aggregates used as base course materials of flexible road pavements. They pointed out that design criteria for gravel base course should consider permeability, filter performance and suffusion requirements.

Table 3.2: Results of seepage tests (from Skempton and Brogan 1994).

Test samples	**A**	**B**	**C**	**D**
Porosity, η (%)	34	37	37.5	36.5
D_{15} (mm)	0.60	0.90	0.98	1.6
C_U	24	10	7	4.5
Permeability, k (cm/s)	0.45	0.84	0.86	1.8
Filter ratio of components, D_{c15}/D_{f85}	11	3.9	3.2	3.2
Stability index, $(H/F)_{min}$	0.14	0.98	1.6	2.8
Critical gradient, i_c, in test	0.20	0.34	1.0	1.0

Note: Samples A and B, with $(H/F)_{min} < 1$, were assessed as Internally Unstable, whereas Samples C and D were assessed as Internally Stable.

Chapuis et al. (1996) carried out downward flow seepage tests on 2 aggregates, namely crushed limestones and crushed gravels (0.075 – 20 mm), having grain-size distribution curves as shown in Figure 3.21. The tests showed that gravels represented by Curve 1 and 3 were internally stable, whereas gravels represented by Curve 2 was internally unstable.

Foster and Fell (1999a, 2001)

Foster and Fell (1999a, 2001) investigated the factors which influenced the no erosion and continuing erosion filter boundaries. Their investigation involved analysing experimental data on hundreds of filter tests carried out by others, reviewing the performance of filters in existing dams, and carrying out continuing erosion filter (CEF) tests. Based on the results of their investigation, they proposed that the boundaries of filter test behaviour are related to D_{F15} of the filter, some characteristic sizes of the base materials, namely D_{B85}, D_{B90} and D_{B95}, and also the fines content of the base materials.

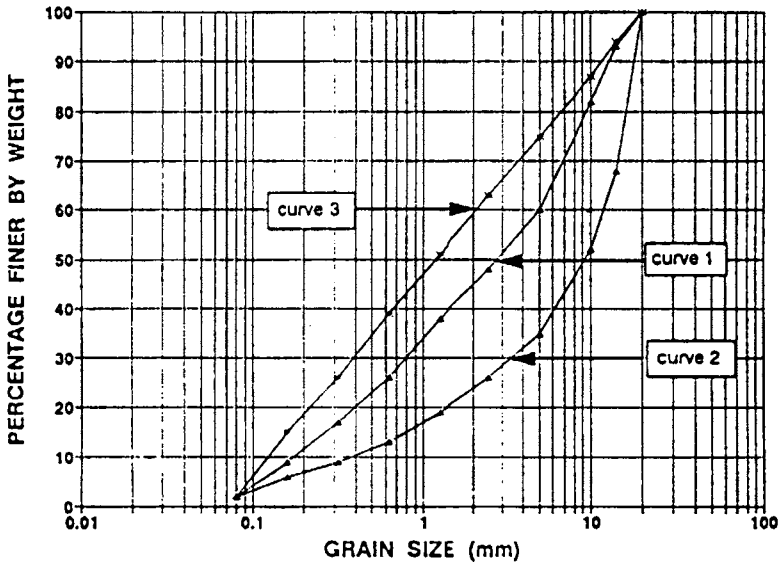

(Curves 1 and 3 – Stable; Curve 2 – Unstable)

Figure 3.21: Samples selected for seepage tests (Chapuis et al. 1996).

Foster and Fell (1999a, 2001) investigations are not directly related to the study of the internal instability of a soil. Their investigations, however, provide useful information to help assessing the likelihood of moving of fine soil particles through the voids of a coarser soil skeleton, as happens in the suffusion process.

3.2.4 Investigations on internal instability of cohesive soils by others

Sun (1989)

Unlike the investigations by others, Sun (1989) investigations were focused on cohesive clay-silt-sand mixtures rather than cohesionless sand-gravel mixtures. Sun (1989) carried out laboratory tests on 16 clayey/silty sands. The grain-size distribution curves of the 16 test samples are shown in Figure 3.22 and Figure 3.23. The test samples were 1" (25.4 mm) thick and 2.8" (71.1 mm) in diameter, and were tested in a pressurised flexible wall permeameter under an upward hydraulic gradient of 20. Figure 3.24 shows a schematic diagram of the test apparatus.

Sun's proposed method of assessing the internal stability of a soil involves splitting a soil into a coarse fraction (*c*) and a fine fraction (*f*) at any arbitrary point along its grain-

size distribution curve. At any arbitrary dividing point, *i*, represented by particle size, D_i, along the grain-size distribution curve, there corresponds a constriction size $D_{Ci} = 0.25 D_i$, and a characteristic size $d_{50i\,Fine}$ representing the d_{50} size of the fine fraction. The controlling constriction size, D_C^*, is defined as the D_{Ci} value at a particular dividing point, D_i, which maximises the ratio $D_{Ci}/d_{50i\,Fine}$. According to Sun, the internal stability of a clayey/silty sand depends on the parameters $D_C^*/d_{50\,Fine}^*$, and F_C^*, where F_C^* represents the fraction by weight finer than size D_C^*. A boundary separating the unstable soils and the stable soils was proposed as shown in Figure 3.25. The boundary corresponds to a hydraulic gradient of 20. According to Sun, the inclined section of the boundary would vary according to the hydraulic gradient, and would become less steep if the hydraulic gradient is less than 20.

The seepage tests by Sun (1989) were carried out under a very high hydraulic gradient of 20 to 1, which would not be experienced in embankment dam cores or their foundations. The very high gradients across the 25.4 mm thick test sample may well have cracked the sample, and the process involved may not be suffusion, but erosion along a crack.

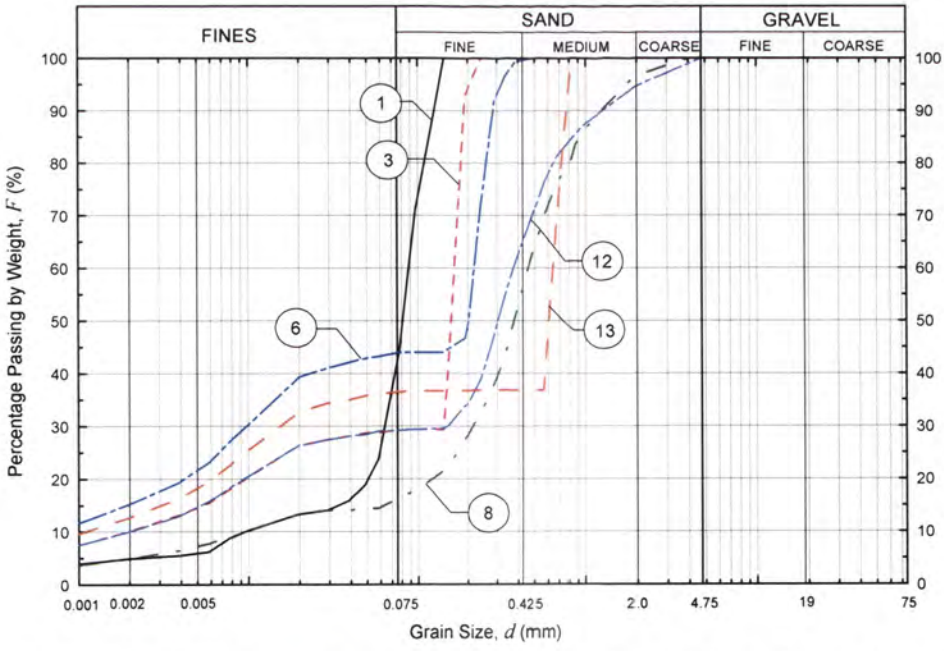

Figure 3.22: Soil samples tested to be internally stable by Sun (1989).

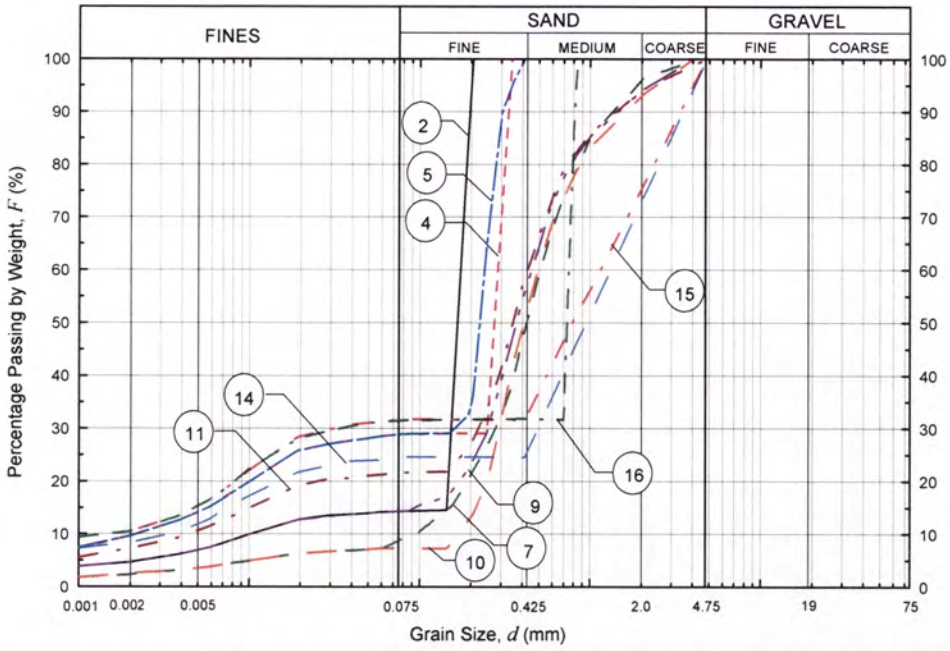

Figure 3.23: Soil samples tested to be internally unstable by Sun (1989).

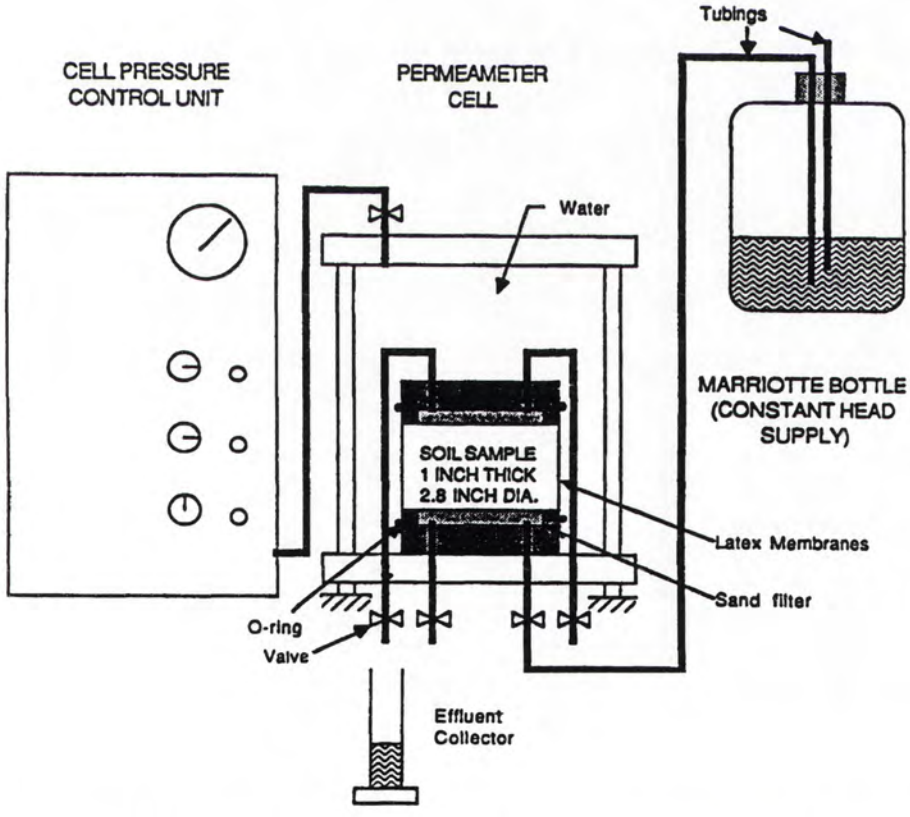

Figure 3.24: Schematic drawing showing setup of test equipment (Sun 1989).

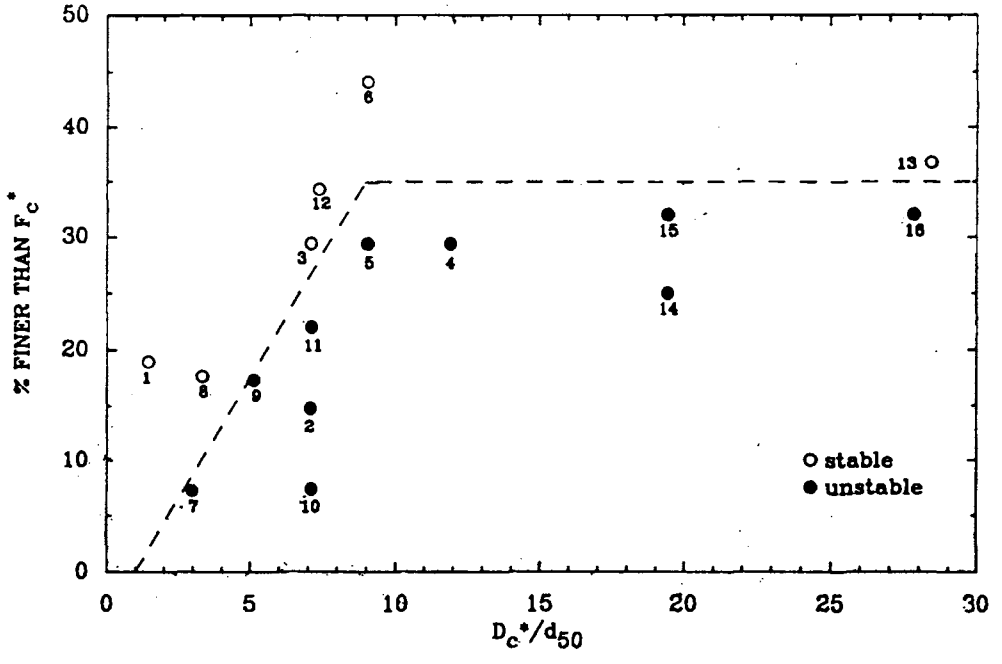

Figure 3.25: Assessment of internal stability (Sun 1989).

3.2.5 Investigations of soils which do not self filter

A few previous investigators considered an internally unstable soil as one which did not self filter. They divided a soil into a coarse fraction and a fine fraction, and applied empirical filter design rules to test the ability of the coarse fraction to filter the fine fraction of the soil.

Kézdi (1969)

Kézdi (1969) divided a soil into a coarse fraction (*c*) and a fine fraction (*f*) at one point along its grain-size distribution curve. He applied the rule for designing protective filter to the two fractions treating the fine fraction as the base, and the coarse fraction as the filter. That is:

$$\frac{D_{c15}}{D_{f85}} < 4 < \frac{D_{c15}}{D_{f15}} \qquad \text{Eqn 3.11}$$

The above rule for designing protective filter is generally credited to Terzaghi (1939), and was verified experimentally by Bertram (1940). Kézdi (1969) hypothesized that a soil which satisfied $D_{c15}/D_{f85} < 4$ at any arbitrary dividing point along its grain-size distribution curve would be self-filtering, and would therefore be internally stable.

The second part of equation 3.11, represented by $4 < D_{c15}/D_{f15}$, is a requirement to ensure adequate drainage capacity of a filter, and is irrelevant to the study of internal stability.

de Mello (1975)

de Mello (1975) briefly described a quantitative evaluation of skip-graded (gap-graded) materials. The proposed method is similar to Kézdi (1969) method, but the proposed filter criterion is $D_{c15}/D_{f85} < 5$, and is applied to gap-graded materials only. Figure 3.26 illustrates the splitting of the grain-size distribution curve of a gap-graded soil into a coarse fraction and a fine fraction.

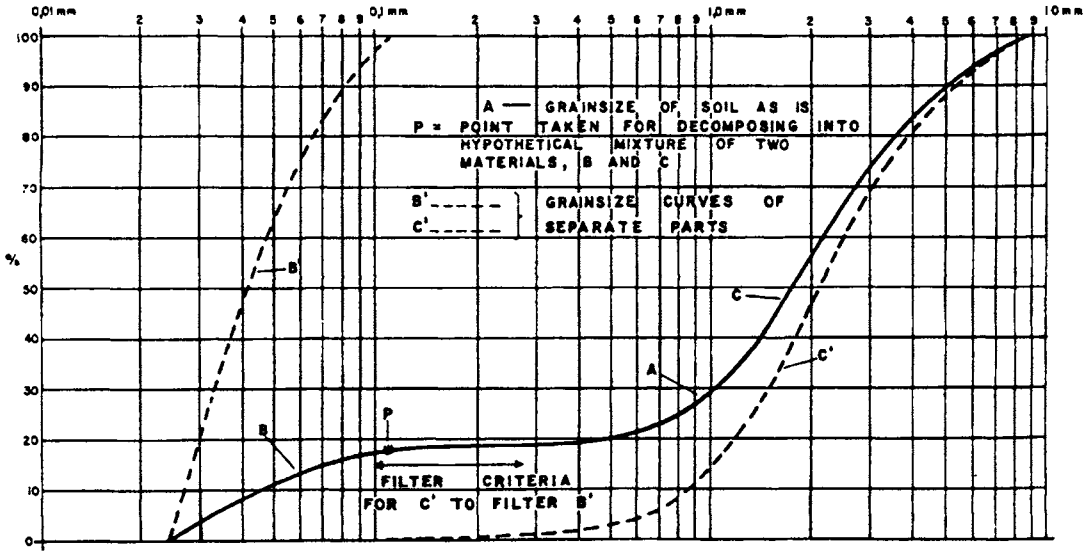

Figure 3.26: Simple test on grain size curve to check unacceptable skip-grading with respect to internal erosion (de Mello 1975).

Sherard (1979)

Sherard (1979) reported that, in his experiences, sinkholes occurred in dams comprised of remarkably similar cohesionless, coarse, broadly graded soils. He attributed this to the soils being internally unstable. For identifying potentially internally unstable soils, he proposed to split a soil into a coarse fraction and a fine fraction at any arbitrary point along its particle size distribution curve, and required that the filter criterion be satisfied at any arbitrary splitting point for a soil to be internally stable. Sherard's method is similar to the methods proposed by Kézdi (1969), and de Mello (1975). Application of the method was not limited to gap-graded soils. The proposed filter criterion is defined by $D_{c15} / D_{f85} < 4$ *to* 5.

3.2.6 Summary

The laboratory test methods used by previous investigators, and a brief description of the soils they tested for investigating the internal instability of a soil are summarised in Table 3.3.

These studies indicate that, for suffusion to occur, the following three criteria have to be satisfied:

Criterion 1: the size of the fine soil particles must be smaller than the size of the constrictions between the coarser particles, which form the primary fabric (i.e. the basic skeleton) of the soil, i.e. the soil is internally unstable;

Criterion 2: the amount of fine soil particles must be less than enough to fill the voids of the primary fabric (If there are more than enough fine soil particles for void filling, the coarser particles will be "floating" in the matrix of fine soil particles, so that a primary fabric comprises mainly of the coarser particles will not exist.);

Criterion 3: the velocity of flow through the soil matrix must be high enough to move the loose fine soil particles through the constrictions between the larger soil particles.

The first two criteria (so called geometrical criteria) are related to the grain-size distribution of a soil, whereas the third criterion (so called hydraulic criteria) is related to the hydraulic force causing movement of the fine soil particles.

Embankment dams having broadly-graded clay-silt-sand-gravel mixtures with cohesive or non-cohesive fines are not uncommon. For example, glacial and alluvial materials and many alluvial soils in dam foundations found in some USA, Swedish, Norwegian and New Zealand embankment dams are broadly-graded, and have significant fines content. The literature review, however, finds no previous attempt to test the internal stability of soils with silt or clay content. Most of the proposed criteria, as introduced in Section 3.2.3 above, for assessing the internal stability of a soil were based on laboratory tests on cohesionless sand-gravel mixtures (e.g. U.S. Army Corps of Engineers (1953), Kenney & Lau (1984, 1985, 1986), Burenkova (1993), Chapuis et al. (1996)). These criteria may not be applicable to broadly-graded silt-sand-gravel mixtures or materials with significant fines content.

Other proposed criteria (e.g. de Mello (1975), Sherard (1979)) are related to self filtering, are purely empirical, and have not been verified as being able to determine if a soil is subject to suffusion by soil tests. These empirical methods are easy to apply, and may successfully identify some potentially internally unstable coarse broadly-graded soils and more particularly gap-graded soils. The validity of these criteria when applied to materials with silty fines is, however, questionable. In addition, soils that are assessed to be not self filter using empirical filter design rules are not necessarily internally unstable within the definition of internal instability used in this thesis. This is due to two main reasons:

i. Most filter rules are conservatives, and a set of filter rules may not apply to all types of soils.

Table 3.3: Summary of investigations on internal instability of soils by others.

Investigators	Method Proposed for Prediction of Internal Instability		Type of Test	Information on Test Samples		
	"Y"es/ "N"o	"Empirical" or Based on Laboratory "Testing"		Description	Particle sizes (mm)	Gradings
Fuller and Thompson (1907)	Y (for prediction of maximum aggregate density)	Testing	Test on density of a mixture of cement and aggregates.	Cement, fine and coarse aggregates.		Not available
U.S. Army Corps of Engineers (1953)	Y	Testing	Downflow seepage test with vibrational forces.	Granular filters.		Not available
Istomina (1957)	Y	Unknown				
Lubochkov (1962, 1965)	Y	Testing	Unkown	Not available		Not available
Kenney, Lau and Clute (1983)	N	Testing	Downward seepage test with vibrational forces (235mm-dia. seepage cell).	Linear and non-linearly graded granular filter materials. (1)	0.2 - 38	Available (15 gradings)
Kenney, Lau and Clute (1984)	N	Testing	Downward seepage test with vibrational forces (235mm-dia. seepage cell).	Narrowly-graded mixtures of uniform medium sand and uniform gravel.	0.3 - 4.75	Available (3 gradings)
Kenney and Lau (1984, 1985, 1986)	Y	Testing	Dry vibration, and downward seepage test (245mm-dia. and 580mm-dia.).	Granular materials. (1)	0.06 - 100	Available (14 gradings)
Lafleur, Mlynarek and Rollin (1989, 1993)	N	Testing	Downward seepage test without bottom filter (197mm-dia. seepage cell).	Mixture of ballotini beads of 14 different sizes.	0.1 - 25	Available (3 gradings)
Sun (1989)	Y	Testing	Upward seepage test (flexible wall permeameter of 71mm-dia.).	Clayey, silty sand.	< 4.75	Available (16 gradings)
Burenkova (1993)	Y	Testing	Dry mixing test, and downward and upward flow seepage test.	22 granular materials.	60 - 100	Available (8 gradings)
Skempton and Brogan (1994)	N	Testing	Upward seepage test (140mm-dia. seepage cell).	Sand-gravel mixtures.	0.06 - 10	Available (4 gradings)
Chapuis et al. (1996)	N	Testing	Downflow rigid-wall permeameter.	Crushed limestone, and crushed natural gravel.	0.075 - 20	Available (3 gradings)

Note : (1) Test results on stable soil samples 20 & 20A, 21 & 21A, 23, and unstable soil sample D were presented in both Kenney, Lau & Clute (1983) and in Kenney & Lau (1984, 85, 86).

ii. One of the essential conditions for internal instability to occur in a soil is that the amount of fine soil particles must be less than enough to fill the voids of the primary fabric formed by the coarse particles of the soil (i.e. geometrical criterion 2 described at the start of this Section). This requirement is not considered in the splitting of a soil into a fine fraction and a coarse fraction when a self filtering rule is applied.

Unlike many other investigators who studied the geometrical criteria governing internal instability, Skempton and Brogan (1994) investigated the hydraulic criteria for the erosion of fine particles in an internally unstable soil. Their findings, however, were based on testing only a few sand-gravel mixtures.

Most previous investigators had ignored the effect of compaction and density on the internal stability of a soil.

The Sun (1989) method is the only method found in the literature for predicting the internally stability of cohesive clay-silt-sand mixtures. The seepage tests by Sun (1989) were carried out under a very high hydraulic gradient of 20 to 1, which would not be experienced in embankment dam cores or their foundations. The very high gradients across the 25.4 mm thick test sample may well have cracked the sample, and the process involved may not be suffusion, but erosion along a crack.

The study of filter behaviour and the study of the internal instability of a soil are closely related as both involve understanding the mechanism by which finer soil particles are moved through the constrictions within a matrix of coarser soil particles. The study of filter behaviour by Kenney et al. (1983, 1985), Lafleur et al. (1993), and Foster and Fell (1999a, 2001) helps understanding the movement of finer soil particles through the constrictions within a soil matrix.

3.3 EXPERIMENTAL INVESTIGATION OF INTERNAL INSTABILITY OF SOILS AT UNSW

3.3.1 Objective of experimental investigation

As described in Section 3.1, the objectives of the experimental investigations are three-fold, namely

i. to investigate the factors which affect the internal stability of soils;
ii. to investigate the validity of applying currently available methods in assessing the internal stability of silt-sand-gravel or clay-silt-sand-gravel mixtures, and to propose appropriate methods for assessing the internal stability of these soils; and
iii. to study the hydraulic conditions at which erosion of fine particles from within the coarse soil matrix occurs in an internally unstable soil.

Two series of laboratory tests, namely the downward flow (DF) seepage test and the upward flow (UF) seepage test, have been carried out. The DF test was used to find out whether or not a soil sample is internally unstable, whereas the UF was carried out to identify the vertical hydraulic gradient across a soil sample at which internal erosion of finer soil particles was observed. Two different levels of vertical hydraulic gradients were observed. The first level corresponds to the onset of erosion of fine particles indicated by the cloudiness of the flow and movement of finer particles within the soil as detected by changes in the particle size distribution. The second level corresponds to more severe erosion indicated by the rapid increase in flow rate and the "boiling" phenomenon. At this stage the process is no longer one of suffusion alone.

3.3.2 Downward flow (DF) seepage test

Overview

In the DF test, a test sample is exposed to a high constant seepage gradient inside a seepage cell. If the test sample is internally unstable, selective erosion of the finer

particles of the test sample is expected to happen, resulting in a change in the grain-size distribution of the test sample after the test. If the test sample is stable, selective erosion of the finer particles of the test sample will not take place, and the grain-size distribution of the test sample will remain unchanged after the test.

The DF test is carried out on a soil sample until the measured flow rate, and the pressures inside the soil sample become steady, and the colour of the effluent becomes clear, indicating that erosion, if any, has completed.

Apparatus

The main apparatus of the DF test comprises a cylindrical aluminium seepage cell of 300-mm internal diameter containing the soil sample to be tested. Water is supplied from a constant head tank located approximately 2.5 m above the seepage cell. The seepage cell is placed inside a transparent overflow tank which serves to maintain a constant water head at the downstream side of the apparatus. With this arrangement, an average seepage gradient, $i \approx 8$ is maintained across the 300 mm thick soil sample. The seepage gradient within the test sample, however, varies throughout the depth of the sample during the test. Higher seepage gradient can be achieved by raising the constant head water supply tank to a higher level. Water pressures within the soil sample are measured by four piezometers embedded at different depths of the soil sample. The pressures measured by the piezometers are recorded automatically in a digital computer at regular time intervals through the use of pressure transducers connected to the piezometers, and an electronic data logger. The tips of the piezometers are set at 100 mm, 150 mm, 200 mm and 250 mm from the top face of the test sample. The overflow chute at the lower tank facilitates measurement of the rate of flow through the system. The 25 mm single-sized aggregates on top of the 300 mm thick soil samples serve to break up the incoming flow so as to ensure more uniform water pressure on the upper surface of the soil sample. The drainage layer at the bottom of the seepage cell is made up of 20 mm single-sized aggregates. The equivalent opening size of the drainage layer is between 2 mm to 5 mm (i.e. $D_{15}/9$ to $D_{15}/4$, where D_{15} is 20 mm). These equivalent opening sizes are considered large enough to allow passage of fine soil particles washed out of an internally unstable test sample during the downflow seepage test. Previous investigators showed that the erodible fine fraction of an internally

unstable soil would not comprise more than 30% by weight of the soil. The D_{30} of most of the test samples were finer than 2 mm, which is smaller than the equivalent opening size of the bottom drainage layer. A few gap-graded test samples, for examples samples 9, 10, 13, 14A, and 15, whose grain-size distribution curves are shown in Figure 3.32 and Figure 3.33, have D_{30} as large as 6 mm, but the majority of the fine soil particles in these gap-graded samples were finer than 2 mm. Some coarse soil samples, e.g. A2, A3, B1, B2 and C1, whose grain-size distribution curves are shown in Figure 3.34, have D_{30} between 8 to 15 mm. Test results indicated that selective erosion of fine particles from these samples did not appear to have been significantly affected by clogging of the bottom drainage layer. The bottom drainage layer has to support the weight of the soil sample and the water load. Aggregates coarser than 20 mm have not been used in the bottom drainage layer to avoid excessive collapse of the lower part of a test sample into the voids of the drainage layer under the water load. The bottom drainage layer is, however, sufficiently fine to act as a filter to the soils tested based on Sherard and Dunnigan (1989) filter criteria provided the soils are internally stable.

A schematic diagram and a photograph of the DF test apparatus are shown in Figure 3.27 and Figure 3.28, respectively.

Soil particle density, Atterberg limits and compaction properties of soils tested

Soil particle density and Atterberg limit tests were carried out on the soil samples according to relevant Australian Standards.

Standard compaction tests were carried out on each of the soil samples to obtain information on standard maximum dry density and optimum water content. This information was essential for controlling the dry density and the moulding water content of the test specimens.

Moulding water content and dry density of test specimens

Test samples were prepared at the standard optimum water content (*OWC*). To achieve the desired moulding water content, the appropriate amount of water was added to the soil sample, which was then cured for at least two days before a test sample was

prepared. Water content tests were carried out on surplus soil trimmed from the compaction mould so as to find out the actual moulding water content of the test sample.

Test samples were prepared at either 90% or 95% of the standard maximum dry density of the soil sample. The dry density of a test sample was controlled by adjusting the total mass of soil of the specified moulding water content to be used for forming the compacted test sample. The 300 mm thick test sample was compacted in 5 layers using a tamping rod. For each layer, a known amount of soil was compacted to a pre-calculated thickness corresponding to the desired dry density. Finally, the mass and the water content of the completed test sample were measured so as to calculate the actual dry density of the sample.

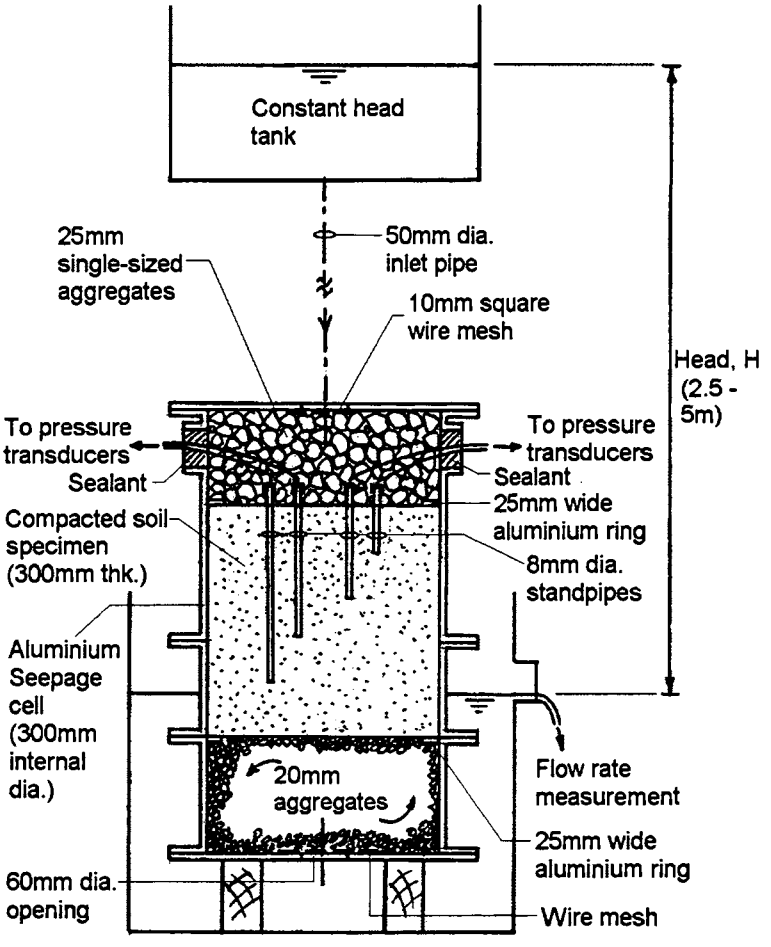

Figure 3.27: Schematic diagram of the downward flow seepage test assembly.

Figure 3.28: Downward flow seepage test apparatus.

Monitoring of hydraulic gradient and flow rate

All of the DF tests were carried out with an upstream water head of 2.5 m. This head corresponded to a hydraulic gradient of about 8 across the 300 mm thick compacted soil sample. As the test proceeded, water pressure at 4 different depths of the test samples was automatically recorded by piezometers connected to pressure transducers and electronic data-loggers. The tips of the piezometers were positioned at 100 mm, 150 mm, 200 mm and 250 mm below the top face of the test sample. The piezometers were intended to provide information on the pressure distribution across the depth of the test sample and to serve as an indicator of whether or not erosion had completed and a steady condition had been reached. Plots of total head versus time are presented in Appendix N. Total head is the pressure head plus the datum head. The pressure head, in metre, is computed from the pressure recorded by the piezometers, and the datum head is taken as the height, also in metre, of the piezometer tip above the bottom face of

the test sample, assuming the zero datum is at the bottom face of the test sample. A review of the piezometer data for some downflow seepage tests, for example tests DF1, DF5, DF9, indicated that the piezometers readings were sometimes erratic. For example, the recorded pressure for DF1 was approximately 48 kN/m^2, which was too high and inconsistent with a water head of 2.5 m. In some other tests, the total head at a higher piezometer was lower than the total head at a lower piezometer. This might be due to the formation of a preferential flow path along the piezometer tube of the higher piezometer which caused a significant reduction in the pressure head at the higher piezometer. In view of the inconsistencies in the piezometer readings in some DF tests, the piezometer readings have not been used for analysing the pressure distribution across the depth of a test sample.

The rate of water flow through the test sample was estimated at regular time intervals by measuring the volume of effluent collected from the overflow chute of the lower tank within a specified period of time (e.g. 20 seconds).

Colour of the flow

The colour of the effluent provided an indication of whether or not erosion was taking place, and was recorded during the test. No attempt was made to measure the sizes and amount of soil particles in the effluent, as erosion of the soil sample can be detected by post-test grain-size distribution analysis of the soil sample, and it is very time consuming to collect, dry and carry out particle size distribution analysis of the eroded soil given the large quantities of water flowing through the sample.

Grain-size distribution analysis

All soil samples, except sample "RD" which was a naturally occurring soil, were formed by blending silt, sand and gravel. Some tests were carried out on samples of clay-silt-sand-gravel mixtures. Grain-size distribution analysis was carried out on each of the blended samples to ensure that the desired grain-size distribution was achieved before the samples were tested.

After a DF test, the soil sample was carefully taken out from the seepage cell, and grain-size distribution analyses were carried out on sub-samples taken from 4, 5 or 6 different

depths of the soil sample to study the effect of internal erosion on the grain-size distribution of the soil sample. The depths below the top surface for obtaining sub-samples for post test grain-size distribution analysis are as follows:

Number of sub-samples	Sampling depths (mm)
4	0 – 75, 75 – 150, 150 – 225, 225 – 300.
5	0 – 60, 60 – 120, 120 – 180, 180 – 240. 240 – 300.
6	0 – 50, 50 – 100, 100 – 150, 150 – 200, 200 – 250, 250 – 300.

3.3.3 Upward flow (UF) seepage test

Overview

During an UF test, the hydraulic gradient across a test sample is gradually increased by raising slowly in steps the level of the upstream water supply tank. Signs of erosion of the test sample are observed as the hydraulic gradient across the test sample increases. For some test samples, a point may be reached when the hydraulic gradient is high enough to cause instability of the soil, as indicated by the "boiling" phenomenon. Internally unstable soils are expected to show signs of erosion and instability at relatively lower hydraulic gradients than stable soils.

Apparatus

The apparatus of the UF test is similar in design to that of the DF test. The main difference is that the direction of water flow in the UF test is from the bottom upward. The upper end of the seepage cell is left open to allow for the observation of the erosion process. The water tank supplying water to the system can be raised or lowered so as to control the seepage gradient across the 250 mm thick soil sample. The thickness of the soil sample in the UF test is 50 mm thinner than that in the DF test so as to reduce the likely arching effect due to restraints by the sides of the seepage cell. A thinner soil sample also implies that the apparatus can apply a higher hydraulic gradient across the

thickness of the sample. An overflow pipe fitted at the top part of the seepage cell allows for measurement of the rate of flow through the system.

The UF test on a test sample is continued until instability is observed in the test sample, or until the highest achievable hydraulic gradient is applied if instability does not occur.

A schematic diagram and a photograph of the UF test apparatus are shown in Figure 3.29 and Figure 3.30, respectively.

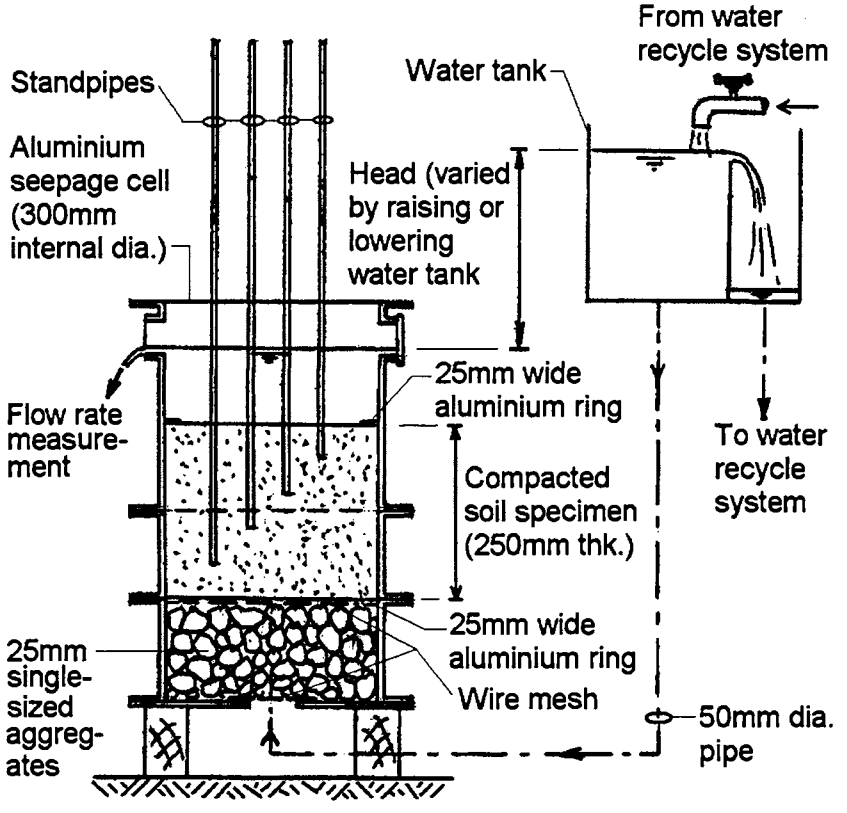

Figure 3.29: Schematic diagram of the upward flow seepage test assembly.

Sample preparation and measurement and control of test variables in the UF Test

The method for the control of the moulding water content and density of the test sample for the UF test is similar to that for the DF test.

In the UF test, water pressures within the test specimen were recorded manually by reading the heights of the water columns in the plastic standpipes. The pressure head within the test sample is measured by 4 standpipes whose tips are located at 50 mm, 100 mm, 150 mm, and 200 mm below the upper surface of the test specimen. The rate of water flow through the test sample was estimated at regular time intervals by measuring the volume of effluent collected from the overflow pipe near the top of the seepage cell within a specified period of time (e.g. 20 seconds). Colour of the effluent and signs of erosion are also recorded during an UF test.

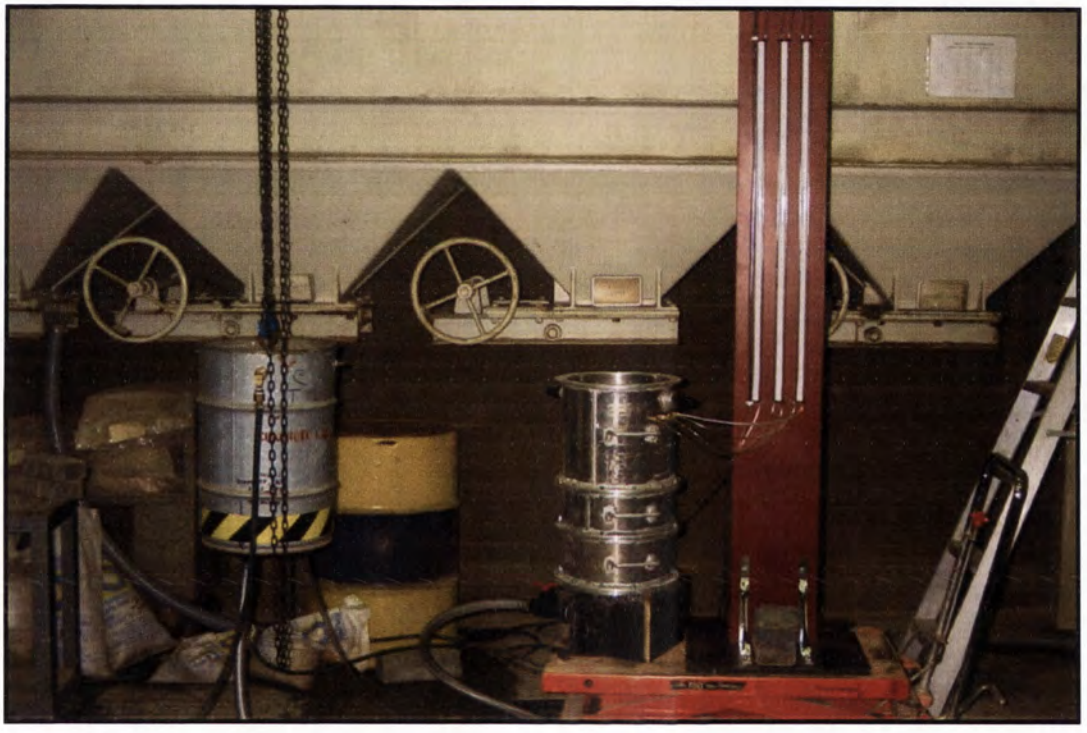

Figure 3.30: Upward flow seepage test apparatus.

3.3.4 Properties of soil samples

Origin of soil samples

Table 3.4 shows a test schedule consisting of 24 DF tests and 18 UF tests intended to test the effects of the fines content, the plasticity of the fines, gap-grading and soil density on internal stability. A total of 20 soil samples were included in the test

schedule. 19 out of the 20 soil samples were formed by blending clay (kaolin), silt (silica), fine to medium sand (Nepean Sand), coarse sand (5 mm Blue Metal), fine gravel (10 mm Basalt and 20 mm Blue Metal), and coarse gravel (25 to 75 mm Pukaki) to achieve the desired fines content, grading, and plasticity of the fines. Nepean Sand is a river sand obtained from the western part of Sydney. The Blue Metal aggregates are crushed basaltic rock. The 25 to 75 mm Pukaki is the over-sized rounded particles of a glacial till obtained near Pukaki Dam in New Zealand.

Table 3.4: Schedule of DF tests and UF tests.

Test sample	Approximate fines content of sample (%)	Sample with plastic fines (Kaolin) "Y" or "N"	Sample gap-graded "Y" or "N"	Compaction (as % of standard max. dry density)	Seepage Tests	
					Downward flow	Upward flow
1, 1A	10	N	N	95%	DF1	UF1
				90%	DF5	UF2
2R	20	N	N	95%	DF2R	UF3
3R	40	N	N	95%	DF3R	UF4
4R	5	N	N	95%	DF4	UF5
5	10	Y	N	95%	DF13	UF13
				90%	DF14	DF14
6	20	Y	N	95%	DF10	UF10
7	40	Y	N	95%	DF16	UF16
9	10	N	Y	95%	DF6	UF6
10	20	N	Y	95%	DF7	UF7
				90%	DF8	UF8
11	40	N	Y	95%	DF9	UF9
13	10	Y	Y	95%	DF11	UF11
14A	20	Y	Y	95%	DF12	UF12
				90%	DF15	UF15
15	40	Y	Y	95%	DF17	UF17
RD	Natural soil			95%	DF18	UF18
A2	Well-graded gravels with fines content < 15%	N	N	95%	DF24	
A3				95%	DF23	
B1				95%	DF22	
B2				95%	DF21	
C1				95%	DF20	
D1				95%	DF25	

Note : All test samples were prepared at optimum water content.

The remaining soil sample (abbreviated "RD") is a glacial till taken from Tasmania, and with particles larger than 9.5mm removed.

The grain-size distribution curves of the materials used for blending for the test samples are shown in Figure 3.31. Table 3.5 shows the mix proportions for the various blended

test samples, and Table 3.6 summarises the grading characteristics of the test samples. Figure 3.32, Figure 3.33 and Figure 3.34 show the grain-size distribution curves of the twenty test samples.

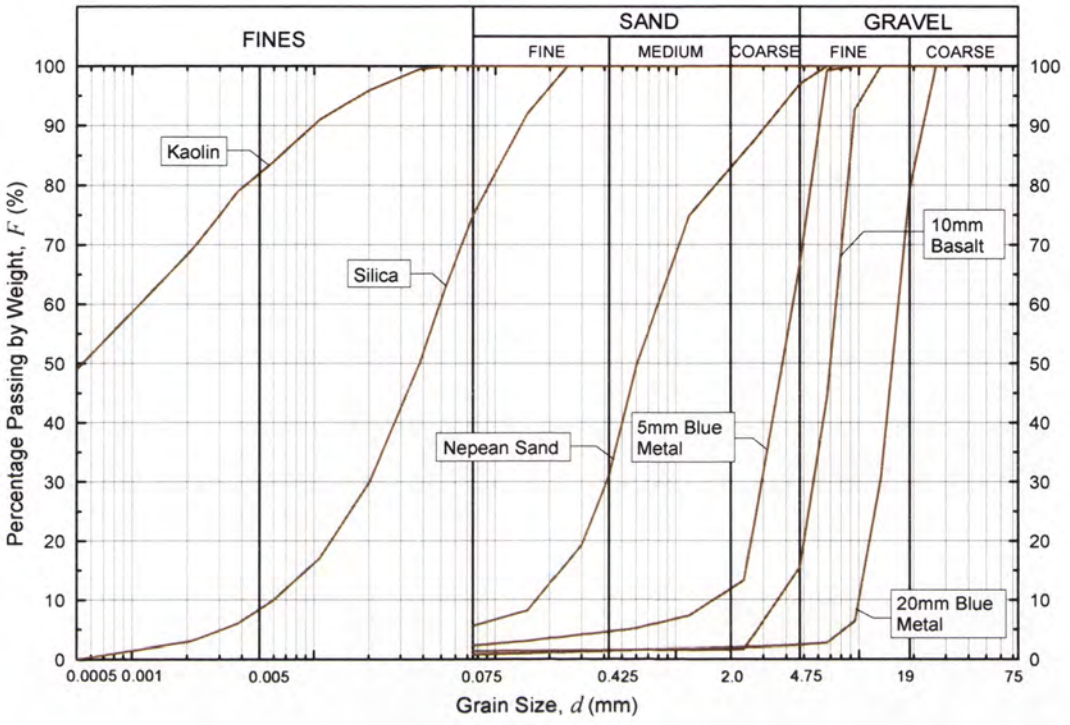

Figure 3.31: Grain-size distribution curves of the materials used for blending for the test samples.

Soil plasticity

Blended soil samples, namely samples 5, 6, 7, 13, 14A and 15, which contain kaolin, were tested to be slightly plastic. The Liquid Limits and Plasticity Indices of these samples are in the range of 23 to 30% and 9 to 13%, respectively. Soil sample "RD", and other blended soil samples without kaolin were tested to be non-plastic.

Table 3.5: Mix proportions for test samples in downward flow tests and upward flow tests.

Mix Sample	Mix Proportions of Ingredients (%)									Grain-size distribution curve	Seepage Tests	
	Kaolin	Silica	Nepean Sand	5mm Blue Metal	10mm Basalt	20mm Blue Metal	Rounded gravel from "Pukaki"				Downflow	Upflow
							25-38mm	38-51mm	51-76mm			
1		10.52	25.70	16.18	23.80	23.80				Fig. 3.32	DF1	UF1, UF2
1A		10.52	25.70	16.18	23.80	23.80				Fig. 3.32	DF5	
2R		24.01	24.01	18.01	18.01	15.96				Fig. 3.32	DF2R	UF3
3R		50.90	28.28	6.11	9.05	5.66				Fig. 3.32	DF3R	UF4
4R		3.23	27.42	32.26	24.19	12.90				Fig. 3.32	DF4	UF5
5	5.88	1.18	41.20	34.73	11.77	5.24				Fig. 3.33	DF13, DF14	UF13, UF14
6	11.18	8.20	34.16	27.33	12.30	6.83				Fig. 3.33	DF10	UF10
7	21.75	21.84	24.12	18.99	8.55	4.75				Fig. 3.33	DF16	UF16
9		11.92	0.00	9.54	60.67	17.87				Fig. 3.33	DF6	UF6
10		25.67	0.00	0.00	54.59	19.74				Fig. 3.33	DF7, DF8	UF7, UF8
11		52.87	0.00	0.00	26.43	20.70				Fig. 3.33	DF9	UF9
13	5.51	4.54	0.00	9.74	61.95	18.26				Fig. 3.33	DF11	UF11
14A	10.89	11.09	0.00	0.00	57.30	20.72				Fig. 3.33	DF12, DF15	UF12, UF15
15	21.49	24.11	30.50	23.90	0.00	0.00				Fig. 3.33	DF17	UF17
RD	N/A	N/A	N/A	N/A	N/A	N/A	N/A	N/A	N/A	Fig. 3.32	DF18	UF18
A2		18.70	6.08	6.08	6.08	12.15	23.88	10.03	17.01	Fig. 3.34	DF24	
A3		9.45	9.45	9.45	6.30	12.60	24.74	10.39	17.63	Fig. 3.34	DF23	
B1		13.07	11.53	11.53	11.53	11.53	12.73	11.06	17.05	Fig. 3.34	DF22	
B2		13.42	12.59	6.99	3.50	6.99	14.55	20.98	20.98	Fig. 3.34	DF21	
C1		6.91	9.60	3.84	3.84	31.82	12.80	15.18	16.01	Fig. 3.34	DF20	
D1		11.36	11.36	11.36	11.36	11.36	14.77	11.36	17.05	Fig. 3.34	DF25	

Note: 1. RD is a glacial till sample taken from Tasmania, and with particles larger than 9.5mm removed.
2. Samples for tests DF5, DF8, DF14, DF15, UF2, UF8, UF14, and UF15 were compacted to 90% standard maximum dry density. Samples for all other tests were compacted at 95% standard maximum dry density.

Table 3.6: Grading characteristics of the test samples.

Test sample (See Note 1)	Fines Content (<0.075mm) (%)	Sand Fraction (0.075 - 4.75mm) (%)	Gravel Fraction (> 4.75mm) (%)	Percentage of Kaolin (%)	Presence of Plastic Fines "Yes/No"	Gap-graded (See Note 2) "Yes/No"	Soil Classification (USCS)	(See Note 3)			(See Note 3)	
								d_{10} (mm)	d_{30} (mm)	d_{60} (mm)	Coefficient of Uniformity $C_U = d_{60}/d_{10}$	Coefficient of Curvature $C_C = d_{30}^2/(d_{60}*d_{10})$
1 & 1A	14.6	35.1	50.3	0	N	N	GM	0.057	0.772	6.152	108	1.7
2R	21.0	32.5	46.5	0	N	N	GM	0.028	0.376	5.487	194	0.9
3R	42.3	37.6	20.1	0	N	N	SM	0.012	0.046	0.475	39	0.4
4R	4.9	45.1	50.0	0	N	N	GW	0.258	1.841	5.420	21	2.4
5	9.8	49.7	40.5	5.9	Y	N	SW, SC	0.082	0.682	4.787	58	1.2
6	21.4	50.5	28.1	11.2	Y	N	SC	0.004	0.323	2.833	734	9.5
7	41.3	34.3	24.4	21.8	Y	N	SC	0.001	0.027	0.937	1789	1.5
9	11.2	12.4	76.4	0	N	Y	GP, GM	0.066	5.150	7.561	115	53
10	24.3	12.0	63.7	0	N	Y	GM	0.022	2.407	6.611	304	40
11	44.4	11.8	43.8	0	N	Y	GM	0.011	0.039	5.307	493	0.03
13	10.9	13.0	76.1	5.5	Y	Y	GP, GC	0.065	5.089	7.182	111	56
14A	18.9	6.1	75.0	10.9	Y	Y	GC	0.007	5.177	8.384	1186	452
15	33.1	7.2	59.7	21.5	Y	Y	GC	0.001	0.063	7.765	5709	0.4
RD	21.7	77.9	0.4	0	N	N	SM	0.006	0.129	0.313	53	9.0
A2	14.2	11.2	74.6	0	N	N	GM	0.042	6.529	33.047	793	31.0
A3	8.5	15.6	75.9	0	N	N	GP, GM	0.132	6.096	31.684	241	8.9
B1	13.4	23.6	63.0	0	N	N	GM	0.054	2.954	15.486	285	10.4
B2	12.8	20.6	66.6	0	N	N	GM	0.062	3.572	36.363	583	5.6
C1	7.4	15.7	76.8	0	N	N	GP, GM	0.229	8.258	25.454	111	11.7
D1	12.3	25.8	61.9	0	N	N	GM	0.042	2.794	11.456	273	16.3

Notes :

1. Samples 1 and 1A have the same compositions but mixed in different batches.
2. A gap-graded soil is one which is deficient of materials in a particular particle size range. Gap-graded samples 9, 10, 13, 14A and 15 are deficient in fine to medium sand (sizes between 0.075 - 2.0mm). Gap-graded sample 11 is deficient in medium to coase sand (sizes between 0.425 - 4.75mm).
3. d_X represents the "X% finer" particle size. In other words, X% by weight of the soil's particles are finer than d_X.

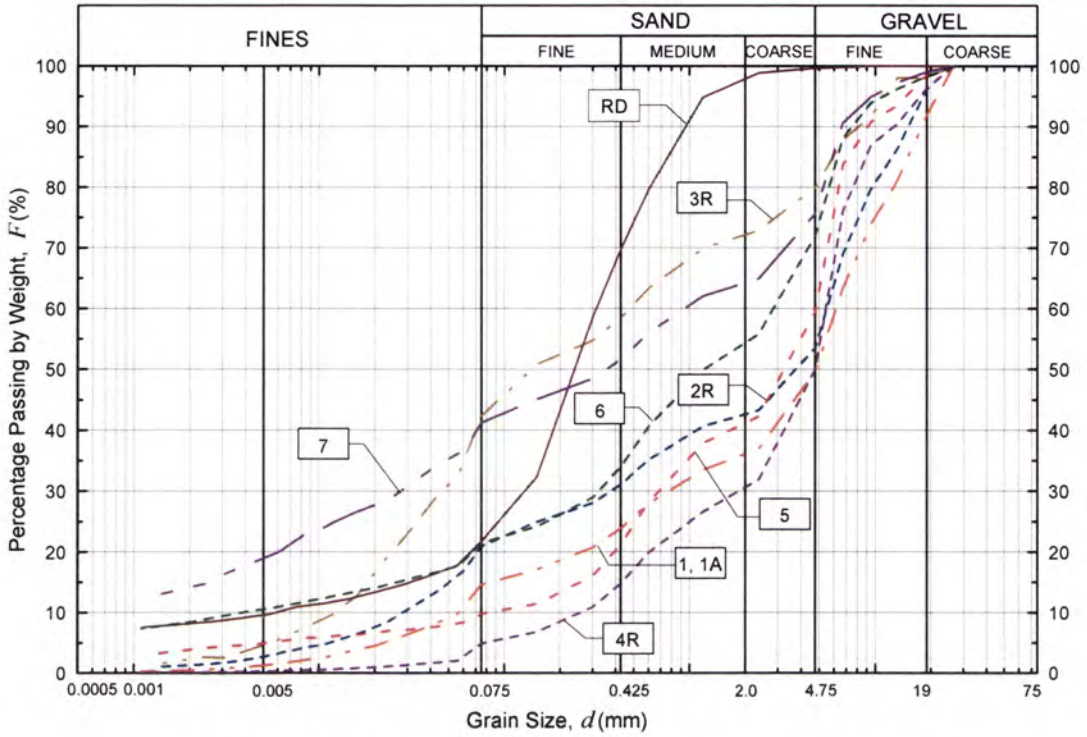

Figure 3.32: Grain-size distribution curves of sample "RD" and well-graded samples of silt-sand-fine gravel mixtures or clay-silt-sand-fine gravel mixtures.

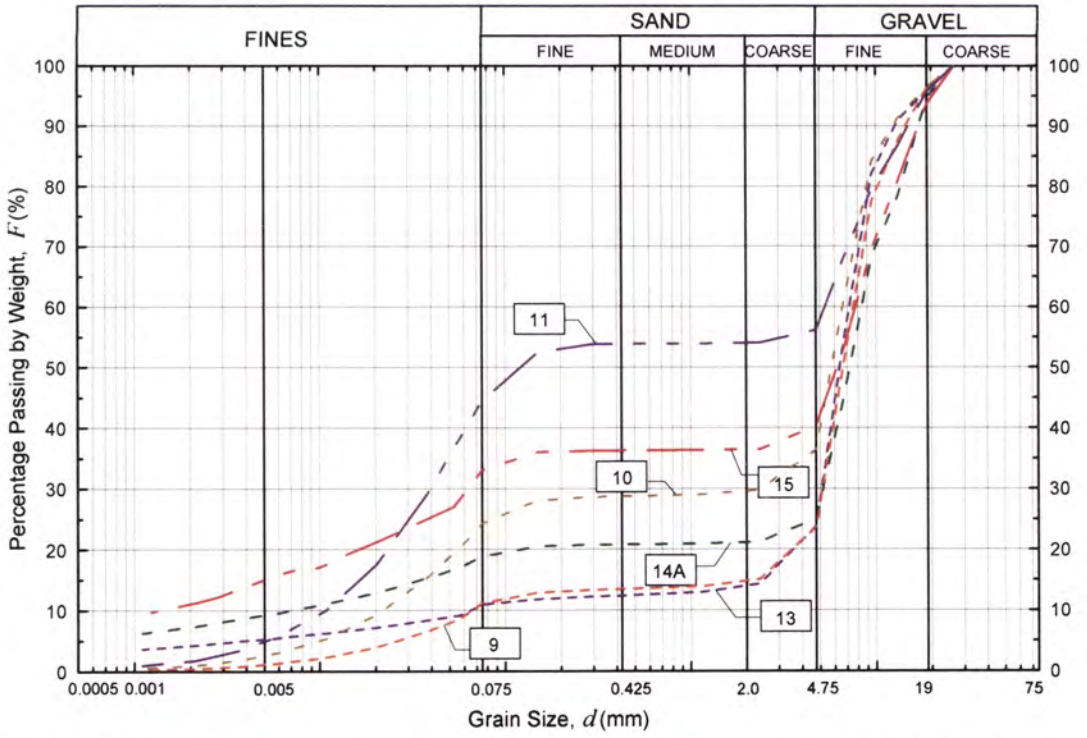

Figure 3.33: Grain-size distribution curves of gap-graded test samples made of silt-sand-fine gravel or clay-silt-sand-fine gravel mixtures.

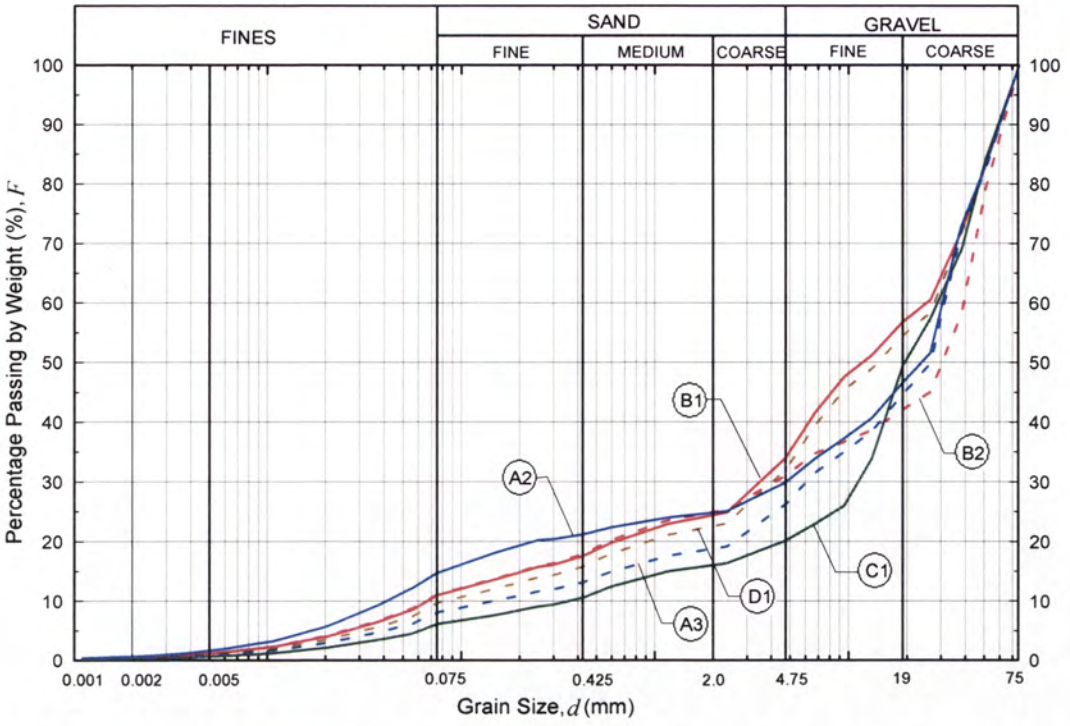

Figure 3.34: Grain-size distribution curves of test samples made of silt-sand-coarse gravel mixtures.

Soil particle density

The soil particle densities of the various materials are summarised in Table 3.7.

Table 3.7: Summary of soil particle densities.

Components	Soil particle density (g/cm^3)
Kaolin	2.58
Silica	2.63
Nepean Sand	2.53
5mm Blue Metal	2.55
10mm Basalt	2.71
20mm Blue Metal	2.70
Rounded gravel from "Pukaki"	2.69
RD	2.82

The above particle densities were used for calculating the average particle densities of the test samples using equation 3.1.

$$G_{s\_avg} = \frac{1}{\sum \frac{f_i}{G_{s\_i}}} \qquad \text{Eqn 3.12}$$

where G_{s_avg}: is the average particle density of a test sample;

f_i: is the proportion by weight of a particular component (e.g. Silica) of the test sample. $\sum f_i = 1$;

G_{s_i}: is the particle density of a particular component as given in Table 3.7.

Standard compaction test

Results of standard compaction tests on the 20 soil samples are summarised in Table 3.8. This information was required for controlling the densities and water contents of the test samples.

3.3.5 Interpretation of test data

DF test

The main purpose of the DF test is to find out if the finer particles of the soil sample are washed out from the sample by the process of suffusion. Any loss of materials will be indicated by a change in the grain-size distribution of the soil. This can be detected by carrying out post-test grain-size distribution analysis on samples taken from different depths of the sample. Figure 3.35 shows the results of post-test grain-size distribution analysis on Sample 10. The obvious shifts in the post-test grain-size distribution curves from the initial curve indicate that the soil sample is internally unstable. Tests which showed only minor changes in post-test grain-size distribution within the accuracy of testing (e.g. curves 2 – 6 in Test 1, Appendix N) or only in the upper layer (e.g. curve 7 in Test 1) were considered non-suffusive.

Results of post-test grain-size distribution analysis on all DF test samples can be found at Appendix N.

Table 3.8: Results of standard compaction tests.

Soil sample	Standard maximum dry density, $\rho_{d\max}$ (t/m^3)	Standard optimum water content, *OWC* (%)
1	2.32	7.5
2R	2.18	9.0
3R	1.97	11.5
4R	2.23	9.5
5	2.12	8.5
6	2.23	7.0
7	2.05	10.0
9	1.94	6.5
10	2.22	8.5
11	1.91	12.0
13	1.92	7.0
14A	2.04	11.0
15	2.09	8.0
RD	1.87	13.5
A2	2.43	6.0
A3	2.41	5.0
B1	2.35	5.5
B2	2.36	5.5
C1	2.34	4.5
D1	2.36	7.0

A graphical technique proposed by Kenney & Lau (1985, 86) can be used to assess the approximate size of the largest particles eroded by the suffusion process, and the approximate fraction of materials eroded by the process. The technique involves extending the initial grain-size distribution curve of the test sample to match the grain-size distribution curve of the same sample after the DF test. Figure 3.36 shows the application of the curve matching technique to DF test no. 8 on Sample 10. By extending the vertical scale of the initial grain-size distribution curve, the initial curve is shifted downward until the coarse part of the curve matches the coarse part of the post-

test grain-size distribution curve. The point at which the matching ends represents the size of the largest particles erodible by suffusion. The fraction of materials loss can be calculated from the amount of shifting of the initial grain-size distribution curve. Figure 3.36 shows that the size of the largest particles erodible by suffusion is in the range of 0.15 to 0.26 mm, whereas the fraction of materials loss is in the range of 5.4 to 17.1%.

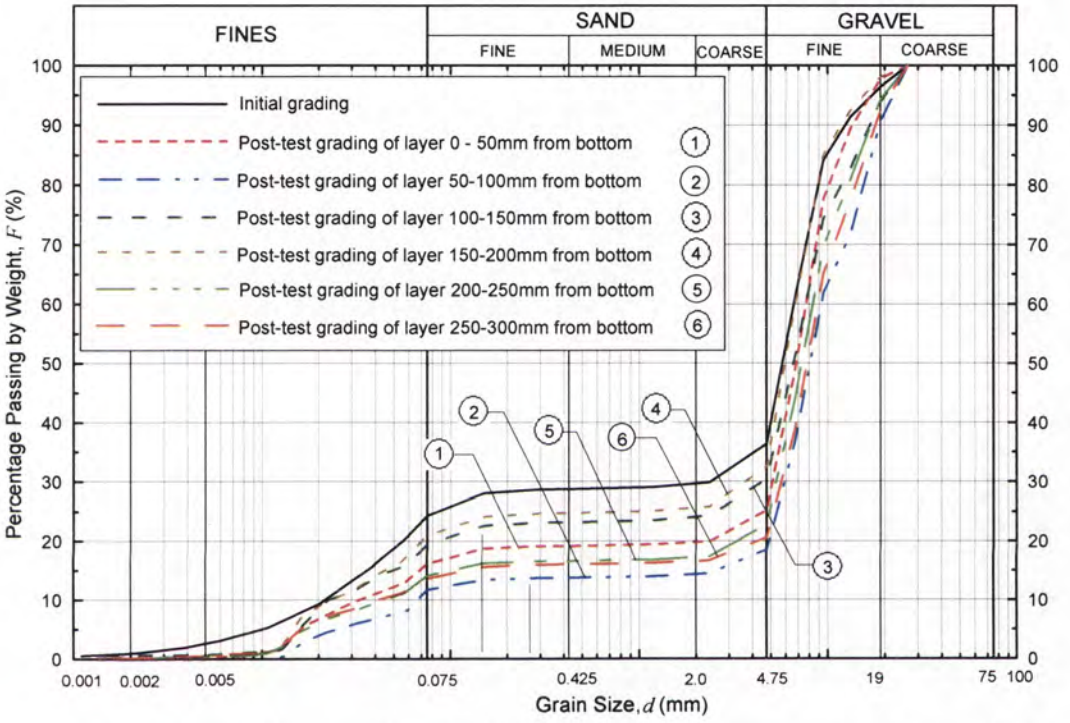

Figure 3.35: DF test No. 8 on Sample 10 - Post-test grain-size distribution analysis on sub-samples taken from various depths of the test sample.

Matching of grain-size distribution curves for the internally unstable soil samples are shown in Appendix O.

UF test

The main purpose of the UF test is to record the change in the flow rate and hydraulic gradient across the test sample, and to record the onset of erosion indicated by the washout of fine particles from the sample. Typical plots of the results of the UF test are shown in Figure 3.37 and Figure 3.38. Figure 3.37 shows the temporal variation of the hydraulic gradients within the test sample, and the seepage rate through the test sample,

whereas Figure 3.38 shows the variation of the average seepage velocity $\overline{V}$ with respect to the average hydraulic gradient I. In Figure 3.38, the gradual increase in the slope of the curve implies that the permeability of the test sample is increasing until a point at $I \approx 1.13$ when the sample starts to "boil" and reaches the zero effective stress condition.

Results of analysis and graphical plots on all UF test samples can be found at Appendix P.

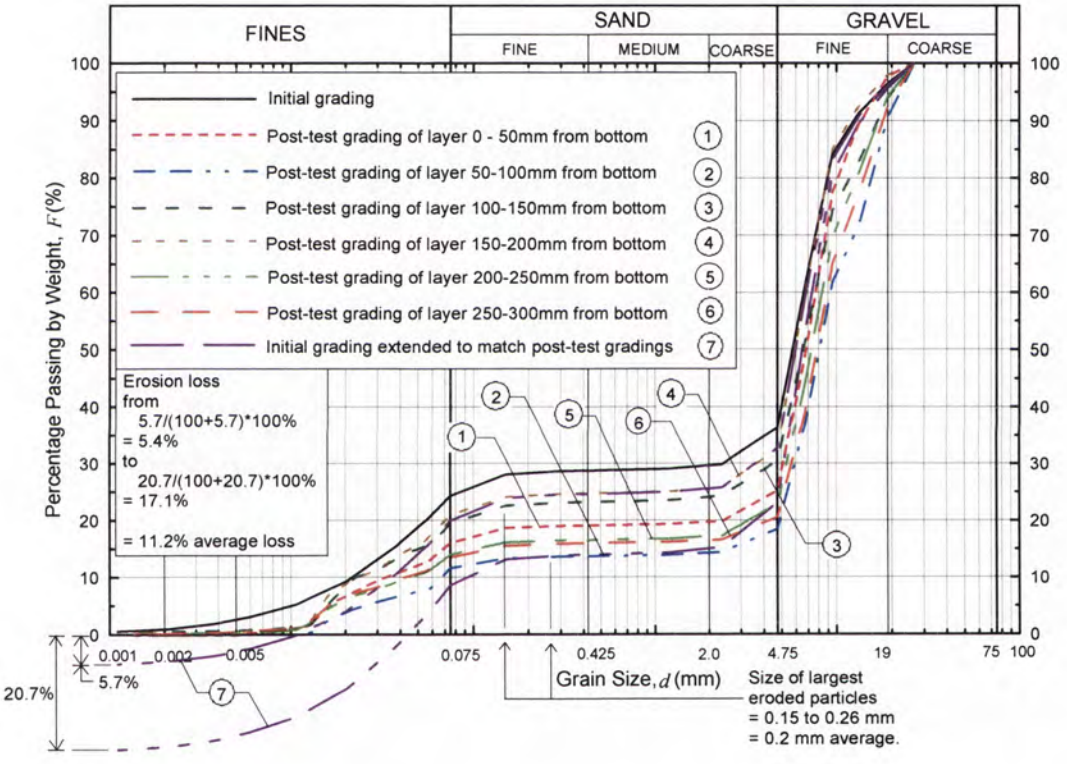

Figure 3.36: DF test No. 8 on Sample 10 – Curve matching for finding the fraction of materials loss by suffusion and the size of the largest erodible particles.

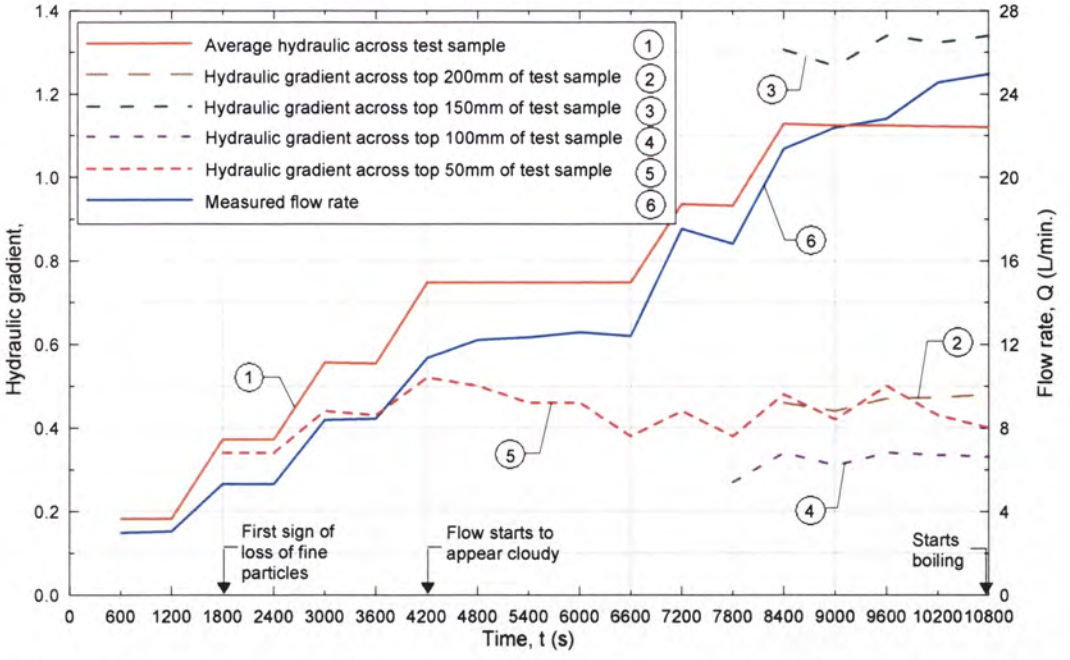

Figure 3.37: UF test No. 8 on Sample No. 10 – Temporal variation of hydraulic gradient and flow rate.

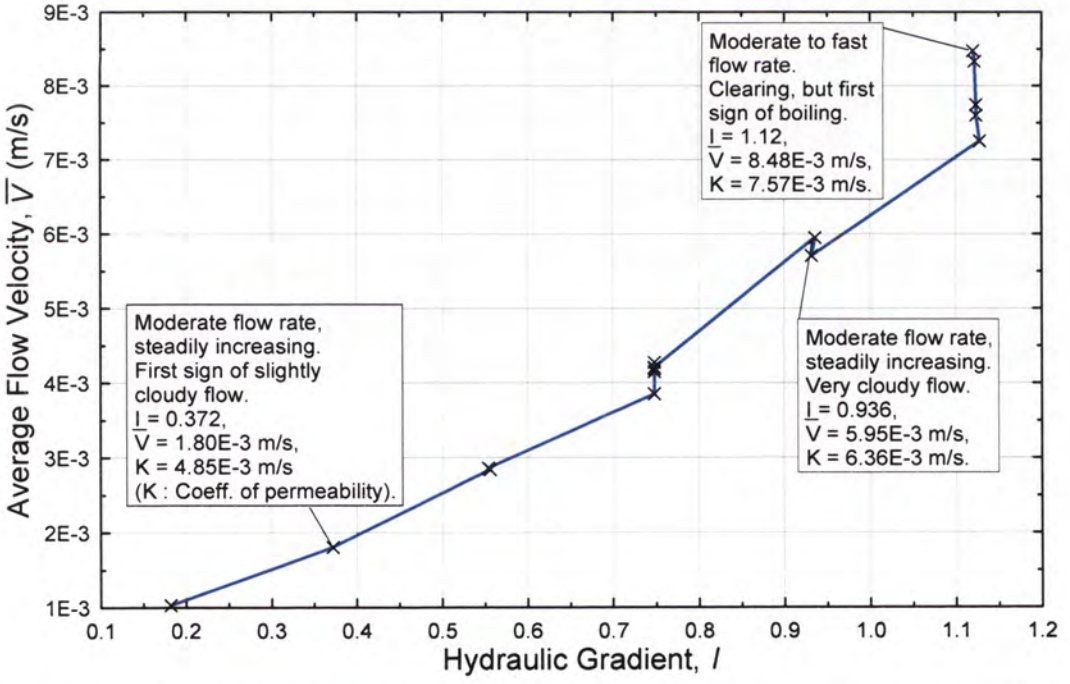

Figure 3.38: UF test No. 8 on Sample No. 10 – Average flow velocity versus hydraulic gradient.

3.4 ANALYSIS OF THE RESULTS OF DOWNWARD FLOW TESTS

3.4.1 Interpretation of test data

A total of 24 DF tests have been carried out on 20 soil samples. 9 out of the 20 soil samples are assessed as internally unstable based on the observations during the DF tests on those samples, and the obvious shift of their grain-size distribution curves from their initial positions after the test. Results of the 24 DF tests are summarised in Table 3.9. Sample 11 showed significant loss of materials in DF test no. 9. Sample 11 is, however, not classified as internally unstable as observations during the test showed the erosion loss was caused by piping along a piping channel through the sample.

For those samples assessed to be internally unstable, namely samples 10, 14A, 15, A2, A3, B1, B2, C1 and D1, their post-test grain-size distribution curves were analysed for the fraction of erosion loss using the curve matching technique described in Section 3.3.15. Results of the analysis are summarised in Table 3.10. For test samples 10 and 14A, ranges of values are given for the results of the curve matching analysis due to the reason that the post-test grain-size distribution of these soil samples varies with depth as revealed by their respectively post-test grain-size distribution curves. The post-test grain-size distribution curve of the bottom layer of the test sample was ignored in the curve matching analysis because the bottom layer usually showed bigger loss of fine particles, due to its contact with the bottom filter layer, when compared to the layers in the middle region of the test sample. The actual fraction of materials loss by suffusion is plotted against the maximum fraction of materials finer than the size of the largest eroded particles in Figure 3.39.

3.4.2 Identification of the factors influencing internal instability

Effects of fines content and gravel content

Figure 3.40 shows a plot of the gravel content versus the fines content for both the internally stable and unstable samples. The plot shows considering scattering of the

data. The internally unstable soils in the data set have fines content ranging from 7.4% to 33.1%, and the internally stable soils have fines content ranging from 4.9% to 44.4%.

The test data do not show any obvious relationship between the fines content and the internal stability of a soil.

Table 3.9: Summary of the results of downward flow tests.

Test sample	Downward flow test no.	Standard Max. Dry Density (t/m^3)	Standard Optimum Water Content (%)	Density Ratio of test specimen (%)	Water Content of test specimen (%)	Average Porosity of test specimen	Material loss due to erosion revealed by post-test grain-size distribution analysis
1, 1A	DF1	2.32	7.7	94.0	7.7	0.169	No Loss
	DF5			89.4	7.8	0.210	No Loss
2R	DF2R	2.13	9.9	95.8	9.5	0.222	No Loss
3R	DF3R	1.89	11.2	94.0	11.7	0.318	No Loss
4R	DF4R	2.23	9.3	93.4	10.0	0.200	No Loss
5	DF13	2.12	8.5	94.2	8.5	0.223	No Loss
	DF14			89.1	8.6	0.265	No Loss
6	DF10	2.23	7.2	95.5	7.2	0.174	No Loss
7	DF16	2.05	9.8	94.2	10.2	0.255	No Loss
9	DF6	1.94	6.3	93.8	5.8	0.323	No Loss
10	DF7	2.22	8.4	94.1	8.4	0.223	Obvious Loss
	DF8			90.0	8.2	0.257	Obvious Loss
11	DF9	1.91	12.1	97.3	12.8	0.303	Obvious Loss (Piping) [1]
13	DF11	1.92	7.1	94.5	6.9	0.323	No Loss
14A	DF12	2.04	11.1	94.6	10.6	0.281	Slight Loss
	DF15			90.0	10.2	0.316	Slight Loss
15	DF17	2.09	8.2	92.3	8.1	0.249	Obvious Loss
RD	DF18	1.87	13.3	94.8	12.9	0.371	No Loss
A2	DF24	2.43	6.1	90.7	5.6	0.173	Obvious Loss
A3	DF23	2.41	5.1	90.5	4.3	0.179	Obvious Loss
B1	DF22	2.35	5.5	91.3	6.5	0.191	Obvious Loss
B2	DF21	2.36	5.7	92.6	5.7	0.176	Obvious Loss
C1	DF20	2.34	4.3	93.9	2.5	0.176	Obvious Loss
D1	DF25	2.36	7.0	95.0	5.0	0.153	Obvious Loss

Note:

1 The observed loss of fines was due to the formation of a pipe through the soil sample, and erosion along the pipe.

Table 3.10: Fraction of material loss by suffusion and size of largest erodible particles assessed by grain-size distribution curve matching technique.

Test sample	Downward flow test no.	Material loss due to erosion revealed by post-test grain-size distribution analysis	Assessment using curve matching technique		
			Size of largest particles eroded (mm)	Fraction finer than the size of the largest particles eroded (%)	Actual fraction of materials loss by suffusion (%)
10	DF7	Obvious Loss	0.15	28.0	9.7 - 17.1 (Avg. 13.4)
	DF8	Obvious Loss	0.15 - 0.26 (Avg. 0.2)	14.0 - 24.0 (Avg. 19.0)	5.4 - 17.1 (Avg. 11.2)
14A	DF12	Slight Loss	0.06	17.5	4.4
	DF15	Slight Loss	0.20	21.0	2.4 - 5.8 (Avg. 4.1)
15	DF17	Obvious Loss	0.16	31.0	7.1
A2	DF24	Obvious Loss	0.60	19.5	15.2
A3	DF23	Obvious Loss	0.80	16.0	6.6
B1	DF22	Obvious Loss	5.00	37.0	20.0
B2	DF21	Obvious Loss	5.00	34.0	17.1
C1	DF20	Obvious Loss	9.50	32.0	15.9
D1	DF25	Obvious Loss	6.00	48.0	26.3

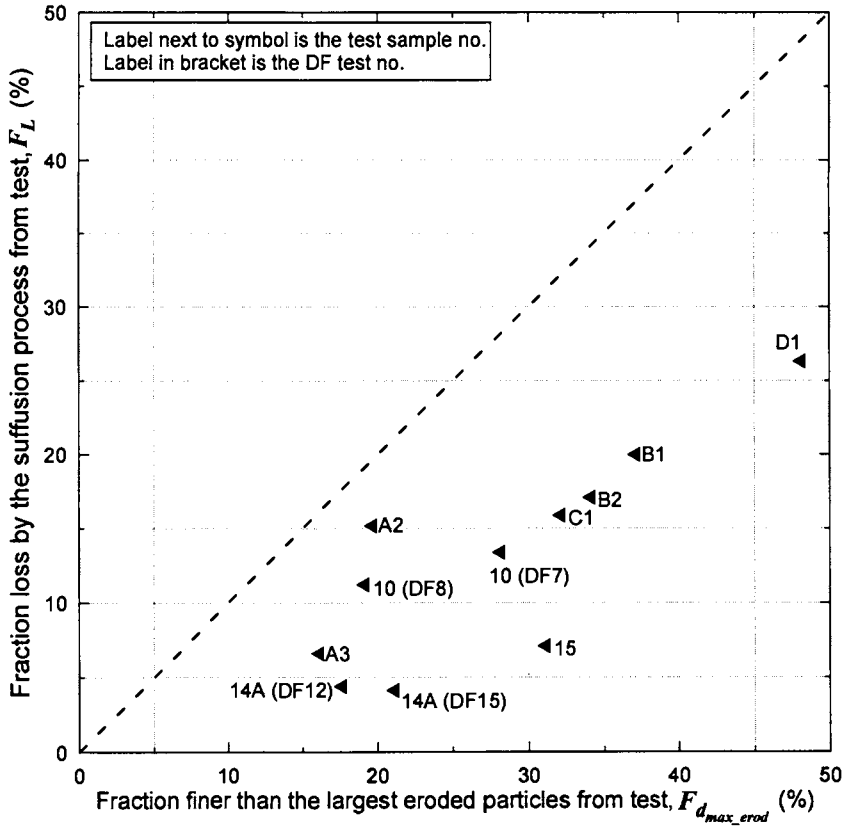

Figure 3.39: Actual fraction of materials loss by suffusion is plotted against the fraction finer than the largest eroded particles.

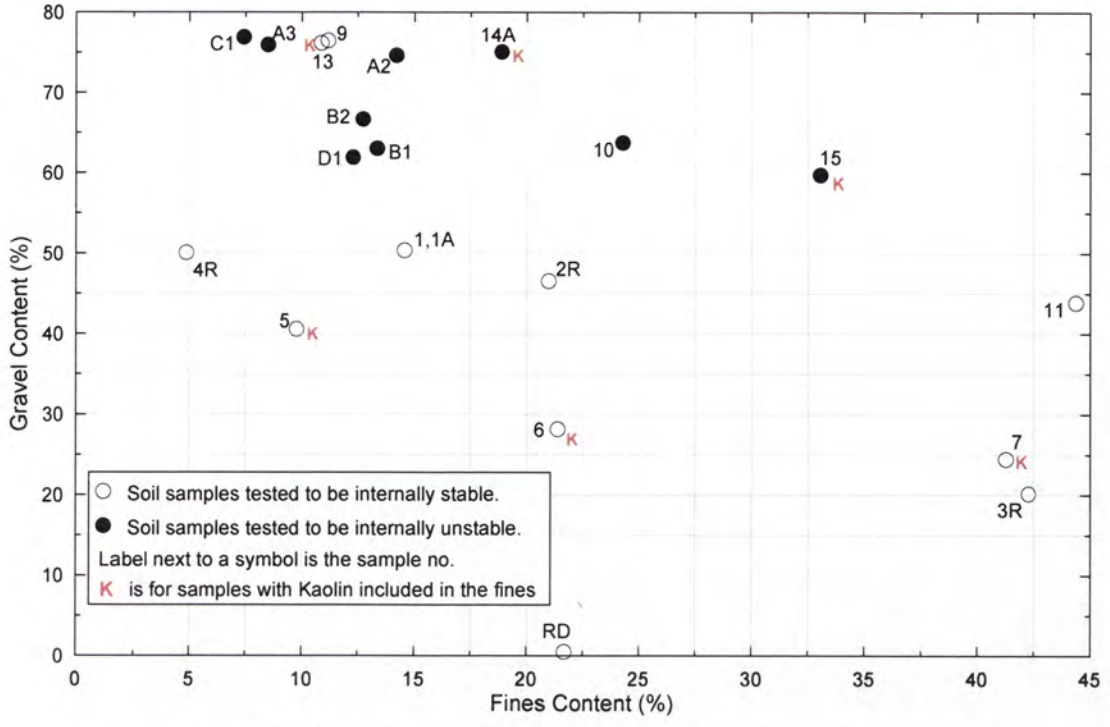

Figure 3.40: Plot of gravel content versus fines content for all test samples.

Figure 3.40 also reveals that all the unstable soil samples are among those having high gravel contents of 60% or above. These soil samples are, in general, widely-graded, and some are gap-graded and deficient in sand content. The observation suggests that widely-graded silty or clayey gravels having a gravel content higher than 60%, and gap-graded gravels deficient in sand content are more vulnerable to suffusion.

Samples 9 and 13, which have high gravel contents and deficient in sand content, however, did not show signs of instability in the DF tests.

Effects of the plasticity of fines

Tests on Atterberg limits indicate that soil samples with kaolin, namely samples 5, 6, 7, 13, 14A and 15, show some degree of plasticity, and the plasticity indices of these mixtures vary within a narrow range of 9 to 13%. It is believed that the presence of clay in a soil may increase its erosion resistance against suffusion in that higher gradients may be needed to initiate erosion. However, samples 14A and 15 (with considerable kaolin contents of 10.9% and 21.5%, respectively) were tested to be internally unstable. It appears that the presence of kaolin clay up to these percentages does not have a significant influence on the internal stability of the soil samples under the high gradient

used in the test. It should, however, be noted that samples 13, 14A and 15 are gap-graded, whereas samples 5, 6, and 7 are well-graded. It is possible that the adverse effect of gap-grading on internal stability is more significant than the stabilising effect of clay.

The above argument does not explain why the gap-graded samples 9 and 13 did not show any signs of instability during the DF tests. One possible reason is that the amount of fine materials loss by suffusion in samples 9 and 13 was too small to effect any noticeable changes in the pressure and flow rate during the DF, and to be detected by the post-test grain-size distribution analysis. The fine materials in samples 9 and 13 are less than 12%, but the erodible fraction may be a lot less than 12%. For example, Table 3.10 and Figure 3.39 show that the assessed erosion loss for Sample 14A is only 4.4%, although the fraction of materials finer than the largest particles eroded was up to 17.5 to 21.0%. For the purposes of this report, it is assumed samples 9 and 13 are internally stable as the tests show.

Effects of gap-grading

Samples 9, 10, 11, 13, 14A and 15 are gap-graded and deficient in sand-sized particles. Samples 10, 14A and 15 showed signs of suffusion during the DF tests, and sample 11 showed signs of piping. Samples 9 and 13 did not show signs of instability during the DF test.

It appears that soil samples which are gap-graded, and have a high gravel content (> 60%) are vulnerable to suffusion.

Effects of soil density

Four soil samples, namely 1 and 1A, 5, 10 and 14A, were each tested at two different compaction densities (i.e. 95% and 90% of the standard maximum dry density). The tests on samples 1 and 1A, and 5 showed no signs of instability. The tests on samples 10 and 14A indicated that the 2 samples were internally unstable. The difference in compacted soil density does not appear to have any significant effect on the results of the DF tests.

It should be noted that all the DF tests were carried out at approximately the same hydraulic gradient of 8. If the tests were carried out at a range of hydraulic gradients, it is possible that tests on the same soil compacted to different densities might show different results under different hydraulic gradients.

3.4.3 Prediction of the internal instability of the UNSW test samples using currently available methods

Overview

Since one of the objectives of the study is to investigate the validity of applying currently available method to predict the internal stability of widely-graded materials, the internal stability of the 20 soil samples has been assessed by a number of currently available methods. This includes the Sherard (1979) method even though this was proposed for identifying soils which will not self filter, rather than those subject to suffusion. Results of the assessment using five of the currently available methods are compared with the actual suffusive behaviour of the soil samples in the DF tests as in Table 3.11. The use of Lubochkov (1965) method and Burenkova (1993) method in the prediction of the sizes of particles eroded by the suffusion process is also discussed in this Section.

Effects of the coefficient of uniformity and the coefficient of curvature on internal instability

Some prediction methods (e.g. the U.S. Army Corps of Engineers (1953) and Istomina (1957)) use the coefficient of uniformity, C_U, as a predictor of internal stability. As shown in Figure 3.41, the coefficient of curvature, C_C, is plotted against C_U for the 20 test UNSW samples. The plot shows considerable scattering of the data. All unstable soil samples have C_U higher than 100. Both the Army Corps method and the Istomina method predict that materials with C_U higher than 20 are internally unstable. Both methods appear to be too conservative in that many stable soil samples have C_U higher than 20. Sample 7, for example, is stable and has a high C_U of approximately 1800.

Table 3.11: Assessment of internal stability of the 20 soil samples using currently available methods.

Test sample	Downward flow test no.	Internal stability based on results of DF Test	Assessment of Internal Instability using methods by Others [2], [3]				
			U.S. Army Corps of Engineers (1953)	Istomina (1957)	Sherard (1979)	Kenney & Lau (1985, 86)	Burenkova (1993)
1, 1A	DF1, DF5	Stable	U	U	U	U	S
2R	DF2R	Stable	U	U	U	U	M
3R	DF3R	Stable	U	U	U	M	S
4R	DF4R	Stable	U	U	U	U	S
5	DF13, DF14	Stable	U	U	U	U	M
6	DF10	Stable	U	U	U	U	M
7	DF16	Stable	U	U	U	U	S
9	DF6	Stable	U	U	U	U	S
10	DF7, DF8	Unstable	U	U	U	S	U
11	DF9	Stable [1]	U	U	U	U	S
13	DF11	Stable	U	U	U	U	S
14A	DF12, DF15	Slightly unstable	U	U	U	U	U
15	DF17	Unstable	U	U	U	U	U
RD	DF18	Stable	U	U	U	U	S
A2	DF24	Unstable	U	U	U	U	U
A3	DF23	Unstable	U	U	U	U	U
B1	DF22	Unstable	U	U	U	U	S
B2	DF21	Unstable	U	U	U	U	U
C1	DF20	Unstable	U	U	U	U	U
D1	DF25	Unstable	U	U	U	U	S

Notes : (1) Sample showed signs of piping, but classified as stable with respect to suffusion.
(2) Details of the various methods can be found in Section 2.
(3) "S" means Stable; "U" means Unstable; "M" means Marginal; "P" means piping.
Box shaded means incorrect prediction.

Data on suffusion seepage tests with information on post-test grain-size distribution analysis are available from the literature, and summarised in Table 3.3 in Section 3.2. Grain-size distribution curves of these data are also presented in Section 3.2. Figure 3.42 shows a plot of C_C versus C_U for a set of 66 test data, including the data of the 20 tests carried out at the University of New South Wales (designated UNSW data), but excluding the test data by Sun (1989). Sun (1989) data were excluded because the samples tested by Sun are cohesive clayey/silty sands rather than the cohesionless silt-sand-gravels tested by others. Sun's test method is also significantly different from the test methods of the other investigators. The plot in Figure 4.4 shows that $C_U \geq 20$ is an

inappropriate criterion for internal instability. Whilst soils with very high C_U appear more likely to be internally unstable, some stable soil samples have very high C_U. On the other hand, Figure 3.42 shows that not all soils with C_U less than 10 are stable.

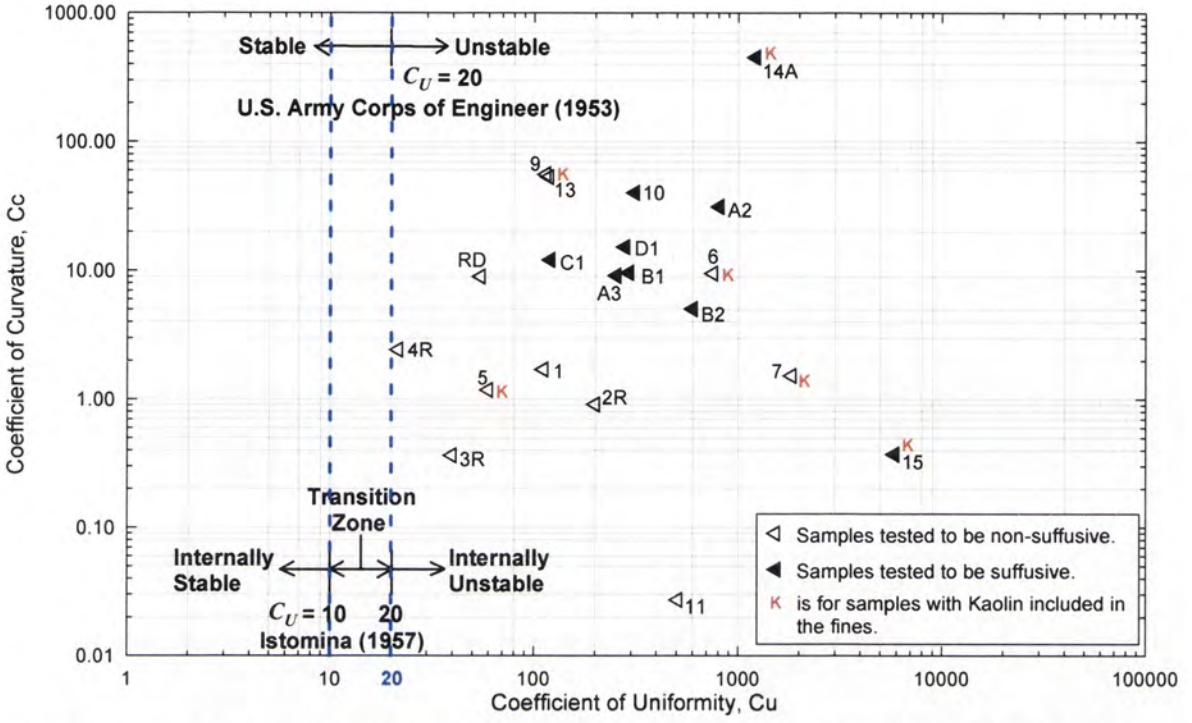

Figure 3.41: Coefficient of curvature versus coefficient of uniformity for 20 UNSW soil samples.

Prediction methods based on splitting a soil into a coarse fraction and a fine fraction and treating the coarse fraction as a filter to the fine fraction

As described in Section 3.2, prediction methods based on splitting a soil into a coarse fraction (*c*) and a fine fraction (*f*) and treating the coarse fraction as a filter to the fine fraction have been proposed by Kézdi (1969), de Mello (1975), Sherard (1979). Sherard's method, which relies on the filter rule $d_{c15}/d_{f85} < 4$ to 5, is more commonly used. These methods were developed to identify soils which will not self filter.

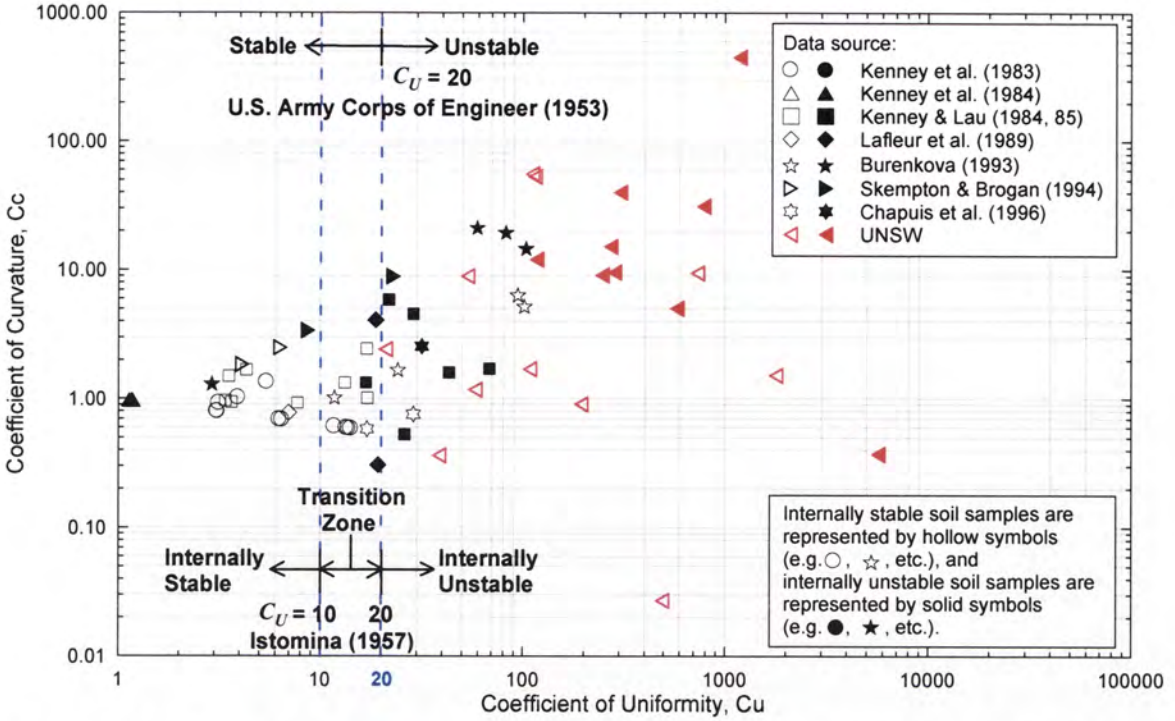

Figure 3.42: Coefficient of curvature versus coefficient of uniformity for all available internal instability test data.

Table 3.11 shows that Sherard (1979) method is too conservative for assessing whether soils are internally unstable and subject to suffusion. All 20 soil samples tested in the DF tests are assessed as not self filtering ("internally unstable"), despite only 9 out of the 20 samples were tested to be internally unstable. Applying the method to all available data (set of 66 data) reveals again that the method is too conservative. About 92.3% of the "internally unstable" samples are correctly assessed as unstable, but only about 55.0% of the stable samples are correctly assessed as stable.

The Sherard (1979) method does not consider the geometrical criterion which requires that the maximum portion of fine erodible materials in a soil cannot be greater than a certain value for suffusion to occur. Sometimes, a grain-size distribution curve is split at a point which indicates that the erodible fraction of the soil is higher than 50%. This is theoretically impossible for suffusion to occur as it implies that the soil consists of coarse particles "floating" in a matrix of the fine particles, and a soil skeleton made up only of the coarser soil particles does not exist.

The use of the filtering criterion defined by $d_{C15}/d_{f85} < 5$ is probably too conservative (c.f. the no erosion boundary defined by $d_{F15}/d_{B85} \leq 9$ (Foster & Fell 1999a, 2001)) for soils with a fines content larger than 85%. The UNSW test data have been re-analysed using a modified curve splitting method based on a less conservative filter rule represented by $d_{C15}/d_{f95} < 9$ (i.e. the continuing erosion boundary (Foster & Fell 1999a, 2001)).

Figure 3.43 and Figure 3.44 show plots of d_{C15}/d_{f95} against the splitting point, d, for the unstable and the stable soil samples, respectively. Figure 3.43 shows that all 9 unstable samples are plotted above the Continuing Erosion Boundary represented by the horizontal line $d_{C15}/d_{f95} = 9$, implying that the modified method has correctly predicted the unstable samples, as the continuing erosion boundary have been exceeded in these samples. Figure 3.44 shows that 3 out of the 11 stable samples are plotted below the continuing erosion boundary when the dividing point, d, is greater than 0.075 mm. Sample 11, which showed signs of piping during the DF test, is plotted above the continuing erosion boundary, but the splitting point, d, represents a fine fraction of about 45%, which is too high for a soil to be susceptible to suffusion. In general, the modified curve splitting method predicts the suffusive characteristics of the UNSW test data quite satisfactorily.

The modified method has also been applied to the Kenney & Lau (1984) test data. As shown in Figure 3.45, 5 out of 6 internally unstable samples tested by Kenney & Lau (1984) are plotted below the continuing erosion boundary, and are interpreted as stable. The method is, therefore, not conservative when applied to Kenney & Lau (1984) data. It appears that methods based on splitting the soil into a fine fraction and a coarse fraction appear to be unviable as a method for predicting internally unstable soils, as it is difficult to establish a filter criterion suitable for all types of soils.

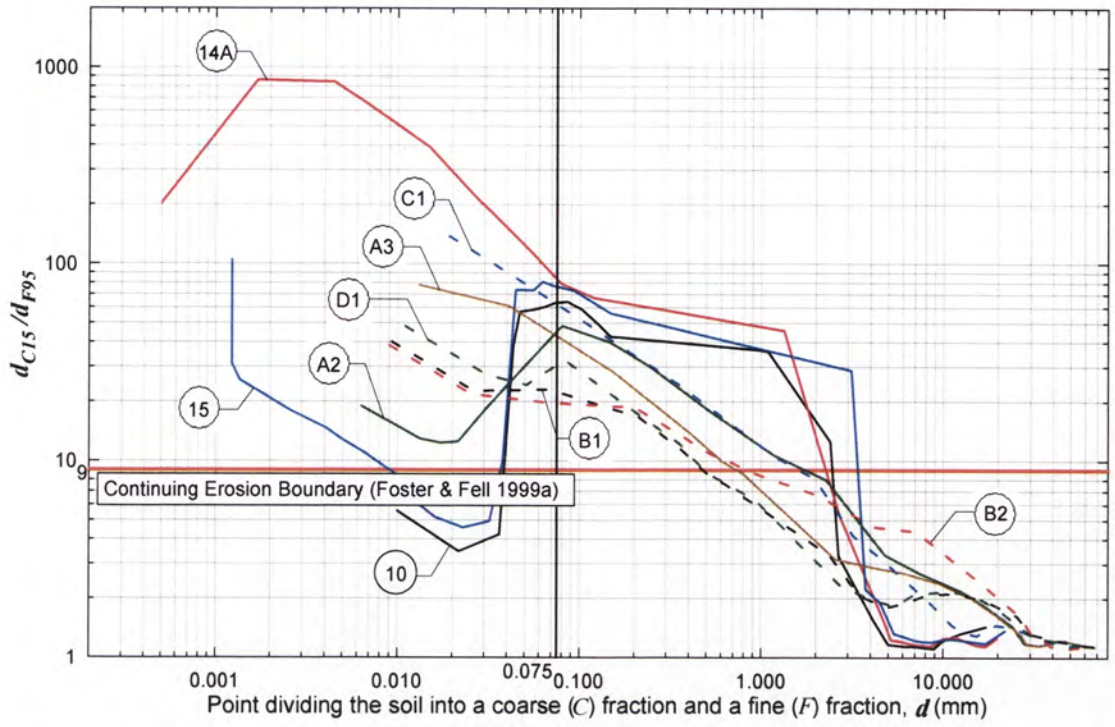

Figure 3.43: d_{C15}/d_{f95} versus dividing point, d for all internally unstable samples tested by UNSW.

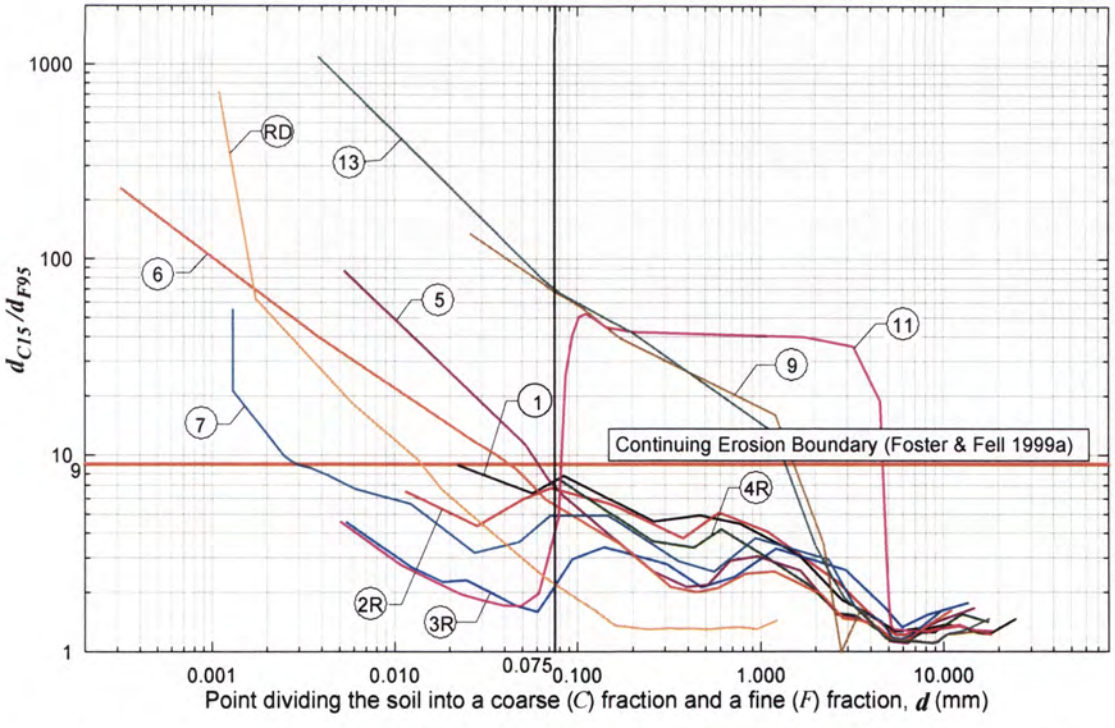

Figure 3.44: d_{C15}/d_{f95} versus dividing point, d for all internally stable samples tested by UNSW.

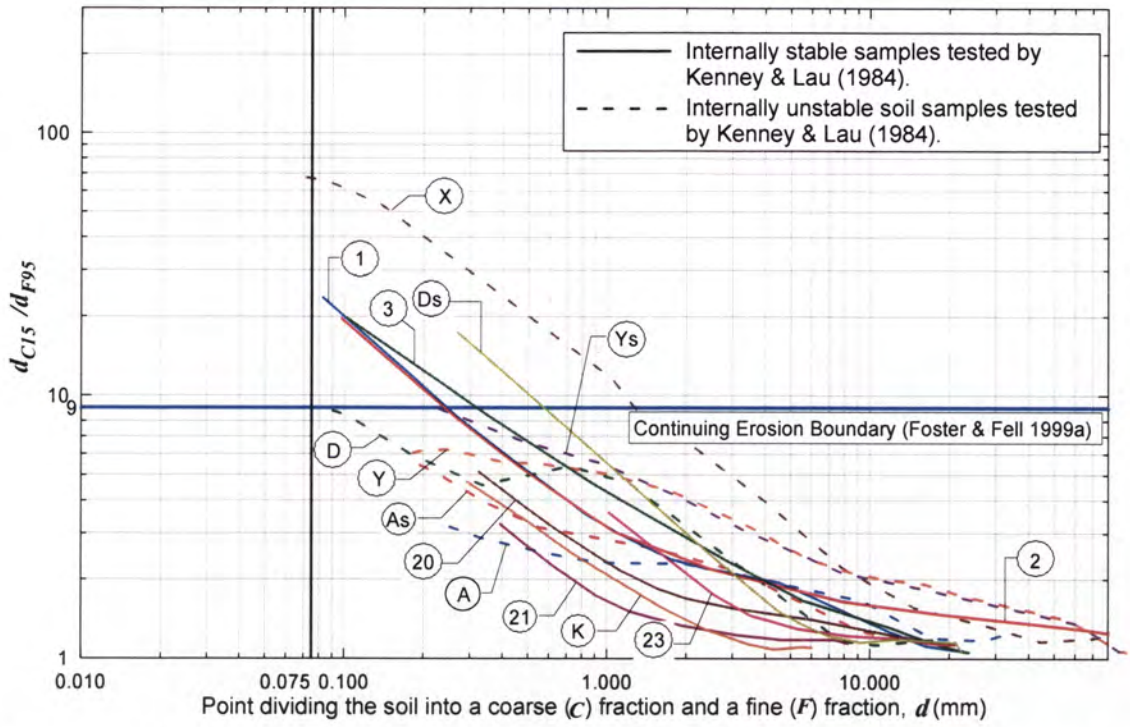

Figure 3.45: d_{C15}/d_{f95} versus dividing point, d for soil samples tested by Kenney & Lau (1984).

Prediction of internal instability using Kenney and Lau (1985, 1986) method

Figure 3.46 and Figure 3.47 show shape curves (*H-F* plots) of the soil samples tested by UNSW. The curves have been prepared in accordance with Kenney & Lau's method. According to Kenney & Lau (1985, 86), the lower boundary $H = 1.0F$ coincides with Fuller & Thompson (1907) criterion for a soil with maximum density, and the upper boundary $H = 1.3F$ coincides with Lubochkov (1962, 1965) criteria for internal stability. The region between the two boundaries represents a transition between the unstable and the stable regions.

Figure 3.46 shows that all 9 unstable samples tested by UNSW are correctly classified as unstable, as they are all plotted below the boundary $H = 1.0F$ for $F < 0.2$. Figure 3.47 shows that 9 out of the 11 stable samples tested by UNSW are incorrectly classified as unstable by Kenney & Lau (1985, 86) method. Only samples 3R and 11 are correctly predicted as stable, as their shape curves are plotted above the boundary $H = 1.3F$ for $F < 0.2$. Figure 3.48 shows a slightly different *H-F* plot in which each soil sample is represented by its (H, F) value at which the stability number (i.e. H/F ratio) is at its minimum value. Figure 3.48 shows clearly that there is a mixture of stable and unstable

soil samples plotted below the boundary $H = 1.0F$. Kenney & Lau's method, therefore, appears to be too conservative when used to predict the suffusive characteristics of the UNSW test samples.

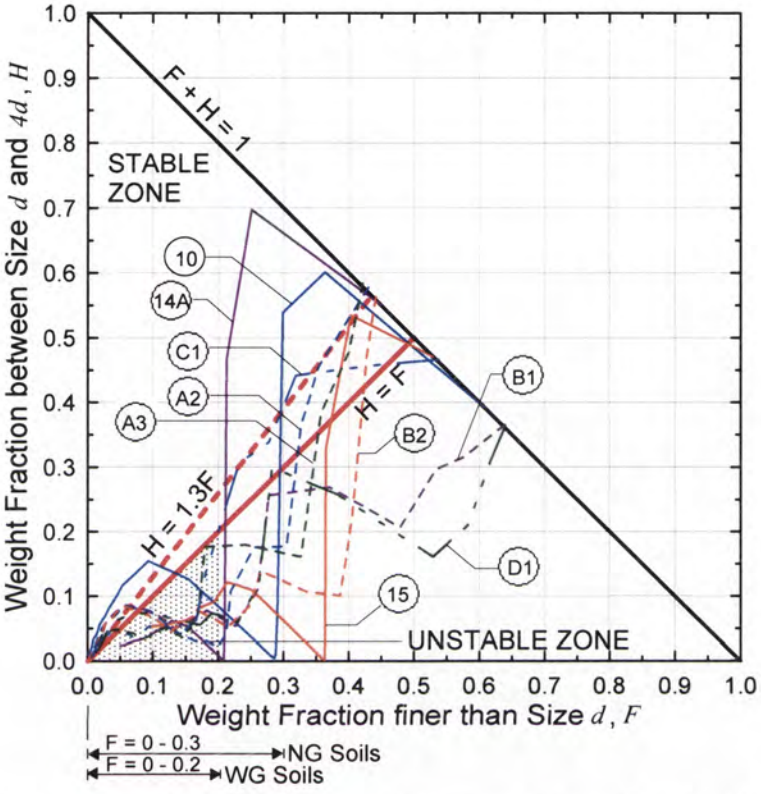

Figure 3.46: *H-F* plots for unstable samples tested by UNSW.

The *H-F* plot in Figure 3.49 summarises the results of prediction for all available test data using Kenney & Lau's method. The plot with 66 data points shows that none of the unstable soil samples are plotted above the boundary $H = 1.3F$. There is, however, a mixture of stable and unstable samples plotted below the boundary $H = 1.0F$.

The above analysis shows that Kenney & Lau (1985, 1986) method is a conservative method for predicting internal instability. The boundary $H = 1.3F$ appears to represent an upper bound for unstable soils. Soils plotted within the boundary (i.e. $H < 1.3F$), can be either internally stable or unstable soils.

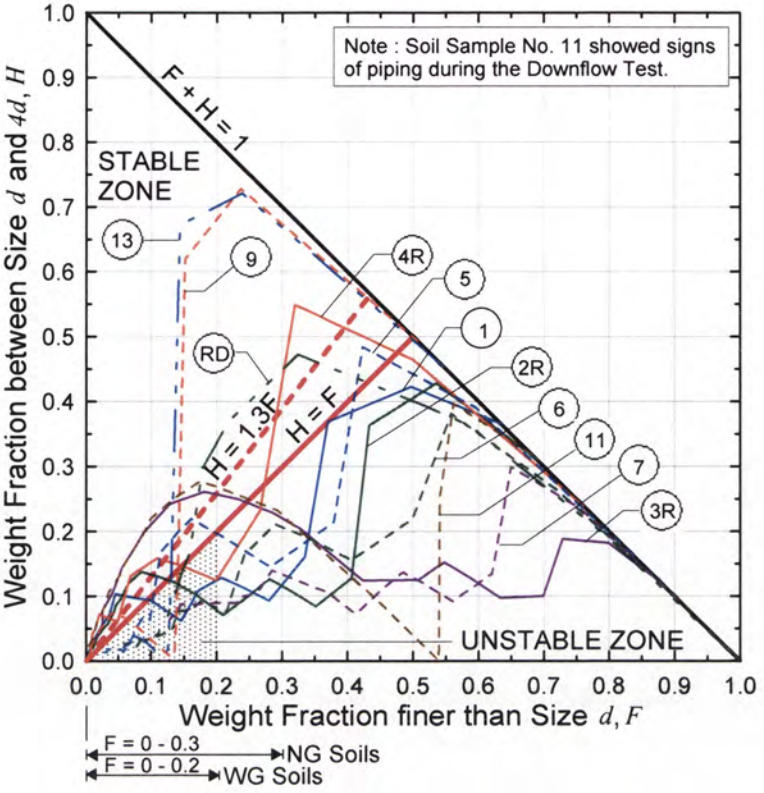

Figure 3.47: *H-F* plots for stable samples tested by UNSW.

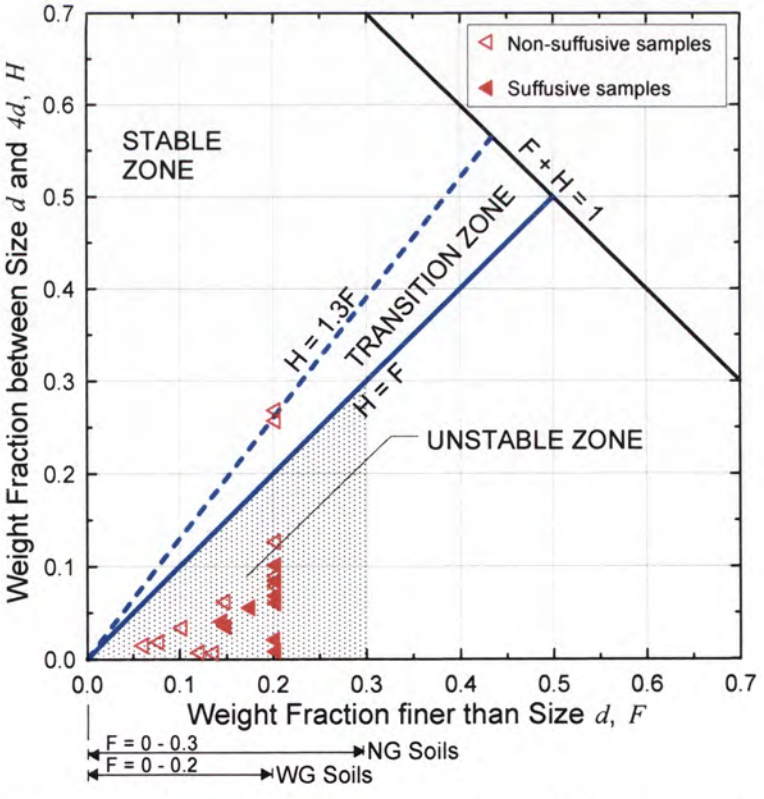

Figure 3.48: Plot of minimum *H/F* ratios (UNSW test data).

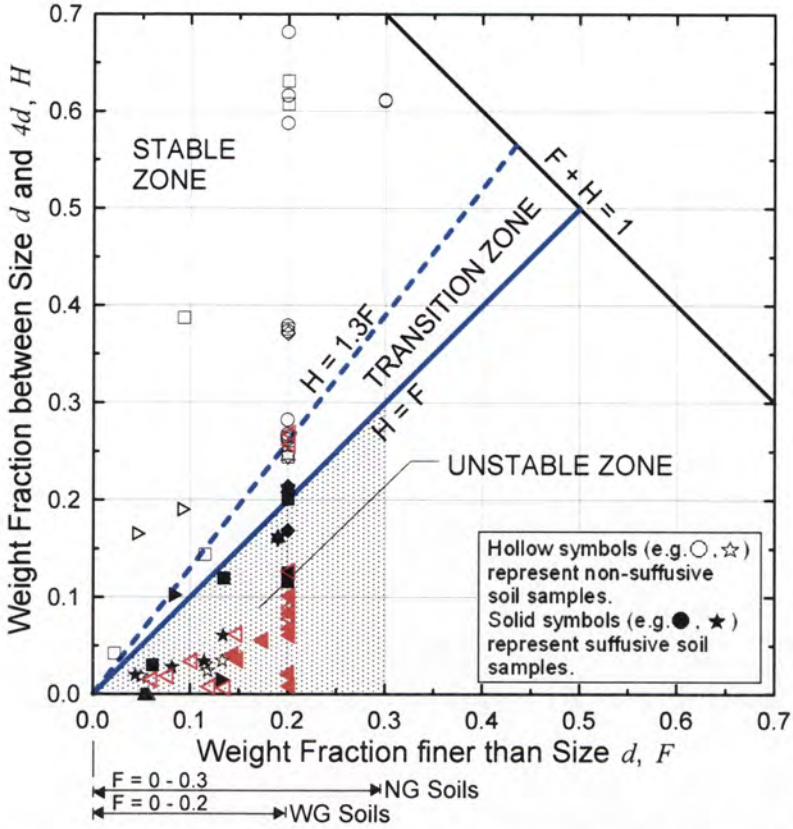

Figure 3.49: Plot of minimum *H/F* ratios for all available test data on silt-sand-gravel and clay-silt-sand-gravel soils.

Prediction of internal instability by Burenkova (1993) method

Figure 3.50 shows the classification of the suffusion characteristics of the 20 UNSW soil samples using Burenkova (1993) method. The figure shows that the lower boundary, represented by $h' = 0.76\log(h'') + 1$, approximately separates the unstable samples from the stable samples if samples B1 and D1 are excluding. 4 stable samples, namely samples 2R, 5, 6 and 11, are plotted only marginally below the lower boundary into the Zone I. Apart from these, Burenkova's method predicts satisfactorily the suffusion characteristics of the UNSW soil samples. Samples B1 and D1 are plotted within Zone II due to high h' values resulted from their unusual shaped grain-size distribution (see Figure 3.34). These distributions may be attributed to the effects of the 50 – 75 mm diameter particles in small samples. Samples B1, and D1 are excluded from the test data set in subsequent analysis, but it should be kept in mind that soils showing these particle size distribution characteristics may be susceptible to internal instability.

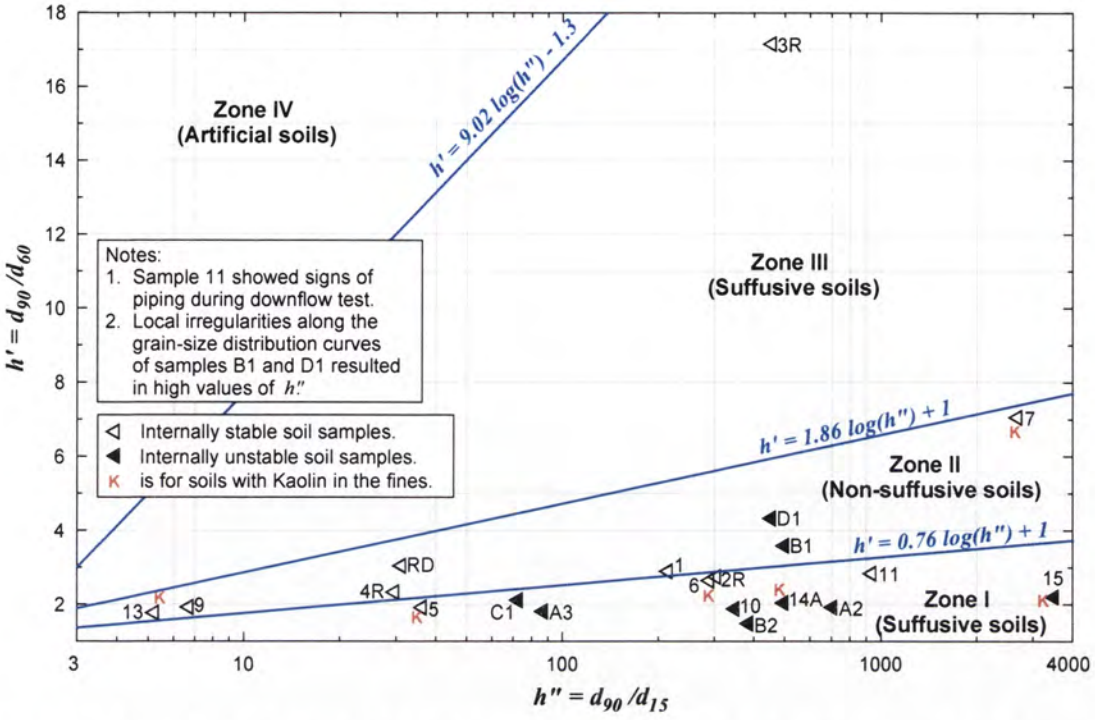

Figure 3.50: Classification of suffusion characteristics based on Burenkova (1993) method (UNSW test data).

The Burenkova (1993) method is also used to classify other available test data, and the results of the classification are shown in Figure 3.51. A few unstable soil samples are plotted above the lower boundary into the non-suffusive zone. This implies that the lower boundary is not conservative in separating the stable soils from the unstable soils. Except for a few stable soil samples plotted marginally below the lower boundary into Zone I, most of the soil samples plotted in Zone I are unstable, as predicted by Burenkova (1993) method, so the lower boundary appears to represent an approximate lower bound for internally stable soils.

It should be noted that to do this analysis Burenkova's method has been extrapolated to include soils having C_U values as high as 5700 in preparing the plots in Figure 3.50 and Figure 3.51. Burenkova's method was based on the test results on samples of C_U values up to 200.

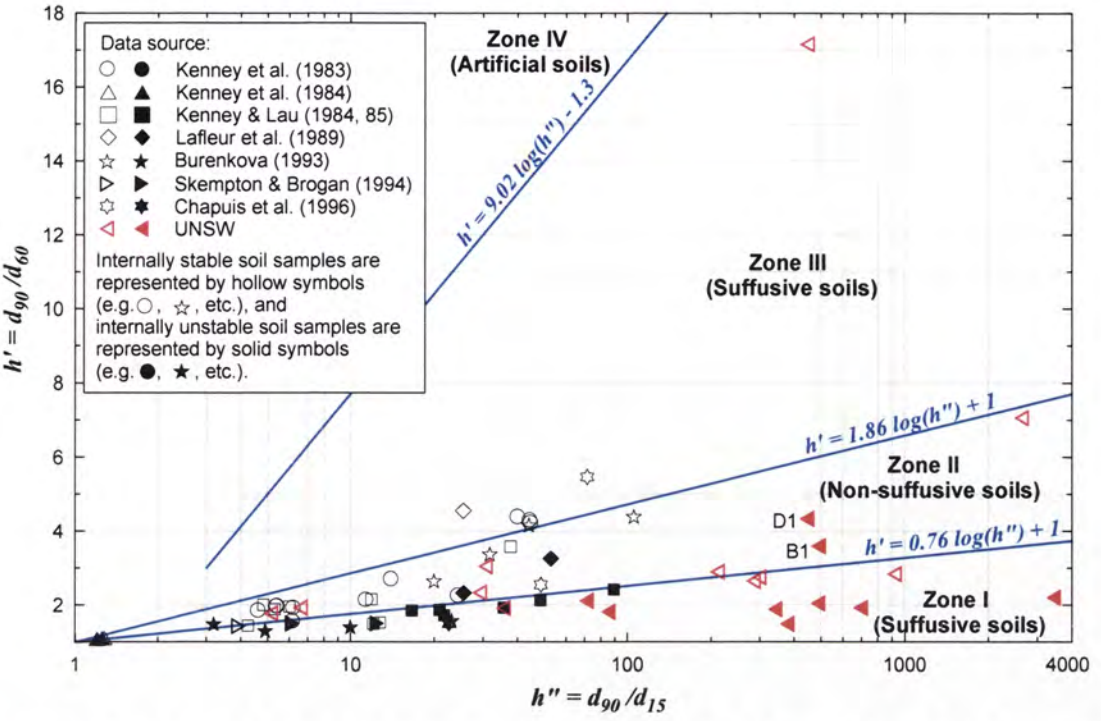

Figure 3.51: Classification of suffusion characteristics for all available test data on silt-sand-gravel and clay-silt-sand-gravel using Burenkova (1993) method.

Prediction of internal instability by Sun (1989) method

The method for predicting internal stability of a soil by Sun (1989) was intended for clayey/silty sands. The Author has, however, applied the method to silt-sand-gravel, clay-silt-sand-gravel soils and sand-gravel soils tested by the authors and others. Figure 3.52 shows the results of classification of the 20 UNSW soil samples using Sun (1989) method. All 9 unstable soil samples are correctly classified as unstable by Sun's method, but 5 of the stable soil samples, namely samples 5, 6, 9, 13 and RD, are incorrectly classified as unstable. This includes 3 samples (5, 6 and 13) which have kaolin included in the fines, so should be applicable to the Sun (1989) method.

The boundary between stable and unstable soils proposed by Sun (1989) implies that the erodible fine fraction of a soil cannot be greater than 35%. Plots of the all test data show that none of the unstable soil samples has an erodible fine fraction (F_C^*) greater than 40%. Possible explanations are either Sun's method is too conservative, or the hydraulic gradient ($i \approx 8$) at which the DF tests were carried out, was not high enough to cause erosion within the soil samples. The boundary proposed by Sun corresponds to

a hydraulic gradient, *i* equal 20. However, the gradient of 8 should have been sufficient when the results of the UF tests are considered, so it is likely that Sun (1989) method is conservative.

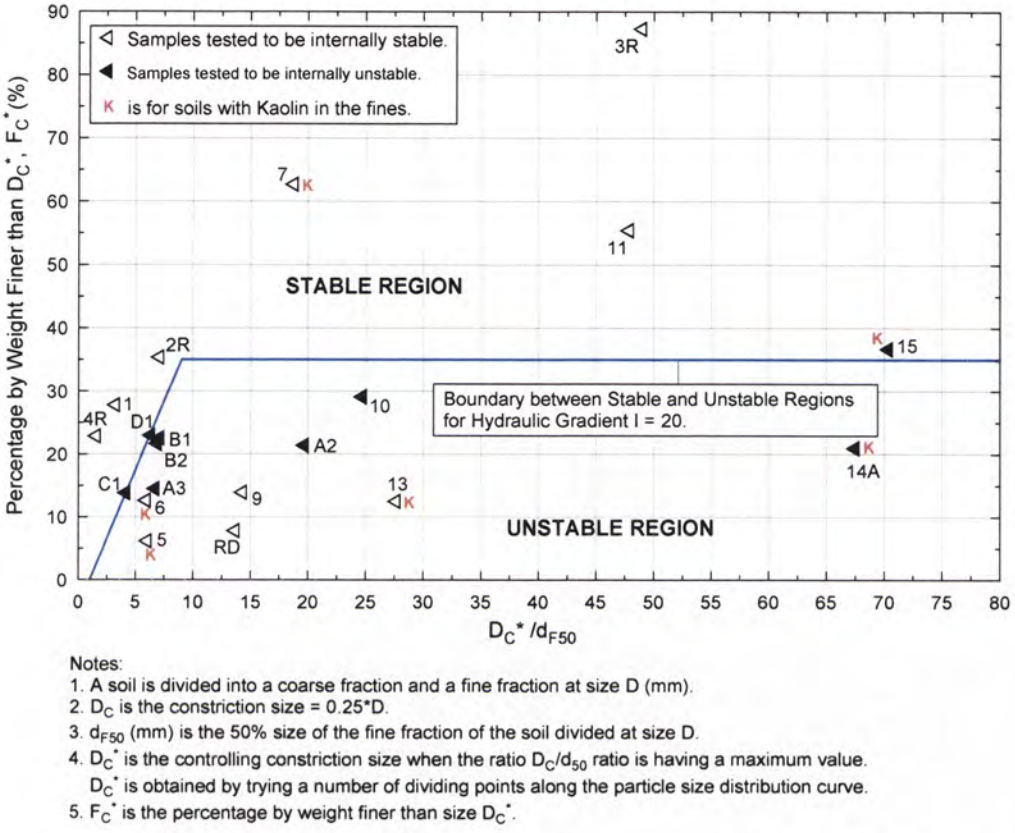

Notes:
1. A soil is divided into a coarse fraction and a fine fraction at size D (mm).
2. D_C is the constriction size = 0.25*D.
3. d_{F50} (mm) is the 50% size of the fine fraction of the soil divided at size D.
4. D_C^* is the controlling constriction size when the ratio D_C/d_{50} ratio is having a maximum value. D_C^* is obtained by trying a number of dividing points along the particle size distribution curve.
5. F_C^* is the percentage by weight finer than size D_C^*.

Figure 3.52: F_C^* versus D_C^*/d_{F50} based on Sun (1989) method for all UNSW internal instability test samples.

Figure 3.53 shows the results of classification of all available test data using Sun (1989) method. The figure shows that a lot of the cohesionless sand-gravel soils, namely those tested to be unstable by Kenney & Lau (1984), are classified as stable by Sun's method. This implies that the method may not be conservative when applied to coarse granular materials.

It should be noted that in the above analysis, Sun's method has been extrapolated to include materials of maximum particle sizes up to 100mm. Sun's method is based on the test results on clayey/silty sand having a maximum particle size of 4.75 mm only.

Clayey/silty sands are believed to have relatively lower tendency to be internally unstable compared to coarse granular materials. This may explain why some unstable coarse granular soils tested by Kenney & Lau (1984) are classified as stable by Sun's method. Sun's method should not be applied to coarse granular soils. As discussed above, it is also possible Sun (1989) tests at high gradients on thin (25 mm) samples may have caused cracking with erosion on the crack, rather than suffusion.

It is clear from the above discussion that the Sun (1989) method for assessing internal instability should not be applied to silt-sand-gravels and to clay-silt-sand-gavels, and may not even be applicable to clayey and silty sands.

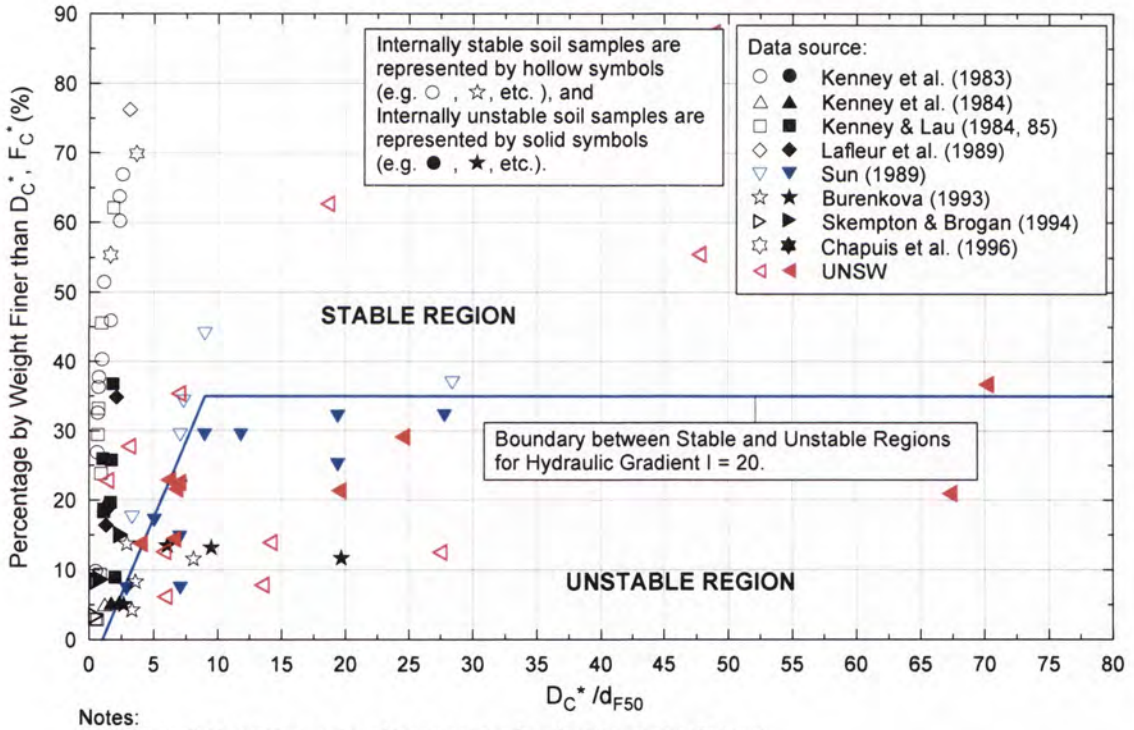

Notes:
1. A soil is divided into a coarse fraction and a fine fraction at size D (mm).
2. D_C is the constriction size = 0.25*D.
3. d_{F50} (mm) is the 50% size of the fine fraction of the soil divided at size D.
4. D_C^* is the controlling constriction size when the ratio D_C/d_{50} ratio is having a maximum value. D_C^* is obtained by trying a number of dividing points along the particle size distribution curve.
5. F_C^* is the percentage by weight finer than size D_C^*.

Figure 3.53: F_C^* versus D_C^*/d_{F50} based on Sun (1989) method for all available internally instability test data.

3.4.4 Prediction of the fraction of materials loss by suffusion and the size of the largest particles eroded

Fraction of materials loss by suffusion

In Section 3.4.2, Table 3.10 summarises the fraction of materials loss by suffusion during the DF tests on internally unstable soil samples. The fraction of materials loss has been estimated by comparing the post-test grain-size distribution curves with the initial grain-size distribution curve of the soil sample using the curve matching technique. Figure 3.39 shows a plot of the actual fraction of materials loss versus the fraction finer than the largest eroded particles. The latter represents the maximum fraction of fine materials that can possibly be eroded by the suffusion process. A similar plot has been prepared, as shown in Figure 3.54, including all the unstable soil samples in the available data. Figure 3.54 shows considerable scattering of the data, and reveals no obvious relationship between the actual fraction of material loss and the possible maximum fraction of erodible materials. This may be due to some physical limitation of erosion, or to test being of limited duration, so not all erodible soil has been eroded.

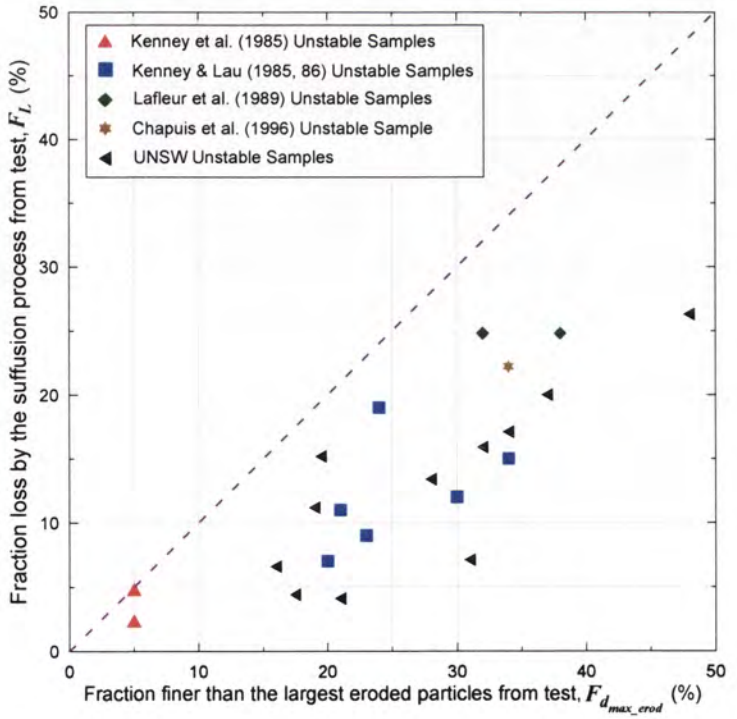

Figure 3.54: Actual fraction of materials loss by suffusion versus maximum fraction of erodible materials (all unstable soil samples in data set).

Prediction of the size of the largest particles eroded by Lubochkov (1965) method

Lubochkov (1965) proposed that a soil would not be susceptible to suffusion when the slope of its grain-size distribution curve was equal to or smaller than a given limit in each grain size interval. His method would lead to the prediction of a maximum particle size than can be eroded in the suffusion process. Details of his method have been described in Section 3.2.3. Lubochkov (1965) method has been used to predict the size of the largest particles eroded for some internally unstable soils in the data set. The predict sizes are compared with the sizes of the largest particles eroded estimating from the curve-matching techniques as shown in Figure 3.55.

Figure 3.55 shows that Lubochkov (1965) method tends to overestimate the sizes of the largest particles eroded by the suffusion process. The overestimation was as high two orders of magnitude in some cases.

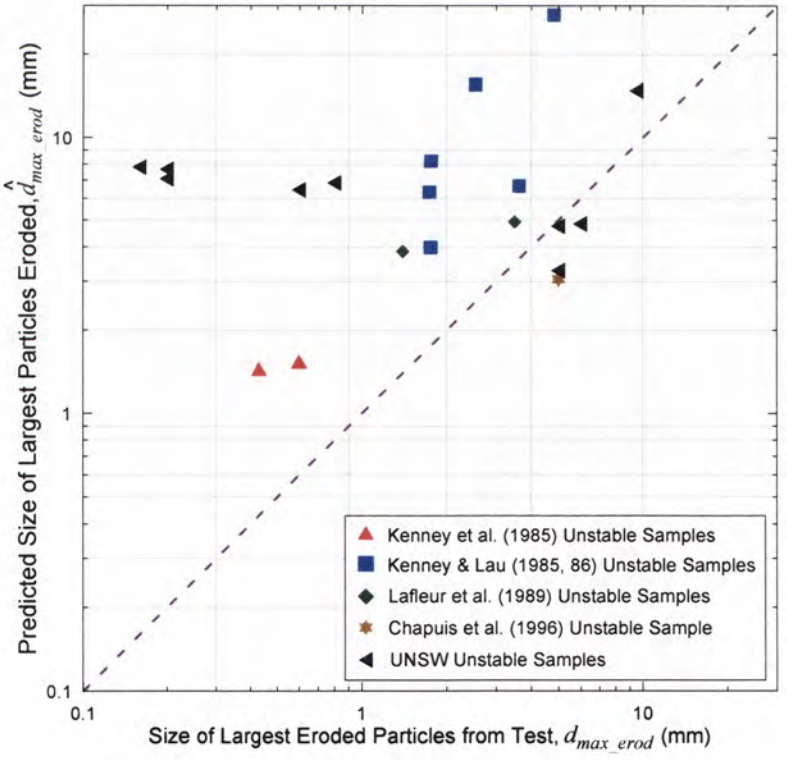

Figure 3.55: Sizes of largest particles eroded predicted by Lubochkov (1965) method versus sizes of largest particles eroded estimated by the curve-matching technique for all samples tested to be internally unstable.

Prediction of the size of the largest particles eroded by Burenkova (1993) method

Burenkova (1993) proposed a method for estimating the particle size, d_{dv}, which divide a soil into a primary fabric, and a fraction of loose fine materials. The method is based on the equation

$$0.55\left(h''\right)^{-1.5} < \frac{d_{dv}}{d_{100}} < 1.87\left(h''\right)^{-1.5} \qquad \text{Eqn 3.13}$$

Figure 3.56 shows a plot of d_{dv}, predicted by equation 3.13 versus the size of the largest erodible particles estimated from the grain-size distribution curve matching technique for all unstable sample in the data set. The plot shows that d_{dv}, estimated for a soil sample by Burenkova's method, is, in most cases, significantly smaller, by as much as 3 log cycles, than the size of the largest erodible particles of the same soil. By definition, d_{dv} should not be smaller than the size of the largest erodible particles. The Burenkova (1993) method, therefore, does not provide a good estimate of the maximum size of erodible particles, or the fraction of erodible materials. It should, however, be noted that Burenkova (1993) method was based on the results of testing granular soils of maximum particle sizes of up to 20mm only, and with C_U values of less than 200. Some of the unstable samples in the data set have C_U values as high as 5700.

3.4.5 Summary

Factors influencing the internal instability of a soil

The fines content of a soil does not appear to have a significant influence on the suffusion characteristics of a soil. Broadly-graded silt-sand-gravel or clay-silt-sand-gravel mixtures having a gravel content of higher than 60% appear to be more susceptible to suffusion. Gap-graded silty/clayey gravels deficient in sand-sized particles also appear to be more susceptible to suffusion.

Soil density and the presence of clay up to the limit tested in the research program do not appear to have a significant influence on the suffusion characteristics of a soil.

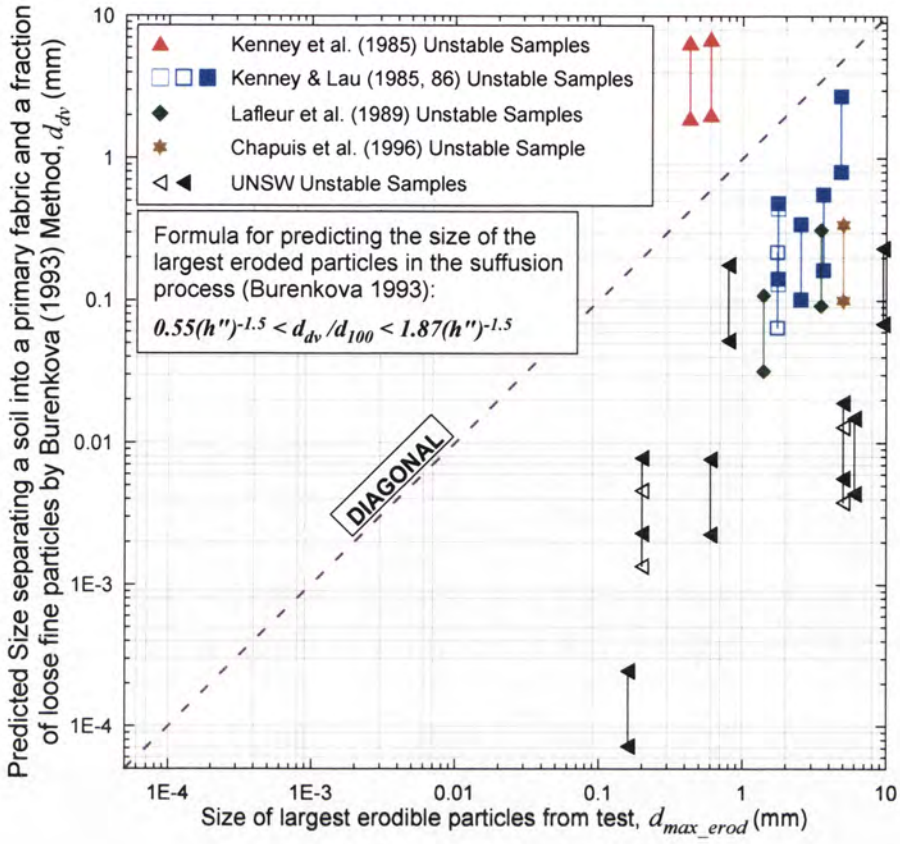

Figure 3.56: d_{dv} estimated by Burenkova (1993) method versus size of largest erodible particles estimated by curve matching technique (all unstable soil samples in data set).

Review of the currently available methods for predicting the internal instability of a soil

Six methods for predicting the suffusion characteristics of a soil have been examined and none has been found to be particularly suitable for predicting the internal stability of broadly-graded silt-sand-gravel or clay-silt-sand-gravel mixtures. Among the 6 methods studied, Kenney & Lau (1985, 86) method and Burenkova (1993) method appear to produce relatively more accurate predictions. Kenney & Lau's method apparently provides an upper bound, represented by $H = 1.3F$, for unstable materials. The method is conservative in that a lot of stable samples are classified as unstable. The lower boundary in Burenkova's method, represented by $h' = 0.76\log(h'') + 1$, is an approximately lower bound for stable materials. The method sometimes classifies unstable materials as stable, and is therefore not always conservative. Table 3.12

provides information on the accuracy of the various methods in the prediction of suffusion characteristics of all the soil samples in the data set.

Table 3.12: Accuracy of various methods used for the prediction of the internal stability of a soil.

Data Source	Data set			Correct predictions			Incorrect predictions	
	Total no. of samples	No. of non-suffusive samples	No. of suffusive samples	Non-suffusive	Suffusive	All soils	Non-suffusive soil predicted as suffusive	Suffusive soil predicted as non-suffusive
Method by U.S. Army Corps of Engineers (1953)								
UNSW (2004) data only	20	11	9	0 (0%)	9 (100%)	9 (45.0%)	11 (100%)	0 (0%)
All available data [1]	66	40	26	25 (62.5%)	19 (73.1%)	44 (66.7%)	15 (37.5%)	7 (26.9%)
Method by Istomina (1957)								
UNSW (2004) data only	20	11	9	0 (0%)	9 (100%)	9 (45.0%)	11 (100%)	0 (0%)
All available data [1]	66	40	26	25 (62.5%)	22 (84.6%)	47 (71.2%)	15 (37.5%)	4 (15.4%)
Method by Sherard (1979) [2]								
UNSW (2004) data only	20	11	9	0 (0%)	9 (100%)	9 (45.0%)	11 (100%)	0 (0%)
All available data [1]	66	40	26	22 (55.0%)	24 (92.3%)	46 (69.7%)	18 (45.0%)	2 (7.7%)
Kenney & Lau (1985, 1986) Method								
UNSW (2004) data only	20	11	9	2 (18.2%)	9 (100%)	11 (55.0%)	9 (81.8%)	0 (0%)
All available data [1]	66	40	26	26 (65.0%)	26 (100%)	52 (78.8%)	14 (35.0%)	0 (0%)
Burenkova (1993) Method								
UNSW (2004) data only	20	11	9	7 (63.6%)	7 (77.8%)	14 (70.0%)	4 (36.4%)	2 (22.2%)
All available data [1]	66	40	26	30 (75.0%)	19 (73.1%)	49 (74.2%)	10 (25.0%)	7 (26.9%)
Sun (1989) Method								
UNSW (2004) data only	20	11	9	6 (63.6%)	6 (77.8%)	12 (60.0%)	5 (36.4%)	3 (22.2%)
All available data	82	46	36	38 (82.6%)	21 (58.3%)	59 (72.0%)	8 (17.4%)	15 (41.7%)

Note : [1] Sun (1989) test data not included.

[2] Sherard (1979) method developed for identifying non-self filtering soils.

Review of the currently available methods for predicting the fraction and the size of the particles eroded by the suffusion process

A review of the methods for predicting the size of the largest erodible particles, namely the Lubochkov (1965) method and Burenkova (1993) method, indicates that these methods cannot provide accurate predictions.

3.5 ANALYSIS OF THE RESULTS OF UPWARD FLOW TESTS

3.5.1 Overview

This section presents the analysis of the results of the UF tests. The analysis aims at identifying factors which might influence the hydraulic gradient at which selective erosion of fine particles by the process of suffusion would initiate, and the critical hydraulic gradient at which the zero effective stress condition, indicated by the phenomenon of "boiling", would occur.

The factors being investigated are the coefficient of uniformity, C_U, the minimum stability number, *H/F* (Kenney and Lau 1984, 85, 86), the fines content and the plasticity of the fines, the porosity, the dry density of the soil, and gap-grading.

The analysis in Sections 3.5.3 to 3.5.6 attempts to identify the relationships, if any, between the hydraulic gradient causing suffusion and the variables, C_U, *H/F*, fines content, and porosity. The analysis in Sections 3.5.7 to 3.5.9 investigates the positive or negative effects of fines content, plasticity of fines, density and grading property on the hydraulic gradients causing suffusion. Rigorous quantitative/statistical analysis was not carried out due to limited test data (14 soil samples only), and the limited number of internally unstable soil samples (3 out of 14 samples) identified from the testing program.

Skempton and Brogan (1994) presented the test data on 4 soil samples (2 internally stable and 2 internally unstable). Apart from this, there was no relevant test data identified from the literature for similar upward flow tests. Grain-size distribution curves of the soil samples tested by Skempton and Brogan (1994) are shown in Figure 3.20 and Table 3.2 in Section 3.2.3.

A summary of the results of the UF tests is presented in Table 3.13. Detailed test records and plots of the results of all 18 UF tests on 14 soil samples are shown in Appendix P.

3.5.2 Definitions

The analysis presented in the section refers to various hydraulic gradients whose meanings are defined as follows:

Critical hydraulic gradient, i_c

It is the hydraulic gradient which causes a zero effective stress condition within a granular cohesionless material (Terzaghi 1948). It occurs when the seepage pore water pressure at a certain level equals the total overburden stress of the soil above that level. i_c is related to the porosity and the specified gravity of soil particles as defined by equation 3.10 in Section 3.2.7. For cohesionless materials, i_c is approximately equal to 1.

Initiating hydraulic gradient, i_{start}

It is defined by the Author as the minimum hydraulic gradient at which erosion of fine particles is first observed. In the UF test, i_{start} corresponded to the hydraulic gradient at which the first sign of erosion of fine particles, indicated by slight cloudiness in the flow, was observed.

Hydraulic gradient at boiling, i_{boil}

It is the minimum hydraulic gradient in the UF test, i_{boil} at which "boiling" at the surface of the test specimen was observed.

In granular cohesionless materials where intergranular forces are controlled by gravity effects, i_{boil} should theoretically be equal to i_c. In silt-sand-gravel or clay-silt-sand-gravel mixtures, i_{boil} observed may be higher than i_c as inter-particle electrochemical forces as well as gravity forces are acting among the soil particles. These electrochemical forces and the weight of the soil particles together act against the uplift force due to the hydraulic gradient. The limited diameter of the seepage cell may allow shear resistance to develop on the sides of the sample, giving artificially high resistance, and $i_{boil} > 1$ in some tests.

Table 3.13: Summary of the results of the 18 UF tests on 14 test samples.

Test sample	Upward flow seepage test no.	Dry density (t/m^3)			Water Content (%)		Average Porosity of test specimen η	Average Specific Gravity of specimen G_s	Theoretical Critical Hydraulic Gradient [1] $(G_s-1)(1-\eta)$	Hydraulic Gradient during Test [2]				Internal Stability observed in Downward Flow seepage test [3]	Coeff. of Uniformity C_U	Coeff. of Curvature C_C
		Standard Max.	Test specimen		Standard Optimum Water Content	Test specimen				Start loss of fines	Extreme cloudiness	Boiling	Highest reached			
			Relative to Max.	Actual												
1	1	2.32	94.1%	2.18	7.7	7.7	0.169	2.62	1.35	2.20	2.54	2.32	2.54	S	108	1.7
	2		89.4%	2.07		7.7	0.210		1.28	0.78	1.17	1.95	2.77			
2	3	2.18	94.5%	2.06	8.9	8.9	0.214	2.62	1.27	0.99	1.38	2.93	2.95	S	194	0.9
3	4	1.97	93.8%	1.85	11.6	11.6	0.292	2.61	1.14	0.73	1.12	Not observed	1.12	S	39	0.4
4R	5	2.23	94.5%	2.11	9.3	9.3	0.191	2.60	1.29	0.80	2.19	3.58	3.98	S	21	2.4
5	13	2.12	94.8%	2.01	8.5	8.8	0.218	2.57	1.23	3.17	3.77	3.97	4.76	S	58	1.2
	14		89.6%	1.90		8.8	0.261		1.16	0.18	Not observed	1.54	1.57			
6	10	2.23	94.9%	2.12	7.2	7.5	0.179	2.58	1.30	Not observed	Not observed	Not observed	5.20	S	734	9.5
7	16	2.05	95.4%	1.95	9.8	10.0	0.246	2.59	1.20	Not observed	Not observed	Not observed	4.80	S	1789	1.5
9	6	1.94	95.0%	1.84	6.3	6.0	0.315	2.68	1.15	0.14	Not observed	Not observed	1.31	S	115	53.2
10	7	2.22	94.8%	2.10	8.4	8.4	0.217	2.69	1.32	0.59	0.78	2.52	2.52	U	304	40.3
	8		90.1%	2.00		8.4	0.256		1.26	0.37	0.94	1.12	1.13			
11	9	1.91	95.0%	1.81	12.1	12.4	0.319	2.67	1.14	0.76	0.68	0.88	0.88	P	493	0.03
13	11	1.92	95.2%	1.83	7.1	6.9	0.318	2.68	1.15	Not observed	Not observed	Not observed	1.12	S	111	55.8
14A	12	2.04	96.0%	1.96	11.1	10.3	0.270	2.68	1.23	0.77	Not observed	3.92	3.92	U (slightly)	1186	452
	15		90.1%	1.84		11.2	0.315		1.15	0.17	0.56	1.33	2.51			
15	17	2.09	94.9%	1.98	8.2	8.3	0.228	2.57	1.21	0.80	Not observed	3.18	4.76	U	5709	0.4
RD	18	1.87	96.0%	1.79	13.3	13.1	0.364	2.82	1.16	Not observed	Not observed	Not observed	4.20	S	53	9

Notes : 1. I_c is the theoretical hydraulic gradient, named as Critical Hydraulic Gradient, at which a cohesionless soil reaches zero effective stress condition due to high pore water pressure.

2. "Start loss of fines" describes the condition when fine soil particles started to be carried out of the test sample by the seepage flow.
"Extreme cloudiness" describes the conditions when many fine soil particles were washed out from the test sample, giving the effluent a very cloudy appearance.
"Boiling" describes the phenomenon when the soil behaves like a boiling liquid due to the effective stress reducing to zero under a high pore pressure condition.
"Highest reached" is the highest hydraulic gradient recorded for the test. It is the highest gradient that could be provided by the test apparatus.

3. "S" stands for internally stable; "U" stands for internally unstable; "P" stands for piping.

3.5.3 Relationship between the hydraulic gradient causing erosion and the coefficient of uniformity of the soil

Figure 3.57 and Figure 3.58 show plots of i_{start} and i_{boil} against the C_U based on the results of UF tests on 14 soil samples. The 4 samples tested by Skempton and Brogan (1994) are also included in the Figures. The plots reveal the following:

- there are considerable scattering of the test data, and a definite relationship between i_{boil} and C_U, and between i_{start} and C_U cannot be identified;
- i_{start} values are less than 1.0 for all soils identified in the DF tests to be internally unstable, with values as low as 0.2. This is consistent with Skempton and Brogan data;
- most internally stable soils also began to erode at gradients less than 1.0. The process of erosion for the internally stable soils is probably "backward erosion", and not suffusion;
- the i_{boil} data are meaningless because they are influenced by the test set up as described above.

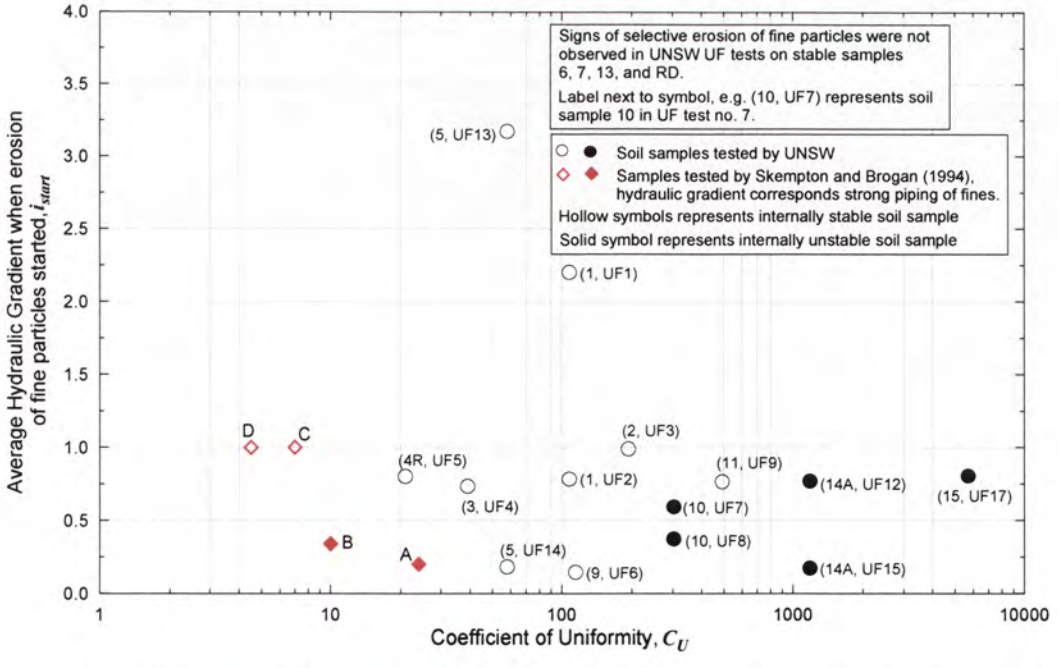

Figure 3.57: Average hydraulic gradient across the test sample at which erosion of fine particles started against coefficient of uniformity.

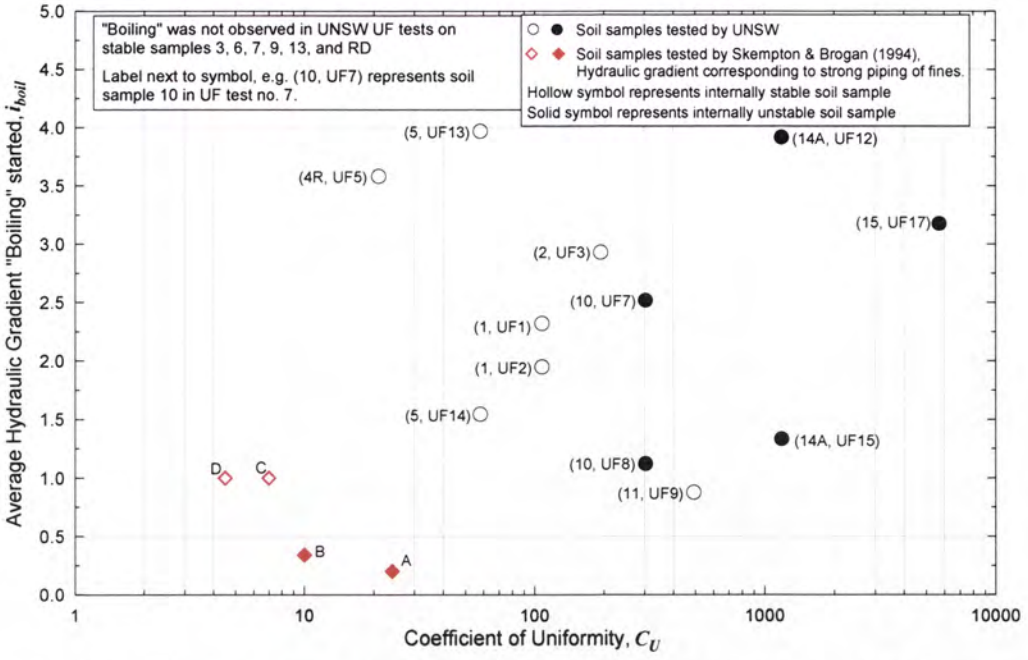

Figure 3.58: Average hydraulic gradient across the test sample at which "boiling" started against coefficient of uniformity.

From Table 3.13, it can be seen that while loss of fine particles begins at low gradients i_{start}, extreme cloudiness only occurs at less than/near the theoretical critical gradient, i_c, for internally unstable soils, and did not occur in two of the internally unstable soils.

3.5.4 Relationship between the hydraulic gradient causing erosion and the minimum stability number H/F of the soil

Based on the results of 4 upward flow seepage tests, Skempton and Brogan (1994) proposed that internally unstable sand-gravel soils, which have minimum stability number, *H/F*, less than 1, would have critical hydraulic gradients, i_c, significantly less than 1, and that transition of i_c from very low to normal values would take place across the boundary represented by $H/F = 1$. Skempton and Brogan's proposition is examined by plotting hydraulic gradient against *H/F* ratio as in Figure 3.59 using the results of the UF tests on 14 soil samples. The 4 samples tested by Skempton and Brogan (1994) are also included in the plot in Figure 3.59.

The plot in Figure 3.59 show considerable scattering of the test data, and a definite relationship between i_{start} and H/F cannot be identified. Skempton and Brogan (1994) proposition that hydraulic gradients causing erosion are dependent on the H/F ratio does not seem to apply to silt-sand-gravel or clay-silt-sand-gravel mixtures.

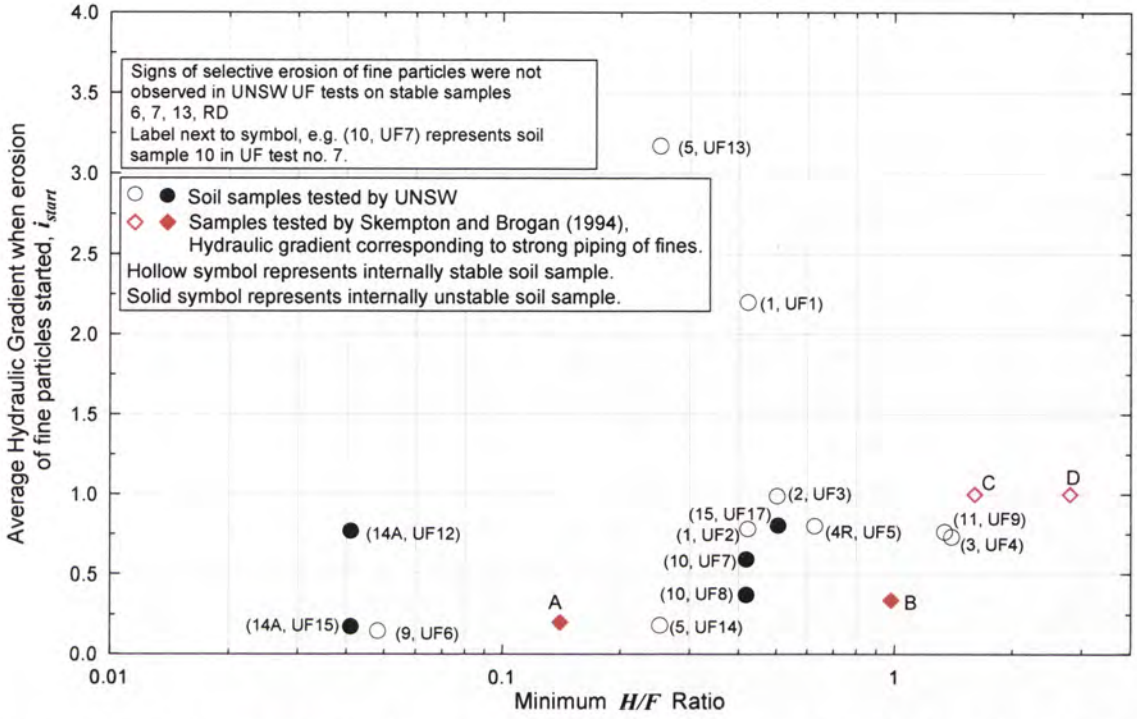

Figure 3.59: Average hydraulic gradient across the test sample at which erosion of fine particles started against Minimum H/F ratio.

3.5.5 Relationship between the hydraulic gradient causing erosion and the fines content of the soil

The fines in a soil are believed to influence the resistance of a soil against internal erosion, as the presence of fines, in particular clayey fines, would provide additional inter-particle electrochemical attraction among the fine soil particles. i_{start} is plotted against fines content in Figure 3.60, and it can be seen that there is no relationship. The plots also do not show any trend that a higher fines content might increase the hydraulic gradients causing suffusion.

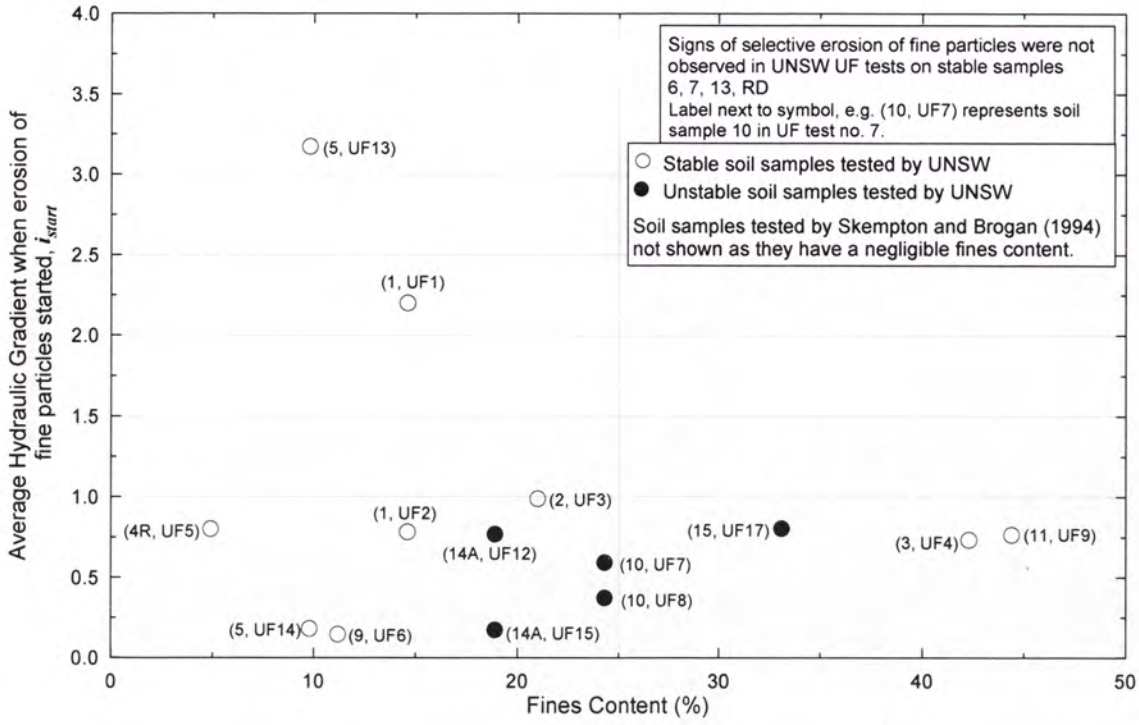

Figure 3.60: Average hydraulic gradient across the test sample at which erosion of fine particles started against fines content (% finer than 0.075mm).

3.5.6 Relationship between the hydraulic gradient causing erosion and the porosity of the soil

As explained in Section 3.5.2, the critical hydraulic gradient, i_c, for cohesionless soils is a function of soil porosity, η, and the specific gravity of the soil grains, G_s. It is, therefore, possible that η should also have an influence on the hydraulic gradients causing erosion in silt-sand-gravel and clay-silt-sand-gravel mixtures.

Figure 3.61 shows a plot of i_{start} against porosity. The plot shows a general trend that i_{start} is lower the higher the porosity of the soil. Scattering of the data is, however, still quite significant so that a definite mathematical relationship between the hydraulic gradients and the porosity cannot be identified.

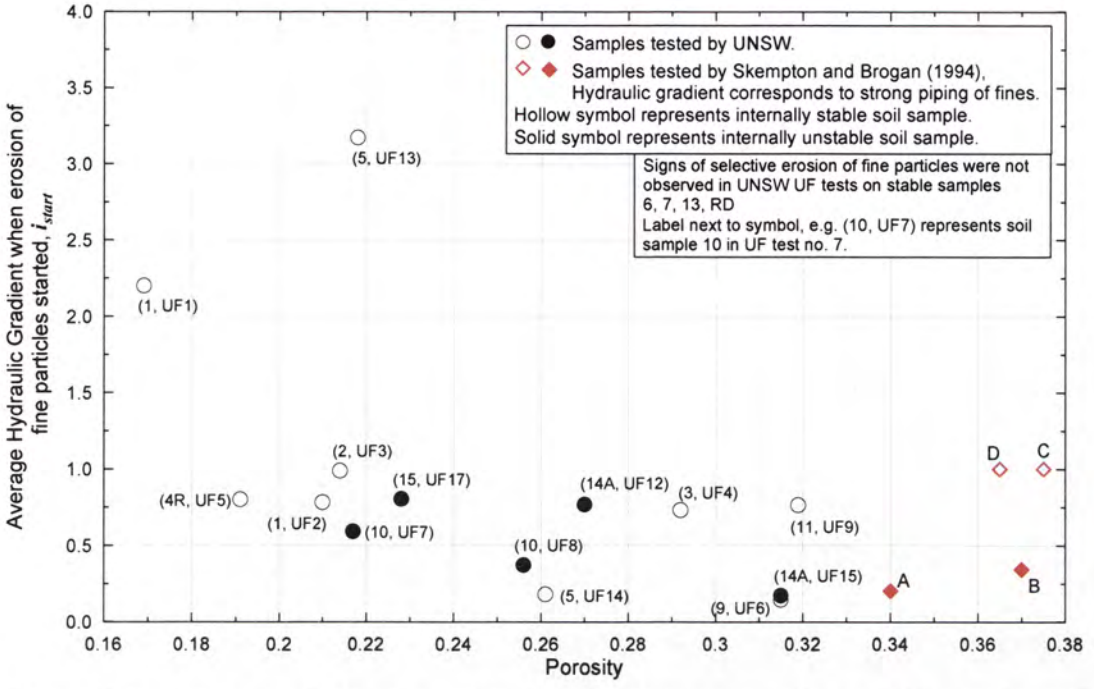

Figure 3.61: Average hydraulic gradient across the test sample at which erosion of fine particles started against porosity.

3.5.7 Effects of plastic fines on the hydraulic gradient causing erosion

Figure 3.62 shows a plot of i_{start} against fines content of the non gap-graded soil samples. On the plot, the soil samples are classified into two groups, namely the silt-sand-gravel mixtures (i.e. soils without plastic fines), and the clay-silt-sand-gravel mixture (i.e. soils with plastic fines). The plot shows that the clay-silt-sand-gravel mixtures have generally higher i_{start} than the silt-sand-gravel mixtures having similar fines content.

Figure 3.63 shows a plot similar to Figure 3.62 but for gap-graded soil samples. The gap-graded clay-silt-sand-gravel mixtures show higher i_{start} than the gap-graded silt-sand-gravel mixtures having similar fines content.

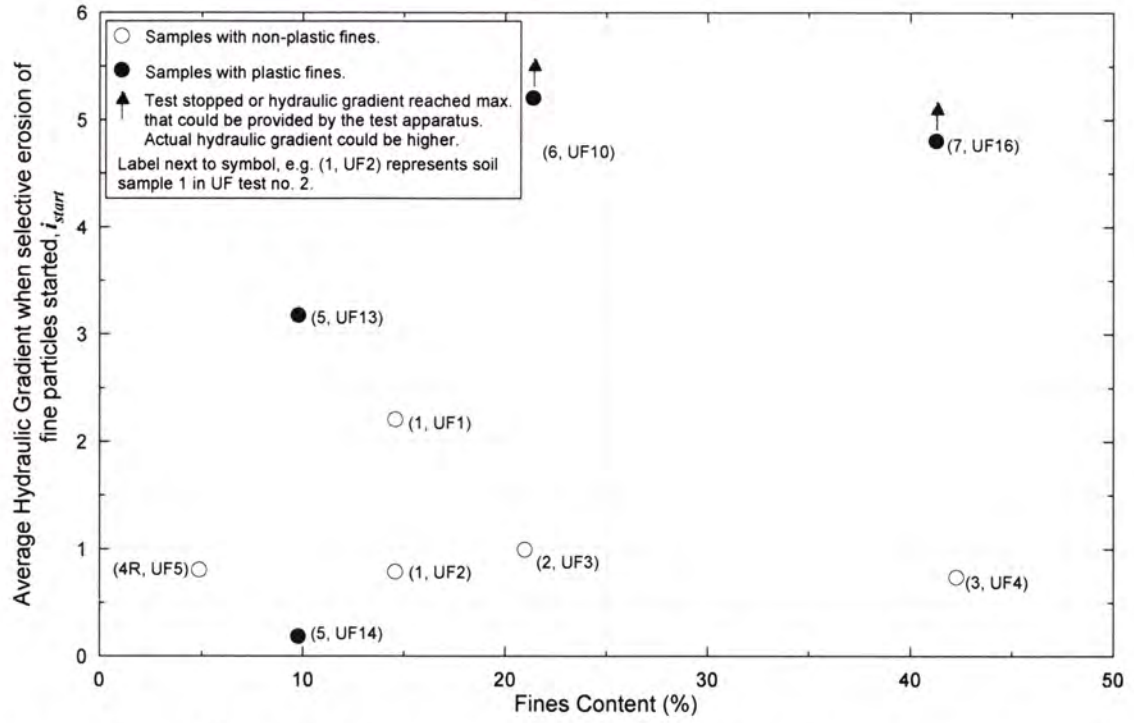

Figure 3.62: Effects of fines content and plasticity of fines on average hydraulic gradient when erosion of fine particles started in non gap-graded samples.

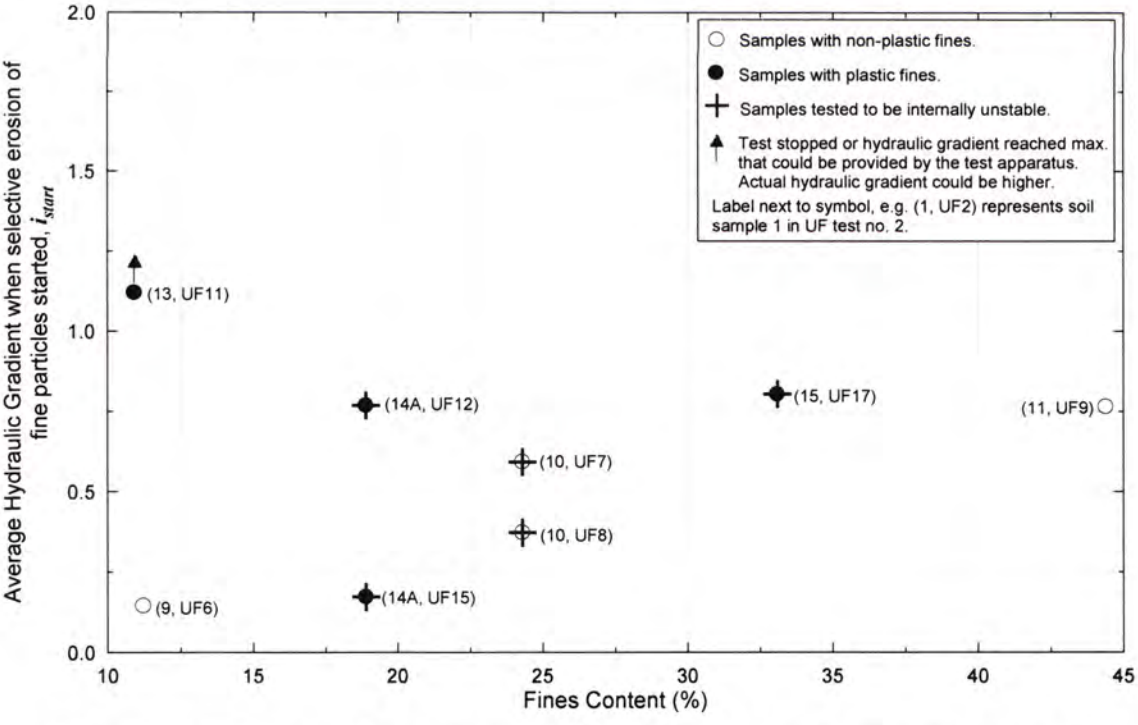

Figure 3.63: Effects of fines content and plasticity of fines on average hydraulic gradient when erosion of fine particles started in gap-graded samples.

The above observations suggest that the presence of clayey fines in a soil might improve its resistance against initiation of suffusion. The plots, however, show no obvious relationship between the fines content and the hydraulic gradients causing erosion.

3.5.8 Effects of dry density on the hydraulic gradient causing erosion

The effects of the soil's dry density on the hydraulic gradient i_{start} causing erosion are revealed by the plot in Figure 3.64. Soil density is expressed as a percentage of the Standard Maximum Dry Density (SMDD). Figure 3.64 shows that soil samples compacted to 95% SMDD have significantly higher i_{start} than the same soil samples compacted to a lower density of 90% SMDD. In some soil samples (e.g. Sample 5), increasing the soil density from 90% to 95% SMDD increases i_{start} significantly from approximately 0.2 to 3.2.

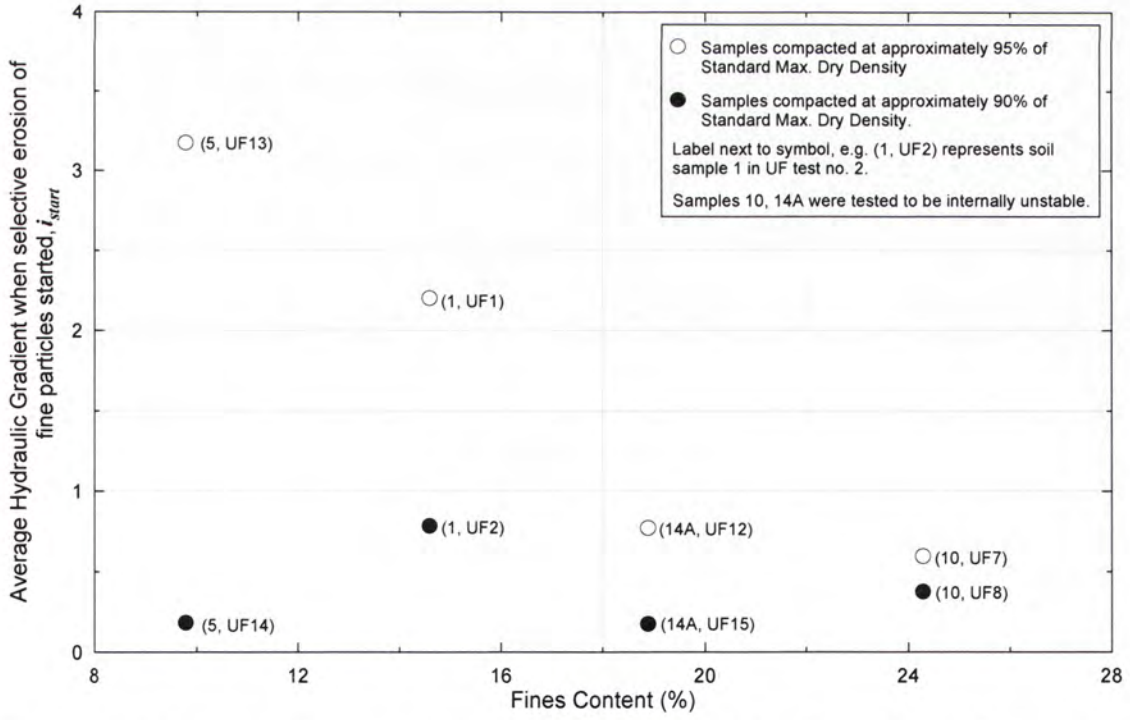

Figure 3.64: Effects of compaction density on average hydraulic gradient when erosion of fine particles started.

3.5.9 Effects of gap-grading on the hydraulic gradient causing erosion

The plot in Figure 3.65 shows the effects of gap-grading of a soil on the hydraulic gradient i_{start} causing erosion. The plot shows that gap-graded soils, in general, have relatively lower i_{start} that non gap-graded soil samples having similar fines content.

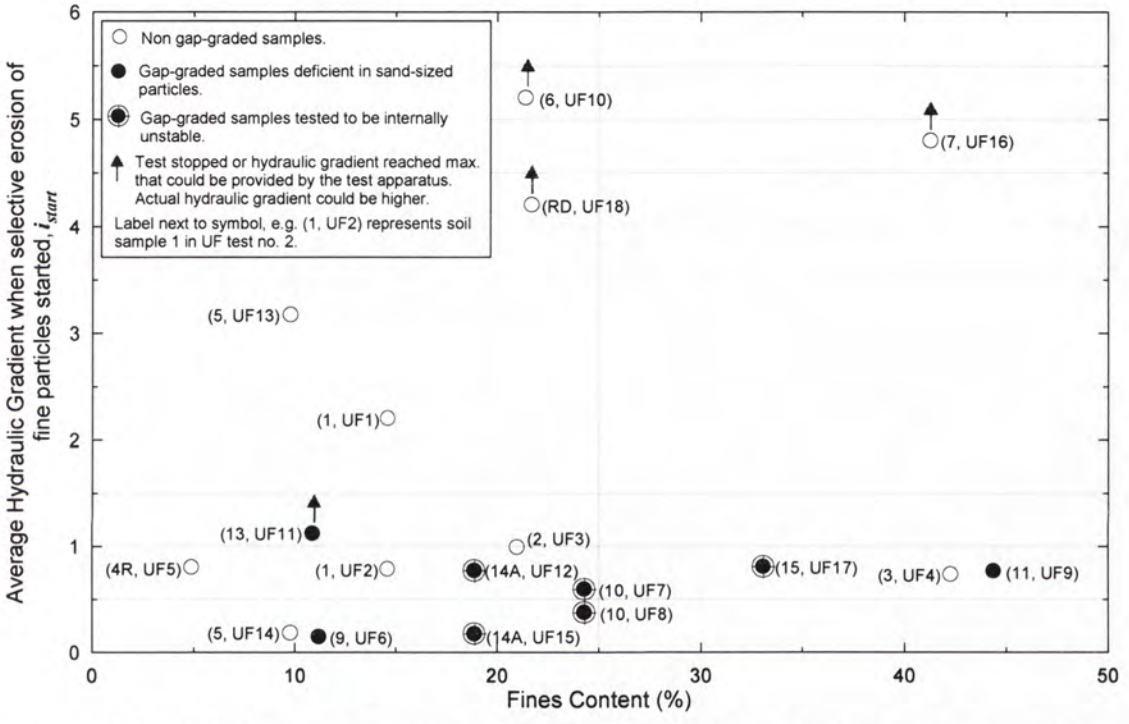

Figure 3.65: Effects of gap-grading on average hydraulic gradient when erosion of fine particles started.

3.5.10 Summary

The results of 18 UF tests on 14 silt-sand-gravel and clay-silt-sand-gravel mixtures, including 3 internally unstable mixtures, have been analysed graphically. A summary of the findings is as follows:

- The i_{boil} data from the tests are not reliable because they are affected by the test setup geometry, with significant shear resistance developing between the soil and the sides of the test cylinder.
- Selective erosion of fine soil particles begins at gradients, i_{start}, less than the theoretical critical gradient, i_c, for all internally unstable soils, and for many internally stable soils. This erosion develops at relatively minor rates, and even in the internally unstable soils, did not lead to "extreme cloudiness" condition when erosion would be obvious.
- No definite mathematical relationship has been identified between the hydraulic gradient i_{start} and the Coefficient of Uniformity, the minimum *H/F* ratio and the fines content.
- There appears to be a general trend that soils with higher porosity would start to erode at lower hydraulic gradients. There is, however, considerable scattering of data that a reliable mathematical relationship cannot be derived between the two variables.
- Soils with clayey fines appear to erode at relatively higher hydraulic gradients than soils having similar fines contents but without clayey fines.
- The density of a soil has a significant effect on the hydraulic gradient i_{start}. The higher the soil density, the higher the i_{start}, given that the fines content of the soils are the same.
- Gap-graded soils erode at relatively lower hydraulic gradient i_{start} than non gap-graded soils with similar fines content.

3.6 PROPOSED METHODS FOR PREDICTION OF INTERNAL INSTABILITY

3.6.1 Fine particles and the primary soil fabric in an internally unstable soil

Phase relationship between the erodible fine particles and the primary soil fabric in an internally unstable soil

As described in Section 3.2.6, one of the geometrical criteria (Criterion 2) for suffusion to occur requires that the amount of fine soil particles be less than enough to fill the voids of the primary fabric of the soil, or else the assumption of a primary soil fabric comprising of the coarse soil particles only will become invalid. This geometrical criterion implies that a certain phase relationship exists between the primary fabric and the fine erodible particles of the soil. This is illustrated by the phase diagram in Figure 3.66.

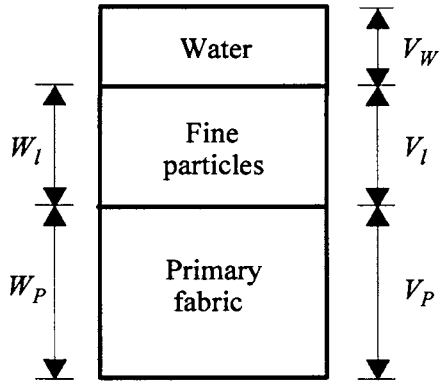

Figure 3.66: Phase diagram showing volume and weight relationships between the primary fabric, and the fine erodible particles in an internally unstable soil.

The meanings of the various symbols in Figure 3.66 are as follows:

V_P: Volume of the coarse particles forming the primary fabric of the soil;

V_l: Volume of the fine erodible particles of the soil;

W_P: Weight of the coarse particles forming the primary fabric of the soil;

W_l: Weight of the fine erodible particles of the soil;

f_P: Weight fraction of the primary fabric of the soil, and is equal to $W_P/(W_P+W_l)$;

f_l: Weight fraction of the fine particles of the soil, and is equal to $W_l/(W_P+W_l)$;

e_P: Void ratio of the primary fabric of the soil;

e_l: Void ratio of the fine erodible particles of the soil.

Since the amount of the fine particles are insufficient to fill up all the voids of the primary fabric, the void ratio, e_P, of the primary fabric, assuming that the fine particles are removed, is given by

$$e_P = \frac{V_w + V_l}{V_P} \text{ or } V_l = e_P V_P - V_W \qquad \text{Eqn 3.14}$$

The void ratio, e_l, of the fine erodible particles packed within the voids of the primary fabric is given by

$$e_l = \frac{V_W}{V_l} \quad \text{or} \quad V_W = e_l V_l \qquad \text{Eqn 3.15}$$

Substituting equation 3.15 into equation 3.14 gives

$$V_l = e_P V_P - e_l V_l \quad \text{or} \quad V_l(1+e_l) = e_P V_P \qquad \text{Eqn 3.16}$$

Dividing both sides of equation 3.16 by $(V_l + V_p)$ gives

$$\frac{V_l}{V_l + V_P}(1+e_l) = \frac{V_P}{V_l + V_P} e_P \qquad \text{Eqn 3.17}$$

If the fine particles and the coarse particles have similar particle densities, the volume ratios can be replaced by weight ratios, and equation 3.17 can be replaced by

$$\frac{W_l}{W_l + W_P}(1+e_l) = \frac{W_P}{W_l + W_P} e_P$$

or simply

$$f_l(1+e_l)=f_P e_p=(1-f_l)\,e_P \qquad \text{Eqn 3.18}$$

Rearranging terms in equation 3.18 gives

$$f_l=\frac{e_P}{1+e_l+e_P} \qquad \text{Eqn 3.19}$$

Equation 3.19 relates the fraction of fine particles of an internally unstable soil to the void ratios of the fine particles and the primary fabric. A similar relationship was presented by Kenney & Lau (1985), as in equation 3.20.

$$f_P \geq \frac{1}{1+e_P(1-\eta_l)} \qquad \text{Eqn 3.20}$$

The symbol, η_l, in equation 3.20 represents the porosity of the fine particles. Equation 3.19 is essentially the same as equation 3.20, but presented in a slightly different form.

Kenney & Lau (1985) suggested that the narrowly-graded (NG) materials tested by them had a dense primary fabric (e_P = 0.7), and loose fine particles (η_l = 0.4), giving $f_P \geq$ 0.7 (i.e. $F <$ 0.3). For the widely-graded (WG) materials tested by them, Kenney & Lau (1985) suggested e_P = 0.4, and η_l = 0.4, giving $f_P \geq$ 0.8 (i.e. $F <$ 0.2). Based on this assessment, Kenney & Lau (1985, 86) stated that their proposed boundary (i.e. $H = 1.0F$) between stable and unstable soils only applied within the region $F <$ 0.3 for NG soils, and $F <$ 0.2 for WG soils (refer Section 3.2.3). Kenney & Lau (1985) implied that the erodible fine fraction of the unstable soils tested by them did not exceed 0.3 (for NG soils), and 0.2 (for WG soils). For unstable soils whose void characteristics are different to those soils tested by Kenney & Lau, we would expect that the fraction of erodible particles would deviate from the values 0.3 or 0.2 predicted by Kenney & Lau (1985).

Maximum possible fraction of erodible fine particles in an internally unstable soil

Typical values of maximum and minimum void ratios for granular soils are given in Table 3.14. A maximum value of f_l is obtained when the coarse particles in an internally unstable material are loosely packed, whilst the fine particles are closely

packed inside the voids formed by the coarse particles. Assume that an unstable material is made up of uniform spheres, and that the primary fabric formed by the larger spheres is loosely packed (e_P = 0.92), whereas the smaller spheres partially filling the voids of the primary fabric is densely packed (e_l = 0.35), the fraction of erodible fine particles predicted by equation 3.19 will be f_l = 0.405 (say 40%). For an unstable widely-graded silt-sand-gravel mixture with maximum e_P = 0.85 (assumed silty sand and gravel), and minimum e_l = 0.3 (assume silty sand), f_l predicted by equation 3.19 is 0.395 (say 40%). In reality, the primary fabric of an internally unstable soil is expected to have lower e_P values due to compaction by surcharge, and the fine particles are expected to be less densely packed with higher e_l values, resulting in f_l lower than 40%.

The above examples indicate that the maximum possible fraction of loose fine particles, f_l, erodible in the suffusion process would very unlikely be higher than 40% (i.e. $F \leq 0.4$) of the total weight of an internally unstable granular soil. UNSW test data and available test data from the literature indicate a maximum F value of not greater than 30% (refer to Figure 3.39 in Section 3.4.2). The proposed limiting value for suffusive soils is expected to remain valid for unstable soils with small clay contents.

Methods for predicting the size of the largest particles erodible by the suffusion process should consider the above proposed limitation that the maximum possible fraction of loose fine particle erodible in the process should not be greater than 40%.

Soils with higher proportions of fine particles will not be susceptible to internal instability and suffusion, but may be subject to backward erosion, and may not self filter.

Table 3.14: Maximum and minimum densities for granular soils (from Lambe & Whitman 1979).

Description	Void Ratio		Porosity (%)		Dry Unit Weight (kN/m³)	
	e_{max}	e_{min}	n_{max}	n_{min}	$\gamma_{d\,min}$	$\gamma_{d\,max}$
Uniform spheres	0.92	0.35	47.6	26.0	—	—
Standard Ottawa sand	0.80	0.50	44	33	14.5	17.3
Clean uniform sand	1.0	0.40	50	29	13.0	18.5
Uniform inorganic silt	1.1	0.40	52	29	12.6	18.5
Silty sand	0.90	0.30	47	23	13.7	20.0
Fine to coarse sand	0.95	0.20	49	17	13.4	21.7
Micaceous sand	1.2	0.40	55	29	11.9	18.9
Silty sand and gravel	0.85	0.14	46	12	14.0	22.9

3.6.2 Proposed methods for predicting internal instability

Combined Kenney and Lau (1985, 1986) and Burenkova (1993)

As discussed in Section 3.4.5, most of the currently available methods are unsatisfactory in predicting the internal stability of widely-graded silt-sand-gravel and clay-silt-sand-gravel mixtures. Among the various predictive methods introduced, the methods by Kenney and Lau (1985, 86), and Burenkova (1993) are comparatively more accurate. The two methods have both merits and demerits. Kenney and Lau's method is accurate in identifying stable soils, but tends to be conservative in that soils identified as internally unstable have a good chance of being internally stable. Burenkova's method is more accurate than Kenney and Lau's method in predicting the suffusive characteristics of the UNSW soil samples, and is less conservative than Kenney and Lau's method. Nevertheless, Burenkova's method is not always conservative in that some unstable soils are predicted as stable. The two methods supplement each other when used together, so if a soil is unstable by both methods, it is most likely unstable, and if it is stable by both methods, it is likely stable. Table 3.15 classifies 64 soil

samples in the data set according to the results of the assessments by both the Kenney & Lau (1985, 86) method and the Burenkova (1993) method. The 64 soil samples exclude samples B1, and D1 in UNSW data set and Sun (1989) test samples. As shown in Table 3.15, 16 internally unstable soil samples and 3 stable soil samples are classified in the group represented by $H < F$, and $h' \leq 0.76\log(h'') + 1$, implying that 84.2% (i.e. 16 out of a total of 19 samples) of the soil samples in this group are internally unstable. Table 3.15 also shows that no internally unstable soil sample, but 15 stable soil samples are classified in the group represented by $H \geq 1.3F$ and $h' > 0.76\log(h'') + 1$, implying that 0% (0 out of a total of 15 soil samples) of the soil samples in this group is internally unstable.

Table 3.15: Classification of all test samples using Kenney & Lau (1985, 1986) method and Burenkova (1993) method.

Classification of test results for 64 soil samples			Kenney & Lau (1985, 86) method			Row total
			$H < F$ (Unstable predicted)	$F \leq H < 1.3F$ (Marginal)	$H \geq 1.3F$ (Stable predicted)	
Burenkova (1993) method	$h' \leq 0.76\log(h'') + 1$ (Unstable predicted)	Un-stable	16 [Note 1] (84.2%)	3 (60.0%)	0 (0%)	19
		Stable	3 [Note 1]	2	5	10
	$h' > 0.76\log(h'') + 1$ (Stable predicted)	Un-stable	4 (26.7%)	1 (20.0%)	0 (0%)	5
		Stable	11	4	15	30
Column Total :			34	10	20	64

Notes

(1): 16 unstable soil samples and 3 stable soil samples were assessed to be in the group represented by $H < F$ and $h' \leq 0.76\log(h'') + 1$. The percentage in bracket is the probability of finding an unstable soil in this group is 84.2% (i.e. 16 out of 19 samples).

(2): F is the fraction by weight of those soil particles finer than particle size d, and H is the fraction between size d and $4d$ (Kenney & Lau 1985, 86).

(3): h' is equal to d_{90}/d_{60}, and h'' is equal to d_{90}/d_{15} (Burenkova 1993).

The Author believes that at this stage there is insufficient test data to set up deterministic rules to classify a soil as either internally unstable or stable. It is more

practical to assess the likelihood of internally instability of a soil by considering the results of classification of the soil using both Kenney and Lau (1985, 86) method and Burenkova (1993) method (or the probabilistic method outlined later in this Section). The proposed scheme for assessing the likelihood of internal instability, as shown in Table 3.16, is based on the results of classification of 64 soil samples in Table 3.15. Based on Table 3.16, a soil is unlikely to be internally unstable if assessment by Kenney & Lau (1985, 86) method indicates $H < F$, and assessment by Burenkova's method indicates $h' > 0.76\log(h'') + 1$. The soil is very unlikely to be internally unstable if $H \geq 1.3F$ for whatever values of h'.

Table 3.16: Method for assessing the likelihood of internal instability of silt-sand-gravel and clay-silt-sand-gravel mixtures using Burenkova (1993) and Kenney and Lau (1985, 1986) methods.

Likelihood of Internal Instability		Kenney & Lau (1985, 1986) method		
		$H < F$	$F \leq H < 1.3F$	$H \geq 1.3F$
Burenkova (1993) method	$h' \leq 0.76\log(h'') + 1$	Likely - Very likely	Neutral - Likely	Very unlikely
	$h' > 0.76\log(h'') + 1$	Unlikely	Very unlikely - Unlikely	Very unlikely

Prediction of internal instability by the probabilistic approach

The distribution of test data representing internally unstable and stable soils as in a h' versus $\log(h'')$ plot of Burenkova (1993) method reveals the pattern that soils having a high value of h'', but a low value of h' are more likely to be internally unstable, whereas soils having high values of h' are less likely to be internally unstable. The pattern suggests that contours for predicting the probability of internal instability can be calculated using a statistical approach. Figure 3.67 and Figure 3.68 show probability contours obtained by logistic regression, using h' and $\log(h'')$ as predicting variables. The contours in Figure 3.67 are based on all available test data excluding the outliers B1, and D1 in the UNSW data set, and the test data by Sun (1989). Figure 3.67 is proposed to be applied to silt-sand-gravel and clay-silt-sand-gravel mixtures with a

plasticity index less than 12% and less than 10% clay size fraction (% passing 0.002mm). The contours are represented by the following equations:

$$p_f = \frac{e^Z}{1+e^Z} \qquad \text{Eqn 3.21}$$

$$Z = 2.378\log(h'') - 3.648h' + 3.701 \qquad \text{Eqn 3.22}$$

Where p_f: is the predicted probability of internal instability;

Z: is the dependent variable of the logistic regression equation;

h': is defined as d_{90}/d_{60} by Burenkova (1993); and

h'': is defined as d_{90}/d_{15} by Burenkova (1993).

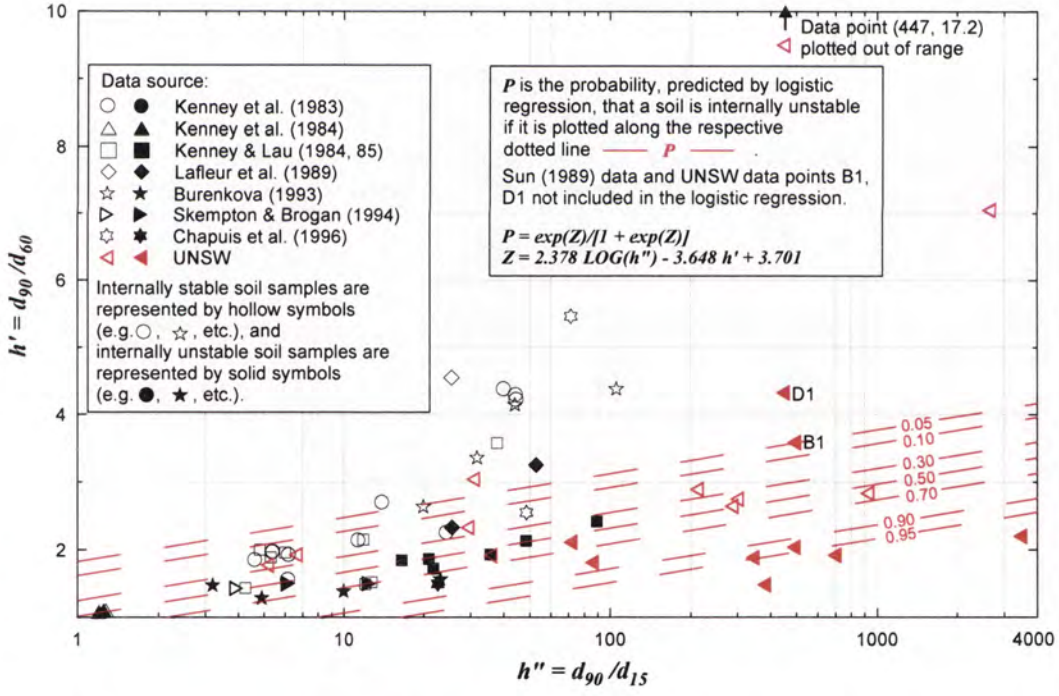

Figure 3.67: Contours of the probability of internal instability for silt-sand-gravel soils and clay-silt-sand-gravel soils of limited clay content and plasticity.

The contours in Figure 3.68 are based on all available test data excluding the test data with kaolin fines by UNSW and the data by Sun (1989). Figure 3.68 is proposed to be

applied to sand-gravel mixtures. The contours in Figure 3.68 are represented by the logistic regression equation 3.23.

$$Z = 3.875\log(h'') - 3.591h' + 2.436 \qquad \text{Eqn 3.23}$$

The contours in Figure 3.68 predict higher probabilities of internal instability than those in Figure 3.68 due to the reason that the more erosion resistant clayey/silty soil samples in the UNSW data set have been excluded.

Burenkova (1993) had a second zone (Zone III) of suffusive soils (see Figure 3.17). The Author did not test soils in this range, but given they would represent soils with a concave downwards shape. Such soils are not common but the Author would expect these to be internally stable.

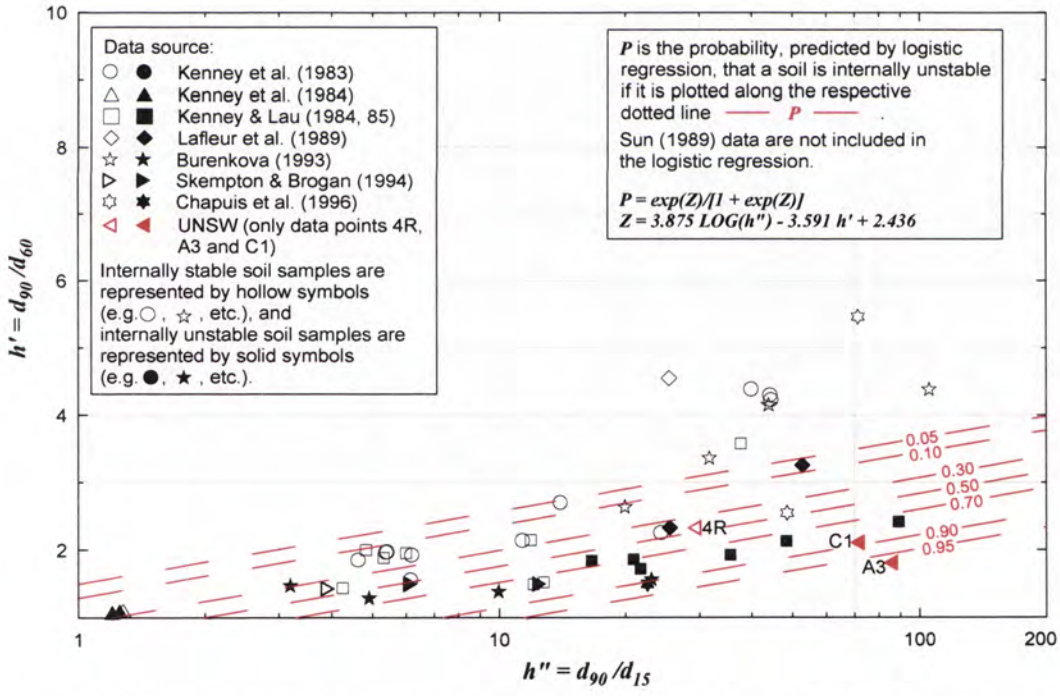

Figure 3.68: Contours of the probability of internal instability for sand-gravel soils with less than 10% non-plastic fines passing 0.075 mm.

3.6.3 Proposed methods for estimating the maximum fraction of erodible particles and the size of the largest erodible soil particles

Overview

It is useful to estimate the size of the largest erodible soil particles, and the fraction that is lost by suffusion in order to assess the changes in the permeability and the filtering ability of the soil. In Section 3.4.4 Figure 3.56, the Burenkova (1993) method for estimating the particle size, d_{dv}, that divides a soil into a primary fabric and a loose fraction, has been shown to underestimate the size of the largest particles eroded by suffusion. The Lubochkov (1965) method (refer to Figure 3.55) was shown to overestimate the size of the largest particles eroded by the suffusion process. This section explores other feasible methods for estimating the size of the largest particles eroded by suffusion.

Method based on the stability number, H/F

An alternative for estimating the maximum fraction of erodible particles is based on Kenney & Lau (1984, 85, 86) method with slight modifications. The procedure is as follows:

Step 1: Prepare a *H-F* plot based on the grain-size distribution curve of a soil.

Step 2: Identify a maximum F value, denoted by $\hat{F}_{\max}$, smaller than 0.4 at which the stability number, H/F, is smaller than 1.3.

Step 3: $\hat{F}_{\max}$ is an estimate of the maximum fraction of erodible particles, and the particle size, $\hat{d}_{\max\_erod}$, corresponding to $\hat{F}_{\max}$ is an estimate of the size of the largest erodible particles.

The above method has employed Kenney & Lau (1984, 1985, 1986) concept that the particles of size d or below will not be adequately protected against erosion if there is insufficient materials within the size range d to $4d$. Whilst Kenney and Lau imposed the criterion that F should be less than 0.3 (for materials with C_U <3), and 0.2 (for materials with C_U >3), the proposed method relaxes the criterion to F < 0.4 due to reasons explained in Section 3.6.1.

The predicted maximum erodible fraction, $\hat{F}_{\max}$ for 20 soil samples are plotted against the maximum erodible fraction, $F_{\max\_erod}$, assessed by comparing the post-test grain-size distribution curves to the initial grain-size distribution curves of the soil samples in Figure 3.69. The plot reveals a reasonably good correlation between the predicted values, $\hat{F}_{\max}$, and the $F_{\max\_erod}$ values assessed from test data.

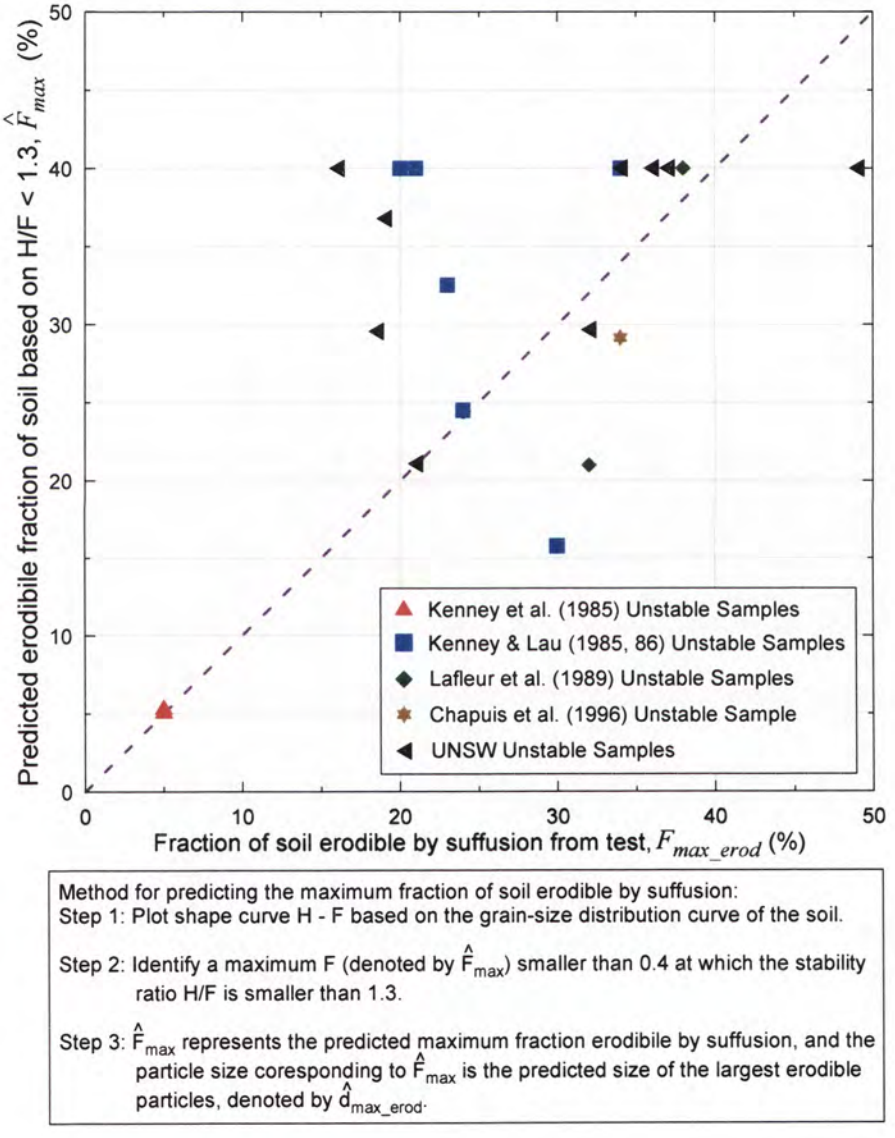

Figure 3.69: Predicted maximum fraction of erodible particles based on $H/F < 1.3$ versus maximum fraction of erodible particles assessed from test data.

The predicted size of the largest erodible particles, $\hat{d}_{\max\_erod}$, are plotted against the size of the largest erodible particles, $d_{\max\_erod}$, assessed by comparing the post-test grain-size distribution curves to the initial grain-size distribution curves of the soil samples in Figure 3.70. The plot reveals that the predicted sizes are, in general, within 1.5 log cycle of the respective particle sizes assessed from test data.

The plots in Figure 3.69 and Figure 3.70 indicate that the proposed method based on Kenney and Lau (1984, 1985, 1986) *H-F* approach provides satisfactory estimates of the maximum fraction of erodible particles, and the size of the largest erodible particles in an internally unstable soil.

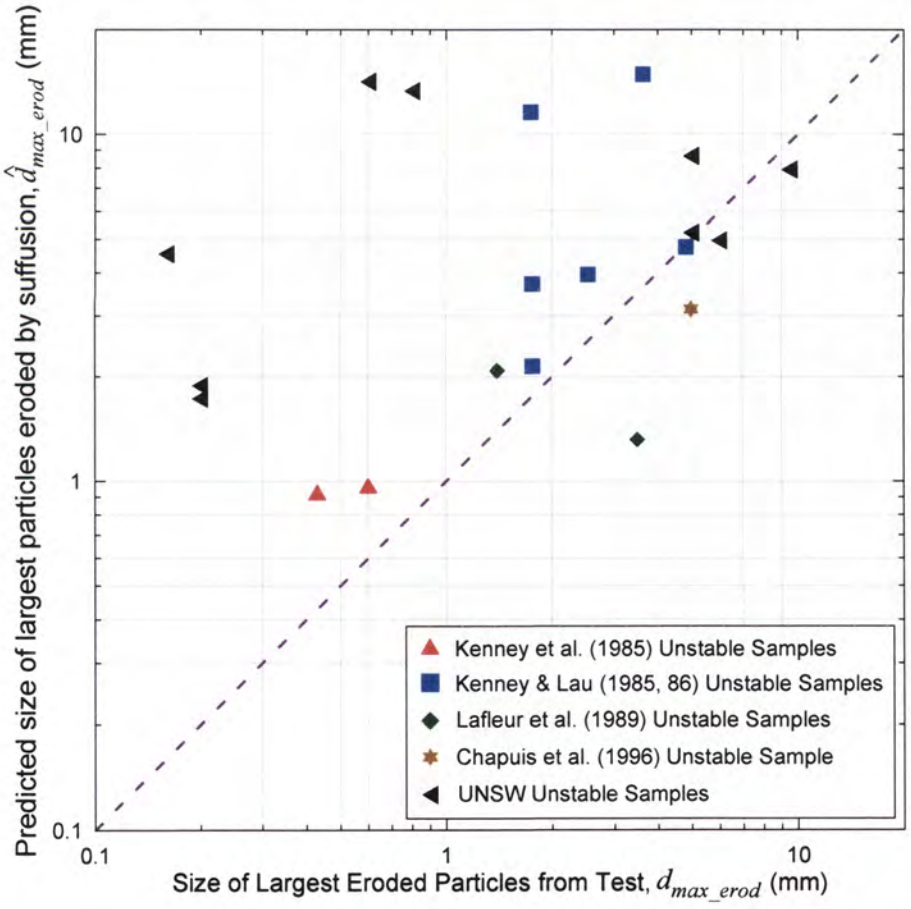

Figure 3.70: Predicted size of largest erodible particles based on $H/F < 1.3$ versus size of largest erodible particles assessed from test data.

Proposed method for gap-graded soils

While the method above should apply to all soils, for gap-graded soils it would be sufficient to assume that the fine part of the soil may be eroded by suffusion. So for example, in Section 3.3.4, Figure 3.33, soil 10, about 25 – 30% could be eroded, corresponding to a maximum size of about 0.1 mm to 0.2 mm.

3.6.4 Estimating the actual fraction of materials eroded by suffusion

It should be noted that the actual fraction of materials eroded by suffusion is always less than the maximum possible erodible fraction discussed in Section 3.6.3 above. If seepage tests have been carried out, and post-test grain-size distribution curves are available, the actual fraction of materials eroded can be estimated from the test data using the grain-size distribution curve matching technique.

Figure 3.39 in Section 3.4.2 shows a plot of the actual fraction of materials eroded versus the maximum possible erodible fraction for 20 soil samples. Both parameters were obtained from the curve matching technique. The plot shows considerable scattering of data. The plot, however, shows that the actual fraction of materials eroded is unlikely to be greater than 30%. The actual fraction of materials erodible might be very close to the maximum possible fraction of erodible materials if the latter is less than 20% of the total weight of the soil.

3.7 CONCLUSIONS

3.7.1 Factors influencing whether a soil is internally unstable

Effects of fines content and gravel content

The experimental investigation reveals no obvious relationship between the fines content and the internal stability of silt-sand-gravel and clay-silt-sand-gravel mixtures.

Effects of plasticity of fines

The experimental investigation shows no significance influence of the plasticity of the fines on the internal stability of clay-silt-sand-gravel mixtures up to the limits of the soils tested – less than 10% clay-sized fraction, and plasticity index less than 12%.

Effects of gap-grading

Gap-graded mixtures with more than 60% gravel-size particles (> 4.75 mm), but lacking sand-sized particles are vulnerable to suffusion. Nevertheless, similar gap-graded mixtures which have a very low fines content (< 10%) did not show significant loss of materials by the process of suffusion. It is possible that the amount of erosion loss was too small to be detected in these mixtures.

Effects of dry density of soil

The results of DF tests do not suggest any significant influence of the dry density of a soil on its internal stability classification, within the range of dry densities investigated (i.e. 90 – 95% of standard maximum dry density).

Nevertheless, results of UF tests do indicate that erosion of fine particles started at comparatively lower hydraulic gradient in samples compacted at lower dry densities/higher porosities.

3.7.2 Currently available methods for assessing internal instability

Using the coefficient of uniformity, C_U, as an indicator (US Army Corps of Engineers (1953), Istomina (1957))

C_U is not an accurate predictor of internal stability. In general, internally unstable soils are more likely to have C_U values higher than 10. Nevertheless, the investigation shows that some internally unstable soils have C_U values lower than 10, and a lot of soils with very high C_U values (> 100) are not internally unstable.

Methods involve splitting a soil into a coarse fraction and a fine fraction (Kézdi 1969, de Mello 1975, Sherard 1979)

Methods involving splitting a soil into a fine fraction and a coarse fraction, and treating the coarse fraction as a filter to the fine fraction are easy to apply. These methods, however, are too conservative for assessing whether a soil is internally unstable and subject to suffusion if the commonly used filter rule represented by $d_{C15}/d_{f85} < 5$ is used to assess the filter compatibility between the coarse and the fine fraction, in that the method tends to classify stable soils as unstable.

The use of a less conservative filter rule, such as the Continuing Erosion Boundary (Foster & Fell 1999a, 2001) represented by $d_{C15}/d_{f95} = 9$, is shown to be unconservative when applied to some coarse granular soils.

It appears that a filter rule suitable for assessing internal instability for most types of soils does not exist without being conservative.

The methods may be able to determine if a soil will self filter, but there is no experimental evidence to support this.

Kenney & Lau (1985, 1986) method

The method using the stability number, *H/F*, as a predictor of internal stability is conservative in that a lot of stable soils are classified as internally unstable soils. The

upper boundary of Kenney & Lau (1985) method, represented by $H = 1.3F$, appears to be an upper bound for unstable soils, in that no internally unstable soils are plotted above the boundary.

Burenkova (1993) method

The method presents a boundary, represented by $h' = 0.76\log(h'') + 1$, which appears to be an approximate lower bound for stable soils. Soils plotted below the boundary are more likely to be unstable than stable. The method is less conservative than Kenney & Lau (1985, 1986) method in that some unstable soils are plotted in the non-suffusive zone (Zone II) above the boundary.

Sun (1989) method for clayey/silty sands

Sun's method was developed for clayey/silty sands. The method predicts some internally unstable coarse granular soils as stable, and is hence unconservative, and should not be applied to clay-silt-sand-gravel and silt-sand-gravel mixtures. Its validity for silty sands and clayey sands is questionable, and these soils may not be susceptible to suffusion.

3.7.3 Proposed methods for assessing internal instability

Combining the Burenkova (1993) method and the Kenney and Lau (1985, 1986) method

By combining the Burenkova (1993) and Kenney and Lau (1985, 1986) methods, a more reliable estimate of whether a soil is internally unstable can be obtained. Table 3.16 can be used to estimate the likelihood of internal instability of a soil.

Proposed probabilistic method based on Burenkova (1993) method for assessing internal instability

The distribution of the internally unstable and stable soil samples in an h' versus log h" plot based on Burenkova (1993) method suggests that a probabilistic approach can be used to predict internal instability. Contours for the probability of internal instability,

calculated by logistic regression, are presented in Section 3.6.2. It is recommended that Figure 3.67 be used for predicting the probability of internal instability for silt-sand-gravel and clay-silt-sand-gravel mixtures with clay-sized fraction less than 10% and plasticity index less than 12%, and Figure 3.68 be used for predicting the probability of internal instability for coarse granular soils with less than 10% non-plastic fines passing 0.075mm sieve.

3.7.4 Currently available method for predicting the fraction of fine materials and the size of the largest particles eroded by the suffusion process

Lubochkov (1965) method and Burenkova (1993)

The Burenkova (1993) method has been found to severely underestimate the size of the largest particles eroded by suffusion, whereas the Lubochkov (1965) method was shown to overestimate the sizes of the largest particles eroded

3.7.5 Proposed method for predicting the fraction of fine materials and the size of the largest particles eroded by the suffusion process

Theoretical maximum possible fraction of fine materials eroded by the suffusion process

The maximum possible fraction of fine particles erodible in the suffusion process would very unlikely be higher than 40% (i.e. $F \leq 0.4$) of the total weight of an internally unstable granular soil based on geometrical criterion 2 (refer Section 3.2.6). UNSW test data and available test data from the literature indicate a maximum F value of not greater than 30%. The proposed limiting value of $F \leq 0.4$ for suffusive soils is expected to remain valid for unstable soils with small clay contents.

Proposed methods for predicting the fraction of fine materials and the size of the largest particles eroded by the suffusion process

The Author proposes a method for predicting the size of the largest particles eroded by the process of suffusion based on dividing a soil into a coarse fraction and a fine fraction. The dividing point, D, is chosen at where the ratio H/F (Kenney & Lau 1985, 86) is minimised for $F < 0.4$, and not greater than 1.3. D is the predicted size of the largest particles eroded by the process of suffusion, and F is the predicted maximum fraction of fine particles that can be eroded.

For gap-graded soils, it can be assumed the fine part of the soil may erode.

3.7.6 Hydraulic gradients causing internal instability in silt-sand-gravel and clay-silt-sand-gravel mixtures

Hydraulic gradient, i_{start}, for initiation of suffusion

Selective erosion of fine soil particles begins at gradients, i_{start}, less than the theoretical critical gradient, i_c, for all internally unstable soils, and for many internally stable soils. For the internally unstable soils tested, all began to erode with gradients of 0.8 or less, with several less than 0.5. This erosion is relatively minor rate, and even in the internally unstable soils, did not lead to "extreme cloudiness" condition when erosion would be obvious.

Relationship between i_{start} and the H/F ratio

No definite mathematical relationship has been identified between the hydraulic gradient i_{start} and the coefficient of uniformity, the minimum H/F ratio and the fines content.

Relationship between i_{start} and the porosity of the soil

There appears to be a general trend that soils with higher porosity would start to erode at lower hydraulic gradients. Loose, higher porosity soils tested began to erode at

gradients less than 0.3. There is, however, considerable scattering of data that a reliable mathematical relationship cannot be derived between the two variables.

Relationship between i_{start} and the plasticity of fines

Soils with clayey (kaolin) fines appear to erode at relatively higher hydraulic gradients than soils having similar fines contents but without clayey fines.

Effects of soil dry density on i_{start}

The dry density of a soil has a significant effect on the hydraulic gradient i_{start}. The higher the soil density, the higher the i_{start}, given that the fines content of the soils are the same.

Effects of gap-grading on i_{start}

Gap-graded soils erode at relatively lower hydraulic gradient i_{start} than non gap-graded soils with similar fines content.

CHAPTER 4

APPLICATIONS

4.1 OVERVIEW

This Chapter presents some examples on the applications of the findings presented in Chapter 2 and Chapter 3 of this thesis. Three examples are presented. The first example explain the use of the initial hydraulic shear stress obtained from the Hole Erosion Test (HET) to aid judgment of the probability of initiation of erosion along a concentrated leak. The second example shows how the Erosion Rate Index obtained from either the HET or the Slot Erosion Test (SET) can be used to estimate the rate of progression of piping erosion. The last example illustrates the use of the methods proposed by the Author in the assessment of the internal instability of some filter materials which do not satisfy the requirements of the technical specification, and the assessment of the fraction of fine materials that might be eroded by the process of suffusion.

The analysis procedures as illustrated by the three examples presented in this Chapter have been applied in a number of dam failure risk assessment projects in Australia.

4.2 PREDICTION OF INITIATION OF EROSION ALONG A CRACK OR CONCENTRATED LEAK

4.2.1 Background

As explained in Chapter 1, development of internal erosion and piping comprises of four phases, viz. the initiation phase, the continuation phase, the progression phase, and the breach formation phase. During the assessment of the probability of internal erosion and piping, there are two main questions to be answered by the risk analyst when studying the initiation phase of internal erosion. The two questions are

(i) what is the probability that a crack/concentrated leak will form in the embankment, or in the foundation?

(ii) in case a crack/concentrated leak presents, what is the probability that piping erosion will initiate along the crack/concentrated leak under certain hydraulic conditions?

Some research has been carried out by Bui et al. (2004, 2005) to predict the formation of cracks in embankment dams using two-dimensional and three-dimensional numerical modeling techniques taking into account the differences in the stiffness of the materials in the various zones of an embankment, the zoning arrangement, the foundation profile of the embankment, the irregularity of the foundation/abutment profile, the stiffness of the foundation materials, the construction sequence, desiccation of materials near the ground surface, etc. The research provides some useful guidelines for estimating the potential of cracking in an embankment dam, the likely locations for cracks to be found, and the extent of cracking. In a number of dam investigation projects in Australia and overseas, trial pits were formed along or near the crest of the embankment to confirm zoning details, and to identify the extent of cracking if any. Numerical modeling and site investigations would provide useful answers to question (i) above.

To answer question (ii) requires the knowledge of the geometry of the cracks, the hydraulic shear stress along the walls of the cracks, and the critical hydraulic shear stress, τ_c, of the soils in the embankment. The Hole Erosion Test can be used to estimate the τ_c.

4.2.2 Hydraulic Shear Stress along the Walls of a Crack

The hydraulics of flow in a crack or pipe is complex because the geometry of the crack/pipe may vary. Nevertheless the cross-section of a crack/pipe and the hydraulic shear stress along the walls of the crack/pipe can be assumed uniform so as to allow an approximate assessment of the hydraulic shear stress, τ, along the walls of the crack/pipe.

For a cylindrical crack/pipe, the average hydraulic shear stress, τ, acting on the walls of the crack is

$$\pi \phi L \tau = (p_1 - p_2)\frac{\pi \phi^2}{4} \qquad \text{Eqn 4.1}$$

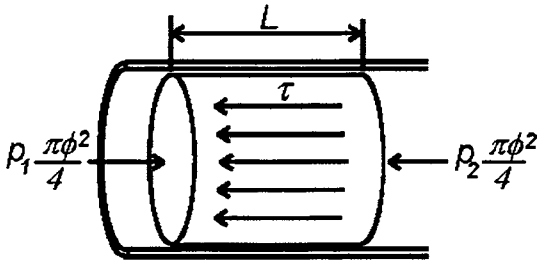

Figure 4.1: Diagram showing the forces acting on a segment of eroding fluid within a cylindrical leak.

Rearranging terms gives

$$\tau = \frac{(p_1 - p_2)}{L}\frac{\phi}{4} = \rho g s \frac{\phi}{4} \qquad \text{Eqn 4.2}$$

where ρ : is the density of water (eroding fluid) in kg/m^3;

g : is the acceleration due to gravity and equal to 9.8 m/s^2;

p_1, p_2 : are the pressures on the upstream and downstream face of the leak, respectively.

s : is the hydraulic gradient across the leak;

L : is the length of the flow path (i.e. length of the leak) in m;

ϕ : is the diameter of the cylindrical leak in m;

For example, the hydraulic shear stress along the walls of a cylindrical crack/pipe, given head loss H_f = 10 m, length L = 4 m, and diameter ϕ = 0.01 m, is

$$\tau = \frac{1000 x 9.8 x 10 x 0.01}{4 x 4} = 61 \text{ N/m}^2 \text{ [or Pa]}$$

A more general formula for the hydraulic shear stress, τ, along a crack/pipe with a uniform cross-sectional area, A, and a wetted perimeter, $\wp$, is given by

$$\tau = \rho g s \frac{A}{\wp} \qquad \text{Eqn 4.3}$$

For an open crack with an uniform width as shown in Figure 4.2, the average hydraulic shear stress, τ, acting on the walls of the crack can be approximated by

$$F_1 - F_2 \cong \tau L(W + H_1 + H_2) \qquad \text{Eqn 4.4}$$

$$F_1 - F_2 = \frac{\rho g W \left(H_1^2 - H_2^2\right)}{2} \qquad \text{Eqn 4.5}$$

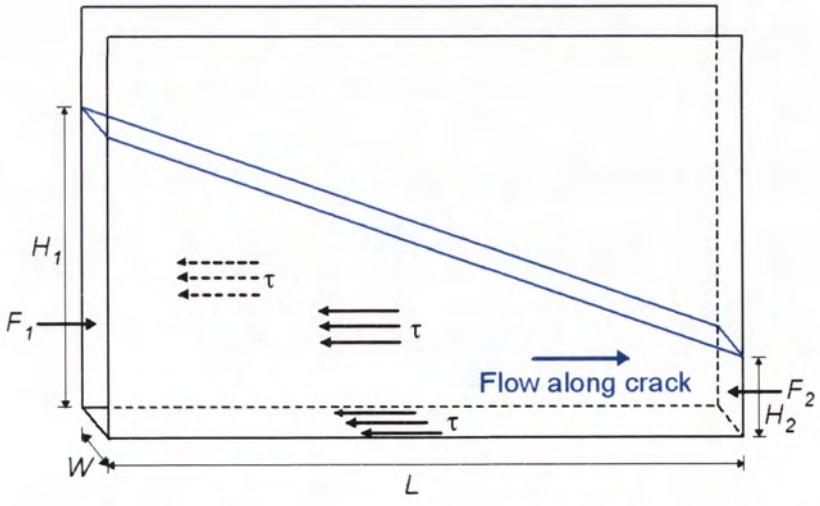

Figure 4.2: Diagram showing the forces acting on a segment of eroding fluid within an open crack or gap.

Combining equations 4.4 and 4.5

$$\tau \cong \frac{\rho g W \left(H_1^2 - H_2^2\right)}{2L(W + H_1 + H_2)} \qquad \text{Eqn 4.6}$$

where W : is the width of the open crack/gap in m;

L : is the length of the crack/gap in m;

H_1, H_2 : are the water heads at the upstream and downstream ends of the crack/gap, respectively.

In case H_2 is very small compared to H_1, equation 4.6 can be further simplified to

$$\tau \cong \frac{\rho g W H_1^2}{2L(W + H_1)} \qquad \text{Eqn 4.7}$$

and if W is also very small compared to H_1,

$$\tau \cong \frac{\rho g W H_1}{2L} \qquad \text{Eqn 4.8}$$

For example, using equation 4.8, the approximate hydraulic shear stress along the wall of an open crack of width 10 mm, with head loss of 3 m over a length of 5 m is

$$\tau = \frac{1000 x 9.8 x 3^2 x 0.01}{2(3+0.01)5} = 29 \text{ N/m}^2 \text{ [or Pa]}$$

Table 4.1 shows approximate values of hydraulic shear stress along the walls of an open crack based on equation 4.8.

Table 4.1: Estimated hydraulic shear stress (N/m^2) from water flowing in an open crack, versus crack width and flow gradient.

Crack Width	**Hydraulic shear stress (N/m^2)**					
	Hydraulic Gradient in Crack (H_1/L)					
(mm)	**0.1**	**0.25**	**0.5**	**1.0**	**2.0**	**5.0**
1	0.5	1.25	2.5	5	10	25
2	1	2.5	5	10	20	50
5	2.5	6	12	25	50	125
10	5	12	25	50	100	250
20	10	25	50	100	200	500
50	25	60	125	250	500	1250
100	50	125	250	500	1000	2500

4.2.3 Hole Erosion Test and Initial Shear Stress

As explained in Chapter 2, HET can be carried out on a soil sample at different test heads in order to find out the minimum test head at which piping erosion will initiate along the pre-formed hole in the soil sample. The hydraulic shear stress due to the minimum test head, named as the initiate shear stress, τ_o, by the Author, is an estimate of the value of the critical hydraulic shear stress, τ_c, of the soil sample.

As a guide to whether erosion will initiate along a crack, an assessment can be made of the hydraulic shear stress, τ, from the estimated crack width and embankment core geometry, and reservoir level. The estimated hydraulic shear stress along the crack can then be compared with the likely initial shear stress, τ_o, for the soil in which the crack is

formed from the HET or approximately from the Erosion Rate Index, I_{HET}, and Figure 4.3 . I_{HET} can be determined from laboratory HETs, or approximately from Table 4.2.

Care should be taken in using this approach because of the uncertainty in τ_c, and the hydraulic shear stress in the crack or pipe.

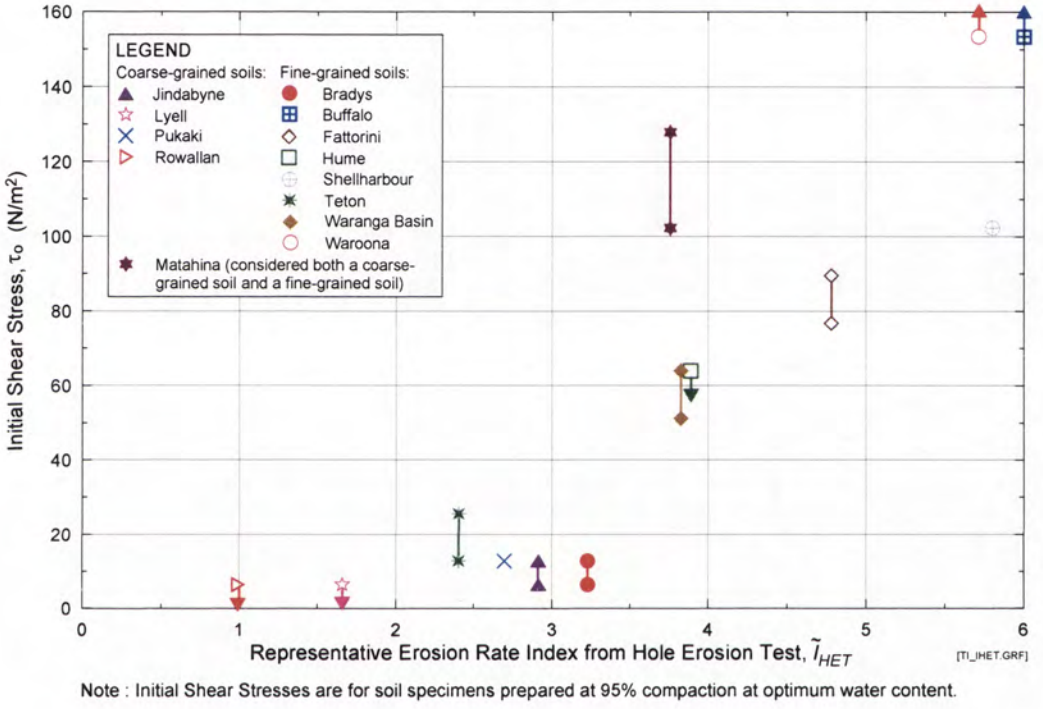

Figure 4.3: Initial Shear Stresses, τ_o versus Representative Erosion Rate Index, $\tilde{I}_{HET}$ (Reproduced from Figure 2.79. of Chapter 2)

Table 4.2: Proposed Guidelines for Preliminary Estimation of the Representative Erosion Rate Index of a Soil (Reproduced from Table 2.25 of Chapter 2).

Parameters	Values	Erosion Rate Index (See Note 1)					
		Extremely rapid	Very rapid	Moderately rapid	Moderately slow	Very slow	Extremely slow
		<2	2 - 3	3 - 4	4 - 5	5 - 6	>6
Predictions for coarse-grained soils (See Note 3):							
USCS Classification	SM	Very likely	Likely	Likely - Neutral	Unlikely	Very unlikely	
(See Note 2)	SC	Neutral - Likely	Very likley		Likely - Neutral	Unlikely	Very unlikely
Degree of Saturation	<70%	Very likely	Likely	Neutral - Unlikely	Unlikely	Very unlikely	
	70 - 80%	Likely	Very Likely		Likely	Unlikely	Very unlikely
	>80%	Neutral	Likely	Very likely	Likely - Neutral	Unlikely	Very unlikely
Fines Content (<0.075mm)	<30%	Very likely	Likely - Neutral	Unlikely	Very unlikely		
	30 - 40%	Neutral - Likely	Very Likely		Likely - Neutral	Unlikely	Very unlikely
	40 - 50%	Unlikely - Neutral	Likely	Very likely	Likely	Neutral - Unlikely	Unlikely
Clay Content (<0.002mm)	<10%	Very likely	Likely - Neutral	Unlikely	Very unlikely		
	10 - 20%	Very likely			Likely - Neutral	Unlikely	Very unlikely
	>20%	Unlikely	Likely - Neutral	Very likely	Likely - Neutral	Unlikely	
Predictions for fine-grained soils (See Note 3):							
USCS Classification	CH	Very unlikely	Unlikely - Neutral	Likely		Very likely	
	MH	Unlikely	Likely	Very likely		Likely	
	CL	Unlikely - Neutral	Likely	Very likely	Likely		
	CL - ML	Neutral - Likely	Very likely		Neutral - Likely	Unlikely	
	ML	Likely	Very likely	Likely - Neutral	Unlikely	Very unlikely	
Degree of Saturation	<70%	Likely - Neutral	Very likely		Likely - Neutral	Unlikely	Very unlikely
	70 - 80%	Unlikely	Neutral - Likely	Very likely		Likely	
	>80%	Unlikely	Unlikely - Neutral	Likely		Very likely	
Soil mineralogy	Kaolinites or illites or chlorites only	Unlikely			Neutral - Likely	Very likely	Likely
	Some smectites or vermiculites	Unlikely	Likely	Very likely		Likely	Unlikely
	With cementing materials (e.g. iron oxides, aluminium oxides, gypsum, etc.)	Unlikely			Neutral - Likely	Very likely	

Notes :

1 Erosion Rate Index is taken as the negative LOG of the Coefficient of Soil Erosion, which is defined as the slope of the rising portion of the curve obtained by plotting the rate of mass removal per unit area against shear stress.

2 Soils used for construction of dam cores usually contains a considerable fraction of fines. Coarse-grained soils used for construction of a dam core are usually SC or SM. It is less common to find dam core materials belonging to GW,GP, GM, GC, SW, or SP.

3 Fine-grained soils means soils containing more than 50% by mass of fines (namely silts and clays). Fines means soil particles finer than 0.075mm. Coarse-grained soils means soils containing less than 50% by mass of fines (namely gravels and sands).

4.3 PREDICTION OF THE RATE OF EROSION ALONG A CONCENTRATED LEAK

4.3.1 Background

The rate of soil erosion is an important factor that affects the rate of progression of piping erosion. The Erosion Rate Index obtained from the HET or the SET provides an indicator of the rate of piping erosion. The lower the value of the index, the faster the rate of increase of the rate of erosion in response to an increase in the hydraulic shear stress, and hence the faster the rate of progression of piping erosion.

In case a reliable value of the Erosion Rate Index is obtained from a series of laboratory HETs, the index can be used in a numerical modeling procedure for estimating the enlargement of a pipe with time due to erosion. A hypothetical embankment dam with a clay core suffering from piping is used as an example in this Section to illustrate the numerical modeling procedure.

The rate of progression of piping erosion has important bearings on dam safety management in that it affects the chance of a successful intervention to prevent the further development of piping into a dam failure. The rate of progression of piping also determines the available warning time for evacuation of the downstream population who are at risk of a dam failure. DeKay and McClelland (1993) and Graham (1999) have indicated that the number of loss of lives due to a dambreak flood depends on the available warning time.

4.3.2 Details of a hypothetical dam suffering from piping

A hypothetical embankment dam suffering from piping through its clay core is shown in Figure 4.4. The following details have been assumed:

- an embankment dam with an impervious puddle clay core not protected by filter zones at its upstream and downstream faces
- the maximum storage depth at Full Supply Level (FSL) is 30 m

- a concentrated leak has developed through the clay core at 10 m below FSL, which is at 130 mAHD. The estimated length of the concentrated leak in the core is 4 m.
- the fill materials at both the upstream and the downstream shoulders are highly permeable.
- the estimated diameter of the concentrated leak is 10 mm when leakage is detected and emergency drawdown of the reservoir is initiated.
- emergency discharge is via a 160m long cast iron pipe with centre line at 100 mAHD (i.e. 30m below FSL).
- storage capacity – level relationship is provided and as shown in Figure 4.4.

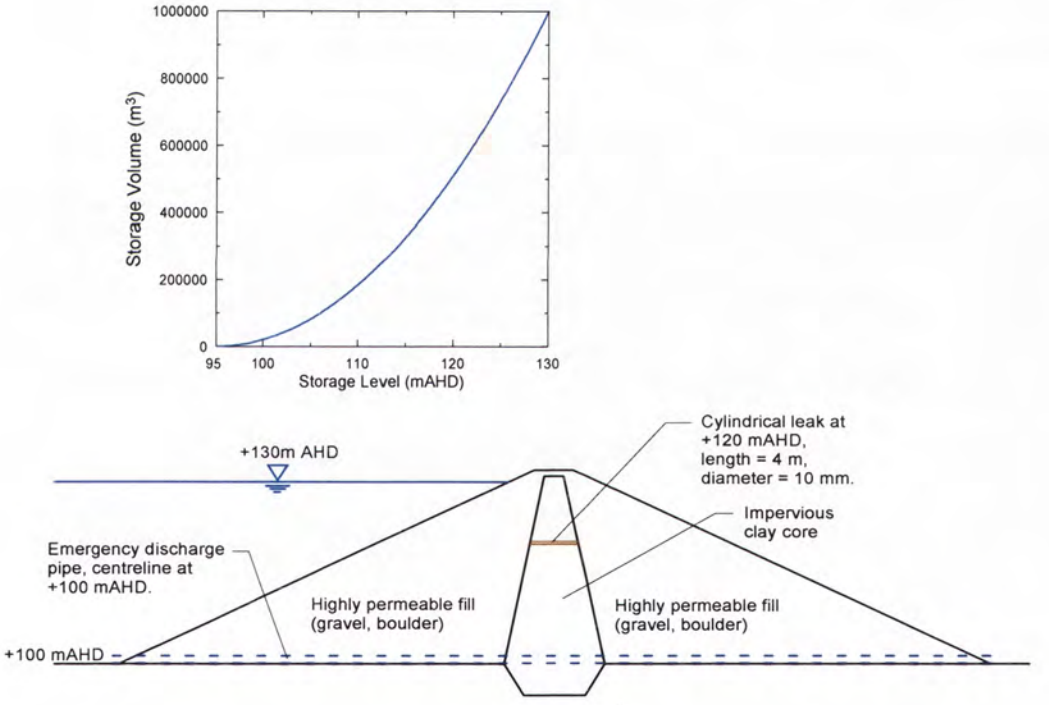

Figure 4.4: Details of a hypothetical embankment dam suffering from piping.

4.3.3 Numerical modeling of piping erosion

The objective of the numerical modeling is to estimate the rate of progression of piping erosion along the pipe in the dam core. The rate of progression of piping is indicated by

the enlargement of the pipe with time. The following assumptions have been made in the numerical modeling:

i. the shape of the concentrated leak/pipe remains circular throughout the course of erosion process
ii. the Critical Shear Stress (τ_c) (i.e. the minimum hydraulic shear stress to initiate soil erosion) is negligible
iii. the pipe can sustain a roof without collapsing despite the pipe is being enlarged by the process of erosion
iv. erosion stops when the reservoir level is lowered to the level of the concentrated leak (i.e. 120 mAHD)

Assumption ii above is a valid assumption in that τ_c of most unsaturated soils is close to zero. This is also a conservative assumption when the erosion rate ($\dot{\varepsilon}$) is estimated from the shear stress (τ) based on the equation

$$\dot{\varepsilon} = C_e(\tau - \tau_c)$$

$$\dot{\varepsilon} \cong C_e \cdot \tau \qquad \text{as } \tau_c \text{ is assumed to be zero.}$$

In the above equation, the Coefficient of Soil Erosion, C_e is equal to $10^{-I_{HET}}$, where I_{HET} is the Erosion Rate Index obtained from the Hole Erosion Test.

Theory and Numerical Modeling Procedure

While the size of the concentrated leak is being enlarged by erosion, the reservoir level is gradually lowered due to discharge via the outlet pipe at 100 mAHD as well as the concentrated leak at 120 mAHD.

The relevant equations for estimating the enlargement of the concentrated leak are:

$$\tau = \rho_w g \frac{H_f}{L}\frac{\phi}{4} = \rho_w g s \frac{\phi}{4} \qquad \text{Eqn 4.9}$$

$$\dot{\varepsilon} \cong C_e \cdot \tau \qquad \text{Eqn 4.10}$$

where H_f is the head loss along the pipe due to friction.

L is the length of the pipe.

ϕ is the diameter of the pipe (varies with time, the initial value is 10mm).

s is the hydraulic gradient across the pipe.

ρ_w is the density of water.

g is the acceleration due to gravity.

The lowering of the storage level can be modeled by a water balance equation (i.e. decrease in reservoir storage = total outflow from the reservoir) using the given storage-level relationship, and equations for estimation friction loss due to flow along a circular pipe. The relevant equations are:

$$\frac{H_f}{L} = \frac{4f}{\phi}\frac{\overline{V}^2}{2g} \qquad \text{(i.e. Darcy-Weisbach equation)} \qquad \text{Eqn 4.11}$$

$$q = \overline{V}\frac{\pi\phi^2}{4} \qquad \text{Eqn 4.12}$$

$$R_e = \frac{\rho_w \overline{V}\phi}{\mu} \qquad \text{Eqn 4.13}$$

where f is the friction loss factor for pipe flow.

ϕ is the diameter of the pipe. For the emergency discharge pipe, ϕ = 1.2 m. For the concentrated leak, ϕ increases with time as erosion progresses.

$\overline{V}$ is the mean velocity of flow along the pipe.

q is the rate of discharge.

R_e is the Reynolds number.

μ is the coefficient of dynamic viscosity of water (10^{-3} kg/ms at 20 °C).

For the emergency discharge pipe, discharge q can be estimated using equations 4.11 and 4.12, in which ϕ and L are constant, and an appropriate f coefficient for a cast iron pipe is 0.0035.

For the pipe through the clay core, combining equations 4.9 and 4.11 gives

$$\tau = \frac{\rho_w f}{2}\overline{V}^2 \qquad \text{Eqn 4.14}$$

Knowing τ, and by assuming an initial value for f, $\overline{V}$ and R_e can be estimated using equations 4.13 and 4.14. Based on Moody's diagram for flow through a circular pipe, the following relationships between f and R_e can be assumed for a rough pipe:

For $R_e \leq 2500$, $f = 16/R_e$ (f= 0.0064 at R_e=2500)

$2500 < R_e \leq 20000$ f varies linearly with log(R_e) from 0.0064 at R_e = 2500 to 0.02 at R_e=20000. Eqn 4.15

$R_e > 20000$ f= 0.02.

Using an iterative procedure, the final values of f, $\overline{V}$ and R_e can be found from equations 4.13, 4.14 and 4.15. The flow rate q through the leak can then be estimated using equation 4.12. The iterative procedure is often not required as R_e is usually larger than 20000, in which case f is equal to 0.02.

43.4 Results of Numerical Analysis

Four different scenarios have been studied and the results are summarised in Table 4.3. Figure 4.5 shows reservoir level and the diameter of the pipe plotted against time for Scenario 1 (i.e. core soil has an I_{HET} of 4 (C_e = 10^{-4} kg/s/m^2 per Pa) and the diameter of the emergency discharge pipe is 1.2 m). The plots show that the diameter of the concentrated leak will be enlarged from 10 mm to about 2.3 m in approximately 3.1 hr. when the storage level is lowered to the level of the pipe.

Table 4.3: Results of numerical modeling of the rate of piping erosion.

Scenarios	I_{HET} of Soil (Note 1)	Diameter of Emergency Discharge Pipe (m)	Findings		
			Time taken to drawdown to level of leak (hr)	Final diameter of the pipe (Note 2) (m)	Graphical plots of water level and pipe diameter
1	4	1.2	3.1	2.3	Figure 4.5
2	4	0.6	2.6	3.4	Figure 4.6
3	5	1.2	5.4	0.02	Figure 4.7
4	5	0.6	27	0.5	Figure 4.8

Notes :

1. Soils having a lower I_{HET} show a larger increase in the erosion rate in response to an increase in the hydraulic shear stress.
2. The initial diameter of the pipe through the dam core is 0.01 m.

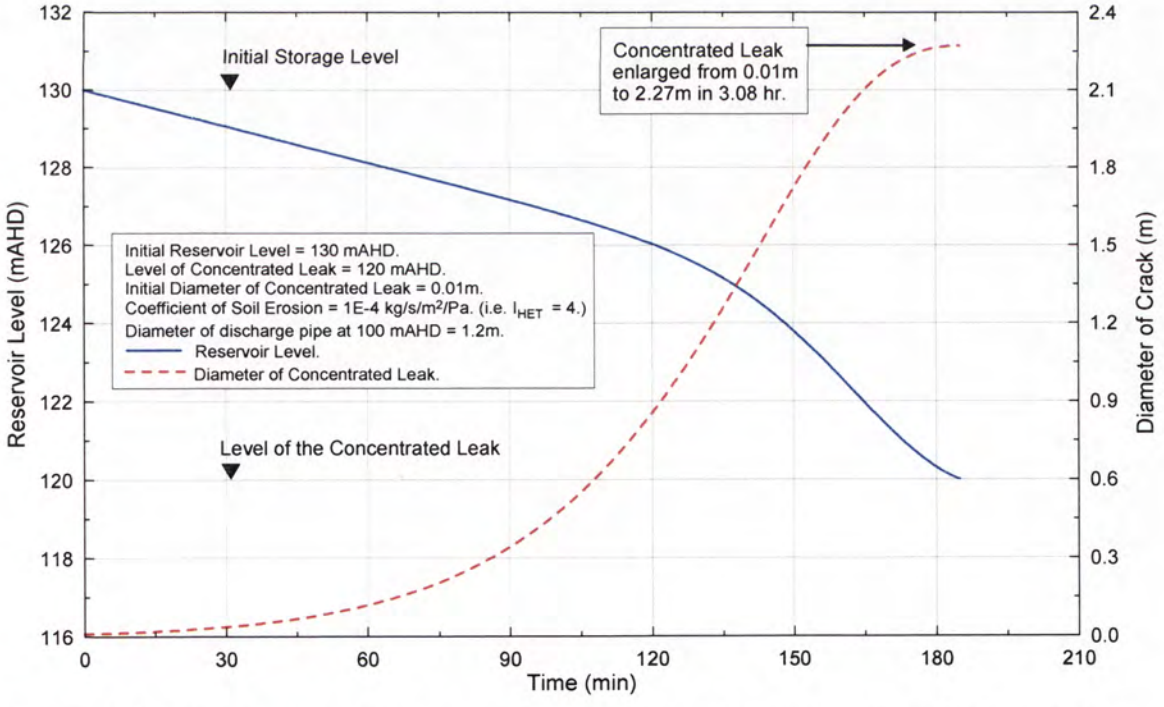

Figure 4.5: Storage level and diameter of concentrated leak versus time for Scenario 1 - I_{HET} = 4, and diameter of emergency discharge pipe = 1.2 m.

For Scenario 2, the emergency discharge pipe has a much smaller discharge rate due to its smaller diameter of 0.6 m. The result, as shown in Figure 4.6, is more severe piping erosion, and the leak is enlarged to 3.4 m in diameter in about 2.6 hr. when the storage level is lowered to the level of the leak. For both Scenarios 1 and 2, the pipe might have already collapsed, and a breach might have developed well before the reservoir level is lowered to the level of the leak.

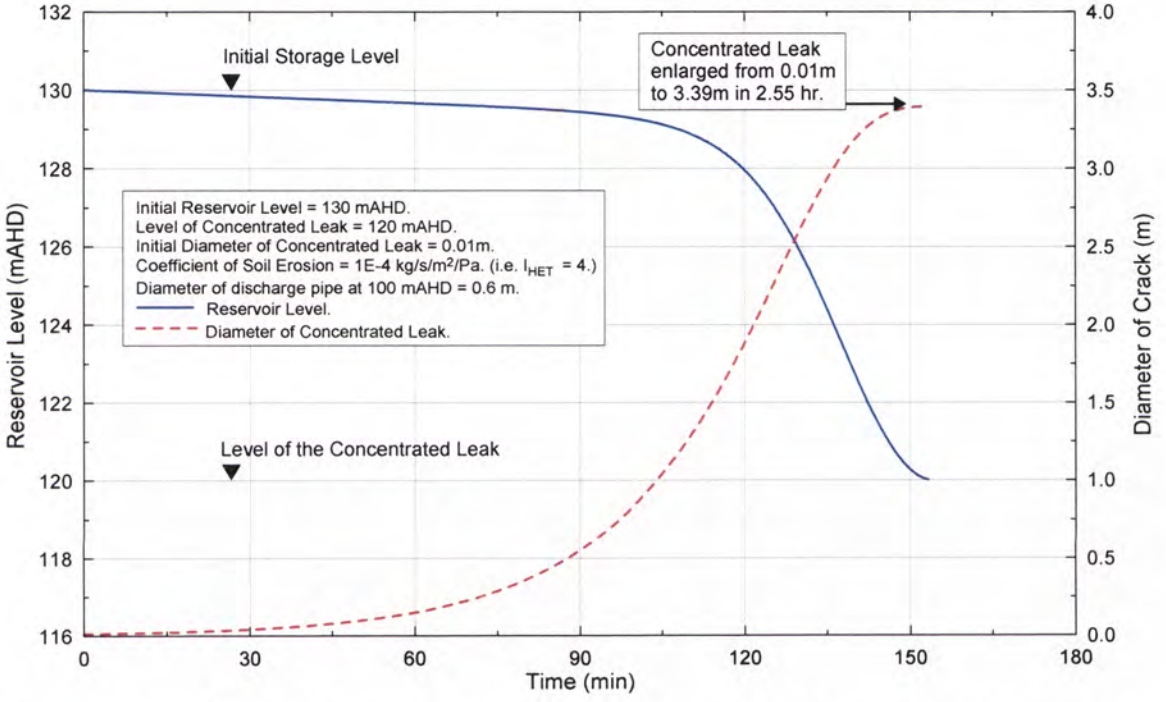

Figure 4.6: Storage level and diameter of concentrated leak versus time for Scenario 2 - I_{HET} = 4, and diameter of emergency discharge pipe = 0.6 m.

For Scenario 3, the dam core is constructed of a more erosion resistant soil (I_{HET} = 5), and the emergency discharge pipe (1.2 m diameter) has a relatively larger discharge capacity. The result, as shown in Figure 4.7, is that the pipe is only slightly enlarged to 0.02 m diameter when the storage level is lowered to the level of the pipe in 5.4 hr.

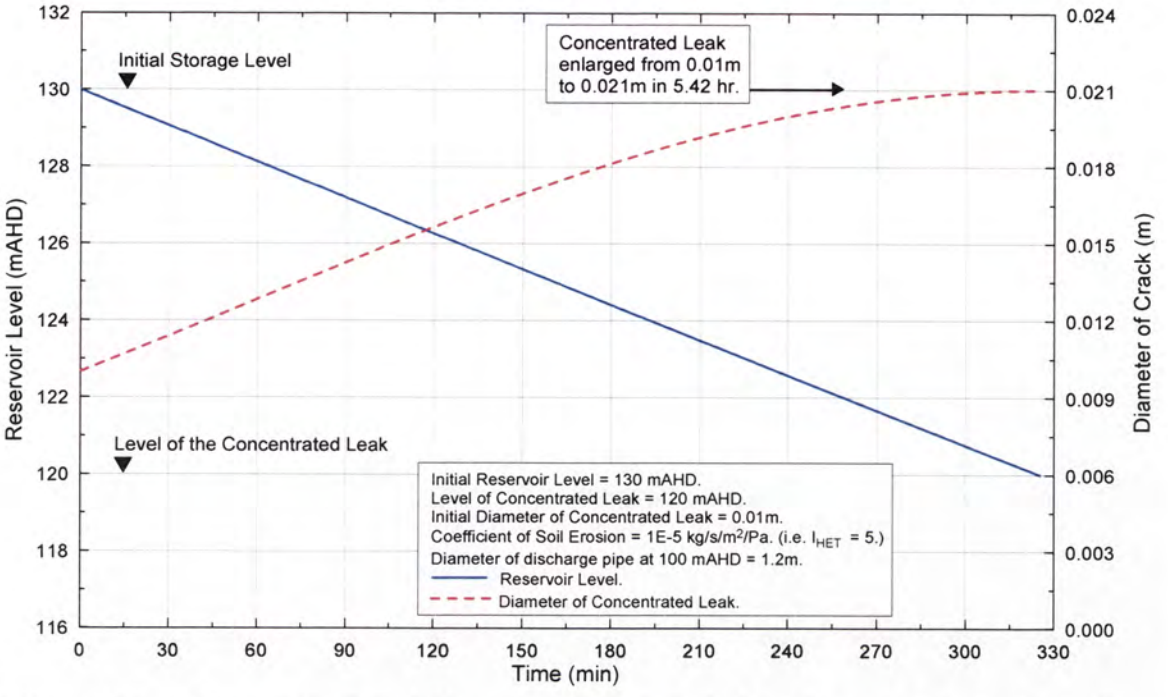

Figure 4.7: Storage level and diameter of concentrated leak versus time for Scenario 3 - I_{HET} = 5, and diameter of emergency discharge pipe = 1.2 m.

Scenario 4 is similar to Scenario 3 except that the emergency discharge pipe has a smaller diameter of 0.6 m and hence a much smaller discharge capacity. The result, as shown in Figure 4.8, is that the pipe is enlarged to 0.5 m diameter when the storage level is lowered to the level of the pipe in 27 hr. For both Scenarios 3 and 4, the chance of a successful intervention to prevent a dam breach appears to be rather high in view of the slow rate of enlargement of the pipe by erosion.

It should be noted that the rate of progression of piping are highly dependent on the I_{HET}, so the above numerical modeling should only be carried out when a reliable values of the I_{HET} have been obtained from a series of HETs.

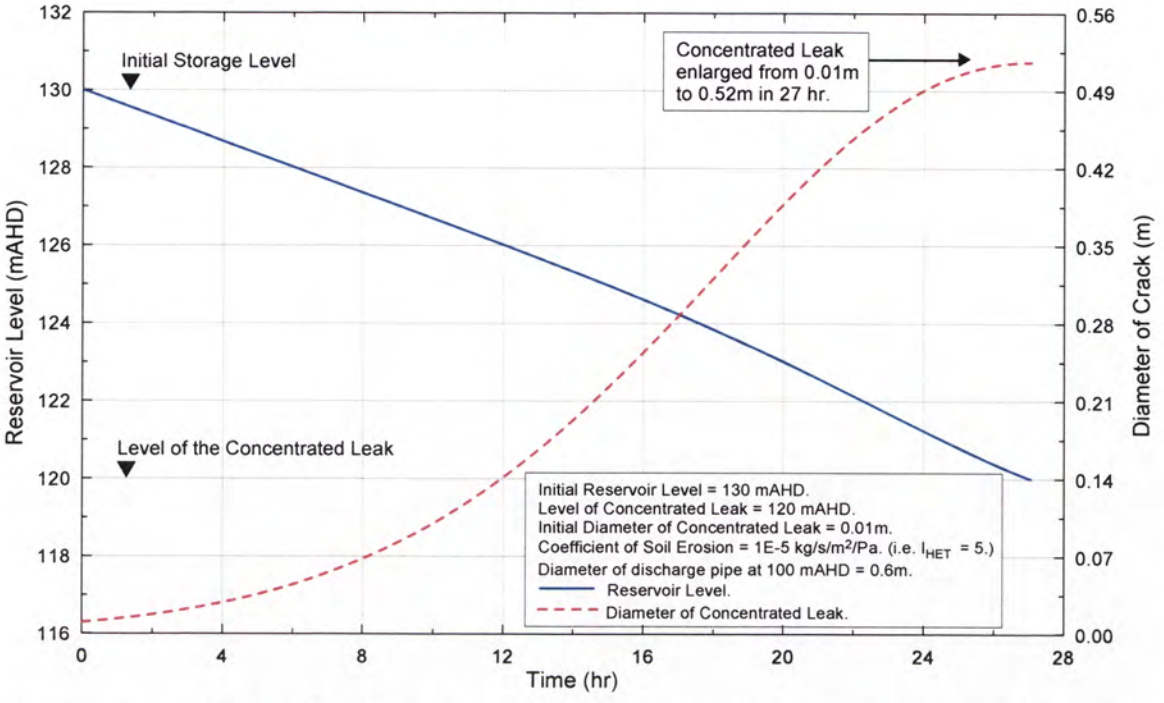

Figure 4.8: Storage level and diameter of concentrated leak versus time for Scenario 4 - I_{HET} = 5, and diameter of emergency discharge pipe = 0.6 m.

4.4 PREDICTION OF INTERNAL INSTABILITY AND EROSION OF FINE MATERIALS BY SUFFUSION

4.4.1 Background

An example is presented in this Section on the use of the methods proposed by the Author to predict the probability of internal instability in some granular filters that do not satisfy the technical specification. The filters have fine contents (% by weight finer than 0.075 mm) higher than specified. The fine soil particles in the filters are believed to be susceptible to erosion by the process of suffusion. The example also illustrates the method proposed by the Author for estimating the maximum fraction of the fine soil particles eroded by suffusion.

4.4.2 Assessing the Probability of Internally Instability

The particle size distribution curves of five different proposed filter materials, designated Filters A, B, C, D and E, are shown in Figure 4.9. Also shown in the figure are the fine and coarse boundaries of acceptable filter materials. All five filters do not satisfy the technical specification in that they contain too much fine materials. The flat portions of their particle size distribution curves suggest that the filters might be internally unstable.

The internal instability of the proposed filter materials has been assessed using Kenney and Lau (1985, 1986) method and Burenkova (1993) method. Kenney and Lau (1985, 1986) method indicates that all five filter materials are internally unstable, as the shape curves of the filters pass below the line represented by $H = 1.0F$ as shown in Figure 4.10. Burenkova (1993) method shows that only Filter C is internally unstable, but all five filters are marginal between internally stable and unstable conditions (refer Figure 4.11).

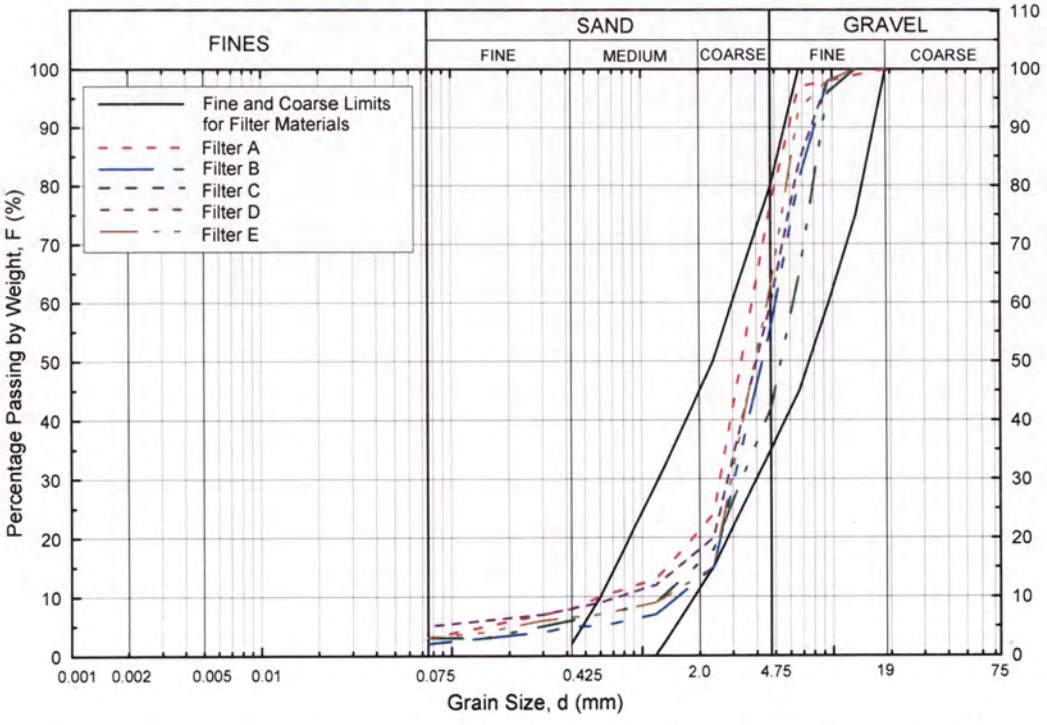

Figure 4.9: Particle size distribution curves of proposed filter materials.

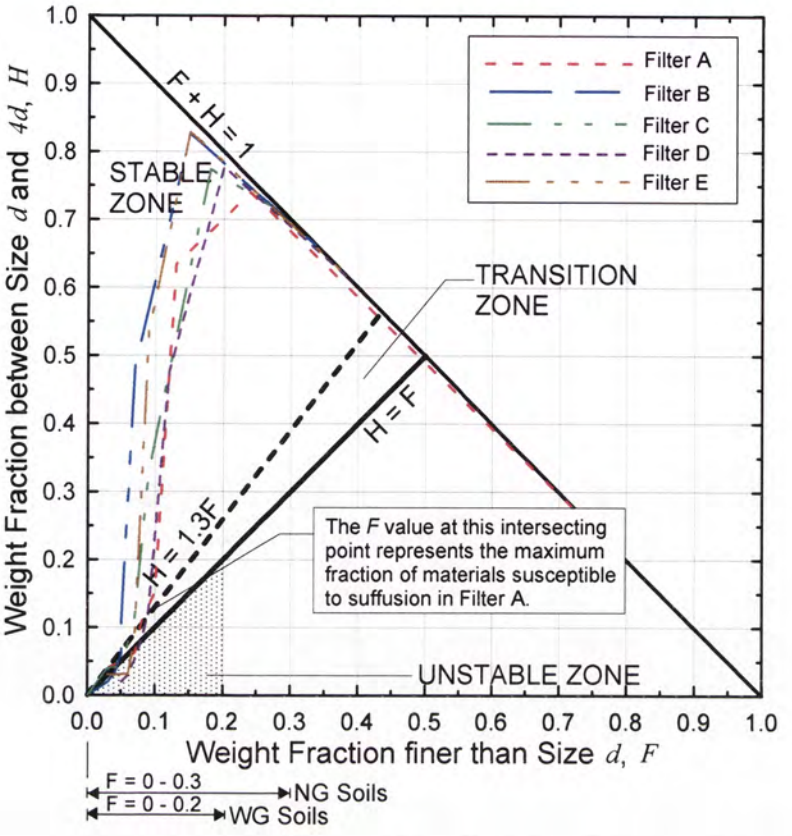

Figure 4.10: Assessment of the internal instability of the proposed filter materials using Kenney and Lau (1985, 1986) method.

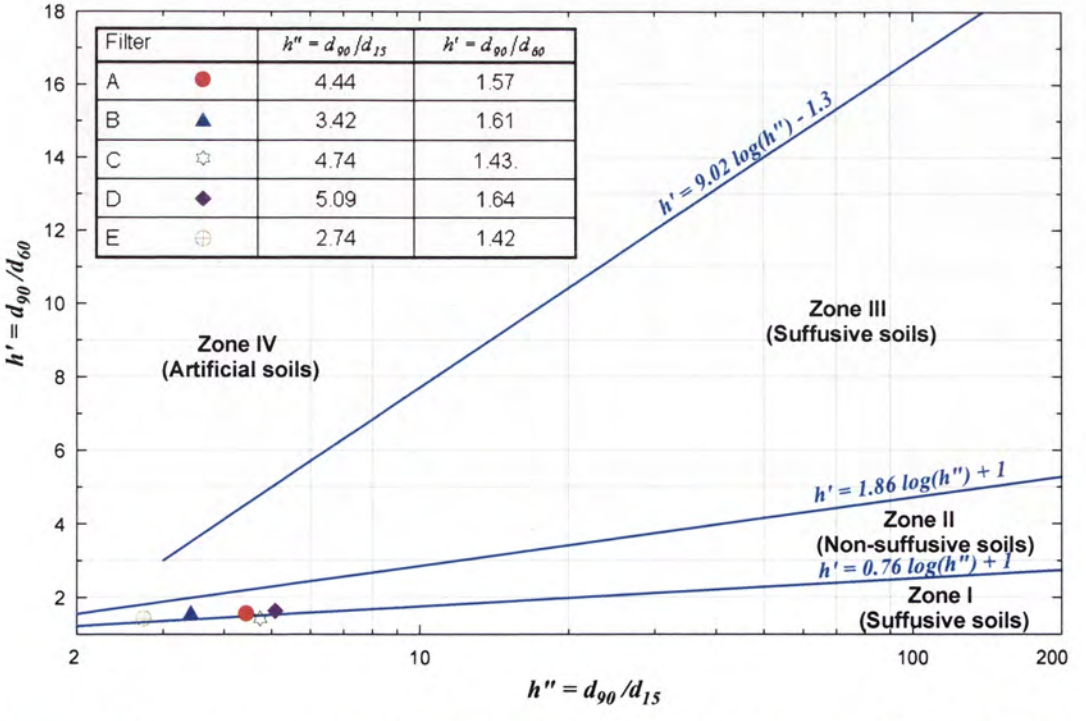

Figure 4.11: Assessment of the internal instability of the proposed filter materials using Burenkova (1993) method.

Figure 4.12 illustrate the use of the probabilistic method proposed by the Author to estimate the probability of internal instability for the five filters. Details of the probabilistic method are explained in Chapter 3, Section 3.6.2. The estimated probability of internal instability for Filters A, B, C, D and E are 0.34, 0.22, 0.48, 0.33, and 0.27, respectively.

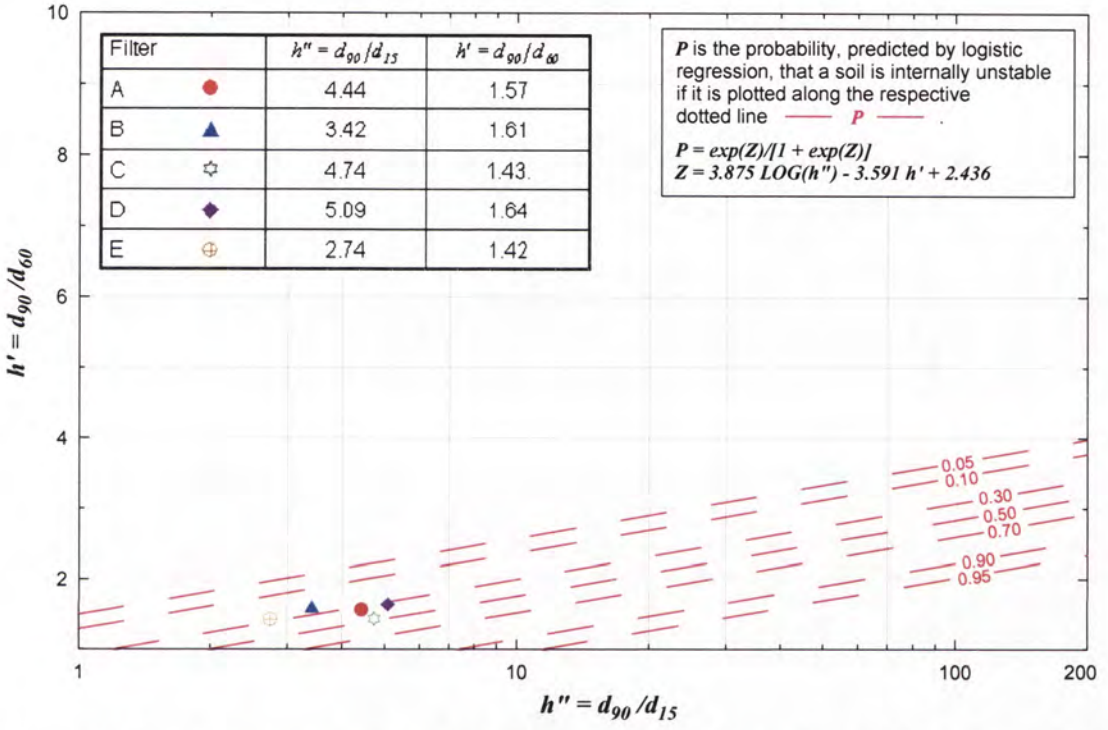

Figure 4.12: Assessment of the probability of internal instability of the proposed filter materials using the method proposed by the Author.

4.4.3 Assessment of the Fraction of Materials Eroded

Due to the high probability of being internally unstable, the five filters have been assessed for loss of fine materials by the process of suffusion. Based on the method proposed by the Author (refer Chapter 3, Section 3.6.3), the unstable fractions susceptible to erosion by suffusion of Filters A, B, C, D and E are assessed to be 8%, 5%, 7%, 9% and 7%, respectively. The unstable fraction is represented by that part of the shape curve passing under $H = 1.3F$ of Kenney and Lau (1985, 1986) shape curves as shown in Figure 4.10.

The particle size distribution curves of the proposed filters will need to be adjusted assuming that the fine fractions assessed above will be lost, and the regraded filters will be re-assessed for their ability to protect the core materials against erosion based on the adopted filter design rules (e.g. Sherard and Dunnigan 1989, Vaughan and Soares 1982, Vaughan and Bridle 2004, Foster and Fell 1999a, 2001).

CHAPTER 5

CONCLUSIONS AND RECOMMENDATIONS

5.1 LABORATORY INVESTIGATION OF PIPING EROSION

5.1.1 Relationship between erosion rate and hydraulic shear stress

Experimental investigations show that the Slot Erosion Tests (SET) and the Hole Erosion Tests (HET) can successfully measure the piping erosion rate of a soil. The tests express erosion rate in the form of an Erosion Rate Index, I defined by:

$$I = -\log(C_e) \qquad \text{Eqn 5.1}$$

$$\dot{\varepsilon} = C_e(\tau - \tau_c) \qquad \text{Eqn 5.2}$$

where $\dot{\varepsilon}$ is the erosion rate per unit area [kg/s/m^2],

C_e is the Coefficient of Soil Erosion [kg/s/m^2/Pa or s/m],

τ is the shear stress [N/m^2 or Pa],

τ_c is the Critical Shear Stress for initiation of erosion [N/m^2 or Pa].

Tests on 13 soil samples show that C_e is in the order of 10^{-1} to 10^{-6} kg/s/m^2/Pa. The corresponding range of values for the Erosion Rate Index, I is > 0 to 6. Soils that erode rapidly have lower I values than soils that erode slowly. The Erosion Rate Index obtained from the SET is denoted by I_{SET}, whereas the Erosion Rate Index obtained from the HET is denoted by I_{HET}.

5.1.2 Effects of dry density and water content on Erosion Rate Index

The Erosion Rate Index of a soil is influenced strongly by the degree of compaction and the water content of the soil. In most of the soil samples tested, a specimen compacted to a higher dry density, and to the wet side of the optimum water content has a higher

Erosion Rate Index (higher erosion resistance) than another specimen of the same soil compacted to a lower dry density, and to the dry side of the optimum water content.

Some coarse-grained, non-plastic soil samples behave differently. These soils have a highest Erosion Rate Index when compacted to a high dry density and to the dry side of optimum.

The erosion resistance of a soil can conveniently be represented by $\tilde{I}$, the Erosion Rate Index of the soil at 95% of standard maximum dry density (SMDD) and at optimum water content (OWC). $\tilde{I}$ is called the Representative Erosion Rate Index of the soil. $\tilde{I}$ can be obtained directly from a test on a specimen at 95% SMDD and OWC, or estimated from results of tests on specimens of different dry densities and water contents using a second order non-linear regression with the dry density and the water content as the independent variables.

5.1.3 Correlation between Erosion Rate Index and other soil properties

For coarse-grained soils, the Erosion Rate Indices show good correlation with water content, degree of saturation, fines content, and the fraction of the soil finer than 0.005 mm.

For fine-grained soils, the Erosion Rate Indices show moderately good correlations with the Degree of Saturation, and dispersivity ratings based on the Pinhole Dispersion Test, Emerson Class Test, SCS Laboratory Dispersion Test and the Sodium Adsorption Ratio.

Correlation analysis indicates that the Representative Erosion Rate Indices of the coarse-grained soil samples show very good correlation with the degree of saturation, the fines content, and the fraction of the soil finer than 0.005 mm. For fine-grained soil samples, only a moderately good correlation exists between the Representative Erosion Rate Indices and the degree of saturation.

5.1.4 Multiple linear regression analysis on test data

Multiple linear regression analysis has been carried out to investigate any possible relationship between the Erosion Rate Index and a group of two or more soil parameters. The analysis provided separate linear regression equations for predicting the Erosion Rate Index for coarse-grained soils and for fine-grained soils. The predictive equations are presented in Section 2.8.3 in Chapter 2. These equations represent multiple linear regression models obtained from statistical analysis of the test data of the SET and the HET. They do not necessarily imply any causal link between the predictor variables and the Erosion Rate Indices, but Table 2.25 in Chapter 2 gives approximately relationship between I_{HET} and soil parameters and is a reasonable guide.

The erosion tests on fine-grained soils show more scattering results. The regression models for the coarse-grained soils provide more satisfactory predictions than the regression models for the fine-grained soils.

5.1.5 Effects of soil mineralogy on erosion properties

Examination of the soil mineral compositions of the soil samples revealed that soils containing smectites and vermiculites appeared to have lower Erosion Rate Indices (lower erosion resistance). There is some evidence that the presence of iron oxide may also act as cementing material reducing the rate of erosion.

5.1.6 Estimation of Critical Shear Stress from the SET and the HET

There is a large degree of inaccuracy in the estimation of the Critical Hydraulic Shear Stress, τ_c, by extrapolating the straight-line plot of erosion rate, $\dot{\varepsilon}$, versus hydraulic shear stress, τ, to the horizontal axis (where $\dot{\varepsilon} = 0$). The τ_c values represented by the intercept of the extrapolated plot at the horizontal axis, do not show any form of strong relationship with other soil properties. The values of τ_c obtained for different specimens of the same soil also vary considerably.

Instead of predicting τ_c by extrapolating the $\dot{\varepsilon}$ versus τ plot, the HET can be used to estimate the minimum test head required to initiate erosion in a soil. The initial shear stress, τ_o corresponding to the minimum test head can be used as an indicator of the soil's resistance against initiation of erosion. In other words, τ_o is an estimate of τ_c.

Results of HETs on specimens of the 13 soil samples compacted to 95% SMDD at OWC show the broad trend that coarse-grained soils have lower τ_o values than the fine-grained soils, and that τ_o value of a fine-grained soil increases as its Erosion Rate Index increases as shown in Figure 2.79, Section 2.5.2, Chapter 2.

5.1.7 Comparison between the Representative Erosion Rate Indices of the Slot Erosion Test and the Hole Erosion Test

The Representative Erosion Rate Indices, $\tilde{I}_{SET}$, based on the test data of the SET show very strong correlation with the Representative Erosion Rate Indices, $\tilde{I}_{HET}$, based on the data of the HET. In addition, $\tilde{I}_{SET}$ and $\tilde{I}_{HET}$ of the same soil have the same order of magnitude. It implies that the two erosion tests will give a similar rating on the erosion rate to the same soil at the standard condition of 95% SMDD and OWC. In addition, one test can provide a check on the results of the other test. Both tests physically model the conditions which would be expected to occur in a crack in a dam.

5.1.8 Special tests

Special tests have been carried out to investigate the effects of prior soaking/saturation (soaked test), salt concentration in the eroding fluid (salt test), and pausing (paused test) on the erosion rate of a soil.

For the soaked tests, the number of cases showing an increase in the value of the Erosion Rate Index due to prior soaking of the test specimen is almost equal to the number of cases showing a decrease in the value of the Erosion Rate Index.

Similarly, for the salt tests, although there were a few tests that showed positive results (i.e. salt water caused slower erosion than tap water), there were as many tests that showed negative results (i.e. salt water caused faster erosion than tap water).

For the paused tests, two out of a total of three tests gave positive results (i.e. pausing caused slower erosion).

Due to the limited number of successful tests, conclusions regarding the special tests cannot be made at this stage.

5.2 INVESTIGATION OF INTERNAL INSTABILITY OF SOILS

5.2.1 Factors influencing whether a soil is internally unstable

Effects of fines content and gravel content

The experimental investigation reveals no obvious relationship between the fines content and the internal stability of silt-sand-gravel and clay-silt-sand-gravel mixtures.

Effects of plasticity of fines

The experimental investigation shows no significance influence of the plasticity of the fines on the internal stability of clay-silt-sand-gravel mixtures up to the limits of the soils tested – less than 10% clay-sized fraction, and plasticity index less than 12%.

Effects of gap-grading

Gap-graded mixtures with more than 60% gravel-size particles (> 4.75 mm), but lacking sand-sized particles are vulnerable to suffusion. Nevertheless, similar gap-graded mixtures which have a very low fines content (< 10%) did not show significant loss of materials by the process of suffusion. It is possible that the amount of erosion loss was too small to be detected in these mixtures.

Effects of soil density

The results of DF tests do not suggest any significant influence of the density of a soil on its internal stability classification, within the range of dry densities investigated (i.e. 90 – 95% of standard maximum dry density).

Nevertheless, results of UF tests do indicate that erosion of fine particles started at comparatively lower hydraulic gradient in samples compacted at lower dry densities/higher porosities.

5.2.2 Methods for assessing internal instability

Using the coefficient of uniformity, C_U, as an indicator (US Army Corps of Engineers (1953), Istomina (1957))

C_U is not an accurate predictor of internal stability. In general, internally unstable soils are more likely to have C_U values higher than 10. Nevertheless, the investigation shows that some internally unstable soils have C_U values lower than 10, and a lot of soils with very high C_U values (> 100) are not internally unstable.

Methods involve splitting a soil into a coarse fraction and a fine fraction (Kézdi 1969, de Mello 1975, Sherard 1979)

These methods are easy to apply. They are, in general, too conservative for assessing whether a soil is internally unstable and subject to suffusion if the commonly used filter rule represented by d_{C15}/d_{f85} <5 is used to assess the filter compatibility between the coarse and the fine fraction. The method tends to classify stable soils as unstable.

The use of a less conservative filter rule, such as the Continuing Erosion Boundary (Foster & Fell 1999, 2001) represented by d_{C15}/d_{f95}= 9, is shown to be unconservative when applied to some coarse granular soils.

It appears that a filter rule suitable for assessing internal instability for most types of soils does not exist without being conservative.

The methods may be able to determine if a soil will self filter, but there is no experimental evidence to support this.

Kenney & Lau (1985, 1986) method using the stability number, H/F, as a predictor of internal stability

The method is conservative in that a lot of internally stable soils are classified as unstable. The upper boundary of Kenney & Lau (1985) method, represented by

$H = 1.3F$, appears to be an upper bound for unstable soils, in that no internally unstable soils are plotted above the boundary.

Burenkova (1993) method

The method presents a boundary, represented by $h' = 0.76\log(h'') + 1$, which appears to be an approximate lower bound for stable soils. Soils plotted below the boundary are more likely to be unstable than stable. The method is less conservative than Kenney & Lau (1985, 1986) method in that some unstable soils are plotted in the non-suffusive zone (Zone II) above the boundary.

Sun (1989) method for clayey/silty sands

Sun's method was developed for clayey/silty sands. The method predicts some internally unstable coarse granular soils as stable, and is hence unconservative, and should not be applied to clay-silt-sand-gravel and silt-sand-gravel mixtures. Its validity for silty sands and clayey sands is questionable, and these soils may not be susceptible to suffusion.

Probabilistic method proposed by the Author

The distribution of the internally unstable and stable soil samples in an h' versus log h'' plot based on Burenkova (1993) method suggests that a probabilistic approach can be used to predict internal instability. Logistic regression models based on experimental data obtained in the current research and experimental data from similar seepage tests carried out by previous investigators are formulated for predicting the probabilities of internal instability, as shown in Figures 3.67 and 3.68, Section 3.6.2, Chapter 3.

5.2.3 Fraction of fine particles eroded by the suffusion process

Theoretical maximum fraction of fine particles eroded in the suffusion process

The fraction of fine particles, f_f, in an internally unstable soil is related to the porosity of the fine particles as well as the porosity of the coarse particles which form the primary soil fabric as expressed in equation 3.20, Section 3.6.1, Chapter 3.

In case that the fine particles are very densely packed (void ratio of fine particles, $e_l \cong$ 0.35) within the voids of the soil skeleton formed by very loosely packed coarse particles (void ratio of the primary soil fabric, $e_P \cong 0.92$), a theoretical maximum possible value of f_l is attained, and is approximately equal to 40%. UNSW test data, and test data from the literature, however, indicate a maximum value of f_l only up to approximately 30%.

The Burenkova (1993) method and Lubochkov (1965) method

The Burenkova (1993) method has been found to severely underestimate the size of the largest particles eroded by suffusion, whereas the Lubochkov (1965) method was shown to overestimate the sizes of the largest particles eroded.

Proposed method for predicting the fraction of fine particles eroded

The method proposed by the Author for predicting the size of the largest particles eroded by the process of suffusion is based on dividing a soil into a coarse fraction and a fine fraction, and treating the coarse fraction as a filter to the fine fraction. The point, *D*, that divides the soil into a coarse fraction and a fine fraction, is chosen at where the ratio *H/F* (Kenney & Lau 1985, 86) is less than 1.3 and is minimised for $F < 0.4$. *D* is the predicted size of the largest particles eroded by the process of suffusion, and *F* is the predicted maximum fraction of fine particles that can be eroded. The reason for limiting $F < 0.4$ is because the theoretical maximum fraction of fine particles in an internally unstable soil has been assessed to be 40% (refer to Chapter 3, Section 3.6.1). UNSW test data and available test data from the literature, however, indicate a maximum *F* value of not greater than 30% (refer to Figure 3.39 in Section 3.4.2).

5.2.4 Hydraulic gradients causing internal instability in silt-sand-gravel and clay-silt-sand-gravel mixtures

Hydraulic gradient, i_{start}, for initiation of erosion by suffusion

Selective erosion of fine soil particles begins at gradients, i_{start}, less than the theoretical critical gradient, i_c, for all internally unstable soils, and for many internally stable soils.

For the internally unstable soils tested, all began to erode with gradients of 0.8 or less, with several less than 0.5. This erosion is relatively minor rate, and even in the internally unstable soils, did not lead to "extreme cloudiness" condition when erosion would be obvious.

Relationship between i_{start}, the H/F Ratio, and the fines content

No definite mathematical relationship has been identified between the hydraulic gradient i_{start} and the coefficient of uniformity, the minimum *H/F* ratio and the fines content.

Relationship between i_{start} and porosity

There appears to be a general trend that soils with higher porosity would start to erode at lower hydraulic gradients. Loose, higher porosity soils tested began to erode at gradients less than 0.3. There is, however, considerable scattering of data that a reliable mathematical relationship cannot be derived between the two variables.

Effects of plastic fines on the value of i_{start}

Soils with clayey (kaolin) fines appear to erode at relatively higher hydraulic gradients than soils having similar fines contents but without clayey fines.

Effects of dry density on the value of i_{start}

The dry density of the soil has a significant effect on the hydraulic gradient i_{start}. The higher the density, the higher the i_{start}, given that the fines content of the soils are the same.

Effects of gap-grading on the value of i_{start}

Gap-graded soils erode at relatively lower hydraulic gradient i_{start} than non gap-graded soils with similar fines content.

5.3 RECOMMENDATIONS

5.3.1 Applications of the Hole Erosion Test and the Slot Erosion Test

Use of the Hole Erosion Test (HET) and the Slot Erosion Test (SET) to find out the erosion properties of a Soil

The HET is recommended as a fast and simple test for assessing the rate of erosion of a soil. The HET assigns an Erosion Rate Index, I_{HET}, to a soil. I_{HET} has values in the range of 0 – 6. The smaller the index, the faster is the rate of erosion for a given shear stress caused by the eroding fluid. When an Erosion Rate Index I_{HET} is quoted for a soil, the percentage compaction and the water content of the test specimen of the soil should also be stated, as I_{HET} is strongly influenced by the degree of compaction and the water content. The Index corresponding to 95% compaction and optimum water content is called the Representative Erosion Rate Index, $\tilde{I}_{HET}$, of the soil.

The SET can also be used to assess the rate of erosion of a soil as a check against the results of the HET. The SET is, however, more costly than the HET due to the use of a much bigger sample of soil per test. The Erosion Rate Index, I_{SET} obtained from the SET on the same soil at the standard conditions of 95% compaction and optimum water content is expected to be in the same order of magnitude as I_{HET} obtained from the HET.

Use of the Erosion Rate Index as a predictor of the rate of piping erosion

Soils are classified into 6 groups by the Author according to their Representative Erosion Rate Index, $\tilde{I}_{HET}$. The 6 groups are :

Group No.	Erosion Rate Index	Description
1	< 2	Extremely rapid
2	2 – 3	Very rapid
3	3 – 4	Moderately rapid

Group No.	Erosion Rate Index	Description
4	4 – 5	Moderately slow
5	5 – 6	Very slow
6	> 6	Extremely slow

The above classification provides a quick guide for the assessment of the rate of progression of piping erosion in a first pass assessment of the risk of internal erosion and piping for an embankment dam.

In case the location and the geometry of a pipe are known, and reliable Erosion Rate Indices are obtained by testing, numerical modelling can be carried out, using the Erosion Rate Indices, to predict the enlargement of the pipe with time. An example is presented in Chapter 4, Section 4.3 to explain the numerical modelling procedure.

Prediction of the Erosion Rate Index without doing HET or SET

If erosion tests have not been carried out to assess the erosion resistance of a soil, predictive equations 5.3 to 5.6 presented in Section 5.1.4 can be used to provide a preliminary estimate of the Erosion Rate Index. The Author strongly recommends carrying out HET rather than using these equations, as the equations are, so far, based on a limited number of soils, and in any case, it will be more economical to do the HET than doing other tests to provide the input data required in the predictive equations.

A qualitative approach is also proposed for predicting the Representative Erosion Rate Index of a soil if HET or SET has not been carried out. A number of soil parameters, namely the degree of saturation, the fines content (< 0.075 mm), the clay content (< 0.005 mm) and the Atterberg Limits, which individually show good correlation with the Representative Erosion Rate Index are used as predictor variables as shown in Table 2.25, Chapter 2. These predictor variables are used independently to estimate the Representative Erosion Rate Index according to the guidelines in Table 2.25. A judgment is made on the final estimated value of the Representative Erosion Rate Index after considering all the values predicted by the individual predictor variables. The table may be used as an aid to judgment in conjunction with the multiple regression

equations. The Author, however, considers that this approach is not as good as doing a HET or SET.

Use of the HET to find out the approximate Critical Hydraulic Shear Stress

It is recommended to use the HET as an approximate test to estimate the erosion resistance of a soil against initiation of erosion. By trying different test heads on different test specimens of a soil, the HET can identify a minimum test head below which the test specimen shows no measurable erosion. The Initial Hydraulic Shear Stress, τ_o, corresponding to the minimum test head in the test, can serve as an indicator of the Critical Hydraulic Shear Stress, τ_c, which is a measure of the soil's resistance against initiation of erosion. Example on the comparison of τ_o with the predicted hydraulic shear stress in a crack is presented in Chapter 4, Section 4.2.

5.32 Recommended method for predicting internal instability

It is recommended to use the logistic regression model presented in Figure 3.67, Chapter 3 for predicting the probability of internal instability in silt-sand-gravel soils and clay-silt-sand-gravel soils of limited clay content (fraction finer than 0.002 mm) of less than 10% and plasticity index less than 12%, and to use Figure 3.68, Chapter 3 for sand-gravel mixtures with less than 10% non-plastic fines.

An approximate method is also recommended for estimating the fraction, *F*, of fine materials eroded in the suffusion process. The method is a modification of the method proposed by Kenney & Lau (1985, 1986), and assumes that *F* cannot be greater than 0.4, and is represented by the point at which the ratio *H/F* is minimised and not greater than 1.3. The size, *D*, of the largest particles eroded in the suffusion process is the largest particles in the fraction *F*. *H* is the fraction of soil particles with size range within *D* to *4D*.

An example on the use of the above proposed methods for assessment internal instability in some filter materials is presented in Chapter 4, Section 4.4.

5.3.3 Proposed further research

Further laboratory investigation using the Hole Erosion Test and Slot Erosion Test

Some testing on some dispersive soil samples using distilled water as the eroding fluid by Mr. S.S. Lim at UNSW has resulted in Erosion Rate Indices which were lower than the indices obtained from tests using tap water as the eroding fluid. Apparently the presence of only a small amount of dissolved solid in the water, as in the case of Sydney tap water (Total Dissolved Solids (TDS) < 100 mg/l), may suppress the dispersive behaviour of some soils. It is recommended to carry out further testing using the HET device to investigate the effects of the electrochemical properties of the eroding fluid on the rate of piping erosion in soils, in particular soils which are dispersive. This should include tests on the rate of erosion, and the initial shear stresses

The Author attempts to saturate the soil by soaking would not have achieved full saturation. Further testing should be done using back-pressure saturation to better investigate the effects of saturation.

The rate of piping erosion may be influenced by the angle of inclination the pipe due to the effect of gravity on entrainment of the eroded soil particles. The effect of gravity can be investigated by further soil testing using the SET device which is set at angle to the horizontal to simulate an upward sloping or downward slope pipe.

There would be benefits in carrying out tests using a rotating cylinder device and the HET to compare the results for initial shear stress. Modifications of the HET to better detect the initiation of erosion would be useful as it is difficult to determine the initial shear stress.

This thesis has not explored the basic mechanism of the erosion process in cohesive soils. From observation, it appears that particle detachment is affected by a slaking process, but there is a need for further research to investigate this.

Testing of the ability of a soil to sustain an open pipe

Testing of some low plasticity or non-plastic soils such as clayey or silty sand in the HET or SET often encountered the situation of having the pre-formed hole/slot blocked by the collapsed soil. Such a property is not undesirable as collapse of the soil into a pipe would block the pipe temporarily and slow down the internal erosion process. In addition, the blockage will result in fluctuating seepage flow which is a good warning signal against internal erosion in an embankment dam. Foster and Fell (1999b) proposed the simple rule that soils having a fines content (fraction fine than 0.075 mm) of greater than 15% are very likely to be able to sustain an open pipe. Simple test, such as the "sand castle" test (Vaughan and Soares 1982) is available to test the ability of a soil to "stand-up" when wetted. The test, however, is more applicable to filter materials. It is recommended to investigate the properties of a soil, such as its grading, density, water content, fines content, plasticity, presence of cementitious materials, soil strength, etc., which are likely to affect the ability of the soil to sustain an open pipe, with an aim to developing methods for assessing the "stand-up" time, and the maximum size of an open pipe that the soil can sustain. Such information is essential in the assessment of the rate of progression of piping, and the likelihood of a dam breach in a risk assessment process.

Further laboratory investigation on internal instability of soils

The number of upward flow seepage tests and downward flow seepage tests carried out under the current research project were limited. More laboratory testing is needed with a wider range of soils placed at varying void ratios, and tested at a range of hydraulic gradients for better understanding of the factors that influence the suffusion process. The additional test data will help to better define the boundary between internally unstable (suffusive) and internally stable (non-suffusive) soils, and/or to derive more accurate regression models, similar to those proposed by the Author, for prediction of the probability of internal instability.

There is still a large uncertainty in the determination of the seepage gradients which will initiate suffusion, and the fraction of erodible materials. Therefore, one of the objectives of the further research should be identifying the factors that influence the hydraulic gradient that causes initiation of suffusion. Another objective is to provide

guidelines for estimating the fraction of erodible materials, and to understand the effect of the hydraulic gradient on the fraction of erodible materials.

It is expected that the hydraulic gradient for initiating suffusion in a horizontal direction is significantly less than the hydraulic gradient for initiating suffusion in a vertically upward direction in the same soil. Tests are hence needed with flow horizontal, and inclined, to better define the gradients at which erosion initiates.

CHAPTER 6

REFERENCES

Acciardi, R. (1984)

Discussions and Closure on *'Erosion in relation to filter design criteria in earth dams'* by Arulanandan, K. and Perry, E.B. Journal of the Geotechnical Engineering Division, ASCE. 110, No. 7, July 1984, pp. 996-1005.

Arulanandan, K., Gillogley, E. and Tully, R. (1980)

Development of a Quantitative Method to Predict Critical Shear Stress and Rate of Erosion of Natural Undisturbed Cohesive Soils. U.S. Army Engineer Waterways Experiment Station, Vicksburg, MS, Technical Report No. GL-80-5.

Arulanandan, K., Loganathan, P. and Krone, R.B. (1975)

Pore and eroding fluid influences on surface erosion of soils. Journal of the Geotechnical Engineering Division, ASCE. 101 (GT1) January 1975, pp. 51-66.

Arulanandan, K. and Perry, E.B. (1983)

Erosion in relation to filter design criteria in earth dams. Journal of the Geotechnical Engineering Division, ASCE. 109(GT5), pp. 682-698.

Arulanandan, K., Sargunam, A., Loganathan, P. and Krone, R.B. (1973)

Application of chemical and electrical parameters to prediction of erodibility. In Soil Erosion: Causes and Mechanisms; Prevention and Control. Special Report 135, Highway Research Board, pp. 42-51.

Atkinson, J.H., Charles, J.A. and Mhach, H.K. (1990)

Examination of erosion resistance of clays in embankment dams. Quarterly Journal of Engineering Geology, London, Vol. 23, 1990, pp. 103-108.

AS1289.3.8.1 (1997)

Dispersion – Determination of Emerson class number of a soil. Australian Standard Methods of Testing Soils for Engineering Purposes.

AS1289.3.8.2 (1997)

Dispersion – Determination of the percent dispersion of a soil. Australian Standard Methods of Testing Soils for Engineering Purposes.

AS1289.3.8.3 (1997)

Dispersion – Determination of pinhole dispersion classification of a soil. Australian Standard Methods of Testing Soils for Engineering Purposes.

ASTM D5852-95 (1995)

Standard Test Method for Erodibility Determination of Soil in the Field or in the Laboratory by the Jet Index Method. American Society of Testing and Materials.

Bertram, G.E. (1940)

An experimental investigation of protective filters. Graduate School of Engineering, Harvard University, Soil Mechanics Series No. 7, January 1940.

Briaud, J.L., Ting, F.C.K., Chen, H.C., Gudavalli, R., Perugu, S. and Wei, G. (1999)

SRICOS: Prediction of scour rate in cohesive soils at bridge piers. ASCE Journal of Geotechnical and GeoEnvironmental Engineering, Vol. 125, No. 4, April 1999, pp. 237-246.

Briaud, J.L., Ting, F.C.K., Chen, H.C., Cao, Y., Han, S.W., and Kwak, K.W. (2001a)

Erosion Function Apparatus for scour rate predicition. ASCE Journal of Geotechnical and GeoEnvironmental Engineering, Vol. 127, No. 2, February 2001, pp. 105-113.

Briaud, J.L., Chen, H.C., Kwak, K.W., Han, S.W. and Ting, F.C.K. (2001b)

Multiflood and multiplayer method for scour rate prediction at bridge piers. ASCE Journal of Geotechnical and GeoEnvironmental Engineering, Vol. 127, No. 2, February 2001, pp. 114-125.

Briaud, J.L., Chen, H.C., Li, P., Nurtjahyo, P. and Wang, J. (2003) *Complex pier scour and contraction scour in cohesive soils.* National Cooperative Highway Reseach Program NCHRP Report 24-15.

Burenkova, V.V. (1993)

Assessment of suffosion in non-cohesive and graded soils. Proceedings, the First International Conference "Geo-Filters", Karlsruhe, Germany, 20–22 October 1992, Filters in Geotechnical and Hydraulic Engineering, Brauns, Heibaum & Schuler (eds), 1993 Balkema, Rotterdam, pp. 357-360.

Bui, H., Fell, R. and Song, C. (2004). *Two and three dimensional numerical modelling of the potential for cracking of embankment dams during construction.* UNICIV Report No. 426, The School of Civil and Environmental Engineering, The University of New South Wales, Sydney.

Bui, H., Tandjiria, V. Fell, R., Song, C. and Khalili, N. (2005). *Two and three dimensional numerical analysis of the potential for cracking of embankment dams – supplementary report.* UNICIV Report R438, The University of New South Wales, ISBN: 85841 405 8.

Cedeño, A.R., Jr. (1998)

Piping in Dams : Tests to Assess the Factors which Affect Progression. CIVL4906 – Project/Thesis, School of Civil and Environmental Engineering, University of New South Wales.

Cedergren, H.R. (1989)

Seepage, Drainage, and FlowNets. Third Edition, 1989, John Wiley & Sons Inc., ISBN 0-471-18053-X.

CFGB (1997)

Internal Erosion: Typology, Detection, Repair. Barrages and Reservoirs No.6. Comité Francais des Grands Barrages, Le Bourget-du-lac Cedex.

Chapuis, R.P. (1986a)

Use of Rotational Erosion Device on Cohesive Soils. Transportation Research Record 1089

Chapuis, R.P. (1986b)

Quantitative measurement of the scour resistance of natural solid clays. Canadian Geotechnical Journal. 23. pp. 132-141.

Chapuis, R.P. (1992)

Similarity of internal stability criteria for granular soils. Canadian Geotechnical Journal, Vol. 29, 1992, pp. 711-713.

Chapuis, R.P. and Gatien, T. (1986)

An improved rotating cylinder technique for quantitative measurements of the scour resistance of clays. Canadian Geotechnical Journal. 23. pp. 83-87.

Chapuis, R.P., Constant, A. and Baass, K.A. (1996)

Migration of fines in 0-20mm crushed base during placement, compaction, and seepage under laboratory conditions. Canadian Geotechnical Journal, Vol. 33, 1996, pp. 168-176.

Christensen, R.W. and Das, B.M. (1973)

Hydraulic erosion of remolded cohesive soils. In Soil Erosion: Causes and Mechanisms; Prevention and Control. Special Report 135, Highway Research Board, pp. 8-19.

de Mello, V.F.B. (1975)

Some lessons from unexpected, real and fictitious problems in earth dam engineering in Brazil. Proceedings, Sixth Regional Conference for Africa on Soil Mechanics and Foundation Engineering, Durban, South Africa, September 1975, Eds. Robertson, A.M.G., and Caldwell, J.A., Volume 2, pp. 285-304.

Decker, R.S. and Dunnigan, L.P. (1977)

Development and Use of the Soil Conservation Service Dispersion Test. In Dispersive Clays, Related Piping, and Erosion in Geotechnical Projects, ASTM STP 623, Eds. Sherard, J.L. and Decker, R.S., American Society for Testing and Materials, 1977, pp. 94-109.

Dekay, M.L. and McClelland, G.H. (1993)

Predicting loss of life in cases of dam failure and flash flood. Risk Analysis, Vol. 13, No. 2, 1993, pp. 193-205.

Dennis, J.E., Gay, D.M. and Welsch, R.E. (1981)

An adaptive nonlinear least-squares algorithm. ACM Transactions on Mathematical Software 7, 3, September 1981.

Dunn, I.S. (1959)

Tractive resistance of cohesive channels. Journal of Soil Mechanics and Foundations Division, ASCE, June 1959, pp. 1 –24.

Emerson, W.W. (1967)

A classification of soil aggregates based on their coherence in water. Australian Journal of Soil Research, 1967, 5, pp. 47-57.

Fell, R., Wan, C.F., Cyganiewicz, J. and Foster, M. (2001)

The Time for Development and Detectability of Internal Erosion and Piping in Embankment Dams and Their Foundations. UNICIV Report R-399, June 2001, ISBN 85841 366 3, the University of New South Wales, Sydney, Australia.

Fell, R., Wan, C.F., Cyganiewicz, J., Foster, M. (2003)

Time for Development of Internal Erosion and Piping in Embankment Dams. Journal of Geotechnical and Geoenvironmental Engineering, ASCE, Vol. 129, No. 4, April 1, 2003, pp 307-314.

Foster, M.A., Fell, R. and Spannagle, M. (1998)

Analysis of embankment dam incidents. UNICIV Report No.R-374, September 1998. The University of New South Wales, Sydney 2052 Australia. ISBN: 85841 349 3.

Foster, M. A. (1999)

The Probability of Failure of Embankment Dams by Internal Erosion and Piping. Thesis submitted in partial fulfilment of the requirements for the degree of Doctor of Philosophy, the University of New South Wales, Sydney, Australia, (1999)

Foster, M.A. and Fell, R. (1999a)

Assessing embankment dam filters which do not satisfy design criteria. UNICIV Report No. R-376, May 1999, School of Civil & Environmental Engineering , the University of New South Wales, Sydney, Australia. ISBN 85841 343 4

Foster, M.A. and Fell, R. (1999b)

A Framework for Estimating the Probability of Failure of Embankment Dams by Internal Erosion and Piping using Event Tree Methods. UNICIV Report R-377 December 1999, the University of New South Wales, Sydney, Australia. ISBN 85841 344 2

Foster, M.A. and Fell, R. (2000)

Use of Event Trees to Estimate the Probability of Failure of Embankment Dams by Internal Erosion and Piping. Transactions, Twentieth International Congress on Large Dams, 19 – 22 September 2000, Beijing, China, Volume 1, Q.76, R.15, pp. 237-259.

Foster, M.A. and Fell, R. (2001)

Assessing embankment dam filters which do not satisfy design criteria. Journal of Geotechnical and Geoenvironmental Engineering, ASCE, Vol. 127, No. 5, May 2001, pp. 398-407.

Foster, M.A., Fell, R. and Spannagle, M. (2000a)

The statistics of embankment dam failures and accidents. Canadian Geotechnical Journal, Ottawa 37, (5), pp. 1000-1024.

Foster, M.A., Fell, R. and Spannagle, M. (2000b)

A method for estimating the relative likelihood of failure of embankment dams by internal erosion and piping. Canadian Geotechnical Journal 37, (5), pp. 1025-1061.

Fuller, W.B. and Thompson, S.E. (1907)

The laws of proportioning concrete. Transactions American Society of Civil Engineers, 59.

Ghebreiyessus, Y.T., Gantzer, C.J., Alberts, E.E. and Lentz, R.W. (1994)

Soil erosion by concentrated flow: shear stress and bulk density. Transactions of the ASAE. 37(6) pp. 1791-1797.

Gibbs, H.J. (1962)

A Study of Erosion and Tractive Force Characteristics in Relation to Soil Mechanics Properties. United States Department of the Interior, Bureau of Reclamation, Division of Engineering Laboratories, Soils Engineering Report No. EM-643, February 23, 1962.

Graham, W.J. (1999)

A procedure for estimating loss of life caused by dam failure. DSO-99-06, US Department of the Interior, Bureau of Reclamation, Denver, CO.

Gray, D.H. (1989)

Discussions on 'Erosion Rate of Dispersive and Nondispersive Clays' by Shaikh, A., Ruff, J.F., Charlie, W.A. and Abt, S.R. Journal of the Geotechnical Engineering Division, ASCE. 115, No. 12, December 1989, pp. 1823 -1824.

Grim, R.E. (1953)

Clay Mineralogy. McGraw-Hill Book Company, Inc. 1953.

Hanson, G.J. (1991)

Development of a Jet Index to Characterize Erosion Resistance of Soils in Earthen Spillways. Transactions of the ASAE. 34(5) pp. 2015-2020.

Hanson, G.J. (1992)

Erosion resistance of compacted soils. Transportation Research Record 1369, pp. 26-30.

Hanson, G.J. and Robinson, K.M. (1993)

The influence of soil moisture and compaction on spillway erosion. Transactions of the ASAE. 36(5) pp. 1349-1352.

Hensel, H.D. (2001)

Report on the identification of components within two clays from the Buffalo Dam, Vic. In Lake Buffalo Future Strategy Phase B2 prepared on behalf of Goulburn-Murray Water, January 2001, Snowy Mountains Engineering Corporation (2001).

Hjeldnes, E.I. and Lavania, B.V.K. (1980)

Cracking, Leakage, and Erosion of Earth Dam Materials. Journal of the Geotechnical Engineering Division, ASCE. 106, No. GT2, February 1980, pp. 117-135.

Istomina, V.S. (1957)

Filtration stability of soils (in Russian). Gostroizdat, Moscow, Leningrad.

Kandiah, A. and Arulanandan, K. (1974)

Hydraulic Erosion of Cohesive Soils. Transportation Research Record No. 497.

Kenney, C. (1984)

Discussions and Closure on '*Erosion in relation to filter design criteria in earth dams*' by Arulanandan, K. and Perry, E.B. Journal of the Geotechnical Engineering Division, ASCE. 110, No. 7, July 1984, pp. 996-1005.

Kenney, T.C., Lau, D. and Clute, G. (1983)

Filter Tests on 235mm diameter specimens of granular materials. University of Toronto, Department of Civil Engineering, Publication 84-07, October 1983, ISBN 0-7727-7060-3.

Kenney, T.C., Lau, D. and Clute, G. (1984)

Stability of Particle Gradations : Tests on Mixtures of Narrowly Graded Materials. University of Toronto, Department of Civil Engineering, Publication 84-08, February 1984.

Kenney, T.C. and Lau, D. (1984)

Stability of Particle Grading of Compacted Granular Filters. University of Toronto, Department of Civil Engineering, Publication 84-06, August 1984, ISBN 0-7727-7058-1.

Kenney, T.C., Chahal, R., Chiu, E., Ofoegbu, I., Omange, G.N. and Ume, C.A. (1985)

Controlling constriction sizes of granular filters. Canadian Geotechnical Journal, Vol. 22, pp. 32-43.

Kenney, T.C. and Lau, D. (1985)

Internal stability of granular filters. Canadian Geotechnical Journal, Vol. 22 No. 2, pp. 215-225.

Kenney, T.C. and Lau, D. (1986)

Internal stability of granular filters : Reply. Canadian Geotechnical Journal, Vol. 23, pp. 420-423.

Kézdi, Á. (1969)

Increase of protective capacity of flood control dikes (in Hungarian). Department of Geotechnics, Technical University of Budapest, Report No. 1.

Kjaernsli, B. and Torblaa, I. (1968)

Horizontal cracks through the core at Hyttejuvet Dam. Publication No. 80, Norwegian Geotechnical Institute, Oslo, Norway, 1968.

Kovács, G. (1981)

Seepage Hydraulics. Elservier Scientific Publishing Company, 1981

Lafleur, J., Mlynarek, J. and Rollin, A.L. (1989)

Filtration of broadly graded cohesionless soils. Journal of Geotechnical Engineering, ASCE, Vol. 115, No. 12, December 1989, pp. 1747-1768.

Lafleur, J., Mlynarek, J. and Rollin, A.L. (1993)

Filter criteria for well graded cohesionless soils. Proceedings, the First International Conference "Geo-Filters", Karlsruhe, Germany, 20–22 October 1992, Filters in Geotechnical and Hydraulic Engineering, Brauns, Heibaum & Schuler (eds), 1993 Balkema, Rotterdam, pp. 97-106.

Lambe, T.W. and Whitman, R.V. (Eds.) (1979)

Soil Mechanics, S.I. Version, Eds. Lambe, T.W. and Whitman, R.V., John Wiley & Sons, New York 1979.

Lyle, W.M. and Smerdon, E.T. (1965)

Relation of compaction and other soil properties to erosion resistance of soils. Transactions of the ASAE, 8(3), pp. 419-422.

Lubochkov, E.A. (1962)

The self-filtering behaviour of non-cohesive soils (in Russian). Izvestia VNIIG, No. 71.

Lubochkov, E.A. (1965)

Graphical and analytical methods for the determination of the properties of non-cohesive soils characterizing suffusion (in Russian). Izvestia VNIIG, No. 78.

Maranha das Neves, E. (1987)

Discussion Report. Proceedings, 9th European Conference on Soil Mechanics and Foundation Engineering, Dublin, Ireland 1987, pp. 1367-1373.

Maranha das Neves, E. (1989)

Analysis of Crack erosion in dam cores. The crack erosion test. de Mello Volume, Sao Paulo, Brazil, pp. 284-298.

Martin, R.T. (1962)

Discussion of Paper by Walter L. Moore and Frank D. Masch, Jr., 'Experiments on the Scour Resistance of Cohesive Sediments'. Journal of Geophysical Research, Vol. 67, No.4, April 1962, pp. 1447 – 1449.

Masch, F.D., Jr., Espey, W.H., Jr., and Moore, W.L. (1963)

Measurements of the Shear Resistance of Cohesive Sediments. Proceedings of the Federal Inter-Agency Sedimentation Conference, Agricultural Research Service, Publication No. 970, Washington, D.C., pp. 151-155.

Mitchell, J.K. (1976)

Fundamentals of Soil Behavior. John Wiley & Sons, Inc., ISBN 0-471-61168-9

Moore, W.L. and Masch, F.D., Jr. (1962)

Experiments on the Scour Resistance of Cohesive Sediments. Journal of Geophysical Research, Vol. 67, No. 4, April 1962, pp. 1437-1449.

Reddi, L.N., Lee, I.M. and Bonala, M.V.S. (2000)

Comparison of Internal and Surface Erosion Using Flow Pump Tests on a Sand-Kaolinite Mixture. Geotechnical Testing Journal, GTJODJ, Vol. 23, No.1, March 2000, pp. 116-122.

Sanchez, R.L., Strutynsky, A.I. and Silver, M.L. (1983)

Evaluation of the Erosion Potential of Embankment Core Materials using the Laboratory Triaxial Erosion Test Procedure. Geotechnical Laboratory, U.S. Army Engineer Waterways Experiment Station, Technical Report GL-83-4, April 1983.

Sargunan, A (1977)

Concept of Critical Shear Stress in Relation to Characterization of Dispersive Clays. In Dispersive Clays, Related Piping, and Erosion in Geotechnical Projects. Symposium, Seventy-ninth Annual Meeting, American Society for Testing and Materials, Chicago, III., 27 June – 2 July 1976, ASTM Special Technical Publication 623, Sherard, J.L. and Decker R.S. eds., pp. 390-397.

Schuler, U (1995)

How to deal with the problem of suffosion. Research and Development in the Field of Dams, Swiss National Committee on Large Dams, 1995, pp. 145-159.

Shaikh, A., Ruff, J.F. and Abt, SR. (1988)

Erosion rate of compacted NA-montmorillonite soils. Journal of Geotechnical Engineering, ASCE. 114(3) pp. 296-305.

Shaikh, A., Ruff, J.F., Charlie, W.A. and Abt, S.R. (1988)

Erosion rate of dispersive and nondispersive clays. Journal of Geotechnical Engineering. 114(5) pp. 589-600.

Sherard, J.L. (1973)

Embankment Dam Cracking. In Embankment Dam Engineering, 1973, Eds. Hirschfeld, R.C. and Poulos, S.J., pp. 271-353.

Sherard, J.L. (1979)

Sinkholes in dams of coarse, broadly graded soils. Transactions, 13th Congress on Large Dams, New Delhi, India, Vol. 2, pp. 25-35.

Sherard, J.L. (1984)

Discussions and Closure on *'Erosion in relation to filter design criteria in earth dams'* by Arulanandan, K. and Perry, E.B. Journal of the Geotechnical Engineering Division, ASCE. 110, No. 7, July 1984, pp. 996-1005.

Sherard, J.L. (1985)

Hydraulic Fracturing in Embankment Dams. Proceedings, Symposium on Seepage and Leakage from Dams and Impoundments, ASCE, 1986, Eds. Volpe, R.L. and Kelly, W.E., pp. 115-141.

Sherard, J.L. and Dunnigan, L.P. (1989)

Critical filters for impervious soils. Journal of the Geotechnical Engineering, ASCE. 115, No. 7, 1989, pp. 927-947.

Sherard, J.L., Decker, R.S. and Ryker, N.L. (1972)

Piping in earth dams of dispersive clay. Proceedings, Specialty Conference on Performance of Earth and Earth-supported Structures, ASCE, 1972, Volume 1, Part 1, pp. 589-626.

Sherard, J.L., Dunnigan, L.P., and Decker, R.S. (1976)

Identification and Nature of Dispersive Soils. Journal of Geotechnical Engineering Division, ASCE. 102, No. GT4, April 1976, pp. 298-312.

Sherard, J.L., Dunnigan, L.P. and Talbot, J.R. (1984)

Filters for silts and clays. Journal of the Geotechnical Engineering Division, ASCE. 110, No. 6, June 1984, pp. 684-699.

Sherard, J.L., Dunnigan, L.P., Decker, R.S. and Steele, E.F. (1976)

Pinhole Test for Identifying Dispersive Soils. Journal of Geotechnical Engineering Division, ASCE. 102, No. GT1, January 1976, pp. 69-85.

Shields, A. (1936)

Application of Similarity Principles and Turbulence Research to Bed-load Movement. In: Ott, W.P. and Unchelen, J.C. (Translators), Mitteilungen der preussischen Nersuchsanstalt fur Wassed Brau end Schiffbuar. Report 167, California Institute of Technology, Pasedena, California

Shrestha, P.L. and Arulanandan, K. (1989)

Discussions on '*Erosion Rate of Dispersive and Nondispersive Clays*' by Shaikh, A., Ruff, J.F., Charlie, W.A. and Abt, S.R., Journal of the Geotechnical Engineering Division, ASCE. 115, No. 12, December 1989, pp. 1824 -1825.

Skempton, A.W. (1953)

The colloidal "activity" of clays. Proceedings, Third International Conference on Soil Mechanics and Foundation Engineering, Switzerland, 1953, 1, pp. 57 – 61.

Skempton A.W. and Brogan, J.M. (1994).

Experiments on piping in sandy gravels. Geotechnique 44, No.3, pp. 449-460.

Statton, C.T. and Mitchell, J.K. (1977)

Influence of Eroding Solution Composition on Dispersive Behaviour of a Compacted Clay Shale. In Dispersive Clays, Related Piping, and Erosion in Geotechnical Projects. Symposium, Seventy-ninth Annual Meeting, American Society for Testing and Materials, Chicago, III., 27 June – 2 July 1976, ASTM Special Technical Publication 623, Sherard, J.L. and Decker R.S. eds., pp. 398-405.

Sun, B.C.B. (1989)

Internal Stability of Clayey to Silty Sands. A dissertation submitted in partial fulfillment of the requirements for the degree of Doctor of Philosophy (Civil Engineering) in the University of Michigan 1989.

Terzaghi, K and Peck, R.B. (1948, 1967)

Soil Mechanics in Engineering Practice. 1st Ed. (1948), 2nd Ed. (1967), John Wiley and Sons, New York.

U.S. Army Corps of Engineers (1953)

Filter Experiments and Design Criteria. Technical Memorandum No. 3-360, Waterways Experiment Station, Vicksburg.

Vaughan, P.R., and Bridle, R.C. (2004)

An update on perfect filters.Long-term benefit and performance of dam. Proceedings, 13th Conference of the British Dam Society and European Club of ICOLD. University of Canterbury, UK, 22-26 June 2004, Thomas Telford, London, pp. 516-531.

Vaughan, P.R., and Soares, H.F. (1982)

Design of filters for clay cores of dams. Journal of Geotechnical Engineering Division, ASCE, 108 (GT1), pp. 17-31.

Von Thun, J.W. (1996)

Understanding Piping and Seepage Failures – The No. 1 Dam Safety Problem in the West. ASDSO Western Regional Conference, Lake Tahoe, Nevada, April 1996.

Wolski, W. (1965)

Model Tests on the Seepage Erosion in the Silty Clay Core of an Earth Dam. Proceedings of the Sixth International Conference on Soil Mechanics and Foundation Engineering, Montreal, 8-15 September 1965, Vol. II, Division 3-6, pp. 583-587.

Published reports and papers

Foster, M.A., Fell, R., Davidson, R. and Wan, C.F. (2001)

Estimation of the Probability of Failure of Embankment Dams by Internal Erosion and Piping using Event Tree Methods. Proceedings, ZSOLD/ANCOLD 2001 Conference on Dams, 3 – 9 November, Auckland, New Zealand.

Wan, C.F. and Fell, R. (2002).

Investigation of internal erosion and piping of soils in embankment dams by the slot erosion test and the hole erosion test. UNICIV Report No. R-412, ISBN: 85841 379 5, School of Civil and Environmental Engineering, The University of New South Wales.

Wan, C.F., Fell, R., and Foster, M.A. Foster (2002)

Experimental investigation of the rate of piping erosion of soils in embankment dams. Proceedings, 2002 ANCOLD Conference on Dams, 19-25 October 2002, Glenelg, Adelaide, South Australia.

Wan, C.F., Fell, R. (2003)

Experimental Investigation of Internal Erosion by the Process of Suffusion in Embankment Dams and their Foundations. Proceedings, 2003 ANCOLD Conference on Dams, 24-29 October 2003, Hobart, Tasmania.

Wan, C.F. and Fell, R. (2004a). *Investigation of rate of erosion of soils in embankment dams.* ASCE Journal of Geotechnical and GeoEnvironmental Engineering, Vol. 130, No. 4, pp. 373-380.

Wan, C.F. and Fell, R. (2004b). *Laboratory tests on the rate of piping erosion of soils in embankment dams.* ASTM Geotechnical Testing Journal, vol.27, No.3, 295-303.

Wan, C.F. and Fell, R. (2004c).

Experimental investigation of internal instability of soils in embankment dams and their foundations. UNICIV Report No.429, School of Civil and Environmental Engineering, The University of New South Wales, Sydney, ISBN 85841 396 5.

Wan, C.F. and Fell, R. (2005)

Investigation of internal erosion by the process of suffusion in embankment dams and their foundations. Workshop on Internal Erosion of Embankment Dams and their Foundations, Aussois, France, 25 – 27 April 2005.

Experimental Investigations of Piping Erosion and Suffusion of Soils in Embankment Dams and their Foundations

by

Chi Fai Wan

A thesis submitted in partial fulfilment
of the requirements for the degree of
Doctor of Philosophy

Volume 2

School of Civil and Environmental Engineering

The University of New South Wales

June 2006

TABLE OF CONTENTS

VOLUME 2

LIST OF APPENDICES

APPENDIX A: SUMMARY OF INTERPRETED RESULTS OF ALL SLOT EROSION TESTS

APPENDIX B: SUMMARY OF INTERPRETED RESULTS OF ALL HOLE EROSION TESTS

APPENDIX C: NON-LINEAR REGRESSION MODELS FOR PREDICTING I_{SET} AND I_{HET} FOR SPECIMEN COMPACTED TO 95% COMPACTION AT OPTIMUM WATER CONTENT

APPENDIX D: CONTOUR PLOTS OF I_{SET} AND I_{HET}

APPENDIX E: PLOTS OF EROSION RATE INDEX AGAINST DRY DENSITY, WATER CONTENT, PERCENTAGE COMPACTION, RATIO OF WATER CONTENT TO OWC, AND DEGREE OF SATURATION

APPENDIX F: PLOTS OF EROSION RATE INDEX AGAINST SAND CONTENT, FINES CONTENT, AND CLAY CONTENT

APPENDIX G: PLOTS OF EROSION RATE INDEX AGAINST LIQUID LIMIT, PLASTICITY INDEX, AND ACTIVITY

APPENDIX H: PLOTS OF EROSION RATE INDEX AGAINST PINHOLE TEST CLASSIFICATION, EMERSON CLASS TEST CLASSIFICATION, PERCENTAGE DISPERSION, *SAR*, AND MAJOR CATION CONTENT

APPENDIX I: SLOT EROSION TEST PROCEDURE

APPENDIX J: HOLE EROSION TEST PROCEDURE

APPENDIX K: X-RAY POWDER DIFFRACTION ANALYSIS OF SOIL SAMPLES

APPENDIX L: REPORT ON THE IDENTIFICATION OF COMPONENTS WITHIN TWO CLAYS FROM THE BUFFALO DAM, VICTORIA BY HENSEL, H.D.

APPENDIX M: SUMMARY OF GRADING INFORMATION OF SOIL SAMPLES TESTED FOR INTERNAL STABILITY BY OTHERS

APPENDIX N: RECORD OF DOWNWARD FLOW SEEPAGE TESTS

APPENDIX O: DOWNWARD FLOW SEEPAGE TESTS – ESTIMATING THE FRACTION OF MATERIALS LOSS BY SUFFUSION USING CURVE MATCHING TECHNIQUE

APPENDIX P: RECORDS OF UPWARD FLOW SEEPAGE TESTS

APPENDIX A

Summary of Interpreted Results of All Slot Erosion Tests

Appendix A – Summary of Interpreted Results of A1 Slot Erosion Tests

Summary of interpreted results of all SETs.

Soil Sample	Max. Dry Unit Weight (Mg/m^3)	Optimum Water Content (%)	Test No.	Test Date	Percentage Compaction (%)	Water Content (%)	Special Treatment (See Note 1)	Duration of erosion test (s)	Coefficient of Soil Erosion C_e (s/m)	Critical Shear Stress (N/m^2)	Coefficient of determination r^2	Remark
Bradys	1.318	35.2%	1	24/11/00	91.5%	34.4%	N	285	7.25E-04	-100.0	0.964	Rate corresponds to time 61 - 196s.
			2	23/11/00	97.0%	37.8%	N	5460	5.22E-05	58.6	0.910	Rate corresponds to time 1005 - 3995s
			3	29/11/00	94.0%	36.2%	N	586	1.65E-04	-470.9	0.911	Rate corresponds to time 2 - 360s.
			4	1/12/00	93.0%	38.0%	N	1200	2.07E-04	73.5	0.957	Rate corresponds to time 527 - 1199s.
			5	3/12/00	97.0%	34.2%	N	540	5.20E-04	7.4	0.813	Rate corresponds to time 167 - 450s.
			6	12/12/00	96.5%	37.5%	N	1290	1.10E-04	-33.4	0.878	Rate corresponds to time 301 - 1289s.
			7	8/12/00	97.5%	35.8%	N	802	3.12E-04	-13.7	0.980	Rate corresponds to time 235 - 540s.
			8	14/12/00	94.0%	34.2%	N	385	7.95E-04	10.9	0.923	Rate corresponds to time 91 - 239s.
			9	16/2/01	96.0%	35.6%	S	7200				Slot blocked
			10	9/8/01	95.5%	35.1%	N	239	8.03E-04	-102.2	0.948	Rate corresponds to time 30 - 120s.
			11	14/9/01	94.5%	35.2%	0.02M	1034	2.87E-04	-20.2	0.883	Rate corresponds to time 118 - 726s.
Buffalo	1.719	19.4%	1	4/9/01	93.5%	15.8%	N	7240	(See Note 2)			Erosion slowed down. Width of slot stabilised at 2.9mm after testing for 2 hrs 40s.
Fattorini	1.696	18.5%	1	1/9/00	97.0%	20.6%	N	7200	(See Note 2)			Erosion slowed down. Width of slot stabilised at 10.4mm after testing for 2 hours .
			2	5/9/00	92.0%	21.3%	N	7200	(See Note 2)			Erosion slowed down. Width of slot stabilised at 5.8mm after testing for 2 hours
			3	6/9/00	95.5%	16.2%	N	390	2.14E-03	2.4	0.840	Rate corresponds to first 101s of erosion. Likely to overestimate rate.
			4	7/9/00	91.5%	16.4%	N	255	2.58E-03	4.1	0.979	Rate corresponds to time 1 - 166s.
			5	8/9/00	92.5%	21.3%	N	7200	(See Note 2)			Erosion slowed down. Width of slot stabilised at 4.1mm after testing for 2 hours .
			6	12/9/00	93.0%	16.4%	N	263	1.87E-03	-13.0	0.967	Rate corresponds to time 1 - 165s.
			7	14/9/00	86.5%	18.2%	N	240	2.71E-03	-1.6	0.857	Rate corresponds to first 81s of erosion. Likely to overestimate rate.
			8	13/9/00	96.0%	18.2%	N	1350	1.94E-04	-48.8	0.954	Rate corresponds to time 242 - 1350s.
			9	13/9/00	91.5%	18.1%	N	700	2.87E-04	-210.4	0.960	Rate corresponds to time 102 - 600s.
			10	19/9/00	88.0%	20.1%	N	3840	1.81E-05	-835.0	0.985	Rotameter found blocked at 1800s. Results not reliable. Rate corresponds to time 1803 - 2700s after unblocking of rotameter.
			10r	29/9/00	92.5%	20.1%	N	7200	(See Note 2)			Erosion slowed down. Width of slot stabilised at 7.9mm after testing for 2 hours .
			11	20/9/00	96.0%	19.8%	N	7200	(See Note 2)			Erosion slowed down. Width of slot stabilised at 6.4mm after testing for 2 hours
			12	21/9/00	94.0%	19.5%	N	7200	(See Note 2)			Erosion slowed down. Width of slot stabilised at 9.2mm after testing for 2 hours .
			13	26/9/00	90.5%	16.7%	S	480	1.13E-04	-1327.4	0.695	Rate corresponds to time 61 - 299s. Low coeff. of determination.
			14	27/9/00	93.0%	17.5%	S	820	2.78E-04	-154.1	0.978	Rate corresponds to time 62 - 600s.
			15	28/9/00	97.5%	16.8%	S	2320	2.61E-04	106.9	0.961	Rate corresponds to time 204 - 2100s.
			16	9/10/00	98.5%	17.5%	P	5400	(See Note 2)			Erosion slowed down. Width of slot stabilised at 8.6mm. Time shown is effective erosion time.
			17	17/11/00	94.5%	19.0%	N	1860	7.12E-05	-317.2	0.839	Rate corresponds to time 2 - 1860s.
			18	21/11/00	95.0%	17.1%	N	864	3.83E-04	-60.7	0.988	Rate corresponds to time 2 - 750s.

Appendix A – Summary of Interpreted Results of Al Slot Erosion Tests

Summary of interpreted results of all SETs (Continued).

Soil Sample	Max. Dry Unit Weight (Mg/m^3)	Optimum Water Content (%)	Test No.	Test Date	Percentage Compaction (%)	Water Content (%)	Special Treatment (See Note 1)	Duration of erosion test (s)	Coefficient of Soil Erosion C_e (s/m)	Critical Shear Stress (N/m^2)	Coefficient of determination r^2	Remark
Hume	1.635	20.8%	1a	1/6/00	98.0%	20.4%	HH	1740	2.45E-04	40.8	0.926	Rate corresponds to first 481s of erosion. Likely to overestimate rate.
			1b	13/6/00	98.0%	21.5%	N	4800	7.57E-05	105.2	0.956	Rate corresponds to time 2401 - 3600s.
			2	9/6/00	98.0%	22.3%	N	5700	2.85E-05	2.8	0.862	Rate corresponds to time 2161 - 5699s.
			3	19/6/00	98.0%	22.2%	N	4020	6.45E-05	-60.3	0.931	Rate corresponds to time 3000 - 4019s.
			4	20/6/00	98.0%	20.8%	N	4500	2.87E-04	215.4	0.855	Rate corresponds to time 2100 - 3600s.
			5	22/6/00	98.0%	19.6%	N	1950	1.56E-03	294.9	0.849	Rate corresponds to time 1321 - 1949s.
			6	22/6/00	95.0%	21.2%	N	2250	5.80E-05	-310.6	0.835	Rate corresponds to time 518 - 1672s.
			7	27/6/00	95.0%	22.6%	N	7200	7.67E-05	140.6	0.949	Rate corresponds to time 2401 - 6000s.
			8	28/6/00	95.0%	20.0%	N	1350	8.79E-05	-366.0	0.637	Rate corresponds to time 601 - 1200s.
			9	30/6/00	90.0%	20.7%	N	660				Depth of slot not measured after test. Insufficient information.
			10	5/7/00	91.5%	23.7%	N	1350	1.94E-04	22.2	0.877	Rate corresponds to time 361 - 1349s.
			11	16/6/00	92.0%	19.4%	N	960	2.45E-04	-119.3	0.833	Rate corresponds to time 31 - 600s.
			12	5/7/00	94.0%	21.3%	P	1020	4.86E-04	163.2	0.711	Rate corresponds to time 661 - 930s (Time shown is effective erosion time).
			12r	18/8/00	97.0%	20.0%	N	3390	3.90E-05	-315.4	0.917	Rate corresponds to time 601 - 1800s.
			13	11/7/00	97.0%	22.8%	S	7800				Slot blocked
			14	12/7/00	93.0%	19.7%	S	8100				Slot blocked
			15	18/7/00	92.5%	17.6%	S	6060				Slot blocked
Jindabyne	1.753	16.2%	1	23/3/01	92.0%	16.7%	N	7200				Slot blocked
			2	26/3/01	91.5%	18.6%	N	220	2.22E-03	34.6	0.985	Rate corresponds to time 61 - 74s. Period for evaluation of erosion rate index is too short that index calculated may not be representative.
			3	27/3/01	97.0%	14.4%	N	628	6.54E-04	32.9	0.984	Rate corresponds to time 121 - 360s.
			4	28/3/01	97.5%	18.6%	N	3900	4.77E-05	-110.4	0.714	Rate corresponds to time 155 - 3000s.
			5	29/3/01	93.5%	18.7%	N	1219	3.00E-04	84.2	0.757	Rate corresponds to time 241 - 420s.
			6	30/3/01	91.0%	15.1%	N	225	1.07E-03	-40.4	0.947	Rate corresponds to time 46 - 120s.
			7	27/7/01	94.5%	16.5%	N	498	1.31E-03	93.2	0.895	Rate corresponds to time 91 - 300s.
			8	9/8/01	94.0%	16.4%	S	7200				Slot blocked.
			9	25/9/01	93.5%	16.5%	0.02M	7200				Slot blocked.
Lyell	1.963	10.1%	1	12/2/01	95.0%	12.3%	N	40				Post test depth measurements were not taken due to excessive slaking of the sample after the test stopped. Insufficient data for estimating erosion rate index.
			2	15/2/01	93.7%	9.6%	N	25	3.95E-02	61.0	0.931	Rate corresponds to time 11 - 23s.
			3	13/2/01	100.0%	11.9%	N	40	5.56E-03	-276.3	0.896	Rate corresponds to time 1 - 14s.
			4	21/2/01	97.5%	8.1%	N		1.56E-02	28.3	0.979	Rate corresponds to time 1 -76s.
			5	4/7/01	96.5%	11.6%	N	45				Rapid erosion caused rapid head loss, and drop in shear stress. Insufficient data for estimating erosion rate index.
			6	5/7/01	97.5%	7.8%	N	249	1.00E-02	45.2	0.956	Rate corresponds to time 31 - 218s.
			7	3/7/01	96.0%	10.0%	N	51				Rapid erosion caused rapid head loss, and drop in shear stress. Insufficient data for estimating erosion rate index.
			8	20/9/01	95.5%	9.8%	0.02M	56	9.57E-03	-37.5	0.896	Rate corresponds to time 40 - 55s.
Matahina	1.805	16.7%	1	29/6/01	94.5%	16.6%	N	7200	(See Note 2)			Erosion slowed down. Width of slot stabilised at 8.8mm after testing for 2 hours
			2	6/7/01	91.0%	14.9%	N	627	1.18E-03	86.5	0.791	Rate corresponds to time 91 - 597s.

Appendix A – Summary of Interpreted Results of Al Slot Erosion Tests

Summary of interpreted results of all SETs (Continued).

Soil Sample	Max. Dry Unit Weight (Mg/m^3)	Optimum Water Content (%)	Test No.	Test Date	Percentage Compaction (%)	Water Content (%)	Special Treatment (See Note 1)	Duration of erosion test (s)	Coefficient of Soil Erosion C_e (s/m)	Critical Shear Stress (N/m^2)	Coefficient of determination r^2	Remark
Pukaki	2.150	8.6%	1	8/6/01	96.0%	8.5%	N	690	3.46E-04	-84.7	0.914	Rate corresponds to time 181 - 240s.
			2	6/6/01	97.5%	10.5%	N	855	8.49E-04	35.8	0.876	Rate corresponds to time 51 - 420s.
			3	15/6/01	98.0%	8.4%	N	768				A second pipe developed. Flow increased but width of slot did not increase. Depth of slot not measured.
			4	6/6/01	96.5%	6.9%	N	160	3.27E-03	-70.4	0.897	Rate corresponds to time 1 - 36s.
			5	12/6/01	96.0%	10.1%	N	568	1.58E-03	52.0	0.937	Rate corresponds to time 51 - 349s.
			6	14/6/01	95.0%	6.9%	N	77	8.61E-03	60.5	1.000	Rate corresponds to time 21 - 29s.
			7	19/6/01	92.5%	10.4%	N	233				A second pipe developed. Flow increased but width of slot did not increase. Depth of slot not measured.
			8	18/6/01	93.5%	8.4%	N	589	3.09E-04	-330.8	0.806	Rate corresponds to time 49 - 360s.
			9	26/6/01	93.0%	10.1%	N	633				A second pipe developed. Flow increased but width of slot did not increase. Depth of slot not measured.
			10	2/7/01	91.0%	6.8%	N	31	9.41E-03	-131.0	0.980	Rate corresponds to time 6 - 11s.
Rowallan	1.868	13.3%	1	1/11/00	97.0%	11.6%	N	28				Slot collapsed and depth of slot could not be measured. Insufficient data for estimating erosion rate index.
			2	3/11/00	97.0%	13.2%	N	18				Slot collapsed and depth of slot could not be measured. Insufficient data for estimating erosion rate index.
			3	6/11/00	93.0%	15.8%	N	1734				Slot collapsed and depth of slot could not be measured. Insufficient data for estimating erosion rate index.
			4	7/11/00	95.5%	16.1%	N	21				Slot collapsed and depth of slot could not be measured. Insufficient data for estimating erosion rate index.
			5	8/11/00	95.5%	16.0%	N	17				Slot collapsed and depth of slot could not be measured. Insufficient data for estimating erosion rate index.
			6	9/11/00	98.5%	13.4%	N	24				Slot collapsed and depth of slot could not be measured. Insufficient data for estimating erosion rate index.
			7	20/2/01	96.0%	13.6%	S	7200				Slot blocked.
			8	23/2/01	98.0%	11.1%	S	101	1.38E-02	21.7	0.953	Rate corresponds to time 1 - 90s.
			9	31/7/01	97.5%	14.8%	N	18	9.21E-02	85.2	0.847	Rate corresponds to time 8 - 11s. Duration of the test was too short that measurements would be rather inaccurate.
			10	3/8/01	96.5%	12.9%	N	151	1.70E-02	50.4	0.831	Rate corresponds to time 32 - 130s.
			11	1/8/01	93.5%	10.9%	N	16	4.03E-02	-31.3	0.930	Rate corresponds to time 1 - 8s. Duration of the test was too short that measurements would be rather inaccurate.
			12	14/9/01	96.0%	13.2%	0.02M	357	1.69E-02	48.8	0.910	Rate corresponds to time 31 - 341s.

Summary of interpreted results of all SETs (Continued).

Soil Sample	Max. Dry Unit Weight (Mg/m^3)	Optimum Water Content (%)	Test No.	Test Date	Percentage Compaction (%)	Water Content (%)	Special Treatment (See Note 1)	Duration of erosion test (s)	Coefficient of Soil Erosion C_e (s/m)	Critical Shear Stress (N/m^2)	Coefficient of determination r^2	Remark
Shellharbour	1.248	40.8%	1a	6/6/00	98.0%	40.0%	HH	6060	7.78E-05	336.4	0.969	Rate corresponds to time 1802 - 3238s.
			1b	8/6/00	98.0%	40.5%	N	7200	3.54E-04	48.0	0.976	Rate corresponds to time 1802 - 7198s.
			1br	23/8/00	95.5%	40.8%	N	7200	3.87E-05	106.0	0.940	Rate corresponds to time 4202 - 7198s.
			2	8/8/00	91.5%	39.7%	N	4620	1.31E-04	130.3	0.902	Rate corresponds to time 1242 - 4200s.
			3	9/8/00	91.5%	43.9%	N	7200	(See Note 2)			Erosion slowed down. Width of slot stabilised at 4.2mm after testing for 2 hours.
			4	29/8/00	92.5%	39.5%	N	7200	1.05E-04	171.9	0.945	Rate corresponds to time 3300 - 6054s.
			5	25/7/00	96.5%	38.5%	N	7200	(See Note 2)			Erosion slowed down. Width of slot stabilised at 5.7mm after testing for 2 hours .
			6	1/8/00	94.5%	40.6%	N	7200	(See Note 2)			Erosion slowed down. Width of slot stabilised at 7.2mm after testing for 2 hours .
			7	23/8/00	91.5%	43.9%	N	7200	1.54E-06	-46.0	0.791	Rate corresponds to time 6002 - 7198s (i.e. the latest stage of the test)
			8	25/7/00	94.0%	38.3%	N	2010	1.85E-04	107.8	0.955	Rate corresponds to time 901 - 1527s.
			9	1/8/00	91.0%	40.3%	N	7200	4.37E-05	130.8	0.951	Rate corresponds to time 3602 - 7198s.
			10	4/8/00	91.5%	42.5%	N	7200	(See Note 2)			Erosion slowed down. Width of slot stabilised at 7.1mm after testing for 2 hours .
			11	21/7/00	92.5%	38.3%	N	1650	1.73E-04	39.2	0.955	Rate corresponds to time 451 - 1649s.
			12	24/8/00	97.0%	39.5%	P	5400	(See Note 2)			Erosion slowed down. Width of slot stabilised at 16.7mm after testing for 3 hours (Equiv. to an effective erosion time of 1.5 hours).
			14	16/8/00	94.5%	37.4%	S	7200				Slot blocked before test
			15	15/8/00	91.0%	38.2%	S	7200				Slot blocked before test
			16	15/11/00	96.5%	39.1%	N	7200	(See Note 2)			Erosion slowed down. Width of slot stabilised at 5.7mm after testing for 2 hours .
			17	18/9/01	94.0%	41.4%	0.02M	7200	(See Note 2)			Erosion slowed down. Width of slot stabilised at 5.4mm after testing for 2 hours .
Teton	1.643	18.3%	1	16/5/01	95.5%	18.1%	N	478	1.12E-03	80.7	0.899	Rate corresponds to time 91 - 220s.
			2	14/5/01	96.0%	20.3%	N	1081	4.90E-04	18.1	0.850	Rate corresponds to time 720 - 1080s.
			3	23/5/01	94.0%	15.7%	N	448	1.20E-03	53.3	0.889	Rate corresponds to time 51 - 210s.
			4	17/5/01	96.5%	16.5%	N	524	6.34E-04	-38.7	0.891	Rate corresponds to time 65 - 180s.
			5	19/7/01	99.0%	20.2%	N (recycled soil)	958	4.07E-04	7.0	1.000	Rate corresponds to time 301 - 399s. Period used for estimating rate appears to be too short.
			6	20/7/01	91.5%	16.5%	N (recycled soil)	171	1.53E-03	-77.8	0.895	Rate corresponds to time 21 - 70s.
Waranga Basin	1.665	19.2%	1	1/5/01	95.0%	19.3%	N	657	9.25E-04	79.1	0.923	Rate corresponds to time 121 - 419s.
			2	2/5/01	94.5%	20.7%	N	3940	8.95E-05	50.6	0.941	Rate corresponds to time 1205 - 3600s.
			3	4/5/01	96.0%	17.3%	N	270	1.30E-03	-37.1	0.899	Rate corresponds to time 31 - 180s.
			4	7/5/01	97.0%	20.8%	N	7200	2.16E-05	-68.9	0.945	Rate corresponds to time 70 - 7190s.
			5	9/5/01	92.5%	21.1%	N	1660	1.70E-04	-62.2	0.884	Rate corresponds to time 62 - 1062s.
			6	10/5/01	91.0%	17.3%	N	165	4.16E-03	63.3	0.971	Rate corresponds to time 31 - 135s.
			7	9/7/01	98.5%	17.0%	N	565	1.12E-03	34.5	0.965	Rate corresponds to time 31 - 300s.
			8	17/7/01	91.0%	19.3%	N	680	5.03E-04	-12.3	0.731	Rate corresponds to time 119 - 360s.
			9	18/7/01	95.5%	19.5%	S	1964	3.23E-05	-890.6	0.929	Rate corresponds to time 712 - 960s.
			10	26/9/01	96.0%	18.8%	0.02M	2397	2.06E-04	47.5	0.946	Rate corresponds to time 204 - 2100s.

Summary of interpreted results of all SETs (Continued).

Soil Sample	Max. Dry Unit Weight (Mg/m^3)	Optimum Water Content (%)	Test No.	Test Date	Percentage Compaction (%)	Water Content (%)	Special Treatment (See Note 1)	Duration of erosion test (s)	Coefficient of Soil Erosion C_e (s/m)	Critical Shear Stress (N/m^2)	Coefficient of determination r^2	Remark
Waroona	1.585	23.0%	1	6/3/01	96.0%	22.7%	N	7200	(See Note 2)			Erosion slowed down. Width of slot stabilised at 4.7mm after testing for 2 hours
			2	7/3/01	99.0%	24.8%	N	7200	(See Note 2)			Erosion slowed down. Width of slot stabilised at 7.8mm after testing for 2 hours .
			3	8/3/01	97.0%	20.9%	N	7200	(See Note 2)			Erosion slowed down. Width of slot stabilised at 5.5mm after testing for 2 hours .
			4	9/3/01	91.0%	25.3%	N	7200	(See Note 2)			Erosion slowed down. Width of slot stabilised at 4.6mm after testing for 2 hours .
			5	13/3/01	96.0%	20.8%	N	7200	4.81E-06	18.0	0.940	Rate corresponds to time 2400 - 5990s.
			6	24/5/01	92.5%	19.0%	N	7200	(See Note 2)			Erosion slowed down. Width of slot stabilised at 1.2mm after testing for 2 hours .
			7	26/7/01	95.5%	19.5%	N	7200	(See Note 2)			Width of slot stabilised at about 2.3mm after testing for 2 hours . Slot partially blocked.

Notes

1. N : represents normal test under a head of 2.5m.
   HH : represents normal test under a higher head of 4.5m.
   S : test specimen soaked in water for at least 18 hrs. before testing.
   P : test paused for 15minutes after each period of 15 minutes of continous erosion.
   0.02M : test using 0.02M NaCl solution as eroding fluid.
   0.005M : test using 0.005M NaCl solution as eroding fluid.
2. Coefficient of Soil Erosion (C_e) for these tests assumed to be 1E-6 $kg/s/m^2$ or smaller.

APPENDIX B

Summary of Interpreted Results of All Hole Erosion Tests

Summary of interpreted results of all HETs.

Soil Sample	Max. Dry Density (Mg/m^3)	Optimum Water Content (%)	Test No.	Test Date	Test head (mm)	Percentage Compaction (%)	Water Content (%)	Special Treatment (See Note 1)	Duration of erosion (s)	Coefficient of Soil Erosion C_e (s/m)	Critical Shear Stress (N/m^2)	Coefficient of determination r^2	Remark
Bradys	1.318	35.2%	1	7/12/00	600	94.0%	35.8%	N	780	1.89E-04	248.04	0.993	Erosion rate index computed for time 356 - 780s.
			2	7/12/00	400	93.5%	35.9%	N	780	3.18E-04	221.85	0.995	Erosion rate index computed for time 367 - 780s.
			3	7/12/00	200	93.5%	35.6%	N	1020	7.37E-04	87.14	0.943	Erosion rate index computed for time 386 - 1020s.
			4	12/12/00	100	94.0%	35.8%	N	1620	1.42E-04	-27.40	0.618	Erosion rate index computed for time 360 - 1440s. Note that coeff. of determination is low.
			5	21/12/00	50	95.5%	34.6%	N	1290	7.31E-04	2.53	0.842	Erosion rate index computed for time 300 - 1020s.
			6	18/12/00	50	92.0%	32.7%	N	810	3.14E-03	17.17	0.901	Erosion rate index computed for time 542 - 660s.
			7	19/12/00	50	98.5%	36.9%	N	5100				Hole blocked.
			8	19/12/00	50	92.5%	37.0%	N	2400				Hole blocked.
			9	18/12/00	50	97.0%	33.7%	N	750	3.35E-03	8.61	0.638	Erosion rate index computed for time 61 - 610s. Note that coeff. of determination is low.
			10	20/12/00	50	95.5%	36.4%	N	2880				Hole blocked.
			11	18/12/00	50	96.0%	32.7%	N	3000				Hole blocked.
			12	21/12/00	50	91.0%	35.9%	N	570	1.49E-03	3.99	0.901	Erosion rate index computed for time 270 - 420s.
			13	21/12/00	50	96.5%	34.2%	N	660	7.39E-03	14.04	0.734	Erosion rate index computed for time 241 - 600s.
			14	16/1/01	50	94.5%	33.7%	N	664	9.58E-03	24.39	0.761	Erosion rate index computed for time 301 - 585s.
			15	26/7/01	50	94.5%	35.1%	N	7200				Hole blocked.
			16	8/8/01	50	94.5%	35.7%	S	7200	2.81E-04	16.05	0.897	Erosion rate index computed for time 1502 - 3298s.
			17	14/09/01	50	95.0%	33.1%	0.02M	7200				Hole blocked.
			18	27/9/01	50	95.5%	34.3%	0.005M	1920	2.07E-02	18.91	0.874	Erosion rate index computed for time 1440 - 1685s.
			19	29/01/02	100	94.5%	35.2%	N	7200				Hole blocked.
			20	4/02/02	100	94.0%	35.6%	S	7200	3.89E-04	83.23	0.928	Erosion rate index computed for time 5252 - 6298s.
Buffalo	1.719	19.4%	1	06/08/01	800	96.0%	18.8%	N	7200	(See Note 2)			Negligible erosion. Flow rate was steady.
			2	07/08/01	1200	95.0%	19.0%	N	7200	(See Note 2)			Negligible erosion. Flow rate was steady.
			3	16/08/01	1200	92.0%	16.7%	N	7200	(See Note 2)			Negligible erosion. Flow rate was steady.
			4	28/08/01	1200	95.0%	18.7%	S	7200	(See Note 2)			Negligible erosion. Flow rate was steady.
			5	24/09/01	1200	94.5%	20.0%	0.02M	7200	(See Note 2)			Negligible erosion. Flow rate was steady.
			6	27/09/01	1200	95.0%	19.7%	0.005M	7200	(See Note 2)			Negligible erosion. Flow rate was steady.
			7	4/02/02	1200	89.5%	15.6%	N	7200	3.45E-06	132.74	0.817	Erosion rate index computed for time 3302 - 4198s. Note short time interval for estimation of erosion rate index, and negligible widening of pre-formed hole after 7200s.
			8	5/03/02	1200	89.0%	15.3%	S	7200	(See Note 2)			Negligible erosion. Flow rate was steady.
			9	4/02/02	1200	93.0%	15.4%	N	7200	2.61E-06	113.91	0.752	Erosion rate index computed for time 3302 - 3898s. Note short time interval for estimation of erosion rate index, relatively low value of coeff. of determination, and negligible widening of pre-formed hole after 7200s.

Summary of interpreted results of all HETs (Continued).

Soil Sample	Max. Dry Density (Mg/m^3)	Optimum Water Content (%)	Test No.	Test Date	Test head (mm)	Percentage Compaction (%)	Water Content (%)	Special Treatment (See Note 1)	Duration of erosion (s)	Coefficient of Soil Erosion C_e (s/m)	Critical Shear Stress (N/m^2)	Coefficient of determination r^2	Remark
Fattorini	1.696	18.5%	1	20/11/00	800	88.5%	18.8%	N	5100				Incomplete information. Erosion rate index not calculated.
			2	20/11/00	600	92.5%	18.7%	N	7200	3.05E-05	605.69	0.906	Erosion rate index computed for time 4802 - 7198s.
			3	20/11/00	600	94.0%	18.4%	N	7200	2.13E-05	479.82	0.916	Erosion rate index computed for time 4802 - 7198s.
			4	22/11/00	700	96.5%	18.8%	N	7200				Erosion rate slowed down gradually. Erosion rate index not calculated.
			5	22/11/00	800	93.5%	18.3%	N	2400	5.15E-05	588.70	0.927	Erosion rate index computed for time 1052 - 1498s.
			6	1/12/00	700	90.5%	17.4%	N	890	4.50E-04	551.44	0.958	Erosion rate index computed for time 541 - 888s.
			7	05/12/00	700	97.5%	20.8%	N	7200	1.29E-05	263.32	0.804	Erosion rate index computed for time 3902 - 7198s.
			8	05/12/00	700	93.5%	21.2%	N	7200	8.68E-06	222.56	0.787	Erosion rate index computed for time 2402 - 6448s.
			9	13/12/00	700	95.0%	17.0%	N	3600				Preformed hole partially blocked. Erosion rate index not calculated.
			10	04/12/00	700	95.0%	15.6%	N	2160	8.60E-05	582.99	0.927	Erosion rate index computed for time 842 - 2158s.
			11	13/12/00	700	94.0%	21.0%	N	7200				Preformed hole partially blocked. Erosion rate index not calculated.
			12	11/12/00	700	91.5%	19.0%	N	2520	1.99E-04	971.60	0.945	Erosion rate index computed for time 1802 - 2518s.
			13	12/12/00	700	96.5%	18.8%	N	7200	4.54E-06	212.33	0.845	Erosion rate index computed for time 6002 - 7198s.
			14	31/07/01	700	95.5%	17.7%	S	7200				Erosion rate slowed down gradually. Erosion rate index not calculated.
Hume	1.635	20.8%	1	22/1/01	700	94.0%	21.4%	N	3784	5.09E-04	197.02	0.807	Erosion rate index computed for time 2852 - 3748s.
			2	23/1/01	600	94.0%	21.4%	N	4380	2.31E-04	284.72	0.787	Erosion rate index computed for time 2702 - 4378s.
			3	24/1/01	500	94.5%	20.8%	N	2430	1.05E-04	189.39	0.787	Erosion rate index computed for time 602 - 2428s.
			4	24/1/01	500	94.5%	21.0%	N	7200	4.27E-05	64.05	0.962	Erosion rate index computed for time 602 - 5998s.
			5	25/1/01	500	92.0%	17.9%	N	3810	2.44E-04	202.35	0.737	Erosion rate index computed for time 2702 - 3600s.
			6	25/1/01	600	97.0%	22.6%	N	5940	3.15E-05	93.84	0.995	Erosion rate index computed for time 1815 - 5940s.
			7	25/1/01	600	91.0%	22.4%	N	4980	1.21E-04	125.33	0.839	Erosion rate index computed for time 1802 - 4978s.
			8	6/2/01	600	97.5%	17.6%	N	7200	1.53E-05	103.61	0.862	Erosion rate index computed for time 2402 - 4498s.
			9	6/2/01	600	94.0%	22.7%	N	5700	3.74E-05	150.14	0.996	Erosion rate index computed for time 2410 - 5700s.
			10	5/2/01	600	94.5%	17.6%	N	7200	3.52E-05	93.05	0.924	Erosion rate index computed for time 4505 - 7195s.
			11	17/8/01	600	95.5%	20.3%	S	6210	3.60E-05	123.71	0.774	Erosion rate index computed for time 902 - 6210s.
			12	17/9/01	600	94.0%	20.3%	0.02M	1440	1.26E-03	307.85	0.972	Erosion rate index computed for time 1082 - 1438s.
Jindabyne	1.753	16.2%	1	20/03/01	600	93.5%	15.7%	N	390	2.51E-03	327.38	0.918	Erosion rate index computed for time 301 - 359s.
			2	20/03/01	200	93.5%	15.6%	N	630	1.93E-03	85.86	0.929	Erosion rate index computed for time 361 - 494s.
			3	21/03/01	50	95.0%	15.3%	N	1815	2.67E-03	19.19	0.951	Erosion rate index computed for time 1261 - 1814s.
			4	23/03/01	50	95.5%	17.6%	N	7200				Pre-formed hole blocked. Erosion rate index not estimated.
			5	28/3/01	50	96.5%	13.8%	N	1380	1.03E-03	7.28	0.896	Erosion rate index computed for time 241 - 1260s.
			6	28/03/01	50	97.0%	15.3%	N	1920	1.72E-03	25.38	0.949	Erosion rate index computed for time 901 - 1259s.
			7	28/03/01	50	98.0%	15.8%	N	2970	2.22E-04	-14.34	0.827	Erosion rate index computed for time 452 - 1798s.
			8	26/03/01	50	97.5%	18.2%	N	7200				Pre-formed hole blocked. Erosion rate index not estimated.
			9	29/03/01	50	95.5%	14.0%	N	1110	1.36E-03	9.68	0.964	Erosion rate index computed for time 241 - 990s.
			10	30/03/01	50	92.0%	17.6%	N	7200				Pre-formed hole blocked. Erosion rate index not estimated.
			11	29/3/01	50	92.0%	16.2%	N	1200	2.96E-03	22.40	0.967	Erosion rate index computed for time 721 - 1110s.
			12	30/03/01	50	90.5%	14.1%	N	660	3.06E-03	14.91	0.861	Erosion rate index computed for time 181 - 509s.
			13	10/08/01	400	95.0%	16.2%	N	1200	5.61E-04	182.03	0.929	Erosion rate index computed for time 781 - 1139s.
			14	09/08/01	100	97.5%	18.3%	N	7200	3.77E-04	46.70	0.891	Erosion rate index computed for time 4802 - 7198s.
			15	20/08/01	50	94.5%	18.9%	N	7200	1.10E-03	19.80	0.926	Erosion rate index computed for time 4502 - 6840s.
			16	31/8/01	50	92.0%	18.0%	N	3930				Pump failed during test. Test results not used.
			17	16/08/01	50	94.5%	15.9%	S	7200				Pre-formed hole blocked. Erosion rate index not estimated.
			18	18/09/01	50	94.0%	16.8%	0.02M	1530	3.68E-03	19.52	0.908	Erosion rate index computed for time 661 - 1289s.
			19	11/02/02	100	96.0%	16.0%	N	1530	1.99E-03	48.33	0.887	Erosion rate index computed for time 1913 - 2220s.
			20	12/02/02	100	96.0%	15.9%	S	7200				Pre-formed hole blocked. Erosion rate index not estimated.
			21	18/09/01	400	94.5%	16.4%	S	2550	9.26E-04	190.62	0.959	Erosion rate index computed for time 2101 - 2511s.

Summary of interpreted results of all HETs (Continued).

Soil Sample	Max. Dry Density (Mg/m^3)	Optimum Water Content (%)	Test No.	Test Date	Test head (mm)	Percentage Compaction (%)	Water Content (%)	Special Treatment (See Note 1)	Duration of erosion (s)	Coefficient of Soil Erosion C_e (s/m)	Critical Shear Stress (N/m^2)	Coefficient of determination r^2	Remark
Lyell	1.963	10.1%	1	13/02/01	50	96.5%	9.5%	N	480	4.38E-02	5.45	0.832	Erosion rate index computed for time 31 - 130s.
			2	13/02/01	50	96.0%	9.8%	N	1339	7.52E-02	7.72	0.959	Erosion rate index computed for time 481 - 749s.
			3	13/02/01	50	96.5%	12.6%	N	1020	6.05E-02	5.55	0.909	Erratic flow rates due to alternate blocking and clearing of pre-formed hole. Estimated erosion rate index computed for time 570 - 675s may not be reliable.
			4	14/2/01	50	98.5%	11.7%	N	1060	8.61E-03	3.20	0.828	Erosion rate index computed for time 31 - 359s.
			5	14/02/01	50	95.0%	7.9%	N	3750	9.39E-03	7.88	0.885	Erosion rate index computed for time 2402 - 3600s.
			6	14/02/01	50	99.5%	9.7%	N	1060	1.04E-02	5.22	0.936	Erosion rate index computed for time 91 - 629s.
			7	16/2/01	50	98.0%	7.5%	N	7200	3.65E-04	15.10	0.886	Erosion rate index computed for time 1352 - 1948s. Note short time interval for estimation of erosion rate index.
			8	16/02/01	50	93.0%	11.6%	N	135	3.37E-02	0.44	0.875	Erosion rate index computed for time 96 - 105s. Note short time interval for estimation of erosion rate index.
			9	23/02/01	50	97.0%	8.0%	N	1800	1.39E-02	15.66	0.976	Erosion rate index computed for time 901 - 1349s.
			10	10/07/01	50	95.5%	9.8%	N	450	1.37E-02	12.06	0.940	Erosion rate index computed for time 122 - 358s.
			11	10/07/01	100	95.0%	9.7%	N	330	9.82E-03	14.21	0.985	Erosion rate index computed for time 106 - 239s.
			12	10/07/01	50	96.5%	11.7%	N	170	7.94E-03	0.25	0.804	Erosion rate index computed for time 50 - 69. Note short time interval for estimation of erosion rate index, and slight collapse of sample after test.
			13	10/07/01	50	92.0%	10.0%	N	210	8.38E-02	12.09	0.910	Erosion rate index computed for time 120 - 162s.
			14	10/07/01	50	91.5%	8.0%	N	540	4.96E-02	19.09	0.970	Erosion rate index computed for time 361 - 471s.
			15	10/07/01	50	95.0%	9.8%	S	115	1.94E-02	1.80	0.865	Erosion rate index computed for time 16 - 34s. Note short time interval for estimation of erosion rate index.
			16	18/09/01	50	97.0%	9.8%	0.02M	1410	1.75E-02	17.90	0.936	Erosion rate index computed for time 781 - 1349s.
			17	30/01/02	50	94.5%	7.5%	N	7200	6.09E-04	16.07	0.919	Erosion rate index computed for time 2852 - 3448s. Note short time interval for estimation of erosion rate index.
			18	11/03/02	50	95.0%	7.5%	S	1980	1.92E-02	8.50	0.908	Erosion rate index computed for time 1426 - 1680s. Note short time interval for estimation of erosion rate index.
Matahina	1.805	16.7%	1	28/06/01	600	95.0%	16.2%	N	7200				Pre-formed hole blocked.
			2	28/06/01	800	95.5%	16.9%	N	7200	2.02E-04	1049.04	0.930	Erosion rate index computed for time 1502 - 2218s.
			3	29/06/01	1000	95.5%	15.8%	N	4560	1.76E-04	402.08	0.886	Erosion rate index computed for time 3452 - 2218s.
			4	02/07/01	1100	94.5%	16.6%	N	7200				Pre-formed hole blocked.
			5	04/07/01	1000	97.0%	18.2%	N	7200	8.03E-06	124.52	0.951	Erosion rate index computed for time 3002 - 7198s.
			6	04/07/01	1000	96.0%	14.3%	N	2220	1.68E-04	585.89	0.938	Erosion rate index computed for time 1502 - 2218s.
			7	06/07/01	1000	96.0%	18.8%	N	6660	8.49E-05	345.16	0.967	Erosion rate index computed for time 4502 - 5848s.
			8	05/07/01	1000	94.5%	14.2%	N	2230	1.09E-04	572.50	0.821	Erosion rate index computed for time 1352 - 2060s.
			9	06/07/01	1000	94.5%	18.5%	N	5220	1.40E-04	339.51	0.961	Erosion rate index computed for time 3152 - 4122s.
			10	09/07/01	1000	92.0%	16.7%	N	2110				Sample collapsed after 2110s.
			11	09/07/01	1000	92.0%	14.7%	N	1770	7.46E-04	311.23	0.895	Erosion rate index computed for time 1352 - 1498s.
			12	05/07/01	1000	95.0%	16.2%	S	4620	8.49E-05	550.41	0.946	Erosion rate index computed for time 2402 - 3448s.
			13	21/09/01	1000	95.5%	15.6%	0.02M	4405				Hole blocked and sample collapsed after 4405s.
			14	26/09/01	1000	94.5%	16.1%	0.005M	2790	6.67E-05	81.88	0.823	Erosion rate index computed for time 1762 - 2622s.
			15	8/02/02	1000	96.5%	16.8%	N	6780	9.32E-05	736.29	0.888	Erosion rate index computed for time 5852 - 6778s.
			16	8/02/02	1000	98.0%	16.9%	N	7200				Pre-formed hole blocked.
			17	12/02/02	1000	97.5%	17.3%	S	7200				Pre-formed hole blocked.

Summary of interpreted results of all HETs (Continued).

Soil Sample	Max. Dry Density (Mg/m^3)	Optimum Water Content (%)	Test No.	Test Date	Test head (mm)	Percentage Compaction (%)	Water Content (%)	Special Treatment (See Note 1)	Duration of erosion (s)	Coefficient of Soil Erosion C_e (s/m)	Critical Shear Stress (N/m^2)	Coefficient of determination r^2	Remark
Pukaki	2.150	8.6%	1	06/06/01	800	95.5%	8.4%	N	79	1.13E-03	-45.42	0.985	Erosion rate index computed for time 36 - 74s. Possible errors in flow measurement due to the fast and short erosion process.
			2	06/06/01	200	95.5%	8.5%	N	468	1.86E-03	71.29	0.965	Erosion rate index computed for time 182 - 448s.
			3	06/06/01	100	95.0%	8.6%	N	1080	5.37E-04	-7.11	0.866	Erosion rate index computed for time 392 - 1078s.
			4	08/06/01	100	96.0%	11.1%	N	930	1.58E-03	12.93	0.917	Erosion rate index computed for time 1 - 359s.
			5	08/06/01	100	94.5%	6.5%	N	3437				Blockage of pre-formed hole, until sample collapsed after 3437s.
			6	08/06/01	100	97.0%	10.7%	N	840	1.97E-03	12.97	0.916	Erosion rate index computed for time 1 - 269s.
			7	13/06/01	100	98.5%	8.1%	N	840	2.00E-03	35.39	0.892	Erosion rate index computed for time 391 - 509s.
			8	13/06/01	100	98.5%	6.9%	N	7200				Pre-formed hole blocked
			9	13/06/01	100	97.5%	6.3%	N	5623				Blockage of pre-formed hole, until sample collapsed after 5623s.
			10	14/06/01	100	95.0%	10.6%	N	1020	1.29E-03	17.66	0.937	Erosion rate index computed for time 361 - 609s.
			11	14/06/01	100	93.0%	8.0%	N	660	1.20E-02	31.91	0.979	Erosion rate index computed for time 375 - 554s.
			12	14/06/01	100	92.0%	6.3%	N	180	4.75E-02	31.22	0.966	Erosion rate index computed for time 124 - 164s.
			13	12/07/01	300	98.0%	8.4%	N	240	7.84E-04	-28.75	0.868	Erosion rate index computed for time 76 - 149s.
			14	12/07/01	100	94.5%	10.6%	N	1290	1.91E-03	11.10	0.939	Erosion rate index computed for time 1 - 549s.
			15	13/7/2001	100	96.0%	8.8%	S	1329	2.97E-03	10.60	0.978	Erosion rate index computed for time 271 - 959s.
			16	20/09/01	100	95.0%	8.8%	0.02M	540	8.64E-03	27.63	0.883	Erosion rate index computed for time 151 - 209s.
			17	27/09/01	100	95.0%	8.9%	0.005M	1080	9.35E-04	-3.62	0.944	Erosion rate index computed for time 2552 - 4498s.
			18	7/02/02	100	96.5%	8.4%	S	2700	8.91E-04	-0.07	0.860	Erosion rate index computed for time 1 - 1147s.
			19	6/02/02	100	94.5%	7.6%	N	420	2.45E-02	61.82	0.929	Erosion rate index computed for time 271 - 344s.
Rowallan	1.868	13.3%	1	14/12/00	200	95.5%	12.5%	N	60				Insufficient data for estimation of erosion rate index.
			2	14/12/00	50	95.5%	12.7%	N	318	5.73E-02	8.14	0.907	Erosion rate index computed for time 122 - 280s.
			3	14/12/00	50	95.0%	12.4%	N	165	3.12E-01	10.53	0.975	Erosion rate index computed for time 98 - 140s.
			4	19/12/00	50	94.5%	13.2%	N	210	6.30E-02	11.77	0.948	Erosion rate index computed for time 135 - 180s.
			5	20/12/00	50	92.5%	11.1%	N	292	1.46E-01	6.62	0.926	Erosion rate index computed for time 233 - 284s.
			6	20/12/00	50	97.0%	15.1%	N	60				Insufficient data for estimation of erosion rate index.
			7	20/12/00	50	94.5%	15.0%	N	120	1.99E-01	6.98	0.971	Erosion rate index computed for time 44 - 78s.
			8	20/12/00	50	98.5%	10.5%	N	255	3.61E-01	10.35	0.968	Erosion rate index computed for time 219 - 233s. Note short time interval for estimation of erosion rate index.
			9	16/01/01	50	96.0%	14.0%	N	175	1.28E-01	25.04	0.959	Erosion rate index computed for time 121 - 164s.
			10	16/01/01	50	94.5%	10.8%	N	165	2.05E-01	11.89	0.953	Erosion rate index computed for time 111 - 139s.
			11	16/01/01	50	92.5%	12.7%	N	64	1.20E-01	15.24	0.978	Erosion rate index computed for time 22 - 40s.
			12	16/01/01	50	97.5%	12.8%	N	195	7.75E-02	24.71	0.969	Erosion rate index computed for time 141 - 182s.
			13	23/07/01	50	95.5%	12.8%	S	109				Insufficient data for estimation of erosion rate index.
			14	14/09/01	50	95.5%	12.1%	0.02M	1080	3.74E-02	9.11	0.954	Erosion rate index computed for time 870 - 995s.
			15	26/09/01	50	94.5%	13.0%	0.005M	390	7.24E-02	9.27	0.949	Erosion rate index computed for time 211 - 300s.
			16	5/02/02	50	98.5%	10.0%	S	7200				Pre-formed hole blocked.

Summary of interpreted results of all HETs (Continued).

Soil Sample	Max. Dry Density (Mg/m^3)	Optimum Water Content (%)	Test No.	Test Date	Test head (mm)	Percentage Compaction (%)	Water Content (%)	Special Treatment (See Note 1)	Duration of erosion (s)	Coefficient of Soil Erosion C_e (s/m)	Critical Shear Stress (N/m^2)	Coefficient of determination r^2	Remark
Shellharbour	1.248	40.8%	1	14/11/00	800	96.0%	39.1%	N	7200	(See Note 2)			Erosion rate slowed down gradually. Erosion rate index not calculated.
			2	15/11/00	600	94.0%	39.6%	N	7200	(See Note 2)			Erosion rate slowed down gradually. Erosion rate index not calculated.
			3	16/11/00	700	93.0%	40.2%	N	7200	(See Note 2)			Erosion rate slowed down gradually. Erosion rate index not calculated.
			4	16/11/00	800	91.5%	39.9%	N	7200	2.09E-05	407.28	0.954	Erosion rate index computed for time 2102 - 3898s.
			5	27/11/00	800	91.5%	38.7%	N	1170	1.51E-04	398.32	0.900	Erosion rate index computed for time 541 - 1169s.
			6	28/11/00	800	91.5%	41.7%	N	7200	7.56E-05	369.36	0.973	Erosion rate index computed for time 6152 - 7198s.
			7	28/11/00	800	92.5%	42.6%	N	7200	1.41E-05	419.55	0.869	Erosion rate index computed for time 4202 - 5998s.
			8	29/11/00	800	98.0%	37.2%	N	2520	6.97E-05	340.91	0.843	Erosion rate index computed for time 528 - 1872s.
			9	29/11/00	800	95.0%	37.9%	N	3540	5.97E-05	391.46	0.866	Erosion rate index computed for time 1802 - 3448s.
			10	30/11/00	800	95.5%	44.0%	N	7200	8.83E-06	310.35	0.900	Erosion rate index computed for time 3002 - 7198s.
			11	6/12/00	800	96.0%	41.1%	N	7200	(See Note 2)			Erosion rate slowed down gradually. Erosion rate index not calculated.
			12	23/7/01	900	95.5%	39.7%	N	7200	1.38E-05	472.51	0.926	Erosion rate index computed for time 3902 - 7198s.
			13	24/7/01	1000	95.0%	39.9%	N	7200	1.50E-05	462.77	0.900	Erosion rate index computed for time 2402 - 4498s.
			14	26/7/01	800	95.5%	40.0%	S	7200	4.60E-05	278.82	0.852	Erosion rate index computed for time 1802 - 3598s.
			15	17/9/01	800	95.0%	40.1%	0.02M	7200	8.49E-06	263.95	0.949	Erosion rate index computed for time 4502 - 6598s.
			16	30/01/02	1100	95.0%	40.7%	N	7200	(See Note 2)			Erosion rate slowed down gradually. Erosion rate index not calculated.
			17	1/02/02	1100	94.5%	40.2%	S	7200	(See Note 2)			Erosion rate slowed down gradually. Erosion rate index not calculated.
Teton	1.643	18.3%	1	14/05/01	200	94.0%	17.9%	N	7200				Pre-formed hole blocked. Erosion rate index not estimated.
			2	14/05/01	400	93.0%	18.0%	N	7200				Pre-formed hole blocked. Erosion rate index not estimated.
			2a	18/05/01	500	94.5%	17.7%	N	7200				Pre-formed hole blocked. Erosion rate index not estimated.
			2b	22/05/01	700	96.0%	17.7%	N	3010				Pref-formed hole blocked. Sample collapsed after 3010s.
			3	15/05/01	100	95.0%	19.3%	N	7200				Pre-formed hole blocked. Erosion rate index not estimated.
			3a	22/05/01	200	96.5%	19.7%	N	7200				Pre-formed hole blocked. Erosion rate index not estimated.
			4	15/05/01	100	95.0%	15.6%	N	7200				Pre-formed hole blocked. Erosion rate index not estimated.
			4a	22/05/01	200	95.0%	15.8%	N	4287				Pref-formed hole blocked. Sample collapsed after 4287s.
			5	15/05/01	100	97.5%	19.1%	N	7200				Pre-formed hole blocked. Erosion rate index not estimated.
			10	28/05/01	400	91.5%	16.8%	N	1110	6.03E-03	216.18	0.854	Erosion rate index computed for time 1050 - 1109s. Note short time interval for estimation of erosion rate index.
			11	28/05/01	400	92.5%	19.1%	N	7200				Pre-formed hole blocked. Erosion rate index not estimated.
			12	31/07/01	200	95.0%	18.0%	N	1590	1.81E-03	12.90	0.843	Pre-formed hole partially blocked and rate of erosion accelerated near the end of the test. Erosion rate index computed for time 600 - 1522s
			13	31/07/01	400	96.5%	18.3%	N	2453	4.48E-03	57.39	0.928	Pref-formed hole partially blocked during earlier stage of test. Erosion rate index computed for time 2101 - 2451s.
			14	01/08/01	500	96.0%	17.8%	N	2431	3.16E-03	21.04	0.889	Pref-formed hole partially blocked during earlier stage of test. Erosion rate index computed for time 1725 - 2429s.
			15	01/08/01	200	98.0%	15.3%	N	2718	3.48E-03	15.17	0.923	Pref-formed hole partially blocked during earlier stage of test. Erosion rate index computed for time 2250 - 2699s.
			16	06/08/01	200	98.0%	19.3%	N	7200				Pre-formed hole blocked. Erosion rate index not estimated.
			17	02/08/01	200	93.0%	19.8%	N	7200				Pre-formed hole blocked. Erosion rate index not estimated.
			18	02/08/01	200	92.0%	15.8%	N	3590	7.42E-03	17.65	0.935	Pref-formed hole partially blocked during earlier stage of test. Erosion rate index computed for time 3001 - 3588s.
			19	02/08/01	50	96.5%	17.8%	S	7200				Pre-formed hole blocked. Erosion rate index not estimated.
			20	19/09/01	50	95.0%	17.3%	0.02M	7200				Pre-formed hole blocked. Erosion rate index not estimated.
			21	5/02/02	400	96.5%	18.5%	N	1020	3.46E-03	102.89	0.960	Erosion rate index computed for time 810 - 905s. Note short time interval for estimation of erosion rate index.
			22	6/02/02	400	95.0%	18.2%	S	240	5.67E-03	161.47	0.955	Erosion rate index computed for time 106 - 224s.

Summary of interpreted results of all HETs (Continued).

Soil Sample	Max. Dry Density (Mg/m^3)	Optimum Water Content (%)	Test No.	Test Date	Test head (mm)	Percentage Compaction (%)	Water Content (%)	Special Treatment (See Note 1)	Duration of erosion (s)	Coefficient of Soil Erosion C_e (s/m)	Critical Shear Stress (N/m^2)	Coefficient of determination r^2	Remark
Waranga Basin	1.665	19.2%	1	27/04/01	800	96.5%	18.5%	N	1470	1.02E-04	332.18	0.885	Erosion rate index computed for time 242 - 1468s.
			2	27/04/01	600	95.0%	19.3%	N	2550	3.99E-05	108.71	0.699	Erosion rate index computed for time 600 - 2548s.
			3	30/04/01	500	95.0%	18.6%	N	4380	6.32E-04	430.25	0.830	Erosion rate index computed for time 3452 - 4348s.
			4	02/05/01	500	95.5%	20.4%	N	6920	5.69E-05	143.89	0.817	Erosion rate index computed for time 2402 - 5548s.
			5	03/05/01	500	94.5%	16.7%	N	2920	5.01E-04	307.68	0.902	Erosion rate index computed for time 1802 - 2698s.
			6	03/05/01	500	97.5%	20.6%	N	7200	2.97E-05	193.86	0.754	Erosion rate index computed for time 3602 - 5848s.
			7	30/04/01	500	97.5%	18.7%	N	2749	2.81E-04	347.97	0.952	Erosion rate index computed for time 1952 - 2548s.
			8	07/05/01	500	97.0%	17.1%	N	4020	1.62E-04	148.68	0.944	Erosion rate index computed for time 2102 - 3448s.
			9	07/05/01	500	92.0%	20.9%	N	7200	3.11E-05	220.64	0.946	Erosion rate index computed for time 3302 - 5998s.
			10	04/05/01	500	92.0%	19.0%	N	2200	3.20E-04	328.36	0.947	Erosion rate index computed for time 1502 - 2172s.
			11	08/05/01	500	91.5%	17.1%	N	1819	8.98E-04	414.88	0.876	Erosion rate index computed for time 1352 - 1798s.
			12	08/05/01	500	92.0%	18.3%	S	7200				Pre-formed hole blocked
			13	30/05/01	500	95.0%	18.5%	S	7200				Pre-formed hole blocked
			14	12/07/01	400	94.0%	20.0%	N	6256	1.45E-04	238.33	0.757	Erosion rate index computed for time 4802 - 5880s.
			15	18/07/01	500	98.0%	20.3%	N	7200	(See Note 2)			Erosion rate slowed down gradually. Erosion rate index not calculated.
			16	19/07/01	500	93.5%	22.0%	N	7200	(See Note 2)			Erosion rate slowed down gradually. Erosion rate index not calculated.
			17	20/09/01	500	96.0%	18.0%	0.02M	3660	1.51E-04	103.67	0.837	Erosion rate index computed for time 2250 - 3148s.
			18	27/09/01	500	95.5%	18.7%	0.005M	3480	9.13E-05	249.39	0.918	Erosion rate index computed for time 1352 - 3298s.
			19	27/09/01	600	95.4%	18.6%	S	7200	9.77E-06	78.80	0.921	Erosion rate index computed for time 4502 - 7198s.

Summary of interpreted results of all HETs (Continued).

Soil Sample	Max. Dry Density (Mg/m^3)	Optimum Water Content (%)	Test No.	Test Date	Test head (mm)	Percentage Compaction (%)	Water Content (%)	Special Treatment (See Note 1)	Duration of erosion (s)	Coefficient of Soil Erosion C_e (s/m)	Critical Shear Stress (N/m^2)	Coefficient of determination r^2.	Remark
Waroona	1.585	23.0%	1	02/03/01	600	97.0%	22.7%	N	7200	(See Note 2)			Negligible erosion. Erosion Rate Index not estimated.
			2	02/03/01	800	94.5%	22.6%	N	7200	(See Note 2)			Negligible erosion. Erosion Rate Index not estimated.
			3	02/03/01	800	95.0%	22.3%	N	7200	(See Note 2)			Negligible erosion. Erosion Rate Index not estimated.
			4	07/03/01	1000	95.5%	22.2%	N	7200	(See Note 2)			Negligible erosion. Erosion Rate Index not estimated.
			5	07/03/01	1200	95.5%	22.8%	N	7200	(See Note 2)			Negligible erosion. Erosion Rate Index not estimated.
			6	08/03/01	1200	97.0%	22.2%	N	7200	(See Note 2)			Negligible erosion. Erosion Rate Index not estimated.
			7	13/3/2001	1200	92.0%	23.0%	N	7200	(See Note 2)			Negligible erosion. Erosion Rate Index not estimated.
			8	14/3/2001	1200	98.0%	24.1%	N	7200	(See Note 2)			Negligible erosion. Erosion Rate Index not estimated.
			9	14/3/2001	1200	95.5%	23.7%	N	7200	1.20E-05	159.10	0.884	Erosion rate index computed for time 1652 - 4498s.
			10	15/3/2001	1200	92.5%	24.9%	N	7200	(See Note 2)			Negligible erosion. Erosion Rate Index not estimated.
			11	15/3/2001	1200	96.5%	21.0%	N	7200	(See Note 2)			Erosion rate slowed down gradually. Erosion rate index not calculated.
			12	16/3/2001	1200	95.0%	20.8%	N	7200	1.79E-05	580.47	0.940	Erosion rate index computed for time 4502 - 6148s.
			13	16/3/2001	1200	89.0%	19.8%	N	7200	(See Note 2)			Erosion rate slowed down gradually. Erosion rate index not calculated.
			14	16/7/01	1200	95.5%	22.1%	N	7200	(See Note 2)			Negligible erosion. Erosion Rate Index not estimated.
			15	16/7/01	1200	91.5%	25.7%	N	7200	4.93E-05	153.54	0.909	Erosion rate index computed for time 1802 - 3148s.
			16	17/07/01	1200	89.0%	18.6%	N	326	1.13E-03	380.03	0.891	Erosion rate index computed for time 152 - 324s.
			17	18/07/01	1200	94.0%	23.2%	S	7200	2.05E-05	494.83	0.854	Erosion rate index computed for time 5552 - 6598s.
			18	19/09/01	1200	95.0%	22.5%	0.02M	7200	3.73E-06	124.35	0.853	Erosion rate index computed for time 602 - 3298s.
			19	31/01/02	1200	88.5%	18.7%	N	7200	1.51E-05	688.99	0.839	Erosion rate index computed for time 5624 - 6898s.
			20	31/01/02	1200	89.5%	18.4%	N	7200	3.53E-05	878.24	0.927	Erosion rate index computed for time 5102 - 6748s.
			21	1/02/02	1200	91.5%	18.4%	N	7200	3.18E-05	634.50	0.916	Erosion rate index computed for time 4500 - 6148s.

Notes

1. N : represents normal test under a head of 2.5m.
   HH : represents normal test under a higher head of 4.5m.
   S : test specimen soaked in water until no further swell before testing.
   0.02M : test using 0.02M NaCl solution as eroding fluid.
   0.005M : test using 0.005M NaCl solution as eroding fluid.
2. Coefficient of Soil Erosion (C_e) for these tests assumed to be 1E-6 $kg/s/m^2$ or smaller.

APPENDIX C

Non-linear Regression Models for Predicting I_{SET} and I_{HET} for Specimen Compacted to 95% Compaction at Optimum Water Content

Table C1 Coefficients of non-linear regression models for predicting I_{SET} for a specimen compacted to 95% compaction at optimum water content.

Soil Sample	Chosen Regression Model	Coefficients for regression model						Predicted I_{SET} at 95% Compaction and OWC
		a	b	c	d	e	f	
Bradys	2	0.455	0.030	-2.673	0.031	0.000	0.000	3.352
Buffalo		Only one test was done. Not enough data for regression analysis.						
Fattorini	4	-172.044	3.681	0.765	0.000	-0.019	0.000	4.443
Hume	3	-413.721	8.796	-5.268	0.058	-0.046	0.000	4.154
Jindabyne	2	-8.642	0.126	-5.192	0.056	0.000	0.000	3.294
Lyell	1	-11.185	0.134	0.001	0.000	0.000	0.000	1.575
Matahina		Only two tests were done. Not enough data for regression analysis.						
Pukaki	6	-8.253	0.124	-5.193	0.056	0.000	-0.368	3.491
Rowallan	1	-55.476	0.590	-0.698	0.000	0.000	0.000	0.606
Shellharbour	4	-868.759	18.453	0.404	0.000	-0.097	0.000	5.632
Teton	1	-2.910	0.063	0.037	0.000	0.000	0.000	3.087
Waranga Basin	4	205.481	-4.393	0.443	0.000	0.024	0.000	3.334
Waroona	1	7.063	-0.012	0.020	0.000	0.000	0.000	5.929
	2	7.794	-0.019	-1.007	0.011	0.000	0.000	5.942
	3	123.160	-2.461	-0.528	0.006	0.013	0.000	5.819
	4	166.459	-3.380	-0.019	0.000	0.018	0.000	5.769
	5	4.532	0.013	0.062	0.000	0.000	0.028	5.782
	6	4.984	0.009	-0.202	0.003	0.000	0.025	5.801
	7	-49.949	1.158	0.085	0.000	-0.006	0.035	5.803
	8	-67.087	1.524	-0.250	0.004	-0.008	0.033	5.833
	9	7.023	-2.724	0.956	0.000	0.000	0.000	5.929
	None of the models is particularly good. Average I_{SET} of the 9 models taken =							5.845

Table C2 Coefficients of non-linear regression models for predicting I_{HET} for a specimen compacted to 95% compaction at optimum water content.

Soil Sample	Chosen Regression Model	Coefficients for regression model						Predicted I_{HET} at 95% Compaction and OWC
		a	b	c	d	e	f	
Bradys	6	-21.510	0.260	-11.849	0.137	0.000	0.307	3.230
Buffalo	9	8.729	2.720	4.520	0.000	0.000	0.000	6.089
Fattorini	4	-420.880	8.865	0.181	0.000	-0.046	0.000	4.780
Hume	5	-9.707	0.143	0.119	0.000	0.000	0.087	3.891
Jindabyne	1	-7.763	0.112	0.056	0.000	0.000	0.000	2.915
Lyell	9	-11.538	29.543	-5.222	0.000	0.000	0.000	1.657
Matahina	4	438.265	-9.436	0.062	0.000	0.051	0.000	3.760
Pukaki	5	-6.371	0.095	0.294	0.000	0.000	-0.125	2.700
Rowallan	6	-2.407	0.036	-2.430	0.025	0.000	-0.067	0.994
Shellharbour	5	-20.021	0.272	0.118	0.000	0.000	-0.144	5.802
Teton	5	-4.543	0.073	-0.228	0.000	0.000	-0.097	2.404
Waranga Basin	5	-10.458	0.150	0.462	0.000	0.000	0.130	3.828
Waroona	9	3.214	29.608	4.331	0.000	0.000	0.000	5.713

APPENDIX D

Contour Plots of I_{SET} and I_{HET}

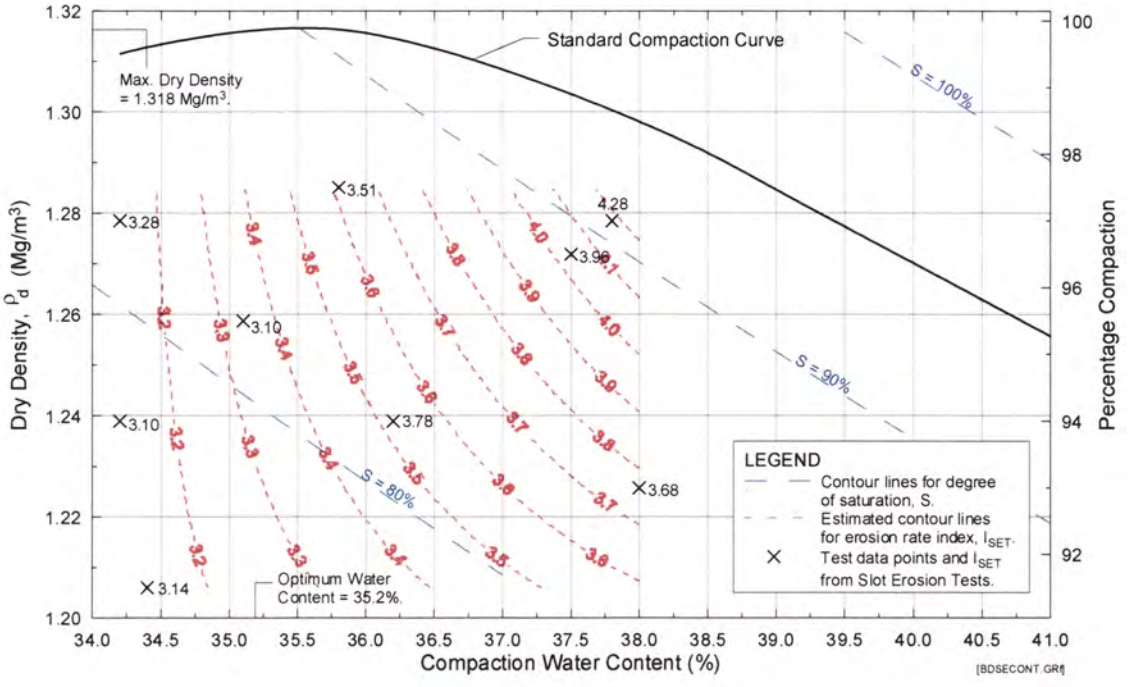

Figure D1a Erosion Rate Indices, I_{SET} based on SETs on soil sample Bradys.

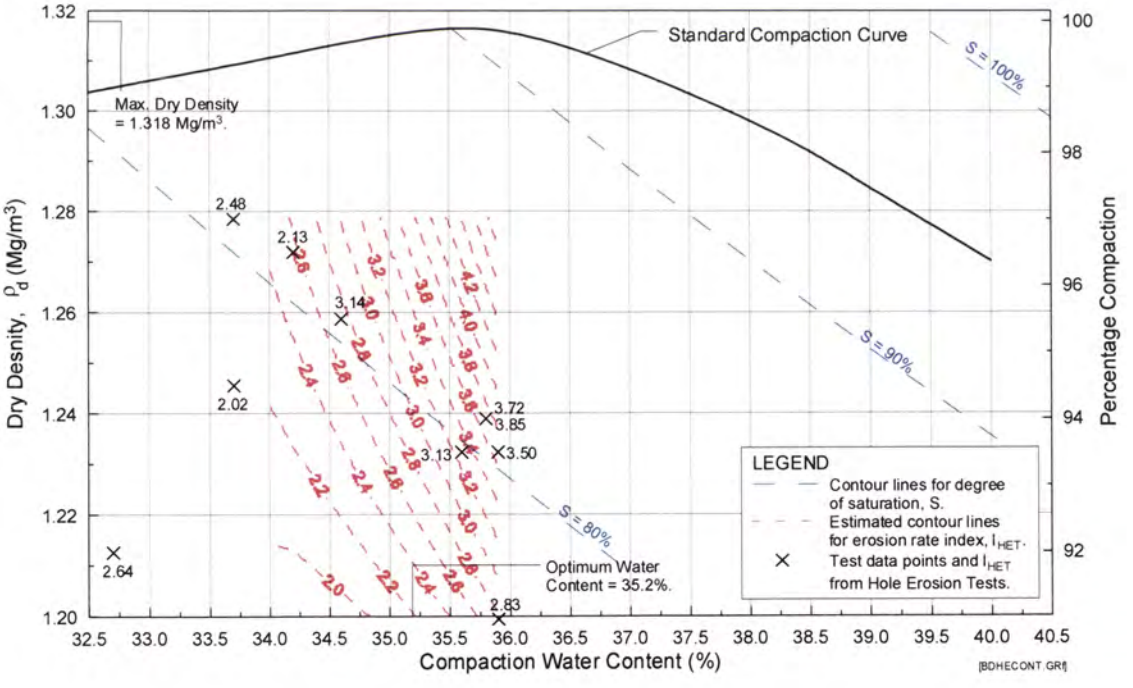

Figure D1b Erosion Rate Indices, I_{HET} based on HETs on soil sample Bradys.

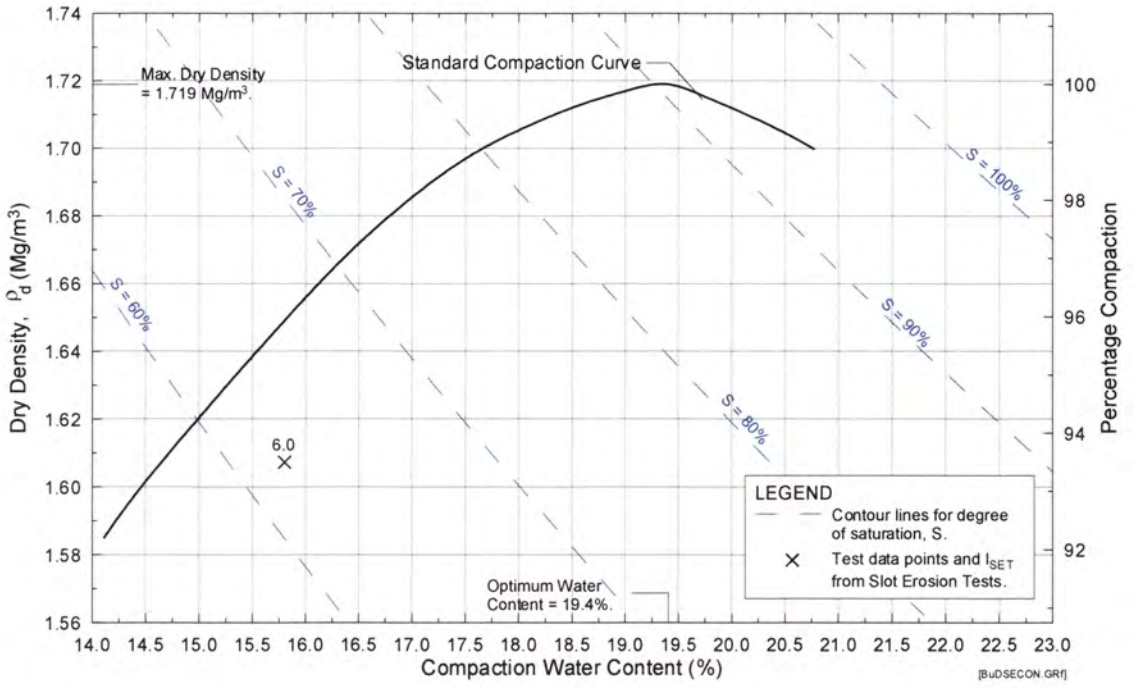

Figure D2a Erosion Rate Indices, I_{SET} based on SETs on soil sample Buffalo.

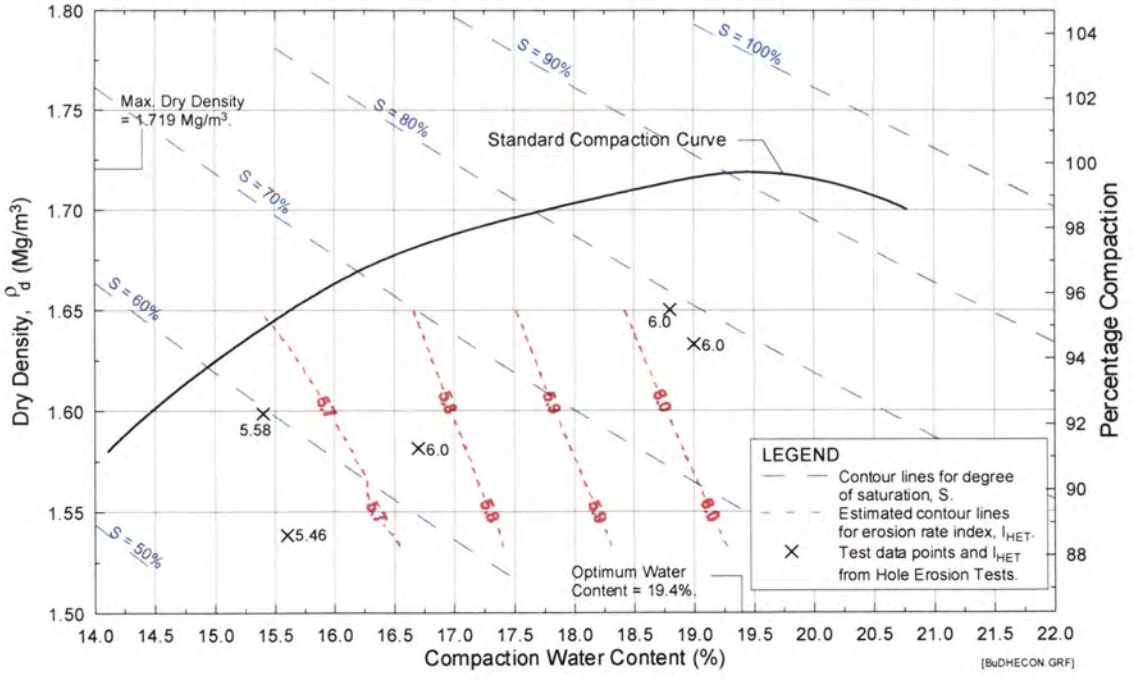

Figure D2b Erosion Rate Indices, I_{HET} based on HETs on soil sample Buffalo.

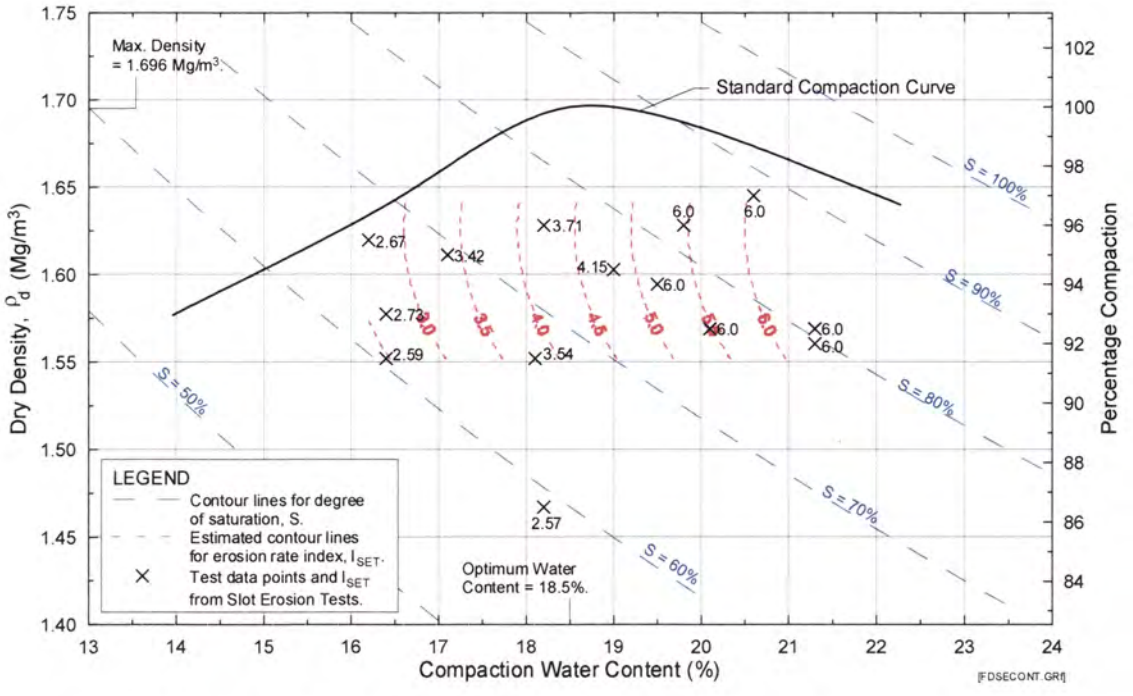

Figure D3a Erosion Rate Indices, I_{SET} based on SETs on soil sample Fattorini.

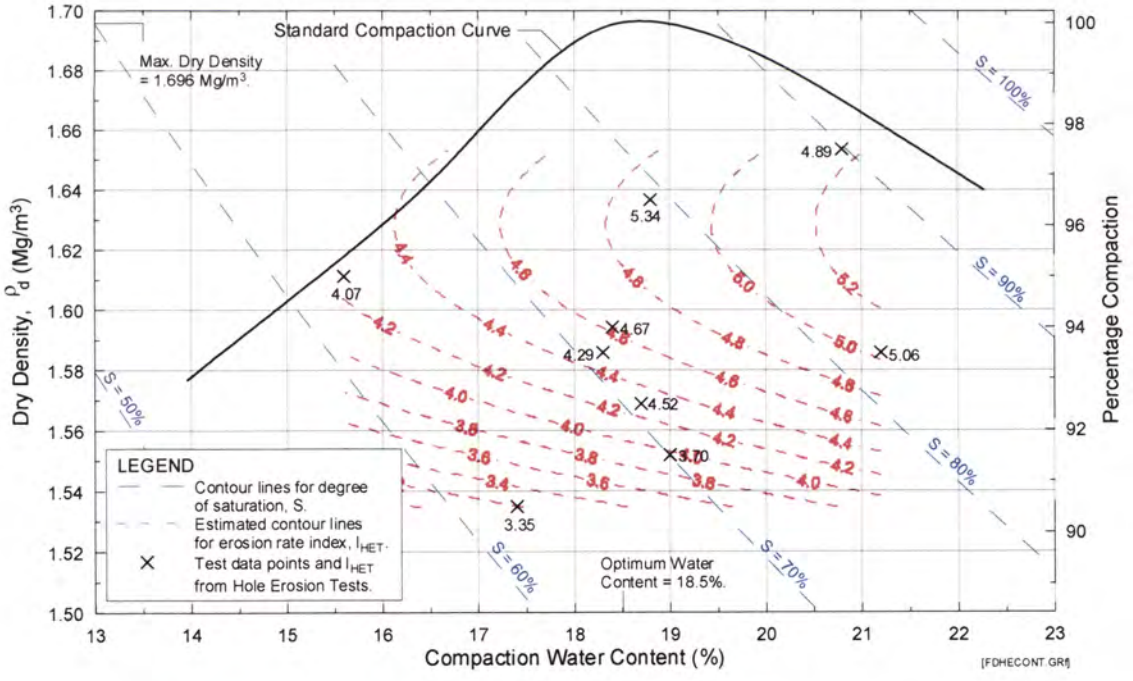

Figure D3b Erosion Rate Indices, I_{HET} based on HETs on soil sample Fattorini.

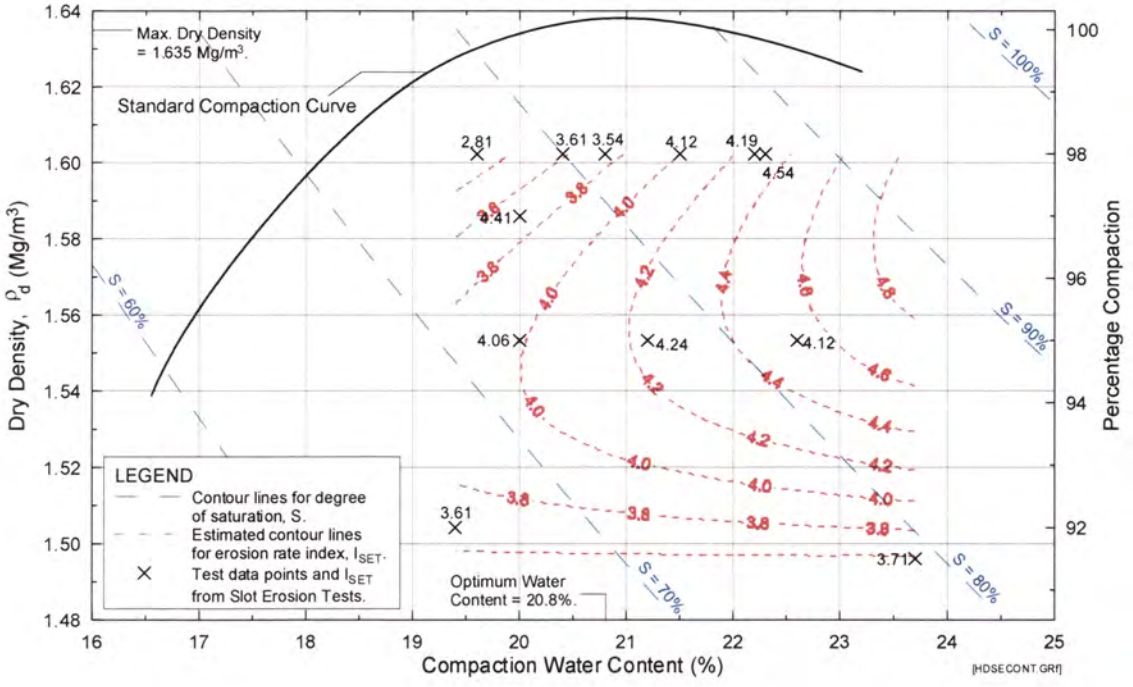

Figure D4a Erosion Rate Indices, I_{SET} based on SETs on soil sample Hume.

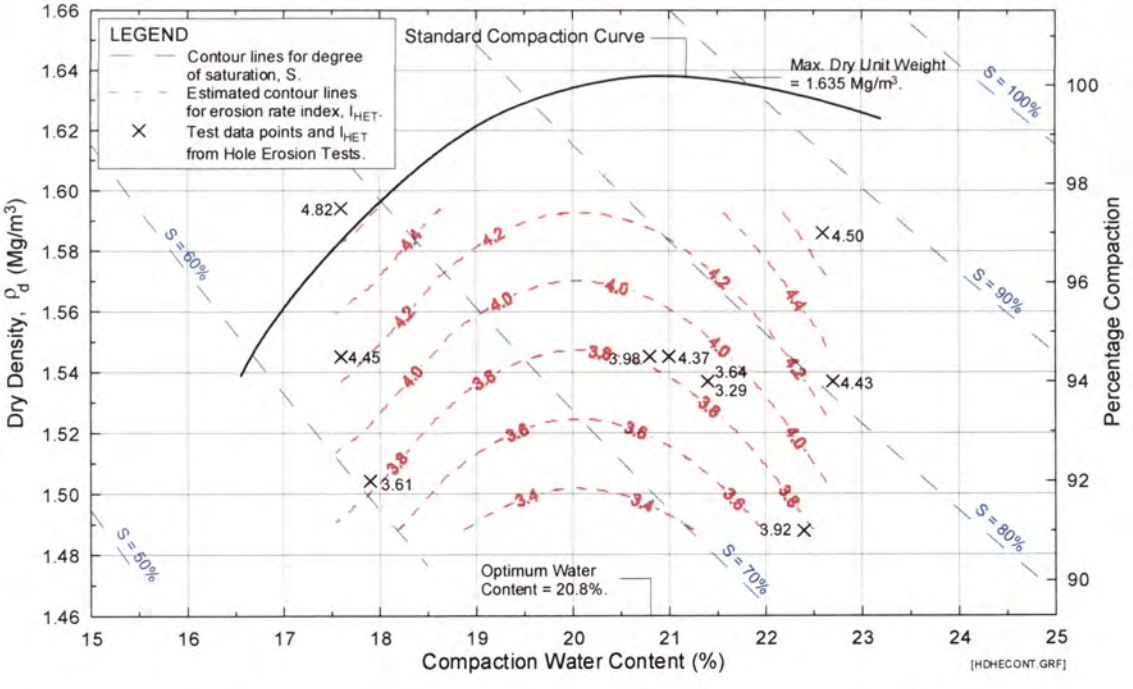

Figure D4b Erosion Rate Indices, I_{HET} based on HETs on soil sample Hume.

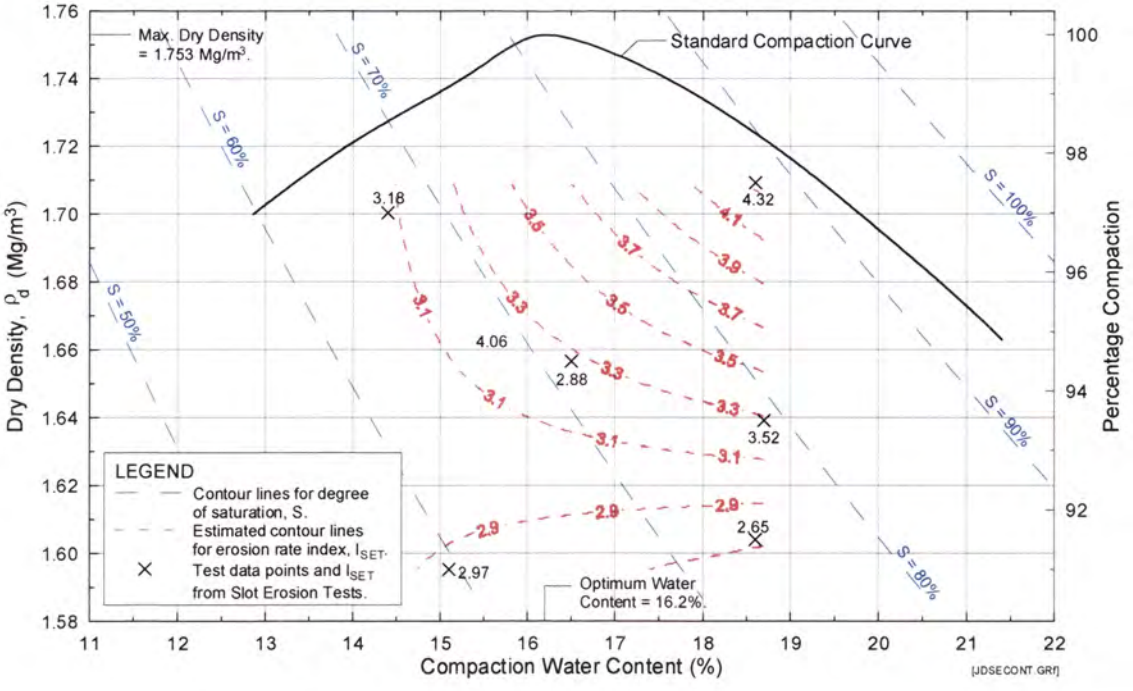

Figure D5a Erosion Rate Indices, I_{SET} based on SETs on soil sample Jindabyne.

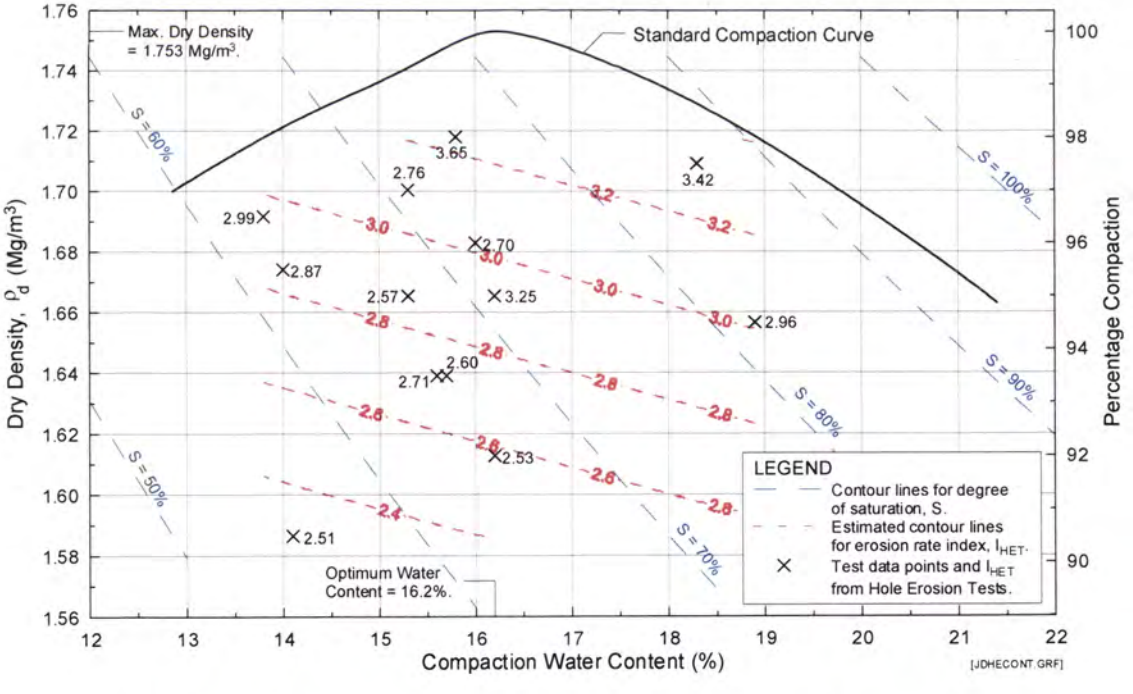

Figure D5b Erosion Rate Indices, I_{HET} based on HETs on soil sample Jindabyne.

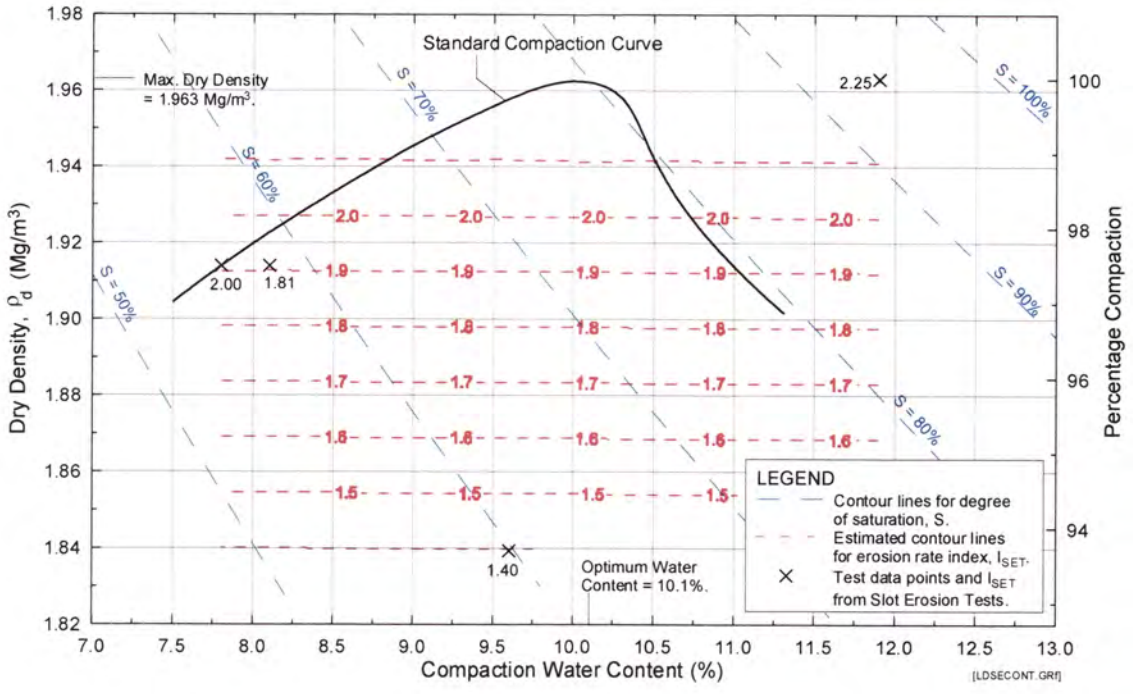

Figure D6a Erosion Rate Indices, I_{SET} based on SETs on soil sample Lyell.

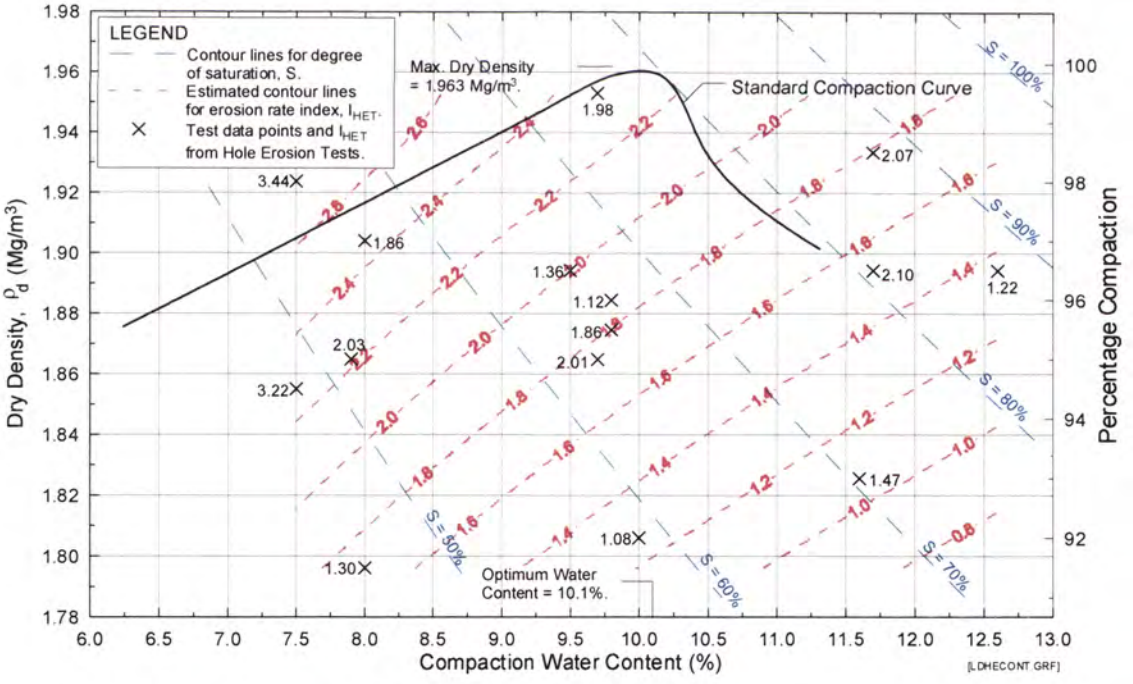

Figure D6b Erosion Rate Indices, I_{HET} based on HETs on soil sample Lyell.

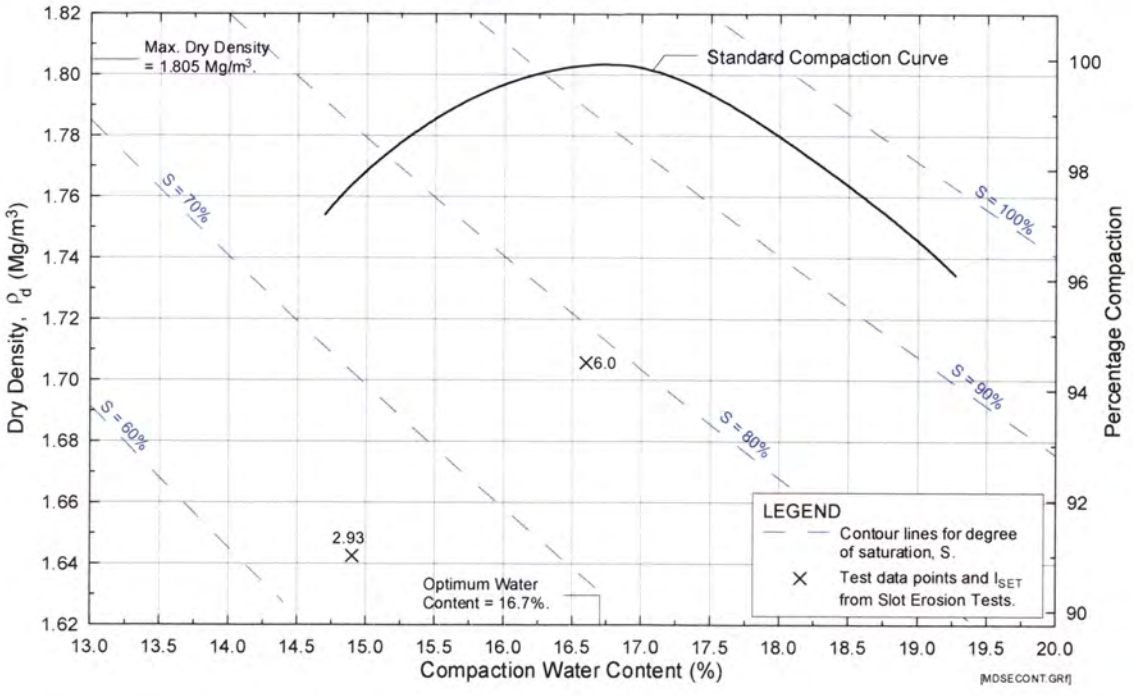

Figure D7a Erosion Rate Indices, I_{SET} based on SETs on soil sample Matahina.

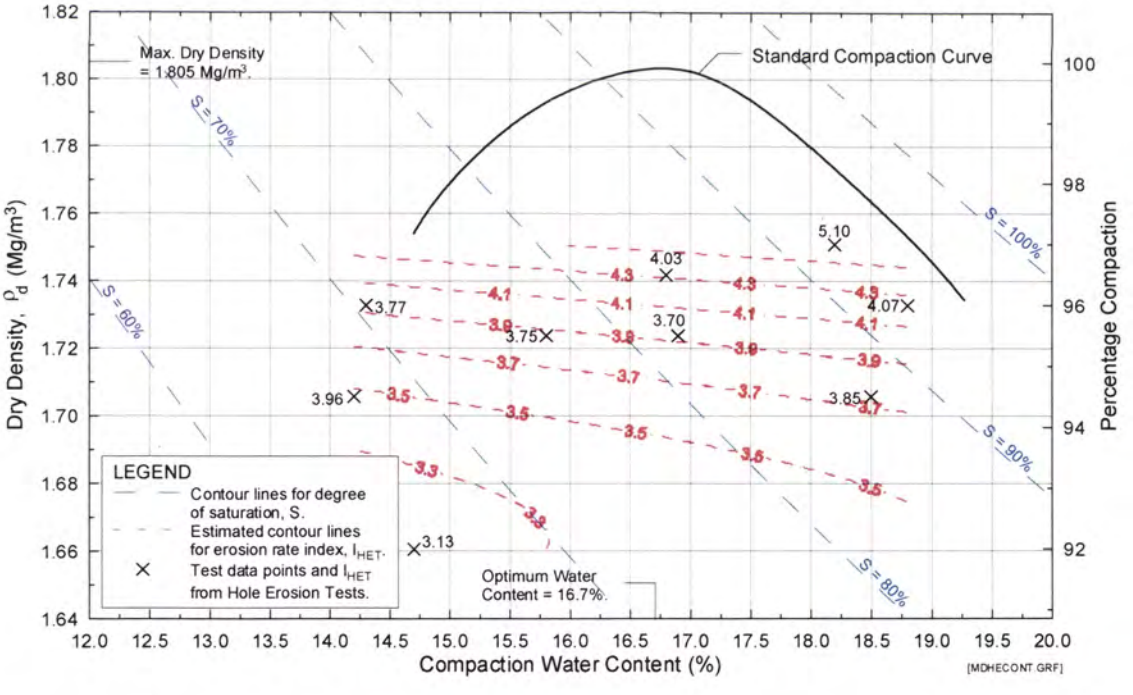

Figure D7b Erosion Rate Indices, I_{HET} based on HETs on soil sample Matahina.

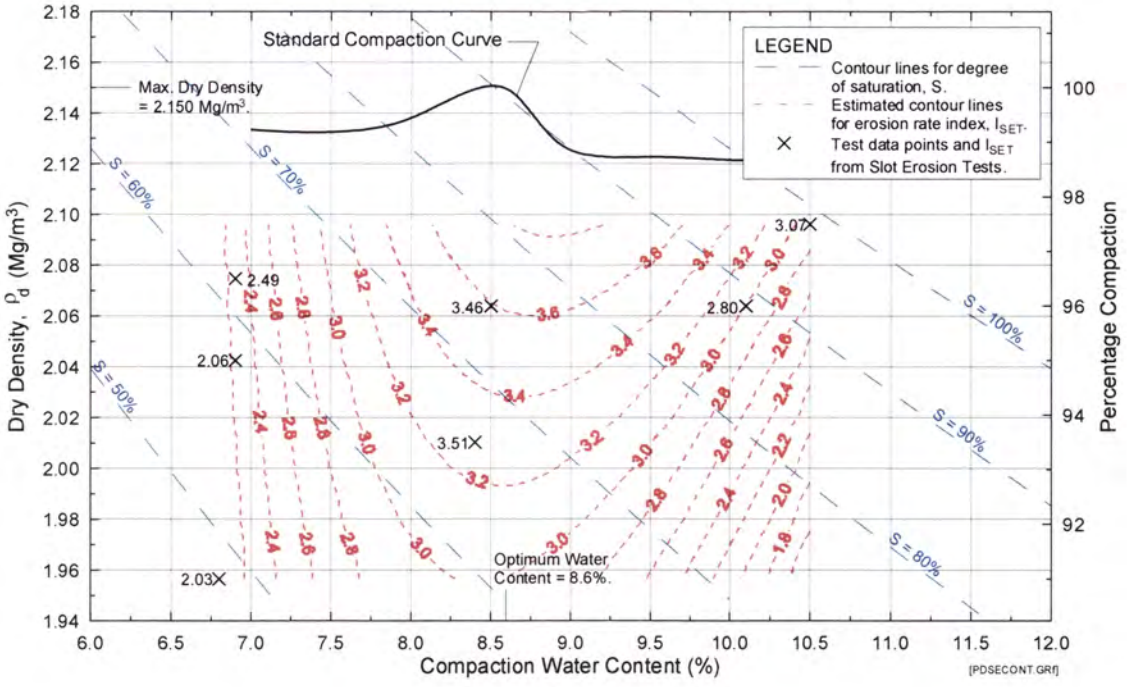

Figure D8a Erosion Rate Indices, I_{SET} based on SETs on soil sample Pukaki.

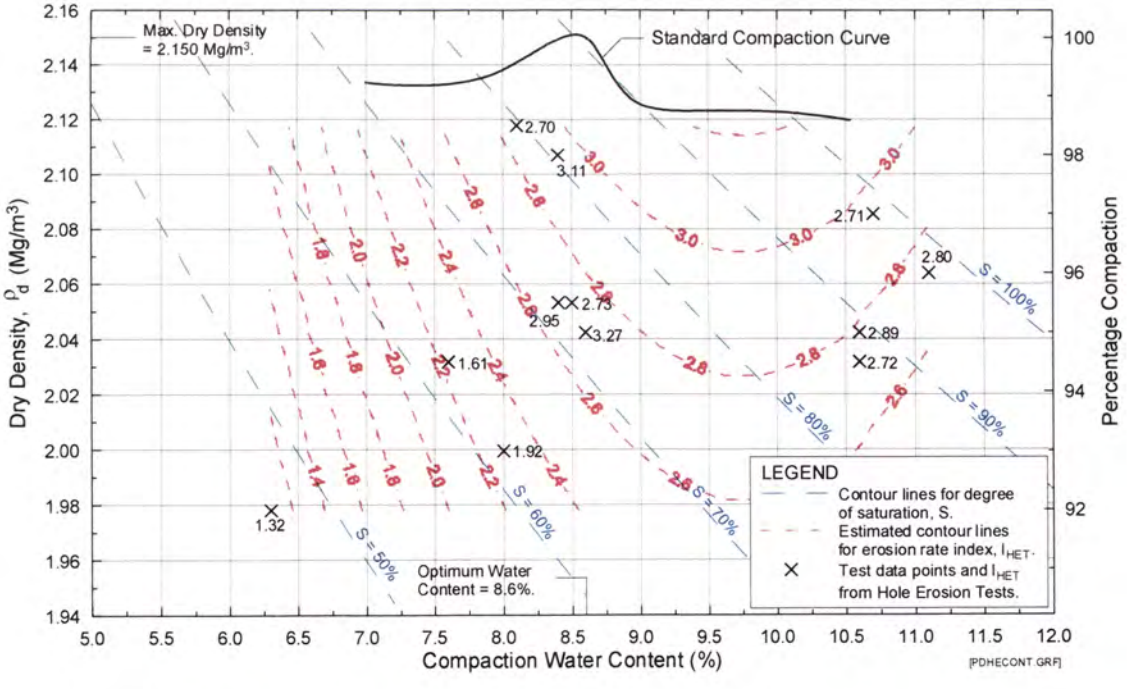

Figure D8b Erosion Rate Indices, I_{HET} based on HETs on soil sample Pukaki.

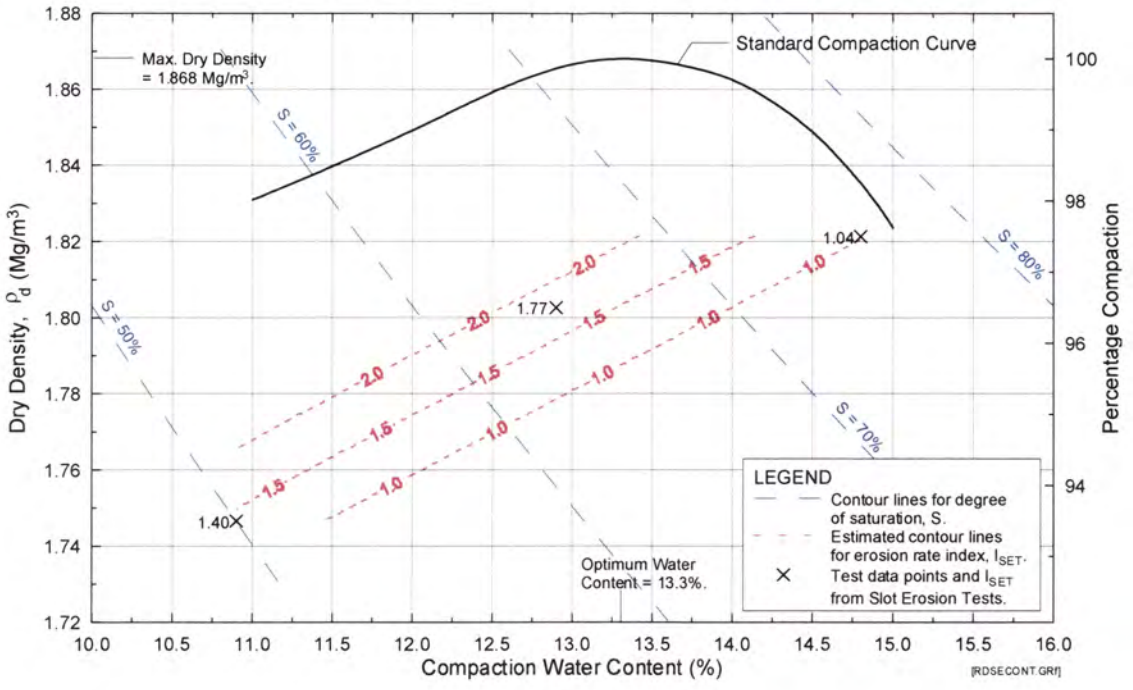

Figure D9a Erosion Rate Indices, I_{SET} based on SETs on soil sample Rowallan.

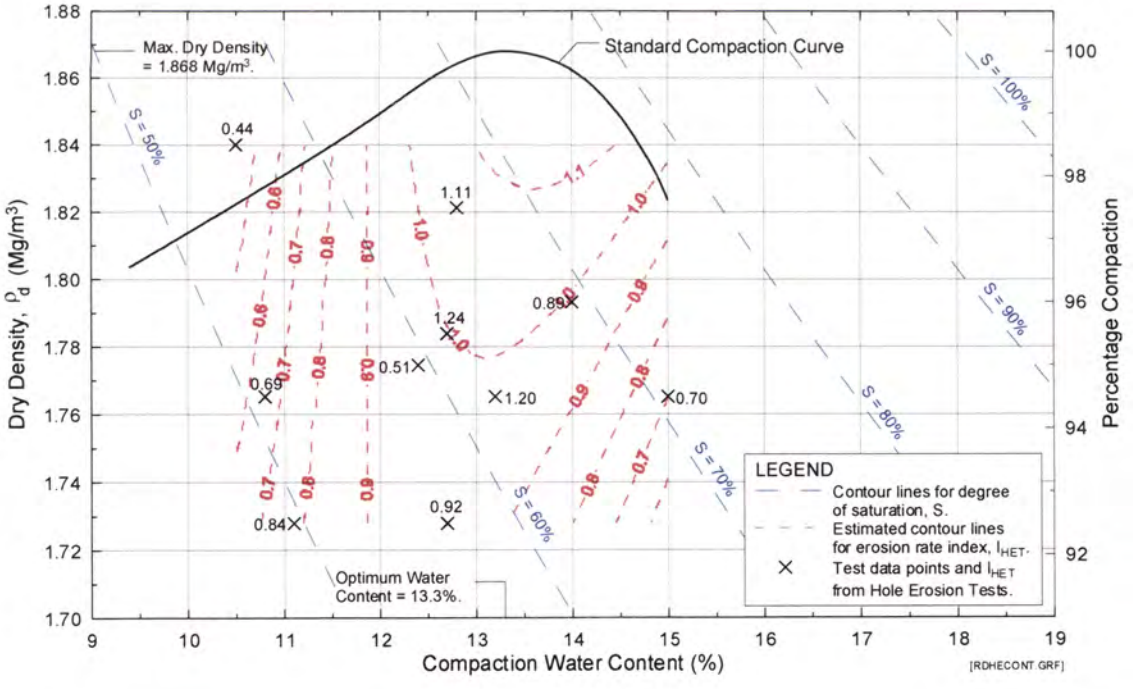

Figure D9b Erosion Rate Indices, I_{HET} based on HETs on soil sample Rowallan.

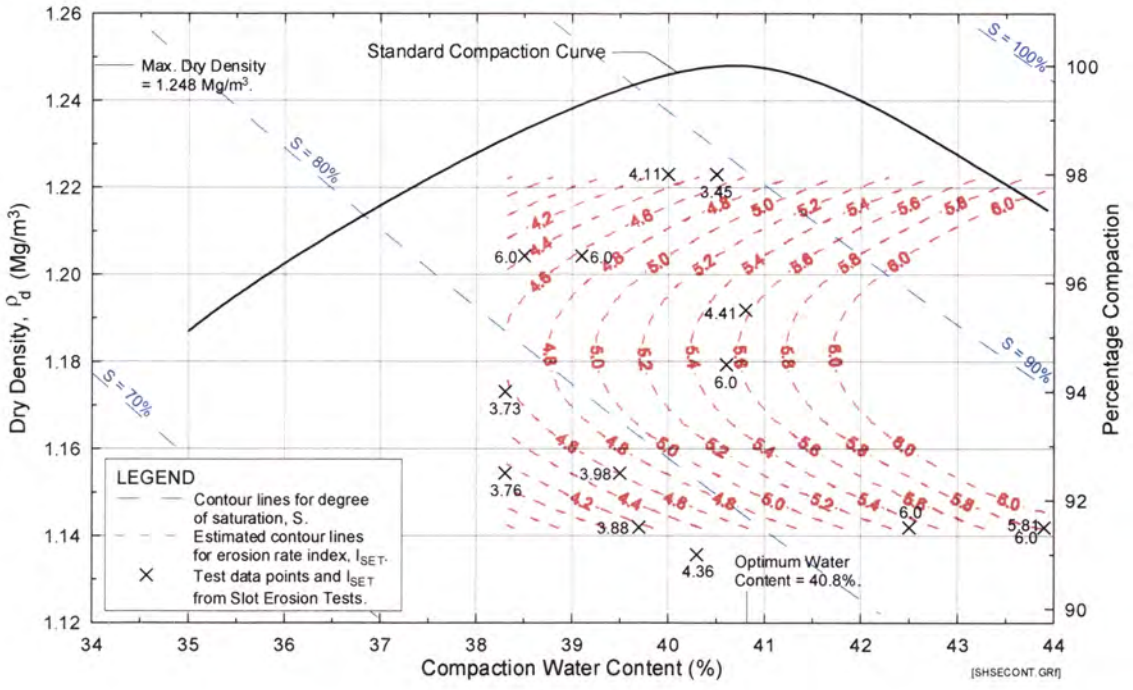

Figure D10a Erosion Rate Indices, I_{SET} based on SETs on soil sample Shellharbour.

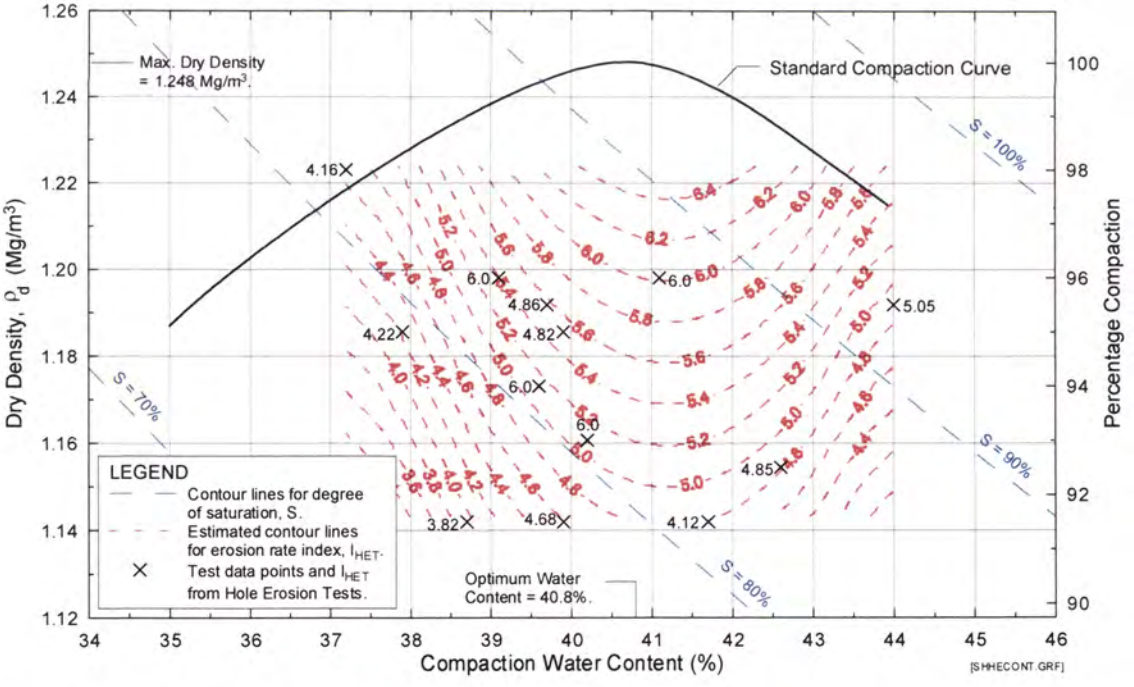

Figure D10b Erosion Rate Indices, I_{HET} based on HETs on soil sample Shellharbour.

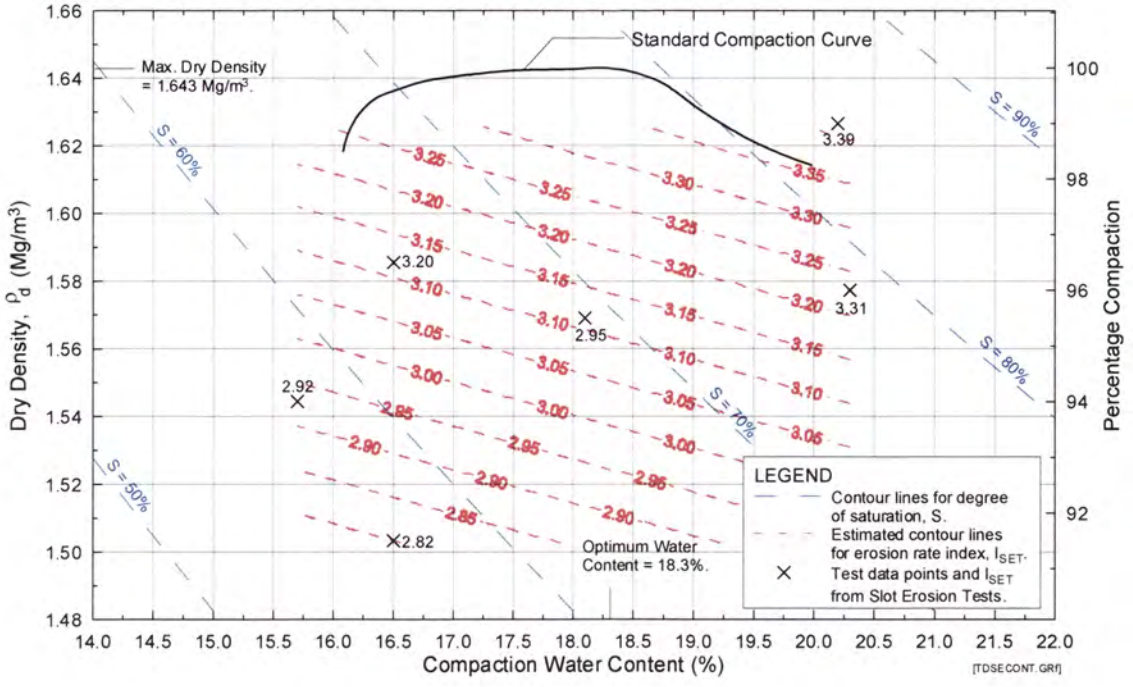

Figure D11a Erosion Rate Indices, I_{SET} based on SETs on soil sample Teton.

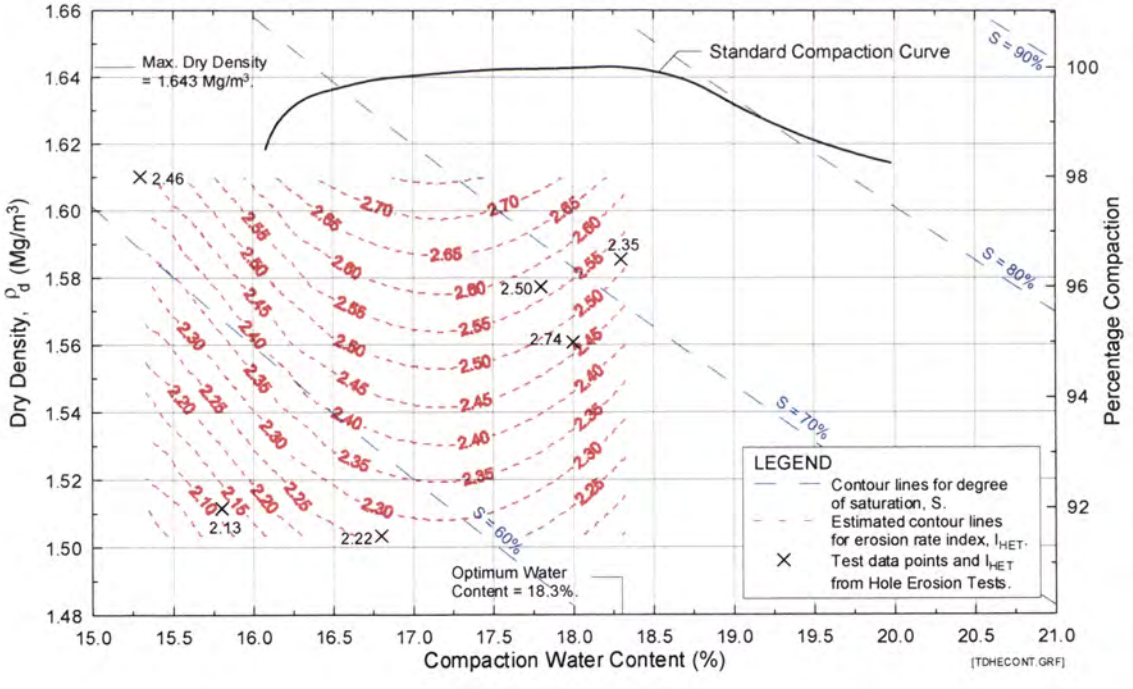

Figure D11b Erosion Rate Indices, I_{HET} based on HETs on soil sample Teton.

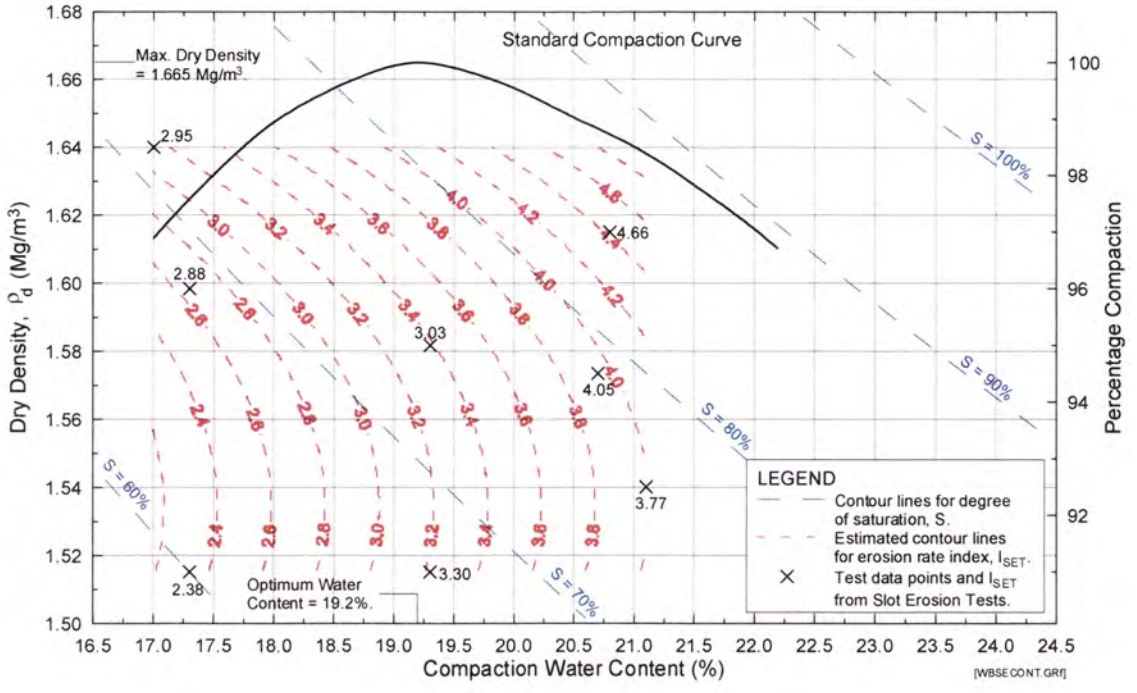

Figure D12a Erosion Rate Indices, I_{SET} based on SETs on soil sample Waranga Basin.

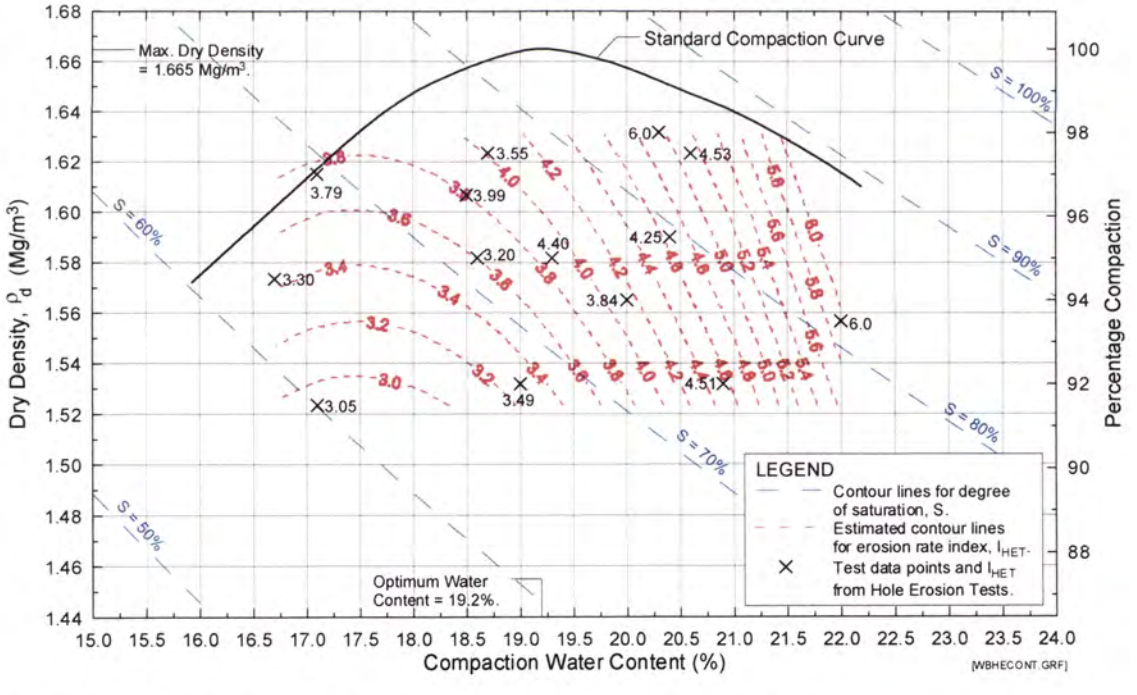

Figure D12b Erosion Rate Indices, I_{HET} based on HETs on soil sample Waranga Basin.

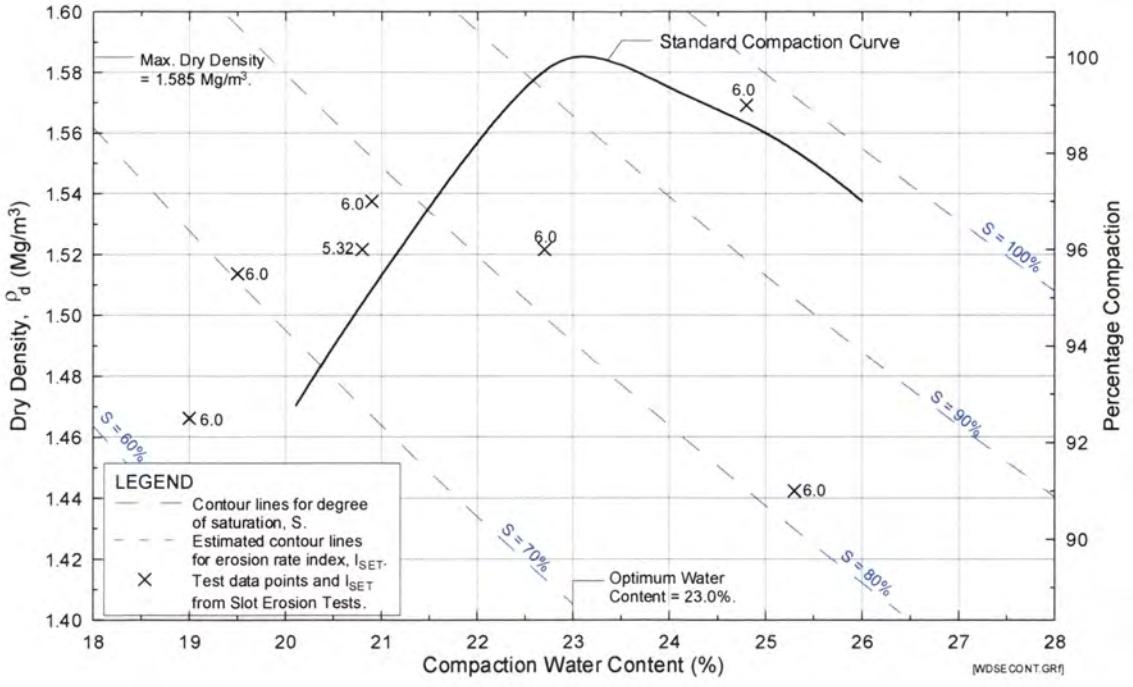

Figure D13a Erosion Rate Indices, I_{SET} based on SETs on soil sample Waroona.

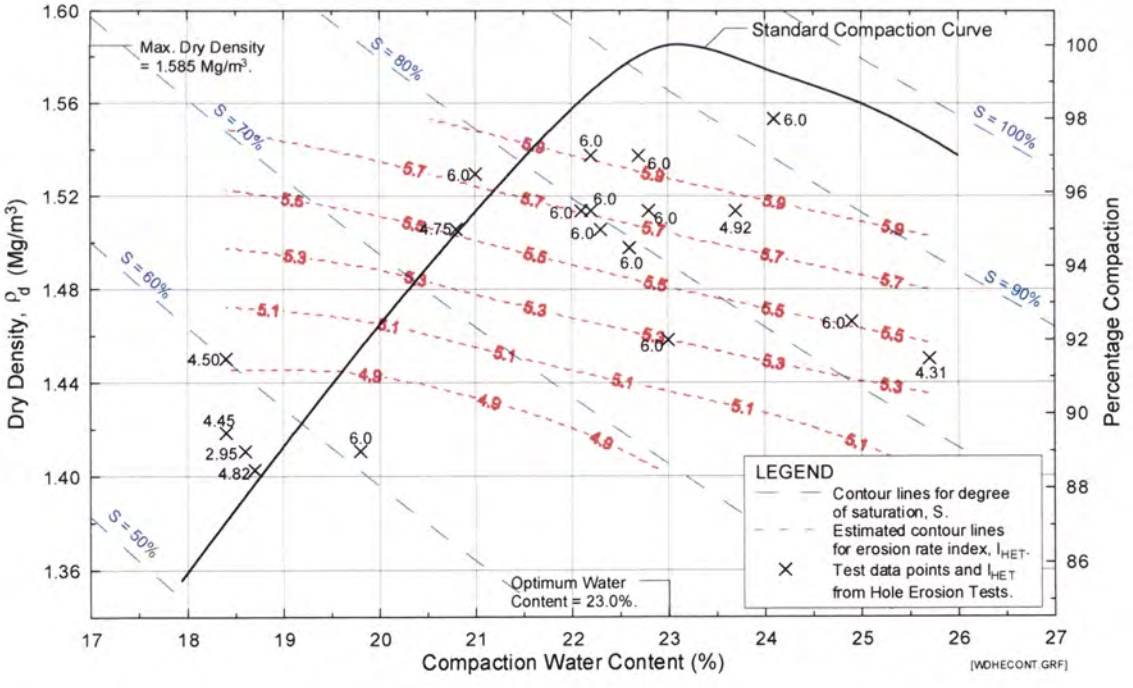

Figure D13b Erosion Rate Indices, I_{HET} based on HETs on soil sample Waroona.

APPENDIX E

Plots of Erosion Rate Index against Dry Density, Water Content, Percentage Compaction, Ratio of Water Content to OWC, and Degree of Saturation

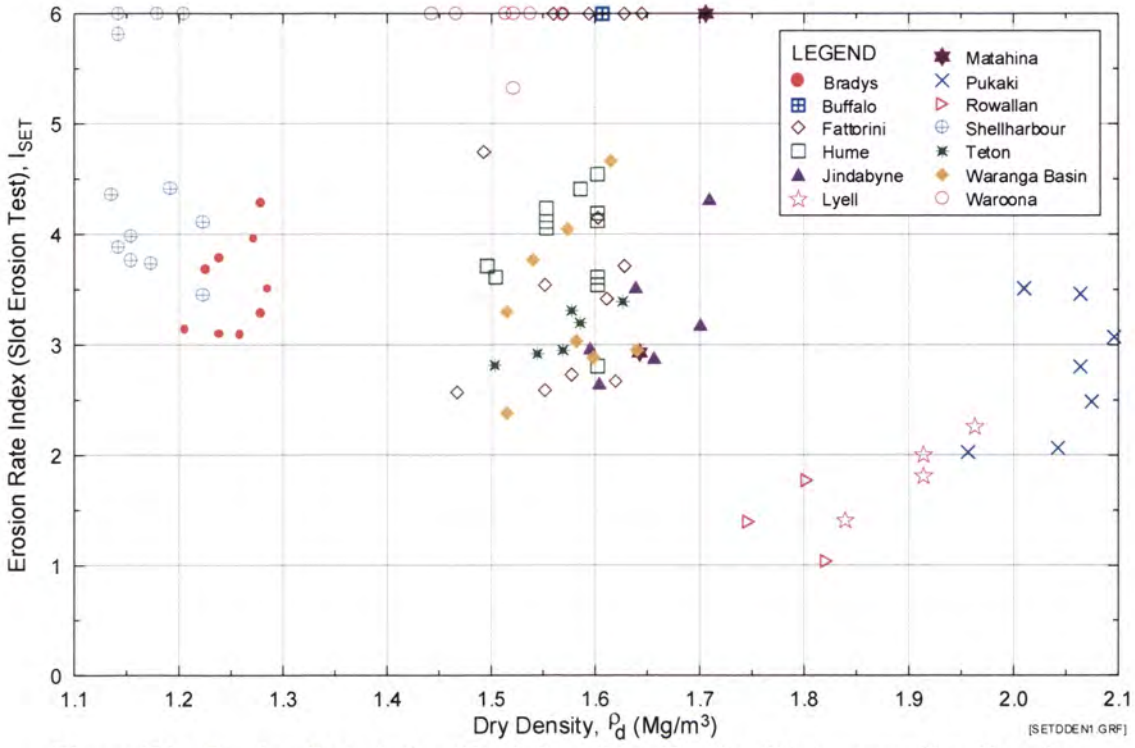

Figure E1a Erosion Rate Index (I_{SET}) from Slot Erosion Test versus Dry Density.

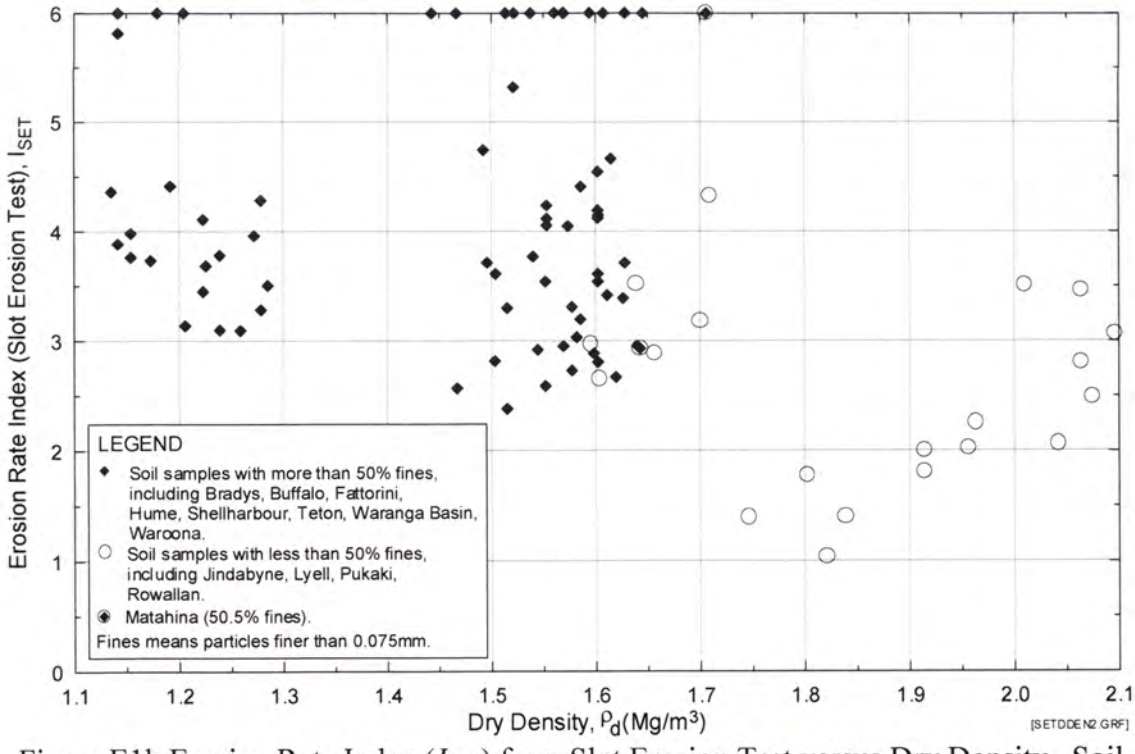

Figure E1b Erosion Rate Index (I_{SET}) from Slot Erosion Test versus Dry Density. Soil samples classified into fine-grained soils and coarse-grained soils.

Appendix E - Plots of Erosion Rate Index against Dry Density, Water Content, Percentage Compaction, Ratio of Water Content to OWC, and Degree of Saturation

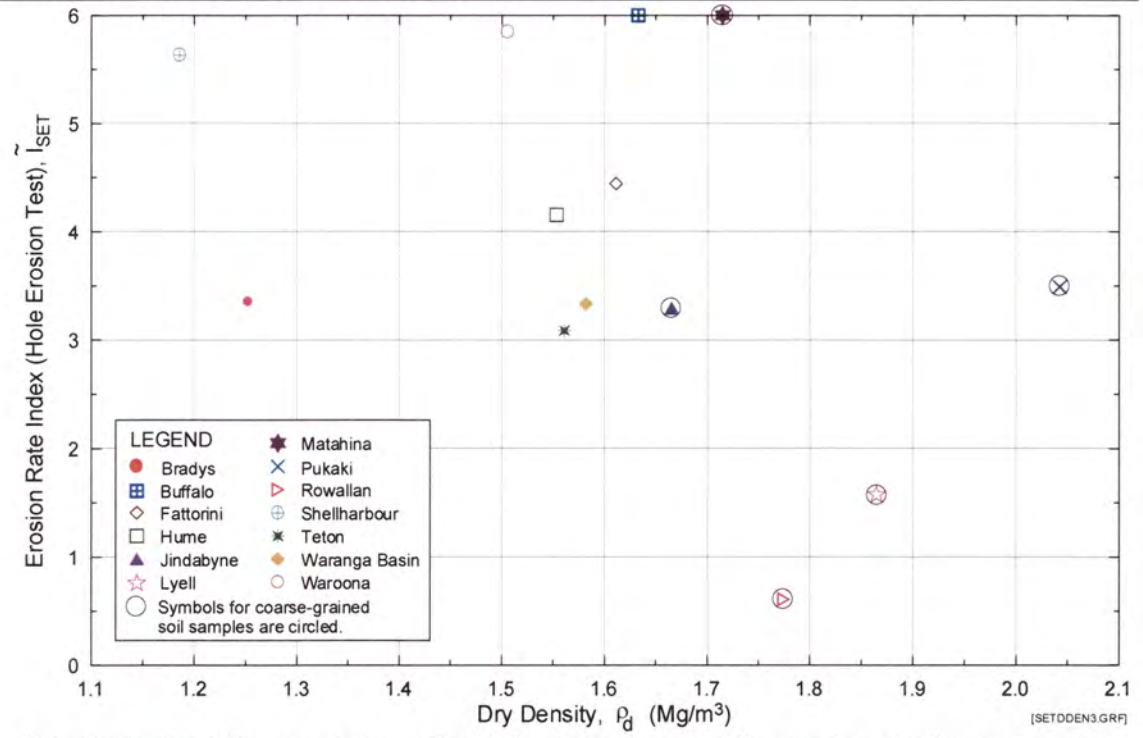

Note : Erosion Rate Indice presented are predicted indices for specimens at 95% compaction and optimum water content.

Figure E1c Predicted Representative Erosion Rate Index ($\tilde{I}_{SET}$) from Slot Erosion Test versus 95% Standard Maximum Dry Density ($\rho_{d\max}$).

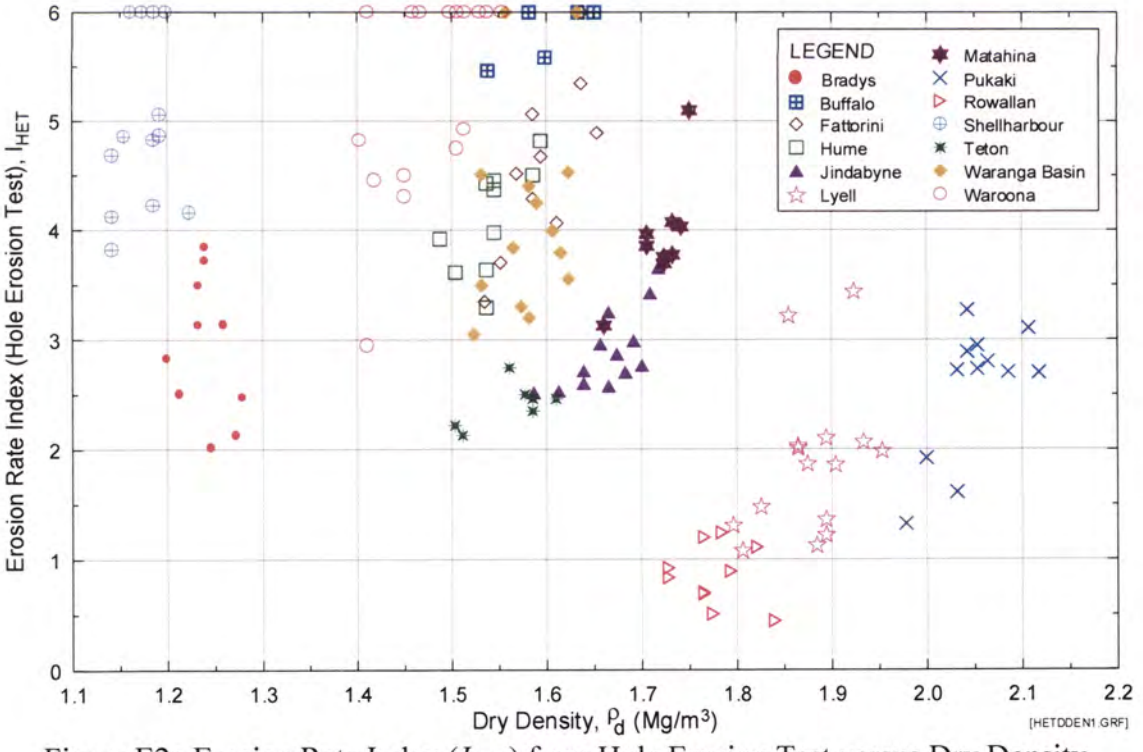

Figure E2a Erosion Rate Index (I_{HET}) from Hole Erosion Test versus Dry Density.

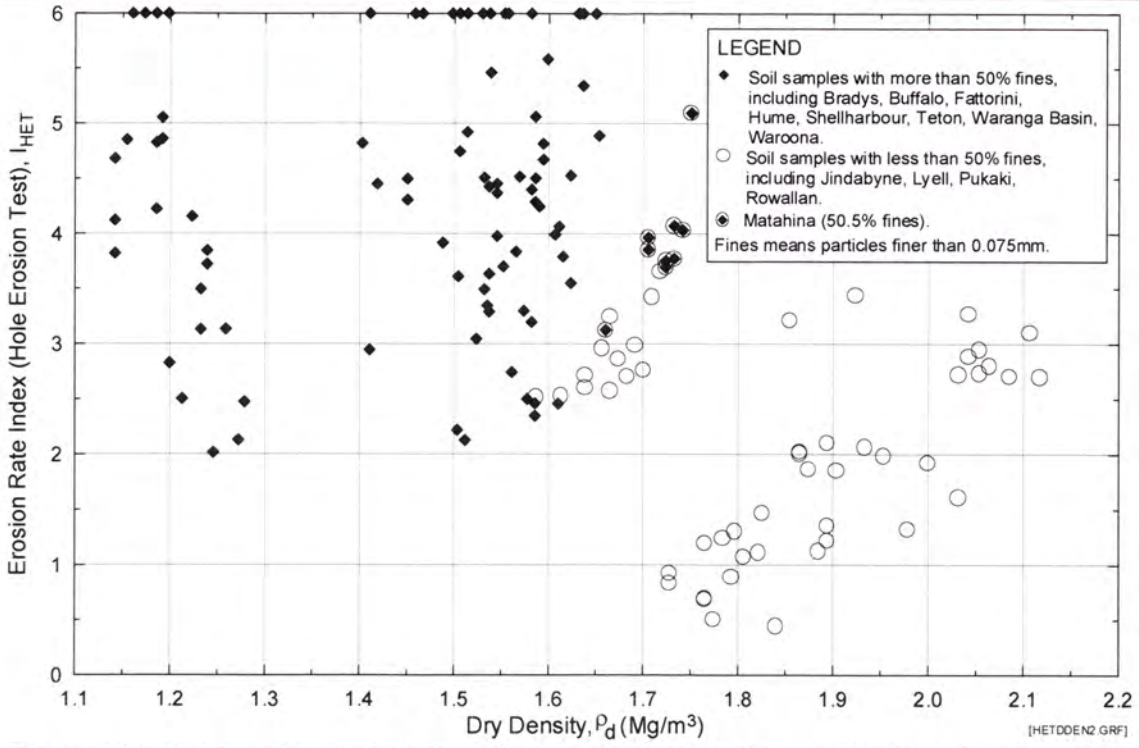

Figure E2b Erosion Rate Index (I_{HET}) from Hole Erosion Test versus Dry Density. Soil samples classified into fine-grained soils and coarse-grained soils.

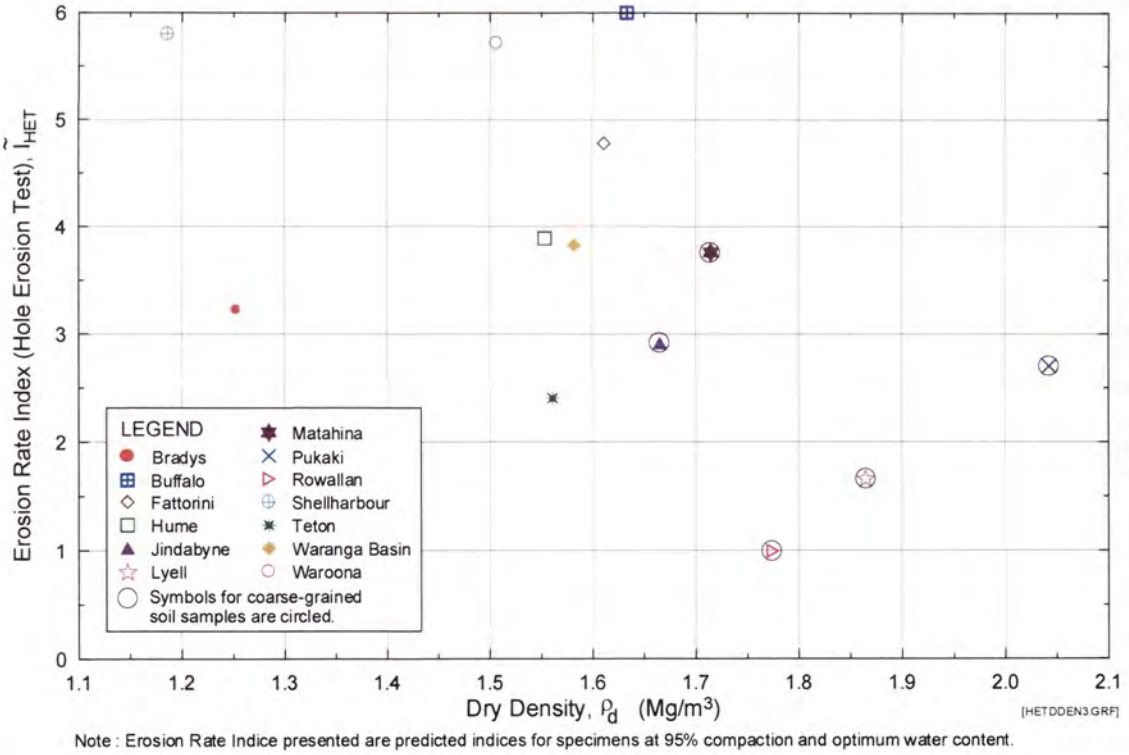

Note : Erosion Rate Indice presented are predicted indices for specimens at 95% compaction and optimum water content.

Figure E2c Predicted Representative Erosion Rate Index ($\tilde{I}_{HET}$) from Hole Erosion Test versus Dry Density (ρ_d).

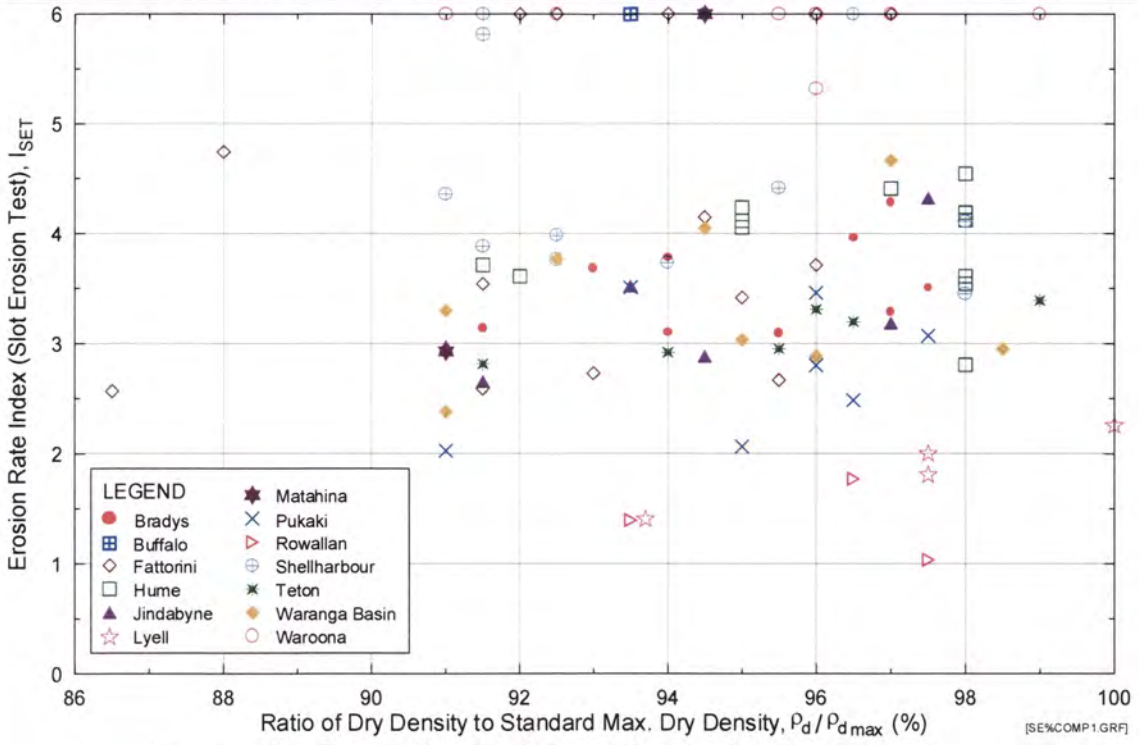

Figure E3a Erosion Rate Index (I_{SET}) from Slot Erosion Test versus Percentage Compaction ($\rho_d / \rho_{d_{max}}$).

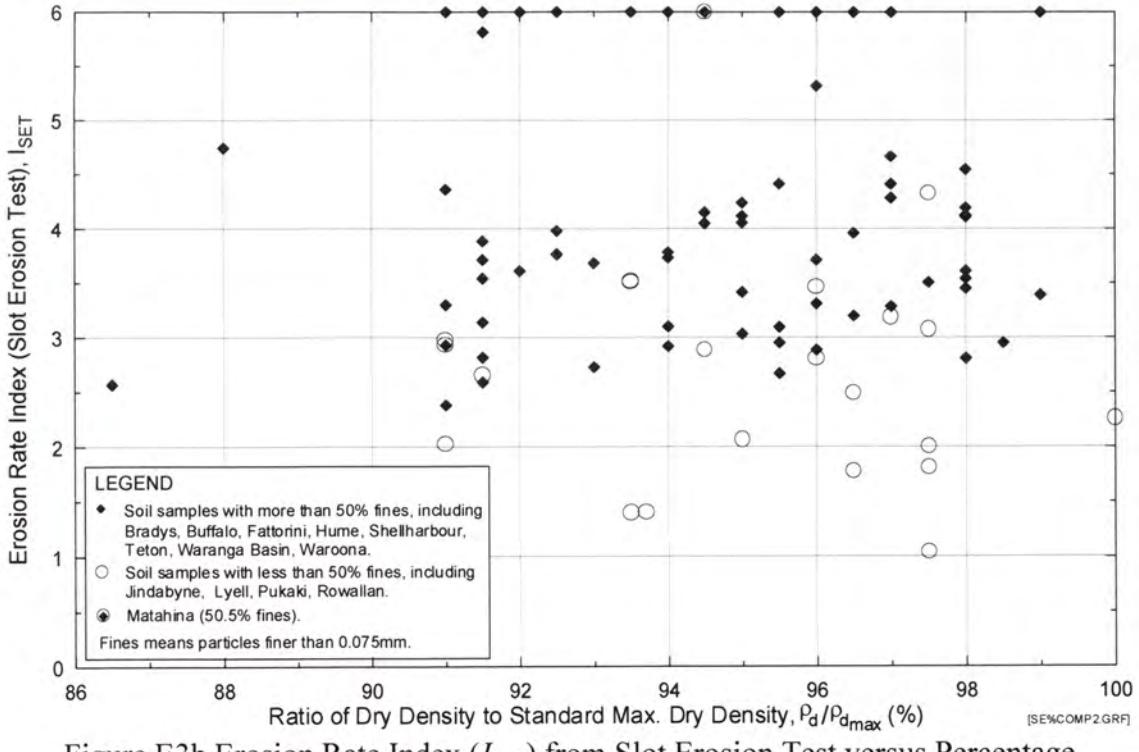

Figure E3b Erosion Rate Index (I_{SET}) from Slot Erosion Test versus Percentage Compaction ($\rho_d / \rho_{d_{max}}$). Soil samples classified into fine-grained soils and coarse-grained soils.

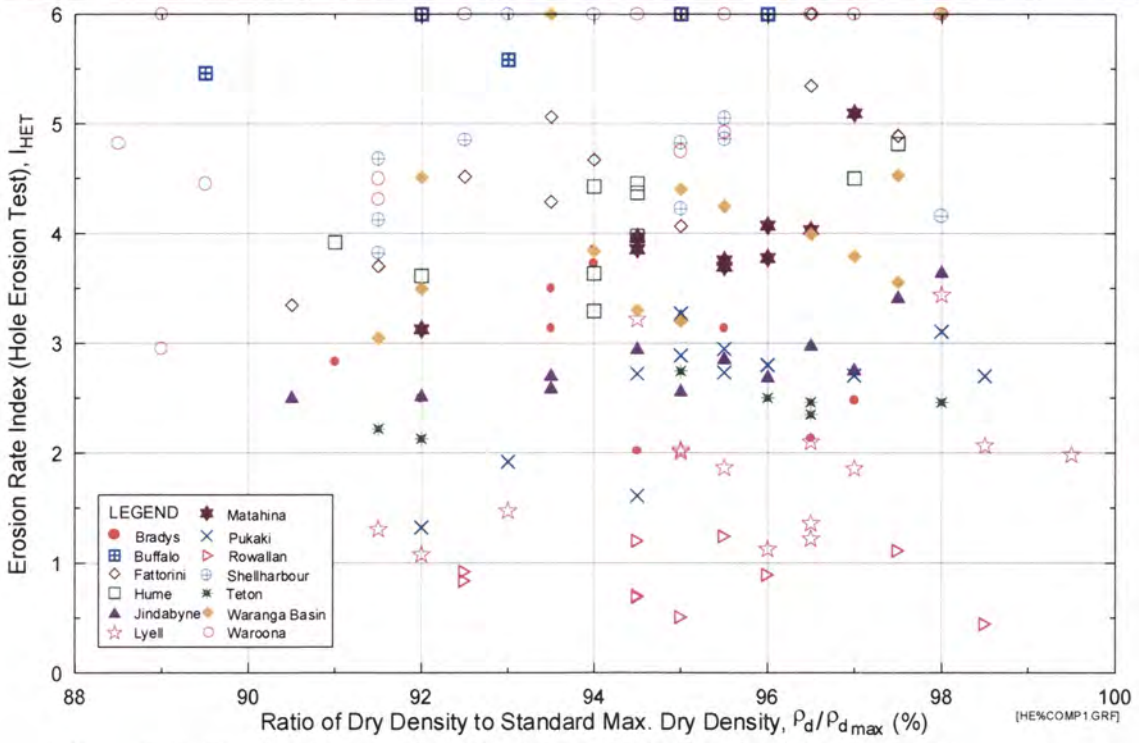

Figure E4a Erosion Rate Index (I_{HET}) from Hole Erosion Test versus Percentage Compaction ($\rho_d / \rho_{d_{max}}$).

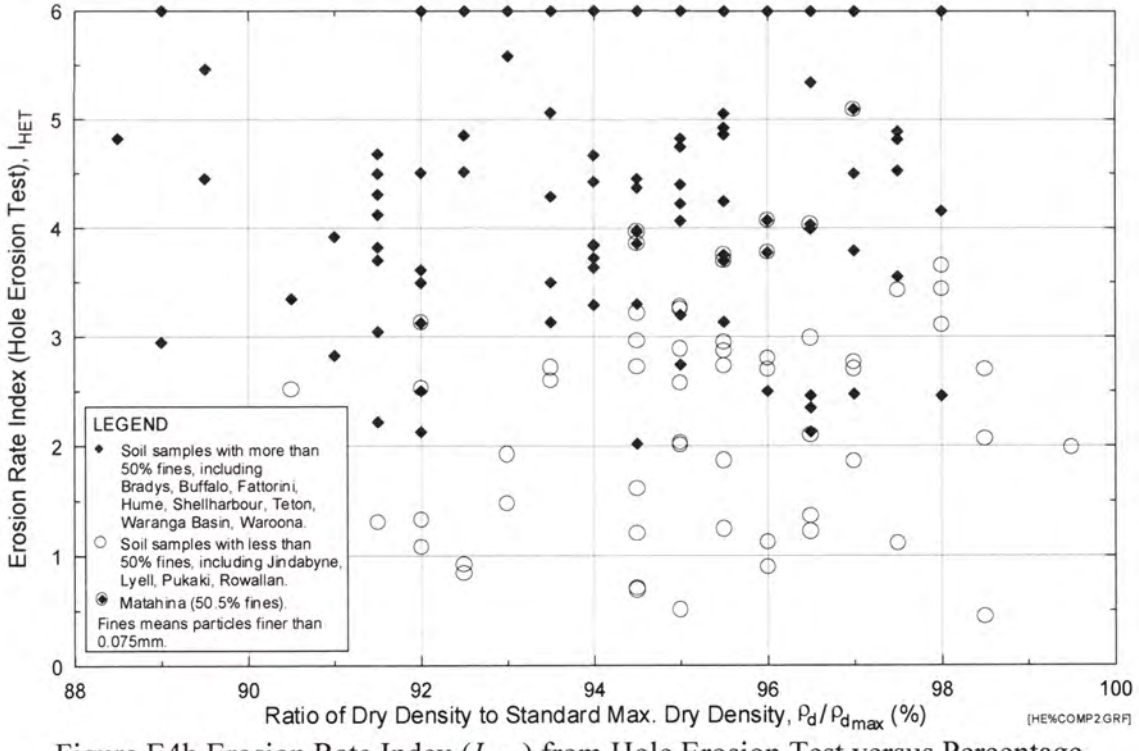

Figure E4b Erosion Rate Index (I_{HET}) from Hole Erosion Test versus Percentage Compaction ($\rho_d / \rho_{d_{max}}$). Soil samples classified into fine-grained soils and coarse-grained soils.

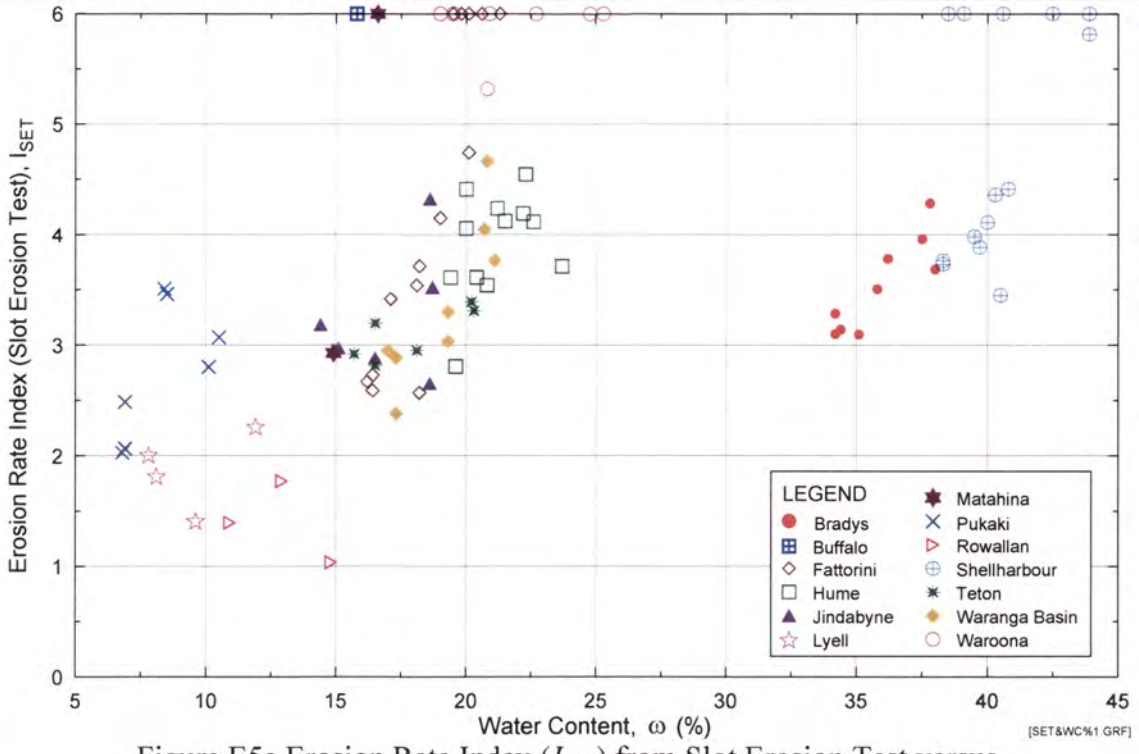

Figure E5a Erosion Rate Index (I_{SET}) from Slot Erosion Test versus Water Content (ω).

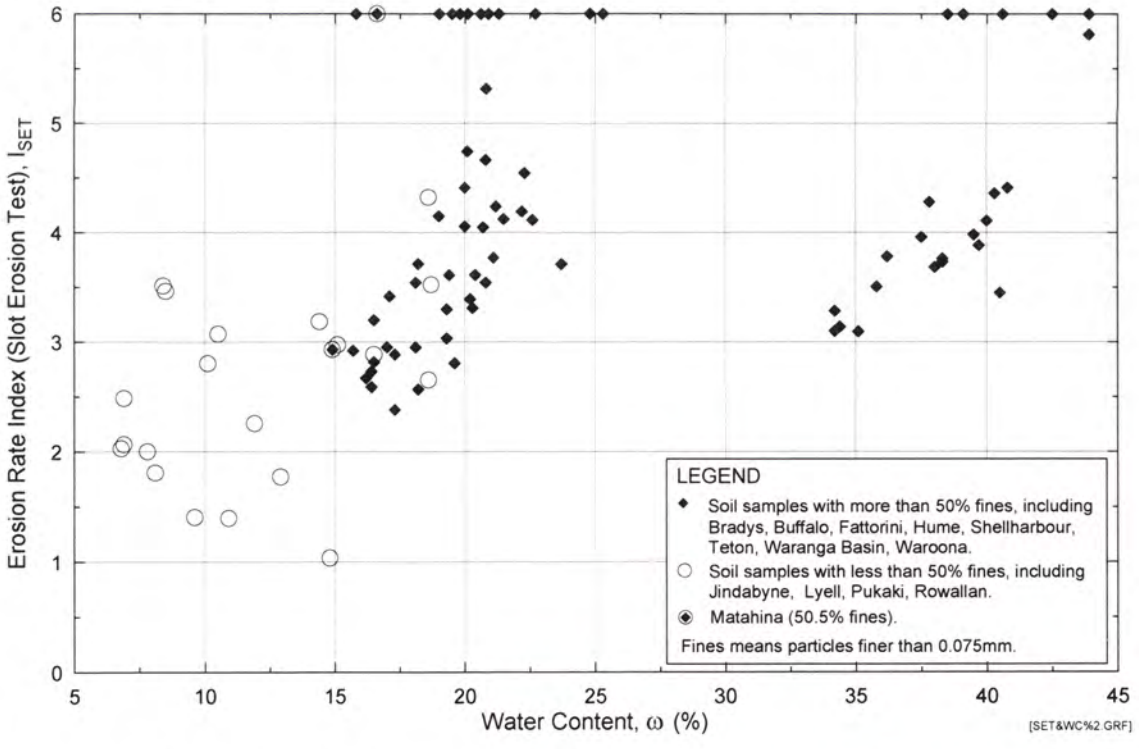

Figure E5b Erosion Rate Index (I_{SET}) from Slot Erosion Test versus Water Content (ω). Soil samples classified into fine-grained soils and coarse-grained soils.

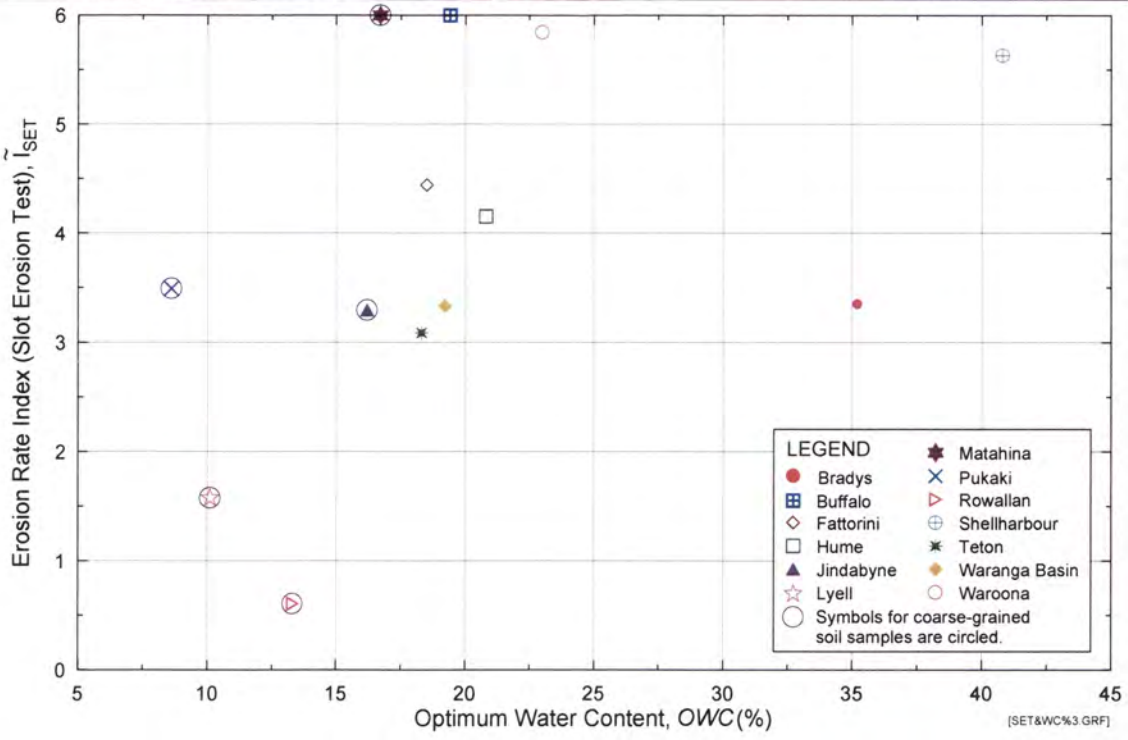

Note : Erosion Rate Indices presented are predicted indices for specimens at 95% compaction and optimum water content.

Figure E5c Predicted Representative Erosion Rate Index ($\tilde{I}_{SET}$) from Slot Erosion Test versus Optimum Water Content (*OWC*).

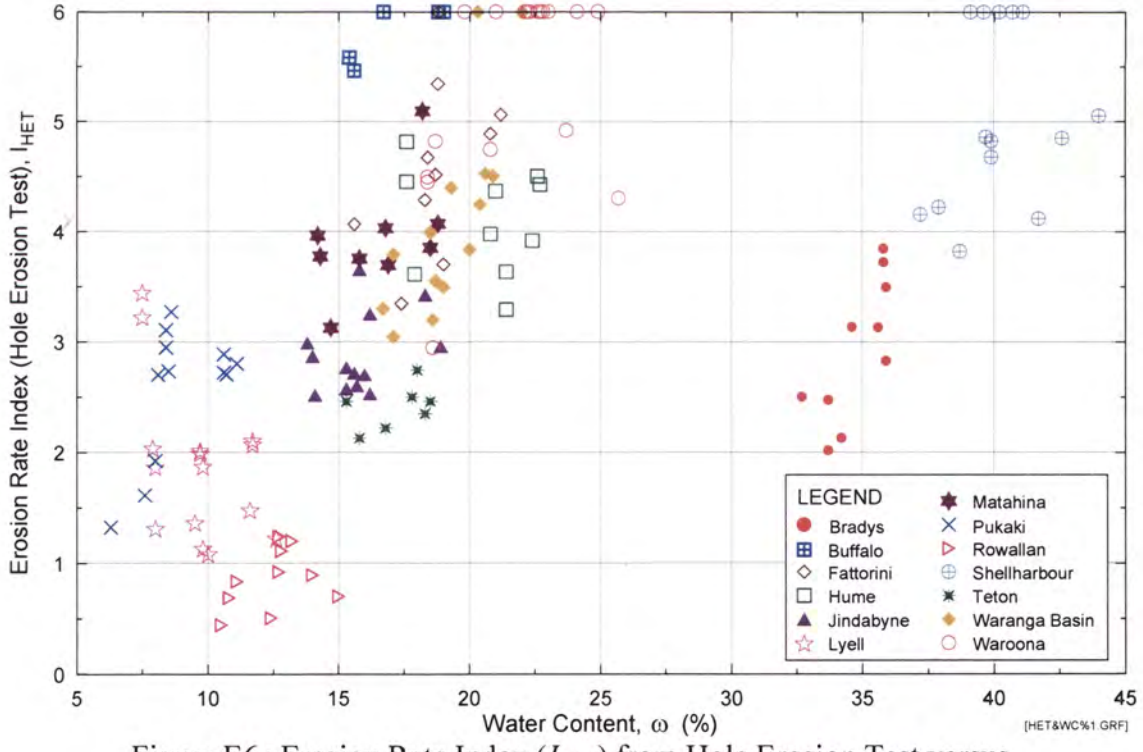

Figure E6a Erosion Rate Index (I_{HET}) from Hole Erosion Test versus Water Content (ω).

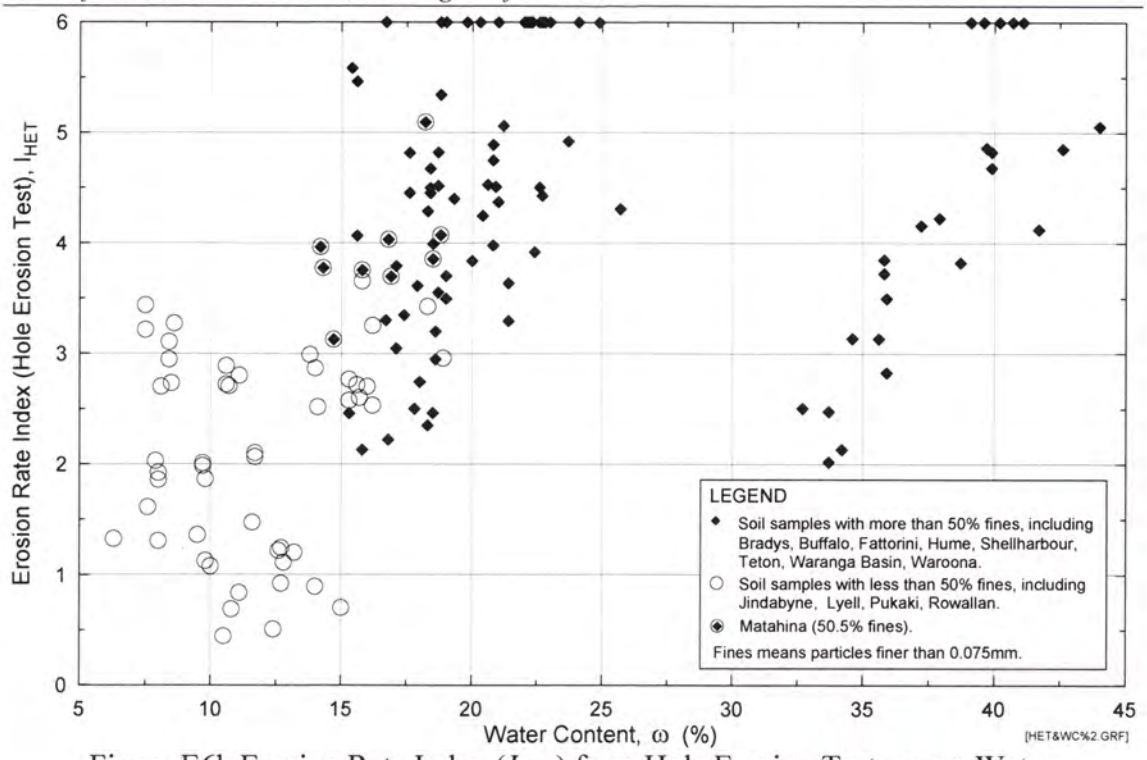

Figure E6b Erosion Rate Index (I_{HET}) from Hole Erosion Test versus Water Content (ω). Soil samples classified into fine-grained soils and coarse-grained soils.

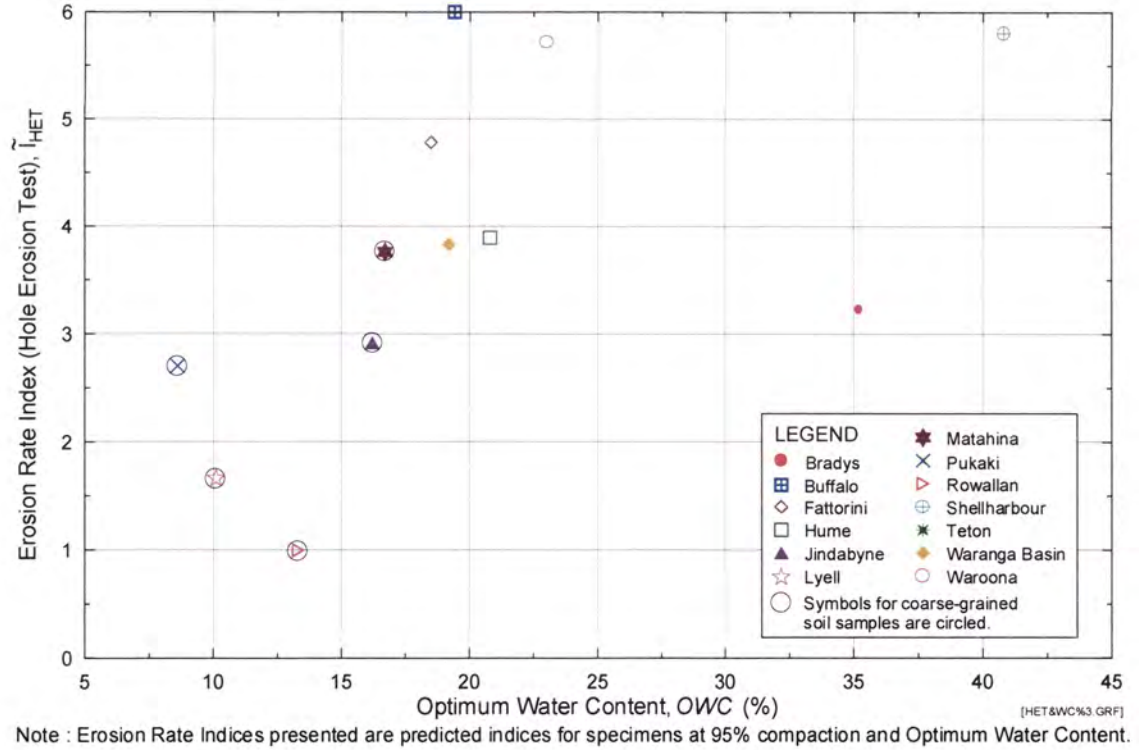

Note : Erosion Rate Indices presented are predicted indices for specimens at 95% compaction and Optimum Water Content.

Figure E6c Predicted Representative Erosion Rate Index ($\tilde{I}_{HET}$) from Hole Erosion Test versus Optimum Water Content (*OWC*).

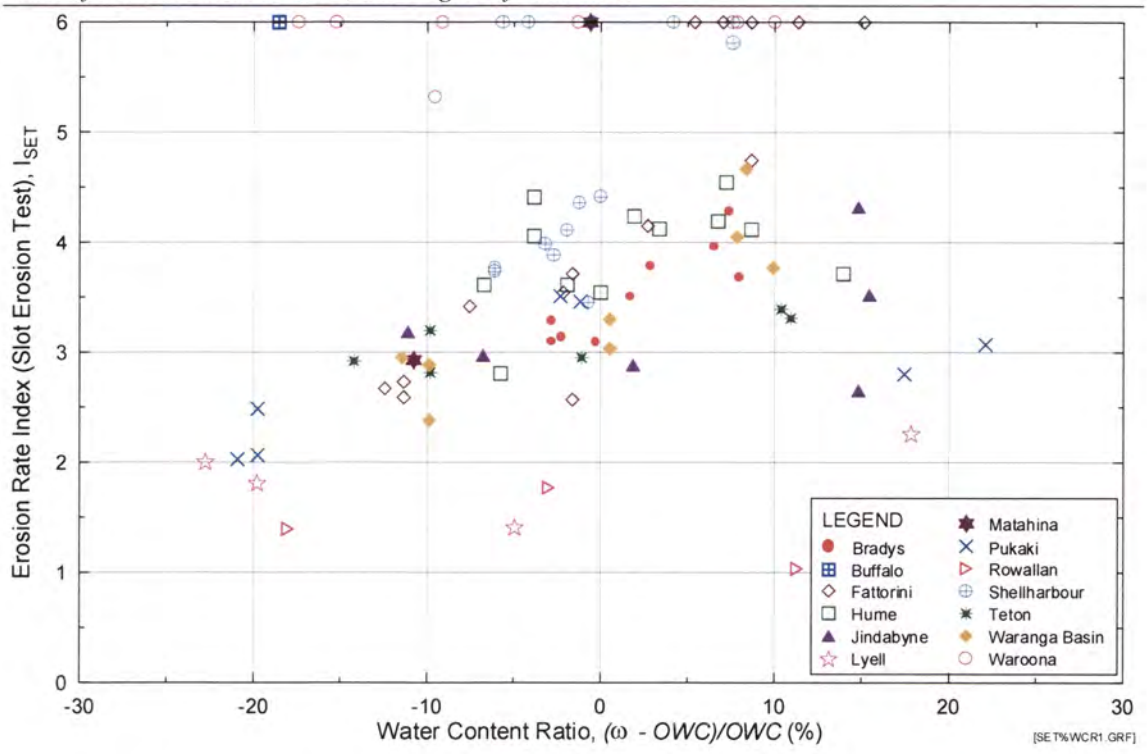

Figure E7a Erosion Rate Index (I_{SET}) from Slot Erosion Test versus Water Content Ratio ($\Delta\omega_r$).

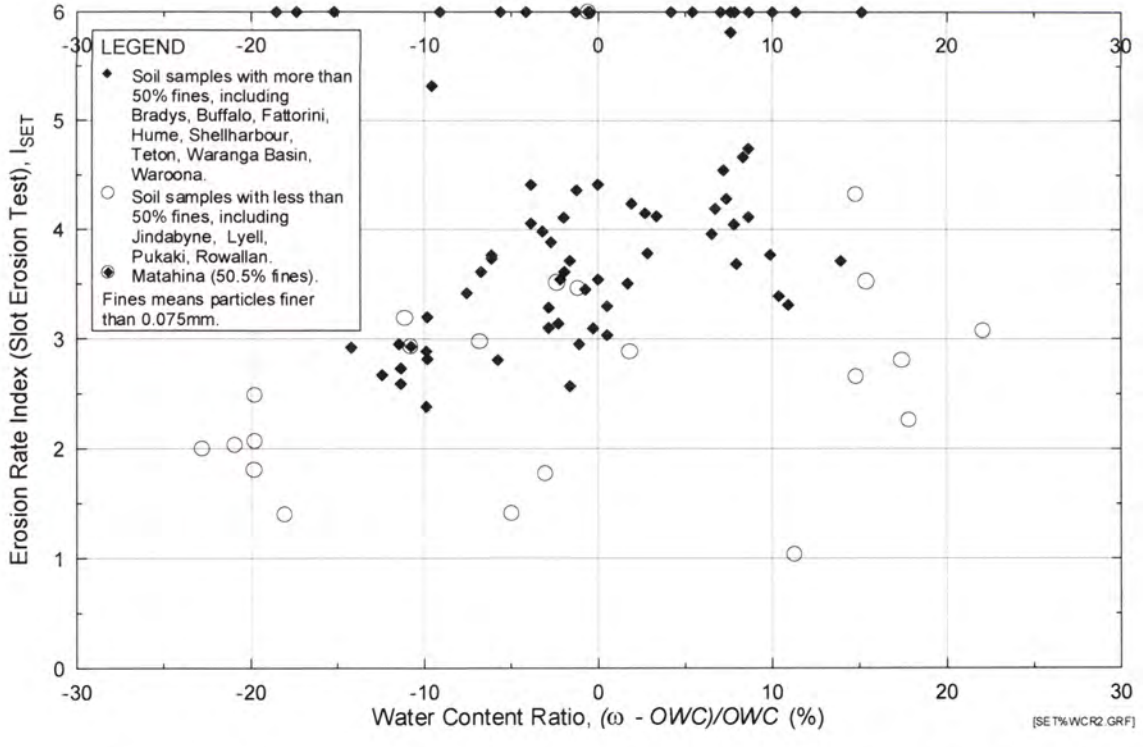

Figure E7b Erosion Rate Index (I_{SET}) from Slot Erosion Test versus Water Content Ratio ($\Delta\omega_r$). Soil samples classified into fine-grained soils and coarse-grained soils.

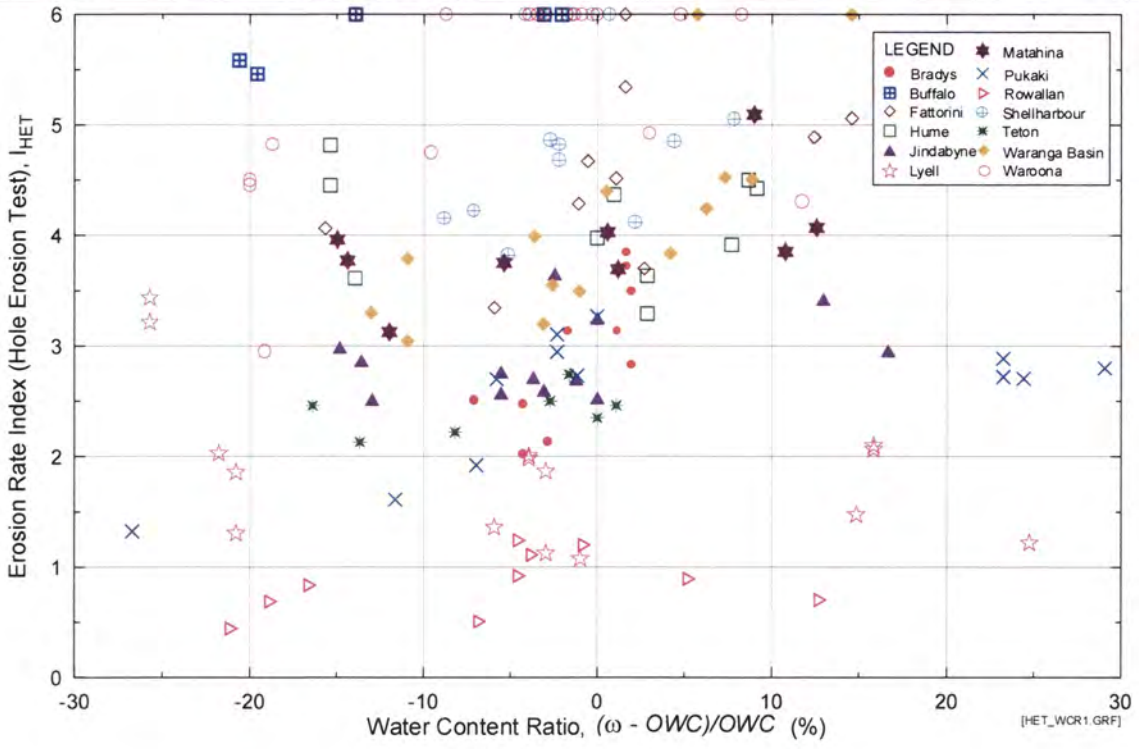

Figure E8a Erosion Rate Index (I_{HET}) from Hole Erosion Test versus Water Content Ratio ($\Delta\omega_r$).

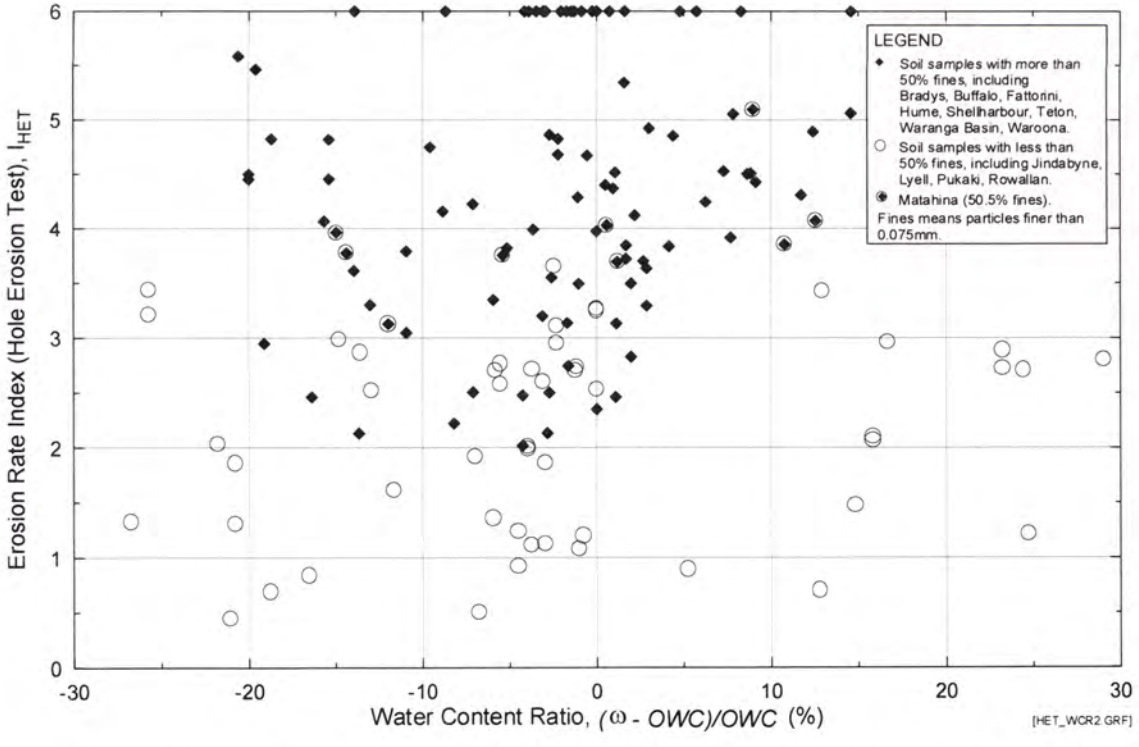

Figure E8b Erosion Rate Index (I_{HET}) from Hole Erosion Test versus Water Content Ratio ($\Delta\omega_r$). Soil samples classified into fine-grained soils and coarse-grained soils.

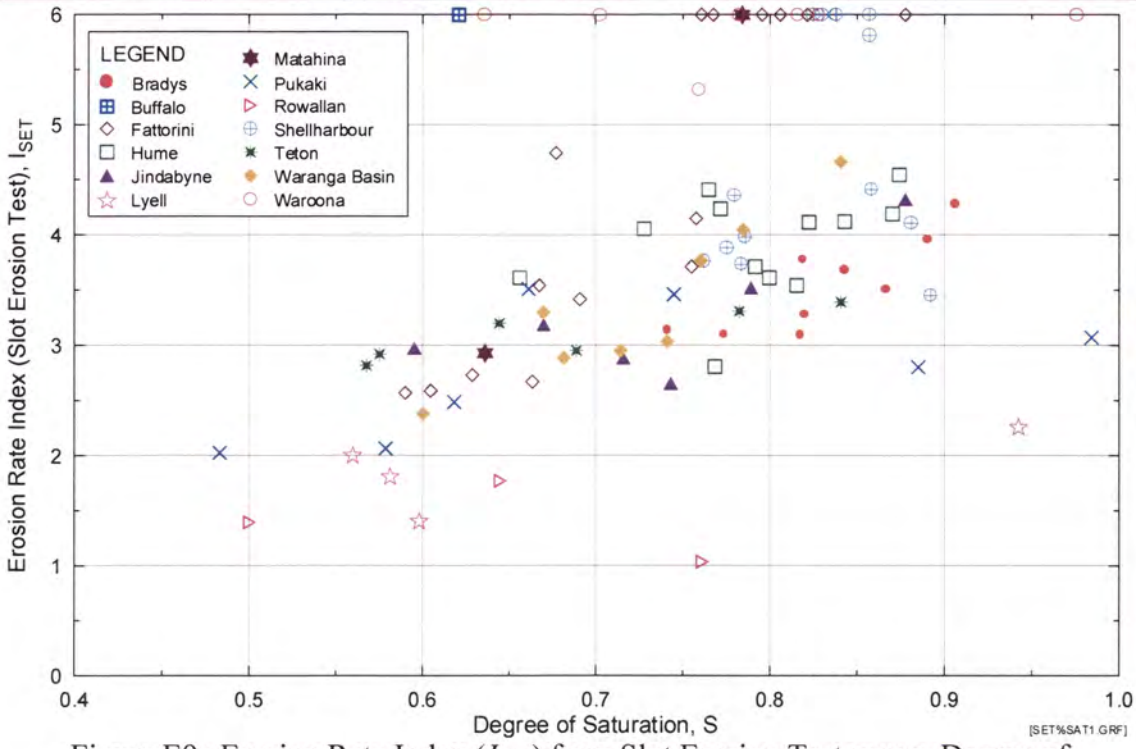

Figure E9a Erosion Rate Index (I_{SET}) from Slot Erosion Test versus Degree of Saturation.

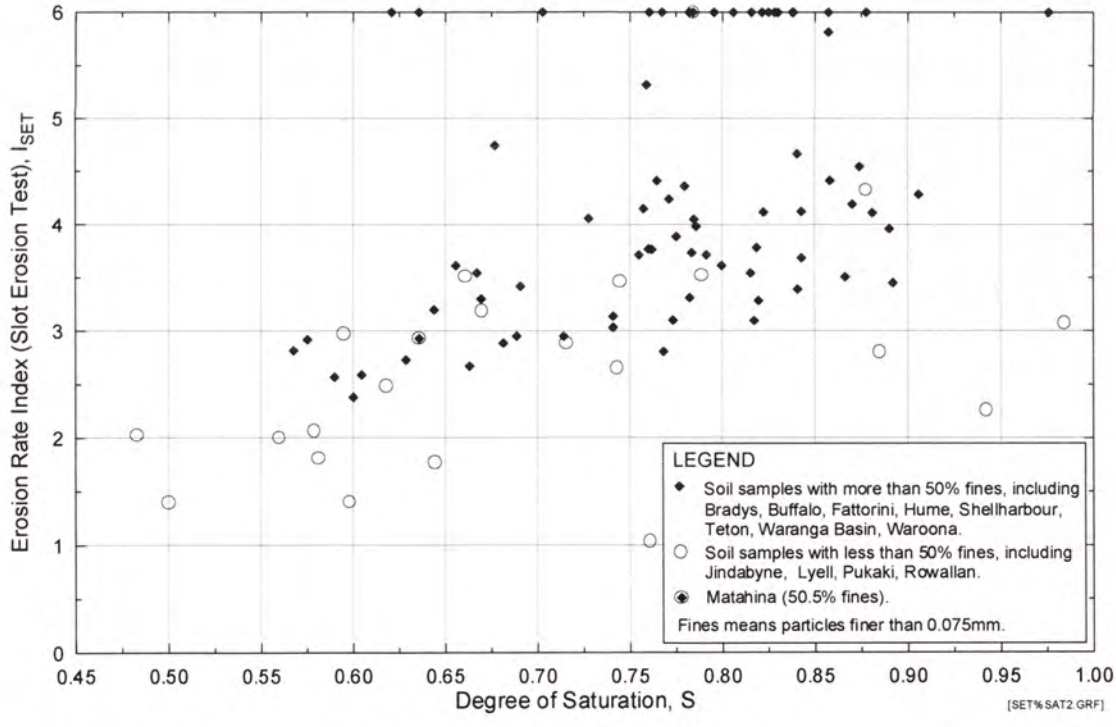

Figure E9b Erosion Rate Index (I_{SET}) from Slot Erosion Test versus Degree of Saturation. Soil samples classified into fine-grained soils and coarse-grained soils.

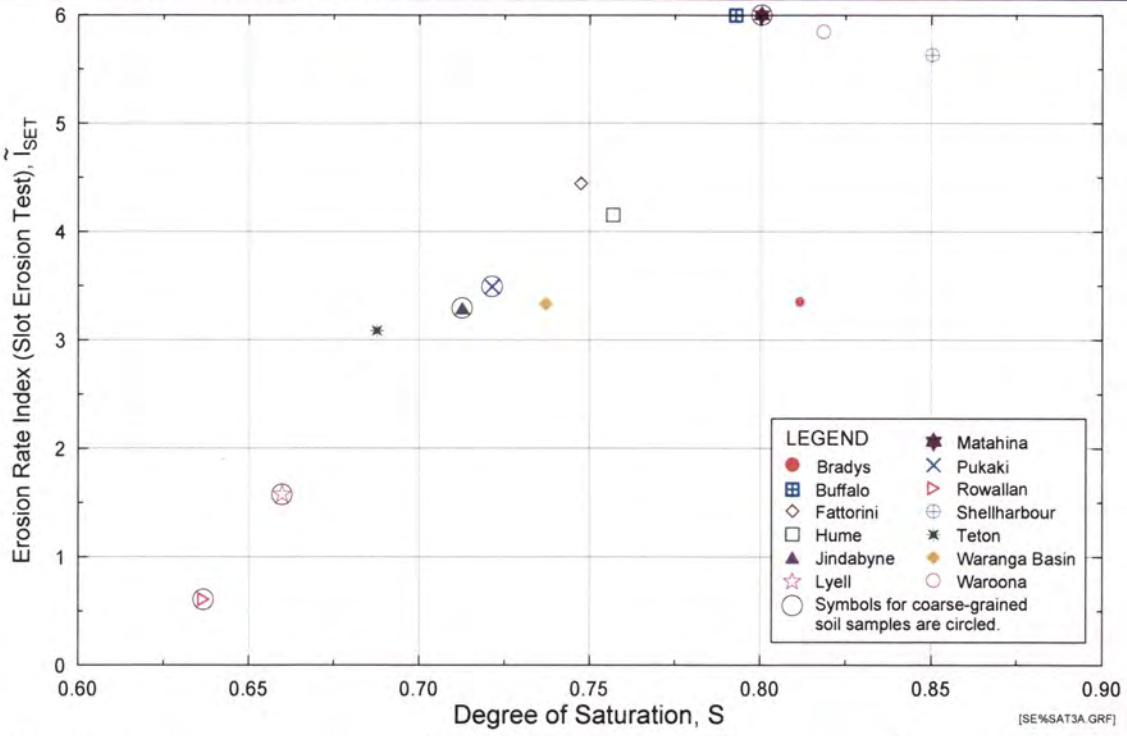

Note : Erosion rate indices presented are predicted indices for specimens at 95% compaction and Optimum Water Content.

Figure E9c Predicted Erosion Rate Index ($\tilde{I}_{SET}$) from Slot Erosion Test versus Degree of Saturation.

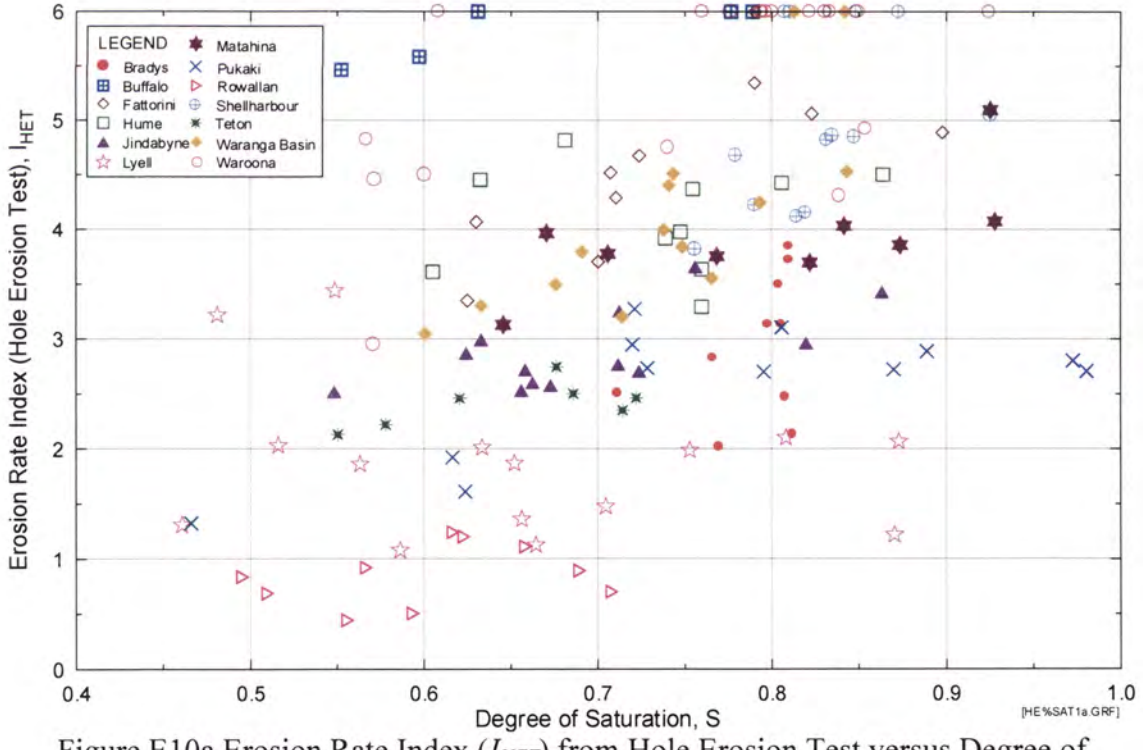

Figure E10a Erosion Rate Index (I_{HET}) from Hole Erosion Test versus Degree of Saturation.

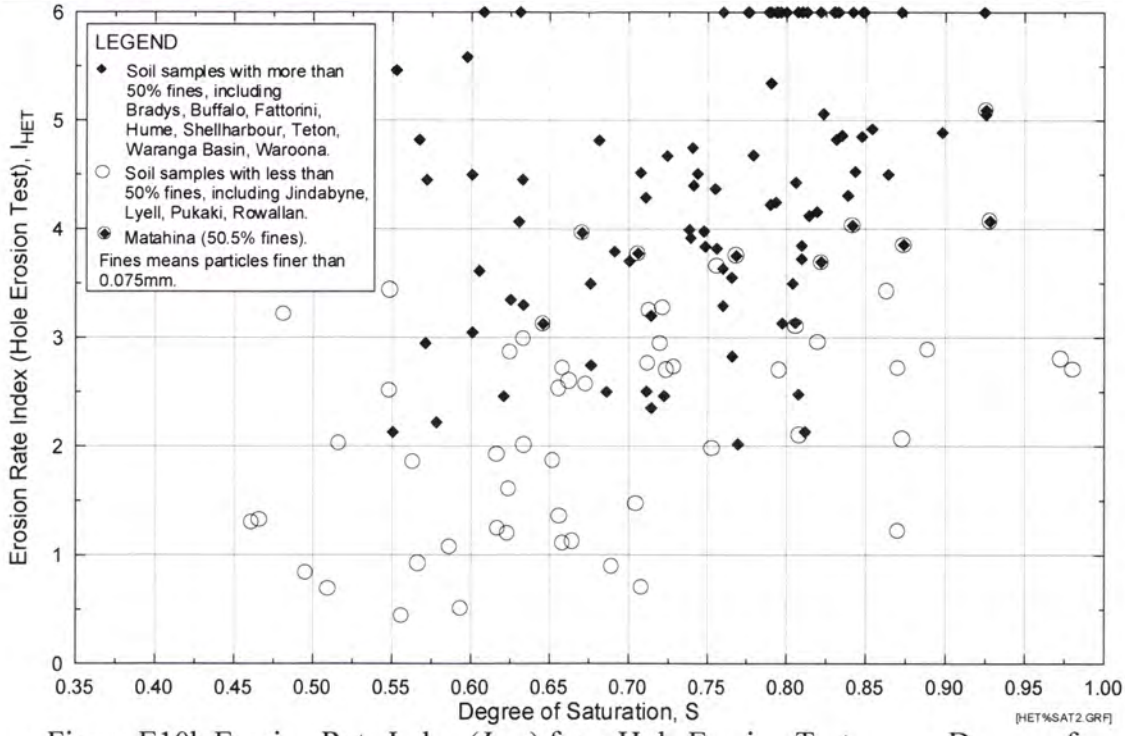

Figure E10b Erosion Rate Index (I_{HET}) from Hole Erosion Test versus Degree of Saturation. Soil samples classified into fine-grained soils and coarse-grained soils.

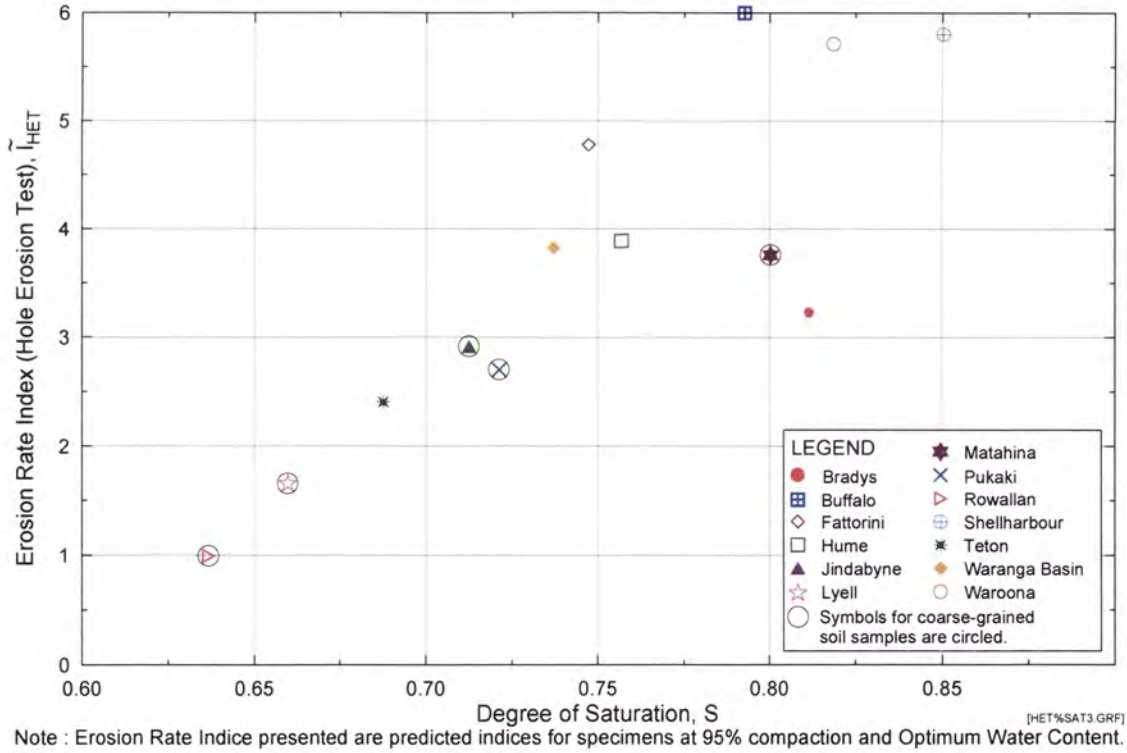

Note : Erosion Rate Indice presented are predicted indices for specimens at 95% compaction and Optimum Water Content.

Figure E10c Predicted Erosion Rate Index ($\tilde{I}_{HET}$) from Hole Erosion Test versus Degree of Saturation.

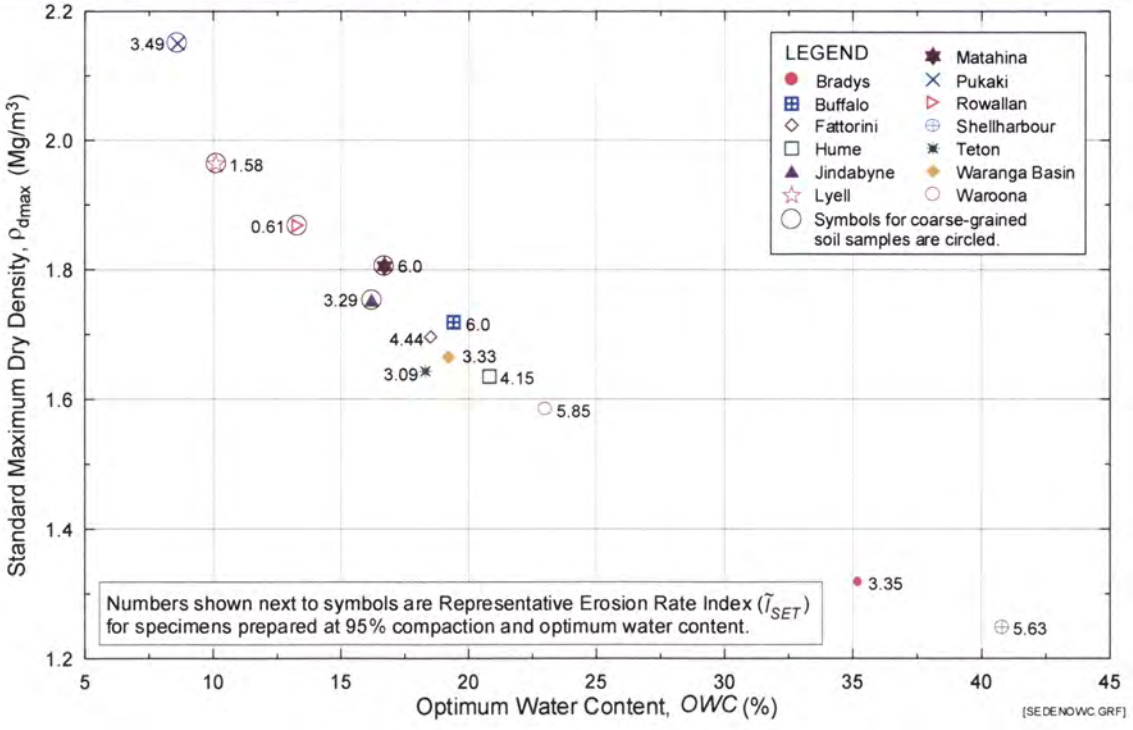

Figure E11a Representative Erosion Rate Index ($\tilde{I}_{SET}$) from Slot Erosion Test versus Standard Maximum Dry Density ($\rho_{d_{max}}$) and Optimum Water Content (*OWC*).

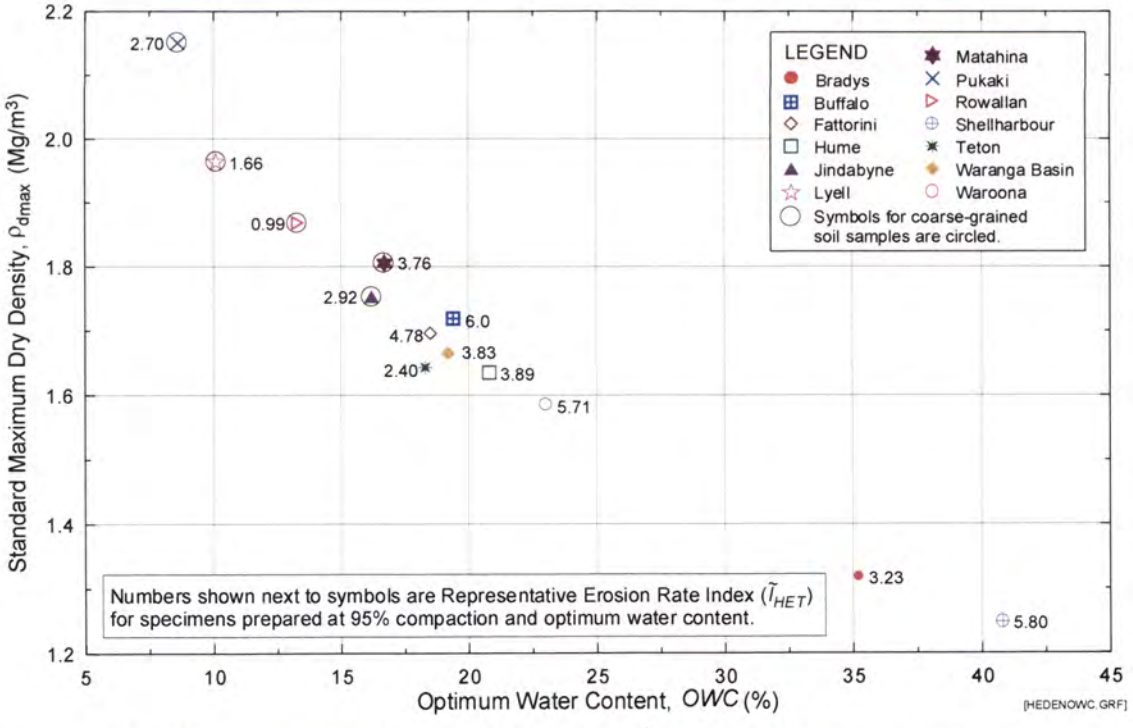

Figure E11b Representative Erosion Rate Index ($\tilde{I}_{HET}$) from Hole Erosion Test versus Standard Maximum Dry Density ($\rho_{d_{max}}$) and Optimum Water Content (*OWC*).

APPENDIX F

Plots of Erosion Rate Index against Sand Content, Fines Content, and Clay Content

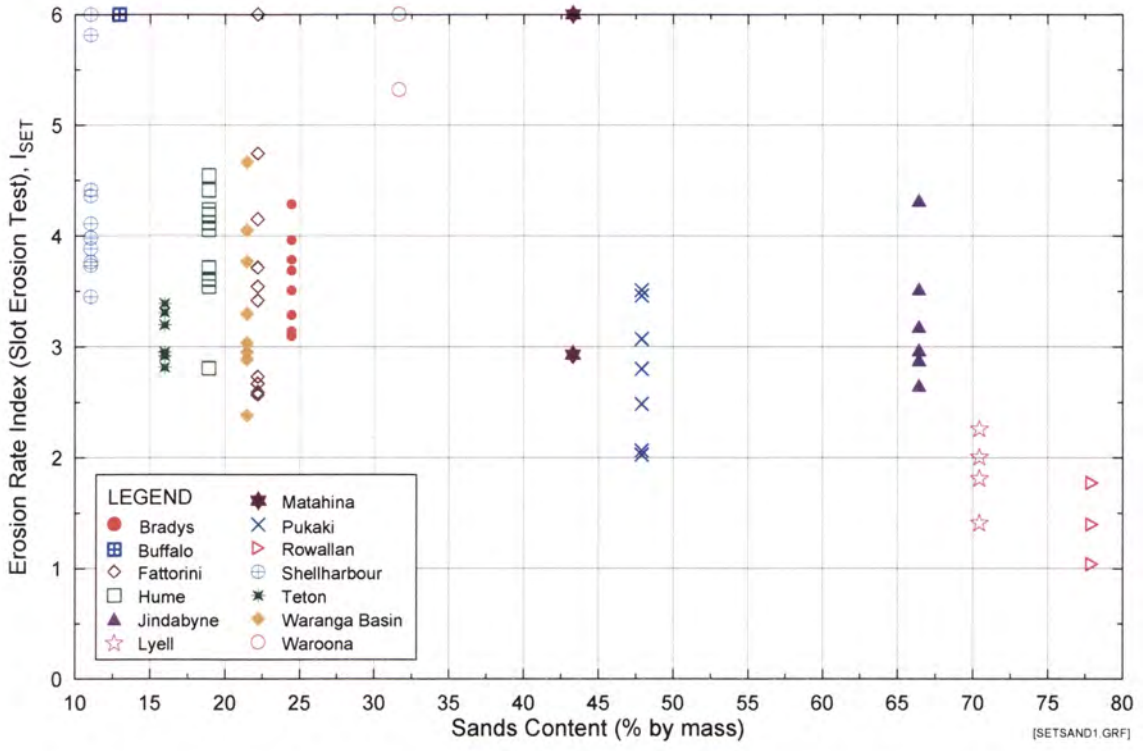

Figure F1a Erosion Rate Index (I_{SET}) from Slot Erosion Test versus Sand Content.

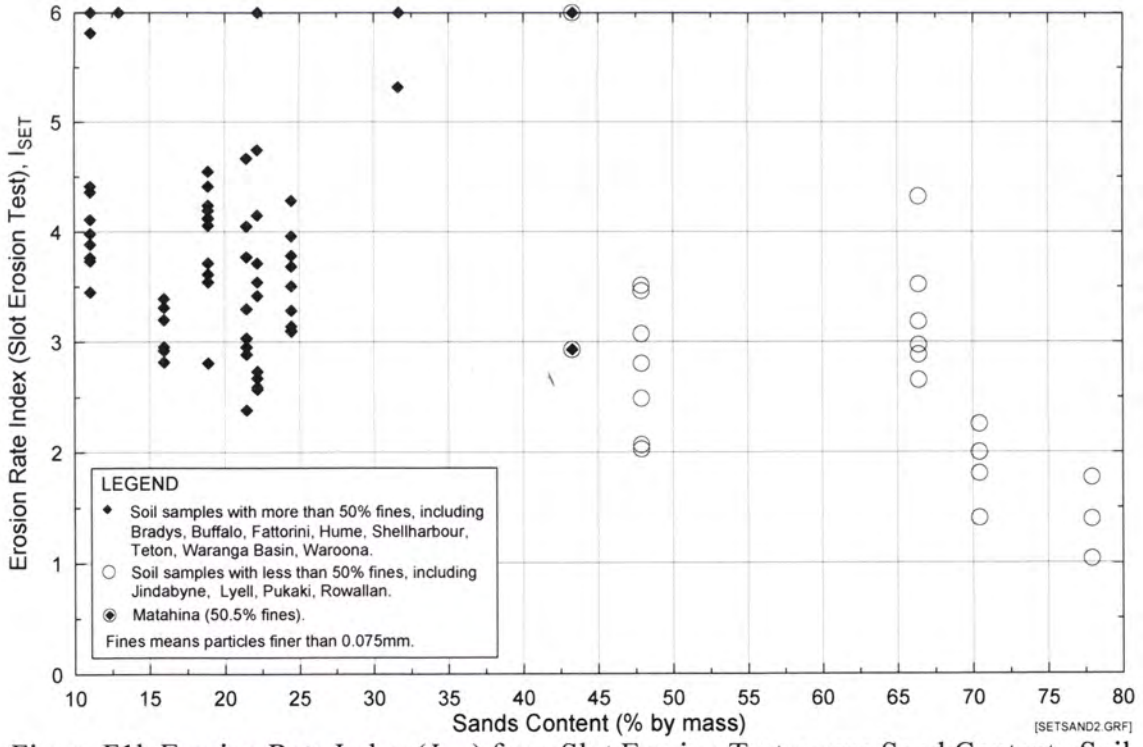

Figure F1b Erosion Rate Index (I_{SET}) from Slot Erosion Test versus Sand Content. Soil samples classified into fine-grained soils and coarse-grained soils.

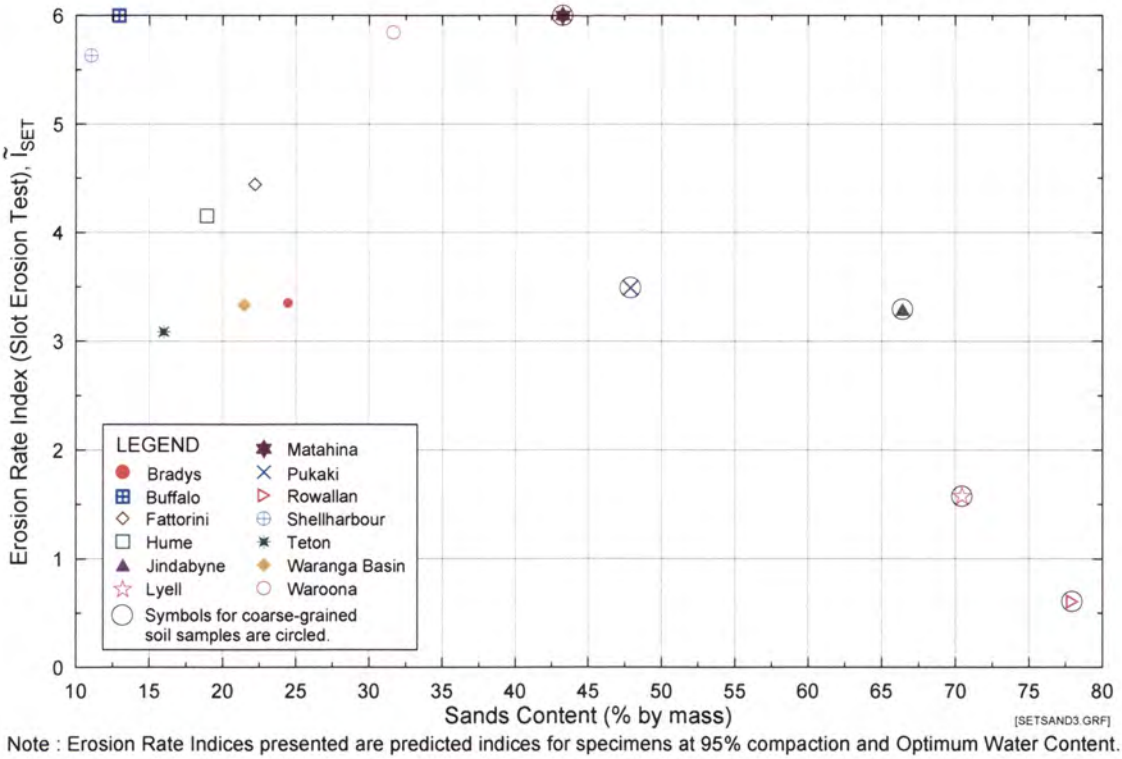

Note : Erosion Rate Indices presented are predicted indices for specimens at 95% compaction and Optimum Water Content.

Figure F1c Predicted Representative Erosion Rate Index ($\tilde{I}_{SET}$) from Slot Erosion Test versus Sand Content.

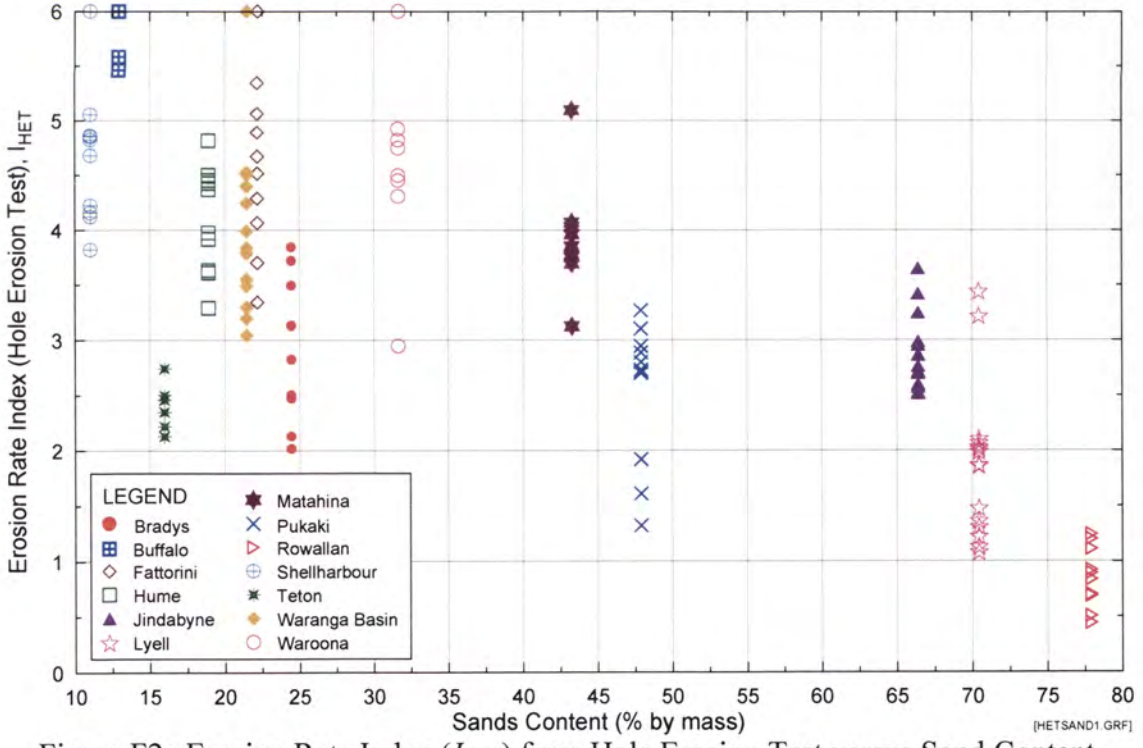

Figure F2a Erosion Rate Index (I_{HET}) from Hole Erosion Test versus Sand Content.

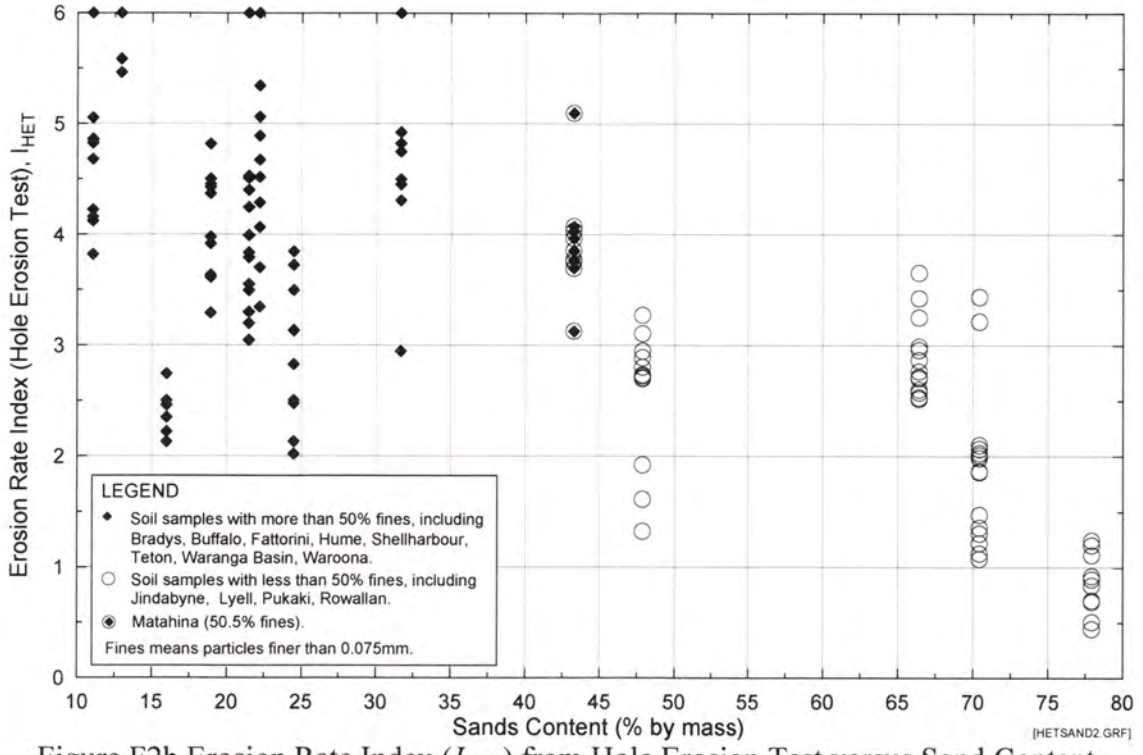

Figure F2b Erosion Rate Index (I_{HET}) from Hole Erosion Test versus Sand Content. Soil samples classified into fine-grained soils and coarse-grained soils.

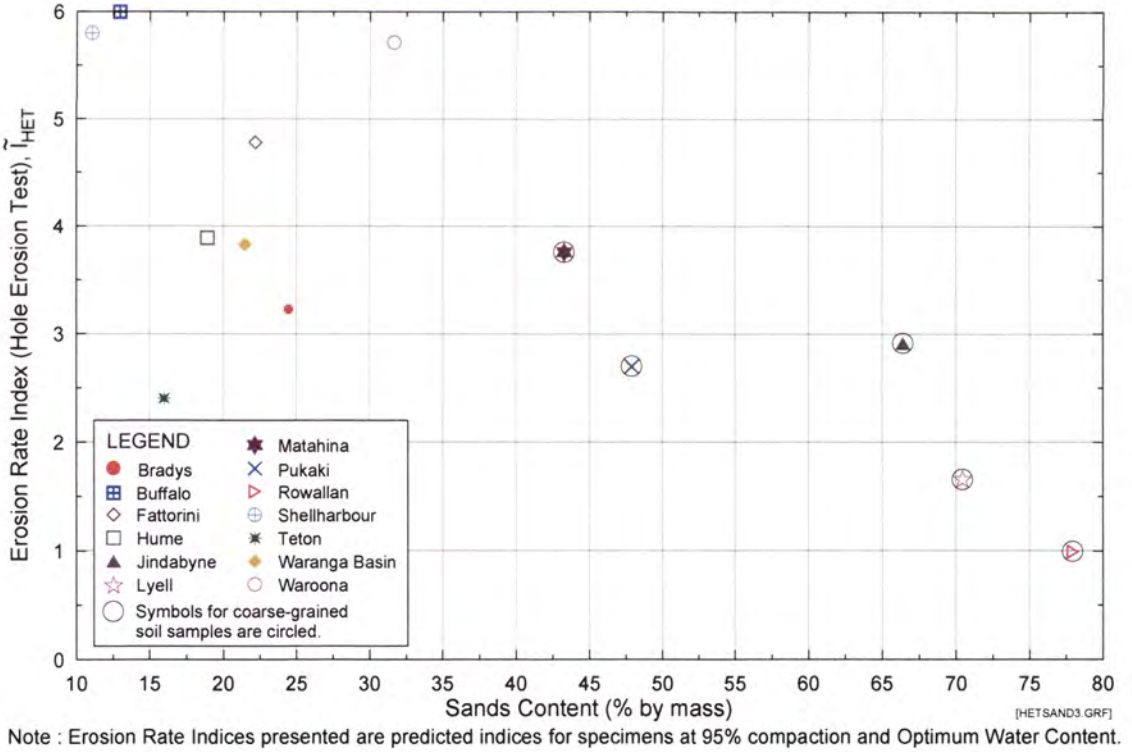

Note : Erosion Rate Indices presented are predicted indices for specimens at 95% compaction and Optimum Water Content.

Figure F2c Predicted Representative Erosion Rate Index ($\tilde{I}_{HET}$) from Hole Erosion Test versus Sand Content.

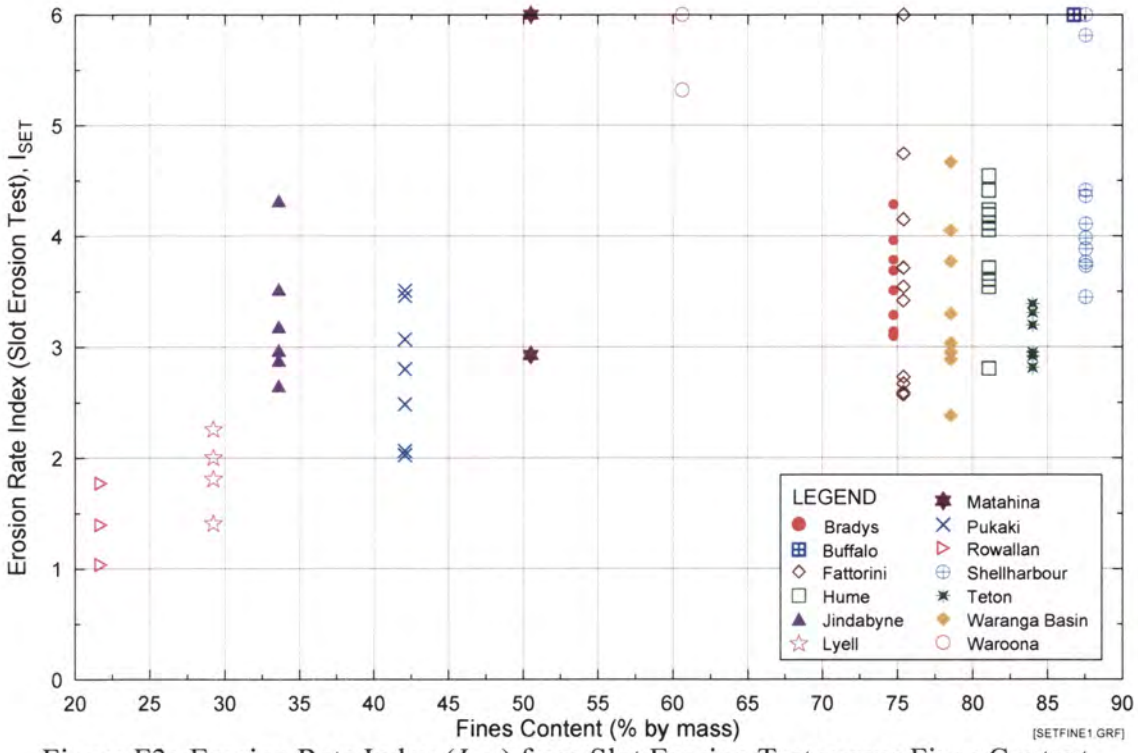

Figure F3a Erosion Rate Index (I_{SET}) from Slot Erosion Test versus Fines Content.

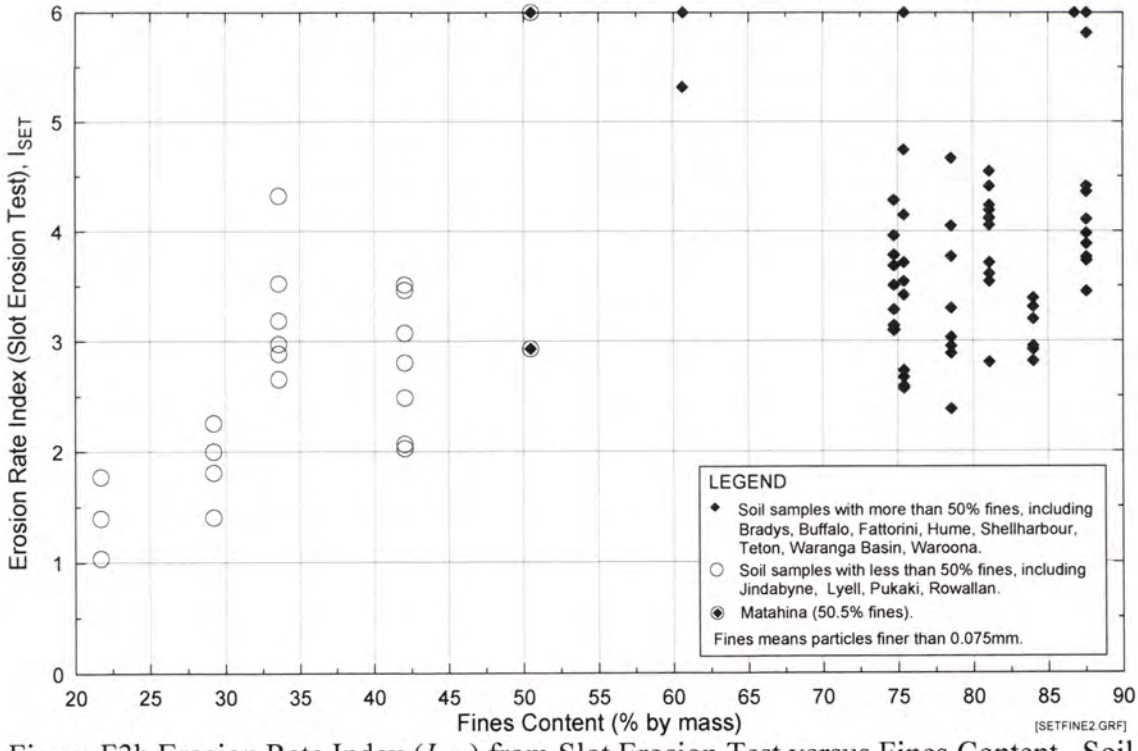

Figure F3b Erosion Rate Index (I_{SET}) from Slot Erosion Test versus Fines Content. Soil samples classified into fine-grained soils and coarse-grained soils.

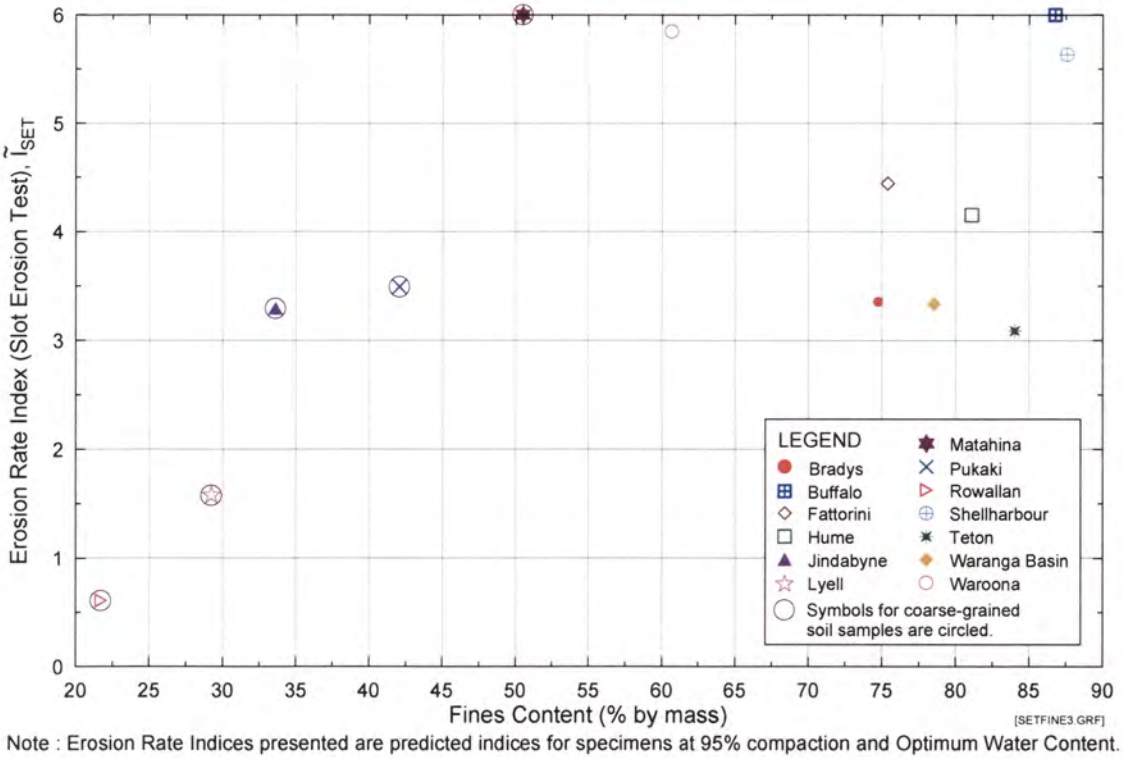

Note : Erosion Rate Indices presented are predicted indices for specimens at 95% compaction and Optimum Water Content.

Figure F3c Predicted Representative Erosion Rate Index ($\tilde{I}_{SET}$) from Slot Erosion Test versus Fines Content.

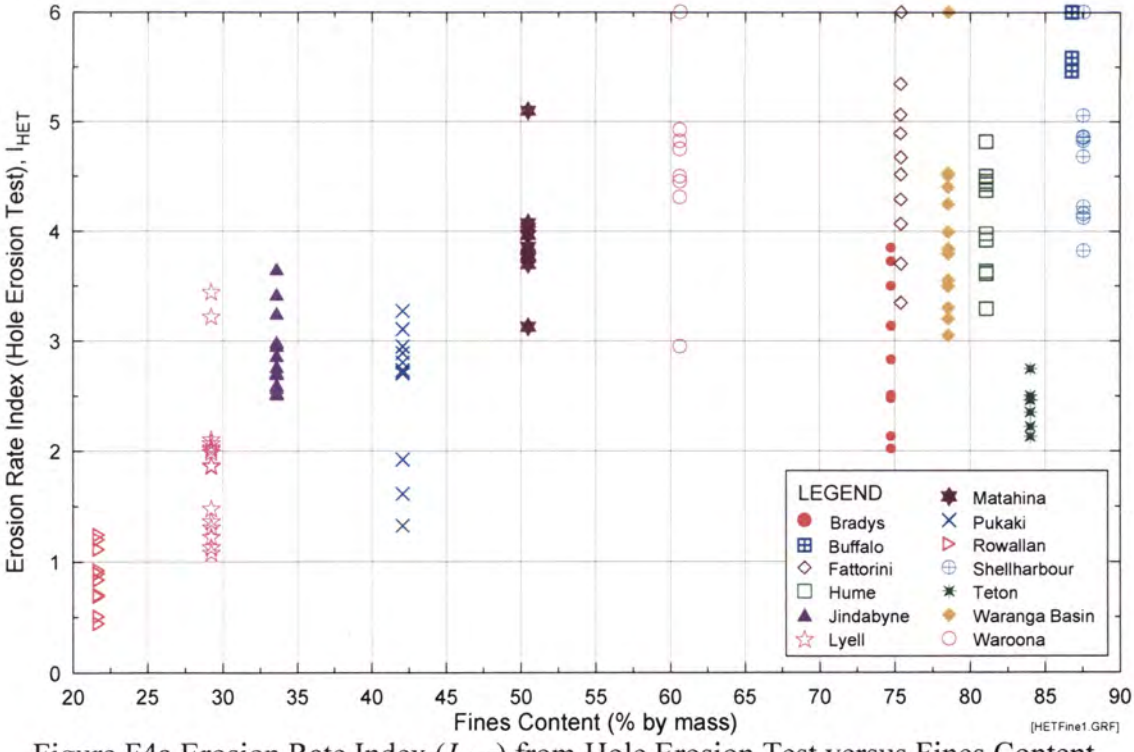

Figure F4a Erosion Rate Index (I_{HET}) from Hole Erosion Test versus Fines Content.

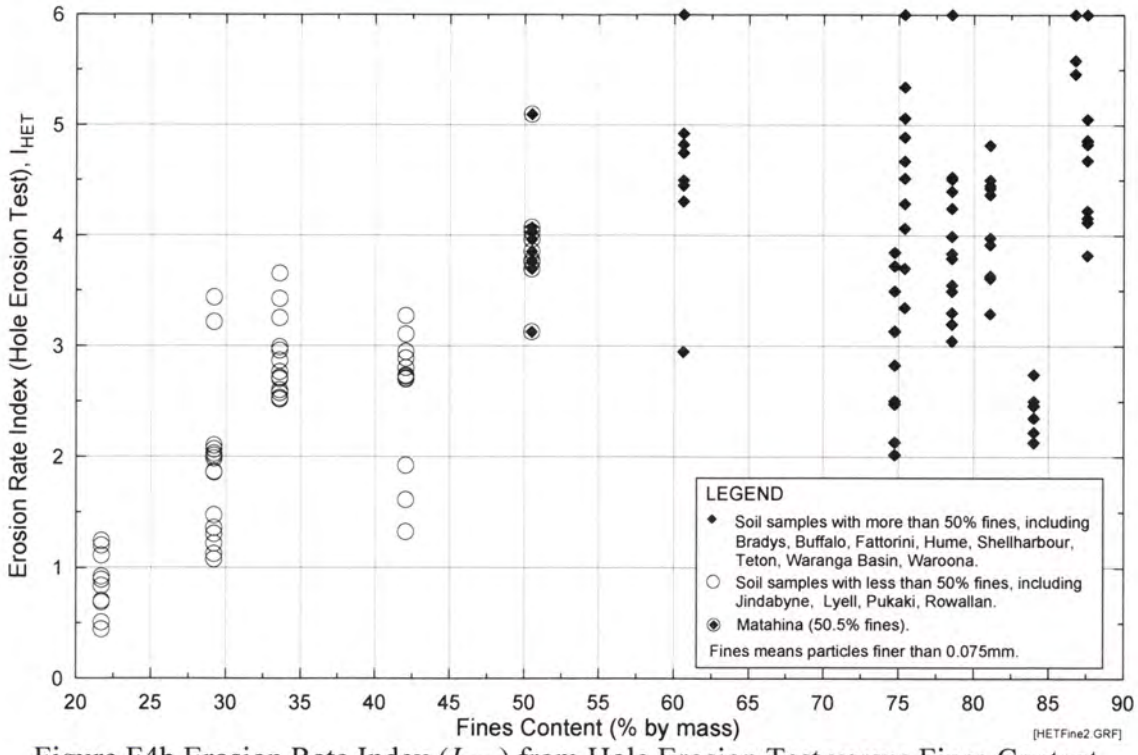

Figure F4b Erosion Rate Index (I_{HET}) from Hole Erosion Test versus Fines Content. Soil samples classified into fine-grained soils and coarse-grained soils.

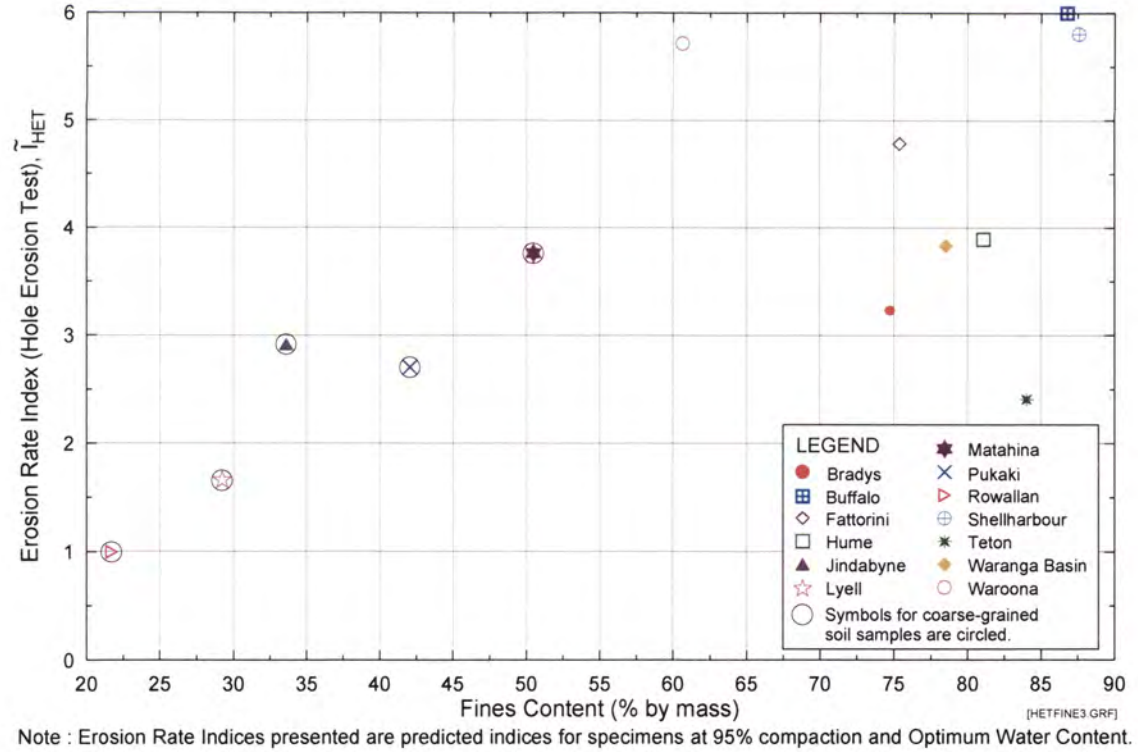

Note : Erosion Rate Indices presented are predicted indices for specimens at 95% compaction and Optimum Water Content.

Figure F4c Predicted Representative Erosion Rate Index ($\tilde{I}_{HET}$) from Hole Erosion Test versus Fines Content.

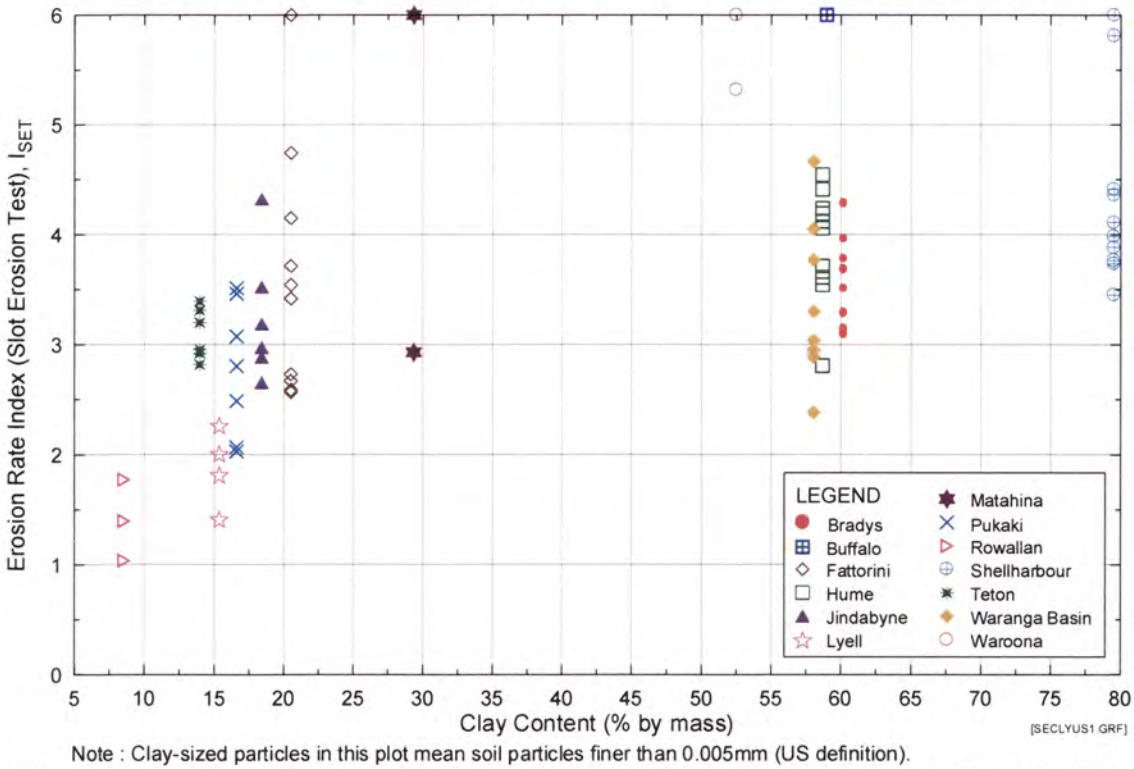

Note : Clay-sized particles in this plot mean soil particles finer than 0.005mm (US definition).

Figure F5a Erosion Rate Index (I_{SET}) from Slot Erosion Test versus Clay Content (US definition).

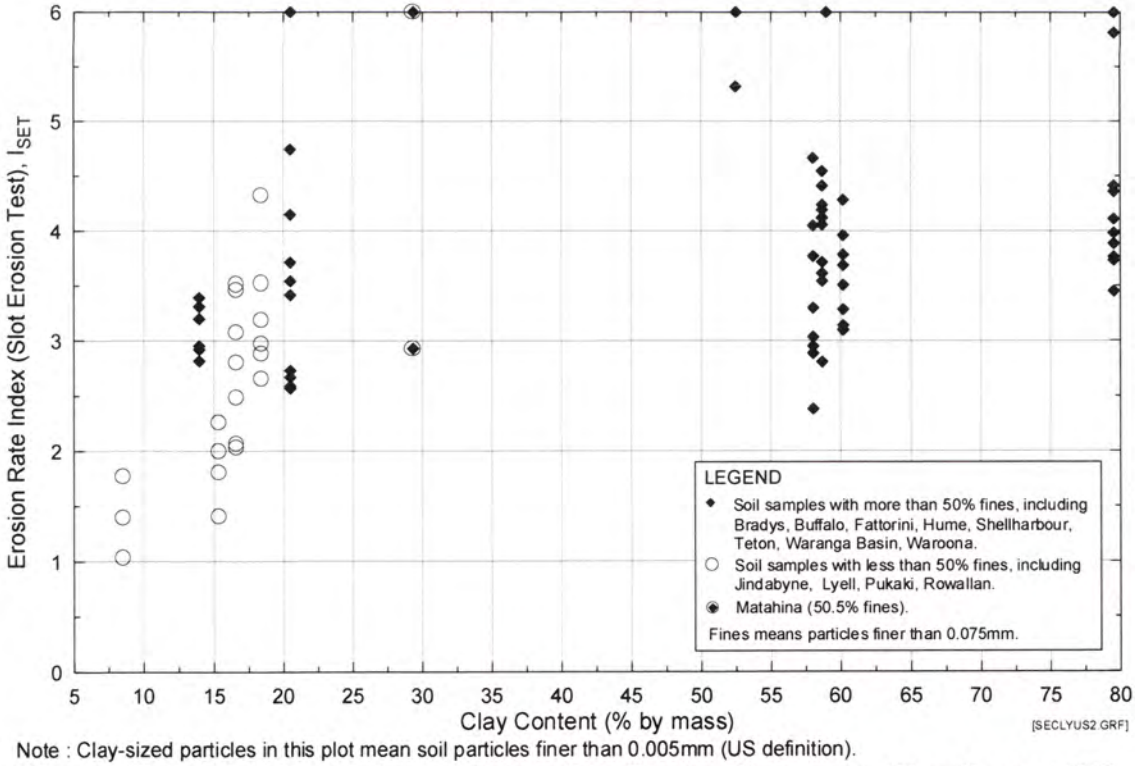

Note : Clay-sized particles in this plot mean soil particles finer than 0.005mm (US definition).

Figure F5b Erosion Rate Index (I_{SET}) from Slot Erosion Test versus Clay Content (US definition). Soil samples classified into fine-grained and coarse-grained soils.

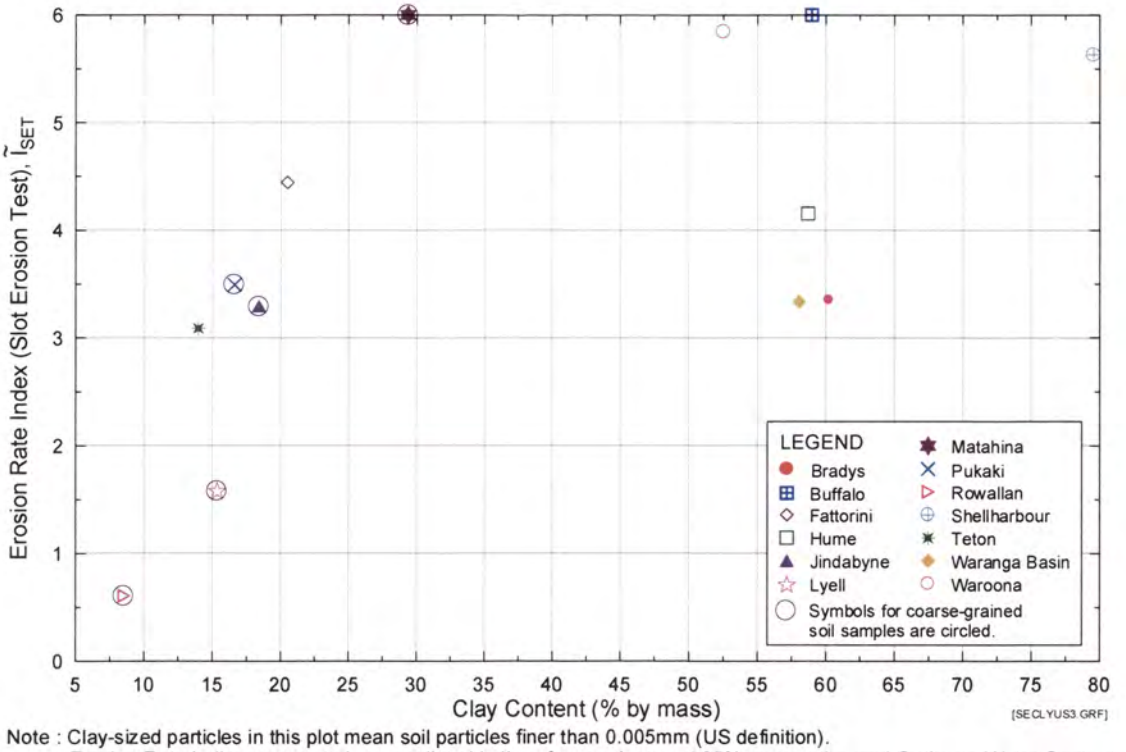

Note : Clay-sized particles in this plot mean soil particles finer than 0.005mm (US definition).
Erosion Rate Indices presented are predicted indices for specimens at 95% compaction and Optimum Water Content.

Figure F5c Predicted Representative Erosion Rate Index ($\tilde{I}_{SET}$) from Slot Erosion Test versus Clay Content (US definition).

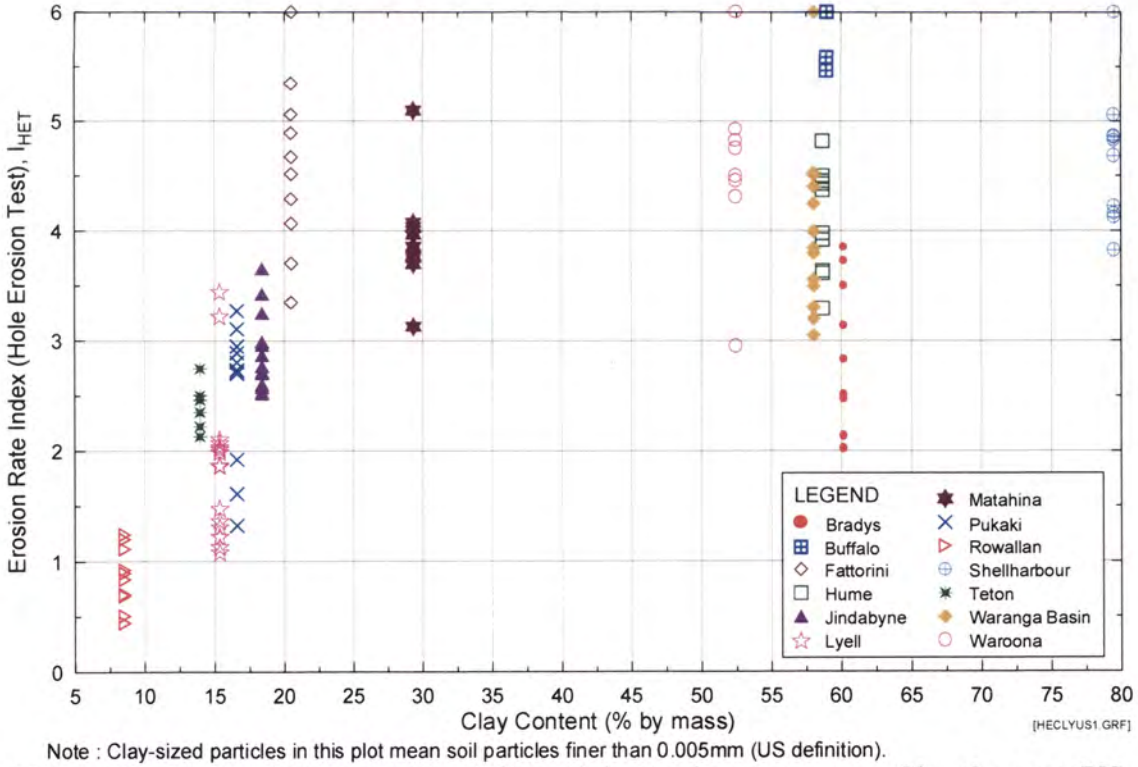

Note : Clay-sized particles in this plot mean soil particles finer than 0.005mm (US definition).

Figure F6a Erosion Rate Index (I_{HET}) from Hole Erosion Test versus Clay Content (US definition).

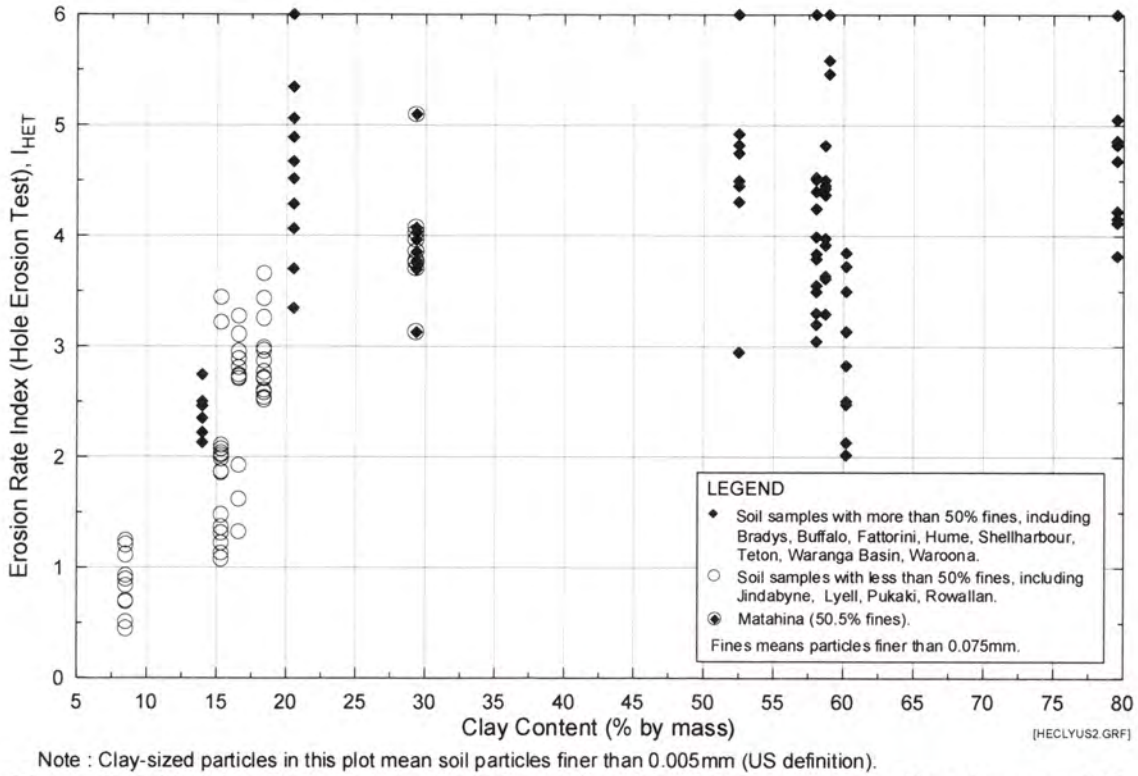

Note : Clay-sized particles in this plot mean soil particles finer than 0.005mm (US definition).

Figure F6b Erosion Rate Index (I_{HET}) from Hole Erosion Test versus Clay Content (US definition). Soil samples classified into fine-grained and coarse-grained soils.

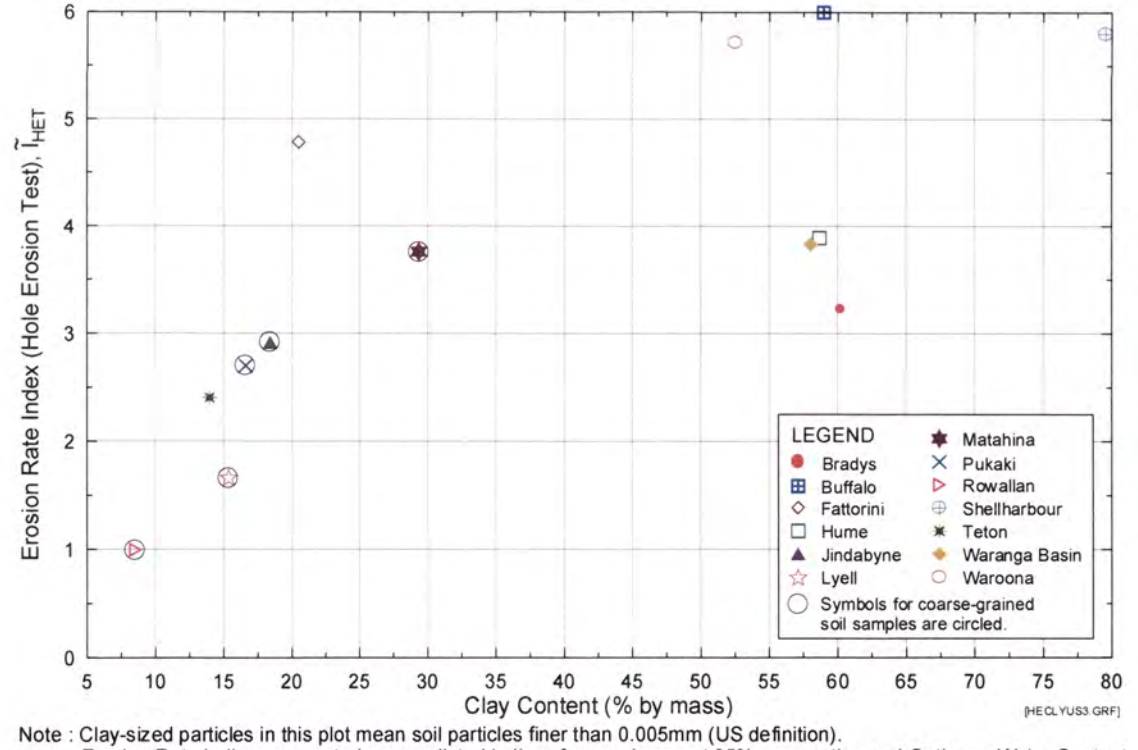

Note : Clay-sized particles in this plot mean soil particles finer than 0.005mm (US definition).
Erosion Rate Indices presented are predicted indices for specimens at 95% compaction and Optimum Water Content.

Figure F6c Predicted Representative Erosion Rate Index ($\tilde{I}_{HET}$) from Hole Erosion Test versus Clay Content (US definition).

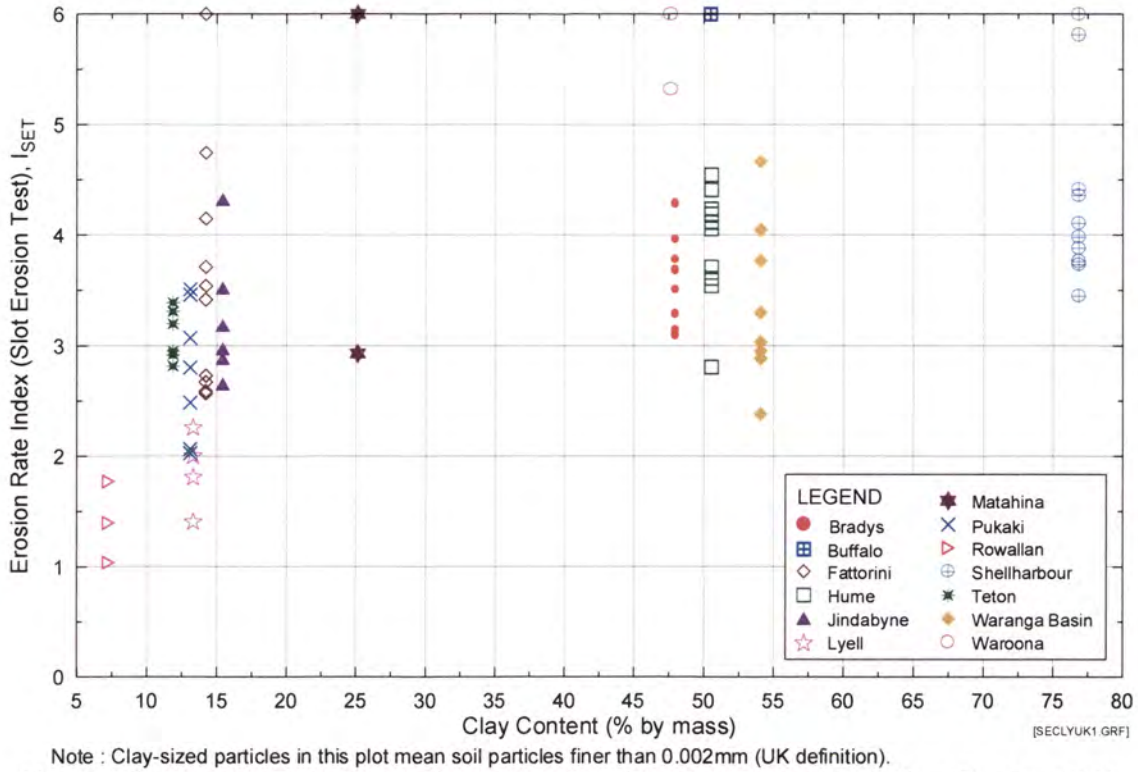

Note : Clay-sized particles in this plot mean soil particles finer than 0.002mm (UK definition).

Figure F7a Erosion Rate Index (I_{SET}) from Slot Erosion Test versus Clay Content (UK definition).

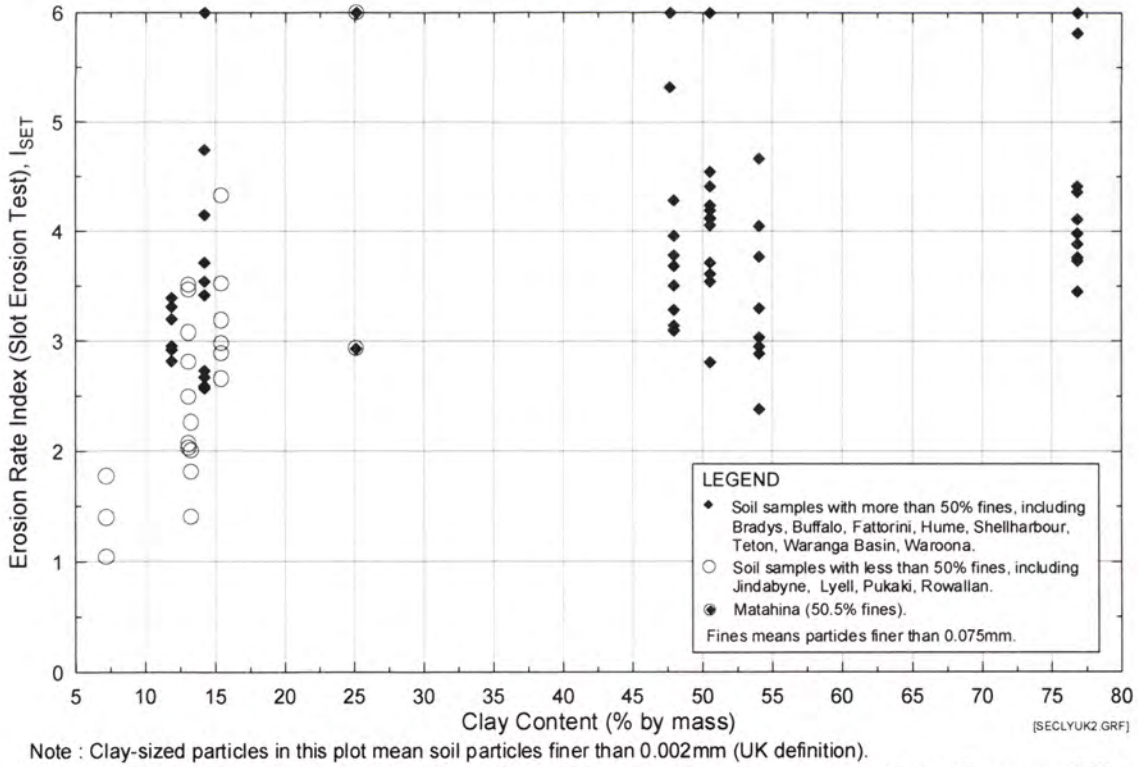

Note : Clay-sized particles in this plot mean soil particles finer than 0.002mm (UK definition).

Figure F7b Erosion Rate Index (I_{SET}) from Slot Erosion Test versus Clay Content (UK definition). Soil samples classified into fine-grained and coarse-grained soils.

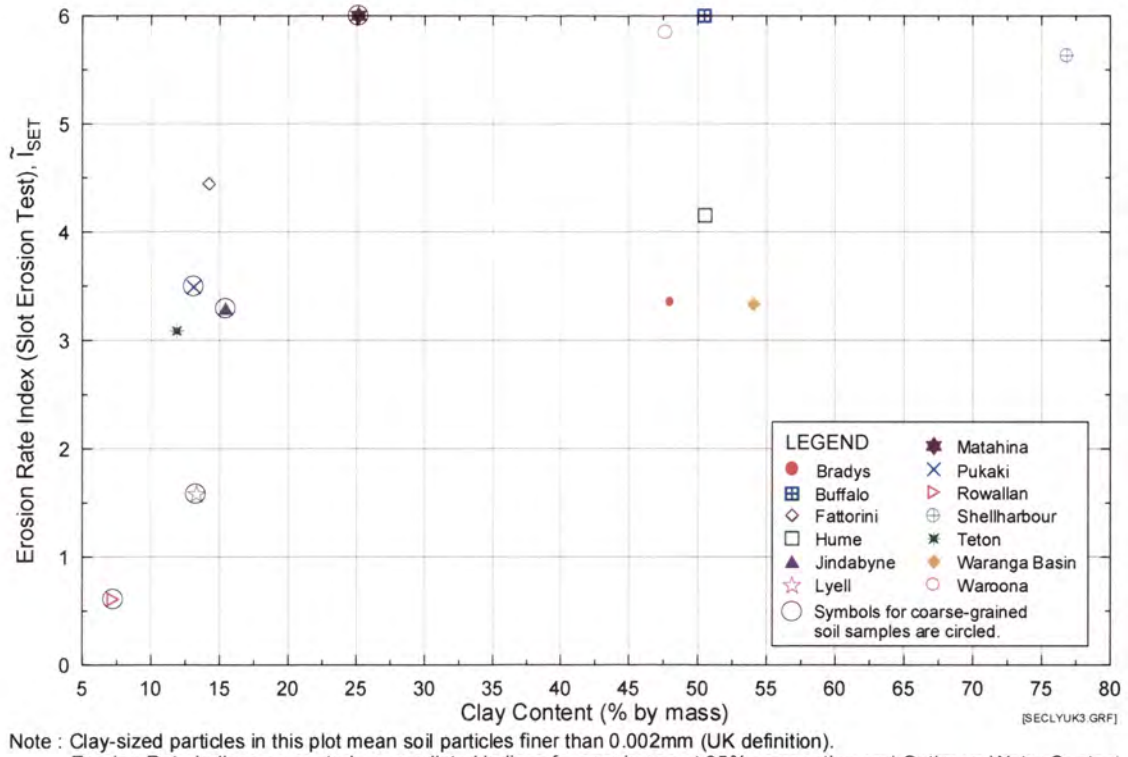

Note : Clay-sized particles in this plot mean soil particles finer than 0.002mm (UK definition).
Erosion Rate Indices presented are predicted indices for specimens at 95% compaction and Optimum Water Content.

Figure F7c Predicted Representative Erosion Rate Index ($\tilde{I}_{SET}$) from Slot Erosion Test versus Clay Content (UK definition).

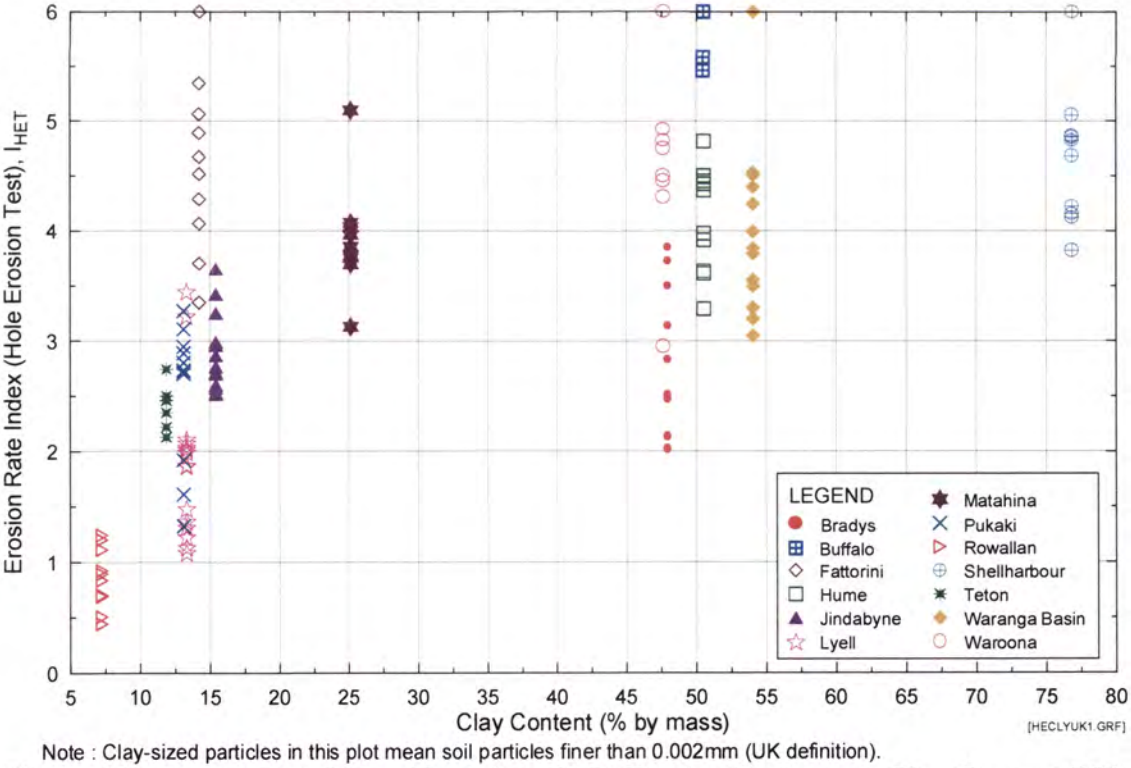

Note : Clay-sized particles in this plot mean soil particles finer than 0.002mm (UK definition).

Figure F8a Erosion Rate Index (I_{HET}) from Hole Erosion Test versus Clay Content (UK definition).

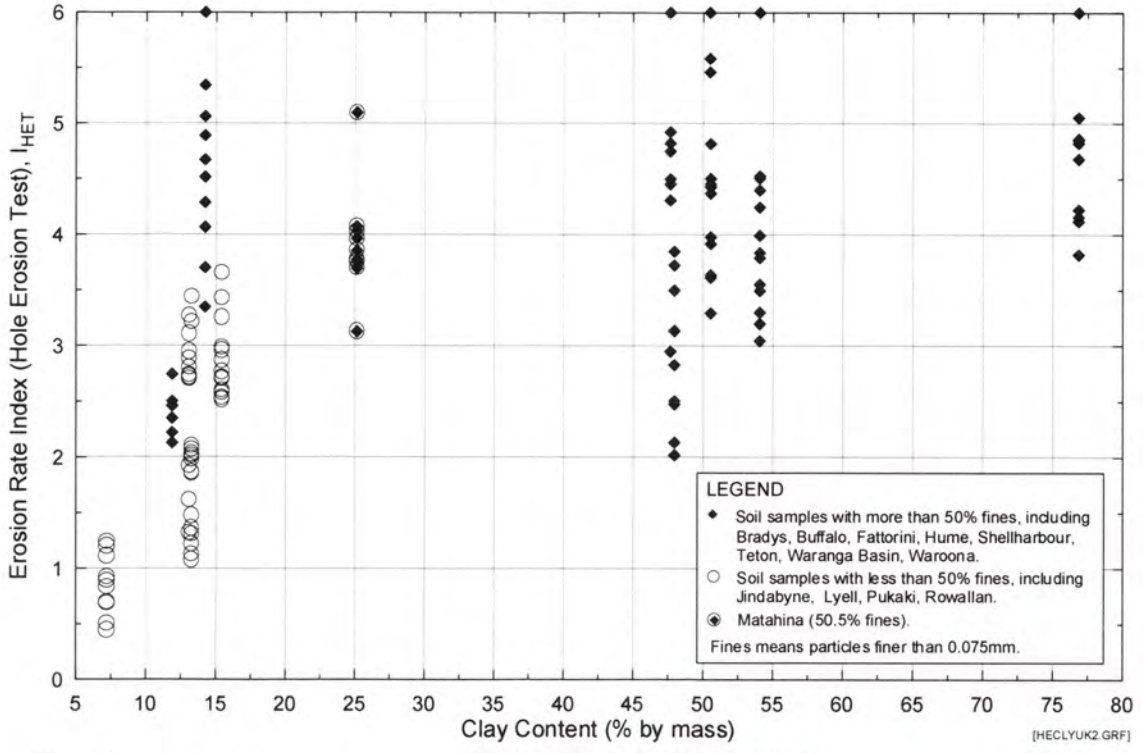

Note : Clay-sized particles in this plot mean soil particles finer than 0.002mm (UK definition).

Figure F8b Erosion Rate Index (I_{HET}) from Hole Erosion Test versus Clay Content (UK definition). Soil samples classified into fine-grained and coarse-grained soils.

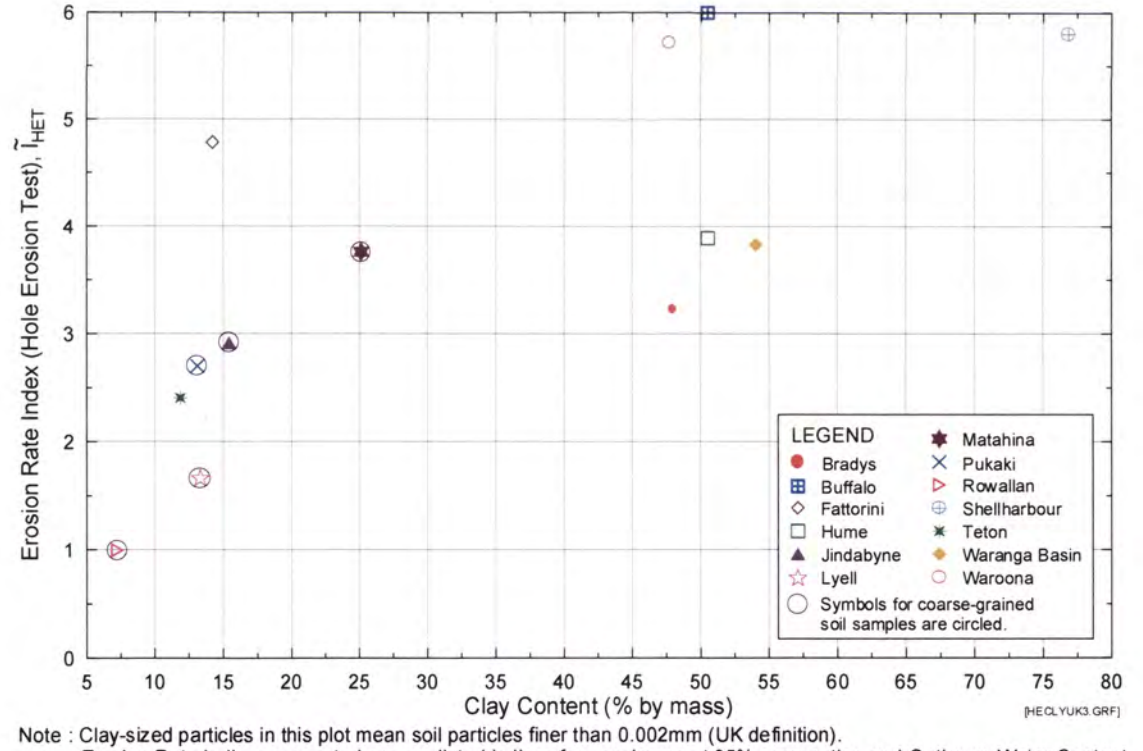

Note : Clay-sized particles in this plot mean soil particles finer than 0.002mm (UK definition).
Erosion Rate Indices presented are predicted indices for specimens at 95% compaction and Optimum Water Content.

Figure F8c Predicted Representative Erosion Rate Index ($\tilde{I}_{HET}$) from Hole Erosion Test versus Clay Content (UK definition).

APPENDIX G

Plots of Erosion Rate Index against Liquid Limit, Plasticity Index, and Activity

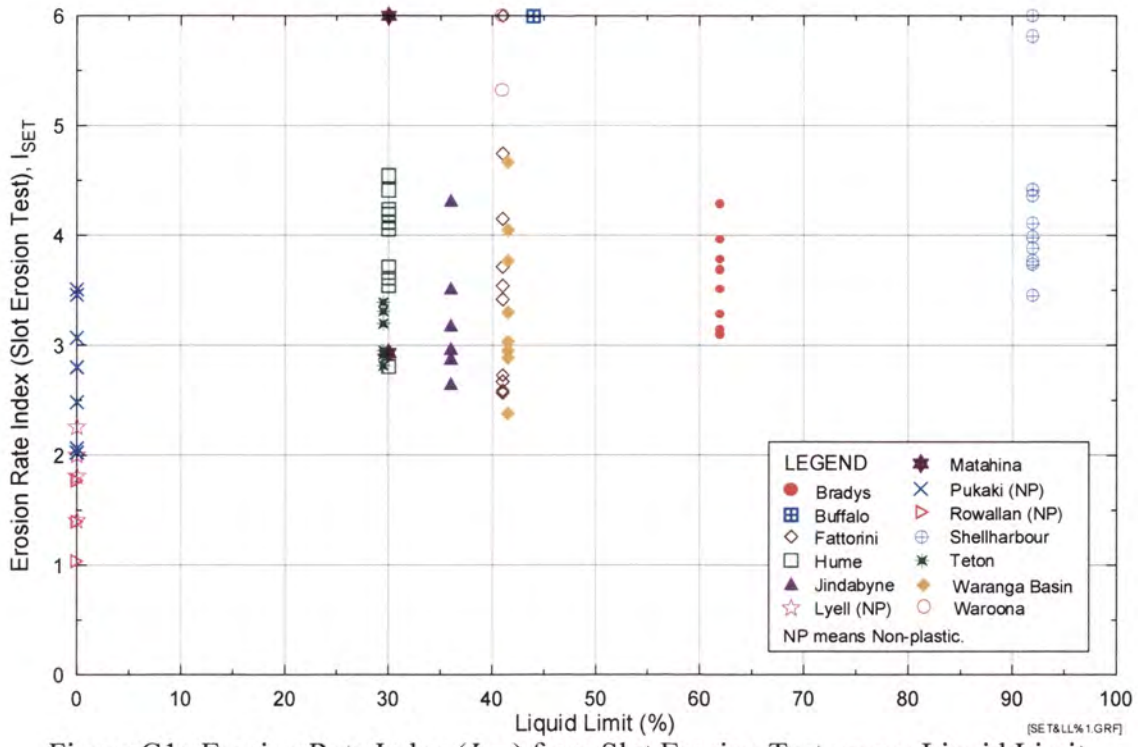

Figure G1a Erosion Rate Index (I_{SET}) from Slot Erosion Test versus Liquid Limit.

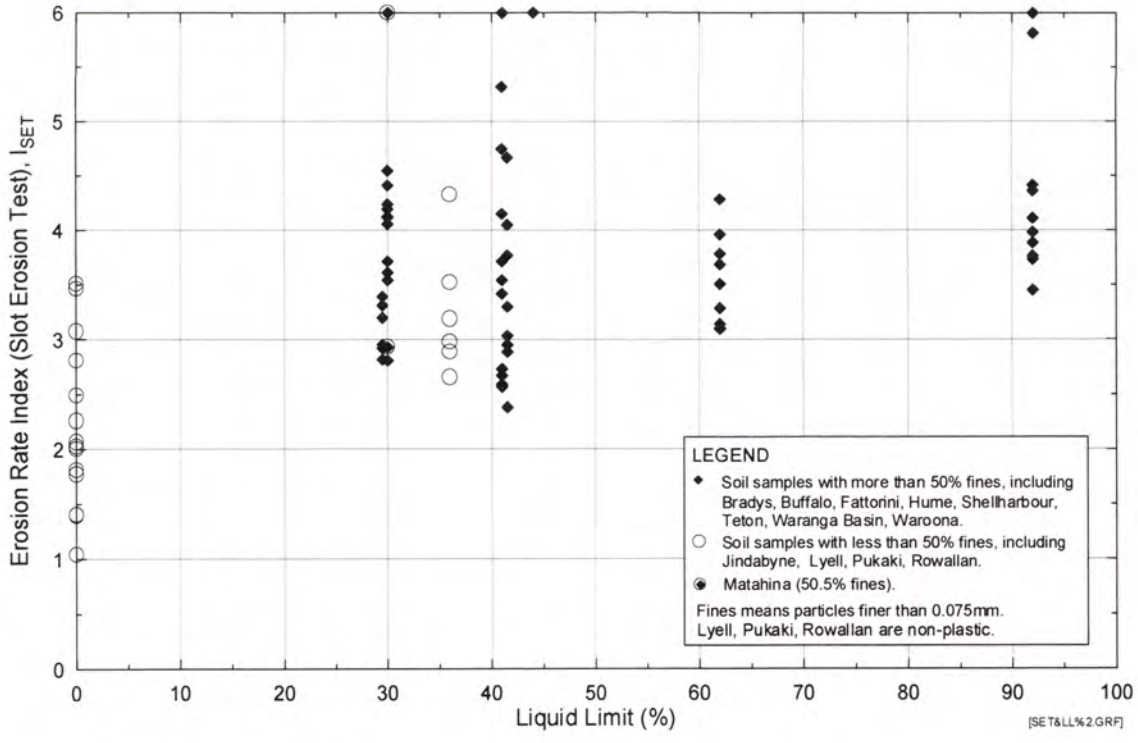

Figure G1b Erosion Rate Index (I_{SET}) from Slot Erosion Test versus Liquid Limit. Soil samples classified into fine-grained and coarse-grained soils.

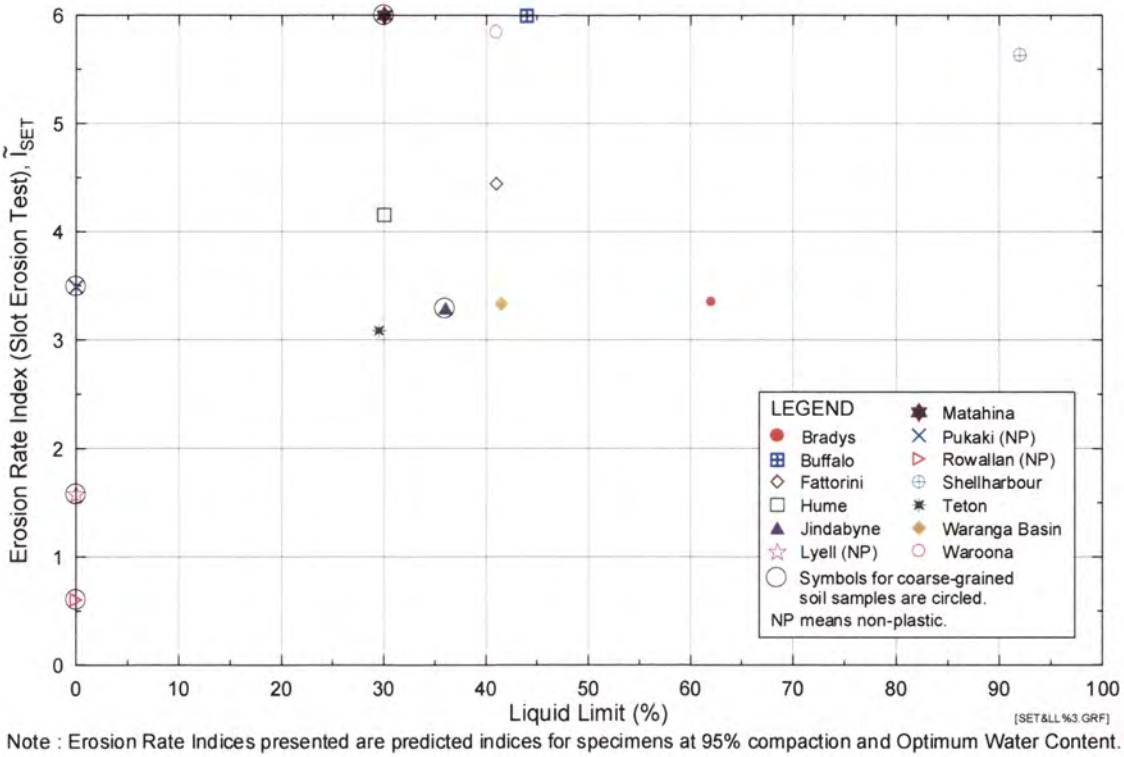

Note : Erosion Rate Indices presented are predicted indices for specimens at 95% compaction and Optimum Water Content.

Figure G1c Predicted Erosion Rate Index ($\tilde{I}_{SET}$) from Slot Erosion Test versus Liquid Limit.

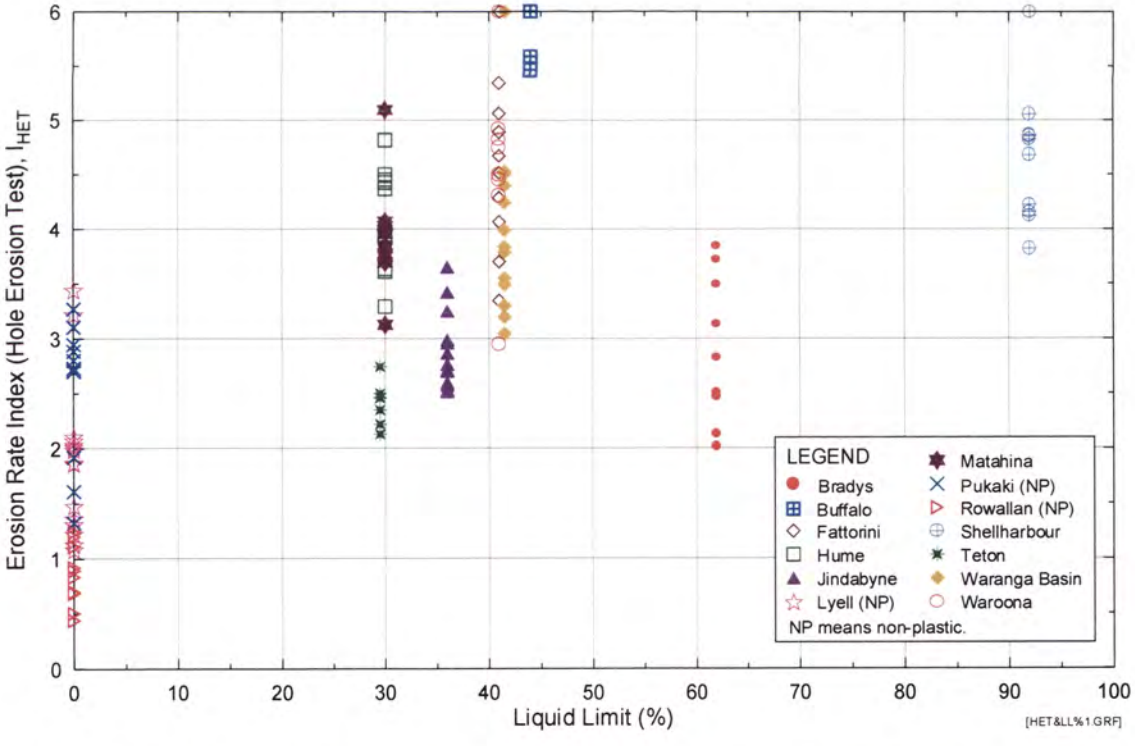

Figure G2a Erosion Rate Index (I_{HET}) from Hole Erosion Test versus Liquid Limit.

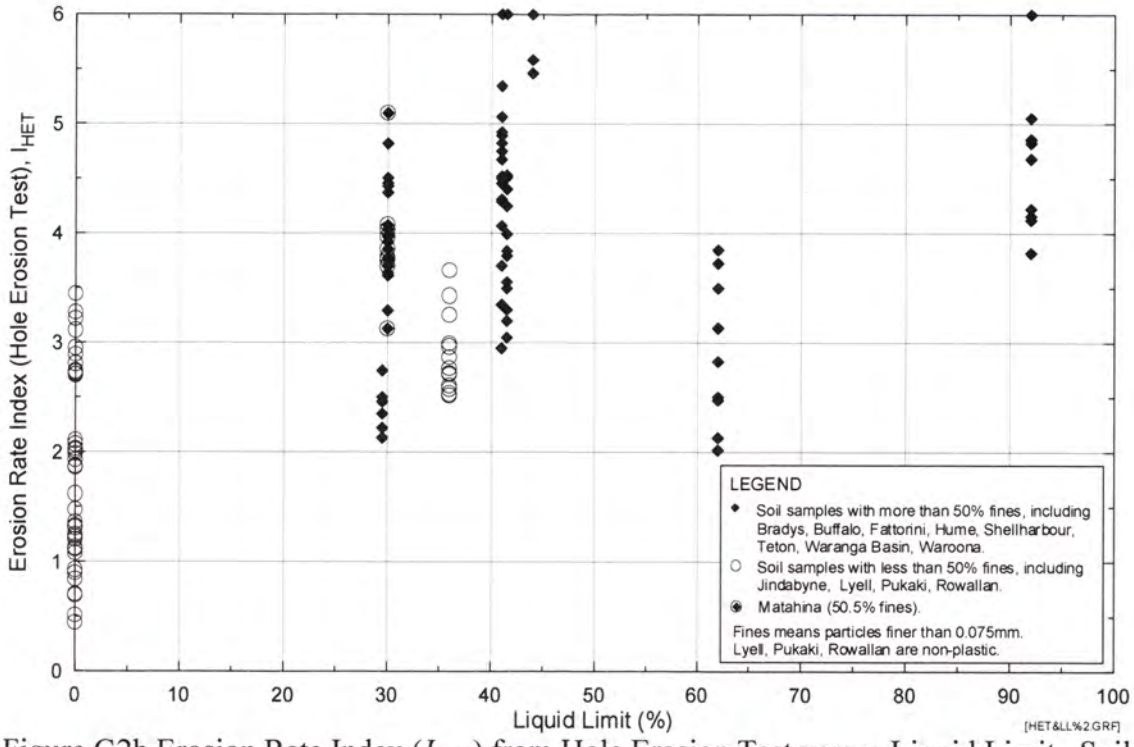

Figure G2b Erosion Rate Index (I_{HET}) from Hole Erosion Test versus Liquid Limit. Soil samples classified into fine-grained and coarse-grained soils.

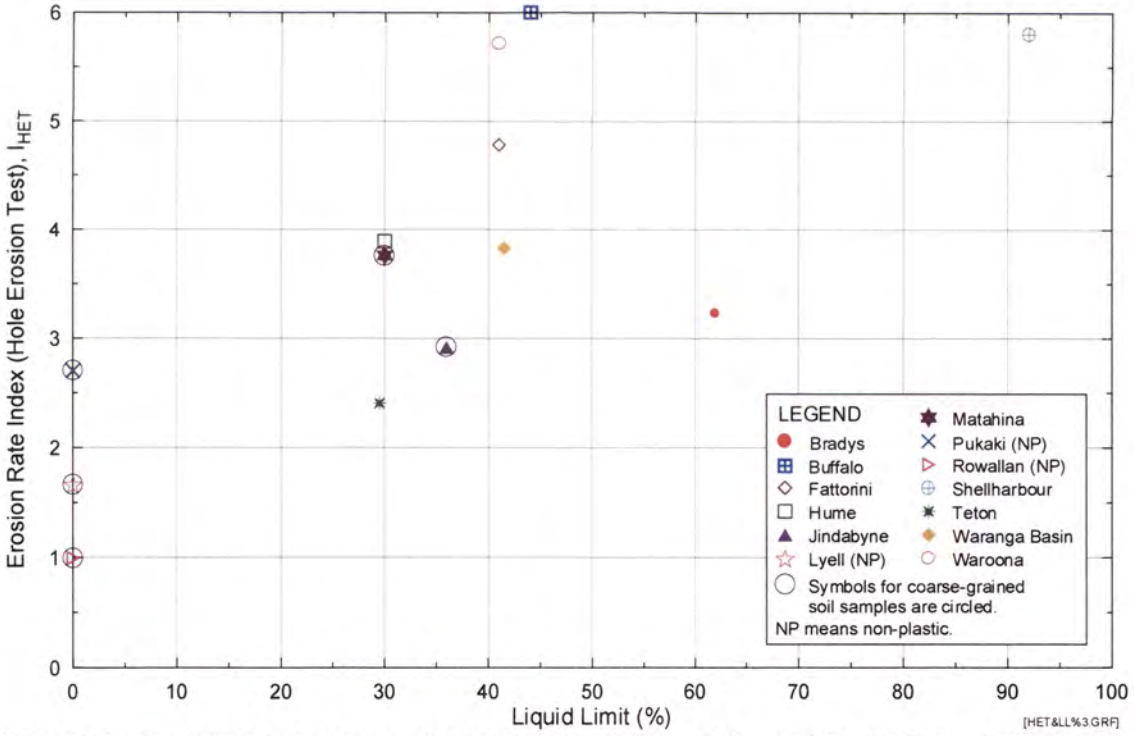

Note : Erosion Rate Indices presented are predicted indices for specimens at 95% compaction and Optimum Water Content.

Figure G2c Predicted Erosion Rate Index ($\tilde{I}_{HET}$) from Hole Erosion Test versus Liquid Limit.

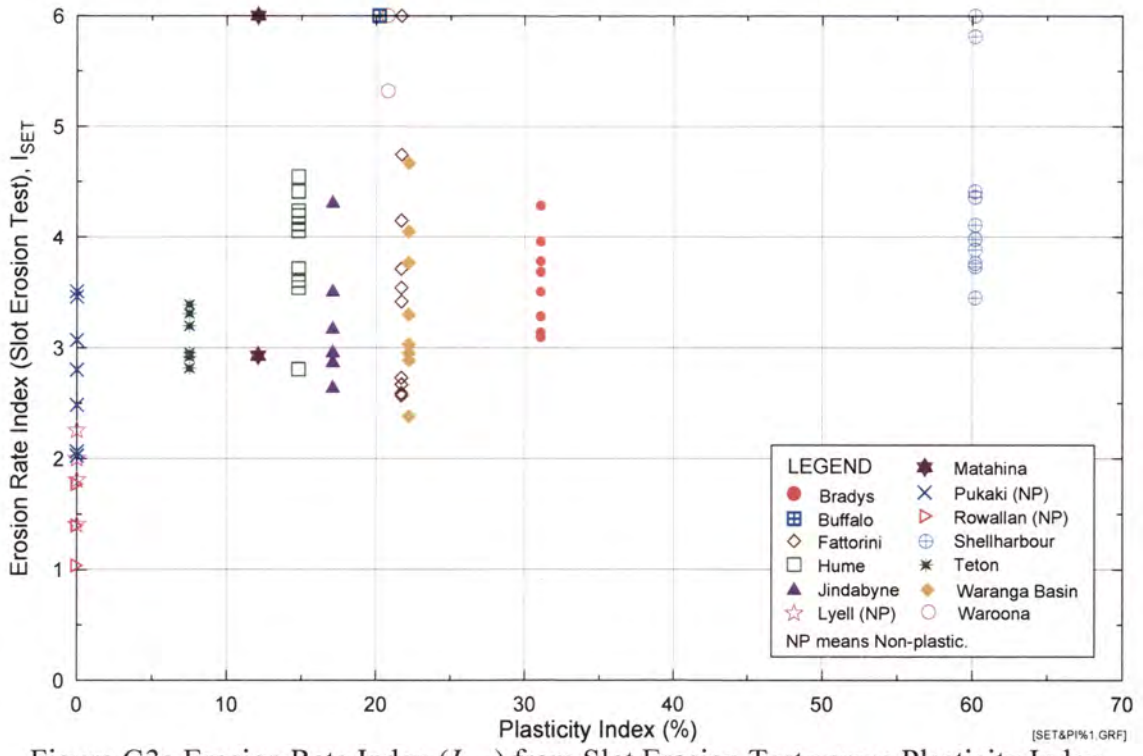

Figure G3a Erosion Rate Index (I_{SET}) from Slot Erosion Test versus Plasticity Index.

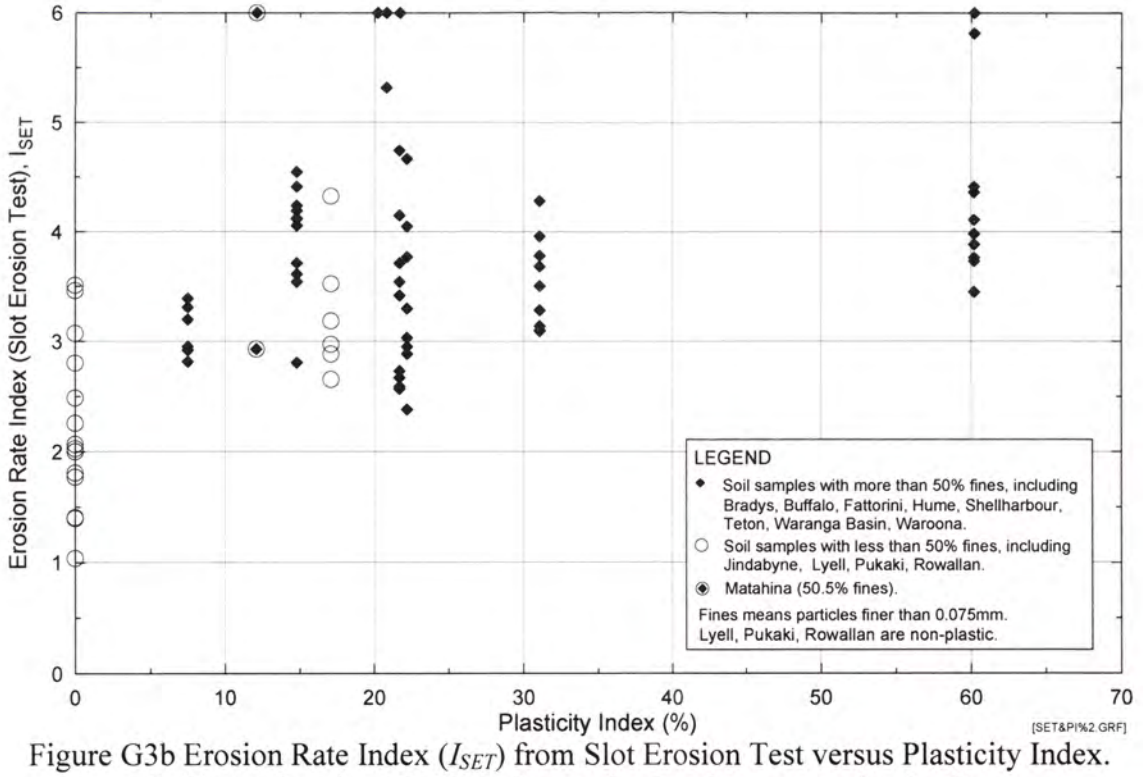

Figure G3b Erosion Rate Index (I_{SET}) from Slot Erosion Test versus Plasticity Index. Soil samples classified into fine-grained and coarse-grained soils.

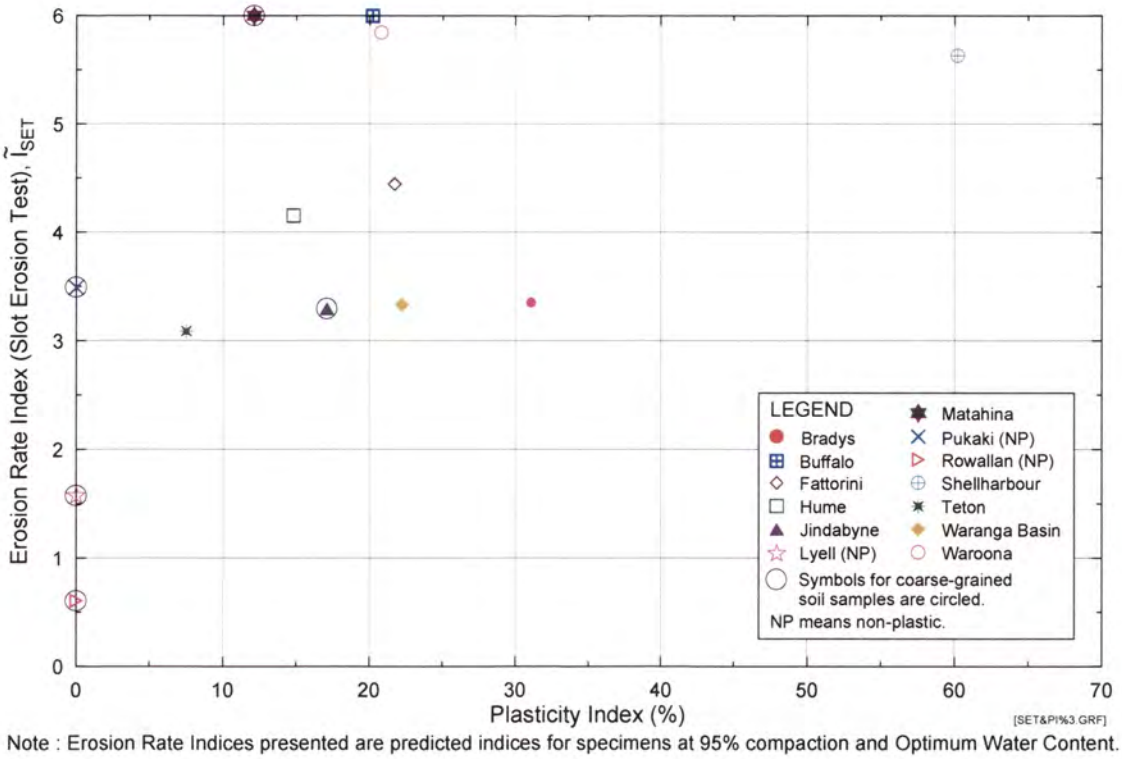

Note : Erosion Rate Indices presented are predicted indices for specimens at 95% compaction and Optimum Water Content.

Figure G3c Predicted Erosion Rate Index ($\tilde{I}_{SET}$) from Slot Erosion Test versus Plasticity Index.

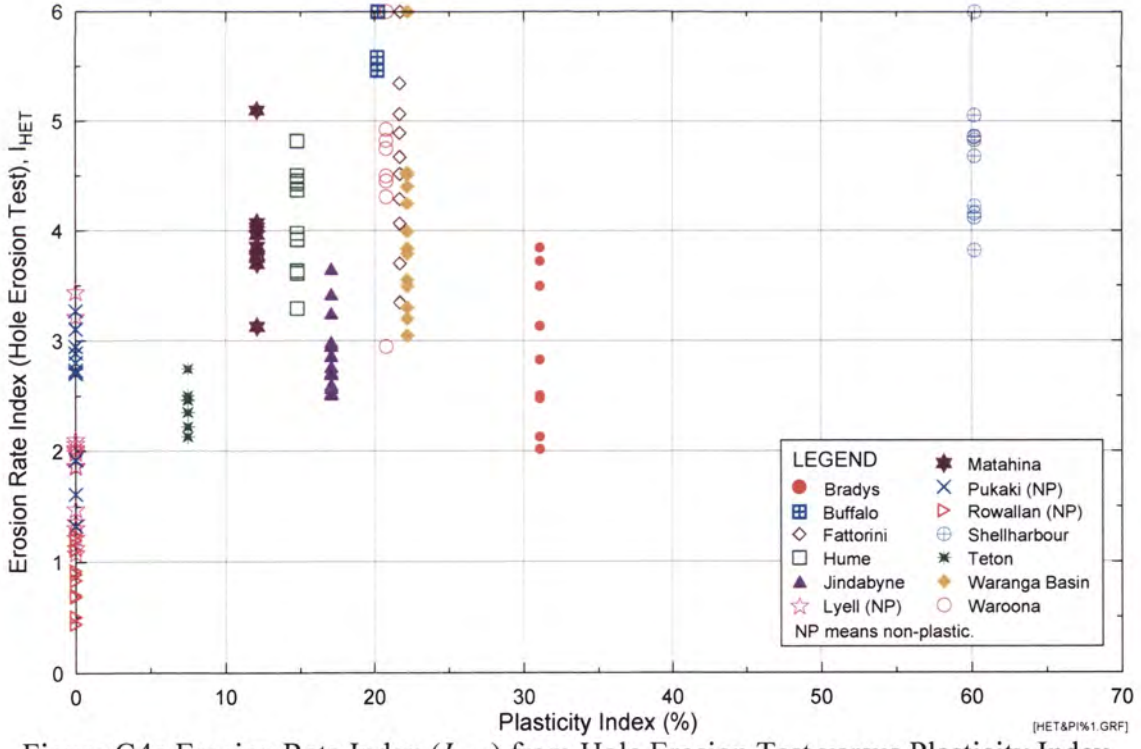

Figure G4a Erosion Rate Index (I_{HET}) from Hole Erosion Test versus Plasticity Index.

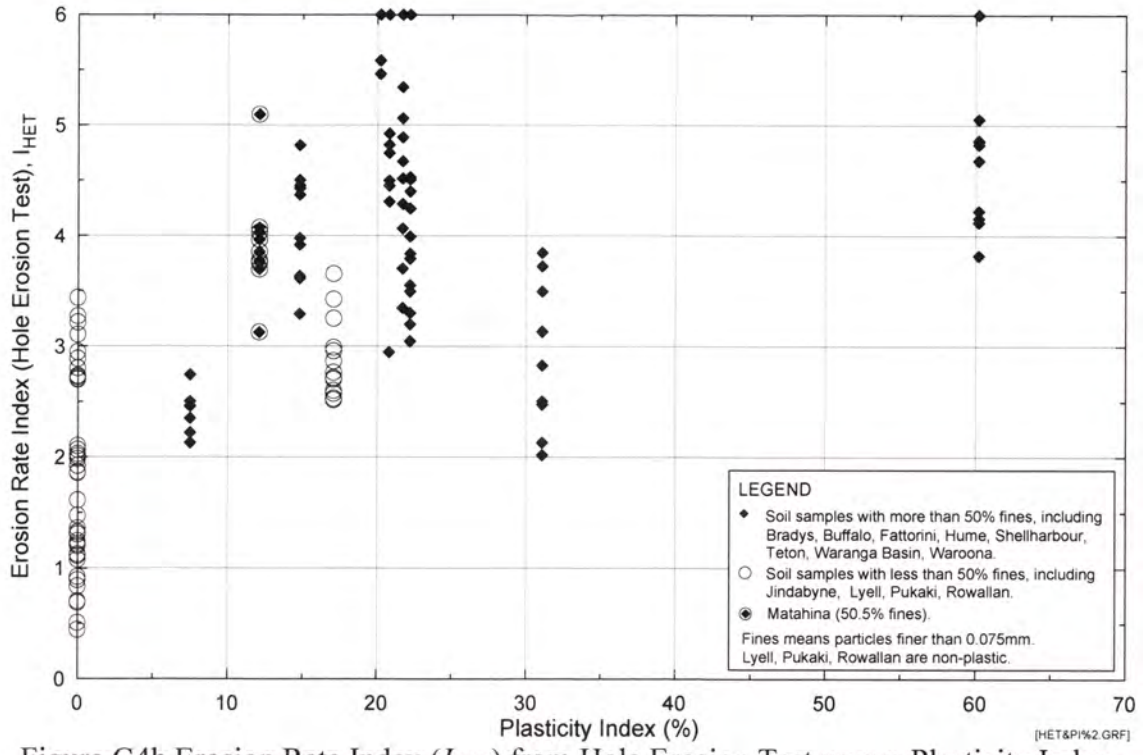

Figure G4b Erosion Rate Index (I_{HET}) from Hole Erosion Test versus Plasticity Index. Soil samples classified into fine-grained and coarse-grained soils.

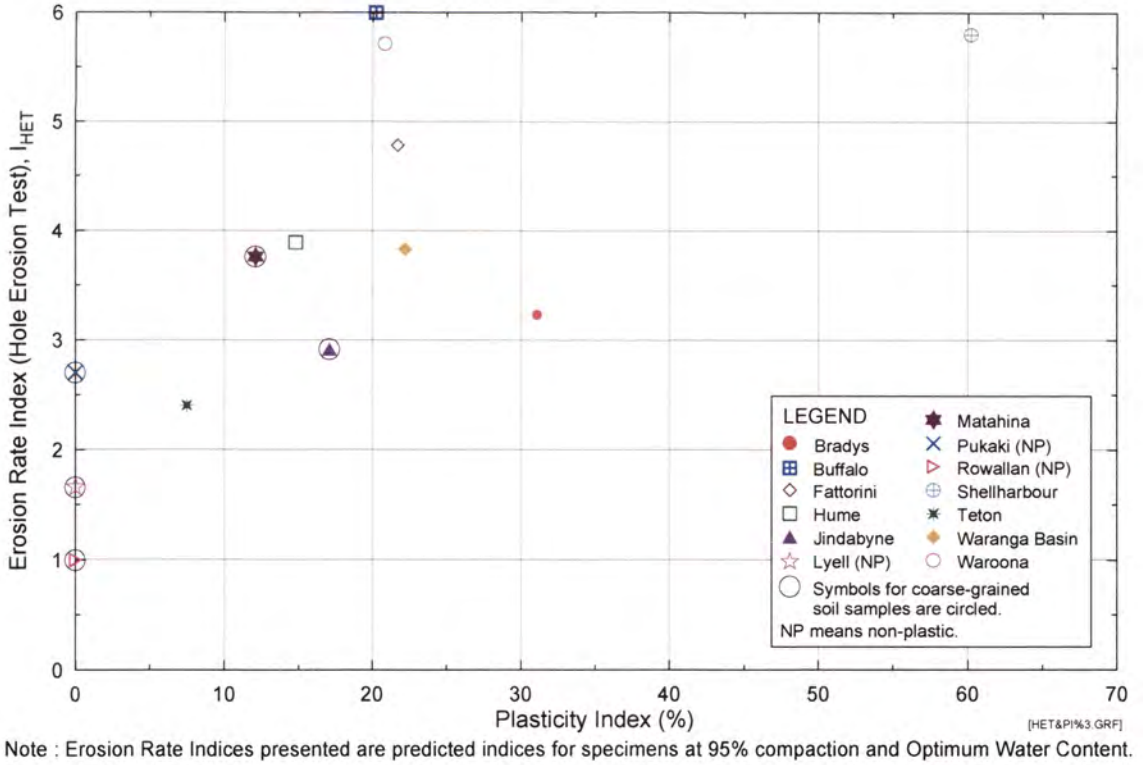

Note : Erosion Rate Indices presented are predicted indices for specimens at 95% compaction and Optimum Water Content.

Figure G4c Predicted Erosion Rate Index ($\tilde{I}_{HET}$) from Hole Erosion Test versus Plasticity Index.

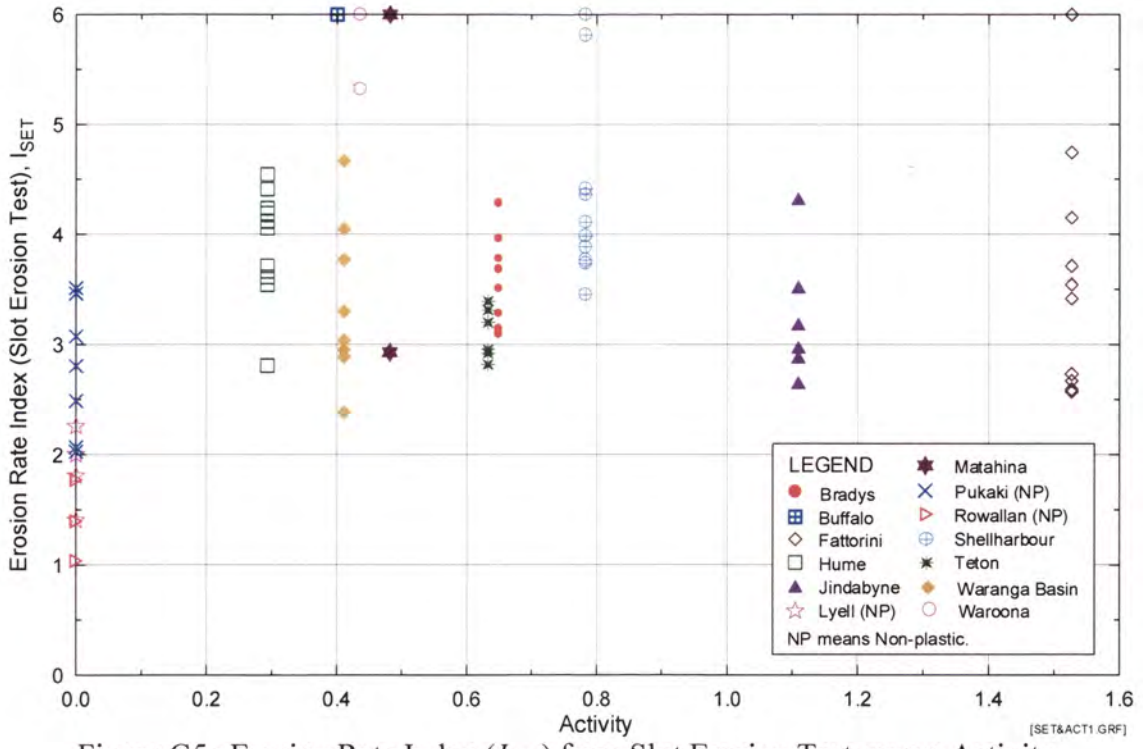

Figure G5a Erosion Rate Index (I_{SET}) from Slot Erosion Test versus Activity.

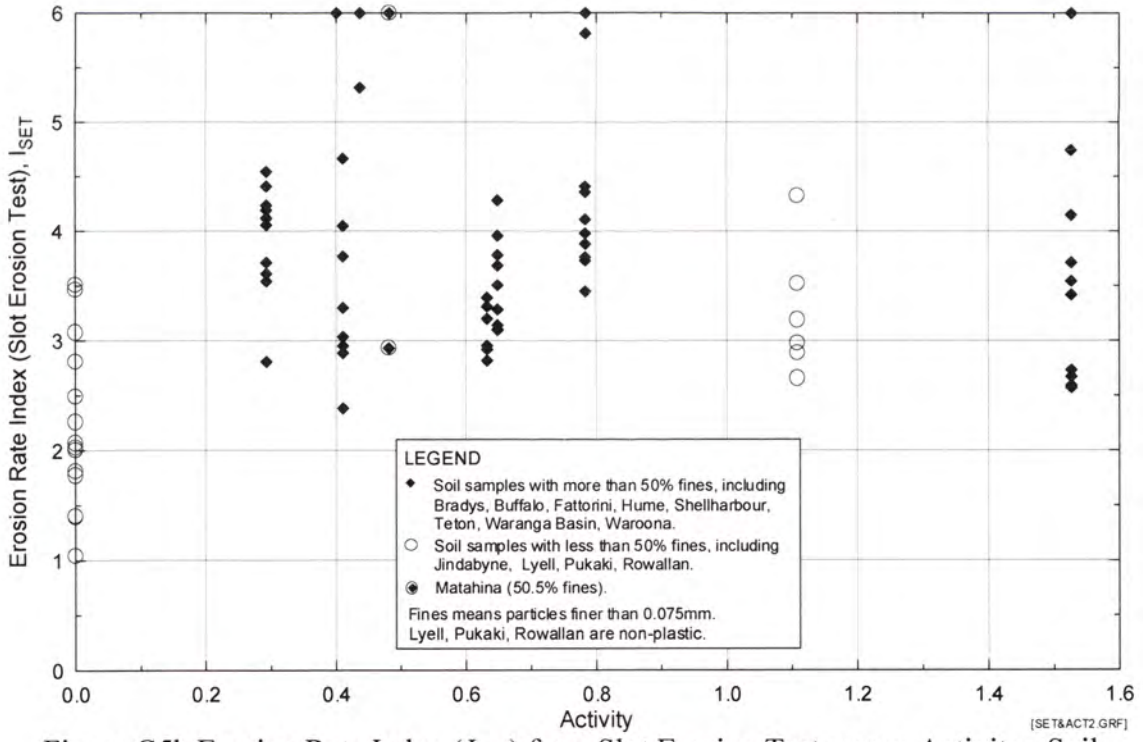

Figure G5b Erosion Rate Index (I_{SET}) from Slot Erosion Test versus Activity. Soil samples classified into fine-grained and coarse-grained soils.

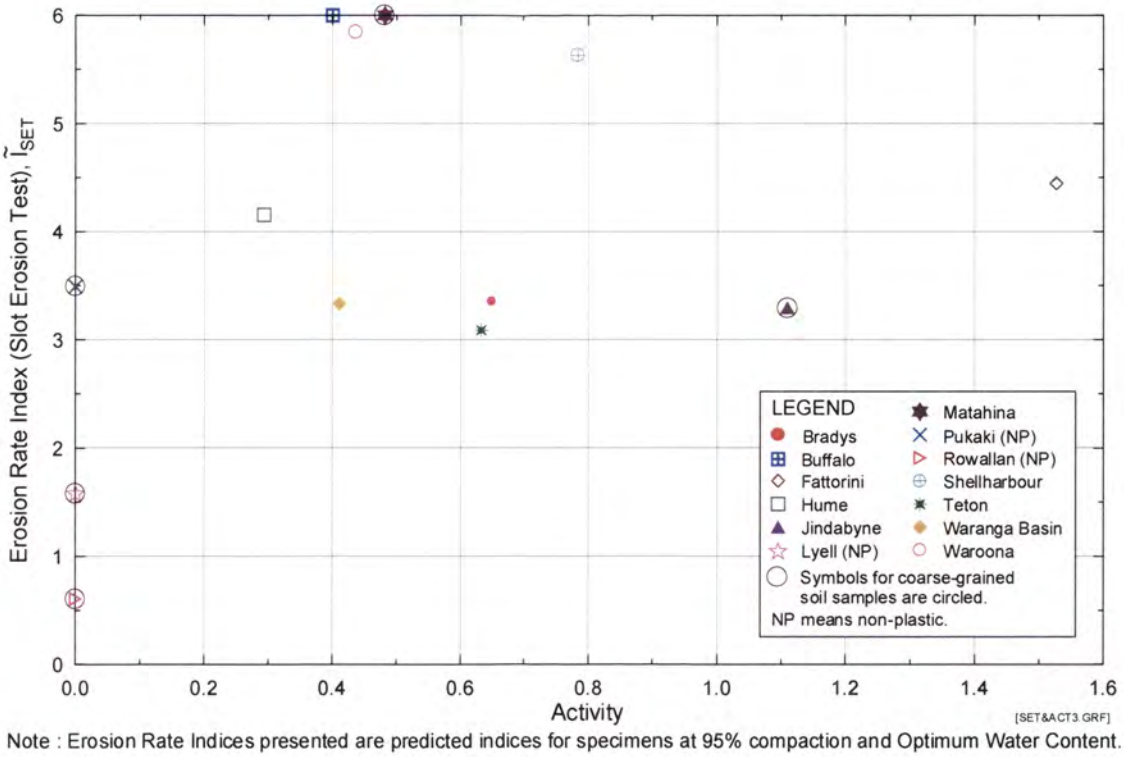

Note : Erosion Rate Indices presented are predicted indices for specimens at 95% compaction and Optimum Water Content.

Figure G5c Predicted Erosion Rate Index ($\tilde{I}_{SET}$) from Slot Erosion Test versus Activity.

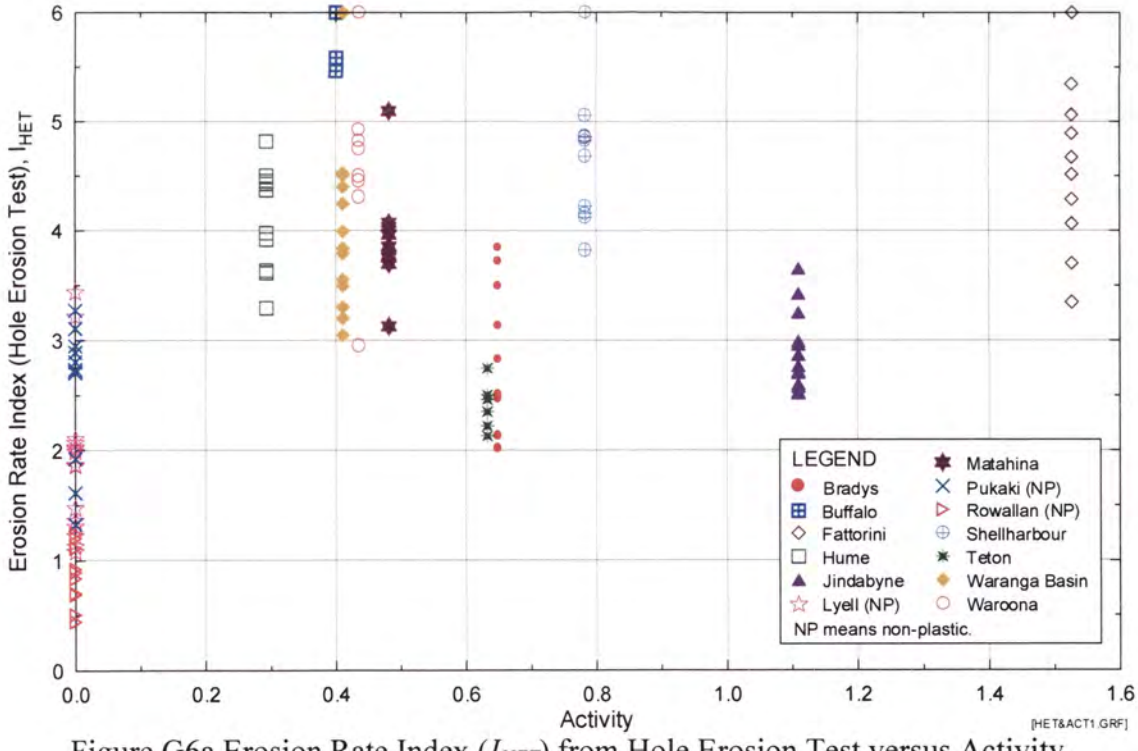

Figure G6a Erosion Rate Index (I_{HET}) from Hole Erosion Test versus Activity.

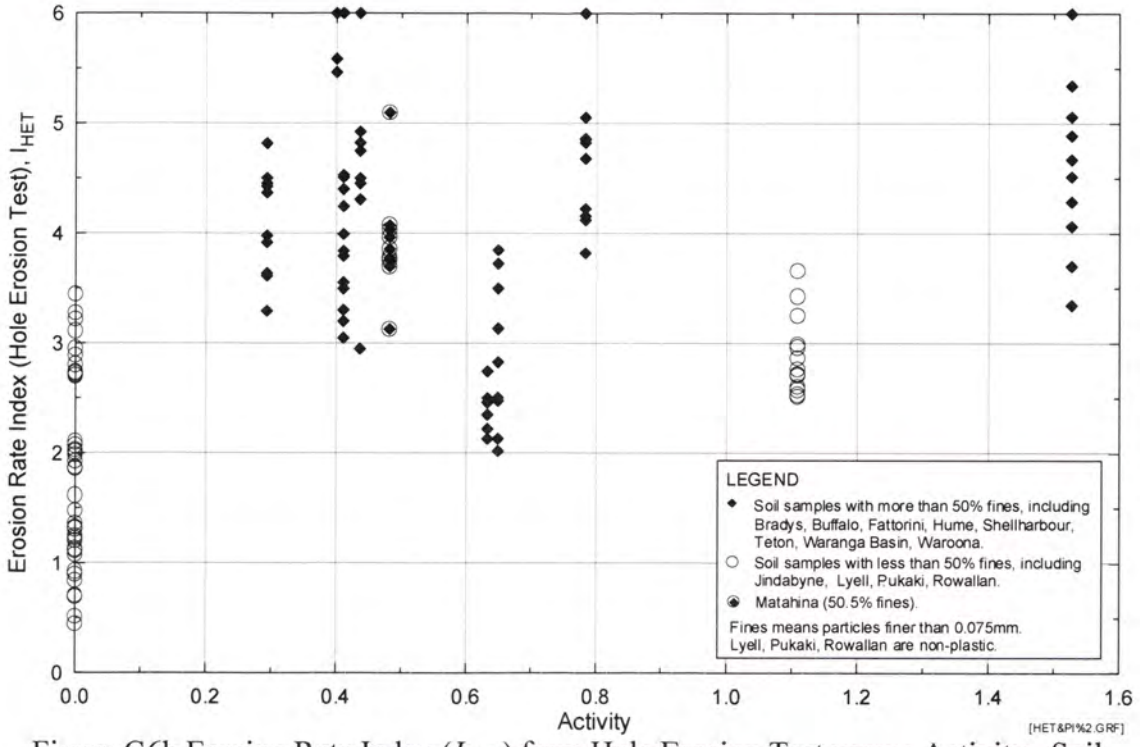

Figure G6b Erosion Rate Index (I_{HET}) from Hole Erosion Test versus Activity. Soil samples classified into fine-grained and coarse-grained soils.

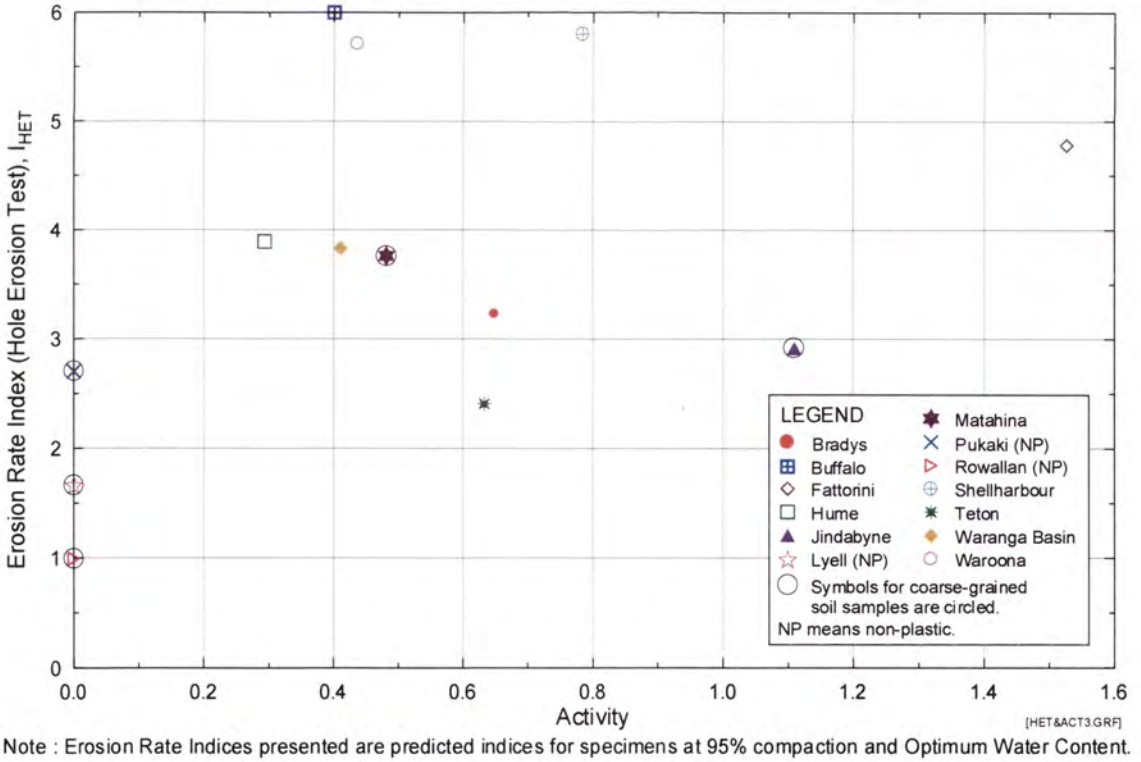

Note : Erosion Rate Indices presented are predicted indices for specimens at 95% compaction and Optimum Water Content.

Figure G6c Predicted Erosion Rate Index (I_{HET}) from Hole Erosion Test versus Activity.

APPENDIX H

Plots of Erosion Rate Index against Pinhole Test Classification, Emerson Class Test Classification, Percentage Dispersion, SAR, and Major Cation Content

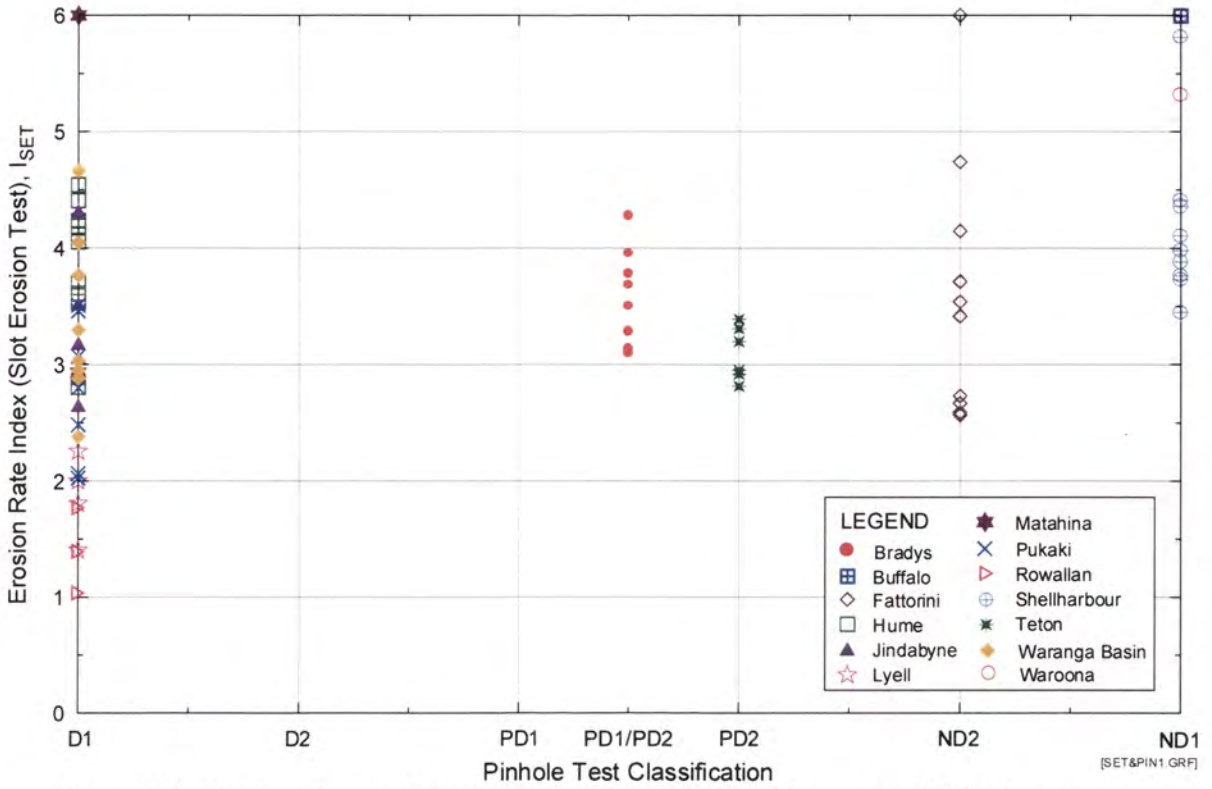

Figure H1a Erosion Rate Index (I_{SET}) from Slot Erosion Test versus Pinhole Test Classification.

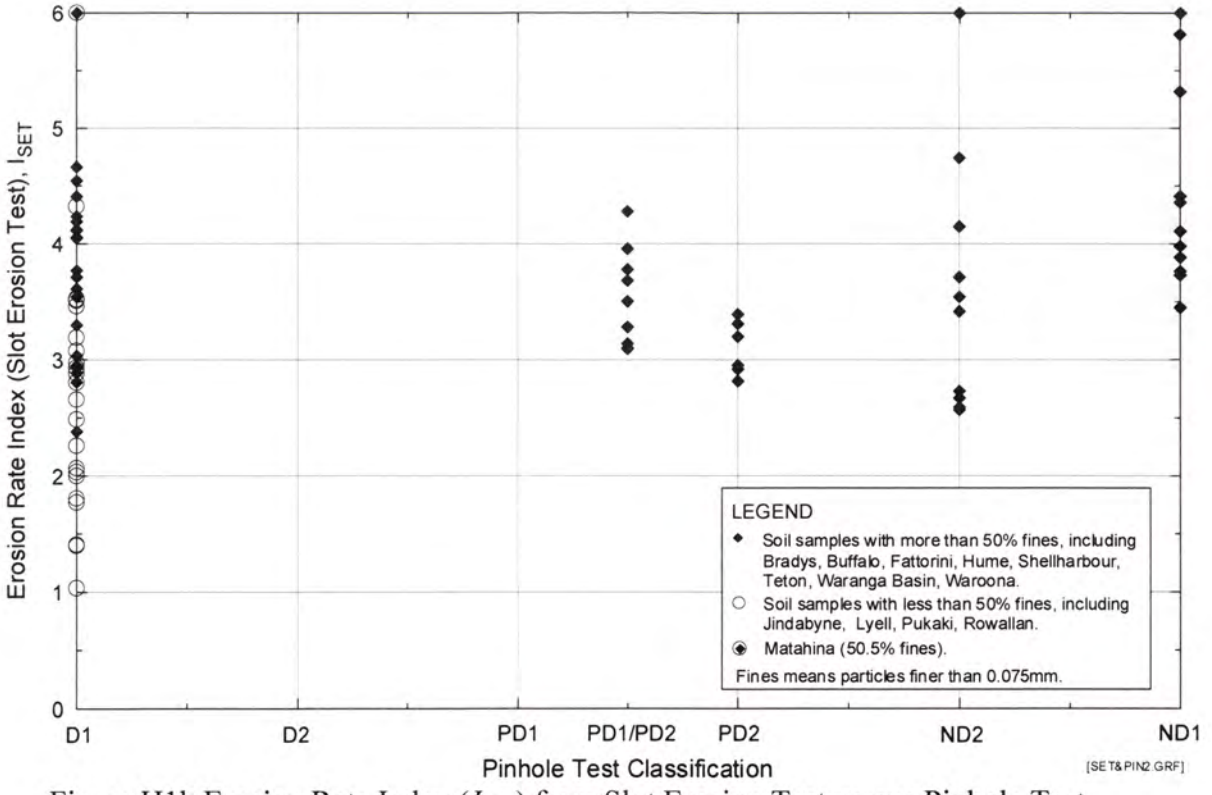

Figure H1b Erosion Rate Index (I_{SET}) from Slot Erosion Test versus Pinhole Test Classification. Soil samples classified into fine-grained and coarse-grained soils.

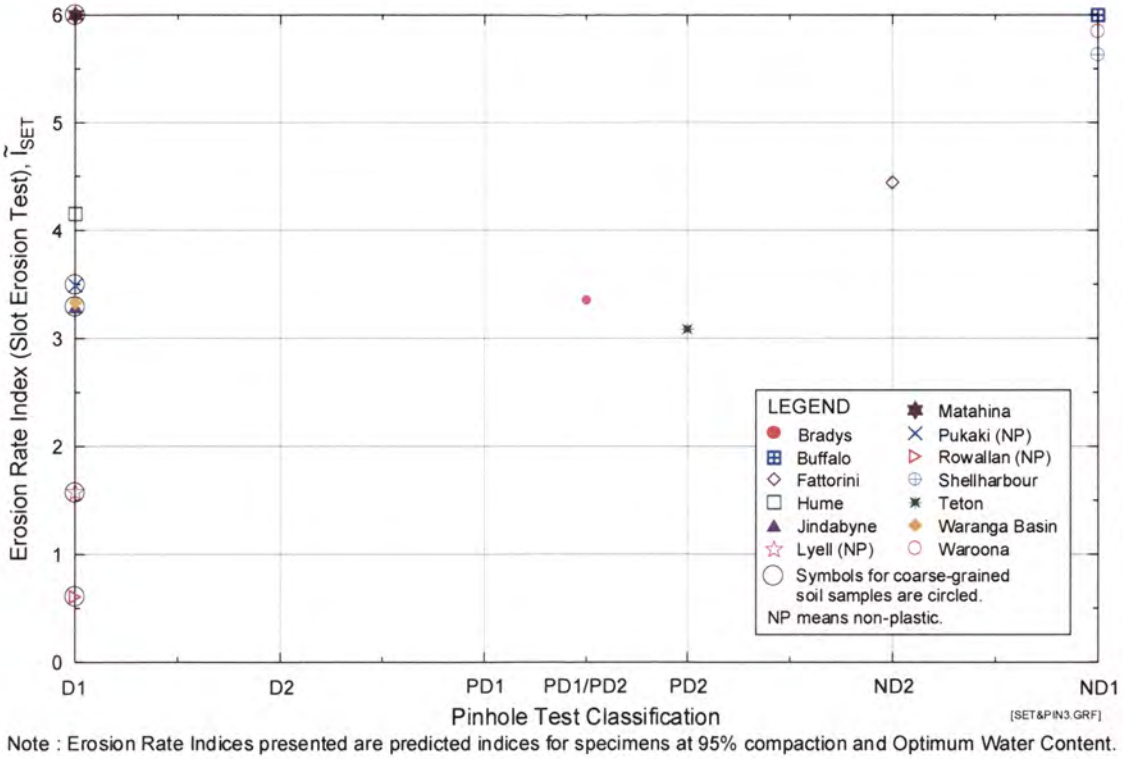

Note : Erosion Rate Indices presented are predicted indices for specimens at 95% compaction and Optimum Water Content.

Figure H1c Predicted Erosion Rate Index ($\tilde{I}_{SET}$) from Slot Erosion Test versus Pinhole Test Classification.

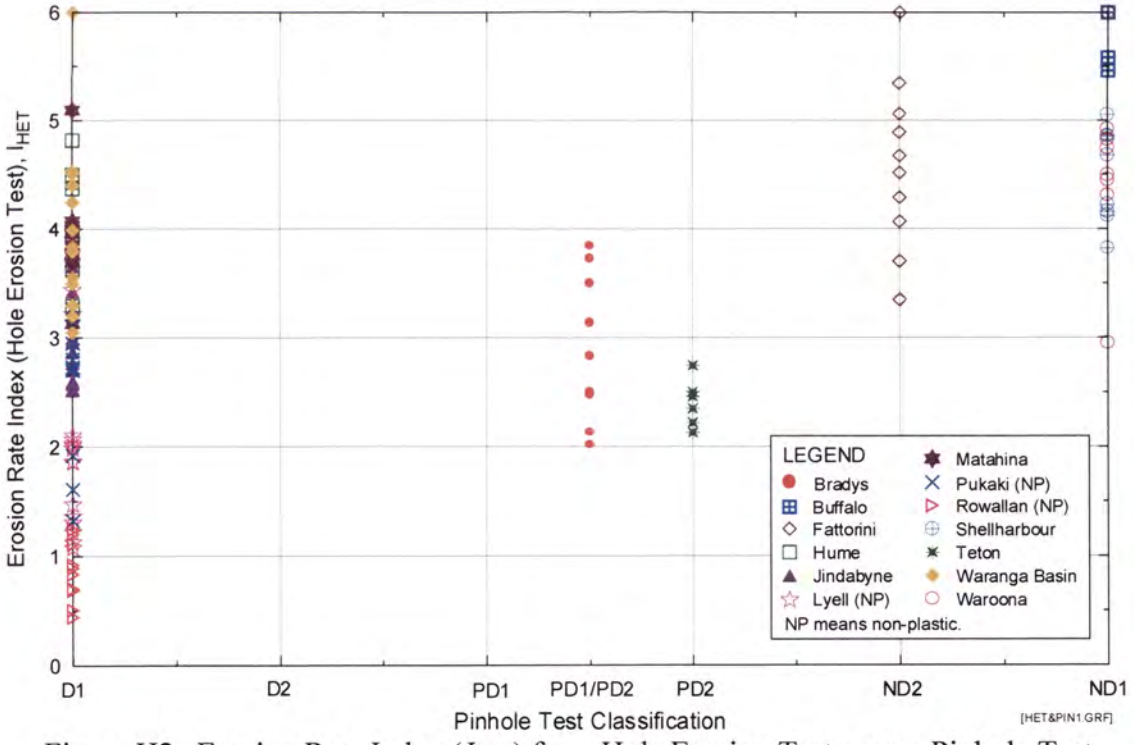

Figure H2a Erosion Rate Index (I_{HET}) from Hole Erosion Test versus Pinhole Test Classification.

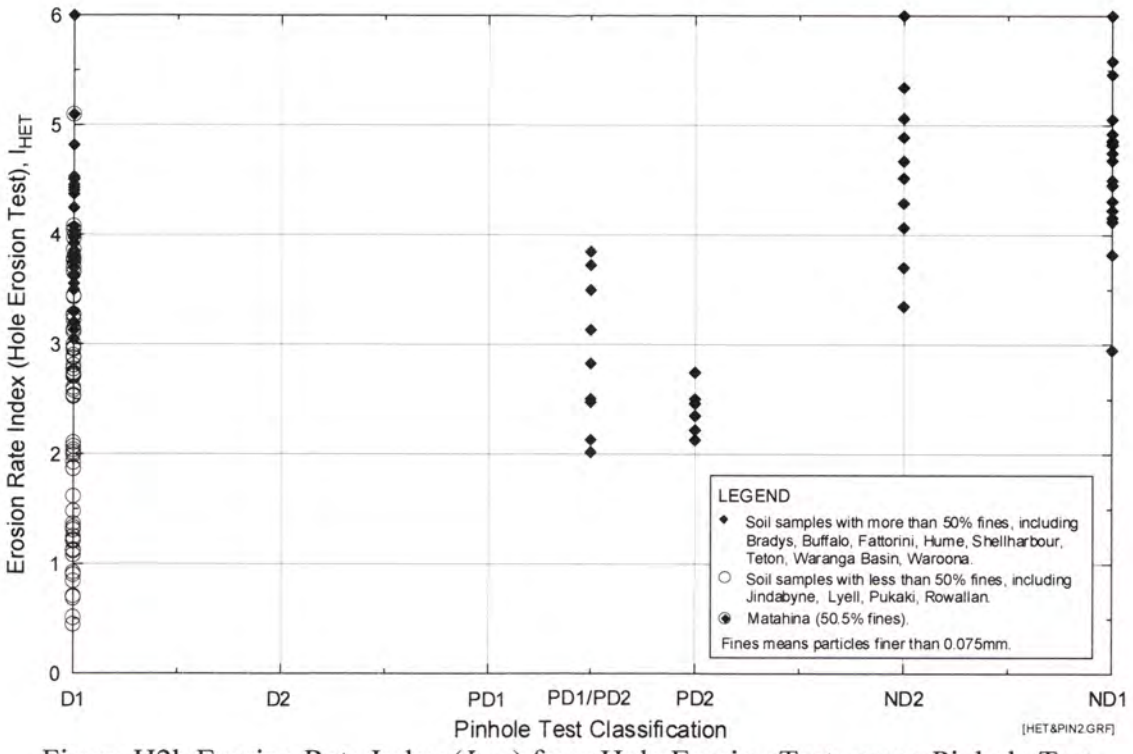

Figure H2b Erosion Rate Index (I_{HET}) from Hole Erosion Test versus Pinhole Test Classification. Soil samples classified into fine-grained and coarse-grained soils.

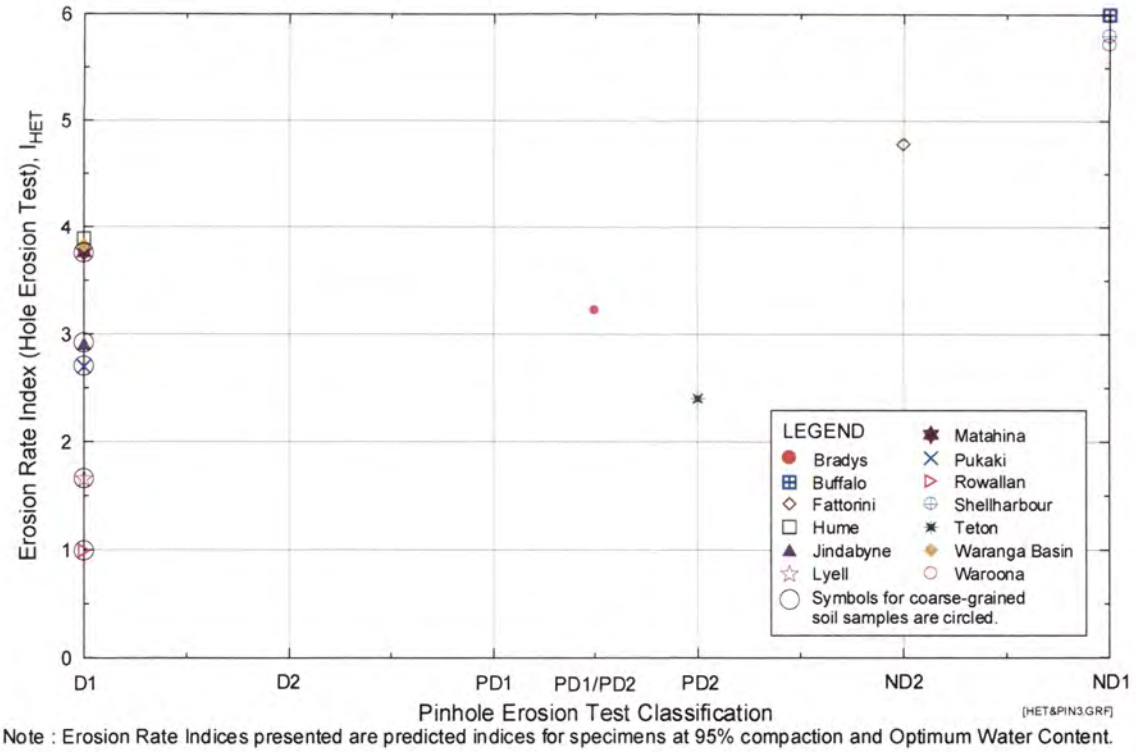

Note : Erosion Rate Indices presented are predicted indices for specimens at 95% compaction and Optimum Water Content.

Figure H2c Predicted Erosion Rate Index ($\tilde{I}_{HET}$) from Hole Erosion Test versus Pinhole Test Classification.

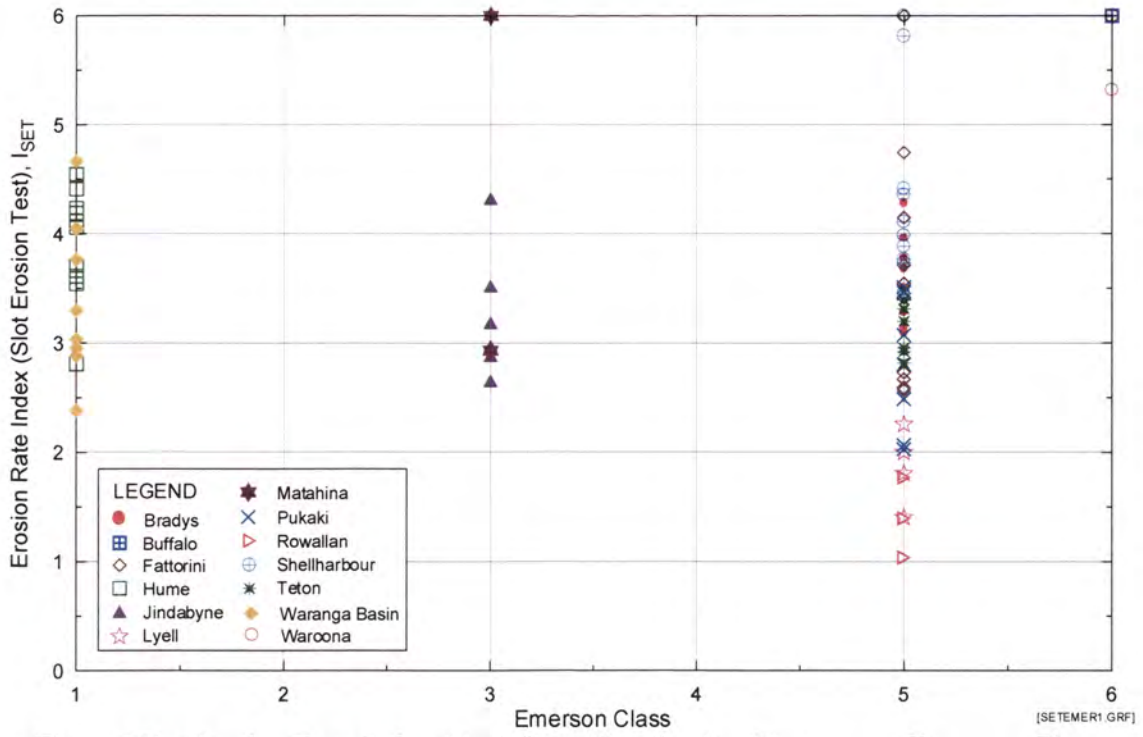

Figure H3a Erosion Rate Index (I_{SET}) from Slot Erosion Test versus Emerson Class.

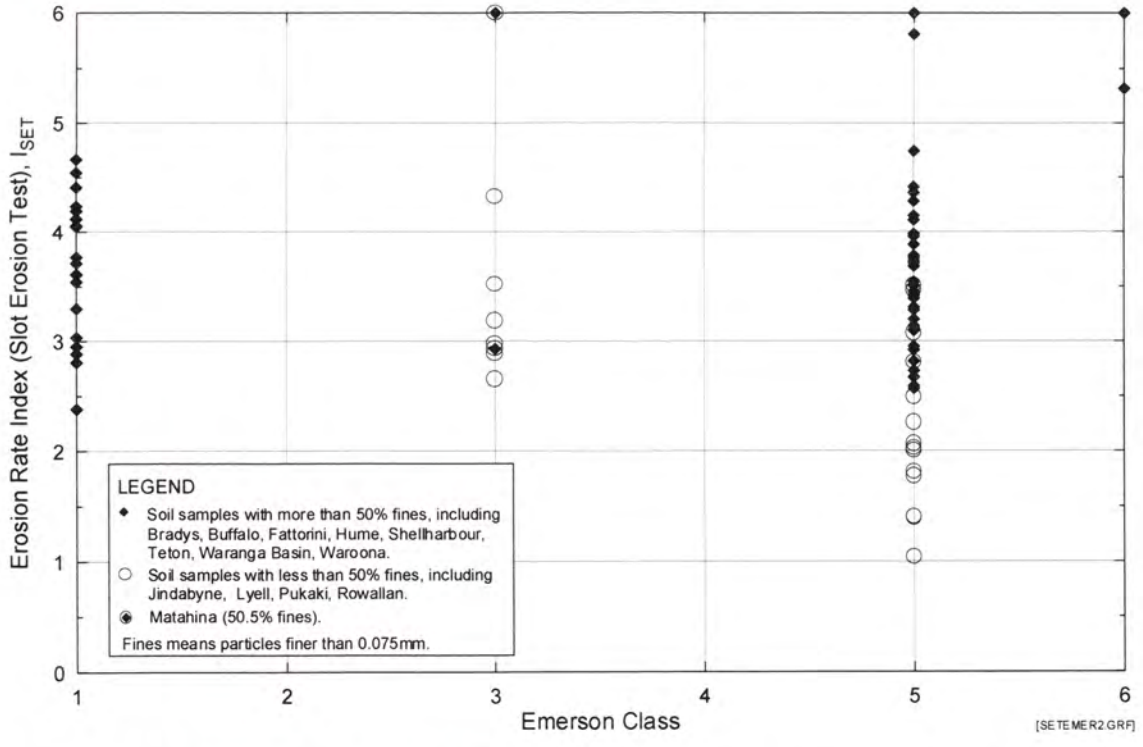

Figure H3b Erosion Rate Index (I_{SET}) from Slot Erosion Test versus Emerson Class. Soil samples classified into fine-grained and coarse-grained soils.

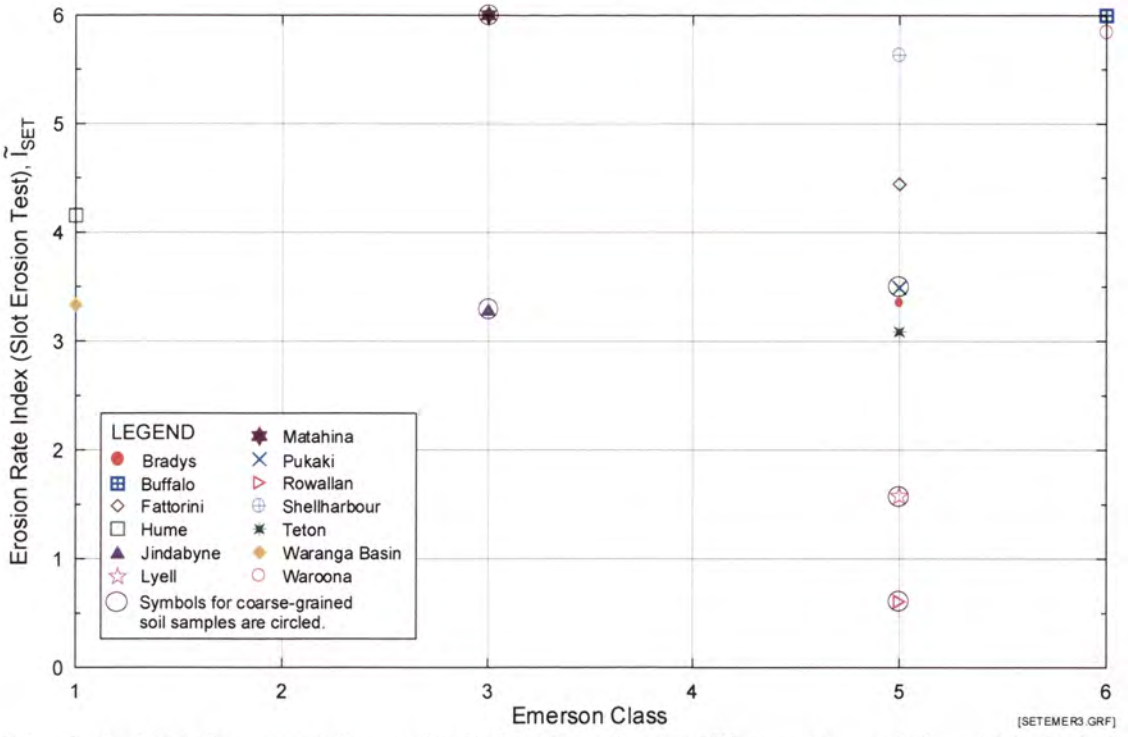

Note : Erosion Rate Indices presented are predicted indices for specimens at 95% compaction and Optimum Water Content.

Figure H3c Predicted Erosion Rate Index ($\tilde{I}_{SET}$) from Slot Erosion Test versus Emerson Class.

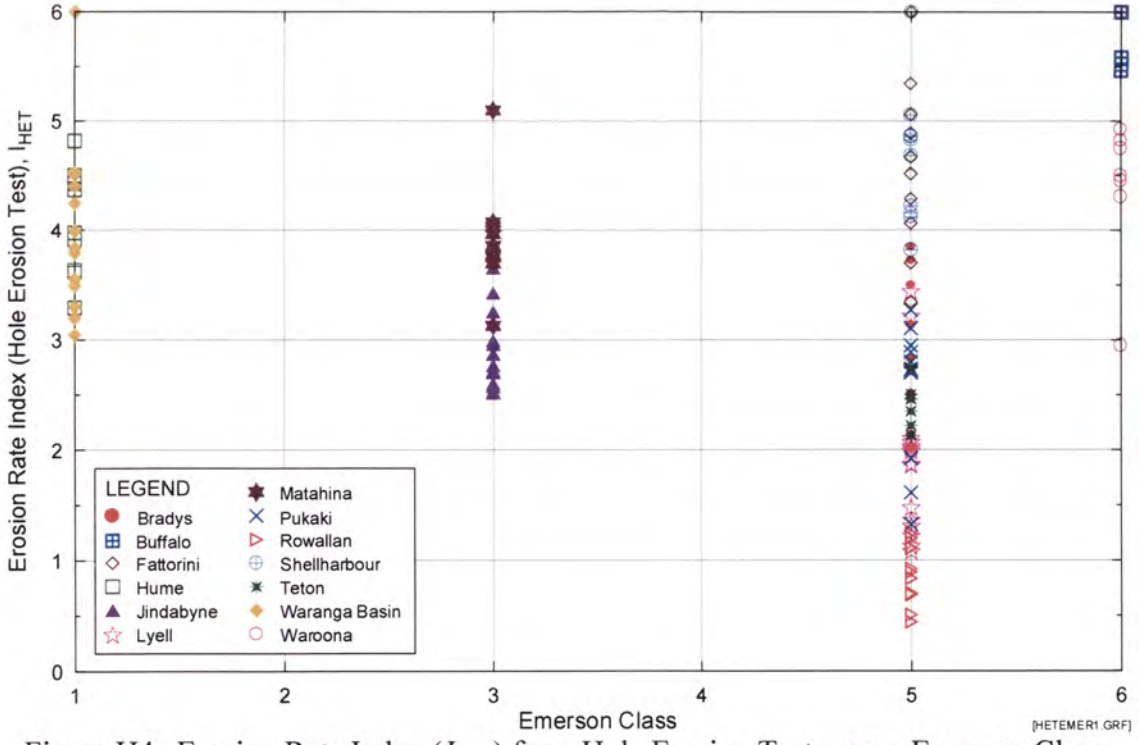

Figure H4a Erosion Rate Index (I_{HET}) from Hole Erosion Test versus Emerson Class.

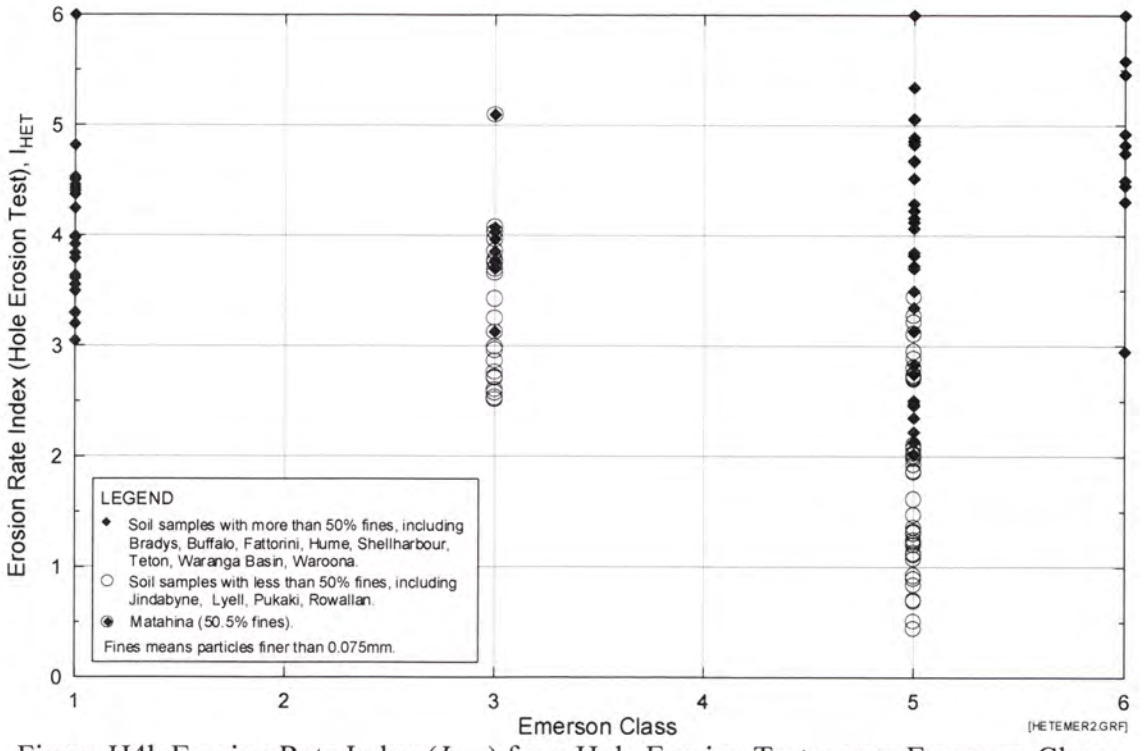

Figure H4b Erosion Rate Index (I_{HET}) from Hole Erosion Test versus Emerson Class. Soil samples classified into fine-grained and coarse-grained soils.

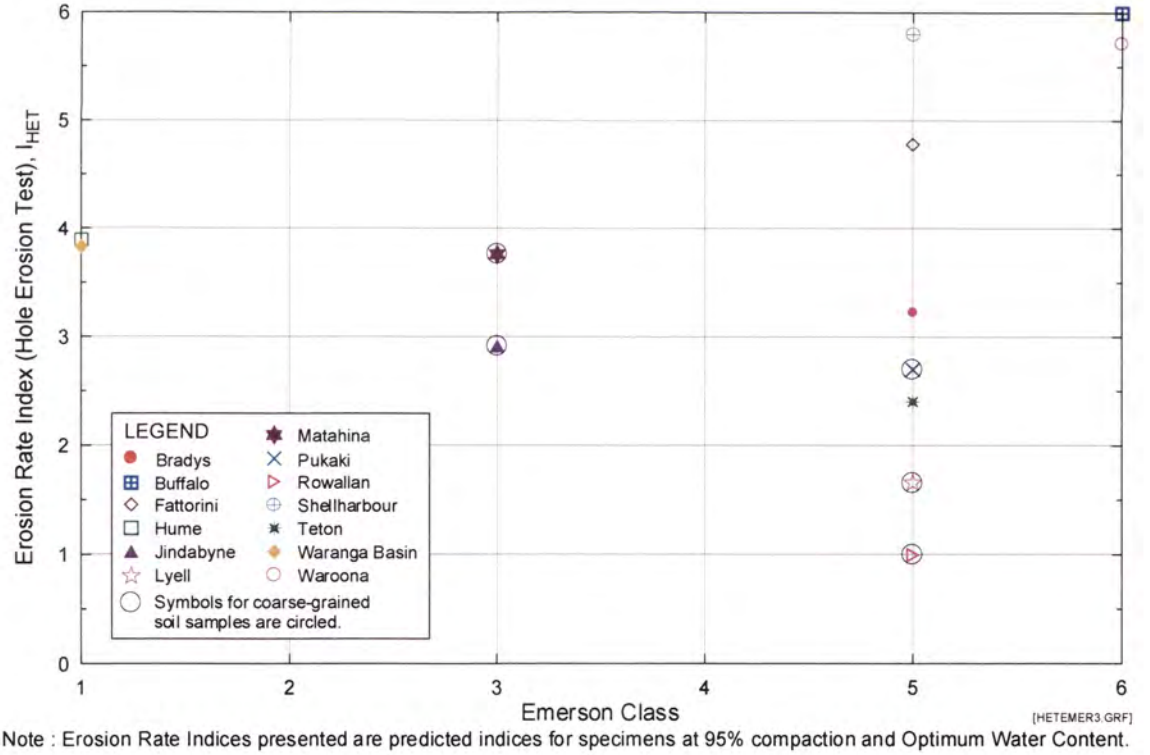

Note : Erosion Rate Indices presented are predicted indices for specimens at 95% compaction and Optimum Water Content.

Figure H4c Predicted Erosion Rate Index ($\tilde{I}_{HET}$) from Hole Erosion Test versus Emerson Class.

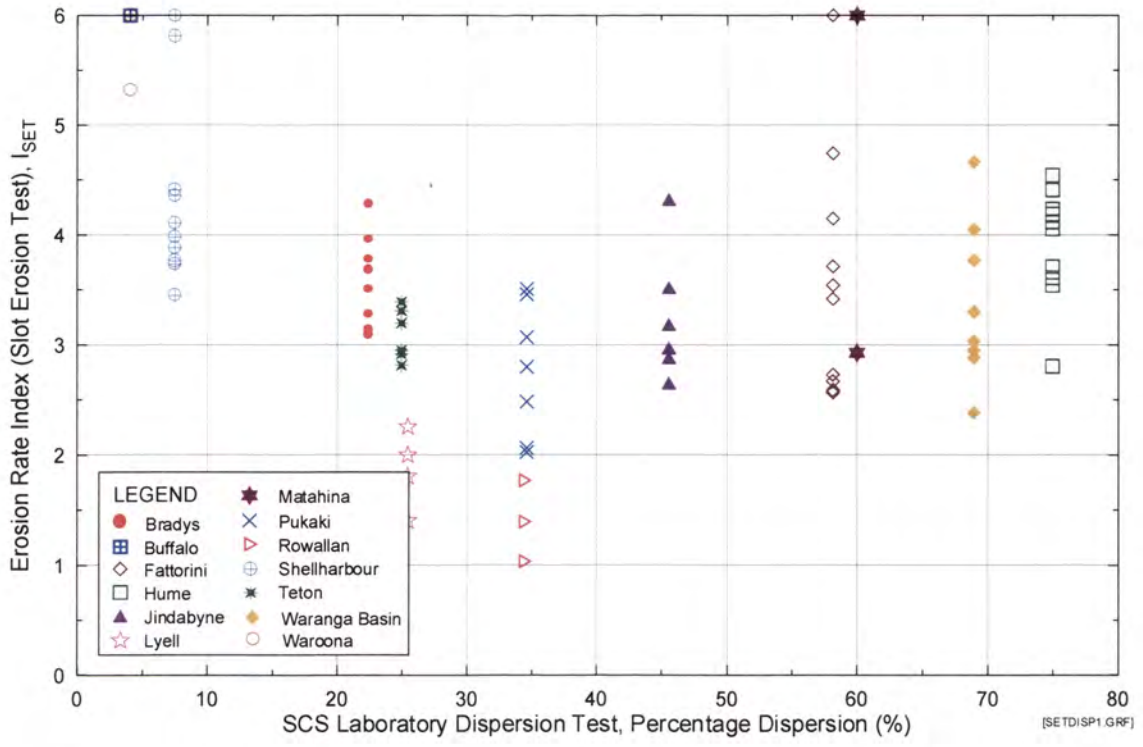

Figure H5a Erosion Rate Index (I_{SET}) from Slot Erosion Test versus Percentage Dispersion.

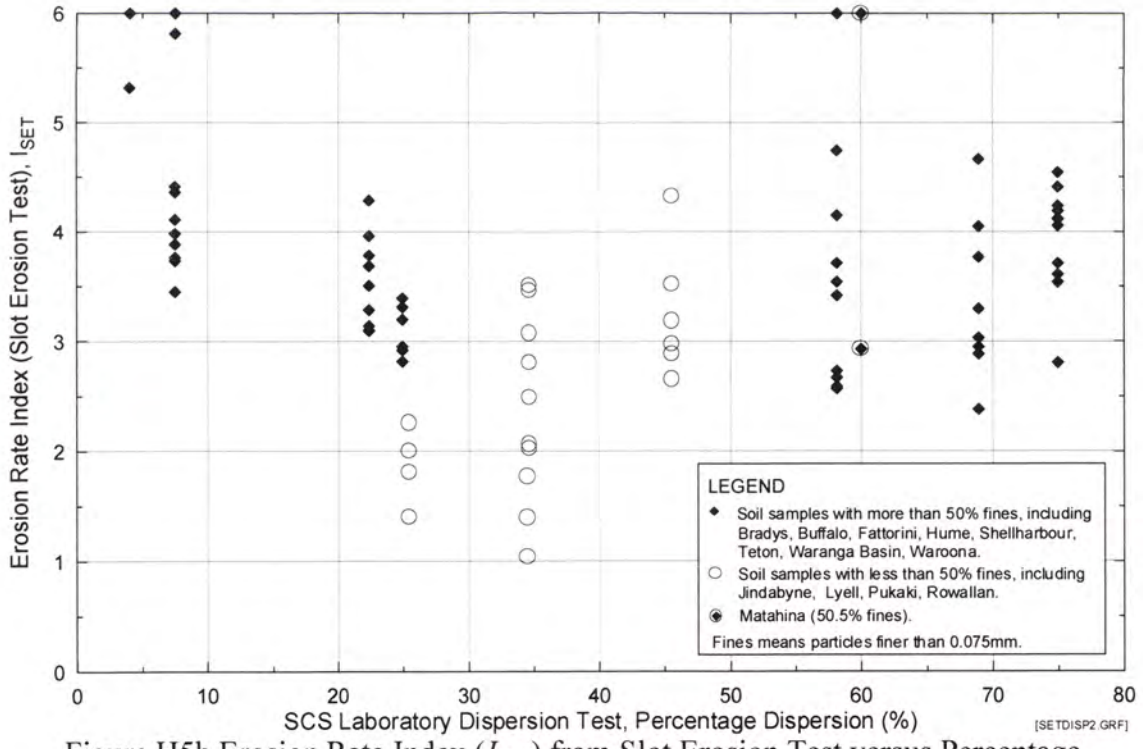

Figure H5b Erosion Rate Index (I_{SET}) from Slot Erosion Test versus Percentage Dispersion. Soil samples classified into fine-grained and coarse-grained soils.

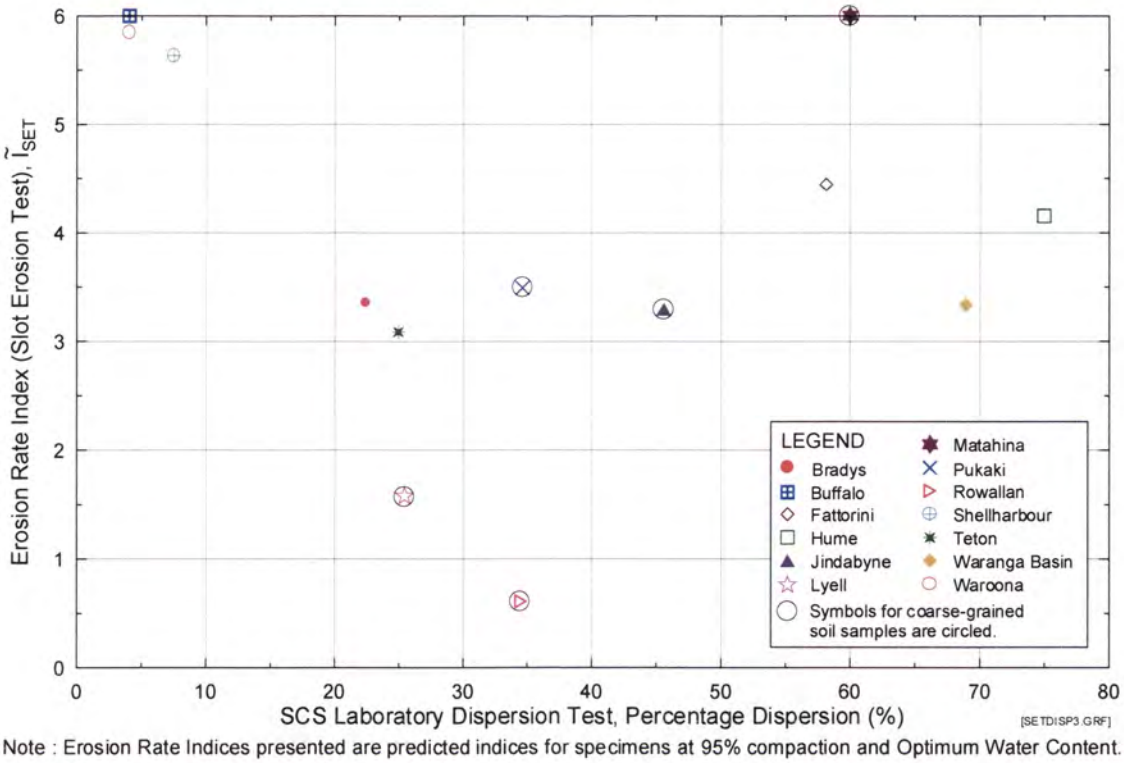

Note : Erosion Rate Indices presented are predicted indices for specimens at 95% compaction and Optimum Water Content.

Figure H5c Predicted Erosion Rate Index ($\tilde{I}_{SET}$) from Slot Erosion Test versus Percentage Dispersion.

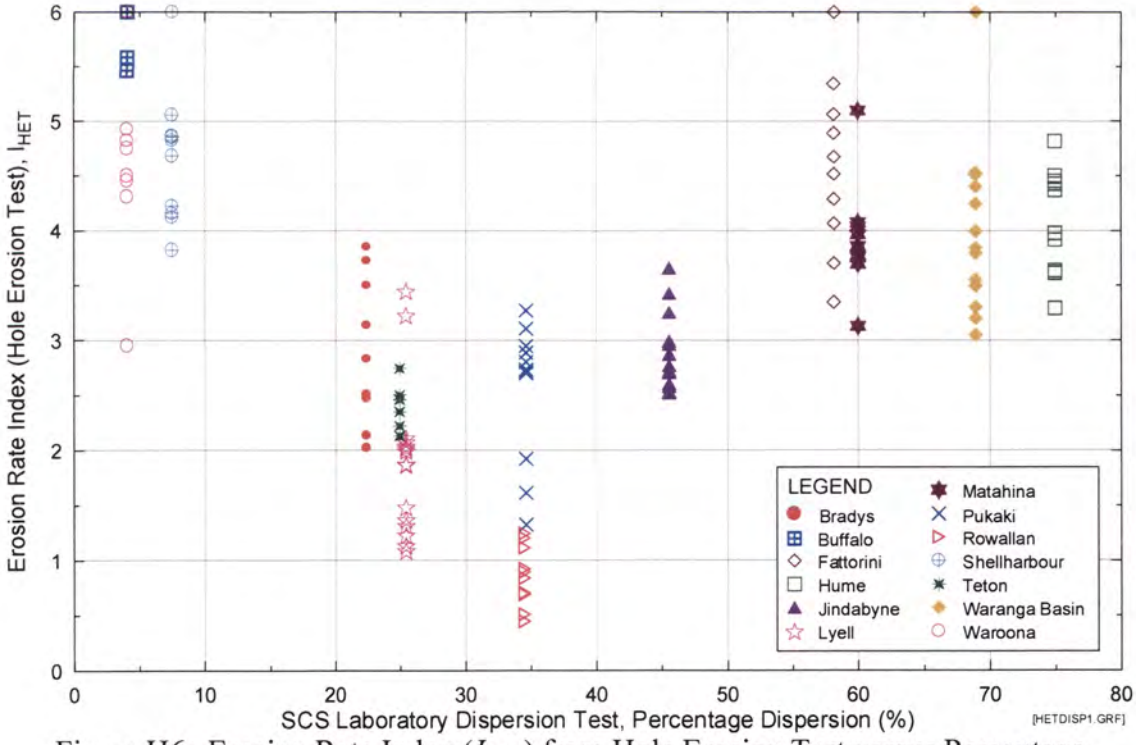

Figure H6a Erosion Rate Index (I_{HET}) from Hole Erosion Test versus Percentage Dispersion.

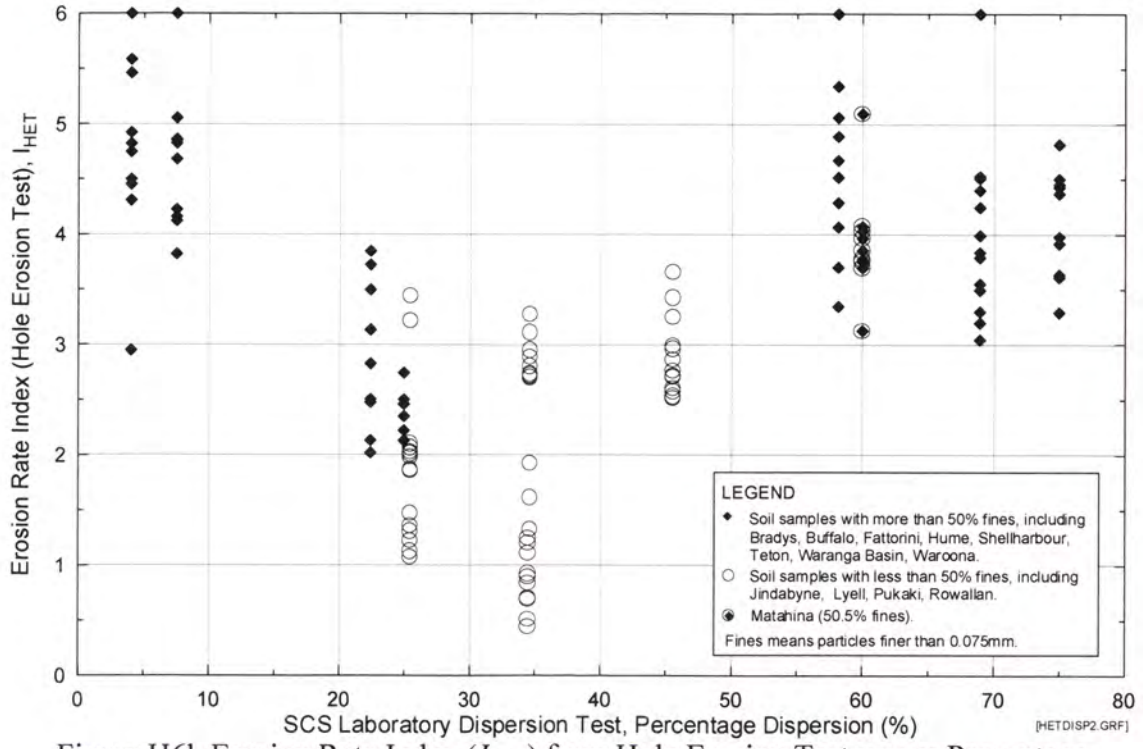

Figure H6b Erosion Rate Index (I_{HET}) from Hole Erosion Test versus Percentage Dispersion. Soil samples classified into fine-grained and coarse-grained soils.

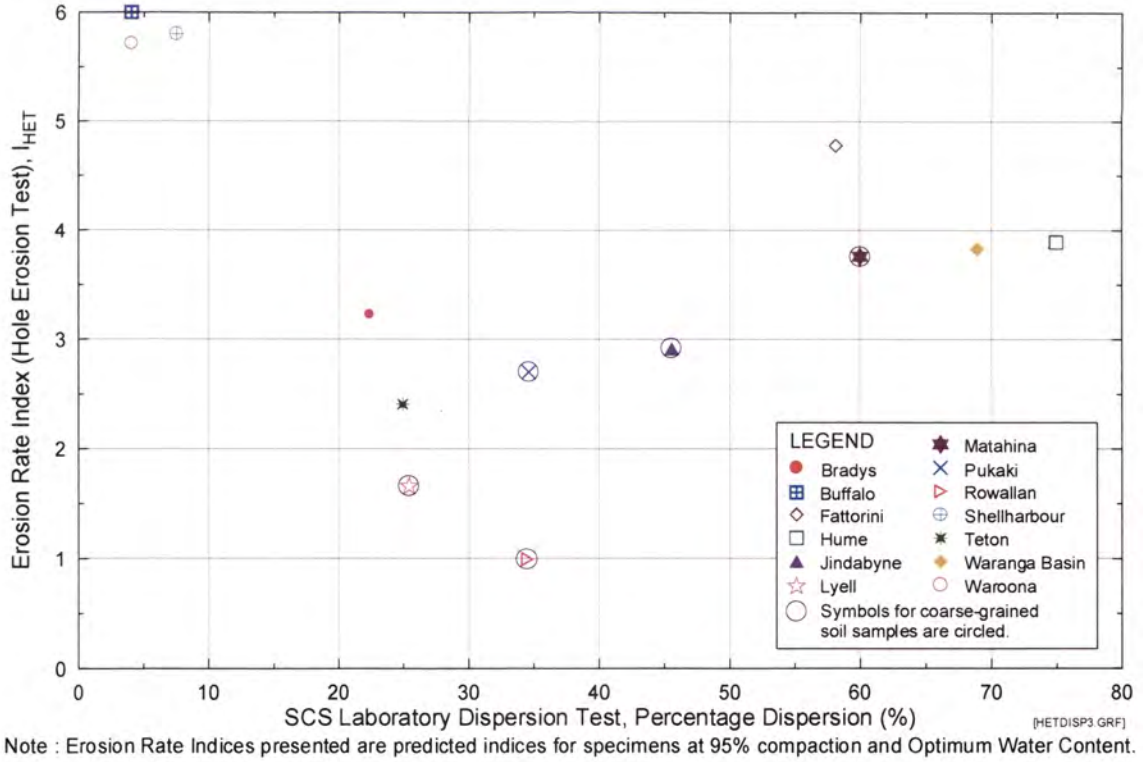

Note : Erosion Rate Indices presented are predicted indices for specimens at 95% compaction and Optimum Water Content.

Figure H6c Predicted Erosion Rate Index ($\tilde{I}_{HET}$) from Hole Erosion Test versus Percentage Dispersion.

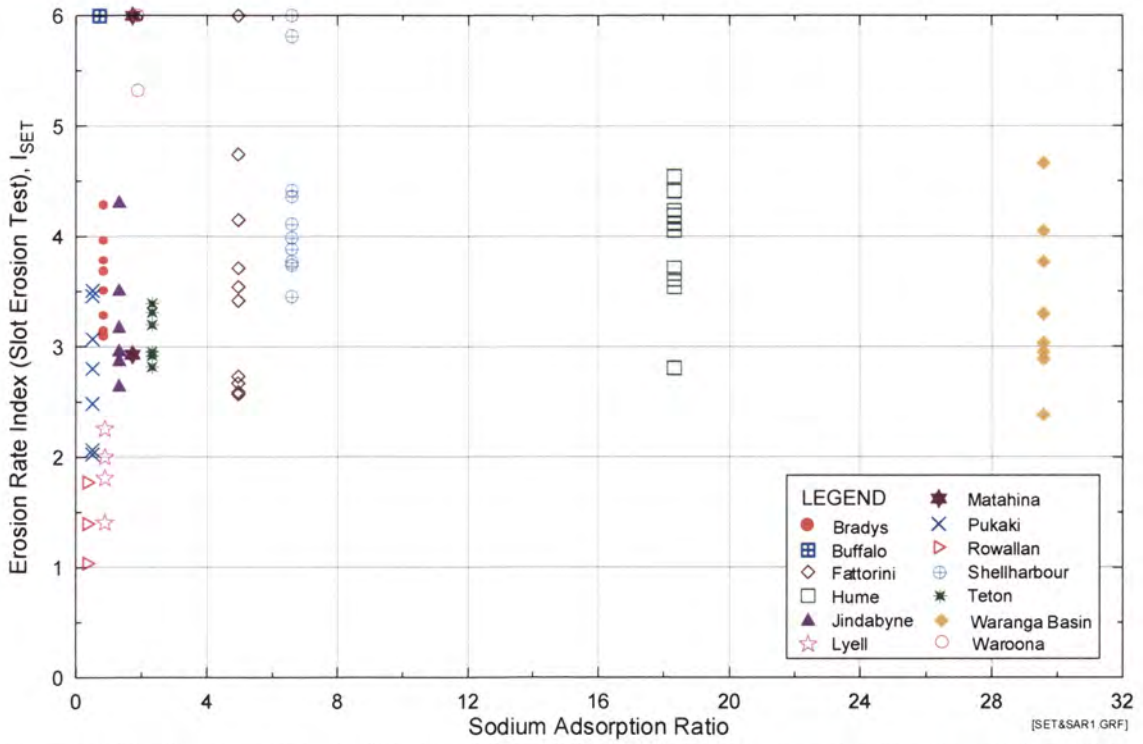

Figure H7a Erosion Rate Index (I_{SET}) from Slot Erosion Test versus Sodium Adsorption Ratio.

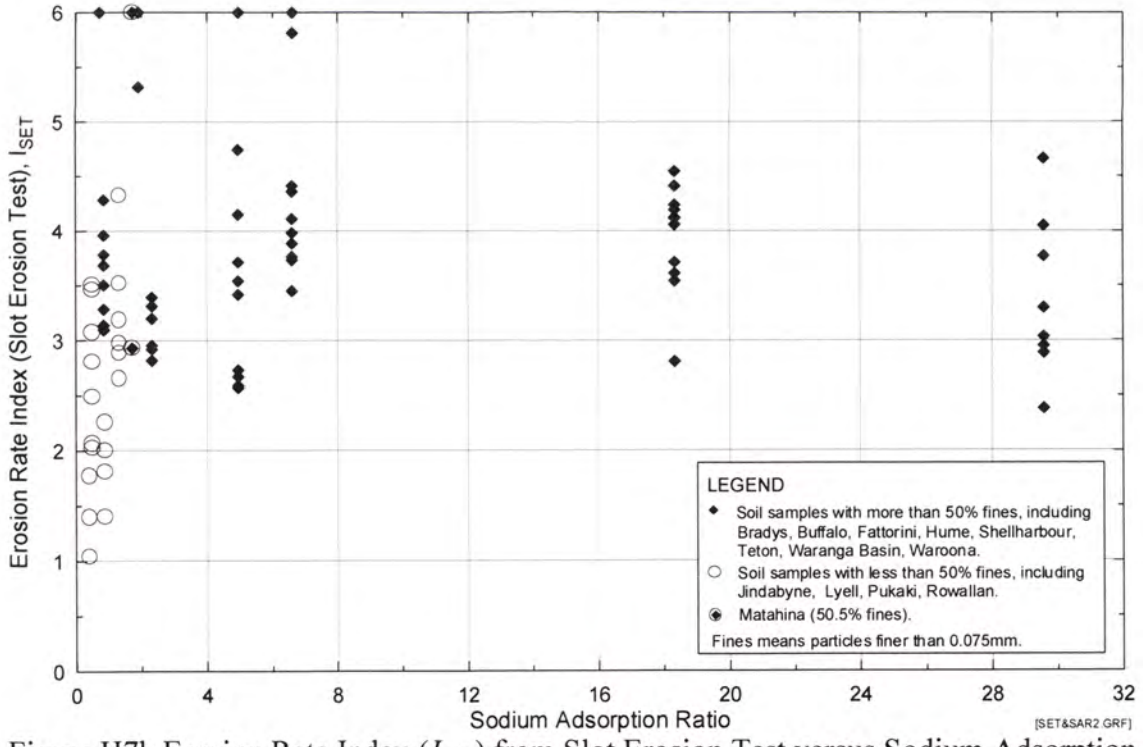

Figure H7b Erosion Rate Index (I_{SET}) from Slot Erosion Test versus Sodium Adsorption Ratio. Soil samples classified into fine-grained and coarse-grained soils.

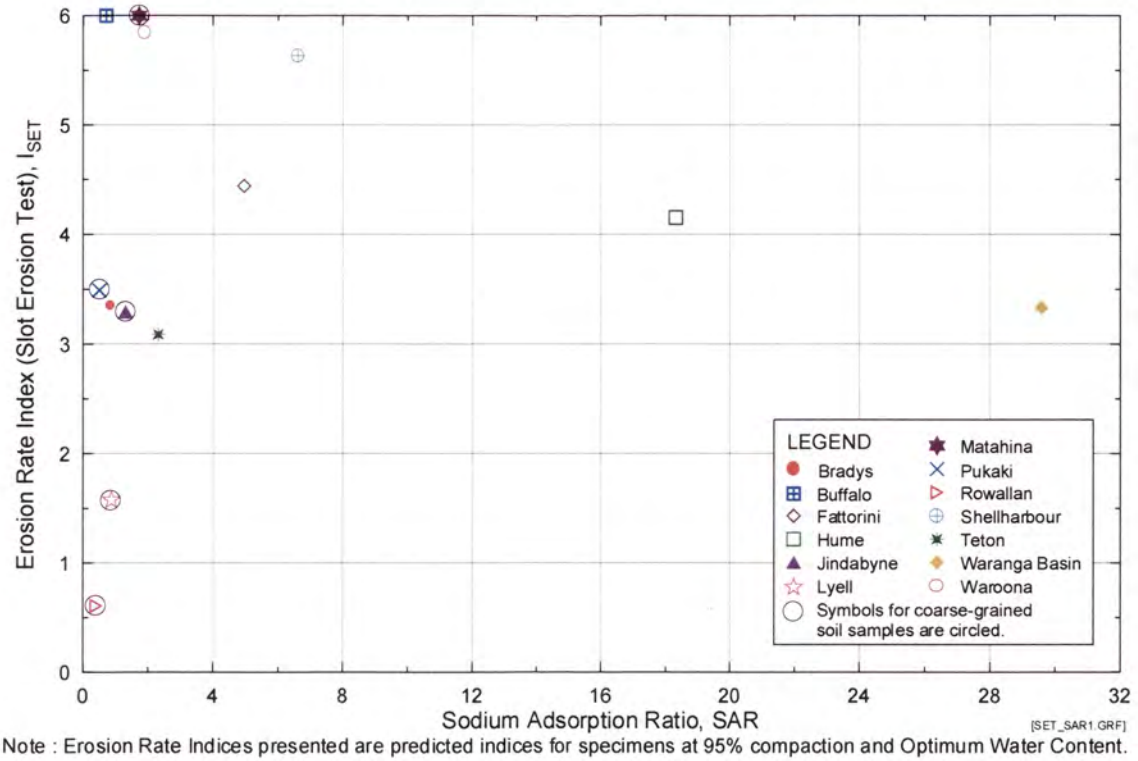

Note : Erosion Rate Indices presented are predicted indices for specimens at 95% compaction and Optimum Water Content.

Figure H7c Predicted Erosion Rate Index (I_{SET}) from Slot Erosion Test versus Sodium Adsorption Ratio.

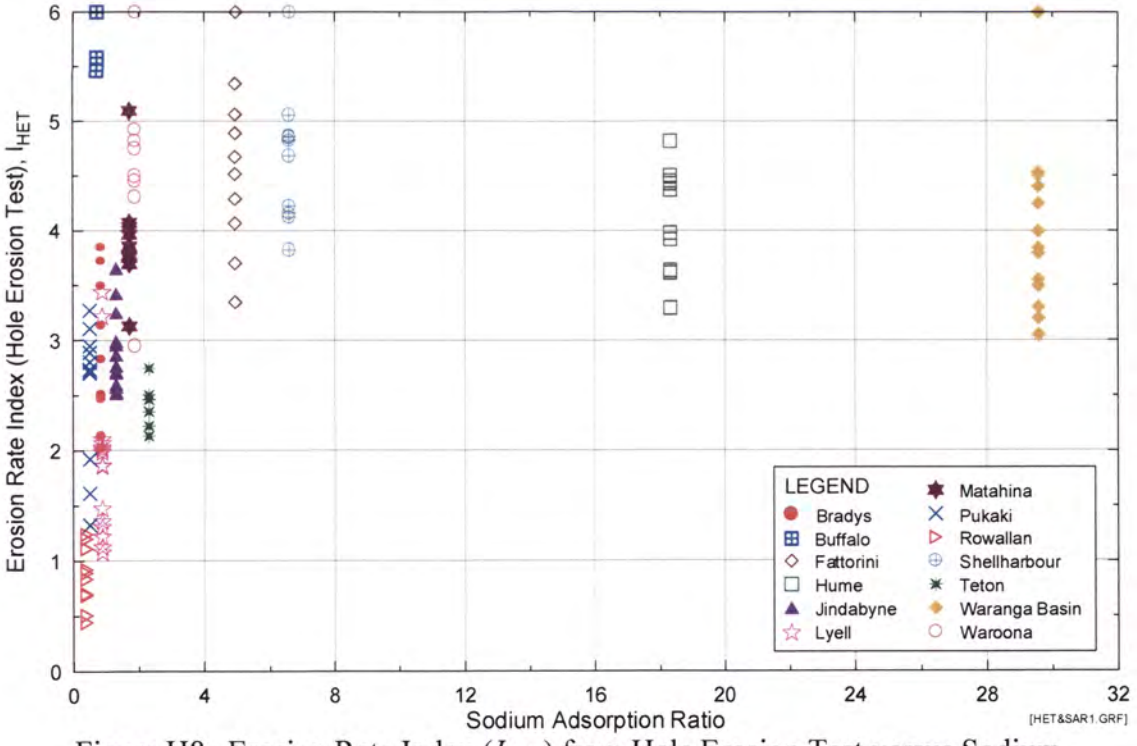

Figure H8a Erosion Rate Index (I_{HET}) from Hole Erosion Test versus Sodium Adsorption Ratio.

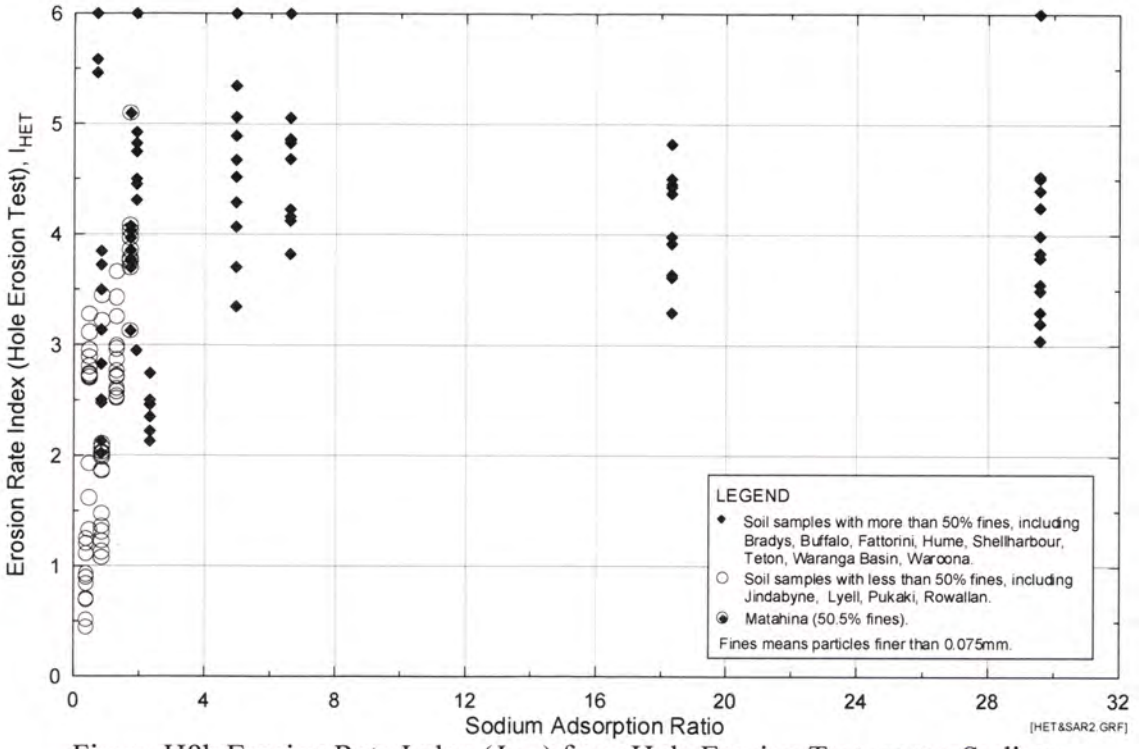

Figure H8b Erosion Rate Index (I_{HET}) from Hole Erosion Test versus Sodium Adsorption Ratio. Soil samples classified into fine-grained and coarse-grained soils.

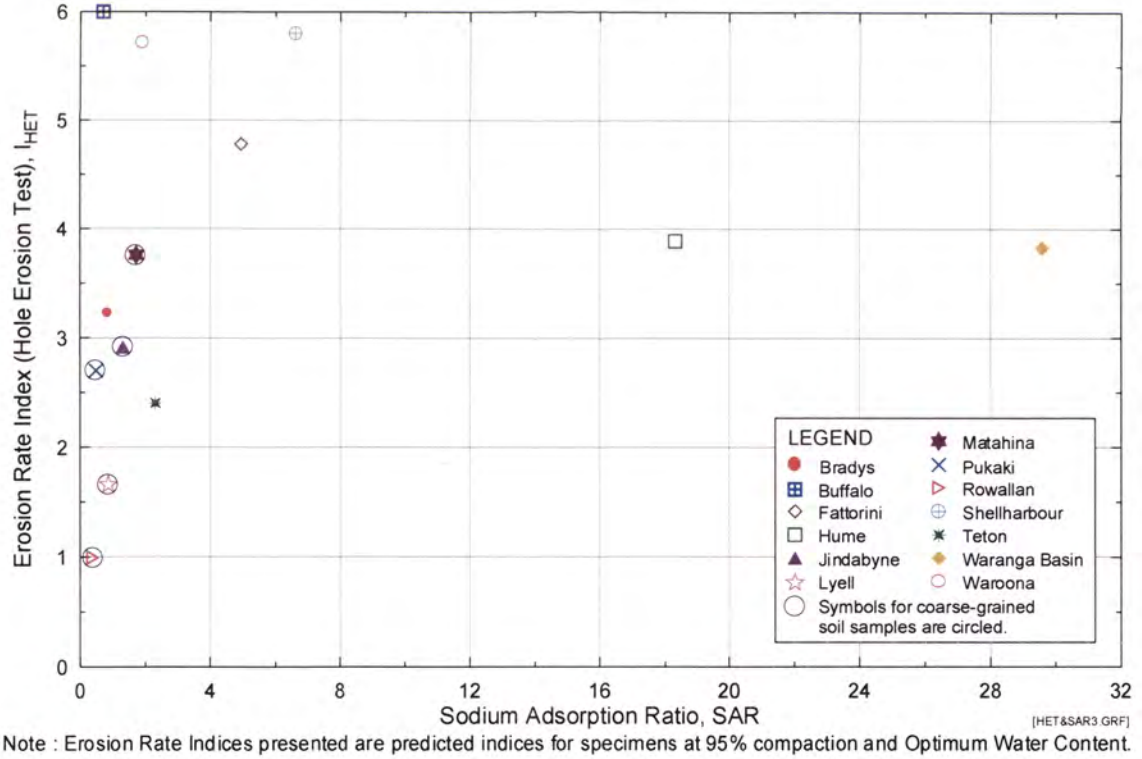

Note : Erosion Rate Indices presented are predicted indices for specimens at 95% compaction and Optimum Water Content.

Figure H8c Predicted Erosion Rate Index ($\tilde{I}_{HET}$) from Hole Erosion Test versus Sodium Adsorption Ratio.

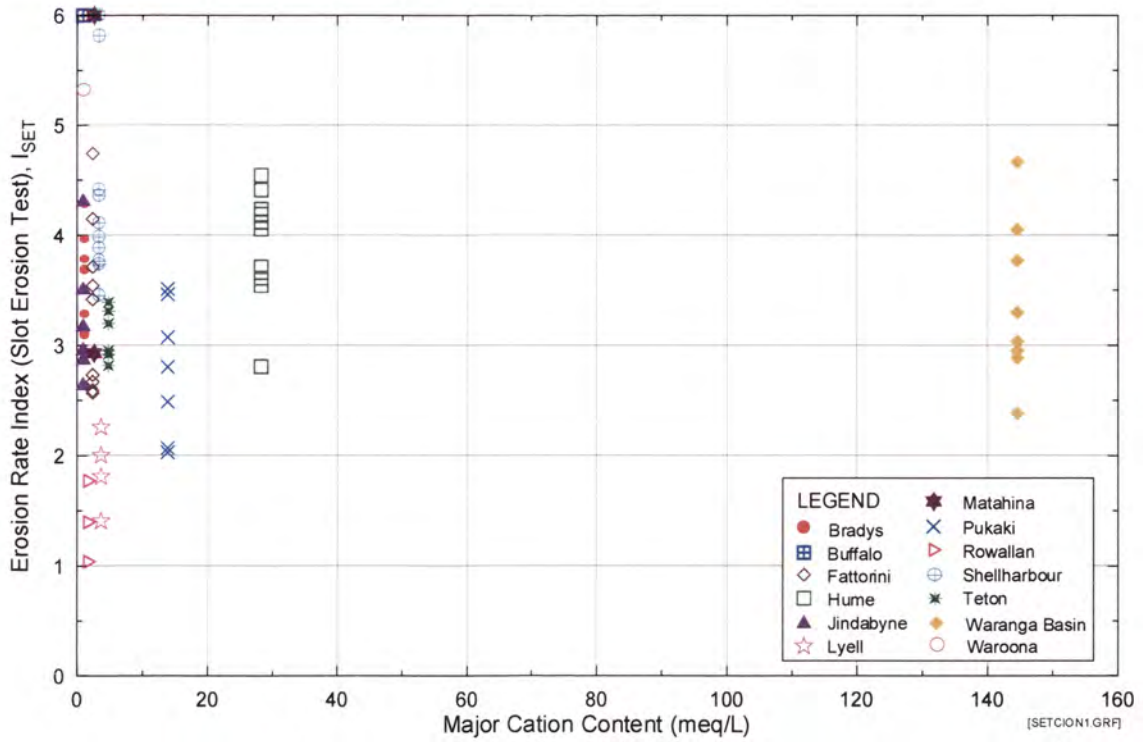

Figure H9a Erosion Rate Index (I_{SET}) from Slot Erosion Test versus Major Cation Content.

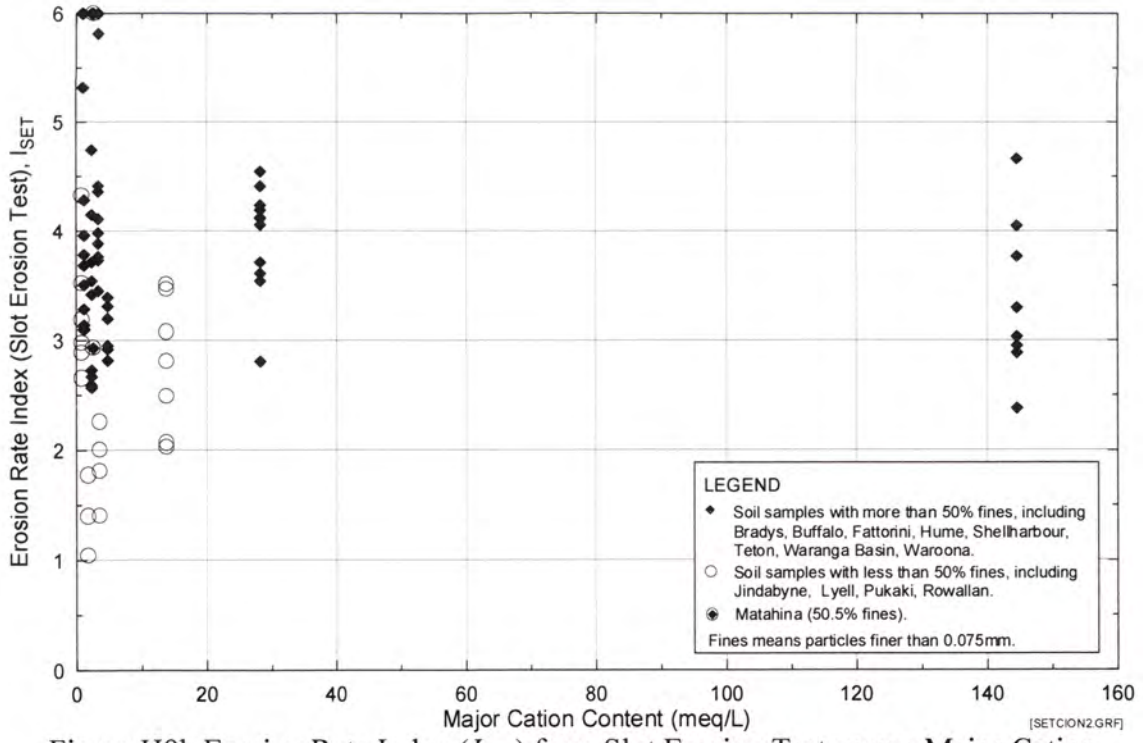

Figure H9b Erosion Rate Index (I_{SET}) from Slot Erosion Test versus Major Cation Content. Soil samples classified into fine-grained and coarse-grained soils.

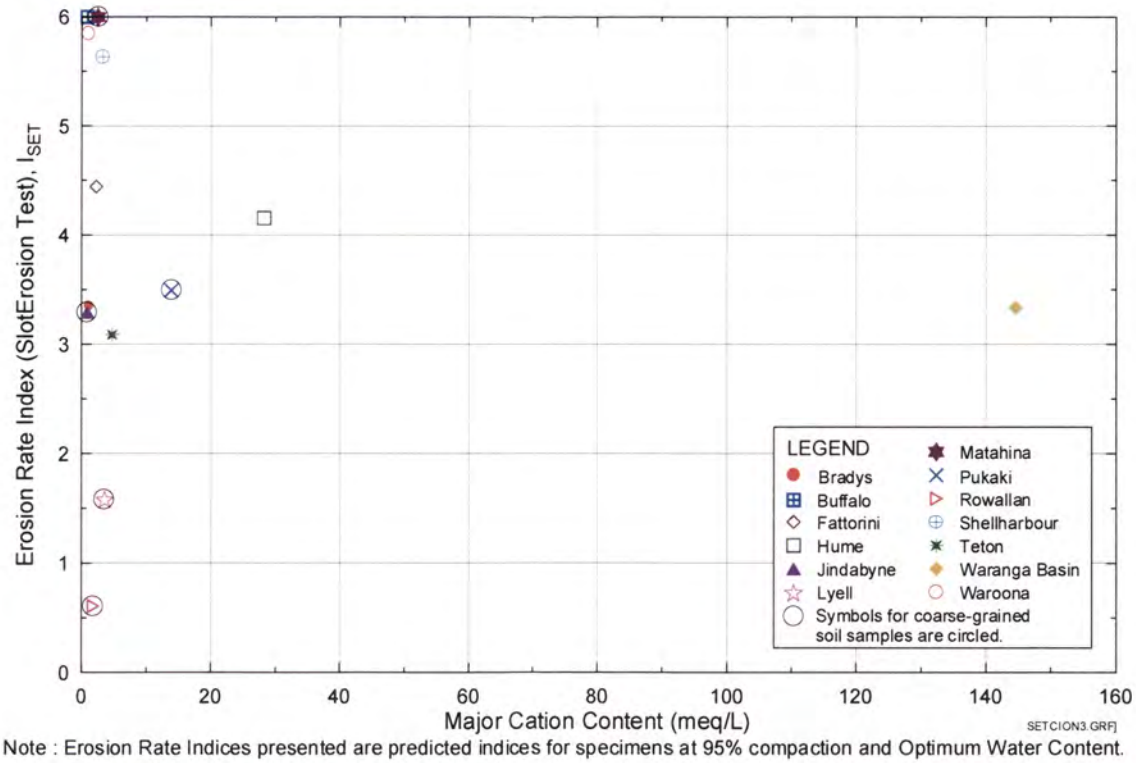

Note : Erosion Rate Indices presented are predicted indices for specimens at 95% compaction and Optimum Water Content.

Figure H9c Predicted Erosion Rate Index (I_{SET}) from Slot Erosion Test versus Major Cation Content.

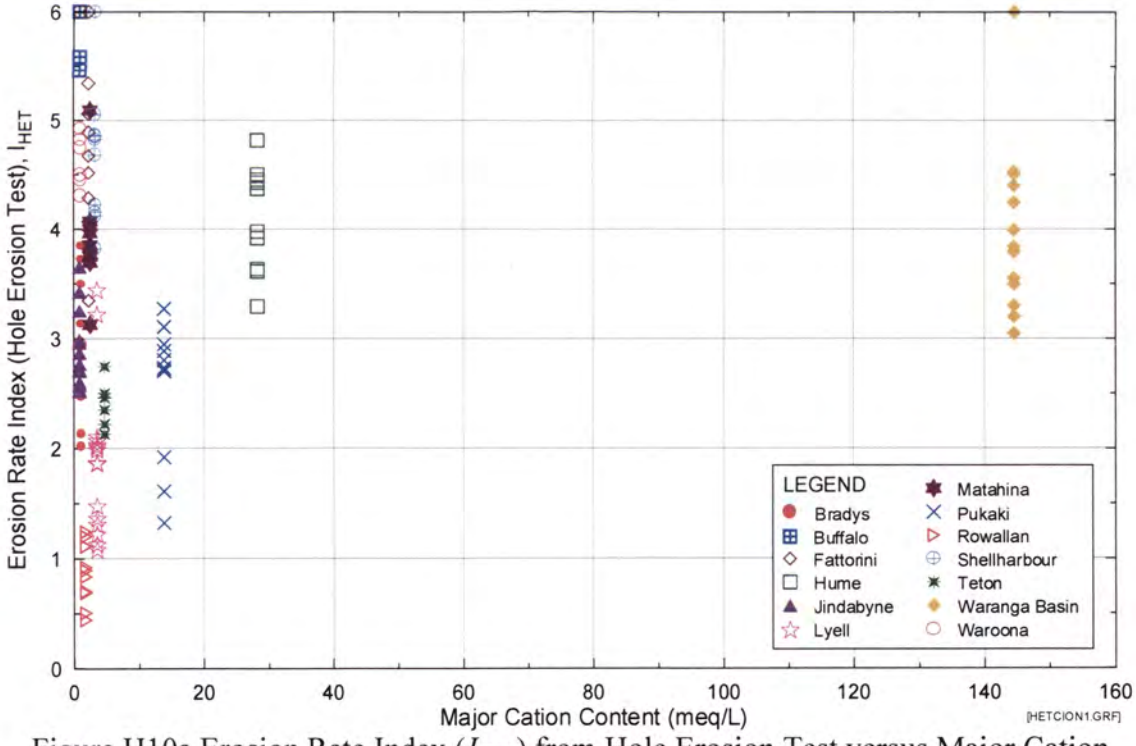

Figure H10a Erosion Rate Index (I_{HET}) from Hole Erosion Test versus Major Cation Content.

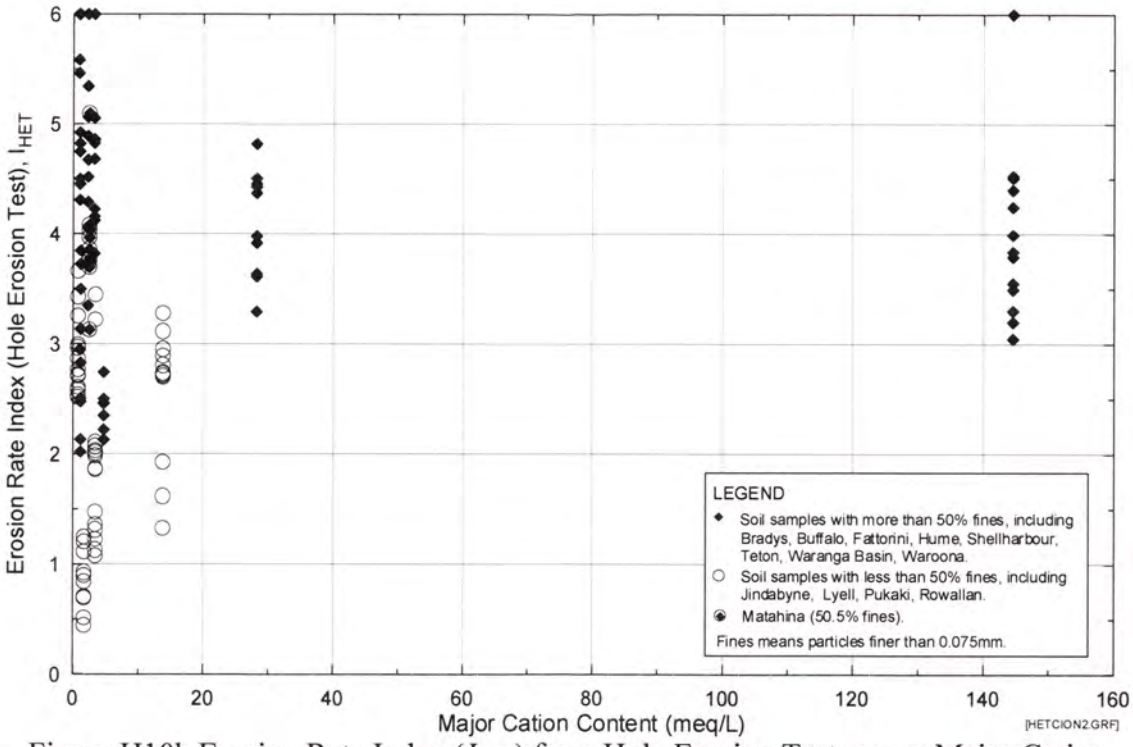

Figure H10b Erosion Rate Index (I_{HET}) from Hole Erosion Test versus Major Cation Content. Soil samples classified into fine-grained and coarse-grained soils.

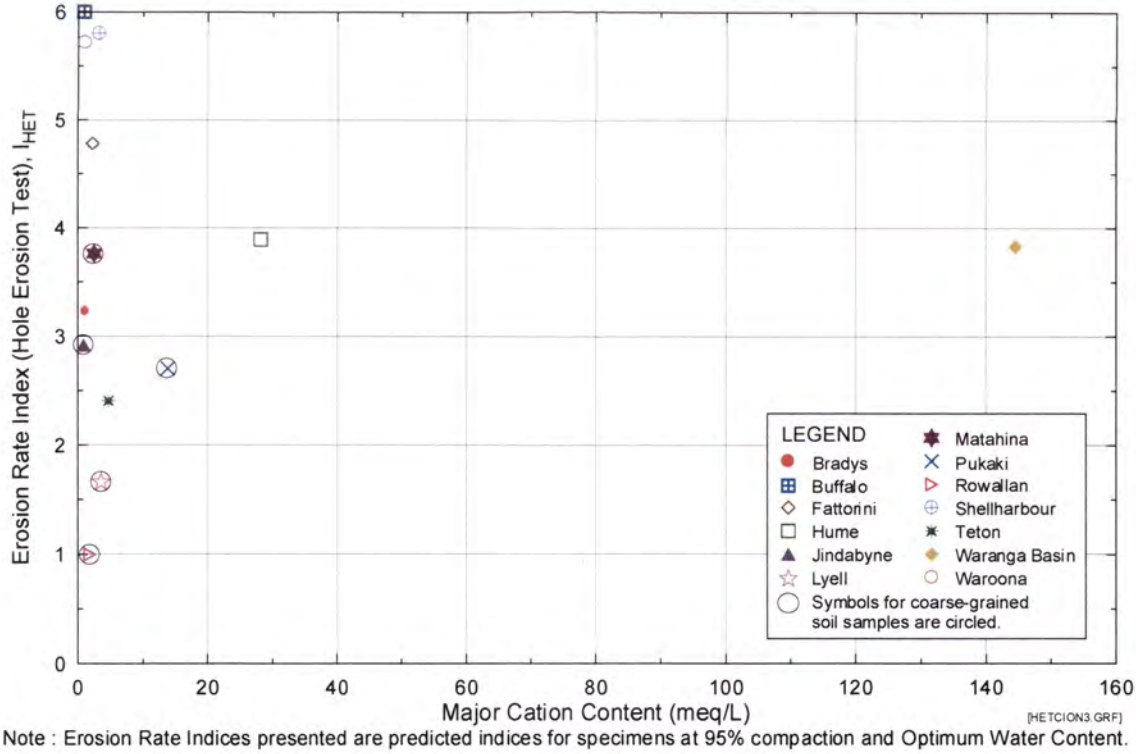

Note : Erosion Rate Indices presented are predicted indices for specimens at 95% compaction and Optimum Water Content.

Figure H10c Predicted Erosion Rate Index ($\tilde{I}_{HET}$) from Hole Erosion Test versus Major Cation Content.

APPENDIX I

Slot Erosion Test Procedure

SLOT EROSION TEST PROCEDURE

(Revised June 2002)

SCOPE

1. SOIL PREPARATION
2. SAMPLE PREPARATION
3. TEST PREPARATION
4. TEST PROCEDURE
5. POST TEST MEASUREMENTS
6. POST TEST ANALYSIS
7. CLEANING AND REASSEMBLY

SLOT EROSION TEST PROCEDURE

(Revised June 2002)

SCOPE

This presentation is a detailed coverage of all test aspects of the Slot Erosion Test.

1. SOIL PREPARATION

(a) Six (6) bags each having an approximate mass of 5kg of the particular soil sample are selected.
(b) Thoroughly mix the soils from each of the six bags, and return the soils to the appropriate bag.
(c) Take the moisture content (*mc*), according to AS1289.2.1.1-1992, for each bag.
(d) Calculation of the compacted height of each layer:
    (i) Open Excel file SLOT.XLS
    (ii) Enter the desired values for compaction and *mc*.
    (iii) Enter the measured values for moisture content.
    (iv) Use results from the spreadsheet to determine layer heights and water to be added to achieve the desired parameters. It may be necessary to reduce the mass of each bag by equal amounts to obtain approximately equal layer heights. The total compacted height of the six layers is 105mm.
(e) Place the sample in a tray on a top pan balance and add the desired amount of water added using an atomiser.
(f) The sample is then mixed thoroughly and placed back in the bag to cure. Curing time will be dependent on the particular soil.

2. SAMPLE PREPARATION

Detailed engineering drawings of the Slot Erosion Test mould and collar are shown in Figures 1 and 2 respectively.

(a) Clean the 20mm form ply top.
(b) Affix this false timber top to the aluminium mould **using low torque and no silicone sealant** using the countersunk screws and nuts.
(c) Rotate the mould through 180 degrees.
(d) Ensure the base-mating surface is clean.
(e) Position the four cleaned piping strips (providing a slot thickness of 2.2mm) and two end retaining plates.
(f) Weigh the mould at this stage. This enables the actual compaction ratio to be determined, when the soil mass and the moisture content of the scraped top layer are used in calculations.

(g) Insert the two end spacers; then attach the aluminium protection collar to the mould. Then attach the compaction support braces.
(h) Starting at one end, evenly distribute one bag of soil, using five equal portions, ensuring that the strips stay together. Carefully work along the mould ensuring even distribution of the soil. Compact the layer to the calculated height. This height can be measured using a straight edge and digital calipers. **Compaction of this first layer is very important as this contains the "slot".**
(i) Repeat step (h) for layers 2, 3, 4, 5 and 6.
(j) Remove the collar and end spacers and trim layer 6 with a straight edge to ensure a completely flat surface.
(k) Weigh the mould.
(l) Trimmed soil is tested for moisture content in accordance with AS1289.2.1.1-1992, and pore fluid is tested for chemical composition (if required).
(m) Place a silicone bead along the soil/mould wall interface and along the mating surfaces. See Figure 3 for sealant application points.
(n) Place the aluminium base plate on the mould and fasten using supplied bolts and nuts, from the centre outwards in a circular pattern.
(o) Clean off any excess silicone sealant.
(p) Carefully rotate the mould through 180 degrees and remove the formply top by tapping sideways and sliding it off. **Do not use any other method, as the compacted soil will adhere to it.**
(q) Carefully remove the four piping strips starting at the centre by prising out with small screwdriver.
(r) Carefully remove the end retaining plates
(s) Place the 10 x 10mm-wire mesh in the inlet chamber and distribute 20mm aggregate in the chamber taking care not to taking care not to block the openings. This includes the slot.
(t) Place another silicone bead on the top surface in a similar manner to the base, along the soil/mould wall interfaces and the mating surfaces, ensuring that it does enter the slot when the top is secured.
(u) Secure the perspex top in the same manner as the base. **Do not over tighten.**
(v) Cover up both the inlet and outlet pipefitting and allow the soil specimen to equilibrate for 24 hours.

3. TEST PREPARATION

(a) Carefully transfer the mould assembly to the hydraulic trolley and position it on the locating bracket with the inlet to the left.
(b) Make two uniform size labels for the test using the label form template LABEL.DOC.
(d) Install pressure gauges in the inlet and outlet chambers.
(e) Connect the constant head system, comprising the supply tanks, pump, constant head tank and overflow. The upstream constant head tank should be securely supported on the tower and initially set to provide a head of approximately **4.5m** or **2.5m** at the upstream side.
(f) Connect the rotameter to the inlet end of the sample box, making sure to flush the rotameter before connecting. **Close valve after connecting to prevent introduction of water into the system upstream end.**

(g) Secure the outlet pipe to the downstream constant head tank at the outlet end of the sample box.
(h) Position the two timers – one facing the discharge point, with the other facing outwards from the mould assembly.
(i) Set up and level the tripod for the digital camera.
(j) Frame the camera.
(k) Fill the outlet tank to the top of the weir. Ensure there is an adequate water supply at hand to replace that used in flooding the outlet chamber.
(l) Record the water temperature of the supply tank.
(m) Ensure that the rubber seals at the top of the pressure gauges are released and that the bleed valves on both gauges are open.

4. TEST PROCEDURE

(a) Carefully open the downstream valve and introduce water into the outlet chamber, filling the outlet chamber and flooding the slot. **It is very important that care is exercised when carrying out this operation, to prevent erosion caused by the rapid passage of water along the slot.** Close the bleed valve when all air is expelled and shut the valve at the outlet end. Immediately top up the downstream tank.
(b) Fully open the inlet valve and fill the inlet chamber until all air is expelled. Close the bleed valve and inlet valve.
(c) Collect a water sample from the constant head tank for testing of salt concentration (if required).
(d) Take a camera shot at zero time.
(e) Fully turn on the valve at the inlet end, and then fully turn on the valve at the outlet end. Note inlet pressure and flow reading, and start the two timers.
(f) Take photos and record discharge flow rates, along with upstream and downstream pressure readings at 30 seconds, 1 minute, 2 minutes, and 5 minutes. It may be necessary to increase the frequency of readings if erosion is rapid.
(g) Monitor the test at 5-minute intervals. If there is no noticeable erosion and the flow rate does not change after 3 consecutive readings increase the interval to 10 minutes.
(h) If there is no noticeable erosion and the flow rate does not change after 3 consecutive readings at 10-minute intervals increase the interval time to 15 minutes.
(i) Continue monitoring the test at 15minute intervals until the test duration has reached 2 hours, at which point the test is deemed to have been completed. During this period, if there is no change in discharge flow rate, indicating no erosion, the test operator may elect not to take a photograph.
(j) The test may be completed sooner if either of the following conditions is reached.
    (i) Flowrate indicated on the rotameter exceeds 110 L/min
    (ii) The erosion path reaches the soil/mould wall interfaces.
(k) At test completion take a photograph, and trace the erosion path on the perspex top using a non-permanent marker.
(l) Close the outlet valve, and then the inlet valve.
(m) Turn off the pump and begin dismantling equipment.
(n) Having removed inlet and outlet connections, drain excess water.
(o) The mould is now ready for tracings to be reproduced.

5. POST TEST MEASUREMENTS

(b) Place pre cut tracing paper over the perspex top and secure with adhesive tape.
(c) Trace over the erosion path on the perspex top with the same colour marker used during the test.
(d) Record test number and catalogue the tracing.
(e) Use soil scrapers to carefully break the seal and remove the perspex top cover.
(f) Measure the final depth of the pipe at intervals of 50mm.

6. POST TEST ANALYSIS

(a) Download the images from the digital camera, and save them systematically into a file according to the soil type and test number.
(b) Select a number of images that show the progression of the eroded slot over time to the completion of the test.
(c) Convert these selected images into Bitmap format for viewing in the program Turbo CAD Version 5.
(d) Select the length of the mould deemed to be unaffected by end effects during the test, and measure the area of the mould minus these end portions using Turbo CAD for the first image.
(e) Measure the area of the eroded slot along the same length of the mould as determined in (d).
(f) Repeat steps (d) and (e) for each consecutive image selected.
(g) Convert the results obtained for the mould area and slot area for each image to scale.
(h) Divide the value for eroded slot area by the length of the mould used in each image to obtain the average slot width for that time.
(i) Using the post test tracing, check the final average slot width obtained from the final image in (h).
(j) Enter the average slot width and corresponding time into the summary spreadsheet: Slot Erosion Test – Analysis of Test Data.

7. CLEANING AND REASSEMBLY

(a) Remove the soil from the mould using soil scrapers, high-pressure water and scrubbing action, and discard it.
(b) Using perspex scrapers clean all remnants of sealant on the mould and perspex top.
(c) Wipe the form ply base with a damp cloth and reassemble the mould system.

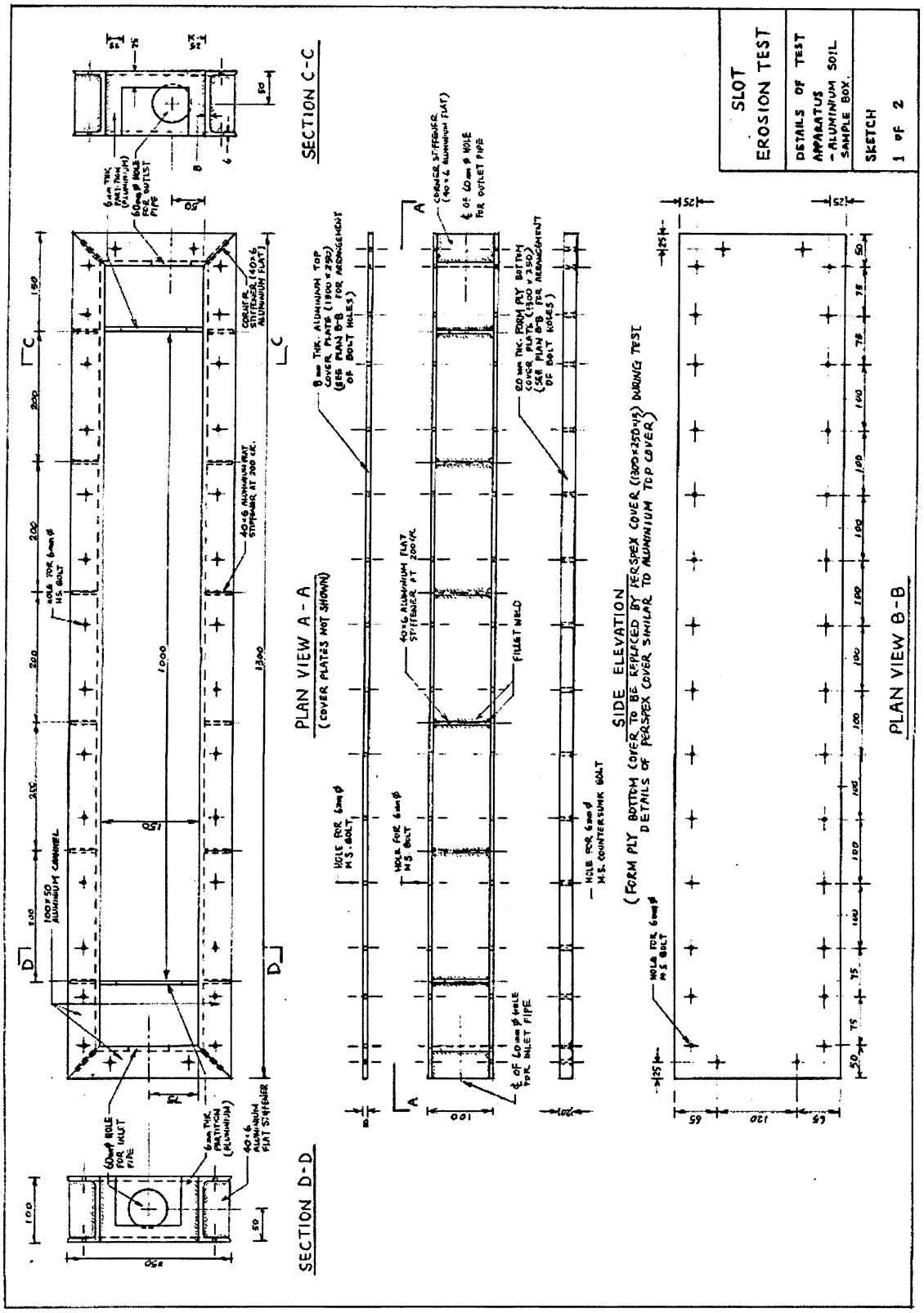

Figure 1 Slot Erosion Test mould

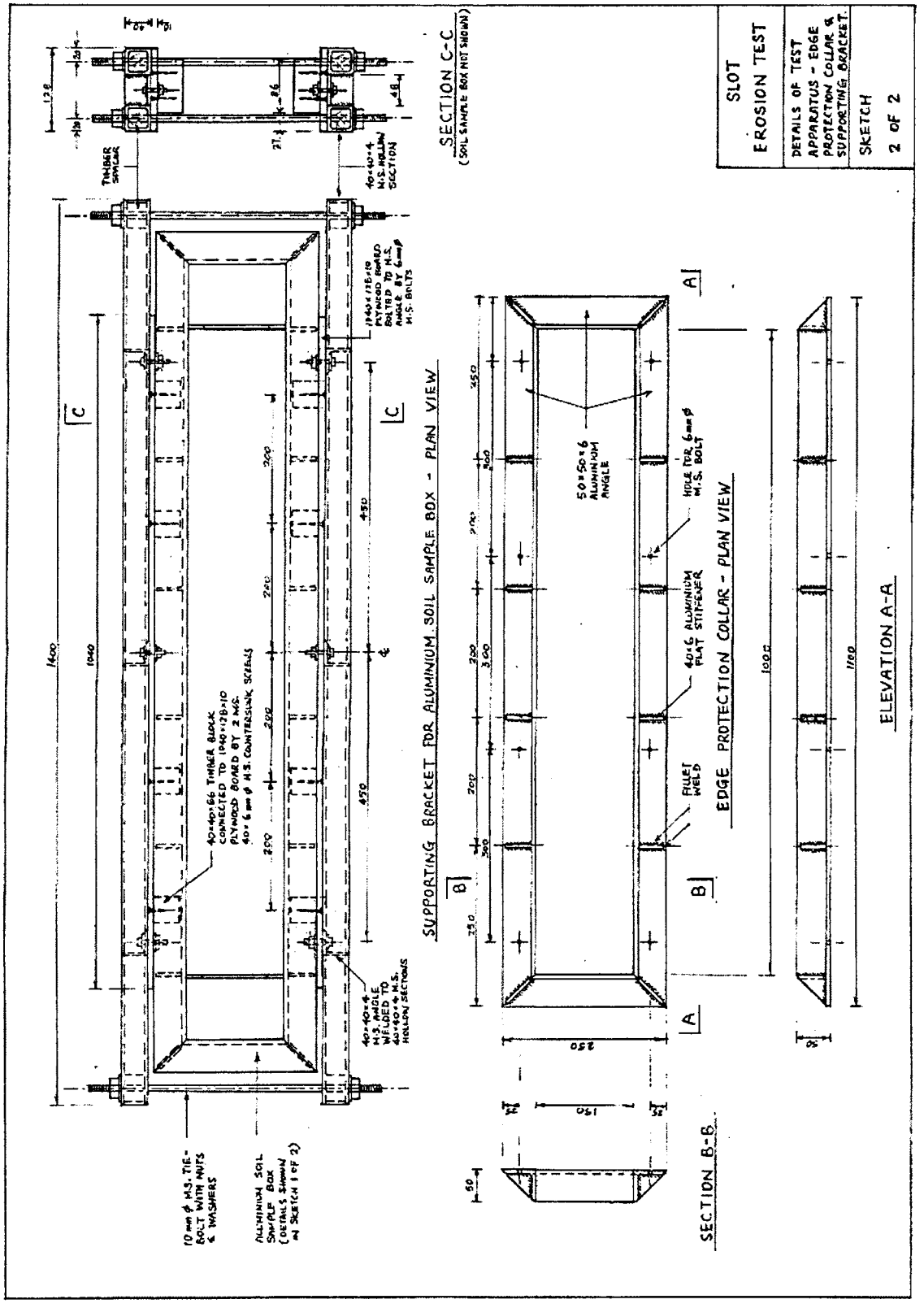

Figure 2 Mould collar

Plan View – Top

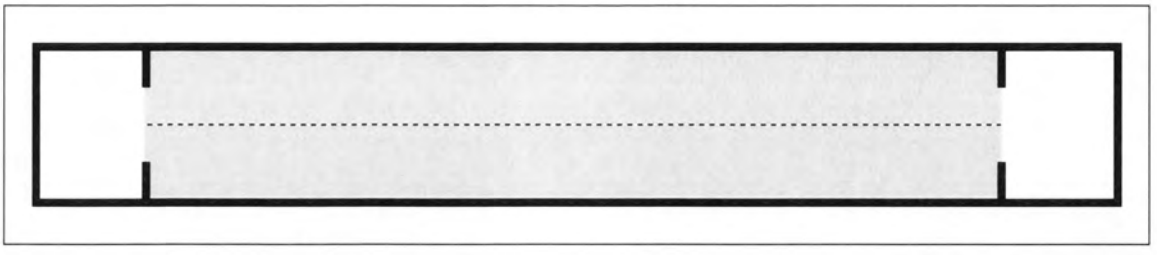

Elevation View

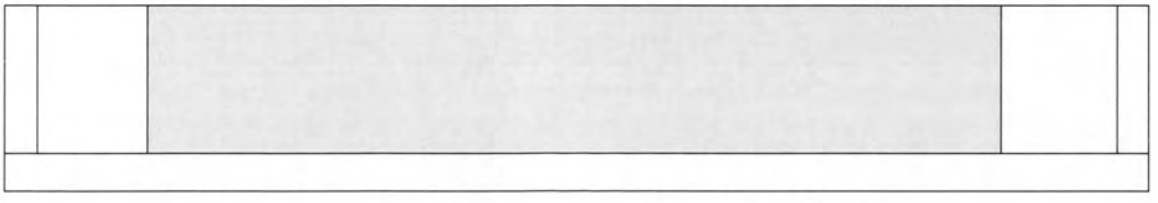

Plan View – Base

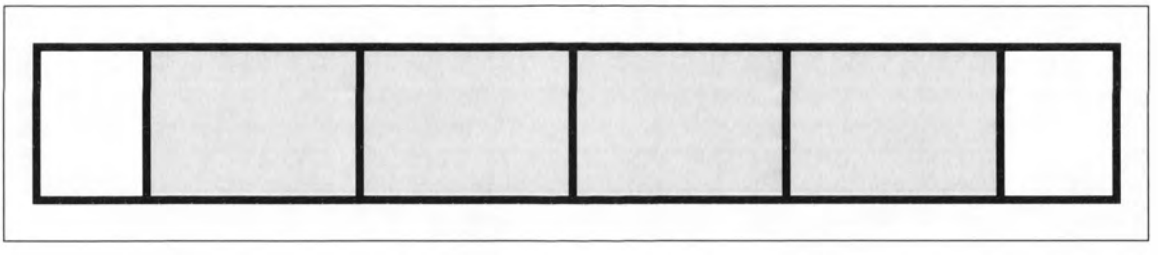

Sealant Application

Figure 3 Sealant application

APPENDIX J

Hole Erosion Test Procedure

HOLE EROSION TEST PROCEDURE

(Revised July 2002)

SCOPE

1. SOIL PREPARATION
2. SAMPLE PREPARATION
3. TEST PREPARATION
4. TEST PROCEDURE
5. POST TEST MEASUREMENTS
6. CLEANING AND REASSEMBLY

HOLE EROSION TEST PROCEDURE

(Revised July 2002)

SCOPE

This presentation is a detailed coverage of all test aspects of the Hole Erosion Test.

1. SOIL PREPARATION

(a) The soils used in Hole Erosion Tests have been sieved through a 6.7mm sieve, properly sub-sampled and bagged. One bag having an approximate mass of 5kg of the particular soil sample is selected.
(b) Thoroughly mix the soil from the bag, and return the soil to the bag.
(c) Take the moisture content (*mc*), according to AS1289.2.1.1-1992, for the bag.
(d) Calculation of the desired compaction control parameters:
    (i) Open Excel file FTE.XLS
    (ii) Enter the desired values for compaction and *mc*.
    (iii) Enter the measured value for moisture content.
    (iv) Use results from the spreadsheet to determine layer heights and water to be added for achieving the desired parameters.
(e) The sample is placed on a tray over a balance and the desired amount of water added using an atomiser.
(f) The sample is then mixed thoroughly and placed back in the bag to cure. Curing time will be dependent on the particular soil.

2. SAMPLE PREPARATION

A detailed engineering drawing of the Hole Erosion Test apparatus is shown in Figure 1.

(a) Clean the test mould, base and collar.
(b) Weigh the mould at this stage. This enables the actual compaction ratio to be determined, when the soil mass and the moisture content of the scraped top layer are used in calculations.
(c) Assemble the mould.
(d) Evenly distribute the first portion of soil. Compact the layer to the calculated height. This height can be measured using a straight edge and digital calipers.
(e) Repeat step (d) for layers 2 and 3.
(f) Remove the collar and trim layer 3 with a straight edge to ensure a completely flat surface.
(g) Remove the mould base and weigh the mould.
(h) Trimmed soil is tested for moisture content in accordance with AS1289.2.1.1-1992, and pore fluid is tested for chemical composition (if required).

(i) Cover up both the upper and lower faces of the mould and allow the soil specimen to equilibrate for at least three hours.

(j) Once the specimen has cured sufficiently, remove the upper and lower covers and transfer the mould to the drill press. Using a 6mm drill bit, drill a hole in the center of the mould along the longitudinal axis of the soil sample.

3. TEST PREPARATION

(a) Carefully transfer the mould to the test apparatus on the hydraulic trolley. Fix the mould between the upper and lower Perspex chambers and tighten.

(b) Raise or lower the trolley to the required height and insert the relevant wooden supports to secure the trolley at that height.

(c) Install the pressure pipes to the inlet and outlet chambers.

(d) Connect the constant head system, comprising the supply tanks, pump, constant head tank and overflow. The upstream constant head tank should be securely supported on the tower and initially set to provide a head of approximately **1.5m** at the upstream side.

(e) **Close the inlet valve after connecting to prevent introduction of water into the system upstream end.**

(f) Secure the outlet pipe to the downstream constant head tank at the outlet end of the sample box.

(g) Position the two timers – one facing the discharge point, with the other facing outwards from the mould assembly.

4. TEST PROCEDURE

(a) Record the water temperature of the supply tank.

(b) Ensure that the valves on both inlet and outlet chambers are open.

(c) Carefully fill the outlet tank to the top of the weir, thus introducing water into the outlet chamber, filling the outlet chamber and flooding the pipe. **It is very important that care is exercised when carrying out this operation, to prevent erosion caused by the rapid passage of water along the pipe**. Close the bleed valve when all air is expelled. Immediately top up the downstream tank.

(d) Fully open the inlet valve and fill the inlet chamber and start the two timers.

(e) Record discharge flowrates, along with upstream and downstream pressure at consecutive readings of 1 minute. It may be necessary to increase the frequency of readings if erosion is rapid.

(f) If there is no noticeable erosion and the flow rate does not change after 3 consecutive readings increase the interval to 2 minutes.

(g) If there is no noticeable erosion and the flow rate does not change after 3 consecutive readings at 2-minute intervals, increase the interval time to 5 minutes.

(h) Continue monitoring the test at 5-minute intervals until the test duration has reached 2hours, at which point the test is deemed to have been completed.

(i) The test may be completed sooner if either of the following conditions is reached.
    (i) Flowrate indicated by outflow measurement exceeds 12 L/min
    (ii) The erosion path reaches the soil/mould wall interfaces.

(j) At test completion close the inlet valve.

(k) Turn off the pump.

(l) Having removed inlet and outlet connections, drain excess water and begin dismantling equipment.

5. POST TEST MEASUREMENTS

(a) Photograph the upstream and downstream ends of the pipe with the appropriate label after the sample has dried sufficiently after the test to allow for extruding the test specimen from the mould.
(b) Measure the final width of the pipe at intervals of 28mm ($1/5^{th}$ positions), and measure the distance of erosion into the upstream and downstream ends of the pipe.

6. CLEANING AND REASSEMBLY

(a) Remove the soil from the mould using the soil extruder and discard it.
(b) Using a wire brush clean all remnants of soil on the mould, and reassemble the mould.

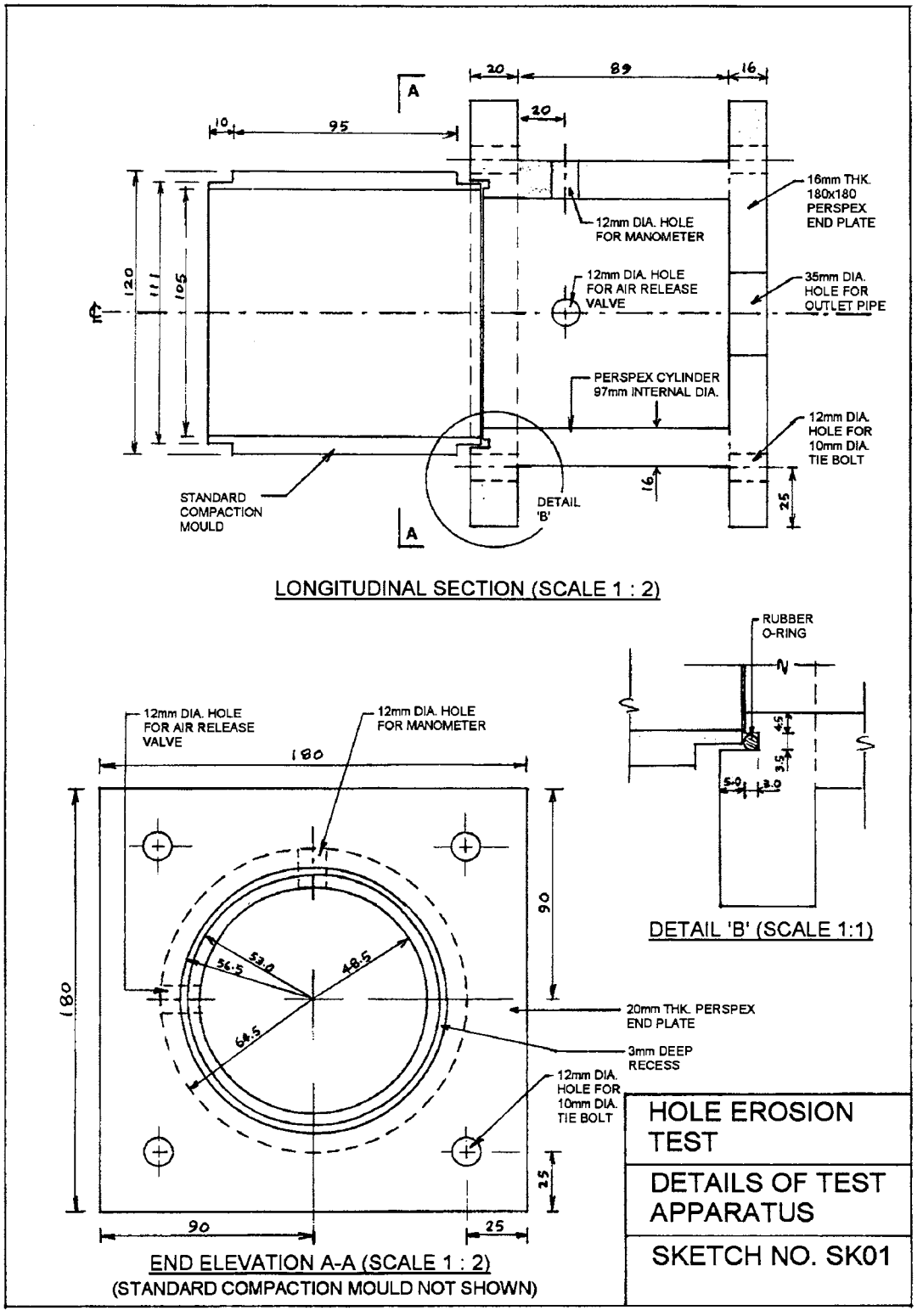

Figure 1 Hole Erosion Test Apparatus

APPENDIX K

X-Ray Powder Diffraction Analysis of Soil Samples

X-RAY POWDER DIFFRACTION ANALYSIS OF EIGHT SOIL SAMPLES

By

Dr Ervin Slansky
School of Geology
THE UNIVERSITY OF NEW SOUTH WALES

For

School of Civil and
Environmental Engineering
(Mr Chi-Fai-Wan)

April 2001

X-RAY POWDER DIFFRACTION ANALYSIS OF EIGHT SOIL SAMPLES

The work involved in the preparation of this report was undertaken in the X-ray Diffraction Laboratory of the School of Geology, University of New South Wales.

Samples Received

Eight soil samples were received for X-ray powder diffraction analysis:

1. Hume Bank 1 (Tertiary Alluvial)
2. Fattorini Dam
3. Shellharbour (Basalt)
4. Brady's Dam
5. Waroona Dam (Embankment Fill (granite))
6. Lyell Dam (granite)
7. Jindabyne Dam
8. Rowallan Dam

Analytical Data

The analysis was carried out by monochromatized CuKα radiation using a Philips X'Pert system. All samples were examined as received and as oriented aggregates of the clay fraction (< 2μm *e.s.d.*) obtained by centrifugation from samples dispersed in water. The oriented specimens on glass slides were prepared by the membrane filter transfer method and subsequently examined air dry, after ethylene glycol solvation and after heating to 400°C for one hour. This is a standard procedure for the identification of clay minerals.

The data from the natural (as received) powdered specimens were processed by computer; a search match program included in WINPlot (CSIRO, Division of Soils) was used for the identification of mineral phases. The program uses the current ICCD (International Centre for Diffraction Data) Powder Diffraction File™ covering experimental data (sets 1 to 50) as well as calculated patterns (sets (70 and higher).

The results of the X-ray powder diffraction analysis of the natural (as received) as well as the oriented samples of the clay fraction are given in Tables 1 and 2, respectively. The diffractometer traces obtained in the course of the examination are

attached. The principal peaks of significant minerals are marked using the following abbreviations:

an = anatase
cl = chlorite
flsp = feldspar(s)
gibb = gibbsite
goeth = goethite
gyps = gypsum
hall = halloysite
hem = hematite
ill = illite
kaol = kaolinite
mic = mica
m-l = mixed-layer mica/smectite
qtz = quartz
sm = smectite
verm = vermiculite

Comment

The X-ray examination of the **samples as received** showed a variety of mineral compositions apparently reflecting different provenance of the samples submitted. Of the common non-clay rock forming minerals *quartz* and *feldspar(s)* are the most widespread, the former being generally more abundant than the latter except for the samples from Lyell and Rowallan Dams.

In the **clay fraction** of the samples examined *kaolinite* is the most frequently occurring mineral. *Illite* is second in the incidence of occurrence, while *smectite* was identified in only a half of the samples submitted. Mixed-layer *mica/smectite* occurs in a larger quantity in one sample only (Fattorini). *Vermiculite* and *chlorite* were identified each in one instance only. The latter mineral may contain some extraneous expandable layers as it slightly contracts when heated.

Ervin Slansky, RNDr, PhD
April 21, 2001

Table 1
Mineral Composition of Samples as Received

Sample / Mineral	Hume Bank 1	Fattorini Dam	Shellharbour	Brady's Dam
Quartz	A-M	A	M	A
Feldspar(s	S	S	A-M	T
Kaolinite	M-S	S	-	M
Illite/mica	M-S	T	T	T
Smectite	S-T	S-T	-	S
Mixed-layer mica/smectite	-	T	T	-
Halloysite	-	-	M	-
Goethite	T-S	S	S	-
Hematite	-	-	S	-
Gibbsite	-	-	-	-
Anatase	T	S	T	T
Siderite	T	-	-	-
Calcite	-	-	?T	?T
Gypsum	-	-	-	-
Jarosite	-	-	-	-

Table 1 Cont'd.

Sample / Mineral	Waroona Dam	Lyell Dam	Jindabyne Dam	Rowallan Dam
Quartz	A	M	A	A
Feldspar(s	S-T	A	M	M
Kaolinite	M	S-T	S	S
Illite/mica	T	-	M	S
Smectite	-	-	T-S	-
Vermiculite	-	T	-	-
Mixed-layer mica/smectite	-	-	-	-
Chlorite	-	-	-	S
Goethite	T	-	-	-
Hematite	-	-	-	-
Gibbsite	M-S	-	-	-
Anatase	-	T	-T	?T
Siderite	-	-	-	-
Calcite	-	-	-	-
Gypsum	-	-	-	-
Jarosite	-	T	T	-

Table 2
Mineral Composition of the Clay Fraction

Sample / Mineral	Hume Bank 1	Fattorini Dam	Shellharbour	Brady's Dam
Kaolinite	M (30)	M (23)	D**	D (79)
Illite/mica	A (51)	A (57)	-	-
Mixed-layer mica/smectite	-	*	T	-
Smectite	S (19)	S (20)	-	M (21)
Vermiculite	-	-	-	-

* estimate for both illite/mica and mixed-layer mica/smectite
** kaolin mineral is halloysite

Table 2 Cont'd.

Sample / Mineral	Waroona Dam	Lyell Dam	Jindabyne Dam	Rowallan Dam
Kaolinite	D (87)	D	A (53)	M
Illite/mica	S (13)	-	M (30)	-
Mixed-layer mica/smectite	-	-	-	-
Smectite	-	-	S (17)	T
Vermiculite	-	S	-	-
Chlorite	-	-	-	A***

*** may contain some expandable layers

The letters D, A, M, S, T denote semi-quantitative estimates of mineral percentages:

D = dominant (>60%)
A = abundant (60 - 40 %)
M = moderate (40 - 20%)
S = small (20 - 5%)
T = traces (<5%)

The numbers in brackets in Table 2 are semi-quantitative estimates of clay minerals by the method of Griffin (in Carver, *Procedures in Sedimentary Petrology*, New York 1970) using peak heights.

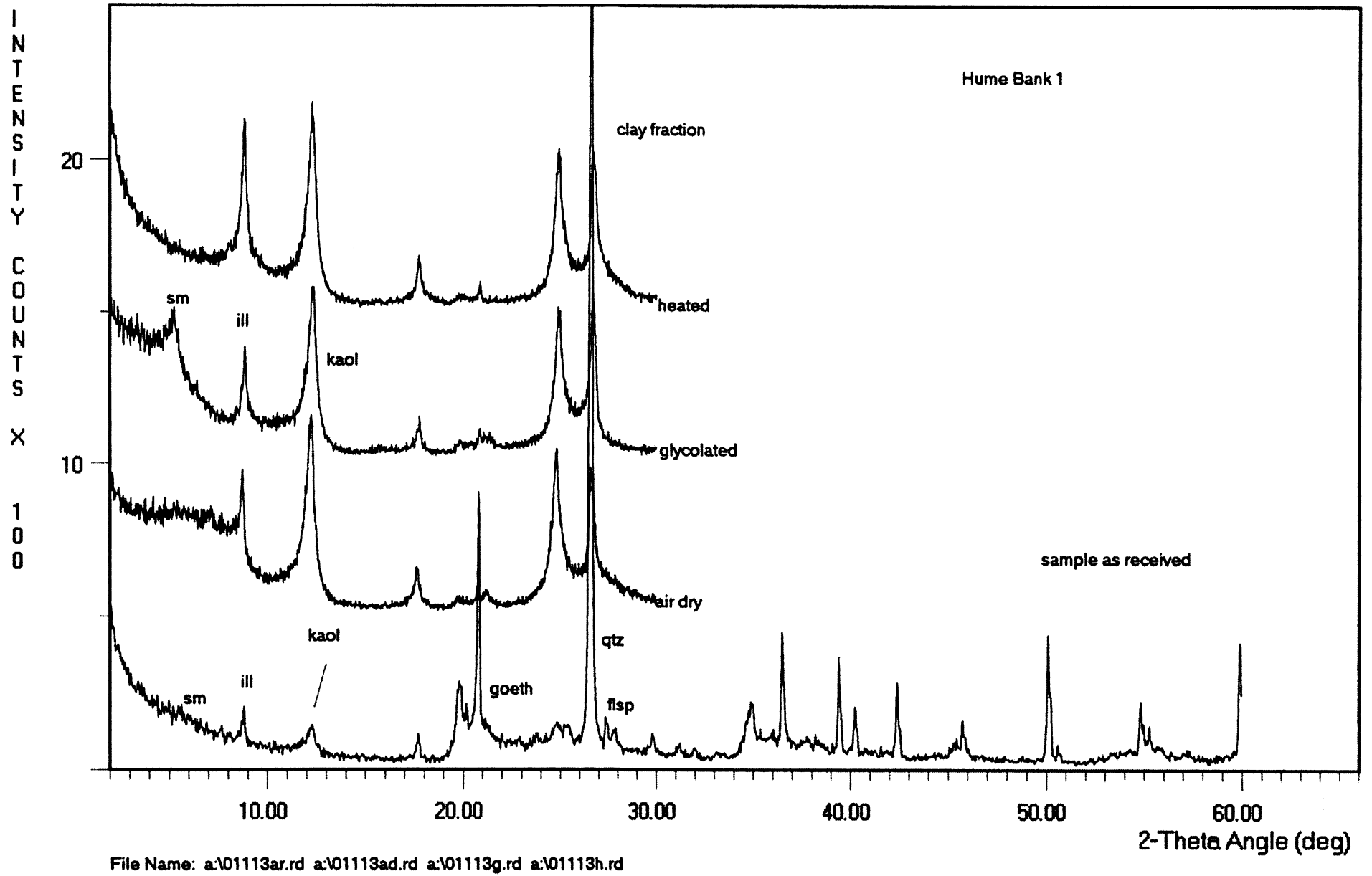

File Name: a:\01113ar.rd a:\01113ad.rd a:\01113g.rd a:\01113h.rd

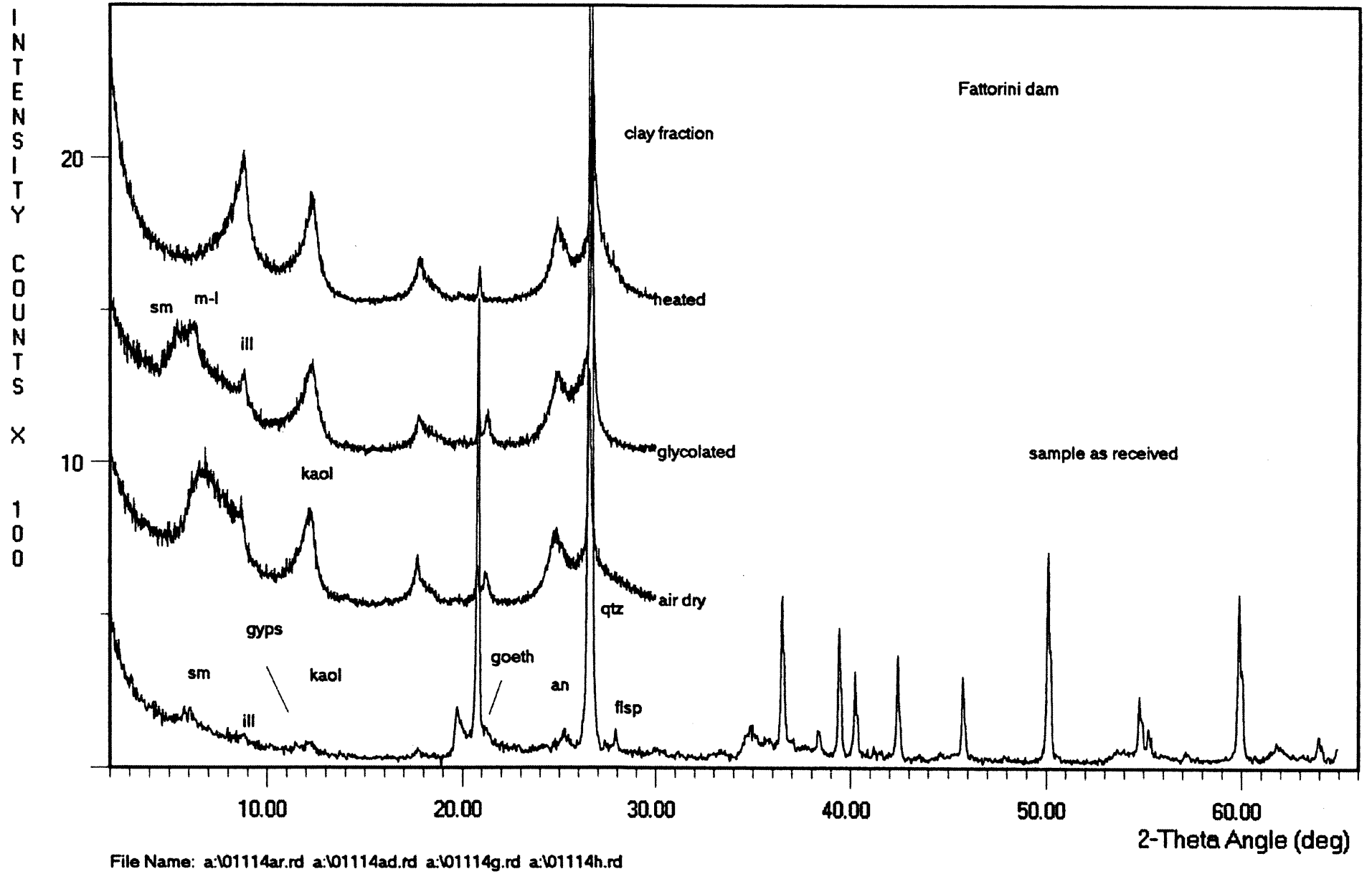
INTENSITY COUNTS X 100
20
10
Fattorini dam
clay fraction
heated
glycolated
air dry
sample as received
sm
m-l
ill
kaol
gyps
sm
kaol
ill
goeth
an
qtz
flsp
10.00
20.00
30.00
40.00
50.00
60.00
2-Theta Angle (deg)
File Name: a:\01114ar.rd a:\01114ad.rd a:\01114g.rd a:\01114h.rd

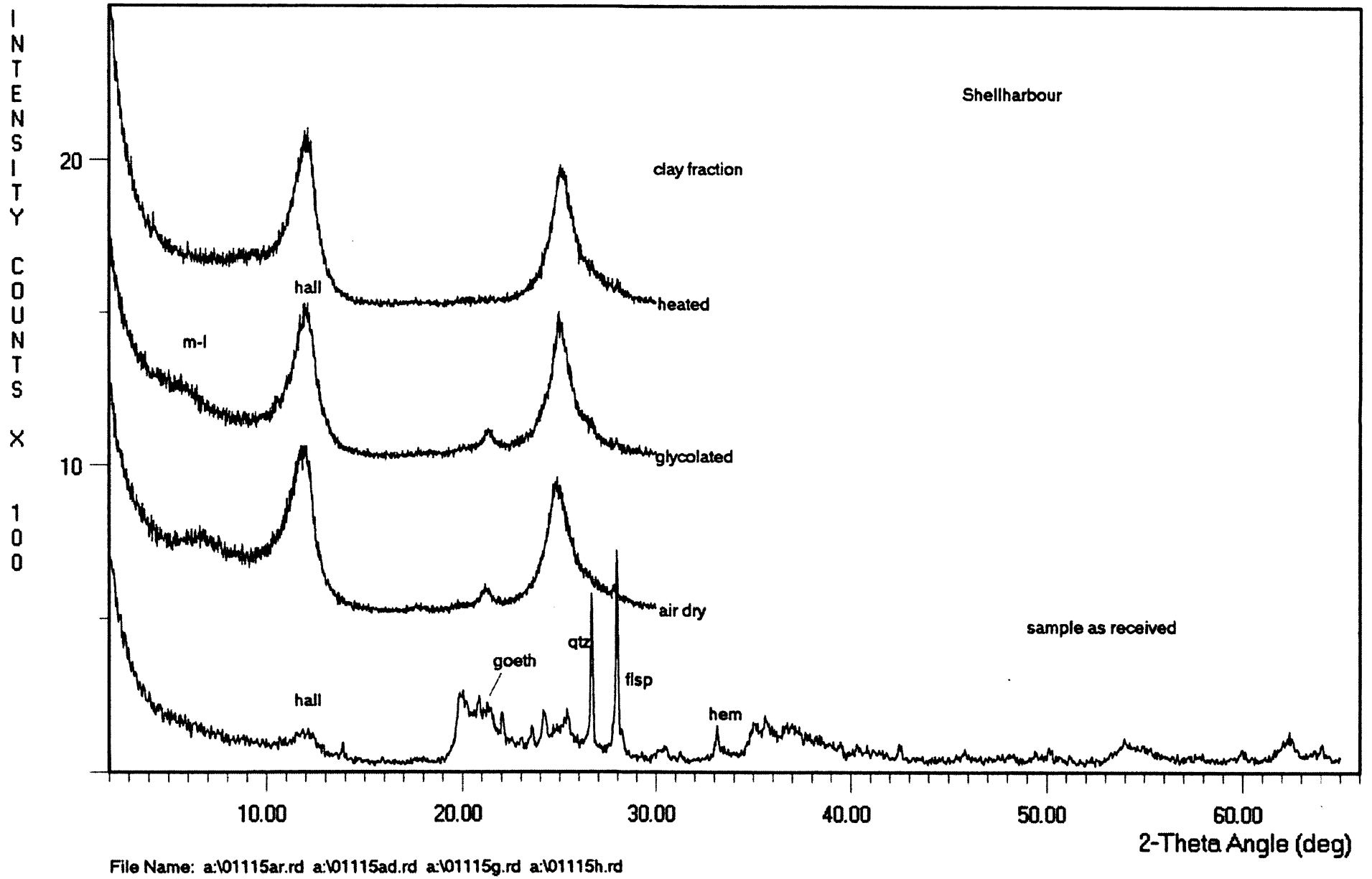
INTENSITY COUNTS X 100
20
10
Shellharbour
clay fraction
hall
heated
m-l
glycolated
air dry
sample as received
qtz
goeth
flsp
hall
hem
10.00
20.00
30.00
40.00
50.00
60.00
2-Theta Angle (deg)
File Name: a:\01115ar.rd a:\01115ad.rd a:\01115g.rd a:\01115h.rd

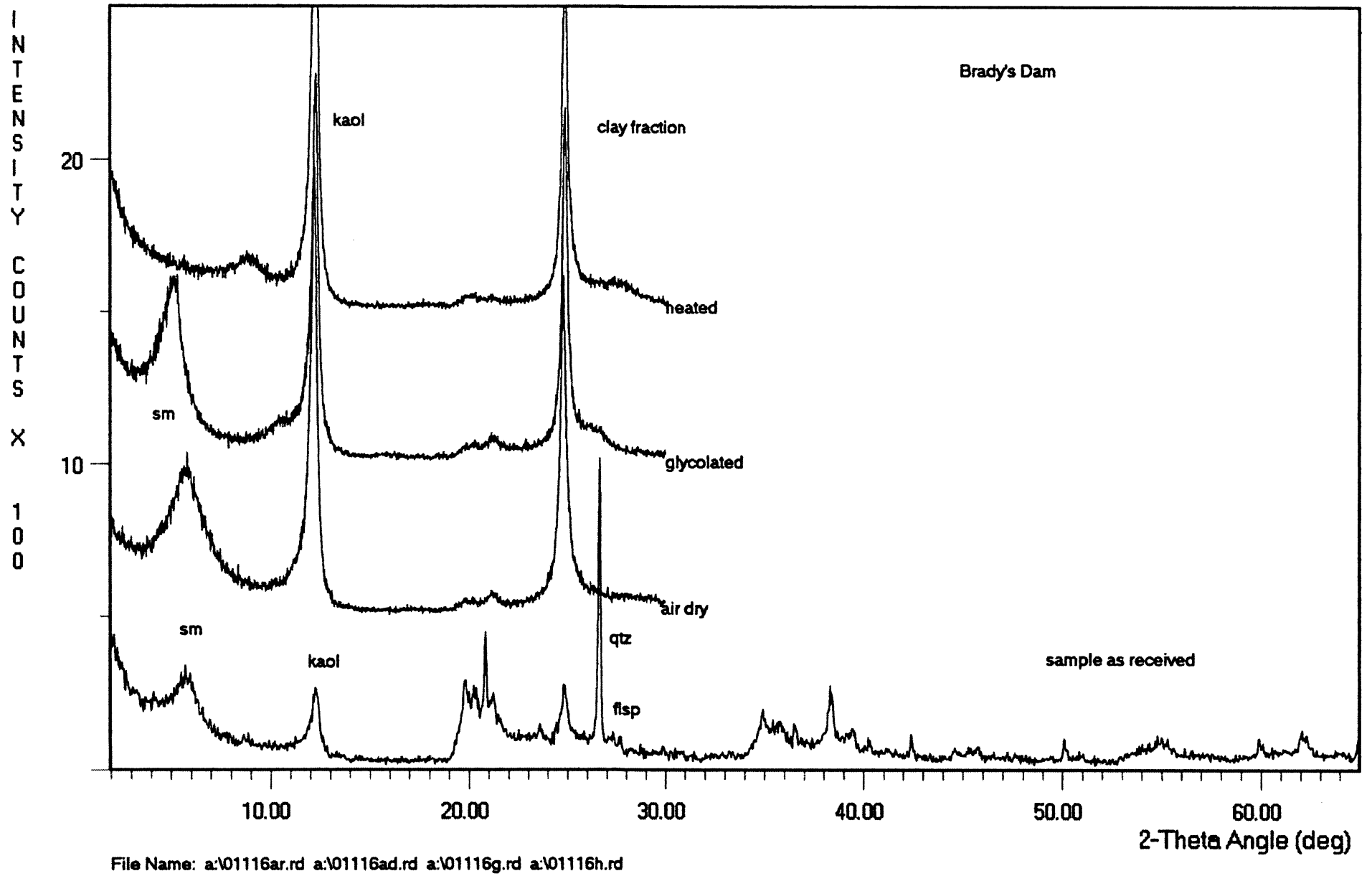
INTENSITY COUNTS X 100
20
10
Brady's Dam
kaol
clay fraction
heated
sm
glycolated
air dry
sm
kaol
qtz
fisp
sample as received
10.00
20.00
30.00
40.00
50.00
60.00
2-Theta Angle (deg)
File Name: a:\01116ar.rd a:\01116ad.rd a:\01116g.rd a:\01116h.rd

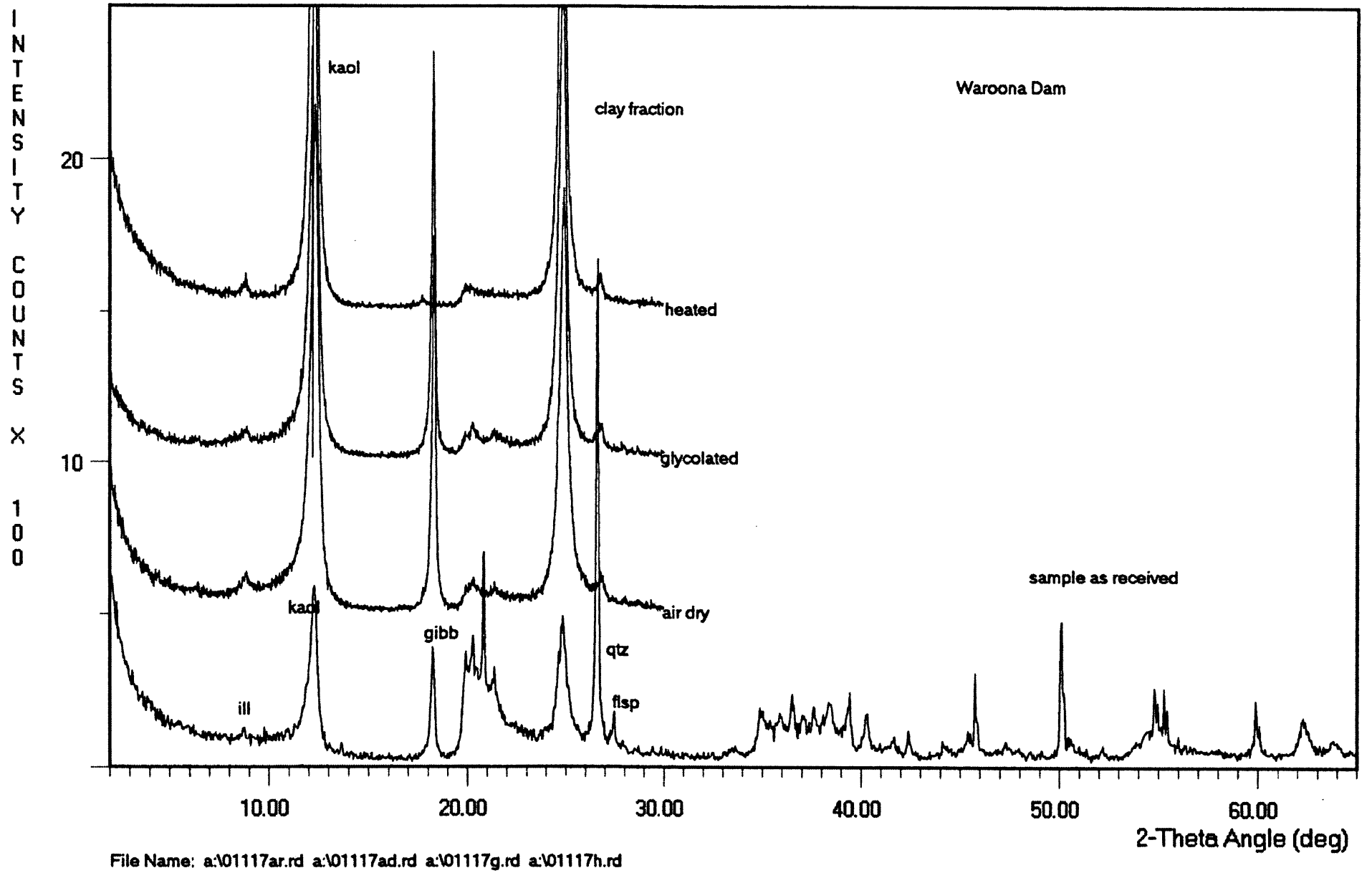

File Name: a:\01117ar.rd a:\01117ad.rd a:\01117g.rd a:\01117h.rd

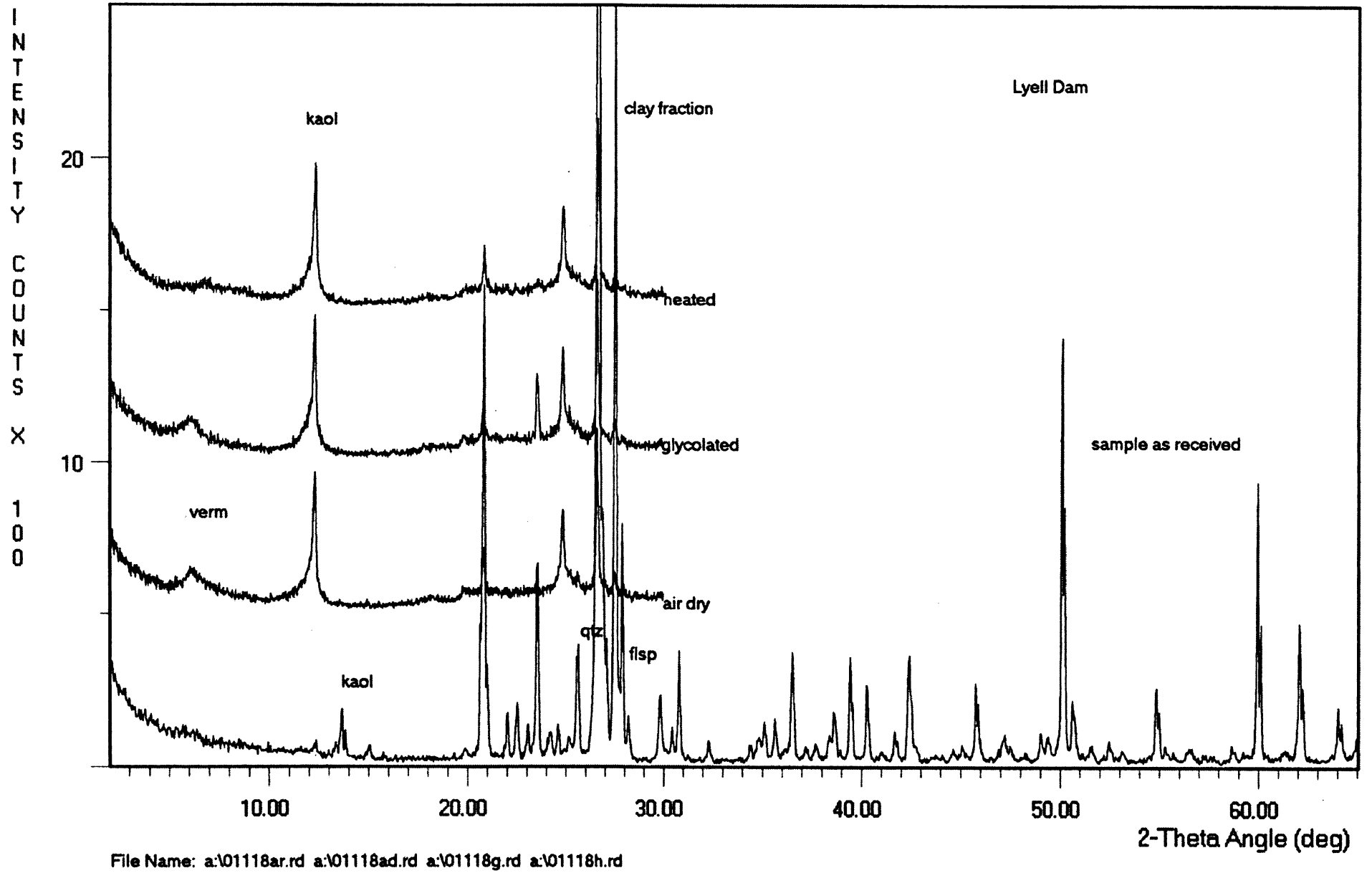
INTENSITY COUNTS X 100
20
10
kaol
clay fraction
Lyell Dam
heated
glycolated
sample as received
verm
air dry
qtz
flsp
kaol
10.00
20.00
30.00
40.00
50.00
60.00
2-Theta Angle (deg)
File Name: a:\01118ar.rd a:\01118ad.rd a:\01118g.rd a:\01118h.rd

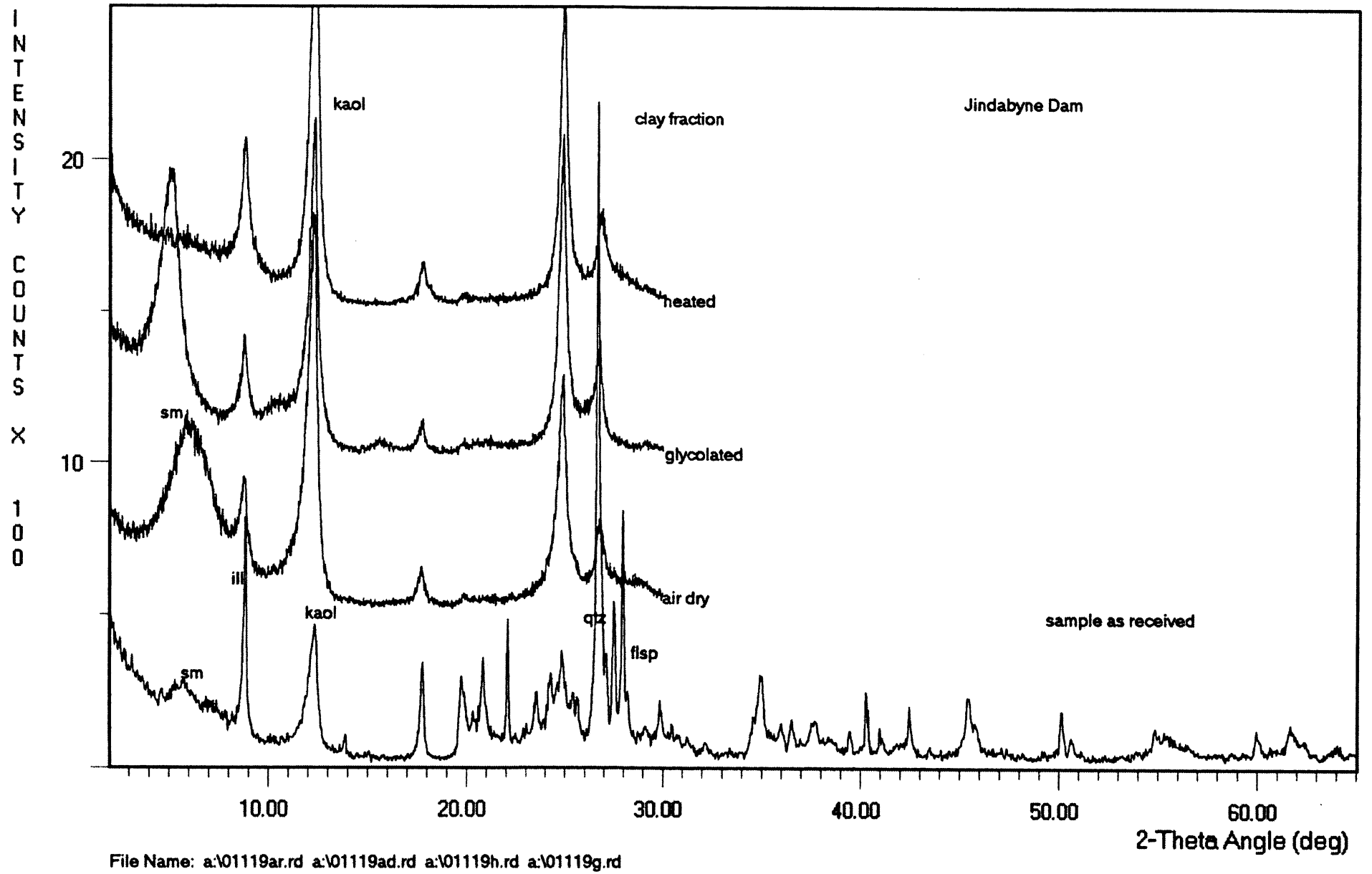

File Name: a:\01119ar.rd a:\01119ad.rd a:\01119h.rd a:\01119g.rd

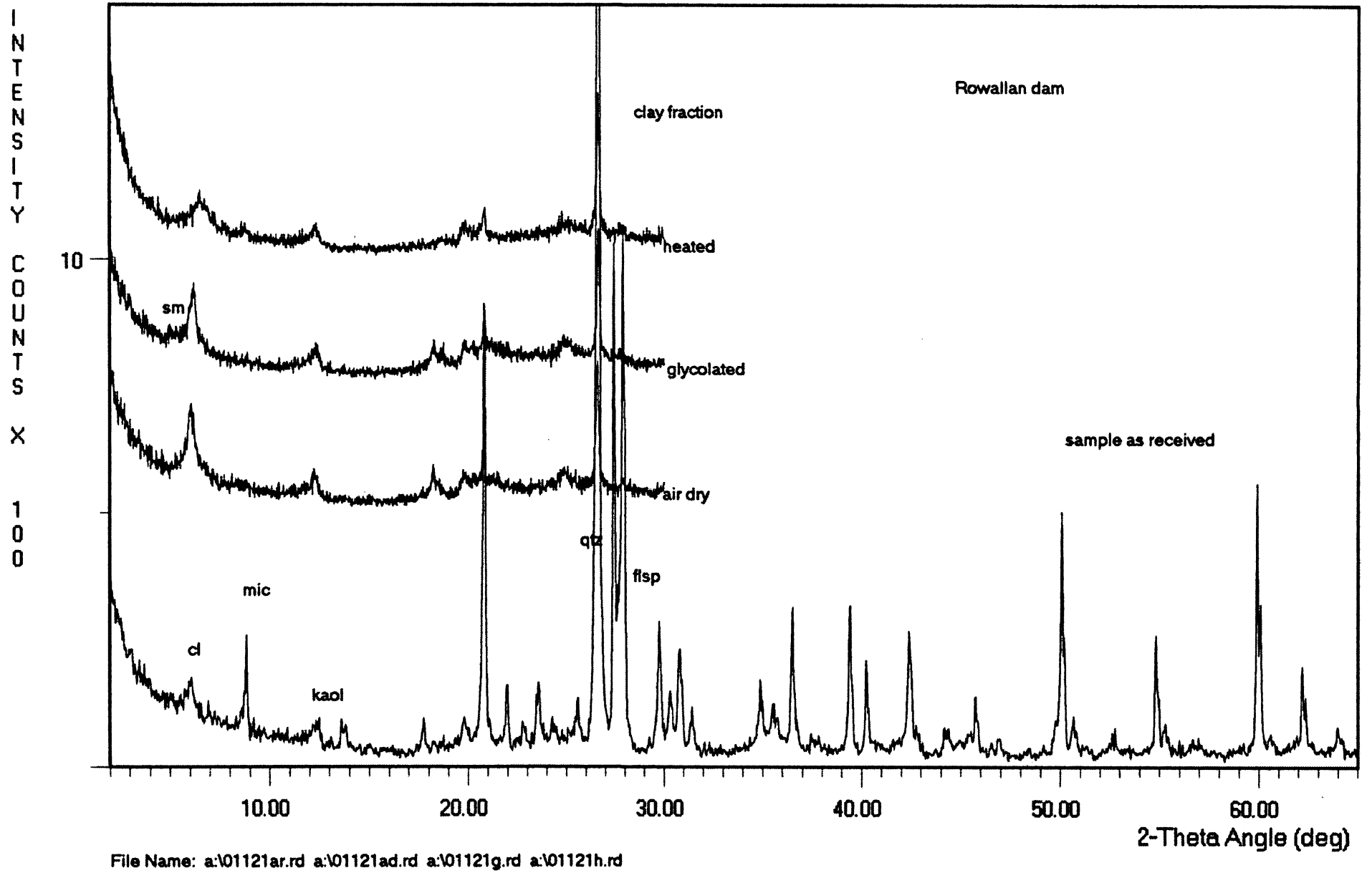

File Name: a:\01121ar.rd a:\01121ad.rd a:\01121g.rd a:\01121h.rd

X-RAY POWDER DIFFRACTION ANALYSIS OF FIVE SOIL SAMPLES

By

Dr Ervin Slansky
School of Geology
THE UNIVERSITY OF NEW SOUTH WALES

For

School of Civil and
Environmental Engineering
(Mr Chi-Fai-Wan)

October 2001

X-RAY POWDER DIFFRACTION ANALYSIS OF FIVE SOIL SAMPLES

The work involved in the preparation of this report was undertaken in the X-ray Diffraction Laboratory of the School of Geology, University of New South Wales.

Samples Received

Five soil samples were received for X-ray powder diffraction analysis:

1. Warranga Basin
2. Pukaki
3. Matahina
4. Teton
5. Buffalo

Analytical Data

The analysis was carried out by monochromatized CuKα radiation using a Philips X'Pert system. All samples were examined as received and as oriented aggregates of the clay fraction (< 2μm e.*s.d.*) obtained by centrifugation from samples dispersed in water. The oriented specimens on glass slides were prepared by the membrane filter transfer method and subsequently examined air dry, after ethylene glycol solvation and after heating to 400°C for one hour. This is a standard procedure for the identification of clay minerals.

The data from the natural (as received) powdered specimens were processed by computer; a search match program included in WINPlot (CSIRO, Division of Soils) was used for the identification of mineral phases. The program uses the current ICCD (International Centre for Diffraction Data) Powder Diffraction File™ covering experimental data (sets 1 to 50) as well as calculated patterns (sets (70 and higher).

The results of the X-ray powder diffraction analysis of the natural (as received) as well as the oriented samples of the clay fraction are given in Tables 1 and 2, respectively. The diffractometer traces obtained in the course of the examination are attached (Figures 1 to 5). The principal peaks of significant minerals are marked using the following abbreviations:

Amp = amphibole
an = anatase
calc = calcite
chl = chlorite
flsp = feldspar(s)
m/ill = mica- illite
kaol = kaolinite
qtz = quartz
sid = siderite
sm = smectite
verm = vermiculite or mixed-layer vermiculite/ chlorite

Comment

The X-ray examination of the **samples as received** showed *quartz* to be the most abundant non-clay rock-forming mineral. *Feldspar(s)* are also widespread, but occur in variable quantity from abundant to traces. The rest of non-clay minerals are present in insignificant amounts and because of that sometimes are questionable.

The **clay fraction** of the samples is varied. *Kaolinite* and *chlorite* are less abundant than *mica/Illite*. *Smectite* occurs in a larger quantity in two samples only (Matahina and Teton). A mineral close to vermiculite or *vermiculite/chlorite* was identified in samples from Pukaki and Buffalo, respectively. In both instances the content of this mineral is very small.

Ervin Slansky, RNDr, PhD
October 8, 2001

Table 1
Mineral Composition of Samples as Received

Sample Mineral	Warranga	Pukaki	Matahina	Teton	Buffalo
Quartz	A	A	A	A	D
Feldspar(s	T	A	A-M	S	T-S
Kaolinite	S	-	S	S	S
Illite/mica	S	S	S	S	S
Smectite	T	T	S	S	-
Chlorite	-	S	-	T	S
Vermiculite or Vermiculite/chlorite	-	T	-	-	T
Goethite	T	-	-	?T	T
Hematite	?T	-	-	T-S	T
Anatase	?T	-	?T	?T	T-S
Siderite	?T	?T	-	T-S	-
Calcite	-	-	?T	S	-
Gypsum	-	-	T	-	?T
Jarosite			?T	?T	?T

The letters D, A, M, S, T denote semi-quantitative estimates of mineral percentages:

D = dominant (>60%)
A = abundant (60 - 40 %)
M = moderate (40 - 20%)
S = small (20 - 5%)
T = traces (<5%)

Table 2
Mineral Composition of the Clay Fraction

Sample Mineral	Warranga	Pukaki	Matahina	Teton	Buffalo
Kaolinite and/or Chlorite	23	14*	14	17	25
Illite/mica	59	50	59	29	52
Smectite and/or Vermiculite or Vermiculite/ Chlorite	17	36**	27***	54***	23

* chlorite only
** smectite and vermiculite or vermiculite/chlorite
*** smectite only

The numbers in brackets in Table 2 are semi-quantitative estimates of clay minerals by the method of Griffin (in Carver, *Procedures in Sedimentary Petrology*, New York 1970) using peak heights.

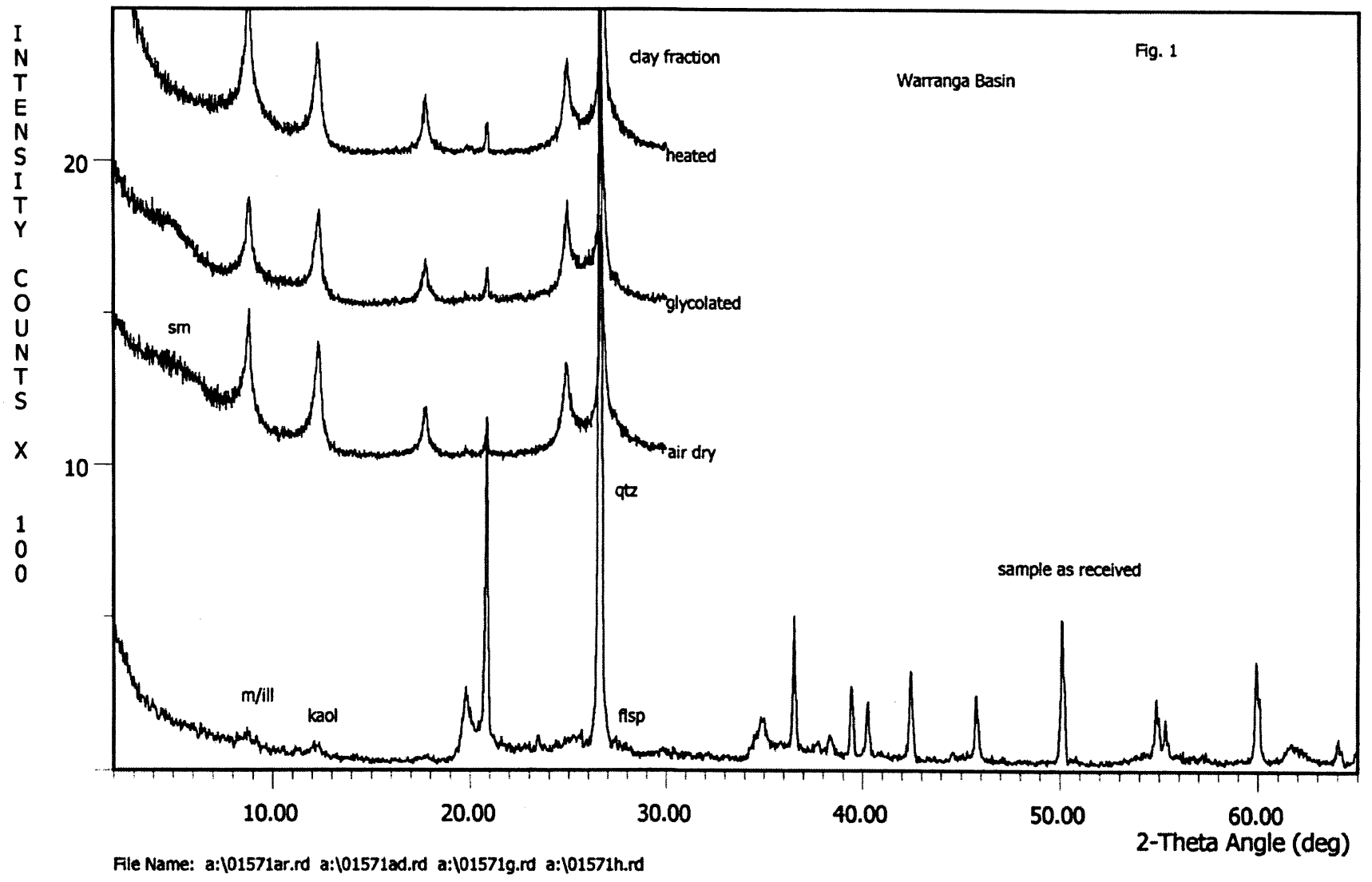

Fig. 1

Warranga Basin

File Name: a:\01571ar.rd a:\01571ad.rd a:\01571g.rd a:\01571h.rd

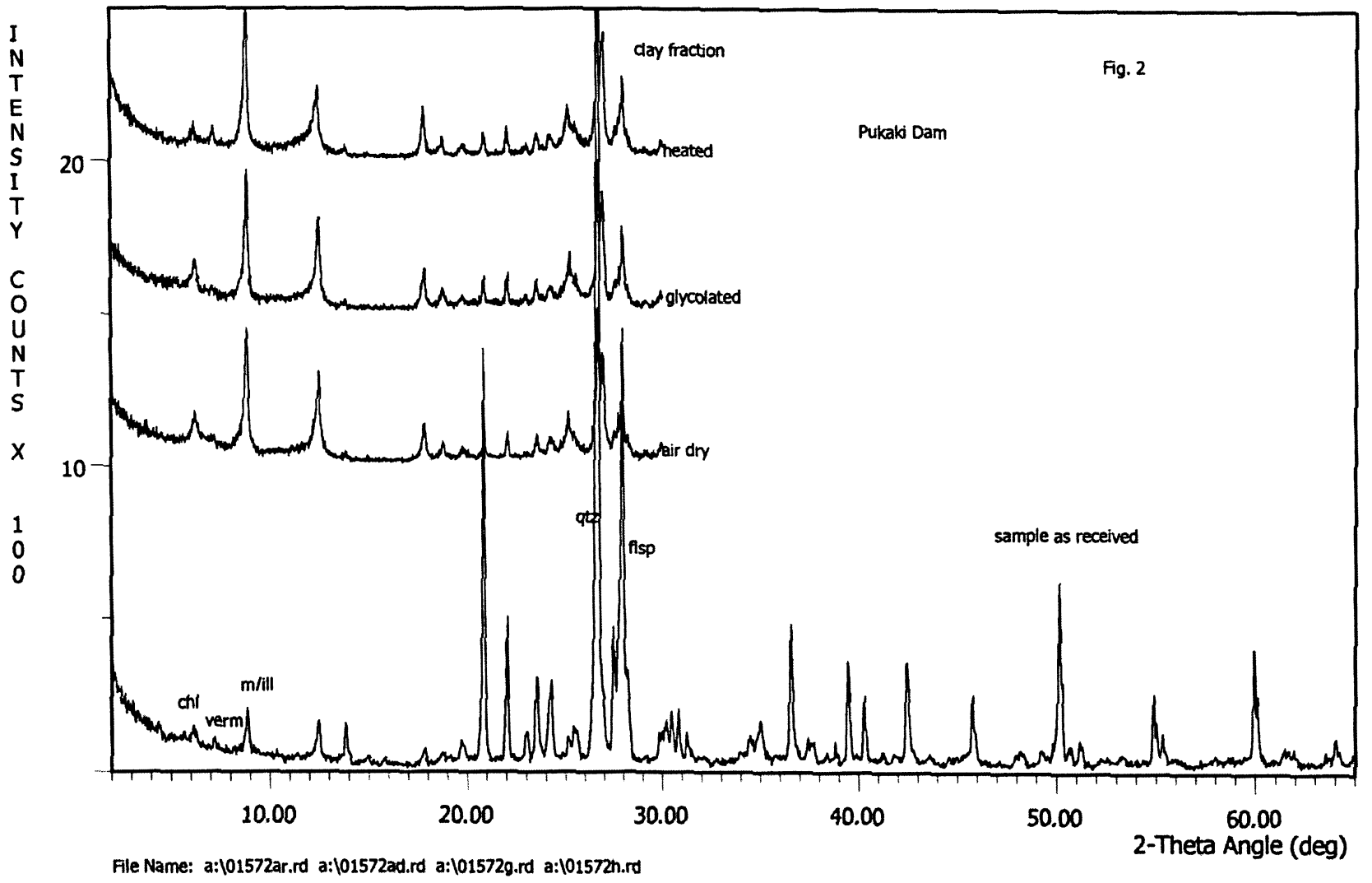
INTENSITY COUNTS X 100
20
10
clay fraction
heated
glycolated
air dry
sample as received
Pukaki Dam
Fig. 2
qtz
flsp
chl
verm
m/ill
10.00
20.00
30.00
40.00
50.00
60.00
2-Theta Angle (deg)
File Name: a:\01572ar.rd a:\01572ad.rd a:\01572g.rd a:\01572h.rd

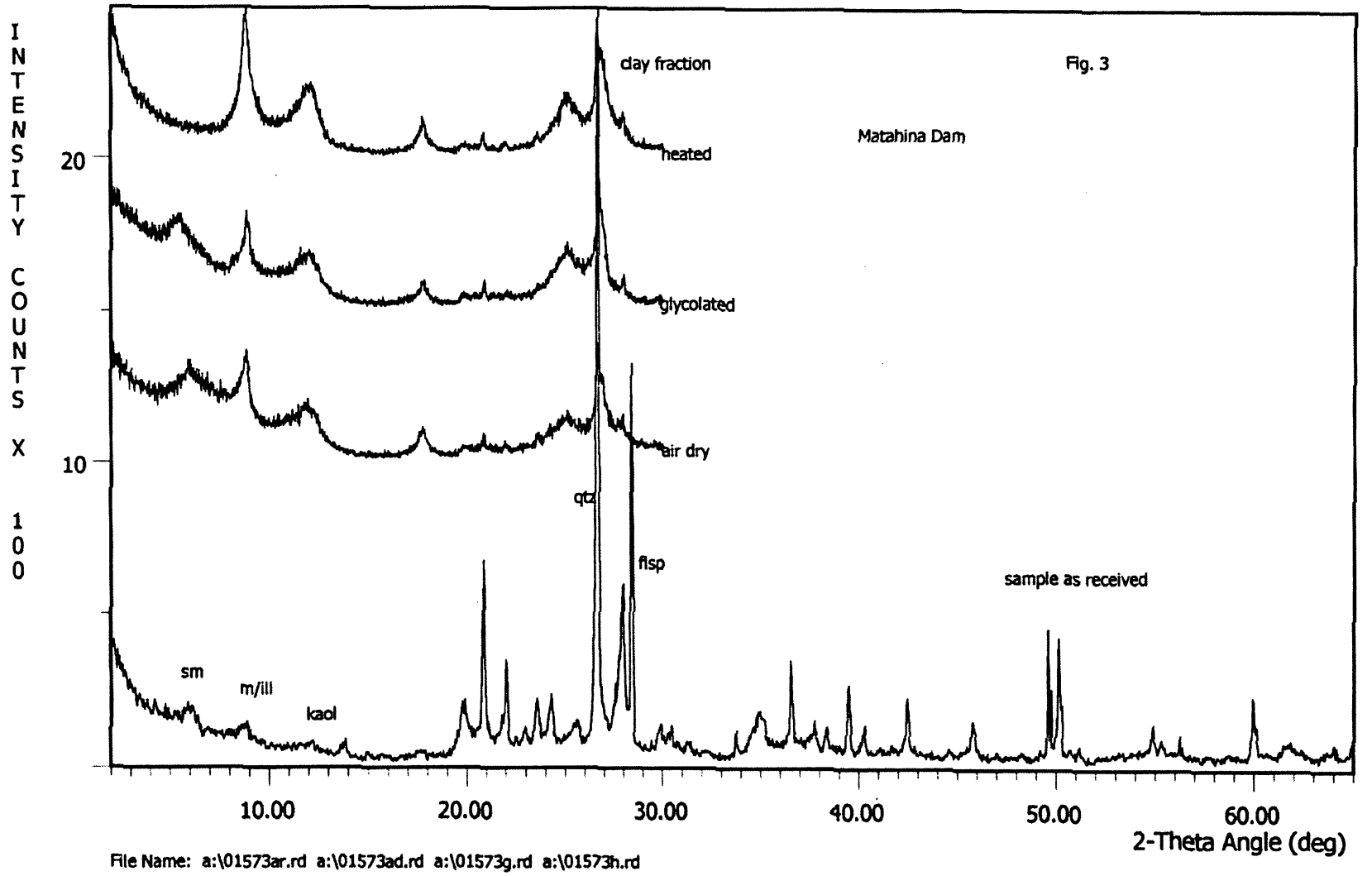
INTENSITY COUNTS X 100
20
10
clay fraction
heated
glycolated
air dry
qtz
flsp
sm
m/ill
kaol
Matahina Dam
sample as received
10.00
20.00
30.00
40.00
50.00
60.00
2-Theta Angle (deg)
File Name: a:\01573ar.rd a:\01573ad.rd a:\01573g.rd a:\01573h.rd

Fig. 3

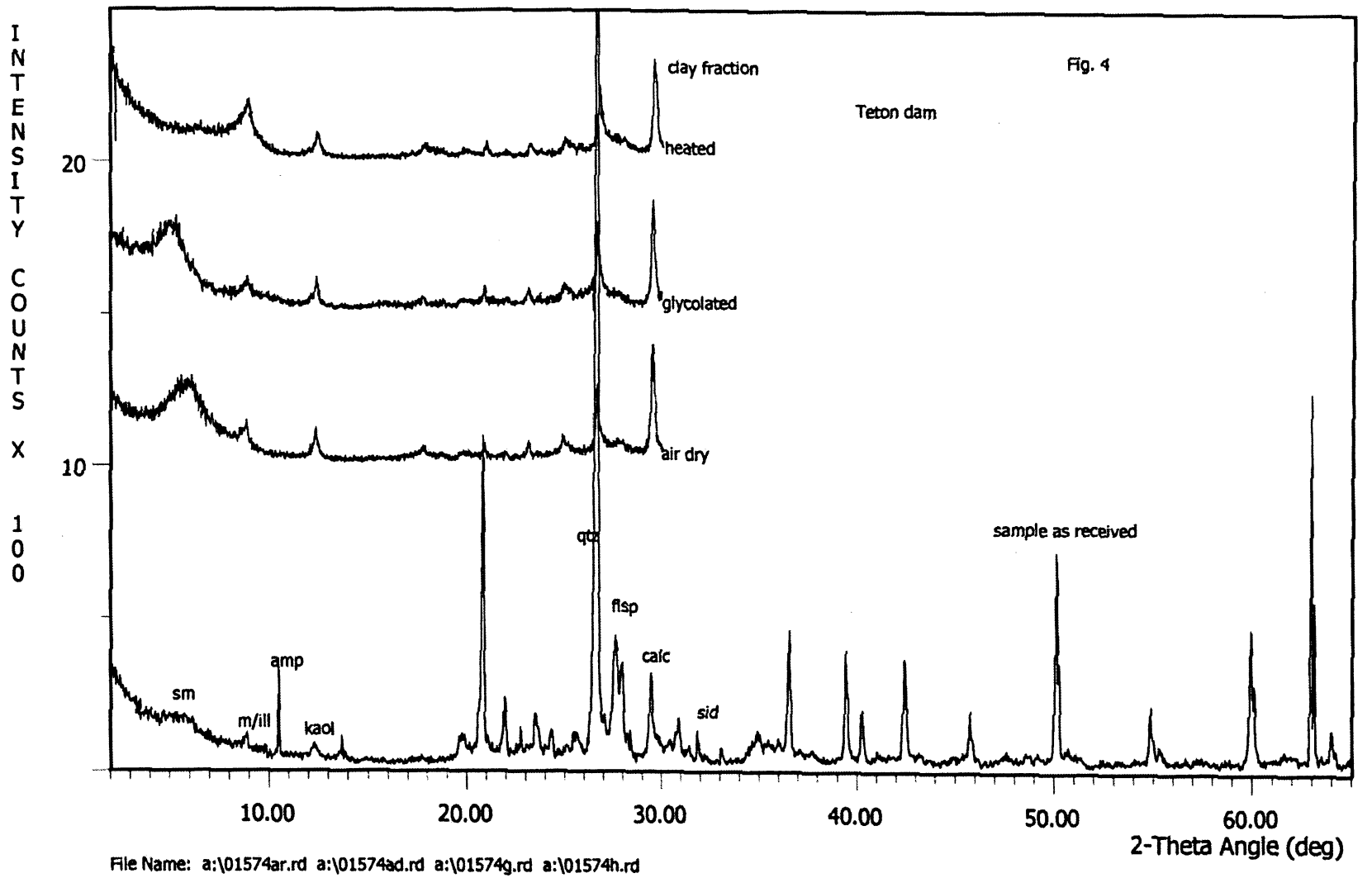
INTENSITY COUNTS X 100
20
10
clay fraction
heated
glycolated
air dry
sample as received
Teton dam
Fig. 4
qtz
flsp
calc
sid
amp
sm
m/ill
kaol
10.00
20.00
30.00
40.00
50.00
60.00
2-Theta Angle (deg)
File Name: a:\01574ar.rd a:\01574ad.rd a:\01574g.rd a:\01574h.rd

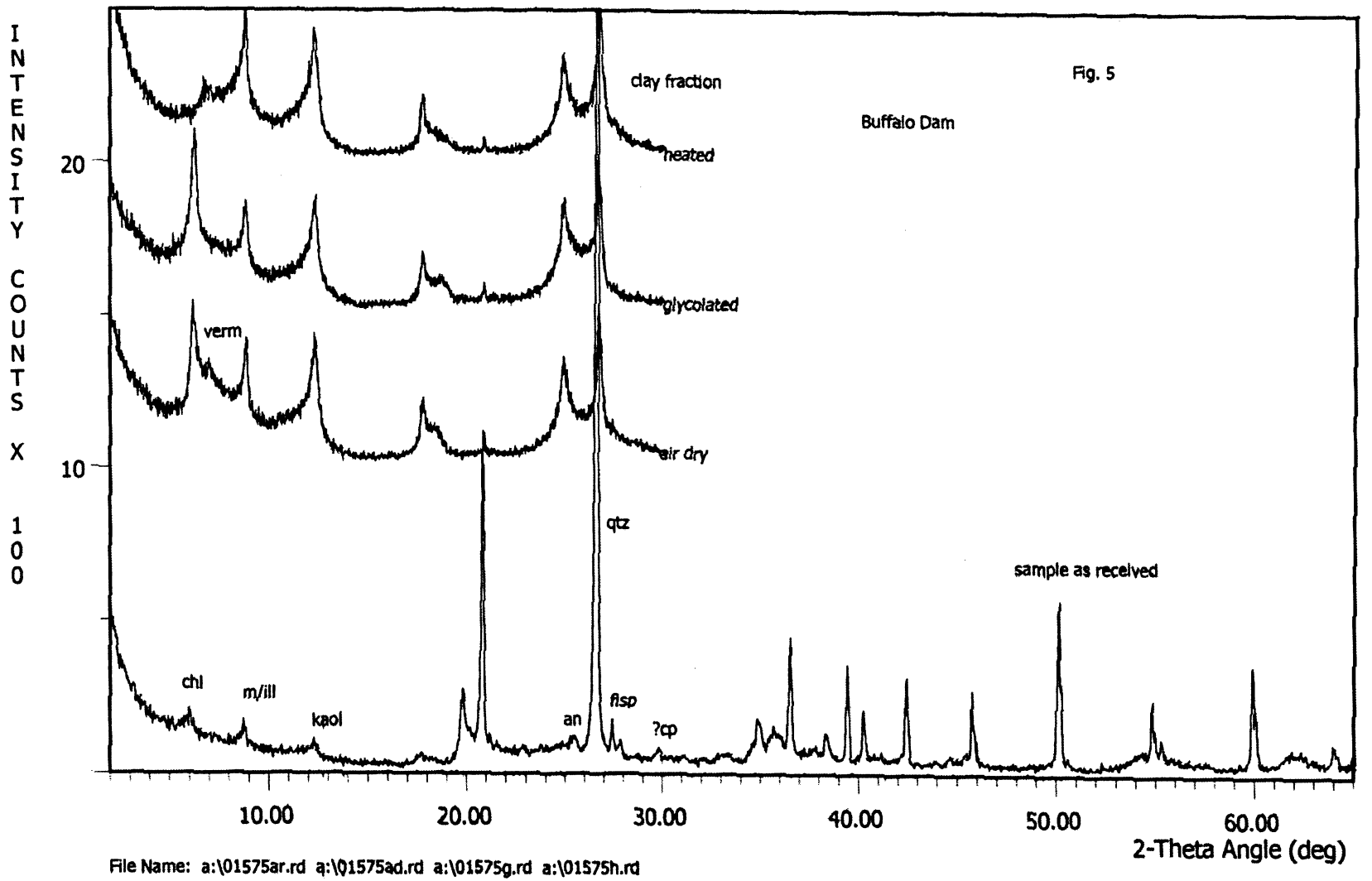
INTENSITY COUNTS X 100
20
10
clay fraction
heated
glycolated
air dry
sample as received
verm
chl
m/ill
kaol
qtz
an
fisp
?cp
10.00
20.00
30.00
40.00
50.00
60.00
2-Theta Angle (deg)
Fig. 5
Buffalo Dam
File Name: a:\01575ar.rd a:\01575ad.rd a:\01575g.rd a:\01575h.rd

APPENDIX L

Report on the identification of components within two clays from the Buffalo Dam, Victoria by Hensel, H.D.

In "Lake Buffalo Future Strategy Phase B2 prepared on behalf of Goulburn-Murray Water, January 2001, Snowy Mountains Engineering Corporation"

Report on the identification of components within two clays from the Buffalo Dam, Vic

Client: Peter Darling (Smec)

Situation: Buffalo Dam, VIC

Problem: Dark chocolate-coloured and dark reddish-brown clays from the dam wall have high residual strengths. Compaction problems have occurred using these clays. The problems associated with the compaction of the clays could be a function of the mineralogy, such as the presence of significant quantities of halloysite

Brief: To identify and quantify the various components within the clay samples using a variety of methods such as X-Ray diffraction analysis, reflected optical microscopy, and if required, other sophisticated techniques such as SEM (scanning electron microscope) and possibly TEM (transmission electron microscope). Quantification is done using a computer programme called SIROQUANT

Methods: The clay-rich samples (TP2 and TP3) were each subjected to a bulk run from which a quantitative analysis was derived using a sophisticated computer programme called SIROQUANT. The bulk run involves the entire sample, i.e. no size limits. Each sample was then treated so that only the platy minerals plus all the clays were collected (<2μ fraction). Oriented sections were prepared and several X-Ray diffraction patterns were obtained after a range of chemical treatments. One of these treatments (using formamide) is a diagnostic test for halloysite. Another, glycolation, is a test for the presence of smectite (swelling clay). Separate runs were also necessary to establish the presence or absence of chlorite and vermiculite.

Results: The bulk run for TP2 showed it to consist of the following mineralogy:

quartz	55%
muscovite	13%
hydrated iron oxide	8%
haematite	1%
kaolinite	13%
vermiculite	4%
feldspar	5%

The clay fraction consisted mainly of kaolinite and muscovite with some minor vermiculite. There was no indication of any halloysite nor smectite. The bulk run for TP3 showed it to consist of:

quartz	52%
muscovite	11%
hydrated iron oxide	9%
haematite	3%
kaolinite	22%
smectite	1%
feldspar	3%

The clay fraction consisted mainly of kaolinite with lesser amounts of muscovite and minor smectite. Again there was no indication of any halloysite. TP2 also contained a trace of chlorite and some vermiculite and TP3 contained some vermiculite which, together with smectite, was interlayered with some of the muscovite.

Cation exchange coefficients for the clay fractions and bulk samples produced the following results:

TP2 clay	31.5	TP2 bulk	7.4
TP3 clay	28.6	TP3 bulk	6.9

Discussion: Neither sample contained any halloysite and only TP3 contained some smectite. The cation exchange coefficients for both samples are typical for kaolinitic clays.

Two aspects are noteworthy from the results of the SIROQUANT analyses. Firstly, the amount of quartz in the bulk sample is extremely high. When the amount of feldspar is added to this (55-60% of total mineralogy) the structure of this "clay" is unlikely to behave as a "normal" clay-rich sample. Although this high level of granularity commonly leads to a moderately flocculent structure this could not be convincingly demonstrated using optical methods. The main reasons for this are the low total amount of platy minerals (clays and micas) and the way they are incorporated within the hydrated iron oxide, i.e. they cannot behave physically as a mass of platy minerals. Importantly, it was essential to undertake an X-ray diffraction analysis of this type of sample because of the masking effect of the hydrated iron oxide. Without this procedure it would not have been possible to establish the amount of clays in these samples.

Secondly, the amount of hydrated iron oxide is also very high. Indeed, it is likely to be a little higher than shown because the peak for the mineral goethite falls directly behind the very strong quartz peak. During soil formation, especially in krasnozems, both iron and aluminium are mobilized by fluids in a process known as ferralization (fe + al). This mobilization, plus continuous remobilization, dissolution and precipitation, generally leads to a dense network of veinlets in the B horizon that are dominated by hydrated iron oxide. The effect of this is to produce encrusted clumps or pods the contents of which might be dominated by platy clays. When the soil is excavated or displaced the network of veinlets and crusts are broken up. Depending on the abundance of the hydrated iron oxide network and the amount of moisture in

cementation by a hydrated iron oxide adds some strength to the soil and this could be contributing to the high residual strength of your samples. Optical microscopy demonstrated the abundant small-scale variation that occurs within these clays, i.e. pockets of clay and fluid pathways. But most importantly it showed the encrustation (by hydrated iron oxide) of every small soil particle. It also clearly demonstrated the additional hardness of this crust by the way each soil particle behaved during the grinding procedure employed in thin-section manufacture. Many of the 'cores' of the soil particles were eroded away but the rims remained intact. Photograph 1 illustrates this effect.

Investigations using a scanning electron microscope (SEM) to confirm the relationship between the clay distribution, soil structure and the distribution of the hydrated iron oxide as outlined above were not definitive because of the high amount of physical disturbance of the clay. Although there was clearly an abundance of hydrated iron oxide in the samples the fine network of veinlets had become too fragmented during the multiple "processing" that the clay samples had undergone. As a result a systematic physical relationship between the iron oxide and the clay could not be established with this method.

Several SEM photographs of the clays are enclosed showing a very mixed composition with relatively large grains of quartz, composite clay plates and altered mica. A number of "spots" were analyzed for major elements but results are only qualitative. Kaolinite, quartz and altered mica were clearly identified. However, the large amount of very fine ?films of Fe tended to "contaminate" the chemical analyses. Optical microscopy again highlighted the abundance of the quartz (Photograph 2) but because of the general fine grainsize of the quartz and the way the clays have become incorporated within a mass of hydrated iron oxide there was little convincing evidence to suggest that the soils had a flocculated texture.

Conclusion: A series of investigations to account for the high residual strengths of the two "clay" samples from the Mt Buffalo area have revealed that because of the low actual clay mineral and platy mineral concentrations (30% and 34%) and the very high amount of quartz and feldspar (>50%), the samples do not and cannot behave in the same way as would a clay-rich sample. In effect, these "clays" are not clays at all but a mixture of unevenly grained sand and platy minerals that have been incorporated within a mass of hydrated iron oxide. Soil-forming processes have contributed further to a "sandy" texture by producing encrustations of hydrated iron oxide around all soil particles. It has been demonstrated that these encrustations are significantly stronger physically than the clay-rich pockets that form the cores of the soil particles.

Dr. H. D. Hensel
(HENSEL GEOSCIENCES)
9th January, 2001

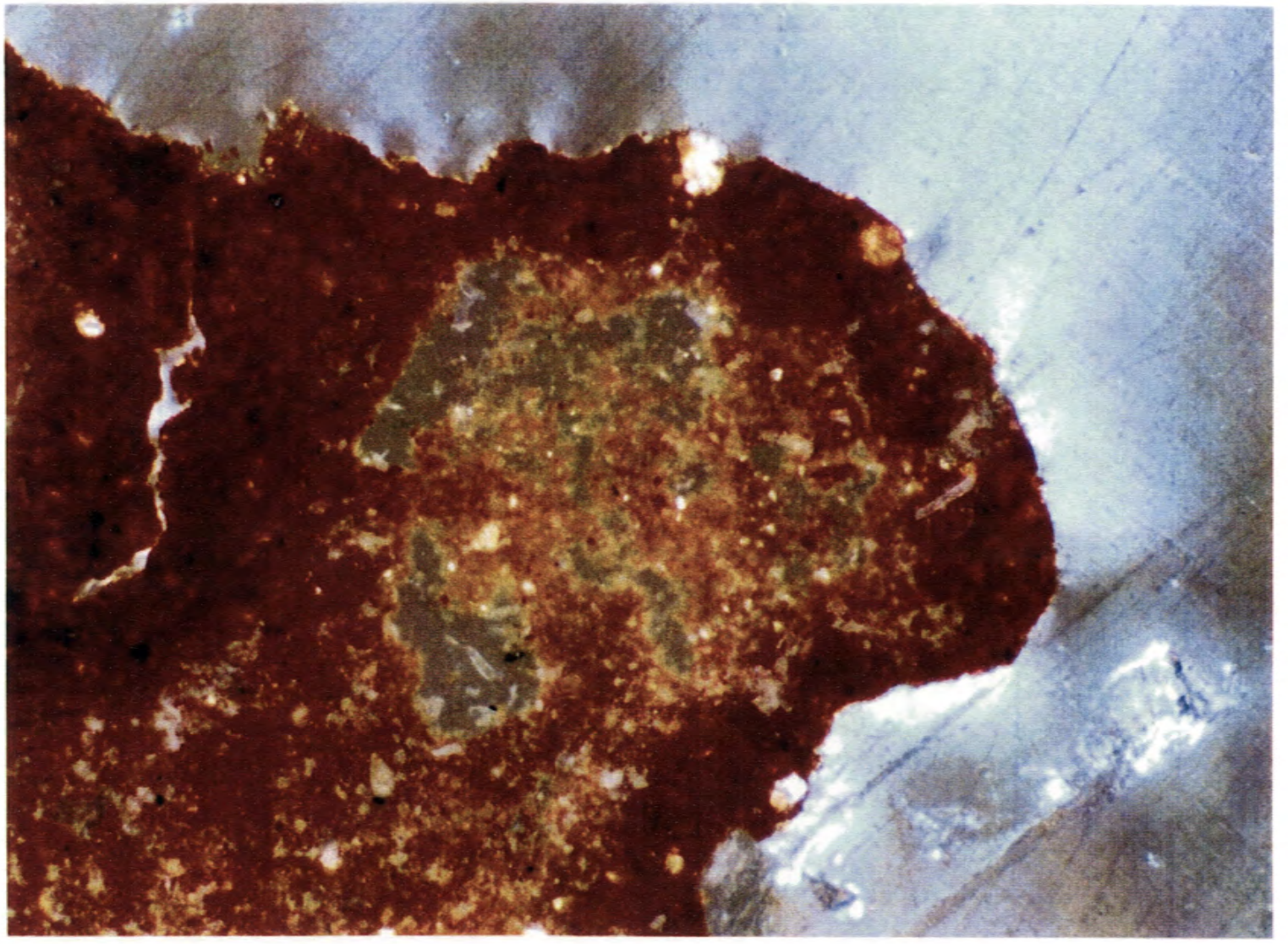

Photograph 1

TP3 - A view in ordinary transmitted light showing the thick encrustation (by hydrated iron oxide) of soil particles. Note the thinning and disappearance of relatively softer clay-rich material away from the crusts. Scale: side of photograph is 2mm

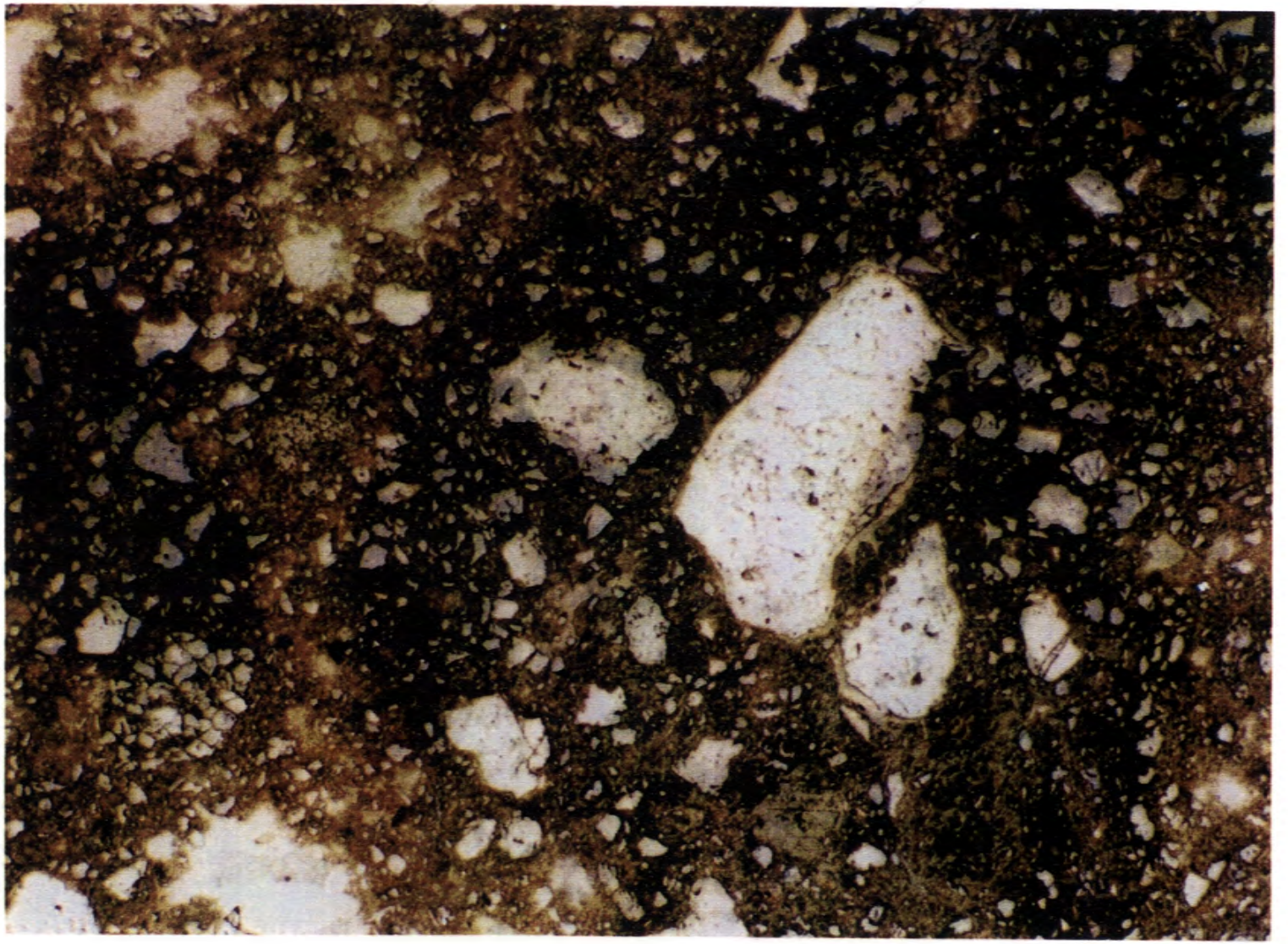

Photograph 2

TP2 - A general view in non-polarized reflected light showing the abundant quartz in these samples. Note the very uneven grainsize of the crystals and their general angularity. Also evident are some textural and mineralogical variations within this soil. Scale: side of photograph is 2mm

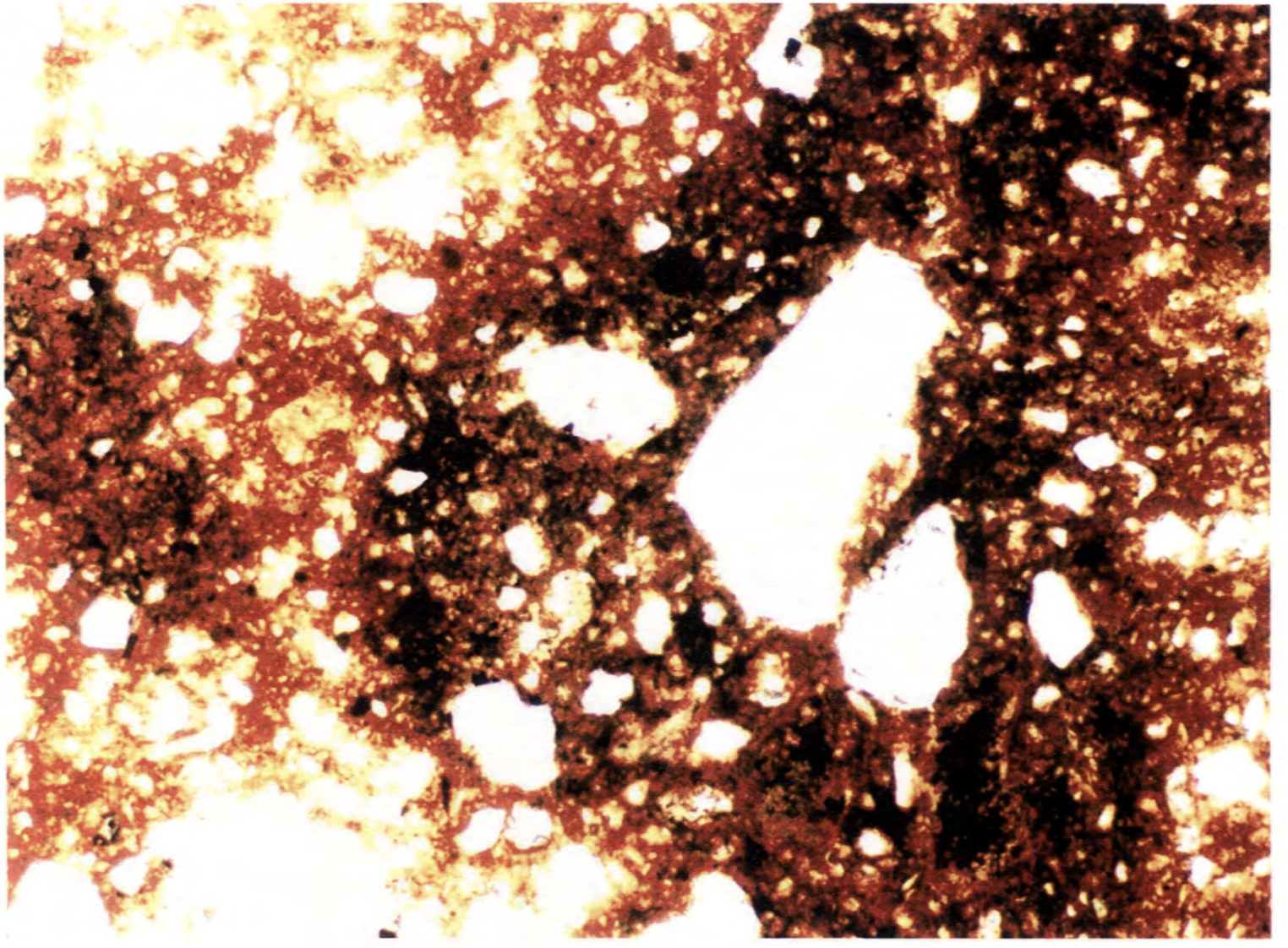

Photograph 3

TP2 - The same view in ordinary transmitted light as photograph 2 showing a much lower percentage of quartz. This emphasizes the need to produce several types of thin-sections to provide accurate information. Scale: side of photograph is 2mm

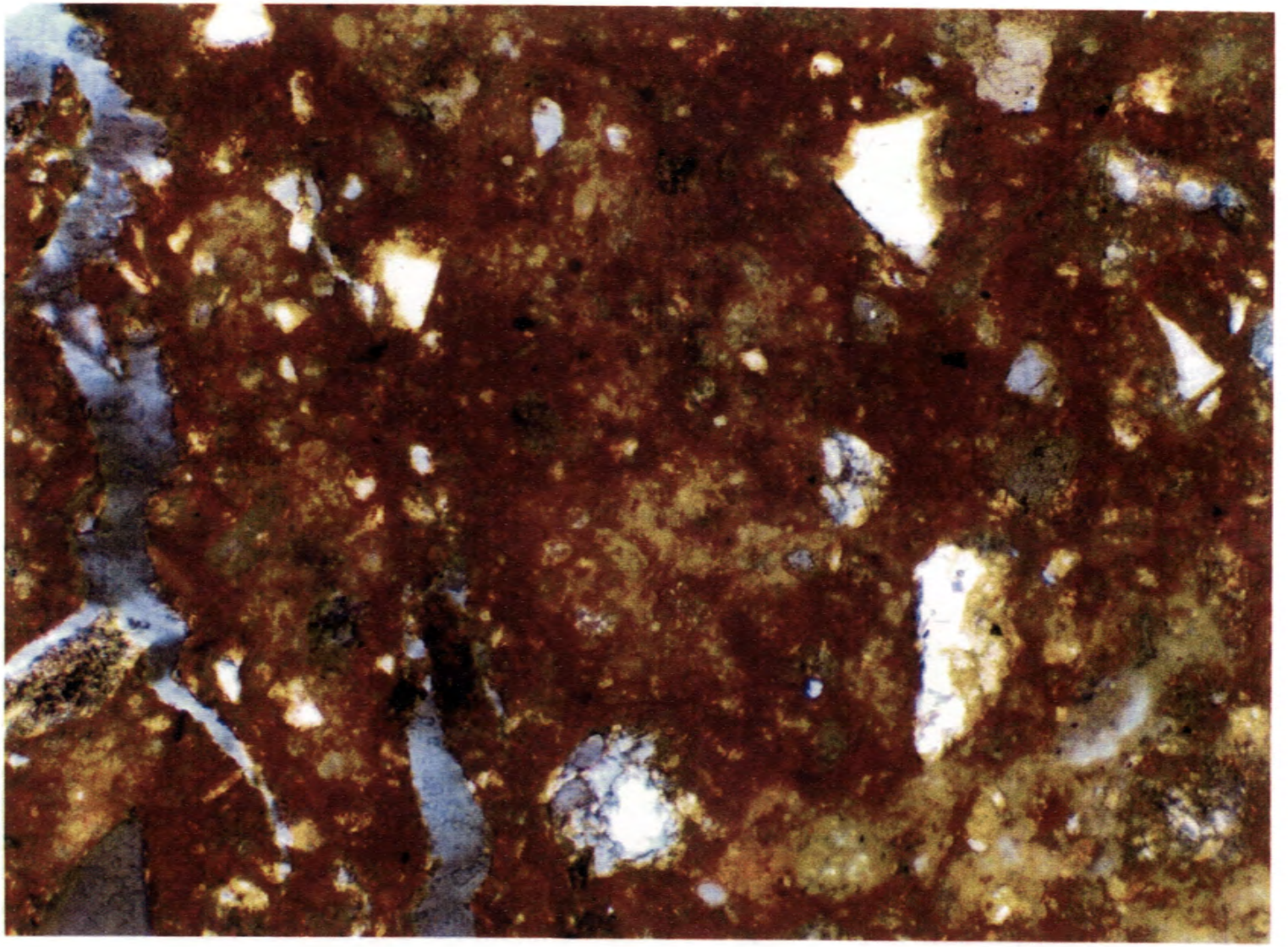

Photograph 4

TP2 - A moderately magnified view in ordinary transmitted light highlighting the small-scale structural heterogeneities. The lighter areas have been less affected by ferruginization processes in the soil. Scale: side of photograph is 1mm

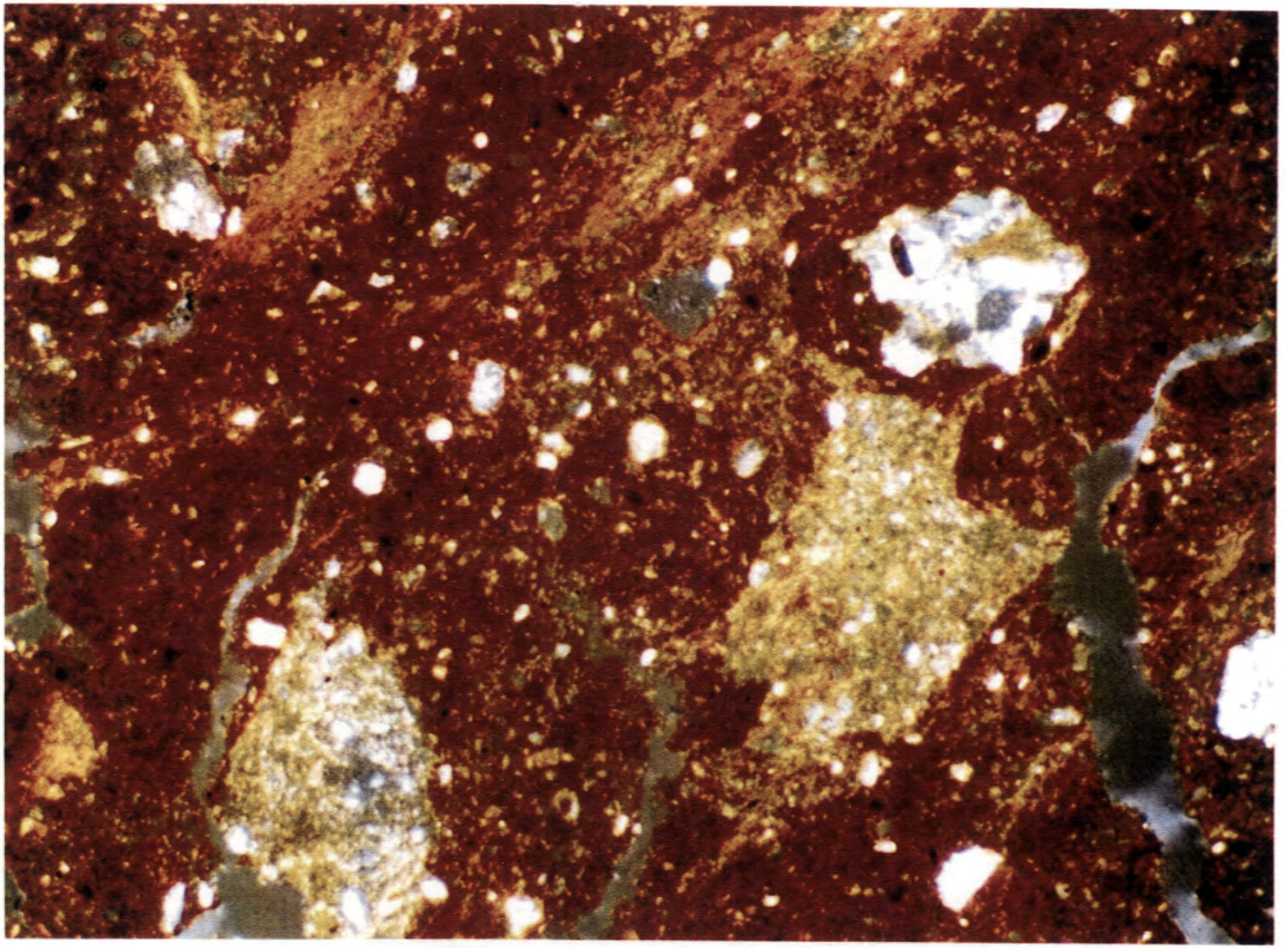

Photograph 5

TP3 - A view in polarized transmitted light again showing small-scale strucutral variations. Also shown are three large lithic fragments of different origins. Note also the abundant cracking. Scale: side of photograph is 2mm

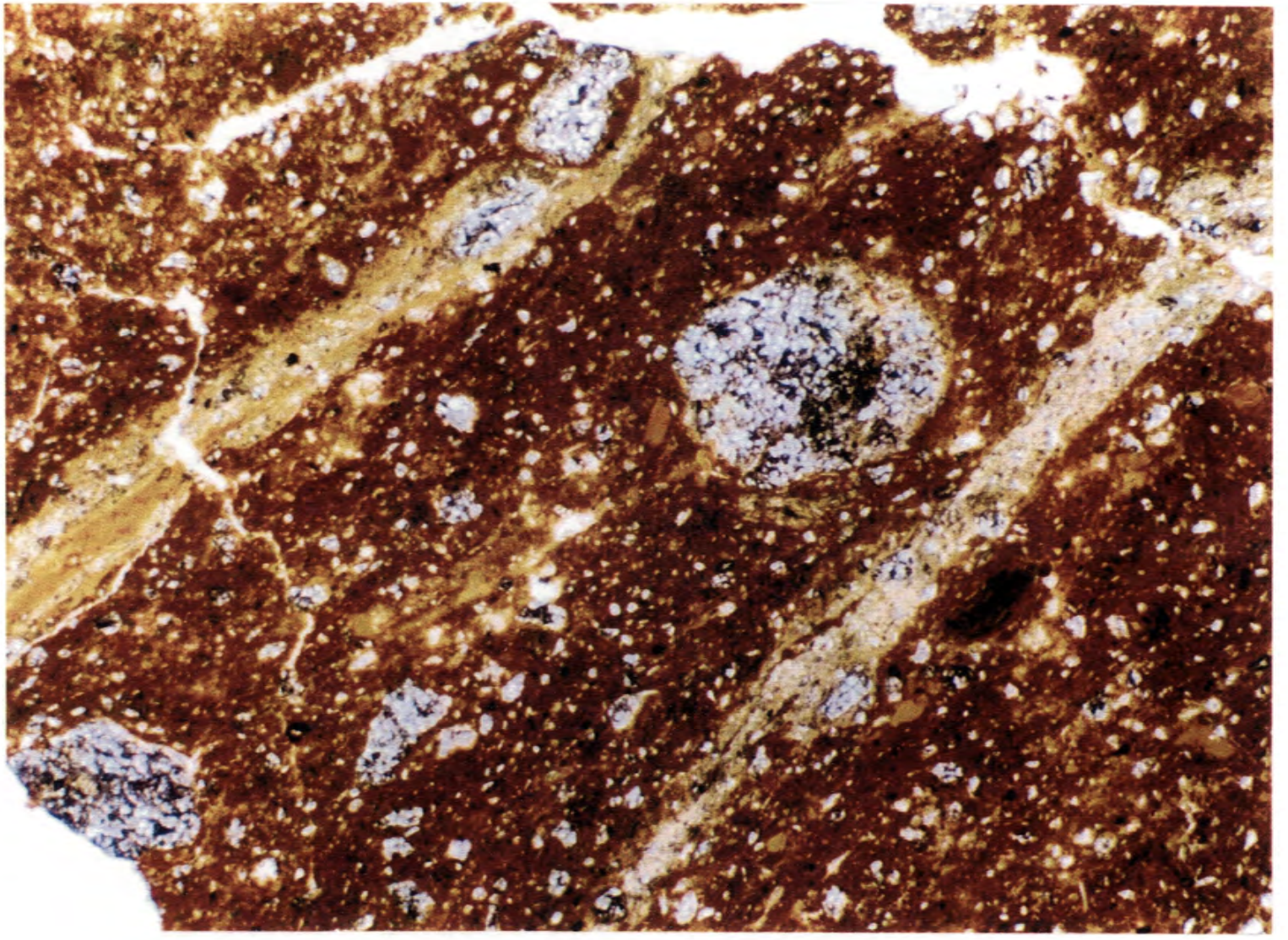

Photograph 6

TP3 - A section of this sample in ordinary light showing abundant and uneven-grained quartz in addition to well-developed fluid pathways containing a high proportion of smectite. Mineralogical detail such as this can be achieved by extra thin thin-sectioning. Scale: side of photograph is 2mm

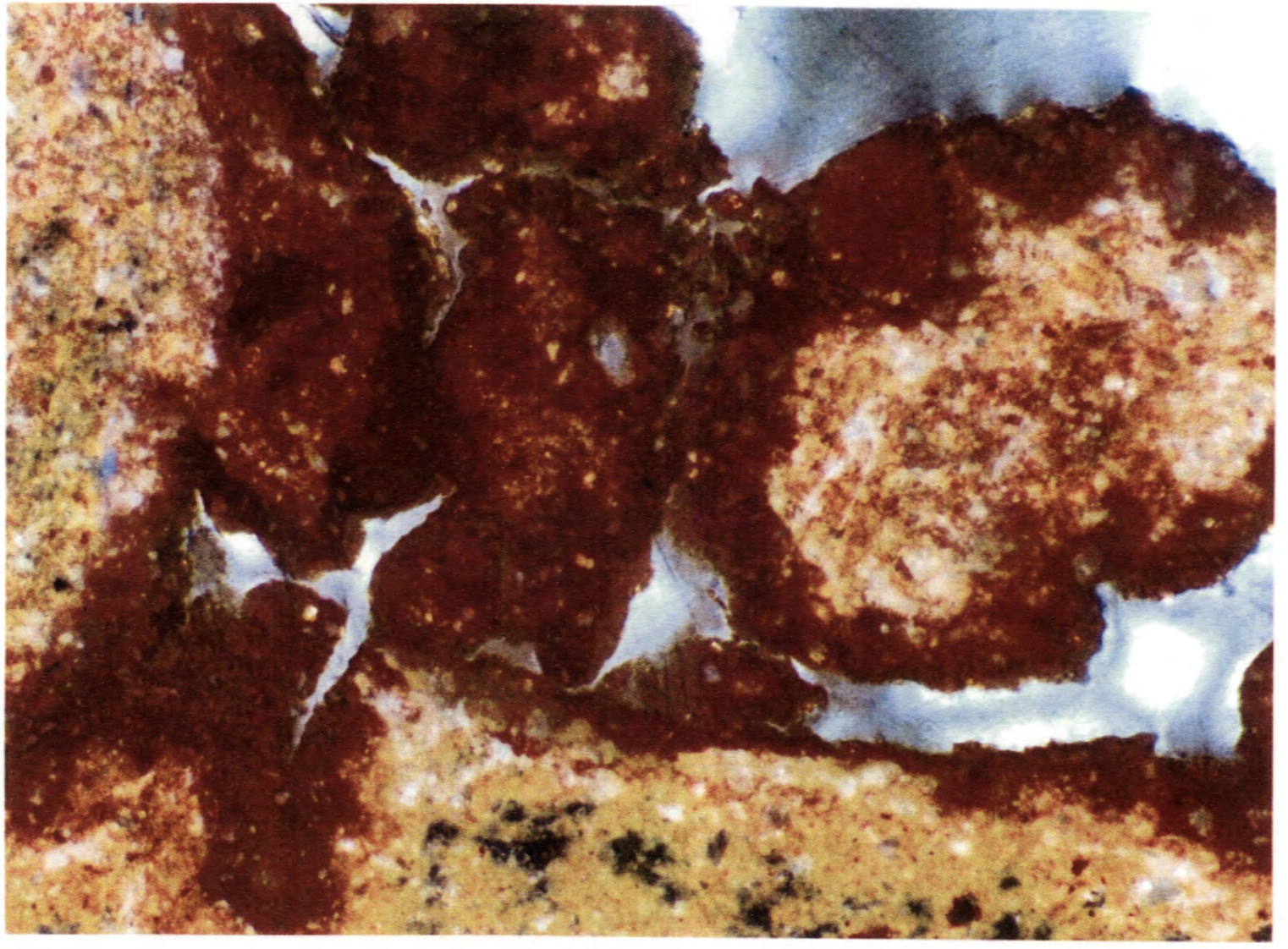

Photograph 7

TP3 - Another example of ferruginous crust formation providing additional strength to individual soil particles. Scale: side of photograph is 2mm

TP2-1

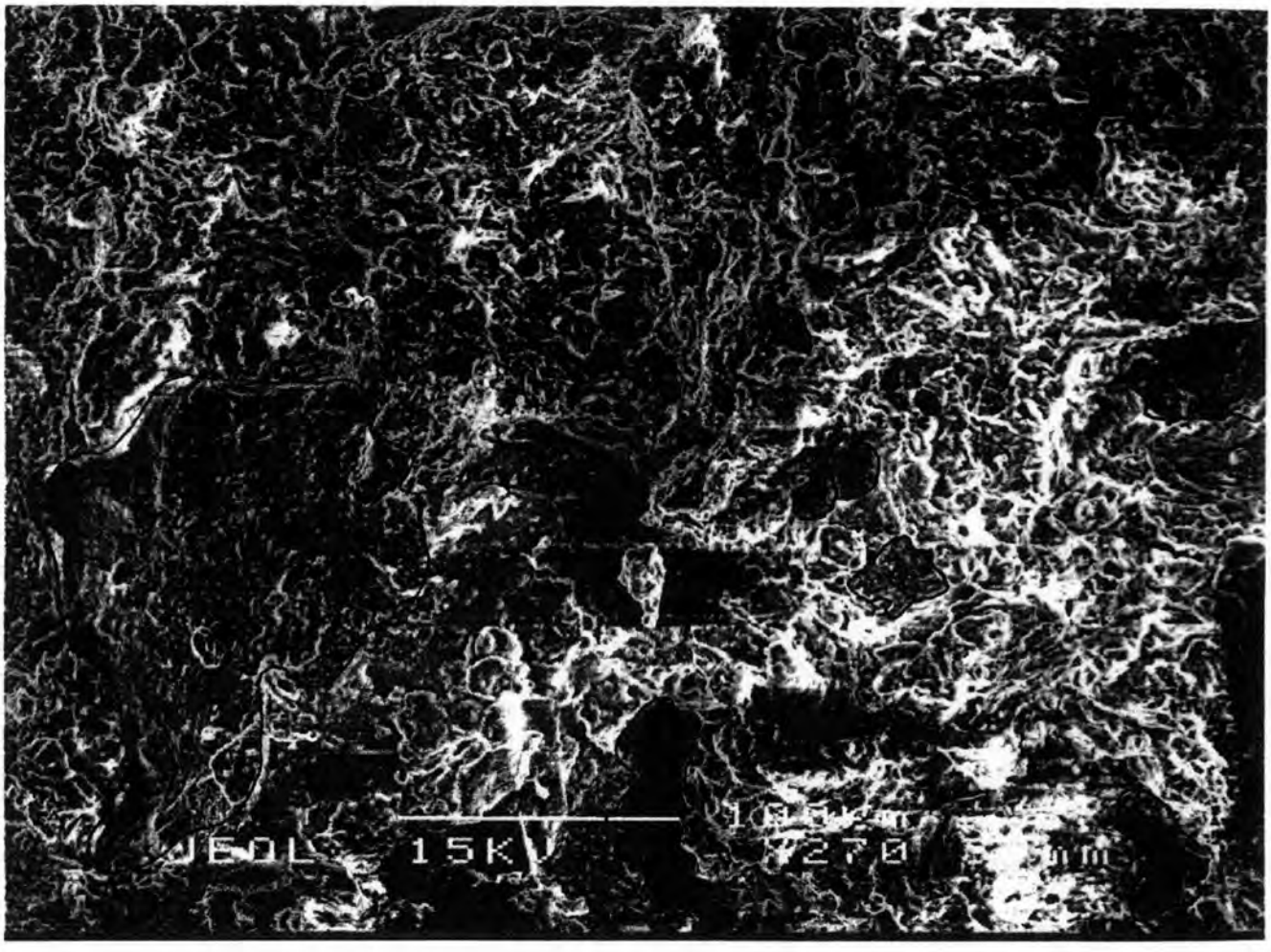

Q : quartz

x 270

TPN2-2

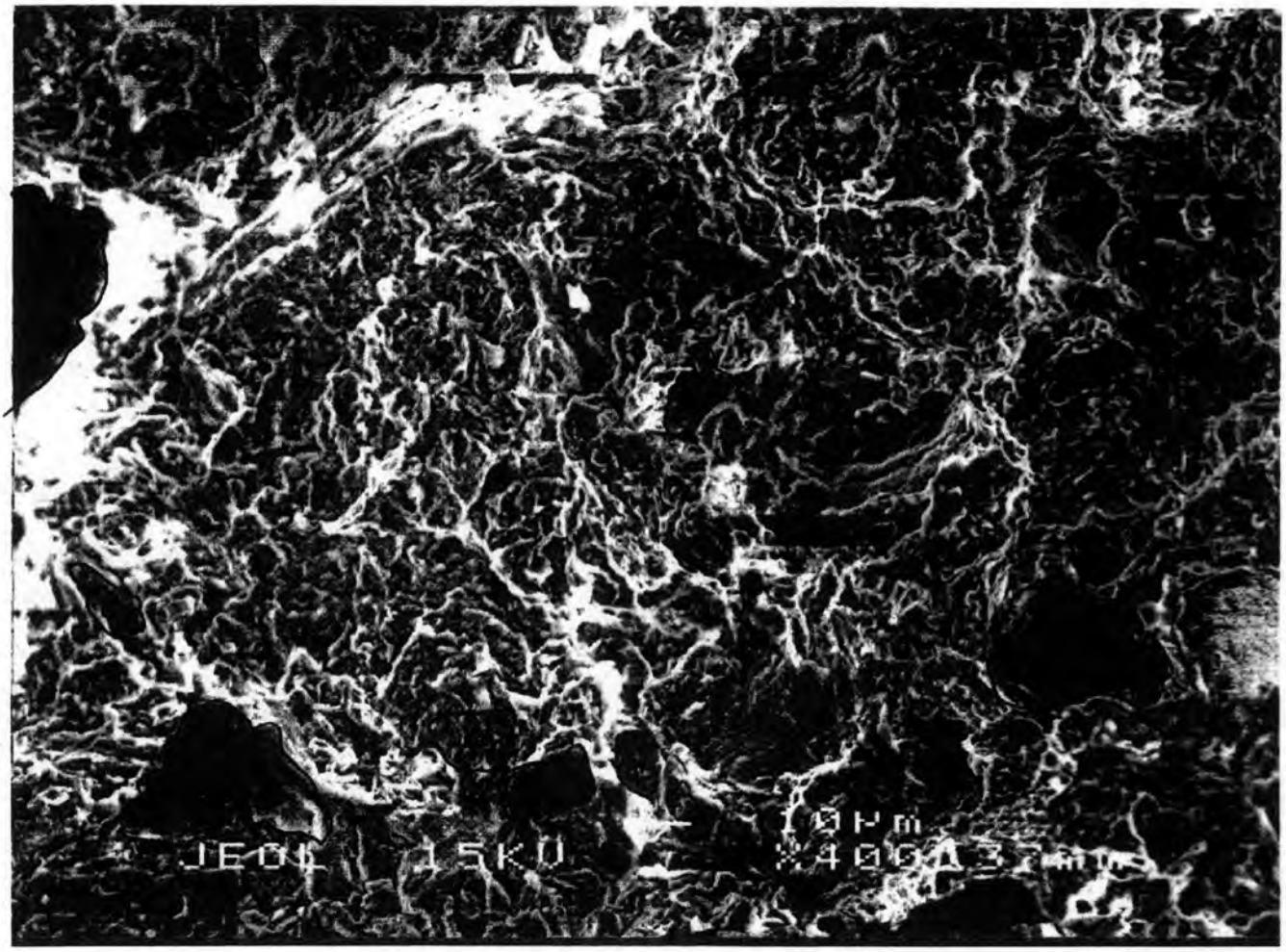

Q = quartz

Photo basically shows flattened layer silicate material in a poorly reflecting matrix overlying quartz.

x 400

TP2-3

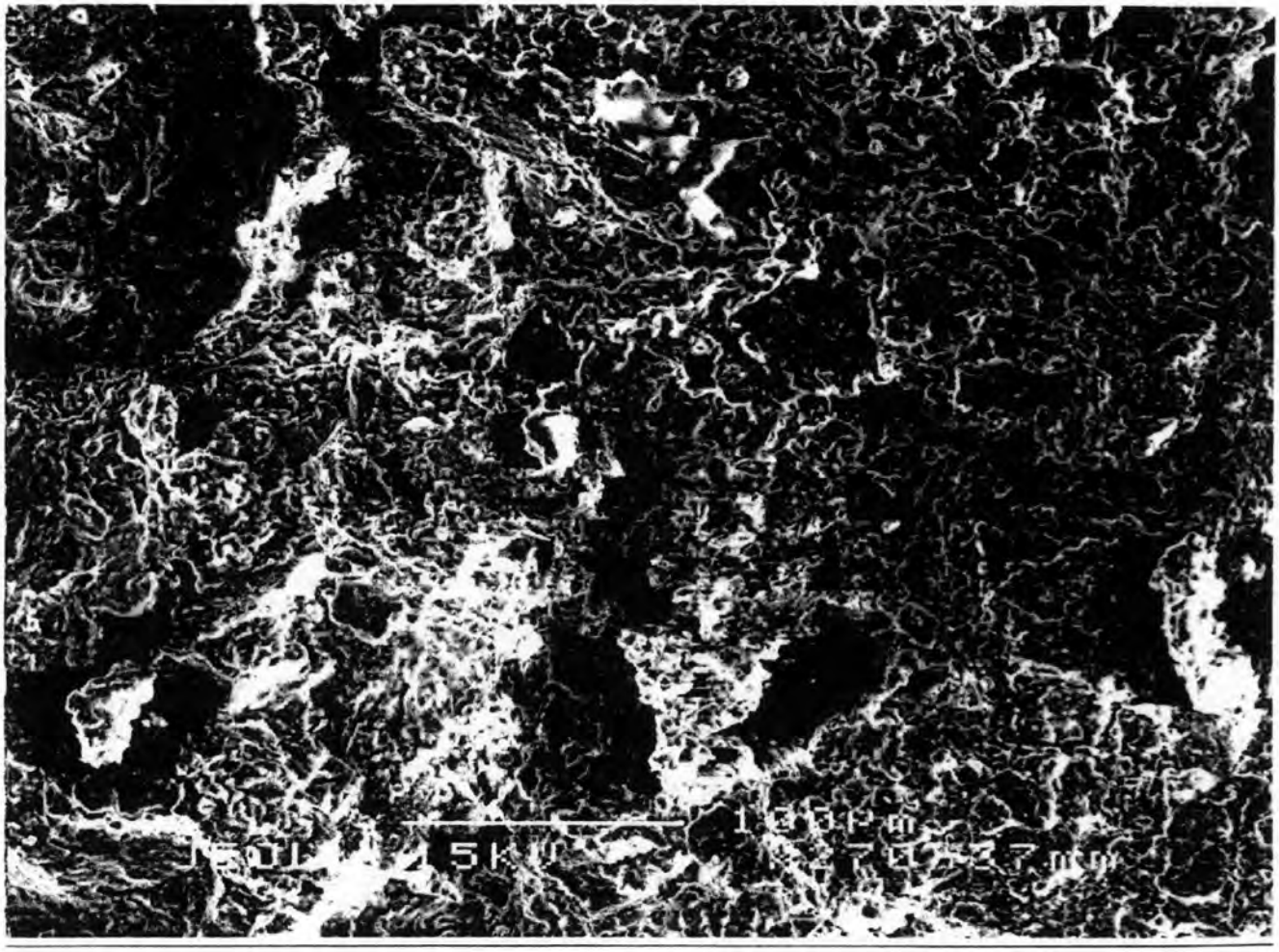

x 270 Abundant quartz

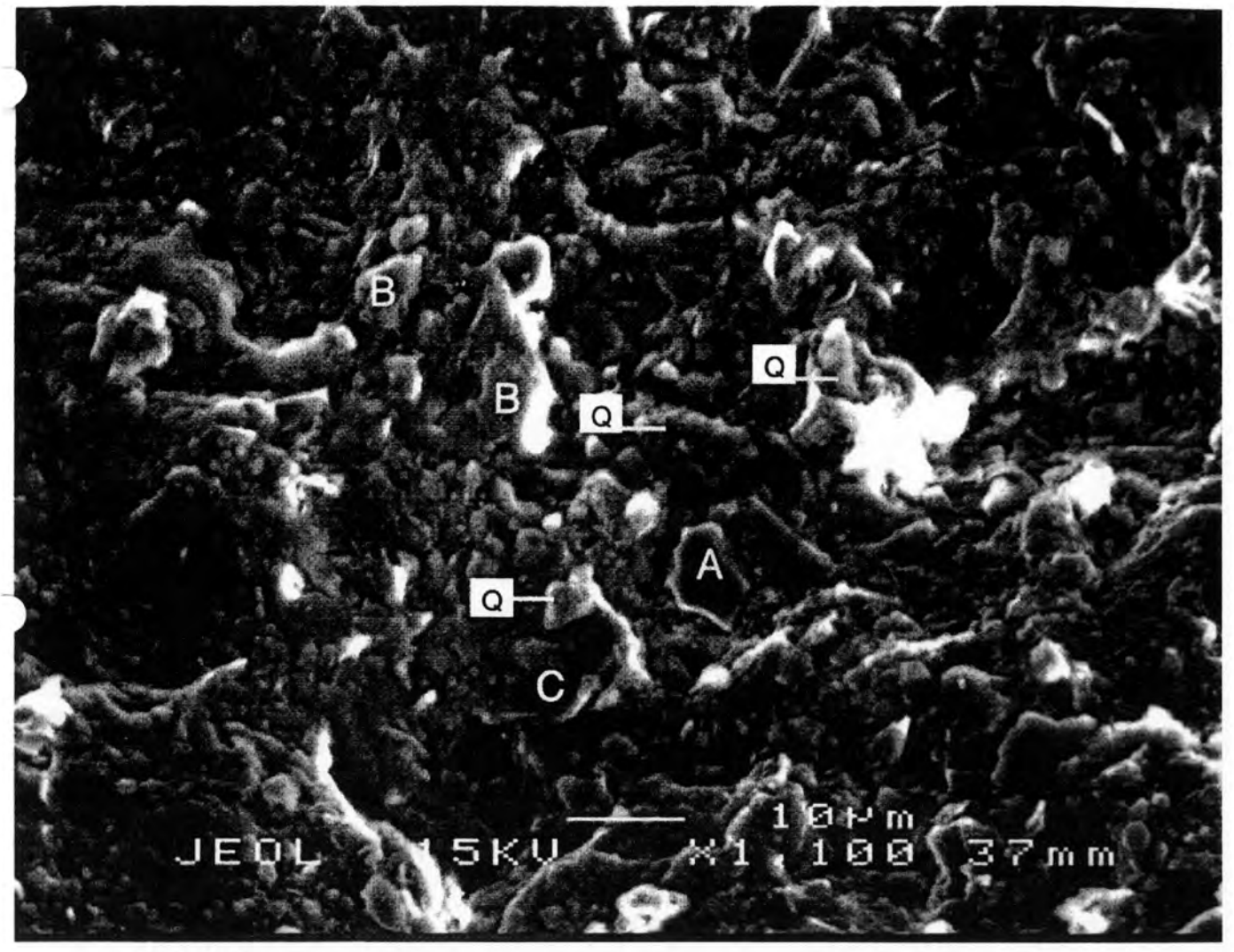

TP3-1

Q-quartz
A, B, C refer to XRF spectra attached

A = "dirty" quartz

B = vermiculite or v. altered biotite

C = "dirty" kaolinite

Magnification = X 1100

2-1 A

3-1

A

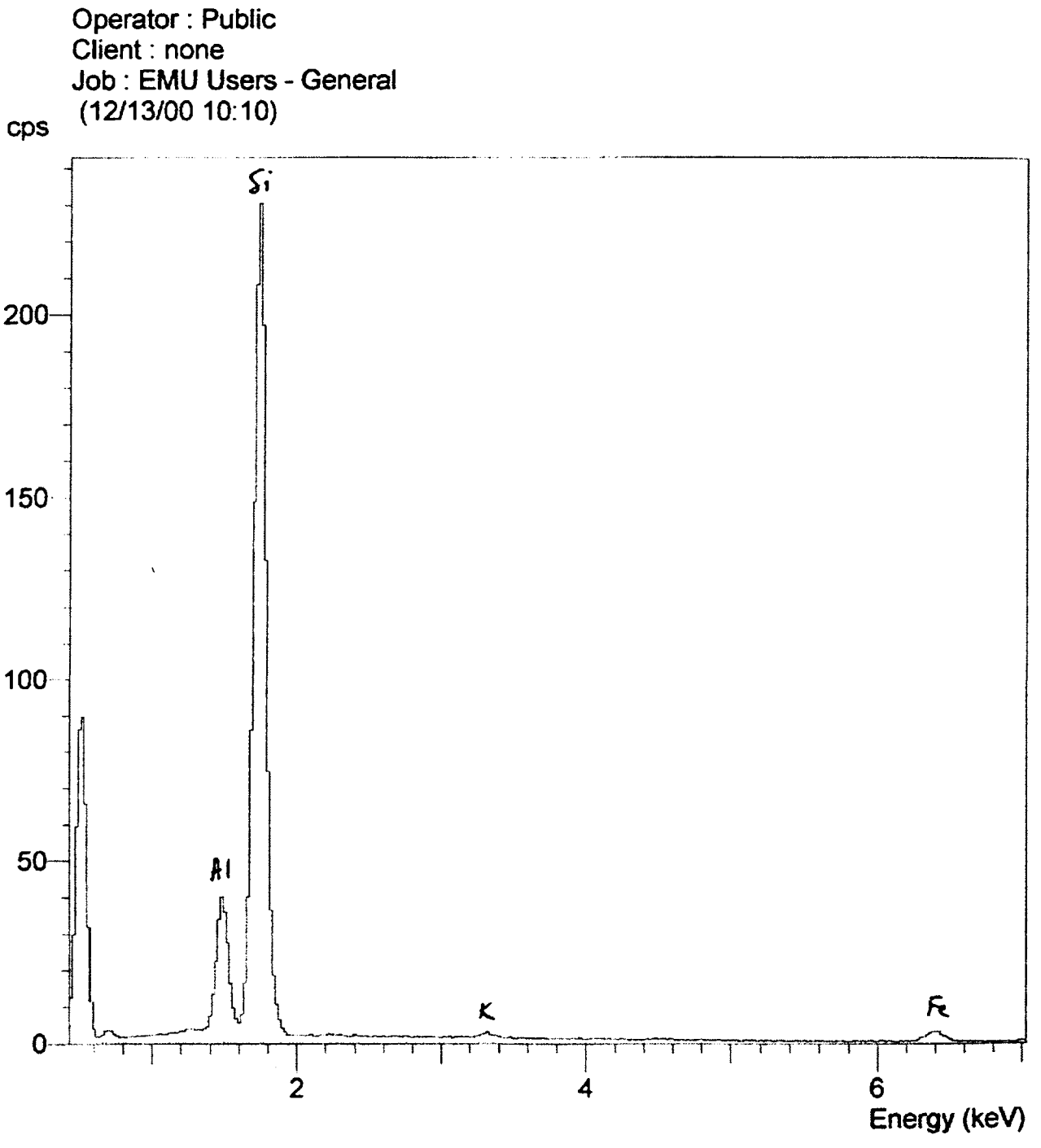
Operator : Public
Client : none
Job : EMU Users - General
(12/13/00 10:10)
cps
Si
Al
K
Fe
200
150
100
50
0
2
4
6
Energy (keV)

3-1

B

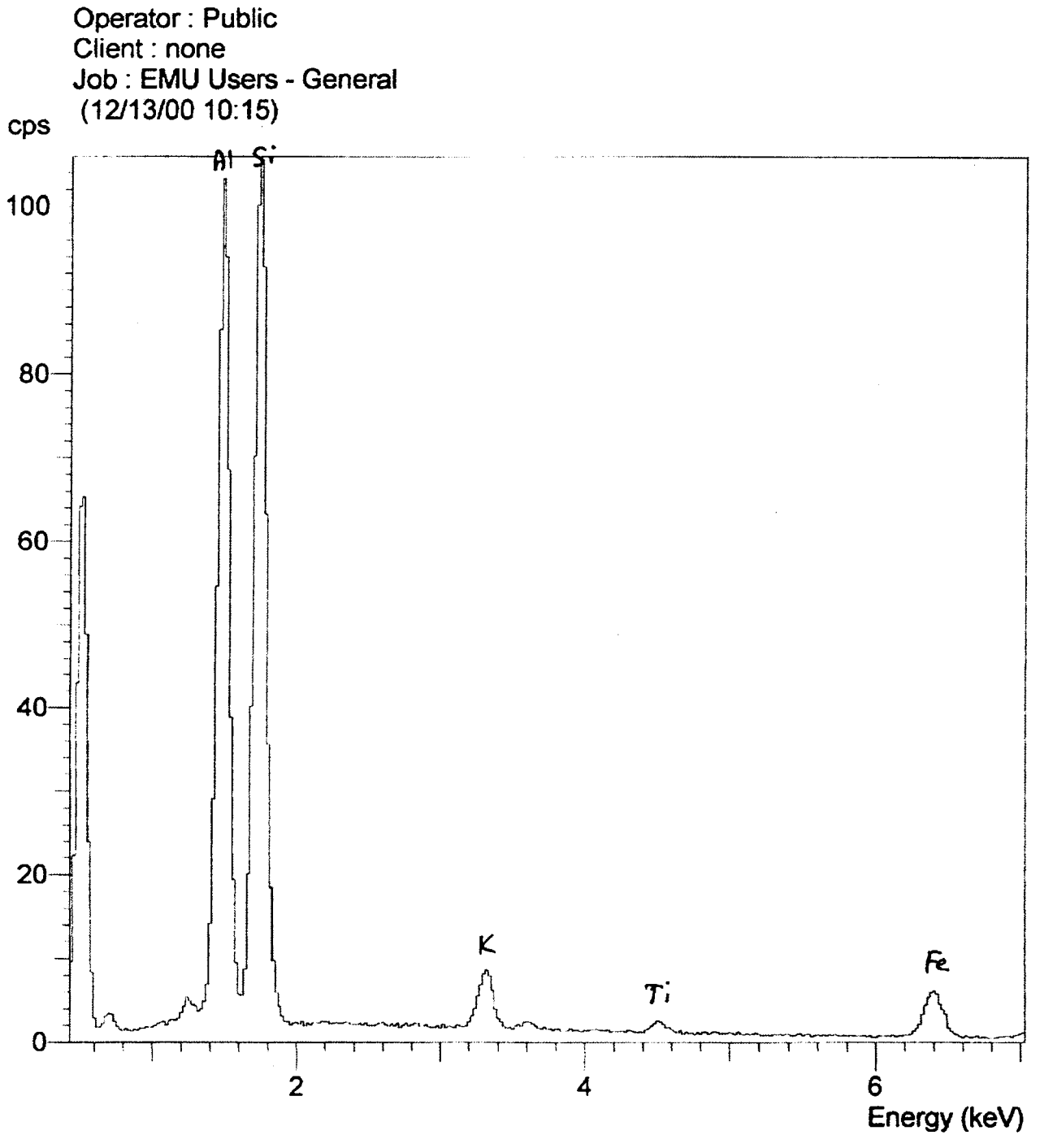
Operator : Public
Client : none
Job : EMU Users - General
(12/13/00 10:15)
cps
100
80
60
40
20
0
Al
Si
K
Ti
Fe
2
4
6
Energy (keV)

3-1

C

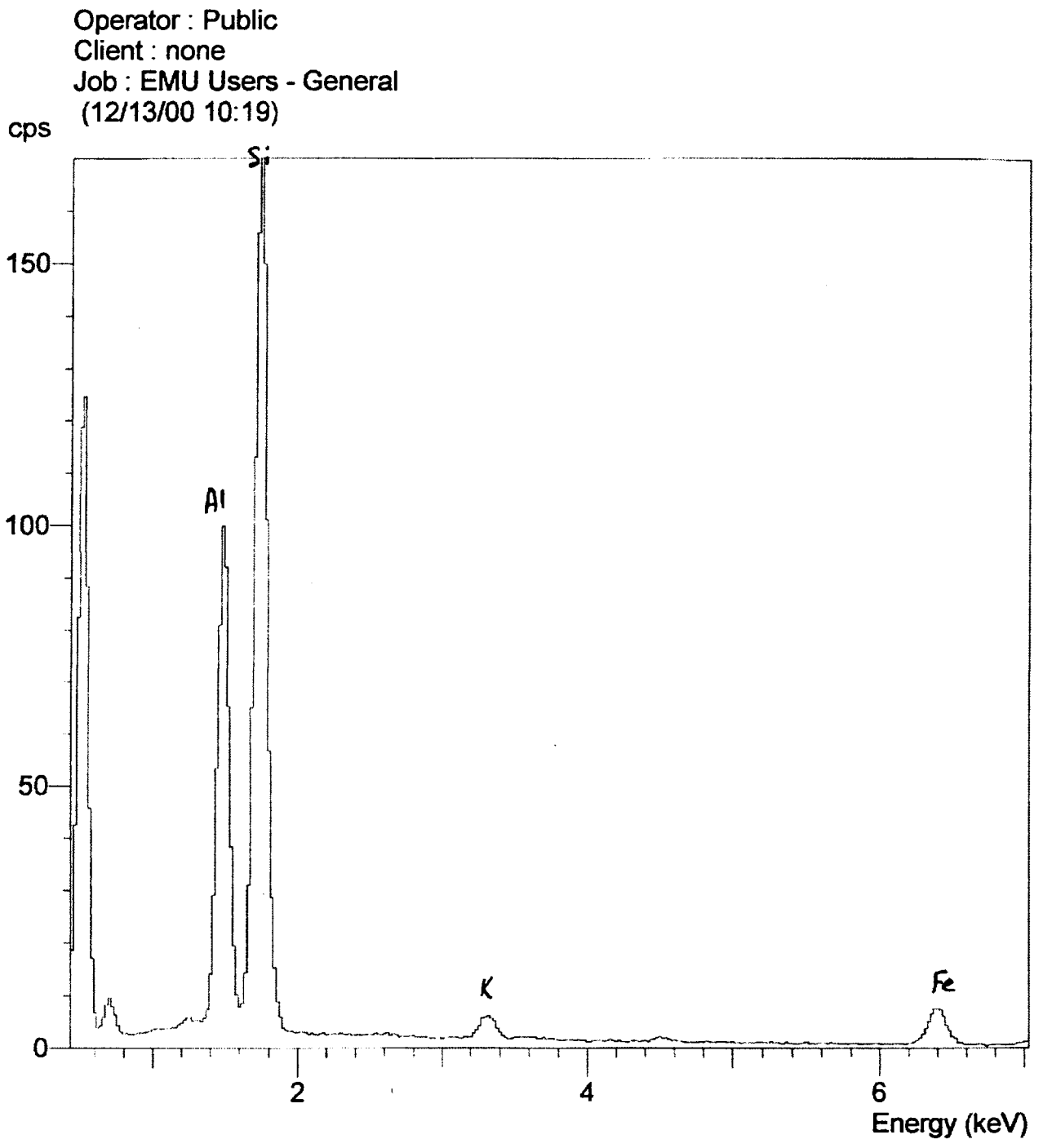
Operator : Public
Client : none
Job : EMU Users - General
(12/13/00 10:19)
cps
150
100
50
0
Si
Al
K
Fe
2
4
6
Energy (keV)

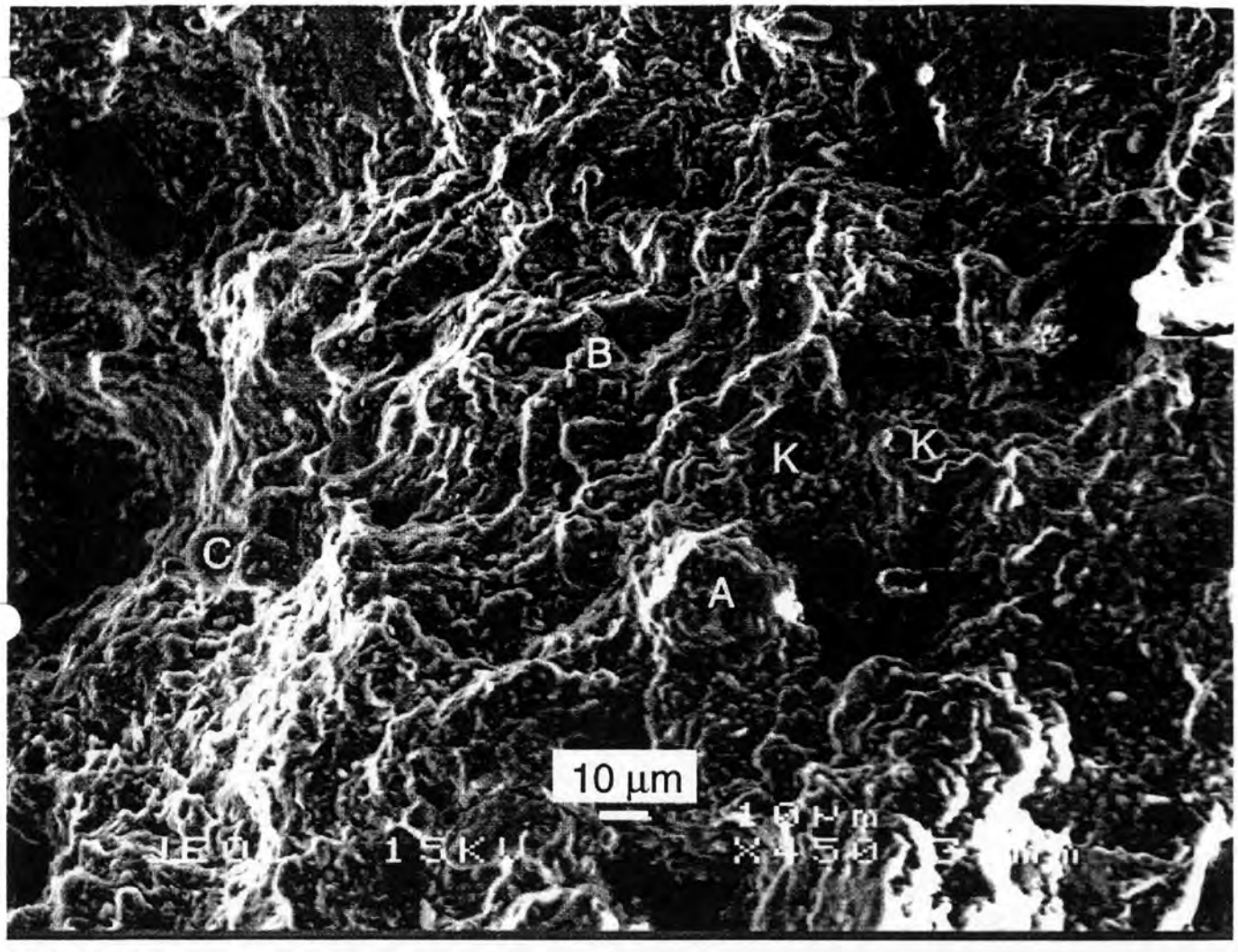

TP3-2
K-kaolin
A,B,C refer to XRF spectra attached

A = "dirty" (~~illegible~~) Kaolinite

B = (~~illegible~~) altered biotite

C = (~~illegible~~) vermiculite plus hydrated iron oxide

Magnification = x 450

3-2

A

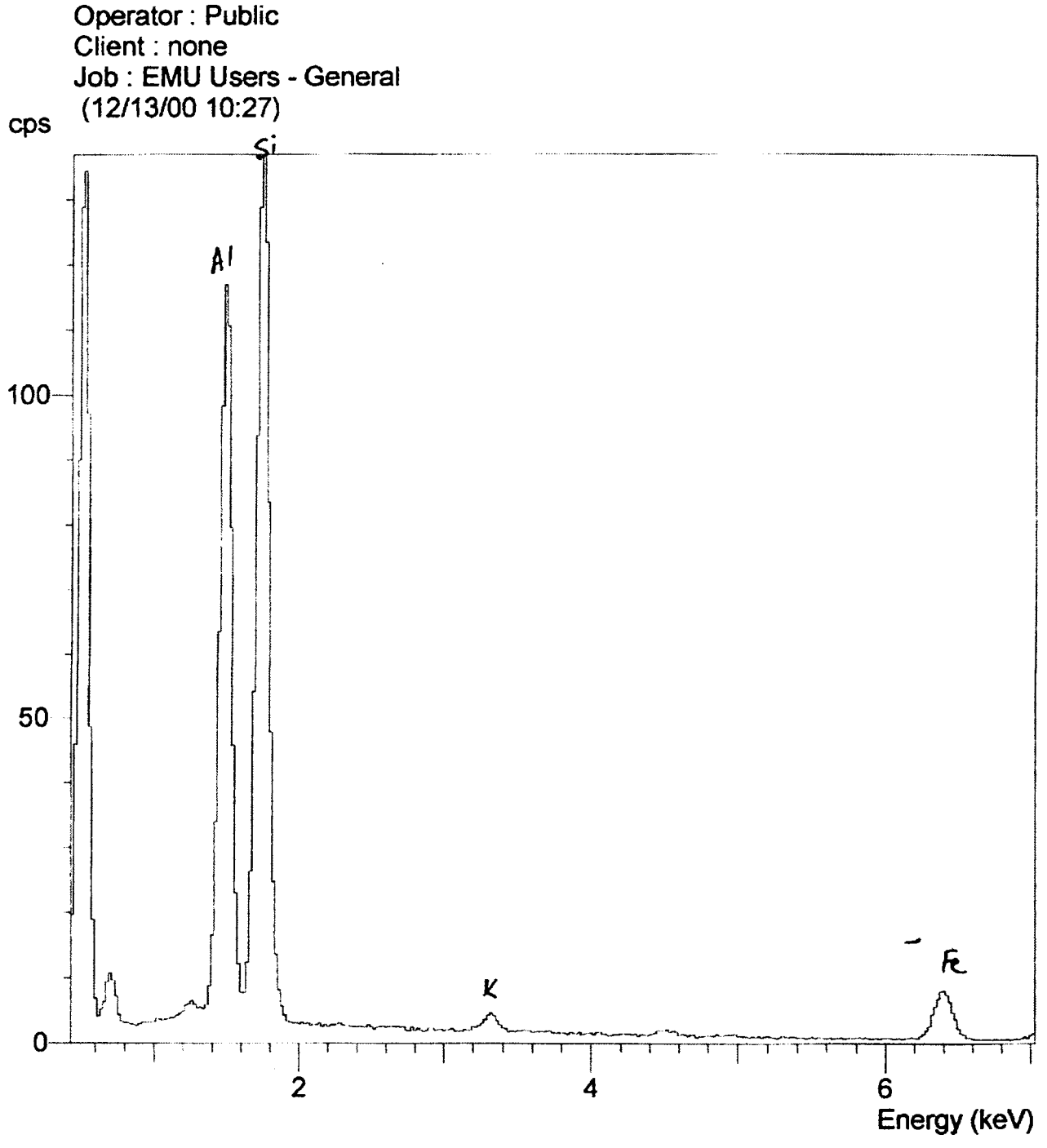

"dirty" kaolinite (i.e. too much Fe and some K)

3-2

B

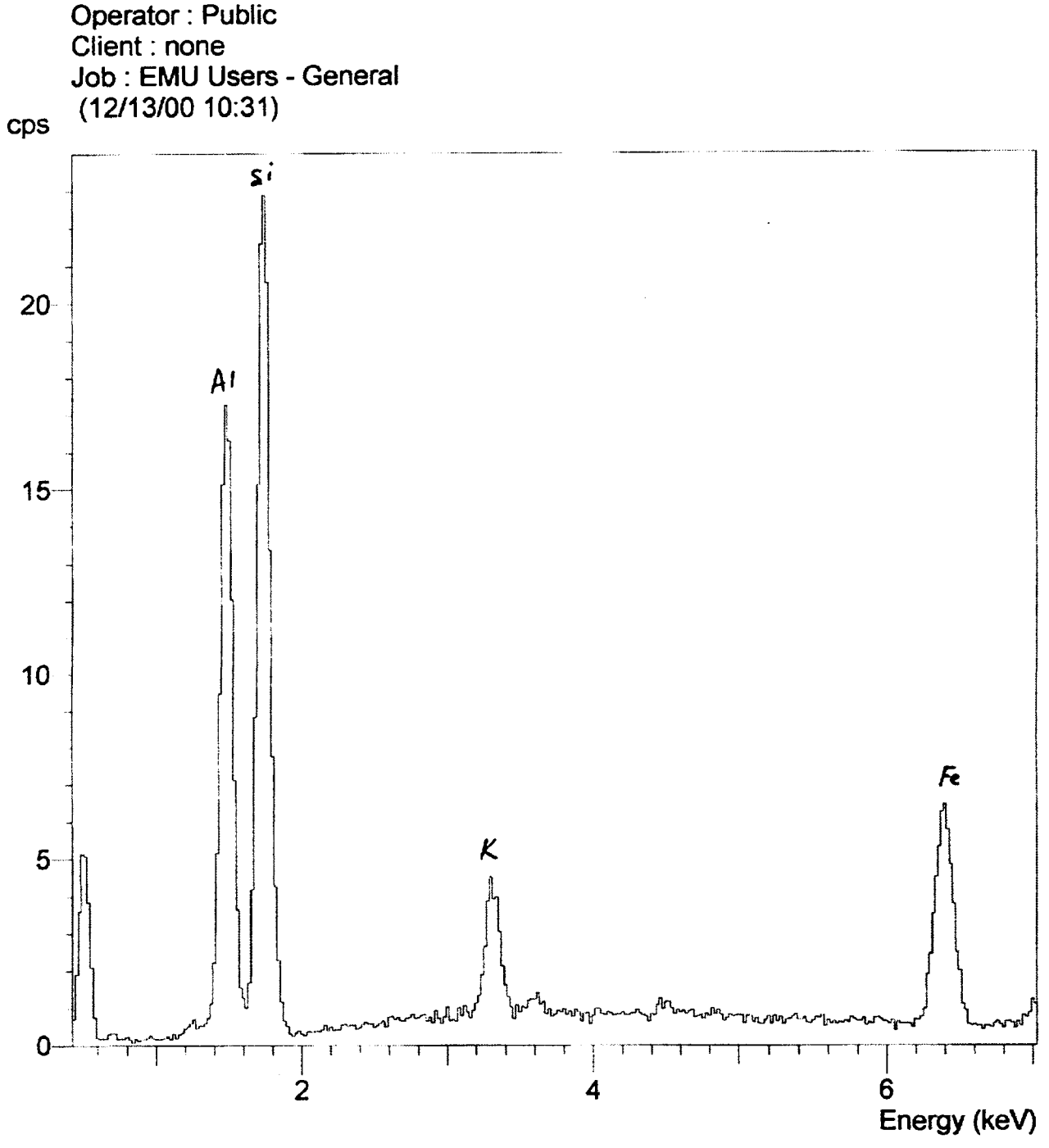

altered iron-rich mica

3-2

C

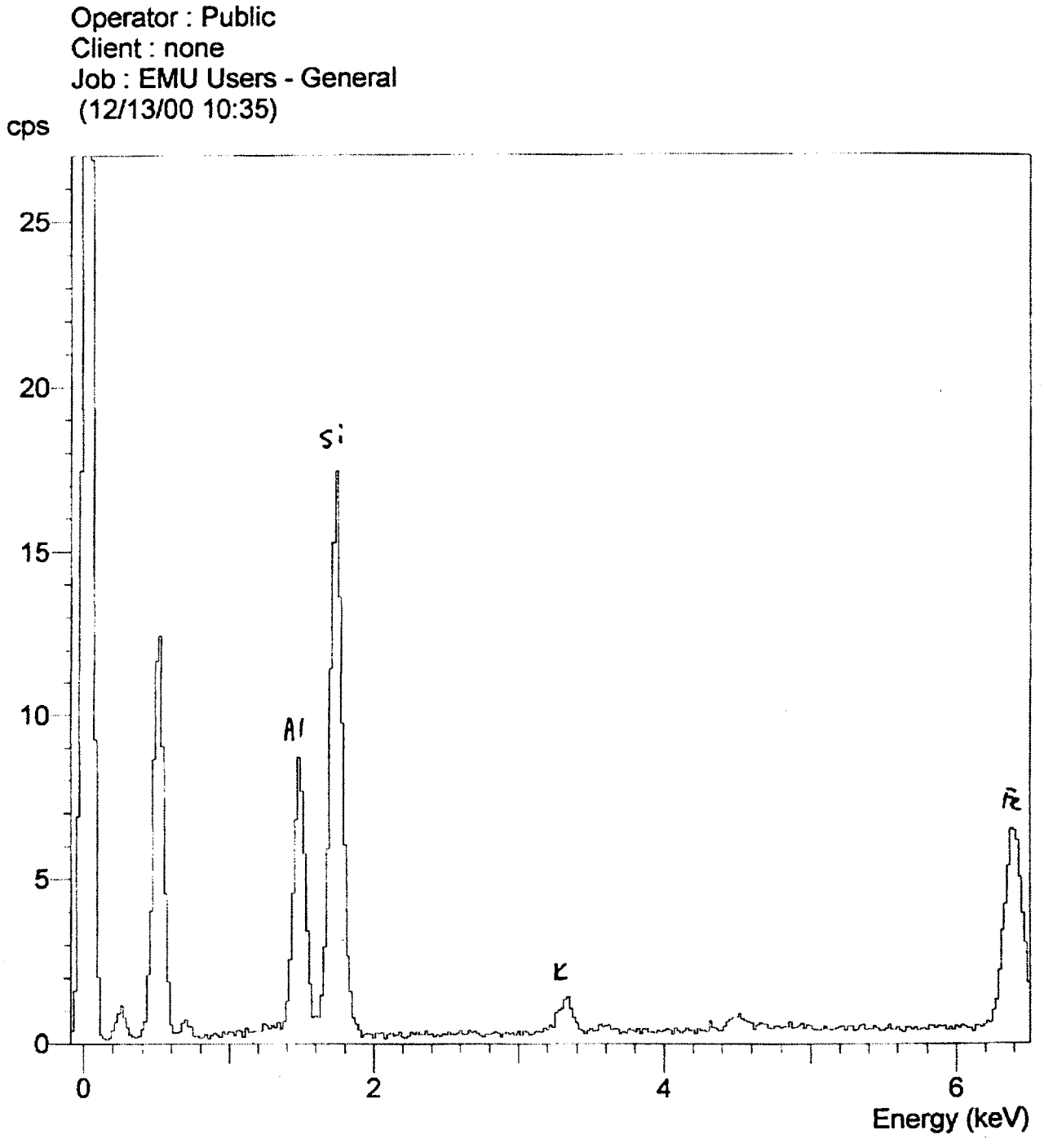

? vermiculite plus hydrated iron oxide

APPENDIX M

Summary of grading information of soil samples tested for internal stability by others

Table B1 Summary of grading information of soil samples tested for internal stability by others.

Investigator	Sample name	Internal stability	Clay Content (<0.005mm)	Fines Content (<0.075mm)	Sand Fraction (0.075 - 4.75mm)	Gravel Fraction (> 4.75mm)	USCS	Gap-grading Deficiency in size range (mm)	Coeff. of Uniformity	Coeff. of Curvature
			(%)	(%)	(%)	(%)			Cu	Cc
Kenney et al. (1983)	1	S	0.0	0.0	60.0	40.0	SP		3.1	0.80
Kenney et al. (1983)	2	S	0.0	0.0	100.0	0.0	SP		3.1	0.80
Kenney et al. (1983)	3	S	0.0	0.0	64.1	35.9	SP		6.2	0.69
Kenney et al. (1983)	4	S	0.0	0.0	36.2	63.8	GW		6.4	0.69
Kenney et al. (1983)	6	S	0.0	0.0	44.3	55.7	GW		14.1	0.59
Kenney et al. (1983)	7	S	0.0	0.0	51.8	48.2	SP		13.8	0.59
Kenney et al. (1983)	8	S	0.0	0.0	58.6	41.4	SP		13.4	0.59
Kenney et al. (1983)	9	S	0.0	0.0	70.0	30.0	SP		11.7	0.61
Kenney et al. (1983)	22	S	0.0	0.0	56.3	43.7	SP		3.9	1.02
Kenney et al. (1983)	24	S	0.0	0.0	30.8	69.2	GP		3.1	0.93
Kenney et al. (1983)	25	S	0.0	0.0	16.3	83.7	GW		5.4	1.35
Kenney et al. (1985)	A-B	S	0.0	0.0	88.5	11.5	SP	0.9 - 3.5	1.2	0.97
Kenney et al. (1985)	A-C	U	0.0	0.0	90.4	9.6	SP	0.75 - 3.5	1.1	0.98
Kenney et al. (1985)	A-D	U	0.0	0.0	91.1	8.9	SP	0.45 - 3.5	1.2	0.97
Kenney & Lau (1984, 85)	1	S	0.0	0.9	29.9	69.2	GW		13.2	1.32
Kenney & Lau (1984, 85)	2	S	0.0	0.6	30.4	69.0	GW		17.1	1.01
Kenney & Lau (1984, 85)	3	S	0.0	0.3	26.7	73.0	GW		17.0	2.44
Kenney & Lau (1984, 85)	20	S	0.0	0.0	42.6	57.4	GW		7.7	0.92
Kenney & Lau (1984, 85)	21	S	0.0	0.0	71.5	28.5	SP		3.6	0.94
Kenney & Lau (1984, 85)	23	S	0.0	0.0	25.7	74.3	GP		3.4	0.97
Kenney & Lau (1984, 85)	K	S	0.0	0.0	80.6	19.4	SP		4.3	1.67
Kenney & Lau (1984, 85)	Ds	S	0.0	0.0	16.6	83.4	GP		3.5	1.49
Kenney & Lau (1984, 85)	A	U	0.0	0.0	42.2	57.8	GW		26.0	0.53
Kenney & Lau (1984, 85)	As	U	0.0	0.0	36.1	63.9	GW		16.8	1.33
Kenney & Lau (1984, 85)	D	U	0.0	0.0	30.3	69.7	GP		21.8	5.85
Kenney & Lau (1984, 85)	X	U	0.0	1.3	14.5	84.2	GP		28.8	4.57
Kenney & Lau (1984, 85)	Y	U	0.0	0.0	28.0	72.0	GW		68.0	1.71
Kenney & Lau (1984, 85)	Ys	U	0.0	0.0	23.0	77.0	GW		43.1	1.60

Table B1 (Cont'd) Summary of grading information of soil samples tested for internal stability by others.

Investigator	Sample name	Internal stability	Clay Content (<0.005mm)	Fines Content (<0.075mm)	Sand Fraction (0.075 - 4.75mm)	Gravel Fraction (> 4.75mm)	USCS	Gap-grading Deficiency in size range (mm)	Coeff. of Uniformity	Coeff. of Curvature
			(%)	(%)	(%)	(%)			Cu	Cc
Lafleur et al. (1989)	M42	S	0.0	0.0	80.9	19.1	SP		7.0	0.78
Lafleur et al. (1989)	M6	U	0.0	0.0	62.0	38.0	SP	0.75 - 2.5	19.3	0.31
Lafleur et al. (1989)	M8	U	0.0	0.0	43.5	56.5	GP		18.8	4.08
Sun (1989)	1	S	5.9	42.3	57.7	0.0	SM		9.2	4.80
Sun (1989)	3	S	14.6	29.2	70.8	0.0	SM	0.03 - 0.15	84.7	29.05
Sun (1989)	6	S	21.7	43.9	56.1	0.0	SM	0.04 - 0.2	297.2	0.60
Sun (1989)	8	S	7.3	16.2	83.8	0.0	SM		48.9	10.61
Sun (1989)	12	S	14.7	29.2	70.8	0.0	SM	0.03 - 0.15	189.4	30.95
Sun (1989)	13	S	18.3	36.5	63.5	0.0	SM	0.04 - 0.6	493.2	0.41
Sun (1989)	2	U	7.0	14.3	85.7	0.0	SM	0.02 - 0.15	16.9	13.22
Sun (1989)	4	U	14.2	28.9	71.1	0.0	SM	0.04 - 0.25	126.9	66.35
Sun (1989)	5	U	14.2	28.9	71.1	0.0	SM	0.03 - 0.15	111.5	49.72
Sun (1989)	7	U	3.5	8.7	91.3	0.0	SP, SM		5.5	1.62
Sun (1989)	9	U	7.0	14.3	85.7	0.0	SM	0.03 - 0.075	44.2	13.51
Sun (1989)	10	U	3.5	7.3	92.7	0.0	SP, SM		2.9	1.04
Sun (1989)	11	U	10.7	21.6	78.3	0.1	SM	0.03 - 0.15	97.2	25.57
Sun (1989)	14	U	11.9	24.6	75.1	0.4	SM	0.03 - 0.25	388.0	9.71
Sun (1989)	15	U	15.4	31.7	68.0	0.3	SM	0.04 - 0.425	797.9	0.59
Sun (1989)	16	U	15.4	31.5	68.5	0.0	SM	0.04 - 0.7	404.4	1.37

Table B1 (Cont'd) Summary of grading information of soil samples tested for internal stability by others.

Investigator	Sample name	Internal stability	Clay Content (<0.005mm)	Fines Content (<0.075mm)	Sand Fraction (0.075 - 4.75mm)	Gravel Fraction (> 4.75mm)	USCS	Gap-grading Deficiency in size range (mm)	Coeff. of Uniformity	Coeff. of Curvature
			(%)	(%)	(%)	(%)			Cu	Cc
Burenkova (1993)	11	S	0.6	3.3	26.2	70.5	GW		11.8	1.01
Burenkova (1993)	12	S	0.0	5.9	31.9	62.2	GW, GM		24.1	1.65
Burenkova (1993)	13	S	4.2	9.4	35.1	55.4	GP, GM		93.9	6.33
Burenkova (1993)	14	S	0.4	9.8	39.6	50.6	GP, GM		101.4	5.16
Burenkova (1993)	1	U	1.8	6.4	6.5	87.2	GP, GM		59.4	21.09
Burenkova (1993)	2	U	0.0	0.2	5.6	94.2	GP		2.9	1.29
Burenkova (1993)	3	U	0.0	5.7	9.0	85.3	GP, GM		82.1	19.35
Burenkova (1993)	4	U	0.0	5.2	11.6	83.2	GP, GM		103.3	14.54
Skempton & Brogan (1994)	C	S	0.0	0.0	73.6	26.4	SW		6.3	2.49
Skempton & Brogan (1994)	D	S	0.0	0.0	67.3	32.7	SP		4.1	1.84
Skempton & Brogan (1994)	A	U	0.0	1.0	72.2	26.8	SP	0.25 - 0.8	22.9	8.91
Skempton & Brogan (1994)	B	U	0.0	0.8	72.2	27.0	SP		8.7	3.39
Chapuis et al. (1996)	1	S	0.0	1.1	58.0	40.8	SP		28.8	0.76
Chapuis et al. (1996)	3	S	0.0	0.7	73.5	25.8	SP		17.0	0.58
Chapuis et al. (1996)	2	U	0.0	1.6	32.9	65.5	GW		31.6	2.55

APPENDIX N

Record of downward flow seepage tests

Downward flow test No. 1 Test Records

DOWNWARD FLOW SUFFUSION TEST
Test Record

Test No/Date :	**Suffusion Downflow 001 09/11/01**
Soil Sample :	**Suffusion Test Blend No. 1**
Standard max. dry density :	2.319 Mg/m^3
Optimum water content (OWC) :	7.70%
Targeted dry density relative to Standard max. dry density :	95.0%
Actual dry density from test:	94.0%
Water content during conditioning :	7.70%
Targeted moisture content :	7.70%
Actual water content from test :	7.70%
Fluid for conditioning soil :	Sydney tap water
Eroding fluid :	Sydney tap water
Eroding fluid mean temperature :	21.6 °C
Data Log File Name :	DF1b, DF1c
Time/Date of compaction of sample :	10.00am 8/10/01
Time/Date of Commencement of Test :	11.10am 11/10/01

Mix Ingredient	Mix Proportion (%)
Clay Q38	0.00
Silica 60G	10.52
Nepean Sand	25.70
5mm Blue Metal	16.18
10mm Bassalt	23.80
20mm Blue Metal	23.80
Total	100.00

Time (From Commencement) (hr)	Time (From Commencement) (min)	Flowrate (L/min)	Observations
0.00	0	0.00	Test Started. Extremely low initial flow. Sligthly cloudy appearance after 25 sec.
70.00	4200	0.50	Clear, and very low steady flow
71.00	4260	0.47	Clear, and very low steady flow
73.67	4420	0.47	Clear, and very low steady flow
74.67	4480	0.47	Clear, and very low steady flow
75.67	4540	0.45	Clear, and very low steady flow
77.42	4645	0.44	Clear, and very low steady flow
94.00	5640	0.37	Clear, and very low steady flow. Test stopped.

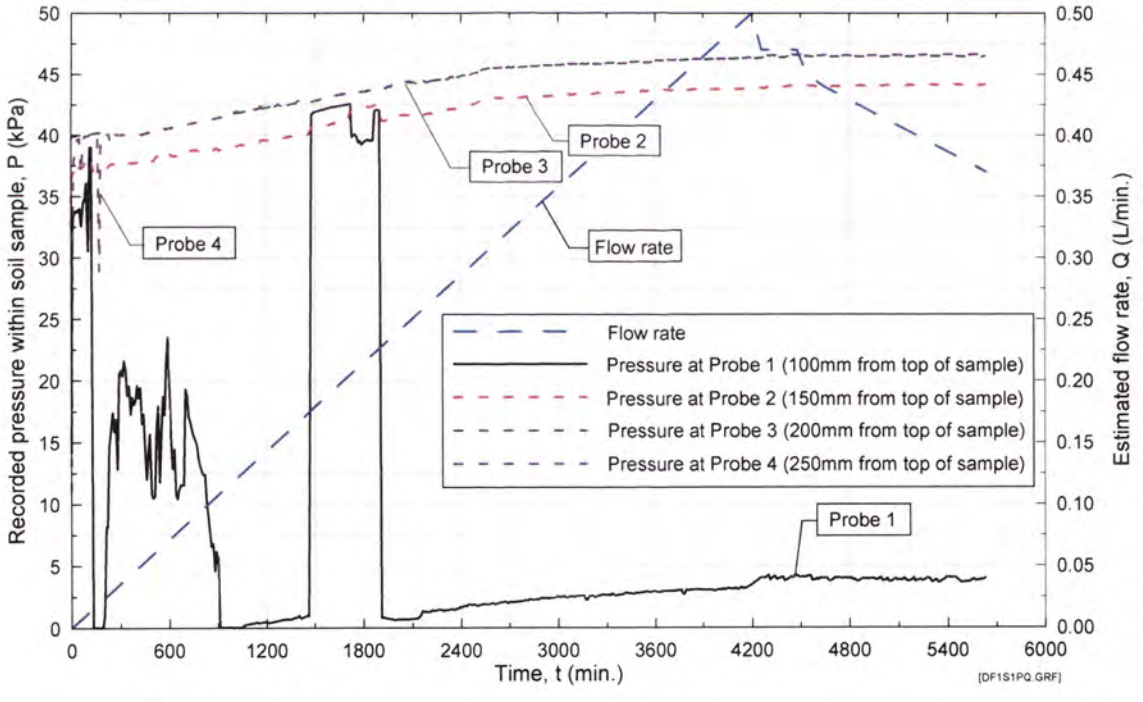

DF Test No. 1 on Sample 1 – Recorded pressure and flow rate. Sample compacted to 94% of Standard Max. Dry Density.

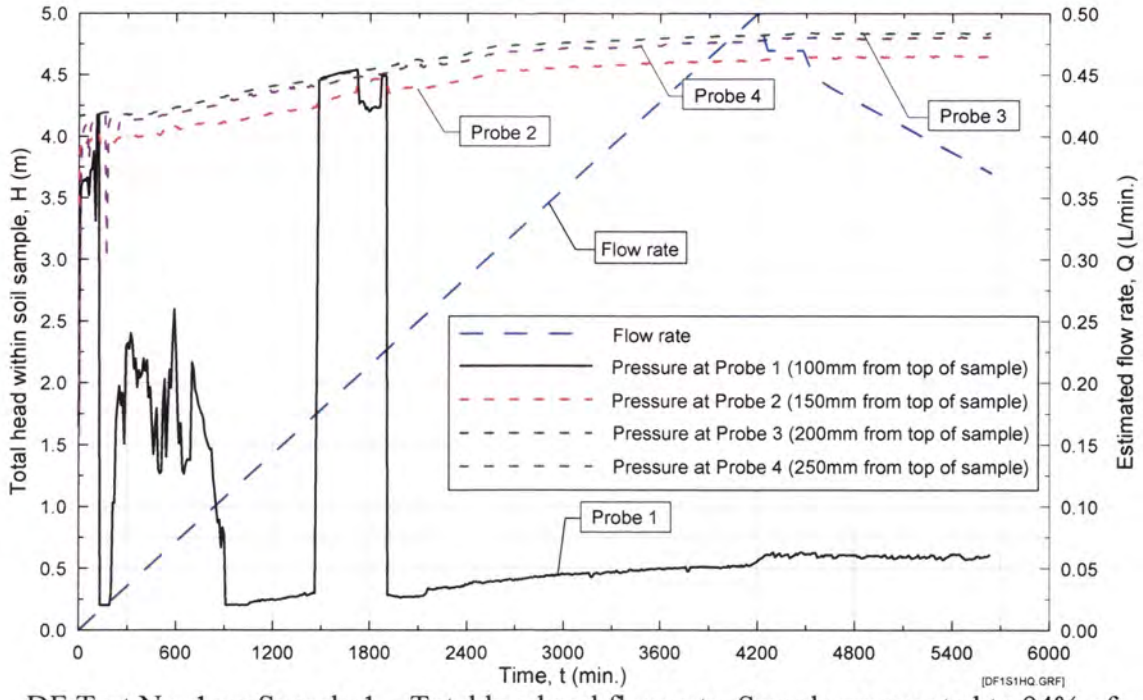

DF Test No. 1 on Sample 1 – Total head and flow rate. Sample compacted to 94% of Standard Max. Dry Density.

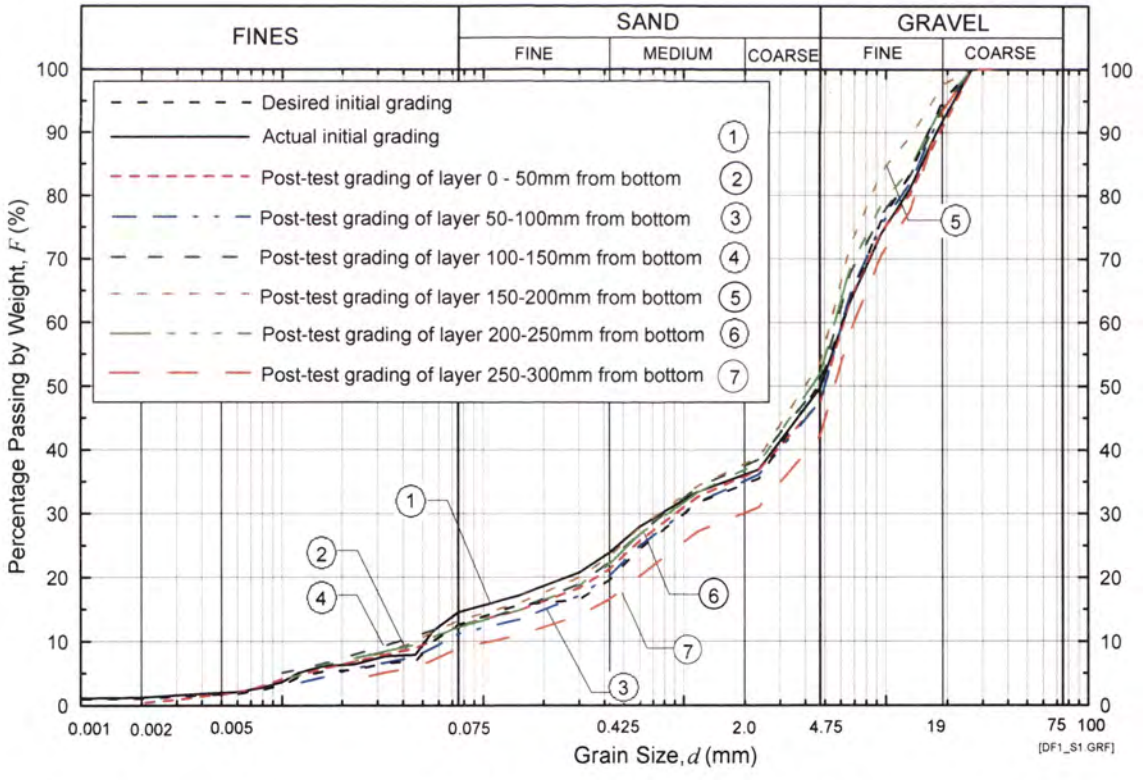

DF Test No. 1 on Sample 1 - Initial and post-test grain-size distribution analysis. Sample compacted to 94% of Standard Max. Dry Density.

Downward flow test No. 5 Test Records

DOWNWARD FLOW SUFFUSION TEST
Test Record

Test No/Date :	**Suffusion Downflow 005 9/04/02**	
Soil Sample :	**Suffusion Test Blend No. 1a**	
Standard max. dry density :	2.319	Mg/m^3
Optimum water content (OWC) :	7.70%	
Targeted dry density relative to Standard max. dry density :	90.0%	
Actual dry density from test:	89.4%	
Water content during conditioning :	7.70%	
Targeted moisture content :	7.70%	
Actual water content from test :	7.84%	
Fluid for conditioning soil :	Sydney tap water	
Eroding fluid :	Sydney tap water	
Eroding fluid mean temperature :	21.6	°C
Data Log File Name :	DF5a, DF5b, DF5c, DF5d	
Time/Date of compaction of sample :	pm 8/04/02	
Time/Date of Commencement of Test :	10.20am 9/04/02	

Mix Ingredient	Mix Proportion (%)
Clay Q38	0.00
Silica 60G	10.52
Nepean Sand	25.70
5mm Blue Metal	16.18
10mm Bassalt	23.80
20mm Blue Metal	23.80
Total	100.00

Time (From Commencement) (hr)	Time (From Commencement) (min)	Flowrate (L/min)	Observations
0.00	0	0.00	Test Started. Slight cloudiness near base, extremely low outflow.
0.05	3	0.04	Slightly cloudy near base, and slowly increasing throughout. Extremely low outflow.
0.67	40	0.05	Slightly cloudy near base, and slowly increasing throughout. Extremely low outflow.
1.00	60	0.09	Slightly cloudy near base, and slowly increasing throughout. Extremely low outflow.
2.75	165	0.13	Slightly cloudy near base, and slowly increasing throughout. Extremely low outflow.
3.75	225	0.16	Slightly cloudy near base, and slowly clearing throughout. Extremely low outflow.
5.55	333	0.14	Slightly cloudy near base. Extremely low outflow. Test paused, then restarted.
5.67	340	0.15	Mostly clear throughout. Extremely low outflow.
11.67	700	0.13	Mostly clear throughout. Extremely low outflow. Test stopped.

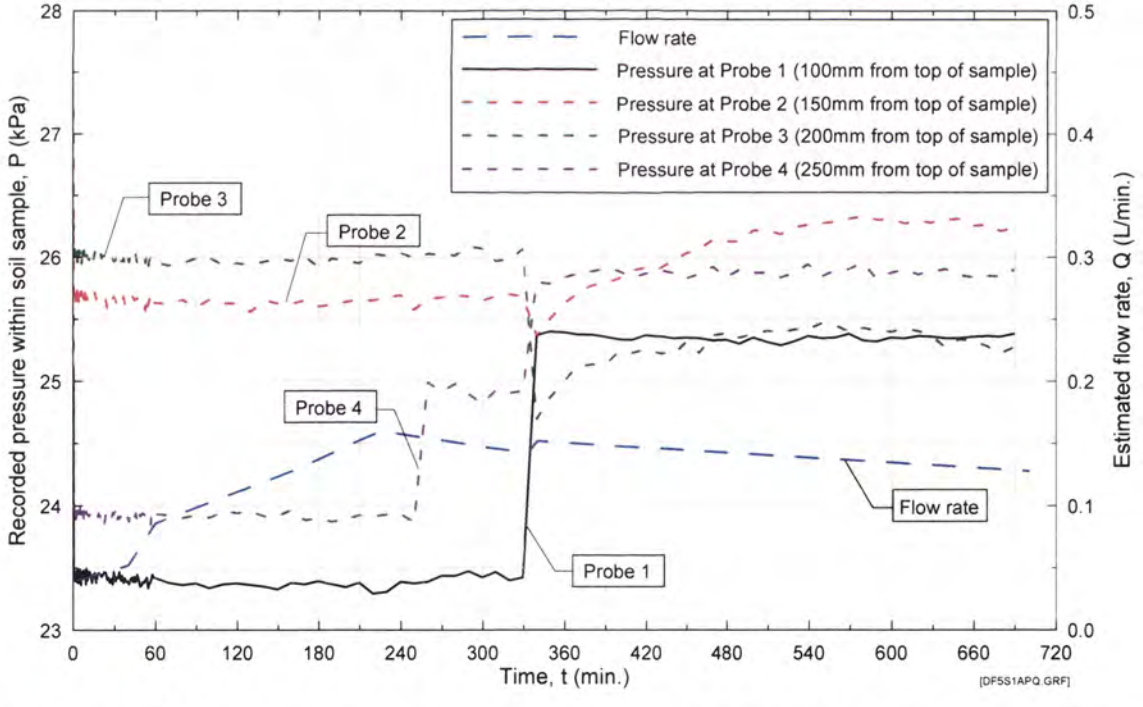

DF Test No. 5 on Sample 1A – Recorded pressure and flow rate. Sample compacted to 89.4% of Standard Max. Dry Density.

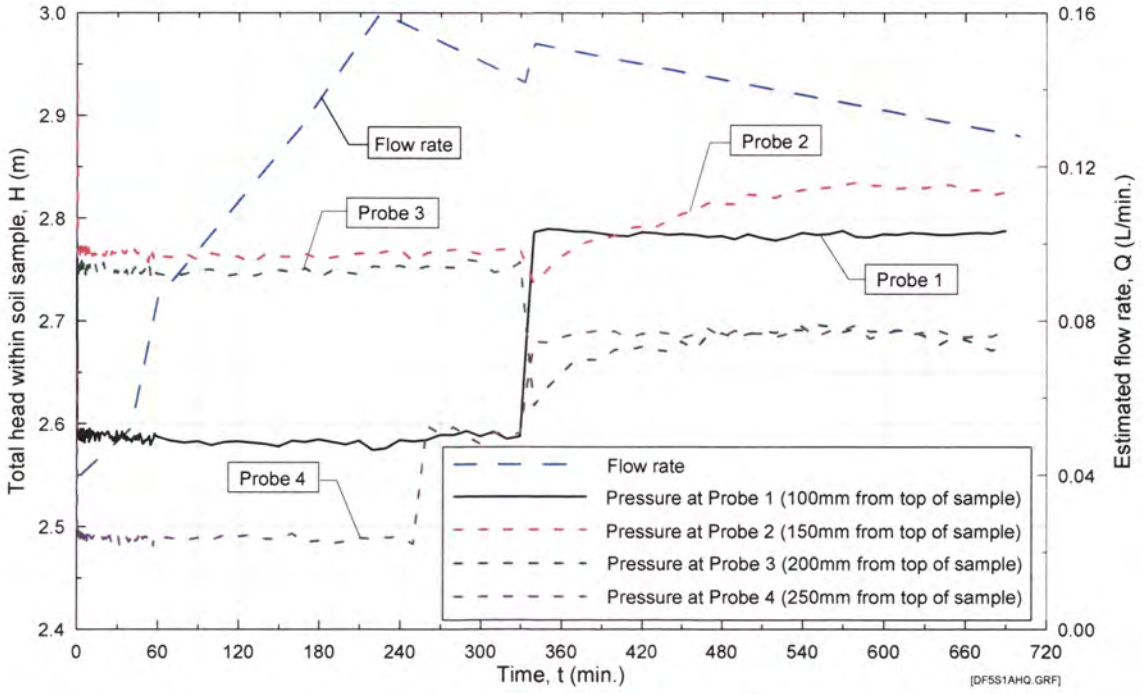

DF Test No. 5 on Sample 1A – Total head and flow rate. Sample compacted to 89.4% of Standard Max. Dry Density.

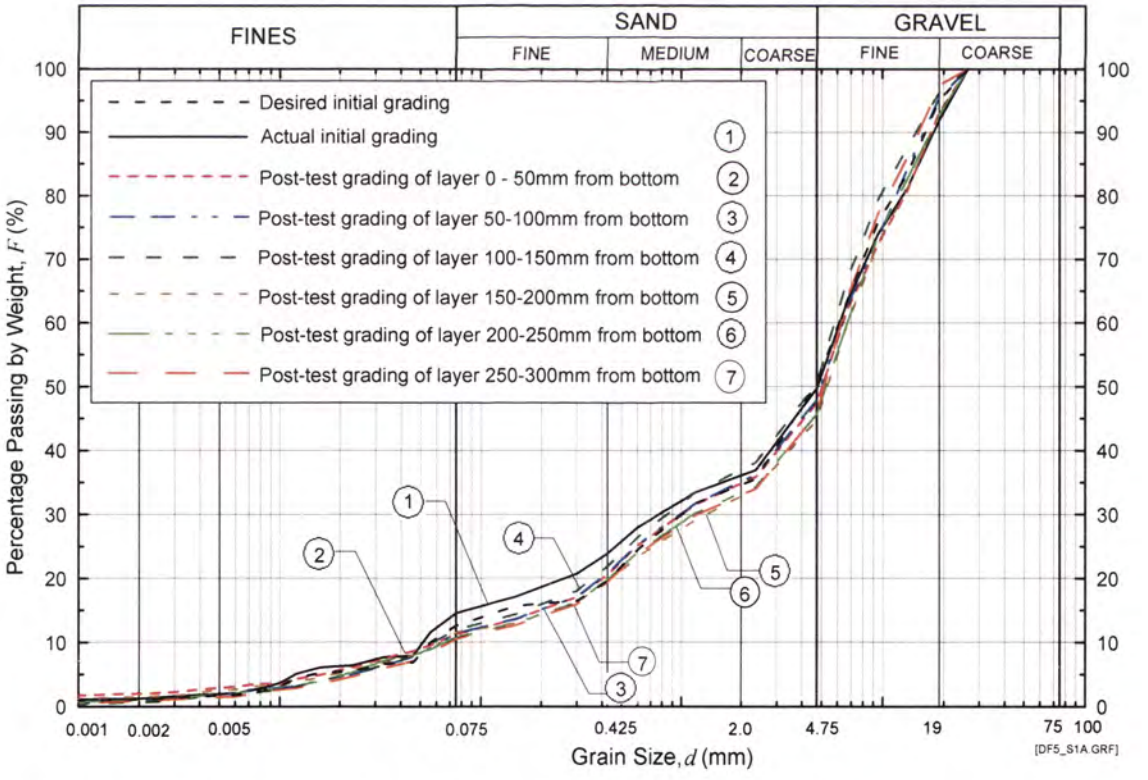

DF Test No. 5 on Sample 1A - Initial and post-test grain-size distribution analysis. Sample compacted to 89.4% of Standard Max. Dry Density.

Downward flow test No. 2R Test Records

DOWNWARD FLOW SUFFUSION TEST
Test Record

Test No/Date :	**Suffusion Downflow 002R 2/12/02**
Soil Sample :	**Suffusion Test Blend No. 2R**
Standard max. dry density :	2.125 Mg/m^3
Optimum water content (OWC) :	9.86%
Targeted dry density relative to Standard max. dry density :	95.0%
Actual dry density from test:	95.8%
Water content during conditioning :	9.86%
Targeted moisture content :	9.86%
Actual water content from test :	9.53%
Fluid for conditioning soil :	Sydney tap water
Eroding fluid :	Sydney tap water
Eroding fluid mean temperature :	21.6 °C
Data Log File Name :	DF2Ra, DF2Rb, DF2Rc
Time/Date of compaction of sample :	10.00am 8/10/01
Time/Date of Commencement of Test :	11.10am 11/10/01

Mix Ingredient	Mix Proportion (%)
Clay Q38	0.00
Silica 60G	24.01
Nepean Sand	24.01
5mm Blue Metal	18.01
10mm Bassalt	18.01
20mm Blue Metal	15.96
Total	100.00

Time (From Commencement) (hr)	Time (From Commencement) (min)	Flowrate (L/min)	Observations
0.00	0	0.00	Test Started. Very low flow and very slight cloudiness at base initially.
0.08	5	0.39	Slightly cloudy at base, and cloudiness slowly increasing. Very low flow.
0.20	12	0.45	Cloudy and very low flow. Cloudiness increasing, and flow fluctuating.
0.33	20	0.41	Cloudy and very low flow. Cloudiness increasing, and flow fluctuating.
0.50	30	0.42	Cloudy and very low flow. Cloudiness increasing, and flow fluctuating.
0.67	40	2.28	Very cloudy and low flow. Cloudiness and flow increasing steadily.
0.75	45	3.45	Very cloudy and low flow. Cloudiness and flow increasing steadily.
0.83	50	6.84	Very cloudy and moderate flow. Cloudiness and flow increasing steadily.
0.92	55	7.62	Cloudy and moderate flow. Clearing slightly, and flow increasing slowly.
1.00	60	8.55	Cloudy and moderate flow. Clearing slightly, and flow increasing slowly.
1.08	65	9.12	Cloudy and moderate flow. Clearing slightly, and flow increasing slowly.
1.17	70	9.33	Cloudy and moderate flow. Clearing slightly, and flow increasing slowly.
1.33	80	10.59	Cloudy and moderate flow. Clearing slightly, and flow increasing slowly.
1.50	90	11.64	Cloudy and moderate flow. Clearing slightly, and flow increasing slowly.
1.67	100	12.00	Slightly cloudy and moderate flow. Clearing slightly, and flow increasing slowly.
2.00	120	14.34	Slightly cloudy and moderate flow. Clearing slightly, and flow increasing slowly.
2.33	140	15.96	Mostly clear and moderate flow. Continuing to clear, and flow increasing slowly.
2.67	160	16.20	Mostly clear and moderate flow. Continuing to clear, and flow increasing slightly.
3.00	180	16.80	Clear and moderate flow. Pressure stabilising, and flow increasing slightly. Stop test.

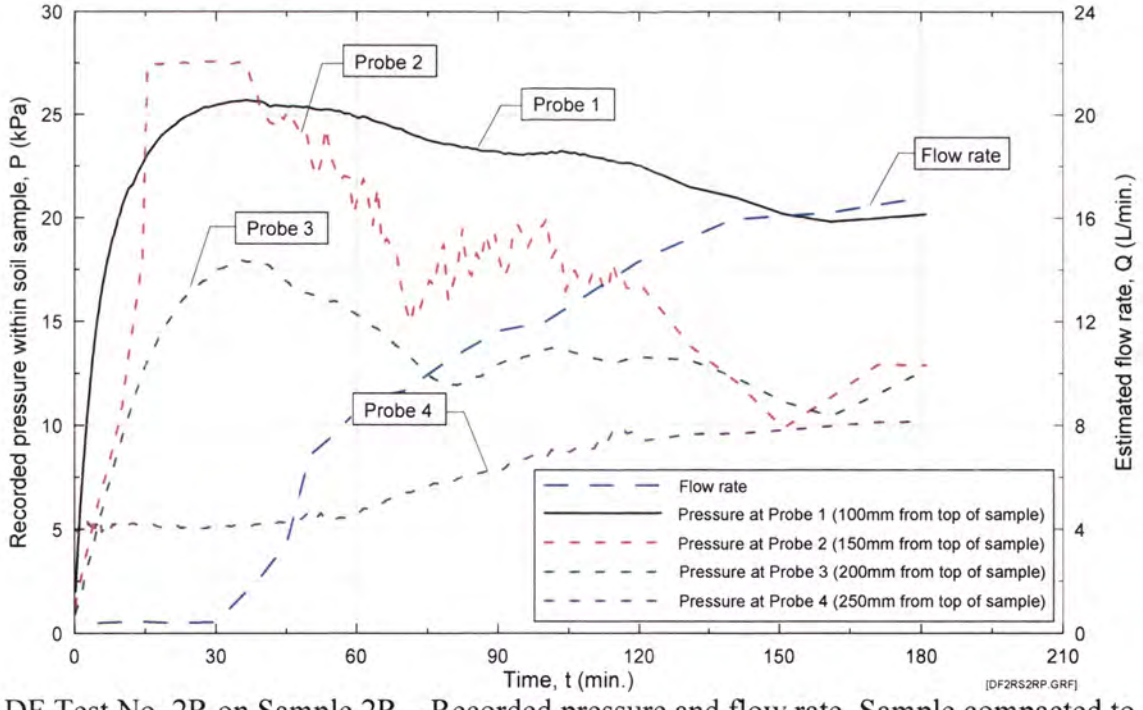

DF Test No. 2R on Sample 2R – Recorded pressure and flow rate. Sample compacted to 95.8% of Standard Max. Dry Density.

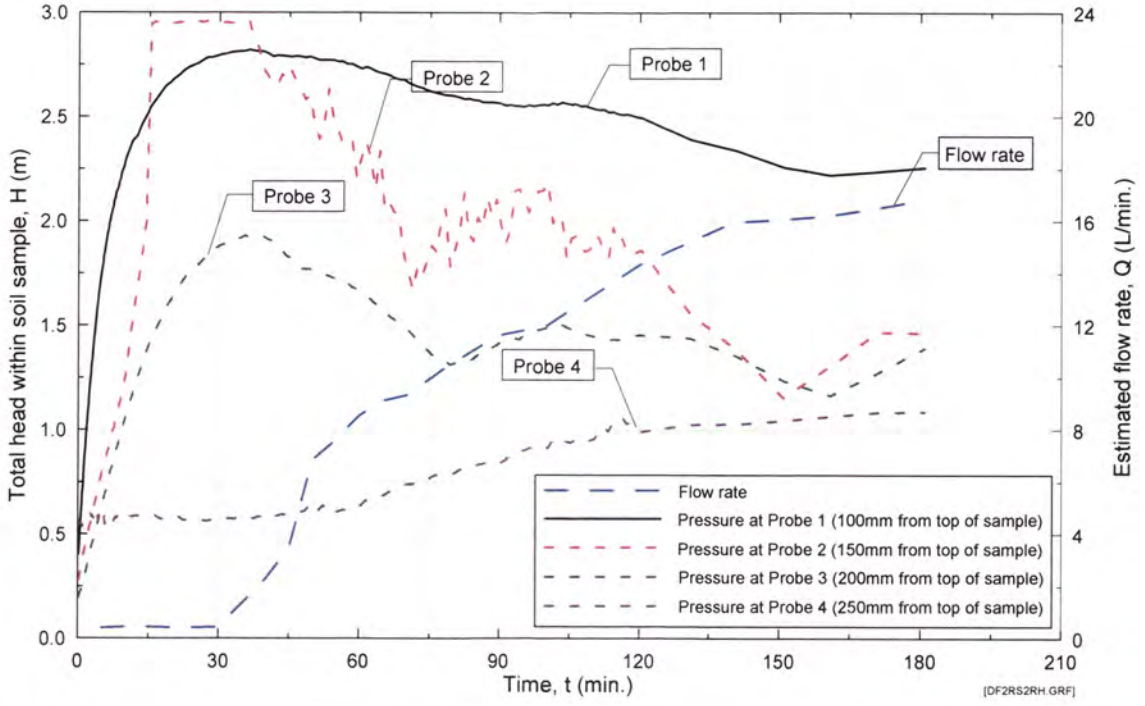

DF Test No. 2R on Sample 2R – Total head and flow rate. Sample compacted to 95.8% of Standard Max. Dry Density.

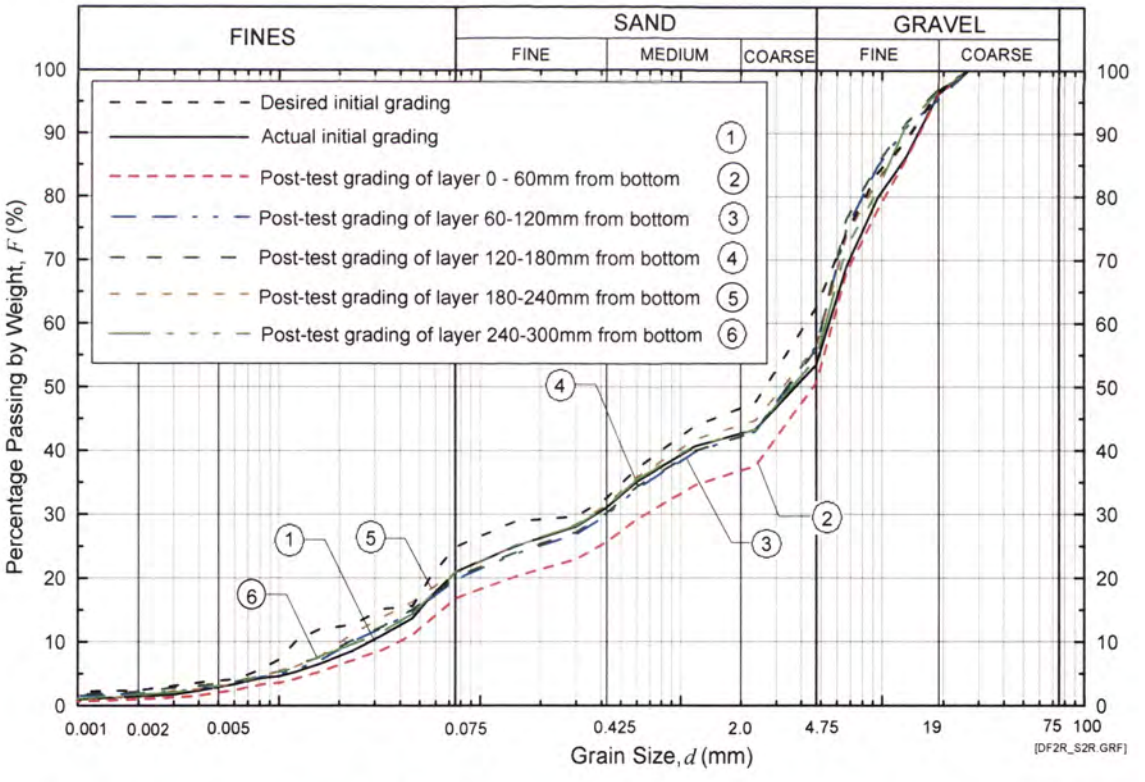

DF Test No. 2R on Sample 2R - Initial and post-test grain-size distribution analysis. Sample compacted to 95.8% of Standard Max. Dry Density.

Downward flow test No. 3R Test Records

DOWNWARD FLOW SUFFUSION TEST
Test Record

Test No/Date :	**Suffusion Downflow 003R 9/12/02**
Soil Sample :	**Suffusion Test Blend No. 3R**
Standard max. dry density :	1.892 Mg/m^3
Optimum water content (OWC) :	11.16%
Targeted dry density relative to Standard max. dry density :	95.0%
Actual dry density from test:	94.0%
Water content during conditioning :	11.16%
Targeted moisture content :	11.16%
Actual water content from test :	11.68%
Fluid for conditioning soil :	Sydney tap water
Eroding fluid :	Sydney tap water
Eroding fluid mean temperature :	21.6 °C
Data Log File Name :	DF3Ra, DF3Rb, DF3Rc, DF3Rd
Time/Date of compaction of sample :	1.00pm 6/12/02
Time/Date of Commencement of Test :	1.00pm 9/12/02

Mix Ingredient	Mix Proportion (%)
Clay Q38	0.00
Silica 60G	50.90
Nepean Sand	28.28
5mm Blue Metal	6.11
10mm Bassalt	9.05
20mm Blue Metal	5.66
Total	100.00

Time (From Commencement) (hr)	Time (From Commencement) (min)	Flowrate (L/min)	Observations
0.00	0	0.00	Test Started. Clear, no outflow.
0.03	2	0.00	Clear, no outflow.
0.15	9	0.00	Clear, no outflow.
0.33	20	0.01	Clear, extremely low outflow.
1.00	60	0.04	Slightly cloudy appearance near base and increasing slowly. Extremely low outflow.
1.43	86	0.03	Slightly cloudy near base, extremely low outflow.
2.00	120	0.03	Slightly cloudy near base, extremely low outflow.
3.00	180	0.02	Slightly cloudy near base, extremely low outflow.
4.00	240	0.02	Slightly cloudy near base, extremely low outflow.
4.50	270	0.02	Slightly cloud near base, extremely low outflow. Test paused, then restarted.
4.67	280	0.01	Slightly cloudy near base, extremely low outflow.
7.00	420	0.01	Slightly cloudy near base, extremely low outflow.
10.00	600	0.01	Slightly cloudy near base, extremely low outflow. Test stopped.

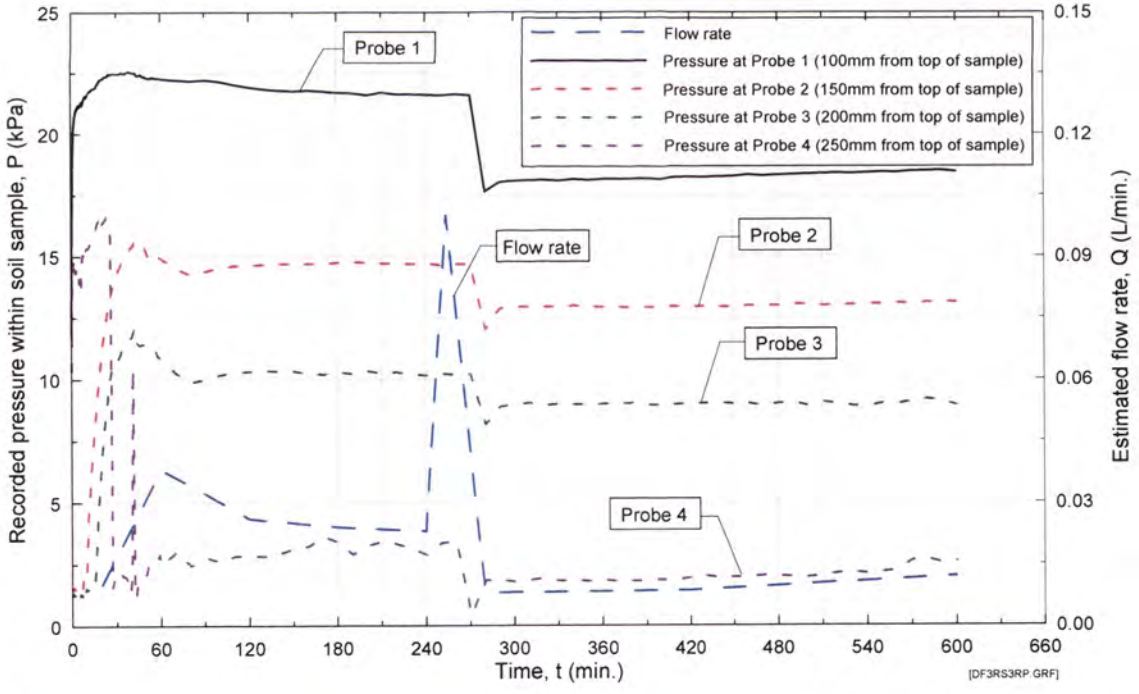

DF Test No. 3R on Sample 3R – Recorded pressure and flow rate. Sample compacted to 94.0% of Standard Max. Dry Density.

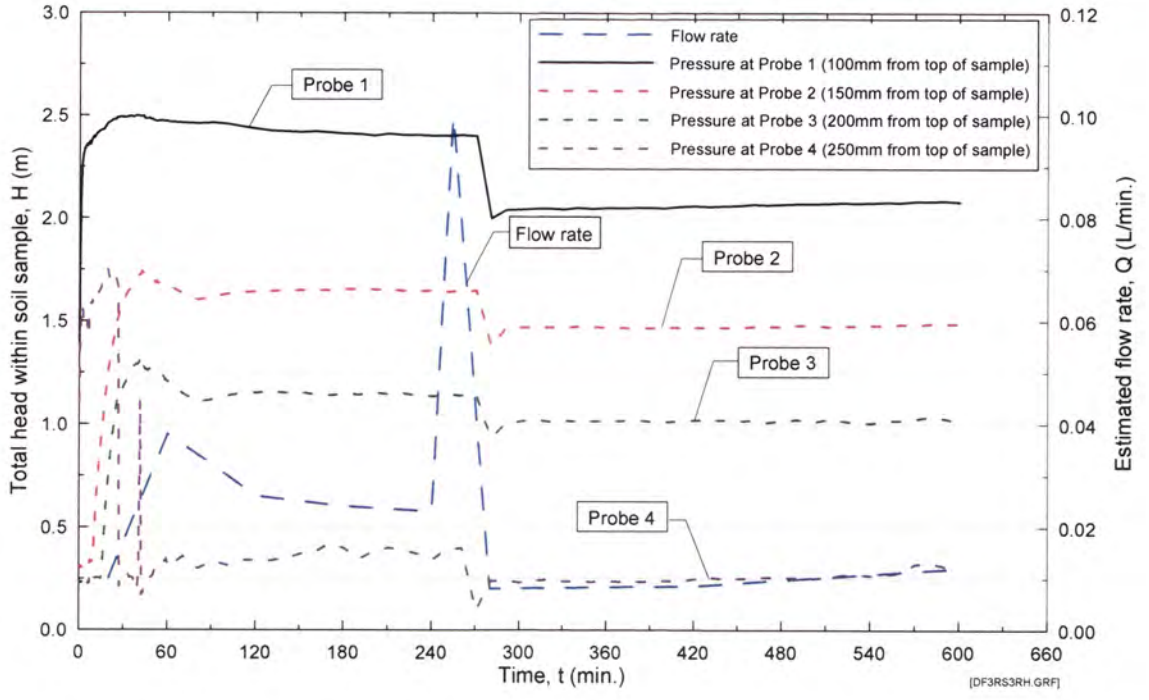

DF Test No. 3R on Sample 3R – Total head and flow rate. Sample compacted to 94.0% of Standard Max. Dry Density.

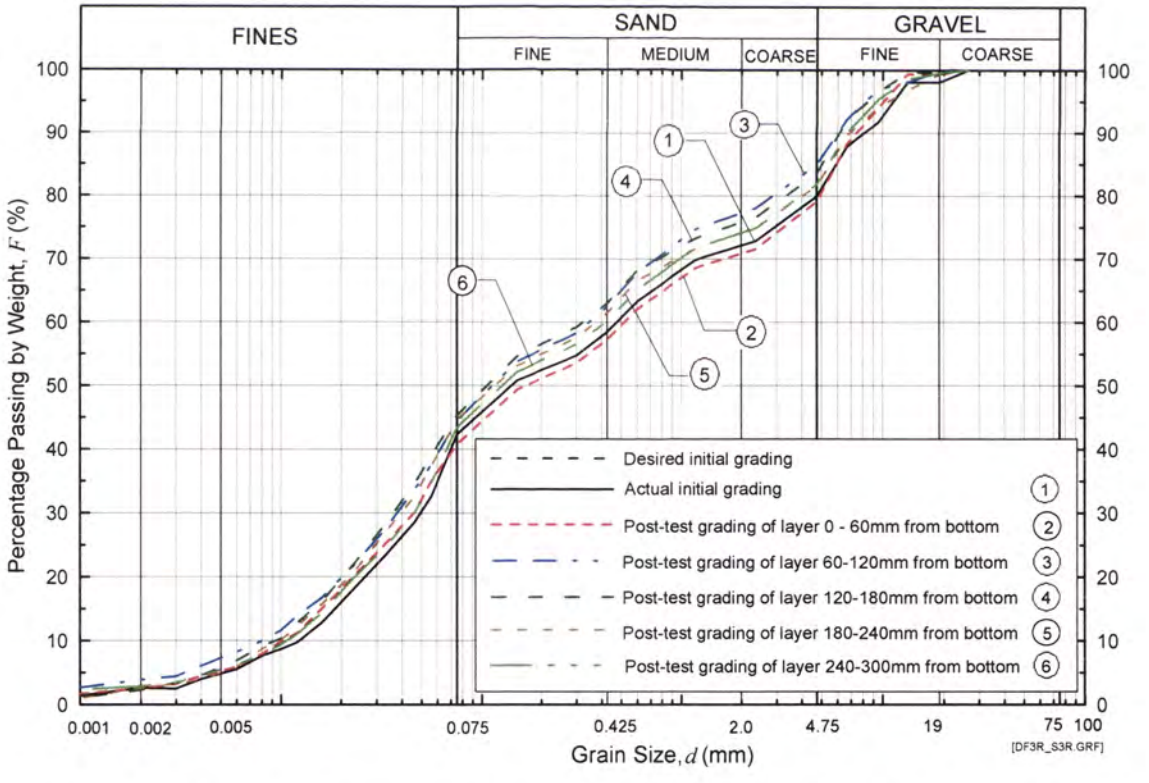

DF Test No. 3R on Sample 3R - Initial and post-test grain-size distribution analysis. Sample compacted to 94.0% of Standard Max. Dry Density.

Downward flow test No. 4R Test Records

DOWNWARD FLOW SUFFUSION TEST
Test Record

Test No/Date :	**Suffusion Downflow 004 2/04/02**
Soil Sample :	**Suffusion Test Blend No. 4R**
Standard max. dry density :	2.229 Mg/m^3
Optimum water content (OWC) :	9.30%
Targeted dry density relative to Standard max. dry density :	95.0%
Actual dry density from test:	93.4%
Water content during conditioning :	9.30%
Targeted moisture content :	9.30%
Actual water content from test :	9.98%
Fluid for conditioning soil :	Sydney tap water
Eroding fluid :	Sydney tap water
Eroding fluid mean temperature :	21.6 °C
Data Log File Name :	DF4a, DF4b, DF4c, DF4d
Time/Date of compaction of sample :	1.00pm 6/12/02
Time/Date of Commencement of Test :	1.00pm 9/12/02

Mix Ingredient	Mix Proportion (%)
Clay Q38	0.00
Silica 60G	3.23
Nepean Sand	27.42
5mm Blue Metal	32.26
10mm Bassalt	24.19
20mm Blue Metal	12.90
Total	100.00

Time (From Commencement) (hr)	Time (From Commencement) (min)	Flowrate (L/min)	Observations
0.00	0	0.00	Test Started. Slight cloudiness, extremely low outflow.
0.03	2	0.12	Very cloudy near base, and slowly increasing throughout. Extremely low outflow.
0.08	5	0.16	Very cloudy near base, and slowly increasing throughout. Extremely low outflow.
0.22	13	0.14	Very cloudy near base, and slowly increasing throughout. Extremely low outflow.
0.33	20	0.16	Very cloudy near base, and slowly increasing throughout. Extremely low outflow.
0.70	42	0.12	Very cloudy near base, and slowly increasing throughout. Extremely low outflow.
1.00	60	0.12	Very cloudy near base, and slowly increasing throughout. Extremely low outflow.
2.00	120	0.14	Very cloudy throughout. Extremely low outflow.
4.00	240	0.14	Very cloudy throughout. Extremely low outflow.
5.00	300	0.14	Slightly cloudy throughout, and slowly clearing. Extremely low outflow.
6.33	380	0.12	Slightly cloudy, extremely low outflow. Test paused, then restarted.
6.50	390	0.08	Slightly cloudy throughout, and slowly clearing. Extremely low outflow.
12.50	750	0.08	Slightly cloudy throughout, and slowly clearing. Extremely low outflow. Test stopped.

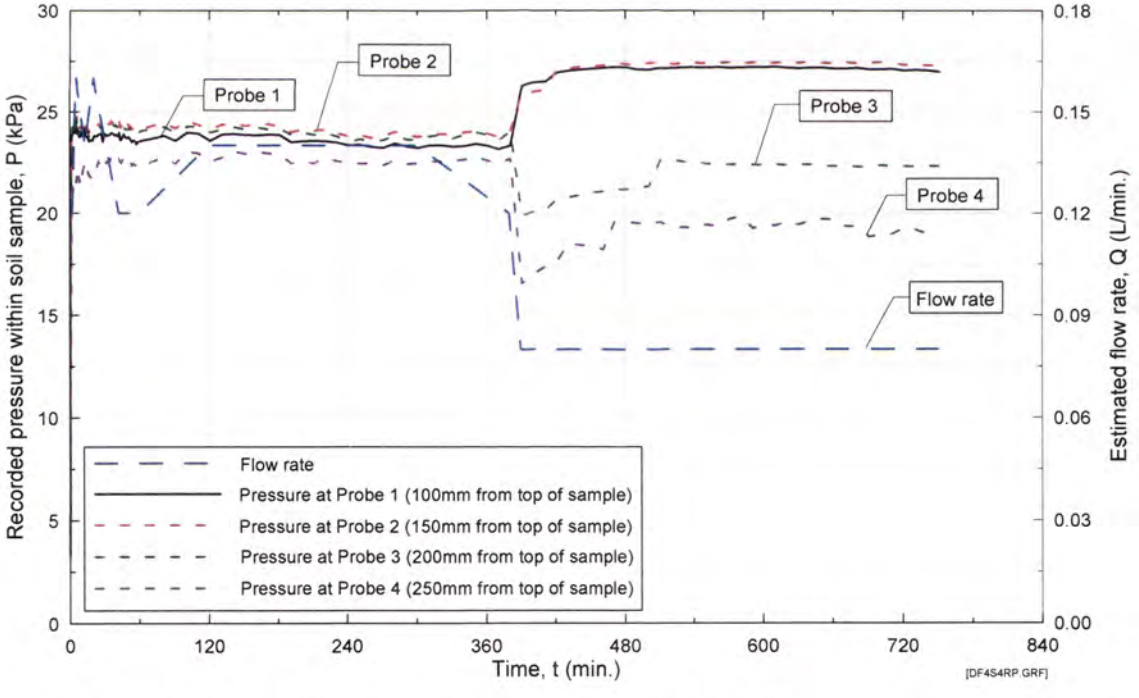

DF Test No. 4R on Sample 4R – Recorded pressure and flow rate. Sample compacted to 93.4% of Standard Max. Dry Density.

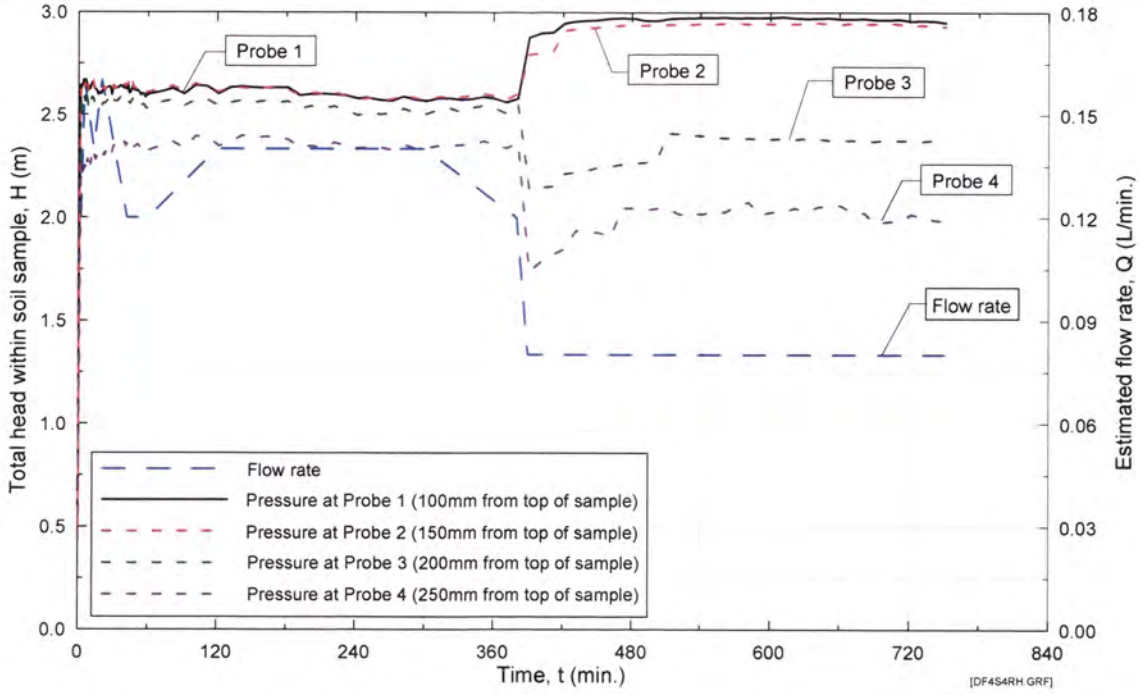

DF Test No. 4R on Sample 4R – Total head and flow rate. Sample compacted to 93.4% of Standard Max. Dry Density.

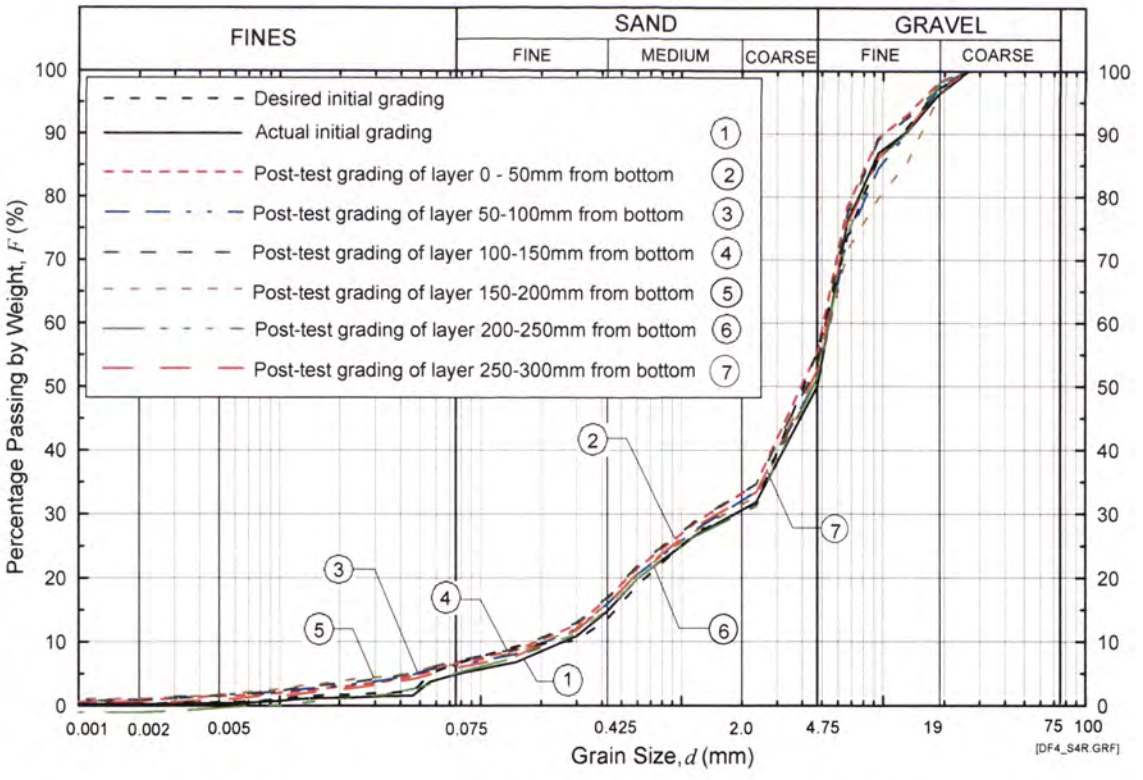

DF Test No. 4R on Sample 4R - Initial and post-test grain-size distribution analysis. Sample compacted to 93.4% of Standard Max. Dry Density.

Downward flow test No. 13 Test Records

DOWNWARD FLOW SUFFUSION TEST
Test Record

Test No/Date :	**Suffusion Downflow 013 1/10/02**
Soil Sample :	**Suffusion Test Blend No. 5**
Standard max. dry density :	2.119 Mg/m^3
Optimum water content (OWC) :	8.48%
Targeted dry density relative to Standard max. dry density :	95.0%
Actual dry density from test:	94.2%
Water content during conditioning :	8.48%
Targeted moisture content :	8.48%
Actual water content from test :	8.49%
Fluid for conditioning soil :	Sydney tap water
Eroding fluid :	Sydney tap water
Eroding fluid mean temperature :	21.6 °C
Data Log File Name :	DF13a, DF 13b.
Time/Date of compaction of sample :	am 30/09/02
Time/Date of Commencement of Test :	am 1/10/02

Mix Ingredient	Mix Proportion (%)
Clay Q38	5.88
Silica 60G	1.18
Nepean Sand	41.20
5mm Blue Metal	34.73
10mm Bassalt	11.77
20mm Blue Metal	5.24
Total	100.00

Time (From Commencement) (hr)	Time (From Commencement) (min)	Flowrate (L/min)	Observations
0.00	0.0	0.00	Test Started. Slightly cloudy near base, very low outflow.
0.07	4.3	1.71	Slightly cloudy near base, and increasing slowly. Low outflow, fluctuating slightly.
0.14	8.3	1.62	Slightly cloudy near base, and increasing slowly. Low outflow, fluctuating slightly.
0.24	14.3	1.53	Slightly cloudy near base, and increasing slowly. Low outflow, fluctuating slightly.
0.40	24.0	1.50	Slightly cloudy. Low outflow, fluctuating slightly.
0.57	34.0	1.47	Slightly cloudy. Low outflow, fluctuating slightly.
0.87	52.0	1.47	Slightly cloudy. Low outflow, fluctuating slightly.
1.23	74.0	1.53	Slightly cloudy. Low outflow, fluctuating slightly.
1.63	98.0	1.56	Slightly cloudy, and clearing slowly. Low outflow, fluctuating slightly.
2.17	130.0	1.62	Slightly cloudy, and clearing slowly. Low outflow, fluctuating slightly.
2.42	145.0	1.62	Mostly clear. Low outflow, fluctuating slightly.
2.60	156.0	1.68	Mostly clear. Low outflow, fluctuating slightly.
2.80	168.0	1.68	Clear, low outflow. Test stopped.

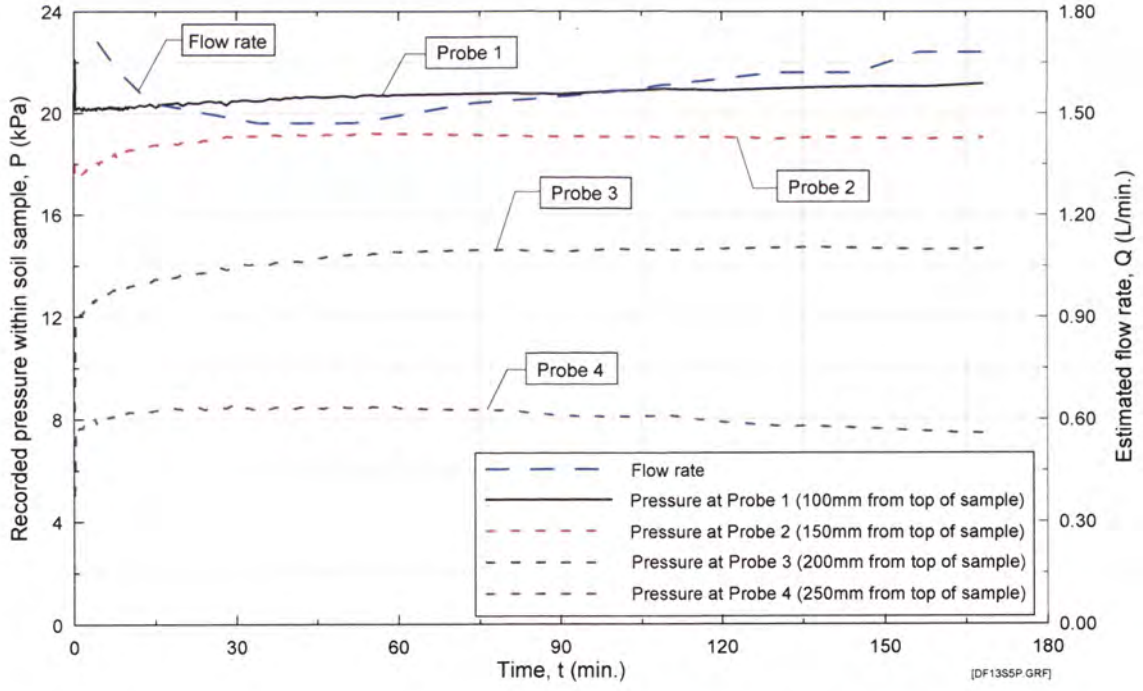

DF Test No. 13 on Sample 5 – Recorded pressure and flow rate. Sample compacted to 94.2% of Standard Max. Dry Density.

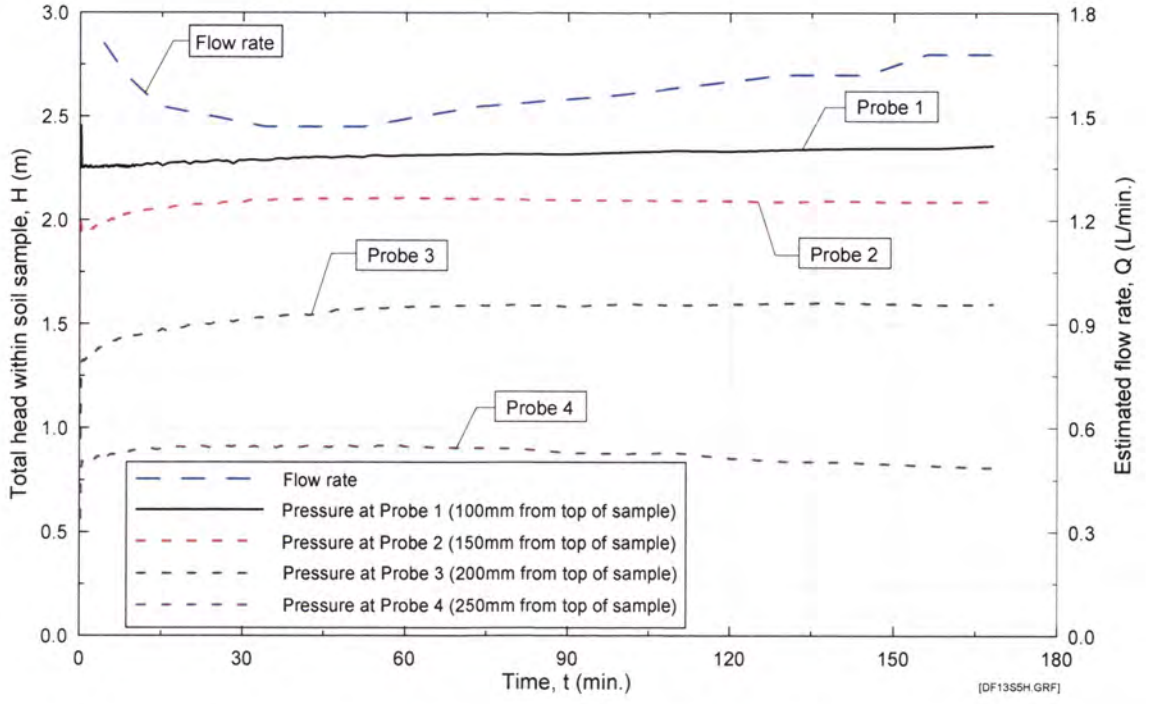

DF Test No. 13 on Sample 5 – Total head and flow rate. Sample compacted to 94.2% of Standard Max. Dry Density.

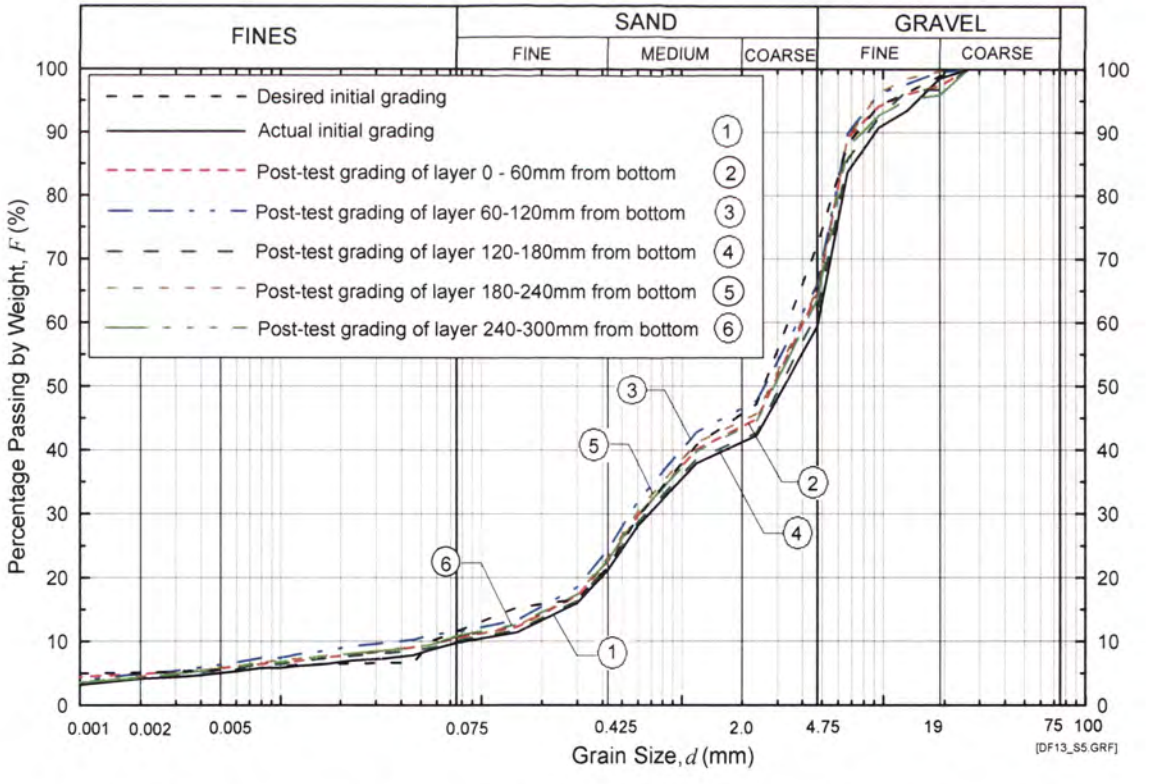

DF Test No. 13 on Sample 5 - Initial and post-test grain-size distribution analysis. Sample compacted to 94.2% of Standard Max. Dry Density.

Downward flow test No. 14 Test Records

DOWNWARD FLOW SUFFUSION TEST
Test Record

Test No/Date :	**Suffusion Downflow 014 27/10/02**
Soil Sample :	**Suffusion Test Blend No. 5**
Standard max. dry density :	2.119 Mg/m^3
Optimum water content (OWC) :	8.48%
Targeted dry density relative to Standard max. dry density :	90.0%
Actual dry density from test:	89.1%
Water content during conditioning :	8.48%
Targeted moisture content :	8.48%
Actual water content from test :	8.62%
Fluid for conditioning soil :	Sydney tap water
Eroding fluid :	Sydney tap water
Eroding fluid mean temperature :	21.6 °C
Data Log File Name :	DF14a, DF 14b, DF 14c.
Time/Date of compaction of sample :	am 21/10/02
Time/Date of Commencement of Test :	am 22/10/02

Mix Ingredient	Mix Proportion (%)
Clay Q38	5.88
Silica 60G	1.18
Nepean Sand	41.20
5mm Blue Metal	34.73
10mm Bassalt	11.77
20mm Blue Metal	5.24
Total	100.00

Time (From Commencement) (hr)	Time (From Commencement) (min)	Flowrate (L/min)	Observations
0.00	0.0	0.00	Test Started. Slightly cloudy near base, very low outflow.
0.08	5.0	3.12	Slightly cloudy near base, and increasing slowly. Low outflow, fluctuating slightly.
0.17	10.0	2.94	Cloudy. Low outflow, fluctuating slightly.
0.50	30.0	2.70	Cloudy. Low outflow, fluctuating slightly.
2.83	170.0	3.00	Slightly cloudy. Low outflow, fluctuating slightly.
3.50	210.0	3.06	Mostly clear. Low outflow, fluctuating slightly.
4.42	265.0	3.24	Mostly clear. Low outflow, fluctuating slightly.
5.17	310.0	3.33	Mostly clear. Low outflow, fluctuating slightly.
6.17	370.0	3.33	Mostly clear. Low outflow, fluctuating slightly.
6.83	410.0	3.42	Clear. Low outflow, fluctuating slightly. Test stopped.

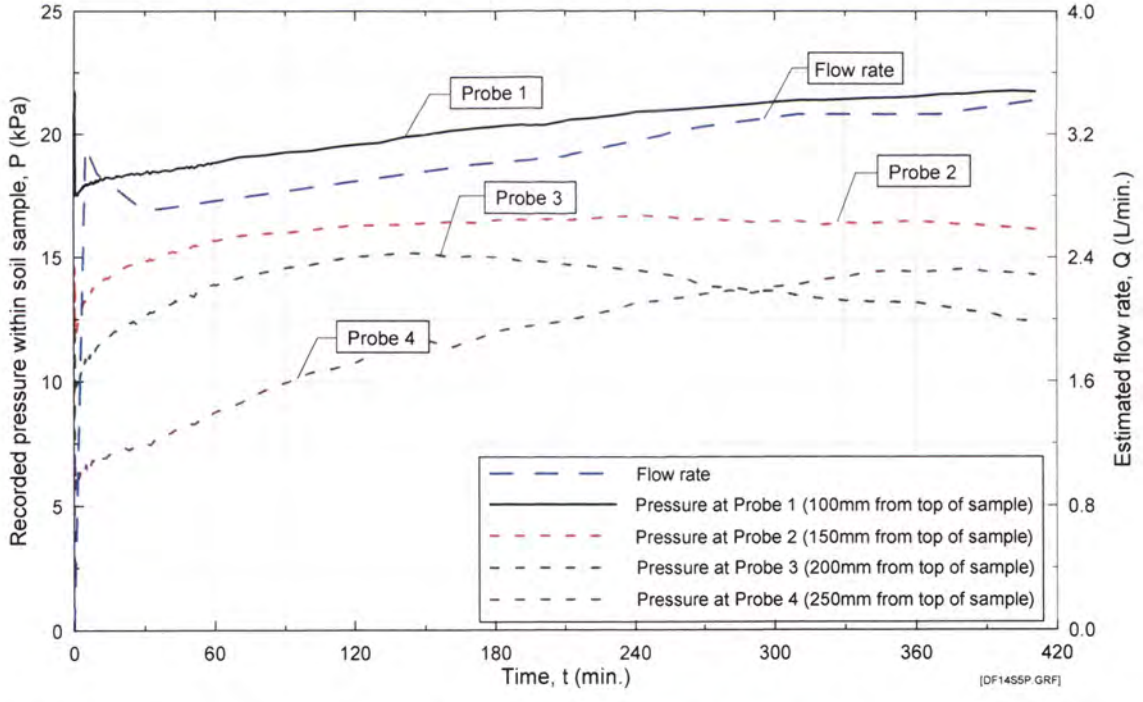

DF Test No. 14 on Sample 5 – Recorded pressure and flow rate. Sample compacted to 89.1% of Standard Max. Dry Density.

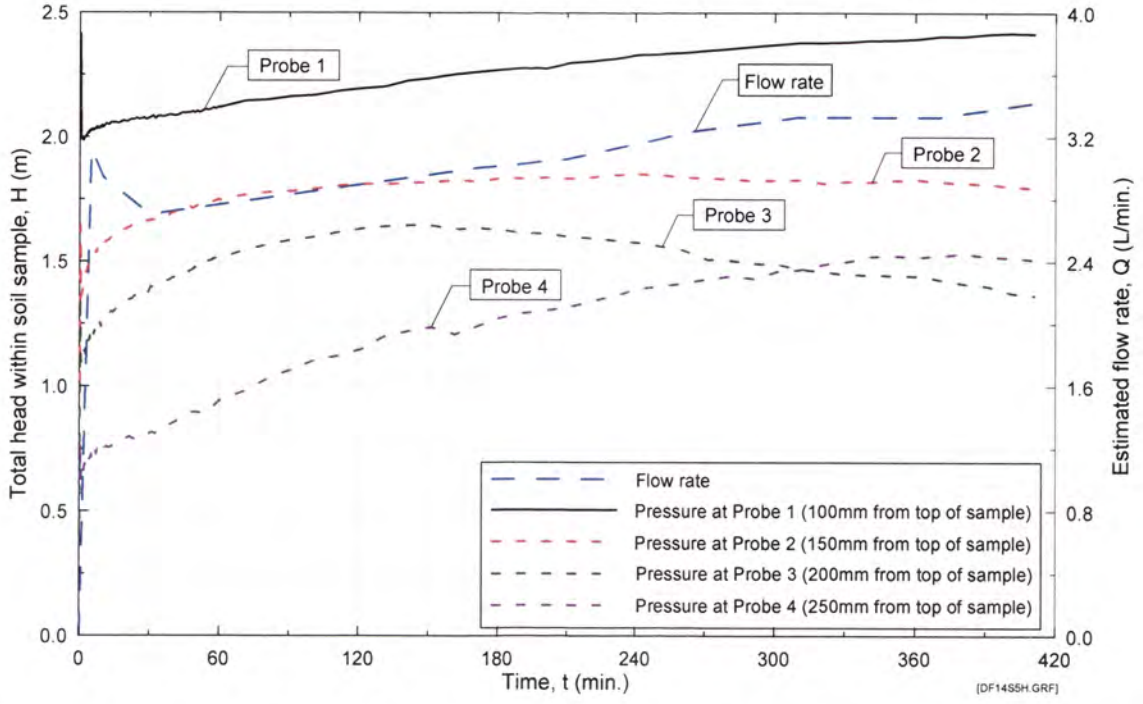

DF Test No. 14 on Sample 5 – Total head and flow rate. Sample compacted to 89.1% of Standard Max. Dry Density.

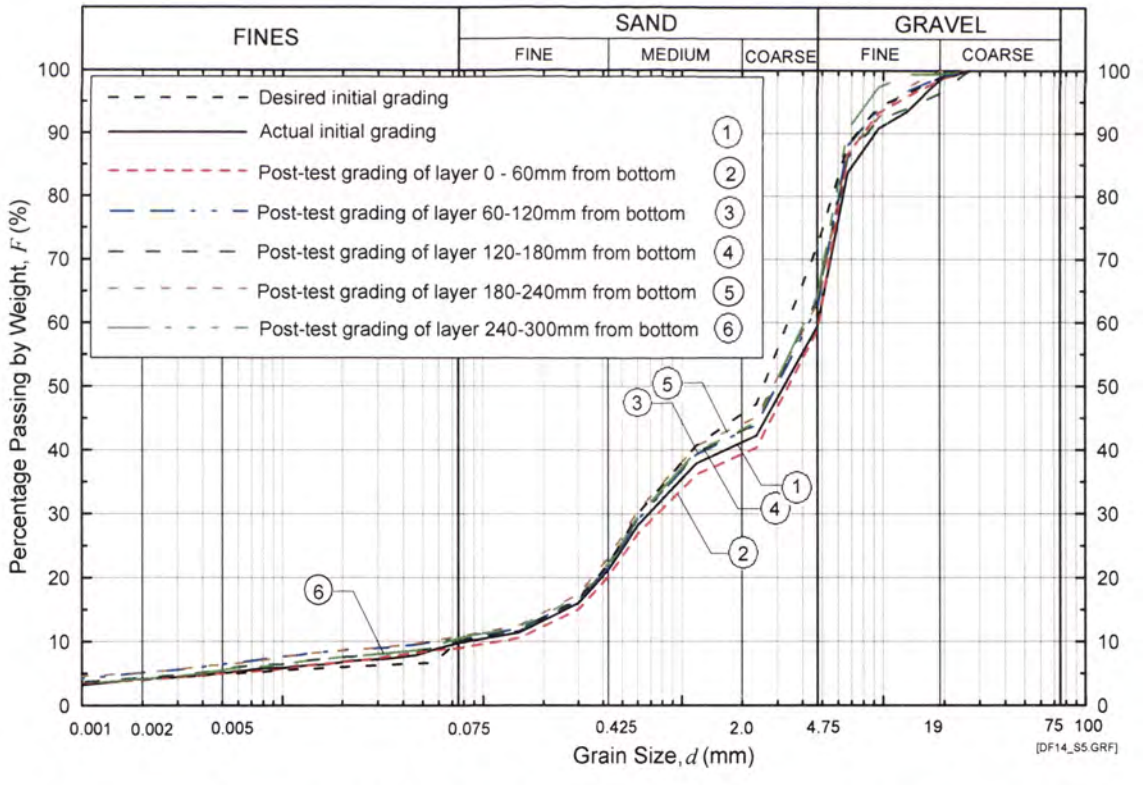

DF Test No. 14 on Sample 5 - Initial and post-test grain-size distribution analysis. Sample compacted to 89.1% of Standard Max. Dry Density.

Downward flow test No. 10 Test Records

DOWNWARD FLOW SUFFUSION TEST
Test Record

Test No/Date :	**Suffusion Downflow 010 14/03/02**
Soil Sample :	**Suffusion Test Blend No. 6**
Standard max. dry density :	2.234 Mg/m^3
Optimum water content (OWC) :	7.18%
Targeted dry density relative to Standard max. dry density :	95.0%
Actual dry density from test:	95.5%
Water content during conditioning :	7.18%
Targeted moisture content :	7.18%
Actual water content from test :	7.24%
Fluid for conditioning soil :	Sydney tap water
Eroding fluid :	Sydney tap water
Eroding fluid mean temperature :	21.6 °C
Data Log File Name :	DF10a, DF 10b, DF 10c, DF 10d.
Time/Date of compaction of sample :	am 14/03/02
Time/Date of Commencement of Test :	2.30pm 14/03/02

Mix Ingredient	Mix Proportion (%)
Clay Q38	11.18
Silica 60G	8.20
Nepean Sand	34.16
5mm Blue Metal	27.33
10mm Bassalt	12.30
20mm Blue Metal	6.83
Total	100.00

Time (From Commencement) (hr)	Time (From Commencement) (min)	Flowrate (L/min)	Observations
0.00	0	0.00	Test Started. Slightly cloudy at base. Very low outflow.
0.08	5	0.81	Slightly cloudy at base, and increasing slowly. Very low outflow, fluctuating slightly.
0.15	9	0.84	Slightly cloudy at base, and increasing slowly. Very low outflow, fluctuating slightly.
0.22	13	0.81	Slightly cloudy at base, and increasing slowly. Very low outflow, fluctuating slightly.
0.33	20	0.78	Slightly cloudy at base, and increasing slowly. Very low outflow, fluctuating slightly.
0.53	32	0.78	Slightly cloudy at base, and increasing slowly. Very low outflow, fluctuating slightly.
1.00	60	0.75	Slightly cloudy at base, and increasing slowly. Very low outflow, fluctuating slightly.
1.25	75	0.78	(As above) Test paused, then restarted.
1.33	80	0.81	Slightly cloudy, and clearing slowly. Very low outflow, fluctuating slightly.
2.00	120	0.78	Slightly cloudy, and clearing slowly. Very low outflow, fluctuating slightly.
5.00	300	0.78	Mostly clear. Very low outflow, and fluctuating slightly.
6.00	360	0.78	Mostly clear. Very low outflow, and fluctuating slightly. Test stopped.

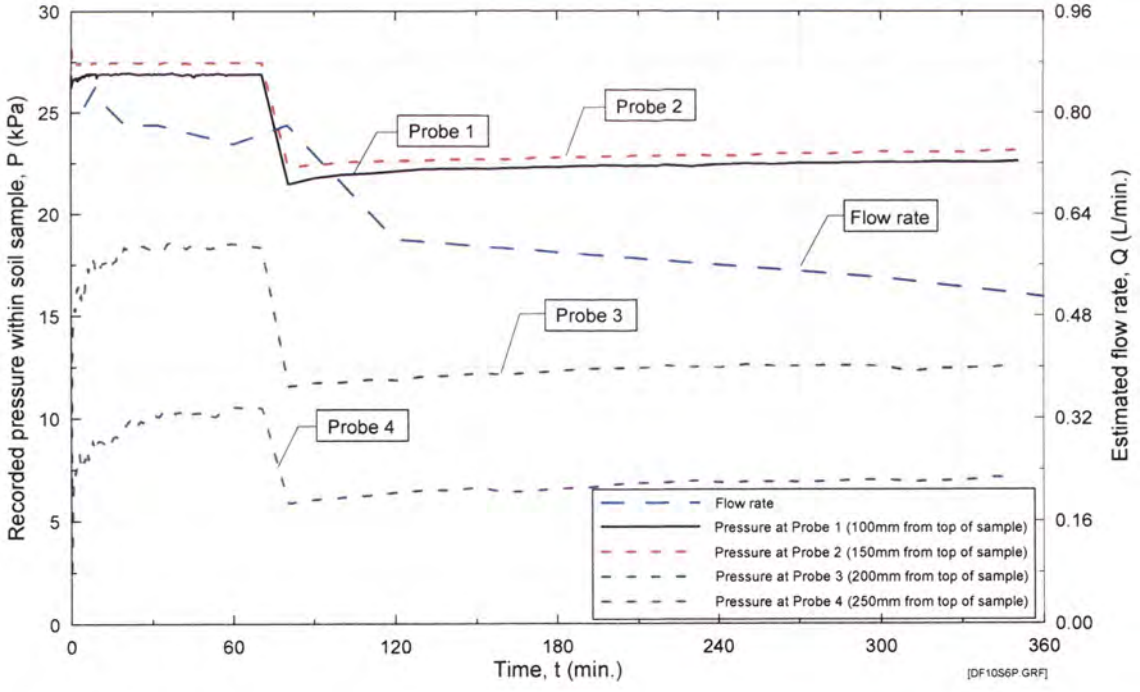

DF Test No. 10 on Sample 6 – Recorded pressure and flow rate. Sample compacted to 95.5% of Standard Max. Dry Density.

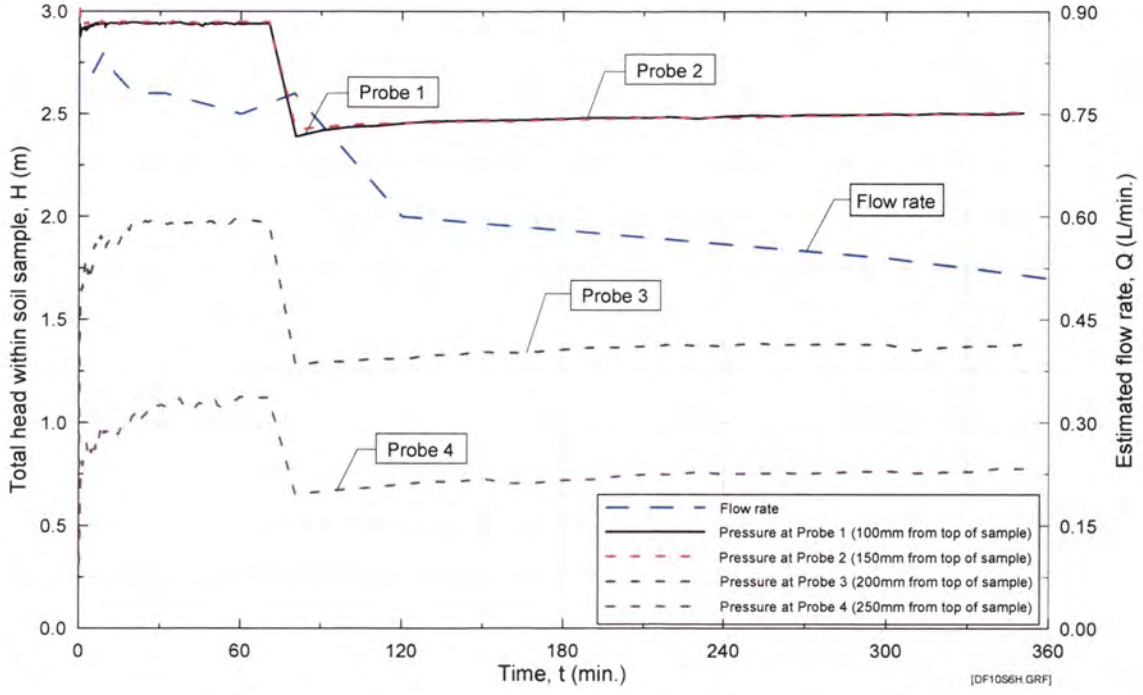

DF Test No. 10 on Sample 6 – Total head and flow rate. Sample compacted to 95.5% of Standard Max. Dry Density.

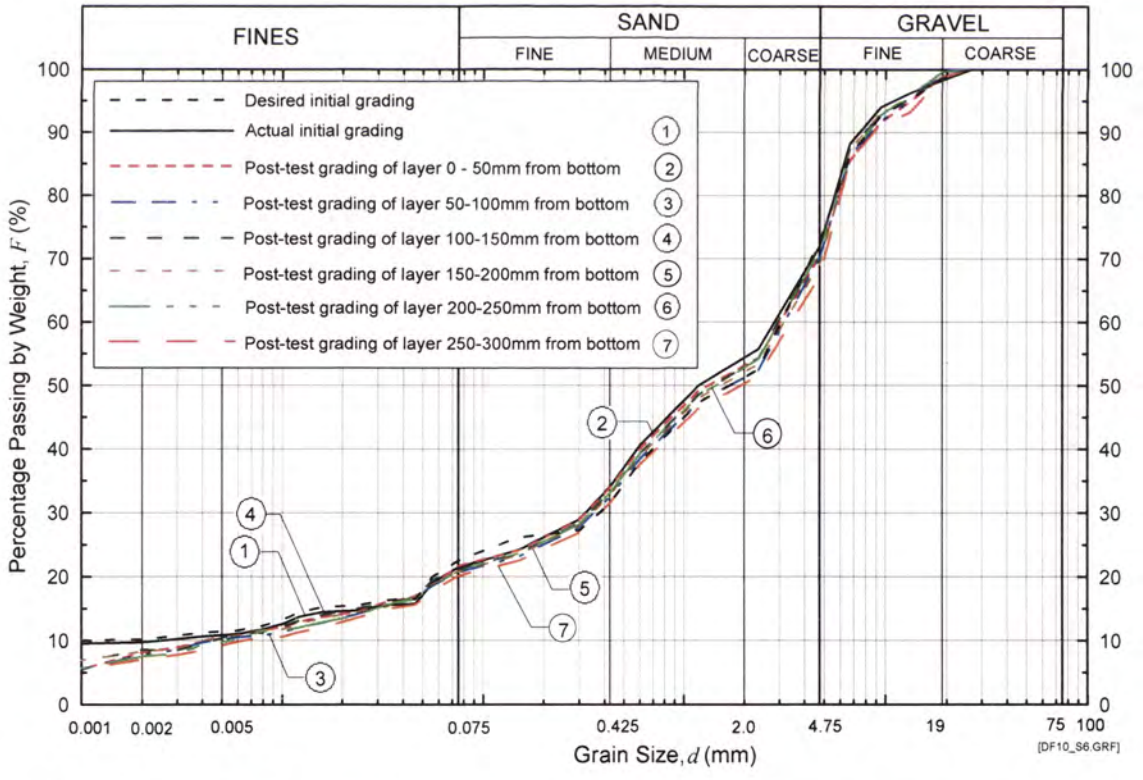

DF Test No. 10 on Sample 6 - Initial and post-test grain-size distribution analysis. Sample compacted to 95.5% of Standard Max. Dry Density.

Downward flow test No. 16 Test Records

DOWNWARD FLOW SUFFUSION TEST
Test Record

Test No/Date :	**Suffusion Downflow 016 27/08/02**
Soil Sample :	**Suffusion Test Blend No. 7**
Standard max. dry density :	2.046 Mg/m^3
Optimum water content (OWC) :	9.81%
Targeted dry density relative to Standard max. dry density :	95.0%
Actual dry density from test:	94.2%
Water content during conditioning :	9.81%
Targeted moisture content :	9.81%
Actual water content from test :	10.21%
Fluid for conditioning soil :	Sydney tap water
Eroding fluid :	Sydney tap water
Eroding fluid mean temperature :	14.4 °C
Data Log File Name :	DF 16a, DF 16b, DF 16c.
Time/Date of compaction of sample :	pm 23/08/02 + am 26/08/02
Time/Date of Commencement of Test :	am 27/08/02

Mix Ingredient	Mix Proportion (%)
Clay Q38	21.75
Silica 60G	21.84
Nepean Sand	24.12
5mm Blue Metal	18.99
10mm Bassalt	8.55
20mm Blue Metal	4.75
Total	100.00

Time (From Commencement) (hr)	Time (From Commencement) (min)	Flowrate (L/min)	Observations
0.00	0.0	0.00	Test Started. Slightly cloudy near base, no outflow.
0.07	4.0	0.00	Slightly cloudy near base, and slowly increasing. No outflow.
0.09	5.5	0.63	Slightly cloudy near base, and slowly increasing. Low outflow, slowly increasing.
0.17	10.0	0.81	Slightly cloudy near base, and slowly increasing. Low outflow, slowly increasing.
0.28	17.0	0.75	Slightly cloudy near base, and slowly increasing. Low outflow, slowly increasing.
0.45	27.0	1.14	Very cloudy. Low outflow, slowly increasing.
0.65	39.0	1.62	Very cloudy. Low outflow, slowly increasing.
0.83	50.0	2.16	Very cloudy. Low outflow, slowly increasing.
1.42	85.0	6.45	Very cloudy. Low outflow, slowly increasing.
1.87	112.0	32.82	Very cloudy. Moderate outflow, steadily increasing.
2.00	120.0	35.16	Cloudy, slowly clearing. Moderate outflow, steadily increasing.
2.17	130.0	39.12	Cloudy, slowly clearing. Moderate outflow, steadily increasing.
2.33	140.0	37.38	Cloudy, slowly clearing. Moderate outflow, fluctuating.
2.55	153.0	42.90	Cloudy, slowly clearing. Moderate outflow, steadily increasing.
2.83	170.0	45.90	Cloudy, slowly clearing. Moderate outflow, steadily increasing.
3.08	185.0	45.78	Cloudy, slowly clearing. Moderate outflow, fluctuating.
3.22	193.0	47.88	Cloudy, slowly clearing. Moderate outflow, steadily increasing.
3.32	199.0	47.63	Cloudy, slowly clearing. Moderate outflow, fluctuating.
3.40	204.0	41.70	Cloudy, slowly clearing. Moderate outflow, fluctuating.
3.47	208.0	36.96	Cloudy, slowly clearing. Moderate outflow, fluctuating.
3.50	210.0	40.00	Cloudy, slowly clearing. Moderate outflow, fluctuating. Test stopped.

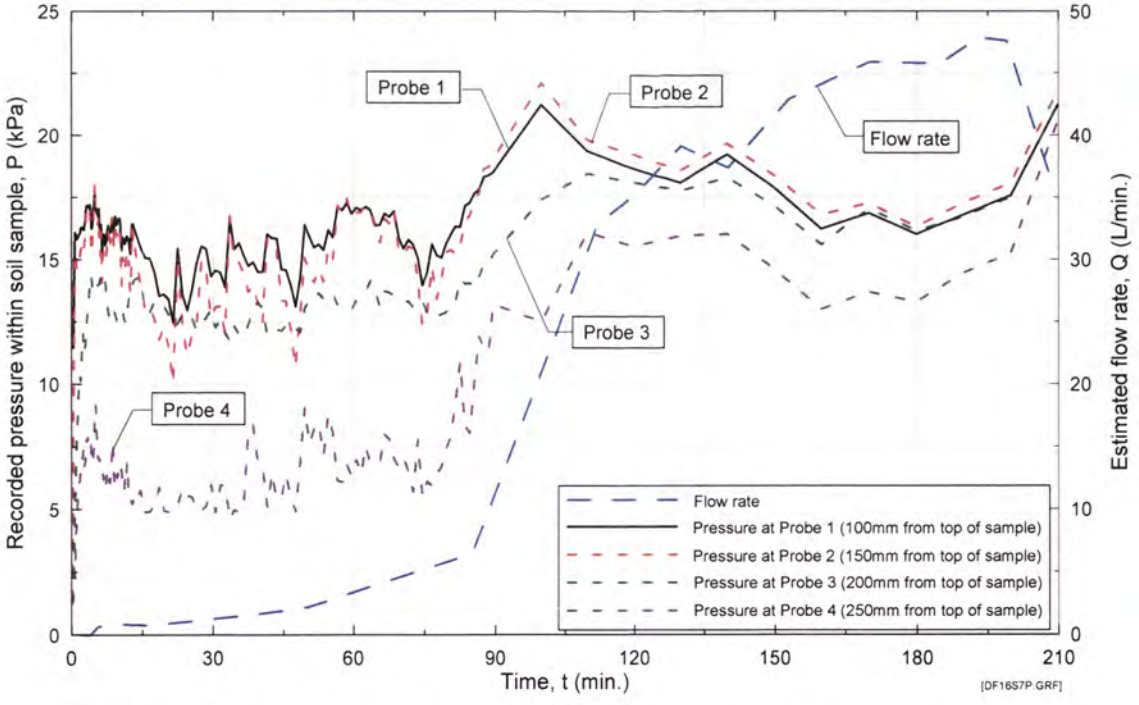

DF Test No. 16 on Sample 7 – Recorded pressure and flow rate. Sample compacted to 94.2% of Standard Max. Dry Density.

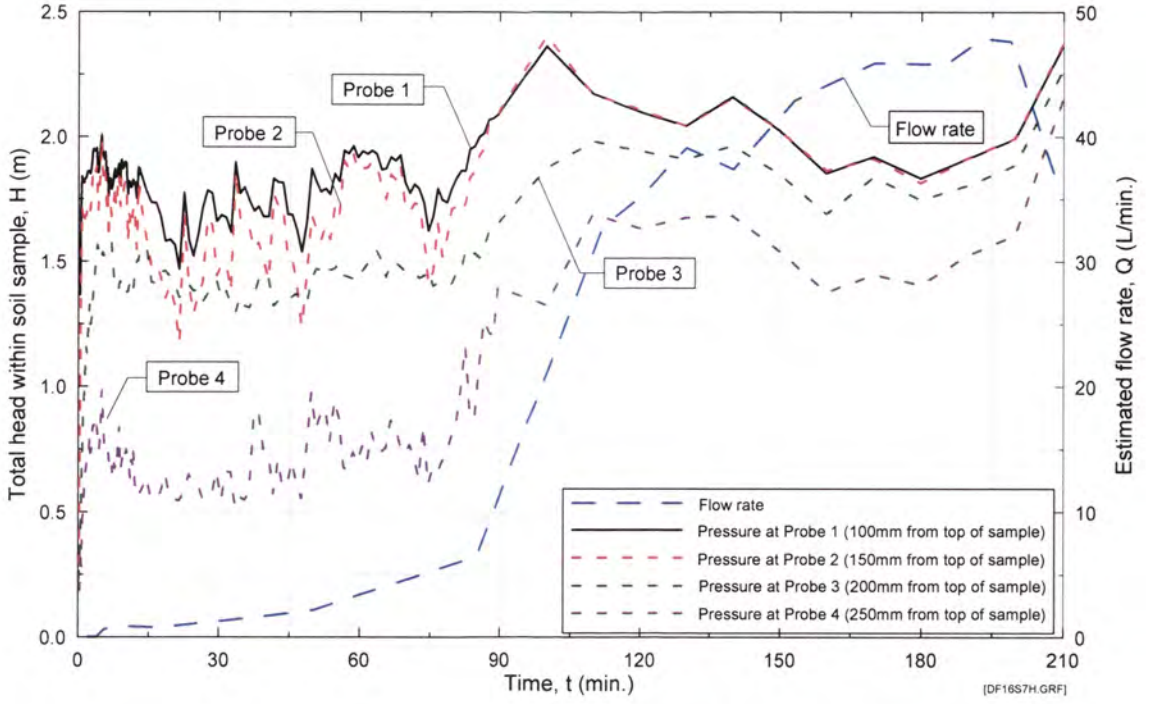

DF Test No. 16 on Sample 7 – Total head and flow rate. Sample compacted to 94.2% of Standard Max. Dry Density.

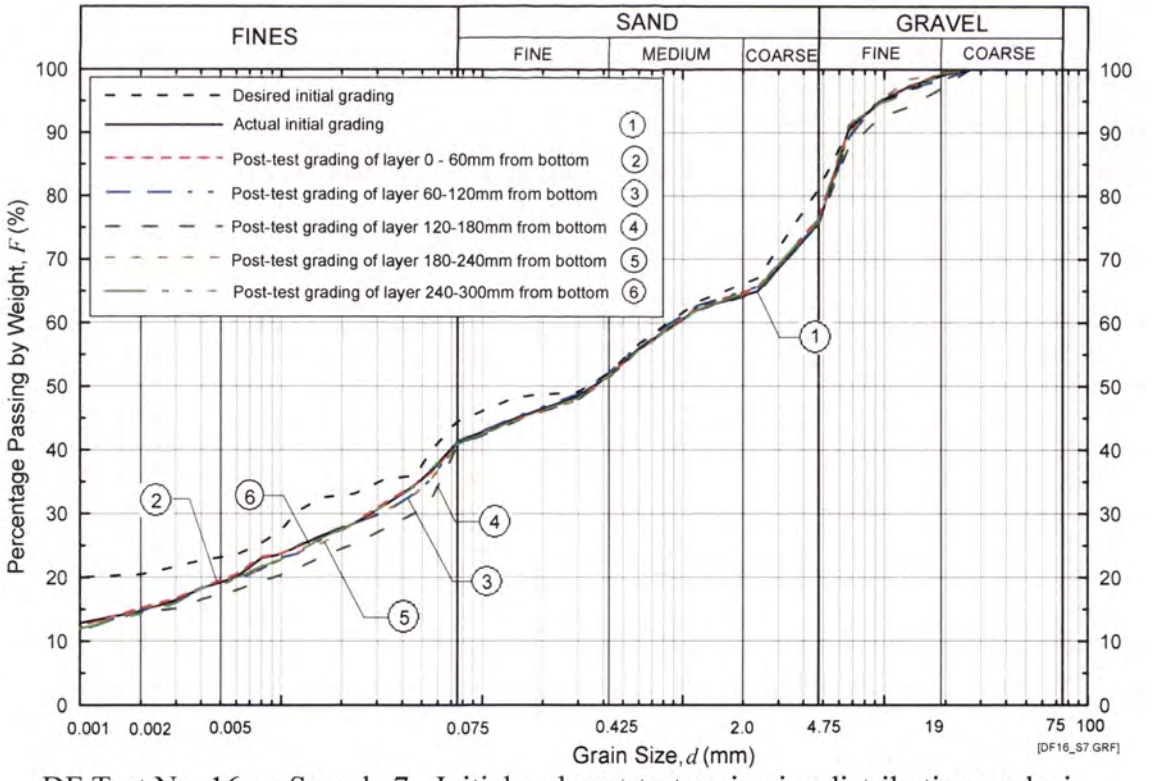

DF Test No. 16 on Sample 7 - Initial and post-test grain-size distribution analysis. Sample compacted to 94.2% of Standard Max. Dry Density.

Downward flow test No. 6 Test Records

DOWNWARD FLOW SUFFUSION TEST
Test Record

Test No/Date :	**Suffusion Downflow 006 14/05/02**
Soil Sample :	**Suffusion Test Blend No. 9**
Standard max. dry density :	1.935 Mg/m^3
Optimum water content (OWC) :	6.25%
Targeted dry density relative to Standard max. dry density :	95.0%
Actual dry density from test:	93.8%
Water content during conditioning :	6.25%
Targeted moisture content :	6.25%
Actual water content from test :	5.76%
Fluid for conditioning soil :	Sydney tap water
Eroding fluid :	Sydney tap water
Eroding fluid mean temperature :	21.6 °C
Data Log File Name :	DF6a
Time/Date of compaction of sample :	pm 13/05/02
Time/Date of Commencement of Test :	9.20am 14/05/02

Mix Ingredient	Mix Proportion (%)
Clay Q38	0.00
Silica 60G	11.92
Nepean Sand	0.00
5mm Blue Metal	9.54
10mm Bassalt	60.67
20mm Blue Metal	17.87
Total	100.00

Time (From Commencement) (hr)	Time (min)	Flowrate (L/min)	Observations
0.00	0	0.00	Test Started. Extremely cloudy, extremely rapid outflow.
0.08	4.5	137.70	Extremely cloudy, extremely rapid outflow.
0.10	6	139.00	Cloudy, extremely rapid outflow.
0.13	8	133.60	Clear, extremely rapid outflow.
0.20	12	135.00	Clear, extremely rapid outflow. Test stopped.

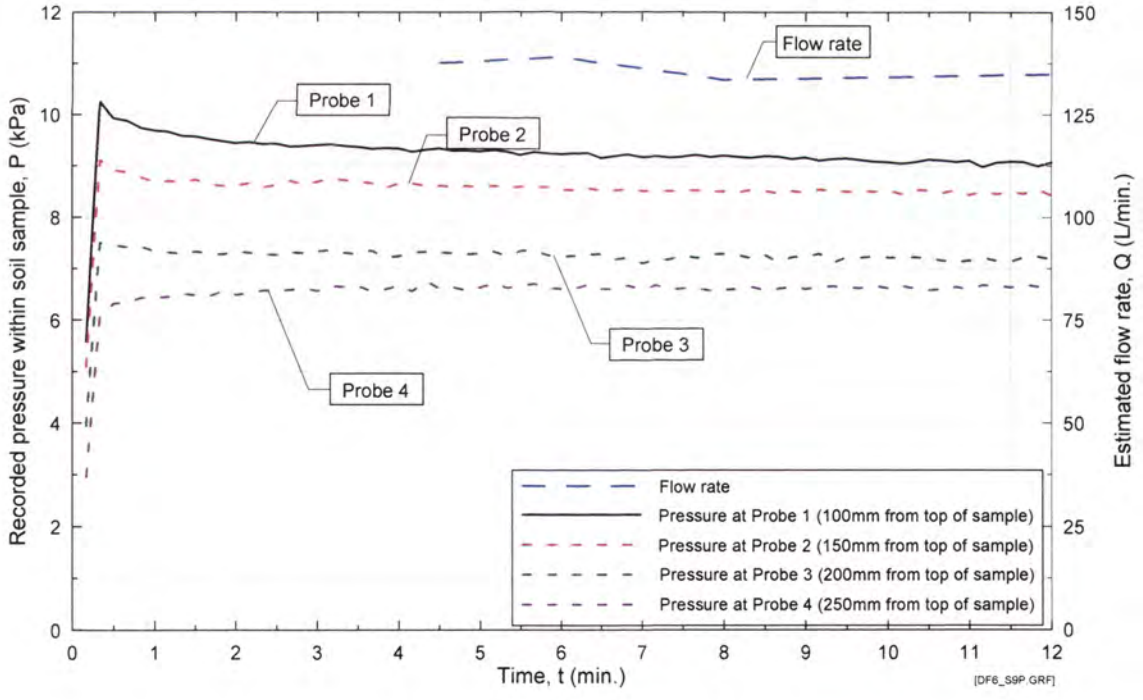

DF Test No. 6 on Sample 9 – Recorded pressure and flow rate. Sample compacted to 93.8% of Standard Max. Dry Density.

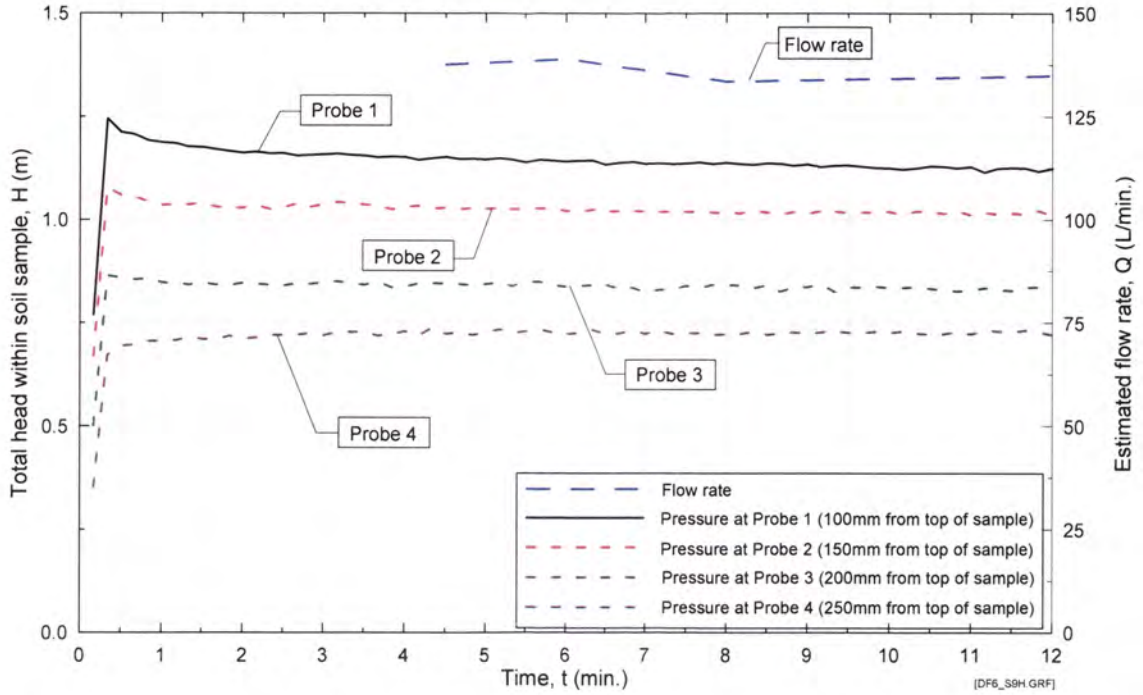

DF Test No. 6 on Sample 9 – Total head and flow rate. Sample compacted to 93.8% of Standard Max. Dry Density.

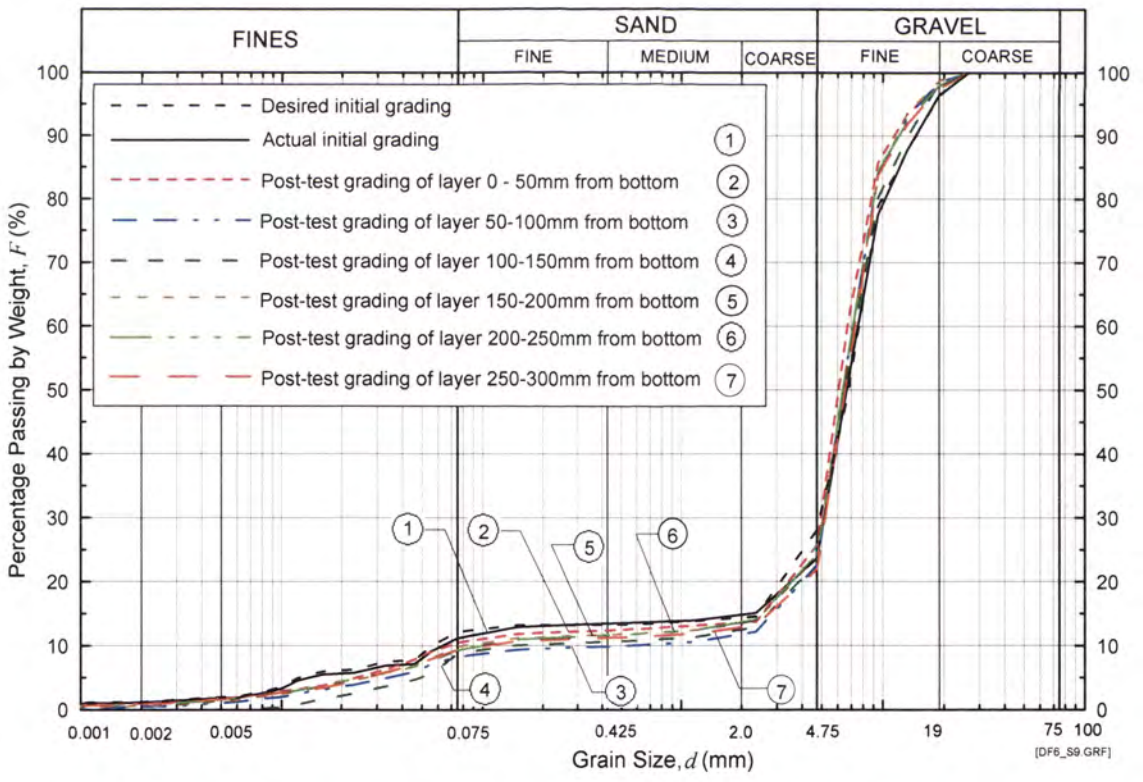

DF Test No. 6 on Sample 9 - Initial and post-test grain-size distribution analysis. Sample compacted to 93.8% of Standard Max. Dry Density.

Downward flow test No. 7 Test Records

DOWNWARD FLOW SUFFUSION TEST
Test Record

Test No/Date :	**Suffusion Downflow 007 26/11/01**
Soil Sample :	**Suffusion Test Blend No. 10**
Standard max. dry density :	2.219 Mg/m^3
Optimum water content (OWC) :	8.44%
Targeted dry density relative to Standard max. dry density :	95.0%
Actual dry density from test:	94.1%
Water content during conditioning :	8.44%
Targeted moisture content :	8.44%
Actual water content from test :	8.44%
Fluid for conditioning soil :	Sydney tap water
Eroding fluid :	Sydney tap water
Eroding fluid mean temperature :	21.6 °C
Data Log File Name :	DF7a, DF7b
Time/Date of compaction of sample :	am 26/11/01
Time/Date of Commencement of Test :	3.00pm 26/11/01

Mix Ingredient	Mix Proportion (%)
Clay Q38	0.00
Silica 60G	25.67
Nepean Sand	0.00
5mm Blue Metal	0.00
10mm Bassalt	54.59
20mm Blue Metal	19.74
Total	100.00

Time (From Commencement) (hr)	Time (From Commencement) (min)	Flowrate (L/min)	Observations
0.00	0	0.00	Test Started. Very cloudy, very rapid outflow.
0.03	1.5	28.50	Slightly cloudy, very rapid outflow.
0.08	5	29.46	Slightly cloudy, very rapid outflow.
0.27	16	31.20	Slightly cloudy, very rapid outflow.
1.00	60	33.36	Clear, very rapid outflow. Test stopped.

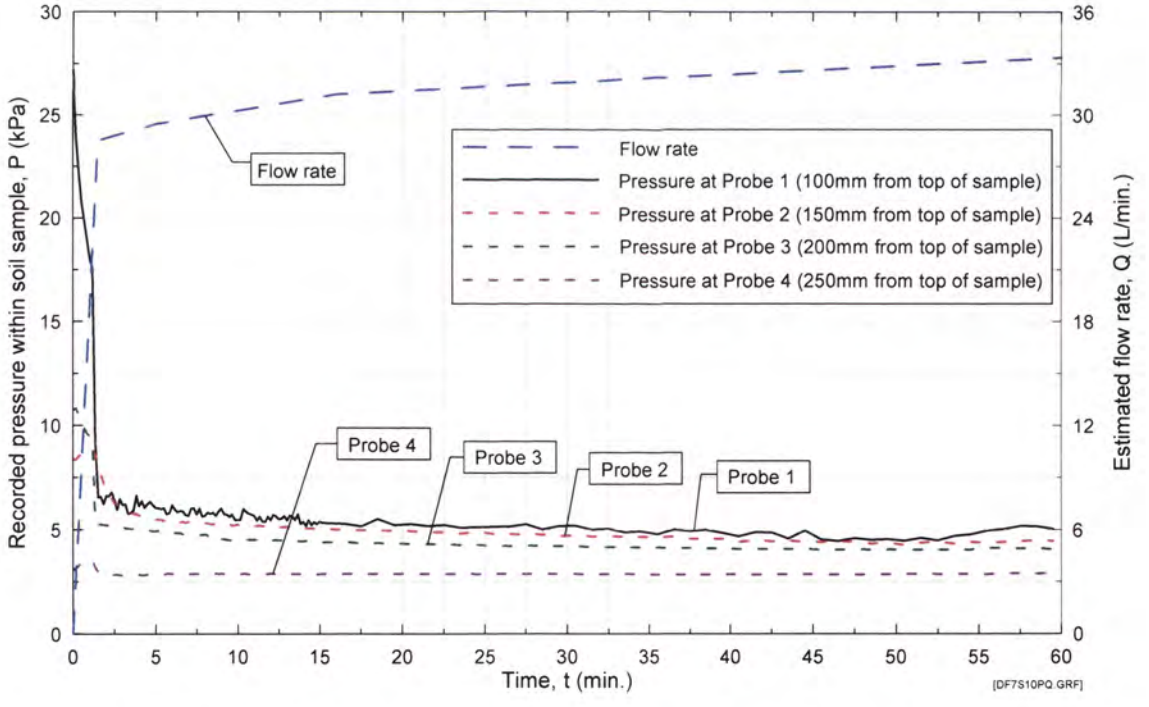

DF Test No. 7 on Sample 10 – Recorded pressure and flow rate. Sample compacted to 94.0% of Standard Max. Dry Density.

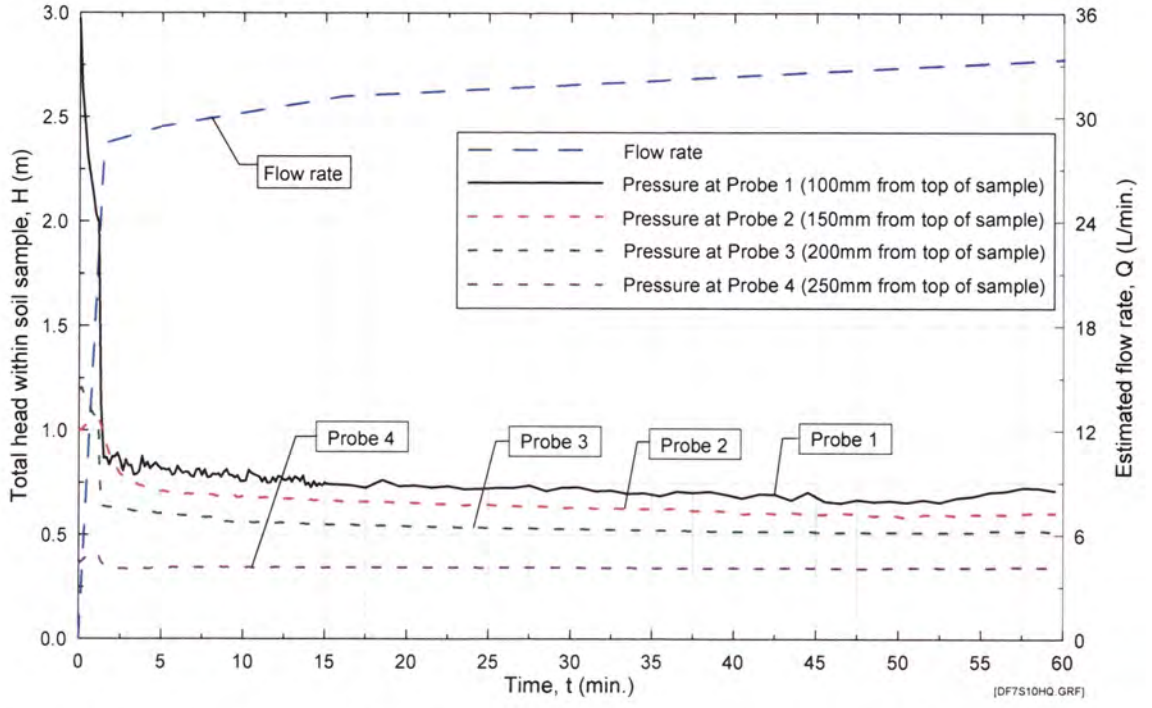

DF Test No. 7 on Sample 10 – Recorded pressure and flow rate. Sample compacted to 94.0% of Standard Max. Dry Density.

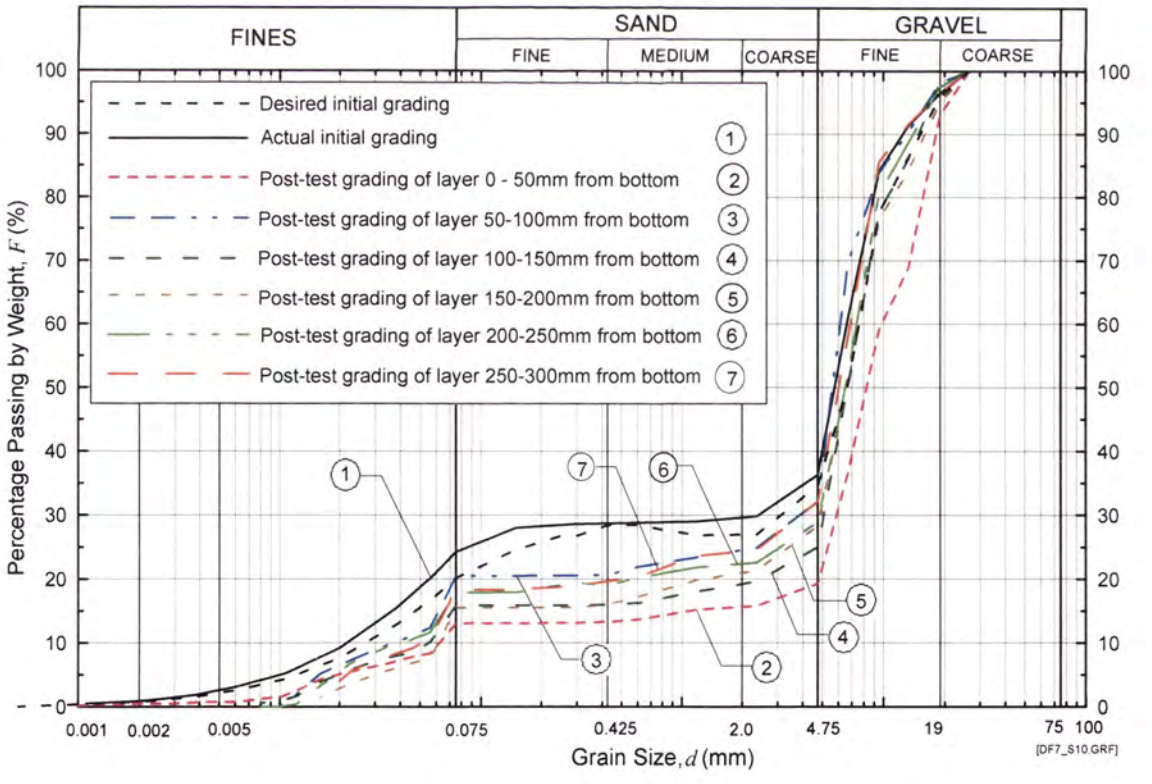

DF Test No. 7 on Sample 10 - Initial and post-test grain-size distribution analysis. Sample compacted to 94.0% of Standard Max. Dry Density.

Downward flow test No. 8 Test Records

DOWNWARD FLOW SUFFUSION TEST
Test Record

Test No/Date :	**Suffusion Downflow 008 13/03/02**
Soil Sample :	**Suffusion Test Blend No. 10**
Standard max. dry density :	2.219 Mg/m^3
Optimum water content (OWC) :	8.44%
Targeted dry density relative to Standard max. dry density :	90.0%
Actual dry density from test:	90.0%
Water content during conditioning :	8.44%
Targeted moisture content :	8.44%
Actual water content from test :	8.20%
Fluid for conditioning soil :	Sydney tap water
Eroding fluid :	Sydney tap water
Eroding fluid mean temperature :	21.6 °C
Data Log File Name :	DF8a
Time/Date of compaction of sample :	am 12/03/02
Time/Date of Commencement of Test :	9.00am 13/03/02

Mix Ingredient	Mix Proportion (%)
Clay Q38	0.00
Silica 60G	25.67
Nepean Sand	0.00
5mm Blue Metal	0.00
10mm Bassalt	54.59
20mm Blue Metal	19.74
Total	100.00

Time (From Commencement) (hr)	Time (min)	Flowrate (L/min)	Observations
0.00	0	0.00	Test Started. Extremely cloudy, extremely rapid outflow.
0.03	1.5	140.00	Cloudy, extremely rapid outflow.
0.08	4.5	156.00	Slightly cloudy, extremely rapid outflow.
0.14	8.5	139.00	Clear, extremely rapid outflow.
0.21	12.67	145.00	Clear, extremely rapid outflow. Test stopped.

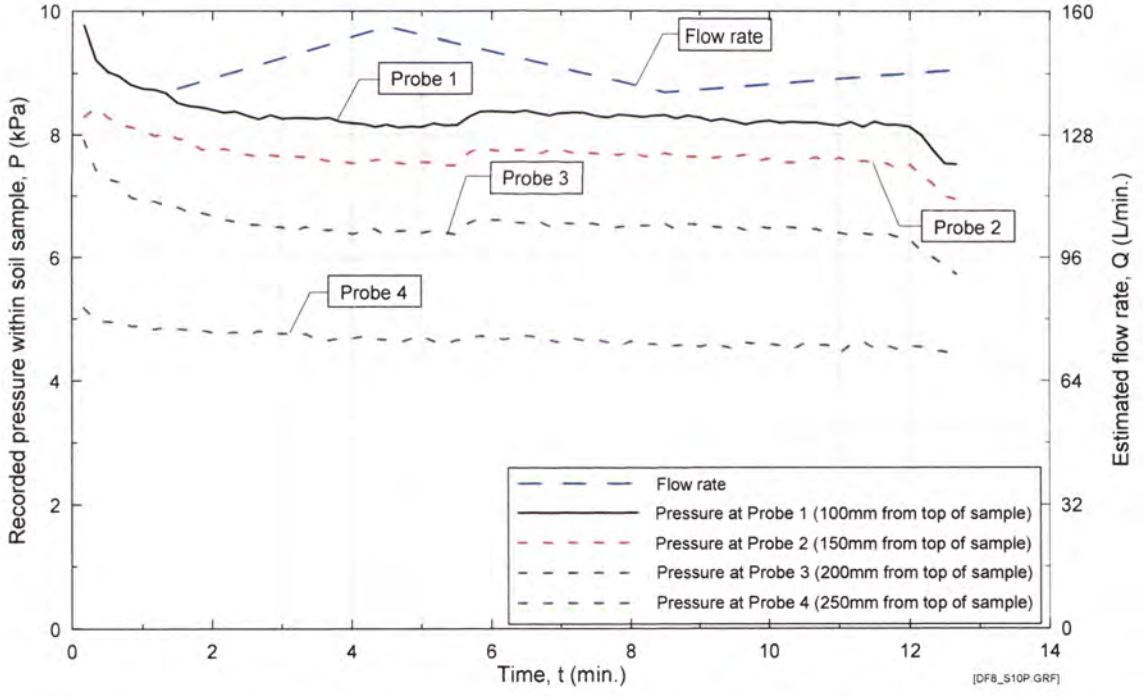

DF Test No. 8 on Sample 10 – Recorded pressure and flow rate. Sample compacted to 90.0% of Standard Max. Dry Density.

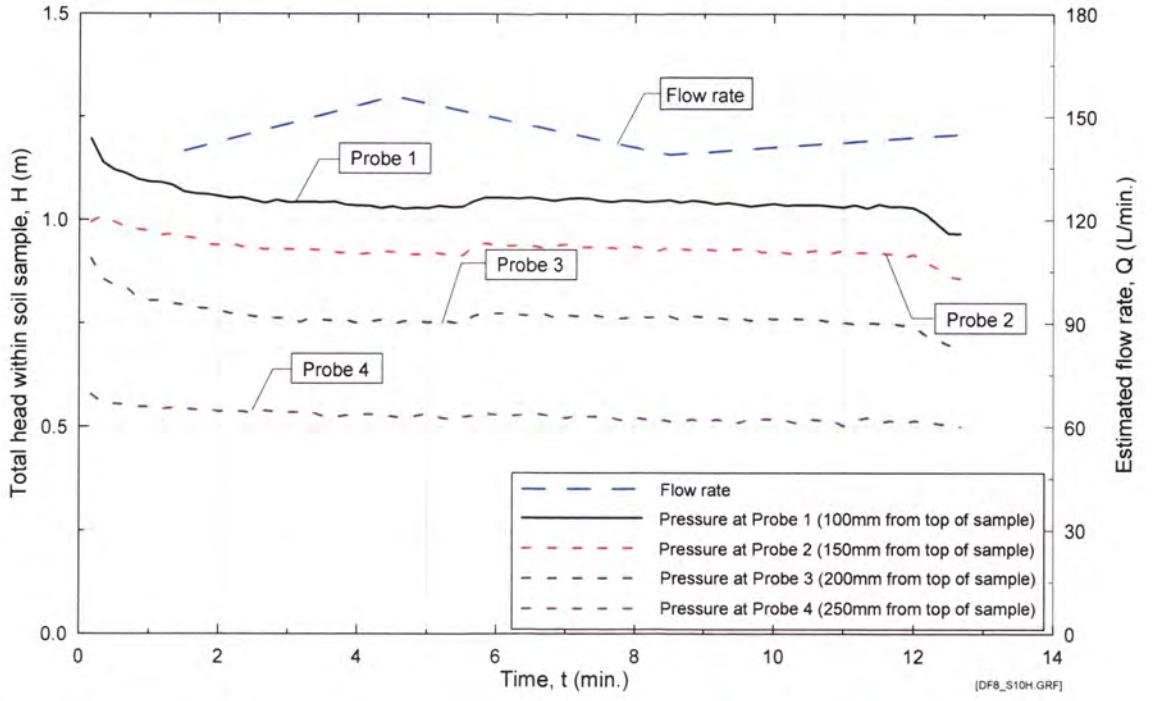

DF Test No. 8 on Sample 10 – Total head and flow rate. Sample compacted to 90.0% of Standard Max. Dry Density.

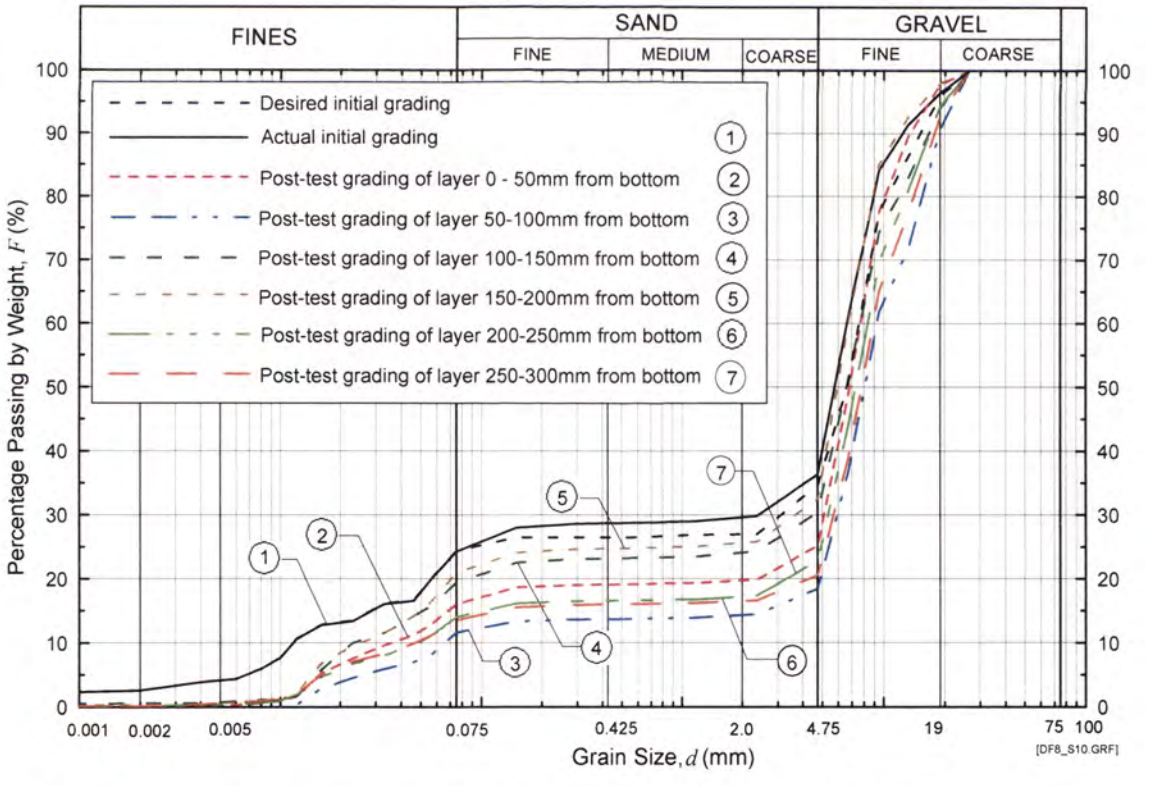

DF Test No. 8 on Sample 10 - Initial and post-test grain-size distribution analysis. Sample compacted to 90.0% of Standard Max. Dry Density.

Downward flow test No. 9 Test Records

DOWNWARD FLOW SUFFUSION TEST
Test Record

Test No/Date :	**Suffusion Downflow 009 17/05/02**
Soil Sample :	**Suffusion Test Blend No. 11**
Standard max. dry density :	1.91 Mg/m^3
Optimum water content (OWC) :	12.06%
Targeted dry density relative to Standard max. dry density :	95.0%
Actual dry density from test:	97.3%
Water content during conditioning :	12.06%
Targeted moisture content :	12.06%
Actual water content from test :	12.81%
Fluid for conditioning soil :	Sydney tap water
Eroding fluid :	Sydney tap water
Eroding fluid mean temperature :	21.6 °C
Data Log File Name :	DF9a
Time/Date of compaction of sample :	pm 15/05/02 - am 16/05/02
Time/Date of Commencement of Test :	10.00am 17/05/02

Mix Ingredient	Mix Proportion (%)
Clay Q38	0.00
Silica 60G	52.87
Nepean Sand	0.00
5mm Blue Metal	0.00
10mm Bassalt	26.43
20mm Blue Metal	20.70
Total	100.00

Time (From Commencement) (hr)	Time (min)	Flowrate (L/min)	Observations
0.00	0	0.00	Test Started. Very cloudy at base. Moderate outflow, and increasing.
0.03	1.5	20.00	Very cloudy at base. High outflow, and increasing.
0.03	1.83	30.00	Very cloudy through most of mould. High outflow, and increasing.
0.04	2.2	50.00	Extremely cloudy throughout mould. Very high outflow, and increasing.
0.06	3.65	80.00	Very cloudy throughout mould. Extremely high outflow, and increasing.
0.07	4	140.00	Cloudy throughout mould. Extremely high outflow. Test stopped.

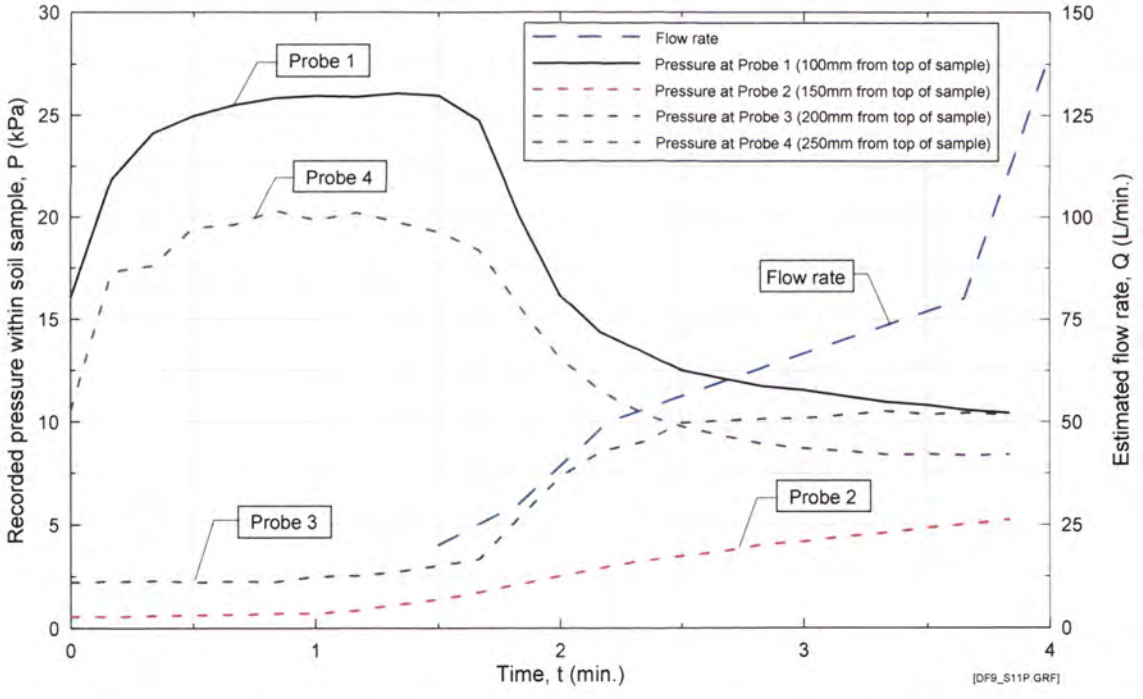

DF Test No. 9 on Sample 11 – Recorded pressure and flow rate. Sample compacted to 97.3% of Standard Max. Dry Density.

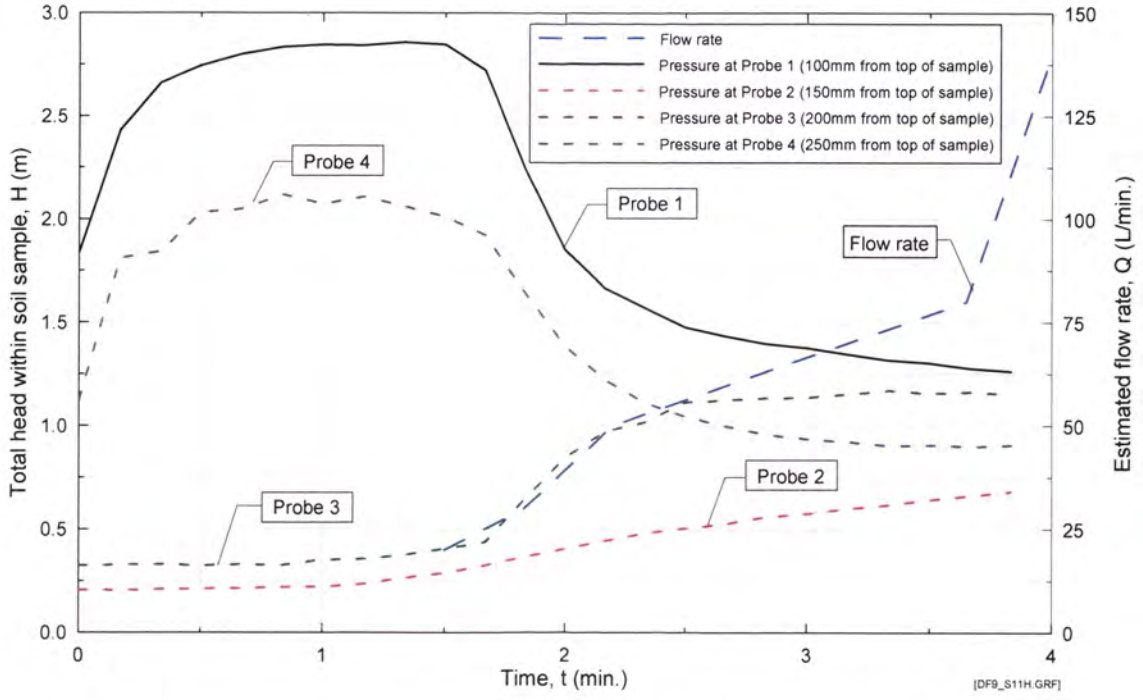

DF Test No. 9 on Sample 11 – Total head and flow rate. Sample compacted to 97.3% of Standard Max. Dry Density.

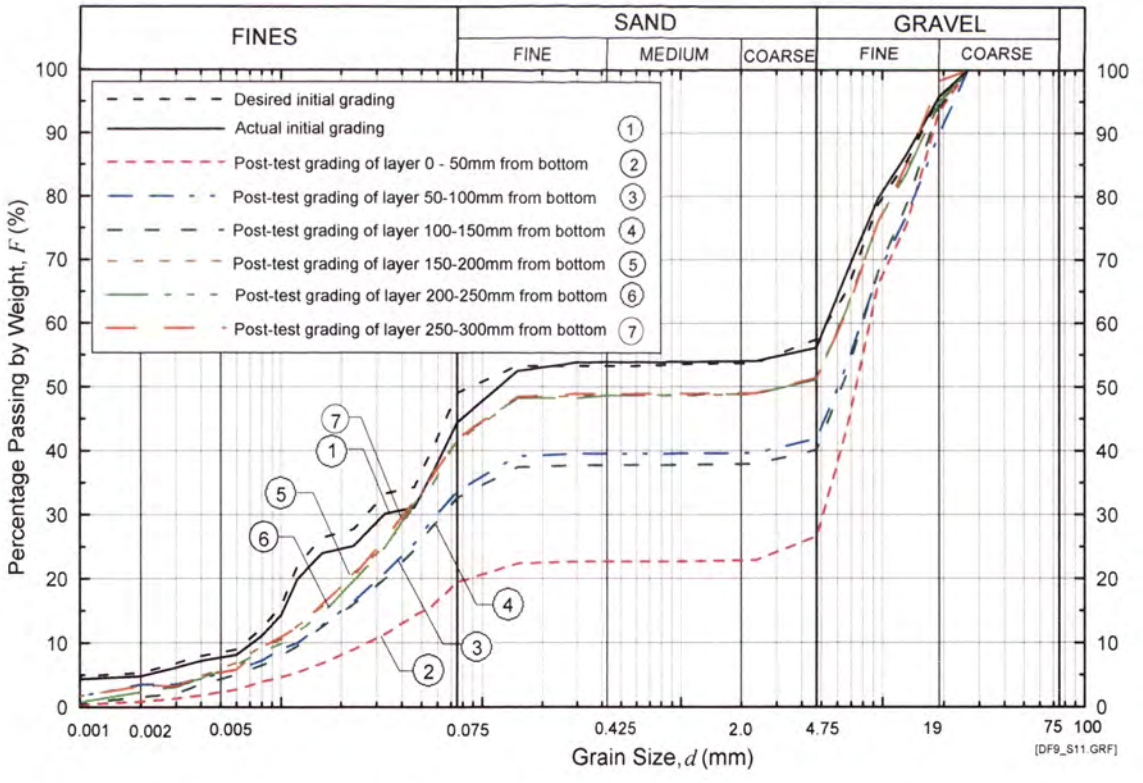

DF Test No. 9 on Sample 11 - Initial and post-test grain-size distribution analysis. Sample compacted to 97.3% of Standard Max. Dry Density.

Downward flow test No. 11 Test Records

DOWNWARD FLOW SUFFUSION TEST
Test Record

Test No/Date :	**Suffusion Downflow 011 3/06/02**
Soil Sample :	**Suffusion Test Blend No. 13**
Standard max. dry density :	1.921 Mg/m^3
Optimum water content (OWC) :	7.10%
Targeted dry density relative to Standard max. dry density :	95.0%
Actual dry density from test:	94.5%
Water content during conditioning :	7.10%
Targeted moisture content :	7.10%
Actual water content from test :	6.91%
Fluid for conditioning soil :	Sydney tap water
Eroding fluid :	Sydney tap water
Eroding fluid mean temperature :	21.6 °C
Data Log File Name :	DF11a.
Time/Date of compaction of sample :	am 3/06/02
Time/Date of Commencement of Test :	am 4/06/02

Mix Ingredient	Mix Proportion (%)
Clay Q38	5.51
Silica 60G	4.54
Nepean Sand	0.00
5mm Blue Metal	9.74
10mm Bassalt	61.95
20mm Blue Metal	18.26
Total	100.00

Time (From Commencement) (hr)	Time (From Commencement) (min)	Flowrate (L/min)	Observations
0.00	0	0.00	Test Started. Very cloudy, extremely rapid outflow.
0.06	3.5	123.60	Mostly clear, extremely rapid outflow.
0.13	7.5	121.80	Clear, extremely rapid outflow.
0.18	10.5	129.00	Clear, extremely rapid outflow.
0.23	13.5	125.60	Clear, extremely rapid outflow.
0.27	16	124.00	Clear, extremely rapid outflow. Test stopped.

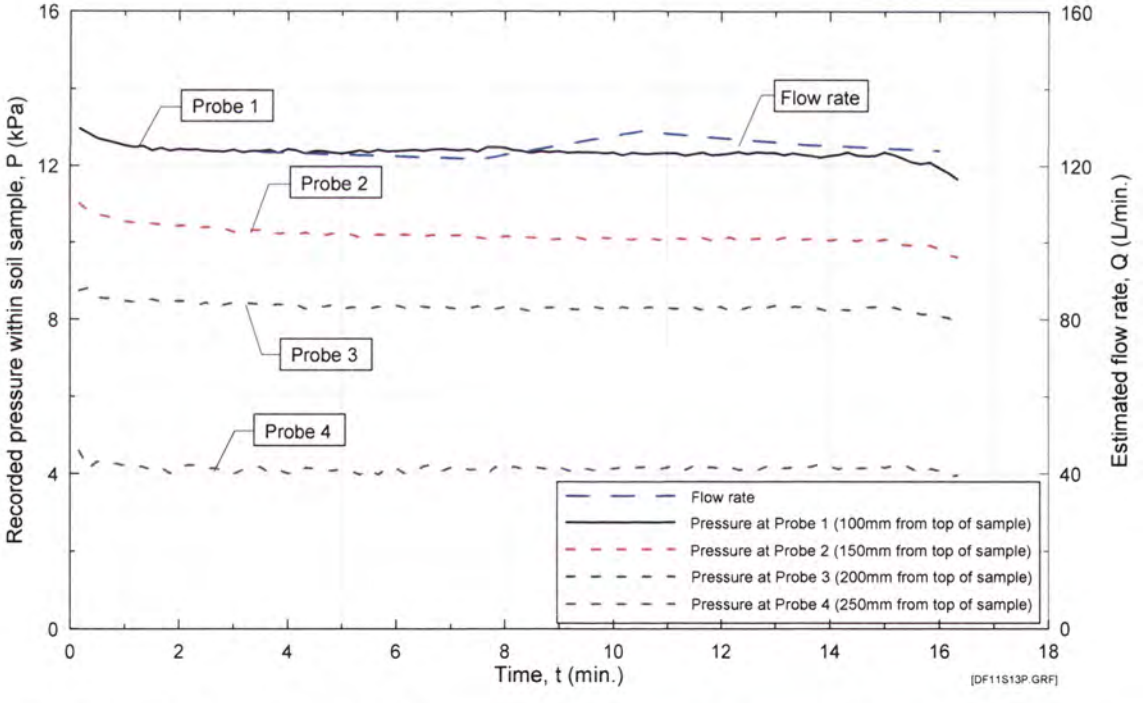

DF Test No. 11 on Sample 13 – Recorded pressure and flow rate. Sample compacted to 94.5% of Standard Max. Dry Density.

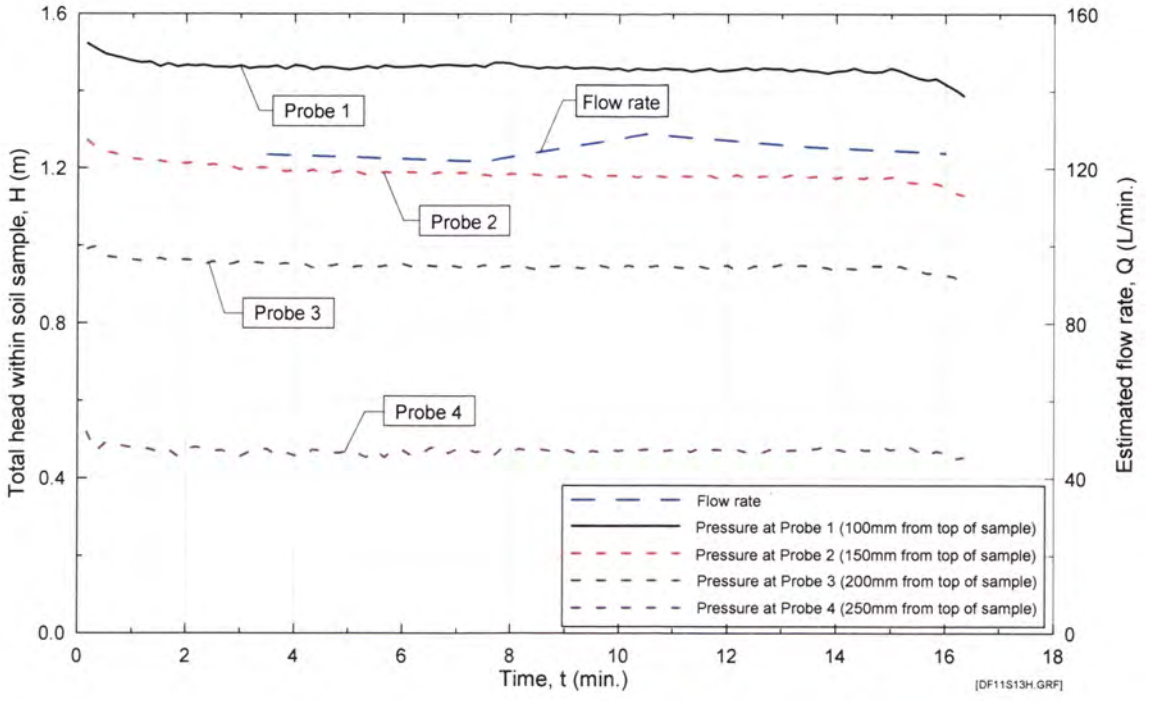

DF Test No. 11 on Sample 13 – Total head and flow rate. Sample compacted to 94.5% of Standard Max. Dry Density.

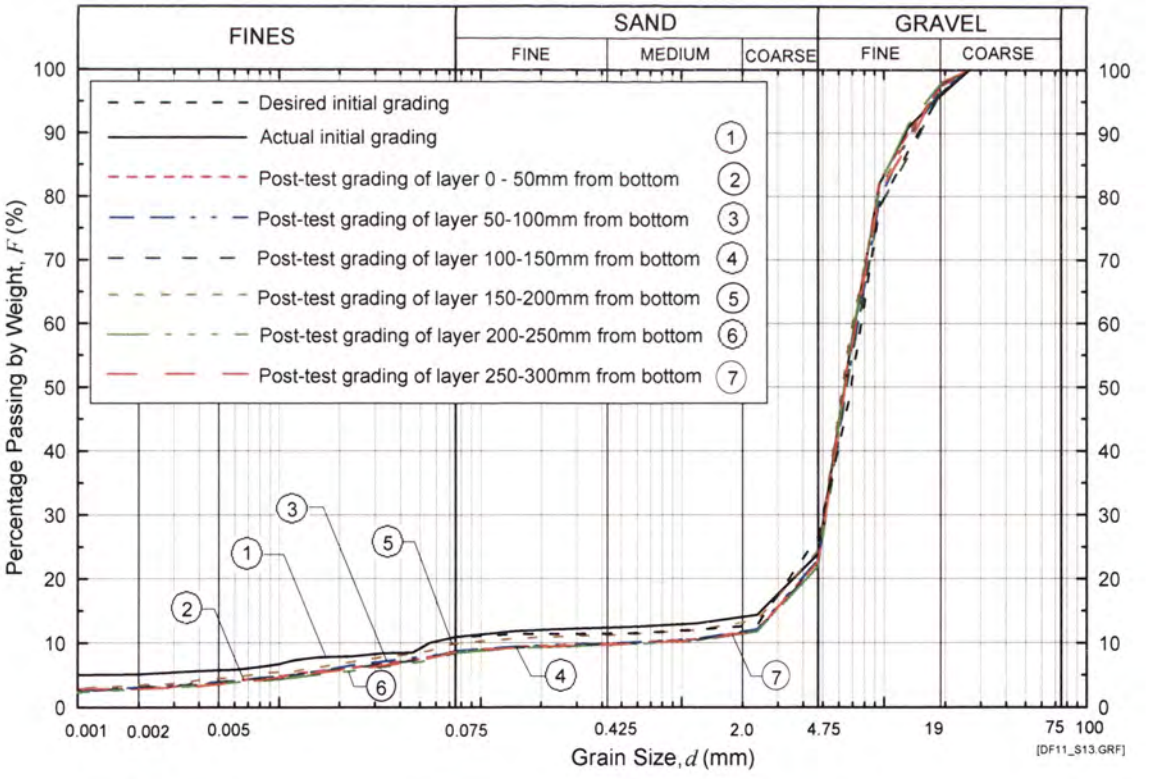

DF Test No. 11 on Sample 13 - Initial and post-test grain-size distribution analysis. Sample compacted to 94.5% of Standard Max. Dry Density.

Downward flow test No. 12 Test Records

DOWNWARD FLOW SUFFUSION TEST
Test Record

Test No/Date :	**Suffusion Downflow 012 8/07/02**
Soil Sample :	**Suffusion Test Blend No. 14**
Standard max. dry density :	2.040 Mg/m^3
Optimum water content (OWC) :	11.10%
Targeted dry density relative to Standard max. dry density :	95.0%
Actual dry density from test:	94.6%
Water content during conditioning :	11.10%
Targeted moisture content :	11.10%
Actual water content from test :	10.56%
Fluid for conditioning soil :	Sydney tap water
Eroding fluid :	Sydney tap water
Eroding fluid mean temperature :	21.6 °C
Data Log File Name :	DF12a.
Time/Date of compaction of sample :	am 3/06/02
Time/Date of Commencement of Test :	am 4/06/02

Mix Ingredient	Mix Proportion (%)
Clay Q38	10.90
Silica 60G	11.08
Nepean Sand	0.00
5mm Blue Metal	0.00
10mm Bassalt	57.30
20mm Blue Metal	20.72
Total	100.00

Time (From Commencement) (hr)	Time (From Commencement) (min)	Flowrate (L/min)	Observations
0.00	0.0	0.00	Test Started. Very cloudy, very rapid outflow.
0.05	3.0	81.80	Mostly clear, very rapid outflow.
0.09	5.5	82.80	Clear, very rapid outflow.
0.13	7.5	90.00	Clear, very rapid outflow.
0.16	9.5	86.00	Clear, very rapid outflow.
0.19	11.5	95.20	Clear, very rapid outflow.
0.23	13.5	94.80	Clear, very rapid outflow.
0.27	16.0	83.60	Clear, very rapid outflow.
0.32	19.0	86.80	Clear, very rapid outflow.
0.34	20.5	83.40	Clear, very rapid outflow.
0.37	22.0	88.20	Clear, very rapid outflow.
0.40	24.0	89.40	Clear, very rapid outflow.
0.42	25.0	89.00	Clear, very rapid outflow. Test stopped.

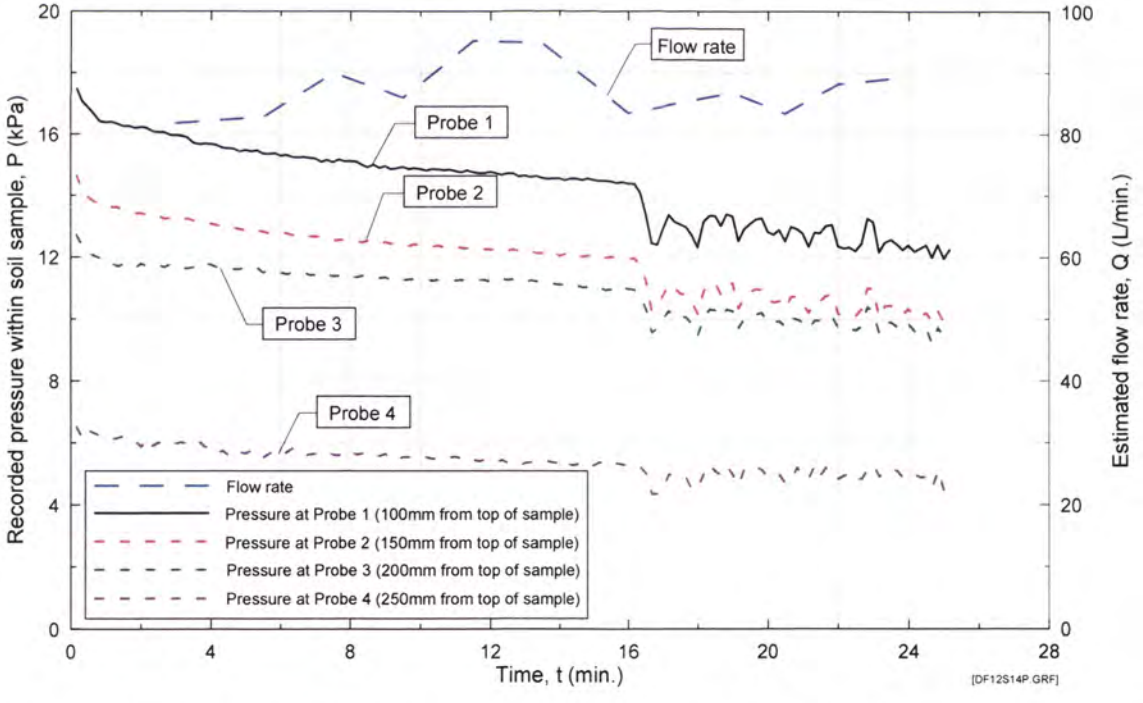

DF Test No. 12 on Sample 14A – Recorded pressure and flow rate. Sample compacted to 94.6% of Standard Max. Dry Density.

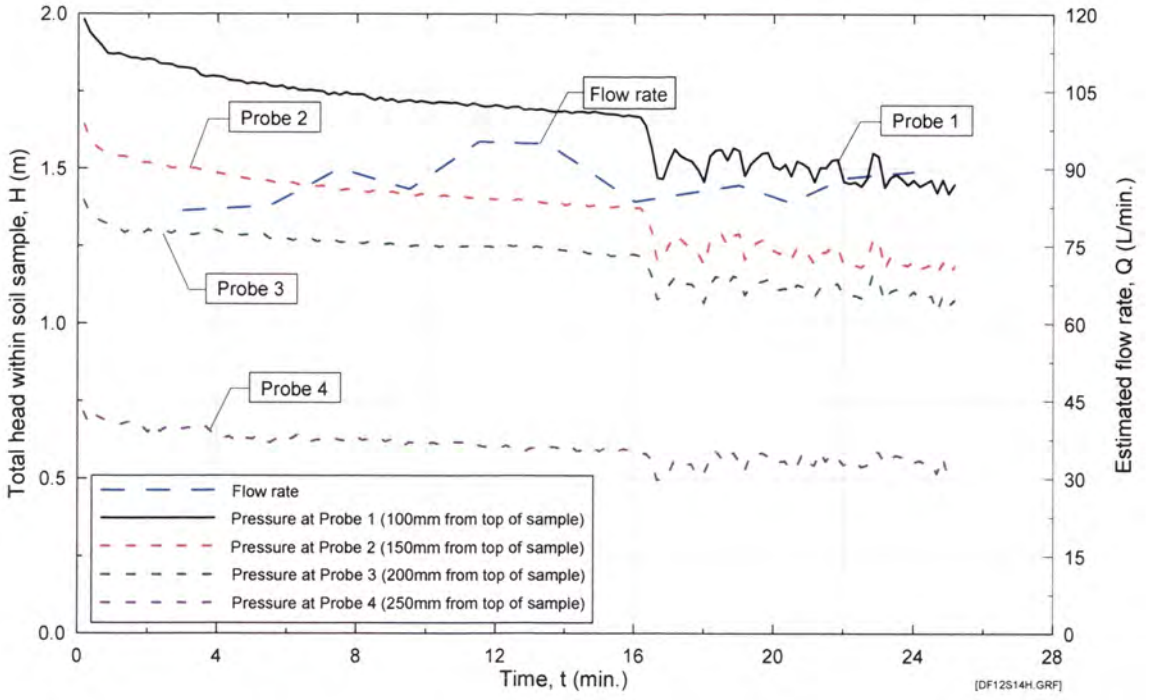

DF Test No. 12 on Sample 14A – Total head and flow rate. Sample compacted to 94.6% of Standard Max. Dry Density.

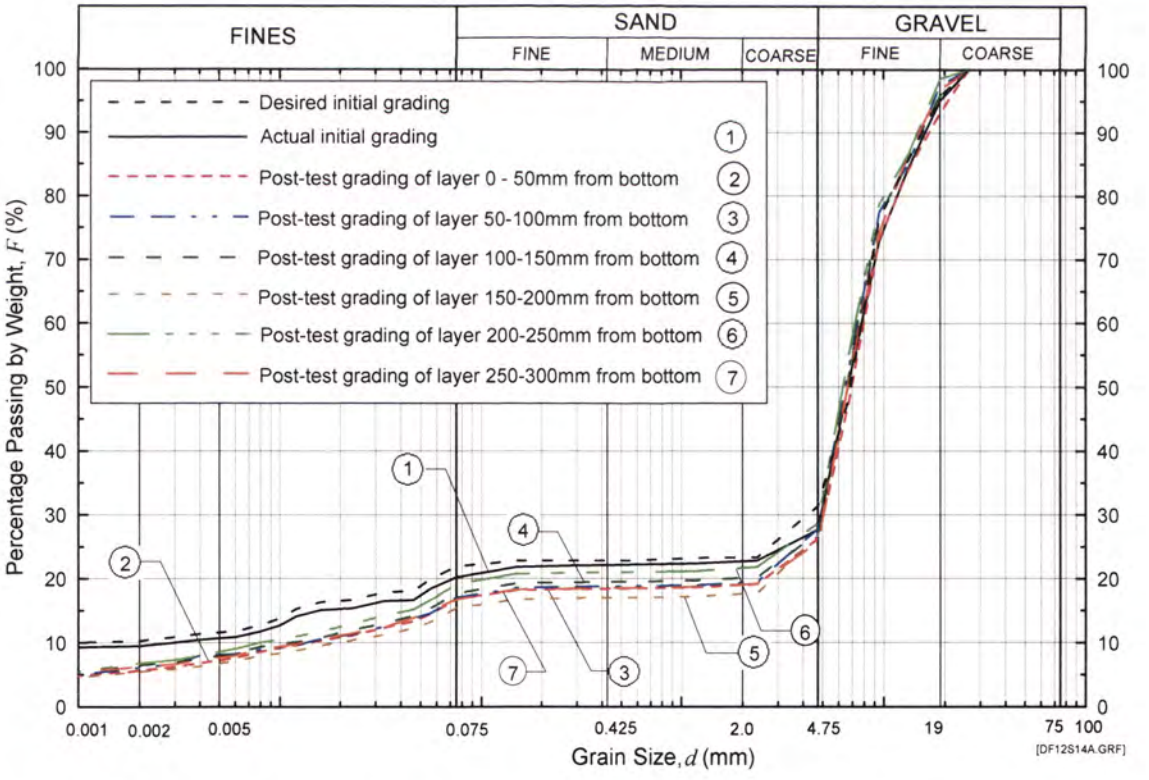

DF Test No. 12 on Sample 14A - Initial and post-test grain-size distribution analysis. Sample compacted to 94.6% of Standard Max. Dry Density.

Downward flow test No. 15 Test Records

DOWNWARD FLOW SUFFUSION TEST
Test Record

Test No/Date :	**Suffusion Downflow 015 6/06/02**
Soil Sample :	**Suffusion Test Blend No. 14a**
Standard max. dry density :	2.040 Mg/m^3
Optimum water content (OWC) :	11.10%
Targeted dry density relative to Standard max. dry density :	90.0%
Actual dry density from test:	90.0%
Water content during conditioning :	11.10%
Targeted moisture content :	11.10%
Actual water content from test :	10.23%
Fluid for conditioning soil :	Sydney tap water
Eroding fluid :	Sydney tap water
Eroding fluid mean temperature :	21.6 °C
Data Log File Name :	DF15a
Time/Date of compaction of sample :	am 5/06/02
Time/Date of Commencement of Test :	am 6/06/02

Mix Ingredient	Mix Proportion (%)
Clay Q38	10.89
Silica 60G	11.09
Nepean Sand	0.00
5mm Blue Metal	0.00
10mm Bassalt	57.30
20mm Blue Metal	20.72
Total	100.00

Time (From Commencement) (hr)	Time (From Commencement) (min)	Flowrate (L/min)	Observations
0.00	0.0	0.00	Test Started. Very cloudy near base, very rapid outflow.
0.03	1.5	109.00	Very cloudy. Extremely high outflow, fluctuating slightly.
0.06	3.5	110.00	Very cloudy, starting to clear slightly. Extremely high outflow, fluctuating slightly.
0.09	5.5	109.60	Slightly cloudy, clearing steadily. Extremely high outflow, fluctuating slightly.
0.13	7.5	108.20	Mostly clear. Extremely high outflow, fluctuating slightly.
0.17	10.0	112.00	Mostly clear. Extremely high outflow, fluctuating slightly.
0.20	12.0	110.00	Mostly clear. Extremely high outflow, fluctuating slightly.
0.23	14.0	116.80	Clear. Extremely high outflow, fluctuating slightly.
0.27	16.0	112.60	Clear. Extremely high outflow, fluctuating slightly.
0.30	18.0	122.60	Clear. Extremely high outflow, fluctuating slightly.
0.33	19.5	119.80	Clear. Extremely high outflow, fluctuating slightly.
0.35	21.0	129.00	Clear. Extremely high outflow, fluctuating slightly.
0.38	23.0	119.60	Clear. Extremely high outflow, fluctuating slightly.
0.41	24.5	121.80	Clear. Extremely high outflow, fluctuating slightly. Test stopped.

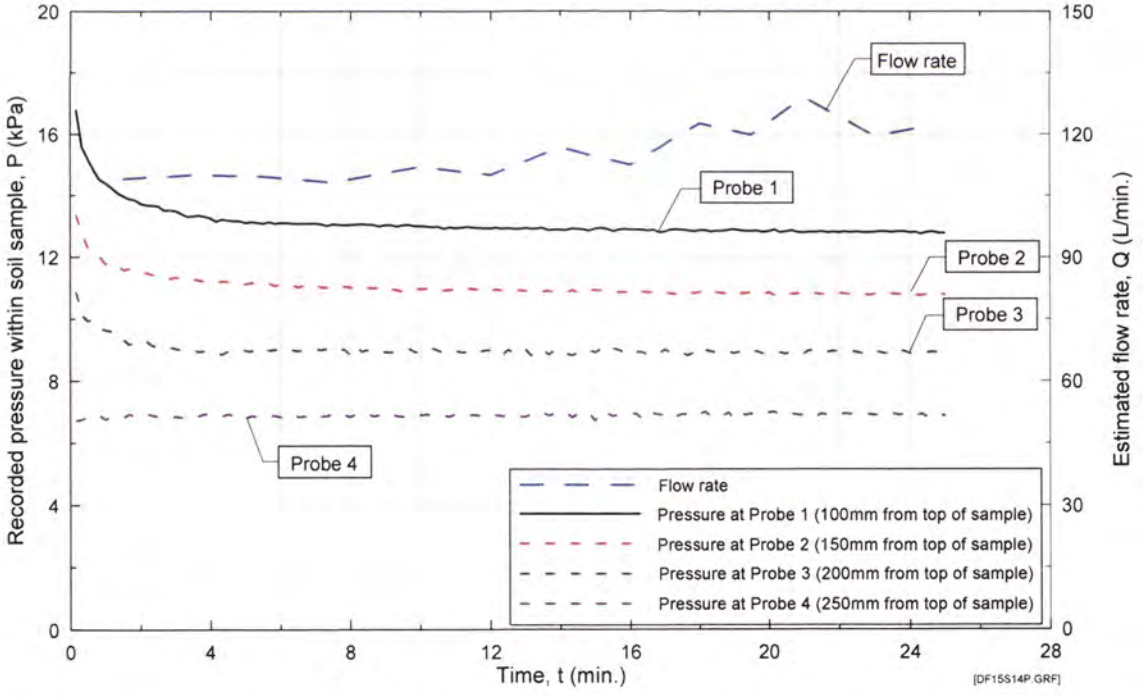

DF Test No. 15 on Sample 14A – Recorded pressure and flow rate. Sample compacted to 90.0% of Standard Max. Dry Density.

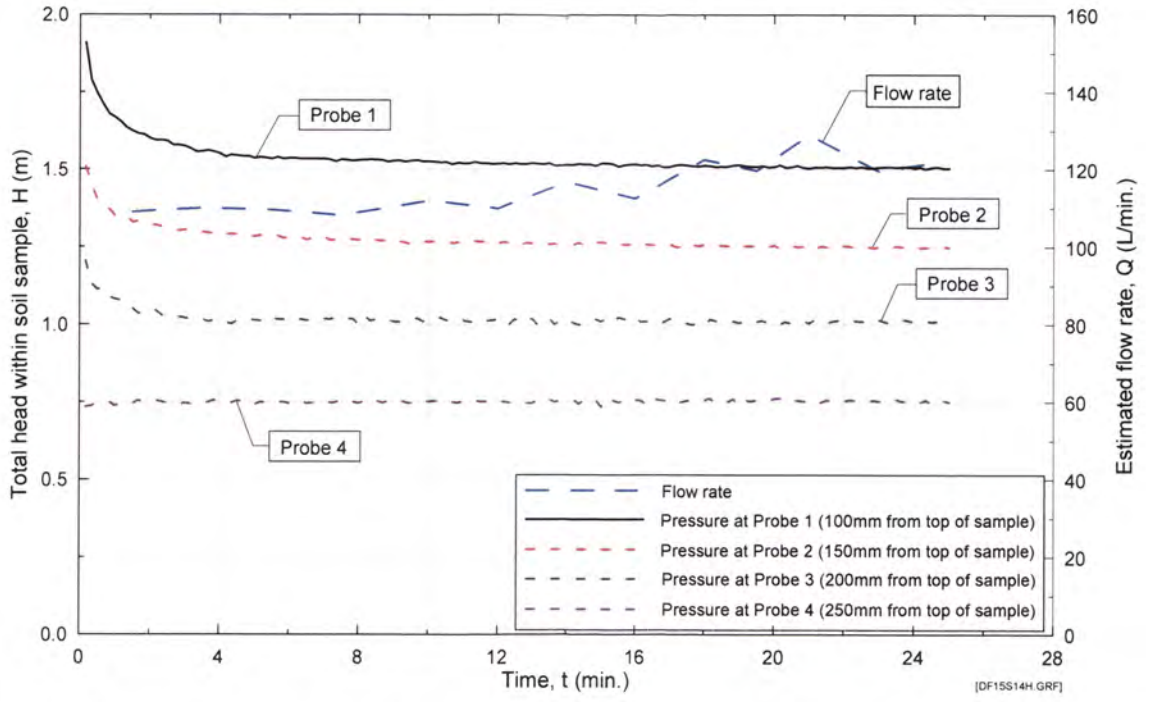

DF Test No. 15 on Sample 14A – Total head and flow rate. Sample compacted to 90.0% of Standard Max. Dry Density.

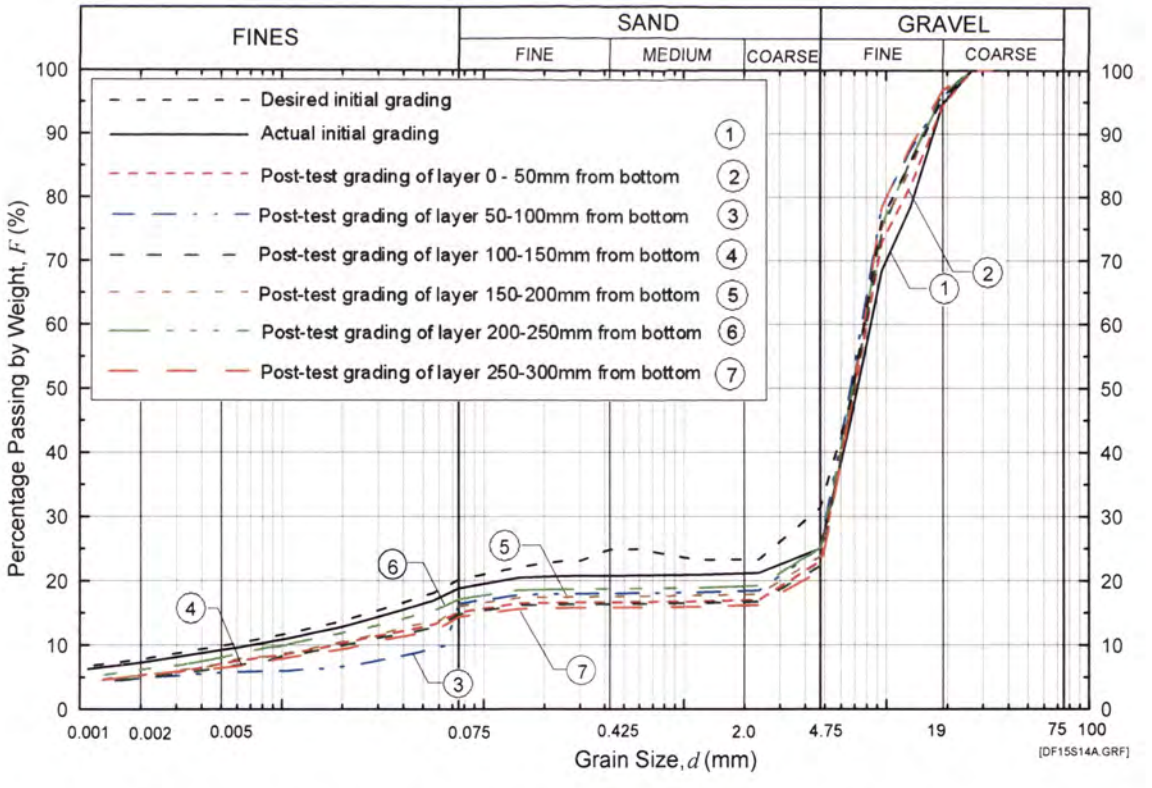

DF Test No. 15 on Sample 14A - Initial and post-test grain-size distribution analysis. Sample compacted to 90.0% of Standard Max. Dry Density.

Downward flow test No. 17 Test Records

DOWNWARD FLOW SUFFUSION TEST
Test Record

Test No/Date :	**Suffusion Downflow 017 18/09/02**
Soil Sample :	**Suffusion Test Blend No. 15**
Standard max. dry density :	2.090 Mg/m^3
Optimum water content (OWC) :	8.20%
Targeted dry density relative to Standard max. dry density :	95.0%
Actual dry density from test:	92.3%
Water content during conditioning :	8.20%
Targeted moisture content :	8.20%
Actual water content from test :	8.10%
Fluid for conditioning soil :	Sydney tap water
Eroding fluid :	Sydney tap water
Eroding fluid mean temperature :	14.4 °C
Data Log File Name :	DF 17a.
Time/Date of compaction of sample :	pm 13/09/02 + am 16/09/02
Time/Date of Commencement of Test :	am 18/09/02

Mix Ingredient	Mix Proportion (%)
Clay Q38	21.49
Silica 60G	24.11
Nepean Sand	30.50
5mm Blue Metal	23.90
10mm Bassalt	0.00
20mm Blue Metal	0.00
Total	100.00

Time (From Commencement) (hr)	Time (From Commencement) (min)	Flowrate (L/min)	Observations
0.00	0.0	0.00	Test Started. Slightly cloudy near base and increasing, low outflow.
0.03	1.7	50.00	Very cloudy. High outflow. and steadily increasing.
0.12	7.0	70.44	Slightly cloudy, slowly clearing. High outflow, slowly increasing.
0.15	9.0	73.80	Slightly cloudy, slowly clearing. High outflow, slowly increasing.
0.19	11.5	79.92	Slightly cloudy, slowly clearing. High outflow, slowly increasing.
0.22	13.0	77.04	Slightly cloudy, slowly clearing. High outflow, fluctuating slightly.
0.25	15.0	79.32	Slightly cloudy, slowly clearing. High outflow, fluctuating slightly.
0.28	17.0	80.40	Slightly cloudy, slowly clearing. High outflow, fluctuating slightly.
0.32	19.0	85.68	Slightly cloudy, slowly increasing again. High outflow, slowly increasing.
0.35	21.0	89.64	Slightly cloudy, slowly increasing again. High outflow, slowly increasing.
0.38	23.0	85.80	Slightly cloudy, slowly clearing. High outflow, fluctuating slightly.
0.42	25.0	89.16	Slightly cloudy, slowly clearing. High outflow, fluctuating slightly.
0.45	27.0	100.20	Slightly cloudy, increasing. Very high outflow, steadily increasing. Test stopped.

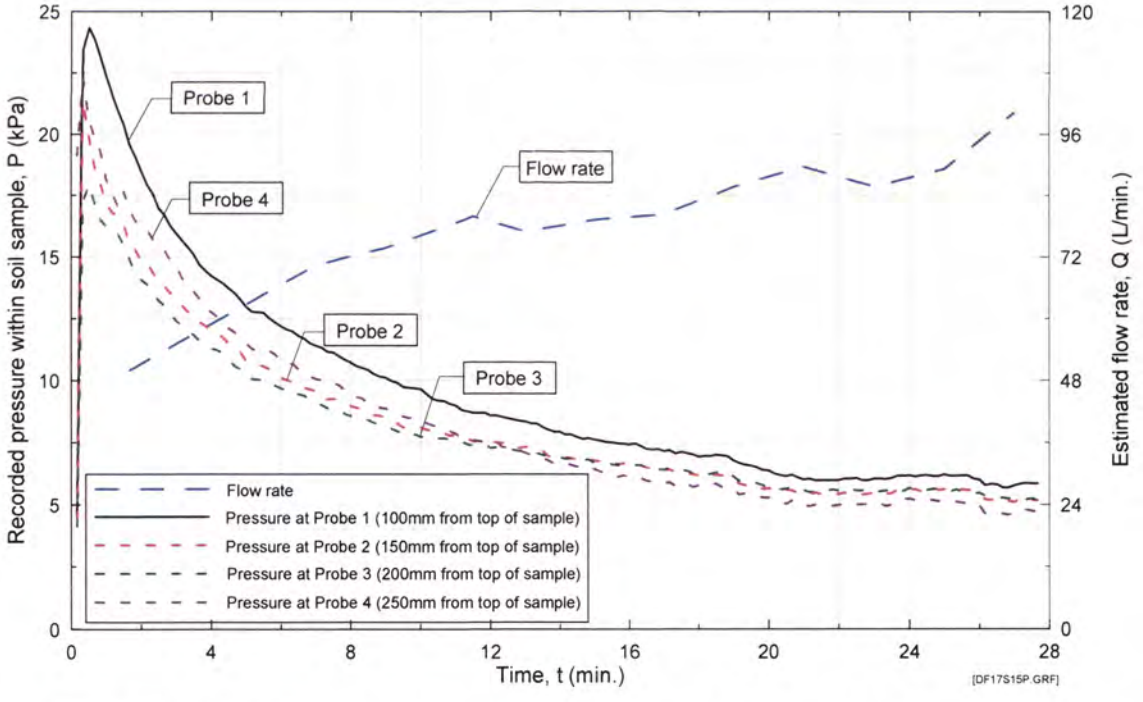

DF Test No. 17 on Sample 15 – Recorded pressure and flow rate. Sample compacted to 92.3% of Standard Max. Dry Density.

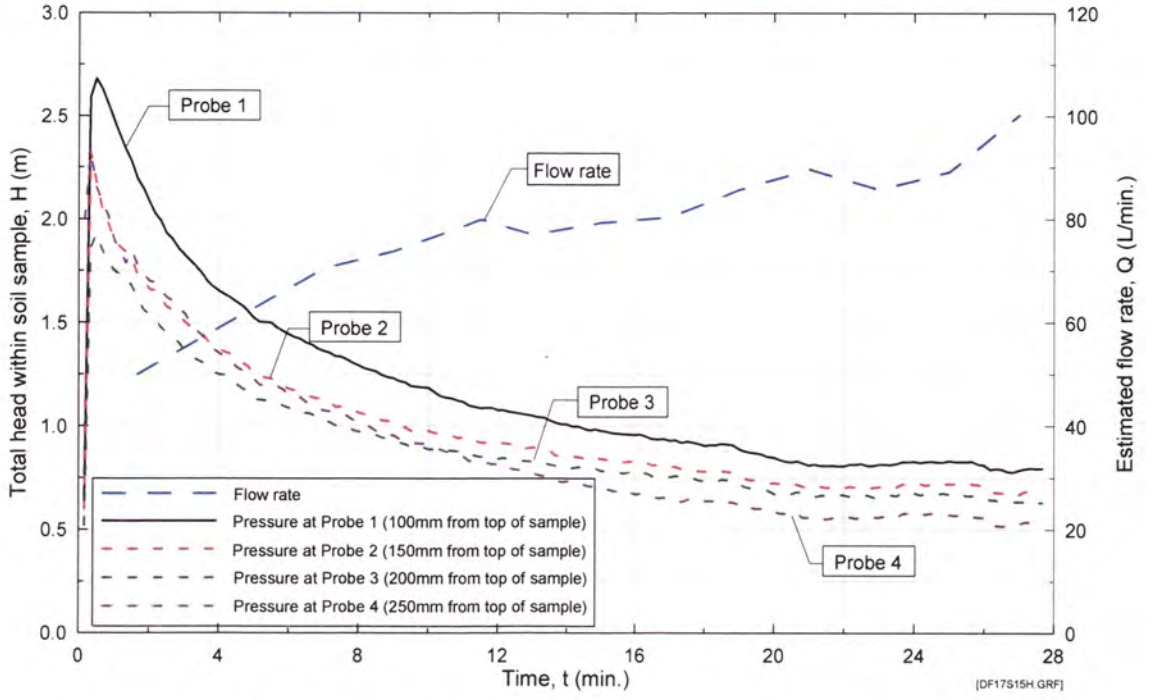

DF Test No. 17 on Sample 15 – Total head and flow rate. Sample compacted to 92.3% of Standard Max. Dry Density.

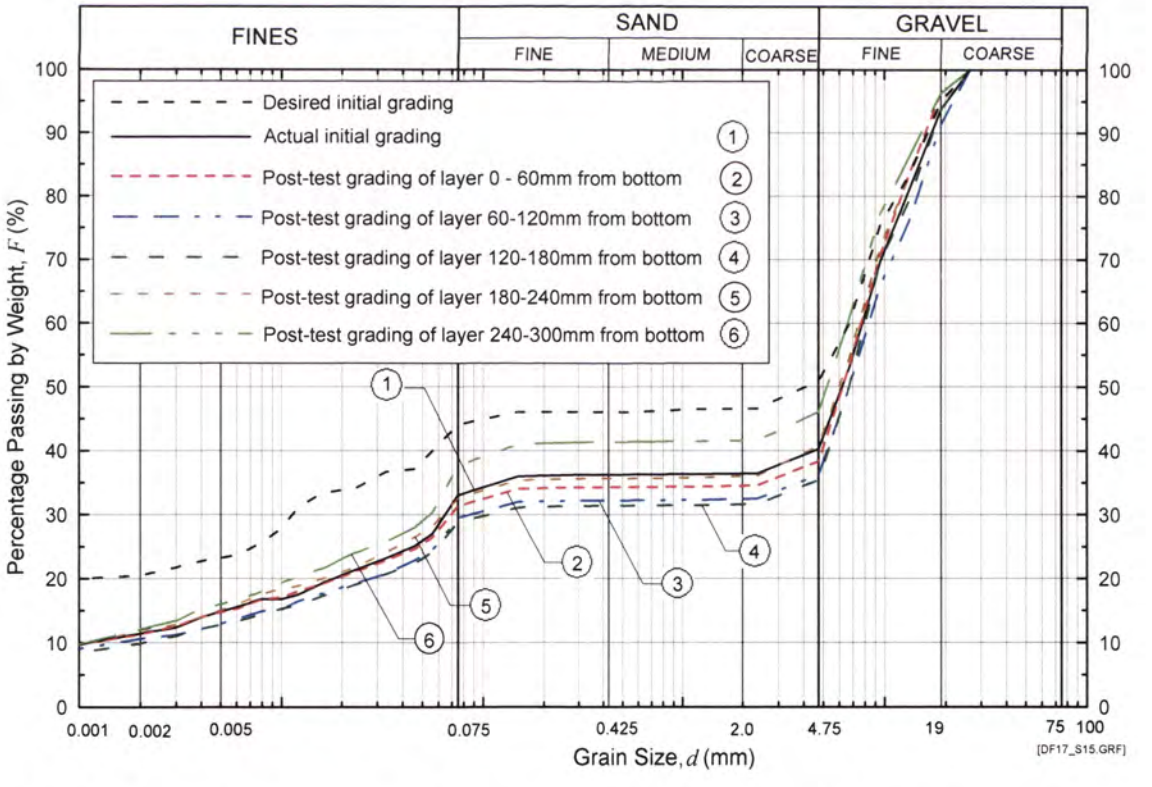

DF Test No. 17 on Sample 15 - Initial and post-test grain-size distribution analysis. Sample compacted to 92.3% of Standard Max. Dry Density.

Downward flow test No. 18 Test Records

DOWNWARD FLOW SUFFUSION TEST
Test Record

Test No/Date :	**Suffusion Downflow 018 (020) 10/07/02**
Soil Sample :	**Suffusion Test Blend No. 17 (Rowallan Dam)**
Standard max. dry density :	1.868 Mg/m^3
Optimum water content (OWC) :	13.30%
Targeted dry density relative to Standard max. dry density :	95.0%
Actual dry density from test:	94.8%
Water content during conditioning :	13.30%
Targeted moisture content :	13.30%
Actual water content from test :	12.90%
Fluid for conditioning soil :	Sydney tap water
Eroding fluid :	Sydney tap water
Eroding fluid mean temperature :	14.4 °C
Data Log File Name :	DF 20a, DF 20b, DF 20c, DF 20d.
Time/Date of compaction of sample :	am 9/07/02
Time/Date of Commencement of Test :	am 11/07/02

Mix Ingredient	Mix Proportion (%)
Rowallan Dam	100.00

Time (From Commencement) (hr)	Time (From Commencement) (min)	Flowrate (L/min)	Observations
0.00	0.0	0.00	Test Started. Clear, no visible erosion. Extremely low outflow.
0.03	2.0	0.03	Clear, no visible erosion. Extremely low outflow.
3.29	197.5	0.03	Clear, no visible erosion. Extremely low outflow.
4.99	299.3	-	Clear, no visible erosion. Extremely low outflow. Test paused, then restarted.
11.37	682.0	0.04	Clear, no visible erosion. Extremely low outflow.
11.40	684.3	0.03	Clear, no visible erosion. Extremely low outflow. Test started.

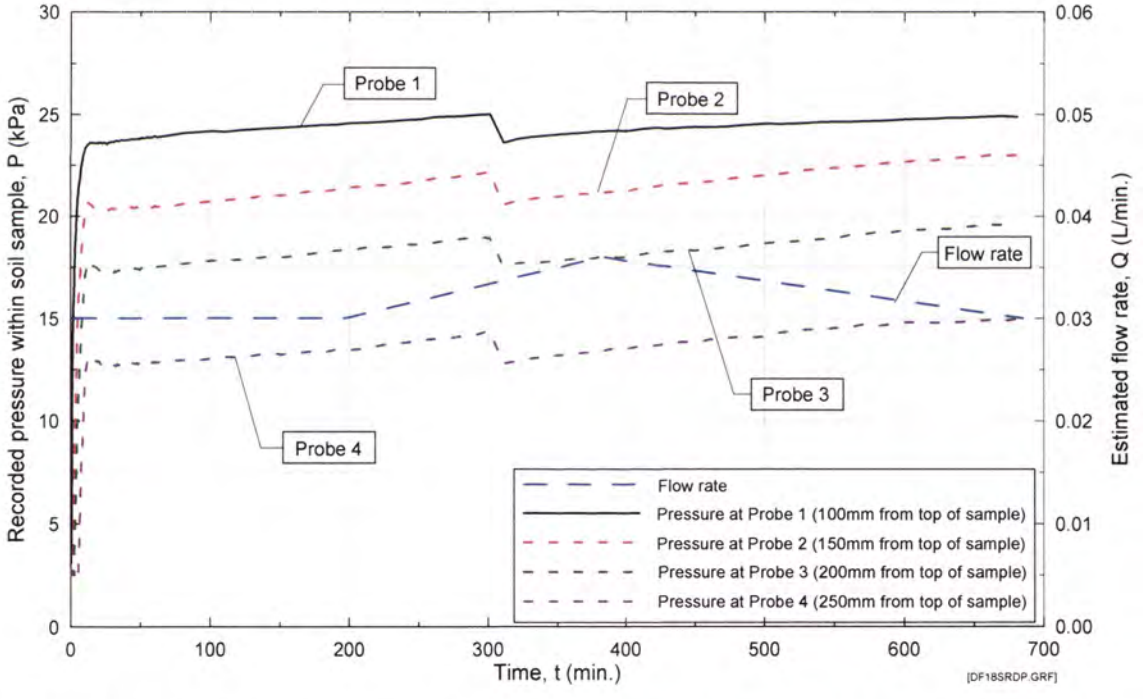

DF Test No. 18 on Sample RD – Recorded pressure and flow rate. Sample compacted to 94.8% of Standard Max. Dry Density.

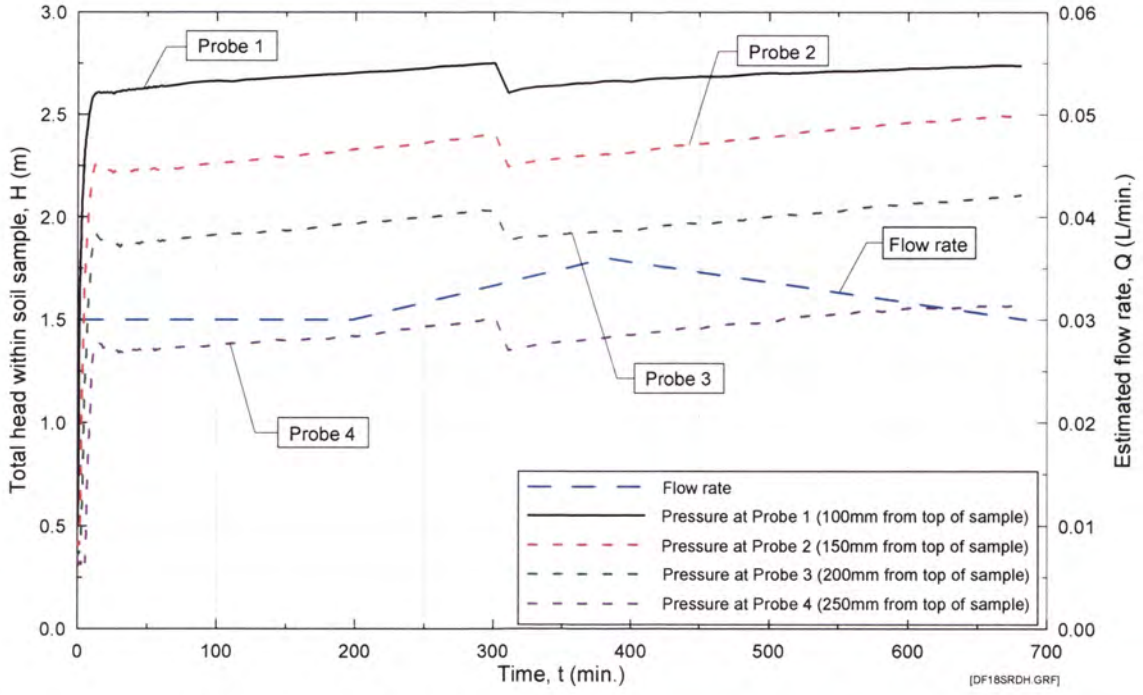

DF Test No. 18 on Sample RD – Total head and flow rate. Sample compacted to 94.8% of Standard Max. Dry Density.

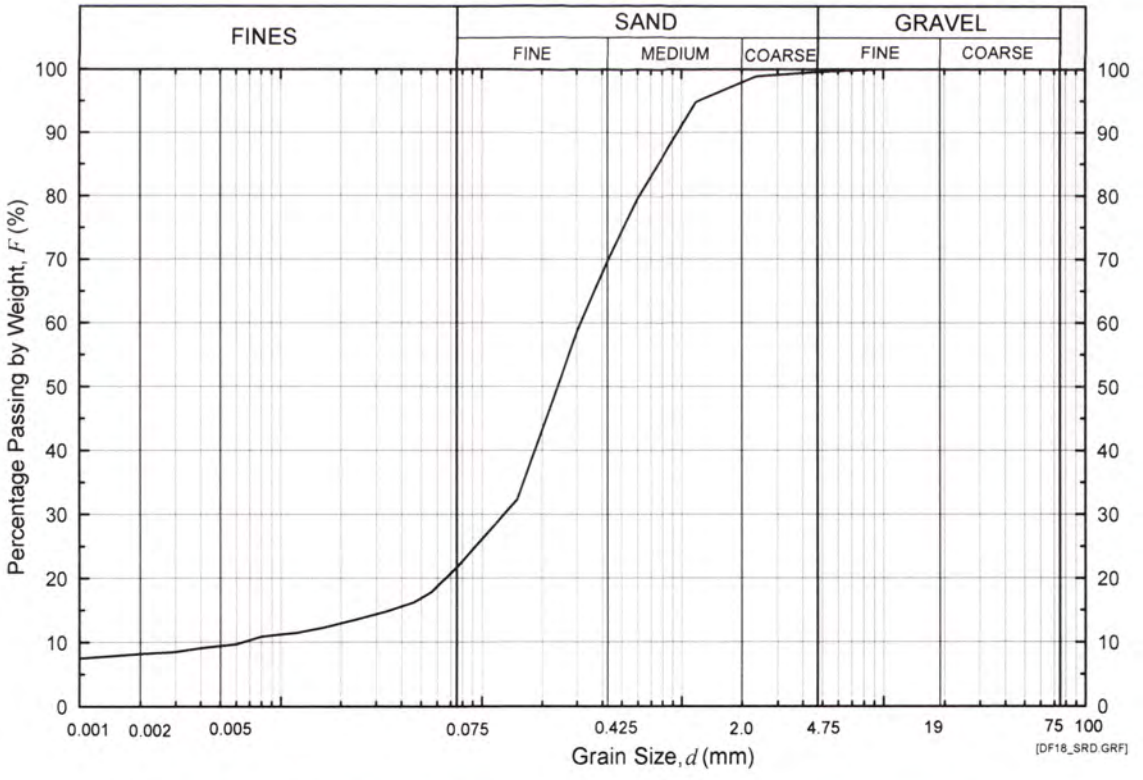

DF Test No. 18 on Sample RD - Initial grain-size distribution analysis. (Sample showed no obvious change during the DF test. No post-test grain-size distribution analysis was carried out.)

Downward flow test No. 24 Test Records

DOWNWARD FLOW SUFFUSION TEST
Test Record

Test No/Date :	**Suffusion Downflow 024 21/11/03**
Soil Sample :	**Suffusion Test Blend A2**
Standard max. dry density :	2.428 Mg/m^3
Optimum water content (OWC) :	6.14%
Targeted dry density relative to Standard max. dry density :	95.0%
Actual dry density from test:	90.7%
Water content during conditioning :	6.14%
Targeted moisture content :	6.14%
Actual water content from test :	5.55%
Fluid for conditioning soil :	Sydney tap water
Eroding fluid :	Sydney tap water
Eroding fluid mean temperature :	14.4 °C
Data Log File Name :	DF 24a.
Time/Date of compaction of sample :	pm 20/11/03
Time/Date of Commencement of Test :	am 21/11/03

Mix Ingredient	Mix Proportion (%)
Silica 60G	18.70
Nepean Sand	6.08
5mm Blue Metal	6.08
10mm Bassalt	6.08
20mm Blue Metal	12.15
pukaki 25-38	23.88
pukaki 38-51	10.027
pukaki 51-76	17.013
Total	100.00

Time (From Commencement) (hr)	Time (From Commencement) (min)	Flowrate (L/min)	Observations
0.00	0.0	0.00	Test Started. Extremely cloudy near base and increasing, rapid outflow increase.
0.02	2.0	98.10	Extremely cloudy. Very high outflow, becoming steady.
0.04	4.0	102.30	Extremely cloudy. Very high outflow, fluctuating slightly.
0.06	6.0	101.25	Very cloudy, clearing slightly. Very high outflow, fluctuating slightly.
0.08	8.0	90.90	Cloudy, clearing slightly. Very high outflow, slowing slightly.
0.10	10.0	86.55	Cloudy, clearing slightly. Very high outflow, slowing slightly.
0.12	12.0	88.00	Slightly cloudy, slowly clearing. Very high outflow, fluctuating slightly.
0.14	14.0	85.50	Slightly cloudy, slowly clearing. Very high outflow, fluctuating slightly.
0.16	16.0	85.05	Slightly cloudy, slowly clearing. Very high outflow, fluctuating slightly.
0.18	18.0	87.00	Slightly cloudy, slowly clearing. Very high outflow, fluctuating slightly.
0.20	20.0	79.95	Mostly clear, clearing slightly. Very high outflow, fluctuating slightly.
0.22	22.0	85.50	Mostly clear, clearing slightly. Very high outflow, fluctuating slightly.
0.24	24.0	73.95	Clear. Very high outflow, slowing slightly.
0.26	26.0	72.00	Clear. Very high outflow, slowing slightly.
0.28	28.0	62.85	Clear. Very high outflow, slowing slightly.
0.30	30.0	65.28	Clear. High outflow, fluctuating slightly.
0.33	32.5	66.30	Clear. High outflow, fluctuating slightly. Test stopped.

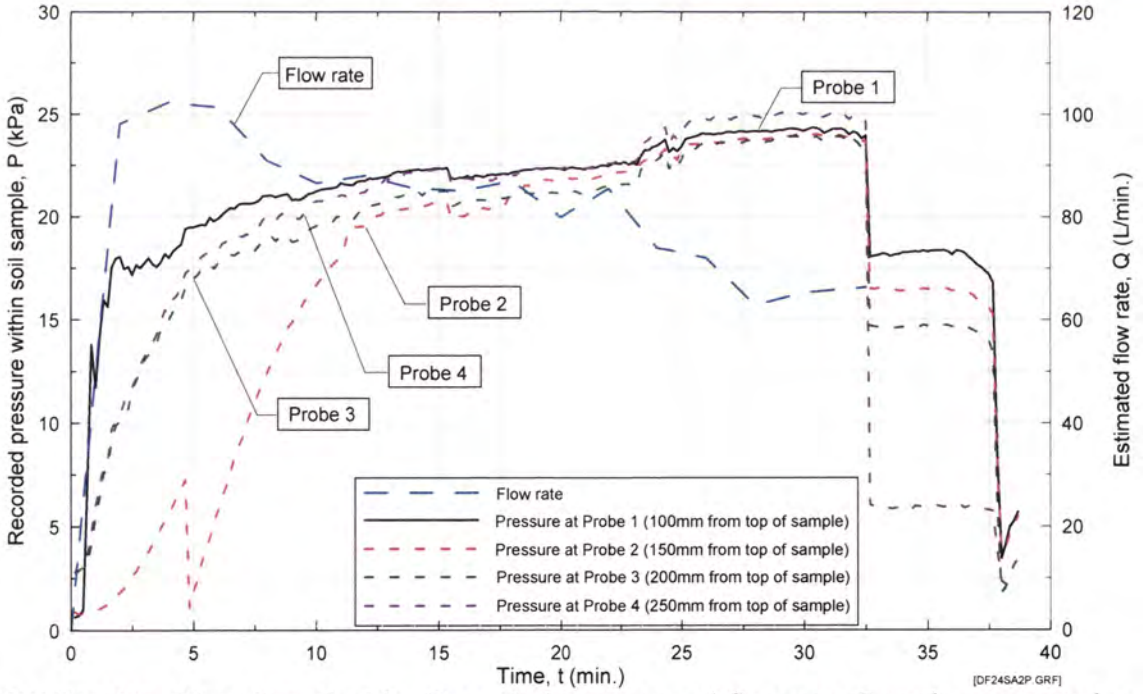

DF Test No. 24 on Sample A2 – Recorded pressure and flow rate. Sample compacted to 90.7% of Standard Max. Dry Density.

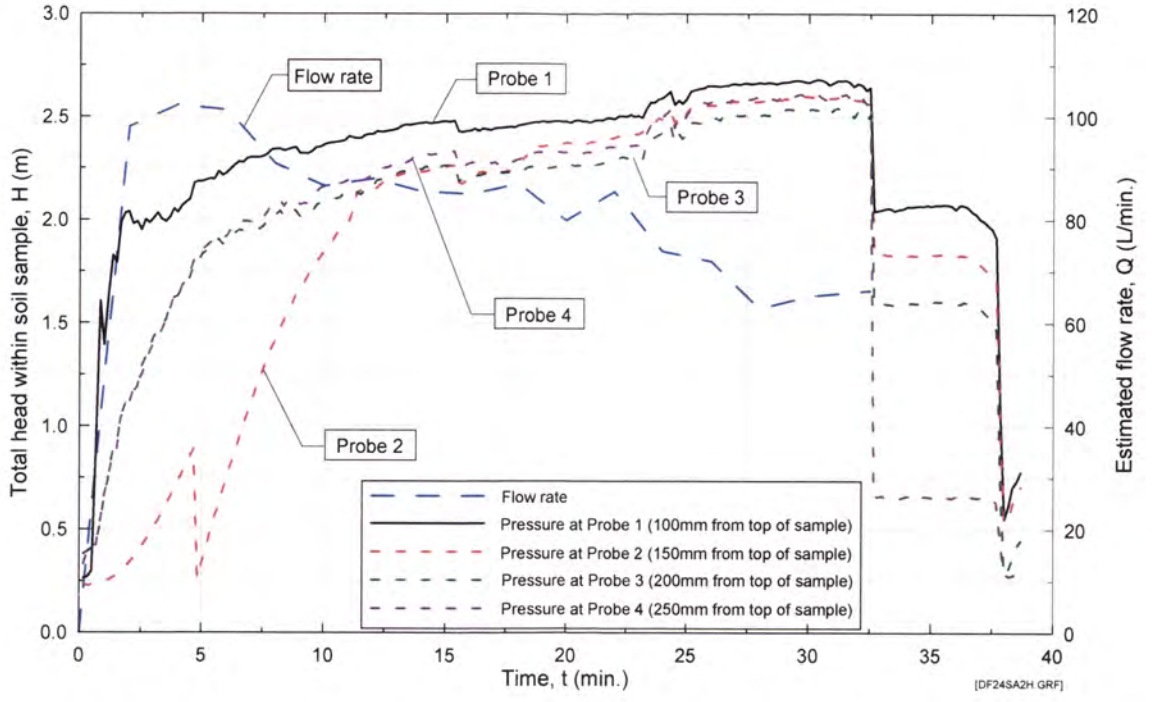

DF Test No. 24 on Sample A2 – Total head and flow rate. Sample compacted to 90.7% of Standard Max. Dry Density.

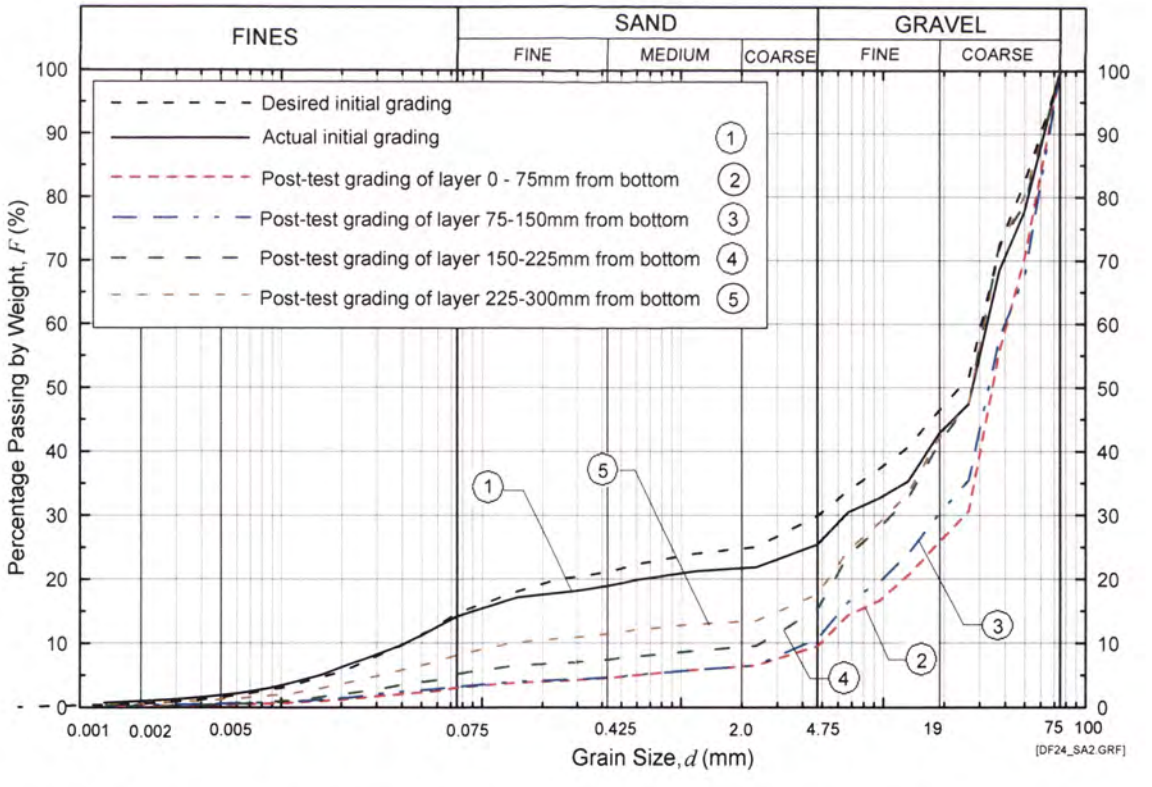

DF Test No. 24 on Sample A2 - Initial and post-test grain-size distribution analysis. Sample compacted to 90.7% of Standard Max. Dry Density.

Downward flow test No. 23 Test Records

DOWNWARD FLOW SUFFUSION TEST
Test Record

Test No/Date :	**Suffusion Downflow 023 27/10/03**
Soil Sample :	**Suffusion Test Blend A3**
Standard max. dry density :	2.409 Mg/m^3
Optimum water content (OWC) :	5.14%
Targeted dry density relative to Standard max. dry density :	95.0%
Actual dry density from test:	90.5%
Water content during conditioning :	5.14%
Targeted moisture content :	5.14%
Actual water content from test :	4.32%
Fluid for conditioning soil :	Sydney tap water
Eroding fluid :	Sydney tap water
Eroding fluid mean temperature :	14.4 °C
Data Log File Name :	DF 23a.
Time/Date of compaction of sample :	pm 24/10/03
Time/Date of Commencement of Test :	am 27/10/03

Mix Ingredient	Mix Proportion (%)
Silica 60G	9.45
Nepean Sand	9.45
5mm Blue Metal	9.45
10mm Bassalt	6.30
20mm Blue Metal	12.60
pukaki 25-38	24.74
pukaki 38-51	10.39
pukaki 51-76	17.63
Total	100.00

Time (From Commencement) (hr)	Time (From Commencement) (min)	Flowrate (L/min)	Observations
0.00	0.0	0.00	Test Started. Extremely cloudy near base and increasing, moderate outflow.
0.02	2.0	66.40	Extremely cloudy, moderate outflow and steady.
0.05	4.5	66.40	Very cloudy and clearing slightly, moderate outflow and steady.
0.07	6.5	62.10	Very cloudy and clearing slightly, moderate outflow and steady.
0.09	8.5	68.80	Cloudy and clearing slowly, moderate outflow and steady.
0.11	10.5	66.30	Slightly cloudy and clearing slowly, moderate outflow and steady.
0.13	12.5	64.20	Slightly cloudy and clearing slowly, moderate outflow and steady.
0.15	14.5	64.00	Mostly clear and continuing to clear slowly, moderate outflow and steady.
0.17	16.5	68.70	Mostly clear and continuing to clear slowly, moderate outflow and steady.
0.19	18.5	63.60	Mostly clear and continuing to clear slowly, moderate outflow and steady.
0.21	20.5	64.40	Mostly clear and continuing to clear slowly, moderate outflow and steady.
0.23	22.5	64.50	Mostly clear and continuing to clear slowly, moderate outflow and steady.
0.25	24.5	63.70	Mostly clear and continuing to clear slowly, moderate outflow and steady.
0.27	26.5	66.00	Clear, moderate outflow and steady.
0.29	28.5	63.20	Clear, moderate outflow and steady.
0.31	30.5	62.90	Clear, moderate outflow and steady.
0.33	32.5	65.00	Clear, moderate outflow and steady.
0.35	34.5	66.20	Clear, moderate outflow and steady.
0.37	36.5	61.60	Clear, moderate outflow and steady.
0.38	38.5	58.40	Clear, moderate outflow and steady. Test stopped.

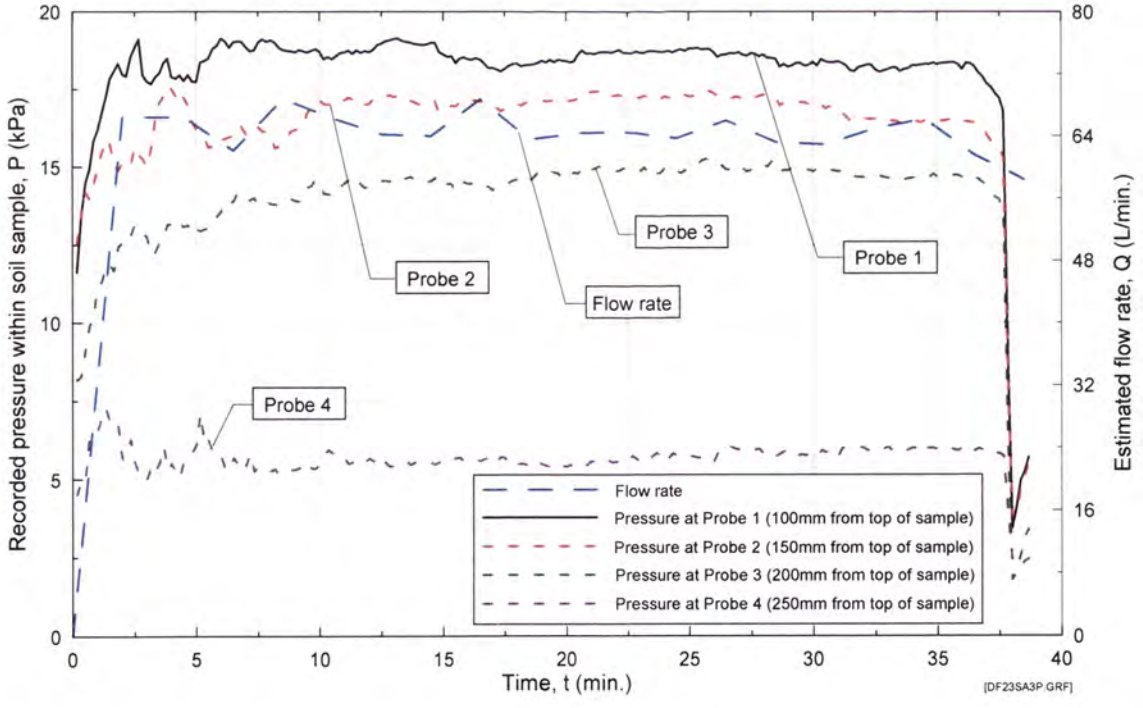

DF Test No. 23 on Sample A3 – Recorded pressure and flow rate. Sample compacted to 90.5% of Standard Max. Dry Density.

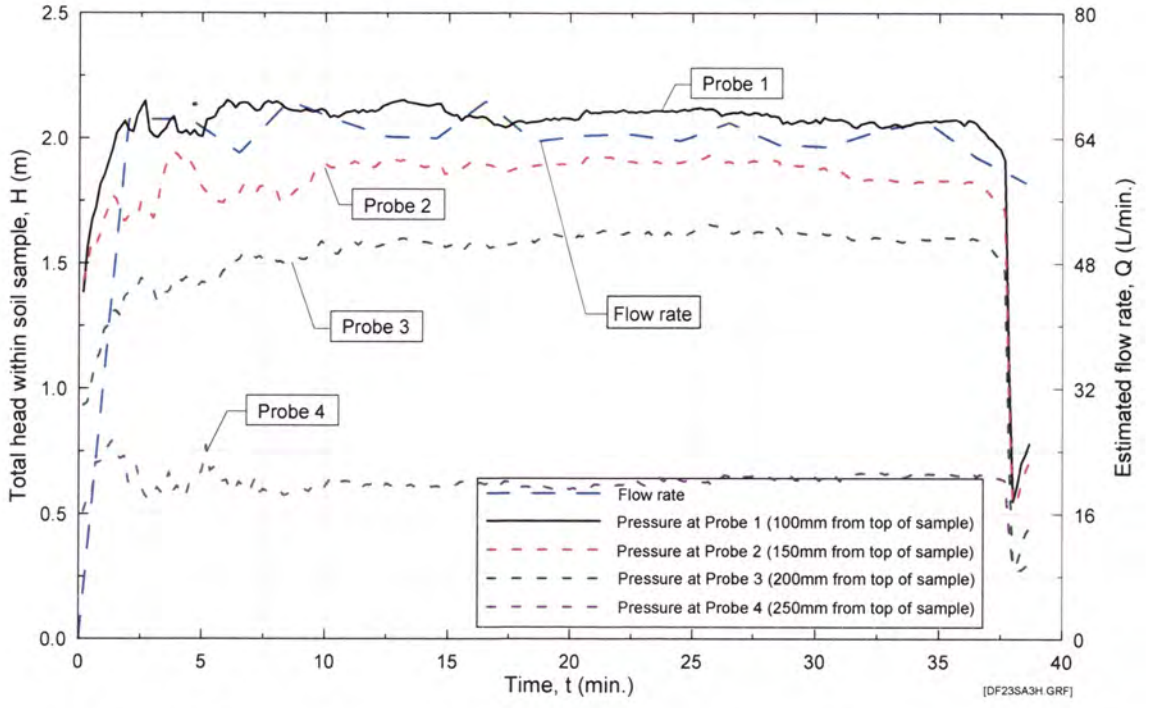

DF Test No. 23 on Sample A3 – Total head and flow rate. Sample compacted to 90.5% of Standard Max. Dry Density.

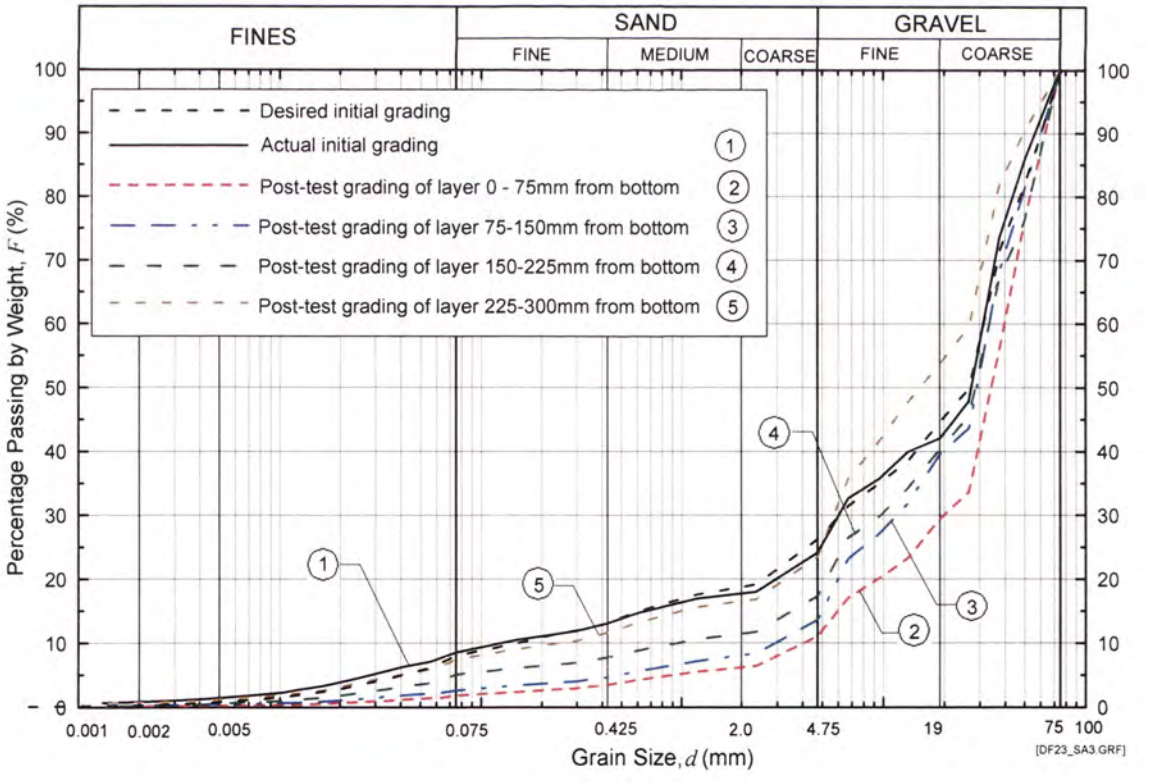

DF Test No. 23 on Sample A3 - Initial and post-test grain-size distribution analysis. Sample compacted to 90.5% of Standard Max. Dry Density.

Downward flow test No. 22 Test Records

DOWNWARD FLOW SUFFUSION TEST
Test Record

Test No/Date :	**Suffusion Downflow 022 21/10/03**
Soil Sample :	**Suffusion Test Blend B1**
Standard max. dry density :	2.348 Mg/m^3
Optimum water content (OWC) :	5.49%
Targeted dry density relative to Standard max. dry density :	95.0%
Actual dry density from test:	91.3%
Water content during conditioning :	5.53%
Targeted moisture content :	5.53%
Actual water content from test :	6.51%
Fluid for conditioning soil :	Sydney tap water
Eroding fluid :	Sydney tap water
Eroding fluid mean temperature :	14.4 °C
Data Log File Name :	DF 22a, DF 22b.
Time/Date of compaction of sample :	pm 20/10/03
Time/Date of Commencement of Test :	am 21/10/03

Mix Ingredient	Mix Proportion (%)
Silica 60G	13.07
Nepean Sand	11.53
5mm Blue Metal	11.53
10mm Bassalt	11.53
20mm Blue Metal	11.53
pukaki 25-38	12.73
pukaki 38-51	11.06
pukaki 51-76	17.05
Total	100.00

Time (From Commencement) (hr)	Time (From Commencement) (min)	Flowrate (L/min)	Observations
0.00	0.0	0.00	Test Started. Cloudy base, increasing rapidly. Low outflow, increasing rapidly.
0.03	3.0	66.20	Extremely cloudy. Moderate outflow, and steady.
0.05	5.0	70.10	Very cloudy, and clearing slowly. Moderate outflow, and fluctuating slightly.
0.07	7.0	65.00	Very cloudy, and clearing slowly. Moderate outflow, and fluctuating slightly.
0.09	9.0	64.00	Cloudy, and clearing slowly. Moderate outflow, and fluctuating slightly.
0.11	11.0	55.50	Cloudy, and clearing slowly. Moderate outflow, and fluctuating slightly.
0.13	13.0	67.00	Slightly cloudy, slowly clearing. Moderate outflow, fluctuating slightly.
0.15	15.0	66.40	Slightly cloudy, slowly clearing. Moderate outflow, fluctuating slightly.
0.17	17.0	65.00	Slightly cloudy, slowly clearing. Moderate outflow, fluctuating slightly.
0.19	19.0	63.10	Slightly cloudy, slowly clearing. Moderate outflow, fluctuating slightly. Test paused/restarted.
0.22	22.0	65.20	Slightly cloudy, slowly clearing. Moderate outflow, fluctuating slightly.
0.29	29.0	70.30	Mostly clear, slowly clearing. Moderate outflow, fluctuating slightly.
0.31	31.0	69.60	Mostly clear, slowly clearing. Moderate outflow, fluctuating slightly.
0.33	33.0	69.90	Mostly clear, slowly clearing. Moderate outflow, fluctuating slightly.
0.35	35.0	70.70	Clear. Moderate outflow, fluctuating slightly.
0.37	37.0	67.80	Clear. Moderate outflow, fluctuating slightly.
0.39	39.0	66.20	Clear. Moderate outflow, fluctuating slightly.
0.41	41.0	66.30	Clear. Moderate outflow, fluctuating slightly.
0.43	43.0	69.00	Clear. Moderate outflow, fluctuating slightly.
0.45	45.0	68.80	Clear. Moderate outflow, fluctuating slightly.
0.47	47.0	67.50	Clear. Moderate outflow, fluctuating slightly. Test stopped.

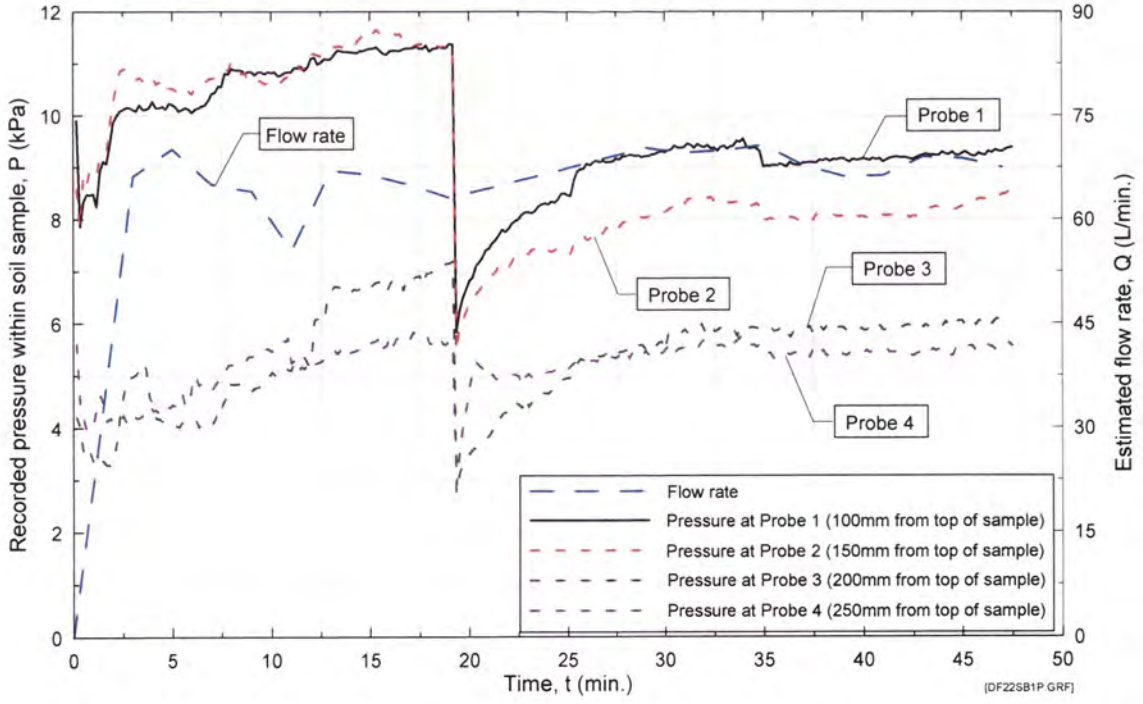

DF Test No. 22 on Sample B1 – Recorded pressure and flow rate. Sample compacted to 91.3% of Standard Max. Dry Density.

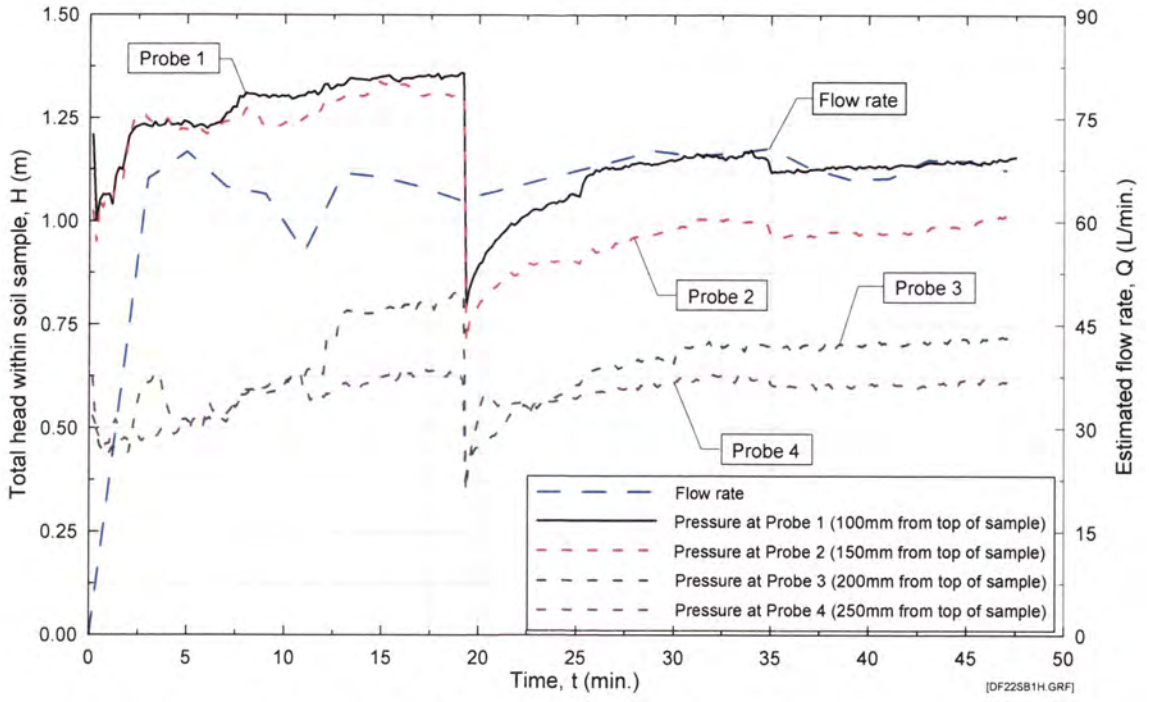

DF Test No. 22 on Sample B1 – Total head and flow rate. Sample compacted to 91.3% of Standard Max. Dry Density.

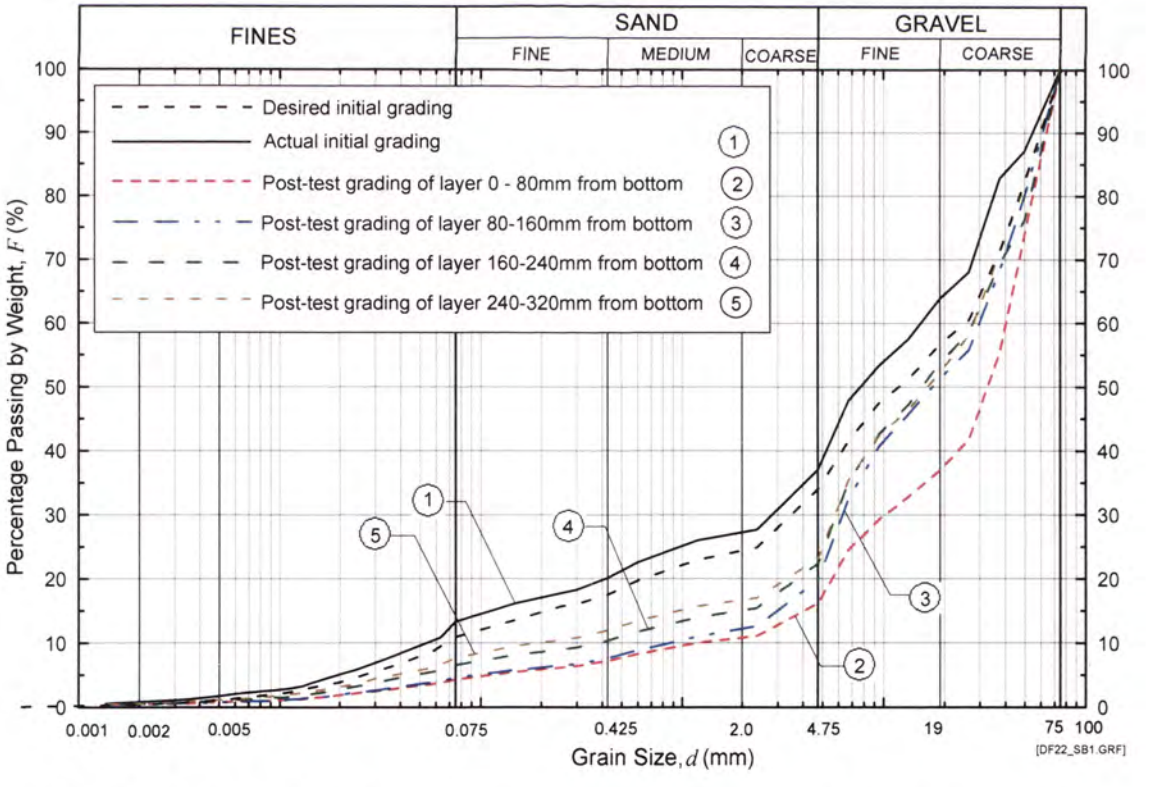

DF Test No. 22 on Sample B1 - Initial and post-test grain-size distribution analysis. Sample compacted to 91.3% of Standard Max. Dry Density.

Downward flow test No. 21 Test Records

DOWNWARD FLOW SUFFUSION TEST
Test Record

Test No/Date :	**Suffusion Downflow 021 3/10/03**
Soil Sample :	**Suffusion Test Blend B2 (rpt of test 19.)**
Standard max. dry density :	2.360 Mg/m^3
Optimum water content (OWC) :	5.73%
Targeted dry density relative to Standard max. dry density :	95.0%
Actual dry density from test:	92.6%
Water content during conditioning :	5.73%
Targeted moisture content :	5.73%
Actual water content from test :	5.73%
Fluid for conditioning soil :	Sydney tap water
Eroding fluid :	Sydney tap water
Eroding fluid mean temperature :	14.4 °C
Data Log File Name :	DF 21a, DF 21b, DF 21c.
Time/Date of compaction of sample :	pm 2/10/03
Time/Date of Commencement of Test :	am 3/10/03

Notes: Flow rate estimated.

Mix Ingredient	Mix Proportion (%)
Silica 60G	13.42
Nepean Sand	12.59
5mm Blue Metal	6.99
10mm Bassalt	3.50
20mm Blue Metal	6.99
pukaki 25-38	14.55
pukaki 38-51	20.98
pukaki 51-76	20.98
Total	100.00

Time (From Commencement) (hr)	Time (From Commencement) (min)	Flowrate (L/min)	Observations
0.00	0.0	0.00	Test Started. Slightly cloudy near base and increasing, low outflow.
0.01	0.7	50.00	Extremely cloudy. Moderate outflow, and increasing slightly. *
0.02	1.4	50.00	Extremely cloudy. Moderate outflow, and decreasing slightly. *
0.02	2.0	51.36	Very cloudy, slowly clearing. Moderate outflow, fluctuating slightly.
0.04	4.0	39.48	Very cloudy, slowly clearing. Moderate outflow, fluctuating slightly.
0.05	5.5	34.20	Very cloudy, slowly clearing. Moderate outflow, fluctuating slightly.
0.07	7.0	33.72	Very cloudy, slowly clearing. Moderate outflow, fluctuating slightly.
0.08	8.5	32.10	Slightly cloudy, slowly clearing. Moderate outflow, decreasing slightly.
0.10	10.0	33.00	Slightly cloudy, slowly clearing. Moderate outflow, decreasing slightly.
0.12	11.5	33.00	Slightly cloudy, slowly clearing. Moderate outflow, decreasing slightly.
0.13	13.0	31.92	Slightly cloudy, slowly clearing. Moderate outflow, decreasing slightly.
0.15	14.5	32.94	Slightly cloudy, slowly clearing. Moderate outflow, fluctuating slightly.
0.18	18.5	32.16	Slightly cloudy, slowly clearing. Moderate outflow, fluctuating slightly.
0.20	20.5	31.68	Slightly cloudy, slowly clearing. Moderate outflow, fluctuating slightly.
0.22	22.5	33.00	Slightly cloudy, slowly clearing. Moderate outflow, fluctuating slightly.
0.25	25.3	31.50	Mostly clear, slowly clearing. Moderate outflow, steady.
0.29	29.5	30.66	Mostly clear, slowly clearing. Moderate outflow, steady.
0.35	35.5	31.14	Mostly clear, slowly clearing. Moderate outflow, steady.
0.40	40.5	30.96	Clear. Moderate outflow, fluctuating slightly.
0.46	45.5	30.84	Clear. Moderate outflow, fluctuating slightly.
0.53	53.5	29.64	Clear. Moderate outflow, fluctuating slightly.
1.01	60.5	28.80	Clear. Moderate outflow, fluctuating slightly.
1.12	72.5	28.68	Clear. Moderate outflow, fluctuating slightly.
1.42	102.0	28.38	Clear. Moderate outflow, fluctuating slightly.
2.02	122.0	28.14	Clear. Moderate outflow, fluctuating slightly.
2.14	134.5	27.76	Clear. Moderate outflow, fluctuating slightly.
2.55	175.0	27.08	Clear. Moderate outflow, fluctuating slightly.
3.21	201.5	29.56	Clear. Moderate outflow, fluctuating slightly.
3.46	226.0	27.76	Clear. Moderate outflow, fluctuating slightly.
4.14	254.0	26.80	Clear. Moderate outflow, fluctuating slightly.
4.43	283.0	26.52	Clear. Moderate outflow, fluctuating slightly.
5.00	300.0	26.96	Clear. Moderate outflow, fluctuating slightly. Test stopped.

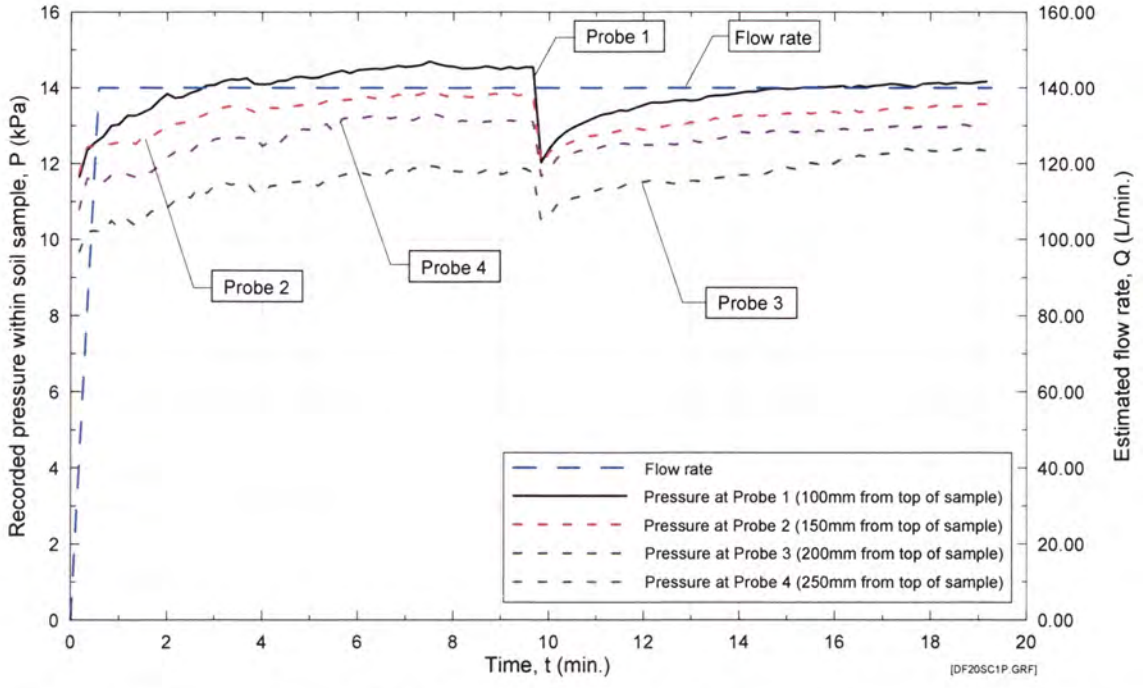

DF Test No. 21 on Sample B2 – Recorded pressure and flow rate. Sample compacted to 92.6% of Standard Max. Dry Density.

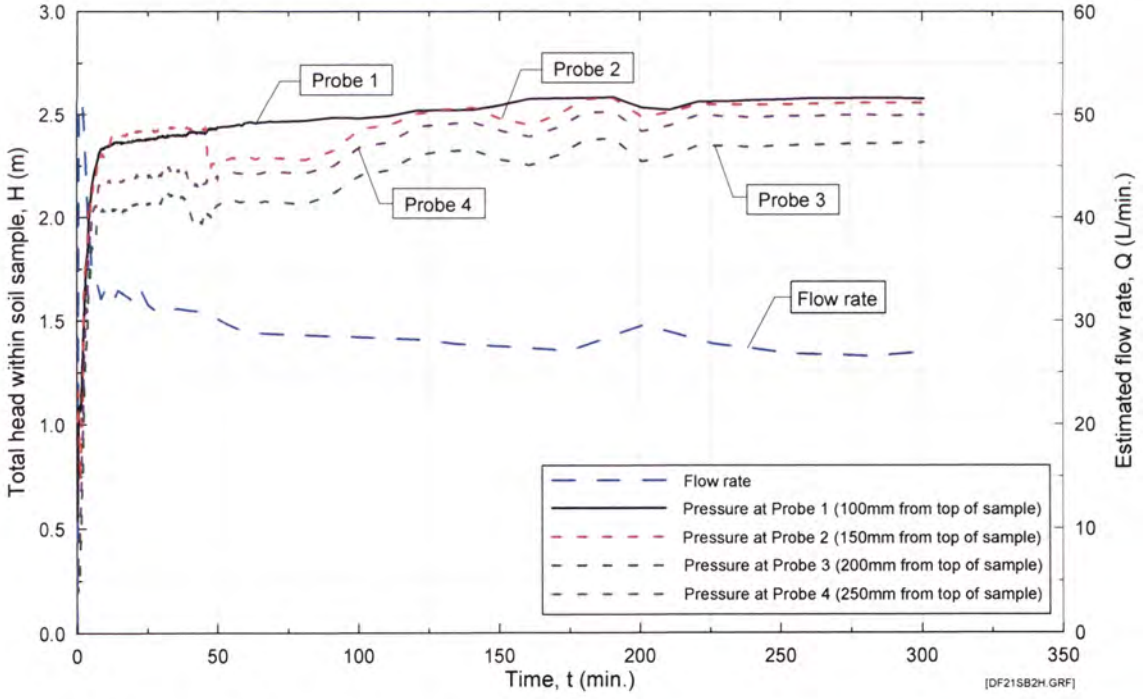

DF Test No. 21 on Sample B2 – Total head and flow rate. Sample compacted to 92.6% of Standard Max. Dry Density.

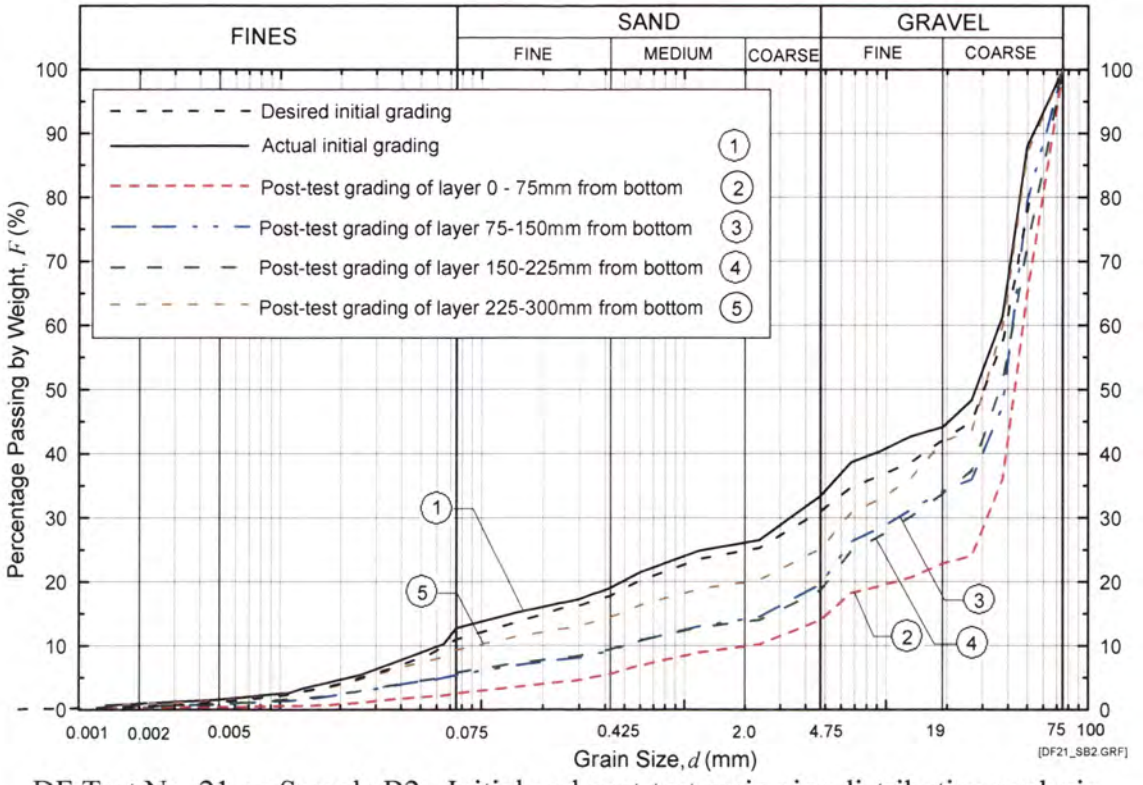

DF Test No. 21 on Sample B2 - Initial and post-test grain-size distribution analysis. Sample compacted to 92.6% of Standard Max. Dry Density.

Downward flow test No. 20 Test Records

DOWNWARD FLOW SUFFUSION TEST
Test Record

Test No/Date :	**Suffusion Downflow 020 31/09/03**	
Soil Sample :	**Suffusion Test Blend C1**	
Standard max. dry density :	2.341	Mg/m^3
Optimum water content (OWC) :	4.29%	
Targeted dry density relative to Standard max. dry density :	95.0%	
Actual dry density from test:	93.9%	
Water content during conditioning :	4.29%	
Targeted moisture content :	4.29%	
Actual water content from test :	2.47%	
Fluid for conditioning soil :	Sydney tap water	
Eroding fluid :	Sydney tap water	
Eroding fluid mean temperature :	14.4	°C
Data Log File Name :	DF 18a, DF 18b.	
Time/Date of compaction of sample :	pm 30/09/03	
Time/Date of Commencement of Test :	am 31/09/03	

Mix Ingredient	Mix Proportion (%)
Silica 60G	6.91
Nepean Sand	9.60
5mm Blue Metal	3.84
10mm Bassalt	3.84
20mm Blue Metal	31.82
pukaki 25-38	12.8
pukaki 38-51	15.18
pukaki 51-76	16.01
Total	100.00

* Note: Flow rate readings are approximations only due to rapid flow rate.

Time (From Commencement) (hr)	Time (From Commencement) (min)	Flowrate * (L/min)	Observations
0.00	0.0	0.00	Test Started. Very cloudy near base and increasing, rapidly increasing outflow.
0.01	0.6	140.00	Very cloudy. High outflow, and steadily increasing.
0.02	1.5	140.00	Very cloudy. Very high outflow, and steady.
0.02	2.0	140.00	Cloudy, starting to clear slightly. Very high outflow, and steady.
0.04	4.5	140.00	Slightly cloudy, continuing to clear slowly. Very high outflow, and steady.
0.06	6.0	140.00	Mostly clear, and continuing to clear slowly. Very high outflow, and steady.
0.09	9.0	140.00	Clear. Very high outflow, and steady.
0.10	9.8	140.00	Clear. Very high outflow, and steady. Test paused, then restarted.
0.10	10.0	140.00	Slightly cloudy, continuing to clear slowly. Very high outflow, and steady.
0.11	11.3	140.00	Mostly clear, and continuing to clear slowly. Very high outflow, and steady.
0.12	12.3	140.00	Clear. Very high outflow, and steady.
0.19	19.3	140.00	Clear. Very high outflow, and steady. Test stopped.

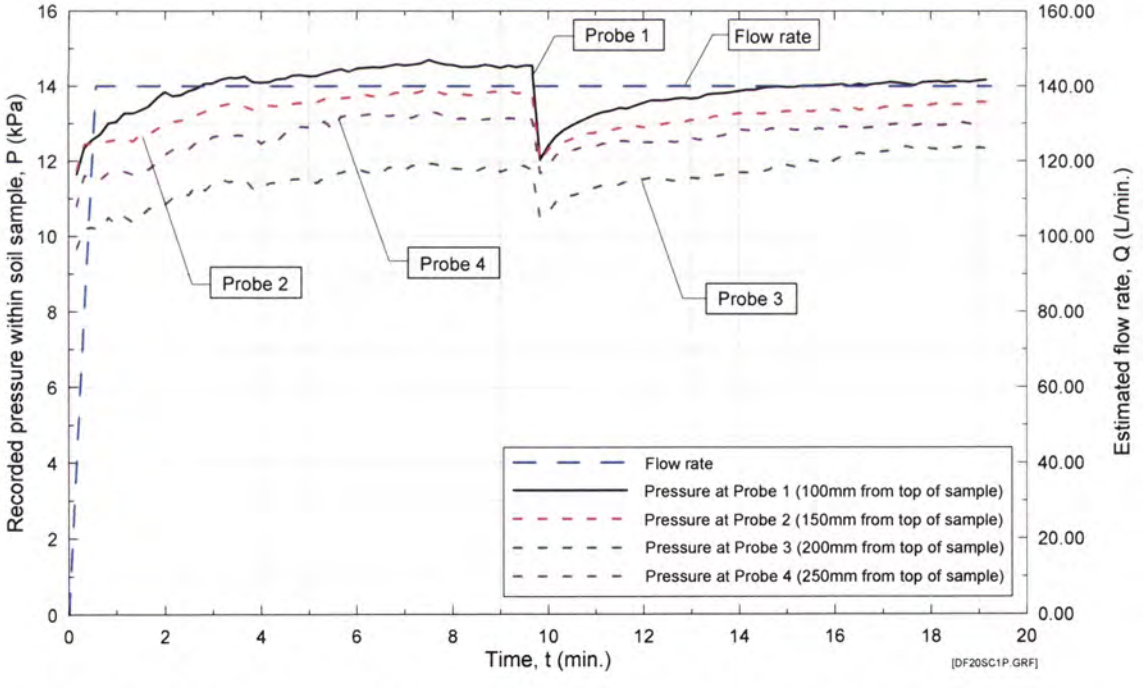

DF Test No. 20 on Sample C1 – Recorded pressure and flow rate. Sample compacted to 93.9% of Standard Max. Dry Density.

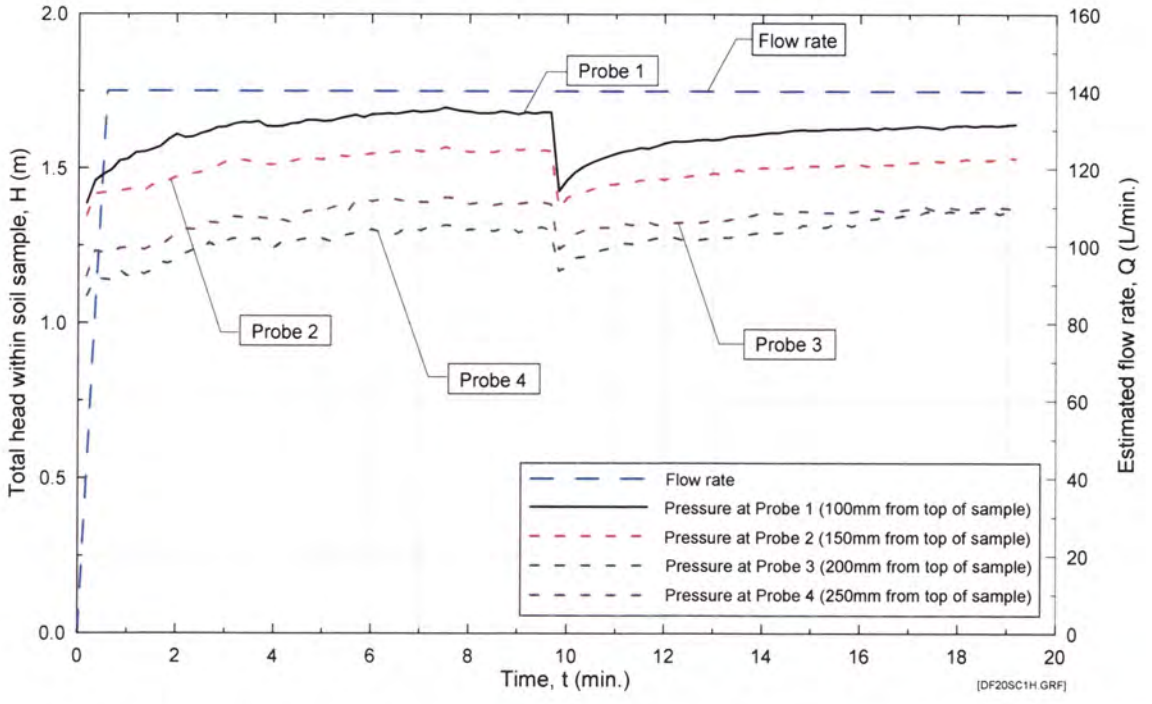

DF Test No. 20 on Sample C1 – Total head and flow rate. Sample compacted to 93.9% of Standard Max. Dry Density.

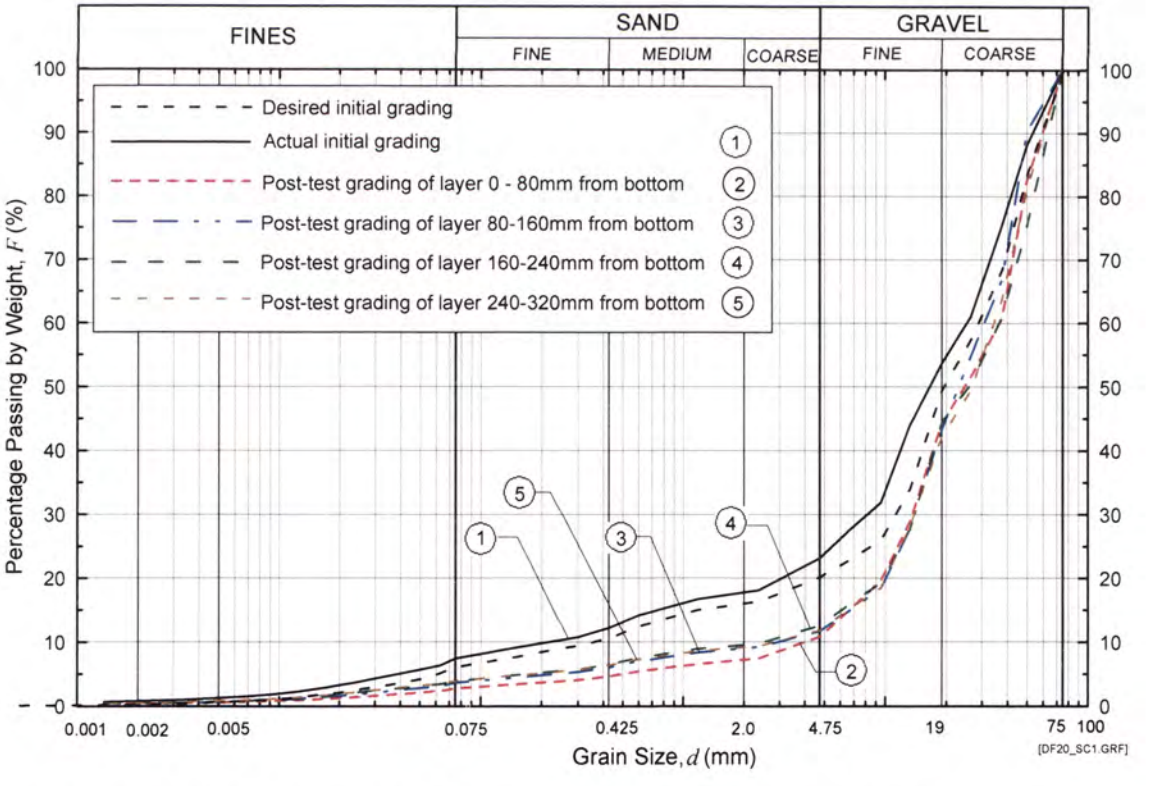

DF Test No. 20 on Sample C1 - Initial and post-test grain-size distribution analysis. Sample compacted to 93.9% of Standard Max. Dry Density.

Downward flow test No. 25 Test Records

DOWNWARD FLOW SUFFUSION TEST
Test Record

Test No/Date :	**Suffusion Downflow 025 25/11/03**
Soil Sample :	**Suffusion Test Blend D1**
Standard max. dry density :	2.363 Mg/m^3
Optimum water content (OWC) :	6.99%
Targeted dry density relative to Standard max. dry density :	95.0%
Actual dry density from test:	95.0%
Water content during conditioning :	6.99%
Targeted moisture content :	6.99%
Actual water content from test :	5.03%
Fluid for conditioning soil :	Sydney tap water
Eroding fluid :	Sydney tap water
Eroding fluid mean temperature :	14.4 °C
Data Log File Name :	DF 25a, DF 25b, DF 25c.
Time/Date of compaction of sample :	pm 21/11/03
Time/Date of Commencement of Test :	am 25/11/03

Mix Ingredient	Mix Proportion (%)
Silica 60G	11.36
Nepean Sand	11.36
5mm Blue Metal	11.36
10mm Bassalt	11.36
20mm Blue Metal	11.36
pukaki 25-38	14.773
pukaki 38-51	11.36
pukaki 51-76	17.045
Total	100.00

Time (From Commencement) (hr)	Time (From Commencement) (min)	Flowrate (L/min)	Observations
0.00	0.0	0.00	Test Started. Very cloudy near base and increasing, rapid outflow increase, becoming moderate.
0.04	2.5	26.22	Extremely cloudy. Moderate outflow, and steady.
0.06	3.3	26.34	Extremely cloudy. Moderate outflow, and steady.
0.06	3.8	24.72	Very cloudy, slowly clearing. Moderate outflow, slowly decreasing.
0.16	9.8	24.20	Very cloudy, slowly clearing. Moderate outflow, slowly decreasing.
0.19	11.2	21.20	Cloudy, slowly clearing. Moderate outflow, slowly decreasing.
0.42	25.0	19.44	Slightly cloudy, slowly clearing. Moderate outflow, fluctuating slightly.
0.57	34.0	19.50	Slightly cloudy, slowly clearing. Moderate outflow, fluctuating slightly.
0.73	44.0	18.99	Mostly clear, clearing slightly. Moderate outflow, fluctuating slightly.
1.07	64.0	18.81	Clear. Moderate outflow, fluctuating slightly.
1.43	86.0	18.51	Clear. Moderate outflow, fluctuating slightly.
1.68	101.0	18.33	Clear. Moderate outflow, fluctuating slightly.
2.20	132.0	17.79	Clear. Moderate outflow, fluctuating slightly.
2.73	164.0	18.06	Clear. Moderate outflow, fluctuating slightly.
3.25	195.0	17.91	Clear. Moderate outflow, fluctuating slightly. Test stopped.

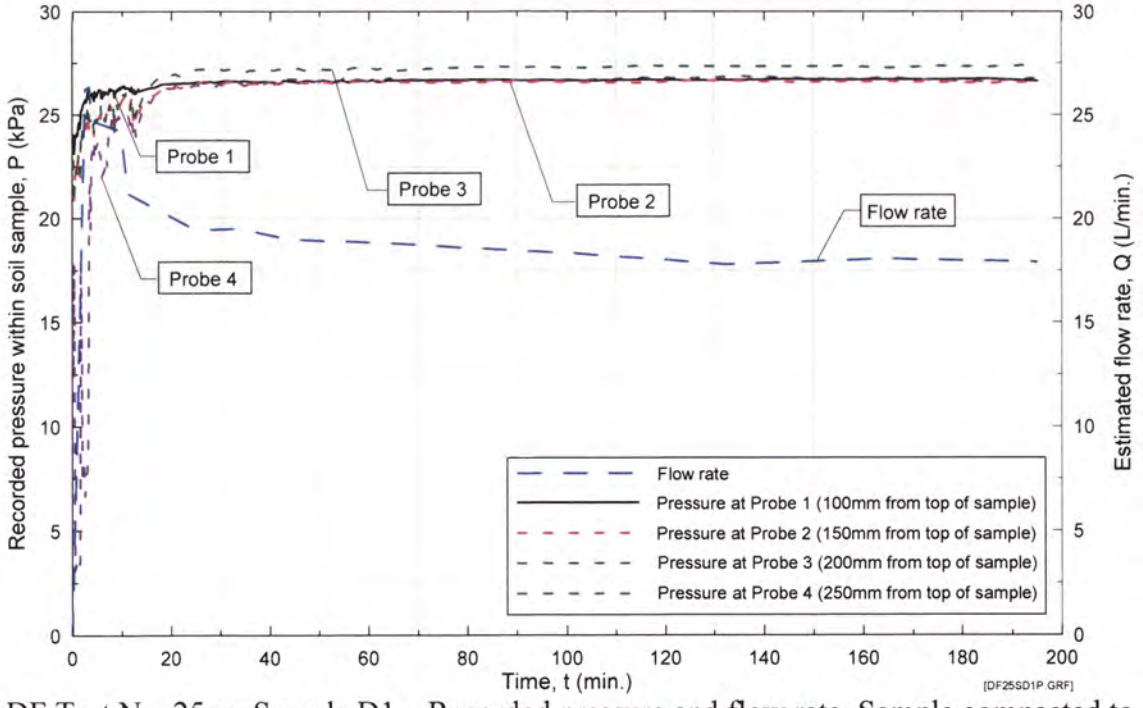

DF Test No. 25 on Sample D1 – Recorded pressure and flow rate. Sample compacted to 95.0% of Standard Max. Dry Density.

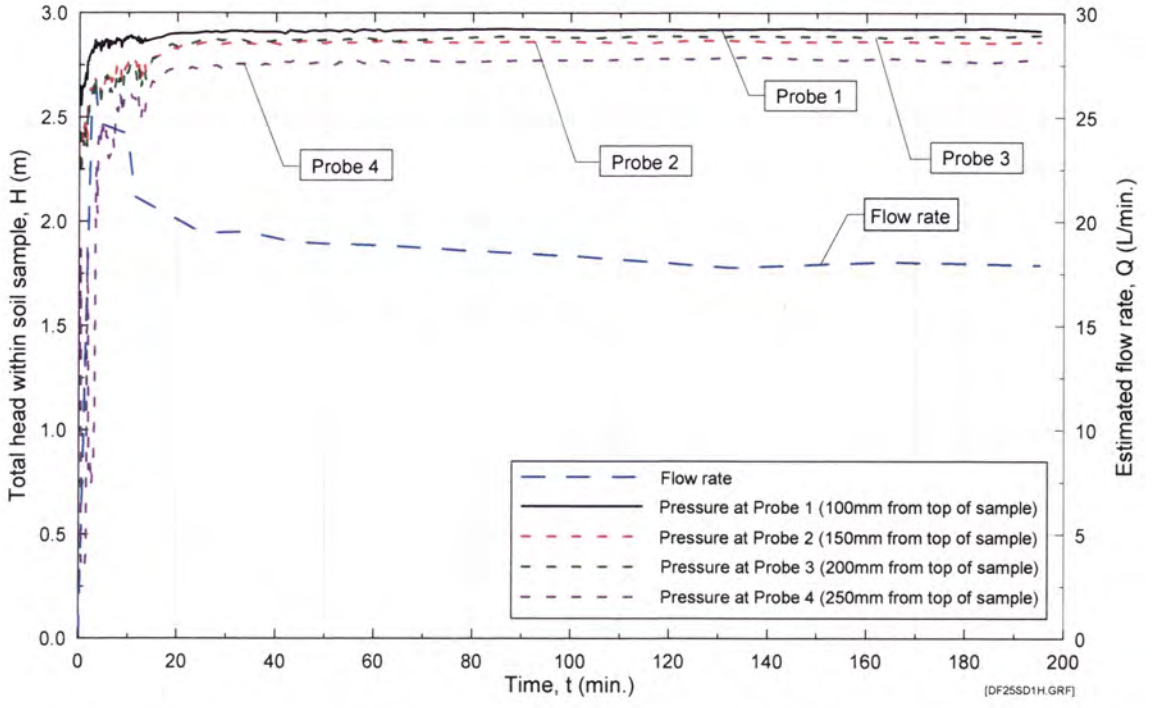

DF Test No. 25 on Sample D1 – Total head and flow rate. Sample compacted to 95.0% of Standard Max. Dry Density.

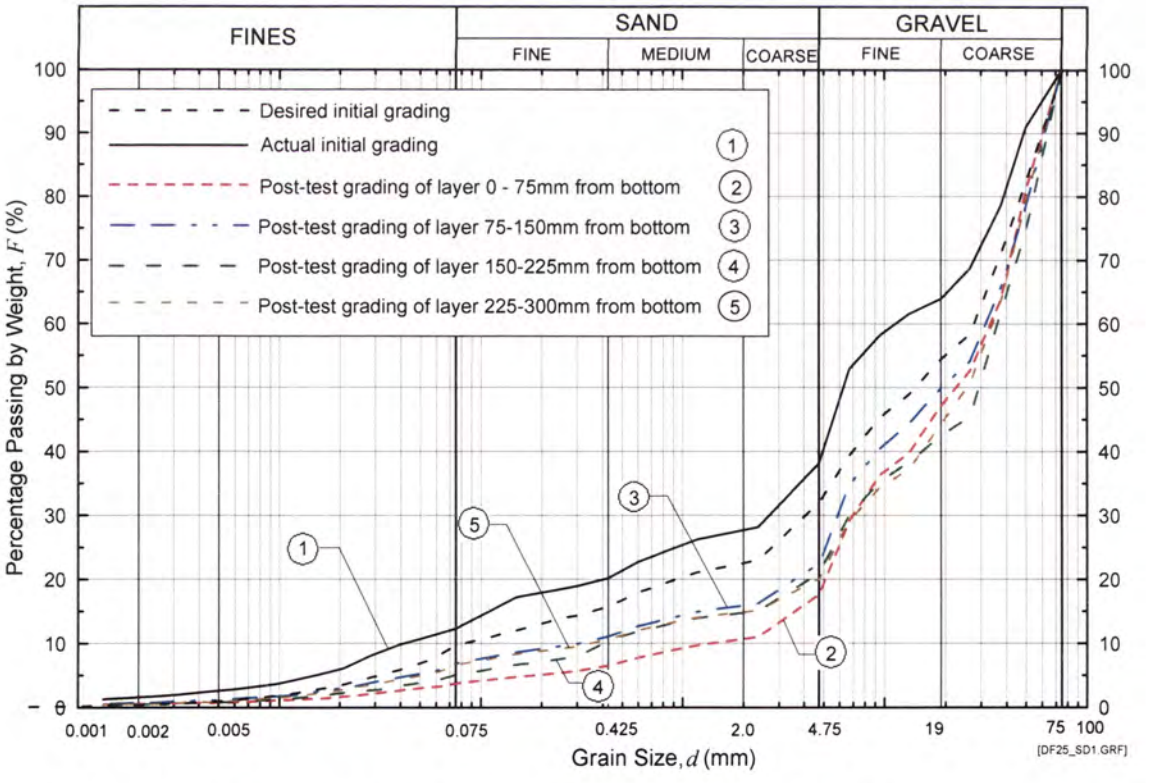

DF Test No. 25 on Sample D1 - Initial and post-test grain-size distribution analysis. Sample compacted to 95.0% of Standard Max. Dry Density.

APPENDIX O

Downward flow seepage tests – Estimating the fraction of materials loss by suffusion using curve matching technique

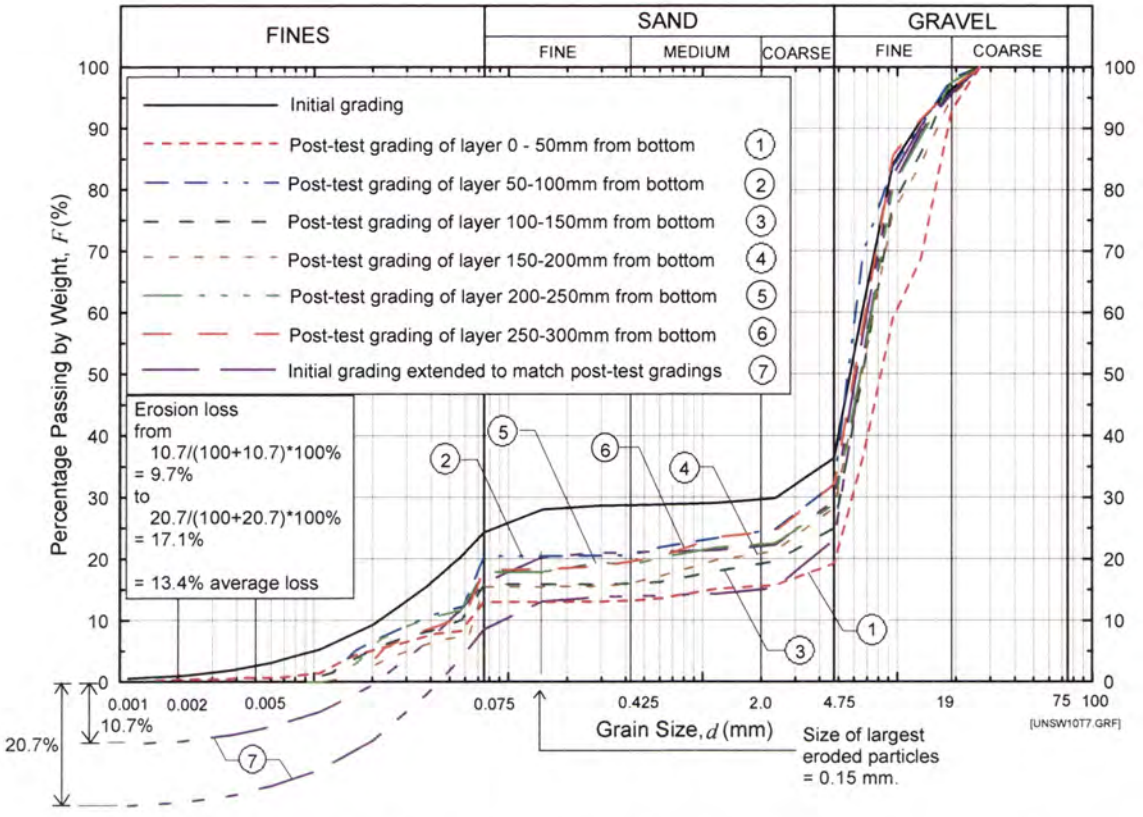

Figure O1 Downward flow seepage test DF7 on Sample 10 – Curve matching.

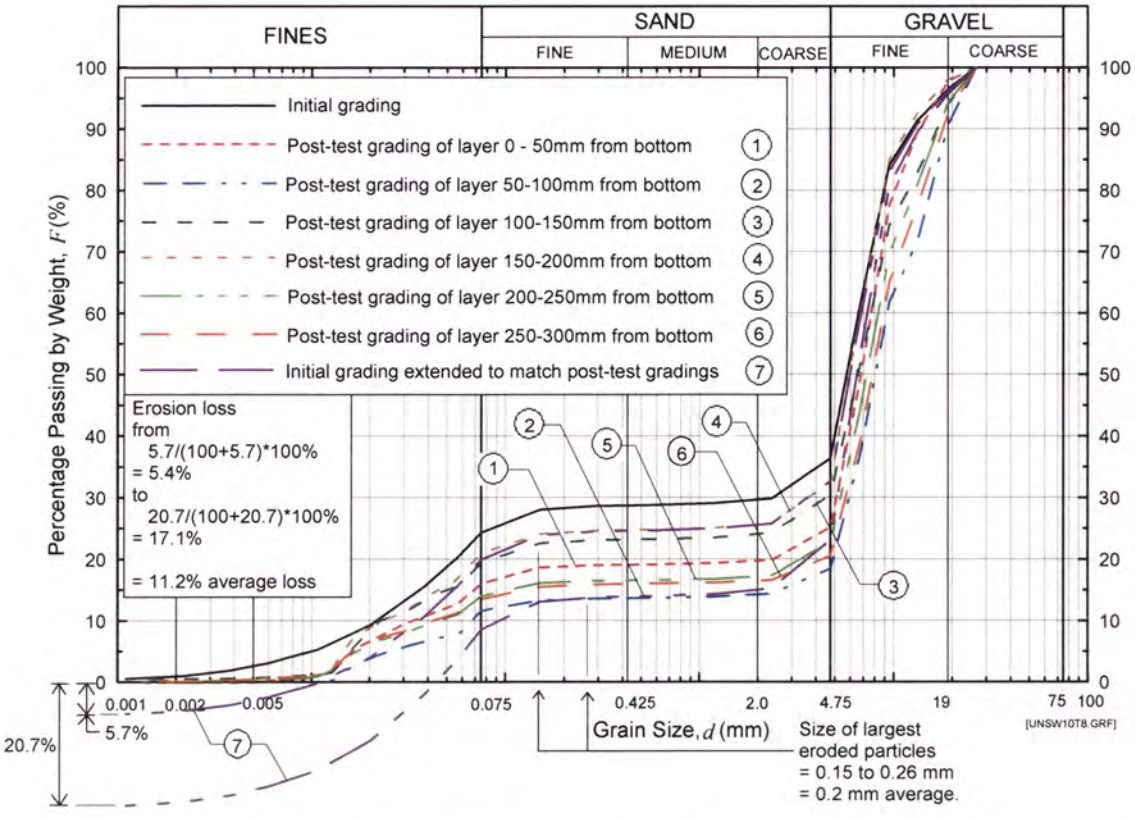

Figure O2 Downward flow seepage test DF8 on Sample 10 – Curve matching.

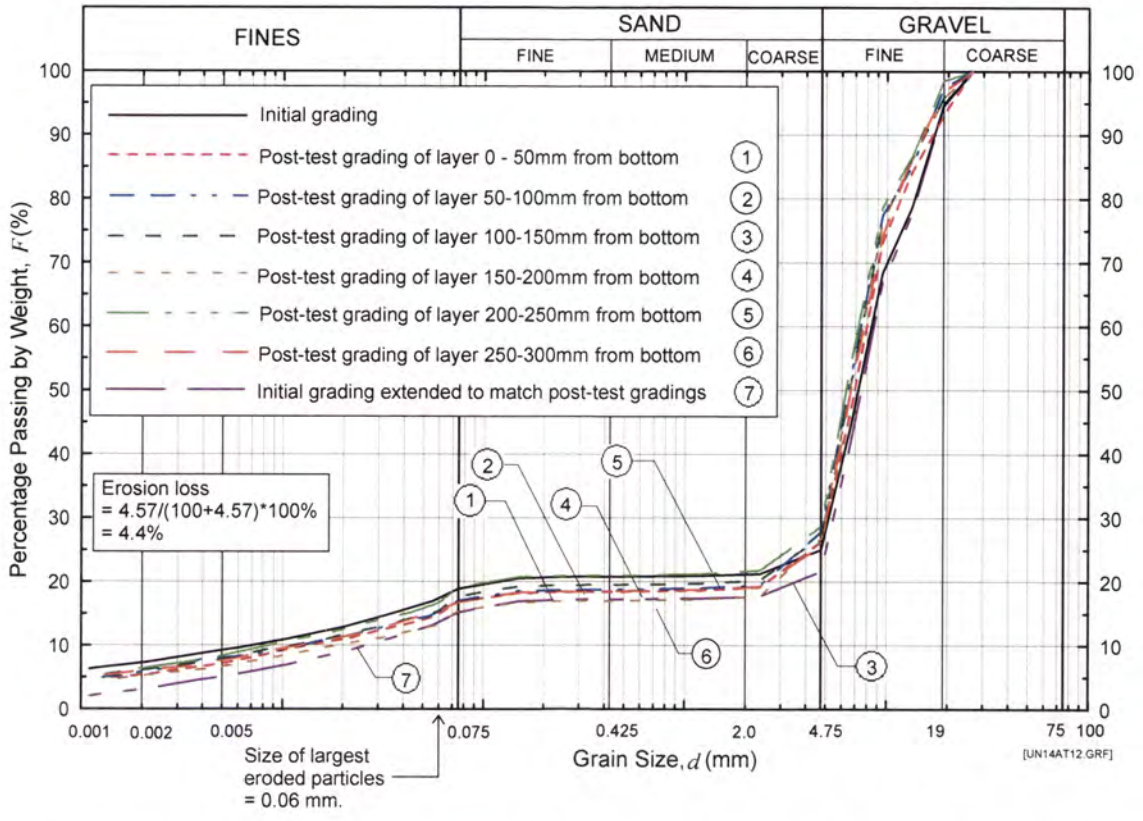

Figure O3 Downward flow seepage test DF12 on Sample 14A – Curve matching.

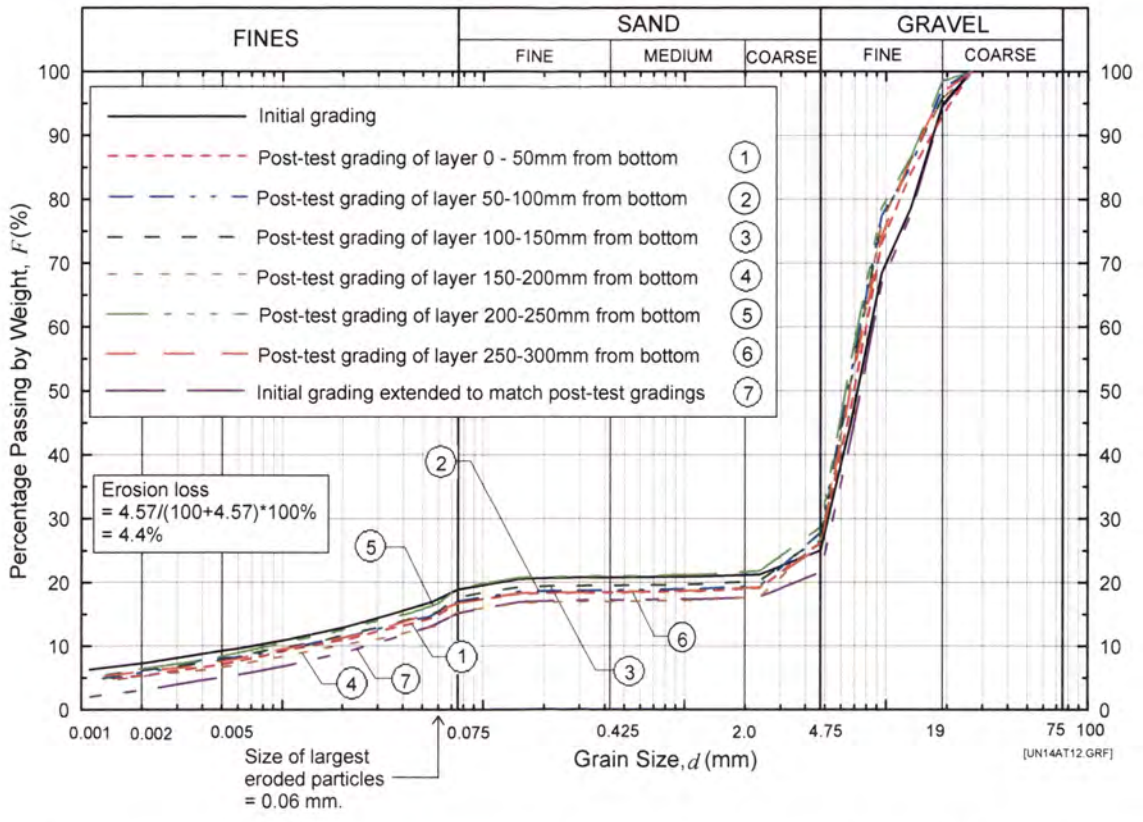

Figure O4 Downward flow seepage test DF15 on Sample 14A – Curve matching.

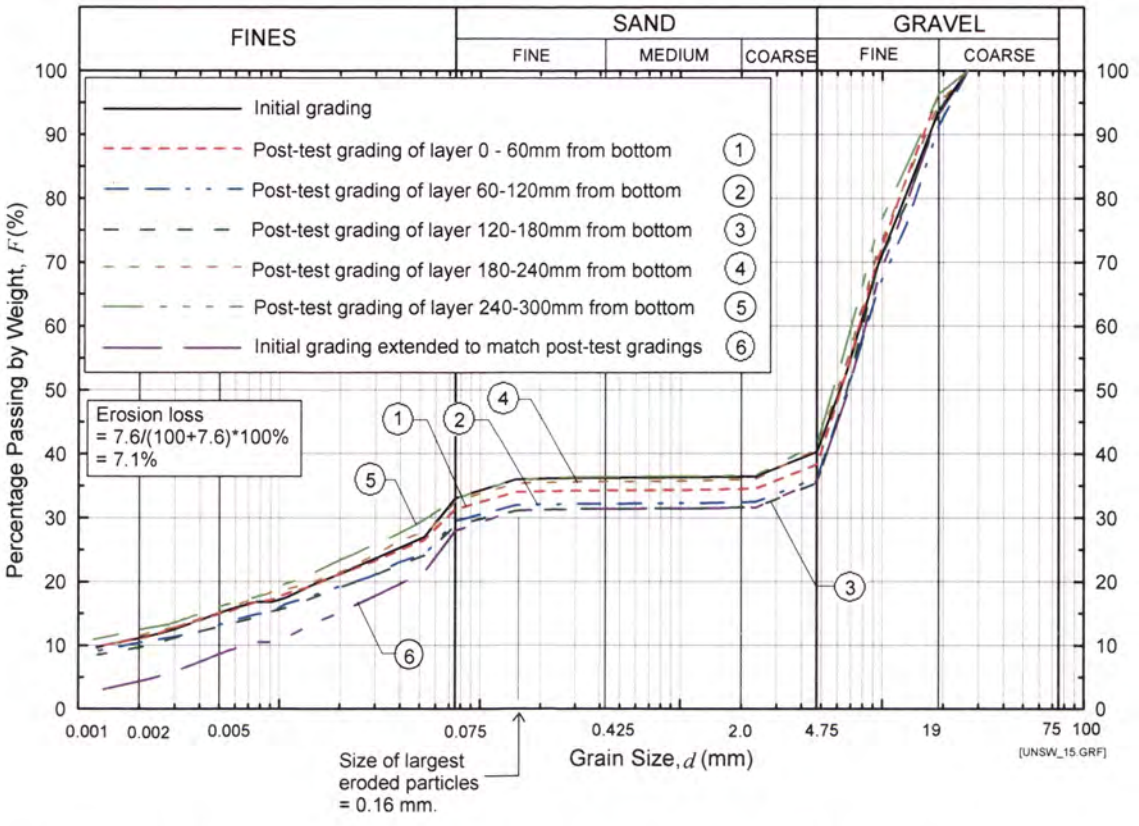

Figure O5 Downward flow seepage test DF17 on Sample 15 – Curve matching.

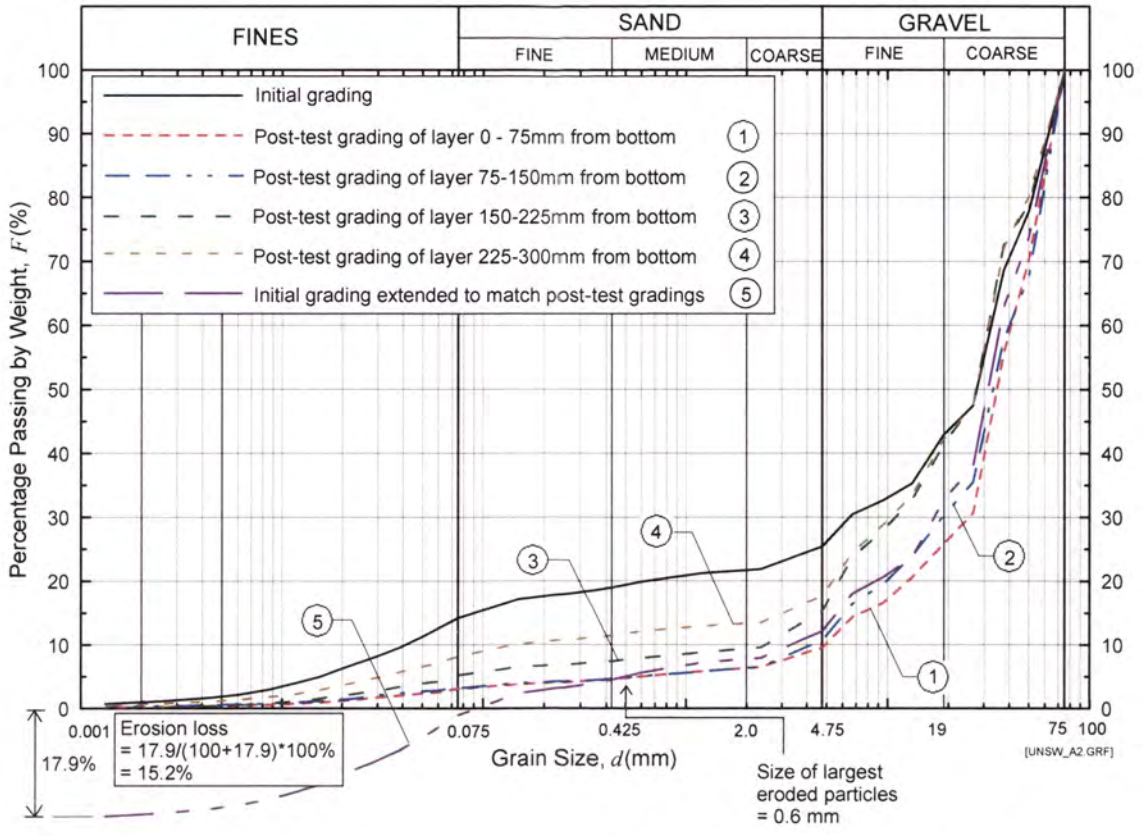

Figure O6 Downward flow seepage test DF24 on Sample A2 – Curve matching.

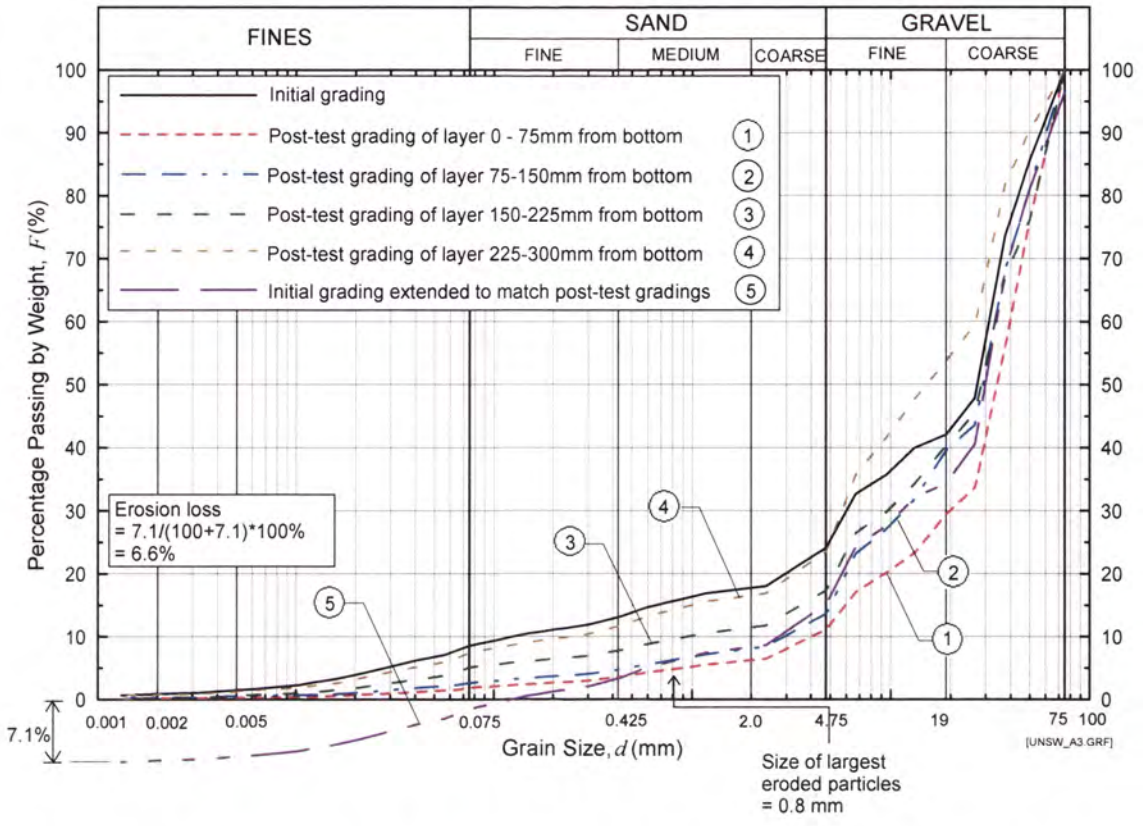

Figure O7 Downward flow seepage test DF23 on Sample A3 – Curve matching.

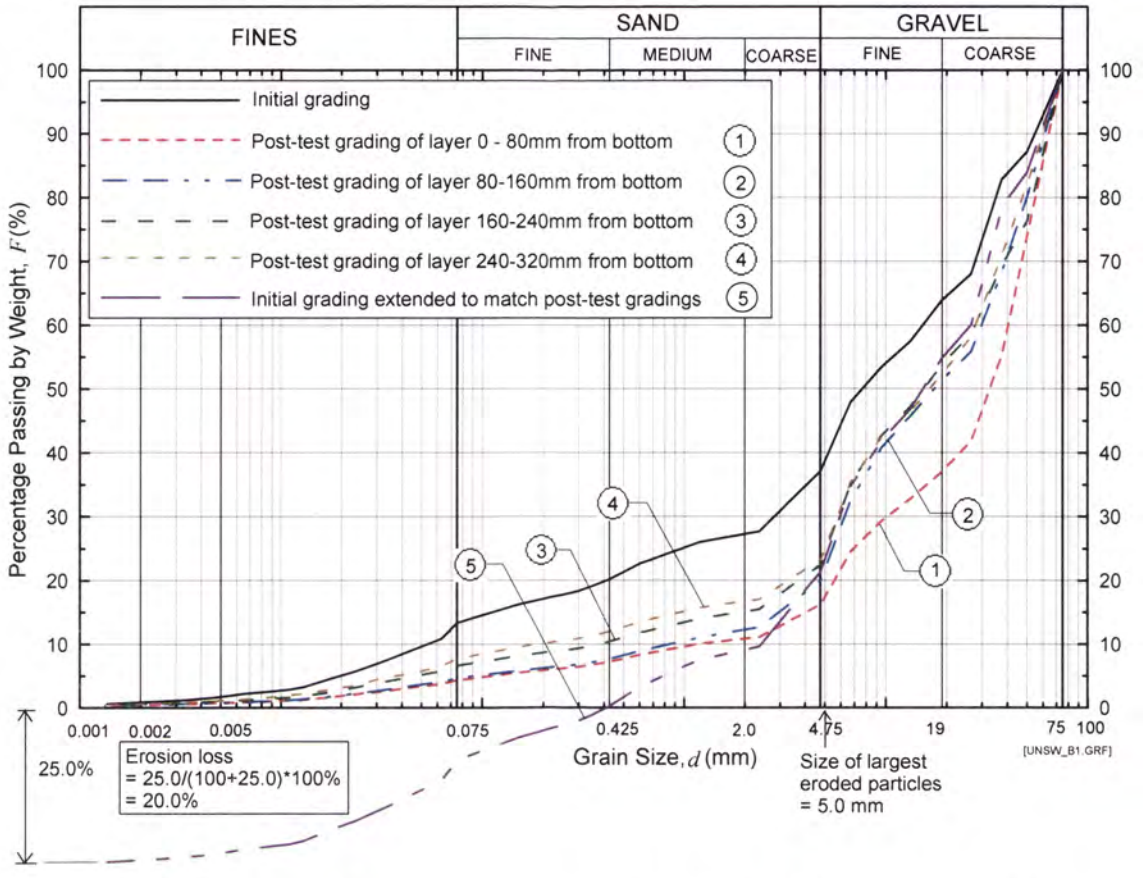

Figure O8 Downward flow seepage test DF22 on Sample B1 – Curve matching.

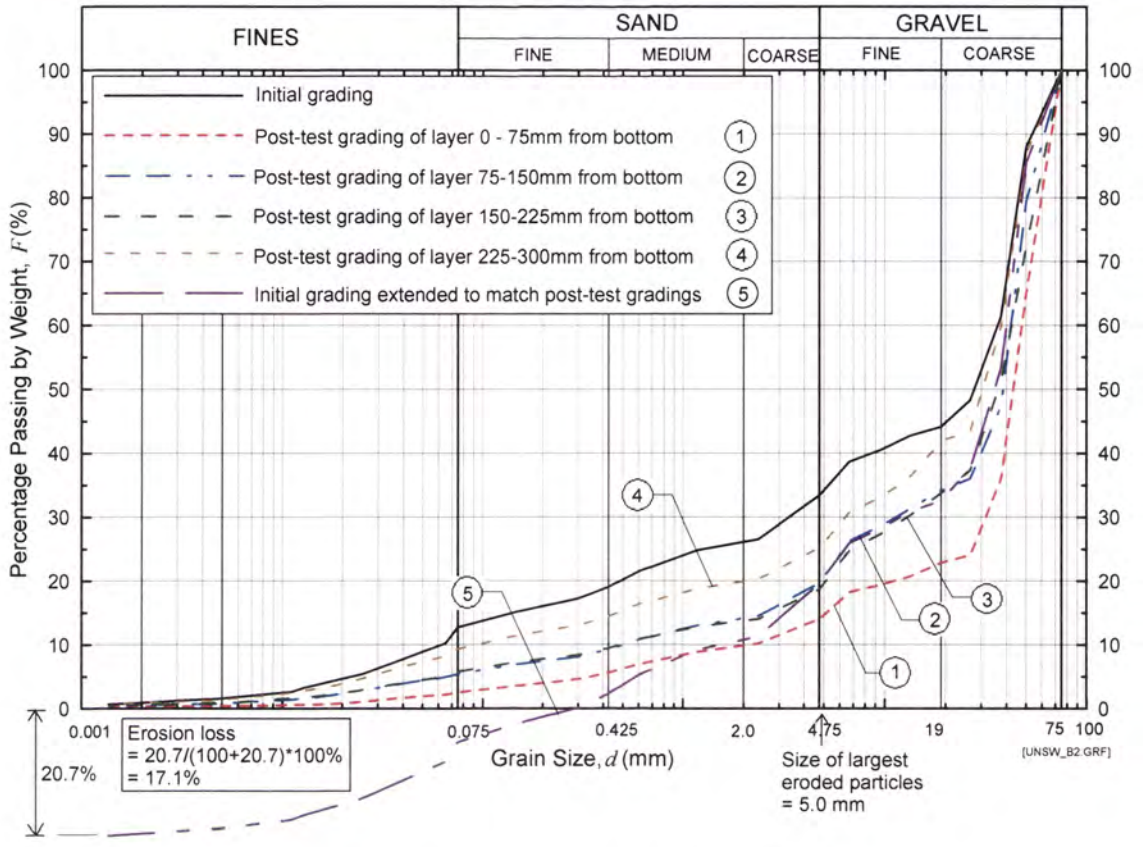

Figure O9 Downward flow seepage test DF21 on Sample B2 – Curve matching.

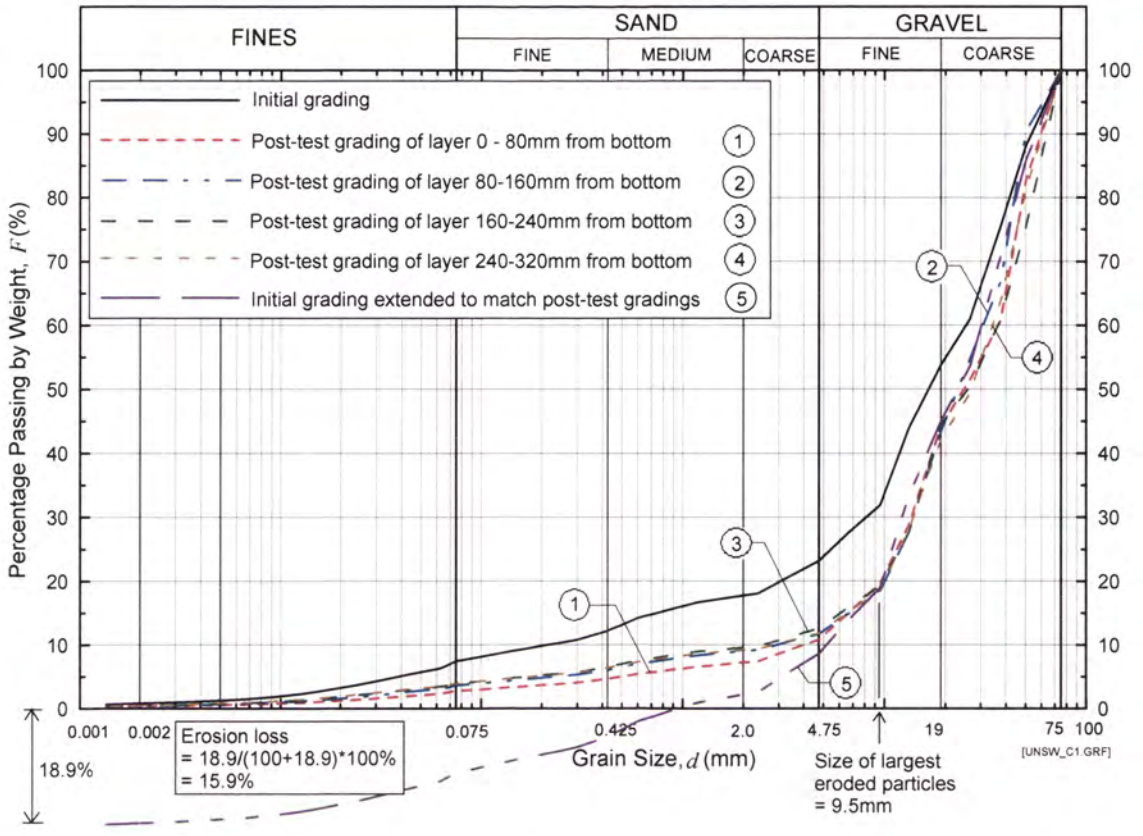

Figure O10 Downward flow seepage test DF20 on Sample C1 – Curve matching.

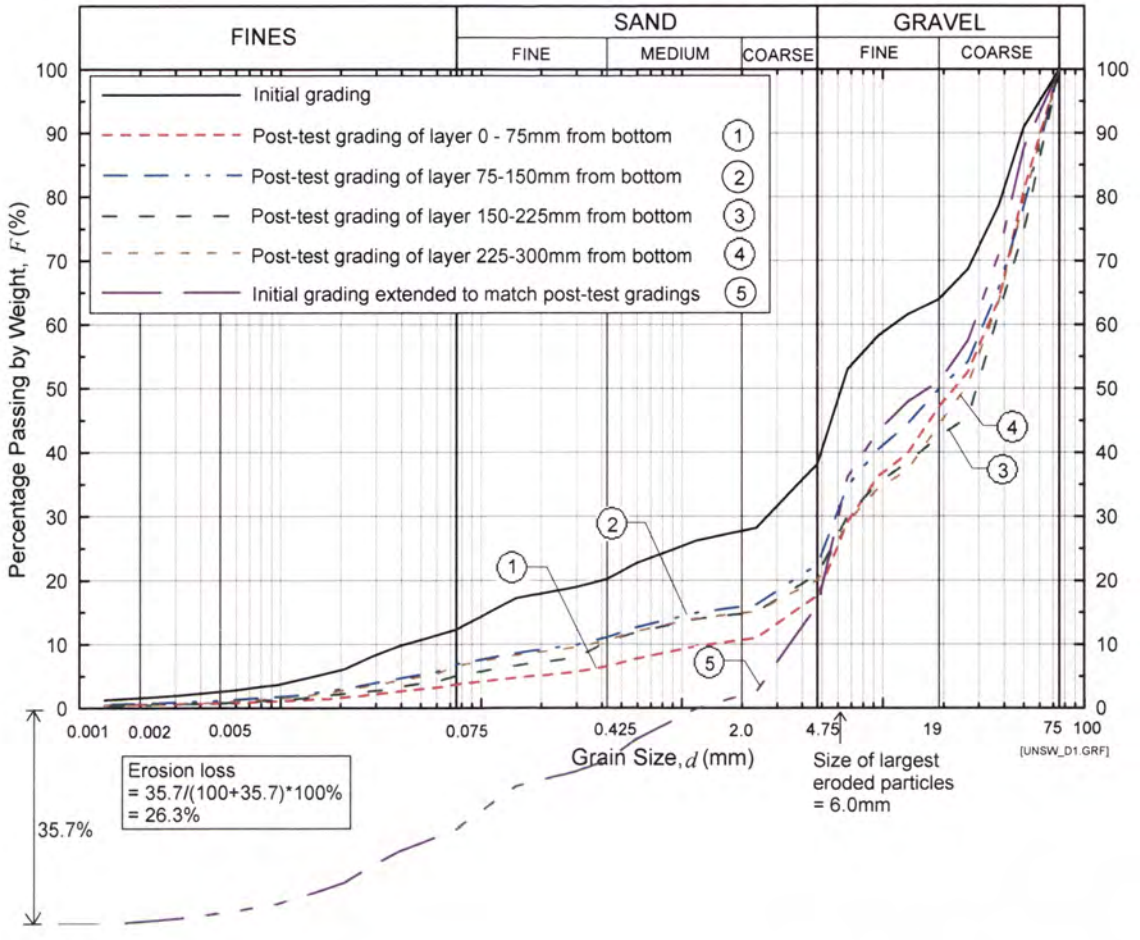

Figure O11 Downward flow seepage test DF25 on Sample D1 – Curve matching.

APPENDIX P

Records of upward flow seepage tests

Upward flow test No. UF1 Test Records

UPWARD FLOW SUFFUSION TEST
Test Data

Test No. :	**Suffusion Upflow 001 08/10/01**	
Soil Sample :	**Suffusion Test Blend No. 1**	
Max. dry density :	2.319	Mg/m3
Optimum moisture content (OWC) :	7.70%	
Relative compaction :	95.0%	
Actual compaction from test:	94.1%	
Moisture content during conditioning :	7.70%	
Targeted moisture content :	7.70%	
Moisture content from test :	7.70%	
Fluid for conditioning soil :	tap water	
Eroding fluid :	tap water	
Eroding fluid mean temperature :	21.6	°C
Time/Date of Commencement of Soaking :	10.00am 8/10/01	
Time/Date of Commencement of Test :	11.10am 11/10/01	

Mix Ingredient	Mix Proportion (%)
Clay Q38	0.00
Silica 60G	10.52
Nepean Sand	25.70
5mm Blue Metal	16.18
10mm Bassalt	23.80
20mm Blue Metal	23.80
Total	100.00

Time (From Commencement) (mins)	Time (s)	Flowrate (L/min)	Head (mm) Inlet	200mm From top surface of sample	150mm From top surface of sample	100mm From top surface of sample	50mm From top surface of sample	Water Surface within cell. (See note)	Observations
15.00	900	0.000	50.0	0.0	0.0	0.0	3.0	5.5	Test started. Clear. No outflow.
30.00	1800	0.000	50.0	0.0	0.0	0.0	0.0	5.5	Clear. No outflow.
45.00	2700	0.000	50.0	0.0	0.0	0.0	0.0	5.5	Clear. No outflow.
60.00	3600	0.000	100.0	0.0	0.0	0.0	0.0	5.5	Clear. No outflow.
75.00	4500	0.000	100.0	0.0	0.0	0.0	0.0	5.5	Clear. No outflow.
90.00	5400	0.000	100.0	0.0	0.0	0.0	0.0	5.5	Clear. No outflow.
105.00	6300	0.000	150.0	0.0	0.0	0.0	0.0	5.5	Clear. No outflow.
120.00	7200	0.000	150.0	0.0	0.0	0.0	0.0	5.5	Clear. No outflow.
135.00	8100	0.000	150.0	0.0	0.0	0.0	0.0	5.5	Clear. No outflow.
150.00	9000	0.000	200.0	0.0	0.0	0.0	0.0	6.0	Clear. No outflow.
165.00	9900	0.000	200.0	0.0	0.0	0.0	0.0	6.0	Clear. No outflow.
180.00	10800	0.000	200.0	0.0	0.0	0.0	0.0	6.0	Clear. No outflow.
195.00	11700	0.000	250.0	0.0	0.0	0.0	0.0	6.0	Clear. No outflow.
210.00	12600	0.000	250.0	0.0	0.0	0.0	0.0	6.0	Clear. No outflow.
225.00	13500	0.000	250.0	0.0	0.0	0.0	0.0	6.0	Clear. No outflow.
240.00	14400	0.000	300.0	0.0	0.0	0.0	0.0	6.0	Clear. No outflow.
255.00	15300	0.000	300.0	0.0	0.0	0.0	0.0	6.0	Clear. No outflow.
270.00	16200	0.000	300.0	0.0	0.0	0.0	0.0	6.0	Clear. No outflow.

Upward flow test No. UF1 Test Records (Cont'd)

Time (From Commencement) (mins)	Time (s)	Flowrate (L/min)	Head (mm)						Observations
			Inlet	200mm From top surface of sample	150mm From top surface of sample	100mm From top surface of sample	50mm From top surface of sample	Water Surface within cell. (See note)	
285.00	17100	0.000	350.0	0.0	0.0	0.0	0.0	6.0	Clear. No outflow. Test paused, then restarted.
300.00	18000	0.000	350.0	0.0	0.0	0.0	0.0	6.0	Clear. No outflow.
315.00	18900	0.001	350.0	1.0	0.0	0.0	0.0	5.5	Clear. Very low outflow.
330.00	19800	0.001	400.0	18.0	0.0	0.0	0.0	6.0	Clear. Very low outflow.
345.00	20700	0.001	400.0	82.0	0.0	0.0	0.0	6.0	Clear. Very low outflow.
360.00	21600	0.001	400.0	100.0	5.0	0.0	0.0	6.0	Clear. Very low outflow.
375.00	22500	0.008	450.0	163.0	51.0	0.0	0.0	6.0	Clear. Very low outflow.
390.00	23400	0.010	450.0	200.0	97.0	0.0	0.0	6.0	Clear. Very low outflow.
405.00	24300	0.010	450.0	235.0	120.0	0.0	0.0	5.5	Clear. Very low outflow.
420.00	25200	0.010	500.0	271.0	148.0	0.0	0.0	5.5	Clear. Very low outflow.
435.00	26100	0.008	500.0	302.0	172.0	0.0	0.0	5.5	Clear. Very low outflow.
450.00	27000	0.008	500.0	325.0	187.0	0.0	0.0	6.0	Clear. Very low outflow.
465.00	27900	0.012	550.0	357.0	207.0	0.0	0.0	5.5	Slightly cloudy appearance. Very low outflow.
480.00	28800	0.013	550.0	388.0	222.0	0.0	0.0	5.5	Slightly cloudy appearance. Very low outflow.
495.00	29700	0.012	550.0	414.0	235.0	0.0	0.0	5.5	Slightly cloudy appearance. Very low outflow.
510.00	30600	0.018	600.0	440.0	250.0	0.0	0.0	5.5	Slightly cloudy appearance. Very low outflow.
525.00	31500	0.018	600.0	440.0	250.0	0.0	0.0	5.5	Slightly cloudy appearance. Very low outflow.
540.00	32400	0.014	600.0	481.0	274.0	0.0	0.0	5.5	Slightly cloudy appearance. Very low outflow. Test paused, then restarted.
555.00	33300	2.730	642.0	397.0	548.0	0.0	9.0	14.0	Extremely Cloudy. Steady outflow.
560.00	33600	7.586	630.0	398.0	545.0	510.0	10.0	14.0	Extremely Cloudy. Steady outflow.
562.00	33720	8.040	616.0	398.0	538.0	305.0	11.0	21.0	Extremely Cloudy. Steady outflow.
564.00	33840	7.680	612.0	397.0	534.0	258.0	14.0	21.0	Extremely Cloudy. Steady outflow.
566.00	33960	7.680	613.0	397.0	534.0	245.0	16.0	20.0	Extremely Cloudy. Steady outflow.
568.00	34080	8.100	610.0	397.0	534.0	234.0	21.0	21.0	Appearance slightly less cloudy. Steady outflow.
570.00	34200	9.240	601.0	396.0	533.0	295.0	75.0	22.0	Appearance slightly less cloudy. Steady outflow.
575.00	34500	9.720	599.0	396.0	532.0	172.0	88.0	22.0	Appearance slightly less cloudy. Steady outflow.
580.00	34800	9.240	599.0	396.0	532.0	147.0	84.0	22.0	Appearance slightly less cloudy. Steady outflow.
585.00	35100	9.840	601.0	395.0	531.0	143.0	81.0	22.0	Appearance slightly less cloudy. Steady outflow.
595.00	35700	9.480	600.0	394.0	531.0	139.0	77.0	22.0	Cloudiness increasing. Outflow increasing slightly.
600.00	36000	10.440	593.0	394.0	531.0	137.0	67.0	22.0	Cloudiness increasing. Outflow increasing slightly.
605.00	36300	9.900	597.0	393.0	530.0	120.0	64.0	22.0	Cloudiness decreasing slightly. Outflow increasing slightly. Fines noticeably 'boiling'
610.00	36600	9.960	596.0	393.0	530.0	114.0	61.0	22.0	Cloudiness decreasing slightly. Outflow increasing slightly. Fines noticeably 'boiling'
615.00	36900	9.960	598.0	392.0	529.0	106.0	55.0	22.0	Cloudiness decreasing slightly. Outflow increasing slightly. Fines noticeably 'boiling'
620.00	37200	10.200	598.0	392.0	528.0	105.0	57.0	22.0	Cloudiness decreasing slightly. Outflow increasing slightly. Fines noticeably 'boiling'
625.00	37500	9.840	593.0	391.0	528.0	105.0	58.0	22.0	Cloudiness decreasing slightly. Outflow increasing slightly. Fines noticeably 'boiling'
630.00	37800	10.680	648.0	391.0	527.0	182.0	73.0	22.0	Cloudiness decreasing slightly. Outflow increasing slightly. Fines noticeably 'boiling'
635.00	38100	10.440	652.0	390.0	527.0	175.0	47.0	22.0	Cloudiness decreasing slightly. Outflow increasing slightly. Fines noticeably 'boiling'
640.00	38400	11.100	648.0	390.0	527.0	205.0	43.0	22.0	Slightly cloudy appearance. Outflow increasing more noticeably. 'Piping' visible. Test Stopped.

Note : Deduct 6mm to give true depth of water from water surface to top of test sample within seepage cell.

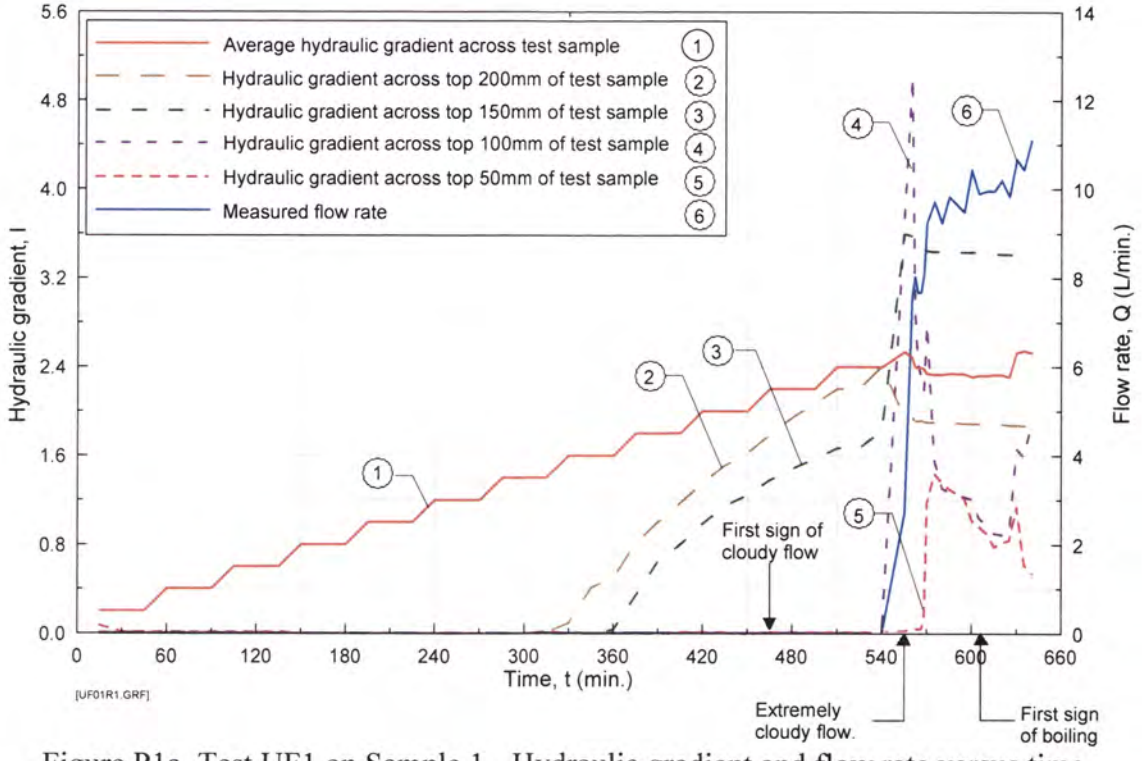

Figure P1a Test UF1 on Sample 1 - Hydraulic gradient and flow rate versus time. Sample compacted to 94% of Standard Maximum Dry Density.

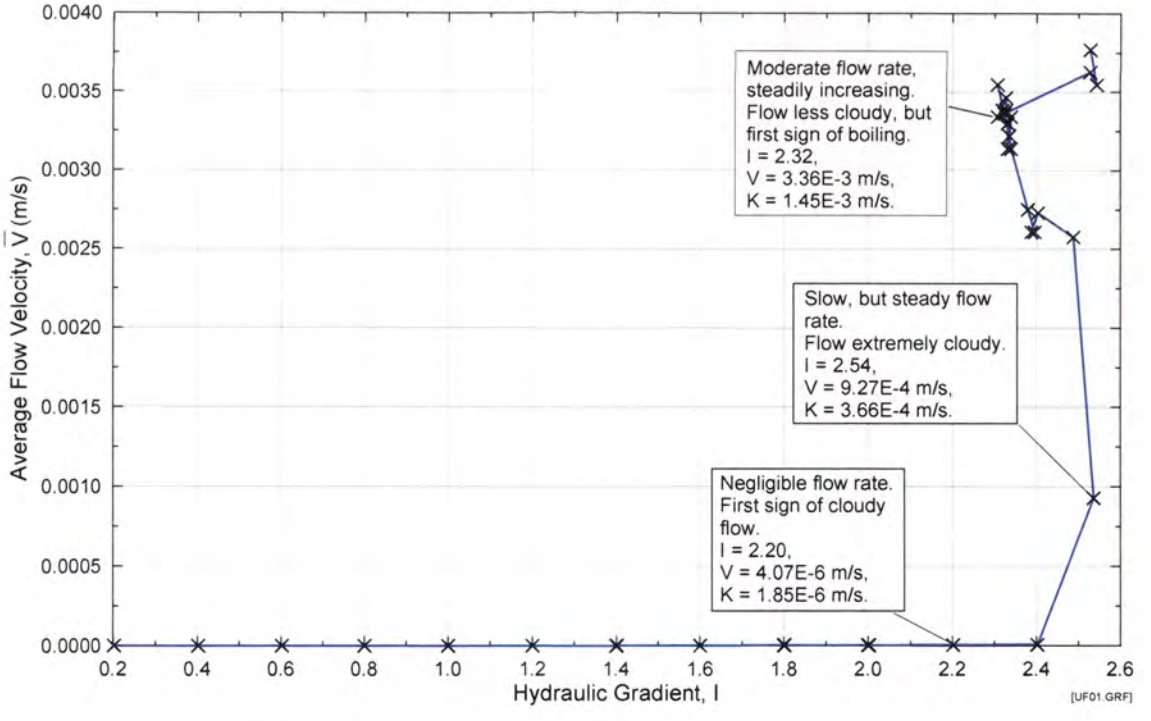

Figure P1b Test UF1 on Sample 1 – Average flow velocity versus average hydraulic gradient. Sample compacted to 94% of Standard Maximum Dry Density.

Upward flow test No. UF2 Test Records

UPWARD FLOW SUFFUSION TEST
Test Data

Test No. :	**Suffusion Upflow 002 16/10/01**
Soil Sample :	**Suffusion Test Blend No. 1**
Max. dry density :	2.319 Mg/m3
Optimum moisture content (OWC) :	7.70%
Relative compaction :	90.0%
Actual compaction from test:	89.4%
Moisture content during conditioning :	7.70%
Targeted moisture content :	7.70%
Moisture content from test :	7.70%
Fluid for conditioning soil :	tap water
Eroding fluid :	tap water
Eroding fluid mean temperature :	21.6 °C
Time/Date of Commencement of Soaking :	2.00pm 16/10/01
Time/Date of Commencement of Test :	10.30am 17/10/01

Mix Ingredient	Mix Proportion (%)
Clay Q38	0.00
Silica 60G	10.52
Nepean Sand	25.70
5mm Blue Metal	16.18
10mm Bassalt	23.80
20mm Blue Metal	23.80
Total	100.00

Time (From Commencement) (mins)	Time (s)	Flowrate (L/min)	Head (mm) Inlet	200mm From top surface of sample	150mm From top surface of sample	100mm From top surface of sample	50mm From top surface of sample	Water Surface within cell. (See note)	Observations
15.00	900	0.360	50.0	0.0	0.0	0.0	0.0	7.0	Clear. Very low outflow.
30.00	1800	0.360	50.0	0.0	0.0	0.0	0.0	7.0	Clear. Very low outflow.
45.00	2700	0.380	50.0	0.0	0.0	0.0	0.0	7.0	Clear. Very low outflow.
60.00	3600	0.720	100.0	0.0	0.0	0.0	0.0	7.0	Clear. Very low outflow.
75.00	4500	0.780	100.0	0.0	0.0	0.0	0.0	7.0	Clear. Very low outflow.
90.00	5400	0.750	100.0	0.0	0.0	0.0	0.0	7.0	Clear. Very low outflow.
105.00	6300	1.170	150.0	0.0	0.0	0.0	0.0	8.0	Clear. Very low outflow.
120.00	7200	1.220	150.0	0.0	0.0	0.0	0.0	8.0	Clear. Very low outflow.
135.00	8100	1.290	150.0	0.0	0.0	0.0	0.0	9.5	Clear. Very low outflow.
150.00	9000	1.830	200.0	0.0	0.0	0.0	0.0	10.0	Clear. Very low outflow. Test paused, then restarted.
165.00	9900	1.890	200.0	0.0	0.0	0.0	0.0	10.5	Slightly cloudy appearance. Very low outflow.
180.00	10800	1.830	200.0	0.0	0.0	0.0	0.0	10.5	Slightly cloudy appearance. Very low outflow.
195.00	11700	2.100	250.0	0.0	0.0	0.0	0.0	11.0	Slightly cloudy appearance. Very low outflow.
210.00	12600	2.430	250.0	0.0	0.0	0.0	0.0	11.5	Slightly cloudy appearance. Very low outflow.
225.00	13500	2.370	250.0	0.0	0.0	0.0	0.0	11.5	Slightly cloudy appearance. Very low outflow.
240.00	14400	5.280	300.0	0.0	0.0	0.0	0.0	12.5	Cloudy appearance. Low outflow. Test paused, then restarted.
255.00	15300	4.440	300.0	0.0	0.0	0.0	0.0	14.0	Very cloudy appearance. Low outflow.
270.00	16200	4.680	297.0	0.0	0.0	0.0	0.0	14.0	Very cloudy appearance. Low outflow.

Upward flow test No. UF2 Test Records (Cont'd)

Time (From Commencement) (mins)	Time (s)	Flowrate (L/min)	Head (mm)						Observations
			Inlet	200mm From top surface of sample	150mm From top surface of sample	100mm From top surface of sample	50mm From top surface of sample	Water Surface within cell. (See note)	
285.00	17100	4.980	350.0	0.0	0.0	0.0	0.0	14.5	Very cloudy appearance. Low outflow.
300.00	18000	5.280	348.0	0.0	0.0	0.0	0.0	15.5	Very cloudy appearance. Low outflow.
315.00	18900	5.550	347.0	0.0	0.0	0.0	0.0	16.0	Very cloudy appearance. Low outflow.
330.00	19800	5.880	400.0	0.0	0.0	0.0	0.0	16.5	Very cloudy appearance. Low outflow.
345.00	20700	6.240	399.0	195.0	0.0	0.0	0.0	17.0	Very cloudy appearance. Low outflow.
360.00	21600	6.600	399.0	235.0	0.0	0.0	0.0	17.0	Very cloudy appearance. Low outflow.
375.00	22500	6.840	445.0	270.0	0.0	0.0	23.0	18.0	Very cloudy appearance. Low outflow.
390.00	23400	7.440	445.0	301.0	142.0	0.0	28.0	18.5	Slightly cloudy appearance. Low outflow.
405.00	24300	6.840	446.0	332.0	182.0	18.0	17.0	18.5	Clear. Low outflow.
420.00	25200	8.040	500.0	373.0	233.0	101.0	18.0	19.0	Slightly cloudy appearance. Fines boiling. Moderate outflow.
435.00	26100	8.280	500.0	403.0	286.0	144.0	17.0	19.0	Slightly cloudy appearance. Fines boiling. Moderate outflow.
450.00	27000	7.800	500.0	424.0	323.0	161.0	17.0	20.0	Slightly cloudy appearance. Fines boiling. Moderate outflow.
465.00	27900	8.100	550.0	450.0	370.0	174.0	18.0	20.0	Slightly cloudy appearance. Fines boiling. Moderate outflow.
480.00	28800	8.280	550.0	471.0	436.0	180.0	17.0	20.0	Slightly cloudy appearance. Fines boiling. Moderate outflow.
495.00	29700	8.160	551.0	487.0	465.0	187.0	17.0	20.0	Slightly cloudy appearance. Fines boiling. Moderate outflow.
510.00	30600	8.400	600.0	517.0	492.0	197.0	17.0	20.0	Slightly cloudy appearance. Fines boiling. Moderate outflow.
525.00	31500	8.310	600.0	534.0	501.0	198.0	17.0	20.0	Slightly cloudy appearance. Fines boiling. Moderate outflow.
555.00	33300	8.550	604.0	555.0	499.0	198.0	17.0	20.0	Slightly cloudy appearance. Fines boiling. Moderate outflow.
570.00	34200	9.180	654.0	596.0	531.0	205.0	16.0	20.0	Slightly cloudy appearance. Fines boiling. Moderate outflow.
575.00	34500	9.000	654.0	603.0	532.0	207.0	16.0	20.0	Slightly cloudy appearance. Fines boiling. Moderate outflow.
585.00	35100	8.820	660.0	613.0	532.0	212.0	16.0	20.0	Slightly cloudy appearance. Fines boiling. Moderate outflow.
600.00	36000	9.000	660.0	620.0	532.0	218.0	16.0	20.0	Slightly cloudy appearance. Fines boiling. Moderate outflow.
615.00	36900	9.300	706.0	647.0	566.0	235.0	16.0	20.0	Slightly cloudy appearance. Fines boiling. Moderate outflow.
630.00	37800	9.300	706.0	665.0	567.0	246.0	16.0	20.0	Cloudy appearance. Boiling of fines increasing. Moderate outflow.
645.00	38700	9.450	706.0	677.0	569.0	252.0	16.0	20.0	Cloudy appearance. Boiling of fines increasing. Moderate outflow. Test stopped.

Note : Deduct 6mm to give true depth of water from water surface to top of test sample within seepage cell.

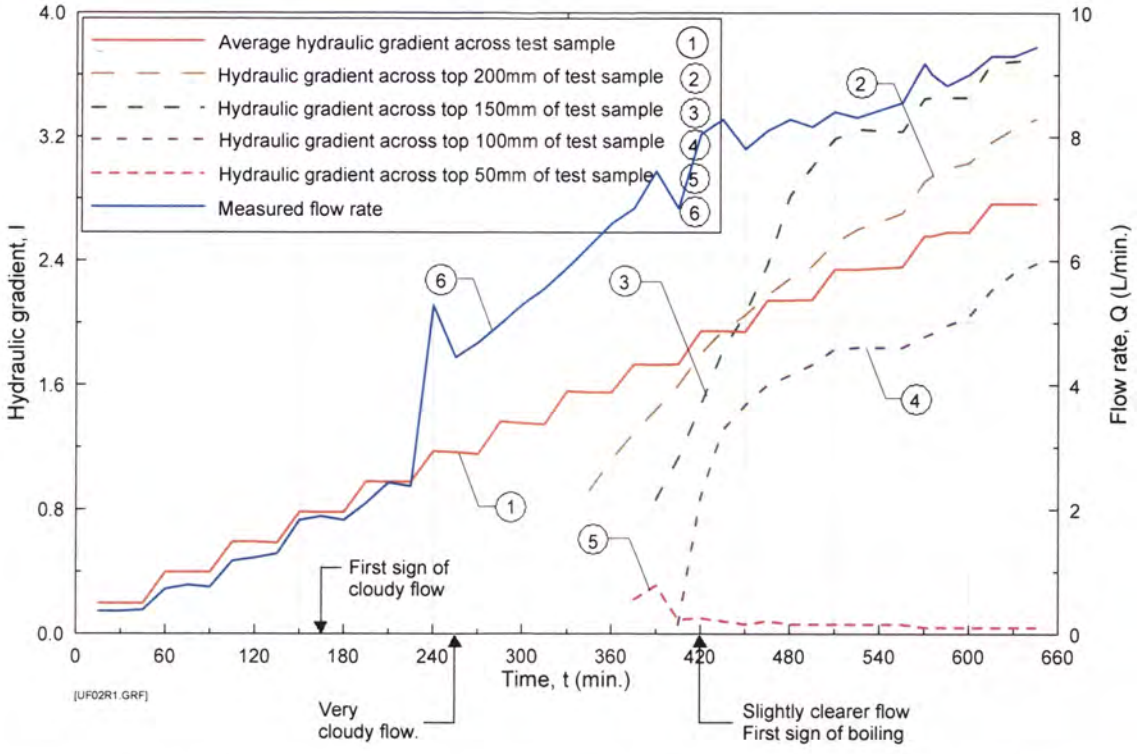

Figure P2a Test UF2 on Sample 1 - Hydraulic gradient and flow rate versus time. Sample compacted to 89.5% of Standard Maximum Dry Density.

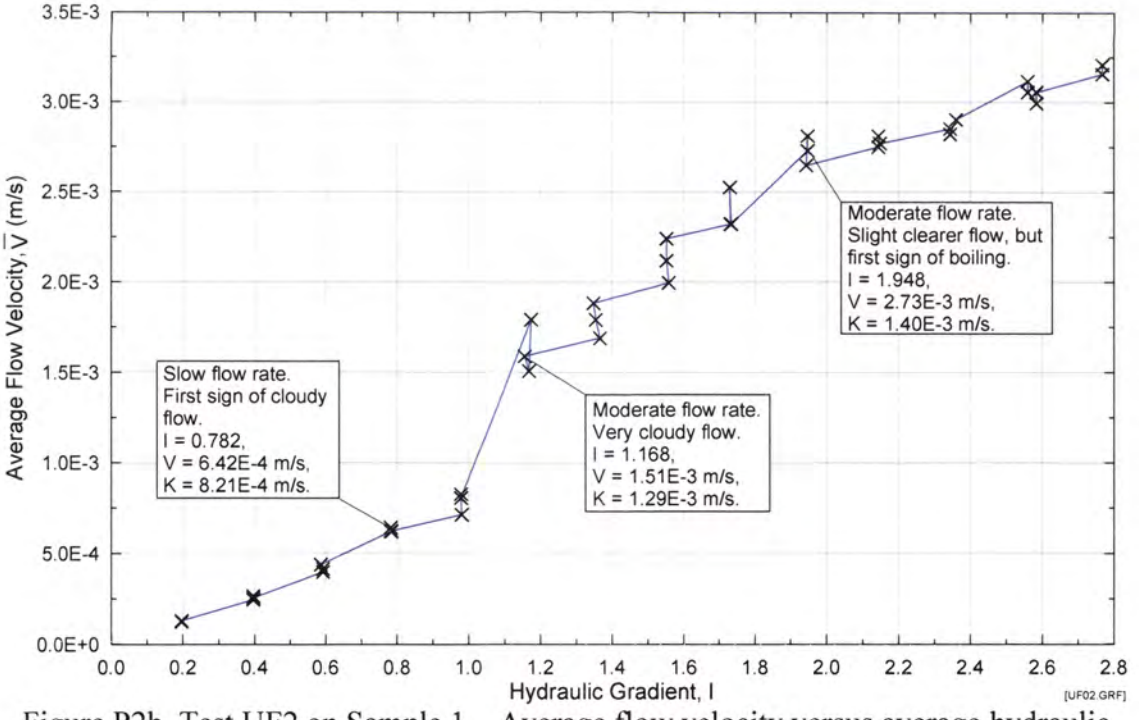

Figure P2b Test UF2 on Sample 1 – Average flow velocity versus average hydraulic gradient. Sample compacted to 89.5% of Standard Maximum Dry Density.

Upward flow test No. UF3 Test Records

UPWARD FLOW SUFFUSION TEST
Test Data

Test No. :	**Suffusion Upflow 003 22/10/01**	
Soil Sample :	**Suffusion Test Blend No. 2**	
Max. dry density :	2.175	Mg/m3
Optimum moisture content (OWC) :	8.88%	
Relative compaction :	95.0%	
Actual compaction from test:	94.5%	
Moisture content during conditioning :	8.88%	
Targeted moisture content :	8.88%	
Moisture content from test :	8.88%	
Fluid for conditioning soil :	tap water	
Eroding fluid :	tap water	
Eroding fluid mean temperature :	18.6	°C
Time/Date of Commencement of Soaking :	9.45am 22/10/01	
Time/Date of Commencement of Test :	9.00am 23/10/01	

Mix Ingredient	Mix Proportion (%)
Clay Q38	0.00
Silica 60G	24.01
Nepean Sand	24.01
5mm Blue Metal	18.01
10mm Bassalt	18.01
20mm Blue Metal	15.97
Total	100.00

Time (From Commencement) (mins)	Time (s)	Flowrate (L/min)	Head (mm) Inlet	200mm From top surface of sample	150mm From top surface of sample	100mm From top surface of sample	50mm From top surface of sample	Water Surface within cell. (See note)	Observations
10.00	600	0.000	50.0	0.0	0.0	0.0	0.0	6.0	Test started. Clear. No outflow.
20.00	1200	0.048	50.0	0.0	0.0	0.0	0.0	6.0	Clear. Very low outflow.
30.00	1800	0.135	100.0	0.0	0.0	0.0	0.0	7.0	Clear. Very low outflow.
40.00	2400	0.090	100.0	0.0	0.0	0.0	0.0	7.0	Clear. Very low outflow.
50.00	3000	0.156	150.0	0.0	0.0	0.0	0.0	7.0	Clear. Very low outflow.
60.00	3600	0.164	150.0	0.0	0.0	0.0	0.0	7.5	Clear. Very low outflow.
70.00	4200	0.267	200.0	0.0	0.0	0.0	0.0	7.5	Clear. Very low outflow.
80.00	4800	0.303	200.0	0.0	0.0	0.0	0.0	8.0	Clear. Very low outflow.
90.00	5400	0.408	250.0	0.0	0.0	0.0	4.0	8.0	Slightly cloudy appearance. Very low outflow.
100.00	6000	0.498	250.0	0.0	0.0	0.0	4.0	9.0	Clear. Very low outflow. Test paused, then restarted.
110.00	6600	0.510	250.0	0.0	0.0	0.0	4.0	9.0	Slightly cloudy appearance. Very low outflow.
120.00	7200	0.708	300.0	0.0	0.0	0.0	4.0	9.0	Slightly cloudy appearance. Very low outflow.
130.00	7800	0.792	300.0	0.0	0.0	0.0	4.0	9.5	Slightly cloudy appearance. Very low outflow.
140.00	8400	0.708	300.0	0.0	0.0	0.0	4.0	9.5	Slightly cloudy appearance. Very low outflow.
150.00	9000	0.972	350.0	0.0	0.0	0.0	4.0	10.0	Slightly cloudy appearance. Very low outflow.
160.00	9600	1.008	350.0	0.0	0.0	0.0	4.0	10.0	Cloudy appearance. Very low outflow.
170.00	10200	1.185	400.0	0.0	0.0	0.0	4.0	10.0	Cloudy appearance. Very low outflow.
180.00	10800	1.230	400.0	0.0	0.0	0.0	4.0	10.0	Cloudy appearance. Very low outflow.

Upward flow test No. UF3 Test Records (Cont'd)

Time (From Commencement) (mins)	Time (s)	Flowrate (L/min)	Head (mm)						Observations
			Inlet	200mm From top surface of sample	150mm From top surface of sample	100mm From top surface of sample	50mm From top surface of sample	Water Surface within cell. (See note)	
190.00	11400	1.350	450.0	0.0	0.0	0.0	5.0	10.0	Cloudy appearance. Very low outflow.
200.00	12000	1.590	450.0	0.0	0.0	0.0	6.0	10.5	Cloudy appearance. Very low outflow.
210.00	12600	2.120	448.0	0.0	0.0	0.0	6.0	11.5	Cloudy appearance. Low outflow.
220.00	13200	2.280	446.0	0.0	0.0	0.0	7.0	12.0	Slightly cloudy appearance. Low outflow.
230.00	13800	2.190	446.0	0.0	0.0	0.0	7.0	12.5	Slightly cloudy appearance. Low outflow.
240.00	14400	2.430	500.0	0.0	0.0	0.0	7.0	12.5	Slightly cloudy appearance. Low outflow.
250.00	15000	2.460	500.0	0.0	0.0	0.0	7.0	13.0	Slightly cloudy appearance. Low outflow.
260.00	15600	2.535	550.0	0.0	0.0	0.0	8.0	13.0	Slightly cloudy appearance. Low outflow.
270.00	16200	2.880	550.0	0.0	0.0	0.0	8.0	14.0	Slightly cloudy appearance. Low outflow.
280.00	16800	2.910	550.0	0.0	77.0	0.0	8.0	14.0	Slightly cloudy appearance. Low outflow.
290.00	17400	3.030	600.0	25.0	99.0	0.0	8.0	14.0	Slightly cloudy appearance. Low outflow.
300.00	18000	3.000	600.0	59.0	140.0	0.0	8.0	14.5	Slightly cloudy appearance. Low outflow.
310.00	18600	3.570	650.0	97.0	177.0	0.0	9.0	14.5	Slightly cloudy appearance. Low outflow.
320.00	19200	3.300	650.0	129.0	206.0	0.0	9.0	15.0	Slightly cloudy appearance. Low outflow.
330.00	19800	3.390	650.0	160.0	234.0	0.0	9.0	15.0	Slightly cloudy appearance. Low outflow.
340.00	20400	4.920	700.0	195.0	266.0	0.0	10.0	15.5	Slightly cloudy appearance. Low outflow.
350.00	21000	4.830	700.0	222.0	287.0	0.0	10.5	16.5	Slightly cloudy appearance. Low outflow.
360.00	21600	5.400	695.0	249.0	312.0	0.0	11.0	17.0	Slightly cloudy appearance. Low outflow.
370.00	22200	5.220	697.0	275.0	338.0	0.0	11.5	18.0	Slightly cloudy appearance. Low outflow.
380.00	22800	5.550	750.0	300.0	363.0	0.0	12.0	19.0	Slightly cloudy appearance. Low outflow.
390.00	23400	5.280	750.0	323.0	385.0	0.0	12.0	18.5	Slightly cloudy appearance. Low outflow. Test Paused and Restarted.
405.00	24300	10.920	750.0	44.0	101.0	0.0	19.0	24.0	Very cloudy appearance. Fines boiling. Moderate outflow.
410.00	24600	10.320	750.0	67.0	140.0	0.0	18.0	23.0	Very cloudy appearance. Fines boiling. Moderate outflow.
415.00	24900	10.920	750.0	85.0	165.0	0.0	18.0	23.0	Cloudy appearance. Fines boiling. Moderate outflow.
420.00	25200	10.500	750.0	103.0	188.0	8.0	18.0	23.0	Cloudy appearance. Fines boiling. Moderate outflow.
425.00	25500	10.980	750.0	123.0	212.0	18.0	18.0	23.0	Cloudy appearance. Boiling of fines increasing. Moderate outflow. Test stopped.

Note : Deduct 6mm to give true depth of water from water surface to top of test sample within seepage cell.

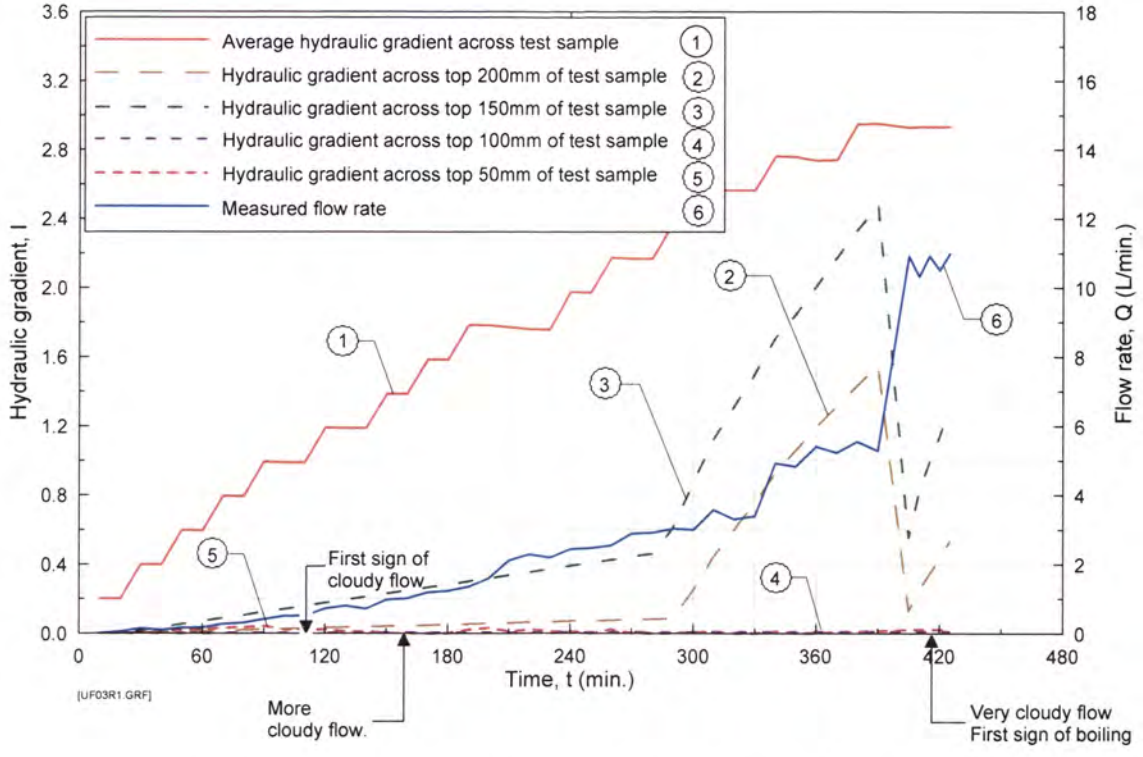

Figure P3a Test UF3 on Sample 2 - Hydraulic gradient and flow rate versus time. Sample compacted to 94.5% of Standard Maximum Dry Density.

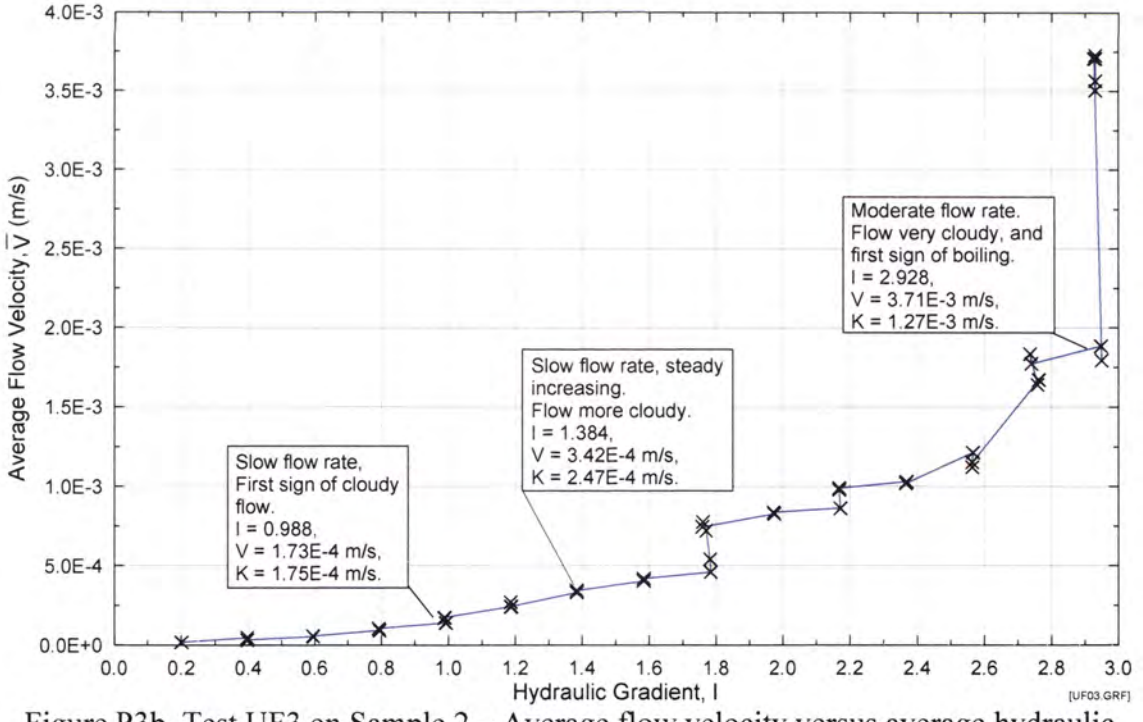

Figure P3b Test UF3 on Sample 2 – Average flow velocity versus average hydraulic gradient. Sample compacted to 94.5% of Standard Maximum Dry Density.

Upward flow test No. UF4 Test Records

UPWARD FLOW SUFFUSION TEST
Test Data

Test No. :	**Suffusion Upflow 004 25/10/01**	
Soil Sample :	**Suffusion Test Blend No. 3**	
Max. dry density :	1.968	Mg/m3
Optimum moisture content (OWC) :	11.61%	
Relative compaction :	95.0%	
Actual compaction from test:	93.8%	
Moisture content during conditioning :	11.61%	
Targeted moisture content :	11.61%	
Moisture content from test :	11.61%	
Fluid for conditioning soil :	tap water	
Eroding fluid :	tap water	
Eroding fluid mean temperature :	21.6	°C
Time/Date of Commencement of Soaking :	4.00pm 25/10/01	
Time/Date of Commencement of Test :	8.30am 30/10/01	

Mix Ingredient	Mix Proportion (%)
Clay Q38	0.00
Silica 60G	50.90
Nepean Sand	28.28
5mm Blue Metal	6.11
10mm Bassalt	9.05
20mm Blue Metal	5.66
Total	100.00

Time (From Commencement) (mins)	Time (s)	Flowrate (L/min)	Head (mm) Inlet	200mm From top surface of sample	150mm From top surface of sample	100mm From top surface of sample	50mm From top surface of sample	Water Surface within cell. (See note)	Observations
10.00	600	0.000	50.0	0.0	0.0	0.0	0.0	2.0	Clear. No outflow.
20.00	1200	0.000	50.0	0.0	0.0	0.0	0.0	2.0	Clear. No outflow.
30.00	1800	0.000	100.0	0.0	0.0	0.0	0.0	2.0	Clear. No outflow.
40.00	2400	0.000	100.0	0.0	0.0	0.0	0.0	2.0	Clear. No outflow.
50.00	3000	0.000	150.0	0.0	0.0	0.0	0.0	2.0	Clear. No outflow.
60.00	3600	0.002	150.0	89.0	0.0	0.0	0.0	2.0	Clear. No outflow.
65.00	3900	6.540	200.0	112.0	0.0	0.0	0.0	23.0	Very cloudy appearance. Rapid flow increase. Now moderate outflow.
70.00	4200	13.770	200.0	106.0	0.0	0.0	0.0	23.0	Very Cloudy appearance. Steady flow increase. High outflow.
75.00	4500	13.590	200.0	86.0	0.0	0.0	0.0	23.0	Very Cloudy appearance. Steady flow increase. High outflow.
80.00	4800	13.620	200.0	98.0	0.0	0.0	0.0	23.0	Very Cloudy appearance. Steady flow increase. High outflow.
85.00	5100	16.470	250.0	91.0	0.0	0.0	0.0	24.0	Very Cloudy appearance. Steady flow increase. High outflow.
90.00	5400	16.950	250.0	93.0	0.0	55.0	0.0	24.0	Very Cloudy appearance. Steady flow increase. High outflow.
95.00	5700	16.920	250.0	92.0	0.0	58.0	0.0	24.0	Very Cloudy appearance. Steady flow increase. High outflow.
100.00	6000	17.100	250.0	91.0	0.0	63.0	0.0	24.0	Very Cloudy appearance. Steady flow increase. High outflow.
105.00	6300	17.100	250.0	91.0	0.0	63.0	0.0	24.0	Cloudy appearance. Steady flow increase. High outflow.
110.00	6600	19.500	300.0	93.0	7.0	68.0	0.0	25.0	Very Cloudy appearance. Steady flow increase. High outflow.
115.00	6900	20.040	300.0	94.0	17.0	67.0	0.0	25.5	Cloudy appearance. Steady flow increase. High outflow.
120.00	7200	19.980	300.0	93.0	23.0	68.0	0.0	26.0	Cloudy appearance. Steady flow increase. High outflow.
125.00	7500	20.220	300.0	91.0	26.0	68.0	0.0	26.0	Cloudy appearance. Steady flow increase. Very high outflow. Test stopped.

Note : Deduct 6mm to give true depth of water from water surface to top of test sample within seepage cell.

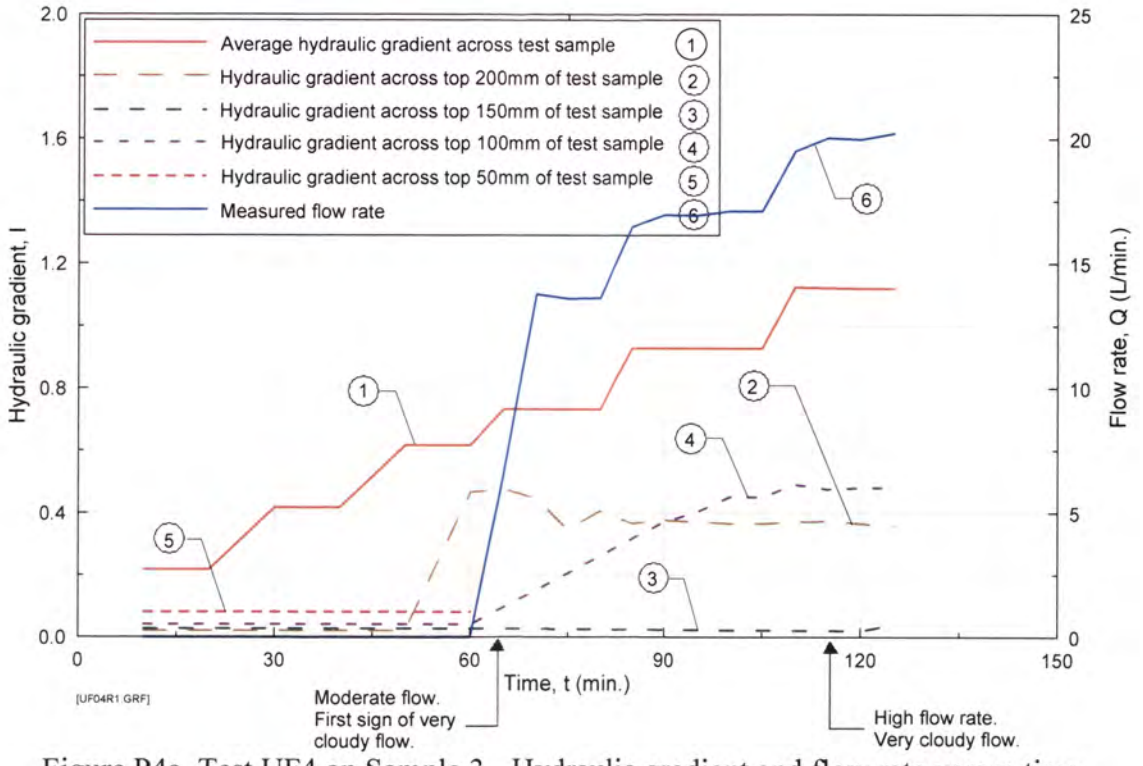

Figure P4a Test UF4 on Sample 3 - Hydraulic gradient and flow rate versus time. Sample compacted to 94.0% of Standard Maximum Dry Density.

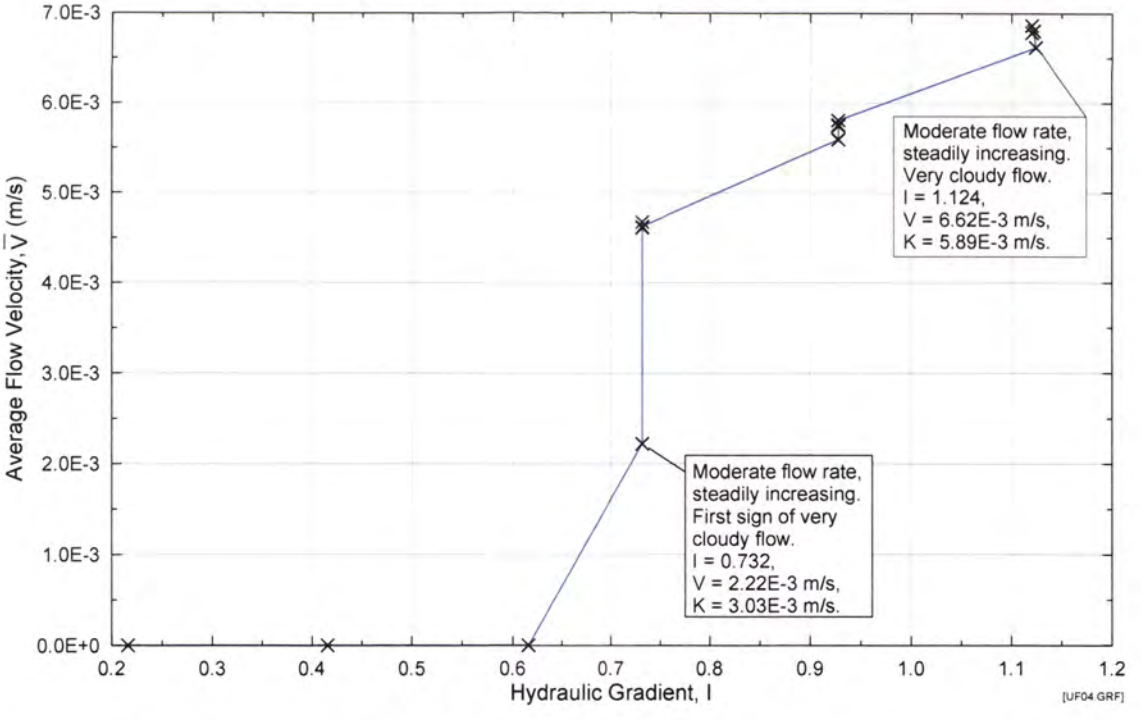

Figure B4b Test UF4 on Sample 3 – Average flow velocity versus average hydraulic gradient. Sample compacted to 94.0% of Standard Maximum Dry Density.

Upward flow test No. UF5 Test Records

UPWARD FLOW SUFFUSION TEST
Test Data

Test No. :	**Suffusion Upflow 005 05/11/01**
Soil Sample :	**Suffusion Test Blend No. 4R**
Max. dry density :	2.229 Mg/m3
Optimum moisture content (OWC) :	9.30%
Relative compaction :	95.0%
Actual compaction from test:	94.5%
Moisture content during conditioning :	9.30%
Targeted moisture content :	9.30%
Moisture content from test :	9.30%
Fluid for conditioning soil :	tap water
Eroding fluid :	tap water
Eroding fluid mean temperature :	21.6 °C
Time/Date of Commencement of Soaking :	2.00 pm 05/11/01
Time/Date of Commencement of Test :	10.20 am 06/11/01

Mix Ingredient	Mix Proportion (%)
Clay Q38	0.00
Silica 60G	3.23
Nepean Sand	27.42
5mm Blue Metal	32.26
10mm Bassalt	24.19
20mm Blue Metal	12.90
Total	100.00

Time (From Commencement) (mins)	Time (s)	Flowrate (L/min)	Head (mm) Inlet	200mm From top surface of sample	150mm From top surface of sample	100mm From top surface of sample	50mm From top surface of sample	Water Surface within cell. (See note)	Observations
10.00	600	0.195	50.0	0.0	0.0	0.0	0.0	3.0	Test started. Clear. Very low outflow.
20.00	1200	0.195	50.0	0.0	0.0	0.0	0.0	5.0	Clear. Very low outflow.
30.00	1800	0.330	100.0	0.0	0.0	0.0	0.0	5.0	Clear. Very low outflow.
40.00	2400	0.330	100.0	0.0	0.0	0.0	0.0	5.0	Clear. Very low outflow.
50.00	3000	0.455	150.0	0.0	0.0	0.0	0.0	5.0	Clear. Very low outflow.
60.00	3600	0.450	150.0	0.0	0.0	0.0	0.0	5.0	Clear. Very low outflow.
70.00	4200	0.650	200.0	0.0	0.0	0.0	0.0	6.0	Slightly cloudy appearance. Very low outflow.
80.00	4800	0.640	200.0	0.0	0.0	0.0	0.0	6.0	Slightly cloudy appearance. Very low outflow.
90.00	5400	0.840	250.0	155.0	0.0	0.0	0.0	7.0	Slightly cloudy appearance. Very low outflow.
100.00	6000	0.840	250.0	182.0	0.0	81.0	0.0	7.5	Slightly cloudy appearance. Very low outflow.
110.00	6600	0.900	300.0	225.0	0.0	122.0	0.0	7.5	Slightly cloudy appearance. Very low outflow.
120.00	7200	0.915	300.0	225.0	0.0	124.0	0.0	7.5	Slightly cloudy appearance. Very low outflow.
130.00	7800	1.020	350.0	268.0	0.0	150.0	0.0	8.0	Slightly cloudy appearance. Very low outflow.
140.00	8400	0.990	350.0	270.0	0.0	151.0	0.0	8.0	Slightly cloudy appearance. Very low outflow.
150.00	9000	1.110	400.0	312.0	105.0	174.0	0.0	8.5	Slightly cloudy appearance. Very low outflow.
160.00	9600	1.080	400.0	316.0	160.0	174.0	0.0	8.5	Slightly cloudy appearance. Very low outflow.
170.00	10200	1.050	450.0	362.0	167.0	193.0	0.0	9.0	Slightly cloudy appearance. Very low outflow.
180.00	10800	0.960	450.0	367.0	163.0	199.0	0.0	9.0	Slightly cloudy appearance. Very low outflow.

Upward flow test No. UF5 Test Records (Cont'd)

Time (From Commencement) (mins)	Time (s)	Flowrate (L/min)	Head (mm)						Observations
			Inlet	200mm From top surface of sample	150mm From top surface of sample	100mm From top surface of sample	50mm From top surface of sample	Water Surface within cell. (See note)	
190.00	11400	1.065	500.0	414.0	195.0	217.0	0.0	9.0	Slightly cloudy appearance. Very low outflow.
200.00	12000	1.080	500.0	418.0	195.0	218.0	0.0	9.0	Slightly cloudy appearance. Very low outflow.
210.00	12600	1.200	550.0	464.0	229.0	243.0	0.0	9.0	Cloudy appearance. Very low outflow.
220.00	13200	1.140	550.0	469.0	227.0	240.0	0.0	9.0	Cloudy appearance. Very low outflow.
230.00	13800	1.230	600.0	519.0	262.0	257.0	0.0	9.5	Cloudy appearance. Very low outflow.
240.00	14400	1.200	600.0	527.0	239.0	274.0	0.0	9.5	Cloudy appearance. Very low outflow.
250.00	15000	1.230	650.0	576.0	228.0	291.0	9.0	9.5	Cloudy appearance. Very low outflow.
260.00	15600	1.215	650.0	580.0	233.0	293.0	9.0	9.5	Cloudy appearance. Very low outflow.
270.00	16200	1.320	700.0	628.0	229.0	330.0	8.0	9.5	Cloudy appearance. Very low outflow.
280.00	16800	1.260	700.0	633.0	220.0	326.0	8.0	9.5	Cloudy appearance. Very low outflow.
290.00	17400	1.245	750.0	683.0	231.0	351.0	6.0	9.0	Cloudy appearance. Very low outflow.
300.00	18000	1.305	750.0	684.0	236.0	336.0	8.0	9.0	Cloudy appearance. Very low outflow.
310.00	18600	1.470	800.0	733.0	283.0	332.0	10.0	9.0	Cloudy appearance. Very low outflow.
320.00	19200	1.515	800.0	733.0	278.0	330.0	10.0	9.0	Cloudy appearance. Very low outflow.
330.00	19800	1.560	850.0	779.0	359.0	338.0	13.0	9.0	Cloudy appearance. Very low outflow.
340.00	20400	1.500	850.0	784.0	376.0	349.0	13.0	9.0	Cloudy appearance. Very low outflow.
350.00	21000	1.515	900.0	833.0	396.0	358.0	12.0	9.0	Cloudy appearance. Very low outflow. Test paused, then restarted
360.00	21600	2.850	900.0	822.0	563.0	347.0	21.0	11.0	Very cloudy appearance. Low outflow. Boling fines.
370.00	22200	2.820	900.0	830.0	727.0	480.0	17.0	11.0	Very cloudy appearance. Low outflow. Boling fines.
380.00	22800	3.000	950.0	866.0	850.0	480.0	20.0	12.0	Very cloudy appearance. Low outflow. Boling fines.
390.00	23400	3.000	950.0	858.0	841.0	497.0	20.0	12.0	Very cloudy appearance. Low outflow. Boling fines.
400.00	24000	3.090	1000.0	886.0	873.0	482.0	17.0	12.0	Very cloudy appearance. Low outflow. Boling fines.
410.00	24600	3.210	1000.0	867.0	857.0	513.0	17.0	12.0	Cloudy appearance. Low outflow. Boling fines.
420.00	25200	3.270	1000.0	875.0	861.0	495.0	17.0	12.0	Cloudy appearance. Low outflow. Boling fines.
430.00	25800	3.210	1000.0	880.0	863.0	502.0	17.0	12.5	Slightly cloudy appearance. Low outflow. Boling fines and sand.
435.00	26100	3.270	1000.0	874.0	857.0	495.0	17.0	12.5	Slightly cloudy appearance. Low outflow. Boling fines and sand.
440.00	26400	3.210	1000.0	874.0	855.0	495.0	17.0	12.5	Slightly cloudy appearance. Low outflow. Boling fines and sand increasing. Test stopped.

Note : Deduct 6mm to give true depth of water from water surface to top of test sample within seepage cell.

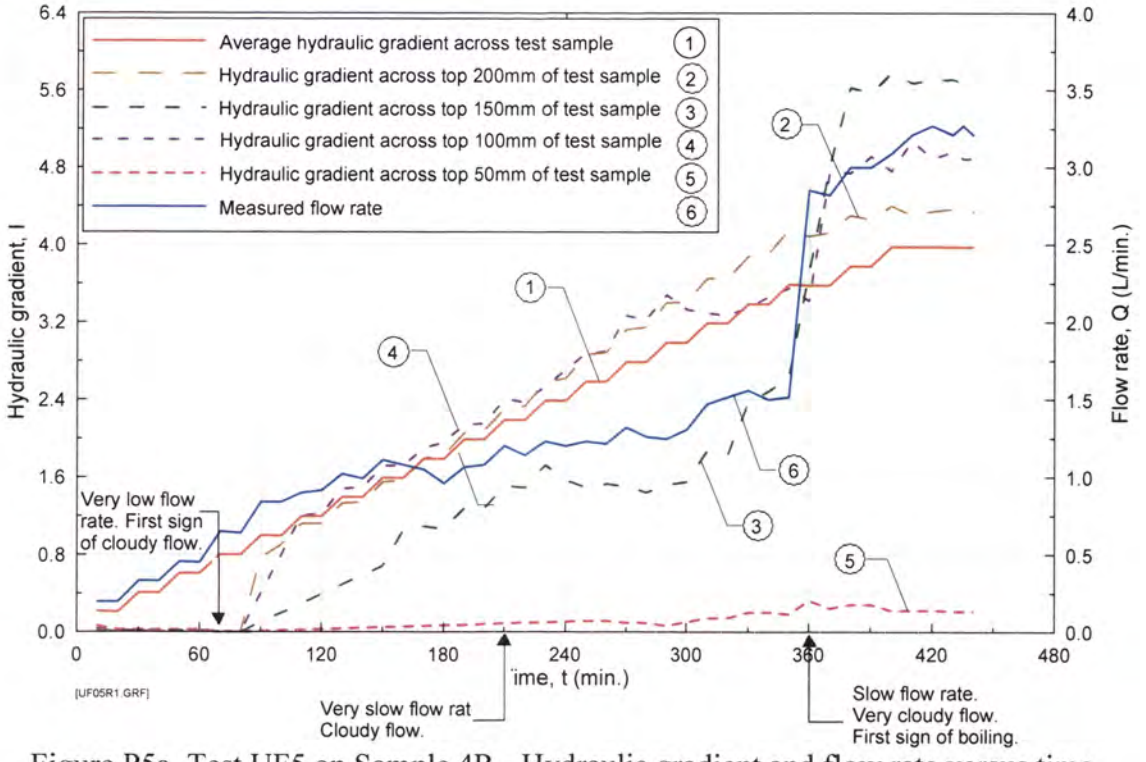

Figure P5a Test UF5 on Sample 4R - Hydraulic gradient and flow rate versus time. Sample compacted to 94.5% of Standard Maximum Dry Density.

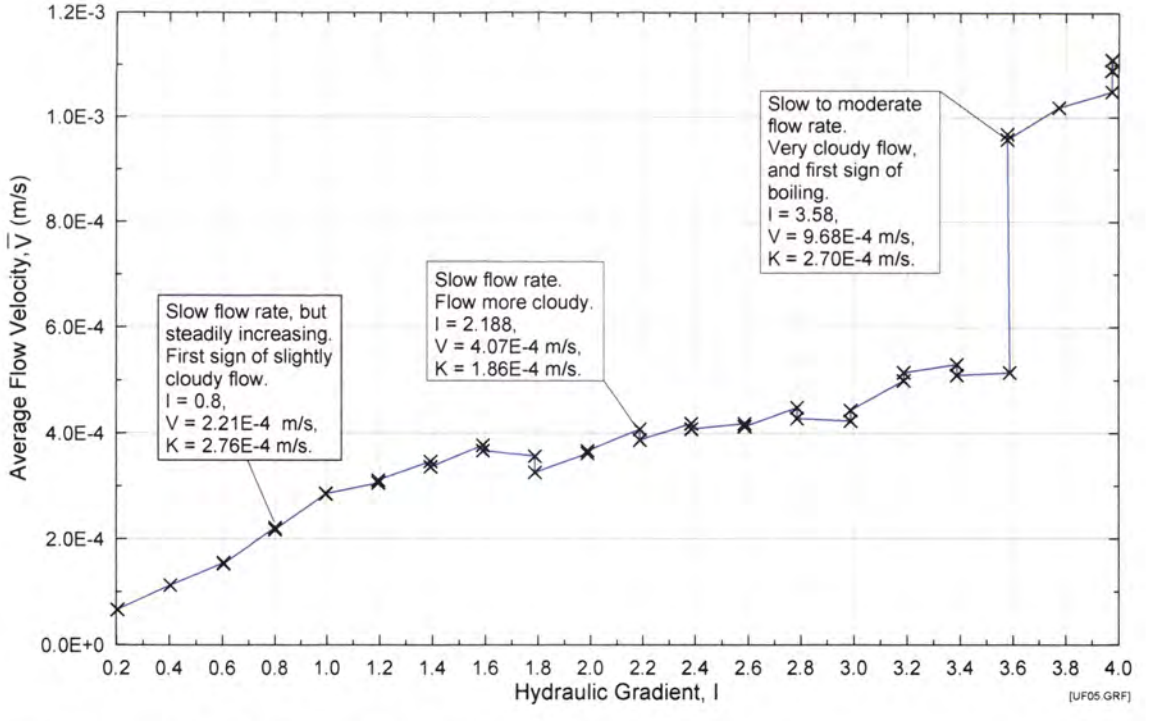

Figure P5b Test UF5 on Sample 4R – Average flow velocity versus average hydraulic gradient. Sample compacted to 94.5% of Standard Maximum Dry Density.

Upward flow test No. UF6 Test Records

UPWARD FLOW SUFFUSION TEST
Test Data

Test No. :	**Suffusion Upflow 006 18/01/02**	
Soil Sample :	**Suffusion Test Blend No. 9**	
Max. dry density :	1.935	Mg/m3
Optimum moisture content (OWC) :	6.25%	
Relative compaction :	95.0%	
Actual compaction from test:	95.0%	
Moisture content during conditioning :	6.25%	
Targeted moisture content :	6.25%	
Moisture content from test :	6.01%	
Fluid for conditioning soil :	tap water	
Eroding fluid :	tap water	
Eroding fluid mean temperature :	23.2	°C
Time/Date of Commencement of Soaking :	2.20 pm 18/01/02	
Time/Date of Commencement of Test :	9.00 am 21/01/02	

Mix Ingredient	Mix Proportion (%)
Clay Q38	0.00
Silica 60G	11.92
Nepean Sand	0.00
5mm Blue Metal	9.54
10mm Bassalt	60.67
20mm Blue Metal	17.88
Total	100.00

Time (From Commencement) (mins)	Time (s)	Flowrate (L/min)	Head (mm) Inlet	200mm From top surface of sample	150mm From top surface of sample	100mm From top surface of sample	50mm From top surface of sample	Water Surface within cell. (See note)	Observations
10.00	600	9.480	50.0	33.0	0.0	20.0	18.0	20.0	Test started. Slightly cloudy appearance. Moderate outflow, and slowly increasing.
20.00	1200	9.420	50.0	33.0	0.0	22.0	18.0	21.0	Clear. Moderate outflow, and slowly increasing.
30.00	1800	13.350	100.0	45.0	0.0	27.0	22.0	22.0	Slightly cloudy appearance. Moderate outflow, and slowly increasing.
40.00	2400	12.870	100.0	45.0	0.0	27.0	22.0	22.0	Clear. Moderate outflow, and slowly increasing.
50.00	3000	13.410	100.0	45.0	0.0	27.0	22.0	22.0	Clear. Moderate outflow, and slowly increasing.
60.00	3600	17.100	150.0	55.0	0.0	31.0	25.0	24.0	Slightly cloudy appearance. Moderate outflow, and slowly increasing.
70.00	4200	16.140	150.0	55.0	9.0	31.0	25.0	24.0	Clear. Moderate outflow, and slowly increasing.
80.00	4800	17.220	150.0	55.0	9.0	31.0	25.0	24.0	Clear. Moderate outflow, and slowly increasing.
90.00	5400	19.560	200.0	63.0	16.0	34.0	27.0	25.0	Slightly cloudy appearance. Moderate outflow, and slowly increasing.
100.00	6000	19.140	200.0	63.0	16.0	34.0	27.0	25.0	Clear. Moderate outflow, and slowly increasing.
110.00	6600	19.080	200.0	63.0	16.0	34.0	27.0	25.0	Clear. Moderate outflow, and slowly increasing.
120.00	7200	19.920	250.0	69.0	46.0	38.0	29.0	26.0	Slightly cloudy appearance. Moderate outflow, and slowly increasing.
130.00	7800	20.640	250.0	69.0	46.0	38.0	29.0	26.0	Clear. High outflow, and slowly increasing.
140.00	8400	21.540	250.0	69.0	47.0	38.0	29.0	26.0	Clear. High outflow, and slowly increasing.
150.00	9000	21.540	250.0	69.0	48.0	38.0	30.0	26.0	Clear. High outflow, and slowly increasing.
160.00	9600	23.100	300.0	77.0	52.0	40.0	32.0	27.0	Slightly cloudy appearance. High outflow, and slowly increasing.
170.00	10200	22.500	300.0	77.0	52.0	40.0	32.0	27.0	Clear. High outflow, and slowly increasing.
180.00	10800	22.440	300.0	76.0	52.0	40.0	32.0	27.0	Clear. High outflow, and slowly increasing.
190.00	11400	25.380	350.0	83.0	56.0	43.0	34.0	28.0	Slightly cloudy appearance. High outflow, and slowly increasing.
200.00	12000	25.200	350.0	83.0	56.0	43.0	34.0	28.0	Clear. Very high outflow, and slowly increasing.

Note : Deduct 6mm to give true depth of water from water surface to top of test sample within seepage cell.

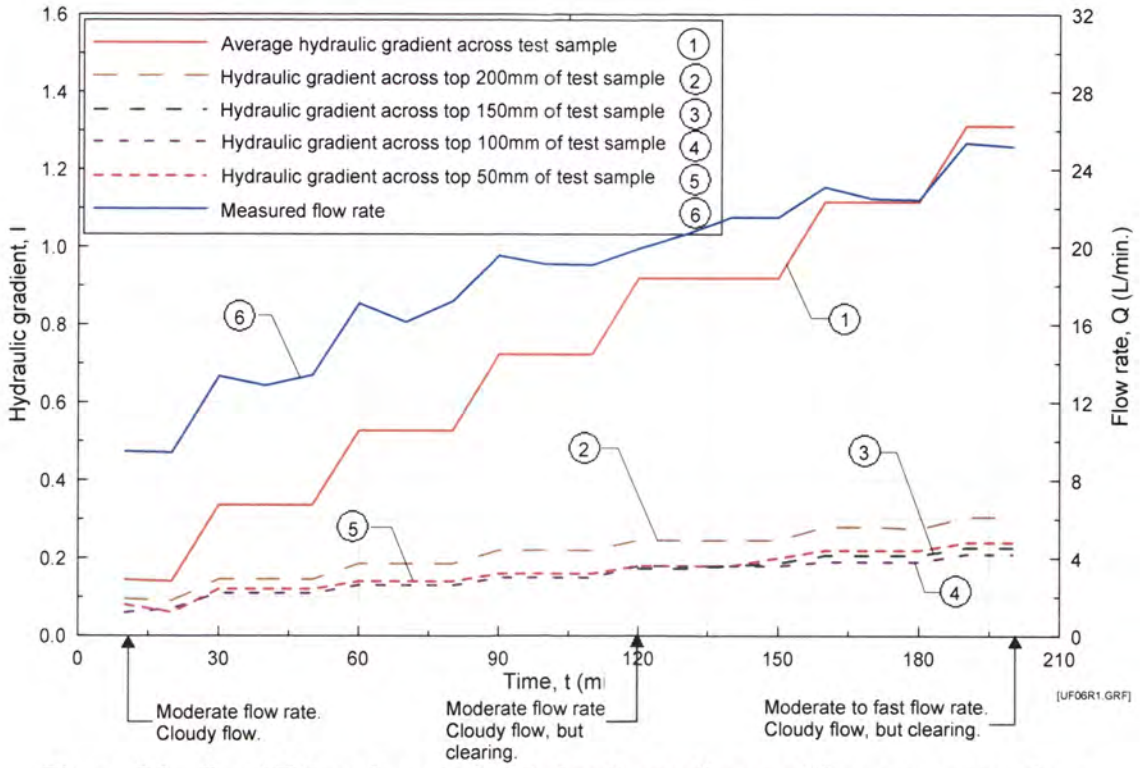

Figure P6a Test UF6 on Sample 9 - Hydraulic gradient and flow rate versus time. Sample compacted to 95.0% of Standard Maximum Dry Density.

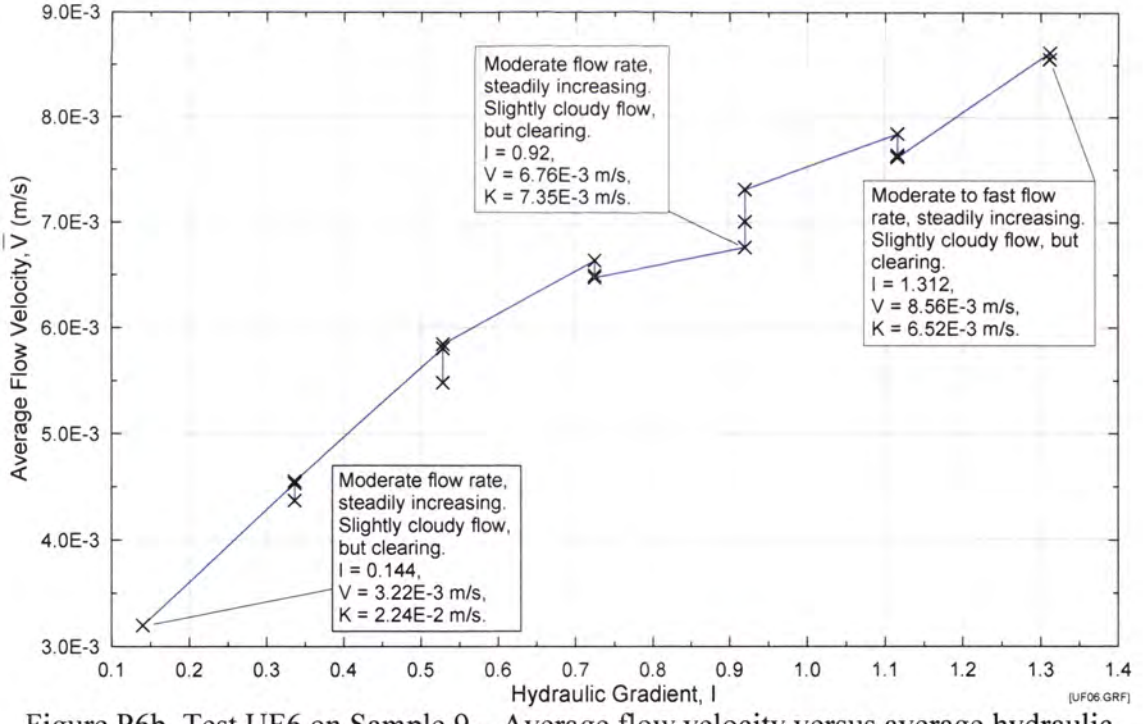

Figure P6b Test UF6 on Sample 9 – Average flow velocity versus average hydraulic gradient. Sample compacted to 95.0% of Standard Maximum Dry Density.

Upward flow test No. UF7 Test Records

UPWARD FLOW SUFFUSION TEST
Test Data

Test No. :	**Suffusion Upflow 007 16/11/01**	
Soil Sample :	**Suffusion Test Blend No. 10**	
Max. dry density :	2.219	Mg/m3
Optimum moisture content (OWC) :	8.44%	
Relative compaction :	95.0%	
Actual compaction from test:	94.8%	
Moisture content during conditioning :	8.44%	
Targeted moisture content :	8.44%	
Moisture content from test :	8.44%	
Fluid for conditioning soil :	tap water	
Eroding fluid :	tap water	
Eroding fluid mean temperature :	20.2	°C
Time/Date of Commencement of Soaking :	9.30 am 15/1/01	
Time/Date of Commencement of Test :	8.40 am 16/11/01	

Mix Ingredient	Mix Proportion (%)
Clay Q38	0.00
Silica 60G	25.67
Nepean Sand	0.00
5mm Blue Metal	0.00
10mm Bassalt	54.59
20mm Blue Metal	19.74
Total	100.00

Time (From Commencement) (mins)	Time (s)	Flowrate (L/min)	Head (mm) Inlet	200mm From top surface of sample	150mm From top surface of sample	100mm From top surface of sample	50mm From top surface of sample	Water Surface within cell. (See note)	Observations
10.00	600	0.670	50.0	0.0	0.0	0.0	0.0	5.0	Test started. Clear. Very low outflow.
20.00	1200	0.650	50.0	0.0	0.0	0.0	0.0	5.0	Clear. Very low outflow.
30.00	1800	1.080	100.0	0.0	0.0	0.0	0.0	6.0	Clear. Very low outflow.
40.00	2400	1.100	100.0	0.0	0.0	0.0	0.0	6.0	Clear. Very low outflow.
50.00	3000	1.800	150.0	0.0	0.0	0.0	0.0	8.0	Slightly cloudy. Low outflow, and slowly increasing.
60.00	3600	1.800	150.0	0.0	0.0	0.0	0.0	8.0	Slightly cloudy. Low outflow, and slowly increasing.
70.00	4200	2.720	200.0	0.0	0.0	0.0	0.0	10.0	Cloudy. Low outflow, and slowly increasing.
80.00	4800	2.760	200.0	0.0	0.0	0.0	0.0	10.0	Cloudy. Low outflow, and slowly increasing.
90.00	5400	3.690	250.0	0.0	0.0	0.0	0.0	11.0	Cloudy. Low outflow, and slowly increasing.
100.00	6000	3.810	250.0	0.0	0.0	0.0	0.0	12.0	Slightly cloudy. Low outflow, and slowly increasing.
110.00	6600	4.050	250.0	0.0	0.0	0.0	0.0	12.0	Slightly cloudy. Low outflow, and slowly increasing.
120.00	7200	3.990	250.0	0.0	0.0	0.0	0.0	12.5	Slightly cloudy. Low outflow, and slowly increasing.
130.00	7800	4.890	300.0	0.0	0.0	0.0	0.0	13.0	Cloudy. Low outflow, and slowly increasing.
140.00	8400	5.010	300.0	0.0	0.0	0.0	0.0	13.0	Cloudy. Moderate outflow, and slowly increasing.
150.00	9000	5.040	300.0	0.0	0.0	48.0	0.0	14.0	Cloudy. Moderate outflow, and slowly increasing.
160.00	9600	6.090	350.0	0.0	0.0	48.0	0.0	15.0	Cloudy. Moderate outflow, and slowly increasing.
170.00	10200	6.300	350.0	0.0	0.0	48.0	0.0	15.0	Cloudy. Moderate outflow, and slowly increasing.
180.00	10800	6.450	350.0	29.0	0.0	49.0	0.0	15.0	Slightly cloudy. Moderate outflow, and slowly increasing.

Upward flow test No. UF7 Test Records (Cont'd)

Time (From Commencement) (mins)	Time (s)	Flowrate (L/min)	Head (mm) Inlet	200mm From top surface of sample	150mm From top surface of sample	100mm From top surface of sample	50mm From top surface of sample	Water Surface within cell. (See note)	Observations
190.00	11400	6.510	350.0	62.0	0.0	50.0	0.0	15.5	Slightly cloudy. Moderate outflow, and slowly increasing.
200.00	12000	8.070	400.0	100.0	0.0	61.0	0.0	17.0	Cloudy. Moderate outflow, and slowly increasing.
210.00	12600	8.100	400.0	130.0	0.0	68.0	0.0	17.5	Cloudy. Moderate outflow, and slowly increasing.
220.00	13200	10.710	450.0	164.0	0.0	80.0	0.0	20.0	Cloudy. High outflow, and slowly increasing.
230.00	13800	10.740	450.0	185.0	0.0	84.0	0.0	20.0	Cloudy. High outflow, and slowly increasing.
240.00	14400	12.750	500.0	211.0	0.0	96.0	0.0	21.0	Cloudy. High outflow, and slowly increasing.
250.00	15000	13.320	500.0	232.0	0.0	95.0	0.0	21.0	Cloudy. High outflow, and slowly increasing.
260.00	15600	13.470	500.0	249.0	59.0	96.0	0.0	22.0	Cloudy. High outflow, and slowly increasing.
270.00	16200	13.890	500.0	262.0	81.0	96.0	0.0	22.0	Cloudy. High outflow, and slowly increasing.
280.00	16800	13.840	500.0	272.0	83.0	95.0	0.0	22.0	Slightly cloudy. High outflow, and slowly increasing.
290.00	17400	16.020	550.0	287.0	94.0	104.0	0.0	23.0	Cloudy. High outflow, and slowly increasing.
300.00	18000	16.770	550.0	299.0	94.0	104.0	0.0	23.0	Cloudy. High outflow, and slowly increasing.
310.00	18600	16.770	550.0	307.0	94.0	105.0	0.0	23.0	Cloudy. High outflow, and slowly increasing.
320.00	19200	20.820	600.0	321.0	114.0	111.0	0.0	24.0	Cloudy. Very high outflow, and slowly increasing.
330.00	19800	19.320	600.0	330.0	114.0	114.0	0.0	25.0	Slightly cloudy. Very high outflow, and slowly increasing.
340.00	20400	20.160	600.0	337.0	110.0	110.0	0.0	25.0	Slightly cloudy. Very high outflow, and slowly increasing.
350.00	21000	24.660	650.0	350.0	124.0	122.0	0.0	26.5	Cloudy. Extremely high outflow, and steadily increasing. Sands boling. Stop test.

Note : Deduct 6mm to give true depth of water from water surface to top of test sample within seepage cell.

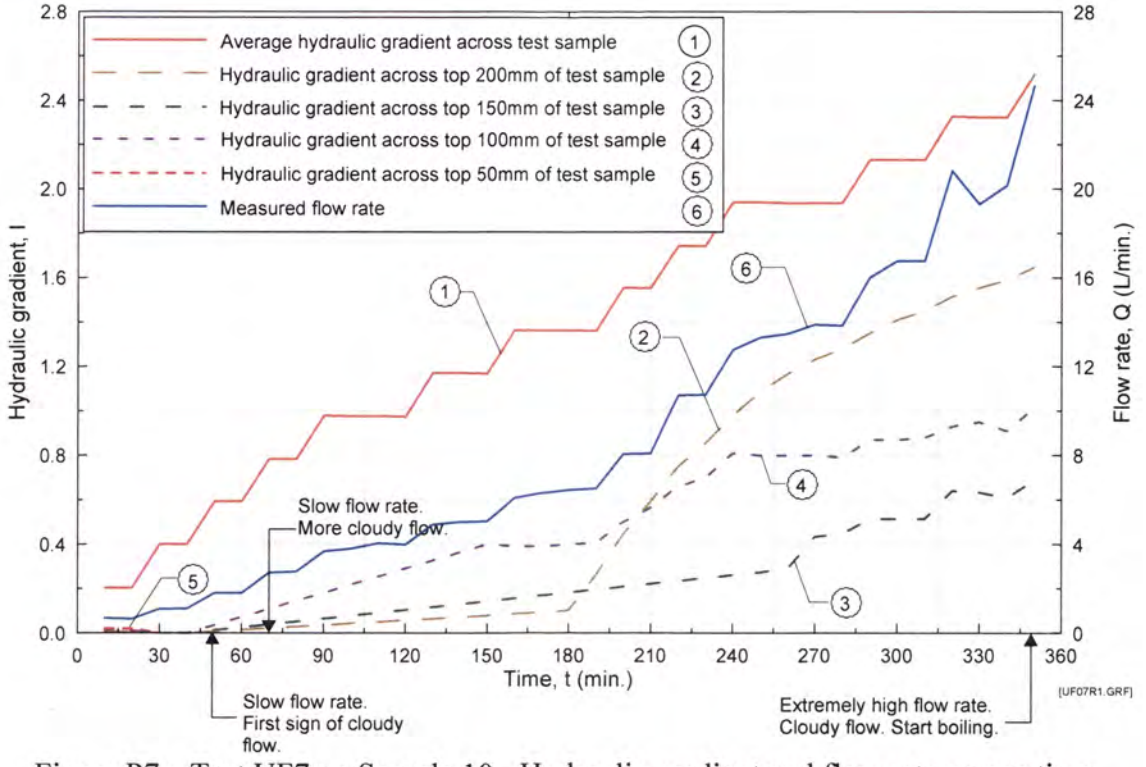

Figure P7a Test UF7 on Sample 10 - Hydraulic gradient and flow rate versus time. Sample compacted to 95.0% of Standard Maximum Dry Density.

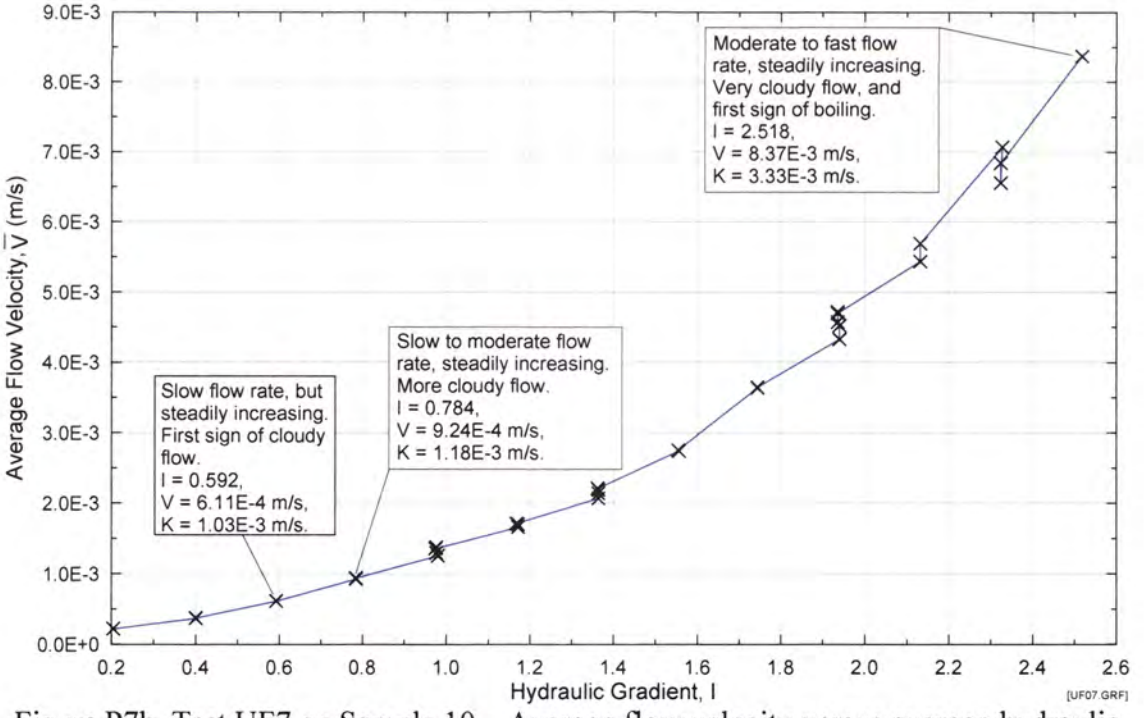

Figure P7b Test UF7 on Sample 10 – Average flow velocity versus average hydraulic gradient. Sample compacted to 95.0% of Standard Maximum Dry Density.

Upward flow test No. UF8 Test Records

UPWARD FLOW SUFFUSION TEST
Test Data

Test No. :	**Suffusion Upflow 008 22/11/01**	
Soil Sample :	**Suffusion Test Blend No. 10**	
Max. dry density :	2.219	Mg/m3
Optimum moisture content (OWC) :	8.44%	
Relative compaction :	90.0%	
Actual compaction from test:	90.1%	
Moisture content during conditioning :	8.44%	
Targeted moisture content :	8.44%	
Moisture content from test :	8.44%	
Fluid for conditioning soil :	tap water	
Eroding fluid :	tap water	
Eroding fluid mean temperature :	18.5	°C
Time/Date of Commencement of Soaking :	10.30 am 22/11/01	
Time/Date of Commencement of Test :	9.20 am 23/11/01	

Mix Ingredient	Mix Proportion (%)
Clay Q38	0.00
Silica 60G	25.67
Nepean Sand	0.00
5mm Blue Metal	0.00
10mm Bassalt	54.59
20mm Blue Metal	19.74
Total	100.00

Time (From Commencement) (mins)	Time (s)	Flowrate (L/min)	Head (mm) Inlet	200mm From top surface of sample	150mm From top surface of sample	100mm From top surface of sample	50mm From top surface of sample	Water Surface within cell. (See note)	Observations
10.00	600	2.970	50.0	0.0	0.0	0.0	0.0	10.5	Test started. Slightly cloudy appearance. Low outflow, and slowly increasing.
20.00	1200	3.030	50.0	0.0	0.0	0.0	0.0	10.5	Clear. Low outflow, and slowly increasing.
30.00	1800	5.310	100.0	0.0	0.0	0.0	24.0	13.0	Slightly cloudy appearance. Moderate outflow, and slowly increasing.
40.00	2400	5.310	100.0	0.0	0.0	0.0	24.0	13.0	Clear. Moderate outflow, and slowly increasing.
50.00	3000	8.370	150.0	0.0	0.0	0.0	33.0	17.0	Slightly cloudy appearance. Moderate outflow, and slowly increasing.
60.00	3600	8.430	150.0	0.0	0.0	0.0	33.0	17.5	Clear. Moderate outflow, and slowly increasing.
70.00	4200	11.340	200.0	0.0	0.0	0.0	39.0	19.0	Slightly cloudy appearance. High outflow, and slowly increasing.
80.00	4800	12.210	200.0	0.0	0.0	0.0	38.0	19.0	Clear. High outflow, and slowly increasing.
90.00	5400	12.330	200.0	0.0	0.0	0.0	36.0	19.0	Clear. High outflow, and slowly increasing.
100.00	6000	12.570	200.0	0.0	0.0	0.0	36.0	19.0	Clear. High outflow, and slowly increasing.
110.00	6600	12.390	200.0	0.0	0.0	0.0	32.0	19.0	Clear. High outflow, and slowly increasing.
120.00	7200	17.520	250.0	0.0	0.0	0.0	38.0	22.0	Very cloudy appearance. High outflow, and slowly increasing.
130.00	7800	16.800	250.0	0.0	0.0	44.0	36.0	23.0	Very cloudy appearance. High outflow, and slowly increasing.
140.00	8400	21.360	300.0	110.0	214.0	52.0	42.0	24.0	Very cloudy appearance. Very high outflow, and slowly increasing.
150.00	9000	22.380	300.0	107.0	209.0	50.0	40.0	25.0	Cloudy appearance. Very high outflow, and slowly increasing.
160.00	9600	22.800	300.0	113.0	220.0	53.0	44.0	25.0	Slightly cloudy appearance. Very high outflow, and slowly increasing.
170.00	10200	24.540	300.0	114.0	218.0	53.0	41.0	25.5	Slightly cloudy appearance. Very high outflow, and slowly increasing.
180.00	10800	24.960	300.0	116.0	221.0	53.0	40.0	26.0	Clear, though sands boiling. Extremely high outflow, and slowly increasing. Stop test.

Note : Deduct 6mm to give true depth of water from water surface to top of test sample within seepage cell.

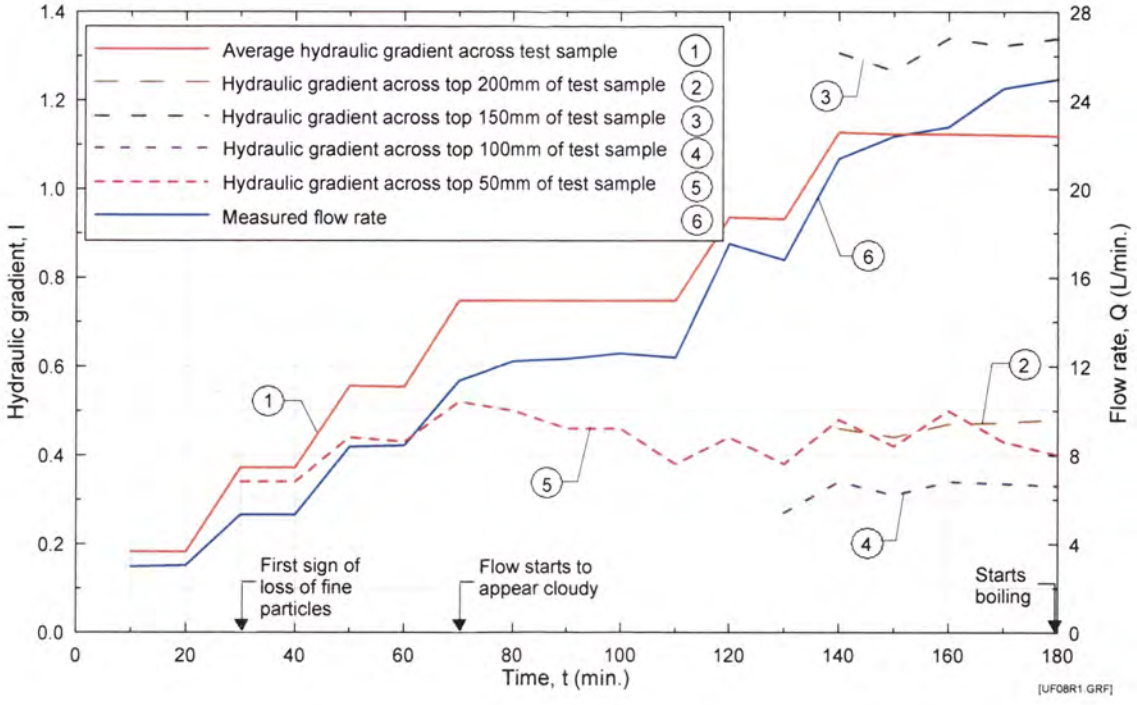

Figure P8a Test UF8 on Sample 10 - Hydraulic gradient and flow rate versus time. Sample compacted to 90.0% of Standard Maximum Dry Density.

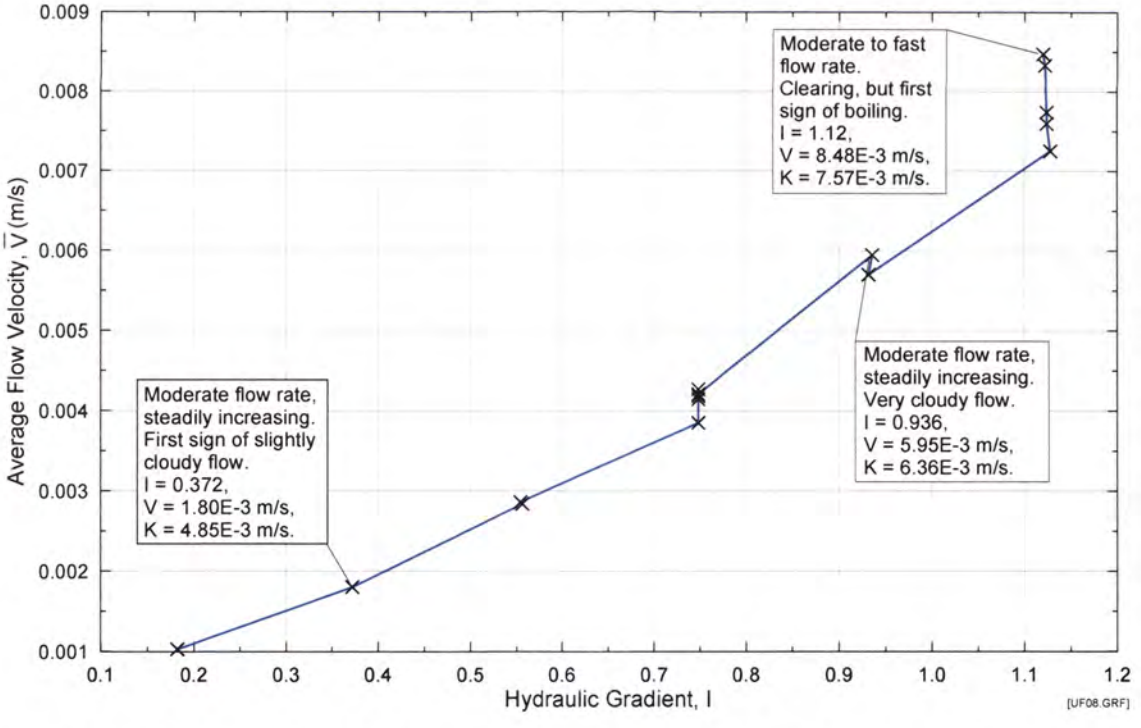

Figure P8b Test UF8 on Sample 10 – Average flow velocity versus average hydraulic gradient. Sample compacted to 90.0% of Standard Maximum Dry Density.

Upward flow test No. UF9 Test Records

UPWARD FLOW SUFFUSION TEST
Test Data

Test No. :	**Suffusion Upflow 009 22/01/02**	
Soil Sample :	**Suffusion Test Blend No.11**	
Max. dry density :	1.910	Mg/m3
Optimum moisture content (OWC) :	12.06%	
Relative compaction :	95.0%	
Actual compaction from test:	95.0%	
Moisture content during conditioning :	12.06%	
Targeted moisture content :	12.06%	
Moisture content from test :	12.36%	
Fluid for conditioning soil :	tap water	
Eroding fluid :	tap water	
Eroding fluid mean temperature :	24.1	°C
Time/Date of Commencement of Soaking :	1.30 pm 22/01/02	
Time/Date of Commencement of Test :	10.20 am 23/01/02	

Mix Ingredient	Mix Proportion (%)
Clay Q38	0.00
Silica 60G	52.86
Nepean Sand	0.00
5mm Blue Metal	0.00
10mm Bassalt	26.43
20mm Blue Metal	20.70
Total	100.00

Time (From Commencement) (mins)	Time (s)	Flowrate (L/min)	Head (mm) Inlet	200mm From top surface of sample	150mm From top surface of sample	100mm From top surface of sample	50mm From top surface of sample	Water Surface within cell. (See note)	Observations
10.00	600	0.000	50.0	0.0	0.0	0.0	0.0	8.0	Test started. Very cloudy appearance. No outflow.
20.00	1200	0.000	50.0	0.0	0.0	0.0	0.0	8.0	Very cloudy appearance. No outflow.
30.00	1800	0.000	100.0	0.0	0.0	0.0	0.0	8.0	Very cloudy appearance. No outflow.
40.00	2400	0.000	100.0	0.0	0.0	0.0	0.0	8.0	Very cloudy appearance. No outflow.
50.00	3000	0.000	150.0	0.0	0.0	0.0	0.0	8.0	Very cloudy appearance. No outflow.
60.00	3600	0.000	150.0	0.0	0.0	0.0	0.0	8.0	Very cloudy appearance. No outflow.
70.00	4200	4.980	200.0	12.0	0.0	0.0	0.0	15.0	Very cloudy appearance. Moderate outflow, and rapidly increasing.
80.00	4800	17.250	200.0	54.0	0.0	0.0	33.0	34.0	Very cloudy appearance. High outflow, and slowly increasing.
90.00	5400	17.070	200.0	50.0	43.0	27.0	32.0	36.0	Very cloudy appearance. Fines piping. High outflow, and fluctuating.
100.00	6000	17.010	200.0	48.0	44.0	37.0	30.0	36.0	Very cloudy appearance. Fines piping. High outflow, and fluctuating.
110.00	6600	20.580	250.0	48.0	46.0	41.0	33.0	37.0	Very cloudy appearance. Fines piping. Very high outflow, and increasing slowly.
120.00	7200	21.900	250.0	47.0	45.0	40.0	33.0	37.0	Very cloudy appearance. Fines and sands piping. Very high outflow, and increasing slowly. Stop tes

Note : Deduct 6mm to give true depth of water from water surface to top of test sample within seepage cell.

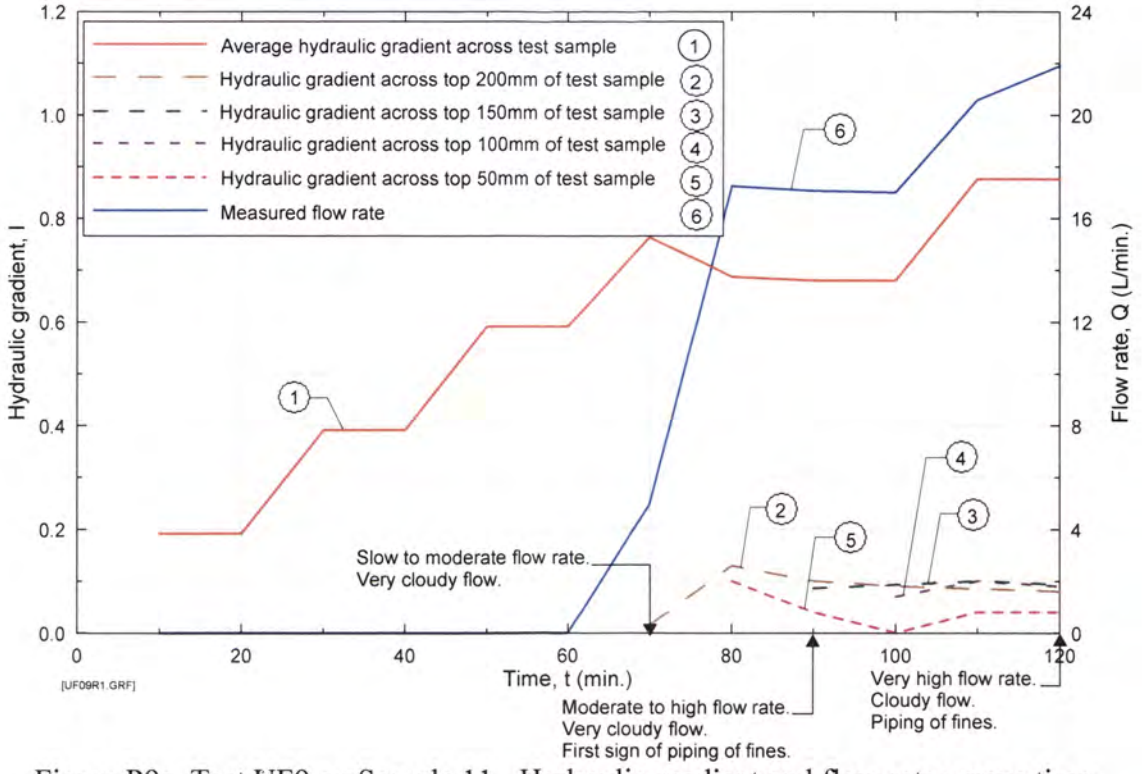

Figure P9a Test UF9 on Sample 11 - Hydraulic gradient and flow rate versus time. Sample compacted to 95.0% of Standard Maximum Dry Density.

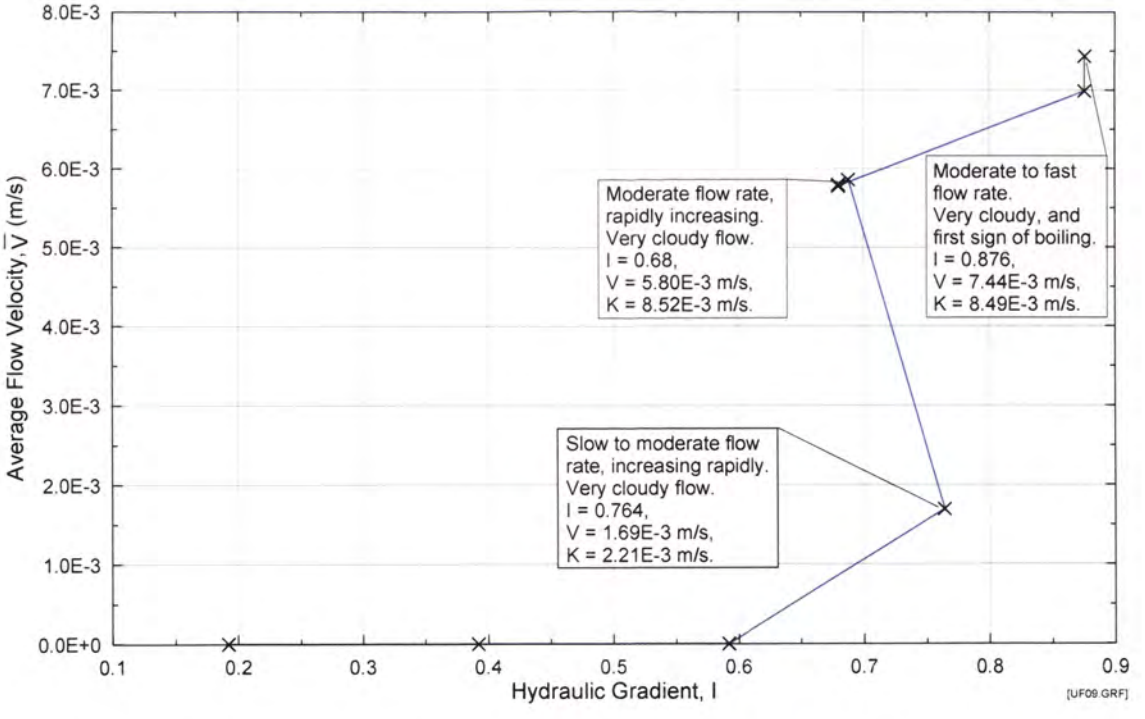

Figure P9b Test UF9 on Sample 11 – Average flow velocity versus average hydraulic gradient. Sample compacted to 95.0% of Standard Maximum Dry Density.

Upward flow test No. UF10 Test Records

UPWARD FLOW SUFFUSION TEST
Test Data

Test No. :	**Suffusion Upflow 010 07/02/02**	
Soil Sample :	**Suffusion Test Blend No. 6**	
Max. dry density :	2.234	Mg/m3
Optimum moisture content (OWC) :	7.18%	
Relative compaction :	95.0%	
Actual compaction from test:	94.9%	
Moisture content during conditioning :	7.18%	
Targeted moisture content :	7.18%	
Moisture content from test :	7.46%	
Fluid for conditioning soil :	tap water	
Eroding fluid :	tap water	
Eroding fluid mean temperature :	21.6	°C
Time/Date of Commencement of Soaking :	2.00pm 7/02/02	
Time/Date of Commencement of Test :	1.20pm 11/02/02	

Mix Ingredient	Mix Proportion (%)
Clay Q38	11.18
Silica 60G	8.20
Nepean Sand	34.16
5mm Blue Metal	27.33
10mm Bassalt	12.30
20mm Blue Metal	6.83
Total	100.00

Time (From Commencement) (mins)	Time (s)	Flowrate (L/min)	Head (mm) Inlet	200mm From top surface of sample	150mm From top surface of sample	100mm From top surface of sample	50mm From top surface of sample	Water Surface within cell. (See note)	Observations
10.00	600	0.006	150.0	0.0	0.0	0.0	0.0	5.0	Test started. Clear. Very low outflow.
20.00	1200	0.006	150.0	0.0	0.0	0.0	0.0	5.0	Clear. Very low outflow.
30.00	1800	0.014	200.0	0.0	0.0	0.0	0.0	5.0	Clear. Very low outflow.
40.00	2400	0.016	200.0	0.0	0.0	0.0	0.0	5.0	Clear. Very low outflow.
50.00	3000	0.020	250.0	0.0	0.0	0.0	0.0	5.0	Clear. Very low outflow.
60.00	3600	0.018	250.0	0.0	0.0	0.0	0.0	5.5	Clear. Very low outflow.
70.00	4200	0.024	300.0	0.0	0.0	0.0	0.0	5.5	Clear. Very low outflow.
80.00	4800	0.028	300.0	0.0	0.0	0.0	0.0	5.5	Clear. Very low outflow.
90.00	5400	0.030	350.0	0.0	0.0	0.0	0.0	5.5	Clear. Very low outflow.
100.00	6000	0.036	350.0	0.0	0.0	0.0	0.0	6.0	Clear. Very low outflow.
110.00	6600	0.040	400.0	0.0	0.0	0.0	0.0	6.0	Clear. Very low outflow.
120.00	7200	0.044	400.0	0.0	0.0	0.0	0.0	6.0	Clear. Very low outflow.
130.00	7800	0.044	450.0	0.0	0.0	0.0	0.0	6.0	Clear. Very low outflow.
140.00	8400	0.050	450.0	0.0	0.0	0.0	0.0	7.0	Clear. Very low outflow.
150.00	9000	0.048	500.0	0.0	0.0	0.0	0.0	7.0	Clear. Very low outflow.
160.00	9600	0.060	500.0	0.0	34.0	0.0	0.0	7.0	Clear. Very low outflow. Test paused, then restarted.
170.00	10200	0.068	550.0	0.0	65.0	40.0	0.0	7.0	Clear. Very low outflow.
180.00	10800	0.074	550.0	0.0	67.0	48.0	0.0	7.0	Clear. Very low outflow.

Upward flow test No. UF10 Test Records (Cont'd)

Time (From Commencement) (mins)	Time (s)	Flowrate (L/min)	Head (mm)						Observations
			Inlet	200mm From top surface of sample	150mm From top surface of sample	100mm From top surface of sample	50mm From top surface of sample	Water Surface within cell. (See note)	
190.00	11400	0.074	600.0	0.0	76.0	60.0	1.0	7.0	Clear. Very low outflow.
200.00	12000	0.076	600.0	0.0	76.0	60.0	1.0	7.0	Clear. Very low outflow.
210.00	12600	0.082	650.0	0.0	78.0	61.0	1.0	7.0	Clear. Very low outflow.
220.00	13200	0.084	650.0	0.0	79.0	62.0	1.0	7.0	Clear. Very low outflow.
230.00	13800	0.092	700.0	0.0	88.0	67.0	1.0	7.0	Clear. Very low outflow.
240.00	14400	0.094	700.0	0.0	88.0	67.0	1.0	7.0	Clear. Very low outflow.
250.00	15000	0.098	750.0	0.0	96.0	73.0	1.0	7.0	Clear. Very low outflow.
260.00	15600	0.102	750.0	0.0	96.0	74.0	1.0	7.0	Clear. Very low outflow.
270.00	16200	0.106	800.0	0.0	102.0	80.0	1.0	7.0	Clear. Very low outflow.
280.00	16800	0.110	800.0	0.0	103.0	81.0	1.0	7.0	Clear. Very low outflow.
290.00	17400	0.110	850.0	0.0	104.0	82.0	1.0	7.0	Clear. Very low outflow.
300.00	18000	0.118	850.0	0.0	100.0	79.0	1.0	7.0	Clear. Very low outflow.
310.00	18600	0.116	900.0	0.0	104.0	83.0	1.0	7.0	Clear. Very low outflow.
320.00	19200	0.118	900.0	0.0	104.0	83.0	1.0	7.0	Clear. Very low outflow.
330.00	19800	0.120	950.0	0.0	110.0	88.0	1.0	7.0	Clear. Very low outflow.
340.00	20400	0.120	950.0	0.0	110.0	88.0	1.0	7.0	Clear. Very low outflow.
350.00	21000	0.124	1000.0	0.0	110.0	88.0	1.0	7.0	Clear. Very low outflow.
360.00	21600	0.124	1000.0	0.0	98.0	87.0	1.0	7.0	Clear. Very low outflow.
370.00	22200	0.126	1050.0	0.0	110.0	90.0	1.0	7.0	Clear. Very low outflow.
380.00	22800	0.128	1050.0	0.0	112.0	90.0	1.0	7.0	Clear. Very low outflow.
390.00	23400	0.124	1100.0	0.0	115.0	92.0	1.0	7.0	Clear. Very low outflow.
400.00	24000	0.124	1100.0	0.0	115.0	92.0	1.0	7.0	Clear. Very low outflow.
410.00	24600	0.126	1150.0	0.0	117.0	95.0	1.0	7.0	Clear. Very low outflow.
420.00	25200	0.126	1150.0	0.0	117.0	95.0	1.0	7.0	Clear. Very low outflow.
430.00	25800	0.128	1200.0	0.0	119.0	97.0	1.0	7.0	Clear. Very low outflow.
440.00	26400	0.126	1200.0	0.0	119.0	97.0	1.0	7.0	Clear. Very low outflow.
450.00	27000	0.136	1250.0	0.0	121.0	99.0	1.0	7.0	Clear. Very low outflow.
460.00	27600	0.138	1250.0	0.0	121.0	99.0	1.0	7.0	Clear. Very low outflow.
470.00	28200	0.140	1300.0	0.0	123.0	101.0	1.0	7.0	Clear. Very low outflow.
480.00	28800	0.140	1300.0	0.0	123.0	101.0	1.0	7.0	Clear. Very low outflow. Limit of test head, test stopped.

Note : Deduct 6mm to give true depth of water from water surface to top of test sample within seepage cell.

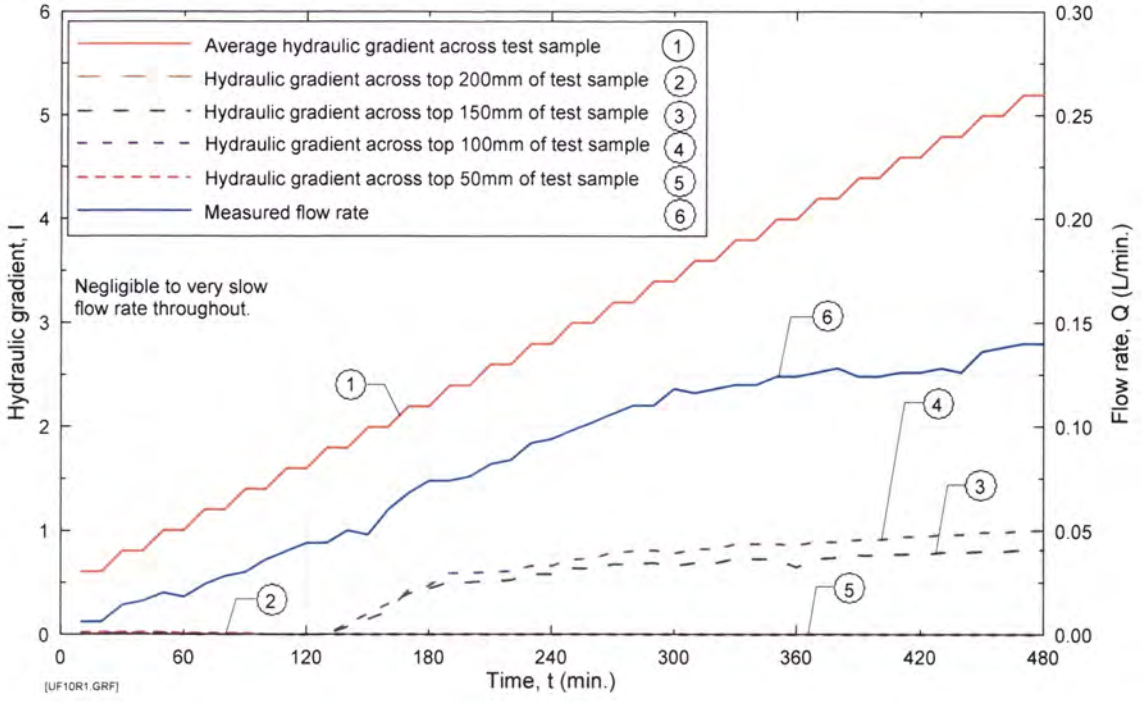

Figure P10a Test UF10 on Sample 6 - Hydraulic gradient and flow rate versus time. Sample compacted to 95.0% of Standard Maximum Dry Density.

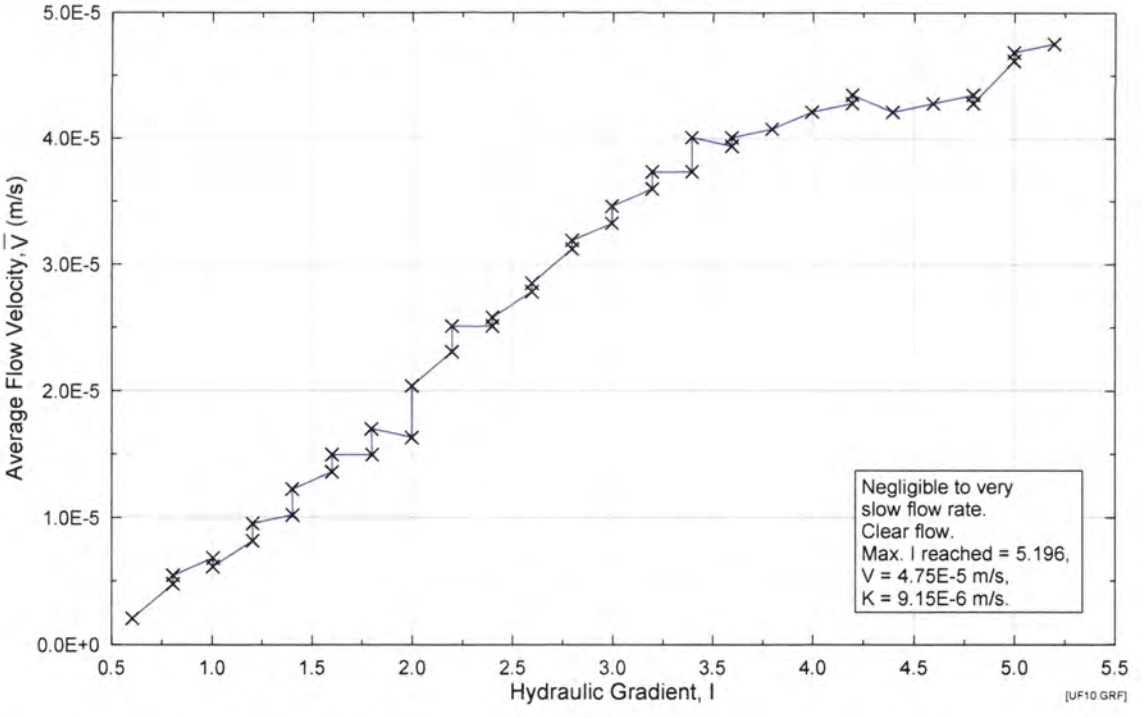

Figure P10b Test UF10 on Sample 6 – Average flow velocity versus average hydraulic gradient. Sample compacted to 95.0% of Standard Maximum Dry Density.

Upward flow test No. UF11 Test Records

UPWARD FLOW SUFFUSION TEST
Test Data

Test No. :	**Suffusion Upflow 011 19/02/02**	
Soil Sample :	**Suffusion Test Blend No. 13**	
Max. dry density :	1.921	Mg/m3
Optimum moisture content (OWC) :	7.10%	
Relative compaction :	95.0%	
Actual compaction from test:	95.2%	
Moisture content during conditioning :	7.10%	
Targeted moisture content :	7.10%	
Moisture content from test :	6.87%	
Fluid for conditioning soil :	tap water	
Eroding fluid :	tap water	
Eroding fluid mean temperature :	21.6	°C
Time/Date of Commencement of Soaking :	2.00pm 7/02/02	
Time/Date of Commencement of Test :	1.20pm 11/02/02	

Mix Ingredient	Mix Proportion (%)
Clay Q38	5.51
Silica 60G	4.54
Nepean Sand	0.00
5mm Blue Metal	9.84
10mm Bassalt	61.95
20mm Blue Metal	18.26
Total	100.00

Time (From Commencement) (mins)	Time (s)	Flowrate (L/min)	Head (mm) Inlet	200mm From top surface of sample	150mm From top surface of sample	100mm From top surface of sample	50mm From top surface of sample	Water Surface within cell. (See note)	Observations
10.00	600	5.670	50.0	30.0	21.0	19.0	12.0	17.0	Test started. Clear. Moderate outflow.
20.00	1200	5.730	50.0	30.0	21.0	19.0	13.0	18.0	Clear. Moderate outflow.
30.00	1800	9.000	100.0	52.0	36.0	33.0	17.0	21.0	Clear. Moderate outflow.
40.00	2400	9.060	100.0	52.0	36.0	33.0	17.0	21.0	Clear. Moderate outflow.
50.00	3000	11.340	150.0	75.0	49.0	44.0	21.0	23.0	Clear. High outflow.
60.00	3600	11.490	150.0	75.0	49.0	44.0	21.0	23.0	Clear. High outflow, and fluctuating slightly.
70.00	4200	10.980	150.0	75.0	49.0	44.0	21.0	23.0	Clear. High outflow, and fluctuating slightly.
80.00	4800	11.220	150.0	75.0	49.0	44.0	21.0	23.0	Clear. High outflow, and fluctuating slightly.
90.00	5400	14.040	200.0	95.0	60.0	52.0	22.0	23.0	Clear. High outflow.
100.00	6000	13.980	200.0	95.0	60.0	52.0	22.0	23.0	Clear. High outflow.
110.00	6600	16.650	250.0	117.0	73.0	61.0	27.0	24.0	Clear. High outflow.
120.00	7200	16.080	250.0	116.0	74.0	62.0	27.0	24.0	Clear. High outflow, and fluctuating slightly. Test paused and then restarted.
130.00	7800	15.870	250.0	114.0	72.0	61.0	27.0	24.0	Clear. High outflow, and fluctuating slightly.
140.00	8400	16.260	250.0	114.0	72.0	61.0	27.0	24.0	Clear. High outflow, and fluctuating slightly.
150.00	9000	16.260	250.0	115.0	72.0	61.0	27.0	24.0	Clear. High outflow, and fluctuating slightly.
160.00	9600	19.140	300.0	133.0	82.0	70.0	28.0	25.0	Clear. Very high outflow, and fluctuating slightly.
170.00	10200	18.390	300.0	134.0	82.0	71.0	28.0	25.0	Clear. Very high outflow, and fluctuating slightly.
180.00	10800	17.940	300.0	134.0	82.0	71.0	28.0	25.0	Clear. Very high outflow, and fluctuating slightly.
190.00	11400	17.760	300.0	134.0	82.0	71.0	28.0	25.0	Clear. Very high outflow, and fluctuating slightly. Test stopped.

Note : Deduct 6mm to give true depth of water from water surface to top of test sample within seepage cell.

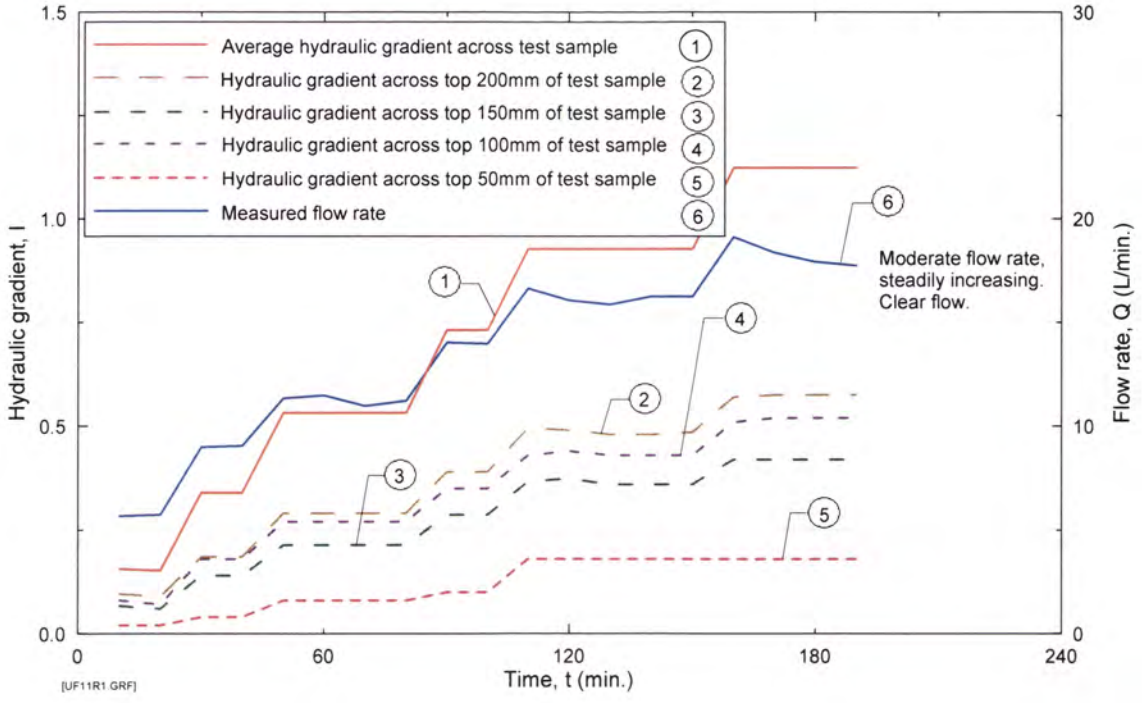

Figure P11a Test UF11 on Sample 13 - Hydraulic gradient and flow rate versus time. Sample compacted to 95.0% of Standard Maximum Dry Density.

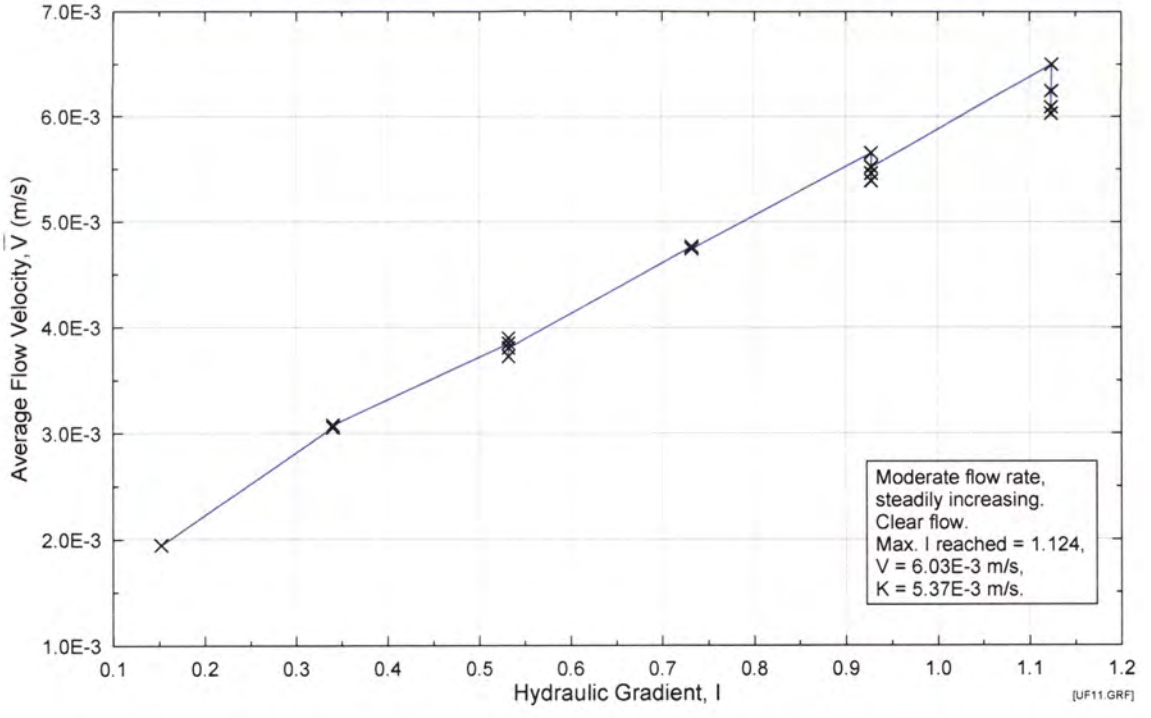

Figure P11b Test UF11 on Sample 13 – Average flow velocity versus average hydraulic gradient. Sample compacted to 95.0% of Standard Maximum Dry Density.

Upward flow test No. UF12 Test Records

UPWARD FLOW SUFFUSION TEST
Test Data

Test No. :	**Suffusion Upflow 012 4/03/02**
Soil Sample :	**Suffusion Test Blend No. 14a**
Max. dry density :	2.040 Mg/m3
Optimum moisture content (OWC) :	11.10%
Relative compaction :	95.0%
Actual compaction from test:	96.0%
Moisture content during conditioning :	11.10%
Targeted moisture content :	11.10%
Moisture content from test :	10.30%
Fluid for conditioning soil :	tap water
Eroding fluid :	tap water
Eroding fluid mean temperature :	22.4 °C
Time/Date of Commencement of Soaking :	10.30 am 01/03/02
Time/Date of Commencement of Test :	9.00am 04/03/02

Mix Ingredient	Mix Proportion (%)
Clay Q38	10.89
Silica 60G	11.08
Nepean Sand	0.00
5mm Blue Metal	0.00
10mm Bassalt	57.30
20mm Blue Metal	20.72
Total	100.00

Time (From Commencement) (mins)	Time (s)	Flowrate (L/min)	Head (mm) Inlet	200mm From top surface of sample	150mm From top surface of sample	100mm From top surface of sample	50mm From top surface of sample	Water Surface within cell. (See note)	Observations
10.00	600	1.420	50.0	0.0	0.0	29.0	5.0	10.0	Test started. Clear. Low outflow.
20.00	1200	1.440	50.0	0.0	0.0	29.0	5.0	10.0	Clear. Low outflow.
30.00	1800	2.140	100.0	0.0	0.0	56.0	6.0	11.0	Clear. Low outflow.
40.00	2400	2.140	100.0	0.0	63.0	56.0	6.0	11.0	Clear. Low outflow.
50.00	3000	2.880	150.0	136.0	105.0	82.0	9.0	13.0	Clear. Low outflow.
60.00	3600	2.860	150.0	138.0	106.0	82.0	9.0	13.0	Clear. Low outflow.
70.00	4200	3.580	200.0	183.0	137.0	106.0	10.0	14.0	Slightly cloudy appearance and bubbling, Low outflow.
80.00	4800	3.600	200.0	175.0	139.0	106.0	10.0	14.0	Clear. Low outflow.
90.00	5400	4.140	250.0	224.0	180.0	130.0	11.0	14.0	Slightly cloudy appearance and bubbling, Low outflow.
100.00	6000	4.140	250.0	224.0	180.0	130.0	11.0	14.0	Clear. Low outflow.
110.00	6600	5.000	300.0	248.0	191.0	153.0	12.0	14.0	Slightly cloudy appearance and bubbling, Moderate outflow.
120.00	7200	5.020	300.0	246.0	183.0	153.0	12.0	15.0	Clear. Moderate outflow.
130.00	7800	5.660	350.0	285.0	230.0	179.0	13.0	15.0	Slightly cloudy appearance and bubbling, Moderate outflow.
140.00	8400	5.700	350.0	285.0	209.0	178.0	13.0	15.0	Clear. Moderate outflow.
150.00	9000	6.420	400.0	319.0	232.0	199.0	14.0	16.0	Slightly cloudy appearance and bubbling, Moderate outflow.
160.00	9600	6.420	400.0	319.0	230.0	199.0	14.0	17.0	Clear. Moderate outflow.
170.00	10200	7.140	450.0	361.0	261.0	220.0	15.0	18.0	Slightly cloudy appearance and bubbling, Moderate outflow.
180.00	10800	7.460	450.0	330.0	282.0	216.0	15.0	19.0	Clear. Moderate outflow.

Upward flow test No. UF12 Test Records (Cont'd)

Time (From Commencement) (mins)	Time (s)	Flowrate (L/min)	Head (mm)						Observations
			Inlet	200mm From top surface of sample	150mm From top surface of sample	100mm From top surface of sample	50mm From top surface of sample	Water Surface within cell. (See note)	
190.00	11400	7.540	450.0	330.0	282.0	219.0	15.0	20.0	Clear. Moderate outflow.
200.00	12000	8.260	500.0	366.0	306.0	238.0	20.0	21.0	Slightly cloudy appearance and bubbling, Moderate outflow.
210.00	12600	8.140	500.0	365.0	305.0	236.0	20.0	21.0	Clear. Moderate outflow.
220.00	13200	8.980	550.0	400.0	330.0	257.0	22.0	21.0	Slightly cloudy appearance and bubbling, Moderate outflow.
230.00	13800	9.220	550.0	400.0	326.0	258.0	22.0	21.0	Clear. Moderate outflow.
240.00	14400	9.040	550.0	400.0	326.0	258.0	22.0	21.0	Clear. Moderate outflow.
250.00	15000	10.120	600.0	432.0	346.0	273.0	22.0	22.0	Slightly cloudy appearance and bubbling, High outflow.
260.00	15600	10.180	600.0	430.0	345.0	272.0	25.0	22.0	Clear. High outflow.
270.00	16200	10.880	650.0	464.0	407.0	296.0	26.0	23.0	Slightly cloudy appearance and bubbling, High outflow.
280.00	16800	10.900	650.0	462.0	405.0	289.0	28.0	23.0	Clear. High outflow.
290.00	17400	11.520	700.0	497.0	425.0	309.0	26.0	24.0	Slightly cloudy appearance and bubbling, High outflow.
300.00	18000	11.940	700.0	495.0	421.0	303.0	28.0	24.0	Clear. High outflow.
310.00	18600	12.000	700.0	494.0	417.0	302.0	27.0	24.0	Clear. High outflow.
320.00	19200	12.180	750.0	522.0	439.0	320.0	29.0	25.0	Slightly cloudy appearance and bubbling, High outflow.
330.00	19800	14.460	750.0	521.0	435.0	321.0	29.0	25.0	Clear. High outflow, and fluctuating.
340.00	20400	13.050	750.0	517.0	426.0	317.0	27.0	25.0	Clear. High outflow, and fluctuating.
350.00	21000	14.280	800.0	549.0	452.0	337.0	29.0	25.0	Slightly cloudy appearance and bubbling, High outflow.
360.00	21600	13.950	800.0	547.0	447.0	299.0	29.0	25.0	Clear. High outflow, and fluctuating.
370.00	22200	15.810	850.0	573.0	469.0	302.0	31.0	25.0	Slightly cloudy appearance and bubbling, Very high outflow.
380.00	22800	15.150	850.0	570.0	482.0	284.0	31.0	25.0	Clear. Very high outflow, and fluctuating.
390.00	23400	16.380	900.0	600.0	504.0	295.0	31.0	25.0	Clear. Very high outflow, and fluctuating.
400.00	24000	16.500	900.0	596.0	491.0	290.0	31.0	25.0	Clear. Very high outflow, and fluctuating.
410.00	24600	16.860	950.0	625.0	505.0	302.0	33.0	26.0	Slightly cloudy appearance and bubbling, Very high outflow.
420.00	25200	17.730	950.0	622.0	503.0	304.0	36.0	26.0	Clear. Very high outflow, and fluctuating.
430.00	25800	17.640	950.0	619.0	500.0	302.0	33.0	26.0	Clear. Very high outflow, and fluctuating.
440.00	26400	18.000	1000.0	641.0	516.0	312.0	34.0	27.0	Slightly cloudy appearance and bubbling, Very high outflow.
450.00	27000	19.080	1000.0	637.0	512.0	312.0	34.0	27.0	Clear, with fines bubbling more. Very high outflow, and fluctuating. Stop test.

Note : Deduct 6mm to give true depth of water from water surface to top of test sample within seepage cell.

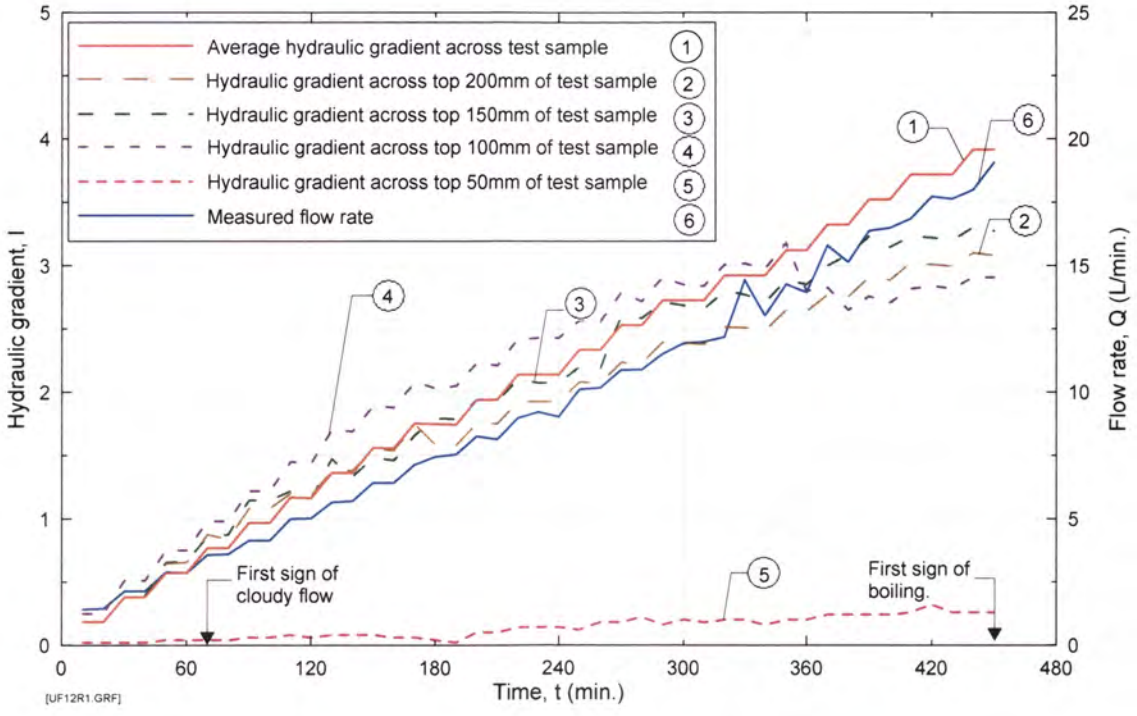

Figure P12a Test UF12 on Sample 14A - Hydraulic gradient and flow rate versus time. Sample compacted to 96.0% of Standard Maximum Dry Density.

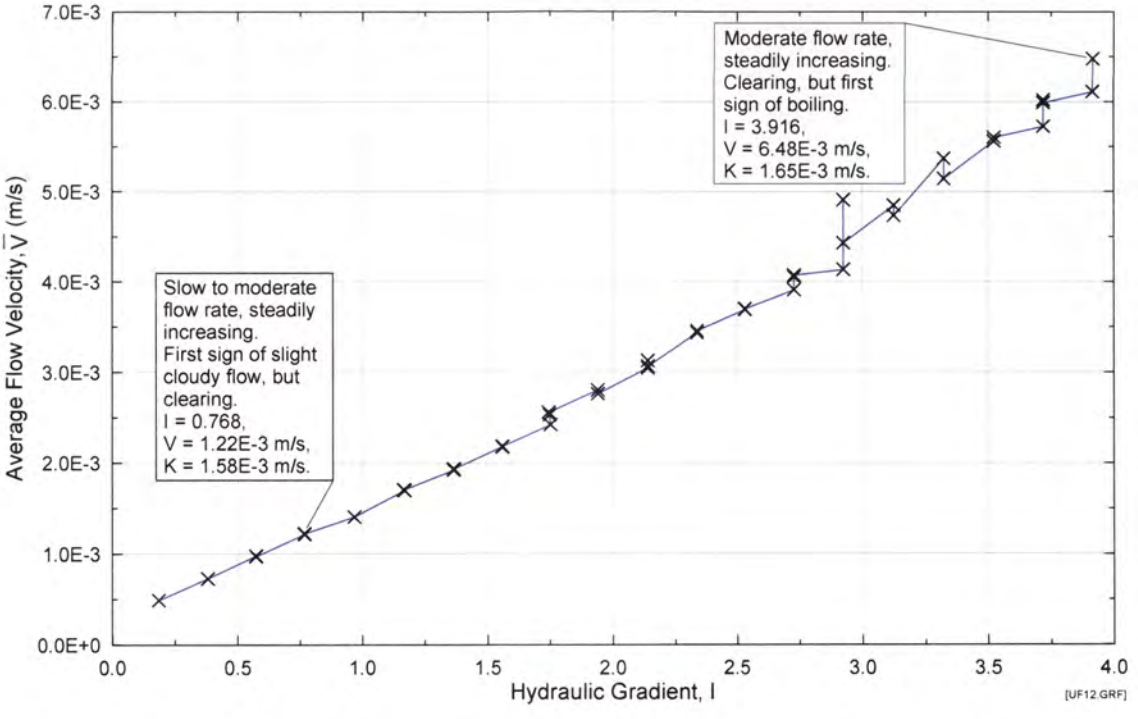

Figure P12b Test UF12 on Sample 14A – Average flow velocity versus average hydraulic gradient. Sample compacted to 96.0% of Standard Maximum Dry Density.

Upward flow test No. UF13 Test Records

UPWARD FLOW SUFFUSION TEST
Test Data

Test No. :	**Suffusion Upflow 013 01/10/02**	
Soil Sample :	**Suffusion Test Blend No. 5**	
Max. dry density :	2.119	Mg/m3
Optimum moisture content (OWC) :	8.48%	
Relative compaction :	95.0%	
Actual compaction from test:	94.8%	
Moisture content during conditioning :	8.48%	
Targeted moisture content :	8.48%	
Moisture content from test :	8.83%	
Fluid for conditioning soil :	tap water	
Eroding fluid :	tap water	
Eroding fluid mean temperature :	20.5 °C	
Time/Date of Commencement of Soaking :	10.30 am 30/09/02	
Time/Date of Commencement of Test :	10.00am 01/10/02	

Mix Ingredient	Mix Proportion (%)
Clay Q38	5.89
Silica 60G	1.18
Nepean Sand	41.20
5mm Blue Metal	34.73
10mm Bassalt	11.77
20mm Blue Metal	5.24
Total	100.00

Time (From Commencement) (mins)	Time (s)	Flowrate (L/min)	Head (mm) Inlet	200mm From top surface of sample	150mm From top surface of sample	100mm From top surface of sample	50mm From top surface of sample	Water Surface within cell. (See note)	Observations
10.00	600	0.0120	50.0	0.0	0.0	0.0	0.0	6.0	Test started. Clear. Very low outflow, increasing very slightly.
20.00	1200	0.0120	50.0	0.0	0.0	0.0	0.0	6.0	Clear. Very low outflow, increasing very slightly.
30.00	1800	0.0240	100.0	0.0	0.0	0.0	0.0	6.0	Clear. Very low outflow, increasing very slightly.
40.00	2400	0.0240	100.0	0.0	0.0	0.0	0.0	6.0	Clear. Very low outflow, increasing very slightly.
50.00	3000	0.0360	150.0	0.0	0.0	0.0	0.0	6.0	Clear. Very low outflow, increasing very slightly.
60.00	3600	0.0360	150.0	0.0	0.0	0.0	0.0	6.0	Clear. Very low outflow, increasing very slightly.
70.00	4200	0.4500	200.0	0.0	0.0	0.0	0.0	6.0	Clear. Very low outflow, increasing very slightly.
80.00	4800	0.4500	200.0	0.0	0.0	0.0	0.0	6.0	Clear. Very low outflow, increasing very slightly.
90.00	5400	0.5700	250.0	0.0	0.0	0.0	0.0	7.0	Clear. Very low outflow, increasing very slightly.
100.00	6000	0.5400	250.0	0.0	0.0	0.0	0.0	7.0	Clear. Very low outflow, increasing very slightly.
110.00	6600	0.6450	300.0	291.0	200.0	0.0	0.0	7.0	Clear. Very low outflow, increasing very slightly.
120.00	7200	0.6600	300.0	293.0	215.0	0.0	0.0	7.0	Clear. Very low outflow, increasing very slightly.
130.00	7800	0.8400	350.0	330.0	240.0	0.0	0.0	7.0	Clear. Very low outflow, increasing very slightly.
140.00	8400	0.8400	350.0	341.0	250.0	0.0	0.0	7.0	Clear. Very low outflow, increasing very slightly.
150.00	9000	0.9600	400.0	380.0	285.0	0.0	0.0	7.0	Clear. Very low outflow, increasing very slightly.
160.00	9600	0.9600	400.0	388.0	292.0	0.0	0.0	7.0	Clear. Very low outflow, increasing very slightly.
170.00	10200	1.2000	450.0	427.0	301.0	15.0	0.0	8.0	Clear. Very low outflow, increasing very slightly.
180.00	10800	1.2000	450.0	432.0	305.0	24.0	0.0	8.0	Clear. Very low outflow, increasing very slightly.

Upward flow test No. UF13 Test Records (Cont'd)

Time (From Commencement) (mins)	Time (s)	Flowrate (L/min)	Head (mm) Inlet	200mm From top surface of sample	150mm From top surface of sample	100mm From top surface of sample	50mm From top surface of sample	Water Surface within cell. (See note)	Observations
190.00	11400	1.3500	500.0	472.0	340.0	95.0	0.0	8.0	Clear. Very low outflow, increasing very slightly.
200.00	12000	1.3500	500.0	478.0	344.0	100.0	0.0	9.0	Clear. Very low outflow, increasing very slightly.
210.00	12600	1.5600	550.0	518.0	360.0	98.0	0.0	10.0	Clear. Very low outflow, increasing very slightly.
220.00	13200	1.5600	550.0	523.0	366.0	103.0	0.0	10.0	Clear. Very low outflow, increasing very slightly.
230.00	13800	1.8000	600.0	562.0	427.0	125.0	0.0	11.0	Clear. Very low outflow, increasing very slightly.
240.00	14400	1.8000	600.0	569.0	431.0	126.0	1.0	11.0	Clear. Very low outflow, increasing very slightly.
250.00	15000	2.0700	650.0	612.0	447.0	136.0	1.0	11.0	Clear. Low outflow, increasing very slightly.
260.00	15600	2.0700	650.0	615.0	448.0	136.0	1.0	11.0	Clear. Low outflow, increasing very slightly.
270.00	16200	2.2800	700.0	659.0	479.0	144.0	1.0	12.0	Clear. Low outflow, increasing very slightly.
280.00	16800	2.2800	700.0	660.0	479.0	145.0	2.0	12.0	Clear. Low outflow, increasing very slightly.
290.00	17400	2.4500	750.0	707.0	511.0	152.0	3.0	12.0	Clear. Low outflow, increasing very slightly.
300.00	18000	2.4600	750.0	708.0	511.0	153.0	4.0	12.0	Clear. Low outflow, increasing very slightly.
310.00	18600	2.7000	800.0	731.0	532.0	159.0	8.0	13.0	Slightly cloudy. Low outflow, increasing slightly.
320.00	19200	2.7000	800.0	733.0	533.0	159.0	9.0	13.0	Slightly cloudy. Low outflow, increasing slightly.
330.00	19800	3.0000	850.0	800.0	550.0	164.0	20.0	13.0	Slightly cloudy, occasional bubbles. Low outflow, increasing slightly.
340.00	20400	3.0000	850.0	800.0	546.0	167.0	47.0	13.0	Slightly cloudy, occasional bubbles. Low outflow, increasing slightly.
350.00	21000	3.3600	900.0	848.0	590.0	170.0	44.0	13.0	Slightly cloudy, occasional bubbles. Low outflow, increasing slightly.
360.00	21600	3.3600	900.0	848.0	590.0	170.0	44.0	13.0	Slightly cloudy, occasional bubbles. Low outflow, increasing slightly.
370.00	22200	3.4200	950.0	913.0	582.0	185.0	67.0	13.0	Cloudy and increasing, occasional bubbles increasing. Low outflow, increasing slightly.
380.00	22800	3.4800	950.0	916.0	583.0	187.0	78.0	13.0	Cloudy and increasing, occasional bubbles increasing. Low outflow, increasing slightly.
390.00	23400	3.6400	1000.0	969.0	569.0	180.0	103.0	14.0	Cloudy and increasing, occasional bubbles increasing, fines piping. Low outflow, increasing slightly.
400.00	24000	3.6400	1000.0	969.0	569.0	180.0	108.0	14.0	Cloudy and increasing, occasional bubbles increasing, fines piping. Low outflow, increasing slightly.
410.00	24600	4.3800	1050.0	1024.0	577.0	117.0	161.0	14.0	Cloudy and increasing, occasional bubbles increasing, fines piping. Low outflow, increasing slightly.
420.00	25200	4.3800	1050.0	1024.0	577.0	117.0	157.0	15.0	Cloudy and increasing, occasional bubbles increasing, fines piping. Low outflow, increasing slightly.
430.00	25800	5.1600	1100.0	1076.0	590.0	79.0	149.0	15.0	Cloudy and increasing, occasional bubbles increasing, fines piping. Moderate outflow, increasing slightly.
440.00	26400	5.1600	1100.0	1077.0	591.0	71.0	144.0	15.0	Cloudy and increasing, occasional bubbles increasing, fines piping. Moderate outflow, increasing slightly.
450.00	27000	5.7000	1150.0	1129.0	590.0	69.0	143.0	16.0	Cloudy and increasing, occasional bubbles increasing, fines piping. Moderate outflow, increasing slightly.
460.00	27600	5.7600	1150.0	1130.0	588.0	66.0	140.0	16.0	Cloudy and increasing, occasional bubbles increasing, fines piping. Moderate outflow, increasing slightly.
470.00	28200	6.3900	1200.0	1180.0	647.0	79.0	139.0	17.0	Very cloudy, bubbles increasing, fines piping increasing. Moderate outflow, increasing slowly.
480.00	28800	6.6300	1200.0	1180.0	652.0	81.0	140.0	17.0	Very cloudy, bubbles increasing, fines piping increasing. Moderate outflow, increasing slowly. Stop Test.

Note : Deduct 6mm to give true depth of water from water surface to top of test sample within seepage cell.

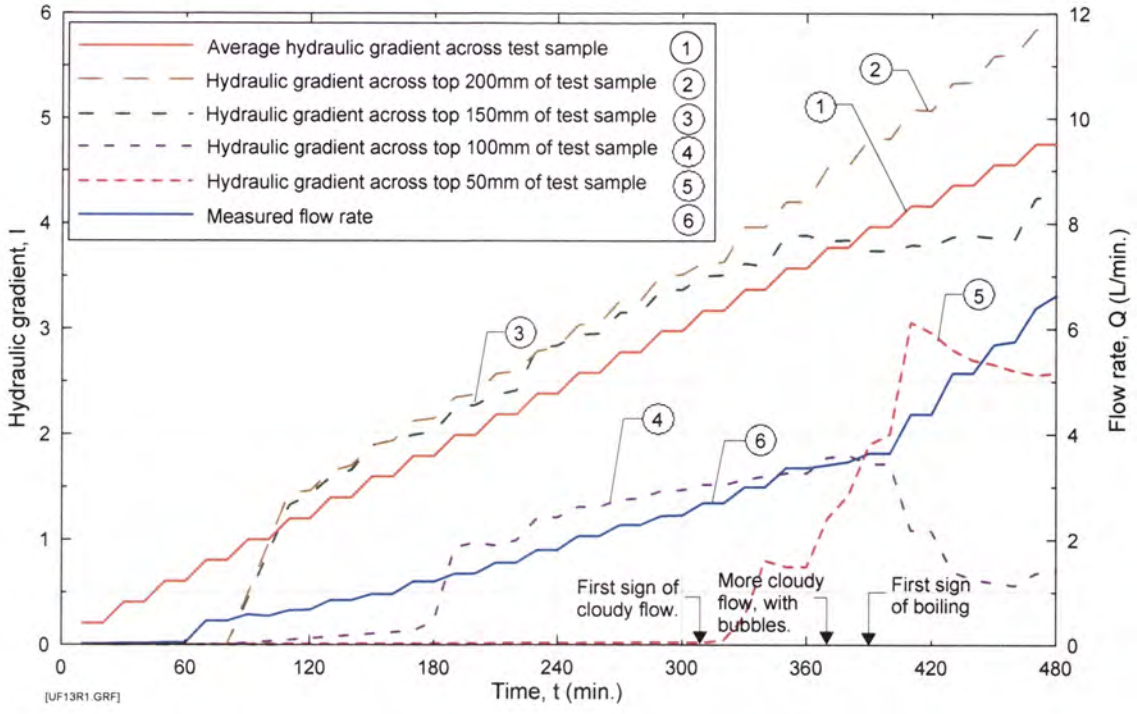

Figure P13a Test UF13 on Sample 5 - Hydraulic gradient and flow rate versus time. Sample compacted to 95.0% of Standard Maximum Dry Density.

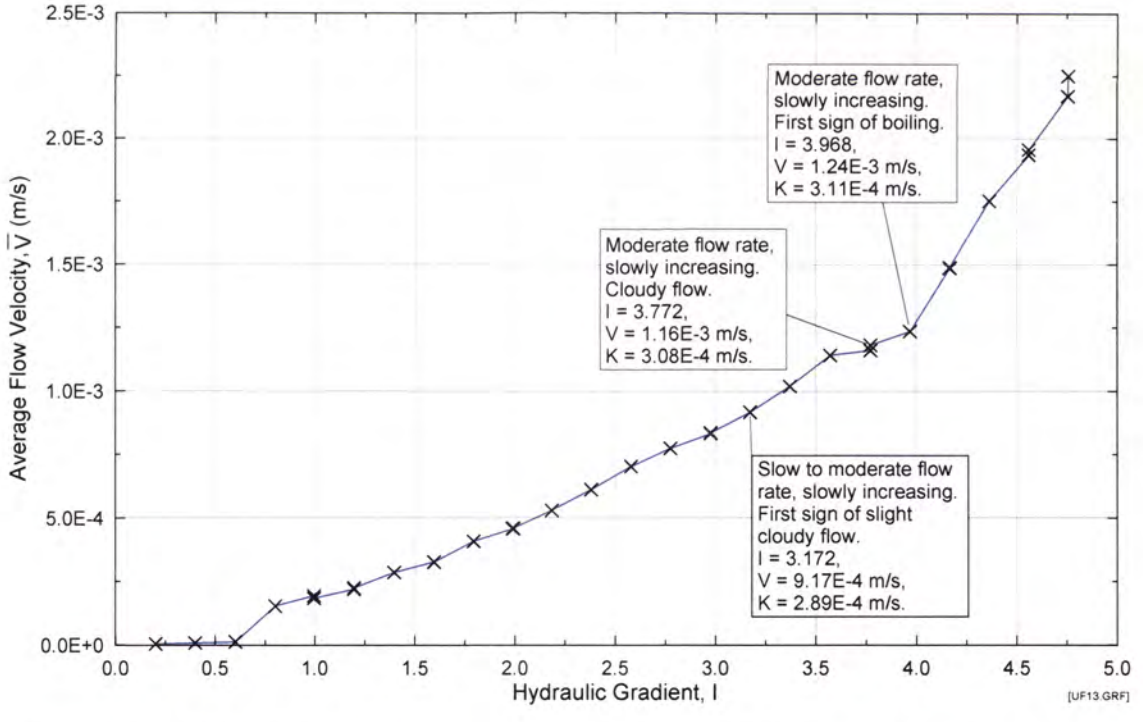

Figure P13b Test UF13 on Sample 5 – Average flow velocity versus average hydraulic gradient. Sample compacted to 95.0% of Standard Maximum Dry Density.

Upward flow test No. UF14 Test Records

UPWARD FLOW SUFFUSION TEST
Test Data

Test No. :	**Suffusion Upflow 014 28/10/02**
Soil Sample :	**Suffusion Test Blend No. 5**
Max. dry density :	2.119 Mg/m3
Optimum moisture content (OWC) :	8.48%
Relative compaction :	90.0%
Actual compaction from test:	89.6%
Moisture content during conditioning :	8.48%
Targeted moisture content :	8.48%
Moisture content from test :	8.81%
Fluid for conditioning soil :	tap water
Eroding fluid :	tap water
Eroding fluid mean temperature :	20.2 °C
Time/Date of Commencement of Soaking :	9.30 am 28/10/02
Time/Date of Commencement of Test :	11.00 am 28/10/02

Mix Ingredient	Mix Proportion (%)
Clay Q38	5.89
Silica 60G	1.18
Nepean Sand	41.20
5mm Blue Metal	34.73
10mm Bassalt	11.77
20mm Blue Metal	5.24
Total	100.00

Time (From Commencement) (mins)	Time (s)	Flowrate (L/min)	Head (mm) Inlet	200mm From top surface of sample	150mm From top surface of sample	100mm From top surface of sample	50mm From top surface of sample	Water Surface within cell. (See note)	Observations
10.00	600	0.0000	50.0	39.0	34.0	0.0	6.0	11.0	Test started. Slightly cloudy. Very low outflow, increasing very slightly.
20.00	1200	0.0480	50.0	39.0	34.0	0.0	6.0	11.0	Slightly cloudy. Very low outflow, increasing very slightly.
30.00	1800	0.1050	100.0	82.0	69.0	0.0	6.0	12.0	Slightly cloudy. Very low outflow, increasing very slightly.
40.00	2400	0.0990	100.0	84.0	72.0	0.0	6.0	12.0	Slightly cloudy. Very low outflow, increasing very slightly.
50.00	3000	0.1320	150.0	118.0	101.0	0.0	7.0	12.0	Slightly cloudy. Very low outflow, increasing very slightly.
60.00	3600	0.1320	150.0	120.0	101.0	0.0	7.0	12.0	Slightly cloudy. Very low outflow, increasing very slightly.
70.00	4200	0.1680	200.0	156.0	130.0	0.0	7.0	12.0	Slightly cloudy. Very low outflow, increasing very slightly.
80.00	4800	0.1710	200.0	158.0	134.0	0.0	7.0	12.0	Slightly cloudy. Very low outflow, increasing very slightly.
90.00	5400	0.1860	250.0	195.0	159.0	0.0	8.0	12.5	Slightly cloudy. Very low outflow, increasing very slightly.
100.00	6000	0.1800	250.0	195.0	158.0	0.0	8.0	12.5	Slightly cloudy. Very low outflow, increasing very slightly.
110.00	6600	0.2130	300.0	230.0	186.0	44.0	8.0	13.0	Slightly cloudy. Very low outflow, increasing very slightly.
120.00	7200	0.2070	300.0	230.0	186.0	45.0	8.0	13.0	Slightly cloudy. Very low outflow, increasing very slightly.
130.00	7800	0.2400	350.0	265.0	213.0	59.0	8.0	13.0	Slightly cloudy. Very low outflow, increasing very slightly.
140.00	8400	0.2460	350.0	265.0	213.0	59.0	8.0	13.0	Slightly cloudy. Very low outflow, increasing very slightly.
150.00	9000	0.3030	400.0	294.0	220.0	65.0	8.0	13.0	Slightly cloudy. Very low outflow, increasing very slightly.
160.00	9600	0.3000	400.0	295.0	223.0	69.0	8.0	13.0	Slightly cloudy. Very low outflow, increasing very slightly.
170.00	10200	10.5000	400.0	250.0	200.0	69.0	30.0	20.0	Very cloudy, steady piping of fines. High outflow, increasing very rapidly.
180.00	10800	20.6400	400.0	139.0	103.0	68.0	58.0	37.0	Very cloudy, steady piping of fines. Very high outflow, increasing very rapidly.
190.00	11400	21.6000	400.0	142.0	105.0	68.0	59.0	37.0	Very cloudy, steady piping of fines. Extremely high outflow, fluctuating slightly.
200.00	12000	21.6000	400.0	142.0	103.0	67.0	56.0	37.0	Very cloudy, steady piping of fines. Extremely high outflow, fluctuating slightly.
204.00	12240	21.1200	400.0	144.0	104.0	67.0	57.0	37.0	Very cloudy, steady piping of fines. Extremely high outflow, fluctuating slightly. Test stopped.

Note : Deduct 6mm to give true depth of water from water surface to top of test sample within seepage cell.

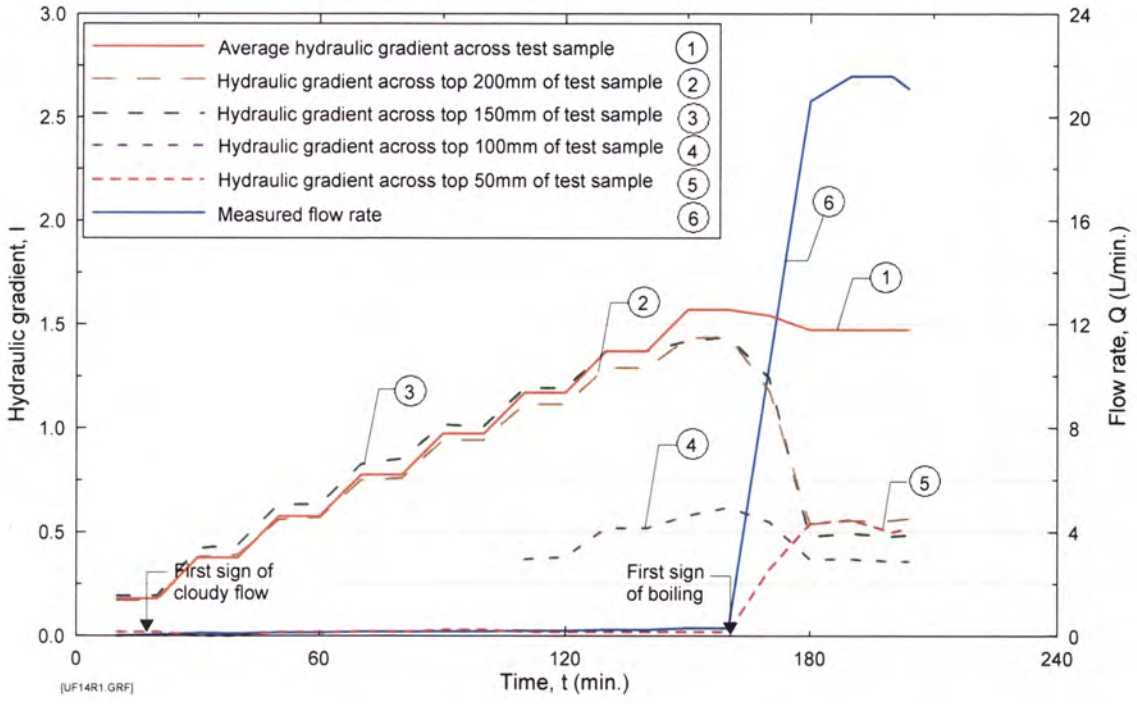

Figure P14a Test UF14 on Sample 5 - Hydraulic gradient and flow rate versus time. Sample compacted to 89.5% of Standard Maximum Dry Density.

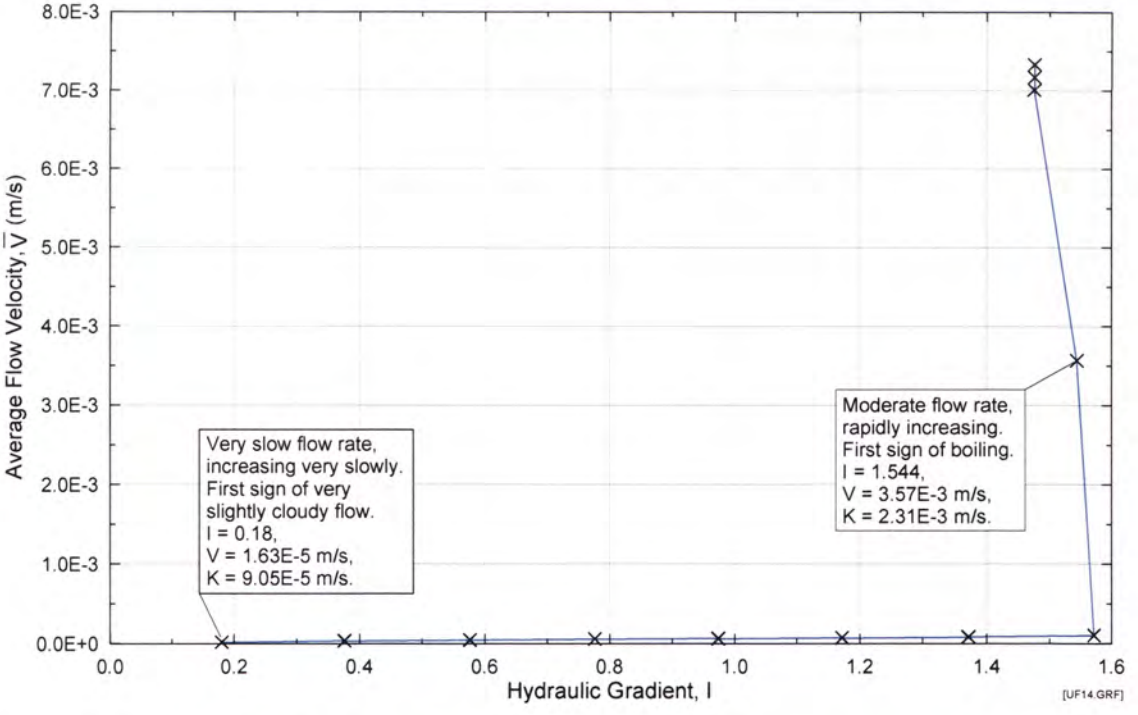

Figure P14b Test UF14 on Sample 5 – Average flow velocity versus average hydraulic gradient. Sample compacted to 89.5% of Standard Maximum Dry Density.

Upward flow test No. UF15 Test Records

Test No. :	**Suffusion Upflow 015 8/03/02**
Soil Sample :	**Suffusion Test Blend No. 14a**
Max. dry density :	2.040 Mg/m3
Optimum moisture content (OWC) :	11.10%
Relative compaction :	90.0%
Actual compaction from test:	90.1%
Moisture content during conditioning :	11.10%
Targeted moisture content :	11.10%
Moisture content from test :	11.22%
Fluid for conditioning soil :	tap water
Eroding fluid :	tap water
Eroding fluid mean temperature :	22.0 °C
Time/Date of Commencement of Soaking :	10.30 am 01/03/02
Time/Date of Commencement of Test :	9.00am 04/03/02

Mix Ingredient	Mix Proportion (%)
Clay Q38	10.89
Silica 60G	11.08
Nepean Sand	0.00
5mm Blue Metal	0.00
10mm Bassalt	57.30
20mm Blue Metal	20.72
Total	100.00

Time (From Commencement) (mins)	Time (s)	Flowrate (L/min)	Head (mm) Inlet	200mm From top surface of sample	150mm From top surface of sample	100mm From top surface of sample	50mm From top surface of sample	Water Surface within cell. (See note)	Observations
10.00	600	1.920	50.0	0.0	0.0	0.0	1.0	13.0	Test started. Slightly cloudy, slight bubbling.. Very low outflow, increasing very slightly.
20.00	1200	1.960	50.0	40.0	34.0	27.0	14.0	13.0	Clear. Very low outflow, increasing very slightly.
30.00	1800	3.080	100.0	76.0	63.0	48.0	28.0	14.0	Slightly cloudy, slight bubbling. Low outflow, increasing very slightly.
40.00	2400	3.080	100.0	77.0	62.0	47.0	28.0	14.0	Clear. Low outflow.
50.00	3000	4.300	150.0	107.0	83.0	67.0	43.0	15.0	Cloudy, regular bubbling. Low outflow, increasing very slightly.
60.00	3600	4.340	150.0	107.0	83.0	67.0	40.0	15.0	Clear. Low outflow, increasing very slightly.
70.00	4200	5.500	200.0	140.0	105.0	79.0	67.0	17.0	Cloudy, regular bubbling. Moderate outflow, increasing very slightly.
80.00	4800	5.560	200.0	139.0	105.0	79.0	67.0	17.0	Clear. Moderate outflow, increasing very slightly.
90.00	5400	6.660	250.0	171.0	133.0	96.0	72.0	20.0	Cloudy, regular bubbling. Moderate outflow, increasing very slightly.
100.00	6000	6.750	250.0	169.0	132.0	96.0	72.0	20.0	Clear. Moderate outflow, increasing very slightly.
110.00	6600	7.200	250.0	162.0	127.0	95.0	71.0	20.0	Clear. Moderate outflow, increasing very slightly.
120.00	7200	6.990	250.0	161.0	127.0	94.0	72.0	20.0	Clear. Moderate outflow, fluctuating slightly.
130.00	7800	8.550	300.0	189.0	154.0	112.0	76.0	21.0	Cloudy, regular bubbling. Moderate outflow, increasing very slightly.
140.00	8400	8.400	300.0	187.0	152.0	112.0	76.0	21.0	Clear. Moderate outflow, fluctuating slightly.
150.00	9000	9.270	350.0	207.0	166.0	120.0	81.0	23.0	Cloudy, regular bubbling, slight boiling of fines. Moderate outflow, increasing very slightly.
160.00	9600	9.450	350.0	200.0	157.0	115.0	62.0	23.0	Slightly cloudy, slight boiling of fines. Moderate outflow, increasing slightly.
170.00	10200	9.870	350.0	204.0	158.0	116.0	62.0	23.0	Clear, slight boiling of fines. Moderate outflow, fluctuating slightly.
180.00	10800	9.600	350.0	204.0	157.0	116.0	61.0	23.0	Clear, slight boiling of fines. Moderate outflow, fluctuating slightly.

Upward flow test No. UF15 Test Records (Cont'd)

Time (From Commencement) (mins)	Time (s)	Flowrate (L/min)	Head (mm)						Observations
			Inlet	200mm From top surface of sample	150mm From top surface of sample	100mm From top surface of sample	50mm From top surface of sample	Water Surface within cell. (See note)	
190.00	11400	11.880	400.0	218.0	165.0	119.0	54.0	24.0	Cloudy, regular bubbling, moderate boling of fines. High outflow, increasing very slightly.
200.00	12000	11.940	400.0	217.0	164.0	118.0	54.0	24.0	Clear, slight boiling of fines. High outflow, fluctuating slightly.
210.00	12600	13.440	450.0	228.0	174.0	122.0	53.0	25.0	Cloudy, regular bubbling, moderate boling of fines. High outflow, increasing very slightly.
220.00	13200	13.650	450.0	226.0	172.0	122.0	52.0	25.0	Clear, slight bubbling, slight boiling of fines. High outflow, fluctuating slightly.
230.00	13800	13.860	450.0	225.0	172.0	122.0	53.0	25.0	Clear, slight bubbling, slight boiling of fines. High outflow, fluctuating slightly.
240.00	14400	13.620	450.0	225.0	172.0	124.0	53.0	25.0	Clear, slight bubbling, slight boiling of fines. High outflow, fluctuating slightly.
250.00	15000	15.120	500.0	243.0	182.0	131.0	56.0	25.0	Very cloudy, regular bubbling, moderate boling of fines. Very high outflow, increasing very slightly.
260.00	15600	14.730	500.0	242.0	182.0	133.0	57.0	25.0	Slightly cloudy, slight bubbling, slight boiling of fines. Very high outflow, fluctuating slightly.
270.00	16200	16.560	550.0	259.0	190.0	136.0	54.0	26.0	Very cloudy, regular bubbling, moderate boling of fines. Very high outflow, increasing very slightly.
280.00	16800	16.620	550.0	257.0	192.0	143.0	54.0	27.0	Slightly cloudy, slight bubbling, slight boiling of fines. Very high outflow, fluctuating slightly.
290.00	17400	17.970	600.0	271.0	199.0	149.0	53.0	27.0	Very cloudy, regular bubbling, moderate boling of fines. Very high outflow, increasing very slightly.
300.00	18000	18.030	600.0	269.0	198.0	149.0	53.0	27.0	Slightly cloudy, slight bubbling, slight boiling of fines. Very high outflow, fluctuating slightly.
310.00	18600	20.160	650.0	282.0	206.0	149.0	53.0	28.0	Very cloudy, regular bubbling, moderate boling of fines. Extremely high outflow, increasing very slightly.
320.00	19200	21.000	650.0	282.0	206.0	149.0	53.0	28.0	Slightly cloudy, slight bubbling, slight boiling of fines. Extremely high outflow, fluctuating slightly. Test stopped.

Note : Deduct 6mm to give true depth of water from water surface to top of test sample within seepage cell.

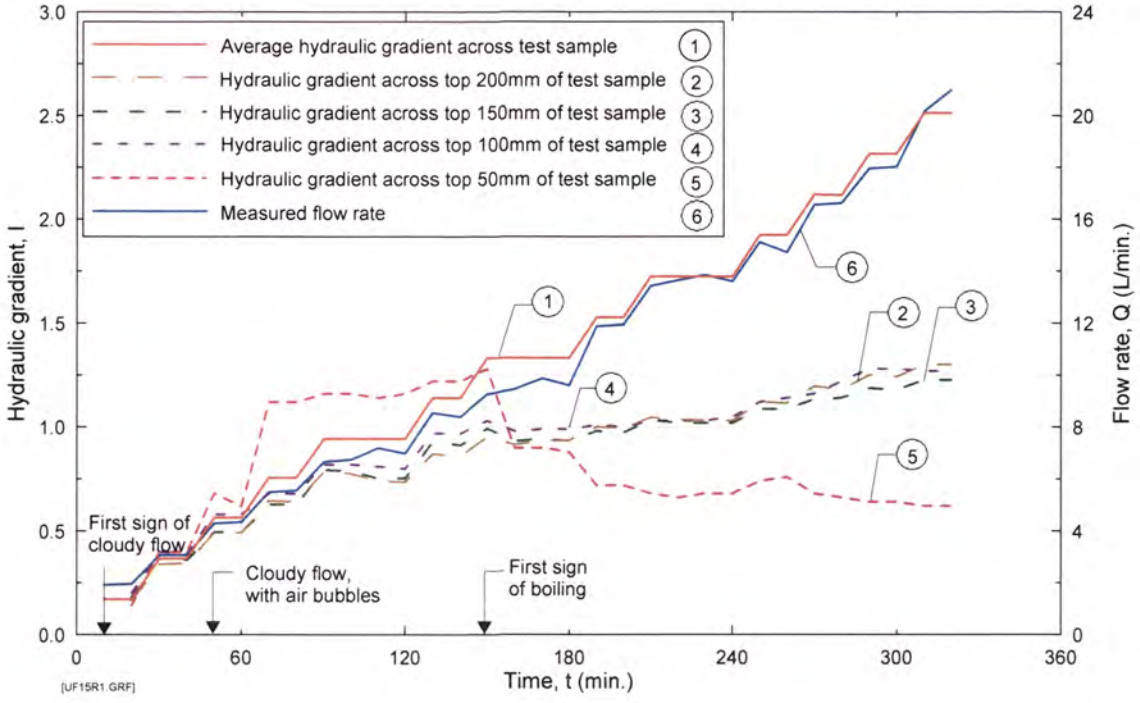

Figure P15a Test UF15 on Sample 14A - Hydraulic gradient and flow rate versus time. Sample compacted to 90.0% of Standard Maximum Dry Density.

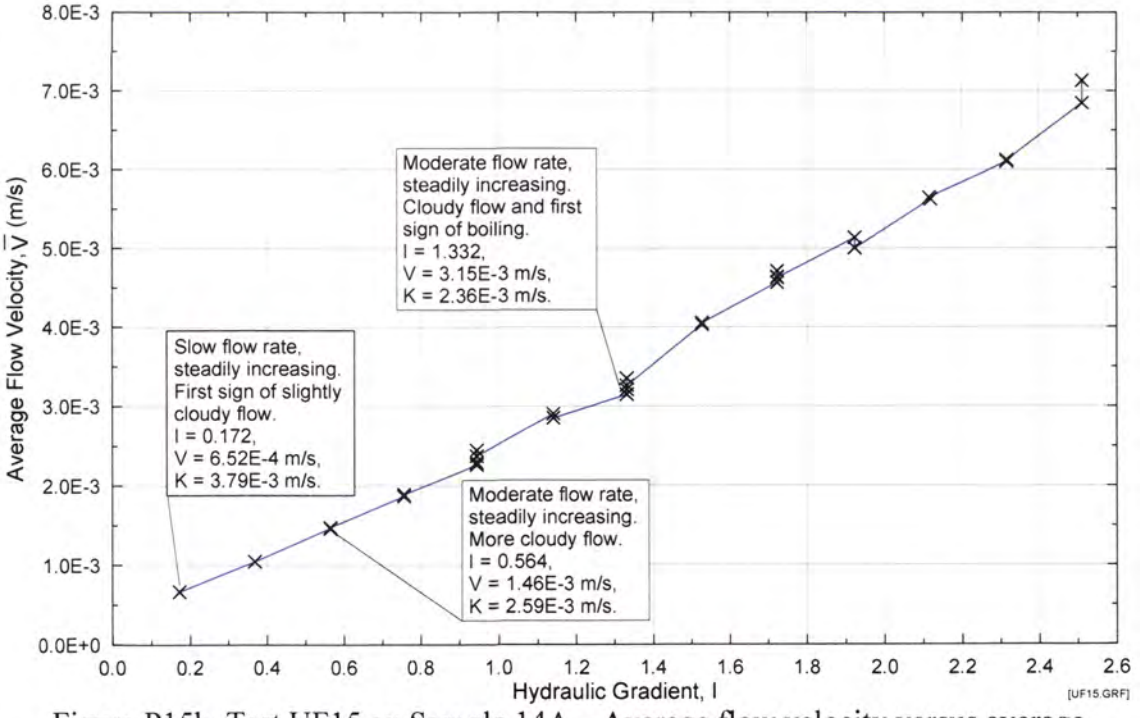

Figure P15b Test UF15 on Sample 14A – Average flow velocity versus average hydraulic gradient. Sample compacted to 90.0% of Standard Maximum Dry Density.

Upward flow test No. UF16 Test Records

UPWARD FLOW SUFFUSION TEST
Test Data

Test No. :	**Suffusion Upflow 016 29/08/02**
Soil Sample :	**Suffusion Test Blend No. 7**
Max. dry density :	2.046 Mg/m3
Optimum moisture content (OWC) :	9.81%
Relative compaction :	95.0%
Actual compaction from test:	95.4%
Moisture content during conditioning :	9.81%
Targeted moisture content :	9.81%
Moisture content from test :	9.99%
Fluid for conditioning soil :	tap water
Eroding fluid :	tap water
Eroding fluid mean temperature :	15.3 °C
Time/Date of Commencement of Soaking :	10.30 am 23/08/02
Time/Date of Commencement of Test :	9.00am 29/08/02

Mix Ingredient	Mix Proportion (%)
Clay Q38	21.75
Silica 60G	21.84
Nepean Sand	24.12
5mm Blue Metal	18.99
10mm Bassalt	8.55
20mm Blue Metal	4.75
Total	100.00

Time (From Commencement) (mins)	Time (s)	Flowrate (L/min)	Head (mm) Inlet	200mm From top surface of sample	150mm From top surface of sample	100mm From top surface of sample	50mm From top surface of sample	Water Surface within cell. (See note)	Observations
0.00	0	0.0000	0.0	0.0	0.0	0.0	0.0	5.0	Test started
10.00	600	0.0028	200.0	0.0	0.0	0.0	0.0	5.0	Clear. Extremely low outflow.
20.00	1200	0.0004	200.0	0.0	0.0	0.0	0.0	5.0	Clear. Extremely low outflow.
30.00	1800	0.0003	250.0	0.0	0.0	0.0	0.0	5.0	Clear. Extremely low outflow.
40.00	2400	0.0003	250.0	0.0	0.0	0.0	0.0	5.0	Clear. Extremely low outflow.
50.00	3000	0.0016	300.0	0.0	0.0	0.0	0.0	5.0	Clear. Extremely low outflow.
60.00	3600	0.0034	300.0	0.0	0.0	0.0	0.0	5.0	Clear. Extremely low outflow.
70.00	4200	0.0105	350.0	0.0	0.0	0.0	0.0	5.0	Clear. Extremely low outflow.
80.00	4800	0.0035	350.0	0.0	0.0	0.0	0.0	5.0	Clear. Extremely low outflow.
90.00	5400	0.0050	400.0	0.0	0.0	0.0	0.0	5.0	Clear. Extremely low outflow.
100.00	6000	0.0061	400.0	0.0	0.0	0.0	0.0	5.0	Clear. Extremely low outflow.
110.00	6600	0.0050	450.0	0.0	0.0	0.0	0.0	5.0	Clear. Extremely low outflow.
120.00	7200	0.0040	450.0	0.0	0.0	0.0	0.0	5.0	Clear. Extremely low outflow.
130.00	7800	0.0060	500.0	0.0	0.0	0.0	0.0	5.0	Clear. Extremely low outflow.
140.00	8400	0.0075	500.0	0.0	0.0	0.0	0.0	5.0	Clear. Extremely low outflow.
150.00	9000	0.0100	550.0	0.0	0.0	0.0	0.0	5.0	Clear. Extremely low outflow.
160.00	9600	0.0129	550.0	0.0	0.0	0.0	0.0	5.0	Clear. Extremely low outflow.
170.00	10200	0.0130	600.0	0.0	0.0	0.0	0.0	5.0	Clear. Extremely low outflow.

Upward flow test No. UF16 Test Records (Cont'd)

Time (From Commencement) (mins)	Time (s)	Flowrate (L/min)	Head (mm) Inlet	200mm From top surface of sample	150mm From top surface of sample	100mm From top surface of sample	50mm From top surface of sample	Water Surface within cell. (See note)	Observations
180.00	10800	0.0130	600.0	0.0	0.0	0.0	0.0	5.0	Clear. Extremely low outflow.
190.00	11400	0.0162	650.0	0.0	0.0	0.0	0.0	5.0	Clear. Extremely low outflow.
200.00	12000	0.0150	650.0	0.0	0.0	0.0	0.0	5.0	Clear. Extremely low outflow.
210.00	12600	0.0180	700.0	0.0	0.0	0.0	0.0	5.0	Clear. Extremely low outflow.
220.00	13200	0.0204	700.0	0.0	0.0	0.0	0.0	5.0	Clear. Extremely low outflow.
230.00	13800	0.0200	750.0	0.0	0.0	0.0	0.0	5.0	Clear. Extremely low outflow.
240.00	14400	0.0204	750.0	0.0	0.0	0.0	0.0	5.0	Clear. Extremely low outflow.
250.00	15000	0.0220	800.0	0.0	0.0	0.0	0.0	5.0	Clear. Extremely low outflow.
260.00	15600	0.0232	800.0	0.0	0.0	0.0	0.0	5.0	Clear. Extremely low outflow.
270.00	16200	0.0220	850.0	0.0	0.0	0.0	0.0	5.0	Clear. Extremely low outflow.
280.00	16800	0.0232	850.0	0.0	0.0	0.0	0.0	5.0	Clear. Extremely low outflow.
290.00	17400	0.0230	900.0	0.0	0.0	0.0	0.0	5.0	Clear. Extremely low outflow.
300.00	18000	0.0242	900.0	0.0	0.0	0.0	0.0	5.0	Clear. Extremely low outflow.
310.00	18600	0.0240	950.0	0.0	0.0	0.0	0.0	5.0	Clear. Extremely low outflow.
320.00	19200	0.0234	950.0	0.0	0.0	0.0	0.0	5.0	Clear. Extremely low outflow.
330.00	19800	0.0252	1000.0	0.0	13.0	0.0	0.0	5.0	Clear. Extremely low outflow.
340.00	20400	0.0246	1000.0	0.0	28.0	0.0	0.0	5.0	Clear. Extremely low outflow.
350.00	21000	0.0250	1050.0	0.0	40.0	0.0	0.0	5.0	Clear. Extremely low outflow.
360.00	21600	0.0260	1050.0	0.0	48.0	0.0	0.0	5.0	Clear. Extremely low outflow.
370.00	22200	0.0260	1100.0	0.0	60.0	0.0	0.0	5.0	Clear. Extremely low outflow.
380.00	22800	0.0262	1100.0	0.0	67.0	0.0	0.0	5.0	Clear. Extremely low outflow.
390.00	23400	0.0360	1150.0	0.0	80.0	0.0	0.0	5.0	Clear. Extremely low outflow.
400.00	24000	0.0380	1150.0	0.0	89.0	0.0	0.0	5.0	Clear. Extremely low outflow.
410.00	24600	0.0400	1200.0	0.0	100.0	0.0	0.0	5.0	Clear. Extremely low outflow.
420.00	25200	0.0416	1200.0	0.0	103.0	0.0	0.0	5.0	Clear. Extremely low outflow.
430.00	25800	0.0406	1200.0	0.0	106.0	0.0	0.0	5.0	Clear. Extremely low outflow. Maximum test head. Stop test.

Note : Deduct 6mm to give true depth of water from water surface to top of test sample within seepage cell.

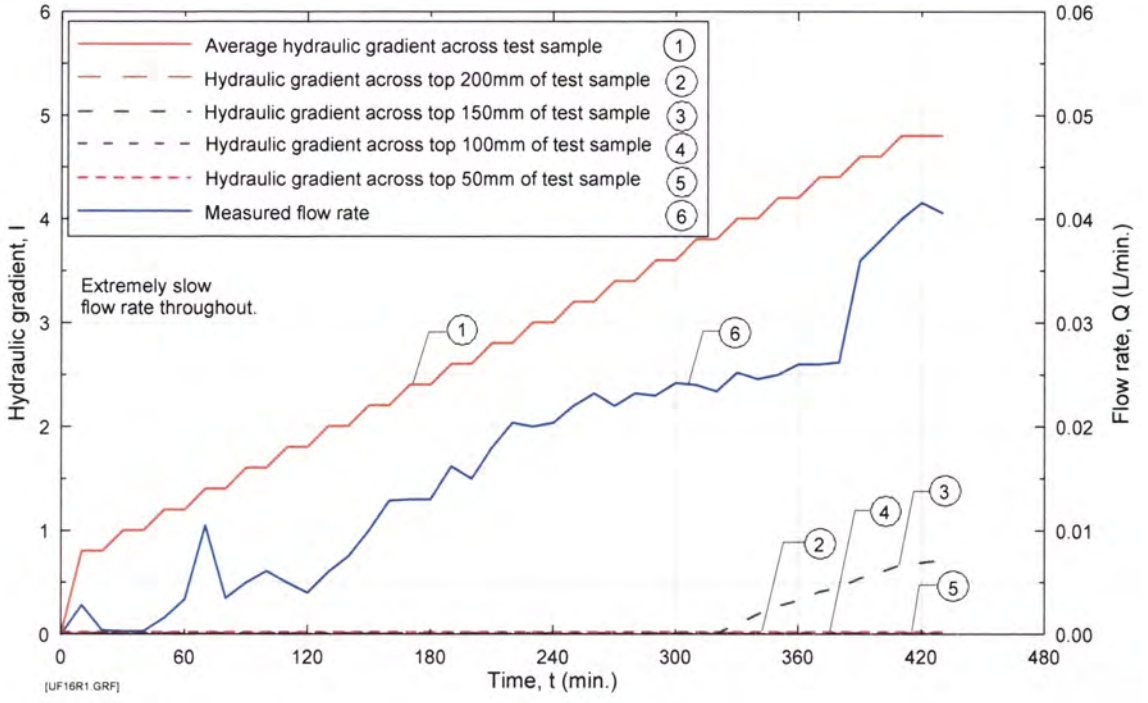

Figure P16a Test UF16 on Sample 7 - Hydraulic gradient and flow rate versus time. Sample compacted to 95.5% of Standard Maximum Dry Density.

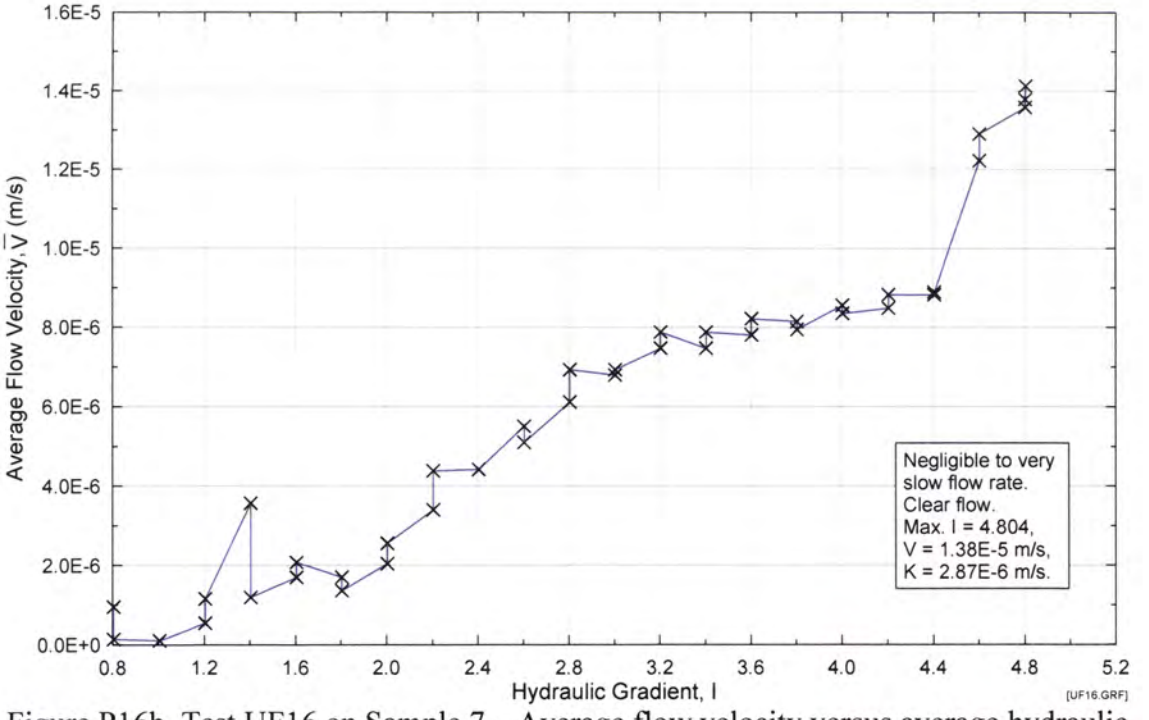

Figure P16b Test UF16 on Sample 7 – Average flow velocity versus average hydraulic gradient. Sample compacted to 95.5% of Standard Maximum Dry Density.

Upward flow test No. UF17 Test Records

UPWARD FLOW SUFFUSION TEST
Test Data

Test No. :	**Suffusion Upflow 017 20/09/02**
Soil Sample :	**Suffusion Test Blend No. 15**
Max. dry density :	2.090 Mg/m3
Optimum moisture content (OWC) :	8.20%
Relative compaction :	95.0%
Actual compaction from test:	94.9%
Moisture content during conditioning :	8.20%
Targeted moisture content :	8.20%
Moisture content from test :	8.34%
Fluid for conditioning soil :	tap water
Eroding fluid :	tap water
Eroding fluid mean temperature :	18.4 °C
Time/Date of Commencement of Soaking :	10.30 am 19/09/02
Time/Date of Commencement of Test :	9.00am 20/09/02

Mix Ingredient	Mix Proportion (%)
Clay Q38	21.49
Silica 60G	24.11
Nepean Sand	0.00
5mm Blue Metal	0.00
10mm Bassalt	30.50
20mm Blue Metal	23.90
Total	100.00

Time (From Commencement) (mins)	Time (s)	Flowrate (L/min)	Head (mm) Inlet	200mm From top surface of sample	150mm From top surface of sample	100mm From top surface of sample	50mm From top surface of sample	Water Surface within cell. (See note)	Observations
10.00	600	0.0000	50.0	0.0	0.0	0.0	0.0	5.0	Test started. Clear. No outflow.
20.00	1200	0.0000	50.0	0.0	0.0	0.0	0.0	5.0	Clear. No outflow.
30.00	1800	0.0000	100.0	0.0	0.0	0.0	0.0	5.0	Clear. No outflow.
40.00	2400	0.0000	100.0	0.0	0.0	0.0	0.0	5.0	Clear. No outflow.
50.00	3000	0.0200	150.0	0.0	0.0	0.0	0.0	5.0	Clear. Extremely low outflow.
60.00	3600	0.0300	150.0	0.0	0.0	0.0	0.0	5.0	Clear. Extremely low outflow.
70.00	4200	0.0630	200.0	0.0	0.0	0.0	0.0	5.0	Slightly cloudy. Extremely low outflow.
80.00	4800	0.0630	200.0	0.0	0.0	0.0	0.0	5.0	Slightly cloudy. Extremely low outflow.
90.00	5400	0.0900	250.0	0.0	0.0	0.0	0.0	5.0	Slightly cloudy. Extremely low outflow.
100.00	6000	0.0900	250.0	0.0	0.0	0.0	0.0	5.0	Slightly cloudy. Extremely low outflow.
110.00	6600	0.1380	300.0	0.0	0.0	0.0	0.0	5.0	Slightly cloudy. Extremely low outflow.
120.00	7200	0.1440	300.0	0.0	0.0	0.0	0.0	6.0	Slightly cloudy. Extremely low outflow.
130.00	7800	0.4000	350.0	0.0	0.0	0.0	0.0	6.0	Slightly cloudy. Extremely low outflow. Test paused, then restarted.
140.00	8400	0.4560	350.0	47.0	4.0	0.0	3.0	7.0	Slightly cloudy. Extremely low outflow.
150.00	9000	0.4500	350.0	260.0	54.0	0.0	3.0	7.0	Slightly cloudy. Extremely low outflow.
160.00	9600	0.5790	400.0	301.0	88.0	0.0	3.0	9.0	Slightly cloudy. Very low outflow.
170.00	10200	0.5880	400.0	318.0	103.0	0.0	4.0	9.0	Slightly cloudy. Very low outflow.
180.00	10800	0.6360	450.0	336.0	135.0	0.0	4.0	9.0	Slightly cloudy. Very low outflow.

Upward flow test No. UF17 Test Records (Cont'd)

Time (From Commencement) (mins)	Time (s)	Flowrate (L/min)	Head (mm)						Observations
			Inlet	200mm From top surface of sample	150mm From top surface of sample	100mm From top surface of sample	50mm From top surface of sample	Water Surface within cell. (See note)	
190.00	11400	0.6540	450.0	340.0	150.0	0.0	4.0	9.0	Slightly cloudy. Very low outflow.
200.00	12000	0.6900	500.0	362.0	159.0	0.0	4.0	9.0	Slightly cloudy. Very low outflow.
210.00	12600	0.7500	500.0	371.0	169.0	0.0	4.0	9.0	Slightly cloudy. Very low outflow.
220.00	13200	0.8220	550.0	377.0	182.0	3.0	4.0	11.0	Slightly cloudy. Very low outflow.
230.00	13800	0.8820	550.0	361.0	195.0	6.0	4.0	11.0	Slightly cloudy. Very low outflow.
240.00	14400	1.0440	600.0	373.0	203.0	7.0	5.0	11.0	Slightly cloudy. Low outflow.
250.00	15000	1.0440	600.0	377.0	210.0	7.0	5.0	11.0	Slightly cloudy. Low outflow.
260.00	15600	1.3620	650.0	404.0	219.0	11.0	6.0	11.0	Slightly cloudy. Low outflow.
270.00	16200	1.3680	650.0	408.0	218.0	11.0	6.0	11.0	Slightly cloudy. Low outflow.
280.00	16800	1.9500	700.0	430.0	218.0	12.0	7.0	13.0	Slightly cloudy. Low outflow.
290.00	17400	1.9800	700.0	430.0	216.0	12.0	7.0	13.0	Slightly cloudy. Low outflow.
300.00	18000	2.0850	750.0	455.0	165.0	6.0	7.0	12.0	Slightly cloudy. Low outflow. Test paused, then restarted.
310.00	18600	2.1450	750.0	466.0	195.0	7.0	8.0	12.0	Slightly cloudy. Low outflow.
320.00	19200	2.2500	800.0	485.0	220.0	9.0	8.0	12.0	Clear, occasional bubbles and piping. Low outflow.
330.00	19800	2.2050	800.0	489.0	243.0	9.0	8.0	12.0	Clear, occasional bubbles and piping. Low outflow.
340.00	20400	2.3250	850.0	526.0	264.0	9.0	8.0	12.0	Clear, occasional bubbles and piping. Low outflow.
350.00	21000	2.3400	850.0	529.0	274.0	9.0	8.0	13.0	Clear, occasional bubbles and piping. Low outflow.
360.00	21600	2.4450	900.0	551.0	293.0	9.0	8.0	13.0	Clear, occasional bubbles and piping. Low outflow.
370.00	22200	2.5200	900.0	551.0	300.0	10.0	8.0	13.0	Clear, occasional bubbles and piping. Low outflow.
380.00	22800	2.7400	900.0	553.0	312.0	33.0	8.0	13.0	Clear, occasional bubbles and piping. Low outflow.
390.00	23400	2.7200	900.0	555.0	314.0	34.0	9.0	13.0	Clear, occasional bubbles and piping. Low outflow.
400.00	24000	2.8000	950.0	593.0	322.0	32.0	9.0	13.0	Clear, occasional bubbles and piping. Low outflow.
410.00	24600	2.8600	950.0	600.0	328.0	36.0	9.0	13.0	Clear, occasional bubbles and piping. Low outflow.
420.00	25200	3.3300	1000.0	633.0	335.0	36.0	10.0	14.0	Slightly cloudy, bubbling and piping slightly more. Low outflow.
430.00	25800	3.3300	1000.0	627.0	335.0	33.0	10.0	14.0	Slightly cloudy, bubbling and piping slightly more. Low outflow.
440.00	26400	3.4500	1050.0	655.0	340.0	37.0	10.0	14.0	Slightly cloudy, bubbling and piping slightly more. Low outflow. Test paused, then restarted.
450.00	27000	3.5100	1050.0	615.0	314.0	37.0	10.0	14.0	Slightly cloudy, bubbling and piping slightly more. Low outflow.
460.00	27600	4.0800	1100.0	620.0	314.0	43.0	12.0	14.0	Slightly cloudy, bubbling and piping slightly more. Low outflow.
470.00	28200	4.1400	1100.0	628.0	345.0	45.0	11.0	14.0	Slightly cloudy, bubbling and piping slightly more. Low outflow.
480.00	28800	4.4280	1150.0	639.0	358.0	49.0	12.0	15.0	Slightly cloudy, bubbling and piping slightly more. Low outflow.
490.00	29400	4.4700	1150.0	633.0	368.0	49.0	12.0	15.0	Slightly cloudy, bubbling and piping slightly more. Low outflow.
500.00	30000	4.8600	1200.0	670.0	381.0	53.0	12.0	16.0	Slightly cloudy, bubbling and piping slightly more. Low outflow.
510.00	30600	4.9800	1200.0	680.0	384.0	55.0	13.0	16.0	Slightly cloudy, bubbling and piping slightly more. Moderate outflow. Maximum head, stop test.

Note : Deduct 6mm to give true depth of water from water surface to top of test sample within seepage cell.

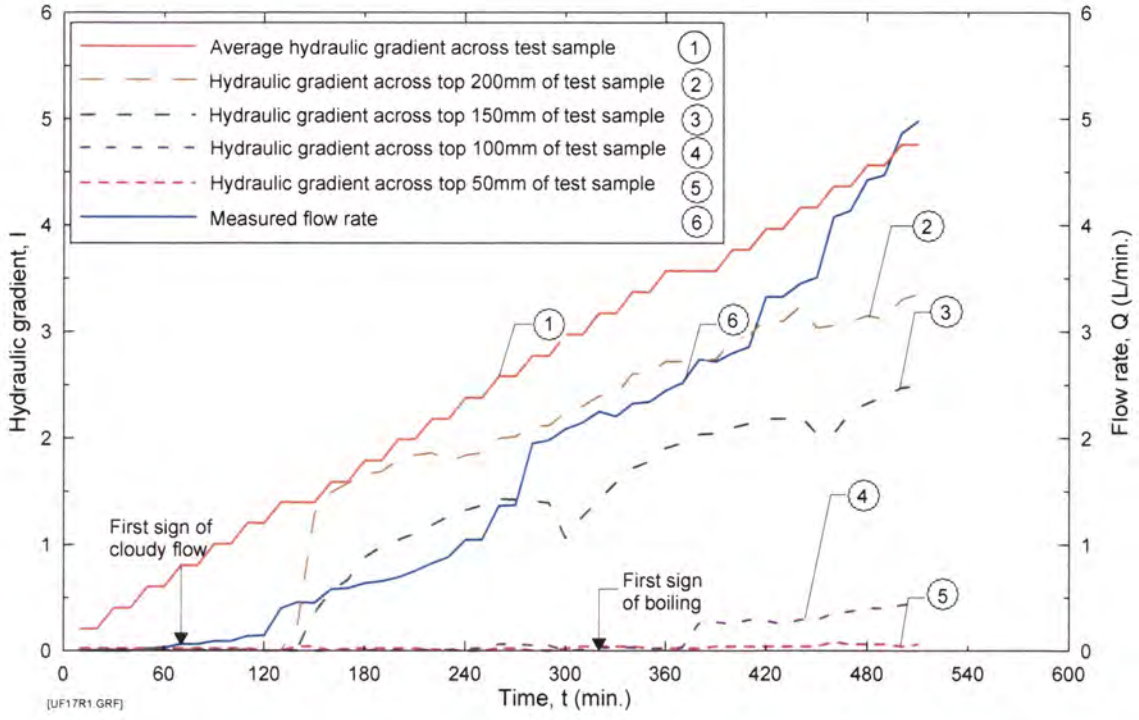

Figure P17a Test UF17 on Sample 15 - Hydraulic gradient and flow rate versus time. Sample compacted to 95.0% of Standard Maximum Dry Density.

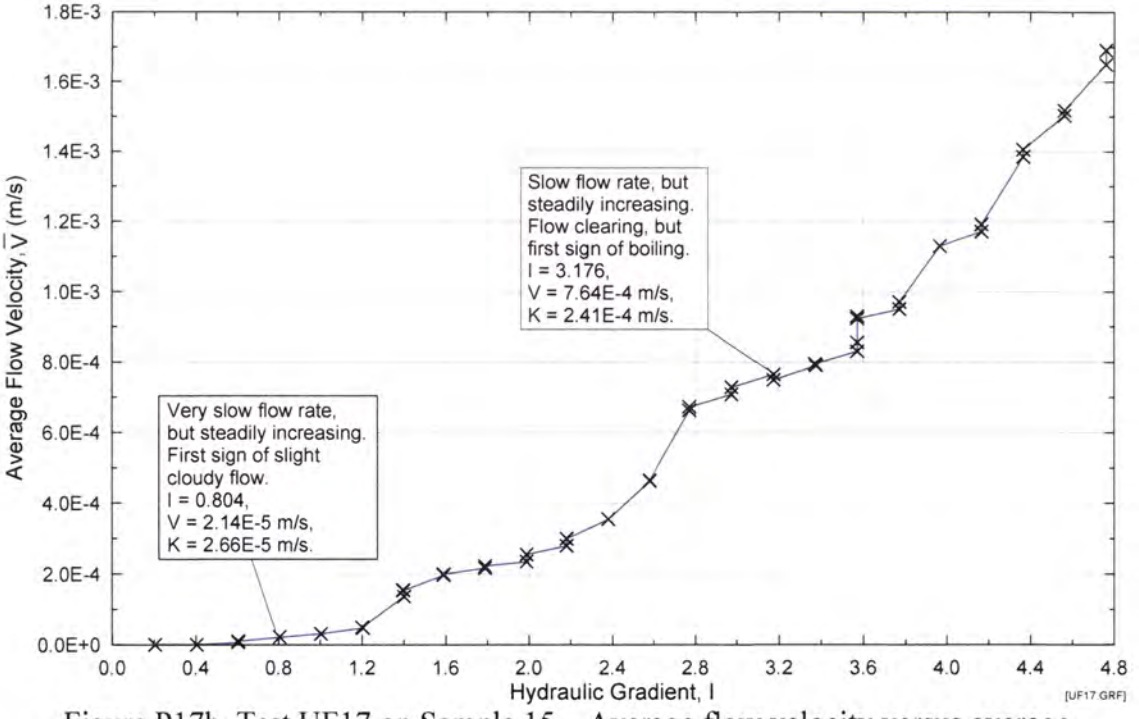

Figure P17b Test UF17 on Sample 15 – Average flow velocity versus average hydraulic gradient. Sample compacted to 95.0% of Standard Maximum Dry Density.

Upward flow test No. UF18 Test Records

UPWARD FLOW SUFFUSION TEST
Test Data

Test No. :	**Suffusion Upflow 018 4/04/02**
Soil Sample :	**Suffusion Test Blend No. 17 (Rowallan Dam)**
Max. dry density :	1.868 Mg/m3
Optimum moisture content (OWC) :	13.30%
Relative compaction :	95.0%
Actual compaction from test:	96.0%
Moisture content during conditioning :	13.30%
Targeted moisture content :	13.30%
Moisture content from test :	13.11%
Fluid for conditioning soil :	tap water
Eroding fluid :	tap water
Eroding fluid mean temperature :	21.7 °C
Time/Date of Commencement of Soaking :	10.30 am 01/03/02
Time/Date of Commencement of Test :	9.00am 04/03/02

Mix Ingredient	Mix Proportion (%)
Rowallan Dam	100.00
Total	100.00

Time (From Commencement) (mins)	Time (s)	Flowrate (L/min)	Head (mm) Inlet	200mm From top surface of sample	150mm From top surface of sample	100mm From top surface of sample	50mm From top surface of sample	Water Surface within cell. (See note)	Observations
10.00	600	0.002	50.0	0.0	0.0	0.0	0.0	7.0	Test started. Clear. Extremely low outflow.
20.00	1200	0.001	50.0	0.0	0.0	0.0	0.0	7.0	Clear. Extremely low outflow.
30.00	1800	0.001	100.0	0.0	0.0	0.0	0.0	7.0	Clear. Extremely low outflow.
40.00	2400	0.001	100.0	0.0	0.0	0.0	0.0	7.0	Clear. Extremely low outflow.
50.00	3000	0.001	150.0	0.0	0.0	0.0	0.0	7.0	Clear. Extremely low outflow.
60.00	3600	0.002	150.0	0.0	0.0	0.0	0.0	7.0	Clear. Extremely low outflow.
70.00	4200	0.002	200.0	0.0	0.0	0.0	0.0	7.0	Clear. Extremely low outflow.
80.00	4800	0.002	200.0	100.0	0.0	0.0	5.0	7.0	Clear. Extremely low outflow.
90.00	5400	0.008	250.0	125.0	117.0	13.0	8.0	7.0	Clear. Extremely low outflow.
100.00	6000	0.011	250.0	126.0	117.0	17.0	8.0	7.0	Clear. Extremely low outflow.
110.00	6600	0.012	300.0	143.0	121.0	26.0	10.0	7.0	Clear. Extremely low outflow.
120.00	7200	0.012	300.0	143.0	121.0	28.0	10.0	7.0	Clear. Extremely low outflow.
130.00	7800	0.016	350.0	157.0	129.0	37.0	13.0	7.0	Clear. Extremely low outflow.
140.00	8400	0.016	350.0	157.0	129.0	37.0	13.0	7.0	Clear. Extremely low outflow.
150.00	9000	0.017	400.0	157.0	130.0	42.0	13.0	7.0	Clear. Extremely low outflow.
160.00	9600	0.017	400.0	157.0	130.0	42.0	13.0	7.0	Clear. Extremely low outflow.
170.00	10200	0.016	450.0	145.0	126.0	38.0	12.0	7.0	Clear. Extremely low outflow.
180.00	10800	0.014	450.0	143.0	125.0	38.0	12.0	7.0	Clear. Extremely low outflow.

Upward flow test No. UF18 Test Records (Cont'd)

Time (From Commencement) (mins)	Time (s)	Flowrate (L/min)	Head (mm)						Observations
			Inlet	200mm From top surface of sample	150mm From top surface of sample	100mm From top surface of sample	50mm From top surface of sample	Water Surface within cell. (See note)	
190.00	11400	0.016	500.0	153.0	127.0	41.0	13.0	7.0	Clear. Extremely low outflow.
200.00	12000	0.016	500.0	153.0	127.0	41.0	13.0	7.0	Clear. Extremely low outflow.
210.00	12600	0.016	550.0	150.0	127.0	40.0	12.0	7.0	Clear. Extremely low outflow.
220.00	13200	0.014	550.0	147.0	125.0	40.0	12.0	7.0	Clear. Extremely low outflow.
230.00	13800	0.016	600.0	155.0	127.0	43.0	13.0	7.0	Clear. Extremely low outflow.
240.00	14400	0.016	600.0	152.0	127.0	43.0	13.0	7.0	Clear. Extremely low outflow.
250.00	15000	0.016	650.0	161.0	129.0	45.0	13.0	7.0	Clear. Extremely low outflow.
260.00	15600	0.018	650.0	160.0	129.0	45.0	13.0	7.0	Clear. Extremely low outflow.
270.00	16200	0.020	700.0	162.0	131.0	47.0	14.0	7.0	Clear. Extremely low outflow.
280.00	16800	0.020	700.0	158.0	130.0	47.0	14.0	7.0	Clear. Extremely low outflow.
290.00	17400	0.020	750.0	160.0	134.0	50.0	14.0	7.0	Clear. Extremely low outflow.
300.00	18000	0.020	750.0	160.0	134.0	50.0	14.0	7.0	Clear. Extremely low outflow.
310.00	18600	0.022	800.0	154.0	133.0	49.0	13.0	7.0	Clear. Extremely low outflow.
330.00	19800	0.021	800.0	158.0	131.0	50.0	13.0	7.0	Clear. Extremely low outflow.
350.00	21000	0.021	800.0	158.0	131.0	50.0	13.0	7.0	Clear. Extremely low outflow.
360.00	21600	0.021	850.0	156.0	132.0	53.0	14.0	7.0	Clear. Extremely low outflow.
370.00	22200	0.021	850.0	152.0	131.0	50.0	13.0	7.0	Clear. Extremely low outflow.
380.00	22800	0.021	900.0	158.0	132.0	54.0	15.0	7.0	Clear. Extremely low outflow.
390.00	23400	0.021	900.0	157.0	132.0	54.0	14.0	7.0	Clear. Extremely low outflow.
400.00	24000	0.024	950.0	167.0	135.0	57.0	16.0	7.0	Clear. Extremely low outflow.
410.00	24600	0.024	950.0	167.0	135.0	57.0	16.0	7.0	Clear. Extremely low outflow.
420.00	25200	0.024	1000.0	159.0	135.0	57.0	15.0	7.0	Clear. Extremely low outflow.
430.00	25800	0.025	1000.0	159.0	135.0	57.0	15.0	7.0	Clear. Extremely low outflow.
440.00	26400	0.025	1050.0	159.0	135.0	57.0	15.0	7.0	Clear. Extremely low outflow.
450.00	27000	0.025	1050.0	161.0	136.0	58.0	16.0	7.0	Clear. Extremely low outflow. Test stopped.

Note : Deduct 6mm to give true depth of water from water surface to top of test sample within seepage cell.

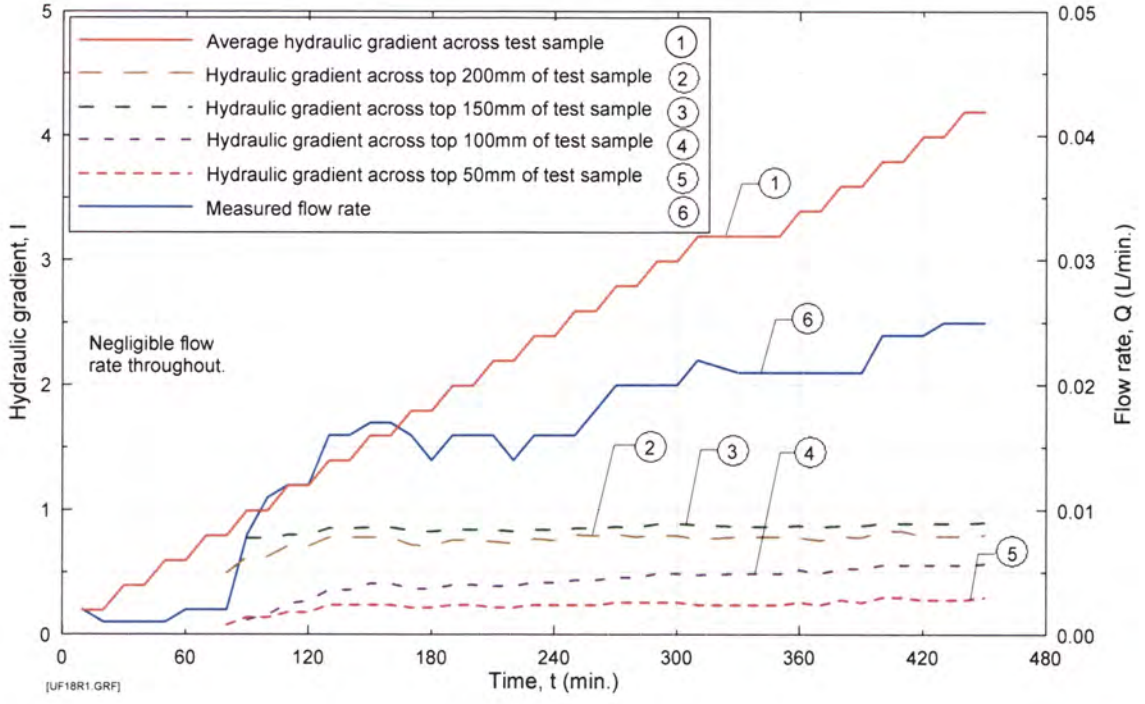

Figure P18a Test UF18 on Sample RD - Hydraulic gradient and flow rate versus time. Sample compacted to 96.0% of Standard Maximum Dry Density.

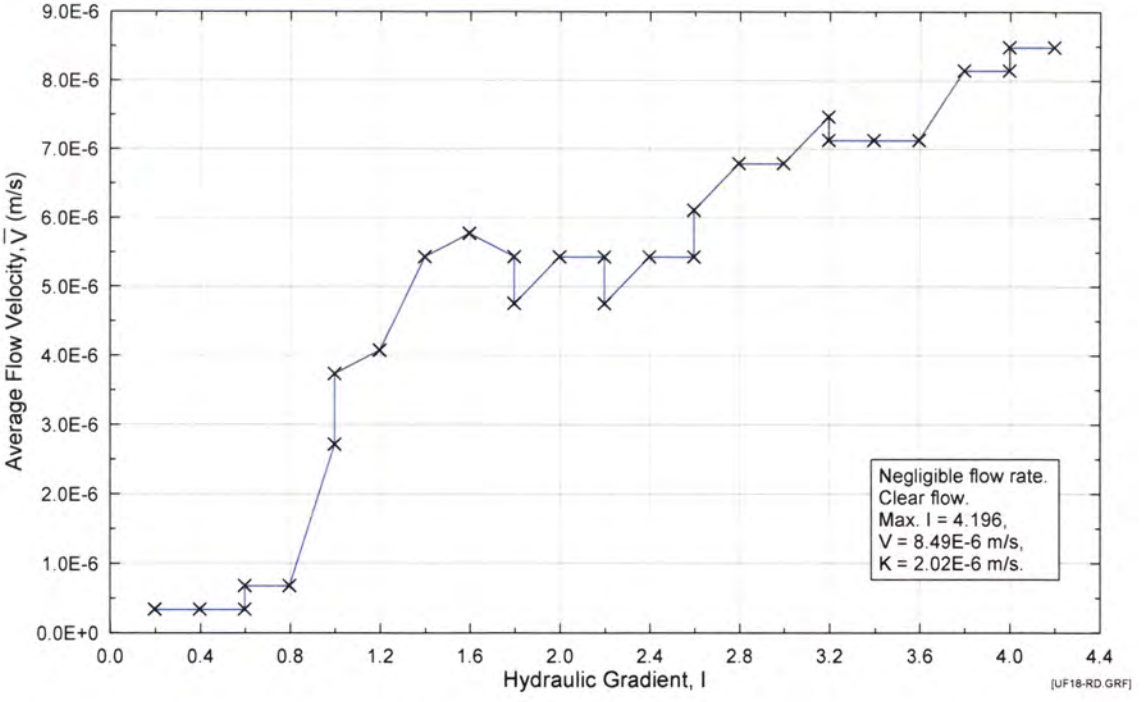

Figure P18b Test UF18 on Sample RD – Average flow velocity versus average hydraulic gradient. Sample compacted to 96.0% of Standard Maximum Dry Density.